ENCYCLOPEDIA OF

Physical Science and Technology

THIRD EDITION

Inorganic Chemistry

Table of Contents
(Subject Area: Inorganic Chemistry)

Article	*Authors*	Pages in the Encyclopedia
Actinide Elements	*Siegfried Hübener*	Pages 211-236
Bioinorganic Chemistry	*Brian T. Farrer and Vincent L. Pecoraro*	Pages 117-139
Boron Hydrides	*Herbert Beall and Donald F. Gaines*	Pages 301-316
Coordination Compounds	*R. D. Gillard*	Pages 739-760
Dielectric Gases	*L. G. Christophorou and S. J. Dale*	Pages 357-371
Electron Transfer Reactions	*Gilbert P. Haight, Jr.*	Pages 347-361
Halogen Chemistry	*Marianna Anderson Busch*	Pages 197-222
Inclusion (Clathrate) Compounds	*Jerry L. Atwood*	Pages 717-729
Inorganic Exotic Molecules	*Joel F. Liebman, Kay Severin and Thomas M. Klapötke*	Pages 817-838
Liquid Alkali Metals	*C. C. Addison*	Pages 661-671
Main Group Elements	*Russell L. Rasmussen, Joseph G. Morse and Karen W. Morse*	Pages 1-30
Mesoporous Materials, Synthesis	*Robert Mokaya*	Pages 369-381
Metal Cluster Chemistry	*D. F. Shriver*	Pages 407-409
Metal Hydrides	*Holger Kohlmann*	Pages 441-458
Metal Particles and Cluster Compounds	*Allan W. Olsen and Kenneth J. Klabunde*	Pages 513-550
Nano sized Inorganic Clusters	*Leroy Cronin, Achim Müller and Dieter Fenske*	Pages 303-317
Noble Metals (Chemistry)	*Hubert Schmidbaur and John L. Cihonski*	Pages 463-492
Noble-Gas Chemistry	*Gary J. Schrobilgen*	Pages 449-461
Periodic Table (Chemistry)	*N. D. Epiotis and D. K. Henze*	Pages 671-695
Rare Earth Elements and Materials	*Zhiping Zheng and John E. Greedan*	Pages 1-22

Actinide Elements

Siegfried Hübener
Forschungszentrum Rossendorf

I. Discovery, Occurrence, and Synthesis of the Actinides
II. Radioactivity and Nuclear Reactions of Actinides
III. Applications of Actinides
IV. Actinide Metals
V. Actinide Ions
VI. Actinide Compounds and Complexes

GLOSSARY

Actinyl ion Dioxo actinide cations MO_2^+ and MO_2^{2+}.

Decay chain A series of nuclides in which each member transforms into the next through nuclear decay until a stable nuclide has been formed.

Lanthanides Fourteen elements with atomic numbers 58 (cerium) to 71 (lutetium) that are a result of filling the $4f$ orbitals with electrons.

Nuclear fission The division of a nucleus into two or more parts, usually accompanied by the emission of neutrons and γ radiation.

Nuclide A species of atom characterized by its mass number, atomic number, and nuclear energy state. A radionuclide is a radioactive nuclide.

Primordial radionuclides Nuclides which were produced during element evolution and which have partly survived since then due to their long half-lives.

Radioactivity The property of certain nuclides of showing radioactive decay in which particles or γ radiation are emitted or the nucleus undergoes spontaneous fission.

Speciation Characterization of physical and chemical states of (actinide) species in a given (chemical) environment.

Transactinide elements Artificial elements beyond the actinide elements, beginning with rutherfordium (Rf), element 104. The heaviest elements, synthesized until now, are the elements 114, 116, and 118. At present, bohrium (Bh), element 107, is the heaviest element which has been characterized chemically; chemical studies of element 108, hassium (Hs), and element 112 are in preparation.

THE ACTINIDE ELEMENTS (actinoids) comprise the 14 elements with atomic numbers 90–103, which follow actinium in the periodic table: thorium (Th), protactinium (Pa), uranium (U), neptunium (Np), plutonium (Pu), americium (Am), curium (Cm), berkelium (Bk), californium (Cf), einsteinium (Es), fermium (Fm), mendelevium (Md), nobelium (No), and lawrencium (Lr). The actinides constitute a unique series of elements which are formed by the progressive filling of the $5f$ electron shell. Although not formally an actinide element, actinium (Ac;

atomic number 89) is usually included in discussions about the actinides.

According to the International Union of Pure and Applied Chemistry (IUPAC), the name actinoid is preferable to actinide because the ending "-ide" normally indicates a negative ion. However, owing to wide current use, "actinide" is still allowed.

I. DISCOVERY, OCCURRENCE, AND SYNTHESIS OF THE ACTINIDES

A. Naturally Occurring Actinides

All of the isotopes of the actinide elements are radioactive, and only four of the primordial isotopes, ^{232}Th, ^{235}U, ^{238}U, and ^{244}Pu, have a sufficient long half-life for there to be any of these isotopes left in nature. Only three actinide elements and actinium were known as late as 1940. In addition to thorium and uranium, protactinium and actinium have been found to exist in uranium and thorium ores due to the ^{238}U [Eq. (1)] and ^{235}U [Eq. (2)] decay series:

$$^{238}_{92}U \xrightarrow{-\alpha} {}^{234}_{90}Th \xrightarrow{-\beta^-} {}^{234}_{91}Pa \xrightarrow{-\beta^-} {}^{234}_{92}U, \qquad (1)$$

$$^{235}_{92}U \xrightarrow{-\alpha} {}^{231}_{90}Th \xrightarrow{-\beta^-} {}^{231}_{91}Pa \xrightarrow{-\alpha} {}^{227}_{89}Ac. \qquad (2)$$

It was not until 1971 that the existence of primordial ^{244}Pu in nature in trace amounts was shown by D. C. Hoffman and co-workers.

Uranium was the first actinide element to be discovered. M. H. Klaproth showed in 1789 that pitchblende contained a new element and named it uranium after the then newly discovered planet Uranus. Uranium is now known to comprise 2.1 ppm of the Earth's crust, which makes it about as abundant as arsenic or europium. It is widely distributed, with the principal sources being in Australia, Canada, South Africa, and the United States. The two most important oxide minerals of uranium are uraninite (U_3O_8; 50–90% uranium), a variety of which is called pitchblende, and carnotite ($K_2(UO_2)(VO_4)_2 \cdot 3H_2O$; 54% uranium). A very common uranium mineral is autunite ($Ca(UO_2)_2(PO_4)_2 \cdot nH_2O$, $n = 8$–12). Natural uranium consists of 99.3% ^{238}U and 0.72% of the fissionable isotope ^{235}U. A third important isotope, ^{233}U, does not occur in nature but can be produced by thermal-neutron irradiation of ^{232}Th [Eq. (3)]:

$$^{232}_{90}Th + {}^{1}_{0}n \rightarrow {}^{233}_{90}Th \xrightarrow{-\beta^-} {}^{233}_{91}Pa \xrightarrow{-\beta^-} {}^{233}_{92}U. \qquad (3)$$

This process converts thorium to fissionable fuel in a breeder reactor.

Thorium was discovered by J. J. Berzelius in 1828 when he isolated a new oxide from a Norwegian ore then known as thorite. He named the oxide thoria, and the metal he obtained by reduction of its tetrachloride with potassium he named thorium. (Later, in 1841, B. Peligot used the same method to prepare uranium metal for the first time.) Thorium constitutes 8.1 ppm of the Earth's crust and is thus as abundant as boron. Converted by neutron irradiation to ^{233}U, it could yield an amount of neutron-fissile material several hundred times the amount of the naturally occurring fissile uranium isotope ^{235}U. The principal thorium ore is monazite, a mixture of rare-earth and thorium phosphates containing up to 30% ThO_2. Monazite sands are widely distributed throughout the world. In Canada thorium is recovered from uranothorite (a mixed thorium-uranium silicate accompanied by pitchblende) as a co-product of uranium. Rarer minerals thorianite (90% ThO_2) and thorite ($ThSiO_4$; 62% thorium) have been found in the western United States and New zealand. Natural thorium is 100% ^{232}Th.

In 1913 protactinium was discovered by K. Fajans and O. Göhring, who identified ^{234m}Pa as an unstable member of the ^{238}U decay series. They named the new element brevium because of its short half-life of 1.15 min. In 1918 the longer-lived isotope ^{231}Pa, with a half-life of 32,800 years, was identified independently by two groups, O. Hahn and L. Meitner, and F. Soddy and J. A. Cranston, as a product of ^{235}U decay. Since the name brevium was obviously inappropriate for such a long-lived radioelement, it was changed to protactinium, thus naming element 91 as the parent of actinium. Protactinium is one of the rarest of the naturally occurring elements. Although not worth extracting from uranium ores, protactinium becomes concentrated in residues from uranium processing plants.

Actinium was discovered by A. Debierne in 1899. Its name is derived from the Greek word for beam or ray, referring to its radioactivity. The natural occurrence of the longest lived actinium isotope ^{227}Ac, with a half-life of 21.77 years, is entirely dependent on that of its primordial ancestor, ^{235}U. The natural abundance of ^{227}Ac is estimated to be $5.7 \cdot 10^{-10}$ ppm. The most concentrated actinium sample ever prepared from a natural raw material consisted of about 7 μg of ^{227}Ac in less than 0.1 mg of La_2O_3.

B. Synthetic Actinides

Stimulated by the discovery of the neutron in 1932 by J. Chadwick and the first synthesis of artificial radioactive nuclei using α particle-induced nuclear reactions in 1934 by F. Joliot and I. Curie, many attempts were made to produce transuranium elements by neutron irradiation of uranium. In 1934, E. Fermi and later O. Hahn, L. Meitner, and F. Strassmann reported that they had created transuranium elements. But in 1938, O. Hahn and F. Strassmann showed that the radioactive species produced by neutron

irradiation of uranium were in fact fission fragments resulting from the nuclear fission of uranium! Thus, the early search for transuranium elements led to one of the greatest discoveries of the 20th century.

The first transuranium element, neptunium, was discovered in 1940 by E. M. McMillan and P. H. Abelson. They were able to chemically separate and identify element 93 formed in the following reaction sequences [Eq. (4)]:

$$^{238}_{92}\mathrm{U} + ^{1}_{0}n \rightarrow ^{239}_{92}\mathrm{U} \xrightarrow[23\ \mathrm{min}]{-\beta^-} ^{239}_{93}\mathrm{Np} \xrightarrow[2.3\ \mathrm{days}]{-\beta^-} ^{239}_{94}\mathrm{Pu}. \qquad (4)$$

They showed that element 93 has chemical properties similar to those of uranium and not those of an eka-rhenium as suggested on the basis of the periodic table of that time. To distinguish it from uranium, element 93 was reduced by SO_2 and precipitated as a fluoride. This new element was named neptunium after Neptune, the planet discovered after Uranus. In 1952, trace amounts of ^{237}Np were found in uranium of natural origin, formed by neutron capture in uranium.

It was obvious to the discoverers of neptunium that ^{239}Np should β decay to the isotope of element 94 with mass number 239, but they were unable to identify it. However, up to the end of 1940, G. T. Seaborg, E. M. McMillan, J. W. Kennedy, and A. C. Wahl succeeded in identifying ^{238}Pu in uranium, which was bombarded with deuterons produced in the 60-in. cyclotron at the University of California in Berkeley [Eq. (5)]:

$$^{238}_{92}\mathrm{U} + ^{2}_{1}\mathrm{H} \rightarrow 2^{1}_{0}n + ^{238}_{93}\mathrm{Np} \xrightarrow[2.1\ \mathrm{days}]{-\beta} ^{238}_{94}\mathrm{Pu}. \qquad (5)$$

Element 94 was named plutonium after the planet discovered last, Pluto. In 1941, the first 0.5 μg of the fissionable isotope ^{239}Pu were produced by irradiating 1.2 kg of uranyl nitrate with cyclotron-generated neutrons. In 1948, trace amounts of ^{239}Pu were found in nature, formed by neutron capture in uranium. In chemical studies, plutonium was shown to have properties similar to uranium and not to osmium as suggested earlier. The actinide concept advanced by G. T. Seaborg, to consider the actinide elements as a second f transition series analogous to the lanthanides, systematized the chemistry of the transuranium elements and facilitated the search for heavier actinide elements. The actinide elements americium (95) through fermium (100) were produced first either via neutron or helium-ion bombardments of actinide targets in the years between 1944 and 1955.

Element 96, curium, was produced in 1944 by the bombardment of ^{239}Pu with helium ions in the Berkeley 60-in. cyclotron, and soon after it was found that ^{241}Pu, formed from ^{239}Pu by two successive neutron captures in a nuclear reactor, decays under β^- particle emission to give ^{241}Am. Earlier attempts to produce and chemically separate americium and curium failed, believing that they would have chemical properties similar to uranium, neptunium, and plutonium. Once it was recognized that these elements, according to G. T. Seaborg's actinide concept, might have properties similar to europium and gadolinium, the use of proper chemical procedures led to success. By analogy to europium (named after Europe) and gadolinium (named after Johan Gadolin, a Finnish rare-earth chemist), for elements 95 and 96 the names americium after the continent of America and curium to honor Pierre and Marie Curie were proposed. The elements with the atomic numbers 97 and 98 at first could not be produced by irradiation with neutrons, because β^- decaying isotopes of curium were not known. By 1949 sufficient amounts of ^{241}Am and ^{242}Cm had been accumulated to make it possible to produce elements 97 and 98 in helium-ion bombardments. The α particle-emitting species produced in the bombardments could be identified as isotopes of elements 97 and 98, which were named berkelium and californium after the city and state of discovery.

Elements 99 and 100, named einsteinium and fermium to honor Albert Einstein and Enrico Fermi, were unexpectedly synthesized in the first U. S. thermonuclear explosion in 1952. The successive capture of numerous neutrons by ^{238}U and subsequent β^- decay chains ended in the β stable nuclides ^{253}Es and ^{255}Fm. From tons of coral collected at the explosion area, hundreds of atoms of the new elements could be separated and positively identified. Further attempts to produce still heavier elements in underground nuclear tests or in high-flux nuclear reactors failed. ^{257}Fm is the heaviest nuclide which can be produced using neutron-capture reactions, owing to the very short half-lives of the heavier fermium isotopes and their spontaneous fission instead of β^- decay. To produce element 101, mendelevium, only about 10^9 atoms of ^{253}Es were made available for a bombardment with helium ions in the Berkeley 60-in. cyclotron. For the first time an element was discovered in "one-atom-at-a-time" experiments on the basis of only 17 produced atoms recoiling from the einsteinium target. The discoverers of element 101, A. Ghiorso, B. G. Harvey, G. R. Choppin, S. G. Thompson, and G. T. Seaborg, suggested the name mendelevium in honor of the Russian chemist Dmitri I. Mendeleev, who was the first to use a periodic system of the elements to predict the chemical properties of undiscovered elements.

The synthesis of element 102 was even more complicated, because a fermium target to apply the bombardment with helium ions was not available. In order to make use of lighter target elements, heavier ions had to be accelerated. The discovery of element 102 was first reported in 1957 by an international group working at the Nobel Institute of Physics in Stockholm. The name nobelium in honor of

Alfred Nobel was immediately accepted by the IUPAC. However, experiments at Berkeley and the Kurchatov Institute in Moscow showed that the original Swedish claim to have prepared element 102 was in error. Attempts to synthesize and identify isotopes of element 102 in heavy ion bombardments of actinide targets dragged on for many years at the laboratories in Berkeley and Dubna, Russia. Thus, scientists from Berkeley suggested that the credit for the discovery should be shared. But, in 1993 the IUPAC-IUPAP Transfermium Working Group concluded that the Dubna laboratory finally achieved an undisputed synthesis.

Also, the discovery of element 103, the last actinide element, was contested by Berkeley and Dubna for a long time. At Berkeley mixtures of californium isotopes were bombarded with boron ions, whereas at Dubna the bombardment of americium targets with oxygen ions was applied. Finally, both groups accepted the conclusion of the Transfermium Working Group, that full confidence was built up over a decade with credit for discovery of element 103 attaching to work in both Berkeley and Dubna. The name lawrencium after E. O. Lawrence, the inventor of the cyclotron, suggested by A. Ghiorso and co-workers from Berkeley and accepted by IUPAC, was finally recommended by IUPAC in 1997 together with the names for the transactinide elements up to element 109.

Table I summarizes the discovery or synthesis of all of the actinide elements.

II. RADIOACTIVITY AND NUCLEAR REACTIONS OF ACTINIDES

All isotopes of the actinides and actinium are radioactive. Table II presents data on several of the most available and important of these. The unstable, radioactive actinide nuclei decay by emission of α particles, electrons, or positrons (β^- or β^+ decay, respectively). Alternatively to the emission of a positron, the unstable nucleus may capture an electron of the electron shell of the atom (symbol ε). In most cases the radioactive decay leads to an excited state of the new nucleus, which gives off its excitation energy in the form of one or several photons (γ rays). In some cases a metastable state results that decays independently of the way it was formed. Spontaneous fission (symbol sf) is another mode of radioactive decay, which was discovered in 1940 by G. N. Flerov and K. A. Petrzhak.

The numerous radionuclides present in thorium and uranium ores are members of genetic correlated radioactive decay series, which are represented in Fig. 1. In all of these decay series, only α and β^- decay are observed. With emission of an α particle ($^4_2$He), the atomic number is reduced by 2, the mass number by 4. With emission of a β^- particle, the mass number remains unchanged, whereas the atomic number increases by 1. As a result, in these decay series the mass number can differ only by multiples of 4 and there are four such families, designated $4n+0$ (thorium series), $4n+1$ (neptunium series), $4n+2$ (uranium or uranium-radium series), and $4n+3$ (actinium series). The neptunium series is missing in nature. It was probably present in nature for some million years after the genesis of the elements, but decayed due to the relatively short half-life of ^{237}Np, compared with the age of the Earth (about $5 \cdot 10^9$ years). Each series contains a number of short-lived nuclides, and the final members of each series are stable nuclides. α Decay is the dominant decay mode of long-lived heavy nuclei with atomic numbers $Z > 83$. With increasing atomic numbers spontaneous fission begins to compete with α decay. For ^{238}U the probability of spontaneous fission is about 10^{-4}% of that of α decay and is already about 90% for ^{256}Fm.

The radioactive decay is the simplest form of a nuclear reaction according to equation [Eq. (6)]:

$$\mathrm{A} \rightarrow \mathrm{B} + \mathrm{x} + \Delta E. \tag{6}$$

This is a mononuclear reaction. In nuclear science, however, binuclear reactions are generally understood by the term "nuclear reaction." They are described by the general equation [Eq. (7)]:

$$\mathrm{A} + \mathrm{x} \rightarrow \mathrm{B} + \mathrm{y} + \Delta E, \tag{7}$$

where A is the target nuclide, x is the projectile, B is the product nuclide, and y is the particle or photon emitted. Equations (3)–(5) are examples for neutron- and deuteron-induced nuclear reactions. With heavy ions (heavier than α particles) as projectiles, the heaviest actinides have been synthesized. Targets made from heavy actinide nuclides such as ^{248}Cm and ^{249}Bk have been used to synthesize several transactinide elements in heavy-ion reactions.

Nuclear fission of actinides is, without doubt, the most important nuclear reaction. Nuclear fission by thermal neutrons may be described by the general equation [Eq. (8)]:

$$\mathrm{A} + \mathrm{n} \rightarrow \mathrm{B} + \mathrm{D} + \nu\mathrm{n} + \Delta E. \tag{8}$$

The fission products B and D have mass numbers in the range between about 70 and 160, the number of neutrons emitted is $\nu \approx 2$–3, and the energy set free by fission is $\Delta E \approx 200$ MeV. This energy is relatively high, because the binding energy per nucleon is higher for the fission products than for the actinide nuclei. In the case of nuclei with even proton and odd neutron numbers, such as ^{233}U, ^{235}U, and ^{239}Pu, the binding energy of an additional neutron is particularly high, and the barrier against fission is easily surmounted. Therefore, these nuclides have high fission yields for fission by thermal neutrons.

TABLE I Discovery or Synthesis of Actinide Elements

Atomic number	Element	Symbol	Investigators	Source or synthesis	Isotope first discovered	Most stable isotope	Source of name
89	Actinium	Ac	A. Debierne (1899)	Uranium ore	^{227}Ac	^{227}Ac	Greek word for ray
90	Thorium	Th	J. J. Berzelius (1828)	Thorium ore	^{232}Th	^{232}Th	Scandinavian god of war, Thor
91	Protactinium	Pa	K. Fajans, O. Göhring (1913)	Uranium ore concentrates	^{234}Pa	^{234}Pa	Parent of actinium
92	Uranium	U	M. H. Klaproth (1789)	Pitchblende	^{238}U	^{238}U	Planet Uranus
93	Neptunium	Np	E. M. McMillan, P. Abelson (1940)	Bombardment of uranium with neutrons: $^{238}_{92}U + ^{1}_{0}n \rightarrow$ $^{239}_{92}U \xrightarrow[23\,\text{min}]{-\beta^-} {}^{239}_{93}Np$	^{239}Np	^{237}Np	Planet Neptune
94	Plutonium	Pu	G. T. Seaborg, E. M. McMillan, J. W. Kennedy, A. Wahl (1940)	Bombardment of uranium with deuterons: $^{238}_{92}U + ^{2}_{1}H \rightarrow$ $2^{1}_{0}n + ^{238}_{93}Np$ $\xrightarrow[2.1\,\text{days}]{-\beta^-} {}^{238}_{94}Pu$	^{238}Pu	^{244}Pu	Planet Pluto
95	Americium	Am	G. T. Seaborg, R. A. James, L. O. Morgan, A. Ghiorso (1944)	Bombardment of plutonium with neutrons: $^{239}_{94}Pu + 2^{1}_{0}n \rightarrow$ $^{241}_{94}Pu \xrightarrow{-\beta^-} {}^{241}_{95}Am$	^{241}Am	^{243}Am	America
96	Curium	Cm	G. T. Seaborg, R. A. James, A. Ghiorso (1944)	Bombardment of plutonium with helium ions: $^{239}_{94}Pu + ^{4}_{2}He \rightarrow$ $^{242}_{96}Cm + ^{1}_{0}n$	^{242}Cm	^{247}Cm	Pierre and Marie Curie
97	Berkelium	Bk	S. G. Thompson, A. Ghiorso, G. T. Seaborg (1949)	Bombardment of americium with helium ions: $^{241}_{95}Am + ^{4}_{2}He$ $\rightarrow ^{243}_{97}Bk + 2^{1}_{0}n$	^{243}Bk	^{247}Bk	Berkeley, CA
98	Californium	Cf	S. G. Thompson, K. Street, A. Ghiorso, G. T. Seaborg (1950)	Bombardment of curium with helium ions: $^{242}_{96}Cm + ^{4}_{2}He$ $\rightarrow ^{245}_{98}Cf + ^{1}_{0}n$	^{245}Cf	^{251}Cf	California
99	Einsteinium	Es	Workers at Berkeley, Argonne, and Los Alamos (1952)	Discovered in the fallout of the first thermonuclear explosion as a result of uranium bombardment with fast neutrons: $^{238}_{92}U + 15^{1}_{0}n \rightarrow$ $^{253}_{92}U \xrightarrow{-7\beta^-} {}^{253}_{99}Es$	^{253}Es	^{252}Es	Albert Einstein

Continues

TABLE I (*continued*)

Atomic number	Element	Symbol	Investigators	Source or synthesis	Isotope first discovered	Most stable isotope	Source of name
100	Fermium	Fm	Workers at Berkeley, Argonne, and Los Alamos (1952)	Discovered in the fallout of the first thermonuclear explosion as a result of uranium bombardment with fast neutrons: $^{238}_{92}U + 17^{1}_{0}n \rightarrow {}^{255}_{92}U \xrightarrow{-8\beta^-} {}^{255}_{100}Fm$	^{255}Fm	^{257}Fm	Enrico Fermi
101	Mendelevium	Md	A. Ghiorso, B. H. Harvey, G. R. Choppin, S. G. Thompson, G. T. Seaborg (1955)	Bombardment of einsteinium with helium ions: $^{253}_{99}Es + {}^{4}_{2}He \rightarrow {}^{256}_{101}Md + {}^{1}_{0}n$	^{256}Md	^{258}Md	Dimitri Mendeleev
102	Nobelium	No	E. D. Donets, V. A. Shegolev, V. A. Ermakov (1966)	Bombardment of americium with nitrogen ions: $^{243}_{95}Am + {}^{15}_{7}N \rightarrow {}^{254}_{102}No + 4^{1}_{0}n$	^{254}No	^{259}No	Alfred Nobel
103	Lawrencium	Lr	Workers at both Berkeley and Dubna (1961–1971)	Bombardments of actinide targets with heavy ions	(^{258}Lr)	^{262}Lr	Ernest Lawrence

III. APPLICATIONS OF ACTINIDES

The practical importance of the actinide elements derives mainly from their nuclear properties. The principal application is in the production of nuclear energy. Controlled fission of fissile nuclides in nuclear reactors is used to provide heat to generate electricity. The fissile nuclides ^{233}U, ^{235}U, and ^{239}Pu constitute an enormous, practically inexhaustible, energy source.

Several actinide nuclides have found other applications. Heat sources made from kilogram amounts of ^{238}Pu have been used to drive thermoelectric power units in space vehicles. In medicine, ^{238}Pu was applied as a long-lived compact power unit to provide energy for cardiac pacemakers and artificial organs. ^{241}Am has been used in neutron sources of various sizes on the basis of the (α,n) reaction on beryllium. The monoenergetic 59-keV γ radiation of ^{241}Am is used in a multitude of density and thickness determinations and in ionization smoke detectors. ^{252}Cf decays by both α emission and spontaneous fission. One gram of ^{252}Cf emits $2.4 \cdot 10^{12}$ neutrons per second. ^{252}Cf thus provides an intense and compact neutron source. Neutron sources based on ^{252}Cf are applied in nuclear reactor start-up operations and in neutron activation analysis.

Nuclear energy and the application of actinide elements in other fields may promise mankind a prosperous future; however, whether the promise becomes a reality depends on the solution of numerous technological, economic, social, and international problems. Technical problems are related to the safe operation of nuclear reactors, reprocessing, and waste disposal, to the prevention of environmental contamination with radioactive and toxic substances, and to the prevention of the diversion of plutonium for an uncontrolled manufacture of nuclear weapons. All these technical and technological problems are soluble, but the future of nuclear energy depends also on the solution of other problems of acute global concern.

IV. ACTINIDE METALS

A. Preparation of Actinide Metals

All of the actinide elements are metals with physical and chemical properties changing along the series from those typical of transition elements to those of the lanthanides. Several separation, purification, and preparation techniques have been developed considering the different properties of the actinide elements, their availability, and application. Powerful reducing agents are necessary to produce the metals from the actinide compounds. Actinide metals are produced by metallothermic reduction of halides, oxides, or carbides, followed by the evaporation in vacuum or the thermal dissociation of iodides to refine the metals.

The metallothermic reduction of halides was the first method to be successfully applied. Actinium metal can

TABLE II Important Isotopes of the Actinide Elements

Atomic number	Element	Isotope	Half-life	Mode of decay
89	Actinium	^{227}Ac	21.7 years	β^-(0.986), α(0.014), γ
		^{228}Ac	6.15 h	β^-
90	Thorium	^{232}Th	$1.405 \cdot 10^{10}$ years	α,
91	Protactinium	^{231}Pa	32760 years	α, γ
		^{234}Pa	6.70 h	β^-
92	Uranium	^{235}U	$7.038 \cdot 10^8$ years	α
		^{238}U	$4.468 \cdot 10^9$ years	α
93	Neptunium	^{237}Np	$2.144 \cdot 10^6$ years	α
94	Plutonium	^{238}Pu	87.7 years	α
		^{239}Pu	$2.411 \cdot 10^4$ years	α
		^{242}Pu	$3.733 \cdot 10^5$ years	α
		^{244}Pu	$8.08 \cdot 10^7$ years	α(0.999), sf(0.001)
95	Americium	^{241}Am	432.2 years	α, γ
		^{243}Am	7370 years	α
96	Curium	^{242}Cm	162.8 days	α
		^{244}Cm	18.10 years	α
		^{248}Cm	$3.40 \cdot 10^5$ years	α(0.916), sf(0.084)
97	Berkelium	^{247}Bk	1380 years	α(<100%)
		^{249}Bk	320 days	β^-(0.99999), α(0.00001)
98	Californium	^{249}Cf	351 years	α
		^{251}Cf	898 years	α
		^{252}Cf	2.645 year	α(0.969), sf(0.031)
99	Einsteinium	^{252}Es	471.7 days	α(0.76, ε(0.24)
		^{253}Es	20.47 days	α
		^{254}Es	275.7 days	α
100	Fermium	^{252}Fm	25.39 h	α(0.99998), sf(0.00002)
		^{255}Fm	20.07 h	α
		^{256}Fm	157.6 min	sf(0.919), α(0.081)
101	Mendelevium	^{255}Md	27 min	ε(0.92), α(0.08)
		^{256}Md	78.1 min	ε(0.907), α(0.093)
102	Nobelium	^{259}No	58 min	α(0.75), ε(0.25)
103	Lawrencium	^{260}Lr	3.0 min	α(0.75), ε(0.25)

be produced by reducing AcF_3 with lithium at 1200°C. Small amounts of actinium can be obtained from residues of uranium processing. Gram amounts of ^{227}Ac has been produced synthetically at Mol, Belgium, by neutron irradiation of ^{226}Ra [Eq. (9)]:

$$^{226}_{88}\mathrm{Ra} + {}^{1}_{0}n \rightarrow {}^{227}_{88}\mathrm{Ra} + \gamma \xrightarrow[42.2\,\mathrm{min}]{-\beta^-} {}^{227}_{91}\mathrm{Ac}. \qquad (9)$$

Both thorium and uranium occur to a significant extent in nature, and industrial processes have been developed for the production of these elements.

Thorium is produced commercially from monazite sands. After mining, the monazite sands are concentrated magnetically and then treated with either hot, concentrated sulfuric acid or hot, concentrated sodium hydroxide. The acid treatment dissolves the thorium phosphate present, while the basic process converts the phosphates to insoluble hydroxides. The separation of thorium from the uranium and rare-earth phosphates after the acid process can be carried out by selective precipitation of the thorium and rare earth phosphates and then by using a solvent extraction process to remove the thorium. When the alkali opening method is used, the insoluble hydroxides are dissolved in nitric acid and the thorium and uranium(VI) species are extracted, leaving the lanthanides in the aqueous phase. The thorium and uranium can then be separated by further solvent extraction.

Thorium metal can be produced in several ways. In the most common process, thorium oxide is reduced with calcium [Eq. (10)]:

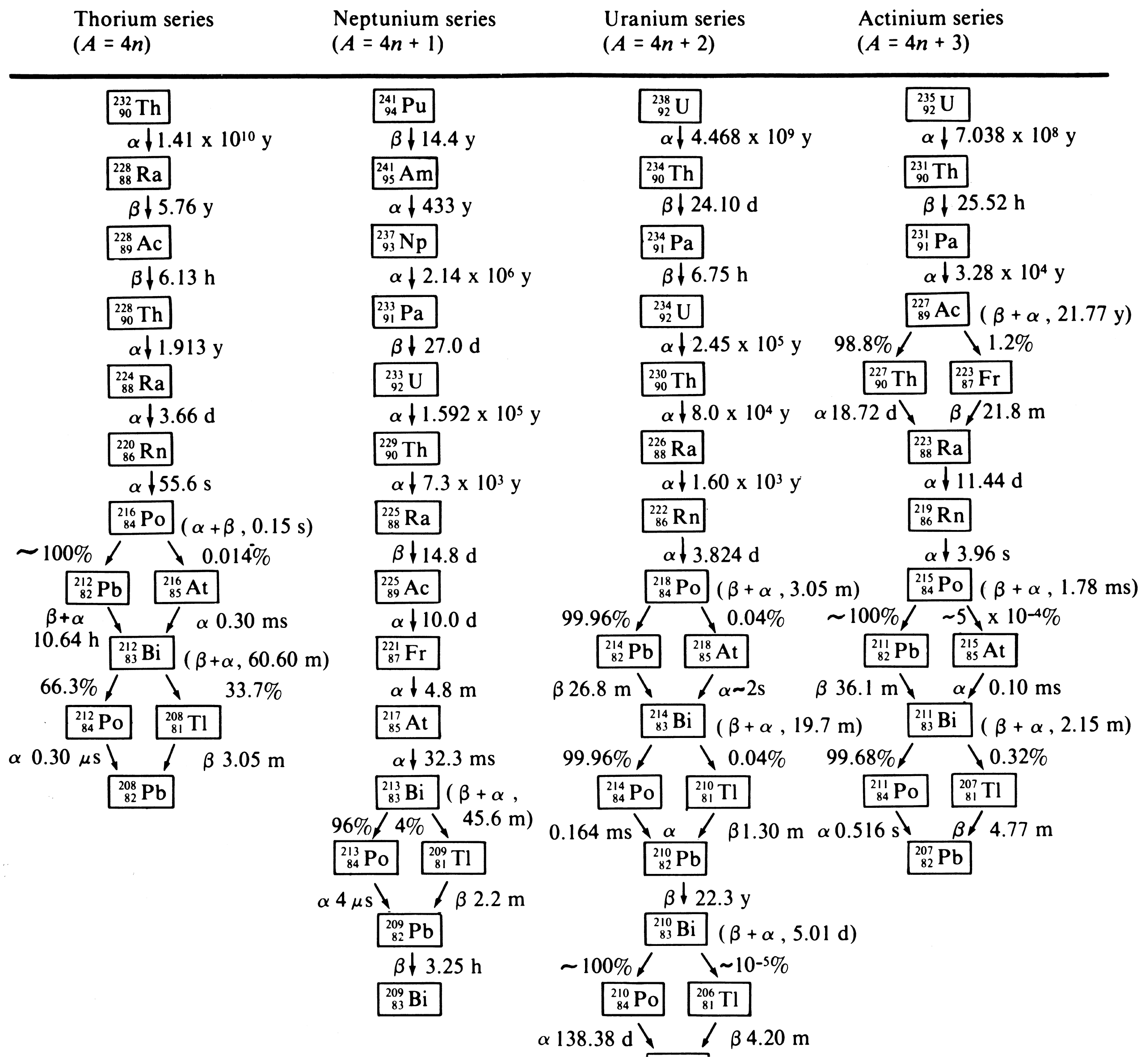

FIGURE 1

$$ThO_2 + 2Ca \xrightarrow[\text{Ar}]{1000^\circ C} Th + 2CaO. \quad (10)$$

The reaction mass is leached with water and dilute acid, leaving thorium metal powder. Very pure thorium metal can be prepared by the van Arkel process involving the thermal decomposition of ThI_4.

To obtain significant quantities of protactinium, a separation procedure was developed for extracting protactinium from the sludge that was left after the ether extraction of uranium at the Springfields refinery. The process yielded 127 g of pure ^{231}Pa from 60 tons of sludge. Protactinium metal can be obtained by reducing PaF_4 with barium vapor at 1300°C, followed by increasing the temperature to 1600°C to produce a bead of protactinium metal. Single-crystal protactinium metal is obtained by a modified van Arkel process starting from the carbide.

More then 150 minerals containing uranium are known. Typically, however, uranium ores contain only about 0.1% uranium. In the commercial production of uranium metal, the ore is crushed, concentrated, roasted, and in most cases leached with sulfuric acid in the presence of an oxidizing agent such as manganese dioxide or chlorate ions to convert all of the uranium to uranyl sulfato complexes. Carbonate leaching is used to extract uranium from ores containing minerals such as calcite. The recovery of uranium

from leach solutions can be affected by ion exchange, solvent extraction, and chemical precipitation. Most leach solutions are now treated by anion-exchange methods or solvent extraction or both for purification prior to precipitation. The two principal methods of precipitation are now neutralization with ammonia or the precipitation of uranium peroxide, $UO_4 \cdot xH_2O$, with hydrogen peroxide. The precipitates ("yellow cake") are dried and ignited to U_3O_8 or UO_3, depending on temperature. To produce nuclear-grade material, these raw products are normally further refined by solvent extraction or fluoride volatility processes. The purified uranium is converted to UO_3, reduced with hydrogen to UO_2, and converted to UF_4 with hydrogen fluoride. The UF_4 can either be reduced to uranium metal or fluorinated to UF_6 for isotope enrichment by gaseous diffusion.

The production of uranium metal usually involves the reduction of UF_4 with magnesium at 700°C. The metal may be refined by molten-salt electrolysis followed by zone melting. Because of the low melting point of uranium, the van Arkel process is not as feasible as for thorium and protactinium.

The principal source of neptunium (^{237}Np) is irradiated nuclear reactor fuel based on ^{235}U. A slightly modified Purex (plutonium-uranium recovery by extraction) process can be used to separate neptunium from uranium, plutonium, and fission products during reprocessing of nuclear reactor fuel. Ion-exchange methods are used for the final purification and concentration. Neptunium metal is produced by reduction of NpF_4 with calcium metal using iodine as a booster. Refining is accomplished by vacuum melting. Plutonium was the first synthetic actinide element to be produced on a large scale. It is produced in nuclear reactors by the so-called pile reactions [Eqs. (11) and (4)]:

$$^{238}_{92}\mathrm{U} + ^{1}_{0}n \rightarrow \text{fission products} + 2.5\mathrm{n} + \sim 200\,\mathrm{MeV} \qquad (11)$$

$$^{238}_{92}\mathrm{U} + ^{1}_{0}n \rightarrow ^{239}_{92}\mathrm{U} \xrightarrow[23\,\mathrm{min}]{-\beta^-} ^{239}_{93}\mathrm{Np} \xrightarrow[2.3\,\mathrm{days}]{-\beta^-} ^{238}_{92}\mathrm{Pu} \qquad (4)$$

The most widely employed method for plutonium reprocessing used today in almost all of the world's reprocessing plants is the Purex (plutonium-uranium reduction extraction) process. Tributylphosphate (TBP) is used as the extraction agent for the separation of plutonium from uranium and fission products. In effecting a separation, advantage is taken of differences in the extractability of the various oxidation states and in the thermodynamics and kinetics of oxidation reduction of uranium, plutonium, and impurities. Various methods are in use for the conversion of plutonium nitrate solution, the final product from fuel reprocessing plants, to the metal. The reduction of plutonium halides with calcium proved to be the best method for metal production, and PuF_4 is most commonly used as the starting material. The crude plutonium metal may be refined by electrolysis in molten salts.

Americium and curium can be obtained from the aqueous waste of the Purex process. This americium is a mixture of ^{241}Am and ^{243}Am. Isotopically pure ^{241}Am, the decay product of ^{241}Pu, can be obtained from aged plutonium. Solvent extraction and ion-exchange procedures are used to recover americium from waste streams. Americium metal is produced by lanthanum reduction of the oxide, followed by vacuum distillation of the americium at 1400°C.

^{243}Cm and ^{244}Cm are minor constituents of nuclear waste. Gram quantities of ^{242}Cm and ^{244}Cm were produced by neutron irradiations of ^{241}Am and plutonium, respectively. The Tramex process based on the extraction with tertiary amines and high-pressure ion-exchange systems was developed for the recovery of curium. Curium metal is advantageously produced by thorium reduction of the oxide, followed by vacuum distillation of the metal at 2000°C.

Weighable quantities of the transcurium elements berkelium (^{249}Bk), californium (^{252}Cf), and einsteinium (^{253}Es) for use in research are produced in the high-flux nuclear reactors HFIR at Oak Ridge and SM-2 at Dimitrovgrad, Russia. ^{257}Fm in picogram quantities was produced only at Oak Ridge. Targets containing plutonium, americium, and curium are irradiated in the high-flux reactors and then processed. After target dissolution followed by impurity, rare-earth, and curium removal, the transcurium elements are separated by high-pressure cation exchange using ammonium α-hydroxyisobutyrate as the eluent. Berkelium metal in microgram to milligram amounts is produced by reducing BkF_3 or BkF_4 with lithium metal, followed by the removal of lithium fluoride at 1200°C from the less volatile berkelium metal. The more volatile californium, einsteinium, and fermium metals can be prepared by reduction of the oxides with lanthanum metal, followed by a distillation of the actinide metals. To prepare the metals free of a supporting material at least a few milligrams of metal have to be distilled.

Californium is the heaviest actinide for which data like the enthalpy of sublimation have been determined directly with bulk quantities of about 2 mg of pure metal. Due to the limited availability of the heaviest actinides down to the "one-atom-at-a-time" scale, the preparation of the metals becomes an integral part of an experiment for studying the metals. Unusual experimental approaches like the measurement of partial pressures of the actinide under study over an alloy, studies of diffusion of actinide atoms in metals, and adsorption studies of actinide atoms onto metal surfaces by thermochromatography have been reported.

To obtain and stabilize the actinides under study in the elemental/metallic state, the reduction of actinide oxides with lanthanum metal and the desorption of actinide atoms from metals like tantalum, titanium, and zirconium have been applied successfully.

B. Properties of Actinide Metals

1. Electronic Structure

The electronic ground state configurations of the gaseous actinide atoms consist of the closed-shell electronic structure of the noble gas radon, a partly filled $5f$ shell, and two to four electrons in the $6d$ and $7s$ states. The electronic ground state configurations for the actinides and, for comparison, the lanthanides are given in Table III.

The filling of the f shell is a common feature of both lanthanides and actinides. However, there are remarkable differences in the properties of the $4f$ and $5f$ electrons. The $4f$ orbitals of the lanthanides and the $5f$ actinide orbitals have the same angular part of the wave function but differ in the radial part. The $5f$ orbitals also have a radial node, while the $4f$ orbitals do not. The major differences between actinide and lanthanide orbitals depend, then, on the relative energies and spatial distributions of these orbitals. The $5f$ orbitals have a greater spatial extension relative to the $7s$ and $7p$ than the $4f$ orbitals have relative to the $6s$ and $6p$. This allows a small covalent contribution from the $5f$ orbitals, whereas no compounds in which $4f$ orbitals are used exist. In fact, the $4f$ electrons are so highly localized that they do not participate in chemical bonding, whereas the $5d$ and $6s$ valence electrons overlap as for the transition elements. The energies of the $5f$, $6d$, $7s$, and $7p$ orbitals are comparable over a range of atomic numbers, and since the orbitals overlap spatially, bonding can involve any or all of them. This is especially important in the first half of the actinide series. Oxidation states up to +7 are available, and the electronic structure of an actinide in any given oxidation state may vary from compound to compound and in solution, depending on the ligands, because the small differences in energy between the $5f$, $6d$, $7s$, and $7p$ orbitals can be compensated within the range of chemical bonding energies.

With increasing atomic number, the $5f$ electrons become increasingly localized as a consequence of insufficient screening. Beginning with americium, the $5f$ electrons do not participate in bonding, similar to the $4f$ electrons in the lanthanides. In the heaviest actinides, the $5f$ electrons appear even more localized than the analogous $4f$ electrons. This conclusion is supported by the tendency to form the divalent oxidation state well before the end of the actinide series.

In the region of the heaviest actinides, relativistic effects may become noticeable. Due to the relativistic mass increase of the electrons, which are strongly accelerated in the vicinity of a highly charged nucleus, the spherical $7s$ and $7p_{1/2}$ orbitals have high electron densities near the nucleus, whereas the $6d$ and $5f$ orbitals become destabilized. Thus, the ground state configuration for lawrencium was predicted to be [Rn]$5f^{14}d^07s^2p^1$ instead of the [Rn]$5f^{14}d^17s^2$ configuration, which might be expected by analogy with lutetium.

The $5f$ electrons of the lighter actinide metals through plutonium have highly extended wave functions. Thus,

TABLE III Ground State Electronic Configurations of $5f$ and $4f$ Elements

Atomic number	Symbol	Element	Electronic structure [Rn] plus	Atomic number	Symbol	Element	Electronic structure [Xe] plus
89	Ac	Actinium	$6d7s^2$	57	La	Lanthanum	$5d6s^2$
90	Th	Thorium	$6d^27s^2$	58	Ce	Cerium	$4f5d6s^2$
91	Pa	Protactinium	$5f^26d7s^2$ or $5f6d^27s^2$	59	Pr	Praseodymium	$4f^36s^2$
92	U	Uranium	$5f^36d7s^2$	60	Nd	Neodymium	$4f^46s^2$
93	Np	Neptunium	$5f^57s^2$	61	Pm	Promethium	$4f^56s^2$
94	Pu	Plutonium	$5f^67s^2$	62	Sm	Samarium	$4f^66s^2$
95	Am	Americium	$5f^77s^2$	63	Eu	Europium	$4f^76s^2$
96	Cm	Curium	$5f^76d7s^2$	64	Gd	Gadoliniuum	$4f^75d6s^2$
97	Bk	Berkelium	$5f^86d7s^2$ or $5f^97s^2$	65	Tb	Terbium	$4f^96s^2$
98	Cf	Californium	$5f^{10}7s^2$	66	Dy	Dysprosium	$4f^{10}6s^2$
99	Es	Einsteinium	$5f^{11}7s^2$	67	Ho	Holmium	$4f^{11}6s^2$
100	Fm	Fermium	$5f^{12}7s^2$	68	Er	Erbium	$4f^{12}6s^2$
101	Md	Mendelevium	$5f^{13}7s^2$	69	Tm	Thulium	$4f^{13}6s^2$
102	No	Nobelium	$5f^{14}7s^2$	70	Yb	Ytterbium	$4f^{14}6s^2$
103	Lr	Lawrencium	$5f^{14}6d^07s^2p^1$ or $(5f^{14}6d^17s^2)$	71	Lu	Lutetium	$4f^{14}5d6s^2$

these delocalized or itinerant $5f$ electrons are involved in the metallic bonding as a part of the conduction band formed together with the $6d$ and $7s$ electrons. The band character of the delocalized $5f$ electrons is inhibitory to the development of magnetism. Within the framework of a simple model of the metallic bond, the metal is an array of ions held together by quasi-free conduction electrons, and a metallic valence can be defined as the contribution of outer electrons each atom gives to the "sea" of bonding conduction electrons. Conversely, the metallic valence is the charge left per atom when the bonding electrons have been stripped off. In this approach, the first five actinides after actinium, thorium up to plutonium, are considered as having metallic valences greater than three.

As the atomic number increases, the radial extension and the bandwidth of the $5f$ electrons decreases. From americium on the $5f$ electrons are localized, nonbonding, and carry a magnetic moment. The actinide metals americium to californium and lawrencium are trivalent metals. Einsteinium to nobelium are divalent metals due to very high promotion energies needed to promote one f electron to the metallic bonding state as known from ytterbium in the lanthanide series. Thus, the actinide series displays more complex electronic structures than does the lanthanide series; not only in the first half of thek series.

2. Crystal Structures

Actinide crystal structures are more complicated and diversified than the corresponding lanthanide metal structures. Information about the crystal structures of the actinide metals is given in Table IV.

Actinium and thorium have no f electrons and behave like transition metals with a body-centered cubic structure of thorium. Neptunium and plutonium have complex, low-symmetry, room-temperature crystal structures and exhibit multiple phase changes with increasing temperature due to their delocalized $5f$ electrons. For plutonium metal, up to six crystalline modifications between room temperature and 915 K exist. The f electrons become localized for the heavier actinides. Americium, curium, berkelium, and californium all have room-temperature, double hexagonal, close-packed phases and high-temperature, face-centered cubic phases. Einsteinium, the heaviest actinide metal available in quantities sufficient for crystal structure studies on at least thin films, has a face-centered cubic structure as typical for a divalent metal.

3. Physical Properties

The radioactivity of the actinides along with their limited availability makes their experimental investigation in most cases notoriously difficult. Therefore, data on physical properties of the actinide metals are very limited. Data on selected physical and thermodynamic properties are presented in Table V.

Proceeding along the $5f$ series, the high melting points of Th and Pa reflect their transition metal character, Np and Pu have very low melting points due to f-orbital reflection, the melting points rise over Am to Cm, and they then again decrease. The maximum at Cm reflects both its half-filled $5f$ shell and the presence of a d-type valence electron. The decreasing melting points of the transcurium elements reflect the onset of s-type bonding and the loss of d bonding in the divalent metals. The melting point of Lr is expected to be as high as that of Cm, assuming d bonding, but should be lower if it behaves like a p element due to relativistic effects.

Looking at transport and magnetic properties along the actinide series, superconductivity under atmospheric pressure (Th, Pa), superconductivity under high pressure (U), exchange reinforced Pauli paramagnetism without superconductivity (Np, Pu), superconductivity under atmospheric pressure (Am), and finally magnetic ordering and absence of superconductivity (Cm, Bk, Cf) are successively encountered. Measurements of electrical, magnetic, or electronic properties of the heaviest actinides beyond californium have been missing up to now.

4. Thermodynamic Properties

One of the fundamental properties of a metal is its enthalpy of sublimation. The enthalpy of sublimation of a metal, which is a measure of its cohesive energy, is related to the electronic structure in both the solid and its vapor. The enthalpies of sublimation of the actinide metals thorium through californium have been determined directly by vapor pressure measurements using the pure metals, those of einsteinium and fermium by measuring partial pressures over alloys. Estimates of the enthalpies of sublimation for the actinide metals californium through nobelium have also been made based on thermochromatographic measurements of the adsorption of actinide atoms on metals. The experimental enthalpies of sublimation clearly reflect the trends and changes in the electronic properties of the actinide metals when progressing across the series. Thus, there is further evidence for metallic divalency well before the end of the actinide series.

5. Alloying Behavior

Experimental studies of actinide alloys have been carried out with Np, Am, Cm, Bk, Es, and Fm, and far more extensive studies have been carried out with the actinide metals of technological importance, Th, U, and Pu. The

TABLE IV Crystal Structure of the Actinide Metals

Atomic number	Melting point (K)	Phase	Crystal symmetry[a]	Space group	Stability range (K)	Lattice parameters a (Å)	b (Å)	c (Å)	β (deg)	Metallic valence	Temp. (K)	Density (g cm^{-3})	Metallic radii (Å)
89	1320	Ac	fcc	Fm3m	<1320	5.314				3	293	10.06	1.88
90	2023	α-Th	fcc	Fm3m	<1633	5.180				4	293	11.72	1.798
		β-Th	bcc	Im3m	1633–2023	4.11					1698		1.78
91	1845	α-Pa	bct	I4/mmm	<1200	3.921		3.235		≥4		15.43	1.631
		β-Pa	fcc	Fm3m	1200–1845	5.018						12.31	1.777
92	1408	α-U	eco	Cmcm	<941	2.853	5.865	4.955		≥4	293	19.060	1.56
		β-U	t	P4$_2$mnm	941–1049	10.759	10.759	5.656			993	18.11	
		γ-U	bcc	Im3m	1049–1408	3.525					1078	18.06	1.55
93	913	α-Np	o	Pnma	<553	6.663	4.723	4.887		≥3	293	20.45	1.55
		β-Np	t	P4/nmm	553–849	4.897		3.388			586	19.36	
		γ-Np	bcc	Im3m	849–913	3.52					873	18.00	1.54
94	913.2	α-Pu	m	P2$_1$Im	<398	6.183	4.822	10.963	101.79	≥3	294	19.86	1.58
		β-Pu	bcm	12/m	398–488	9.284	10.463	7.859	92.13		463	17.70	1.59
		γ-Pu	fco	Fddd	488–593	3.159	5.768	10.162			508	17.14	1.589
		δ-Pu	fcc	Fm3m	593–736	4.637					593	15.92	1.644
		δ'-Pu	bct	14/mmm	736–756	3.34		4.44			738	6.00	1.644
		ε-Pu	bcc	Im3m	756–913.2	3.363					763	16.51	1.594
95	1449	α-Am	dhcp	P6$_3$/mmc	<1347	3.468		11.248		3	293	13.671	1.730
		β-Am	fcc	Fm3m	1347–1449	4.894					295	13.65	1.730
96	1681	α-Cm	dhcp	P6$_3$/mmc	<1550	3.496		11.33		3	293	13.51	1.745
		β-Cm	fcc	Fm3m	1550–1681	5.039							1.79
97	1323	α-Bk	dhcp	P6$_3$/mmc	<1250	3.416		11.068		3	293	14.79	1.704
		β-Bk	fcc	Fm3m	1250–1323	4.999					293	13.24	1.764
98	1173	α-Cf	dhcp	P6$_3$/mmc	<863	3.39		11.01		3		15.1	1.69
		β-Cf	fcc	Fm3m		4.94						13.7	1.75
		γ-Cf	fcc	Fm3m		5.75						8.70	2.03
99	1130	(α-Es)	hcp	P6$_3$/mmc	<573	3.98		6.50		2			
		(β-Es)	fcc	Fm3m		5.71							2.03
100		Fm	fcc							2			2.00
101		Md	fcc							2			1.985
102		No	fcc							2			1.97
103		Lr	bcc							3			1.66

[a] bcc, body-centered cubic; dhcp, double hexagonal close-packed; fcc, face-centered cubic; hcp, hexagonal close-packed; m, monoclinic; bcm, body-centered monoclinic; o, orthorhombic; eco, end-centered orthorhombic; fco, face-centered orthorhombic; t, tetragonal; bct, body-centered tetragonal.

complex and variable electronic properties of the actinides are reflected in their alloying behavior also. Varying the composition can result in properties ranging from superconductivity to magnetism. There is a huge number of possible intermetallic compounds because of the many possible valence states of the actinides itself. The itinerant f-electron metals protactinium through plutonium are mutually soluble. Uranium and plutonium form a number of isomorphous compounds due to their similarity in size. The trivalent actinide metals are expected to be mutually soluble in one another. The same should hold for the divalent metals einsteinium through nobelium, but they should not alloy with the higher valent actinide metals.

A large number of intermetallic compounds of the actinide metals with transition metals and with elements of the aluminium and silicon groups are known. All have metallic properties. Compounds with AnX_3 stoichiometry have the $AuCu_3$-, $TiNi_3$-, $MgCd_3$-, or $PuAl_3$-type structure. At AnX_2, stoichiometry Laves phases having the $MgCu_2$-type or $MgZn_2$-type structures are found very often, especially when the partner is an Fe- or Ni-group transition metal. At AnX the NaCl-type structure and at the

TABLE V Selected Physical and Thermodynamic Properties of Actinide Elements

Symbol	Boiling point (K, 1 atm)	Enthalpy of fusion, ΔH_{fus} (kJ mol^{-1})	Enthalpy of sublimation, ΔH^0_{298} (kJ mol^{-1})	Electrical resistivity ($\mu\Omega$ cm, 295 K)
Ac	(3200)		(418)	
Th	(5000)	14	598	14
Pa	(4230)	16.7	570	18
U	3818	19.7	536	31
Np	(4174)	5.23	465	123
Pu	(3508)	2.82	342	138
Am	(2067)	14.4	284	67
Cm	(3383)	13.8	387	86
Bk	(2900)	7.91	310	
Cf	(1745)	7.51	196	
Es	(1269)	9.40	133(167)[a]	
Fm	(1350)		143(143)[a]	
Md			(136)[a]	
No			(134)[a]	

[a] Values in parentheses are estimates based on thermochromatographic measurements.

AnX_5 stoichiometry $AuBe_5$-- and $CaCu_5$-type structures are found.

V. ACTINIDE IONS

A. Oxidation States

The oxidation states of the actinide elements are listed in Table VI. Unlike the lanthanide elements, for which the dominant oxidation state is +3, the actinides exhibit a broad range of oxidation states, ranging from +2 to +7 in solution. The proximity of $5f$, $6d$, and $7s$ energy levels in the lighter actinides results in a variety of oxidation states up to +7. The stability of the higher oxidation states decreases with increasing atomic number. From americium on, a more lanthanide-like behavior is exhibited. The most stable oxidation state of the heavier actinides with the exception of No is +3; however, in contrast to the analogous lanthanides, the divalent oxidation state appears well before the end of the actinide series. Thus, in comparison with the analogous $4f$ electrons, the $5f$ electrons in the latter part of the actinide series appear more tightly bound.

With the exception of thorium and protactinium, all of the actinide elements show a +3 oxidation state in aqueous solution. A stable +4 state is observed in the elements thorium through plutonium and in berkelium. The oxidation state +5 is well established for the elements protactinium through americium, and the +6 state is well established in the elements uranium through americium. The oxidation state +2 first appears at californium and becomes increasingly more stable in proceeding to nobelium.

For any oxidation state, the ionic radii decrease regularly with increasing atomic number as a consequence of the decreased shielding by f electrons of the outer valence electrons from the increasing effective nuclear charge. This actinide contraction is very similar to the corresponding lanthanide contraction. Table VII summarizes crystallographic ionic radii of lanthanide and actinide ions for coordination numbers 6 and 8.

B. Solution Chemistry

Although many solvents have been studied, the most widely used solvent is still water. Table VIII presents some data on the stability of various actinide ions in water. In aqueous solution the actinide ions present in the oxidation states +1 to +6 are M^+, M^{2+}, M^{3+}, M^{4+}, MO_2^+, and MO_2^{2+}. MO_5^{3-} oxo anions are known for the oxidation state +7. The actinyl ions MO_2^+ and MO_2^{2+} are remarkably stable. The oxygen atoms are linearly coordinated to the actinide metal with short metal-oxygen distances ranging from 1.6 to 2.0 Å for MO_2^{2+}. The strength of the metal-oxygen bond decreases with increasing atomic number in the actinyl ions from uranium to americium.

TABLE VI Oxidation States of the Actinide Elements

Atomic number Symbol	89 Ac	90 Th	91 Pa	92 U	93 Np	94 Pu	95 Am	96 Cm	97 Bk	98 Cf	99 Es	100 Fm	101 Md	102 No	103 Lr
Oxidation states													1?		
							(2)			(2)	(2)	2	2	**2**	
	3	(3)	(3)	3	3	3	**3**	**3**	**3**	**3**	**3**	**3**	**3**	3	**3**
		4	4	4	4	**4**	4	4	4	(4)	4?				
			5	5	**5**	5	5	5?		5?					
				6	6	6	6	6?							
					7	(7)	7?								

Note: Bold type: most stable; ( ): unstable; ?: claimed but not substantiated.

TABLE VII Crystallographic Ionic Radii of Lanthanide and Actinide Ions

Ion Symbol	Coordination number 6				Coordination number 8		
	M^{2+}	M^{3+}	M^{4+}	MO_2^+	M^{3+}	M^{4+}	MO_2^{2+}
La	1.304	1.032			1.162		
Ce	1.278	1.010	0.863		1.138	0.967	
Pr	1.253	0.996	0.847		1.122	0.949	
Nd	1.225	0.983	0.836		1.107	0.936	
Pm	1.206	0.968	0.826		1.090	0.925	
Sm	1.183	0.958	0.815		1.079	0.912	
Eu	1.166	0.946	0.807		1.065	0.903	
Gd	1.140	0.937	0.799		1.055	0.894	
Tb	1.119	0.923	0.792		1.040	0.886	
Dy	1.096	0.912	0.782		1.027	0.874	
Ho	1.075	0.900	0.773		1.014	0.864	
Er	1.056	0.889	0.764		1.003	0.854	
Tm	1.038	0.879	0.756		0.993	0.844	
Yb	1.026	0.869	0.748		0.984	0.835	
Lu		0.863	0.741		0.979	0.827	
Ac	1.41	1.12			1.26		
Th	1.36	1.08	0.932		1.22	1.048	
Pa	1.30	1.05	0.906	0.78	1.20	1.016	
U	1.27	1.028	0.889	0.76	1.160	0.997	0.73
Np	1.24	1.011	0.874	0.75	1.141	0.980	0.72
Pu	1.21	0.995	0.859	0.74	1.123	0.962	0.71
Am	1.194	0.980	0.848		1.106	0.950	
Cm	1.164	0.970	0.841		1.094	0.942	
Bk	1.145	0.955	0.833		1.077	0.932	
Cf	1.125	0.945	0.827		1.066	0.925	
Es	1.102	0.934	0.818		1.053	0.914	
Fm	1.083	0.922	0.811		1.040	0.906	
Md	1.064	0.912	0.803		1.028	0.897	
No	1.052	0.902	0.796		1.017	0.889	
Lr		0.896	0.790		1.010	0.881	

The solution chemistry of the actinide elements can be affected by radiolysis. In principle, the chemistry of an actinide element is independent of its radioactivity. In practice, short-lived isotopes, decaying by α emission or spontaneous fission, cause heating and solvent decomposition with the formation of hydrogen, hydroxide radicals, and hydrogen peroxide from water as well as decomposition products of acids. The decomposition products react with each other and with the actinide element under consideration so that the oxidation state gradually changes. To suppress radiolytic effects, chemical studies with actinide elements should be carried out preferably with long-lived nuclides or on a few-atom basis using radiochemical methods.

Reduction potentials for the actinide elements are given in Table IX. The M^{4+}/M^{3+} and the MO_2^{2+}/MO_2^+ couples are reversible, while the formation and rupture of bonds and the subsequent reorganization of the solvent shell results in nonreversibility of the couples MO_2^{2+}/M^{3+}, MO_2^+/M^{4+}, and MO_2^{2+}/M^{4+}. The redox reactions of UO_2^+, Pu^{4+}, PuO_2^+, and AmO_2^+ are especially complex. In the special case of plutonium, all four ions Pu^{3+}, Pu^{4+}, PuO_2^+, and PuO_2^{2+} can coexist in solution. Pu^{4+} or PuO_2^+ disproportionate into mixtures of all four oxidation states. An initially pure solution of Pu^{4+} in 0.5M hydrochloric acid was reported to contain 26.3% Pu^{3+}, 62.7% Pu^{4+}, 0.5% PuO_2^+, and 10.5% PuO_2^{2+} after 200 h.

In aqueous solution the actinide cations interact with the solvent water. This hydration is a special case of complex ion formation with water as a nucleophilic ligand. The hydrated ions act as acids, splitting off protons from the water molecules of the hydration shell. Their acidity increases with the charge on the central atom. The divalent ions are weak acids. On account of their large radii, the

TABLE VIII Stability of Actinide Ions in Aqueous Solution

Ion	Preparation	Stability
Md^{2+}		Slowly oxidized to Md^{3+}
No^{2+}		Stable
Ac^{3+}		Stable
U^{3+}	Electrolytic reduction (Zn or Na/Hg on UO)	Slowly oxidized by water; rapidly by air to U^{4+}
Np^{3+}	Electrolytic reduction (H_2/Pt)	Stable to water; rapidly oxidized by air to Np^{4+}
$Pü^{3+}$	SO_2, NH_2OH, Zn, U^{4+}, or H_2(Pt) reduction	Stable to water and air; oxidized by its own α radiation to Pu^{4+} (in case of ^{239}Pu)
Am^{3+}	Iodide, SO_2 reduction	Stable; difficult to oxidize
Cm^{3+}		Stable
Bk^{3+}		Stable; can be oxidized to Bk^{4+}
Cf^{3+}		Stable
Es^{3+}		Stable
Fm^{3+}		Stable
Md^{3+}		Stable; can be reduced to Md^{2+}
No^{3+}	Oxidation of No^{2+} with Ce^{4+}	Easily reduced to No^{2+}
Lr^{3+}		Stable
Th^{4+}		Stable
Pa^{4+}	Reduction of PaO^{2+} in HCl (Zn/Hg, Cr^{2+}, or Ti^{3+}); electrolytic reduction	Stable to water; rapidly oxidized by air to Pa(V)
U^{4+}	Air oxidation of U^{3+}; reduction of UO^{2+} (Zn or H_2 with Ni); electrolytic reduction of UO^{2+}	Stable to water; slowly oxidized by air to UO^{2+}
Np^{4+}	Air oxidation of Np^{3+}; Fe^{2+}, SO_2, I^- or H_2(Pt) reduction	Stable to water; slowly oxidized by air to NpO_2^+
Pu^{4+}	BrO_3^-, Ce^{4+}, $Cr_2O_7^{2-}$, HIO_3, or MnO_4^- oxidation in acid; HNO_2, NH_3OH^+, I^-, $3M$ HI, $3M$ HNO_3, Fe^{2+}, $C_2O_4^{2-}$, or HCOOH reduction in acid	Stable in $6M$ acids, disproportionates to Pu^{3+} and PuO_2^+ at lower acidities
Am^{4+}	Electrolytic oxidation of Am^{3+} in $12M$ H_3PO_4	Not stable in water; stable in $15M$ NH_4F CmF_6^{2-}
Cm^{4+}	Dissolution of CmF_4 in $15M$ CsF	stable 1 h at 25°C
Bk^{4+}	$Cr_2O_7^{2-}$ or BrO_3^- oxidation of Bk^{3+}	Reasonably stable in solution, easily reduced to Bk^{3+}
Cf^{3+}	Oxidation of Cf^{3+} using potassium persulfate, stabilization with phosphotungstate	Slowly reduced to Cf^{3+}
PaO_2^+		Stable; reduction difficult
UO_2^+	Electrolytic reduction of UO_2^{2+}; UO_2^{2+} reduction by Zn/Hg or H_2 at pH 2.5	Greatest stability at pH 2.5; disproportionates to U^{4+} and UO_2^{2+}
NpO_2^+	NH_2NH_2, NH_2OH, HNO_2, H_2O_2/HNO_3, Sn^{2+}, or SO_2 reduction of NpO_2^{2+}	Stable; disproportionates only in strong acids
PuO_2^+	Reduction of PuO_2^{2+} by I^-, Fe^{2+}, V^{3+}, SO_2, or U^{4+}	Most stable at low acidity; disproportionates to Pu^{4+} and PuO_2^{2+}
AmO_2^+	Oxidation of Am^{3+} with O_3, $S_2O_8^{2-}$, OCl^-, or by electrolysis	Disproportionates in strong acids to Am^{3+} and AmO_2^{2+}, reduction to Am^{3+} at low acidities by its own α radiation in case of ^{241}Am
UO_2^{2+}		Stable; difficult to reduce
NpO_2^{2+}	Oxidation of Np^{4+} with Ce^{4+}, MnO_4^-, Ag^{2+}, Cl_2, or BrO_3^-	Stable in acidic or complexed solutions
PuO_2^{2+}	Oxidation of Pu^{4+} with BiO_3^-, Ce^{4+}, Ag^{2+} or a number of other reagents	Stable, fairly easy to reduce; slow reduction by its own α radiation
AmO_2^{2+}	Oxidation of Am^{3+}or AmO_2^+ by $S_2O_8^{2-}$ or Ag^{2+}	Stable, rapid reduction by its own α radiation
NpO_5^{3-}	Oxidation of NpO_2^{2+} in alkaline solution by O_3, $S_2O_8^{2-}$, ClO^-, BrO^-, or BiO_3^-	Stable only in alkaline solution
PuO_5^{3-}	Oxidation of PuO_2^{2+} in alkaline solution by O_3, $S_2O_8^{2-}$, ClO^-, or BrO^-	Stable only in alkaline solution, oxidizes water
AmO_5^{3-}	Oxidation of AmO_2^{2+} in alkaline solution by O_3	Stable only in alkaline solution

TABLE IX Reduction Potentials of the Actinide Elements

Atomic number Symbol	89 Ac	90 Th	91 Pa	92 U	93 Np	94 Pu	95 Am	96 Cm	97 Bk	98 Cf	99 Es	100 Fm	101 Md	102 No	103 Lr
Reduction															
$M^{2+} \to M$													−2.53	−2.6	
$M^{3+} \to M$				−1.66	−1.79	−2.00	−2.07	−2.06	−2.00	−1.91	−1.98	−2.07	−1.74	−1.26	−2.1
$M^{4+} \to M$		−1.83	−1.47	−1.38	−1.30	−1.25	−0.90								
$M^{3+} \to M^{2+}$													−0.15	+1.45	
$M^{4+} \to M^{3+}$				−0.55	+0.218	+1.051	+2.62	+3.1	+1.67						
$MO_2^{+} \to M^{3+}$							+1.727								
$MO_2^{2+} \to M^{3+}$						+1.023									
$MO_2^{+} \to M^{4+}$				+0.38	+0.606	+1.17	+0.84								
$MO_2^{2+} \to M^{4+}$				+0.267	+0.94	+1.04	+1.217								
$MO_2^{2+} \to M_2^{+}$				+0.088	+1.159	+0.936	+1.60								
$MO_3^{+} \to M_2^{2+}$	−2.13				+0.04										

Note: Standard reduction potentials in acidic (pH 0) solutions are given in volts vs standard hydrogen electrode.

trivalent actinide ions are also weak acids. The tetravalent ions are the most acidic. The actinyl ions MO_2^{+} and MO_2^{2+} are formed with great speed whenever oxidation to the +5 and +6 states occurs in water. The actinyl ions are considerably less acidic than are the M^{4+} ions and, therefore, have a smaller tendency to undergo hydrolysis. Hydrolysis decreases in the order

$$M^{4+} > MO_2^{2+} > M^{3+} > MO_2^{+}.$$

Hydrolysis may result in the formation of polynuclear species. The M^{4+} ions, and among them especially Pu^{4+}, appear to be particularly prone to polymerization. Colloidal polymers of Pu^{4+} with molecular weights as high as 10^{10} have been observed. Polymer formation and depolymerization are ill defined, and chemical studies may be rendered extremely difficult by the formation of intractable polymers. The formation of polymers can be suppressed by complexation with other ligands such as fluoride ions. Complex ion formation has proved to be extremely important for several fields of pure and applied chemistry of the actinide elements such as their solution chemistry, actinide and nuclear fuel processing and reprocessing using liquid–liquid extraction and ion-exchange methods, or their environmental and biological behavior.

The actinide ions are able to form complexes with various ligands. Complex formation involves an exchange of coordinated water, directly bonded to the central actinide ion, for ligands on the condition that the ligand has an affinity for the actinide ion strong enough to compete with that of the coordinated water. Such exchange results in the formation of inner-sphere complexes. Alternatively, ligands may be attached to coordinated water to form outer-sphere complexes. Strong complexes are mainly of the inner-sphere type. The stability sequences for a given actinide ion seem to be $F^- \gg$ glycolate$^-$ > acetate$^-$ > $SCN^- > NO_3^- > Cl^- > Br^- > I^- > ClO_4^-$ for monovalent ligands and $CO_3^{2-} > EDTA^{4-} > HPO_4^{2-} >$ citrate^{3-} > tartrate^{2-} > oxalate^{2-} > SO_4^{2-} for polyvalent ligands. For a given ligand the stability of the complexes follows the order of the effective charge on the central atom as typical for hard acceptors: $M^{4+} > MO_2^{2+} \simeq M^{3+} > MO_2^{+}$. The reversal in the order of MO_2^{2+} and M^{3+} ions is a result of the higher charge density of MO_2^{2+} because of imperfect shielding by the linear oxygen atoms. High stabilities of complexes formed by hard acceptors are not reflected in exothermic enthalpy changes, but rather in very positive entropy terms due to a large decrease of order as a result of complex formation.

The phosphate anion PO_4^{3-} and organic phosphates are powerful complexing agents for actinide ions, forming complexes that are insoluble in water but soluble in nonpolar aliphatic hydrocarbons. Complexes with such reagents have been used in the separation of the actinide elements by liquid–liquid extraction on a large scale. The actinides, in general, form more stable complexes than do the homologous lanthanide ions. Extraction with tertiary amines and *bis*-2-ethylhexyl hydrogen phosphate has been used to separate the trivalent transplutonium element ions from the lanthanides. Differences in complexation have also been used to separate lanthanides and actinides by ion-exchange techniques. The sorption of actinide ions on cation exchangers varies in the sequence $MO_2^{+} < M^{2+} < MO_2^{2+} < M^{3+} < M^{4+}$. The sorption coefficients of ions of the same charge do not differ widely. Their separation coefficients can be much enhanced, however, by the use of selective, complex-forming eluting agents. Citrate, lactate, and especially α-hydroxoisobutyrate as eluting agents have been proved as

successful for the separation of trivalent lanthanide and actinide ions. A group separation of trivalent actinides and lanthanides may be accomplished also by anion exchange. The trivalent actinide ions form much more stable chloride complexes than do the trivalent lanthanide ions. They are therefore sorbed on anion-exchange resins from concentrated hydrochloric acid, while the lanthanides are not.

C. Magnetic Properties

The actinides exhibit nearly all of the types of magnetism found in transition and lanthanide metals. Thorium behaves like a 6*d* transition metal. The magnetic susceptibility is large, and the temperature dependence is low. The actinide metals protactinium to plutonium do not have ordered ground state moments. Hybridization of 5f and 6*d* levels broadens the f levels and suppresses the formation of localized moments. The temperature-independent paramagnetic susceptibilities indicate an itinerant character of the 5f electrons. From americium on the 5f electrons become localized and the heavy metals are localized magnets, similar to the lanthanide metals. For americium, the susceptibility is large with little temperature dependence. Curium has an antiferromagnetic transition at 65 K, but the face-centered cubic phase shows a ferrimagnetic transition near 200 K. Berkelium metal exhibits high-temperature magnetic behavior like its lanthanide homolog terbium. Californium metal exhibits either ferro- or ferrimagnetic behavior below 51 K and paramagnetic behavior above 160 K.

Actinide compounds and ions exhibit very different magnetic behavior arising from the spin and orbital angular moments of the unpaired electrons. Spin-orbit coupling is about twice that for the lanthanides, and the crystal field strengths for the actinides are an order of magnitude greater. There is a wealth of information about the magnetic properties of various actinide materials which has been reviewed elsewhere.

D. Spectroscopic Properties

Actinide spectra reflect the characteristic features of the 5f orbitals which can be considered as both containing the optically active electrons and belonging to the core of filled shells. The electronic transition spectra of actinide ions in solution are dominated by the structure of the f levels and transitions within the f shell. Free-atom spectra provide more information about the interactions between the 5f and the valence electrons. The emission spectra of the free actinide atoms have an enormous number of lines. In the uranium spectrum, about 100,000 lines have been measured, from which about 2500 lines have been assigned.

In condensed phases, spectra are commonly measured in absorption. Three main types of transitions are observed in the absorption spectra of the actinide ions: (1) Laparte-forbidden f to f transitions, (2) orbitally allowed 5f to 6*d* transitions, and (3) metal to ligand charge transfer. Of these, study of internal f to f transitions has found wide use in the investigation of actinide chemistry. These band usually in the visible and ultraviolet regions, can be easily identified because of their sharpness, and are sensitive to the metal environment. As discussed earlier, the 5f orbitals of the actinide elements are more exposed than the lanthanide 4f orbitals, and therefore, crystal field effects are larger in the 5f series. The f to f transitions for actinide elements may be up to 10 times more intense and twice as broad as those observed for the lanthanides, due to the action of crystal fields. In addition, extra lines resulting from vibronic states coupled to $f \rightarrow f$ states have been observed.

The 5f to 6*d* bands are orbitally allowed and therefore more intense than those of the f to f transitions. They are also usually broader and often observed in the ultraviolet region. The metal to ligand charge-transfer bands are also fully allowed transitions that are broad and occur commonly in the ultraviolet region. When these bands trail into the visible region, they produce the intense colors associated with many of the actinide compounds. Metal-ligand frequencies are also observed in the infrared and Raman spectra of actinide compounds.

Actinide spectra are used in different ways. First, because of their characteristic properties, actinide spectra can be used for the direct speciation of (complexed) actinide ions, the observation and quantification of reactions taking place in solution, or the identification of compounds. On the other hand, actinide spectra can be used to study electronic and physicochemical properties, including information on symmetry, coordination number, or stability constants.

Conventional optical absorption spectrometry has detection limits of between 0.01 and 1 m*M* for the actinides. Highly sensitive spectroscopic methods have been developed, based on powerful laser light sources. Time resolved laser fluorescence spectroscopy (TRLFS), based on the combined measurement of relaxation time and fluorescence wavelength, is capable of speciating Cm(III) down to 10^{-12} mol/L but is restricted to fluorescent species like U(VI) and Cm(III). Spectroscopic methods based on the detection of nonradiative relaxation are the laser-induced photoacoustic spectroscopy (LPAS) and the laser-induced thermal lensing spectroscopy (LTLS). Like conventional absorption spectroscopic methods, these newly developed methods are capable of characterizing oxidation and complexation states of actinide ions but with higher sensitivity.

Methods of growing importance for speciation and complexation studies of actinides are the synchrotron-based X-ray absorption near-edge structure spectroscopy (XANES) and the extended X-ray absorption fine structure spectroscopy (EXAFS).

VI. ACTINIDE COMPOUNDS AND COMPLEXES

A. Binary Compounds

1. Hydrides

Representative actinide hydride compounds are represented in Table X. Actinide metals react readily with hydrogen when heated. The temperature needed for reaction depends on the state of the metal, the amount of surface oxidation on the metal, and the purity and pressure of the hydrogen used. The actinide hydrides are not very thermally stable and are very air and moisture sensitive. The thermal instability of these compounds has been used to obtain finely divided metal via thermal decomposition of the corresponding hydride.

The physicochemical properties of the actinide hydrides are as varied as any in the entire periodic table. Thorium forms a “normal” dihydride like those of Zr and Hf, but also forms Th_4H_{15}, a unique superconductor. The hydrides of protactinium and uranium have cubic structures which have no counterparts in the periodic table. The transuranium element hydrides are more lanthanide like with wide cubic solid solution ranges. Hexagonal phases appear with regularity.

2. Oxides

The actinide oxides have received intensive scrutiny because their refractory nature makes them suitable for use as ceramic fuel elements in nuclear reactors. UO_2 melts at 3150 K, and ThO_2 has the highest melting point of any oxide, about 3465 K. The actinide oxides are complicated by deviations from stoichiometry, polymorphism, and intermediate phases. The sesquioxides are basic, the dioxides are much less basic, and UO_3 is an acid in solid state reactions. The reactivity of these oxides depends greatly on their thermal history. If ignited, they are much more inert. Table XI contains some representative data on actinide oxides.

TABLE X Actinide Hydrides

Compound	Color	Symmetry[a]	Space group	Lattice parameters a (Å)	Lattice parameters c (Å)	M-H Bond length (Å)	Density (g cm^{-3})
AcH_2	Black	fcc	*Fm*3*m*	5.670		2.46	8.35
$ThH_{1.93}$	Black	bct		5.73	4.99	2.39	9.50
ThH_2	Black	bct		4.10	5.03	2.39	9.20
Th_4H_{15}	Black	bcc	$I\bar{4}3d$	9.11		2.29, 2.46	8.29
α-PaH_3	Black	Cubic	*Pm*3*n*	4.150			
β-PaH_3	Black	Cubic	*Pm*3*n*	6.648		2.32	10.57
α-UH_3	Black	Cubic	*Pm*3*n*	4.160		2.32	11.12
β-UH_3	Black	Cubic	*Pm*3*n*	6.644			
NpH_2	Black	fcc	*Fm*3*m*	5.348		2.32	10.41
$NpH_{2.36}$	Black	fcc	*Fm*3*m*	5.346			
$NpH_{2.42}$	Black	fcc	*Fm*3*m*	5.348			
NpH_3	Black	Hexagonal	$P6_3/mmc$	3.777	6.720		9.64
PuH_2	Black	fcc	*Fm*3*m*	5.3594		2.32	10.40
$PuH_{2.5}$	Black	fcc	*Fm*3*m*	5.34			
PuH_3	Black	Hexagonal	$P6_3/mmc$	3.779	6.771	2.18–2.41	9.61
AmH_2	Black	fcc	*Fm*3*m*	5.348		2.316	10.6
$AmH_{2.67}$	Black	fcc	*Fm*3*m*	5.338			
AmH_3	Black	Hexagonal	$P6_3/mmc$	3.764	6.763		9.76
$CmH_{2(+x)}$	Black	fcc	*Fm*3*m*	5.322		2.314	10.7
CmH_3	Black	Hexagonal		3.77	6.73		
$BkH_{2(+x)}$	Black	fcc	*Fm*3*m*	5.25			
$BkH_{3(-x)}$	Black	Trigonal		6.454	6.663		
CfH_{2+x}	Black	Cubic		5.285			

[a] bct, body-centered tetragonal; fcc, face-centered cubic.

TABLE XI Binary Actinide Oxides[a]

Compound	Color	Symmetry[b]	Lattice parameters					
			a (Å)	b (Å)	c (Å)	α (deg)	β (deg)	γ (deg)
Ac_2O_3	White	Hexagonal	4.07		6.29			
ThO_2	White	Cubic	5.5971					
Pa_2O_5	White	fcc	5.446					
$\mathrm{Pa_2O_5}$	White	Tetragonal	5.429		5.503			
$\mathrm{Pa_2O_5}$	White	Hexagonal	3.817		13.220			
$\mathrm{Pa_2O_5}$	White	Rhombohedral	5.424			89.76		
$\mathrm{Pa_2O_5}$	White	Orthorhombic	6.92	4.02	4.18			
$\mathrm{PaO_{2.42}}$-$\mathrm{PaO_{2.44}}$	White	Rhombohedral	5.449			89.65		
$\mathrm{PaO_{2.40}}$-$\mathrm{PaO_{2.42}}$	White	Tetragonal	5.480		5.416			
$\mathrm{PaO_{2.33}}$	White	Tetragonal	5.425		5.568			
$\mathrm{PaO_{2.18}}$-$\mathrm{PaO_{2.21}}$	White	fcc	5.473					
$\mathrm{PaO_2}$	Black	fcc ($\mathrm{CaF_2}$)	5.509					
α-U_3O_8	Dark green	Orthorhombic	6.716	11.960	4.147			
β-$\mathrm{U_3O_8}$	Dark green	Orthorhombic	7.069	11.445	8.303			
α-$\mathrm{U_2O_5}$	Black	Monoclinic	12.40	5.074	6.75		99.2	
β-$\mathrm{U_2O_5}$	Black	Hexagonal	3.813		13.18			
γ-$\mathrm{U_2O_5}$	Black	Monoclinic	5.410	5.481	5.410		90.49	
α-$\mathrm{UO_3}$	Beige	Orthorhombic	6.84	43.45	4.157			
β-$\mathrm{UO_3}$	Orange	Monoclinic	10.34	14.33	3.910		99.03	
γ-$\mathrm{UO_3}$	Yellow	Orthorhombic	9.813	19.93	9.711			
δ-$\mathrm{UO_3}$	Deep red	Cubic	4.16					
ε-$\mathrm{UO_3}$	Brick red	Triclinic	4.002	3.841	4.165	98.10	90.20	120.17
η-$\mathrm{UO_3}$	Brown	Orthorhombic	7.511	5.466	5.224			
$\mathrm{UO_2}$	Dark brown	fcc	5.704					
$\mathrm{Np_2O_5}$	Dark brown	Monoclinic	4.183	6.584	4.086		90.32	
NpO_2	Brown-green	Cubic	5.425					
α-$\mathrm{Pu_2O_3}$	Black	bcc	11.04					
β-$\mathrm{Pu_2O_3}$	Black	Hexagonal	3.841		5.958			
PuO_2	Yellow	fcc	5.3960					
A-$\mathrm{Am_2O_3}$	Red-brown	Hexagonal	3.817		5.96			
B-$\mathrm{Am_2O_3}$	Red-brown	Monoclinic	14.38	3.52	8.92		100.4	
C-$\mathrm{Am_2O_3}$		Cubic	11.03					
AmO_2	Dark brown	fcc	5.374					
A-$\mathrm{Cm_2O_3}$	White	Hexagonal	3.792		5.985			
B-$\mathrm{Cm_2O_3}$	White	Monoclinic	14.282	3.641	8.883		100.29	
C-$\mathrm{Cm_2O_3}$	White	Cubic	11.002					
$\mathrm{CmO_2}$	Black	Cubic	5.3584					
A-$Bk_2\mathrm{O_3}$	Yellow-green	Hexagonal	3.754		5.958			
C-$\mathrm{Bk_2O_3}$	Yellow-green	bcc	10.887					
$\mathrm{BkO_2}$	Brown	fcc	5.3315					
A-$Cf_2\mathrm{O_3}$	Pale green	Hexagonal	3.72		5.69			
B-$\mathrm{Cf_2O_3}$	Pale green	Monoclinic	14.124	3.591	8.809			100.31
C-$\mathrm{Cf_2O_3}$	Pale green	bcc	10.839					
$\mathrm{CfO_2}$	Black	fcc	5.310					
$\mathrm{Es_2O_3}$	Black	bcc	10.766					
$\mathrm{Es_2O_3}$		Monoclinic	14.1	3.59	8.80			100
$\mathrm{Es_2O_3}$		Hexagonal	3.7		6.0			

[a] The most stable oxide of each element is italicized. Where more than one modification exists, the first listed is italicized.

[b] bcc, body-centered cubic; fcc, face-centered cubic.

The wide variety of oxidation states known for the actinides is reflected in the stoichiometry of their binary oxides; however, the highest attainable oxidation state may not be observed. The largest O/M ratio for an f-element binary oxide is achieved in UO_3.

All the solid actinide monoxides which have been reported are now believed to have been oxynitrides, oxycarbides, or hydrides. The highest potential for existence would have the monoxides for the divalent actinide metals einsteinium through nobelium. Only the gaseous monoxides are well-established species. All actinides are known or expected to form gaseous monoxides.

The sesquioxide is known for actinium and all the actinides from plutonium through einsteinium and is probably the highest binary oxide that could be formed for the heaviest actinides with nobelium as an exception, which may only form a solid monoxide. Oxides of the heaviest actinides beyond einsteinium have not been prepared or studied experimentally. The sesquioxides of Pu, Am, and Bk are readily oxidized to their dioxides, whereas those of Cm, Cf, and Es are resistant to air oxidation.

The dioxide is known for all the actinides from thorium through californium. Attempts to prepare einsteinium dioxide have not been successful. All the dioxides crystallize with the fluorite face-centered cubic structure. Actinides that form both a dioxide and a sesquioxide may form complex intermediate oxides, which have O/M ratios between 1.5 and 2.0.

Binary oxides with higher oxygen stoichiometries have been confirmed only for the elements Pa, U, and Np. Numerous phases in the composition range UO_2 to UO_3 have been observed. The reported formation of nonstoichiometric PuO_{2+x} has to be confirmed. Only UO_3 is known for the anhydrous actinide trioxides and is prepared by decomposing uranyl nitrate or a hydrated uranyl hydroxide containing NH_4^+ at 350°C. There are seven crystal modifications of UO_3. Many of these contain oxygen-bridged structures, with uranyl present. δ-UO_3 with its cubic ReO_3 structure consists of linked UO_6 octahedra.

Actinide sulfides, selenides, and tellurides are also known. The sulfides and selenides are generally isostructural, but not with the analogous tellurides. The thermal stability of these compounds decreases in the order sulfides > selenides > tellurides. These compounds are usually prepared via direct reaction of finely divided actinide metal powder with the chalcogen at about 400–600°C. Semimetallic behavior and nonstoichiometry are observed for these compounds.

3. Halides

A wealth of information has been accumulated on actinide halides. The known binary halides range from AnX_2 to AnX_6, and some representative data for these are given in Table XII. The thermal stability of the halides toward reduction of higher oxidation state actinides decreases with increasing atomic number of the halogen.

Truly divalent actinide halides are known only for americium and californium. AnX_2 species for Es have been identified by their absorption spectra. For Fm, Md, and No, AnX_2 halides should be possible if sufficient amounts of these metals could be obtained. ThI_2 is also known, but crystallographic studies of this compound reveal the true formulation to be Th(IV), $2I^-$, and $2e^-$. This compound has some metallic character, including its luster and electrical conductivity.

The actinide trihalides behave similarly to the lanthanide trihalides. The trifluorides through berkelium trifluoride crystallize at room temperature with the LaF_3 hexagonal structure. Nine fluorine atoms are arranged around the actinide in a heptagonal bipyramid geometry. CfF_3 and a second form of BkF_3 have the orthorhombic YF_3 structure, where nine fluorines form an approximate tricapped prism with one fluorine 0.3 Å farther from the metal. All of the trifluorides are high-melting solids, insoluble in water, and only slowly oxidized in air.

The actinide trichlorides are hygroscopic and water soluble and melt between 1030 and 1110 K. They can be obtained by reaction of the metal hydride with HCl at elevated temperatures or by the reaction of CCl_4 with $An(OH)_3$. With the larger actinide(III) ions, the crystal structures of the trichlorides show nine chlorine atoms arranged in a tricapped trigonal prismatic geometry. As the atomic number increases, the three actinide to face-capping-chlorine distances increase relative to the other six chlorines. At californium, a second form of $CfCl_3$ has eight coordination.

$AnBr_3$ compounds can be prepared by reaction of HBr with the proper actinide hydride, hydroxide, oxalate hexahydrate, or oxide. Structures similar to the trichlorides are observed with the structural change from nine coordination to eight coordination occurring with ß-neptunium tribromide. The triiodides to α-americium triiodide have the same eight-coordinate structure found for the heavier bromides and chlorides. From ß-americium triiodide on, the metals are six coordinate. ThI_3 is best formulated as Th(IV), $3I^-$, and $1e^-$.

The best known actinide halides are the tetrahalides, the fluorides being known through californium. All of the AnF_4 species are monoclinic, the metal being eight coordinate with antiprismatic geometry. These compounds, prepared by heating HF with the dioxides, are insoluble in water. The remaining tetrahalides can be prepared by heating the actinide dioxides in CCl_4 ($ThCl_4$ to $NpCl_4$), $Cl_2/SOCl_2$ ($BkCl_4$), or from the elements ($ThBr_4$ to $NpBr_4$ and ThI_4 to UI_4). The tetrachlorides are eight

TABLE XII Binary Actinide Halides

Compound	Color	Symmetry	Lattice parameters					
			a (Å)	b (Å)	c (Å)	α (deg)	β (deg)	γ (deg)
β-ThI_2	Gold	Hexagonal	3.97		31.75			
AmI_2	Black	Monoclinic	7.677	8.311	7.925		98.5	
α-CfI_2	Violet	Hexagonal	4.557		6.992			
β-CfI_2	Violet	Rhombohedral	7.434			35.8		
$AmBr_2$	Black	Trigonal	11.59		7.121			
$CfBr_2$	Amber	Trigonal	11.000		7.109			
$AmCl_2$	Black	Orthorhombic	8.963	7.573	4.532			
PaI_3	Black	Orthorhombic	4.33	14.00	10.02			
UI_3	Black	Orthorhombic	4.328	13.996	9.984			
NpI_3	Purple	Orthorhombic	4.3	14.03	9.95			
PuI_3	Green	Orthorhombic	4.33	13.95	9.96			
α-AmI_3	Yellow	Orthorhombic	4.31	14.03	9.92			
β-AmI_3	Yellow	Hexagonal	7.42		20.55			
CmI_3	White	Hexagonal	7.44		20.4			
BkI_3	Yellow	Hexagonal	7.84		20.87			
CfI_3	Yellow	Hexagonal	7.587		20.814			
EsI_3	Red	Hexagonal	7.53		20.84			
$AcBr_3$		Hexagonal	8.06		4.68			
UBr_3	Red	Hexagonal	7.936		4.438			
α-$NpBr_3$	Green	Hexagonal	7.919		4.392			
β-$NpBr_3$	Green	Orthorhombic	12.618	4.109	9.153			
$PuBr_3$	Green	Orthorhombic	12.65	4.10	9.15			
$AmBr_3$	White	Orthorhombic	12.66	4.064	9.144			
$CmBr_3$	White	Orthorhombic	12.70	4.041	9.135			
$BkBr_3$	Yellow-green	Monoclinic	7.23	12.53	6.83		110.6	
α-$CfBr_3$	Pale green	Monoclinic	7.215	12.423	6.825		110.7	
β-$CfBr_3$	Pale green	Rhombohedral	7.58			56.2		
$EsBr_3$	Straw	Monoclinic	7.27	12.59	6.81		110.8	
$AcCl_3$	White	Hexagonal	7.62		4.55			
UCl_3	Green	Hexagonal	7.442		4.320			
$NpCl_3$	Green	Hexagonal	7.413		4.282			
$PuCl_3$	Green	Hexagonal	7.395		4.246			
$AmCl_3$	Pink	Hexagonal	7.382		4.214			
$CmCl_3$	White	Hexagonal	7.374		4.185			
$BkCl_3$	Green	Hexagonal	7.382		4.127			
β-$CfCl_3$	Green	Hexagonal	7.379		4.090			
α-$CfCl_3$	Green	Orthorhombic	3.859	11.748	8.561			
$EsCl_3$		Hexagonal	7.40		4.07			
AcF_3	White	Trigonal	7.41		7.53			
UF_3	Black	Trigonal	7.181		7.348			
NpF_3	Purple	Trigonal	7.129		7.288			
PuF_3	Violet	Trigonal	7.092		7.254			
AmF_3	Pink	Hexagonal	7.044		7.225			
CmF_3	White	Trigonal	7.019		7.198			
β-BkF_3	Yellow-green	Trigonal	6.97		7.14			
α-BkF_3	Yellow-green	Orthorhombic	6.70	7.09	4.41			
α-CfF_3	Light green	Orthorhombic	6.653	7.039	4.393			
β-CfF_3	Light green	Trigonal	6.945		7.101			

Continues

TABLE XII (*continued*)

Compound	Color	Symmetry	Lattice parameters					
			a (Å)	b (Å)	c (Å)	α (deg)	β (deg)	γ (deg)
ThI_4	White	Monoclinic	13.216	8.069	7.766		98.68	
α-$ThBr_4$	White	Tetragonal	6.737		13.601			
β-$ThBr_4$	White	Tetragonal	8.932		7.963			
$PaBr_4$	Brown	Tetragonal	8.824		7.957			
UBr_4	Brown	Monoclinic	10.92	8.69	7.05		93.15	
$NpBr_4$	Dark red	Monoclinic	10.89	8.74	7.05		94.19	
α-$ThCl_4$	White	Orthorhombic	11.18	5.93	9.09			
β-$ThCl_4$	White	Tetragonal	8.473		7.468			
$PaCl_4$	Green-yellow	Tetragonal	8.377		7.482			
UCl_4	Green	Tetragonal	8.296		7.481			
$NpCl_4$	Red-brown	Tetragonal	8.266		7.475			
ThF_4	White	Monoclinic	12.90	10.93	8.58		126.4	
PaF_4	Brown	Monoclinic	12.86	10.88	8.54		126.3	
UF_4	Green	Monoclinic	12.803	10.792	8.372		126.3	
NpF_4	Green	Monoclinic	12.68	10.66	8.34		126.3	
PuF_4	Pale brown	Monoclinic	12.599	10.573	8.84		126.25	
AmF_4	Tan	Monoclinic	12.538	10.516	8.204		126.8	
CmF_4	Brown	Monoclinic	12.51	10.61	8.20	125.8		
BkF_4		Monoclinic	12.40	10.47	8.12		126.3	
CfF_4	Green	Monoclinic	12.42	10.468	8.126		126.0	
Pa_2F_9	Black	Cubic	8.507					
U_2F_9	Black	Cubic	8.471					
PaI_5	Black	Orthorhombic	7.22	21.20	6.85			
α-$PaBr_5$		Monoclinic	12.69	12.82	9.92		108	
β-$PaBr_5$	Dark red	Monoclinic	8.385	11.205	8.950		91.1	
UBr_5	Brown	Triclinic	7.449	10.127	6.686	89.25	117.56	108.87
$PaCl_5$	Yellow	Monoclinic	8.00	11.42	8.43		106.38	
α-UCl_5	Brown	Monoclinic	7.99	10.69	8.48		91.5	
β-UCl_5	Brown	Triclinic	7.09	9.66	6.36	88.5	117.6	108.5
PaF_5	White	Tetragonal	11.525		5.218			
α-UF_5	Pale blue	Tetragonal	6.512		4.463			
β- UF_5	Pale blue	Tetragonal	11.450		5.207			
NpF_5	Bluish-white	Tetragonal	6.53		4.45			
UCl_6	Dark green	Hexagonal	10.90		6.03			
UF_6	White	Orthorhombic	9.900	8.962	5.207			
NpF_6	Orange	Orthorhombic	9.909	8.997	5.202			
PuF_6	Brown	Orthorhombic	9.95	9.020	5.260			

coordinate with dodecahedral geometry. UBr_4 and $NpBr_4$ are seven coordinate, and UI_4 is octahedral. UCl_4 and $ThCl_4$ are well-known starting materials for the synthesis of organometallic compounds.

Pentahalides are known only to neptunium. All of these compounds are very water sensitive. The pentafluorides and $PaCl_5$ are polymeric seven-coordinate compounds. The geometry is that of a distorted pentagonal bipyramid with double bridging occurring through four of the equatorial atoms. UCl_5 and $PaBr_5$ consist of halogenbridged dimeric An_2X_{10} units.

AnX_6 species are known for fluorides of uranium, neptunium, and plutonium and for UCl_6. The hexafluorides are volatile compounds obtained by fluorinating AnF_4. The highly volatile UF_6 is the compound used for the large-scale isotope separation of ^{235}U from ^{238}U. UCl_6 can be made by the reaction of $AlCl_3$ and UF_6. The hexahalides have octahedral geometry.

Oxyhalides of the actinides are known mainly for the types AnO_2X_2, AnO_2X, $AnOX_2$, and AnOX. They can be prepared by low-temperature hydrolysis or by oxygenating the corresponding halide with oxygen or Sb_2O_3. The hydrolysis of the trihalides results in AnOX species. The higher oxidation states found for AnO_2X_2 compounds confine these to uranium.

4. Compounds with Other Elements

Compounds of actinides with nitrogen, phosphorus, arsenic, antimony, and bismuth have been studied as a result of their refractory nature and possible uses as nuclear fuel materials. Many of these compounds can be prepared by heating a finely divided actinide metal or a hydride of the metal in a sealed tube with the Group 15 element. Borides, carbides, and silicides are also known.

Monocarbides, mononitrides, and other actinide compounds with the general formulation AnX (X = Group 15 and 16 elements) have the face-centered cubic NaCl structure. These compounds are mainly ionic with a partially filled conduction band and, thus, are good conductors of heat and electricity.

Tetragonal compounds of the UX_2 and UXY type, again with X and Y being elements of Group 15 or 16, are also good conductors. Metallic An_3X_4 compounds have body-centered cubic structures.

Table XIII presents some data on these compounds.

TABLE XIII Other Early Actinide Compounds

Compound	Symmetry [a]	Space group	Lattice parameters a (Å)	Lattice parameters b (Å)
UAs	fcc	$Fm3m$	5.7788	
UBi	fcc	$Fm3m$	6.364	
UC	fcc	$Fm3m$	4.961	
UN	fcc	$Fm3m$	4.889	
UP	fcc	$Fm3m$	5.589	
US	Cubic	$Pm3m$	5.4903	
USb	fcc	$Fm3m$	6.203	
USe	fcc	$Fm3m$	5.7399	
UTe	fcc	$Fm3m$	6.150	
NpAs	fcc	$Fm3m$	5.835	
NpC	fcc	$Fm3m$	4.992	
NpN	fcc	$Fm3m$	4.898	
NpP	fcc	$Fm3m$	5.610	
NpS	fcc	$Fm3m$	5.527	
NpSb	fcc	$Fm3m$	6.249	
PuAs	fcc	$Fm3m$	5.855	
PuC	fcc	$Fm3m$	4.974	
PuN	fcc	$Fm3m$	4.9055	
PuP	fcc	$Fm3m$	5.664	
PuS	fcc	$Fm3m$	5.537	
PuSb	fcc	$Fm3m$	6.241	
UP_2	Tetragonal	$P4/nmm$	3.808	7.780
UAs_2	Tetragonal	$P4/nmm$	3.954	8.116
USb_2	Tetragonal	$P4/nmm$	4.272	8.759
UBi_2	Tetragonal	$P4/nmm$	4.445	8.908
α-US_2	Tetragonal	I_1/mcm	10.27	6.32
α-USe_2	Tetragonal	$I4/mcm$	10.772	6.668
UOSe	Tetragonal	$P4/nmm$	3.9035	6.9823
UOTe	Tetragonal	$P4/nmm$	4.004	7.491
UOS	Tetragonal	$P4/nmm$	3.483	6.697
UAsS	Tetragonal	$P4/nmm$	3.884	8.176
UAsSe	Tetragonal	$P4/nmm$	3.962	8.422
UAsTe	Body-centered tetragonal	$I4/mcm$	4.1483	17.2538
UNSe	Tetragonal	$P4/nmm$		
UNTe	Tetragonal	$P4/nmm$		
U_3P_4	bcc	$I\bar{4}3d$	8.207	
U_3As_4	bcc	$I\bar{4}3d$	8.507	
U_3Sb_4	bcc	$I\bar{4}3d$	9.113	
U_3Bi_4	bcc	$I\bar{4}3d$	9.350	
U_3Se_4	bcc	$I\bar{4}3d$	8.760	
U_3Te_4	bcc	$I\bar{4}3d$	9.398	

[a] bcc, body-centered cubic; fcc, face-centered cubic.

B. Oxo Acid Salts

Much of the information on actinide oxo acid salt compounds is provided from studies of the analytical separation chemistry of the actinides, solvent extraction, ion exchange, and precipitation technologies. Little structural information is available on these species. Isolated examples of borates, silicates, nitrites, phosphites, hypophosphites, arsenates, thiosulfates, selenates, selenides, tellurates, and tellurites are known but not well characterized. A much broader chemistry is known for complexes with nitrates, carbonates, phosphates, sulfates, halides, and carboxylates, reflecting the importance of these ions in separation techniques.

The chloride, bromide, bromate, nitrate, and perchlorate anions form water-soluble salts with the actinide M^{3+} ions, which can be isolated by evaporation. Precipitates are formed with hydroxide, fluoride, carbonate, oxalate, and phosphate anions. The actinide M^{4+} ions form insoluble fluorides, iodates, arsenates, and oxalates; the nitrates, sulfates, perchlorates, and sulfides are all water soluble. The MO_2^+ ions can be precipitated from concentrated carbonate solutions as potassium salts. $Na_2U_2O_7$ can be precipitated from alkaline solutions of the uranyl, UO_2^{2+}, ion. The hydroxides or hydrous oxides of any of the actinide ions in all oxidation states are insoluble in water.

Complexes of the actinyl ions with sulfate, nitrate, and carboxylate ions have octahedral, pentagonal

bipyramidal, and hexagonal bipyramidal geometries. The actinyl group is linear with further coordination occurring in the equatorial plane. The oxoanions are often bidentate. The anionic complexes $[An(NO_3)_6]^{2-}$ are also known, having bidentate nitrate ions forming a distorted icosahedron.

Several carboxylates have been prepared, either during separations of An^{4+} ions or for thermal decomposition as a route to the dioxides. Most of the actinide carboxylates can be prepared as hydrates by dissolving the appropriate oxide and hydroxide in carboxylic acid. Formates, acetates, oxalates, xanthates, and carbamates are also known.

C. Organometallic Compounds

A rich and diversified organometallic chemistry of the actinide elements has come into existence in the last three decades of the previous century. High reactivities, unusual reaction paths, catalysis, high coordination numbers, and unique structures continue to reward those working in this area.

The first organoactinide compound was $(\eta^5-C_5H_5)_3UCl$, synthesized by L. T. Reynolds and G. Wilkinson in 1956. The triscyclopentadienyl alkyl and aryl actinide compounds, with a formal coordination number of 10, contain the most stable actinide carbon σ bonds. Later on, compounds containing indenyl and cyclooctatetraenyl groups as the π donor ligands were synthesized. The chemical bonds in these organometallic compounds range from covalent σ bonds to ionic and, thus, provide excellent samples for the study of chemical bonding of the $5f$ elements.

$An(C_5H_5)_4$ and $An(C_5H_5)_3X$ compounds can be prepared via the reaction of $AnCl_4$ with $K(C_5H_5)$. The tetracyclopentadienyl derivatives (thorium through neptunium) contain four π-bonded aromatic rings. This is in contrast to the (two π-, two σ-) bonded cyclopentadienyl rings observed in the structure of tetracyclopentadienyl hafnium and the three π/one σ arrangement found for the corresponding zirconium analogue and is presumably the result of the larger size of the actinide ions. The $An(C_5H_5)_3X$ compounds have a similar structure to that observed for $(\eta^5-C_5H_5)_4U$. The centroids of the three π-bonded aromatic rings occupy three vertices of a tetrahedron, with the fourth occupied by the halogen.

Cyclopentadienyl derivatives of the actinides have received a great deal of attention in the search for alkoxy, alkyl, aryl, allyl, borohydride, amide, and other actinide compounds. The cyclopentadienyl and pentamethylcyclopentadienyl ligands significantly increase the solubility of the actinide in organic solvents, thus allowing their chemistries to be developed. In addition, the reactivity of

TABLE XIV Organometallic Actinide Compounds

Type	Compound[a]	Color
$(\eta^5-C_5H_5)_4An$	Cp_4Th	Colorless
	Cp_4Pa	Orange
	Cp_4U	Red
	Cp_4Np	Brown
$(\eta^5-C_5H_5)_3An$	Cp_3U	Bronze
	Cp_3Pu	Moss green
	Cp_3Am	Rose
	Cp_3Cm	Colorless
	Cp_3Bk	Amber
	Cp_3Cf	Red
$(\eta^5-C_5H_5)_3AnX$	Cp_3ThF	Yellow
	Cp_3ThCl	Colorless
	Cp_3ThBr	Yellow
	Cp_3ThI	Yellow
	Cp_3UF	Green
	Cp_3UCI	Brown
	Cp_3UBr	Dark brown
	Cp_3UI	Brown
	Cp_3NpF	Green
	Cp_3NpCI	Dark brown
$(\eta^5-C_5H_5)_3AnR$	$Cp_3U(CH_3)$	
	$Cp_3U(i\text{-}C_3H_7)$	
	$Cp_3U(n\text{-}C_4H_9)$	Dark red
	$Cp_3U(t\text{-}C_4H_9)$	
	Cp_3U(neopentyl)	Dark red
	Cp_3U(ferrocenyl)	Brown
	Cp_3U(allyl)	Dark brown
	Cp_3U(2-methylallyl)	
	Cp_3U(vinyl)	
	$Cp_3U(C_6H_5)$	Greenish
	$Cp_3U(C_6F_5)$	Dark brown
	$Cp_3U(p\text{-}C_6H_4UCp_3)$	Red-orange
	$Cp_3U(C_2H)$	Yellow-green
	$Cp_3U(C_2C_6H_5)$	Yellow-green
	Cp_3U(*p*-methylbenzyl)	Dark violet
	Cp_3U(benzyl)	Dark violet
	Cp_3U(2-*cis*-2-butenyl)	
	Cp_3U(2-*trans*-2-butenyl)	
	$(C_5H_4)2Fe[UCp_3]_2$	Green
	Cp_3Th(neopentyl)	White
	Cp_3Th(allyl)	White
	$Cp_3Th(i\text{-}C_3H_7)$	White
	Cp_3Th(2-*cis*-2-butenyl)	White
	Cp_3Th(2-*trans*-2-butenyl)	White
	$Cp_3Th(n\text{-}C_4H_9)$	White
$(\eta^5-C_9H_7)_3AnR$	$(C_9H_7)_3U(CH_3)$	Red-brown
	$(C_9H_7)_3Th(CH_3)$	Yellow
	$(C_9H_7)_3Th(n\text{-}C_4H_9)$	Yellow

Continues

TABLE XIV (*continued*)

Type	Compound[a]	Color
$(\eta^5-C_5Me_5)_2AnR_2$	$Cp_2^*U(CH_3)_2$	Orange
	$Cp_2^*Th(CH_3)_2$	White
	$Cp_2^*U(CH_3)Cl$	Red-orange
	$Cp_2^*Th(CH_3)Cl$	White
	$Cp_2^*U[CH_2Si(CH_3)_3]_2$	Orange
	$Cp_2^*Th[CH_2Si(CH_3)_3]_2$	White
	$Cp_2^*U[CH_2Si(CH_3)_3]Cl$	Red
	$Cp_2^*Th[CH_2Si(CH_3)_3]Cl$	White
	$Cp_2^*U[CH_2C(CH_3)_3]_2$	Brown
	$Cp_2^*Th[CH_2C(CH_3)_3]_2$	White
	$Cp_2^*U(CH_2C_6H_5)_2$	Black
	$Cp_2^*U(CH_2C_6H_5)Cl$	Black
	$Cp_2^*Th(CH_2C_6H_5)_2$	White
	$Cp_2^*Th(CH_2C_6H_5)Cl$	White
	$Cp_2^*U(C_6H_5)_2$	Orange-brown
	$Cp_2^*Th(C_6H_5)_2$	White
	$Cp_2^*Th(C_6H_5)Cl$	White
	$Cp_2^*U[C_4(C_6H_5)_4]$	Brown
	$Cp_2^*Th(CH_2CH_3)_2$	White
$(\eta^8-C_8H_8)_2An$	COT_2Th	Yellow
	COT_2U	Green
	COT_2Np	Yellow-red
	COT_2Pu	Red

[a] Cp, cyclopentadienyl; Cp*, pentamethylcyclopentadienyl; COT, cyclooctatetraenyl.

actinide compounds has been found to be a sensitive function of the metal's coligands, and these compounds react readily with alkyllithium and Grignard reagents to give σ-bonded carbon compounds. The resulting alkyl compounds are highly reactive and extremely air and moisture sensitive. Hydrogenolysis yields organoactinide hydrides. The dihydrocarbyls react with carbon monoxide to form metal–oxygen and carbon–carbon double bonds, reactions which are of interest in catalysis.

Some representative organoactinide compounds are given in Table XIV. $(\eta^5-C_5H_5)_2AnCl_2$ compounds are unstable. These compounds disproportionate to $(\eta^5-C_5H_5)_3AnCl$ and $(\eta^5-C_5H_5)AnCl_3$. Compounds of the type $(\eta^5-C_5H_5)_2AnX_2$ have been prepared either by placing the cyclopentadienyl ligands on the metal last or by using charged multidentate acetyl acetonate, dihydrobis(pyrazolyl) borate, or hydrotris(pyrazolyl) borate ligands to stabilize the $(\eta^5-C_5H_5)_2AnX_2$ configuration. Trivalent triscyclopentadienyl compounds of the actinides can be prepared starting from $AnCl_3$. These compounds readily form adducts, and a large number of $(\eta^5-C_5H_5)_3AnL$ complexes have been structurally characterized. $(\eta^5-C_5H_5)_3UCl$ and other organometallic compounds of the $5f$ elements show a greater degree of covalency than their lanthanide analogues.

The reaction of actinide tetrachlorides (thorium through plutonium) with the potassium salt of cyclo-octatetraene (COT) results in the formation of "actocene" complexes, $(\eta^8-C_8H_8)_2An$, named by analogy with ferrocene. All these compounds have a sandwich structure in which two planar COT rings enclose a metal atom.

In the search for catalytically active species, heterobi- and polynuclear molecules containing both U(III) and a transition metal (palladium, platinum, rhodium, or ruthenium) strongly bonded in close proximity but without a direct metal–metal bond were synthesized. Difunctional bridging ligands like cyclopentadienylphosphido ligands were used to form such complexes.

Only recently were the actinide containing metallofullerenes $Am@C_{82}$, $Np@C_{82}$, and $U@C_{82}$, which consist of actinide atoms being encapsulated into the carbon cage of fullerene compounds, prepared and characterized.

SEE ALSO THE FOLLOWING ARTICLES

CRYSTALLOGRAPHY • NUCLEAR CHEMISTRY • RADIOACTIVITY • URANIUM

BIBLIOGRAPHY

Bagnall, K. W. (1972). "The Actinide Elements," Am. Elsevier, New York.

Choppin, G. R., and Rydberg, J. (1980). "Nuclear Chemistry—Theory and Applications," Pergamon, Oxford.

Cotton, F. A., and Wilkinson, G. (1999). "Advanced Inorganic Chemistry," 6th ed., Wiley, New York.

Edelstein, N. M., ed. (1980). "Lanthanide and Actinide Chemistry and Spectroscopy," Am. Chem. Soc., Washington, DC.

Edelstein, N. M., ed. (1982). "Actinides in Perspective," Pergamon, Oxford.

Freeman, A. J., and Darby, J. B., Jr., eds. (1974). "The Actinides: Electronic Structure and Related Properties," Vols. 1 and 2, Academic Press, New York.

Freeman, A. J., and Lander, G. H. (1984, 1985, 1987). "Handbook on Physics and Chemistry of the Actinides," Vols. 1, 2, and 5, North-Holland, Amsterdam.

"Gmelin Handbook of Inorganic Chemistry," Supplement Vol. on Thorium: AIa(1990), A2(1986), A3(1988), A4(1989), A5(1990), C3(1987), C5(1986), C7(1988), D1(1988), D2(1985), D3(1990), E(1985); Supplement Vol. on Uranium: B2(1989), C5(1986), C12(197). Springer-Verlag, Berlin.

Greenwood, N. N., and Earnshaw, A. (1998). "Chemistry of the Elements," 2nd ed., Butterworth-Heinemann, Oxford.

Gschneidner, K. A., Jr., Eyring, L., Choppin, G. R., and Lander, G. H., eds. (1994). "Handbook on the Physics and Chemistry of Rare

Earths, Vol. 18: Lanthanides/Actinides: Chemistry," North-Holland, Amsterdam.
Katz, J. J., Seaborg, G. T., and Morss, L. R., eds. (1986). "The Chemistry of the Actinide Elements," Vols. 1 and 2, Chapman & Hall, London.
Keller, C. (1971). "The Chemistry of the Transuranium Elements," VCH, Weinheim/New York.
Leigh, G. J., ed. (1990). "Nomenclature of Inorganic Chemistry, Recommendations 1990," Blackwell Sci; Oxford.
Lieser, K. H. (1997). "Nuclear and Radiochemistry: Fundamentals and Applications," VCH, Weinheim/New York.
Marks, T. J., and Fischer, R. D., eds. (1979). "Organometallics of the *f*-Elements," Reidel, Dordrecht, Netherlands.
Navratil, J. D., and Schulz, W. W., eds. (1980). "Actinide Separations," Am. Chem. Soc., Washington, DC.
Seaborg, G. T., and Loveland, W. T. (1990). "The Elements Beyond Uranium," Wiley, New York.
Wilkinson, G., Stone, F. G. A., and Abel, E. W., eds. (1982). "Comprehensive Organometallic Chemistry," Vol. 3, Pergamon, Oxford.

Bioinorganic Chemistry

Brian T. Farrer
Vincent L. Pecoraro
University of Michigan

I. Inorganic Ion Uptake and Regulation
II. Inorganic Components of Enzymatic Systems
III. Biomineralization
IV. Medical Uses for Inorganic Compounds

GLOSSARY

Active site The location in an enzyme that is responsible for the binding and catalysis of the substrate.

Cofactor A substance, as an inorganic ion, coenzyme, or vitamin, that activates an enzyme.

Eukaryotic Of or pertaining to an organism that contains one or more cells with a distinct nucleus.

Homeostasis A state of physiological equilibrium produced by a balance of functions and chemical composition within an organism.

Ligand A molecule or part of a molecule that bonds to a metal to form a complex ion.

Oxidation A chemical reaction in which there is an increase in formal charge on an atom. This increase can be brought about by processes such as loss of electrons, addition of an oxygen atom, etc.

Oxidation state A numerical value given to an atom that signifies the number of electrons removed from the proximity of its nucleus relative to the number of electrons present in its elemental form [e.g., iron has eight valence electrons in its elemental form; since in $FeCl_2$ the iron has only six electrons, the oxidation state is $+2$ and the iron is denoted Fe(II) or Fe^{2+}].

Prokaryotic Of or pertaining to a cellular organism, the nucleus of which has no limiting membrane.

Reduction A chemical reaction in which there is a decrease in formal charge on an atom. This decrease can be brought about by processes such as gain of electrons, loss of an oxygen atom, etc.

Reduction potential A quantitative value given to the ease of electron addition to a system. The reduction potential E is related to the standard free energy ΔG° of a half-reaction ($A \rightarrow A^+ + e^-$) by the Nernst equation: $\Delta G^\circ = -nFE$, where n is the number of electrons removed and F is Faraday's constant.

BIOINORGANIC CHEMISTRY is the field of chemistry that is concerned with the role of inorganic elements in biological systems. In the 19th century, the term "organic" was given to the chemistry of life. For several years, the basic elements of life seemed to be hydrogen, carbon, nitrogen, and oxygen, while the other elements seemed only to be abundant in nonliving things: ores, the atmosphere, etc. These other elements were termed "inorganic" or "without life." Within the past half century, it has become obvious that some elements originally denoted "inorganic" play an

essential role in biological systems, giving this area of science the seemingly contradictory title. In fact, in most of the major functions of life—respiration, photosynthesis, reproduction, oxygen transport, and metabolism, to name a few—inorganic ions play an active and essential role.

I. INORGANIC ION UPTAKE AND REGULATION

A. Overview

Microbes, plants, and animals must be able to generate an organized structure from a surrounding disorganized milieu. Table I compares the concentrations of several essential elements in sea water to levels found in human plasma. In most cases, the elements are more concentrated in human plasma. This observation points to the necessity of having an uptake mechanism for inorganic elements in humans. The same requirement is true for all organisms. Not only do organisms need to acquire elements from the environment, they need a mechanism to ensure that toxic concentrations are not attained. This interplay between uptake, storage, and excretion is termed regulation. Homeostasis of these inorganic ions in cells is accomplished by regulating the synthesis of the proteins and small molecules that are involved in the uptake, storage, and discharge of that particular inorganic ion.

A general scheme of inorganic ion regulation is shown in Fig. 1. With the exception of retroviruses, all proteins are encoded in DNA. DNA is transcribed to form RNA by RNA polymerase. RNA is then used to make proteins in the ribosome. Proteins can then be modified to acquire the proper activity. Regulation of the production of enzymes can occur at any of these steps. Regulation of RNA polymerase, ribosome function, and protein function are called transcriptional, translational, and post-translational regulation, respectively. All three types of regulation are employed to control the concentration and location of inorganic ions in a cell. Furthermore, most inorganic ions account for their own regulation. Metal-regulated gene expression can be considered to fall into three categories: (1) maintaining homeostasis of an essential element such as iron or copper, (2) removing or detoxifying elements with no useful biological activity (e.g., mercury or cadmium), and (3) controlling expression of genes that encode proteins that may or may not use the specific element (e.g., zinc fingers).

TABLE I Concentrations of Selected Inorganic Elements in Sea Water and Human Plasma

Inorganic element	Sea water concentration (Molar)	Human plasma concentration (Molar)
Iron	5×10^{-11} to 2×10^{-8}	2.2×10^{-5}
Zinc	8×10^{-8}	1.7×10^{-5}
Copper	1×10^{-8}	1.6×10^{-5}
Molybdenum	1×10^{-7}	1.0×10^{-5}
Cobalt	7×10^{-9}	2.5×10^{-11}
Chromium	4×10^{-9}	5.5×10^{-8}
Vanadium	4×10^{-8}	1.8×10^{-7}
Manganese	7×10^{-9}	1.1×10^{-7}
Nickel	5×10^{-9}	4.4×10^{-8}

B. Acquisition and Regulation of Iron and Other Essential Elements

Iron is one of the most abundant inorganic elements in biology. Iron is essential in processes as diverse as photosynthesis, respiration, and destruction of oxygen species that lead to damage in biomolecules. Iron can also be very toxic. The deleterious side reactions of iron result in detrimental processes in humans such as aging, cancer, and cardiovascular disease. A large excess of iron(III) deposits as rust in a protein called hemosiderin, which accumulates in cell membranes. In thallesemia major, a genetic blood disease, hemosiderin deposits adversely effect cell membrane function. Even more pernicious, iron can react with oxygen or peroxide to form the same oxygen radicals that it is used to prevent. Hydroxyl radical is produced from hydrogen peroxide through a process called the Fenton reaction:

$$Fe^{2+} + H_2O_2 + H^+ \longrightarrow Fe^{3+} + H_2O + OH. \qquad (1)$$

Hydroxyl radical reacts with molecules such as DNA or lipids at diffusion-controlled rates every time it collides with one, and is the cause of lesions to genetic material or cell membranes. Superoxide and peroxynitrite are two additional reactive species that can be formed in the presence of excess Fe(II) as follows:

$$Fe(II) + O_2 \longrightarrow Fe(III) + O_2^- \qquad (2)$$

$$O_2^- + NO \longrightarrow {}^-OONO. \qquad (3)$$

In particular, peroxynitrite has been implicated as an important causative agent of inflammation, nerve damage, and the severe secondary tissue damage following heart attacks and strokes.

Because iron concentrations must be tightly regulated, organisms from archaebacteria to humans have developed complex processes to acquire iron from the environment, transport it through the cell membrane, and insert it into the appropriate enzyme without being released to diffuse freely where it can cause extensive damage to the cell. Given below are two examples of the regulation of iron, one from a prokaryotic organism, the other from humans.

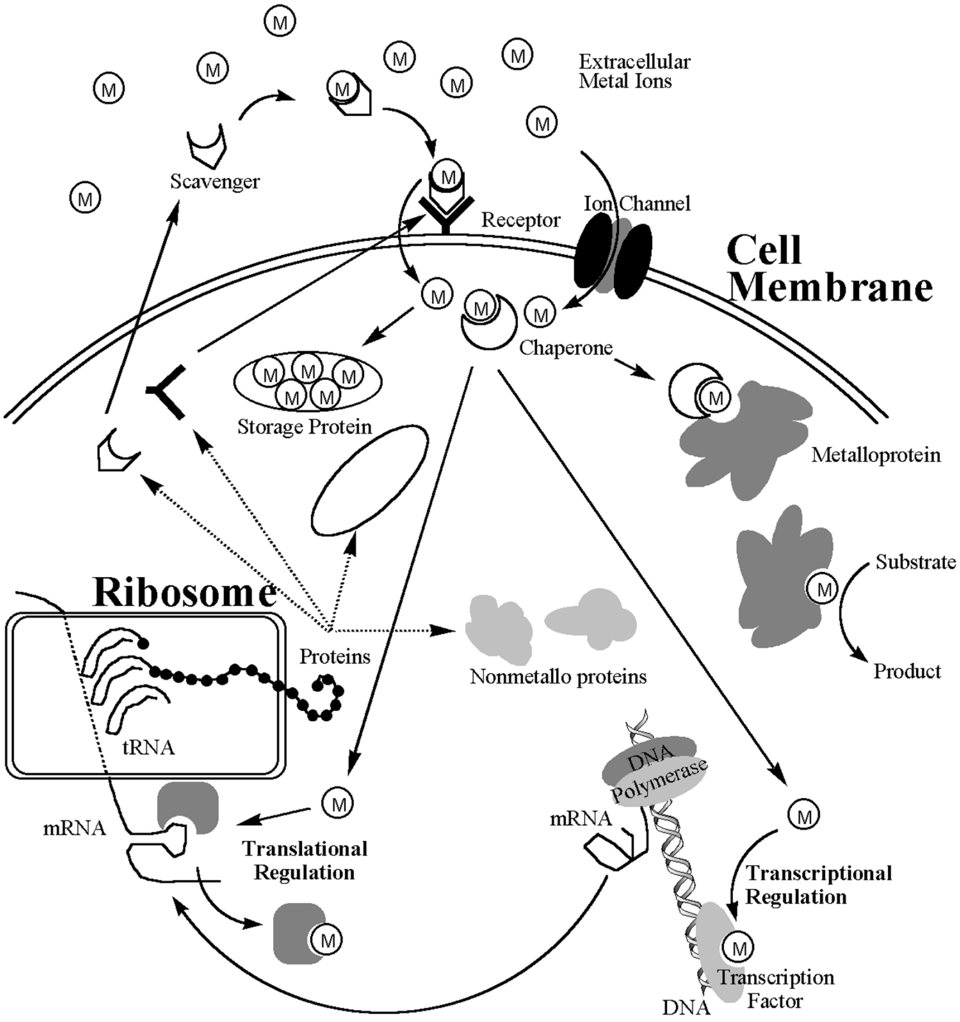

FIGURE 1 General scheme of metal ion uptake and regulation.

1. Iron Regulation in *E. coli*

The Fur (ferric uptake regulation) protein negatively regulates the production of the siderophore enterobactin. Siderophores are small molecules that chelate Fe(III) in the environment and are then transported across the cell membrane, introducing Fe(III) into the cell. Most siderophores use catechol or hydroxamate groups to bind Fe(III). Unicellular organisms must make siderophores in order to extract the highly insoluble Fe(III) from ores or rust. At low intracellular levels of iron, the Fur protein does not bind DNA, and proteins that are responsible for the synthesis and transport of enterobactin across the cell membrane are produced. As the levels of iron are elevated, it binds to DNA and blocks the expression of these proteins, halting the intake of iron when the concentration of iron becomes too high. In this way, iron is directly responsible for *transcriptional* regulation of the synthesis of siderophores that are responsible for its own uptake.

Studies on eukaryotes show that there is a mechanism for iron storage in these cells when the concentration of iron in the cell increases. This process is regulated at the *translational* level (Fig. 1).

2. Iron Regulation in Humans

In humans, iron is transported across the gut by a series of poorly defined processes. Fe(III), ferric ion, is absorbed via a β_3 integrin and mobilferrin, whereas ferrous ion enter the cells via Nramp. Once inside the body, Fe(III) is transported through the serum by transferrin, a protein of molecular weight 63,000 Da. Fe(III)•transferrin is recognized by a receptor protein on the cell surface. Via a process known as cell-mediated endocytosis, the Fe(III)•transferrin/receptor complex induces the external cell membrane to pucker and eventually form a clatharin-coated vesicle in the cytoplasm. After removal of the clatharin, the vesicle (known as an endosome) becomes

acidic and iron is released. Then, the iron is shuttled to sites of utilization (e.g., myoglobin) or storage (ferritin).

In contrast to the analogous bacterial receptors that are regulated transcriptionally, both the transferrin receptor protein and the storage protein ferritin are regulated translationally. After the genes for the proteins are transcribed to mRNA, a section of the mRNA is used to regulate the synthesis of the protein. This region is termed the IRE (iron-responsive element). The IREs associated with transferrin receptor are rich in adenine and uracil bases. These bases do not stabilize RNA structure as well as guanine and cytosine. For ferritin, the IRE is found in the region of mRNA preceding the protein-coding region, whereas the IRE follows the protein-coding region for the transferrin receptor protein. The placement of the IRE is essential for the proper regulation of iron.

The control mechanism for this system is a cytoplasmic protein called the IRP (iron regulatory protein). At low intracellular iron levels, the IRP does not bind iron. Without the iron bound, the protein has a high affinity for the IRE. Under these conditions, the ferritin mRNA is blocked from binding the ribosome and protein is not produced. At the same time, the unstable mRNA for the transferrin receptor protein is stabilized by binding the IRP, which allows protein synthesis to occur for longer periods. As a consequence more iron is brought into the cell and less storage protein is made at low levels of intracellular iron. At high iron levels, the IRP binds four Fe atoms in an "iron–sulfur" cluster. This causes the protein to change its three-dimensional structure to a form that has low affinity for the IRE. Now ferritin mRNA binding to the ribosome is no longer blocked, allowing protein synthesis and, ultimately, iron storage. Concurrently, the transferrin receptor mRNA, now less stable, is rapidly degraded, limiting the iron entering the cell. As a consequence less iron is brought into the cell and more storage protein is made at high levels of intracellular iron.

It is thought that the IRE/IRP system of regulation is very ancient and may represent how the earliest genes were regulated in an RNA world. Other metals such as copper and nickel have separate sets of proteins and genes that regulate the homeostasis of these necessary metals.

C. Regulation of Toxic Inorganic Ions

Some inorganic ions are not necessary to the survival of an organism. In many of these cases, the presence of the metal ion at any concentration is detrimental to that organism. These inorganic ions are purely toxic. For example, mercury, cadmium, and arsenic are toxic to most organisms. It should be noted, however, that these elements are not necessarily toxic to all organisms (e.g., cadmium can enhance the growth of some marine diatoms in the absence of a sufficient supply of zinc.) Below are examples of two different types of biochemical resistance to the toxic ions. The first example is from a prokaryote (Hg^{2+} detoxification), the second from a eukaryote (Cd^{2+} detoxification).

1. Prokaryotic Hg(II) Detoxification

Bacterial mercury regulation and resistance is the classic example of regulated metal resistance. It is accomplished by the *mer* gene. Mercury is a metal that is not essential for life, but is highly toxic. Interestingly, the mechanism for detoxification is through uptake. The explanation for this is that Hg(II) is extremely thiophilic and will bind to available cysteines voraciously. In order to prohibit environmental Hg(II) from binding and disrupting the function of membrane proteins, Hg(II) must be controlled by being brought into the cell and reduced to Hg(0).

The expression of proteins involved in Hg(II) detoxification is regulated by the MerR protein. The MerR protein is always bound as a dimer adjacent to the RNA polymerase binding site of the *mer* gene. In the absence of Hg, MerR holds the DNA in a conformation so that the RNA polymerase binding is blocked and transcription cannot occur. When the mercury binds to MerR, it changes the conformation of the MerR protein–DNA complex and allows RNA polymerase to bind and transcribe the *mer* operon, creating mRNA for the series of enzymes that carry out mercury resistance.

These proteins are MerA, MerT, and MerP. MerP is responsible for scavenging Hg(II) from the environment and bringing it to the cell surface. MerT then transports the Hg(II) across the cell membrane. The Hg(II) is then reduced to Hg(0) by MerA, which uses NADPH as a reductant. The Hg(0) is much less toxic than Hg(II) and is also volatile. Therefore, it is able to diffuse through the membrane out of the cell where it will evaporate out of the surrounding solution.

2. Eukaryotic Cd(II) detoxification

Cadmium is released into the environment by power stations, heating systems, metal-working industries, waste incinerators, and urban traffic and as a by-product of some fertilizers. Its primary mode of toxicity is as an inhibitor to enzymes. For example, by binding to nitrate reductase it inhibits the transport of nitrate and blocks energy flow in plants. In other plants, Cd(II) inhibits Fe(III) reductase leading to Fe(II) deficiency, hence disrupting photosynthesis (see below). In addition, Cd(II) can act as a carcinogen. Unlike iron, however, the cadmium does not produce oxygen radicals. Instead, it inhibits the enzymes responsible for protection against oxygen radicals.

In response to cadmium, the plant cell can respond using a number of defense systems. Some plants bind cadmium via histidine interactions to the cell wall. Cadmium that bypasses the cell wall then must pass the cell membrane. This barrier at least slows the influx of cadmium into the cytoplasm. The cell membrane is usually breached by hijacking an ion channel meant for the influx of another ion. When cadmium enters the cell, the initial cell response is to produce chelating agents, phytochelatins, to bind to the cadmium rendering it ineffective. Phytochelatins are short peptides, typically 5–20 amino acids long, that are synthesized from glutathione and contain repeating γGlu–Cys units.

A very significant mechanism of Cd detoxification is compartmentalization. By limiting the intracellular Cd to vacuoles, the cytoplasmic Cd concentration is decreased and cadmium is effectively removed from the areas where it can be toxic. After the cadmium is complexed to phytochelatins, these complexes can associate with acid-labile sulfur (S^{2-}) to form a higher molecular weight aggregate with higher affinity toward Cd. This complex can then be transported into a vacuole. Here the cadmium is tranferred from the phytochelatin to an organic salt (e.g., citrate, oxalate, or malate) allowing the phytochelatin to return to the cytoplasm to retrieve more cadmium.

For humans, recent data indicate adverse health effects from cadmium exposure may develop in $\sim$1% of the adult population, and in high-risk groups this percentage will be even higher (up to 5%). Smokers have four to five times higher blood cadmium concentrations and twice the kidney cortex concentrations as nonsmokers. In the human body, cadmium is bound to albumin in blood plasma after free cadmium ion has entered the blood stream. This cadmium–albumin complex is recognized by the liver. Once in the liver, it is bound by a proteins called metallothionines (MT). Metallothioneins are small proteins, 4500–8000 Da, that contain a high proportion of cysteine residues (about 30%). These proteins chelate Cd much like the phytochelatins. Free cadmium induces synthesis of MT, protecting the liver from cadmium toxicity. The Cd is returned to the blood stream complexed to MT and is transported to the kidney. There MT is degraded and free cadmium is released to react with sensitive sites or to re-bind to albumin. Because of this loop, cadmium accumulates in the kidney and remains in humans a very long tong time (half-life is 10–15 years). Although plants have metallothionines, their role in the detoxification of heavy metals from plants has yet to be investigated.

D. Regulation of Other Inorganic Ions

While many Americans learn of arsenic poisoning from the classic play "Arsenic and Old Lace," this element represents a significant environmental toxin. Arsenic is found at dangerous concentrations in drinking water in areas throughout southern Asia. As many as 15 million people in that area suffer from arsenic poisoning. Arsenic is found in two forms, arsenate ($As^{V}O_4^{3-}$) and arsenite ($As^{III}O(OH)_2^{-}$). One mechanism of bacterial resistance to arsenic is mediated by genes on the *ars* operon. These genes produce proteins that are responsible for the reduction of arsenate to arsenite, followed by removal of arsenite through an ion pump.

Other metals such as magnesium, silver, chromium, nickel, manganese, zinc, and copper are all regulated by different enzymes, but the general mechanism exhibits characteristics like those described above.

E. Regulation of Expression of Non-Inorganic Proteins

Some regulatory proteins that contain inorganic ions regulate the expression of proteins and enzymes not involved with inorganic ion homeostasis. Unlike the proteins that have been mentioned before, zinc-containing transcription factors do not regulate zinc homeostasis. Cells that are zinc-starved are prone to growth problems because zinc is an integral part of many transcription factors involved in cell proliferation. In fact, humans deficient in zinc have hindered growth. The two most common motifs in zinc transcription factors are the zinc finger and the Zn_2Cys_6 motif, typified by TFIIIA and GAL4, respectively.

TFIIIA was the first zinc finger enzyme to be identified. It contains nine zinc atoms, each stabilizing a region of the peptide known as a zinc finger. Zinc fingers are small regions of the protein (25–30 amino acids long) that fold into a distinctive α-helix–β-sheet conformation in presence of Zn(II) (Fig. 2), allowing the α-helix portion of the structure to recognize DNA through major groove interactions. Most zinc fingers contain two histidines and two cysteines responsible for binding the Zn(II) ion, although some are found with a Cys_3–His zinc ligation. In fact, all nine zinc fingers in TFIIIA contain the consensus sequence (with minor variation) $YXCX_{2,4}CX_3FX_5LX_2HX_{3,4}HX_{2-6}$. When these fingers are placehhd head-to-tail in a protein, they are able to recognize specific sections of DNA. Since the discovery of zinc fingers in TFIIIA, a multitude of proteins have been discovered which contain anywhere from 1 to 37 zinc finger motifs. Many of these proteins are responsible for DNA recognition.

Another family of zinc transcription factors is exemplified by GAL4. GAL4 is responsible for the transcription of genes involved in galactose metabolism in yeast cells. When zinc was initially discovered as a necessary constituent in GAL4, the protein was thought to contain a zinc finger with four ligating cysteines. Further studies

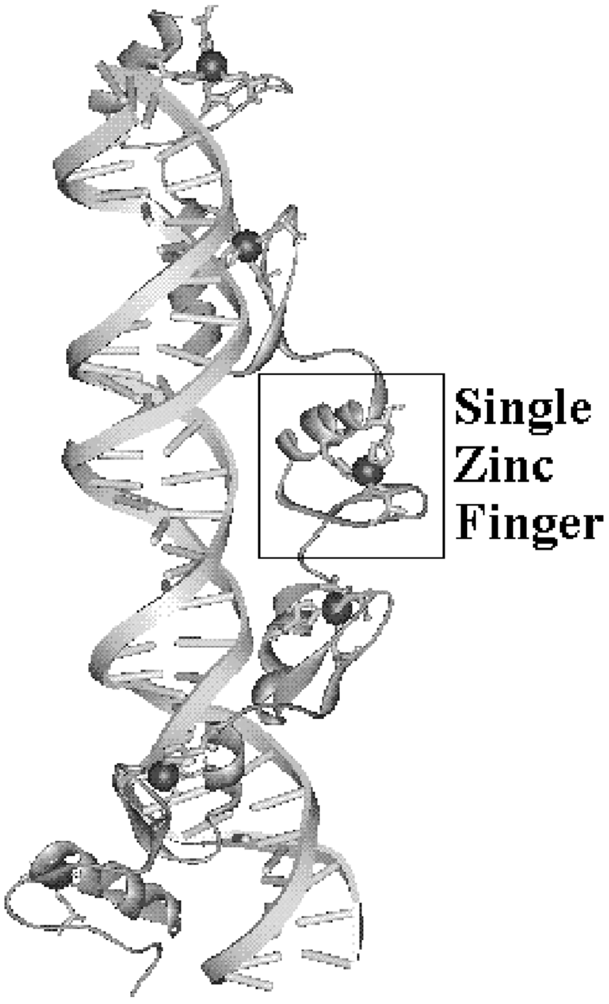

FIGURE 2 Section of transcription factor IIIa bound to DNA: an example of zinc finger binding.

revealed the presence of the binuclear $Zn_2(Cys)_6$ ligation geometry. Similar to the zinc in zinc fingers, the dimeric zinc site in GAL4 stabilizes the DNA-binding domain.

F. Cell Signaling

For a cell to function, it must be able to transmit signals from one compartment of a cell to another. This usually requires transmitting a signal through a cell membrane. This mechanism is usually accomplished through a series of receptors and messengers. Receptors are enzymes that receive the signal from one side of a membrane and transmit it to the other side. Messengers transmit the signal between receptors and ultimately to the proteins that are induced by the signal. Messengers range in size from small molecules and ions to proteins, and are labeled according to the order in which they occur in the signal (e.g., if a hormone binds to a receptor that releases ATP on the other side of a membrane, the hormone is considered the first messenger, while the ATP is a second messenger).

Calcium is one of the most extensively used messengers in biological systems. It is used in the signaling processes of muscle contraction, secretion, protein degradation, and cell division. For a long time, calcium was considered a second messenger. Evidence, however, suggested that the major source of calcium used in signaling comes from the endoplasmic reticulum (ER), which resides entirely within the cell. This observation requires a second messenger to transmit a signal from the outside of a cell through the cytoplasm to the ER, making calcium the third messenger. It was discovered that an organic molecule, inositol triphosphate, acts as the second messenger.

One requirement of a messenger in processes such as muscle contraction that require quick response time is that it must be found in low concentrations in the absence of a signal. This requirement is satisfied for calcium. Although the concentration of calcium in sea water, human plasma, and the ER is about 10 mM, the concentration of calcium within the cytoplasm is 0.0001 mM. This difference provides very dramatic changes in the calcium concentration upon leakage of calcium into the cytoplasm from the ER. This gradient, however, requires very efficient ion channels for calcium (discussed in the next section).

After calcium is released from the ER, one way it transmits the signal to the target protein is through calmodulin. Calmodulin is a protein that can bind four Ca^{2+} ions. The binding of calcium induces a structural change that exposes a methionine-rich region of the protein. Calmodulin then binds to proteins containing a site, a calmodulin-binding domain, that recognizes this methionine-rich region. This interaction can cause structural change in the target protein that regulates its activity. An example of a calmodulin-regulated protein is nitric oxide synthase (NOS). NOS produces nitric oxide, NO, which is a messenger involved in vasodilation and inflammatory response. Calmodulin also activates the ATPase that provides the energy to pump calcium out of the cell against a potential gradient.

G. Ion Channels

To ingest and excrete ions (such as Na^+, K^+, Ca^{2+}, and Cl^-) from and to the surrounding environment, cells must pass these ions through a membrane. In addition, eukaryotic cells are compartmentalized by intracellular membranes that must also be traversed by these ions. There are two types of transport across the cell membranes: mediated and unmediated. Unmediated transport is via simple diffusion, whereas mediated transport occurs through the action of specific carriers. Mediated transport can further

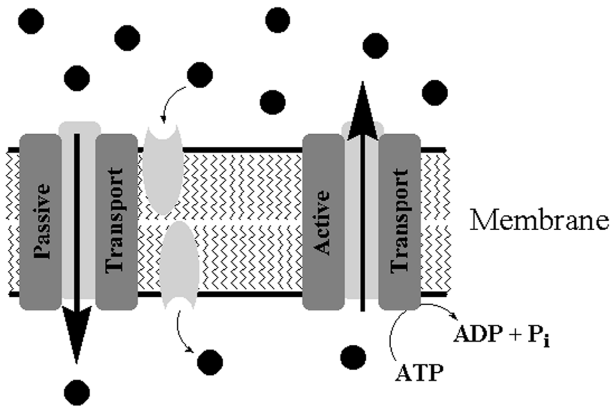

FIGURE 3 Schematic of mediated transport: active and passive ion transport.

be classified into two categories, passive-mediated transport and active-mediated transport (Fig. 3). Passive mediated transport simply increases the rate of concentration equilibration between the two sides of a membrane. Active transport moves ions from areas of low concentration to areas of higher concentration, thus against a potential gradient. To overcome this gradient, active transport must be coupled to an energy-utilizing reaction, usually the hydrolysis of ATP.

Valinomycin is a cyclical molecule that passively mediates transport of K^+ across membranes in the presence of Na^+ and Li^+. Valinomycin binds K^+ octahedrally and encompasses the ion in a shell that is very soluble in the lipophilic membrane. After passing through the membrane, potassium is released on the opposite side. Valinomycin forms a relatively large binding pocket that leads to ion selectivity. Sodium and lithium ions are significantly smaller than the pocket; they do not bind to valinomycin as efficiently and do not result in the structural change that increases valinomycin diffusion through the membrane. Monensin is a similar molecule with a smaller binding pocket, and transfers sodium ions across membranes in a similar fashion.

Active-mediated transport of Ca^{2+} ions from the cytoplasm to the ER or excretion of Ca^{2+} ions from a cell is essential to retain the low concentration of Ca^{2+} necessary for cell signaling (described above). Removal of calcium from the cytoplasm is achieved through the use of a Ca^{2+}–ATPase that is regulated by Ca–calmodulin. The Ca^{2+}–ATPase contains a short polypeptide sequence that blocks Ca^{2+} binding to the ion channel in the absence of Ca–calmodulin. In the presence of Ca–calmodulin, this peptide changes its conformation and allows the binding of calcium, which facilitates binding of ATP. When ATP is hydrolyzed by the enzyme, the structure of the enzyme changes, introducing Ca^{2+} to the other side of the membrane. Calcium is then released and more calcium is bound on the other side of the membrane. This calcium again facilitates binding and hydrolysis of ATP, resulting in transport across the membrane. This cycle continues until the calcium concentration is sufficiently low enough to cause calmodulin to release it. The calmodulin then releases the ATPase and efflux of calcium stops.

II. INORGANIC COMPONENTS OF ENZYMATIC SYSTEMS

A. Overview

Perhaps the classic area of bioinorganic chemistry is the study of enzymatic systems that use inorganic atoms to charry out catalysis. These studies have been undertaken by looking at the enzymes themselves or by examining small molecules that have structural elements found at the active site of the enzyme. This small-molecule modeling approach has provided an invaluable source of data for understanding the electronic structure and chemical mechanism of many complex enzymes. In some respects, bioinorganic chemistry includes all enzymes because soluble enzymes are dissolved in a sea of salt water containing sodium, potassium, and calcium ions that perform some level of perturbation on the structure and/or reactivity of the enzyme. However, this subsection of bioinorganic chemistry is usually limited to those enzymes that bind a specific inorganic cofactor in a specific manner and use it to perform a specific task.

The binding of the metal to the enzyme usually occurs through a set of amino acid ligands. Some amino acid ligands and the ways they bind to metals are shown in Fig. 4. Although this is the most common method of positioning the metal, some enzymes have evolved hydrogen bonding schemes to freeze a solvated inorganic ion in a particular location. Other enzymes will use an exogenous (non amino acid) ligand to help stabilize the metal in the position desired. Still other enzymes use a combination of two or more of these modes of binding.

Among the tasks assigned to inorganic elements in enzymatic systems are stabilization of the protein structure, transfer of electrons, transfer of oxygen, protection from oxidative stress, activation of diatomic molecules such as nitrogen, oxygen, and hydrogen, and harvesting light. Below, a number of these enzymes are organized according to their task and described following a discussion on some general inorganic structures used in these systems.

B. General Structures and Inorganic Cofactors

The metal centers found within enzymatic systems are diverse. Among the "bioinorganic chips" are hemes,

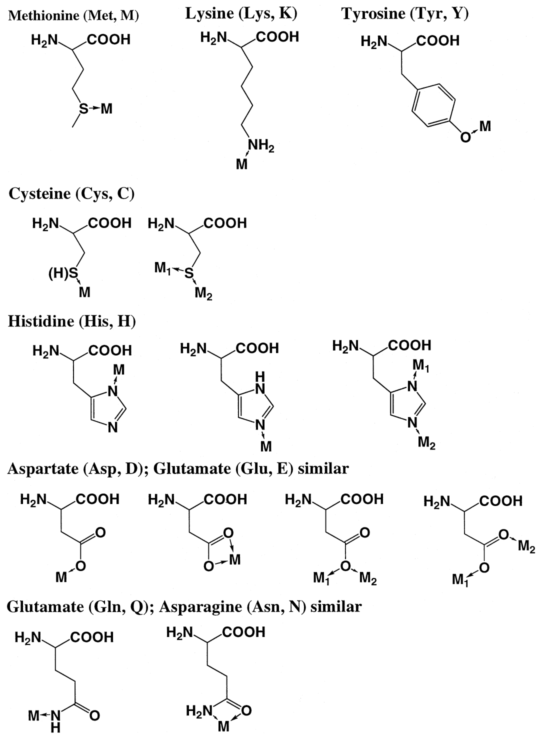

FIGURE 4 Amino acid ligands.

iron–sulfur, and iron–alternate metal–sulfur clusters, the nickel-containing factor F_{430}, chlorophylls, and the cobalt–corrin structure of vitamin B_{12}. In addition, for structures of significant importance, an independent presentation of the specifics of their structures is warranted. Among these are the iron–molybdenum cofactor responsible for nitrogen fixation and the cobalt–corrin structure of vitamin B_{12} and coenzyme B_{12}. Several of the more important bioinorganic cofactors (Fig. 5) will first be discussed independently of the specific proteins or enzymes that contain them.

A heme cofactor contains iron bound to an aromatic organic molecule called a porphyrin. This cofactor is the most ubiquitous of the metal cofactors. Heme function in proteins ranges from electron transfer, to oxygen binding and transport, to oxygen activation and oxidation of organic molecules; functions also include sensing O_2 and CO levels in certain microorganisms. Hemes have been known to contain iron in the +2, +3, and +4 oxidation states. The porphyrin moiety binds the iron in a four-coordinate fashion, leaving available two open coordination sites. One of these sites is almost always bound by an amino acid ligand (histidine, serine, cysteine, etc.), which is designated the proximal ligand. The sixth site, known as the distal ligand, is either bound to another amino acid ligand or an exogenous ligand such as water, or left open to bind substrate.

Porphyrins have two properties that are essential for the proper functioning of the cofactor. First, the four pyrrole-type nitrogen donors are perfectly designed to bind iron either in high-spin or low-spin electronic states. High-spin Fe(II) has unpaired electrons that can interact favorably with paramagnetic molecules such as O_2 to form bonds. Low-spin Fe(II) or either spin state for Fe(III) will not react with O_2. In contrast, electron transfer reactions occur most easily when iron is in the low-spin electronic configuration. Second, the electron donor capacity of the porphyrin, in conjunction with the types of proximal and distal ligands, specifies whether the heme cofactor will be used for oxygen transport or electron transfer, or to form a cation radical. In iron(III) porphyrins, substrates such as hydrogen peroxide can simultaneously oxidize both the metal and the porphyrin to form an Fe(IV)=O(porphyrin$^{+\bullet}$). This highly oxidizing state can insert an oxygen atom into a carbon–hydrogen bond to form epoxides and alcohols.

In modified porphyrins such as chlorophylls, this oxidation can be driven by the absorption of solar energy. Chlorophylls harvest light energy and channel it for use in photosynthesis. Chlorophylls are closely related to porphyrins. In the case of chlorophyll, however, the metal is magnesium and the ligand includes a reduced and modified porphyrin. In photohsystems I and II, chlorophylls form weak dimers, which is one way plants control absorption of the proper solar radiation. The chlorophyll shown in Fig. 5 contains a long alkane chain that helps it associate with the membrane within a chloroplast.

The cobalt center of vitamin B_{12} and coenzyme B_{12} is also similar to a heme. In this case, cobalt is the metal and a corrin is the aromatic ligand. A corrin differs from a porphyrin in two important respects. First, one "meso carbon" that joins the A and D rings of the porphyrin is removed. This alters both the aromaticity of the ring and the size of the metal-binding cavity. Second, a benzimidazole nucleotide linked to the corrin ring can act as the proximal ligand (in another enzyme, methionine synthase, the proximal ligand is replaced by a histidine). Cobalt-containing corrins are designated cobalamins. One forms vitamin B_{12}, cyanocobalamine, when cyanide binds as the distal ligand (R group in Fig. 5). Other important forms of cobalamins are methylcobalamin (R = —CH_3), which is used to transfer methyl groups (e.g., in methionine biosynthesis), and adenosylcobalamin, which uses a radical mechanism to isomerize small organic substrates (e.g., in glutamate mutase). The B_{12} cofactors were the first biological molecules recognized to form metal–carbon bonds.

Iron–sulfur centers are second in the list of most-diverse inorganic cofactors. Iron–sulfur centers are used in electron transfer and to carry out chemical modifications. They can also be employed as structural elements that help stabilize protein structure. The four simplest structures of these

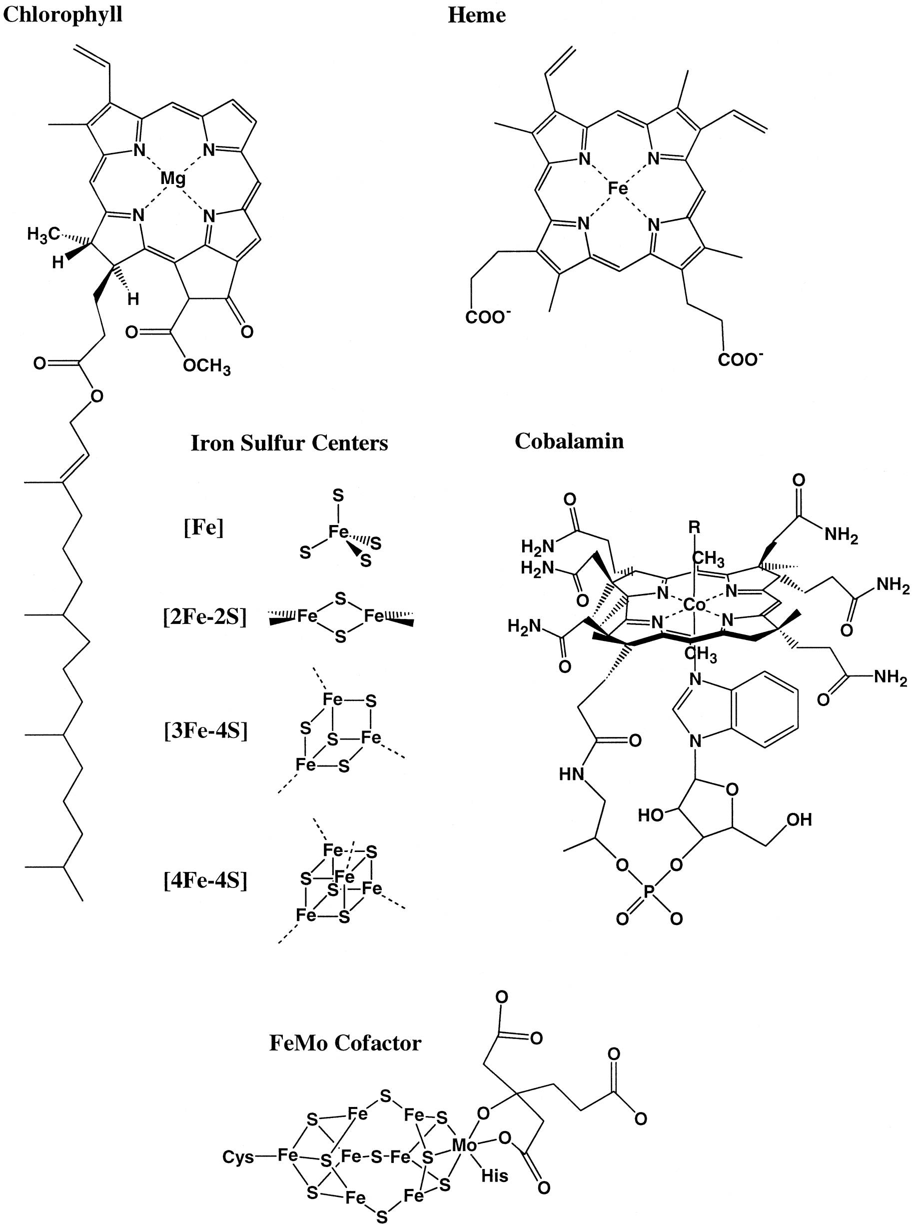

FIGURE 5 A selection of bioinorganic cofactors.

iron–sulfur centers are FeS_4, Fe_2S_2, Fe_3S_4, and Fe_4S_4. The FeS_4 center is a single iron atom bound by four cysteine sulfur atoms. The Fe_2S_2 center contains two bridging sulfides and each iron atom is bound to two amino acid ligands. The Fe_3S_4 structure is similar to the Fe_4S_4 cubane with one iron atom absent.

The iron–molybdenum cofactor of nitrogenase is one of the more complex inorganic cofactors. It consists of seven iron, one molybdenum, and nine sulfur atoms. The cofactor is held in place through an iron–cysteine interaction on one end and a molybdenum–histidine interaction on the other. Another nitrogenase contains a similar center with the molybdenum replaced by vanadium. The contribution of molybdenum and vanadium, two elements not typically associated with biological activity, to the activity of the protein is hotly disputed.

C. Electron Transfer

Many inorganic atoms can undergo facile low-energy redox reactions. With the exception of quinones and flavins, this characteristic is in sharp contrast to classical organic

molecules, where large structural changes, such as bond breaking, usually are coupled to the transfer of electrons. By placing an inorganic atom or cluster of atoms within a protein and tuning the redox properties with the surrounding protein environment, nature can transfer electrons from one location to another within the cell. Furthermore, proteins can set up coupled pathways that enable the facile exchange of electrons from one redox center to another over relatively long distances. Three general types of inorganic sites are used in biology to transfer electrons: hemes, iron–sulfur clusters, and blue copper centers. Each of these will be described below.

The heme proteins that are involved in electron transfer are denoted cytochromes and the best studied of these are the cytochrome c's. Cytochromes are highly water soluble, have relatively low molecular weight (~10 kDa), are highly stable, and are easily purified. Cytochromes are involved solely in the electron transfer cycle between the +2 and +3 oxidation states of iron. The range of reduction potentials for cytochromes is between −100 and +400 mV (vs. NHE). Studies with tuna cytochrome c indicate that there is very little structural difference between the oxidized and reduced forms of the enzyme. This structural rigidity results in extremely fast electron exchange from cytochrome c to its redox partners due to the minimal energy it takes to change the structure during the redox process.

Electron transfer proteins containing one iron atom are called rubredoxins; the class encompassing the two, three, and four iron centers are called ferridoxins. Rubredoxins have reduction potentials between 0 and −100 mV for the transition between Fe^{3+} and Fe^{2+}. The difference in structure between the Fe(III) and Fe(II) proteins is minimal, resulting in extremely fast electron transfer kinetics. Ferridoxins have a much broader range of reduction potentials. The dimeric Fe_2S_2 converts between Fe^{3+}/Fe^{3+} and Fe^{3+}/Fe^{2+} between −150 and −450 mV (NHE) depending on the protein. Fe_3S_4 centers have potentials falling in the range −70 to −460 mV (NHE) for the reduction of $Fe^{3+}/Fe^{3+}/Fe^{3+}$ to $Fe^{3+}/Fe^{3+}/Fe^{2+}$. Four iron centers can undergo two different types of reductions. The first is a transition between $Fe^{3+}/Fe^{3+}/Fe^{2+}/Fe^{2+}$ and $Fe^{3+}/Fe^{2+}/Fe^{2+}/Fe^{2+}$ (−300 to −700 mV, NHE), while the second is a transition between $Fe^{3+}/Fe^{3+}/Fe^{3+}/Fe^{2+}$ and $Fe^{3+}/Fe^{3+}/Fe^{2+}/Fe^{2+}$ (+100 to +400 mV, NHE). Interestingly, no known protein can do both of these reductions without undergoing significant structural change between the two redox processes.

Another general type of electron transfer protein is represented by the blue copper proteins (Fig. 6). The deeply blue color of these proteins results from an extrememly strong interaction between the copper and a cysteine sulfur atom. There are typically three other ligands, two his-

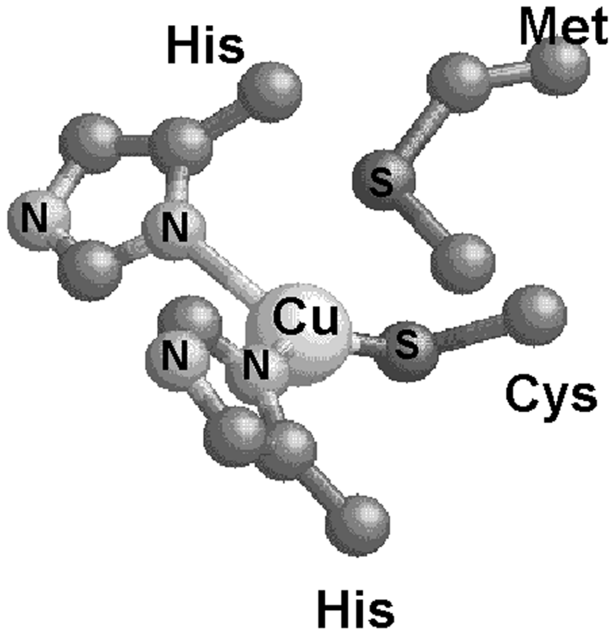

FIGURE 6 A Cys(His)$_2$Met blue copper center.

tidines, and a methionine around the copper forming a distorted trigonal pyramidal geometry. The fourth ligand, methionine, forms an exceptionally weak bond to the copper. The surrounding protein must be rigid and enclosed to block other ligands that form stronger bonds with copper from displacing the methionine. Blue copper proteins, the best known of which are azurin and plastocyanin, cycle between Cu(II) and Cu(I) oxidation states during electron transfer. The reduction potential for blue copper proteins is relatively high (+350 to +250 mV, NHE) stemming from the weak Cu–thiolate interaction. Electron transfer from blue copper centers is two to five orders of magnitude slower than that for the rubredoxins and cytochromes.

D. Photosynthesis and Respiration

The directed transport of electrons over long distances plays a crucial role in two of the most important processes of life: photosynthesis and respiration. Photosynthesis is responsible for harnessing the power of the sun and converting it to chemical energy in the form of ATP. Respiration exploits the highly oxidizing properties of oxygen to burn glucose to synthesize ATP. In photosynthesis, light is used to initiate an electron transfer process that generates a potential gradient across the membrane in chloroplasts. The energy from this gradient is used to produce ATP from ADP and eventually to convert CO_2 to sugars. A consequence of this process is the generation of oxygen from water. The oxygen is then used in respiration to drive the breakdown of glucose, a process which generates

another potential gradient, this time across a mitochondrial membrane. This potential gradient across a mitochondrial membrane is also used to generate ATP from ADP.

1. Photosynthesis

Photosynthesis is the process of converting solar radiation into chemical energy. This occurs in plants, algae, and photosynthetic bacteria. Cyclic photosynthesis (nonoxygenic) only uses photosystem I to capture light, whereas noncyclic (oxygenic) photosynthesis couples the oxidation of water to oxygen with photon capture using both photosystem I and photosystem II reaction centers. Cyclic photosynthesis is a less efficient light-harvesting scheme used by bacteria. The chlorophyll is excited by light, and electrons flow through a series of iron–sulfur clusters. The electrons are used to reduce $NADP^+$. Electrons eventually flow back to reduce the reaction-center chlorophyll through flavoproteins and the heme proteins cytochromes bc_1 and c_2.

In higher organisms, the light reactions of photosynthesis take place in the membrane of chloroplasts. A schematic view of the enzymatic machinery for oxygenic photosynthesis from spinach is shown in Fig. 7a. The photosynthetic machinery lies in the membrane of chloroplasts. By coupling the oxidation of water to oxygen in noncyclic photosynthesis, higher plants efficiently capture solar energy. As shown, many inorganic elements are included in this process. The light vibrationally excites magnesium-containing modified porphyrins called chlorophylls. The vibrational energy is then funneled from these "antenna chlorophyll" to a special pair of chlorophylls, P_{680}. An electron within the special pair is excited and transferred through a series of organic cofactors to a dissociable quinone, Q_B. This quinone passes the electrons to PSI via cytochrome b_6f and plastocyanin (see below). The electron removed from P_{680} is replenished by a cluster of four manganese ions that form the catalytic center of the oxygen-evolving complex (OEC). The OEC is responsible for water oxidation. The manganese cluster accumulates four oxidizing equivalents before converting water to oxygen as given by

$$2H_2O \longrightarrow 4H^+ + 4e^- + O_2. \quad (4)$$

The structure of the manganese cluster has been one of the most controversial areas of bioinorganic chemistry; it is expected that this issue will soon be resolved through X-ray crystallographic analysis.

Cytochrome b_6f is an electron transfer protein that contains several iron sites including hemes and iron–sulfur clusters. This complex migrates through the membrane and transfers the electron to plastocyanin, a blue copper protein. Plastocyanin then transfers the electron to photosystem I, specifically to reduce P_{700}^+, where it rests until P_{700} is excited by energy transferred from light by the chlorophyll surrounding photosystem I.

The electron is then transferred through the membrane via chlorophyll, a quinone, and iron–sulfur clusters to a ferridoxin on the inside of the chloroplast. The electron is then used to generate NADPH, an organic proton and electron carrier, which carries out many chemical transformations inside the chloroplast.

The energy to make ATP is generated by a proton gradient across the membrane, a result of water oxidation (which produces four protons per oxygen molecule formed). The protein ATP synthase converts the energy from this gradient to chemical energy through formation of ATP. The electrons of photosynthesis are used to fix carbon dioxide and produce sugars such as glucose.

2. Respiration

Oxidation of glucose by oxygen to carbon dioxide and water is the overall reaction in respiration:

$$C_6H_{12}O_6 + 6O_2 \longrightarrow 6CO_2 + 6H_2O. \quad (5)$$

This process yields a substantial amount of energy and is harnessed to synthesize 38 ATP molecules from ADP. In eukaryotes, the mitochondria are the site of oxidative metabolism. As with photosynthesis, inorganic elements play essential roles in respiration. In the initial stages of respiration, glucose is broken down into two pyruvate molecules, $C_3H_3O_3^-$, in a process termed glycolysis. This process requires enzymes that contain functional inorganic elements (Table II). Each pyruvate is oxidized by NAD^+ to form acetyl CoA, CH_3CO–SCoA, and carbon dioxide, producing two equivalents of NADH. The acetyl group, CH_3CO^-, is then oxidized by three NAD^+ and one FAD to produce two carbon dioxide molecules and three NADH and one $FADH_2$ in a series of reactions known as the citric acid cycle. The citric acid cycle contains more metalloenzymes. The NADH molecules produced by glycolysis and the citric acid cycle are oxidized by oxygen with a mechanism that produces a total of 34 ATPs per molecule of glucose.

The energy necessary to generate ATP is extracted from the oxidation of NADH and $FADH_2$ by the electron transport chain, a series of four protein complexes, denoted Complexes I–IV (Fig. 7b). NADH is oxidized by Complex I; $FADH_2$ is oxidized by Complex II. Each complex contains multiple redox centers: several iron–sulfur proteins and flavin mononucleotide in Complex I, and three iron–sulfur centers and a heme in Complex II. The electrons are then passed to coenzyme Q, which contains an organic redox center. Coenzyme Q transfers the electrons to Complex III. Complex III contains three hemes and

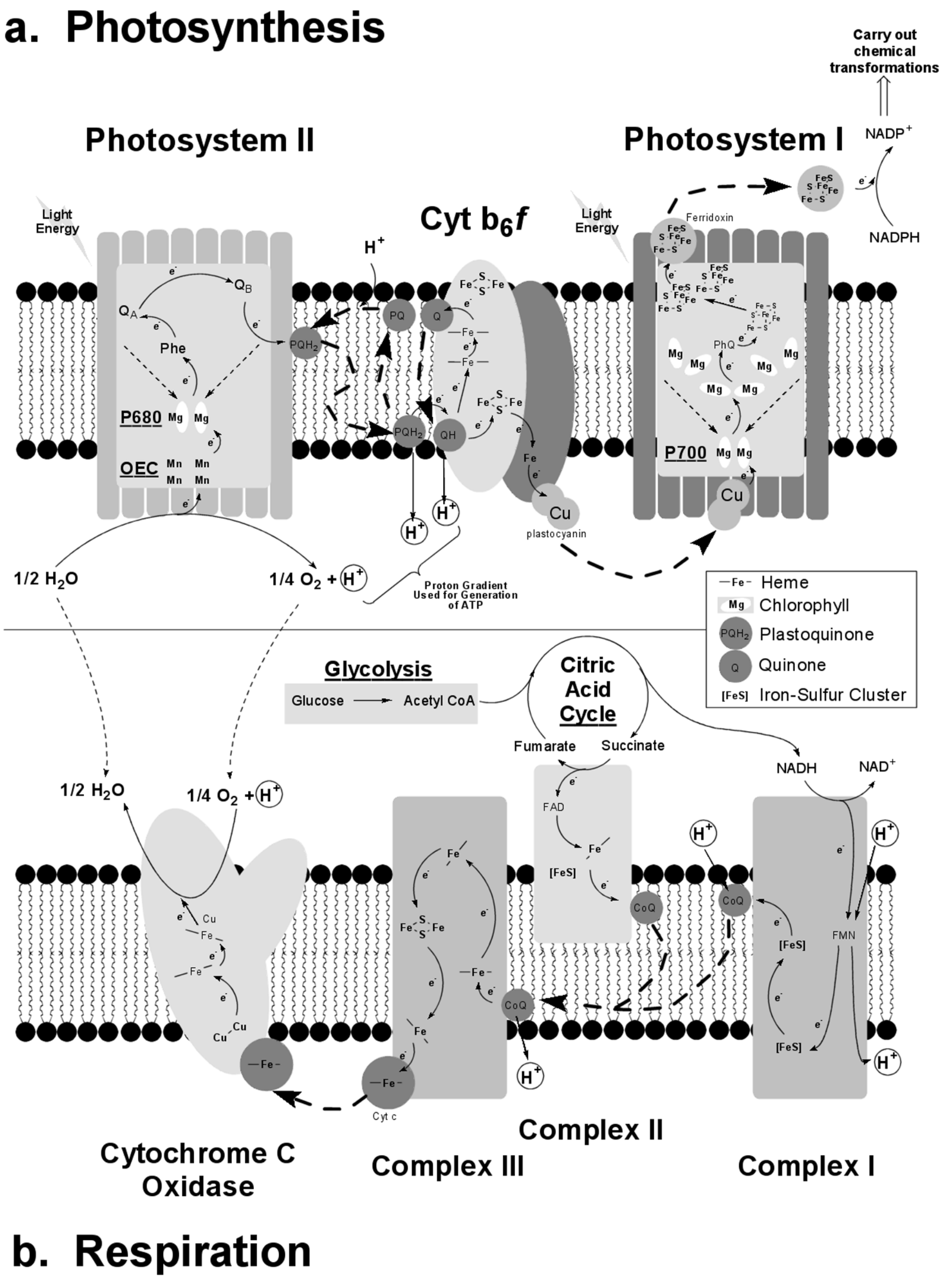

FIGURE 7 Schematic of (a) spinach photosynthesis and (b) aerobic respiration emphasizing the chemical transformations and inorganic cofactors involved.

an Fe–S cluster and transfers the electrons to cytochrome c. Cytochrome c transfers the electrons to cytochrome c oxidase. Here, the electrons are transferred to oxygen, reducing it to water (discussed below).

Complexes I–IV lie within the inner mitochondrial membrane. The proteins of each complex have structures that force the electron transfer pathway to oscillate from the mitochondrial matrix to the intermembrane space. Electron transfer from the matrix to the inner membrane space is coupled to proton transfer across the membrane. However, the return oscillation is not, resulting in a proton gradient. The energy stored in this gradient is used in ATP synthesis to phosphorylate ADP to form ATP, the transporter of energy in a cell.

Enzymes that catalyze the reduction of oxygen to water are called oxidases:

TABLE II Enzymes with Inorganic Cofactors Involved in Glycolysis and the Citric Acid Cycle

Enzyme	Reaction catalyzed	Inorganic cofactor
Glycolysis		
Hexokinase	Glucose ⇛ glucose-6-phosphate	Mg^{2+}•ATP
Phosphofructokinase	Fructose-6-phosphate ⇛ fructose-1,6-bisphosphate	Mg^{2+}•ATP
Phosphoglycerate kinase	1,3-Bisphosphoglycerate ⇛ 3-phosphoglycerate	Mg^{2+}•ADP
Enolase	2-Phosphoglycerate ⇛ phosphoenol pyruvate	Mg^{2+}
Pyruvate kinase	Phosphoenol pyruvate ⇛ pyruvate	Mg^{2+}, K^{2+}
Citric acid cycle		
Aconitase	Citrate ⇛ isocitrate	Fe_4S_4 cluster
Isocitrate dehydrogenase	Isocitrate ⇛ α-ketoglutarate	Mn^{2+} or Mg^{2+}
Succinyl-CoA synthetase	Succinyl-CoA ⇛ succinate	Mn^{2+} or Mg^{2+}
Succinate dehydrogenase	Succinate ⇛ fumarate	Fe_2S_2, Fe_4S_4

$$O_2 + 4H^+ + 4e^- \longrightarrow 2H_2O. \qquad (6)$$

Cytochrome c oxidase, an enzyme that catalyzes this reaction, is located on the membrane of mitochondria. The energy gained from breaking the O═O bond is used in creating a proton gradient across the mitochondrial membrane. This gradient is then used to generate adenine triphosphate (ATP), which is a universal energy transporter in biological systems. Cytochrome c oxidase contains four different metal centers: two hemes (heme a and heme a_3) and two copper sites (Cu_A and Cu_B). The Cu_A site and heme a help to transfer electrons from the electron transport chain to the heme a_3–Cu_B site, where O_2 is reduced to water. Cu_A lies closest to the mitochondrial side of the protein and is responsible for shuttling electrons, one at a time, from cytochrome c to heme a. Cu_A is a dinuclear copper site with the coppers separated by 2.7 Å and bridged by two cysteine sulfurs. Electrons transferred through this site seem to be shared by both copper atoms, which cycle between Cu^{+1}/Cu^{+1} and $Cu^{+1.5}/Cu^{+1.5}$ oxidation states. Heme a, located near the heme a_3–Cu_B site, is ligated by two histidines and is responsible for transferring the electron from the Cu_A site to heme a_3. The heme a_3–Cu_B site is located in the center of the membrane-bound enzyme midway between the inner mitochondrial matrix and cytosol. The heme is bound by a single histidine leaving one site open for dioxygen binding. Interestingly, the copper site, bound by only three histidines, is located only 4.5 Å from the iron site. The iron and copper are in the +2 and +1 oxidation states, respectively, before oxygen is bound. When oxygen is bound, it is quickly reduced by two electrons and protonated by a nearby base to produce an Fe(III)–peroxide/Cu(II) site. Two electrons are shuttled through Cu_A and heme a, further reducing the peroxide to two molecules of water. The resulting Fe(III)/Cu(II) center is reduced by two more electrons from the electron transport chain, regenerating the original Fe(II)/Cu(I) site.

Cyanide poisoning occurs when cyanide, CN^-, irreversibly binds heme a_3 in cytochrome c oxidase and blocks oxygen binding. This binding removes the driving force for the electron transfer pathway from the citric acid cycle to cytochrome oxidase and disrupts the generation of a proton gradient from this transport. Without the proton gradient, ATP synthesis is stopped and energy cannot be transported to the rest of the cell, resulting in cell death and, if the poisoning is severe, death of the organism.

E. Reversible Oxygen Binding

All animals and most microorganisms need oxygen to survive. As mentioned in the previous section, the tremendous amount of energy obtained by breaking the O═O bond is utilized to power the mechanics of the body. However, oxygen is also the origin of one of the most detrimental toxins, hydroxyl radical. As a result, oxygen must be tightly controlled throughout its stay within a multicellular organism. Thus, proteins that transport oxygen from one place to another in an organism are essential. In vertebrates and many invertebrates, this protein is hemoglobin. Three other proteins that reversibly bind oxygen are known: myoglobin, hemocyanin, and hemerythrin, found in muscle tissue, arthropods and mollusks, and marine invertebrates, respectively. Three of these enzymes—hemoglobin, hemocyanin, and hemerythrin—are responsible for oxygen transport; myoglobin is responsible for the storage of oxygen in muscle tissue. The metal centers of these four proteins are shown in Fig. 8 and will be discussed below.

Iron(II) ion and protoporphyrin IX form the heme in hemoglobin and myoglobin. Hemoglobin is four times

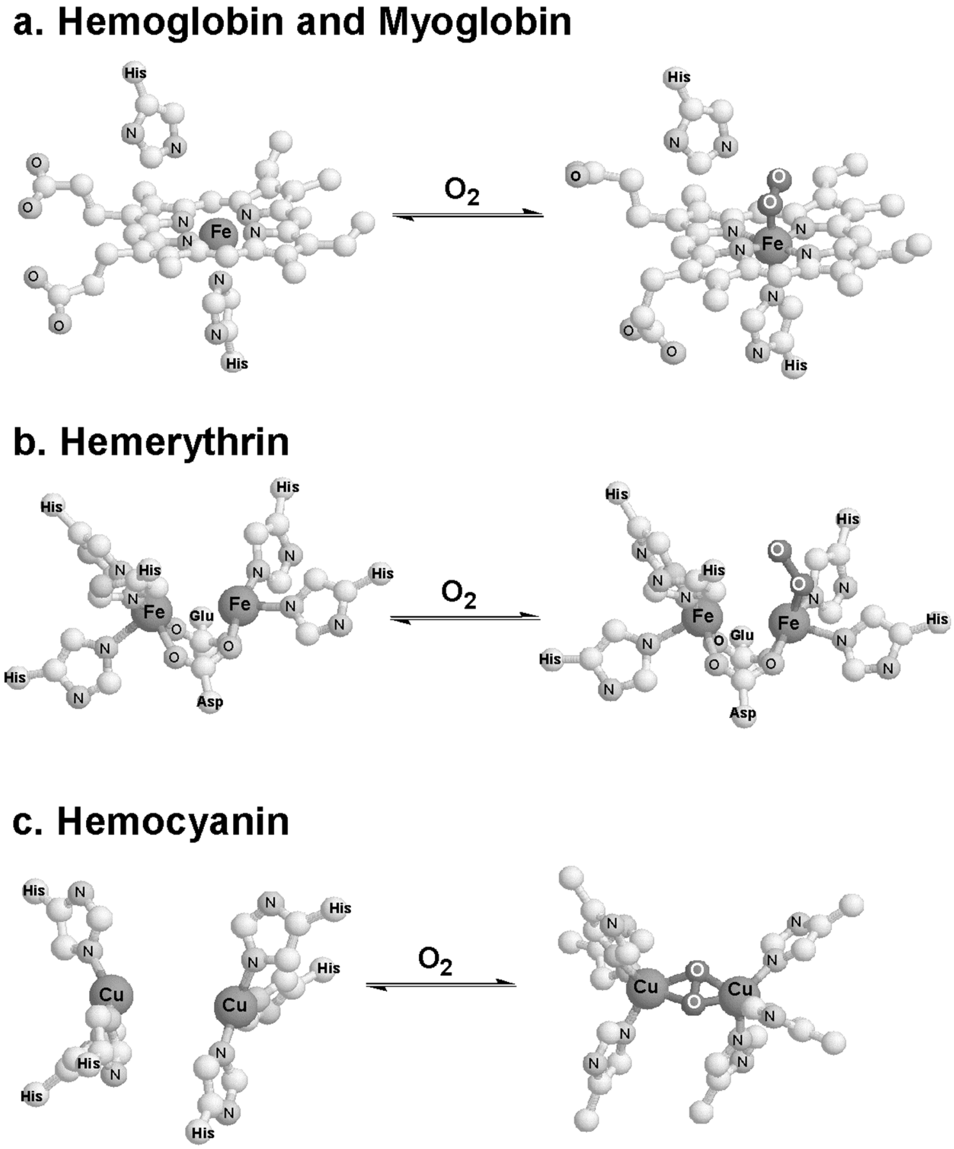

FIGURE 8 Inorganic centers for reversible O_2 binding: (a) hemoglobin and myoglobin, (b) hemerythrin, and (c) hemocyanin.

as large as myoglobin and contains four of these heme groups, whereas myoglobin only contains one. This heme group in both myoglobin and hemoglobin is attached to the protein through a distal histidine–iron bond. The Fe(II) atom protrudes out of the heme plane toward this histidine. Dioxygen binds to the proximal face through one of its atoms, forming a bent Fe—O—O bond (>115°). This bent structure is stabilized by an unligated histidine on the proximal heme face, which forms a hydrogen bond to the oxygen atom that is not bound to the iron. When dioxygen binds, there is evidence that it is reduced by the iron atom forming an Fe(III)–superoxide complex. These changes to the iron cause the metal to move within the heme plane inducing a structural change in hemoglobin that results in increased binding affinity for the other three heme groups. This cooperative binding mechanism enables hemoglobin to obtain oxygen in the lungs, where there is a high concentration of oxygen, and deliver it to areas of the body with lower concentrations of oxygen. In carbon monoxide (CO) poisoning, CO binds to the heme of hemoglobin more strongly than dioxygen. In doing so, CO blocks the transport of oxygen to cells. This mechanism of CO toxicity is less dangerous than the cyanide poisoning described above for cytochrome oxidase.

Hemerythrin is an iron dimer containing eight subunits and is about twice as large as hemoglobin. Each iron is

coordinated to two carboxylate groups of the protein and one hydroxide that are shared between the two irons. One of the irons is six coordinate, filling out its coordination sphere with three histidines. The other iron is five coordinate, with two histidine ligands and one open coordination site. When oxygen binds, it coordinates through this open coordination site. As with hemoglobin and myoglobin, the oxygen is reduced. However, in this case it is reduced by two electrons to form peroxide. The Fe—O—O bond is bent and the structure is stabilized by a hydrogen bond from the unbound oxygen atom to the bridging hydroxyl proton. As with the case of hemoglobin, the change in iron oxidation state may result in a cooperative binding mechanism enabling oxygen to be bound in areas of high oxygen concentration and released in areas of low oxygen concentration.

Hemocyanin is different than hemoglobin, myoglobin, and hemerythrin in that it is a copper enzyme. In fact, it contains two copper atoms both trigonally ligated to three histidine ligands. In the deoxy form, the oxidation state of both of these coppers is one. Oxygen binds hemocyanin symmetrically, with each oxygen atom bound to both coppers. Like hemerythrin, both metals are oxidized, in this case to Cu(II), and the dioxygen is reduced by two electrons to form peroxide. Hemocyanin is the largest of the four oxygen transport proteins; it contains many subunits each outweighing hemoglobin. This complexity probably plays a role in cooperative oxygen binding similar to that of hemoglobin.

F. Protection from Oxidative Stress

Oxygen when it is used as an energy source in biological systems is ultimately reduced to water and excreted. While respiration is extremely efficient, it is not infallible, and occasionally reduced forms of dioxygen are released in cells. This usually occurs via release of superoxide from hemoglobin or as a result of reductants that accumulate after cells have been starved for oxygen for some time (such as after a stroke or heart attack).

Either directly or indirectly, the intermediates of dioxygen reduction—superoxide, hydrogen peroxide, and hydroxyl radical—can be toxic. Two classes of enzymes, the superoxide dismutases (SODs) and the catalases, work in tandem to eliminate superoxide and hydrogen peroxide. SODs catalyze the dismutation of superoxide to oxygen and hydrogen peroxide. Catalases then convert hydrogen peroxide to oxygen and water:

$$\underset{}{O_2} \xrightarrow{e^-} \underset{\text{Oxygen superoxide}}{O_2^-} \xrightarrow{2H^+,e^-} \underset{\text{Hydrogen peroxide}}{H_2O_2} \xrightarrow{H^+,e^-} H_2O + \underset{\text{Hydroxyl redical}}{HO} \xrightarrow{H^+,e^-} \underset{\text{Water}}{2H_2O}$$

There is no enzymatic system to eliminate hydroxyl radical because it reacts so quickly that no enzyme could remove it fast enough to reduce its toxicity. Another very short lived but highly damaging molecule is peroxynitrite ($ONOO^-$), which forms by direct reaction of superoxide with nitric oxide. Because enzymatic intervention is essentially futile with $OH^\bullet$ and $ONOO^-$, cells depend on SODs and catalases to prevent the formation of precursors to these toxic molecules.

There are two major types of SODs, those containing a copper–zinc (Cu/Zn) center in their active site and those containing either iron or manganese. In the Cu/Zn SODs (Fig. 9), the Cu and Zn atoms are connected through an imidazole ring from a histidine. During catalysis, the Cu binds superoxide and cycles between the +1 and +2 oxidation states. Conversion of superoxide to oxygen occurs when the Cu is reduced from +2 to +1, and conversion of superoxide to hydrogen peroxide occurs when Cu is oxidized from +1 to +2. Zinc is present to ensure that the copper has the correct electronic properties to carry out these transformations. A series of mutations in the Cu/Zn SODs has been implicated as the cause of the familial form of amylotropic lateral schelorosis (fALS) known as Lou Gehrig's disease. Manganese (human mitochondria) and iron (bacteria) SODs do not contain a second metal. These SODs carry out the same reaction by cycling between the +2 and +3 oxidation states.

As with the SODs, there are two major types of catalases: one contains a heme group in the active site and

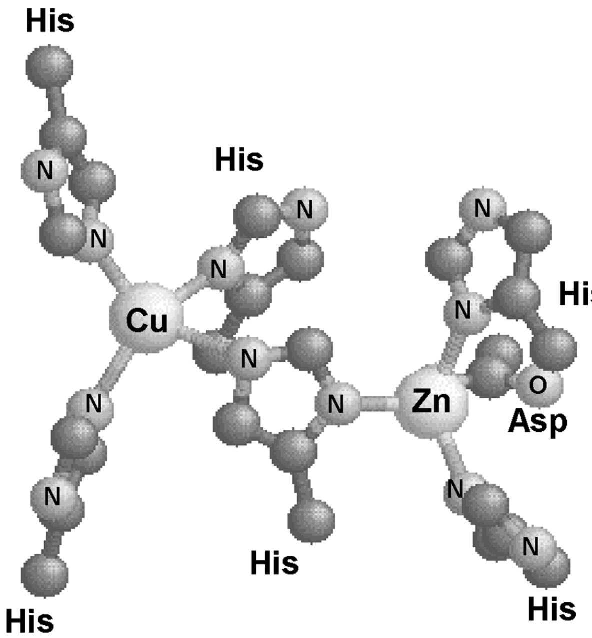

FIGURE 9 Metal center of Cu/Zn superoxide dismutase.

the other contains two manganese atoms. The heme-containing catalases have a tyrosine bound to the iron in the heme. In the reduced state, the iron is in the +3 oxidation state. During the reduction of peroxide to water, the porphyrin and iron are each oxidized by one electron forming a (porphyrin$^+$)Fe(IV)=O. This species, known as Compound I, can oxidize a second hydrogen peroxide to oxygen, completing the catalytic cycle. The manganese catalases, which are far less common than their heme counterparts, contain a manganese dimer where both manganese atoms cycle between +2 and +3 oxidation states during catalysis.

G. Chemical Transformation

In the section on respiration above, it was shown how oxygen reduction to water is used as the engine to produce ATP. Oxygen is also used in the body as a substrate to carry out chemical transformations. Oxygenases are enzymes that activate oxygen for insertion into organic molecules. One class of oxygenases are the cytochromes P450 (cyts P450). Cyts P450 catalyze the NADH (or NADPH) assisted oxidation of organic molecules:

$$O_2 + \text{R–H} + \text{NAD(P)H} \longrightarrow \text{R–OH} + H_2O + \text{NAD(P)}^+. \quad (7)$$

A heme group, porFe^{II}, is attached to the protein through a single iron–cysteine interaction leaving an open coordination site on the iron to bind oxygen. During catalysis, the substrate, R—H, is bound in the active site close to the iron heme. The iron then binds oxygen and reduces it with help from NADH or NADPH. During this reduction, one molecule of water is released and an iron oxo complex (porFe^{V}O or por$^+$Fe^{IV}O) is formed. This iron oxo species is reduced upon reaction with the substrate to produce ROH and porFe^{III}. The iron can be reduced by a $\frac{1}{2}$ NAD(P)H to return to its initial state, porFe^{II}. Using a heme group, cyts P450 are involved in drug, hormone, and cell wall metabolism and other biosynthetic reactions.

The mode of action of azole antifungal agents is binding to cytP450 to block the conversion of ergosterol to lanosterol. The depletion of lanosterol causes severe cell membrane disruption in the fungi. The cyts P450 are also essential for the metabolism of many common drugs such as theophyllen, erythromycin, warfarin, and verapamil. Many isozymes, for example, cyt P450 3A/4, are found in the human liver; however, several of these are known to metabolize, be inhibited by, or be induced by multiple common pharmaceuticals. Hence, evaluation of drug interactions with cytP450 is an important issue in modern pharmaceutical therapies.

Another medically important enzyme, nitric oxide synthase (NOS), has many similarities to cyts P450 and catalyzes the formation of nitric oxide. Nitric oxide is a messenger involved in vasodilation and inflammatory response. The production of nitric oxide is a result of the degradation of the amino acid arginine. Like cytochrome P450, the active center is a heme and the reaction is NAD(P)H dependent. Unlike cytochrome P450s, the current view on the mechanism of NO production does not involve por$^+$Fe^{IV}=O. Instead, the reactive species is believed to be porFe^{III}—OO$^-$. NOS is mediated by Ca^{2+}–calmodulin and does not produce nitric oxide in the absence of calcium.

H. Nitrogen Fixation

Nitrogen fixation is the most important reaction of the biological nitrogen cycle. The presence of nitrogen in molecules other than N_2 is frequently the limiting plant growth requirement. The six-electron reduction of the N≡N bond to form ammonia is ultimately favorable and gives off a significant amount of energy:

$$N_2 + 6H^+ + 6e^- \longrightarrow 2NH_3. \quad (8)$$

However, in the Born–Haber process, the commercial production of ammonia, the formation of the partially reduced intermediates requires high temperature and pressure. Remarkably, by acquiring energy from ATP hydrolysis and coupling the reaction with hydrogen (H_2) formation,

$$N_2 + 16H_2O + 16\text{ATP} + 8e^- \longrightarrow 2NH_3 + H_2 + 16\text{ADP} + 16P_i + 8H^+, \quad (9)$$

microbes are able to convert N_2 to NH_3 at room temperature and pressure. In this way, nature has been able to stabilize the necessary intermediates to carry out the requisite chemistry. The enzyme nitrogenase reduces nitrogen by employing two separate proteins. One of the proteins, the FeMo protein, contains two large cofactors (FeMoCo containing seven irons, nine sulfurs, one molybdenum, and homocitrate, and P clusters with eight iron atoms and seven sulfurs). The other, smaller protein contains an iron–sulfur cluster and is termed the Fe protein. Although both enzymes need to be present for catalysis, the location of nitrogen reduction is the FeMoCo site in the FeMo protein. Electrons are transferred to the FeMo protein by the Fe protein. The process is driven by ATP hydrolysis. The molecular mechanism by which this occurs is under investigation.

I. Nucleotide Metabolism

The reduction of ribonucleic acids (RNAs) to form deoxyribonucleic acids (DNAs) is the first committed step in the biosynthesis of DNA:

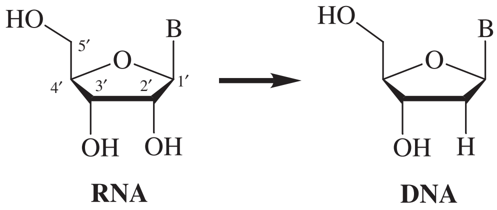

The process involves the removal of a single oxygen atom from the ribose ring. The mechanism by which this occurs is initiated by the removal of a hydrogen atom from the 3′ position of the ring. This mechanism requires the formation of a radical (an unpaired electron) in the interior of a protein. Radicals are very unstable and require care in their formation. The enzymes that carry out this reaction are the ribonucleotide reductases (RRs). There are three classes of RRs. There are two components to the structure of RRs in all three classes. The first component is a metal-containing unit responsible for the generation of radicals. The second is responsible for substrate binding and catalyzing the reaction.

Type I RRs are found in all eukaryotes and in some prokaryotes and require oxygen. Their radical-generating component consists of a di-iron center and a tyrosine. The di-iron center is similar but not identical to that found in hemerythrin. In the resting state, the two irons are both Fe(II). One of the irons is coordinated to a histidine, an aspartate, and a water molecule. A glutamate and oxo bridge both iron atoms. The remaining ligands around the second iron are a histidine and two glutamates. In the presence of oxygen, the di-iron center is oxidized to an Fe(III)–Fe(III) center and a tyrosine radical is generated. This tyrosine can oxidize a cysteine near the substrate. The resulting thiyl radical is directly responsible for the abstraction of a hydrogen atom from the 3′ position of the ribose ring that ultimately leads to the formation of DNA.

The remaining two types of RRs are less well understood than the Type I reductases. Type II RRs require an adenosylcobalamine cofactor (R is adenosyl in Fig. 5), coenzyme B_{12}, for catalysis. They are found in both aerobic and anaerobic bacteria and archae. In an analogous way to the Type I class, a radical is generated on the adenosyl moiety on the cofactor that is used to oxidize a cysteine residue close to the 3′ position on the ribose ring. Type III RRs are found in strictly anaerobic microorganisms. They contain an iron–sulfur cluster. This iron–sulfur cluster along with adenosylmethionine aid in forming a glycine radical that is presumably used to oxidize a cysteine closer to the substrate in much the same way as Type I and II enzymes.

Because RNA is a precursor in the formation of DNA, RRs seemingly are a prerequisite of DNA evolution. On early earth, oxygen was sparse. Therefore, aerobic reductases are not good candidates for this role. An understanding of how Type III reductases work will lead to an understanding of how DNA evolved.

III. BIOMINERALIZATION

A. Overview

Biomineralization is the most glaring example of the misnomer of "bioinorganic" chemistry. It encompasses the formation of largely inorganic minerals by the processes of life. Examples of biomineralization are the formation of calcium phosphate to create bones for structure, calcium carbonate as protective shells, iron oxide to store iron in animal cells, and the formation of magnetite as orientational materials in magnetobacterial cells (Table III). All of these examples demonstrate the precise control of mineral size, structure, shape, orientation, and organization that chemists strive for in the development of novel methods for material syntheses.

B. Four Steps to Biominerals

Organisms generally produce biominerals following a basic four-step process. This process includes supramolecular preorganization, interfacial molecular recognition, vectorial regulation, and cellular processing.

1. Supramolecular preorganization requires the construction of an organized reaction environment prior to the actual mineralization event. In general this involves the self-assembly of lipid vesicles that provide an enclosed space for mineralization. Sometimes a protein construct is made for encapsulating the mineral. The latter is the case of ferritin, the iron storage protein in mammals. Several

TABLE III Examples of Biominerals

Mineral	Formula	Function
Calcium carbonate	$CaCO_3$	Algae exoskeletons, calcium storage in plants
Calcium phosphate	$Ca_{10}(PO_4)_6(OH)_2$	Endoskeletons, teeth, calcium storage
Calcium oxalate	CaC_2O_4	Calcium storage
Barite	$BaSO_4$	Gravity device
Silica	$SiO_2{\bullet}nH_2O$	Algae exoskeletons
Magnetite	Fe_3O_4	Magnetotaxis
Ferrihydrite	$5Fe_2O_3{\bullet}9H_2O$	Iron storage

ferritin subunits assemble to form a large, hollow, spherical ball where iron can be stored in the form of iron oxide.

2. Interfacial molecular recognition involves the controlled nucleation of inorganic structures from aqueous solution confined within the organic structure made in step 1. The general view of this step is that it occurs at functionalized surfaces within the structure. These surfaces serve to initiate and accelerate the growth of inorganic clusters by lowering the activation barrier in much in the same way that an enzyme accelerates a reaction.

3. Vectorial regulation is the assembly of the mineral phase through control of direction and size of crystal growth and termination. This regulation can be brought about by rigid formation of the mineralization structure mentioned in step 1. It also can be brought about by dynamic forces during the mineralization process.

4. Cellular processing is the large-scale cellular activity following the initial mineralization. This process can involve the proper positioning/placement of the mineral or assembly of several minerals to give the final higher ordered architecture with elaborate properties. As an example, caccolith scales are a result of the transport of individual calcite crystals across the cell membrane of marine algae and their extracellular assembly.

C. Ferritin

Perhaps the best-understood process of biomineralization is the storage of iron within ferritin. Mammalian ferritins consist of a protein shell made up of 24 individual peptide subunits (Fig. 10). The resulting structure is roughly a hollow sphere where iron can be stored as ferric oxide.

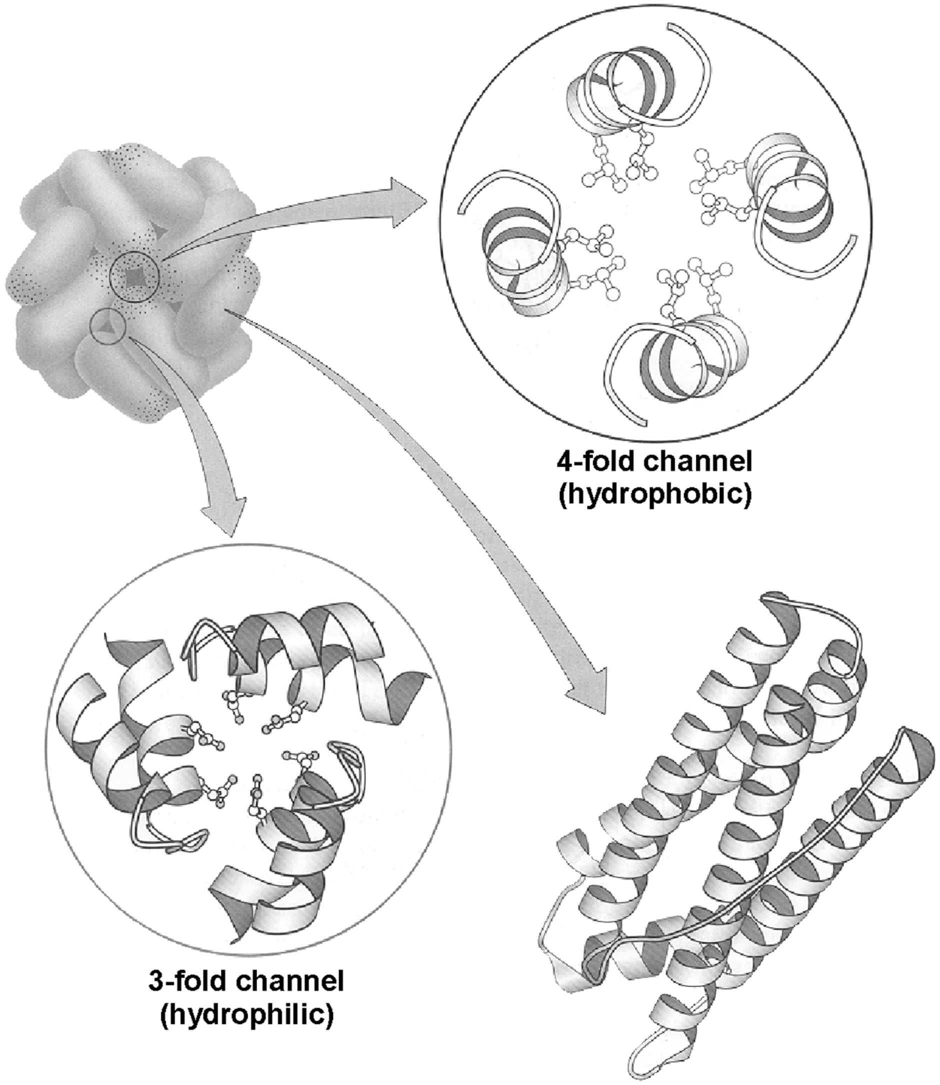

FIGURE 10 The iron storage protein ferritin, a subunit, and the fourfold and threefold channels. Reproduced by permission from Berg, J., and Lippard, S. J. (1994) "Principles of Bioinorganic Chemistry," University Science Books, Mill Valley, CA.

The inside "diameter" is 75 Å and can accommodate up to 4500 iron atoms. The mechanism by which this iron core is formed is under investigation. One interesting problem is the introduction of iron atoms into the interior of the ferritin. There are two channels that might serve as passageways for the iron: a fourfold and a threefold channel. Hydrophobic residues line the interior of the fourfold channel. This channel would serve as a poor entrance for charged ions such as Fe(II) or Fe(III). However, these hydrophobic interactions may play a significant role in the stabilization of the assembly, helping to satisfy step 1 in the formation of biominerals—formation of a supramolecular construct. The threefold channel is lined by several hydrophilic residues and is the more likely candidate for Fe passage. Recently, dimeric Fe(II)-binding sites in the protein shell have been investigated as possible sites of initial introduction of iron into ferritin. At these sites, Fe(II) is oxidized to Fe(III) by oxygen, forming an oxo- or hydroxo-bridged Fe(III) that migrates into the interior of ferritin for storage.

Once the iron is inside the sphere, a site of mineral nucleation is located—step 2 in the biomineralization process. Although the site(s) of nucleation are not known, the walls are lined with carboxylic acids from aspartate and glutamate residues. These are the probable sites of nucleation. After nucleation, the mineral begins to form. The shape is controlled by the protein shell. Studies of the resulting mineral are consistent with octahedrally coordinated iron(III) ions joined by bridging oxide and/or hydroxide ions. A mineral termed ferrihydrite has a similar postulated structure. Because ferritin is used for iron storage agents, the supramolecular structures described in step 4 of Section III.B are not formed.

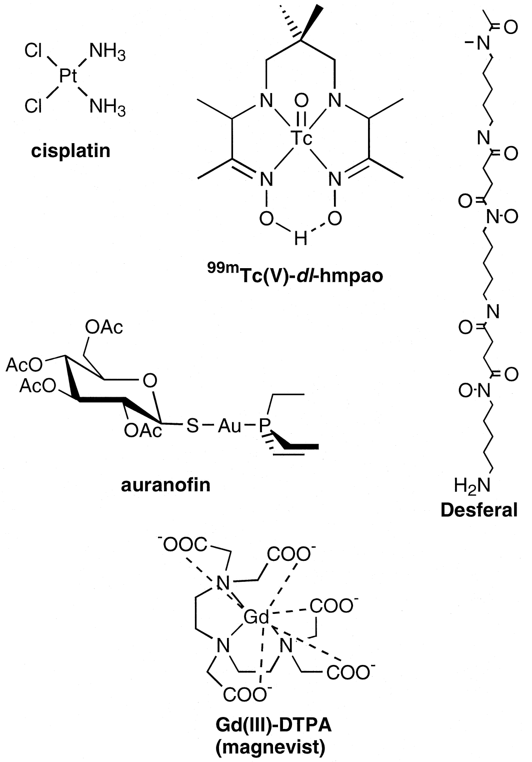

FIGURE 11 Examples of inorganic pharmaceuticals.

IV. MEDICAL USES FOR INORGANIC COMPOUNDS

A. Overview

Inorganic compounds have been used for centuries for their pharmacological properties. Recently, however, the understanding of how inorganic compounds interact with biological molecules has enabled chemists, biologists, and physicians to synthesize and test the medicinal qualities of these compounds in a more systematic way. The unique properties of inorganic compounds enable new mechanisms to be exploited in the treatment of many diseases.

Some of the unique properties being explored include the following: (1) physiologically relevant redox potentials for cancer drugs that cleave DNA and drugs that remove harmful oxygen radicals; (2) ligand exchange for many anticancer drugs, including cisplatin, one of the leading drugs for cancer treatment; (3) photophysical properties, for maladies ranging from psoriasis to cancer; (4) properties of new drugs to treat diabetes without using insulin; (5) radioactivity for use in imaging agents; and (6) paramagnetism for magnetic resonance imaging (MRI) agents. Examples of each of these properties is given below and in Fig. 11. Some of the complexes are already in clinical use, while others are in clinical trials.

In addition to the use of inorganic compounds to treat illnesses, treatments for genetic defects in inorganic ion metabolism and environmental exposure to toxic ions are also discussed. The majority of these disfunctions are treated with some sort of chelation therapy (for overexposure) or metal substitutes (for underexposure). These therapies are briefly discussed below.

B. Redox Chemistry in Medicine

The free radical superoxide, O_2^-, reacts with nitric oxide, NO, to produce damaging peroxinitrite, $OONO^-$. This process has been postulated to be a mediator of ischemia-reperfusion injury as well as inflammatory and vascular diseases. Superoxide dismutases (SODs), enzymes discussed previously, are responsible for converting superoxide to hydrogen peroxide and oxygen. SODs are

not used in therapy because these enzymes have a short retention time in the body and do not cross cell membranes efficiently. Therefore, bioinorganic chemists have designed small molecules that can destroy superoxide and are retained in the body and migrate into cells that are of pharmacological significance. There are a few manganese complexes that have been shown to scavenge superoxide, and research continues to develop effective superoxide dismutase mimics. In addition, a new class of manganese porphyrins are being developed to destroy peroxynitrite.

One family of antitumorigenic compounds used in practice are the bleomycins, natural products that contain iron isolated from *Streptomyces* cultures. Bleomycin sulfate is used in combination chemotherapy for treatment of head and neck cancer. The mechanism of action of bleomycin is believed to include the binding of oxygen to form O_2–Fe(II)–BLM. This complex can accept an electron to produce an active species, O_2^{2-}–Fe(III)–BLM, which can cleave DNA and RNA, ultimately killing the cancer cell.

C. Metal Complexation in Medicine

One mechanism of action for inorganic pharmaceuticals is the binding of the drug to a target biomolecule. A ligand already present on the metal must be lost in order to complex with the target. Inorganic compounds vary widely in both thermodynamic driving force for their binding to biomolecules and kinetic lability of the ligands present on them. This variability is useful in searching for drugs sufficiently stable to reach the targeted biomolecule, exchange ligands, and remain bound to the target until treatment is accomplished. The family of anticancer drugs is typified by cisplatin, a well-studied example of this mode of action.

Cisplatin is a neutral, square planar complex of platinum(II). The mode of action of cisplatin is dependent on the lability of its chloride ligands. When cisplatin crosses the cell membrane, the drug enters an environment that is depleted of chloride ions. This causes the compound to hydrolyze resulting in a charged complex that no longer can diffuse out of the cell. The positively charged drug is attracted to anionic DNA. At this point, bonds are made directly to the nucleobase guanine at the N7 site, the most electron-rich site in nucleic acids. The major cisplatin DNA adduct forms an intrastrand crosslink between adjacent guanines. The new complex is very stable and is unlikely to undergo further ligand exchange. This DNA–Pt(II) adduct cannot be repaired by the cell. The resultant change in DNA structure is thought to block replication through the modified region of the DNA. Whether this is the correct mechanism for drug activity is unknown. Recent studies suggest that these regions may be responsible for binding high-mobility-group (HMG) proteins and inactivating them, resulting in loss of function of the proteins and ultimately death of the platinated cell. Cisplatin and the second-generation drug carboplatin are used in combination chemotherapy for treatment of lung, colorectal, and ovarian cancers. Cisplatin is the most successful drug on the market for testicular cancer. It is not understood why cisplatin is so effective against testicular cancer while having little activity against tumors from many other organs.

Further study on platinum compounds focuses on using different ligands to direct the platinum to different cells in efforts to attack different types of cancers. Other metal complexes show favorable ligand exchange properties and are being evaluated for their anticancer properties. Titanocene dichloride, a titanium(II) compound, is in clinical trials for action against gastrointestinal and breast carcinomas. Compounds of ruthenium(III), known to bind to DNA is much the same way as platinum, are also good candidates for anticancer drugs.

D. Photophysical Properties

Many inorganic compounds show unique properties upon illumination. For example, some have very long excited states due to the flipping of spin of the excited electrons. To return to its preferred state, the electron spin must be flipped back to its original spin. Reaction with triplet oxygen to produce singlet oxygen is one mechanism by which this occurs. Singlet oxygen is cytotoxic, so if the metal complex can be targeted to a diseased area of the body, such as cancerous tissue, the complex can be illuminated and singlet oxygen will result, damaging and, it is hoped, destroying the disease. This mechanism is employed by tin(IV) and lutetium compounds that are presently in clinical trials. Porphyrins, when demetalated, can also be excellent photosensitizers. These molecules can be directly photoactivated or be utilized in conjunction with radiation therapy to increase the concentration of singlet oxygen in tumor cells.

E. Radiopharmaceuticals

Some inorganic isotopes such as ^{99m}Tc and ^{186}Re decay radioactively, giving off radiation (Table IV). This radiation can then be detected using positron emission tomography (PET) or single-photon emission tomography (SPECT). Because the distribution of these molecules in the body can be sensitively monitored, radiologists can use these metal complexes in applications ranging from blood flow monitoring to tumor detection. The ligands coordinating the isotope can be designed to direct the isotope for the desired function.

For example, monoclonal antibodies (mAbs) attached to isotopes can be directed toward cells that recognize the specific antibodies. In one complex, indium-111 is attached to murine mAb B72.3, which is directed to an antigen expressed by many adenocarcinomas. In this way, the indium-111 will be retained in the location of the

TABLE IV Pharmacologically Relevant Radionuclides

Radionuclide	Half-life	Energy (keV)
^{57}Co	271 days	836
^{67}Ga	78 hr	1001
^{99m}Tc	6 hr	140
^{111}In	67 hr	172,247
^{113m}In	104 min	392
^{123}I	13 hr	1,230
^{169}Yb	32 days	207
^{197}Hg	64 hr	159
^{201}Tl	72 hr	135,167

carcinoma. When emission occurs, the presence, size, shape, and location of the carcinoma can be determined. This system is used clinically for diagnosis of colorectal and ovarian cancer.

Among the many imaging agents used in practice are $^{99m}Tc^{V}$ (*dl*-hmpao), used in the evaluation of stroke, $[^{99m}Tc^{I}$ (sestamibi)$]^{+}$, used for myocardia perfusion imaging, and $[^{99m}Tc\text{-MAG3}]^{-}$, used for monitoring renal function. Many more, including more antibody-linked isotopes, are in clinical trials, making radiopharmaceuticals one of the most active and successful areas using inorganic ions in medicine.

F. MRI Contrast Agents

Magnetic resonance imaging (MRI) has become a standard tool for the diagnosis of disease and injury. The strength of MRI is its ability to provide cross-sectional, and in some cases dynamic cross-sectional, images of anatomical regions in any arbitrary plane in the body. The principal property observed in MRI is the magnetic moment of a nucleus, in particular, the hydrogen nuclei in water molecules. The nuclear magnetic moment tends to align in an external magnetic field provided by the MRI apparatus. By perturbing the nuclei with electromagnetic radiation, the return to the original state can then be measured. The speed at which the nuclei return to the original state is dependent on their environment. For example, the signal from nuclei in the blood stream will differ from that in fatty tissue. A series of these measurements results in an image.

Although the process described above yields usable images, the contrast in the image can be enhanced through the use of contrast agents. Contrast agents cause enhanced relaxation of the observed nucleus, leading to the enhancement in signal at the location of the agent. One mechanism employed by contrast agents is an oscillating magnetic field caused by unpaired electron spins to speed the relaxation of the observed nucleus. The inorganic ions Fe(III), Mn(II), and Gd(III) contain five, five, and seven unpaired electrons, respectively, and have been investigated as potential imaging agents. If the metal is bound by a ligand that targets a pathogen, this pathogen is detected using contrast-agent-enhanced MRI (Fig. 12). Several Gd(III)

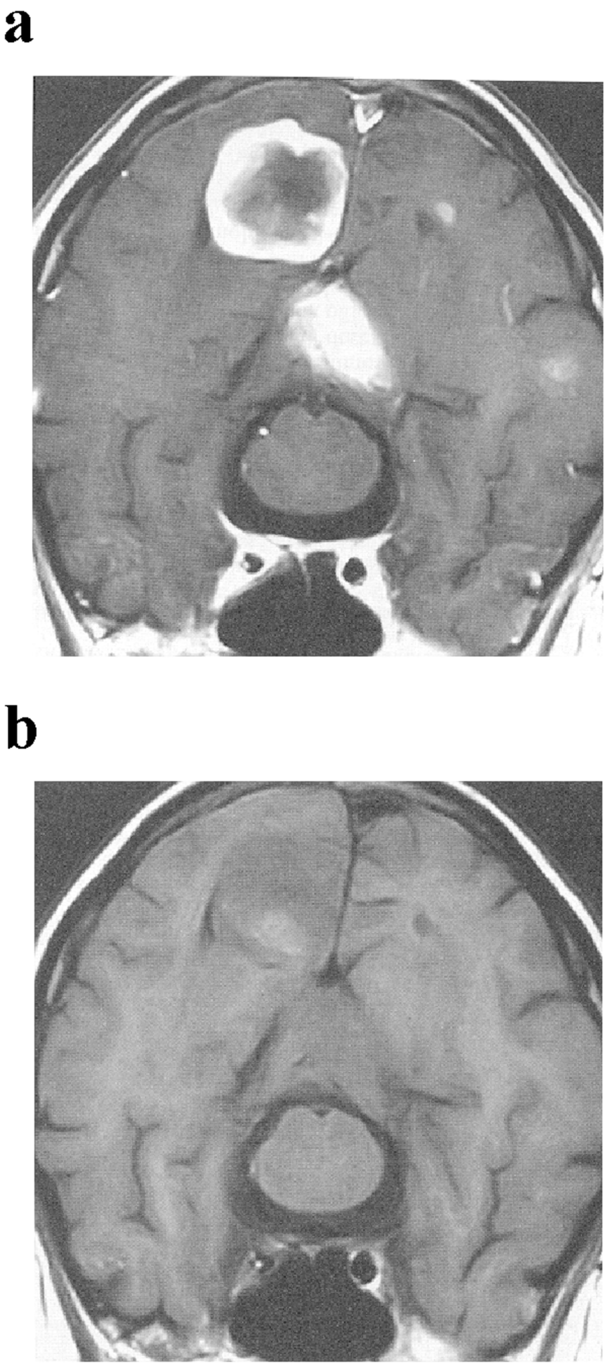

FIGURE 12 Magnetic resonance image (MRI) of the brain metastasis (a) with and (b) without using a contrast agent (Gd-BOPTA). Reproduced by permission from Stark, D. D., and Bradley, W. G., "Magnetic Resonance Imaging, 3rd Edition" Mosby, Inc., St. Louis, Missouri (1999).

agents have been approved for use as tumor imaging agents. Other compounds are being developed for uses as diverse as bowel markers, susceptibility agents for dynamic/functional MRI, blood flow agents, and lymphographic agents. The unique ability of inorganic ions to contain multiple unpaired spins means that MRI contrast agents are exclusively inorganic compounds.

G. Chelation Therapy

When the concentration of an inorganic ion is above the level where the body cannot return it to homeostasis through genetically controlled regulatory pathways, the ion is toxic. Therapy must be provided to a patient to decrease the toxicity of and ultimately remove the inorganic ion from the body. The most widely used method to remove ions from the body is chelation therapy.

Chelation therapy is characterized by addition of a molecule, a chelating agent, that binds to the metal of interest and removes it from the body. Most chelating agents are organic molecules containing multiple thiols, carboxylic acids, alcohols, hydroxamate, or amine groups capable of binding the metal. The effectiveness of a particular chelating agent is dependent on several factors including competing metals and ligands, dynamics of circulation, compartmentalization, and metabolism of the chelating agent. The ideal chelating agent would be one that has an extremely high binding constant and specificity toward the target ion. It would be nontoxic and orally administered. It would be able to diffuse as freely through the body as the target ion and be excreted from the body with high efficiency once it has bound the target ion. In reality, no chelating agents meet all these criteria and few come close.

The siderophore desferriferrioxamine b, Desferal®, is used to treat conditions of iron overload in patients suffering from the genetic blood disorder β-thalassemia major. The drug has a high affinity and specificity for Fe(III) and efficiently removes this ion from the body. The drug must be administered as a subcutaneous infusion as it is not orally active. Patients who do not comply with the rigorous regimen of administration succumb to the fatal effect of iron overload.

H. Inorganic Ion Deficiency

Because certain metal ions are essential for the function of many enzymes, it is imperative not only that they be present in the body, but also that they be transported properly into the necessary cells and to the necessary protein. A dysfunction in any of these mechanisms will be detrimental to an organism. Below are brief descriptions of metal uptake.

In considering ion presence in the body, inorganic chemists are concerned with the amount of a metal complex that is consumed, the types of complexes that are consumed, and the enzymes and processes involved with their transport into the blood stream. In cases of nutritional deficiency of zinc documented in Iran in the 1940s, patients displaying growth retardation, hypogonadism, severe anemia, hepatosplenomegaly, rough and dry skin, and mental lethargy were found to have diets of unleavened bread with negligible intake of animal protein. Geophagia, the practice of clay eating, was also prevalent in the areas of incidence. As a result of this poor diet, zinc was effectively lacking. The anemias were completely corrected by the administration of oral zinc or a combination of animal protein, which contains zinc, and iron sulfate.

Menkes disease is a fatal genetic disorder with a widespread defect in copper transport. Most patients, when untreated, die by 3 years of age. The basic biochemical defect in Menkes patients is an inability to absorb copper through the intestine; the inability to distribute copper to and within cells is also included in the mechanism of Menkes pathology. Treatment with copper histidine, $Cu(His)_2$, is the only available treatment for Menkes disease. Interestingly, no other copper salts have been found to work. The mechanism of efficacy of $Cu(His)_2$ is unclear. One hypothesis is the interplay between histidine and albumin in the transport of copper across membranes.

Another disease related to a dysfunction in copper metabolism is Wilson's disease. Unlike in Menkes' patients, copper in Wilson's patients is readily absorbed through the intestine and into the cell. Within the cell, however, abnormally low levels of the copper-storage protein ceruloplasmin are present. As a result, copper accumulates in the cytosol and is eventually released into the blood stream. The clinical manifestations of Wilson's disease are liver disease and neurological damage.

I. Other Drugs

Several other inorganic compounds that either do not fall into the above categories or whose mechanisms of action are largely unknown are also employed as pharmaceuticals. These include lithium drugs such as Li_2CO_3 for the treatment of manic–depressive disorder. The mechanism of lithium is not fully understood, although it must have an effect on the transmission of neuronal signals. Also included are gold drugs, such as aurofin, for the treatment of arthritis, for which the mode of action also is largely unknown. One theory suggests that the thiophilic nature of gold prevents the formation of disulfide bonds, which can lead to protein insolubility. Another example is bismuth subsalicylate, Pepto-Bismol®, for the treatment of upset stomach and prevention of ulcers. Its mechanism of

action has been linked to radical scavenging. Numerous other inorganic pharmaceuticals are in development. For instance, functionalized manganese porphyrins have been proposed as anti-inflammatory agents. Other manganese macrocycles have been proposed as possible treatments for heart attacks.

Inorganic elements are essential to living systems. They are present in bones and shells, and are a requirement in processes such as nitrogen fixation, photosynthesis, and respiration. In excess, however, most inorganic ions are toxic to biological systems. This polarity requires that most inorganic elements be tightly controlled by organisms while they are present. The knowledge gained by the study of these inorganic systems has led to the discovery and understanding of many pharmaceuticals. Research in the area of bioinorganic chemistry is directed to furthering this knowledge. Novel drugs, new drug targets, and unique methods of making minerals are among the expected outcomes of exploring new and established enzymes, mechanisms of detoxification, and systems that biologically control the synthesis of minerals. Furthermore, bioinorganic chemists are currently working on ways to use inorganic molecules as diagnostic tools to probe biological macromolecules such as DNA. Some scientists are exploring the fundamentals of metalloprotein structure to develop synthetic tools to create medically and industrially useful synthetic proteins. Still others are using the knowledge gained from the study of photosynthesis to explore methods of artificial photosynthesis to help alleviate the global energy crisis. These are a few examples of the current research in bioinorganic chemistry.

SEE ALSO THE FOLLOWING ARTICLES

Bioenergetics • Bioconjugate Chemistry • Biomineralization and Biomimetic Materials • Biopolymers • Electron Transfer Reactions • Environmental Toxins • Enzyme Mechanisms • Inorganic Exotic Molecules • Ion Transport Across Biological Membranes • Nitrogen Cycle, Biological • Nuclear Magnetic Resonance

BIBLIOGRAPHY

Berg, J., and Lippard, S. J. (1994). "Principles of Bioinorganic Chemistry," University Science Books, Mill Valley, CA.

Bertini, I., Gray, H. B., Lippard, S. J., and Valentine, J. S. (1994). "Bioinorganic Chemistry," University Science Books, Mill Valley, CA.

Holm, R. H., and Solomon, E. I. (eds.) (1996). "Special Issue: Bioinorganic Enzymology," *Chem. Rev.* **96**(7).

Mann, S., Webb, J., and Williams, R. J. P. (1989). "Biomineralization: Chemical and Biochemical Perspectives," VCH, New York.

Orvig, C., and Abrams, M. J. (eds.) (1999). "Special Issue: Medicinal Inorganic Chemistry," *Chem. Rev.* **99**(9).

Silver, S., and Walden, W. (1998). "Metal Ions in Gene Regulation," Chapman & Hall, New York.

Voet, D., and Voet, J. G. (1995). "Biochemistry," 2nd ed., Wiley, New York.

Boron Hydrides

Herbert Beall
Worcester Polytechnic Institute

Donald F. Gaines
University of Wisconin-Madison

I. The Boron Hydrides: Their Discovery and Formulas
II. The Structures of Boron Hydrides
III. Bonding Theories
IV. Isoelectronic Compounds: Boron Hydride Anions and Carboranes
V. Reactions of Boron Hydrides
VI. Reactions of Boron Hydride Anions
VII. Reactions of Carboranes
VIII. Metallocarboranes
IX. The Future? Neutron Capture Tumor Therapy

GLOSSARY

Boron hydride (borane) A neutral compound containing only the elements boron and hydrogen.

Boron hydride anion (borane anion) A negatively charged ion containing only the elements boron and hydrogen.

Bridge bond In boron hydrides, boron hydride anions, and their derivatives a three-center, two-electron bond in which a hydrogen atom links two boron or boron and another element located on the edge of the structure.

Carborane A compound containing at least one carbon atom in a framework position that would be occupied by a boron atom in a boron hydride.

Electron deficient compound A compound with insufficient valence electrons to bond all adjacent atoms by ordinary two-center, two-electron bonds.

Three-center bond A bond formed by the overlap of the atomic orbitals of three atoms. Two electrons placed in the bonding orbital resulting from this overlap will create a bonding situation.

THE TERMS BORON HYDRIDES and **boranes** are used synonymously for a family of chemical compounds containing only the elements boron and hydrogen. They do not occur in nature and must be synthesized in the laboratory. Only about 30 of these neutral boron hydride

compounds are known, but they react to form a great variety of other compounds and ions. In addition, the principles of bonding and structure of the boron hydrides, which are somewhat unusual, apply to related compounds in which one or more boron atoms have been replaced by atoms of different elements. The boron hydrides include gases, liquids, and relatively low-melting solids, all of which have symmetrical structures. They have unpleasant odors, are toxic and thermally unstable, and react with moisture and air. Many of the boron hydrides are pyrophoric (inflame spontaneously when exposed to air), and any mixture of these compounds with oxidizing agents has the potential of explosive conflagration.

We will begin this article by considering only the boron hydrides, their formulas, structures, and a sufficient description of the theory of their bonding to understand why these molecules adopt their unique geometries. We will then expand our discussion to closely related compounds that share the same bonding principles and have analogous molecular shapes. The reactions of the boron hydrides and their relatives will then be described in general terms. The formation of interesting metal derivatives will be treated in a separate section. We will also describe possible important applications of these boron compounds.

I. THE BORON HYDRIDES: THEIR DISCOVERY AND FORMULAS

Evidence for the existence of boron hydrides appeared late in the nineteenth century. However, means of handling compounds that are toxic and, especially, pyrophoric were not available, and so serious experimention was precluded. The first study giving actual chemical formulas was reported in 1912 by the German chemist, Alfred Stock. Stock had reacted magnesium metal with boron oxide to form the refractory substance, magnesium boride,

$$6Mg + B_2O_3 \rightarrow 3MgO + Mg_3B_2$$

He then treated the magnesium boride with hydrochloric acid to produce a mixture of volatile boron hydrides, which we will give the general formula B_xH_y.

$$Mg_3B_2 + HCl \rightarrow B_xH_y + 3MgCl_2$$

Handling these compounds required that he invent an apparatus called the *vacuum line* in which chemical operations are performed in a sealed glass system that is under a high vacuum. Subsequently, the vacuum line that Stock invented has been used for all manner of sensitive compounds and is a common and important piece of research laboratory apparatus.

Stock separated the above volatile boron hydride product mixture into pure substances and then determined the chemical formula and physical constants of each. These earliest known boron hyrides are listed in Table I. Note that at room temperature the first two compounds in this table are gases, the next three are liquids, and the last is a solid. New boron hydrides prepared since Stock's work range from B_6H_{12} to $B_{20}H_{26}$.

TABLE I Melting Points and Boiling Points of Stock's Boron Hydrides

Formula	mp (°C)	bp (°C)
B_2H_6	−165.5	−92.5
B_4H_{10}	−120	16
B_5H_9	−46.8	58.4
B_5H_{11}	−123.3	65
B_6H_{10}	−65.1	108
$B_{10}H_{14}$	99.5	ca. 231

The individual boron hydrides are named using a universally employed system. The number of boron atoms in the compound is given by the prefixes di-, tri-, tetra-, penta-, hexa-, etc., preceding the word "borane." The number of hydrogen atoms in the compound follows as an Arabic number in parentheses. Thus B_5H_{11} is called pentaborane(11), pronounced pentaborane eleven.

Most of the boron hydrides are difficult to work with because they are unstable, and their availability is limited. The two exceptions to this are pentaborane(9), B_5H_9, and decaborane(14), $B_{10}H_{14}$. Large quantities of B_5H_9 remain from a military jet fuel program in the 1950s (see Section V). This liquid boron hydride can inflame if exposed to air. However, provided air is excluded B_5H_9 is stable and a large number of its reactions have been explored and documented. The solid boron hydride $B_{10}H_{14}$ does not inflame in the presence of air, and its chemistry has been studied to great advantage both in the vacuum line and on the benchtop. Existing supplies of $B_{10}H_{14}$ are also largely the result of the 1950s jet fuel program.

II. THE STRUCTURES OF BORON HYDRIDES

The actual chemical structures of boron hydrides remained a mystery for decades. The obvious analogy of the formula of diborane(6), B_2H_6, to ethane and of tetraborane(10), B_4H_{10}, to butane tempted speculation that the structures were also analogous. In fact, electron diffraction studies appeared to bear this out for B_2H_6, which was incorrectly reported to have the ethane structure,

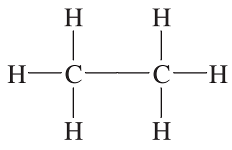

However, making the standard assumption that each bond drawn between two atoms results from the sharing of a pair of electrons, the number of valence electrons available for bonding in B_2H_6 is insufficient. Thus, the seven B—H and B—B bonds would require 7 electron pairs or 14 electrons, but the total number of valence electrons available is only 12, 3 from each boron atom and 1 from each hydrogen atom. Thus the ethane structure is unreasonable and is not observed. Because of the apparent shortage of valence electrons, boron hydrides are often referred to as "electron deficient" compounds.

The correct structure of B_2H_6 was determined by infrared spectroscopy, and this was the only boron hydride structure simple enough to be determined by this means. The actual B_2H_6 structure is

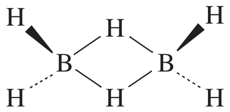

In this structure, the two boron atoms and the hydrogen atoms linking them are coplanar and in the plane of the paper. The other four hydrogen atoms are coplanar with the boron atoms in a plane perpendicular to the plane of the paper. The presence of hydrogen atoms linking or *bridging* boron atoms is a unique characteristic of boron hydride structures.

The structures of 7 of the boron hydrides are given in Fig. 1. In each of these structures boron atoms are shown as filled circles and the hydrogen atoms bonded to the boron atoms are shown as smaller open circles. The hydrogen atoms may be bonded to a single boron atom in which case they are called *terminal hydrogen atoms*, or they may bridge between two boron atoms in which case they are called *bridging hydrogen atoms*. Except for B_2H_6, the framework of the boron atoms in each structure can be described as two or more triangles sharing common edges. Thus the four boron atoms in B_4H_{10} are situated in two triangles sharing one common edge. In B_5H_9 the boron atoms are situated in four triangles each sharing common edges with two other triangles,

Note that Fig. 1 shows the three-dimensional nature of these structures, and that they are not planar.

In every structure shown in Fig. 1, each boron atom is attached by a single bond to a *terminal* hydrogen atom. Some boron atoms are attached to additional hydrogen atoms, either *terminal* or *bridging*, but all of the boron atoms bonded to the additional hydrogen atoms are around the edge of the boron framework. Thus for B_5 H_9, the boron atom at the top of the pyramid bears only a single terminal hydrogen atom whereas the four boron atoms around the base of the pyramidal structure bear both terminal and bridging hydrogen atoms. This observation combined with an electron-counting procedure called "Wade's rules" provides a connection between the shape of the boron framework of a boron hydride and its chemical formula.

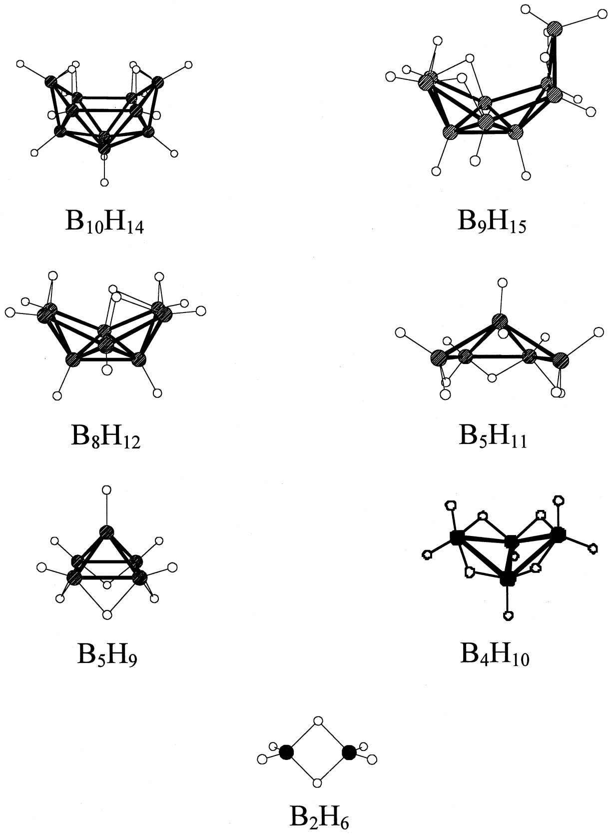

FIGURE 1 The structures of eight of the boron hydrides. Open circles represent boron atoms and filled circles represent hydrogen atoms. [From Shore, S. G. (1975). In "Boron Hydride Chemistry" (E. L. Muetterties, ed.), p. 85, Academic Press, New York, Figure 3.5.]

The application of Wade's rules requires that the ruling geometry of a boron hydride be considered to be a polyhedron having all triangular faces with a boron atom at each vertex. This polyhedron may have one or more of these vertices removed. (A polyhedron with all triangular faces is sometimes called a *deltahedron*.) In the case of B_5 H_9, the complete deltahedron would be an octahedron, and in the actual structure, one of the vertices has been removed to give a square pyramid (Fig. 2), a deltahedral fragment. The number of electrons necessary to hold the boron structure together can be calculated, and this number is always greater than the number of valence electrons provided by the boron atoms in the structure. One additional electron is provided by each of the hydrogen atoms

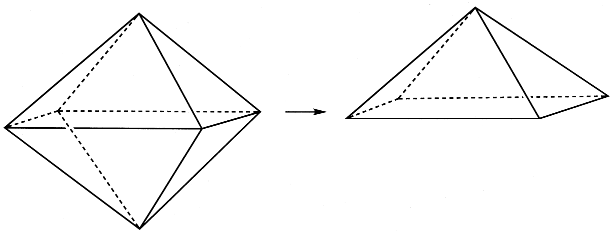

FIGURE 2 Removing a vertex from an octahedron produces a square pyramid.

TABLE III Formulas and Nomenclature for Boron Hydrides Described as Polyhedra with Vertices Removed

Missing vertices	Formula	Designation
0	$B_xH_x^{2-}$	*closo*
1	B_xH_{x+4}	*nido*
2	B_xH_{x+6}	*arachno*
3	B_xH_{x+8}	*hypho*

in the structure and by each negative charge if the species is a negative ion. The number of electrons needed for boron hydride deltahedra and deltahedral fragments of formula B_xH_y is given in Table II.

If no vertices are missing, there are no open edges, and each boron atom bears only a single terminal hydrogen atom. Thus there will be only x electrons from terminal hydrogen atoms for bonding the boron structure together and a charge of −2 will be necessary to provide the necessary electrons. This result means that the chemical formula of any species with a complete deltahedron of boron atoms will be $B_xH_x^{2-}$, and a neutral molecule containing only boron and hydrogen atoms in a closed deltahedron would violate Wade's rules.

If one vertex is missing there will be sufficient electrons for the boron framework if the chemical formula is B_xH_{x+4}, if two vertices are missing the formula will be B_xH_{x+6}, and if three are missing the formula will be B_xH_{x+8}. This information is summarized in Table III along with the designation used to describe each of the four situations.

As an example, these rules can be applied to boron hydrides derived from the pentagonal bipyramid (Fig. 3). With no boron atoms missing from the deltahedron there would be seven boron atoms and the formula would be $B_7H_7^{2-}$. If the boron atom depicted at the bottom of the pentagonal bipyramid is removed, the boron atom structure is a pentagonal pyramid, and the chemical formula would be B_6H_{10}. If one boron atom is removed from the base pentagon of this pentagonal pyramid, the formula would be B_5H_{11}. All of these species, $B_7H_7^{2-}$, B_6H_{10}, and B_5H_{11}, exist. However, the *hypho* species, B_4H_{12}, has never been observed.

TABLE II Calculated Numbers of Electrons Needed to be Supplied by Hydrogen Atoms or Negative Charges for Different Geometries of the Boron Atom Structure Described as Polyhedra with Vertices Removed

Number of missing vertices in boron hydride B_xH_y	Electrons needed from H atom and negative charges
0	$x+2$
1	$x+4$
2	$x+6$
3	$x+8$

III. BONDING THEORIES

The bonding in the boron hydrides is most simply exemplified in B_2H_6. As mentioned above, there are 12 valence electrons, 3 from each boron atom and 1 from each hydrogen, and this is insufficient to bond every pair of adjacent atoms with ordinary single bonds. Each boron atom is connected to two terminal hydrogen atoms and these four single bonds will each require two electrons leaving only four valence electrons to bond the two boron atoms to each other and to the two bridging hydrogen atoms. These four remaining electrons participate in two boron-hydrogen-boron bridge bonds.

Consider one of the boron-hydrogen-boron bridge bonds. As shown in Fig. 4, the bond results from orbital overlap of the spherical orbital on the hydrogen atom and a directed orbital from each of the two boron atoms. Since we are combining three atomic orbitals for the bridge, it is necessary that we form three molecular orbitals from them. The energy diagram for the atomic and molecular orbitals is given in Fig. 5, which shows a bonding molecular orbital at an energy lower than the atomic orbitals, and antibonding molecular orbital at a higher energy than the atomic orbitals, and a nonbonding molecular orbital at about the same energy as the atomic orbitals. A bonding situation occurs when two electrons occupy the lowest energy orbital, and the drop in potential energy can result in a stable molecule. Occupation of the nonbonding molecular

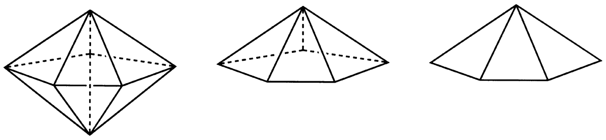

FIGURE 3 Removing vertices from the pentagonal bipyramid.

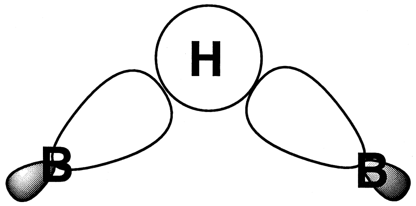

FIGURE 4 Orbital overlap in a boron-hydrogen-boron bridge in B_2H_6.

orbitals would not provide any significant stabilization, and occupation of the antibonding orbitals would produce an unstable situation with a higher potential energy than the unreacted elements.

The boron-hydrogen-boron bridge bond is a two-electron bond and is called a *three-center, two-electron bond* since it bonds three atoms together. Each boron atom is involved in two of these three-center bonds requiring a total of four electrons. The two boron atoms have three valence electrons each, but two of these are involved in bonds to the two terminal hydrogen atoms. Thus each boron atom has one electron remaining for the bridge region of the molecule, and each of the two bridging hydrogen atoms supplies one electron giving a total of four electrons in the bridging region, two for each boron-hydrogen-boron bridge.

The bonding and geometry of the B_2H_6 molecule is the result of the electrons and orbitals of the boron atoms. Each boron atom has three valence electrons but four valence orbitals. For each of these four orbitals to form an ordinary two-center bond, the boron atom would have to supply four valence electrons as is the case of carbon in ethane. Since the boron atom has only three valence electrons there is an "electron deficiency" of one. This will be true of every boron atom in a boron hydride structure. However, a three-center bond uses up three orbitals but only two electrons, and so each three-center bond can offset an electron deficiency of one. Thus in a neutral boron hydride, the use of valence electrons and valence orbitals is balanced if the number of three-center bonds equals the number of boron atoms in the chemical formula, and this result is general for the entire family of neutral compounds.

It is clear that B_2H_6 has two boron atoms and two three-center bonds. The next boron hydride, B_4H_{10}, has four boron-hydrogen-boron bridges to balance the four boron atoms. The situation becomes more complex when we look at the next hydride, B_5H_9. We have already observed that extra hydrogen atoms bridging between two boron atoms can only occur at the edge of the boron hydride molecule. The hydride B_5H_9 has only four borons around its edge and these can only accommodate four bridging hydrogens, one between each pair of adjacent borons. The remaining three-center bond that is necessary is contained within the boron atom framework.

Three boron atoms can form a three-center bond if they are arranged in a triangle, and each has a valence orbital pointing toward the center of the triangle (Fig. 6). These three orbitals can overlap to form a bonding, a nonbonding, and an antibonding orbital, and two electrons can occupy the bonding orbital resulting in a boron-boron-boron, three-center, two-electron bond. Since B_5H_9 requires five three-center bonds and four are boron-hydrogen bridges, we can expect one three-center bond to be in the boron framework. All boron hydrides larger than B_4H_{10} have three center bonds within the boron atom framework, and it is the prevalence of these triangular arrays of boron atoms that give these molecules their characteristic shapes.

Boron hydrides thus contain four different kinds of bonds: ordinary boron-hydrogen bonds, boron-hydrogen-boron three-center bridge bonds, ordinary boron-boron bonds, and boron-boron-boron three-center bonds. W. N. Lipscomb developed a method for determining what combinations of these structural features are possible for a specific boron hydride formula and what are the possible structures. This system is equivalent to the simple bonding rules in organic chemistry that make it possible to translate an empirical formula into possible organic structures.

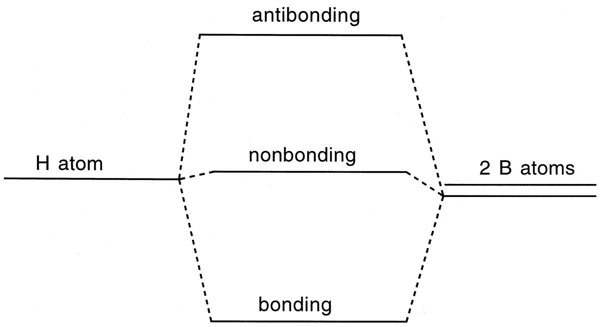

FIGURE 5 Energy levels for bonding, nonbonding, and antibonding orbitals in a boron-hydrogen-boron bridge.

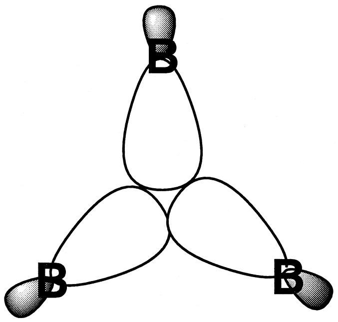

FIGURE 6 Overlap of atomic orbitals of three boron directed toward the center of a triangle and forming a three-center, two-electron, boron-boron-boron bond.

In Lipscomb's method a boron hydride is considered to have one terminal hydrogen atom on every boron atom plus a number of "extra" hydrogen atoms. These "extra" hydrogen atoms may be bridging hydrogens or they may be terminal hydrogen atoms on a boron atom in addition to the one terminal atom already assumed. The general formula for a boron hydride from this point of view is B_pH_{p+q}, where there are p boron atoms each with its terminal hydrogen and q "extra" hydrogen atoms. The variables for the four kinds of bonding features are given by the symbols, s, t, y, and x, where

s = number of three-center, boron-hydrogen-boron, bridge bonds
t = number of three-center boron-boron-boron bonds
y = number of two-center, boron-boron bonds
x = number of terminal hydrogen atoms in excess of one per boron atom

These variables can be related to the values of p and q for a specific boron hydride formula by three *equations of balance*:

1. The total number of three-center bonds $(s + t)$ equals the number of boron atoms p.

$$s + t = p$$

2. The total number of extra hydrogen atoms q equals the number of boron-hydrogen-boron, three-center bonds s plus the number of "extra" terminal hydrogen atoms x.

$$s + x = q$$

3. Considering each boron-terminal hydrogen group p to supply a pair of electrons for the other bonds in the structure, there are p pairs of electrons available. One pair is necessary for each boron-boron-boron, three-center bond t and for each boron-boron, two-center bond y. One electron (half a pair) is necessary for each boron-hydrogen-boron, bridge bond s and for each "extra" terminal hydrogen x beyond the one already assumed on each boron. (Only one electron is necessary for bonds involving hydrogen since the hydrogen atom itself brings in one electron.)

$$p = t + y + \frac{s}{2} + \frac{x}{2}$$

Now, since $q = s + x$, this equation can be simplified to

$$p = t + y + \frac{q}{2}$$

For a particular boron hydride formula B_pH_{p+q} there are four structural unknowns, s, t, y, and x but only three equations. Therefore, a unique solution is not generally possible and there will be a family of solutions for each formula.

For example, three *styx* solutions are possible for B_5H_9,

s	t	y	x
4	1	2	0
3	2	1	1
2	3	0	2

Solutions with negative values for s, t, or y are undefinable. A negative value of x would occur if there were fewer terminal hydrogen atoms than boron atoms, a situation observed in the unusual boron hydride $B_{20}H_{16}$.

A key to the different kinds of bonds in boron hydrides is given in Fig. 7. A structure for the 4, 1, 2, 0 *styx* solution showing the disposition of all the kinds of bonds is

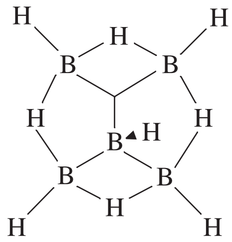

Normally, a number of different structures can be drawn for a specific boron hydride formula, and some selection is necessary. The most favored structures incorporate some symmetry and do not involve bond angles with excessive strain. Often, a number of equivalent but distinct structures that are satisfactory can be drawn for a particular boron hydride. In these cases the positions of the atoms are the same but the disposition of the electrons, that is, the details of the bonding, are different. For example, the structure of B_5H_9 given above can be oriented in four different directions.

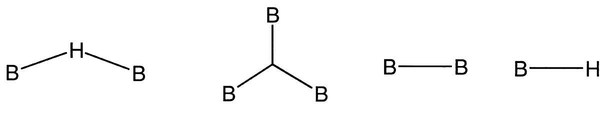

FIGURE 7 Bond types as drawn for boron hydride structures. (a) The bridging, boron-hydrogen-boron, three-center bond, (b) the boron-boron-boron, three-center bond, (c) the boron-boron, two-center bond, and (d) the terminal boron-hydrogen two-center bond.

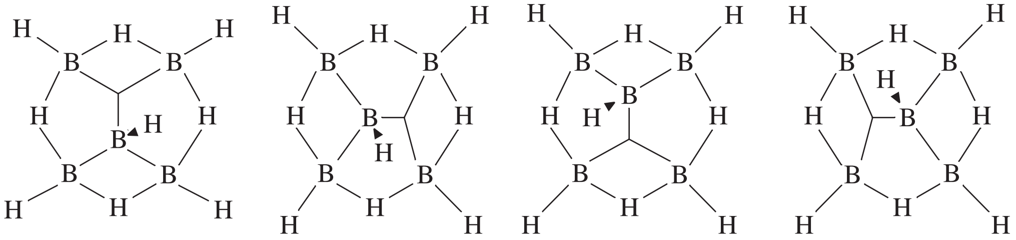

A combination or *resonance hybrid* of these four structures produces a more symmetrical molecule where all of the four borons around the base of the square pyramid are equivalent. This is in agreement with the known structure. As boron hydrides get larger or more symmetrical, the numbers of individual structures making up the hybrid get to the point where it is essentially unmanageable. For these molecules the molecular orbital theory, which constructs orbitals for bonding from the atomic orbitals of multiple atoms, is appropriate.

IV. ISOELECTRONIC COMPOUNDS: BORON HYDRIDE ANIONS AND CARBORANES

We will consider two important groups of compounds that share the same kinds of geometries as boron hydrides, that is, can be viewed as polyhedra or polyhedral fragments. These are the boron hydride anions and carboranes. In many cases the boron hydrides and compounds in these groups are isoelectronic (same number of valence electrons), and in these cases the structures are isostructural with almost the same geometric arrangement of atoms.

A. Boron Hydride Anions

Anions containing only boron and hydrogen are well known. The simplest of these is the borohydride or tetrahydroborate ion BH_4^-, which with its tetrahedral geometry is isoelectronic and isostructural with the methane molecule. The borohydride anion is a very well-known reducing agent in organic chemistry.

The are a number of boron hydride anions with more than one boron atom, and these follow the same bonding principles as the neutral boron hydrides discussed in previous sections. That is, their structures can again be viewed as polyhedra that may have one or more vertices removed. The numbers of the structural features, *s, t, y*, and x, will again depend on equations of balance, which need to be modified to account for the negative charge. For a boron hydride anion with the formula $B_pH_{p+q}^{-c}$ the equations will be

1. The total number of three-center bonds will equal the number of boron atoms minus the charge because each extra electron in the charge will lower the electron deficiency by one.

$$s + t = p - c$$

2. The hydrogen atom balance will be the same as for the neutral boron hydrides.

$$s + x = q$$

3. The electron balance now must include the electrons imparting the charge. Besides the p pairs of electrons from the B—H groups, each negative charge results in one-half a pair more of electrons that are available for the *s, t, y*, and x structural features.

$$p + \frac{c}{2} = t + y + \frac{q}{2}$$

The solution of these equations for the BH_4^- ion are $s = 0$, $t = 0$, $y = 0$, since none of these features is possible with a single boron atom, and $x = 3$. This is a structure with no three-center bonds or boron-boron two-center bonds and with three extra terminal hydrogen atoms on the single boron atom.

The known boron hydride anion with three boron atoms is $B_3H_8^-$, for which the *styx* solutions are 2013 and 1104. Reasonable structures can be built using either of these solutions. X-ray diffraction studies show that the correct structure, at least in the solid phase, is 2013.

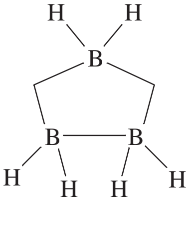

2013

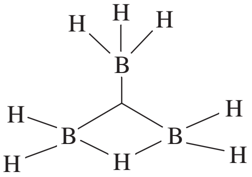

1104

1. Boron Hydride Anions and Wade's Rules

Larger boron hydride anions can be evaluated as polyhedral fragments just as can the neutral boron hydrides

mentioned previously. See Table II for the number of electrons needed for each level of structure, *closo, nido, arachno, and hypho*. Thus, for example, $B_6H_6^{2-}$ and $B_8H_8^{2-}$ are *closo* ions, $B_5H_8^-$, $B_{11}H_{14}^-$, and $B_{10}H_{13}^-$ are *nido* ions, $B_5H_9^{2-}$, $B_5H_{10}^-$, and $B_9H_{14}^-$ are *arachno* ions, and $B_5H_{11}^{2-}$, and $B_5H_{12}^-$ are *hypho* ions.

2. *Closo* Boron Hydride Anions

According to Wade's rules, *closo* boron hydride anions, that is, anions having the structure of a full polyhedron and thus the same number of boron atoms and hydrogen atoms, will have a charge of −2. This family has a number of members, but the most stable and the most studied are $B_{10}H_{10}^{2-}$ and $B_{12}H_{12}^{2-}$. The structures of these two anions are given in Fig. 8. The $B_{10}H_{10}^{2-}$ ion has the geometry of a cube with one side twisted 45° with respect to the opposite side and each of these opposite ends capped so that all faces of the figure are triangles. This is called a *bicapped square antiprism*. The $B_{12}H_{12}^{2-}$ ion has the highly symmetrical geometry of an icosahedron, the Platonic solid with 12 vertices, each indistinguishable from all the others. Likewise it has 20 identical faces and 30 identical edges. The high stability of these ions can be attributed to extensive delocalization of electrons resulting from the high symmetry and polyhedra that are sufficiently large so that bond angle strains on the boron atoms are minimal.

These anions can be prepared by relatively simple, high-yield reactions. The $B_{10}H_{10}^{2-}$ ion is prepared by closure of the neutral boron hydride $B_{10}H_{14}$ in the presence of a base:

$$2(C_2H_5)_3N + B_{10}H_{14} \longrightarrow [(C_2H_5)_3NH]_2B_{10}H_{10} + H_2$$

The proposed mode of closure of $B_{10}H_{14}$ to the $B_{10}H_{10}^{2-}$ ion is shown in Fig. 9.

The $B_{12}H_{12}^{2-}$ ion can be prepared by the reaction of sodium borohydride with $B_{10}H_{14}$:

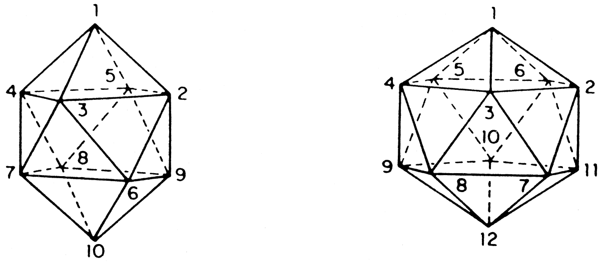

FIGURE 8 The structures and numbering conventions of the boron hydride anions, $B_{10}H_{10}^{2-}$ (left) and $B_{12}H_{12}^{2-}$. Each polyhedral vertex represents a boron atom to which is attached a terminal hydrogen atom directed radially outward. [From Middaugh, R. L. (1975). In "Boron Hydride Chemistry" (E. L. Muetterties, ed.), p. 275, Academic Press, New York, Figure 8.1.]

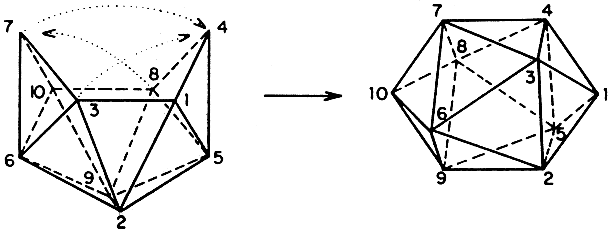

FIGURE 9 The proposed closure of $B_{10}H_{14}$ to the $B_{10}H_{10}^{2-}$ ion. [From Middaugh, R. L. (1975). In "Boron Hydride Chemistry" (E. L. Muetterties, ed.), p. 279, Academic Press, New York, Figure 8.2.]

$$2NaBH_4 + B_{10}H_{14} \longrightarrow Na_2B_{12}H_{12} + 5H_2$$

The reactions of these two ions will be discussed in Section V and have much in common with the reactions of aromatic organic compounds.

B. Carboranes

Since carbon has one more electron than boron, substitution of a boron and a single negative charge in a boron hydride anion with a carbon atom will formally lead to a compound with the same number of electrons and, presumably, a very similar structure to the original boron hydride anion. The new compound is referred to as a carborane, a compound containing only the elements boron, hydrogen, and carbon in which the carbon atom is in a vertex location in the polyhedral framework along with boron atoms. Wade's rules also apply to carboranes which can exist in *closo, nido*, and *arachno* forms. Each carbon atom provides and additional electron to help bond the framework. These carbon atoms are framework atoms and so the number of electrons needed to bond the cage for a *closo* structure is $n_B + n_C + 2$, where n_B is the number of boron atoms in the cage, and n_C is the number of carbon atoms in the cage. Likewise, $n_B + n_C +$ four electrons are necessary for the *nido* structure, etc. According to this counting procedure, $C_2B_3H_7$ has five cage atoms and nine electrons for bonding the cage, five from the five cage atoms, two resulting from the inclusion of two carbon atoms, and the two resulting from the two hydrogen atoms in excess of the five cage atoms. This gives us the $n_B + n_C + 4$ electrons necessary for the *nido* structure indicating that this carborane can be viewed as a deltahedron with one cage atom removed. By this same counting procedure, $C_2B_7H_{13}$ has an *arachno* structure. The structures of several *nido* and *arachno* carboranes are given in Fig. 10. Preparative reactions for *nido* and *arachno* carboranes tend to produce mixtures of products and relatively low yields. For example, B_4H_{10} in the gas phase will react with acetylene to produce at least

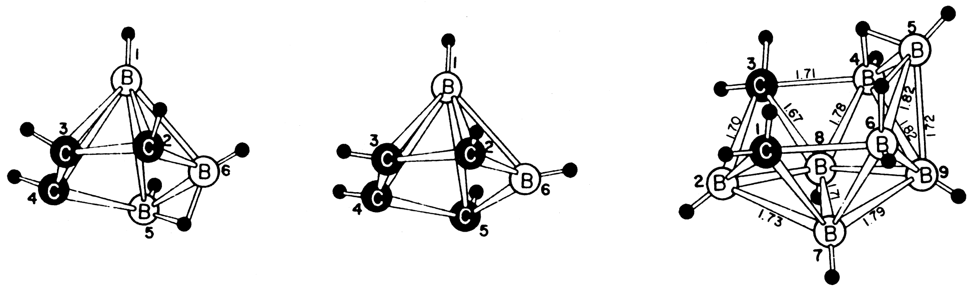

FIGURE 10 The structures of two *nido* (left) and one *arachno* carboranes. The small filled circles represent hydrogen atoms. [From Onak, T. (1975). In "Boron Hydride Chemistry" (E. L. Muetterties, ed.), p. 353, Academic Press, New York, Figures 10.3 and 10.4.]

nine *nido* and *arachno* carboranes and methyl substituted carboranes.

Closo carboranes can be formally constructed from *closo* boron hydride anions by exchanging two boron atoms and two negative charges for two carbon atoms. Thus, the two most important *closo* anions, $B_{10}H_{10}^{2-}$ and $B_{12}H_{12}^{2-}$, are isoelectronic and isostructural with $C_2B_8H_{10}$ and $C_2B_{10}H_{12}$, the former having the geometry of a very slightly distorted bicapped square antiprism and the latter having the geometry of a very slightly distorted icosahedron. The slight distortions in these compounds from the perfect symmetry of the boron hydride anions are the result of the differences in the lengths of bonds formed by boron compared to those formed by carbon.

Of all of the carboranes, by far the most studied are the icosahedral species, $C_2B_{10}H_{12}$. As seen in Fig. 11, three isomers exist. Their systematic names are 1,2-dicarba-*closo*-dodecaborane(12), 1,7-dicarba-*closo*-dodecaborane(12), and 1-12-dicarba-*closo*-dodecaborane(12), but they are generally known as *ortho*-carborane, *meta*-carborane, and *para*-carborane, respectively. They are very stable compounds with many known chemical reactions and derivatives. Their derivatives have been explored for the production of high-temperature resins and elastomers and have found utility for the stationary phases of gas-phase-chromatography columns.

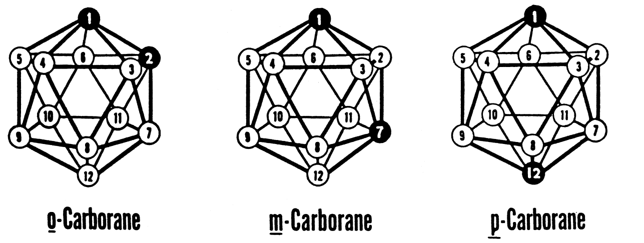

FIGURE 11 The structures and numbering conventions of the three isomers of the icosahedral carboranes. Radially directed, terminal hydrogen atoms at each boron and carbon atom have been omitted. [From Beall, H. (1975). In "Boron Hydride Chemistry" (E. L. Muetterties, ed.), p. 302, Academic Press, New York, Figure 9.1.]

Preparing *ortho*-carborane is the first step in the preparation of the icosahedral carboranes. This compound is made in high yield by a two-step process in which acetylene is inserted into the *nido* cage of $B_{10}H_{14}$. In the first step $B_{10}H_{14}$ is reacted with a Lewis base (L), most usually diethyl sulfide $[(CH_3CH_2)_2S]$.

$$B_{10}H_{14} + 2L \longrightarrow B_{10}H_{12}L_2 + H_2$$

Gaseous acetylene is then passed through a solution of the $B_{10}H_{14}$-Lewis base derivative giving the desired *ortho*-carborane product.

$$B_{10}H_{12}L_2 + HCCH \longrightarrow o\text{-}C_2B_{10}H_{12}$$

It is worth noting that although $B_{10}H_{14}$ has an $n + 4$ electron count and thus should be the result of 1 vertex being removed from an 11-vertex deltahedron, in this reaction it adds two vertices and forms the much more stable icosahedron.

Ortho-carborane is converted to *meta*-carborane in 98% conversion by passage of the vapor through a tube held at 600°C with a residence time of less than a minute. Thermal conversion of *meta*- to *para*-carborane occurs at 700°C, but the product is a mixture of 75% *meta*-carborane and 25% *para*-carborane.

V. REACTIONS OF BORON HYDRIDES

A. Combustion

The great stability of the boron-oxygen bond and the relative instability of the boron hydrides suggests that the combustion of a boron hydride should be a highly exothermic process. In fact, the boron-oxygen bond has a dissociation enthalpy of about 800 kJ/mol, and pentaborane(9), one of

the most stable boron hydrides, is unstable with respect to its elements by 42.7 kJ/mol. The enthalpy of combustion of pentaborane(9) calculated from standard enthalpies of formation is −4512.55 kJ/mol or −71.63 kJ/g assuming the reaction,

$$B_5H_9 + 6O_2 \longrightarrow 2.5B_2O_3 + 4.5H_2O$$

In contrast, pentane has an enthalpy of combustion of only −48.63 kJ/g.

Possible military applications of this high enthalpy of combustion were considered seriously in the 1950s, and several large plants for the manufacture of boron hydrides were established. A "chemical bomber" was envisioned with jet engines that would be propelled by ordinary hydrocarbon fuel except when making attacks at which time the fuel supply would shift over to the higher energy boron hydride. Of possible boron hydrides, the two that were actively considered involved the two most stable of these compounds, B_5H_9 and $B_{10}H_{14}$. Pentaborane(9) is a liquid within a reasonable temperature range but decaborane(14) is a solid. However, substitution of one of the terminal hydrogen atoms on decaborane(14) by a methyl group produced a compound that did not pack in the crystal as well as the much more symmetric decaborane(14) and thus was a liquid at a lower temperature range.

Various problems were to bedevil this project including the pyrophoric nature of the boron hydrides, the fact that the B_2O_3 combustion product was a solid, and that boron nitride, an extreme abrasive, was also produced. Both of these products would be destructive to the internal workings of the jet engine. Furthermore, combustion of the boron hydrides appeared to be incomplete reducing the energy of the reaction. Eventually the project was scrapped, but not before large amounts of B_5H_9 and $B_{10}H_{14}$ had been produced and two lives had been lost in pilot plant accidents.

B. Polymerization and Electric Discharge Reactions

Since they are relatively unstable compounds, boron hydrides are subject to a variety of reactions involving input of energy, either thermal or electric discharge. Pyrolysis of lower boron hydrides such as B_2H_6 or B_4H_{10} results in polymerization producing a mixture of higher boron hydrides up through at least $B_{10}H_{14}$ in sizable quantities plus hydrogen gas as a side product. The preparations of B_5H_9 and $B_{10}H_{14}$ are both based on pyrolysis. In addition to a mixture of volatile boron hydrides, pyrolysis produces a quantity of a yellow, solid material of unknown composition that is capable of inflaming.

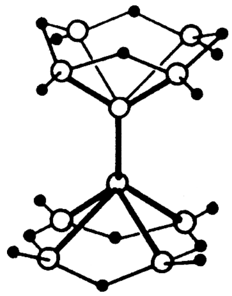

FIGURE 12 The $B_{10}H_{16}$ molecule. [From Shore, S. G., (1975). In "Boron Hydride Chemistry" (E. L. Muetterties, ed.), p. 85, Academic Press, New York, Figure 3.5.]

It is thought that the first step in the pyrolysis of B_2H_6 is its dissociation to the unstable species BH_3,

$$B_2H_6 \longrightarrow 2BH_3,$$

The BH_3 then combines with the B_2H_6 to produce an unstable B_3 hydride, which then undergoes a complex series of reactions with B_2H_6 and other hydrides, stable and unstable, leading to the final mixture of boron hydride products.

Two interesting and unusual boron hydrides are prepared when B_5H_9 and $B_{10}H_{14}$ are passed through a low pressure electric discharge. The product resulting from passing B_5H_9 through the discharge is $B_{10}H_{16}$ with two B_5 cages joined together by the borons at the apex of each square pyramid (B1) (Fig. 12). The electric discharge of $B_{10}H_{14}$ produces $B_{20}H_{16}$, the only boron hydride having fewer hydrogen atoms than boron atoms (Fig. 13). Apparently, there is insufficient space for the hydrogen atoms to bond to the four boron atoms in the concave belt around the molecule.

C. Reactions with Bases

The electrons provided by a base in its reaction with a boron hydride allow ordinary single bonds to be produced at the expense of three-center bonds, and the energy of this bond formation drives the reaction. The simplest examples of this are the cleavage reactions of bases with B_2H_6. Most bases except NH_3 cleave B_2H_6 in what is called a symmetrical manner,

L represents a base such as CH_3NH_2. Note that the starting diborane has a total of six bonds—four ordinary

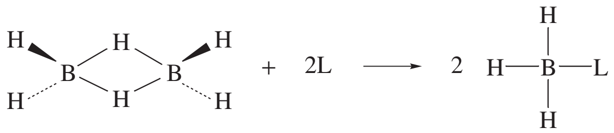

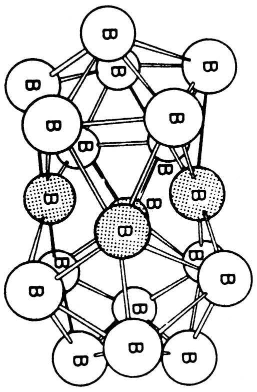

FIGURE 13 The $B_{20}H_{16}$ molecule. All boron atoms except those shaded in gray bear terminal hydrogen atoms. [From Muetterties, E. L., ed. (1975). In "Boron Hydride Chemistry," p. 9, Academic Press, New York, Figure 1.5.]

two-center bonds and two three-center bonds—whereas the two molecules of product have a total of eight bonds, all two-centered.

Ammonia cleaves B_2H_6 in an unsymmetrical manner giving an ionic product with both NH_3 groups bonded to the same boron atom,

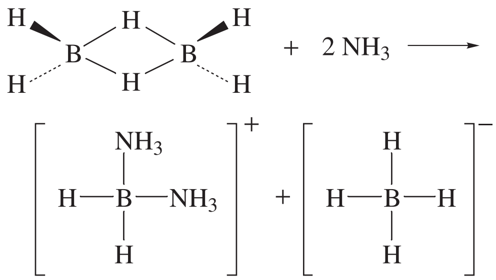

Analogous cleavage reactions have been observed with B_4H_{10} and B_5H_{11}. Such basic cleavage reactions are only observed to occur in boron hydrides in which a boron atom is bonded to the rest of the molecule by two boron-hydrogen-boron, three-center bonds.

Boron hydrides form a considerable number of Lewis base adducts, i.e., compounds in which the Lewis base has become bonded to the boron hydride with the boron framework intact. Such compounds have been observed for B_5H_9, B_6H_{10}, B_8H_{12}, and $B_{10}H_{14}$. The reaction of $B_{10}H_{14}$ with a Lewis base to produce an intermediate necessary for the preparation of *ortho*-carborane has been discussed above. The structure of this adduct is given in Fig. 14.

The bridge hydrogens of a boron hydride are the most acidic, and, in fact, $B_{10}H_{14}$ is a strong acid. Titration of $B_{10}H_{14}$ can be performed with a strong base.

$$B_{10}H_{14} + OH^- \longrightarrow B_{10}H_{13}^- + H_2O$$

Terminal hydrogen atoms in boron hydrides are hydridic, that is, behave as though they have a partial negative charge. Reactions of certain boron hydrides with water can lead to the abstaction of boron atoms and the production of a smaller boron hydride and hydrogen gas,

$$B_6H_{12} + 6H_2O \longrightarrow 2B(OH)_3 + B_4H_{10} + H_2$$

D. Reactions with Reducing Agents

Because of their deficiency in the electrons necessary for the formation of all two-center bonds, reactions of boron hydrides with reducing agents would be expected to proceed easily. Reactive metals will contribute electrons to boron hydrides to produce boron hydride anions, for example,

$$B_2H_6 + 2Na(amalgam) \longrightarrow 2Na^+ + B_2H_6^{2-}$$

$$B_5H_9 + 2Na(amalgam) \longrightarrow 2Na^+ + B_5H_9^{2-}$$

$$B_{10}H_{14} + 2Na \longrightarrow 2Na^+ + B_{10}H_{14}^{2-}$$

E. Reactions with Electrophylic Reagents

Electrophylic substitution is very familiar in substitution reactions of aromatic organic compounds such as the bromination of benzene using aluminum bromide as a catalyst. Such reactions can also be performed on some of the boron hydrides. However, the conditions of electrophylic substitution are rigorous enough that the less stable of the boron hydrides would decompose under the reaction conditions and fail to produce significant isolable products. These reactions have, in fact, been explored in detail for the two more stable hydrides, B_5H_9 and $B_{10}H_{14}$. Since the attacking species in an electrophilic substitution is positively charged or is at the positive end of a dipole, knowledge of the charge distribution on the boron hydride should predict accurately the location of substitution, and this is, in fact, the case.

A very simple method of calculating the charge distributions on boron hydrides can be performed by making the

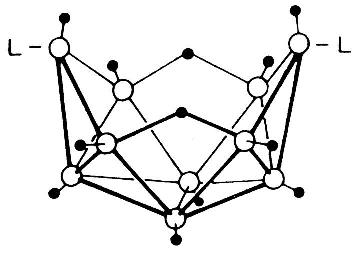

FIGURE 14 The general structure of $B_{10}H_{12}L_2$ compounds, the Lewis base adducts of $B_{10}H_{14}$. L represents a Lewis base such as CH_3CN or $(CH_3)_2S$. [From Shore, S. G. (1975). In "Boron Hydride Chemistry" (E. L. Muetterties, ed.), p.137, Academic Press, New York, Figure 3.40.]

following assumptions of how the two electrons in each bond—two-center or three-center—are shared among the atoms in the bond:

1. The very similar electronegativity of boron and hydrogen result in even sharing of the two electrons in the boron-hydrogen terminal bond.
2. The two electrons in a boron-boron single bond should be shared evenly between the two atoms in the bond.
3. The two electrons in a boron-boron-boron three-center bond should be shared evenly among the three boron atoms, that is, 2/3 of an electron per atom.
4. Of the two electrons in a boron-hydrogen-boron three center bond, one is assigned to the hydrogen in the bridge and 1/2 of an electron is assigned to each boron atom.

These assumptions can be applied to the 4120 *styx* solution of B_5H_9 to give the total number of bonding electrons assigned to each boron atom. Then subtracting this number from the number of valence electrons in the free boron atom gives an approximation of the charge on each atom as shown in Fig. 15a. Averaging the charges of the four boron atoms at the base of the square pyramid to account for hybridizing the possible bonding arrangements to maximize symmetry gives the charges given in Fig. 15b.

According to this reasoning, all electrophilic substitution such as alkylation, electrophilic halogenation, and electrophilic deuteration of B_5H_9 should occur on the boron at the apex of the square pyramid (B1), and this is what is observed.

$$B_5H_9 + CH_3Br \longrightarrow 1\text{–}CH_3B_5H_8 + HBr$$

$$B_5H_9 + DCl \longrightarrow 1\text{–}DB_5H_8 + HCl$$

$$B_5H_9 + Br_2 \longrightarrow 1\text{–}BrB_5H_8 + HBr$$

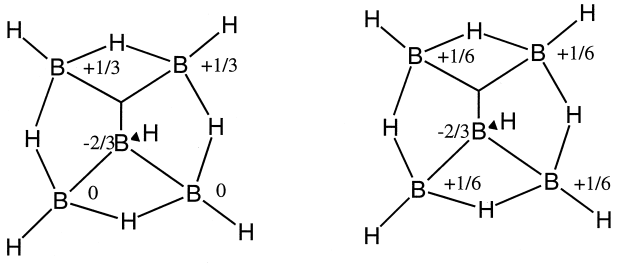

(a) (b)

FIGURE 15 (a) The charges calculated for one form of the bonding of B_5H_9 using the simple model. (b) The same charges averaged so as to increase the molecular symmetry by making the bonding to each of the boron atoms around the base of the square pyramid equivalent.

Calculation of the charge distribution on the boron cage of $B_{10}H_{14}$ is hampered by the large number of possible bonding situations that have to be considered. Molecular orbital calculations, however, show that the boron atoms farthest from the open end of the boron hydride bear the highest negative charges. The most negative boron atoms are B_2 and B_4 (Fig. 16) and the next most are B_1 and B_3. Electrophilic alkylation, halogenation, and deuteration all occur most readily at B_2 and B_4 and next at borons B_1 and B_3.

VI. REACTIONS OF BORON HYDRIDE ANIONS

The *closo* boron hydride anions have been studied considerably more than the open ions, *nido* and *arachno*. The reactions of the open ions are quite varied, and we will consider only a few of these before proceeding to the reactions of the *closo* anions.

A. Open Anions

Some boron hydride anions will add protons to produce neutral boron hydrides and thus provide a method of preparation for the neutral compounds, for example,

$$4HCl + 4B_3H_8^- \longrightarrow 3B_4H_{10} + 4Cl^- + 3H_2$$

$$HCL + B_5H_{12}^- \longrightarrow B_5H_{11} + Cl^- + H_2$$

Some of these ions can complex transition metals, such as the copper(I) complex of $B_3H_8^-$ and triphenylphosphine,

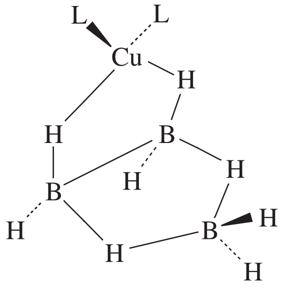

L = triphenylphosphine

B. *Closo* Anions

The properties of the *closo* ions, $B_6H_6^{2-}$, $B_7H_7^{2-}$, $B_8H_8^{2-}$, $B_9H_9^{2-}$, $B_{10}H_{10}^{2-}$, $B_{11}H_{11}^{2-}$, and $B_{12}H_{12}^{2-}$, are roughly similar. We will concentrate on $B_{10}H_{10}^{2-}$ and $B_{12}H_{12}^{2}$, the most familiar and best studied.

Small unipositive cations such as Na^+ and K^+ form soluble salts with the $B_{10}H_{10}^{2-}$ and $B_{12}H_{12}^{2-}$ anions that are

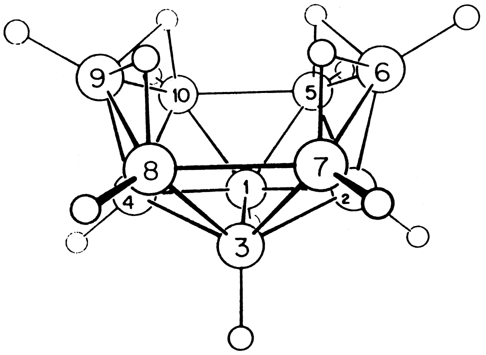

FIGURE 16 The structure and numbering system for the boron atoms in $B_{10}H_{14}$. [From Lipscomb, W. N. (1975). In "Boron Hydride Chemistry" (E. L. Muetterties, ed.), p. 57, Academic Press, New York.]

strong electrolytes. The anions are generally isolated from solution as hydrates. Most dipositive cations such as Sr^{2+} and Fe^{2+} do the same. Large unipositive cations such Tl^{+} and $(CH_3)_4N^{+}$ form salts that are only slightly soluble in water.

A large number of reactions in which H atoms are replaced by other substitutents are known, and the stability of the $B_{10}H_{10}^{2-}$ and $B_{12}H_{12}^{2-}$ cages allows reactions under quite rigorous conditions to proceed with little or no cage degradation. Substitution reactions can be performed with $B_{10}H_{10}^{2-}$ and $B_{12}H_{12}^{2-}$ salts or with H_3O^+ counterions, i.e., the acid form of the anion. Such acid catalysis often leads to facile reactions.

The acid forms of each of these *closo* anions can be fully deuterated in D_2O. Multiple replacement of hydrogen atoms by Cl, Br, and I occurs by reaction of the elemental halogen in the dark and can be forced to full replacement of all hydrogens. Elemental fluorine leads to extensive cage degradation. Substitutions in which nitrogen, oxygen, or sulfur atoms are attached to the boron cage are known as are reactions in which one substitutent is replaced by another. Examples are

$$[H_3O]_2B_{12}H_{12} + CO \longrightarrow B_{12}H_{11}CO^- + \text{dicarbonylated species}$$

$$[H_3O]_2B_{12}H_{12} + CH_3CN \longrightarrow B_{12}H_{11}NCCH_3$$

$$[H_3O]_2B_{12}H_{12} + H_2S \longrightarrow B_{12}H_{11}SH^{2-} \quad \text{(see Section IX)}$$

Note that although the $B_{12}H_{12}^{2-}$ has all equivalent boron atoms, the $B_{10}H_{10}^{2-}$ ion does not. The two boron atoms in *apical* positions that cap the square antiprism are each adjacent to only four other boron atoms whereas the other eight boron atoms in *equatorial* positions are each adjacent to five other boron atoms. In general, the *equatorial* boron atoms in $B_{10}H_{10}^{2-}$ have substitutional reactivity similar to all of the boron atoms in $B_{12}H_{12}^{2-}$, but the *apical* boron atoms in $B_{10}H_{10}^{2-}$ are more susceptible to some substitutions than the *equatorial* and less susceptible to others.

$$[H_3O]_2B_{10}H_{10} + CH_3CN \longrightarrow B_{10}H_9NCCH_3 \text{ (apical)}$$

$$[H_3O]_2B_{10}H_{10} + NH_2C(O)H \longrightarrow B_{10}H_9OC(NH_2)H \text{ (equatorial)}$$

VII. REACTIONS OF CARBORANES

A. *Nido* Carboranes

Electrophilic substitutions can be performed at the boron atoms of *nido* carboranes as they can on the boron hydrides. Charge distributions have been calculated for these compounds and electrophilic substitution occurs, as expected, on boron atoms holding the greatest negative charge. The hydrogen atoms attached to carbon atoms in the carborane cage are weakly acidic and can be abstracted by a very strong base such as butyllithium. Metathesis reactions with halogen compounds can then produce derivatives in which the carborane framework is unchanged, and the new substituents are attached to the carbon atom from which the proton was removed, for example,

$$1,6\text{–}C_2B_4H_6 + 2BuLi \longrightarrow 1,6\text{–}Li_2C_2B_4H_4 + 2BuH\,(Bu = C_4H_9)$$

$$1,6\text{–}Li_2C_2B_4H_4 + 2CH_3I \longrightarrow 1,6\text{–}(CH_3)_2C_2B_4H_4$$

or

$$1,6\text{–}Li_2C_2B_4H_4 + 2Br_2 \longrightarrow 1,6\text{–}Br_2B_4H_4$$

As in boron hydrides, bridge hydrogen atoms are the most acidic and can be removed with metal hydrides. Addition of acid to the carborane anion that is produced usually reforms the original carborane, for example,

$$2,3\text{–}C_2B_4H_8 + NaH \longrightarrow Na\,[2,3\text{–}C_2B_4H_7] + H_2$$

$$Na\,[2,3\text{–}C_2B_4H_7] + HCl \longrightarrow NaCl + 2,3\text{–}C_2B_4H_8$$

B. Icosahedral Carboranes

The much explored chemistry of the icosahedral carboranes has concentrated on metallation followed by metathesis reactions at the carbon atoms and electrophylic substitution at the boron atoms. As with the *nido* carboranes (above) the hydrogen atoms bonded to carbon are slightly acidic. Metallation reactions have been mainly performed using butyllithium and a large number of monofunctional substituents have been substituted onto the carbon atoms of *ortho*-, *meta*-, and *para*-carborane.

With difunctional reagents and the dilithium salts, *ortho*-carborane behaves quite differently than the other two isomers. The proximity of the two carbon atoms on *ortho*-carborane leads to the formation of rings, but for the *meta* and *para* isomers the carbon atoms are remote enough from each other that rings are precluded and polymers can be formed. The *meta* isomer has generally been employed in these reactions since it is easily prepared essentially pure from the *ortho* isomer, whereas preparation of the *para* isomer requires separating it from the *meta* form. Short inorganic and organic links between the carborane residues have been used to prepare carborane resins. Longer and more flexible methyl-siloxane links between *meta* carborane residues have resulted in flexible elastomers with excellent resistance to high temperatures. This resistance may be the result of the bulky carborane cages blocking the formation of siloxane rings, a principle mode of siloxane polymer decomposition.

Electrophylic substitutions have been studied extensively for the icosahedral carboranes. Because of the greater electronegativity of carbon than boron, boron atoms close to the carbon atoms bear slightly positive charges and the most negatively charged boron atoms are as far from the carbons as possible. This means that for *ortho*-carborane, B9 and B12 are most easily substituted under electrophylic conditions such as Friedel-Crafts alkylations and halogenations, and B8 and B10 are next most easily substituted. For *meta*-carborane B9 and B10 are most easily substituted and B5 and B12 are next. Note that in *para*-carborane all boron atoms are equivalent, and each is directly adjacent to a carbon atom. The icosahedral carboranes can undergo photochemical chlorination and products with all boron atoms substituted can be obtained.

VIII. METALLOCARBORANES

The possibility of substituting one boron atom in a boron cage by an atom of another element is realized in a particularly interesting manner in the metallocarboranes in which the boron atom is replaced by an atom of a metal. We will consider icosahedral metallocarboranes, by far the most studied group of compounds and ions in this family. The first step in producing icosahedral metallocarboranes is to remove one boron atom of an icosahedral carborane using a strong base such as ethoxide ion in ethanol. The boron atom removed by the negatively charged base is the boron atom in closest contact to the carbon atoms. This is shown in Fig. 17 for *ortho*- and *meta*- carborane. Note that the boron atom removed is B3 (equivalent to B6) in *ortho*-carborane and B2 (equivalent to B3) in *meta*-carborane.

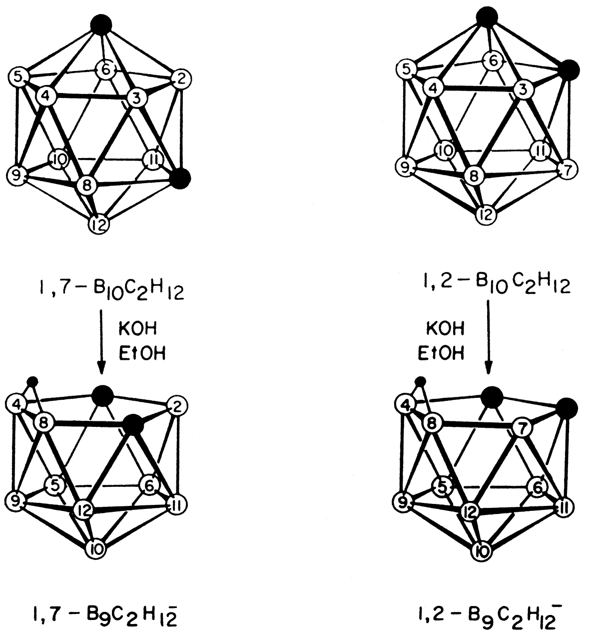

FIGURE 17 The removal of one boron atom from *meta*-carborane (left) and ortho-carborane using the strong base ethoxide ion in ethanol. [From Dunks, G. B., and Hawthorne, M. F. (1975). In "Boron Hydride Chemistry" (E. L. Muetterties, ed.), p. 388, Academic Press, New York, Figure 11.5.]

The reaction equation for either *ortho*- or *meta*-carborane is

$$B_{10}C_2H_{12} + EtO^- + 2EtOH \longrightarrow H_2 + B(OEt)_3 + B_9C_2H_{12}^-$$

In each case this results in an 11-atom cage having a single negative charge in which the open face is a 5-membered ring containing 2 carbon atoms and 3 boron atoms and having 1 bridging hydrogen atom in this open face. Deprotonation of this ion results in removal of the bridging hydrogen atom giving an ion with a double negative charge. For either the *ortho*- or *meta*-carborane isomer the reaction is

$$B_9C_2H_{12}^- \longrightarrow H^+ + B_9C_2H_{11}^{2-}$$

It was immediately recognized by M.F. Hawthorne and coworkers that the open face of either $B_9C_2H_{11}^{2-}$ ion was essentially identical to the cyclopentadienide ion $C_5H_5^-$ in terms of electrons and orbitals. The theoretical description of the open face of the $B_9C_2H_{11}^{2-}$ ion has 6 electrons occupying 5 atomic orbitals directed toward the missing vertex of the icosahedron. The cyclopentadienide ion has six electrons occupying five atomic orbitals oriented perpendicular to the plane of the ion and is well known for its ability to sandwich a metal ion between two cyclopentadienide

rings. When the Fe^{2+} ion is included between two cyclopentadienide rings the result is known as ferrocene, the first and most familiar of the "metal sandwich compounds."

The similarity between the open face of the $B_9C_2H_{11}^{2-}$ ion and the cyclopentadienide ion was first demonstrated by the reaction of $B_9C_2H_{11}^{2-}$ with $FeCl_2$. The product has the metal atom M sandwiched between the open faces of two icosahedra (Fig. 18), and these species have been named *olide complexes* from the Spanish word for "jar." The one metal atom actually completes each of the icosahedra, and so this structure can be viewed as two icosahedra each containing nine boron atoms, two carbon atoms, and one common vertex that is occupied by the metal atom. The sandwich compounds formed with Fe(II), Fe(III), Cr(III), Co(II), Co(III), and Pd(IV) are highly symmetrical as in Fig. 18, but for other metals such as Cu(II), Ni(II), Au(II), Pd(II), and Au(III) the two icosahedral fragments are slipped with respect to each other giving a less symmetrical structure. A wide variety of derivatives of these sandwich compounds have been prepared.

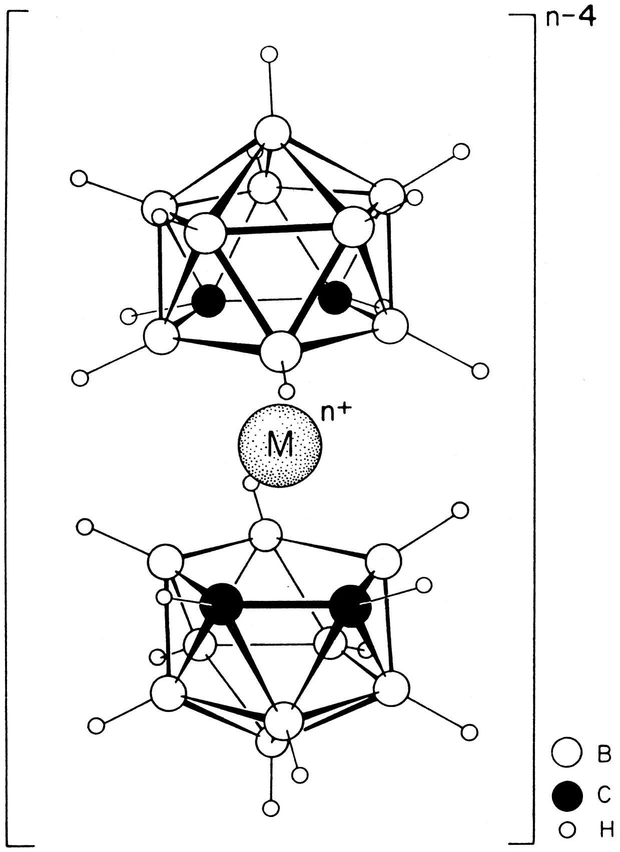

FIGURE 18 The structure of an *olide* sandwich compound in which a transition metal such as Fe^{2+} is complexed to the open faces of two carborane fragments with one boron atom removed. [From Dunks, G. B., and Hawthorne, M. F. (1975). In "Boron Hydride Chemistry" (E. L. Muetterties, ed.), p. 390, Academic Press, New York, Figure 11.7.]

The reaction of an olide complex with a strong base can form a new kind of complex containing two metal atoms and three carborane residues in which the carborane residue at the center has two boron atoms removed (Fig. 19). The central ion is called a *canistide* ion from the Spanish word for "basket."

IX. THE FUTURE? NEUTRON CAPTURE TUMOR THERAPY

We have discussed certain boron hydride species such as the icosahedral carboranes and the *closo* boron hydride anions that are quite stable. A feature of these species compared to other stable boron compounds is that the fraction of their mass that is boron is very high. For example, 75% of the mass of the icosahedral carboranes ($C_2B_{10}H_{12}$) is boron as is 69% of the disodium salt of the *closo* boron hydride anion $B_{12}H_{12}^{2-}$. In contrast, only 17% of the mass of boric acid is boron. Thus boron hydride species can deliver large concentrations of boron to situations where this is desired.

Large concentrations of boron are, in fact, necessary for the therapeutic technique for cancer known as boron neutron capture therapy (BNCT). This unique technique has the promise of destroying tumorous tissue with minimum damage to surrounding tissue that is normal. The basis of BNCT is that the ^{10}B isotope of boron will absorb slow-moving neutrons and give off α-particles in the nuclear reaction,

$$^{10}_{5}B + ^{1}_{0}n \longrightarrow [^{11}_{5}B] \longrightarrow ^{4}_{2}\alpha + ^{7}_{3}Li + \gamma$$

In this reaction, absorption of a neutron converts the ^{10}B to an unstable isomer of ^{11}B, which then decays to the α-particle and a lithium nucleus.

The α-particles liberated by this reaction are at the high energy of about 2.8 million eV. They have a pathlength of about 10 μ, approximately the diameter of one cell. Within this pathlength the α-particle will cause closely spaced, tissue-destroying events, and only a few α-particles released within a cell are sufficient to destroy it. On the other hand, the slow-moving neutrons that initiate the nuclear reaction cause a minimum of tissue damage. Thus, if the ^{10}B can be concentrated in the tumorous tissue, neutron irradiation can result in effective, localized tumor destruction.

The ^{10}B isotope is particularly attractive for this kind of therapy because of its very great capacity to absorb neutrons. This capacity is referred to as neutron cross section and is measured in the units of "barns." A comparison of the neutron cross sections of boron and other elements

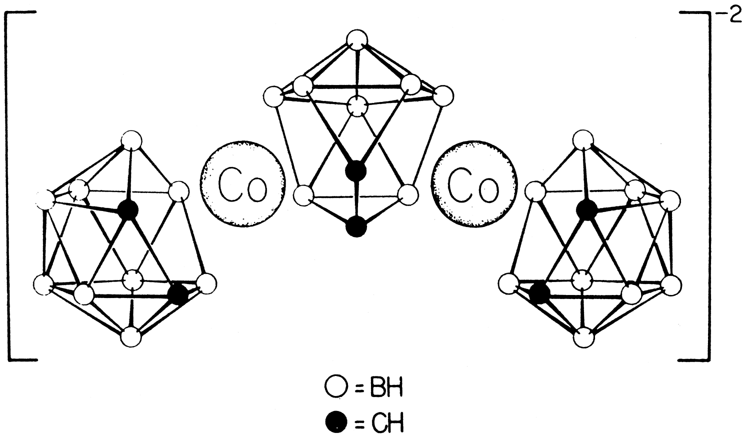

FIGURE 19 A metal complex containing two *olide* ions and two metal atoms enclosing a *canistide* ion. [From Dunks, G. B., and Hawthorne, M. F. (1975). In "Boron Hydride Chemistry" (E. L. Muetterties, ed.), p. 405, Academic Press, New York, Figure 11.25.]

that are prevalent in living tissue is given in Table IV. The other elements in this table will also emit ionizing radiation when neutrons are absorbed, but the much higher neutron cross section of boron means that the radiation will be dominant in the boron-containing regions provided that the concentration of boron is sufficiently high compared to that of the other elements.

Research in the area of BNCT has been directed toward developing methods for delivering boron-containing compounds to tumorous tissue and avoiding the surrounding healthy tissue. A number of different strategies have been employed including boron-containing derivatives of proteins, nucleosides, porphyrins, and antibodies. Particularly relevant to this article are derivatives of the *closo* boron hydride anions, $B_{12}H_{12}^{2-}$ and $B_{10}H_{10}^{2-}$ containing the sulfhydryl group (—SH), which can bind to proteins.

Problems of binding boron-containing compounds to tumorous tissue as well as delivering the slow-moving neutrons to the desired region have yet to be perfected. However, vigorous research continues in this area, and commercial ventures have been initiated.

TABLE IV Thermal Neutron Cross Sections of ^{10}B (barns) Compared with Isotopes of Other Elements

Isotope	Thermal neutron Cross section
^{10}B	3838
^{16}O	0.0002
^{12}C	0.0037
^{1}H	0.332
^{14}N	1.75

[From Barth, R. R., Soloway, A. H., and Fairchild, R. G. (1990). *Scie. Ame.* 100–107.]

SEE ALSO THE FOLLOWING ARTICLES

Hydrogen Bonds • Metal Hydrides

BIBLIOGRAPHY

Beall, H., and Gaines, D. F. (1999). "Chemistry of Pentaborane(9). A Review." *Collect. Czech. Chem. Commun.* **64,** 747–765.

Beall, H., and Gaines, D. F. (1999). "Mechanistic Aspects of Boron Hydride Reactions." *Inorgan. Chem. Acta* 1–10.

Hawthorne, M. F. (1991) "Biochemical Applications of Boron Cluster Chemistry," *Pure Appl. Chem.* **63,** 327–334.

Siebert, W., ed. (1997). "Advances in Boron Chemistry," Royal Society of Chemistry, Cambridge.

Soloway, A. H., Tjarks, W., Barnum, B. A., Rong, F., Barth, R. F., Codogni, I. M., and Wilson, J. G. (1998). "The Chemistry of Neutron Capture Tumor Therapy." *Chem. Rev.* **98,** 1515–1562.

Coordination Compounds

R. D. Gillard
University of Wales, Cardiff, Wales

I. Introduction
II. Formation
III. Electronic Configurations
IV. Shape
V. Biological Metal Complexing
VI. Therapeutic Metal Complexes

GLOSSARY

Brönsted base Proton acceptor.

Chelation Binding of a single ligand to a single metal ion through two (or more) Brönsted donor atoms, making ring structures.

Chrysotherapy Treatment of disease with gold compounds.

Complex Species formed by combination between a metal ion and a ligand.

Coordination Formation of a link between a metal ion and a ligand by the donation of electrons from the ligand to the metal ion.

Coordination number Number of ligand atoms directly attached to a central metal ion in a complex. These directly attached ligands make up the first coordination sphere.

Enantiomers Isomers that are related as an object and its mirror image.

Isoelectronic Pertaining to species (whether molecules, ions, or radicals) that have the same total number of electrons occupying the same orbitals around the same number of nuclei. For example, AlF_6^{3-}, SiF_6^{2-}, PF_6^-, and SF_6 are isoelectronic with each other, as are $[AuCl_2]^-$, $HgCl_2$, and $[TlCl_2]^+$.

Isomerism Existence of more than one distinct substance with the same composition, for example, ammonium cyanate, NH_4NCO, and urea, $(H_2N)_2CO$, both of which are CH_4N_2O in stoichiometry, or potassium fulminate, K(CNO), and potassium cyanate, K(NCO). The distinct substances are called isomers.

Labile Attaining equilibrium rapidly.

Ligand Any moiety bonded to a metal ion in a complex; often denoted by *L* in formulas and equations.

Resolution Separation of enantiomers from one another.

Stability constant Thermodynamic equilibrium constant measuring the ease of formation of a complex ion from its constituents [the metal ion and the ligand(s)].

CHEMISTRY DEALS WITH changes (reactions) of substances such as the conversion of organic matter (e.g., sugar) with dioxygen to carbon dioxide and water:

$$C_6H_{12}O_6 + 6O_2 \rightarrow 6CO_2 + 6H_2O$$

Metal complexes are formed from Brönsted bases (substances with many electrons) and Lewis acids (usually

metal cations, which are positively charged and therefore interact favorably with electron donors). A typical metal complex compound is $[Cu(NH_3)_4](SO_4) \cdot H_2O$, which is made by allowing to crystallize the dark blue solution obtained from adding an excess of strong ammonia to aqueous copper sulfate.

The interaction of ligand with metal ion is often called *coordination*, and the solid compounds that contain metal ions complexed by ligands are called coordination compounds. Typical examples are $K_2[PtCl_4]$, $K_2[PtCl_6]$, $[Pt(NH_3)_4]Cl_2$, and $[Pt(NH_3)_6]Cl_4$.

I. INTRODUCTION

Whenever any metal salt and any Brönsted base (an anion or other molecule with electronegative atoms, such as nitrogen or oxygen, that has the capacity to donate electrons) come into contact, coordination is likely to occur to give a complex compound. For example, when solid nickel chloride (yellow) reacts with a stream of ammonia gas, it is converted to purple hexamminenickel(II) chloride:

$$NiCl_2\,(\text{solid}) + 6NH_3\,(\text{g}) \rightarrow [Ni(NH_3)_6]Cl_2\,(\text{solid})$$

Similarly, on the addition of strong ammonia, a base (in water, $NH_3 + OH_2 \rightleftharpoons NH_4^+ + OH^-$; all four species are present), little by little to a blue aqueous solution of copper(II) sulfate, the final soluble species is the complex tetraammine–copper(II) ion; its stability is clear from the fact that it is formed by the dissolution [Eq. (2)] of the intermediate solid [Eq. (1)]. This solid is basic copper(II) sulfate, known also as several minerals (brocchantite, langite, wroewulfite) in oxidized sulfide ore zones. The word *basic* in the name simply reflects the presence of the hydroxide ion. OH^-, the basic constituent of water.

$$4Cu^{2+}\,(\text{aq}) + SO_4^{2-} + 6OH^- \rightarrow \{Cu_4(SO_4)(OH)_6\} \quad (1)$$

$$\{Cu_4(SO_4)(OH_6)\} + 16NH_3 \rightarrow 4[Cu(NH_3)_4]^{2+} + SO_4^{2-} + 6OH^- \quad (2)$$

The dark blue solution of the tetraammine–copper(II) species in strong aqueous ammonia (Schweitzer's solution) will dissolve cellulose. On acidification, the ammonia is neutralized (protonated forming ammonium ion, NH_4^-) and the cellulose is reforemed (at one time, through spinnerets, to make a commercial fiber).

When silver halide emulsions are used as photographic films, development of the parts exposed to light to give black silver is followed by "fixing," which is simply metal complexing. The unchanged (nonimaged) silver halide (usually chloride and bromide) must be removed before the negative can be handled in daylight. The ligand used is thiosulfate in the form of an aqueous (and therefore ionized) solution of its sodium salt $Na_2S_2O_3 \cdot 5H_2O$, so-called photographer's hypo. The silver halide dissolves:

$$AgX + 2(S_2O_3)^{2-} \rightarrow [Ag(S_2O_3)_2]^{3-} + X^- \quad (3)$$

The sodium salt of the anion, bisthiosulfatoargentate(I), can be crystallized and was said by its discover. Herschel, to have a sweet taste. Oddly, the corresponding compound of the heaviest of the "coinage metals" (copper, silver, gold). $Na_3[Au(S_2O_3)_2] \cdot 2H_2O$ (**1**), also has biological properties, being used under the name Sanochrysine in treating rheumatoid arthritis by chrysotherapy.

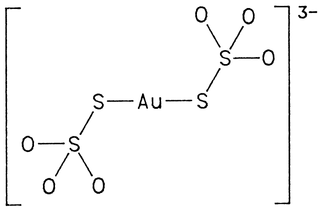

1

The gold ion is linearly bonded by two sulfur atoms.

Leather is a complicated material but contains much protein; it is always a good ligand, because it contains peptide linkages, from which either oxygen or nitrogen can donate electrons to a metal ion, forming a coordinate bond, and in which the many functional groups of the side chains of the amino acids may also interact with metal ions (as shown by the atoms underlined in structure **2**).

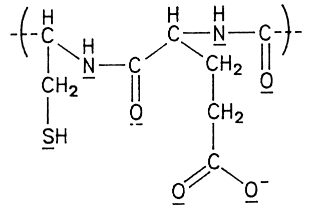

2

This extra element of cross-linking of the polymer (polypeptide) chains by metal ions—in practice, chiefly chromium(III) giving "chrome-leather"—underlies the utility of leather tanning. It is the formatin of coordinated chromium(III) that gives the tan.

Metal ions coordinated by ligands are common, giving rise to effects of striking beauty and great importance. The changes in the color of blood on oxygenation arise because of a change in one ligand on the iron ion in the coordination compound hemoglobin. Many examples of chemotherapy depend on the formation of coordinated metal ions, as in the removal of the excess of copper from patients with Wilson's disease (hepatolenticular degeneration) using

penicillamine (**3**) or triethylenetetramine (**4**). The latter is systematically named 1,4,7,11-tetraazaundecane.

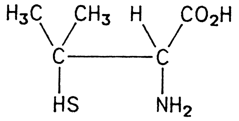

3

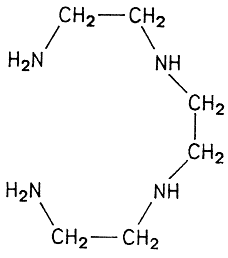

4

II. FORMATION

A. Equilibria between Cations and Donors in Water

When a donor molecule (a Brönsted base, i.e., a proton acceptor) forms a bond by donating electron density to a positive center (a Lewis acid, i.e., an electron acceptor), coordination is said to occur, as shown in Eq. (4).

$$AlCl_3 + Cl^- \rightarrow [AlCl_4]^- \quad (4)$$

More commonly, coordination occurs in solution (often aqueous), to give overall processes of metal complexing such as

$$Ni^{2+}(aq) + 6NH_3 \rightarrow Ni(NH_3)_6^{2+}(aq) \quad (5)$$

In fact, the six water ligands (W) are being replaced, one by one, stepwise, by six ammonia ligands:

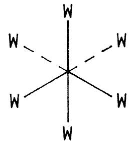

100 %
5

The replacement of one water in **5** by ammonia (A) gives the monosubstituted complex **6**:

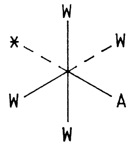

100 %
6

The position marked with an asterisk across from A in **6** (*trans* to A) is unique. The replacement of a second water in **6** by ammonia gives the disubstituted complex; there are in **6** four positions next (*cis*) to A, which gives **7**, and only one across from A (*trans*), which gives **8**:

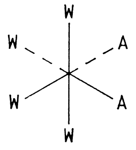

(cis), 80 %
7

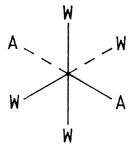

(trans), 20 %
8

If a third W is replaced in **7** or **8** by A, the *trans* (**8**, 20% of the whole) can give only **9**, but the 80% that was *cis* (**7**), gives 40% *mer* (**9**) and 40% *fac* (**10**) for a final result of 60% *mer*-**9** and 40% *fac*-**10**.

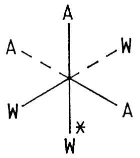

(mer), 60 %
9

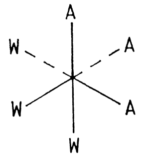

(fac), 40 %
10

A fourth replacement gives, from the 40% *fac* (10), only *cis*-A_4W_2 (since all three Ws are equivalent), but from *mer*, the position marked with an asterisk is unique, giving *trans*-W_2A_4 for one-third of the replacements into mer (A_3W_3) (i.e., 20% of the total, since *mer* was 60% of the whole). Thus, we have 20% *trans*-[MA_4W_2] and 80% *cis*-[MA_4W_2]. The fifth substitution, of course, gives MA_5W.

There is an obvious symmetry to this series of replacements: We may start from MW_6 and replace W by A, or vice versa [Eq. (6)]:

$$MA_6 + W \rightleftharpoons MA_5W_1 \rightleftharpoons MA_4W_2 \rightleftharpoons MA_3W_3$$
$$\rightleftharpoons MA_2W_4 \rightleftharpoons MA_1W_5 \rightleftharpoons MW_6 + A \quad (6)$$

Notice that six-coordinate complex ions [MA_nB_{6-n}], where $2 \leq n \leq 4$, may exist in two forms. In the example above, A is NH_3 and B is H_2O, but the occurrence of two forms (**7** as against **8**, or **9** as against **10**) differing in the arrangement of ligands A and B about the center is quite general.

B. Stability Constants and Relationships among Them

The general form (**7**) of the overall stability constant for the coordination

$$pM^{n+} + qL + rH^{+} \rightleftharpoons [M_pL_qH_r] \qquad (7)$$

is written

$$\beta_{pqr} = [M_pL_qH_r]/[M]^p[L]^q[H^+]^r \qquad (8)$$

For example,

$$Ag^{2+}\,(aq) + 4C_5H_5N\,(aq) \rightleftharpoons [Ag(C_5H_5N)_4]^{2+}\,(aq) \qquad (9)$$

$$\beta_{140} = [Ag(C_5H_5N)_4]/[Ag^{2+}][C_5H_5N]^4 \qquad (10)$$

$$\log \beta_{140} = 25 \qquad (11)$$

These *overall* stability constants describe only the equilibrium of a given stochiometric *composition* of formation of a complex and do not, for example, distinguish between the forms of $[MW_4A_2]$ above [the *trans* (**7**) and the *cis* (**8**)]. These are macroconstants and are a weighted sum of the individual microconstants. For example, the macroconstant β_{120} for Eq. (12) is made up of the two microconstants $\beta_{120(cis)}$ [Eq. (13)] and $\beta_{120(trans)}$ [Eq. (14)]:

$$Ni^{2+}\,(aq) + 2NH_3 \rightleftharpoons [Ni(NH_3)_2(H_2O)_4]^{2+} \qquad (12)$$

$$Ni^{2+}\,(aq) + 2NH_3 \rightleftharpoons cis\text{-}[Ni(NH_3)_2(H_2O)_4]^{2+} \qquad (13)$$

$$Ni^{2+}\,(aq) + 2NH_3 \rightleftharpoons trans\text{-}[Ni(NH_3)_2(H_2O)_4]^{2+} \qquad (14)$$

The constant describing the equilibrium [Eq. (15)] between the forms with the same stoichiometry is simply Eq. (16).

$$cis\text{-}[M(NH_3)_2(H_O)_4]^{2+} \rightleftharpoons trans\text{-}[M(NH_3)_2(H_2O)_4]^{2-} \qquad (15)$$

$$K_{isom} = [trans]/[cis] = \beta_{120(trans)}\beta_{120(cis)} \qquad (16)$$

Reverting to the ammine system above, if everything else were unchanged (if A and W had an equal chance of being attached to M), then the *statistical* proportions shown would apply. Furthermore, if the probability were the same of attaching an ammonia to the metal and removing it from the metal, then we would expect the probability of complexing to be 36 times greater for the first substitution of water by ammonia [Eq. (17)]:

$$MW_6 + NH_3 \rightleftharpoons M(NH_3)W_5 + W \qquad (17)$$

(six equivalent ways forward, only one back) than for replacing the final water ligand by a sixth ammonia [Eq. (18)] (only one possible place where the water can be replaced by ammonia and six ways back where any of the six ammonia ligands can be replaced by water). On these grounds, the *stepwise* equilibrium constants for the formation of $M(NH_3)_6$ decrease (electrical charge on ions is omitted):

$$MW(NH_3)_5 + NH_3 \rightleftharpoons M(NH_3)_6 + W \qquad (18)$$

$$M + L \rightleftharpoons ML \qquad (19)$$

$$K_{110} = [ML]/[M][L] \qquad (20)$$

$$ML + L \rightleftharpoons ML_2 \qquad (21)$$

$$K_{120} = [ML_2]/[ML][L] \qquad (22)$$

$$ML_2 + L \rightleftharpoons ML_3 \qquad (23)$$

$$K_{130} = [ML_3]/[ML_2][L] \qquad (24)$$

So $K_{110} > K_{120} > K_{130}$ on these statistical grounds.

Furthermore, if we consider a similar series [Eqs. (25)–(28)] in which the ligand is an anion, carrying a negative charge, we can see a similar trend due to the effect of charge neutralization (here the ionic charges *are* printed):

$$M^{n+} + L^- \rightleftharpoons (ML)^{(n-1)+} \qquad (25)$$

$$K_{110} = \{[ML]^{(n-1)+}\}/\{[M]^{n+}\}[L^-] \qquad (26)$$

$$(ML)^{(n-1)+} + L^- \rightleftharpoons (ML_2)^{(n-2)+} \qquad (27)$$

$$K_{120} = \{[ML_2]^{(n-2)+}\}/\{[ML]^{(n-1)+}\}[L^-] \qquad (28)$$

The first stepwise complexation, in Eq. (25), involves the neutralization, by mutual Coulombic attraction, of the full n^+ charge of the metal ion by the single negative charge of L^-. However, for the second step, in Eq. (27), the Coulombic interaction is smaller, now being between the same single negative charge on L^- and the less intensely charged (ML) species, with only $(n-1)$ charge. Typically, if M^{n-}were Al^{3-}, and L^- were F^-, the attraction in Eq. (25) would be between a 3+ and a 1− pair, but that in Eq. (27) would be between the 2− of $[AlF]^{2-}$ and the 1− of the fluoride ligand.

In the final stages of stepwise coordination, the negatively charged anionic ligand is being added to an already negatively charged metal species. The Pauling electroneutrality principle reminds us that ligands will add readily only until the affinity for electrons of the central metal ion is essentially satisfied.

Thus, on the grounds both of statistics and of charge interaction, the order $K_{11} > K_{12} > K_{13} > \cdots K_{1n}$ is expected (and almost always observed). Table I lists some examples.

If there is a departure from this order or a sharp, distinct irregularity, something in the system has changed, often the coordination number of the metal ion. For example, with $Cl^- + Fe^{3+}$, K_{11}, K_{12}, and K_{13} decrease steadily but K_{14} shows a sudden drop. This suggests that the octahedral

TABLE I Aqueous Stability Constants (log β_{1n0})[a]

M^{n+}	Ligand	β_{110}	β_{120}	β_{130}	β_{140}
Cu^{2+}	NH_3	4.2	7.7	10.6	12.7
Ni^{2+}	NH_3	2.8	5.04	6.77	7.97
Al^{3+}	F^-	6.1	11.1	14.9	17.7

[a] Note that the overall constants β_{1n0} are the product of stepwise constants $K_{110} \times K_{120} \times \cdots K_{1n0}$, e.g., $\beta_{140} = K_{110} \times K_{120} \times K_{130} \times K_{140}$.

six-coordinated $Fe(OH_2)_6^{3+}$ combines (stepwise) with one, then a second, thean a third Cl^- without change in coordination number but that, at the next addition of chloride, a major change occurs, probably

$$[Fe(OH_2)_3(Cl)_3]^0 + Cl^- \rightleftharpoons [FeCl_4]^-$$

Note that no such discontinuity occurs with fluoride forming complexes with iron(III).

The coordination number of a given metal ion, such as Co^{2+} or Al^{3+} (which indicates the number of ligands attached to it), often varies from ligand to ligand. For example, whereas for aluminum, aqueous chloride forms $[AlCl_4]^-$ and the addition of another chloride ligand (a fifth and a sixth) is not easy, up to six fluoride ligands coordinate rather readily, forming AlF_6^{3-}.

C. Irving–Williams Series

The past discussion has dealt with variation of stability for the coordination compounds of a given metal ion. What about variation for a particular ligand with a range of metal ions? Again, the simple ideas of Coulombic interaction take us a long way. The greater the charge and the smaller, the size of a cation (Lewis acid), the better it will interact with an electron donor (Brönsted base). Thus, for a given ligand, say glycinate (gly-O),

$$K_{110} \text{ for } Na^+ < K_{110} \text{ for } Mg^{2+} < K_{110} \text{ for } Al^{3+}$$

Similarly, for the change in cationic size with constant charge, as in the lanthanides (where the "lanthanide contraction" means that the elements with higher atomic numbers give the smallest 3+ ions) where *only* the metal ion changes, we generally find the stability of a series of coordination compounds to *increase* from lanthanum (atomic number 57) to lutetium (atomic number 71).

The similar decrease in size through the transition series (where the ionic radii of the doubly charged ions M^{2+} decrease from V^{2+} to Zn^{2+}) leads to an increase in stability for coordinated compounds (Fig. 1). The order shown for β_{110} for the second half of the first transition series (Mn < Fe < Co < Ni ≤ Cu > Zn) is the Irving–Williams series. The "double-humped" plot is famous; it summarizes many properties of analogous sets of coordination compounds. Notice that it is the number of d electrons that dictates this shape. The upper dashed plot is for the triply charged metal ions. Naturally, the interaction between M^{3+} and the electrons of a given ligand is better than that of M^{2+}, so the dashed curve of Fig. 1, representing stability constants for triply charged metal ions, like Fe^{3+}, lies above the full curve for doubly charged ions like Fe^{2+}.

D. Inverse Complexing

In the crystal lattice of many solid binary compounds of the type AgI, the metal ion (here Ag^+) will have several anions (here four I^-) surrounding it. This is akin to coordination of metal ion by iodide, giving the complex anions AgI_2^-, AgI_3^{2-}, AgI_4^{3-}, and so on. Conversely, each iodide in solid silver iodide will be surrounded by silver ions. In some cases, chiefly for large central *anions*, complex cations like IAg_2^+, IAg_3^{2+}, and $TeAg_6^{4+}$ exist in aqueous solutions. The formation of a cationic complex by the addition of several positive ions to a central negative ion is called inverse complexing (or sometimes metallocomplexing). Inverse complexes are a chief factor in the dissolution of silver halides in excess of soluble silver salts such as nitrate [Eq. (29)].

$$AgI + AgNO_3 \rightarrow [IAg_2]^+ + NO_3^- \qquad (29)$$

and central inverse complexed units such as $(OM_3)^{y+}$, $(NM_3)^{x+}$ are fairly common. These include $[OIr_3]^{8+}$, in Lecoq de Boisbaudran's compound, $Ir_3O(SO_4)_4$, named for the discoverer of the element gallium; $(OM_3)^{7+}$ in the basic chromium(III), iron(III), and ruthenium(III) acetates $[M_3O(CH_3COO)_6]^+$; and $(Hg_2N)^+$ in Millon's base.

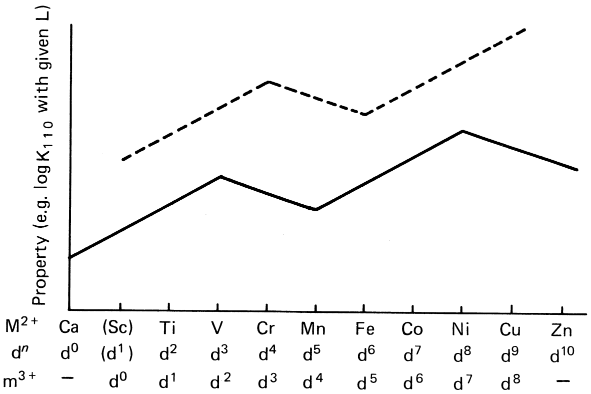

FIGURE 1 Irving–Williams "double-humped" plot (representing the change in properties of the doubly charged ions M^{2+}) for thermodynamic properties of ions of the first transition series. The dashed plot show the related changes for the triply charged M^{3+}.

The phenomena are closely akin to the remarkable dissolution by aqueous solutions of beryllium and zinc salts of their own water, insoluble oxides [Eq. (30)]:

$$2H_2O + MO + 2M^{2+} \rightleftharpoons M_3(OH)_3^{3+} + H^+ \quad (M = Be, Zn) \quad (30)$$

Indeed, whenever the coordination number of a simple anion in a complex is greater than 1, there is an element of "inverse complexing," and interesting properties result. The following are examples:

1. The "oxo-bridged" species, where either O^{2-} or OH^- links two metal ions, as in $[Cl_5RuORuCl_5]^{4-}$; Durrant's anion $[(O_4C_2)_2Co(OH, OH)Co(C_2O_4)_2]^{4-}$; or the famous Werner's hexol $[Co\{(OH)_2Co(NH_3)_4\}_3]^{6+}$. Such bridging ligands carry the symbol μ.
2. Halide bridges. These are common, so that there are many species with two-coordinated halide ligands, as in Pt(II)–Cl–Pt(II), often in the same complex species as one-coordinated "terminal halides." The properties of the terminal and bridging halide ions are quite different.

E. Chelation

Both in nature and in synthetic chemistry, there are many cases of polydonor molecules, each containing several atoms that can coordinate to a metal ion. Often, these several atoms may be so distributed in space that they coordinate to the same metal ion. This is shown in Eq. (31):

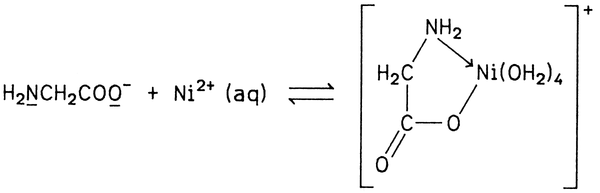

11

(31)

The underlined nitrogen and oxygen atoms of the glycinate ion bind to the same metal ion (here Ni^{2+}), giving a new cyclic structure (**11**) with the five-membered "chelate" ring (NiNCCO). Such di- or polydonor ligands are called chelating. Cyclic molecules (carbocyclic, aliphatic as in cyclohexane; aromatic as in benzene; heterocyclic, aromatic as in pyridine; or alicyclic as in piperidine) are most common when five- or six-membered. The same is true for chelate cycles in coordination compounds. These are formed most readily when five- or six-membered (**12**–**14**; M indicates a metal ion).

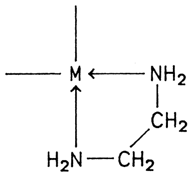

12

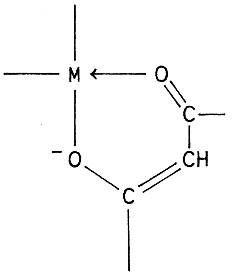

13

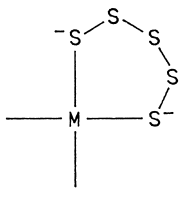

14

The presence of chelate rings stabilizes a molecule, for example, in Eq. (32), where en = 1,2-diaminoethane:

$$[(H_2O)_4Ni(NH_3)_2]^{2+} + en \rightarrow [(H_2O)_4Ni(en)]^{2+} + 2NH_3 \quad (32)$$

Omitting ionic charges and the four water molecules that remain attached to the nickel ion throughout, we obtain

$$K = [Ni(en)][NH_3]^2/[Ni(NH_3)_2][en] = 10^3 \quad (33)$$

Note that this is a macroconstant. Clearly, the relevant equilibrium constant is actually for joining *cis*-nitrogen ligands in pairs [Eq. (34); W indicates a water ligand].

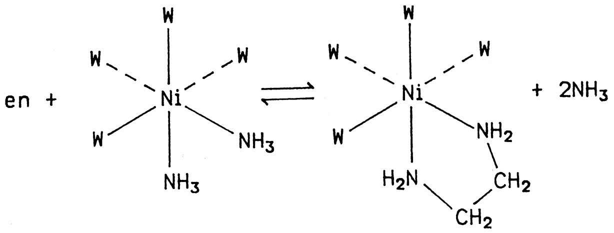

(34)

This stability of chelated coordination is very important in chemical analysis. Two examples of chelated coordination are as follows:

1. The Tchugaev reaction [Eq. (35)] of 2,3-butanedionedioxime (dimethylglyoxime, abbreviated here as H_2DMG) with nickel ions, where the chelated product is a bright red precipitate.

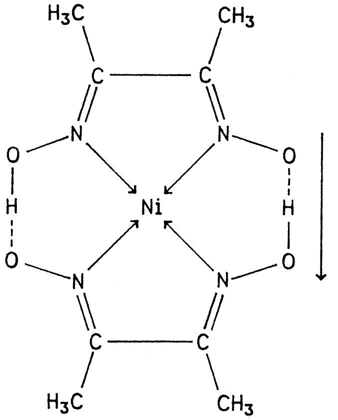

Ni(HDMG)$_2$

(35)

The remarkable stability of this red solid stems from the chelation and the further factors of the short, strong intramolecular hydrogen bonds (O–H---O) and an out-of-plane intermolecular interaction.

2. Complexing, as in Eq. (36), of metal ions by 1,2-diaminoethane-*N,N,N′,N′*-tetraacetate (**15**) from so-called ethylenediaminetetraacetic acid, H_4(EDTA), giving a highly chelated product (**16**).

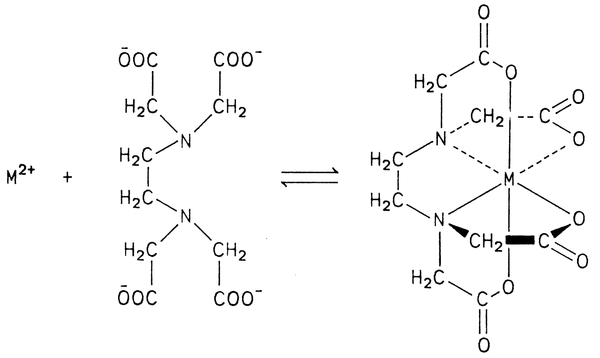

15 **16**

(36)

When the divalent ions, here M^{2+}, are of calcium or magnesium, as in "hard" water, they are sufficiently complexed ("sequestered") by the $EDTA^{4-}$ ligands to render the water "softer."

F. Oxidation States and Their Stability

Coordinating a metal ion (say, Fe^{2+}) to a ligand alters its stability. Coordinating the same ligand to a differently charged ion (e.g., Fe^{3+}) of the same metal (i.e., in a different oxidation state) alters the stability of that ion as well, but usually to a different degree. Such a situation can be analyzed by means of the Nernst equation [Eq. (37)],

$$E = E^0 - 2.303\frac{RT}{nF}\log\frac{[M^{n+}]}{[M^{(n+1)+}]} \qquad (37)$$

or at equilibrium,

$$E^0 = 2.303\frac{RT}{nF}\log\frac{[Fe^{2+}]}{[Fe^{3+}]} \qquad (38)$$

The concentrations $[Fe^{2+}]$ and $[Fe^{3+}]$ here are those of the free, uncomplexed metal ions (i.e., those in a solvent environment). Now, what happens if a coordinating ligand X is added? Both M^{n+} and $M^{(n+1)+}$ (e.g., Fe^{2+} and Fe^{3+}) are bound, but to differing degrees. This depresses the concentration of the two free (aquated) ions differentially. Such binding by the ligand is described by stability constants for the two oidation states, β_{110}^{II} and β_{110}^{III}, so that

$$E = E^0 - 2.303\frac{RT}{nF}\log\frac{[Fe(II)X]}{\beta_{110}^{II}}\frac{\beta_{110}^{III}}{[Fe(III)X]} \qquad (39)$$

If we add a ligand that will bind more tightly with the oxidized ion, $M^{(n+1)+}$ than with M^{n+}, then the potential E will shift strongly.

An extreme example is that, on the addition of cyanide salts (e.g., KCN) to a solution of a cobalt(II) salt in water, cobalt(II) becomes so greatly destabilized relative to its oxidized ion, cobalt(III) (whose cyano complexes are remarkably favored), that the potential for $Co^{3+} + e^- \rightarrow Co^{2+}$ (where $E^0 = +1.84$ V in water in the absence of coordinating agents) becomes -0.82 V. That is, the cobalt couple (extremely strongly oxidizing in water) in now so reducing that it will drive electrons onto protons in the water to give ($H^+ + e^- \rightarrow \frac{1}{2}H_2$) dihydrogen gas.

In a similar way, though silver ion in commonly a good oxidant (i.e., the half-cell $Ag^+ + e^- \rightarrow Ag$ is favored relative to $H^+ + e^- \rightarrow H_2$), in the presence of iodide ions—which diminish the value of $[Ag^+]$ by virtue of the gross insolubility of silver iodide, AgI—silver metal dissolves in hydriodic acid, HI, to give dihydrogen gas.

G. Stability Constants and pH

Most ligands are bases (having lone pairs of electrons), and many examples of coordination may be viewed as competition [e.g., Eq. (40)] for these lone pairs between solvated protons (acid–base equilibria) and other solvated cations:

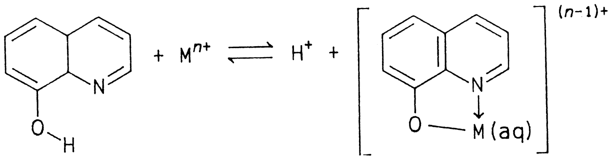

17 **18**

(40)

Clearly, the addition of metal ion (in the form of its salts) to an aqueous solution of the ligand, here

TABLE II Equilibrium Constants *K* for Coordination of Hydroxide[a]

Metal	Ligand	*n*	*x*	log *K*
Pt	2,2-Bipyridyl	2	2	4.3
Pt	5,5′-DMB[b]	2	2	4.8
Pd	5,5′-DMB[b]	2	2	5.5
Pd	HDMG[c]	2	0	5.5

[a] Equivalent to $r = -1$ in β_{pqr}:

$$(ML_n)^{x+} + OH^- \rightarrow [(ML_n)OH]^{(x-1)+}$$

[b] DMB, Dimethyl-2,2′-bipyridyl.

[c] HDMG, "Dimethylglyoxime," 2,3-butanedionedioxime. Equation (35) shows the structure of the analogous $[Ni(DMG)_2]$.

8-hydroxyquinoline (**17**) or *H*-oxinate, displaces some protons, causing a fall in pH. Conversely, the addition of protonic acids to metal complexes such as **18** will reverse this formation and cause the dissociation of the coordinate bond. One common way of measuring stability constants is to set up such competitive equilibria as shown in Eq. (41):

$$2HL + M^{2+} \rightleftharpoons ML_2 + 2H^+ \qquad (41)$$

For example,

$$2H_3NCH_2COO + Cu^{2+} \rightleftharpoons M(H_2NCH_2COO)_2 + 2H^+ \qquad (42)$$

This is done in the presence of concentrations of metal ion from zero to levels comparable with those of ligands.

For aqueous equilibria, where the species M^{n-}, L^-, and OH^- are present, the utility of K_{pqr} is clear. Coordination compounds may contain protons (particularly on polydentate ligands). Values of r (0 in examples so far) represent the involvement of protons in complex formation. Of course, when r is negative, this may arise from loss of a proton from somewhere in the coordination species or, because $[H^+][OH^-] = K_w$, that is, $[OH^-] = K_w[H^+]^{-1}$, it may signify the gain of a hydroxide, as in the examples in Table II.

III. ELECTRONIC CONFIGURATIONS

There are some 70 metallic elements. All metal ions (Lewis acids) form coordination compounds. At present, the coordination compounds of the 27 transition metals are the most widely studied and applied, and this section refers to them. In the periodic table, at the onset of each of the transition series, the energies of the n s, n p, and $(n-1)$ d [or $(n-2)$ f if appropriate] orbitals are so close that they are made to interchange fairly readily. For example, the ground state of the barium atom (atomic number 56, at the start of the third transition series) is $6s^2$, and the atom before it, cesium, has the $6s^1$ ground state. However, for cesium, the next electronic state lies not far from the ground state, and indeed on compression, the conductance of cesium changes sharply, as the d orbital is squeezed below the s orbital. Barium shows a similar transition with pressure, corresponding to a change in configuration from $6s^2$ to $6s^15d^1$. In view of the angled hybrids ($s \mp d$) given by this configuration, the angular (bent) structures as monomers in the vapor phase of MX_2 for M = Ca, X = F; M = Sr, X = Cl, F; M = Ba, X = F, Cl, Br, I are examples of transition metal chemistry. In the same way, although the ground states of the *atoms* of vanadium and nickel are $4s^23d^3$ and $4s^23d^8$, the shrinkage on ionization (which can be regarded as equivalent to the effect of huge pressure) squeezes the 3d orbitals to lower energies than the 4s, so that the ground states of the ions are $3d^3$ and $3d^8$, respectively.

The concept that isoelectronic d^n configurations have related properties is most valuable. In particular, such properties as color, magnetism, and rates of chemical reaction, which depend rather directly on numbers of d-electrons, can be rationalized and predicted. For example, the metal ions whose chiral coordination ions have enough kinetic inertness to be separated (resolved) into long-lasting enantiomers most commonly have six d electrons (n d^6 configurations).

A. Splitting Diagrams for Octahedral Coordination

When six ligands surround a metal ion to give octahedral coordination, the situation for two of the five d orbitals of the metal is shown in Fig. 2. These two orbitals are representative of others like themselves.

1. The d_{yz} orbital is typical of those that "point between" the axes (defined by the six ligands): These three

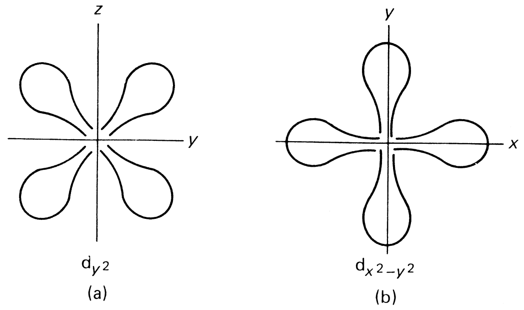

FIGURE 2 Differing spatial distribution of the orbitals (a) d_{yz} (between axes) and (b) $d_{x^2-y^2}$ (along axis).

[d_{yz} (Fig. 2a, **19**), d_{xz} (**20**), and d_{xy} (**21**)] have electron density as far from

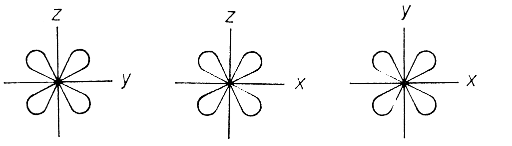

19 **20** **21**

the ligand electron density as possible, and hence are nonbonding.

2. The $d_{x^2-y^2}$ orbital (Fig. 2b) typifies those that point directly at the ligands: These two ($d_{x^2-y^2}$, d_{z^2}) can overlap with ligand orbitals and form good bonds along the axes. From these two metal-centered *d* orbitals and the composite ligand–donor orbitals are formed two bonding and two antibonding combinations, as shown in Fig. 3, representing the overlap of the *s*, *p* (three of these), and d (five) orbitals of the central metal ion with the six equivalent donor orbitals (lone pairs) of the six equivalent ligands of the octahedral complex. Now there are six donor orbitals (two electrons each) on the six ligands, so those 12 electrons will be accommodated in the levels lying up to and including $d_{(\sigma)}$. That diagram is then appropriate to *any* octahedral system, whether or not central atom d electrons are involved. For example, the isoelectronic series AlF_6^{3-}, SiF_6^{2-}, PF_6^-, SF_6 (where the central atom makes bonds using the orbitals 3s, 3p, and 3d) have the electronic structure shown, and in the same way $InCl_6^{3-}$, $SnCl_6^{2-}$, and $SbCl_6^-$ (using the 5s, 5p, and 5d atomic orbitals of the metals) have the same diagram filled, up to and including $d_{(\sigma)}$.

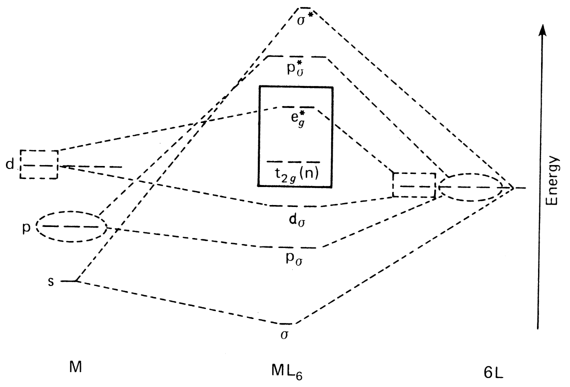

FIGURE 3 Bonding in an octahedral complex, ML_6^{n+}, viewed as a combination (overlap in space) of the s, the p (*x*, *y* and *z*), and the d (*xy*, *yz*, *zx* and $x^2 - y^2$, z^2) orbitals of metal (M) with one, three, and two, respectively, of the six donor orbitals on the six ligands (L). Shown here are the combinations of only those d orbitals that point at ligand lone pairs, that is, the $d_{x^2-y^2}$ and d_{z^2} with selected ligand orbitals. The remaining three of the five d orbitals of the metal (d_{xy}, d_{yz}, d_{zx}) are shown as being unaffected in energy when the complex forms, that is, nonbonding (t_{2g}).

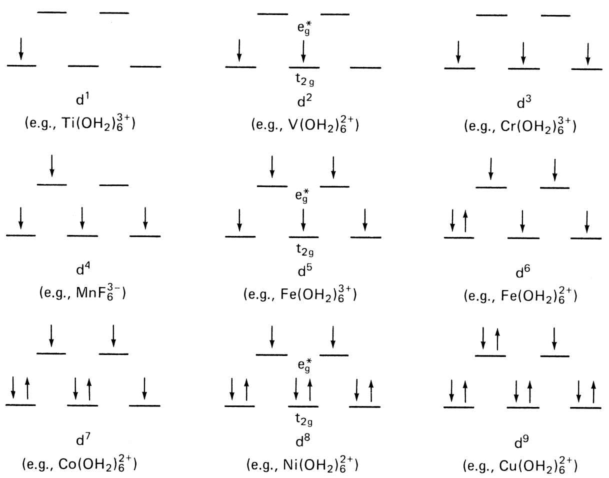

FIGURE 4 Distributions of electrons among the nonbonding (t_{2g}) set and the antibonding (e_g^*) set for ions with various d^n configurations, assuming small values for $\delta E (= e_g^* - t_{2g})$.

B. Spin States

For the transition elements, the metal ion has *n* d electrons, so that those over and above the bonding framework of the 12 originating from the ligands require that the t_{2g} and e_g sets be occupied. This is shown for the d^1–d^9 configurations in Fig. 4 (note that only the nonbonding t_{2g} orbitals, originally d_{xy}, d_{yz}, and d_{zx}, and the antibonding e_g pair are shown, that is, the five molecular orbitals in Fig. 3 enclosed in a solid-line box). This, set of distributions (high spin) assumes Hund's rule. What if Hund's rule is not obeyed? Then, instead of the maximum spin multiplicity (greatest number of unpaired, i.e., parallel, spins, "spin free") as drawn in Fig. 4, the fact that the energy of the e_g^* set is higher than that of t_{2g} will lead to full population of the lower-energy t_{2g} set, with consequent spin pairing ("spin-paired," "low spin"). This will happen where the energy separation ($e_g^* - t_{2g}$) is greatest, which is where the bonds ($L \rightarrow M$ *along* axes *x*, *y*, and *z*) are strongest, since $e_g^* - e_g$ will then be greatest (the nonbonding t_{2g} serves as an unmoving marker between the bonding and antibonding e_g orbitals).

Thus, for d^4–d^7, there are the possible "low-spin" electronic configurations of Fig. 5, quite different from those in Fig. 4, the "high-spin" ones. Table III summarizes the different numbers of unpaired electrons for high- and low-spin complex compounds.

C. Simple Magnetic Properties

One view of the interaction of matter with magnetic fields stems from the electrons acting as revolving charges, setting up a magnetic dipole. Electrons paired in orbitals cancel one another (the small residual effects are lumped

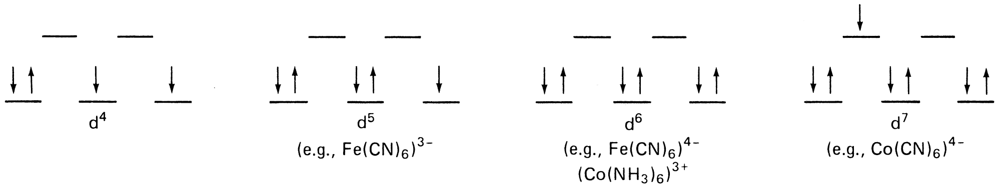

FIGURE 5 Distributions of electrons for ions with d^4–d^7 configurations, where $\Delta E(e_g^* - t_{2g})$ is large.

together under the name *diamagnetism*). Lone (unpaired) electrons give large magnetic moments $\mu > 0$ (paramagnetism) interacting strongly with an applied magnetic field,

$$\mu = [n(n+2)]^{1/2} \tag{43}$$

where n is the number of unpaired electrons: μ is in units of Bohr magnetons (BM). Taking iron(III) as an example, the high-spin (weak-field; see Fig. 4) configuration $(t_{2g})^3(e_g)^2$ with five unpaired electrons as in ferric alum, where the coordination sphere of the iron is $[Fe(OH_2)_6]^{3+}$, gives $\mu = (5 \times 7)^{1/2} = 35^{1/2} = 5.9$ BM per iron. For the low-spin (strong-field; see Fig. 5) ferricyanide ion, where the iron(III) has the configuration $(t_{2g})^5(e_g)^0$, with only one unpaired electron, $\mu = 3^{1/2} = 1.73$ BM. A more systematic name for this spin-paired ion is hexacyanoferrate(III).

D. Colors

As with any other class of matter, if an energy gap in a complex compound matches the energy of an incident photon, absorption occurs. In many coordination compounds, the quantum required for excitation from the ground state is of visible light, so that these compounds are of many colors, often of great beauty. Two chief selection rules decide which of all the possible transitions occur:

TABLE III Occupancy of Orbitals in High- and Low-Spin Octahedral Coordination Compounds[a]

	d^1	d^2	d^3	d^4	d^5	d^6	d^7	d^8	d^9
High spin									
e_g^*	—	—	—	—	—	1	2	3	4
t_{2g}	1	2	3	4	5	5	5	5	5
Unpaired electrons (HS)	1	2	3	4	5	4	3	2	1
S	2	3	4	5	6	5	4	3	2
Low spin									
e_g	—	—	—	—	—	—	1	2	3
t_{2g}	1	2	3	4	5	6	6	6	6
Unpaired electrons (LS)	1	2	3	2	1	0	1	2	1
S	2	3	4	3	2	1	2	3	2
Difference (HS – LS)	0	0	0	2	4	4	2	0	0

[a] HS, High spin; LS, low spin, S denotes spin multiplicity.

1. $s \leftrightarrow p$, $p \leftrightarrow d$ (etc.) atomic transitions are allowed, but $p \leftrightarrow p$, $d \leftrightarrow d$ are not; in more general terms, $g \leftrightarrow u$ is allowed, but $g \leftrightarrow g$, $u \leftrightarrow u$ are forbidden.
2. The spin multiplicity does not change in an allowed transition. It is for this reason that all high-spin d^5 systems are at best weakly colored: There is only the one possible spin-parallel arrangement of five electrons in five d orbitals, so *any* transition must be to a state with different spin multiplicity. Coordination compounds of Mn^{2+} $(3d^5)$ are usually in consequence very pale. Notice that this doubly forbidden character is true for any octahedral six-coodinated *high-spin* ion with five d-electrons. Examples include $[Fe(OH_2)_6]^{3+}$ in alums, which is a weak field environment, but not, of course, $[Fe(CN)_6]^{3-}$, which has its five d-electrons paired.

From the first rule (sometimes called the Laporte rule), any d–d transition in a centrosymmetric molecule is weak. Compared with dyestuffs (often with molar extinction coefficient $\varepsilon \sim 50{,}000$), complex compounds are poor absorbers of photons.

So far, only the electronic configurations for regular octahedral coordination have been given, and color has been described in terms of excitation of an electron by a quantum of visible light from the ground sate to an upper state. The size of the gap E in energy separating the ground and upper states controls the color ($E = h\nu$). The larger the gap, the greater the energy of the photon required to promote an electron across it. The gap depends on the strength of the $M \leftarrow L$ bonds along the axes (see Fig. 3).

In general, descending a triad of transition elements, like cobalt, rhodium, iridium [where the M^{3+} ions have the configurations $(3d)^6$, $(4d)^6$, $(5d)^6$, respectively], the energy gap ΔE in analogous species, say $M(NH_3)_6^{3+}$, increases, as in Table IV. This means, of course, that the compounds become less obviously colored; even the lowest-energy spin-allowed d–d transitions ($5d \rightarrow 5d$) for molecules containing third-row elements go into the ultraviolet.

Taking one metal ion, variation of color arises from the same cause, the variation of the energy gap. For the electronic configuration d^3 in the coordination complexes of chromium(III), for the lowest-energy transition arising

TABLE IV Energy Gaps in Analogous Species Containing Cobalt, Rhodium, and Iridium

Compound	Configuration	Transition	Energy (kK)[a]	Color
$Co(NH_3)_6^{3+}$	$(3d)^6$	$(t_{2g})^6 \rightarrow (t_{2g})^5(e_g)^1$	21.3	Orange-yellow
$Rh(NH_3)_6^{3+}$	$(4d)^6$	$(t_{2g})^6 \rightarrow (t_{2g})^5(e_g)^1$	33.3	White
$Ir(NH_3)_6^{3+}$	$(5d)^6$	$(t_{2g})^6 \rightarrow (t_{2g})^5(e_g)^1$	40.0	White
trans-$[Co(py)_4Cl_2]^{+}$[b]	$(3d)^6$	$(t_{2g})^6 \rightarrow (t_{2g})^5(e_g)^1$	16.0	Green
trans-$[Rh(py)_4Cl_2]^{+}$[b]	$(4d)^6$	$(t_{2g})^6 \rightarrow (t_{2g})^5(e_g)^1$	24.5	Yellow
trans-$[Ir(py)_4Cl_2]^{+}$[b]	$(5d)^6$	—	—	White

[a] 1 kK (kilokayser) = 1000 cm^{-1}.
[b] All are the *trans*-dichloro isomers; py = pyridine, C_5H_5N.

from $(t_{2g})^3 \rightarrow (t_{2g})^2(e_g)^1$, the result of increasing bond strength (i.e., stability) is to increase the ligand field splitting ΔE (Table V).

The order of increasing splitting of the d levels by the ligands is the spectrochemical series: $F^- < OH_2 < NH_3 < NO_2^- < CN^-$. The last entry in Table V shows an example of the baricenter (center of gravity) rule. If the frequency of a particular transition in an environment (MA_6) is ν_1 and that for MB_6 is ν_2, then for $[MA_nB_{6-n}]$ it is the weighted average [Eq. (44)]. Such mixed coordination

$$(n\nu_2 + (6-n)\nu_2)/6 \qquad (44)$$

spheres, where there is more than one type of molecule acting as ligand, are very common. The effects of substituting ammonia by chloride for cobalt(III) $[3d^6]$ and chromium(III) $[(3d)^3]$ are shown in Table VI.

E. Photochemistry

The photochemistry (chemical reactions of molecules in excited electronic states, made by irradiating with light of the appropriate energy to promote them from their ground states) of complex compounds is not as useful as might be expected. In general, the most effective reactions are brought about not by d–d excitation but by other light absorptions, such as charge transfer. For example, on the irradiation of trisoxalatoferrate(III) ion with UV light, the process shown in Eq. (45) takes place through the photochemical excitation shown in Eq. (46).

$$[Fe(C_2O_4)_3]^{3-} \rightarrow [Fe(C_2O_4)_2]^{2-} + CO + CO_2^- \qquad (45)$$

$$\left[Fe(III) \leftarrow (C_2O_4)^{2-}\right] + h\nu \rightarrow \left[Fe(II) - (C_2O_4)^{-}\right]^{+} \qquad (46)$$

TABLE V Colors of d³ Coordination Complexes

Complex	λ[a]	n (=E/h)[b]	Color
$[CrF_6]^{3-}$	671	14.9	Green
$[Cr(OH_2)_6]^{3+}$	575	17.4	Violet
$[Cr(NH_3)_6]^{3+}$	464	21.55	Orange-yellow
$[Cr(CN)_6]^{3-}$	376	26.6	Pale yellow
$[Cr(NC_5H_5)_3Cl]_3^{c}$	629	15.9	Green
$[Cr(OH_2)_4Cl_2]^{+d}$	635	15.75	Green

[a] Wavelength of absorption maximum in nanometers.
[b] Frequency of absorption maximum in kilokaysers (1 kK = 1000 cm^{-1}).
[c] *Mer* isomer; NC_5H_5 is pyridine.
[d] *Trans* isomer.

F. Solvent Effects

Nearly all the basic notions of the chemistry of complex ions are derived from aqueous systems, and striking departures often occur when other solvents are used. For example, the coordination of iron(II) by diimine ligands changes its complexion as follows. In water $\beta_{110} > \beta_{120} \ll \beta_{130}$. The tris species, for example, $[Fe(phen)_3]^{2+}$, in water or isolated from water as salts with chloride and so on is *diamagnetic* (d^6 spin-paired). In *water*, where anions such as chloride are well solvated, paramagnetic solids such as $[Fe(phen)_2Cl_2]$ dismute, as in Eq. (47).

$$6H_2O + 3[Fe(phen)_2Cl_2] \rightarrow 2[Fe(phen)_3]^{2+} + Fe(OH_2)_6^{2+} + 6Cl^- \qquad (47)$$

In acetone and similar nonprotic solvents, the bis species is perfectly stable, and it is now the tris species that is unstable [i.e., $\beta_{120} \gg \beta_{130}$, the opposite of water; see Eq. (48)]. To speak of the spin pairing of the tris species as ligand field stabilization is incorrect, since that stabilization is effective only in water. The remarkable, and often quoted, reversal of the stability constants for adding the second and third chelating ligands to iron(II) ions must actually stem rather from changes in solvation energies of the anions present.

$$[Fe(phen)_3]^{2+} + 2Cl^- \rightarrow [Fe(phen)_2Cl_2] + phen \qquad (48)$$

TABLE VI Mixed Coordination Spheres on Cobalt(III) and Chromium(III)

Compound	ν^a log ε				
	Cobalt		Chromium		Color
$[M(NH_3)_6]^{3+}$	20.7	1.8	21.0	1.6	Orange
$[M(NH_3)_5Cl]^{2+}$	19.4	1.75	19.5	1.6	Pink
trans-$[M(NH_3)_4Cl_2]^+$	16.1	1.4	16.5	1.4	Green
cis-$[M(NH_3)_4Cl_2]^+$	19.1	1.9	19.2	1.9	Green

[a] In kilokaysers (1 kK = 1000 cm^{-1}).

G. Kinetic Properties of Coordination Compounds

Reactions of coordination compounds can be divided into several classes, depending on whether the oxidation state of any atom changes during the transformation of starting materials (factors) into products. No change gives a reaction such as Eq. (49).

$$[Co(NH_3)_5Cl]^{2+} + OH_2 \rightarrow [Co(NH_3)_5(OH_2)]^{3+} + Cl^- \quad (49)$$

Many formations and decompositions or other equilibrations of coordination compounds are extremely rapid. The half-life of a reaction such as the replacement ("substitution") by ammonia of water coordinated to nickel(II) ions is typically microseconds to milliseconds, and there is indeed a convenient distinction (due to Taube) for reactions in solution between kinetically labile and kinetically inert systems. On mixing 0.1 *M* aqueous solutions of the reagents, labile equilibria are fully established within 1 min, whereas inert systems take longer. Many of the ions of the heavier (second and third row) transition elements in several oxidation states (e.g., both Pt^{2+} and Pt^{4+}) are inert, as are many spin-paired d^6 ions (Fe^{2+}, Co^{3+}, Ni^{4+}) and chromium(III) in the first row. Kinetic lability in solution is the rule for coordination compounds containing main group metals. Reactions of solid coordination compounds (like most other solid-state changes) are usually slow. It is this kinetic inertness that has led to the isolation of so many metastable coordination compounds.

The decomposition (via substitution) of hexaamminecobalt(III) salts in acidic water [Eq. (50)] is thermodynamically very favorable; that is, *K* in Eq. (51) is very large, but the rate is extremely small. Solutions of such hexaamminecobalt(III) salts in dilute acid are unchanging for weeks.

$$[Co(NH_3)_6]^{3+} + 6H_3O^+ \rightleftharpoons [Co(OH_2)_6]^{3+} + 6NH_4^+ \quad (50)$$

$$K = [Co(OH_2)_6](NH_4^+)^6/[Co(NH_3)_6](H_3O^+)^6 \quad (51)$$

Isolating the less thermodynamically stable of two interconvertible forms of the same composition (whether it be coordination compounds, allotropes of elements, or any other chemical composition) can be done only if the *rate* of reaching equilibrium is so slow as to render the conversion of the *metastable* isomer to the stable one very protracted. This is a form of Ostwald's law of metastable intermediates. Such rates are slow (minutes < $t_{1/2}$ < years) for the equilibrations of coordinated cobalt(III), chromium(III), a few (spin-paired) d^6 ferrous compounds, such as salts of the ferroin **22a**, tris-1,10-phenanthrolineiron(II) cation, and a few octahedral nickel(II) species with strong field ligands ($3d^8$, e.g., the tris-1,10-phenanthrolinenickel(II) ion **22b**).

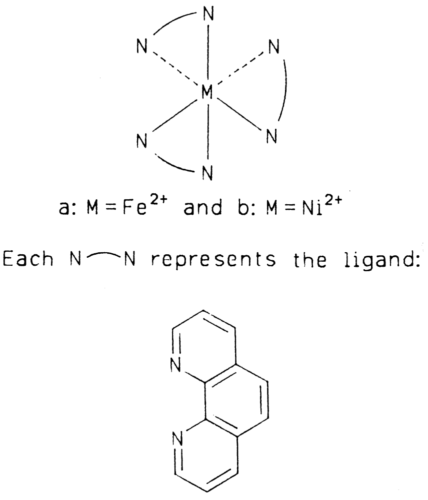

22

Oxidations and reductions are common and important, chiefly because coordination compounds of the transition metals may readily pass (often rapidly) from one oxidation state to another and because one-electron changes are common (whereas elsewhere in the periodic table, this would involve free-radical formation). For example, several named organic reagents utilize half-cells based on coordination compounds.

Typically, Decker's reagent is alkaline ferricyanide [hexacyanoferrate(III)], which may be used to oxidize the pseudobase **23** to the pyridone **24**, as in Eq. (52).

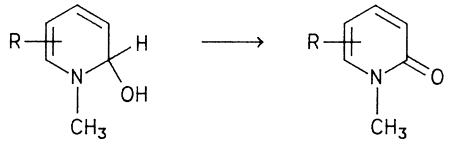

(52)

23 **24**

Many other such reactions occur with changes by a combination of oxidation–reduction and substitution. When Tollens's reagent, $[Ag(NH_3)_2]^+$, oxidizes aldehydes, the

product is silver metal. In Fehling's solution (which he originally called Barreswils's solution) the oxidant (for reducing sugars) is a complex compound of copper(II) with tartrate ions, and in Benedict's solution it is a complex with citrate ions. Sarett's reagent for oxidizing alcohols to aldehydes is a coordination compound of chromium(VI), $Cr(C_5H_5N)_2O_3$, where the chromium(VI) becomes reduced. There are many minor variations of this reaction.

Often, the compound to be oxidized is made a ligand, and the oxidation can then be intramolecular, as in the Dow phenol process [Eq. (53)], where the benzoate of basic copper(II) benzoate is oxidized to salicylate by hydroxide and then carbon dioxide is eliminated to yield phenol.

$$C_6H_5COOCuOH \rightarrow C_6H_5OH + CO_2 + Cu^0 \qquad (53)$$

A degradation of coordinated salicylate [**25**, Eq. (54)] is also typical. This chelating contraction [**25** (six-membered ring) → **26** (five-membered ring)] occurs readily in acid

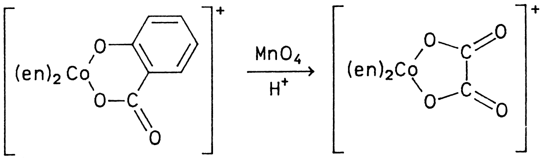

25 **26**

(54)

permanganate. Here is another side to the coin: The metal ion, in this case cobalt(III), somehow prevents the oxalate ion bound to it in **26** from undergoing its normal ("high school") oxidation by permanganate. Such "shielding" effects (loss of normal reactions) on coordination are well known.

Such modifications of the chemistry of ligands attached to metal ions are becoming increasingly important. Not all are oxidation or reduction.

The high-field, spin-paired nitrosopentacyanoferrate ion $[Fe(CN)_5(NO)]^{2-}$, often used as an aqueous solution of its salt—so-called sodium nitroprusside, $Na_2[Fe(CN)_5NO] \cdot 2H_2O$—undergoes many reactions of analytical importance, chiefly as qualitative tests, in which the nitroso ligand becomes modified, usually without detaching from the iron. Examples are the Gmelin test for sulfur in organic matter (Lassaigne sodium fusion to give sulfide, which gives a strong purple color with the FeNO unit) and the Bodlander reaction with sulfite to give a bright red color.

Evens so simple a reaction as acid–base equilibrium in the ligands is strongly modified by metal ions. In Eq. (55),

$$[L_5M(OH_2)]^{n+} \rightleftharpoons [L_5M(OH)]^{(n-1)+} + H^+ \qquad (55)$$

the acid dissociation to form proton and the conjugate base may be strong (e.g., for $L = H_2O$, $M = Fe$, $n = 3$, $pK_a = 2.7$, comparable to that of monochloracetic acid!). Even the acid dissociation of ammonia to give its conjugate base is said to become perceptible when it is attached to a highly charged metal ion, as in Eq. (56).

$$[Pt(NH_3)_6]^{4+}\,(aq) \rightleftharpoons [Pt(NH_3)_5(NH_2)]^{3+} + H^+\,(aq) \qquad (56)$$

Certainly such proton transfers have extremely large rate constants.

In water, nearly all substitutions into a coordination sphere (i.e., of one ligand for another) have a very simple rate equation:

$$\text{Rate} = k[\text{complex}] \qquad (57)$$

That is true whether the rate constant k is large (labile) or small (inert), but tells us nothing about the detailed mechanism.

There are a few situations in which the rate equation is a little more interesting than Eq. (57); for example:

1. Substitution at platinum(II) $[(5d)^8]$; four-coordinated square species. Here, often,

$$\text{Rate} = k[\text{complex}][\text{incoming nucleophile}] \qquad (58)$$

2. "Base hydrolysis" (substitution by hydroxide ion) of coordination compounds of cobalt(III) with ligands containing an N–H group. The unusual rate equation is

$$\text{Rate} = k[\text{complex}][OH^-] \qquad (59)$$

This is commonly thought to imply the presence of a reactive conjugate base, typically via Eqs. (60)–(63):

$$[Co(NH_3)_5Cl]^{2+} + OH^- \rightarrow [Co(NH_3)_4(NH_2)Cl]^+ + H_2O \qquad (60)$$

$$[Co(NH_3)_4(NH_2)Cl]^+ \rightarrow [Co(NH_3)_4(NH_2)]^{2+} + Cl^- \qquad (61)$$

$$[Co(NH_3)_4(NH_2)]^{2+} \rightarrow [Co(NH_3)_4(NH_2)(OH_2)]^{2+} \qquad (62)$$

$$[Co(NH_3)_4(NH_2)(OH_2)]^{2+} + H_2O \rightarrow [Co(NH_3)_5(OH_2)]^{3+} + OH^- \qquad (63)$$

This gives Eq. (64) [with the loss of chloride from the conjugate base, Eq. (61), as the slow-rate-determining step]:

$$\text{Rate} = k[Co(NH_3)_4(NH_2)Cl]^{2+} \qquad (64)$$

$$= kK[Co(NH_3)_5Cl][OH^-] \qquad (65)$$

The base hydrolyses of the much studied cobalt(III) compounds are dominated by this type of equation, whereas the coordination compounds of the equally polarizing

ions chromium(III) and rhodium(III) with ligands capable of forming conjugate bases do not seem to exhibit this behavior.

3. Base hydrolysis (and in a very few cases attack by cyanide or other nucleophiles) on a number of coordination compounds with the ligand C=N. Often, the ligand is part of an aromatic ring. For instance, for all the base hydrolyses such as Eq. (66) (substitution of an N-heterocyclic ligand LL, usually 2,2′-bipyridyl or 1,10-phenanthroline, by hydroxide), although there can obviously be no conjugate base formed by protonic dissociation (there are *no* acidic protons) the rate equations are nevertheless as in Eq. (67):

$$M(LL)_3^{n+} + OH^- \rightarrow [M(LL)_2(OH)(OH_2)]^{(n-1)+} + LL \quad (66)$$

$$\text{Rate} = [M(LL)_3]\left(k_0 + k_1[OH^-] + k_2[OH^-]^2\right) \quad (67)$$

In a similar way, the rate equations for substitution by cyanide ion are as in Eq. (68):

$$\text{Rate} = [M(LL)_3]\left(k_0 + k_1[CN^-] + k_2[CN^-]^2\right) \quad (68)$$

In the latter case, a typical example is the ready reaction of ferroin with cyanide in water to give the Schilt–Barbieri compound:

$$[Fe(phen)_3]^{2+} + 2CN^- \rightarrow [Fe(phen)_2(CN)_2] + phen \quad (69)$$

The most reasonable interpretation (there have been many) is to consider the hydroxide or cyanide as forming first an sp^3-hybridized carbon atom (a pseudobase or Reissert-type adduct, respectively) and then being transmitted from carbon to metal ion. In other words, the change in reactivity of an N-heterocycle on coordination to a metal ion is akin to that of the same N-heterocycle on classical quaternization by an organic agent such as methyl iodide. The unusual rate equation [Eq. (67) or (68)] involving the nucleophile's concentration in first- and second-order terms arises because the rates of these reactions (apparently hydrolysis or substitution by cyanide at the metal ion) are actually controlled by rates of reaction at the ligand (**27** → **28**).

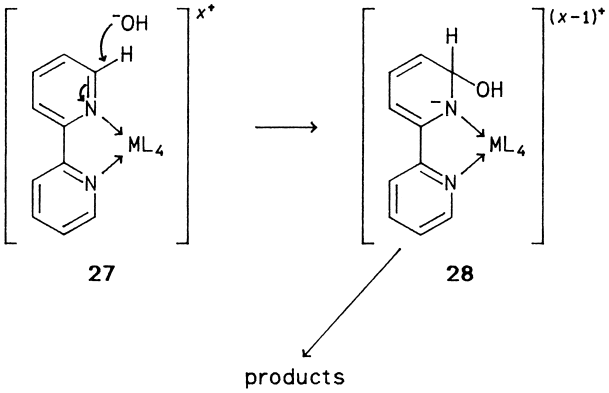

27 **28**

Certainly, the presence of an imine-like carbon atom adjacent to the coordinated nitrogen seems necessary for values of k_1 in rate equations (67) or (68) to be large.

4. The unusually rapid coordination to initially inert aquo metal ions of a few oxo anions (XO_{ny}^{y-}), for example, X = N, $n = 2$, $y = 1$ for ONO^-, may involve a rate-controlling reaction at the oxygen of water (path **29**) rather than the metal (path **30**).

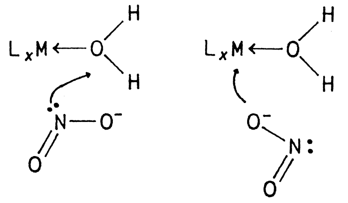

29 **30**

H. Catalysis

If one defines a catalyst as "a species whose activity appears to a higher power in the rate equation than in the stoichiometric equation," many kinds of transformation of coordination compounds may be subject to catalysis. For example, the replacement of fluoride in Eq. (70) has the stoichiometric and rate equations given in Eqs. (71) and (72), respectively. The proton is said to be a catalyst, probably through the intermediate compound (**31**) with hydrogen fluoride as ligands:

$$[Co(NH_3)_5F]^{2+} + H_2O \rightarrow [Co(NH_3)_5(OH_2)]^{3+} + F^- \quad (70)$$

$$K = \frac{[Co(NH_3)_5(OH_2)][F]}{[Co(NH_3)_5F]} \quad (71)$$

$$\text{Rate} = k[Co(NH_3)_5F][H^+] \quad (72)$$

Other ligands that are the conjugate bases of weak Brönsted acids (e.g., NO_2^-) show similar catalysis by a proton. In the case of coordinated nitrite, the proposed protonated intermediates (**32**) may actually be isolated in solid salts [here the nitrate $[Co(NH_3)_5(HONO)](NO_3)_3$]. In both **31** and **32**. A represents the ligand NH_3.

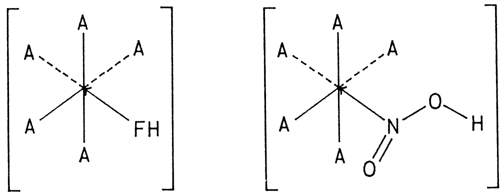

31 **32**

Genesis of the famous Zeise's salt. $K[Pt(C_2H_4)Cl_3]$, made by the slow reaction of potassium tetrachloroplatinate(II) with ethene in water (for ~5 days) is dramatically

$$trans\text{-}[Cr(OH_2)_4Cl_2]^+ + (EDTA)^{4-} \longrightarrow [Cr(EDTA)]^- + 2Cl^- \quad (73)$$

$$[Cr^{II}(OH_2)_4Cl_2]^0 + (EDTA)^{4-} \longrightarrow [Cr(EDTA)]^{2-} \quad (74)$$

(Zn, Green: $trans$-$[Cr(OH_2)_4Cl_2]^+ \rightarrow [Cr^{II}(OH_2)_4Cl_2]^0$; Purple: $[Cr(EDTA)]^{2-} + [Cr(OH_2)_4Cl_2]^+ \rightarrow [Cr(EDTA)]^-$)

catalyzed by a small amount of tin(II) chloride; in its presence, the Zeise's salt forms quickly.

By far the most important catalytic reactions of coordination compounds are those based on oxidation and reduction. Typically, a kinetically labile oxidation state, usually for the first transition series, $3d^{n+1}$, is added to or generated (*in situ*) from an inert one, $3d^n$. An example is shown in Figs. (73) and (74).

Reaction (73) has a very large value of $K = [Cr(EDTA)^-]/[[Cr(OH_2)_4Cl_2]^+][(EDTA)^{4-}]$, so the formation of the purple complex chelated product should be strongly favored, but the half-life is in fact several hours at 15°C. Zinc metal (merely a reducing agent, a source of electrons) rapidly reduces chromium(III) to chromium(II), which is (with its $(3d)^4$ electronic configuration) kinetically labile, and so comes to equilibrium with the $(EDTA)^{4-}$ ligand rapidly ($t_{1/2} = 10^{-7}$ s), forming a quite stable chromium(II)–EDTA compound [Eq. (74); $\beta_{110} \approx 10^{14}$]. The product is now oxidized *rapidly* [Eq. (75)] by electron transfer:

$$[Cr(EDTA)]^{2-} + trans\text{-}[Cr(OH_2)_4Cl_2]^+ \rightarrow [Cr(EDTA)]^- + [Cr(OH_2)_4Cl_2]^0 \quad (75)$$

The same result can be achieved by adding a salt of chromium(II) rather than by forming it *in situ*. Table VII gives some similar redox-catalyzed substitutions. Note that, as in Table VII, whereas the first-row metal ions (here, chromium and cobalt) often have stable oxidation states separated by a single electron [cf. Fe(III) and Fe(II); Cu(II) and Cu(I)], their heavier congeners (here, rhodium and platinum) often have states differing by two charges [cf. Pd(IV) and Pd(II); Au(III) and Au(I)]. The principle of complementarity indicates that, for these heavier metals, such two-electron reductants as primary or secondary alcohols will readily give the catalytic-reduced states.

Many of the most important catalytic activities of coordination compounds and metal ions (particularly iron and copper) are in the electron transport chains of cellular metabolism, where they act as catalysts for the oxidation of organic intermediates. Several other transition metal ions (including vanadium and molybdenum) have important metabolic roles in a variety of organisms. Indeed, recent discoveries suggest that even such metals as chromium and nickel have biological functions.

IV. SHAPE

A. Coordination Number

The formula of a complex compound is established once we know the oxidation state of the metal in the ion and the (coordination) number of ligands attached to it. What can we say about the latter quantity?

The coordination number (i.e., the number of ligand atoms in direct contact with the metal atom) of metal ions

TABLE VII Syntheses via Catalysis

Metal	Inert oxidation state	Electronic configuration	Catalyst	Labile oxidation state	Electronic configuration	Example
Chromium	III	$3d^3$	Zinc	II	$3d^4$	$[Cr(EDTA)]^-$, $[Cr(en)_3]^{3+}$
Cobalt	III	$3d^6$	Charcoal[a]	II	$3d^7$	$Co(NH_3)_6^{3+}$
Rhodium	III	$4d^6$	$R'_3CC\underline{H}ROH$[b]	I	$4d^8$	$[Rh(NH_3)_5Cl]Cl_2$
Platinum	IV	$5d^6$	—	II	$5d^8$	Halo substitution, $[Pt(S_5)_3]^{2-}$

[a] Acts, rather like a graphite electrode, as a source of electrons, i.e., a reducing agent.
[b] The hydrogen underlined here is thought to act as the two-electron source (i.e., $H^- \rightarrow H^+ + 2e^-$).

TABLE VIII Coordination Numbers and Associated Shapes

Coordination number	Shape	Point group	Examples
2[a]	Linear	$C_{\infty h}$	$[CuCl_2]^-$
			$[Ag(NH_3)_2]^+$
4	Tetrahedral	T_d	$[BeF_4]^{2-}$
			$[CoCl_4]^{2-}$
			$[Zn(NH_3)_4]^{2+}$
	Plannar	D_{4h}	$PtCl_4^{2-b}$
			$AuCl_4^{-b}$
			ICl_4^-
5	Pyramidal	C_{4v}	$[OV(OH_2)_4]^{2+}$
	Bipyramidal	D_{3h}	$[InCl_5]^{2-}$
6	Octahedral	O_h	$[AlF_6]^{3-}$
			$[RhCl_6]^{3-}$

[a] On the whole, two coordination is found for the lower oxidation state (I) of the coinage metals (copper, gold, silver) and among their isoelectronic neighbors [e.g., $Hg(OH_2)_2)^{2+}$, $Tl(OH_2)_2^{3+}$].

[b] Note that these are isoelectronic (so the same structure is expected).

in simple coordination compounds varies (as it does in binary and ternary crystalline structures) from 2 up to ~ 12. The most common (all others up to 12 are known) are 2, 4, 5, 6, and (for some of the larger ions—barium and radium; thorium; zirconium, hafnium, and some lanthanides and actinides) 8. Table VIII gives examples of coordination numbers and the associated shapes.

There are many rules of thumb for rationalizing *changes* in coordination number for a particular metal and among metals in general. For a given metal ion with a particular ligand in a particular solvent—usually water—such changes are manifested by sudden discontinuities in properties. With Hg^{2+} in water, the successive stepwise stability constants with chloride are $K_{110} > K_{120} \ggg K_{130} \cdots$. Whereas the first two chloride ligands attach to mercury very well, giving successively $(HgCl)^+$ and $(HgCl_2)^0$, the third one has little affinity. Presumably, the stable linear two-coordinated structure is being altered to a three-coordinated $HgCl_3^-$ (triangular) or four-coordinated $Hg(OH_2)Cl_3^-$ (tetrahedral).

In general, if a particular metal ion in a particular oxidation state manifests, under different circumstances (i.e., with a variety of ligands), more than one coordination number, the changes (based on the Pauling electroneutrality principle) are as follows:

1. Anions have lower coordination numbers than cations:

$$[CoCl_4]^{2-} \quad \text{versus} \quad [Co(OH_2)_6]^{2+}$$
$$[MnCl_4]^{2-} \quad \text{versus} \quad [Mn(OH_2)_6]^{2+}$$

2. The more polarizable the ligand, the lower is the coordination number: $[AlCl_4]^-$, $[AlF_6]^{3-}$.

For any one metal, the ions in increasingly positive oxidation states become smaller [i.e., rFe^{3+} (spin free) $(3d^5) < rFe^{2+}$ (spin free) (d^6); $rCu^{2+}(d^9) < rCu^+(d^{10})$]. The coordination number with a given ligand tends to increase with this shrinkage, perhaps because the more highly charged cation has much increased electron attachment enthaply, requiring more of the same ligands to become electroneutral. Examples (which abound) are $TlCl_6^{3-}$, $TlCl_4^{3-}$; ICl_4^-, ICl_2^-; CuF_6^{3-}, CuF_4^{2-}; $PtCl_6^{2-}$, $PtCl_4^{2-}$; $SnCl_6^{2-}$, $SnCl_3^-$; $Ag(C_5H_5N)_4^{2+}$, $Ag(C_5H_5N)_2^+$; $(AuCl_4)^-$, $(AuCl_2)^-$. In the cases of the electronic configurations d^8 and d^6, for the same metal the interconversion of one state to the other is often called oxidative addition (or reductive elimination in the opposite direction):

$$MCl_4^{2-} + Cl_2 \rightarrow MCl_6^{2-} \qquad (\text{e.g., } M = Pd, Pt) \quad (76)$$

For the same ligand with varying metal ions there is (in crystalline binary compounds) a general tendency for the coordination numbers of the cations to increase on going down a eutropic family (as in SiO_2, GeO_2, SnO_2, PbO_2). This is not as true of isolated complexes in coordination compounds. The sizes of corresponding ions do increase down the three transition series, but this increase is often swamped by the sharing of the effect among several ligands. For example, the bond lengths $M \leftarrow N$ for $Co(NH_3)_6^{3-}$, $Rh(NH_3)_6^{3+}$ and $Ir(NH_3)_6^{3+}$ are sufficiently alike that many triads of their analogous salts, for example, $[M(NH_3)_6](NO_3)_3 \cdot HONO_2$ or $[M(NH_3)_5](OH_2)](NO_3)_3 \cdot HONO_2$, are isostructural for $M = Co$, Rh, Ir.

The growth in size of the s-block ions is well known, as in $rMg^{2+} < rCa^{2+}$ (1.06 Å) $< rSr^{2+}$ (1.33 Å) $< rBa^{2+} < rRa^{2+}$, and the coordination numbers with *like* ligands do tend to increase down these series. However, the metal ions [other than the very small ones of the higher oxidation states, Mn(VII) and the like] of atomic number greater than 19 are all large enough to accommodate the higher coordination numbers (8). For the electropositive elements at the start of the transition series, the lanthanide contraction ensures that $(5d)^n$ ions are about the same size as their $4d^n$ congeners but both are larger than $3d^n$ (e.g., $Ti^{4+} < Zr^{4+} \simeq Hf^{4+}$; $V^{3+} < Nb^{3+} \simeq Ta^{3+}$; $Cr^{3+} < Mo^{3+} \simeq W^{3+}$). Typical complex compounds contain TiF_6^{2-}, ZrF_8^{4-}, and HfF_8^{4-}.

B. Structures and Their Symmetries

The coordination number 4 is fairly common, and there are two limiting shapes, as listed in Table VIII: the planar and the tetrahedral. For main group metals, tetrahedral ions

such as $[BeF_4]^{2-}$, $[AlCl_4]^-$, and $[Zn(NH_3)_4]^{2+}$ are common. For the first transition series, they are quite common among anions and with very polarizable ligands, as in the blue ion $[CoBr_4]^{2-}$ and in the blue β form (so-called for historical reasons: names used to distinguish polymorphic varieties are unsystematic) of $[Co(C_5H_5N)_2Cl_2]$. There is another form of this dimorphic compound, the pink α, which is polymeric in the crystal (through chlorine bridging two cobalt ions) and contains octahedral cobalt(II) ions. The very highly polarizing ions of the highest oxidation states of the central transition elements often have essentially tetrahedral shapes. Some examples are VO_4^{3-}, CrO_4^{2-}, MnO_4^- these being an isoelectronic set; MnO_4^{2-}; FeO_4^{2-} (so-called ferrate); $[CrO_3Cl]^-$, $[TcO_4]^-$, $[ReO_4]^-$, $[OsO_4N]^-$ (osmiamate); and many others.

The planar four-coordinated molecules are of great rarity in main group chemistry (ICl_4^-, XeF_4) but dominate the simple coordination chemistry of spin-paired d^8 species. These crop up among the second and third row platinum and coinage metals, and there are a few examples for $(3d)^8$, chiefly for nickel(II) with strong-field (polarizable) ligands: $[Ni(CN)_4]^{2-}$, $[Pd(NH_3)_4]^{2+}$, $[Pt(NH_3)_2Cl_2]$, $[AuCl_4]^-$.

C. Isomerism

Kinetically labile copper(II) ions, in water, combine with an excess of L-alaninate ligands (LAla-O)$^-$ to give a solution (at pH 8.3) that contains only the uncharged species [Cu(LAla-O)$_2$]. This species, planar about the copper ion, may exist as *cis* (**33**) or *trans* (**34**) isomers. The equilibrium

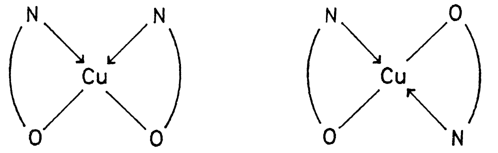

33 **34**

N⌒O represents H$_3$C—CH(NH$_2$)COO$^-$: LAla-O$^-$

ratio in solutions has been said to be

$$K = [trans]/[cis] = 1.5$$

Trans and *cis* isomers must be in labile equilibrium, the copper(II) ion being so rapid in its reactions. Nevertheless, both *trans* and *cis* forms can be obtained as crystals from the solution. A concentrated solution initially deposits Cambridge blue crystals of the *trans* isomer **34**, but if left for a few days these are gradually replaced by the more stable Oxford blue crystals of the *cis* isomer **33**.

TABLE IX Properties of *Cis* and *Trans* Isomers of Square [PtA$_2$B$_2$]

Geometry A	Geometry B	Isomer	μ^a	Other properties
NH_3	Cl	*Cis*	—	$H_2SO_4 \rightarrow$ adduct Drug
NH_3	Cl	*Trans*	—	$H_2SO_4 \rightarrow$ no adduct Not drug
$P(C_2H_5)_3$	Cl	*Cis*	10.6	White
$P(C_2H_5)_3$	Cl	*Trans*	0	Yellow

[a] Dipole moment (in debye units).

The subtlety of metal complex chemistry is manifest in the apparently similar bisglycinatocopper(II) system, the behavior of which is actually opposite to that of alaninate: The initial aqueous solution gives first the metastable crystals of the *cis* isomer, which is slowly replaced by the *trans*.

For the kinetically inert spin-paired d^8 species, such as palladium(II) and platinum(II), this *cis–trans* (geometric) isomerism occurs frequently. Table IX shows some examples. For such compositions as those in Table IX, there is often another kind of isomerism (ionization isomerism) in which the same stoichiometry Pt–2NH$_3$–2Cl is given by such salts as $[Pt(NH_3)_4][PtCl_4]$ and $[Pt(NH_3)_3Cl][Pt(NH_3)Cl_3]$. The former, Magnus's green salt, has columns or chains of platinum ions running through the structure (**35**, A = NH$_3$).

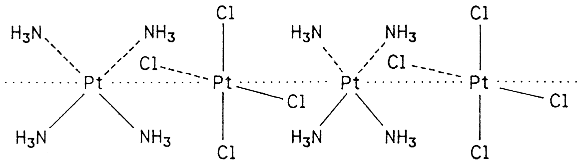

35

Related structures may give rise to desirable electronic properties, such as one-dimensional conductance (along the Pt–Pt axis).

Far and away the most common coordination number is 6, with the ligands arranged at the corners of an octahedron. For metals from atomic number 11 (sodium) upward, more complex ions and compounds contain six-coordinate metal ions than not. Examples of ions are $[Cr(\underline{N}CS)_6]^{3-}$, where the underlining of the N indicates that it is this constituent of the ligand, rather than the sulfur atom, that is directly attached to the metal, $[SnCl_6]^{2-}$, $[Ni(H_2NCH_2CH_2NH_2)_3]^{2+}$, $[Ru(bipy)_3]^{2+}$, and $[Pt(S_5)_3]^{2-}$.

Isomers are particularly common among six-coordinated compounds, although there are many cases for

other coordination numbers. The extraordinarily selective synthesis form the dianion of the natural amino acid L-cysteine as a *bi*dentate ligand at cobalt(III), to give dark green tris-L-cysteinato-(*N*,*S*)-cobaltate(III), illustrates the chief causes of isomerism among coordination compounds.

L-Cysteinate (the doubly charged anion) is represented by structure **36**.

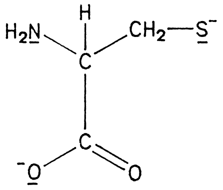

36

The three atoms underlined are all possible donor sites, but since only two are used to form each of the three chelate rings, this ligand could be attched through (1) nitrogen and oxygen (chelated α-amino acidate, with a pendant unattached thiolate, $-CH_2S^-$), (2) sulfur and oxygen (a chelated β-thiocarboxylate, with unattached NH_2), or (3) sulfur and nitrogen (chelated 1-amino-2-thiolate, with pendant carboxylate). This variability of mode of attachment of a ligand is called linkage isomerism. Other ligands with such multiplicity of possible binding sites may be unidentate and include (among several) nitrite attached via nitrogen, for example, $[Co(NH_3)_5(\underline{N}O_2)]$, so-called nitropentamminecobalt(III) ion, a yellow ion; nitrite attached via oxygen, $[Co(NH_3)_5(\underline{O}NO)]^{2+}$, so-called nitritopentamminecobalt(III) ion, a red ion; thiocyanate attached via sulfur, for example, $[Rh(NH_3)_5(\underline{S}CN)]^{2+}$; or "isothiocyanate," nitrogen-bonded $[Rh(NH_3)_5(\underline{N}CS)]^{2+}$.

Representing the bidentate L-cysteinate as N–S, three of these may be coordinated as in **37** or **38**.

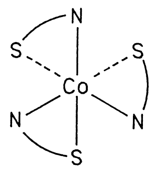

(fac)
37

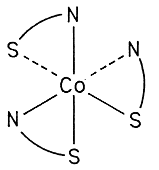

(mer)
38

In the discussion of stepwise stability constants [see Eq. (5)], the more symmetric facial and less symmetric meridional isomers of $[MA_3B_3]$ were distinguished from their probabilities of formation (*mer*-**9**, 60%; *fac*-**10**, 40%). In the present case, only the *fac* isomer is formed. Such geometric isomers have the same composition but different molecular symmetries.

D. Optical Activity

Finally, there are for the *fac* isomer **37** (point group C_3) (and indeed the *mer* isomer **38**, C_1, or for any other geometry that has only axial symmetry, D_3, C_2, and so on) two forms of the molecule that differ, as do right- and left-handed propellers (**39** and **40**). Such an object (molecule) cannot be superimposed on its image in a mirror. The labels attached (by arbitrary convention) to propeller molecules, such as

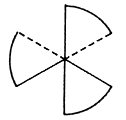

[Δ,L,$R(C_3)$,$P(C_3)$]
39

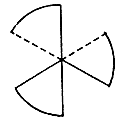

[Λ,D,$S(C_3)$,$M(C_3)$]
40

are shown [from minus (M), plus (P), sinistral (*S*), rectal (*R*); Λ refers to left-helicity about the threefold axis, Δ to right; D and L are for dextro (right) and levo (left)].

E. Stereoselectivity

To distinguish right from left requires an all-one-handed agent (either all right or all left). For an all-right-distinguishing agent, the differing interaction combinations are right–right and right–left. This is the same difference as between shaking hands and holding hands. Isomers formed from differing combinations of right- and left-handed (chiral) parts of molecules are known as diastereoisomers. Natural (optically active) L-cysteine selects the $S(C_3)$ propeller of cobalt(III). Such selection among the posible diastereoisomers is known as stereoselectivity.

The sole product, from among all the possible isomers, is $S(C_3)$-*fac*-$[Co(\text{L-cysteinate-N,S})_3]^{3-}$, which can be readily crystallized as its potassium salt. Such selective syntheses (where one among several possible reactions occurs preferentially rather than at random) are now more readily achieved than hitherto.

Tartaric acid (or its conjugate bases) can select between the right and left hands (**41** and **42**) of DL-$[Co(en)_2(CO_3)]^+$, giving the very stable diastereoisomer **43**. This effectively takes all the L-cobalt centers out of commission, so that on adding symmertric reagents (e.g., $\underline{N}O_2^-$), the only place for reactions is the D-cobalt of **44**, giving the D-$[Co(en)_2(\underline{N}O_2)_2]^+$ ion **45a**. The overall ionic charges on the complex ions **41–46** are omitted, but all the complexed cobalt centers are cobalt(III).

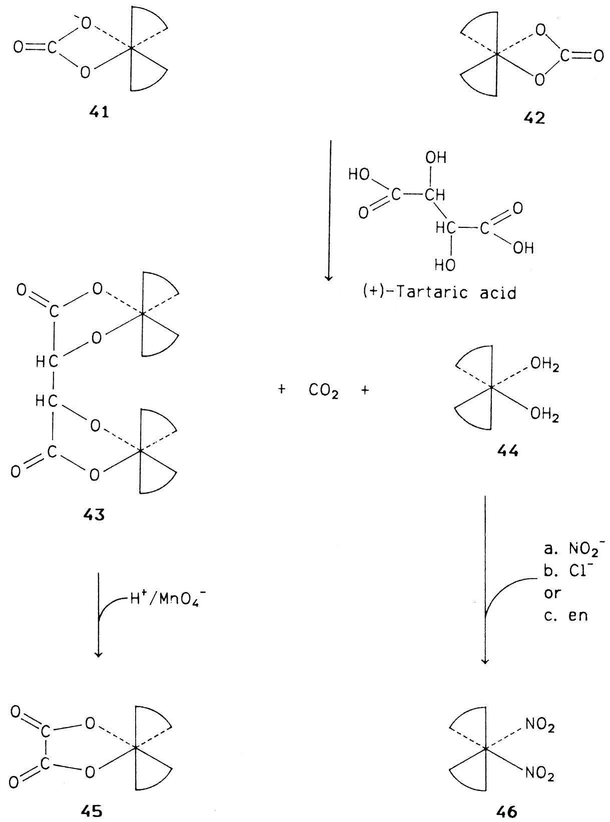

This is a neat dissymmetric synthesis of the product, *cis*-dinitrobis(1,2-diaminoethane)cobalt(III) (**46**), which, in principle, can be done in one reaction vessel.

A similar convenient "one-pot" synthesis of an optically active coordination compound from "off-the-shelf" reagents involves reducing aqueous hexachlororuthenate(IV) ion with dissymmetric (+)-tartaric acid (a natural product) and presumably forming preferentially one of the several possible diastereoisomeric (+)-tartratoruthenium species. On the addition of excess of 2,2′-bipyridyl, it substitutes stereoselectively, giving an excess of (+)-$[Rubipy_3]^{2+}$ over its (−) enantiomer. This product, when racemic, has been used as a photocatalyst in many attempts to catalyze reaction (77), the photolysis of water (as a solar energy utilizer),

$$2H_2O + h\nu \rightarrow 2H_2 + O_2 \qquad (77)$$

A great deal of effort is being made to modify the ligands in this *N*-heterocyclic complex, to improve or alter solubility and oxidation-reduction properties. The final oxidative degradation by acid permanganate of the tartrate ligand in the stable diastereoisomer **43** (this bridging two cobalt ions) gives breakage of the carbon–carbon bond but no rupture of any bond to chiral cobalt(III). Clearly, the handedness of the propeller about cobalt in the product (**45**) is the same as that in the reactant (**43**). This chemical transformation proved that the two chiralities (handedness of propeller) are related and is called a chemical correlation of configuration. Other examples include Eqs. (78)–(80):

$$(+)\text{-}cis\text{-}[Co(en)_2(\underline{N}CS)_2]^+ \rightarrow (+)\text{-}cis\text{-}[Co(en)_2(\underline{N}H_3)_2]^{3+} \qquad (78)$$

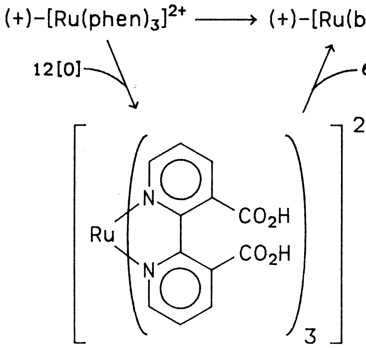

(79)

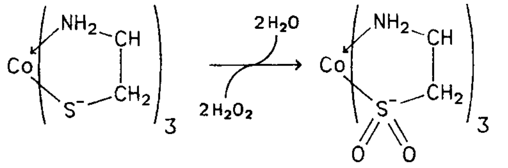

(80)

Equation (80) represents the transformation of coordinated thiolate in the dark green triscysteinate complex of cobalt(III) by oxidation using hydrogen peroxide to the yellow sulfinate. In full, it can be written

$$fac\text{-}[Co(\text{L}Cys)_3]^{3-} + 6H_2O_2 \rightarrow \text{L-}fac\text{-}[Co(\text{L}Cysu\text{-}N,S)_3]^{3-} + 6H_2O \qquad (81)$$

The cysteine sulfinate is abbreviated Cysu, and this dissymmetric yellow anion is a splendid resolving agent for triply charged racemic cations such as $[M(en)_3]^{3+}$ (M = Cr, Co, Rh) or $[M(bipy)_3]^{3+}$(M = Co, Cr). All such chemical correlations of configuration are reactions of coordinated ligands.

F. Resolutions

Selection among diastereoisomers is not, of course, restricted to such intramolecular cases as the tris-(*N*,*S*)-cysteinatocobaltate(III), where all the chiral centers (at the metal ion and in the organic molecules) are in the same molecule. Wherever a single-handed molecule or chiral influence (say, right) interacts with a racemic (50 : 50 right–left) mixture, there are the diastereoisomeric pair of unequal possibilities right–right for the right-handed half of

TABLE X Diastereoisomer Salt Formation

Racemate (X)	Resolving agent (A)	Solvent	LSD[a]
$(NH_4)_2[Pt(S_5)_3]$	$(-)$-$[Ru(bipy)_3](ClO_4)_2$	Acetone	$(-)A(-)X$
$[Co(EDTA)]^-$	L-Histidinium	Water–ethanol	$(+)A(+)X$
$Na[Rh(HN{-}SO_2{-}NH)_2(H_2O)_2]^-$	$(+)$-$H_3CCH(C_6H_5)NH_2$	Water	$(+)A(+)X$
$[Ru(bipy)_3]^{3+}$	$(+)$-$[Co(LCysu)_3]^{3-}$	Water	$(+)_{350}X(+)A$
$[Co(en)_2(NO_2)_2]^+$	$(+)$-$[Co(EDTA)]^-$	Water	$(-)X(+)A$

[a] This column describes the less soluble diastereoisomeric (LSD) slat formed from the resolving agent (A) and one hand of the racemate. It gives (sign of rotation of the cation) (sign of rotation of the anion). This measurement was done at the yellow lines of sodium, except for the $[Rh(biby)_3]^{3+}$ ion, where the rotation is at 350 nm, as indicated by the subscript $(+)_{350}$.

the racemic mixture and right–left for the left-handed half. Table X shows some examples of resolutions.

Pasteur found for organic racemates involving asymmetric tetrahedral carbon atoms that microorganisms (themselves made up of chiral molecules all of one hand; i.e., bacteria are very stereospecific reagents) metabolize one hand much more rapidly than the other. In much the same way, microorganisms show at least stereoselectivity and occasionally, apparently, stereospecificity (100% selection) for those few octahedral chelated compounds that have been studied. For example, racemic *mer*-trisglycinatocobalt(III) serves as a nitrogen source for *Pseudomonas stutzeri*, but only the D hand is consumed; the L is unaffected. This is the best way to obtain this uncharged complex compound in optically active form.

G. Jahn–Teller Effect

For the common four- and six-coordinated shapes, lowering of symmetry by di- or trisubstitution of one ligand by another leads to geometric isomerism (where the shape of the field around the metal ion differs between the two isomers, e.g., fac and mer). Similarly, for the six-coordinated octahedron (O_h), lowering of symmetry by removing reflection elements (center, plane, or improper axis), as in **47**, gives the

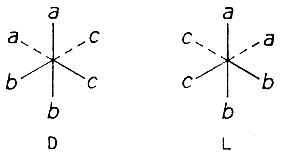

47

possibility of enantiomerism. This is usually done by chelating. Examples of racemates D-**47** + L-**47** are known. Of the several claimed separations of D-**47** from L-**47** (optical resolution) at least that of $[Co(NH_3)_2(NO_2)_2(CN)_2]$ seems authentic.

Quite apart from such modification of essentially symmetric shapes, there is another general effect, causing distortion of symmetric shapes, that is particularly common among coordination compounds of some transition metals (but also known for other species, such as the first electronic excited state of benzene). This is the Jahn–Teller effect. For nonlinear assemblies of nuclei and electrons, unequal occupancy of degenerate orbitals is unstable, and there will be a lower energy state of different geometry in which the nuclear framework has been distorted. Taking the electronic configurations of spin-free d^4 [e.g., Cr(II), Mn(III)] and any d^9 [e.g., Cu(II), Ag(II)] as examples, in octahedral ligand fields the electron occupancy is shown in **48** and **49**,

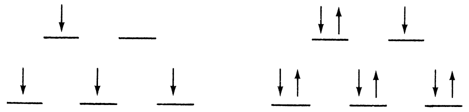

48 **49**

respectively. The Jahn–Teller theorem says that the nuclei will move to lift the degeneracy (i.e., $x = y \neq z$), as in Fig. 6. There are many cases of such distortion. Indeed, either (or both) the ground state or the first excited state of all configurations d^n ($1 \leq n \leq 9$) is subject to Jahn–Teller distortion. Particularly noticeable are departures from regular shape in which the unequally occupied degenerate orbitals are antibonding; some examples are given in Table XI. The energy level diagram for T_d for a particular d^n is the inverse of that for O_h, for the same d^n shown in Figs. 4 and 5.

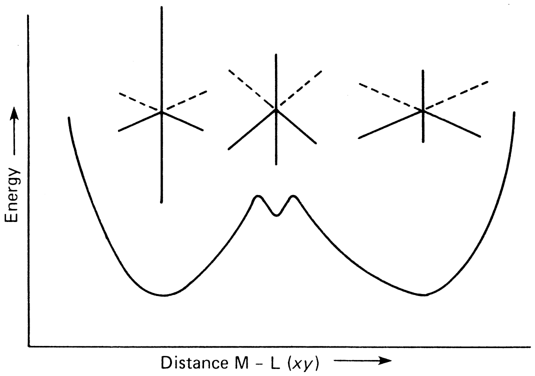

FIGURE 6 Two possible distortions (along normal coordinates) of an octahedral compound MX_6 with all six MX distances equal (center point) to "four short, two long" $MX_4^sX_2^l$ or "two short, four long" $MX_s^2X_4^l$.

V. BIOLOGICAL METAL COMPLEXING

The number of metals known to be essential to a range of living species has increased markedly during the twentieth century, so that the "biological periodic table" is now a large fraction of the periodic table itself. Most of the metal requirements are as trace elements, such as vanadium in mushrooms. The vanadium (in the famous *Amanita muscaria*, the red-capped mushroom with white spots) occurs in the same coordination compound throughout the mushroom. This compound, amavanadin, originally isolated from a Black Forest species, is said to have structure **50**.

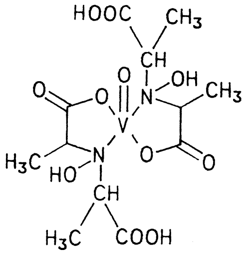

50

Many natural coordination compounds exist—for example, vitamin B_{12}, in which the central metal is cobalt(III), with six ligands, five of which are imine-like or heterocyclic nitrogen, and the sixth an alkyl group (or in the well-known artifact, now called cyanocobalamin, formed during the original isolations, cyanide).

The striking fact about biological metal complex chemistry is its novelty. When first isolated, metal-containing molecules and metal-in-volving systems from living cells almost always turn out to have features that have no real counterpart in known synthetic (*in vitro*) coordination compounds. Much effort has been expended on developing "model systems" to reproduce these natural biochemical ingenuities. For example, the stable carbon–cobalt(III) bond in vitamin B_{12} has been mimicked in the bis-1,2-dionedioximatocobalt(III) moiety (**51**) (the so-called cobaloximes), in which the nitrogen donors of the oxime ligands (whose imine function is very similar to that in N-heterocycles) are held planar by strong intramolecular hydrogen bonds.

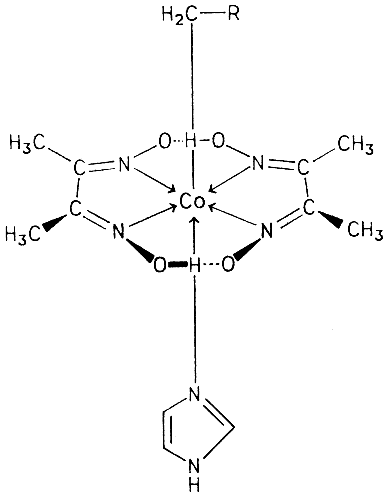

51

One reminder of the power of natural syntheses is the range of iron-binding molecules that have been found in bacteria. Several functional groups have emerged by human design as useful ligands to form stable complex compounds in aqueous media specifically with iron(II) or iron(III). These are shown in Table XII. How wonderful that the same groups are used by all living things. For example, the diimine molecules **52**, caerulomycin A, and **53** (ferropyrimine) of Table VII are very closely akin to the 2,2′-bipyridyl compounds so common in analytical chemistry.

TABLE XI Jahn–Teller Distorted Structures

General shape	Configuration	Ion	Example
O_h, antibonding ($d_{x^2-y^2}$, d_{z^2})	$(3d)^4$	Mn(III)	MnF_3
	$(3d)^4$	Cr(II)	$KCrF_3$
	$(3d)^9$	Cr(II)	K_2CuF_4
T_d, antibonding (d_{xy}, d_{yz}, d_{zx})	$(3d)^8$	—	$NiCr_2O_4$
	$(3d)^8$	—	$Cs_2[CuCl_4]$

VI. THERAPEUTIC METAL COMPLEXES

Whether a solution of a coordination compound is ingested or injected, it enters an aqueous medium and, depending

TABLE XII Some "Specific" Complexing Agents for Aqueous Iron and Natural Analogs

Compound (oxidation state)	Ligand	Natural example
$Fe(OH_2)_6^{3+}$	Salicylate	—
(III)	(2-hydroxybenzoate)	—
	Hydroxamic acids	Ferrioxamine
$Fe(OH_2)_6^{2+}$ (II)	2,2′-Bipyridyl	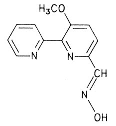 [a] 52 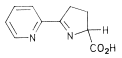 [b] 53

[a] Structure **52** and derivatives known as caerulomycins B, C, and D (all based on the 2,2′-bipyridyl-6-aldoxime moiety) are isolated from *Streptomyces caeruleus*.

[b] Ferropyrimine (**53**) is isolated from the organism *Erwinia rhapontici*, the cause of crown rot in rhubarb, which is also a rich source of the chelating agent $(C_2O_4)^{2-}$, oxalate, or ethane 1,2-dioate.

on concentration, temperature, ionic strength, pH, and so forth, will come to equilibrium with the environment. Establishing the actual nature (*speciation*) of the metal-containing ions and molecules (*species*) that are present in such a given environment is obviously important. It is best done, at present, by a combination of potentiometry [described in Section II.G, Eqs. (41) and (42)] and spectroscopic analysis. The potentiometry defines ranges of possible speciation, and spectroscopy decides among them. Characteristic therapeutic effects [other than those of the separated constituent parts, metal ion and ligand(s) added separately] are therefore to be expected for kinetically inert compounds. Synergic effects are, of course, conceivable for kinetically labile metal ions with particular ligands.

The two best-known therapies involving kinetically inert coordination compounds are chrysotherapy (treatment of rheumatoid arthritis with gold compounds) and the relatively new treatment of certain cancers with platinum compounds.

In chrysotherapy, following earlier uses of "potable gold" and of "colloidal gold," the intact complex compounds (with trade names) used in the form of aqueous solutions are $Na_3[Au(S_2O_3)_2]$ (sanochrysine), sodium gold thiomalate (myocrisin), and a phosphine complex (Solganol). These may have grave side effects but are commonly effective in restoring expression to locked joints. The detailed mechanism of action is unknown, but an intriguing fact is that when two enantiomeric joints are examined, one affected, the other not (such as two elbows), gold is found only in the rheumatic or arthritic joint.

Platinum therapy, discovered by Rosenberg, used *cis*-dichlorodiammineplatinum(II) (see Table IX). This is sold under the names Platinol, *cis*-platin, or Neo-platin. It is thought to act by interfering with nucleic acid replication. Platinosis (a sensitivity, revealed as an allergy, to certain complex compounds of platinum) has become a notifiable industrial disease in France. It has been known since the early years of this century among workers in factories producing platinum chemicals. The novel utility of this simplest of coordination compounds, *cis*-$[Pt(NH_3)_2Cl_2]$, is certainly a major breakthrough in cancer chemotherapy.

Ligands by themselves are often effective drugs or detoxificants. For example, D-penicil-lamine (**3**, a substituted cysteine) is used to mobilize copper deposited in reducing tissues in patients with Wilson's disease (hepatolenticular degeneration), a hereditary defect in copper metabolism. The copper transport protein (ceruloplasmin) of blood plasma is faulty and bonds copper ions less effectively than it should. The enantiomeric L-penicillamine is ineffective as a treatment. If (as may happen) D-penicillamine is either inactive or gives rise to intense nausea, triethylenetetraamine (trien; **4**) is often used.

SEE ALSO THE FOLLOWING ARTICLES

Catalysis, Homogeneous • Catalysis, Industrial • Electron Transfer Reactions • Kinetics (Chemistry) • Ligand Field Concept • Noble Metals • Rare Earth Elements and Materials

BIBLIOGRAPHY

Kauffman, G. B. (ed.) (1994). "Coordination Chemistry, A Century of Progress," ACS Symposium Series 565; American Chemical Society, Washington, D.C.

Wilkinson, G., Gillard, R. D., and McCleverty, J. A. (1987). "Comprehensive Coordination Chemistry," Vols. 1–7, Pergamon Press, Oxford.

Dielectric Gases

L. G. Christophorou
S. J. Dale
Oak Ridge National Laboratory

I. Introduction
II. Basic Physical Processes and Properties
III. Breakdown Strength
IV. Uses of Dielectric Gases
V. Concluding Remarks

GLOSSARY

Breakdown voltage Critical voltage under which a gas makes the transition from an insulator to a conductor.

Dielectric gas Relatively poor conductor or nonconductor of electricity to high applied electrical stress; gas with high breakdown voltage.

Electrical breakdown (or electrical discharge or spark) of a gas Dramatic event whereby the electrical conductivity of an electrically stressed gas increases by many orders of magnitude in times ranging from nanoseconds to milliseconds.

Electronegative gas Electron-attaching gas in which stable negative ions (parent and/or fragment) are produced.

Synergism of gas mixtures Property of gas mixtures whereby they have dielectric strengths exceeding the partial-pressure-weighted dielectric strengths of the individual components making up the gas mixture.

Tailoring gas dielectrics Combination, on the basis of fundamental physicochemical knowledge, of two or more gases to optimize their overall dielectric properties.

A DIELECTRIC GAS IS a gaseous medium consisting of one or more components with a high breakdown voltage (i.e., a gaseous medium that is a relatively poor conductor or a nonconductor of electricity to high applied electrical strength). This article outlines the basic physical processes that determine the dielectric properties of gases and discusses the breakdown strengths of dielectric gases and the main uses of gaseous dielectrics.

I. INTRODUCTION

A gas in its normal state is a perfect insulator. If, however, the gas is electrically stressed, the free electrons present in it gain energy from the applied electric field; when the level of the applied field is such that an appreciable number of these free electrons possess kinetic energies high enough to ionize the gas atoms or molecules, the gas "breaks down" (i.e., it makes the transition from an insulator to a conductor). The minimum critical voltage under which the electrical conductivity of the gas increases by many orders of magnitude is known as the breakdown voltage and the phenomenon itself as electrical breakdown, electrical discharge, or spark.

As mentioned earlier, a dielectric gas is a relatively poor conductor or a nonconductor of electricity to high applied electrical strength (i.e., a gas with a high breakdown voltage). As such, it is used to insulate electrically various types of high-voltage equipment (see Section IV). As we shall see in Section III, the magnitude of the breakdown voltage depends not only on the nature, number density, and temperature of the gas, but also on many other factors such as the type of applied voltage and the geometry, material, and surface condition of the electrodes. The breakdown voltage varies considerably from one gaseous medium to another, and it can be—for certain electronegative gases, for example—over six times larger than the breakdown voltage of atmospheric air, which is the "traditional" gas dielectric (see Section III).

Depending on the form of the applied voltage and the nature and density of the gas, the transition of a gaseous medium from an insulator to a conductor occurs in times ranging from nanoseconds to milliseconds. The transition is critically determined by the behavior of electrons, ions, and photons in the gas, especially by those processes that produce or deplete free electrons. While a multiplicity of physical processes and species, both neutral and charged, play a role in determining the dielectric properties of a gas, it seems that the electron is the key particle, and its interactions with the gas molecules are the critical processes. Knowledge of these processes often allows a prediction of the dielectric properties of the gas and a choice of the appropriate gaseous medium for specific uses.

II. BASIC PHYSICAL PROCESSES AND PROPERTIES

A. Basic Physical Processes

The basic physical processes that determine the properties of dielectric gases involve excited and unexcited atoms and molecules, electrons, positive and negative ions, and photon interactions with the gas and the electrodes. We shall focus on those physical processes that are associated with the gas itself (not with the electrodes), and in Table I we list the principal ones. Basically, all these processes affect

TABLE I Principal Physical Processes in Electrically Stressed Gas Dielectrics

Process number	Process representation	Process description
Group A.	*Electron–molecule interactions*	
1	$e + AB \rightarrow AB + e$	Elastic electron scattering (direct)
2	$e + AB \rightarrow AB^* + e$	Inelastic electron scattering (dirct)
3a	$e + AB \Rightarrow A + B + e$	Dissociation by electron impact
3b	$\Rightarrow A + B^* + e$	Dissociative excitation by electron impact
4a	$e + AB \rightarrow AB^+ + 2e$	Ionization by electron impact
4b	$e + AB \Rightarrow A + B^+ + 2e$	Dissociative ionization by electron impact
5a	$e + AB \rightarrow AB^{-*} \rightarrow AB^-$	Parent negative-ion formation
5b	$\Rightarrow A + B^-$	Dissociative attachment
5c	$\rightarrow AB\ (AB^*) + e$	Elastic (inelastic) electron scattering (indirect)
6	$e + AB \rightarrow A^+ + B^- + e$	Ion-pair formation
Group B.	*Photon–molecule interactions*	
7	$h\nu + AB \rightarrow AB^*$	Photonabsorption
8a	$h\nu + AB \rightarrow AB^+ + e$	Photoionization
8b	$\Rightarrow A + B^+ + e$	Dissociative photoionization
9	$h\nu + AB \rightarrow A + B$	Photodissociation
10	$h\nu + AB^-\ (B^-) \rightarrow AB\ (B) + e$	Photodetachment
11a	$AB^* + C \rightarrow AB + C^+ + e$	Penning ionization
11b	$B^* + C \rightarrow B + C^+ + e$	Penning ionization involving highly excited atoms (e.g., Rydberg states)
Group C.	"*Secondary*" *interactions*	
12	$e + AB^* \rightarrow AB\ (AB^*)$	Electron–positive ion recombination
13	$B^+ + A^- \rightarrow AB\ (AB^*)$	Positive ion–negative ion recombination
14	$AB^- + C \rightarrow AB + C + e$	Collisional detachment
15	$AB^- + C \rightarrow ABC + e$	Associative detachment
16	$AB^- + C \rightarrow AB + C^-$	Electron transfer
17	$AB^- + nC \rightarrow AB^-C_n \quad n \geq 1$	Cluster formation

the dielectric behavior of the gas by their effect(s) on the number density and energies of the free electrons present in the electrically stressed gas. Both the numbers and the energies of the free electrons depend on the gas itself and the density-reduced electric field E/N (E is the applied electric field and N the gas number density). Let us briefly look at the processes in Table I and their expected effect(s) on the dielectric properties of the gas. For convenience, we distinguish three groups of interactions: (1) electron–molecule, (2) photon–molecule, and (3) "secondary." In Table I, AB represents an unexcited and AB^* an excited diatomic or polyatomic molecule, and the double arrows indicate that the reaction can produce a multiplicity of products.

1. Electron–Molecule Interactions

Processes 1 and 2 in Table I are direct elastic and inelastic electron scattering, respectively. Along with process 5c (indirect elastic and inelastic electron scattering, whereby the colliding electron is temporarily captured by the molecule and then released), they crucially determine the energies of the free electrons present in the stressed gas. Their cross sections depend on the electron energy itself and the details of the molecular (atomic) electronic structure. The inelastic electron scattering processes involve excitation of rotational, vibrational, and electronic states, while the elastic scattering does not change the internal energy of the molecule (atom). Although direct electron scattering is nonresonant (i.e., it occurs over a wide range of electron energies), indirect electron scattering is resonant; it usually is very efficient at low ($\lesssim$20 eV) energies and rather significant in establishing the "electron slowing-down" properties of the dielectric gas. Obviously, polyatomic molecules are, as a rule, more efficient in slowing down the electrons than are small molecules or atoms.

Processes 3a and 3b represent the dissociation of molecules by electrons. They can proceed via a multiplicity of channels and thus produce a variety of neutral fragments, some of which, such as B^* in 3b, may be excited and posses sufficient internal energy to ionize an impurity species C present in the dielectric (process 11b) and in this way to increase electron production (B^* can also eject electrons when it collides with a surface). Processes 3a and 3b slow down the electrons present in the gas, as do processes 1, 2, and 5c, but in addition they produce free radicals which can change the number density and the composition of the dielectric gas.

Processes 4a and 4b are the principal ways by which new electrons are generated by electron–molecule collisions (and by which existing ones are slowed down); through process 4b a multiplicity of positive ions can be produced.

Processes 5a and 5b are the main reactions which deplete the electrons present in the dielectric, producing parent 5a and fragment 5b negative ions. In this way the electrons are prevented from causing ionization of the gas. To this end, besides the electron-attachment cross section or the electron-attachment rate constant as a function of electron energy, the binding energy of the attached electron (otherwise known as the electron affinity) must be large to prevent electron detachment (i.e., release of the attached electron). Process 5 has been studied under "isolated conditions" (i.e., very low pressures) and under "multiple collision conditions" (i.e., high pressures) in which the effect of the medium can often be significant. It is a resonant process occurring in the energy range from 0 to ∼20 eV, depending on AB. It crucially affects the breakdown voltage and other properties of the gas dielectric because of its dominant role on the number density of the electrons. Gases with large electron-attachment cross sections are called electronegative or electron-attaching; the cross sections for the electron-attachment resonances decrease with increasing energy, and hence low-energy free electrons can be more efficiently removed from the dielectric (via this process) than can higher energy electrons. Not all gases are electronegative, however, but the good gas dielectrics are, or else contain electronegative additives.

The last process in group A in Table I, process 6, occurs at higher energies than 5, and although it produces negative ions, it does not deplete electrons, it slows them down. In the energy range of interest, its cross section is not appreciable, and its effect on the gas dielectric properties is thought not to be significant.

2. Photon–Molecule Interactions

In the second group of reactions are those between dielectric gas molecules and photons, produced by deexcitation of excited species at high E/N (such as AB^* and B^* in Table I and more likely, excited species produced by recombination processes). Here, three types of processes can increase the number of free electrons in the gas dielectric: photoionization of AB (processes 8a and 8b), photoionization of the negative ions (photodetachment, process 10), and Penning ionization (process 11a or 11b, due to excited species produced via 7 or 3b, respectively). Of course, photons can collide with the electrodes and inject new electrons into the gas dielectric in this way.

3. "Secondary" Interactions

The number density of electrons and ions, and thus the associated space charge effects in nonuniform fields, can be further affected by what can be termed secondary reactions. These can deplete electrons and positive ions

(reaction 12) or positive and negative ions (reaction 13); can collisionally detach electrons from negative ions (reactions 14 and 15) or convert one ionic species to another (reaction 16) (and thus change its stability); or can change the ion's size (and thus its mobility) by clustering (reaction 17). While the role of these processes may be less obvious than the roles of groups A and B, it can, depending on the prevailing conditions, be most significant. For example, the gas dielectric behavior under steep-fronted voltage pulses is affected by the availability of "initiating" electrons produced by reactions 14 and 15. Similarly, corona stabilization (Section III.B) is influenced by the electron–ion (12) and ion–ion (13) recombination processes.

Understanding of the phenomena preceding the transition of the gas from an insulator to a conductor (prebreakdown phenomena) and the mechanisms involved in discharge initiation and development invariably requires basic knowledge on at least a fraction of the processes in Table I. This knowledge comes from two sources: low-pressure beam experiments and high-pressure swarm experiments. In high-pressure swarm experiments, as in electrically stressed gas dielectrics, the free electrons attain an equilibrium energy distribution $f(\varepsilon, E/N)$, and the measured electron trasport coefficients (the electron drift velocity w and the ratio D_T/μ of the transverse diffusion coefficient D_T to the electron mobility μ) are related to the cross sections for the microscopic electron–molecule interactions through $f(\varepsilon, E/N)$. In principle, from a measurement of $w(E/N)$ and $D_T/\mu(E/N)$ and a knowledge of the electron scattering cross section, $f(\varepsilon, E/N)$ can be calculated through the Boltzmann transport equation or by Monte Carlo methods. If, then, for a given gas dielectric the various cross sections are known, they can be integrated over $f(\varepsilon, E/N)$ and used along with the appropriate charge conservation equations to determine the current growth in the gas and predict its breakdown voltage. In practice this is difficult because neither the cross sections nor $f(\varepsilon, E/N)$ is known for the majority of the dielectric gases or gas mixtures, so one resorts to the more easily accessible swarm coefficients to predict the discharge development and behavior.

From high-pressure swarm studies, the coefficients for excitation, detachment, and ion–molecule reactions are obtained as functions of E/N, as well as the primary ionization coefficient α and the effective electron attachment coefficient η. Most of the data are on the latter two coefficients. The coefficients α and η are most significant and are related to the respective ionization, $\sigma_i(\varepsilon)$, and attachment, $\sigma_a(\varepsilon)$, cross sections and $f(\varepsilon, E/N)$ by

$$\frac{\alpha}{N}\left(\frac{E}{N}\right) = \left(\frac{2}{m}\right)^{1/2} w^{-1} \int_I^{\infty} f\left(\varepsilon, \frac{E}{N}\right) \varepsilon^{1/2}\sigma_i(\varepsilon)\, d\varepsilon, \tag{1}$$

$$\frac{\eta}{N_a}\left(\frac{E}{N}\right) = \left(\frac{2}{m}\right)^{1/2} w^{-1} \int_0^{\infty} f\left(\varepsilon, \frac{E}{N}\right) \varepsilon^{1/2}\sigma_a(\varepsilon)\, d\varepsilon, \tag{2}$$

where I is the ionization onset energy, N the total gas number density, and N_a the attaching gas number density; for a unary electronegative gas dielectric $N = N_a$, but for mixtures containing electronegative and nonelectronegative components $N_a < N$.

B. Dielectric Properties

Having elaborated briefly on the basic physical processes occurring in electrically stressed dielectric gases, we can appropriately ask the question: How can the dielectric properties of a gaseous medium be optimized based on knowledge of such processes? To illustrate the type of answer one can get to this question let us see how knowledge of the electron-attaching, electron slowing-down, and electron impact-ionization properties of gases allows one to choose and to tailor gaseous dielectrics. This can be seen by referring to Fig. 1. When the value of E/N is low (e.g., 1.24×10^{-16} V cm^2 in Fig. 1 for N_2), $f(\varepsilon, E/N)$ lies at low energies, and the number of electrons capable of ionizing the gas is negligible (i.e., the gas is an insulator). As the voltage is increased, however, $f(\varepsilon, E/N)$ shifts to higher energies, and for sufficiently high E/N values the number of electrons capable of ionizing the gas is such that the gas makes the transition from an insulator to a conductor. In Fig. 1, $f(\varepsilon, E/N)$ is shown for N_2 at the limiting value of E/N, $(E/N)_{lim}$ ($\simeq 1.3 \times 10^{-15}$ V cm^2) (i.e., the value of E/N at which breakdown occurs). Even at this high E/N value only a small fraction of electrons possess sufficient energy to induce ionization, which, nonetheless, for a non-electron-attaching gas such as N_2, is sufficient to promote gas breakdown. This is designated in Fig. 1 by the shaded area α, which is a measure of the ionization coefficient α/N [Eq. (1)].

For a non-electron-attaching gas and a uniform field, knowledge of α provides a measure of $(E/N)_{lim}$ through the so-called Townsend breakdown criterion,

$$\gamma(e^{\alpha d} - 1) = 1. \tag{3}$$

In Eq. (3), αd is the number of electrons generated by an electron leaving the cathode and arriving as an electron avalanche at the anode (at a distance d from the cathode), and γ is the so-called secondary ionization coefficient, defined as the number of secondary electrons produced perprimary ionization. These secondary-electron processes include (1) electron emission from the cathode as it is struck and photons, positive ions, and metastable molecules and (2) gas processes such as photoionization of the gas. Physically, Eq. (3) states that when each initial

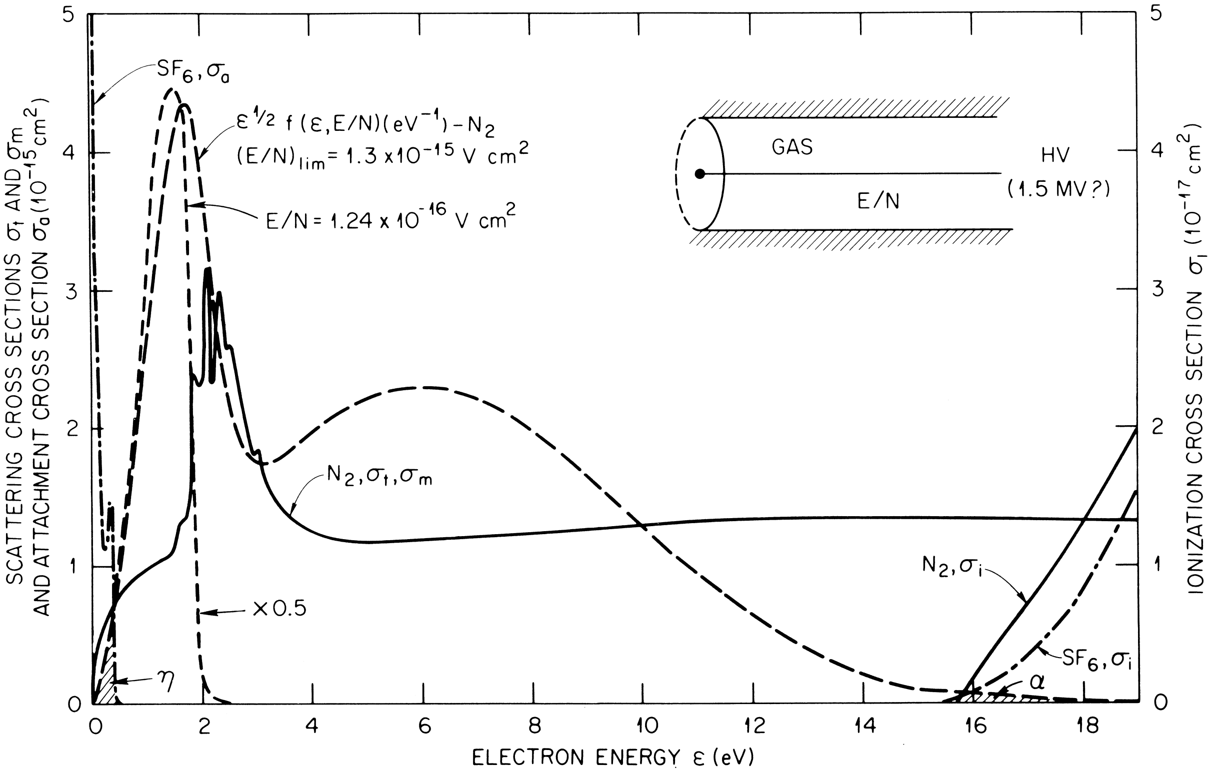

FIGURE 1 Ionization cross section $\sigma_i(\varepsilon)$ for N_2 and SF_6 close to the ionization onset *I*. Electron-scattering cross section as a function of ε for N_2 and electron-attachment cross section $\sigma_a(\varepsilon)$ for SF_6. Normalized electron energy distribution function $\varepsilon^{1/2}f(\varepsilon, E/N)$ as a function of ε for N_2 at two values of E/N. [From Christophorou, L. G., *et al.* (1984). *IEEE Trans, Elect. Insul.* **EI-19,** 550–566.]

electron produces a successor, the current maintains itself and becomes independent of γ.

For an electronegative gas the situation is different because in this case the free electrons can be effectively prevented from initiating breakdown if they attach themselves to gas molecules and form stable negative ions. The total attachment cross section $\sigma_a(\varepsilon)$ for SF_6 is shown in Fig. 1. In general, $\sigma_a(\varepsilon)$ is large at very low energies, and thus only electrons with energies at the extreme low-energy range can be removed efficiently by electron attachment. The shaded area in Fig. 1 that is designated by η is a measure of the effective electron attachment coefficient η/N_a [Eq. (2)]. Knowledge of α/N and η/N_a allows one to predict $(E/N)_{lim}$, which for static uniform fields and a unary gas is defined as the value of E/N at which $\alpha = \eta$, namely,

$$\gamma[\exp\{(\alpha - \eta)d\} - 1] = 1 - \eta/\alpha. \tag{4}$$

Both α/N and η/N_a are functions of E/N (see Figs. 2 and 3). Most often, one measures the so-called effective ionization coefficient $(\alpha - \eta)/N$ (see Fig. 2), and the static uniform field breakdown strength $(E/N)_{lim}$ is defined as the value of E/N for which

$$(\alpha - \eta)/N \equiv \bar{\alpha}/N = 0. \tag{5}$$

Thus (see Fig. 2) for pure SF_6, $(E/N)_{lim} = 3.61 \times 10^{-15}$ V cm^2, and it decreases as N_2 is added in the binary mixture.

For nonuniform fields, $\bar{\alpha}$ is a function of the position between the electrodes, and the breakdown voltage V_s can be calculated from the so-called streamer criterion,

$$\int_0^{x_0} \bar{\alpha}(x)\,dx = k, \tag{6}$$

where x_0 is the length at which the electron avalanche reaches the critical number of electrons ($\sim 10^8$) in the avalanche tip for causing streamer formation. The k is a constant characteristic of the gas. It is generally accepted that photoionization processes play a role in the propagation of the streamer.

For the gas dielectric strength to be optimized, not only must $\sigma_i(\varepsilon)$ be small and $\sigma_a(\varepsilon)$ be large [and extend to high energies to maximize the overlap of $\sigma_a(\varepsilon)$ and $f(\varepsilon, E/N)$, as in Eq. (2)], but the electron energies must be as low as possible because a low-lying $f(\varepsilon, E/N)$ minimizes α and maximizes η. Many studies, however, clearly show that high breakdown strengths require large $\sigma_a(\varepsilon)$. This can be seen from the examples in Fig. 3. As the attachment-rate

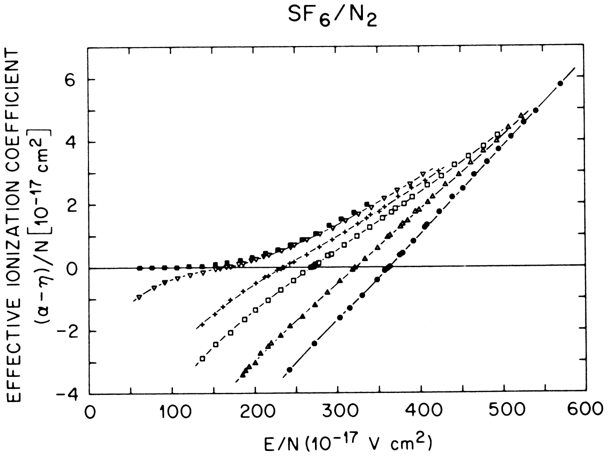

FIGURE 2 Effective ionization coefficient $(\alpha - \eta)/N$ as a function of the density-reduced electric field E/N. Curves are for the following gases and $(E/N)_{\text{lim}}(10^{-17}\ \text{V cm}^2)$: ■ N_2, 130; ∇ 1% SF_6, 160; + 10% SF_6, 235; □ 20% SF_6, 269; △ 50% SF_6, 323; and ● 100% SF_6, 361. [Data from Aschwanden, T. (1984). *In* "Gaseous Dielectrics IV" (L. G. Christophorou and M. O. Pace, eds.), p. 30, Pergamon Press, New York.]

constant, as a function of the mean electron energy $\langle\varepsilon\rangle$, $k_a(\langle\varepsilon\rangle)$, increases, so does the breakdown voltage V_s^R relative to SF_6. Knowledge of $k_a(\langle\varepsilon\rangle)$ or $\sigma_a(\varepsilon)$ led to the identification of many excellent unary gas dielectrics such as the perfluorocarbons (see Table II, which is discussed in Section III).

It is thus apparent that the dielectric properties of gases can be optimized by a combination of two or more gases (i.e., by tailoring multicomponent gas mixtures) designed, for example, to provide the best effective combination of electron-attaching and electron slowing-down components. Basic knowledge on the processes in Table I offers several ways to the systematic development of dielectric gas mixtures. Thus knowledge on the electron-attachment cross section guided the choice of unary gas dielectrics or electronegative components for dielectric gas mixtures, and knowledge on electron scattering at low energies guided the choice of buffer gases for mixtures containing electronegative additives. Of practical significance are mixtures of the strongly electron-attaching gases in Table II with abundant, inert, and inexpensive buffer gases (e.g., N_2), with which they act synergistically: the buffer gas(es) scatter electrons into the energy range in which the electronegative gas(es) capture electrons most efficiently.

Examples of the various types of observed uniform field behavior of the breakdown voltage $(V_s)_{\text{mix}}$ of binary gas mixtures with respect to those $(V_s)_{A,B}$ of the individual components A, B as a function of gas composition are shown in Fig. 4. Figure 4a shows the behavior of $(V_s)_{\text{mix}}$ for binary mixtures of electronegative gases whose $k_a(\langle\varepsilon\rangle)$ is independent of gas number density N. The $(V_s)_{\text{mix}}$ is nearly equal to the sum of the partial-pressure-weighted V_s of the constituent component gases. In Fig. 4b, examples are given of binary mixtures of a buffer gas that slows down electrons efficiently (CO, N_2, or CO_2) and the electronegative gas SF_6. At all gas compositions, the measured $(V_s)_{\text{mix}}$ exceeds the partial-pressure-weighted values of the individual components. This has been referred to as synergism. Similar results are shown in Fig. 4c for mixtures of the strongly electronegative gas c-C_4F_8 and the nonpolar weakly electron-attaching buffer gas CF_4 or the polar buffer gases CHF_3 or 1,1,1-CH_3CF_3, which slow down electrons efficiently via dipole scattering. The $(V_s)_{\text{mix}}$ for the polar gas-containing mixtures far exceeds the partial-pressure-weighted V_s, especially for small percentages of the electronegative gases.

In Fig. 4c the behavior of curve 1 is interesting in that for certain gas compositions the $(V_s)_{\text{mix}}$ exceeds the V_s of either component. This has been observed for other binary mixtures (e.g., 1-C_3F_6/c-C_4F_8; 1-C_3F_6/SO_2; SO_2/SF_6; C_3F_8/SF_6; and OCS/SF_6) for which the electron-attachment properties of one or both of the constituent gases depend on the total gas pressure and the mixture composition. This is clearly seen by the data in Fig. 4d, which show the variation of $(V_s)_{\text{mix}}$ for SF_6/1-C_3F_6 with relative composition and total gas number density.

Many studies on gas mixtures identified binary gas mixtures [e.g., SF_6/N_2, perfluorocarbon/SF_6, and perfluorocarbon/N_2 (or CHF_3)] that can be useful for applications.

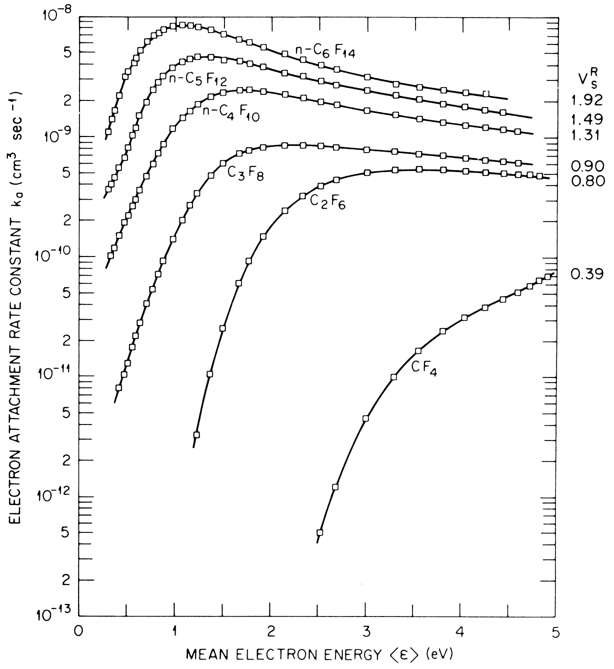

FIGURE 3 Total electron-attachment rate constant k_a as a function of the mean electron energy $\langle\varepsilon\rangle$ for the perfluoroalkanes C_NF_{2N+2} ($N = 1$–6) and their dc uniform field breakdown voltages relative to SF_6. [From Christophorou, L. G., *et al.* (1984), *IEEE Trans. Elect. Insul.* **EI-19,** 550–566.]

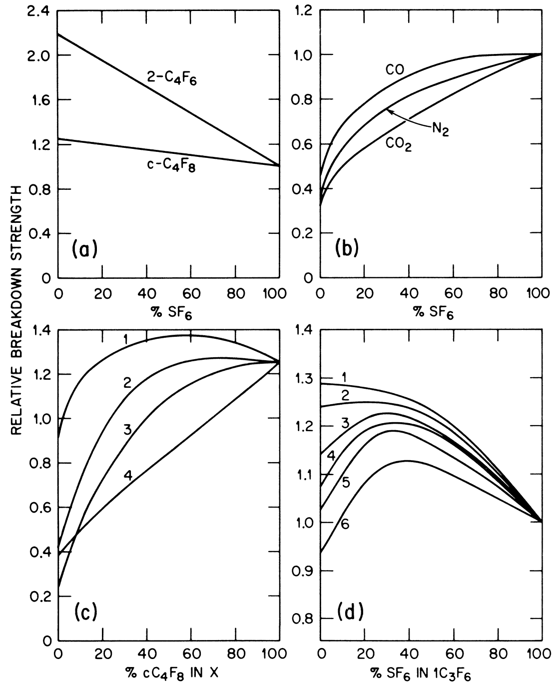

FIGURE 4 Relative breakdown strangth of various gas mixtures. In (c), curves 1–4 are for $x = 1\text{-}C_3F_6$, $1,1,1\text{-}CH_3CF_3$, CHF_3, and CF_4, respectively. In (d), curves 1–6 are for N_{total} (10^{19} cm^{-3}) = 10.00, 7.52, 5.02, 3.76, 2.51, and 1.67 respectively. [Based on data from Christophorou, L. G. (ed.), (1982). "Gaseous Dielectrics III," Pergamon Press, New York; Christophorou, L. G. (ed.). (1984). "Electron–Molecule Interactions and Their Applications," Academic Press, New York; Christophorou, L. G., *et al.* (1984). *IEEE Trans. Elect. Insul.* **EI-19,** 550–566; and Electric Power Research Institute. (1982). "Gases superior to SF_6 for insulation and interruption," **EPRI·EL-2620,** Electric Power Research Institute, Palo Alto, CA [prepared by Westinghouse Electric Corporation].

The SF_6/N_2 mixtures are particularly attractive. Their relatively high dielectric strength (for SF_6 concentrations $\gtrsim$40%) have made the SF_6/N_2 mixtures candidates for high-voltage gas-insulated equipment, especially in low-temperature environments (<-40°C) where pure SF_6 would condense at the normal operating pressures (~4.5 atm); a 50/50 mixture of N_2/SF_6 has a dielectric strength ~85% that of pure SF_6 in uniform fields.

Ternary gaseous mixtures have also been developed to optimize as many of the desirable dielectric properties and characteristics as possible. Such gaseous dielectrics, composed of N_2, SF_6, and small amounts of strongly electronegative perfluorocarbons, show promise for applications.

III. BREAKDOWN STRENGTH

A. Uniform Fields

The range of breakdown potentials for gases is considerable. This can be seen from the selected data on the dc uniform field breakdown strengths V_s^R in Table II, which were measured at approximately atmospheric pressures: The V_s of air is ~50 times higher than that of Ne, and the V_s of SF_6 is ~3.3 times higher than that of air. The highest known V_s (~2.5 times higher than SF_6) are exhibited by strongly electron-attaching polyatomic gases such as the perfluorocarbons in Table II and other polyhalogenated molecules. Weakly electron-attaching or non-electron-attaching gases (Table II) have low V_s values. Nonelectronegative molecular gases with large electron-scattering cross sections have reasonably high V_s values compared, for instance, with the rare gases, in which low-energy electron scattering is totally elastic.

The V_s of a gaseous medium is expected, in accordance with Paschen's law, to be a function only of Nd_s (the product of the gas number density N and the electrode separation d_s); thus, for sufficiently high values of N to the right of the Paschen minimum, $V_s/Nd_s = (E/N)_{lim}$ should be independent of N. This relationship holds for

TABLE II Relative dc Uniform Field Breakdown Strengths V_s^R of Some Dielectric Gases[a]

Gas	$V_s^{R\,b,c}$	Comments
SF_6	1	Most common dielectric gas besides air
C_3F_8	0.90	Strongly and very strongly electron-attaching gases, especially at low energies
$n\text{-}C_4F_{10}$	1.31	
$c\text{-}C_4F_8$	~1.35	
$1,3\text{-}C_4F_6$	~1.50	
$c\text{-}C_4F_6$	~1.70	
$2\text{-}C_4F_8$	~1.75	
$2\text{-}C_4F_6$	~2.3	
$c\text{-}C_6F_{12}$	~2.4	
CF_3H	0.27	Weakly electron-attaching; some (CO, N_2O) are effective in electron slowing-down
CO_2	0.30	
CF_4	0.39	
CO	0.40	
N_2O	0.44	
H_2	0.18	Virtually non-electron-attaching
Air	~0.30	
N_2	0.36	Non-electron-attaching but efficient in electron slowing-down
Ne	0.006	Non-electron-attaching and not efficient in electron slowing-down
Ar	0.07	

[a] Based on data in Christophorou (1984), Meek and Craggs (1978), and Christophorou *et al.* (1984).

[b] Some of the values given are for quasi-uniform fields and may thus be lower than their uniform field values.

[c] The relative values can be put on an absolute scale by multiplying by 3.61×10^{-15} V cm^2, the $(E/N)_{lim}$ of SF_6.

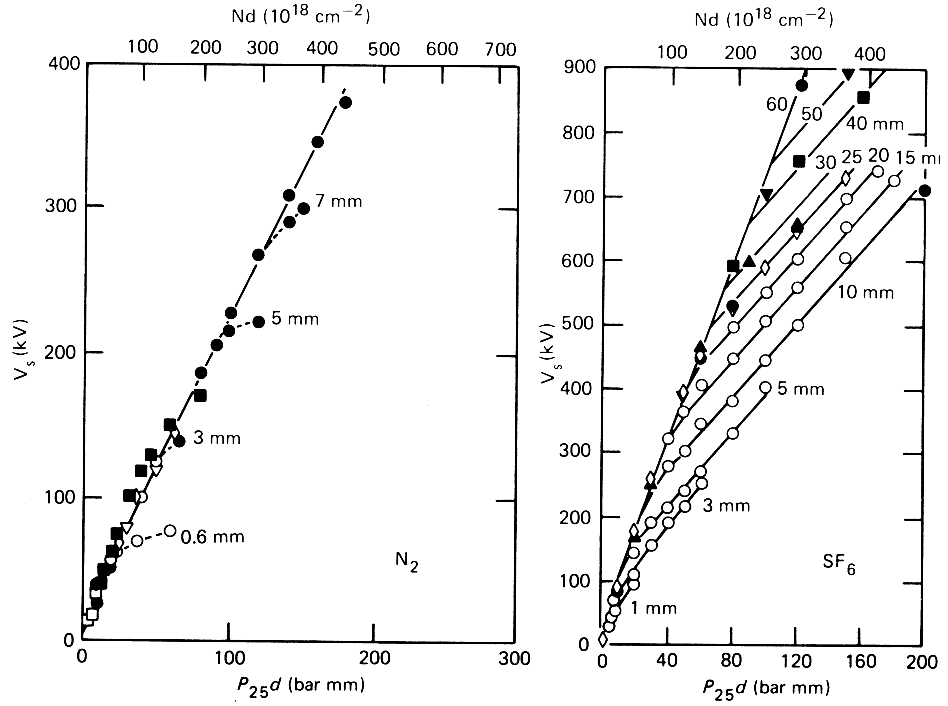

FIGURE 5 Breakdown voltages of N_2 and SF_6 at high *Pd* ($T = 298$ K). [From Meek, J. M., and Craggs, J. D. (eds.). (1978). "Electrical Breakdown of Gases," Wiley, New York.]

most gases at low field strengths and moderate pressures (see Fig. 5). At high field strengths, the V_s varies less than linearly with increasing N for a fixed d_s. This is illustrated by the uniform field data for N_2 and SF_6 shown in Fig. 5 for a number of N and d_s values. It is clear from these data that the deviations are larger for the electronegative gas SF_6 than for the nonelectronegative gas N_2. This pertains to the cause of these deviations, which are generally attributed to the effects of electrode geometry and surface. Changes in field uniformity by surface roughness affects (increases) the value of $\bar{\alpha}/N$ (more so than α/N) principally by decreasing the value of η/N due to the shift of $f(\varepsilon, E/N)$ to higher energies as the field increases at imperfections, scratches, and surface projections.

It has recently been found that Paschen's law can be violated, in a way opposite to that just described [i.e., $(E/N)_{\rm lim}$ increasing rather than decreasing with increasing N], in cases in which it would normally be expected to hold. An example of this type of behavior is shown in Fig. 6, where the $(E/N)_{\rm lim}$ of 1-C_3F_6 (perfluoropropylene) is plotted versus N (or compressibility-corrected pressure). It is seen that $(E/N)_{\rm lim}$ increases with N over a given range, contrary to that of SF_6, which is independent of N. The increase of $(E/N)_{\rm lim}$ with N relates to the decrease with N of $\bar{\alpha}/N$ due to the increase with N of η/N for 1-C_3F_6 (no such increase occurs for SF_6). The saturation in the dependence of $(E/N)_{\rm lim}$ on P is related to the saturation of the increase in $k_a(\langle\varepsilon\rangle)$ with increasing P. A similar violation of Paschen's law has been observed for other gases (e.g., OCS, N_2O, SO_2, and C_3F_8), all of which have electron-attaching properties that are functions of N.

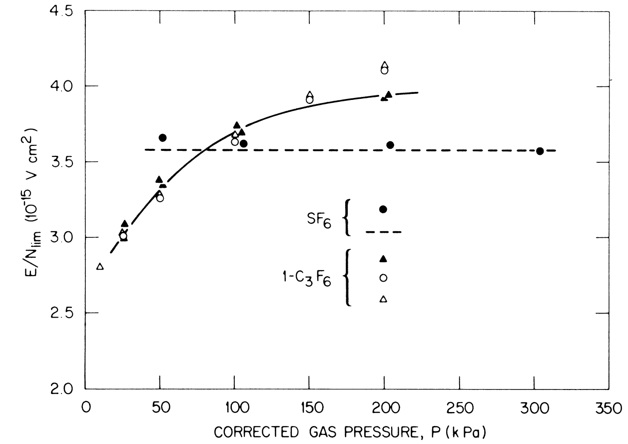

FIGURE 6 $(E/N)_{\rm lim}$ versus pressure *P*, corrected for compressibility, for SF_6 and 1-C_3F_6; the various symbols refer to measurements of different authors. [From Christophorou, L. G. (ed.). (1982). "Gaseous Dielectrics III," Pergamon Press, New York; Christophorou, L. G., and pace, M. O. (eds.). (1984). "Gaseous Dielectrics IV," Pergamon Press, New York.]

B. Nonuniform Fields

A nonuniform field is often characterized by the so-called field utilization factor n, defined as the ratio of the average field E_a to the maximum field E_m, and is a function of the electrode geometry. When the maximum electrical stress in a gas gap is large enough, localized ionization occurs near the high-field electrode without breakdown. This phenomenon is generally known as corona. The charges generated by corona are separated by the electric field and cause field distortion. The space charge produced by corona profoundly affects the breakdown characteristics of the gas. This is illustrated by the breakdown voltage/pressure characteristics of electronegative gases exemplified in Fig. 7 for SF_6. Up to a pressure P_1 the breakdown voltage V_s increases almost linearly with P and considerably exceeds the corona inception voltage V_i. Subsequently, V_s goes through a maximum and then falls, up to pressure P_c' that may coincide with the critical pressure P_c, defined as the pressure for which $V_s = V_i$ (i.e., the pressure at which breakdown occurs directly at the inception voltage without any preceding corona). The pressure range over which $V_s > V_i$ is called the corona stabilization region. In this region, homopolar space charge generated by corona reduces the field near the high-stress electrode. The size and shape of this region and the value of P_c are functions of the field utilization factor n, the applied voltage, and the nature of the gas. Studies have shown that the smaller the field utilization factor (i.e., the more nonuniform the field), the higher the value of P_c (i.e., corona stabilization occurs over a wider range of pressures).

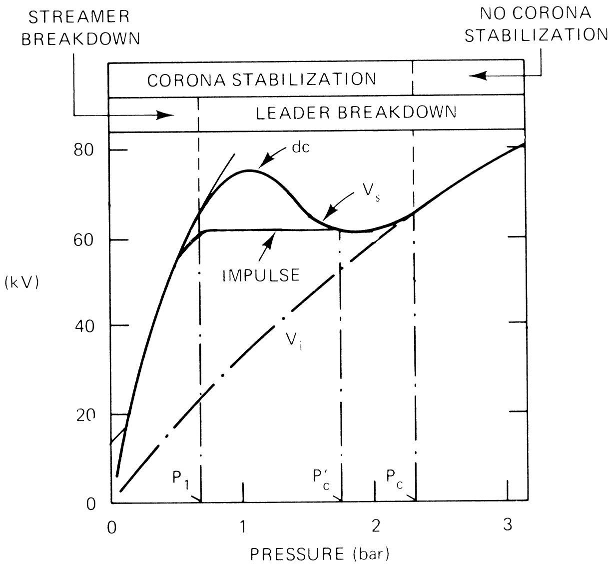

FIGURE 7 Positive dc corona in a point-plane SF_6 gap (radius of point tip, $r_0 = 2$ mm; electrode gap $d = 20$ mm). [From Farish, O. (1983). *In* "Proceedings XVI International Conference on Phenomena in Ionized Gases" (W. Bötticher *et al.*, (eds.). p. 187, Düsseldorf, Germany.)

Under impulse conditions, the behavior of V_s at $P > P_1$ depends on the impulse risetime and on the availability of initiating electrons (i.e., the behavior is strongly dependent on the statistics of discharge initiation). For wavefronts $\gtrsim 100\ \mu$sec, there is time for corona shielding to develop, and the V_s versus P curve is similar to that for dc. For short risetimes (a few microseconds or less), the characteristic is relatively flat between P_i and P_c (see Fig. 7).

In view of the possible significance of the corona stabilization region in the reliability of gas-insulated equipment, systematic studies have been undertaken to tailor dielectric gas mixtures to have improved stabilization. Most such efforts have focused on increasing corona-controlled breakdown of compressed electronegative mixtures containing SF_6 or $SF_6 + N_2$ for both polarities by increasing the negative and positive space charge, respectively, with small amounts of additives that are more electronegative than SF_6 (such as certain perfluorocarbons) for negative polarity and with additives whose ionization threshold energy is much lower than that of SF_6 for positive polarity. Often as little as 1–5% of a suitable electronegative perfluorocarbon additive can effect a substantial increase in the corona stabilization. However, for such mixtures the positive polarity is usually lowered compared with SF_6 or SF_6/N_2. An improvement in the corona stabilization for both positive and negative polarity can be achieved by an additive that is electronegative and has a low ionization potential.

C. Effect of Particles

Another form of nonuniform field breakdown in a gaseous dielectric is that from free conducting particles. Free conducting particles subjected to an electric field in a gaseous medium between the electrodes become levitated when the force exerted on them by the electric field exceeds the gravitational force. With an ac voltage, the particles will bounce on the lower electrode, and the bounce height will increase with the applied voltage. With a dc voltage, the particles can cross the gap between the electrodes as soon as they are levitated. Tests with free conducting particles have shown that the worst type of particles are long, metallic needles or wires. Figure 8 shows the effect of free wire particles in a coaxial electrode system in SF_6 on the ac breakdown voltage as a function of gas pressure and wire length. It is seen that the breakdown voltage is virtually independent of gas pressure for the longer particles and that particle-initiated breakdown occurs at fields considerably lower than those for the uncontaminated system. The effect is usually larger for positive polarity voltages.

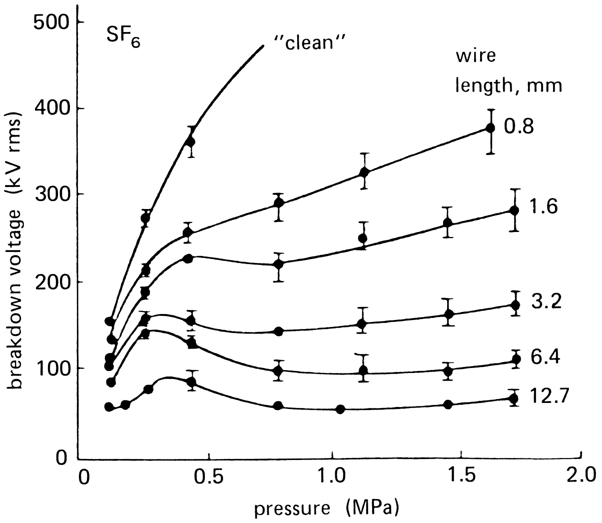

FIGURE 8 The ac breakdown voltage versus pressure in a 150 mm/250 mm coaxial geometry containing free copper wires with 0.4 mm diameter and lengths ranging from 0.8 to 12.7 mm. [From Cookson, A. H., *et al.* (1971). *IEEE Trans. Power App. Syst.* **PAS-90,** 871.]

Although the free conducting particles cause reductions in the V_s of quasi-uniform field electrode geometries, the V_s is higher when the particles are fixed to an electrode. The fixed-particle breakdown voltage/pressure characteristic exhibits the familiar corona stabilization region discussed in the previous section, where $V_s > V_i$ (see Fig. 7). It also has been found that the V_s for free particles with ac voltage corresponds closely to the impulse breakdown voltage with fixed particles. This indicates that the free-particle breakdown mechanism is similar to that of impulse breakdown. For impulse voltages, the corona stabilization process for the fixed particle fails and the impulse breakdown voltage is considerably lower than for ac over the pressure range where the corona stabilization mechanism is dominant. Observations of particle breakdown have shown that as the particle approaches an electrode, discharges occur between the particle and the electrode as a result of their different potentials. The result is a sudden change in the electric field at the particle tip that faces the main gap, which is equivalent to an impulse voltage applied to the particle.

Particle-initiated breakdown is one of the most severe imperfections in gas-insulated apparatus, seriously reducing the dielectric strength of gases and the reliability of gas-insulated apparatus. Obviously, the best way to alleviate the effect of conducting particles is to remove them from the equipment. Various techniques to remove them and to promote particle motion or scavenging into low-field particle traps have been studied and are in use in gas-insulated equipment.

D. Voltage Waveform Effects and Time to Breakdown

When a voltage of sufficient magnitude ($\geq V_s$ for dc) is suddenly applied to a gas-insulated electrode gap, or a gas-insulated conductor, breakdown does not occur instantaneously, but after a finite time $t = t_s + t_f$. The t_s is called the statistical time lag and is the time that elapses between the application of the voltage V ($\geq V_s$) and the occurrence of a free electron in the stressed gas volume which initiates the breakdown process. The t_f is called the formative time lag and is the time interval between the occurrence of the free electron and the collapse of the voltage (i.e., breakdown).

The statistical time lag t_s can vary from nanoseconds to milliseconds (or longer) depending on the time the initiatory electron becomes available when $V \geq V_s$. Initiatory electrons can be produced by cosmic radiation, natural radioactivity from materials, field emission from the cathode surface, or collisional detachment from negative ions in the case of electronegative gases. In experimental apparatus they can be produced intentionally by, for instance, an ultraviolet source, in which case t_s is reduced considerably.

The formative time lag usually varies from nanoseconds to microseconds and is influenced by the overvoltage [$\Delta(V - V_s)$], the field distribution, and, for unsymmetrical fields, the polarity. This is apparent from the data in Fig. 9 on N_2 and SF_6, which were obtained with a square impulse generator having ~2 nsec rise time and ~150 kV amplitude. It is evident that the higher the overvoltage (voltage in excess of V_s), the shorter the t_f at which breakdown occurs. It is also seen that t_f is significantly higher for negative polarity and that it varies considerably with field uniformity, especially for electronegative gases (Fig. 9). The voltage–time characteristics of dielectric gases are of practical importance for the insulation coordination and overvoltage protection of gas-insulated equipment.

E. Gases with Insulator/Conductor Properties

In a number of technologies a gas is needed which is both a good conductor and a good insulator. For example, in pulsed power technologies the key element is a fast repetitive switch. Among a number of switching devices, the diffuse gas discharge switch is promising for a system such as inductive energy storage. The operation of a diffuse discharge switch for inductive storage is characterized by two distinct stages: (1) the conducting (storing) stage, when E/N is small (~3×10^{-17} V cm^2), and (2) the transferring stage (when the stored energy in the inductor is transferred to the load), when E/N is large

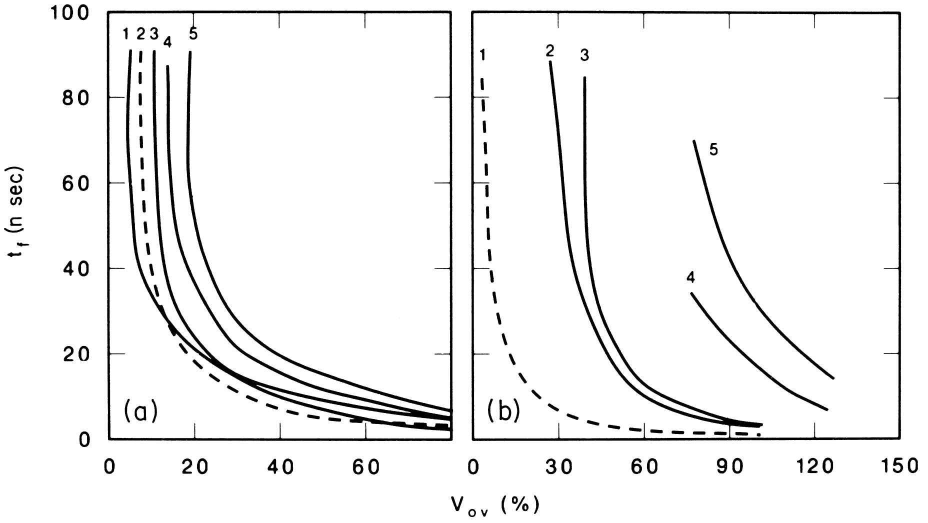

FIGURE 9 Formative time lag versus percentage of overvoltage in (a) N_2 and (b) SF_6 for different field distributions $n \equiv E_a/E_{max}$ (n values of 0.84, 0.54, and 0.32 correspond, respectively, to approximately homogenous, weakly inhomogenous, and inhomogenous fields), $d=4$ mm, and $P=1$ bar. In (a), for N_2, curves 1–5 are (respectively) for $n=0.84$, polarity $+$; $n=0.54$, polarity $+$; $n=0.54$, polarity $-$; $n=0.32$, polarity $+$; and $n=0.32$, polarity $-$. In (b), for SF_6, curves 1–5 are (respectively) for $n=0.84$, polarity $+$; $n=0.54$, polarity $+$; $n=0.54$, polarity $-$; $n=0.32$, polarity $+$; and $n=0.32$, polarity $-$. [Data from Peiffer, W. (1984). *In* "Gaseous Dielectrics IV" (L. G. Christophorou and M. O. Pace, eds.), pp. 329, 331, Pergamon Press, New York.]

($\gtrsim 150 \times 10^{-17}$ V cm^2). The successful operation of such switching devices depends on the availability of a gas that is a good conductor in the conducting stage and a good insulator in the transferring stage. To optimize conduction under the low-E/N conditions of the conducting stage, the electrons produced by the external source (e-beam or laser) must remain free and must have as large a drift velocity w as possible. To optimize the insulating properties under the high-E/N conditions of the transferring stage, the gas must effectively remove electrons by attachment (have a large attachment rate constant at high E/N). These requirements are schematically illustrated in Fig. 10.

Gas mixtures with such desirable characteristics have been reported by various authors. In particular, it has been shown that binary gas mixtures of buffer gases such as Ar and CH_4, whose electron-scattering cross sections have a Ramsauer–Townsend minimum at low energies ($\sim$0.5 eV), and electron-attaching gases such as C_2F_6, and C_3F_8, which attach electrons efficiently at high E/N and have much-reduced electron-attachment rate constants at low E/N, are most appropriate for diffuse discharge switching applications. Such mixtures have distinct maxima in the $w(E/N)$ at E/N values appropriate for the conducting stage of the switch, w values in excess of 10^7 cm sec^{-1}, and breakdown strength $\gtrsim 150 \times 10^{-17}$ V cm^2 for mixtures containing $\gtrsim$10% of the attaching gas.

IV. USES OF DIELECTRIC GASES

The most abundant "traditional" dielectric gas is atmospheric air. It naturally insulates overhead transmission lines that crisscross the countryside. Overhead transmission lines up to 800 kV are presently in service, and

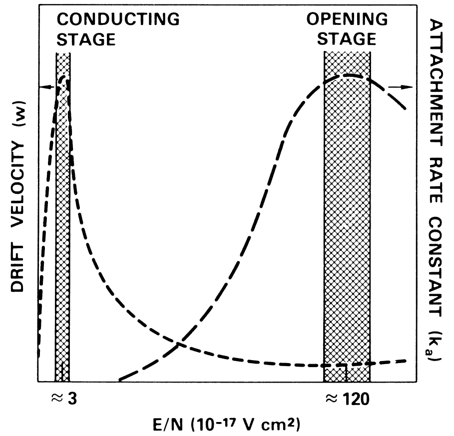

FIGURE 10 Schematic illustration of the desirable characteristics of the $w(E/N)$ and $k_a(E/N)$ functions of the gaseous medium in an externally (e-beam) sustained diffuse discharge switch. Indicated are rough estimates of the E/N values for the conducting and the opening stages of the switch. [From Christophorou, L. G., *et al.* (1983). *In* "Proceedings 4th IEEE International Pulsed Power 1983, Albuquerque, New Mexico" (T. H. Martin and M. F. Rose, eds.), p. 702, Texas Tech University Press, Lubbock, TX.]

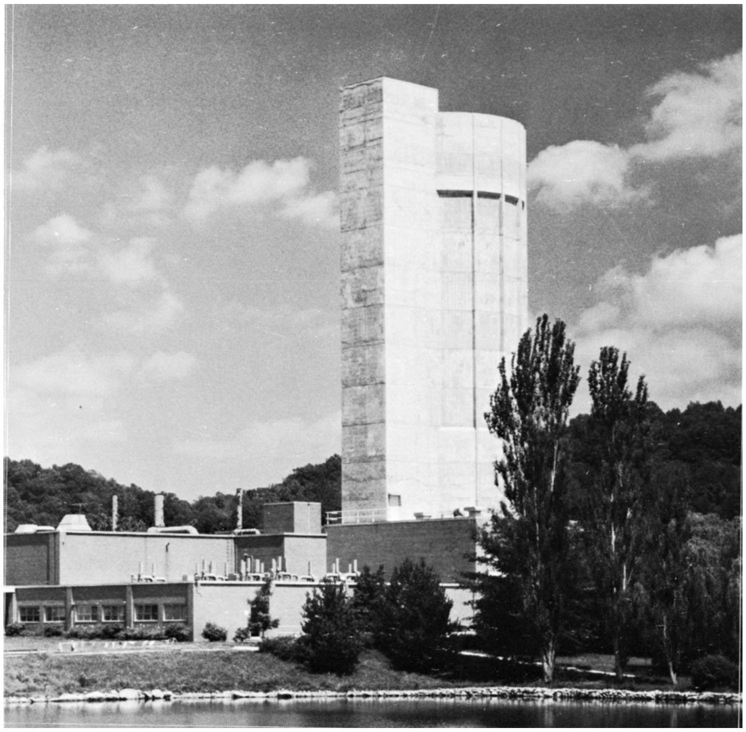

FIGURE 11 A view of Oak Ridge National Laboratory's electrostatic tandemtype heavy ion accelerator, which is insulated with SF_6. (Courtesy of Oak Ridge National Laboratory.)

lines for 1200 kV and higher voltages are under consideration for the future. Early uses of gas dielectrics included the use of N_2 and CO_2 (at pressures up to ~20 atm) in high-voltage standard capacitors. The distinct advantages of gaseous dielectrics (e.g., low weight, excellent recovery characteristics, low dielectric losses, compactness of equipment, and environmental advantages) resulted in their deployment for electrical insulation and arc interruption purposes in a variety of electrical equipment. In this section we briefly mention some of their main uses.

A. Research Equipment

High-voltage power supplies and Van de Graaff-type accelerators are examples of laboratory equipment that employ gas dielectrics for electrical insulation. Most such equipment uses SF_6. Other gases or gas mixtures (e.g., N_2/CO_2 and N_2/SF_6) have occasionally been used.

One of the largest Van de Graaff-type accelerators is the Holifield Heavy Ion Accelerator at Oak Ridge National Laboratory in Tennessee. It uses 0.7 MPa of SF_6 as an insulating gas. With this machine a dc voltage of 34 MV was achieved. A view of this electrostatic tandem-type heavy ion accelerator is shown in Fig. 11.

B. Circuit Breakers

Prior to the 1950s, high-voltage power circuit breakers mainly relied on oil and compressed air for insulation and current interruption. In 1956 the first high-voltage power circuit breaker was put into service at 115 kV, using SF_6 as the insulating and interrupting medium. Since then, circuit breakers with SF_6 gas have been put into service in all distribution and transmission voltage classes from 34.5 through 800 kV with interrupting capabilities in excess of 80 kA. Virtually all new circuit breakers today use a single-pressure chamber (usually at ~6 atm) in which the gas is further compressed with a piston attached to the moving contact and provides an axial gas blast for the are interruption (see Fig. 12). Earlier versions of SF_6 interrupters were of the two-pressure design, where the gas blast for the arc interruption was provided to the arc interruption chamber from a high-pressure (~14.5 atm) reservoir.

A basic requirement for an arc-interrupting medium, besides a high dielectric strength, is a high rate of recovery of its dielectric strength. The ability of SF_6 to recover its dielectric strength quickly after arc interruption along with its rapid thermal recovery and high degree of molecular reconstitution after arcing make it the most attractive arc-interruption gaseous medium.

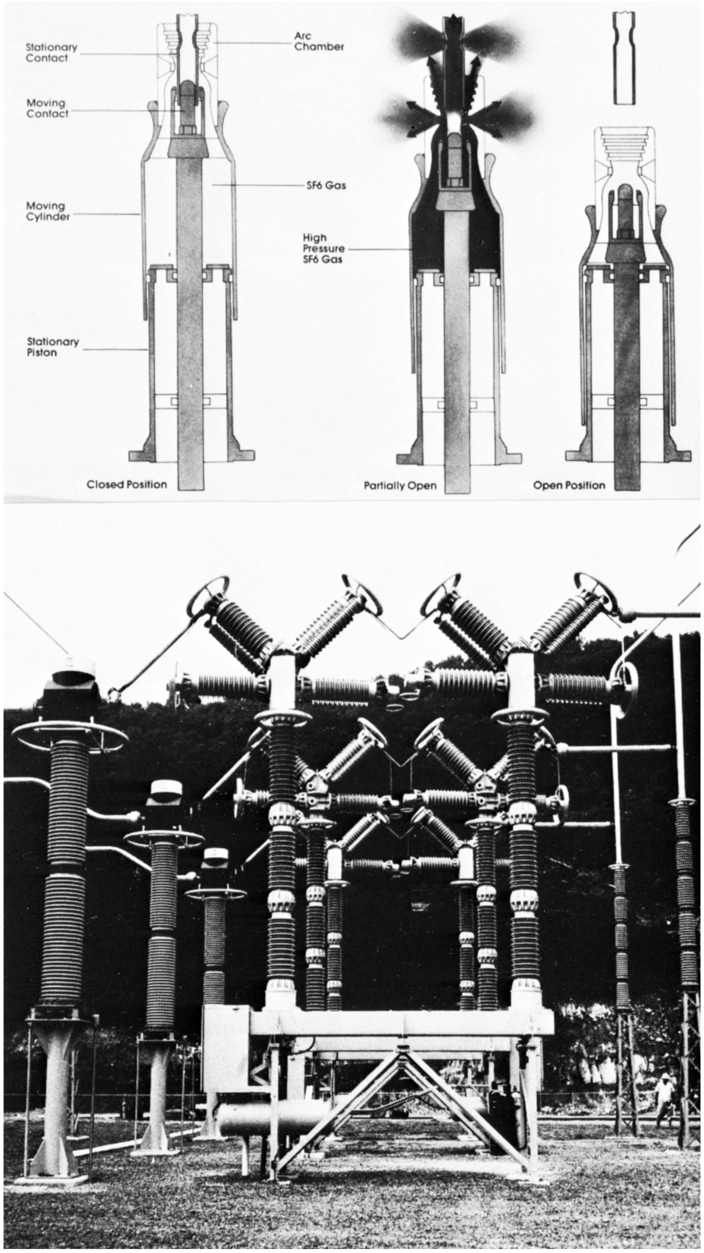

FIGURE 12 Circuit breakers using SF_6 gas. (Courtesy of Westinghouse Electric Corporation.)

A search for other gases/mixtures for use in circuit breakers showed that while no other gaseous medium outperforms SF_6 in circuit breakers, some gases/mixtures can be considered. The performance ratings (based on the critical interruption current I_c for a given surge impedance Z_0) relative to SF_6 of some such media are listed in Table III.

C. Compressed-Gas Insulated Substations

The excellent dielectric strength and arc extinguishing properties of SF_6 facilitated the development of circuit breakers with metal casings, generally called metal clad or dead-tank circuit breakers because the casing or tank is at ground potential. This naturally led to the development of other substation components such as disconnect switches, arresters, interconnecting links (buses), and cables for getaways using the metalclad technology.

The totally enclosed metalclad substations using SF_6 gas (Fig. 13) are significantly more compact than the open-air substations and switchyards. Often, the land required is reduced by as much as 40 times, and the resultant savings in the cost of land are thus significant. Furthermore,

TABLE III Arc Interruption Capabilities of Gases and Gas Mixtures[a,b]

Gas/mixture	$Z_0 = 450\ \Omega$ I_c (kA)	$Z_0 = 450\ \Omega$ $SF_6 = 100$	$Z_0 = 225\ \Omega$ I_c (kA)	$Z_0 = 225\ \Omega$ $SF_6 = 100$
SF_6	21.0	100	26.3	100
SF_6/N_2 (75/25)	17.8	85	20.4	78
$CH_4/CClF_2CF_3$ (50/50)	17.8	85	20.2	77
CF_2CFCF_3/SF_6 (75/25)	17.0	81	20.0	76
CF_3SO_2F/SF_6 (50/50)	16.5	79	18.3	70
SF_6/He (75/25)	15.4	73	20.4	78
SF_6/N_2 (50/50)	14.9	71	17.2	65
CF_2CFCF_3	14.8	70	17.8	68
SF_6/He (50/50)	14.7	70	19.7	75
$CClF_2CF_3/SF_6$ (75/30)	14.0	67	17.6	67
$CHClF_2/SF_6$ (75/25)	13.8	66	14.7	56
$CBrF_3/SF_6$ (75/25)	11.6	55	14.5	55
CF_3SO_2F/SF_6 (75/25)	11.4	54	13.8	52
CF_4	11.1	53	14.6	56
$CBrF_3$	11.1	53	16.8	64
$CClF_2CF_3$	10.8	51	15.4	59

[a] Total pressure = 0.62 Mpa.
[b] Data from Electric Power Research Institute. (1982). "Gases superior to SF_6 for insulation and interruption," EPRI · EL-2620, Electric Power Research Institute, Palo Alto, CA [prepared for Westinghouse Electric Corporation.]

metalclad substations are free from industrial and coastal pollution problems and are esthetically more pleasing. The compactness of gas-insulated substations also offers the option of locating them in the basements of buildings, thus allowing the transmission of power at high voltages straight into urban centers for distribution.

D. Compressed-Gas Insulated Cables

Transmission voltage cables using a compressed gas as the electrical insulation medium have been in commercial use since 1971. The voltage rating ranges from 138 to 800 kV. Such cables are used as getaways from substations to overhead transmission lines, in crossings of two or more transmission lines, in tunnels from hydroelectric and pumped storage generator plants, in river crossings, and so on. They are especially attractive when high-voltage and high-power ratings are required in limited space, when metal-clad substations are connected directly to gas-insulated cables, or when a reduction in fire hazard is required, as in tunnels.

The most common design of compressed-gas insulated cables consists of an aluminum center conductor and a concentrically located outer aluminum enclosure. The conductor is supported by epoxy insulators in the enclosure. SF_6 is the only dielectric gas used for gas-insulated substations and cables. Besides being an excellent dielectric, SF_6 also has good heat transfer characteristics for removing the heat generated by the resistive losses of the conductor to the enclosure. Usually the SF_6 pressure ranges from 3 to 5 bar. A schematic of a typical design of a gas-insulated cable is shown in Fig. 14, and a typical installation is shown in Fig. 13. Some designs include built-in particle traps to improve the reliability of the system.

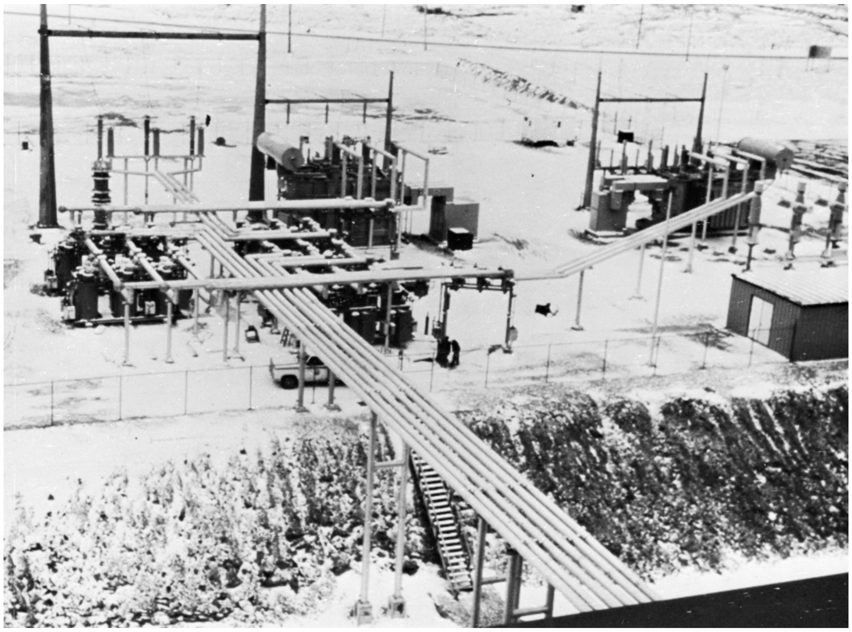

FIGURE 13 Totally enclosed metalclad substation using SF_6 gas as the insulating medium. (Courtesy of Westinghouse Electric Corporation.)

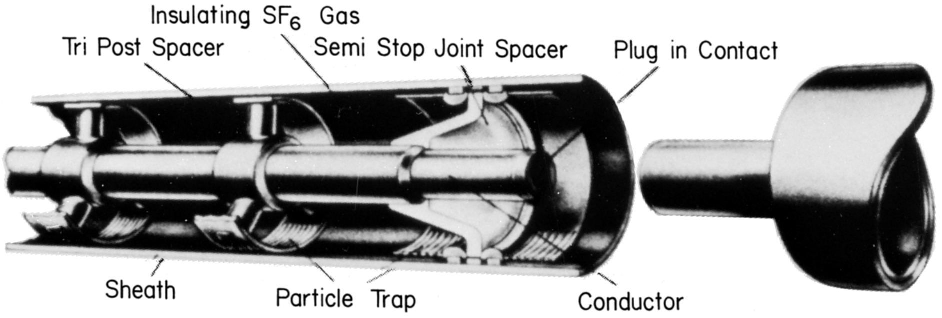

FIGURE 14 Schematic of a compressed-gas insulated (CGI) cable. (Courtesy of Westinghouse Electric Corporation.)

By far the largest use of gas-insulated cables has been in installations that are 100–200 m in length. The longest cable is 700 m (420 kV/1386 MVA). Research and development have been conducted to develop gas-insulated cables using SF_6 for 1200-kV transmission. Three-conductor cables (three-in-one), where the three-phase conductors are arranged in a single enclosure, are also used up to 362 kV transmission voltage. Gas-insulated technology is being further developed by considering flexible enclosure designs for easier installation.

Compressed-gas insulated cables have about two to three times the load-carrying capability of comparable oil-filled cables. Typically, a gas-insulated transmission cable at a 242 kV system voltage can carry 3000 A, equivalent to 1250 MVA, while at 1200 kV, 10,000 A, equivalent to 16 GVA, has been demonstrated.

V. CONCLUDING REMARKS

Recent advances in basic research, especially in electron- and ion-collision physics, have resulted in improved understanding of the dielectric properties of gases. This understanding, in turn, has aided efforts to identify, improve, and tailor new dielectric gases for a variety of electrical insulation needs.

Basic research is still needed to provide better understanding and a sounder scientific basis for the expected expansion in the uses of dielectric gases as insulants in high-voltage transmission and distribution and other high-voltage electrical equipment. The full potential of and benefit from the use of gas dielectrics is yet to be realized. To optimize this benefit, a well-balanced growth in basic and applied research and industrial development in this area is necessary.

SEE ALSO THE FOLLOWING ARTICLES

Atomic and Molecular Collisions • Molecular Electronics • Nanoelectronics • Power Transmission, High Voltage

BIBLIOGRAPHY

Christophorou, L. G. (ed.). (1980). "Gaseous Dielectrics II," Pergamon Press, Oxford.

Christophorou, L. G. (ed.). (1982). "Gaseous Dielectrics III," Pergamon Press, Oxford.

Christophorou, L. G. (ed.). (1984). "Electron–Molecule Interactions and Their Applications," Vols. 1 and 2, Academic Press, New York.

Christophorou, L. G., and Pace, M. O. (eds.). (1984). "Gaseous Dielectrics IV," Pergamon Press, Oxford.

Christophorou, L. G., and Sauers, I. (eds.). (1991). "Gaseous Dielectrics VI," Plenum Press, New York.

Christophorou, L. G., Sauers, I., James, D. R., Rodrigo, H., Pace, M. O., Carter, J. G., and Hunter, S. R. (1984). *IEEE Trans. Elect. Insul.* **EI-19,** 550–566.

Kunhardt, E. E., and Luessen, L. H. (eds.). (1983). "Electrical Breakdown and Discharges in Gases," Plenum Press, New York.

Meek, J. M., and Craggs, J. D. (eds.). (1978). "Electrical Breakdown of Gases," Wiley, New York.

Nasser, E. (1971). "Fundamentals of Gaseous Ionization and Plasma Electronics," Wiley, New York.

Special Issue. (1990). *IEEE Trans. Elect. Insul.* **25** (1, February).

Electron Transfer Reactions

Gilbert P. Haight, Jr.
University of Washington

I. Electron Transfer and Oxidation–Reduction
II. Electron Transfer from Metals to Aqueous H^+
III. Atom Transfer versus Electron Transfer
IV. Electron Transfers between Pairs of Atoms: Numbers of Electrons
V. Inner Sphere and Outer Sphere Transfers
VI. Classification of Electron Transfer Steps
VII. Pathways among Oxidation States
VIII. Electron Transfer in Biological Systems

GLOSSARY

Bridging ligand Atom, molecule, or ion capable of coordinating to both oxidizing and reducing agents and mediating electron transfer between them; such a reaction is called an inner sphere electron transfer.

Cooxidation Three-electron transfer process involving two electron donors; it may occur when both oxalate and alcohol are ligated to Cr(VI) in an activated state and are cooxidized as they transfer three electrons to Cr.

Electron transfer reaction Chemical reaction in which there is a net loss of electrons from one or more atoms or molecules accompanied by a corresponding gain of electrons by other atoms or molecules in a system, as when nonmetal atoms receive electrons from metal atoms to form salts.

Heme iron centers Redox centers in biological systems that contain iron(II) or iron(III) in a porphyrin ring, often with an open site for ligation to small molecules capable of penetrating a hydrophobic pocket.

Hole An active site in an intramolecular electron transfer system with the potential to accept an electron from a donor site.

Iron–sulfur "cubes" Clusters involved in biological electron transfer in a number of enzyme systems.

Multielectron, multipath systems Activated states in which more than one electron may be transferred by more than one orbital pathway in a fairly simple redox reaction such as cooxidation.

Outer sphere electron transfer Electron transfer that occurs when electrons pass between two centers that retain their coordination spheres throughout the transfer process and are not joined by bridging atoms or molecules.

Oxidizing agent Atom or molecule (e.g., a nonmetal atom) that undergoes reduction when it gains electrons from a reducing agent.

Phlogiston An eighteenth-century principle applied to all chemical processes; it can be sensibly identified with the modern concept of the electron.

π and π^* orbitals Orbitals formed by the overlap of p atomic orbitals on nonmetals and $t_{2g}d$ orbitals on transition metals to provide pathways for electron transfer.

Reducing agent Atom or molecule (e.g., a metal atom) that undergoes oxidation when it transfers electrons to an oxidizing agent.

Solvated electron Free electron solvated by a polar solvent such as NH_3 or H_2O in which it has a long enough lifetime to be studied as a chemical entity—electron donor or reducing agent.

Tunneling Quantum-mechanical electron transfer that occurs with little or no activation energy and where no obvious physical pathway for the electron is apparent.

ELECTRON TRANSFER REACTIONS are chemical reactions in which electrons leave a donor atom or a reducing agent and join a receptor atom or an oxidizing agent. This article describes the concepts applied to such reactions from ancient times to present discussions concerning the states of electrons in atomic and molecular orbitals, potentials for initiating transfer, and studies designed to allow postulation of orbital pathways. A tentative effort is made to develop a scheme for classifying such reactions in terms of the nature of the pathways employed and of the numbers of electrons transferred and numbers of pathways used in any given activated state. An early result of supercomputer calculations describing the multiple pathways for an electron to follow from the surface of the protein molecule myoglobin to a heme iron center deep in the interior of the molecule is discussed.

I. ELECTRON TRANSFER AND OXIDATION–REDUCTION

In the reaction of zinc metal with dilute mineral acid, zinc "dissolves" with the evolution of hydrogen gas:

$$Zn + 2H^+ \rightarrow Zn^{2+} + H_2. \quad (1)$$

Zn reduces H^+ to H_2 and is oxidized to Zn^{2+} by transfer of two electrons to two hydrogen ions, which forms hydrogen molecules. The term *reduction* goes back to ancient metallurgy, when ores were said to be reduced to metals. In 1700 the fact that metallurgical reducing agents (charcoal, metals, wood, etc.) also burned in air led to inclusion of such reagents in the phlogiston theory then being applied to nearly all chemical phenomena. Reducing agents were thought to give up phlogiston to the air when they burned and to ores when they were reduced to metals. The reaction above could be described as a phlogiston transfer reaction in which zinc becomes dephlogisticated. Hydrogen gas was described by Cavendish about 1770 as pure, gaseous phlogiston, since it was combustible and capable of reducing ores to metal. Lavoisier's discovery that combustible materials (reducing agents) gained weight by adding oxygen when they burned in air led to the concept of *oxidation* as addition of oxygen and *reduction* as removal of oxygen or to oxidation–reduction reactions as oxygen transfer reactions:

$$2Zn + O_2 \rightarrow 2ZnO$$

and

$$Zn + CuO \rightarrow ZnO + Cu.$$

Early in the twentieth century the structure of metal oxides was deduced to be ionic ($Zn^{2+}O^{2-}$). In electrolysis cells and batteries, addition of electrons at cathodes ($Cu^{2+} + 2e^- \rightarrow Cu$) effected reduction of metal compounds to metal, while at anodes metals were corroded, forming ionic compounds ($Zn \rightarrow Zn^{2+} + 2e^-$) by losing electrons. This led to the general concept that the metal was oxidized when it lost electrons to form positive ions and that positive metal ions were reduced when they gained electrons to form the metal. Table I shows a history of concepts used to describe oxidation–reduction reactions.

A. Identifying Phlogiston as Electrons

There is irony in the fact that the phlogiston theory, which was generally applicable to nearly all chemical systems and processes, was replaced by the oxygen theory, applicable specifically only to classical metallurgy and combustion. If one substitutes the word *electrons* for *phlogiston* in appropriate writings, the early theory makes complete sense. Attempts to identify phlogiston as a weighable substance had to fail because electrons do not exit separately from the atoms and molecules of substances and they are a very small fraction of the weight. All chemical phenomena are explicable in terms of electrons as constituents of atoms and molecules, consistent with the general applicability of the older phlogiston theory.

B. Observation of Electrons and Electron Transfer Processes

Electrons may be observed in electron beams and are undoubtedly released as free charged particles at the high temperatures found in the sun and stars. However, on the surface of the earth they are bound to atomic nuclei

TABLE I Concepts of Oxidation–Reduction Reactions

Process	Oxidizing agents	Reducing agents	Mechanism	Period
Ancient metallurgy	Metal ores	Charcoal, wood		~5000 B.C.
Combustion metallurgy	Air	Metals, charcoal	Phlogiston transfer	A.D. 1700s
	Metal calces	Phlogiston (H_2)		
	Oxygen	Metals, charcoal	Oxygen transfer	A.D. 1800s
	Metal oxides	Hydrogen, carbon monoxide		
Oxidation–reduction	Nonmentals	Metals, charcoal	Electron transfer (atom transfer)	A.D. 1900s
	Metal cations	Nonmental anions		
	High oxidation states	Low oxidation states		
	Anodes	Cathodes		

in atoms and molecules, are indistinguishable from one another, and cannot be observed directly in such states because of the restrictions of the Heisenberg uncertainty principle. We are now able to describe orbitals, or regions in space, in which the probability of finding an electron can be calculated or estimated for points within the region, and we are able to measure or deduce energies for electrons in orbitals. Thus when a reaction is judged to proceed by electron transfer, it can be said that one reagent achieves a state containing more electron(s) than it started with and another less, but nothing can be said from direct observation concerning the fate or role of any individual electrons present during the process.

II. ELECTRON TRANSFER FROM METALS TO AQUEOUS H^+

Figure 1 illustrates several conditions concerning the reaction [Eq. (1)] resulting from the immersion of metallic zinc in dilute sulfuric acid. Parts c and d illustrate the requirements for conduction of electric current in the circuit of this primary cell.

In the wire, electrons move from zinc to copper under the influence of the potential for electron transfer from zinc to hydrogen ions. In the solution, current is carried by positive ions moving toward the copper cathode and negative ions moving toward the zinc anode. Conduction between electrodes and solution is effected by half-reactions, the equations for which add up to Eq. (1). $Zn \rightleftharpoons Zn^{2+} + 2e^-$ (oxidation) "pumps" electrons into the wire and forms zinc cations in solution. $2H^+ + 2e^- \rightleftharpoons H_2$ (gas) (reduction) takes electrons from the wire at the copper, removing hydrogen ions from solution. The potential for electron transfer can be measured with no current flowing, that is, when there is electron transfer equilibrium among reducing agent, oxidizing agent, and electrons in each of the couples employed in reaction (1). Potentials for half-reactions are measured versus the H^+/H_2 potential, taken to be zero.

For the general half-reaction $Red \rightleftharpoons Ox + ne^-$, \ Nernst equation for the potential E is

$$nFE = nFE^0 - RT\ln([Ox]/[Red]),$$

where F is the Faraday, n the number of electrons in the half-reaction, and [ ] represents the molarity or activity of the oxidizing or reducing form of the couple. Some potentials for common half-reactions are given in Table II.

A. Potential Barriers to Electron Transfer

1. Anode hlsion of Cations

The behavior of electrons in Fig. 1 can be postulated from the overall result, namely that although zinc has the potential to transfer electrons to hydrogen ions, there is a barrier to direct contact that requires the hydrogen ions to pick up electrons at copper, which itself does not have

TABLE II Some Half-Reaction Potentials

Half-reaction	Potential E^0(V)
$Mg \rightleftarrows Mg^{2+} + 2e^-$	2.37
$Zn \rightleftarrows Zn^{2+} + 2e^-$	0.76
$H_2 \rightleftarrows 2H^+ + 2e^-$	0.00
$Cu \rightleftarrows Cu^{2+} + 2e^-$	−0.34
$2I^- \rightleftarrows I_2 + 2e^-$	−0.54
$Ag \rightleftarrows Ag^+ + e^-$	−0.80
$O_2 + 4H^+ \rightleftarrows 2H_2O + 4e^-$	−1.23
$2Cl^- \rightleftarrows Cl_2 + 2e^-$	−1.36
$Mn^{2+} + 4H_2O \rightleftarrows MnO_4^- + 8H^+ + 5e^-$	−1.51

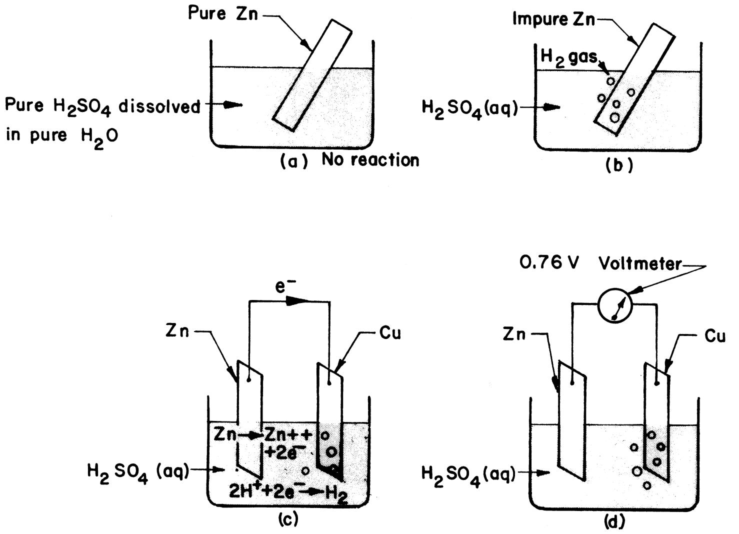

FIGURE 1 Oxidation–reduction: electron transfer. (a) Very pure zinc in very pure sulfuric acid gives no reaction although the potential for hydrogen (H_2) gas evolution is very favorable. (b) When the zinc is impure or has strains in the surface, brisk evolution of hydrogen occurs, or (c) if the zinc is connected by a wire to pure copper that is also immersed in the sulfuric acid solution, brisk evolution of hydrogen occurs at the copper surface ($2H^+ + 2e^- \rightarrow H_2$) and the zinc "dissolves" ($Zn \rightarrow Zn^{2+} + 2e^-$). This arrangement constitutes a primary cell, or battery, which generates electric current as electrons pass from the zinc anode, where oxidation of zinc occurs, to the copper cathode, where reduction of hydrogen ions occurs. (d) Meters inserted in the circuit will measure current flow (amperes) or voltage (0.76 V). The connecting wire and copper cathode provide a favorable path for electron transfer from zinc atoms to hydrogen ions.

the potential to donate electrons to hydrogen ions. In the circuit in Fig. 1, positive cations are repelled by the zinc anode, which suggests that the surface of the zinc in contact with the acid becomes positively charged, which creates a barrier to orbital contact with positive hydrogen ions in solution. No such barrier exists at copper, and the conduction band in the metallic wire provides an avenue for electrons to travel from the zinc surface to the copper surface. Ultrapure aluminum exhibits similar inertia when immersed in very pure sulfuric acid, which suggests a very high potential barrier for direct transfer of electrons from an electropositive metal to hydrogen ions.

2. Removal of the Barrier

Both aluminum and zinc react directly with strongly basic solutions to give hydrogen gas:

$$2Al + 2OH^- + 6H_2O \rightarrow 2Al(OH)_4^- + 3H_2$$

and

$$Zn + 2OH^- + 2H_2O \rightarrow Zn(OH)_4^{2-} + H_2.$$

Evidently the negative hydroxide ion (OH^-) can approach the positive metal surface and provide a path for electrons to reach protons bound to water. A choice among possible sequences of steps involving electron transfer and formation of hydrogen molecules (H_2) cannot be made on the evidence provided here for the nature of a charge barrier to electron transfer at a metal surface.

3. Reductions of Magnesium Anodes

The normal electrochemical process observed at magnesium anodes is the oxidation of magnesium metal ($Mg \rightarrow Mg^{2+} + 2e^-$). However, organic oxidizing agents have been observed to be reduced during the electrolytic oxidation of magnesium in a manner analogous to reduction by Grignard reagents (e.g., RMgBr). Such reductions have been detected some distance from the electrode in flow systems and are attributed to the production of monovalent Mg^+ at the electrode. This ion has an extraordinarily high potential for electron transfer to form the very stable Mg^{2+}, yet it is repelled by the anode before it can donate its remaining valence electron to the electrical circuit and must find a chemical electron acceptor in the solution:

$$Mg \longrightarrow Mg^+ + e^- \text{ (to external wire)}$$

$$Mg^+ + Ox \longrightarrow Red + Mg^{2+}$$

$$\text{(with } e^- \text{ passing from } Mg^+ \text{ to Ox)}$$

Understanding of individual electron transfer processes involves obtaining (to various degrees) knowledge of the following:

1. Potentials of half-reactions—"Is the reaction thermodynamically feasible?"
2. Structures of reactants and products. These can give clues to what must happen in the system to provide sensible pathways for the overall electron transfer to occur.
3. Identification of intermediates—evidence for steps along the way.
4. Kinetics. Reaction rates can be analyzed to postulate steps leading to an activated state, the formula, and the structure of the activated state for electron transfer. Most redox reactions involve very complex rearrangements of atoms and ions as well as electron transfer, as witness the reduction of MnO_4^- to Mn^{2+}. Not only are five electrons accepted by Mn(VII), but eight protons are needed to convert four coordinated oxide ions to water (see Table II).

III. ATOM TRANSFER VERSUS ELECTRON TRANSFER

Chemists have characterized two classes of redox reactions: atom transfer and electron transfer. The classic example of atom transfer involves the aqueous oxidation of sulfite ion by chlorate ion in which ^{18}O atoms initially bound to chlorine are found bound to the product sulfate, which thus precludes exchange of oxygen with water during the process:

$$3SO_3^{2-} + Cl^{18}O_3^- \rightarrow 3\,^{18}OSO_3^{2-} + Cl^-.$$

The rate of the reaction is given by rate $= k[SO_3^{2-}][ClO_3^-][H^+]^2$, consistent with the formation of an activated complex:

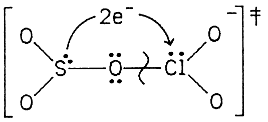

The S and Cl atoms have identical electronic structures as SO_2, produced by two protons acting on SO_3^{2-}, coordinates to an oxygen of ClO_3^-. A positive potential allows sulfur to transfer two electrons to chlorine. This causes scission of the O–Cl bond as water attacks the sulfur, forming SO_4^{2-} containing an oxygen atom originally bound to the chlorine in ClO_3^-.

In a similar way chlorine atoms are transferred in the reaction:

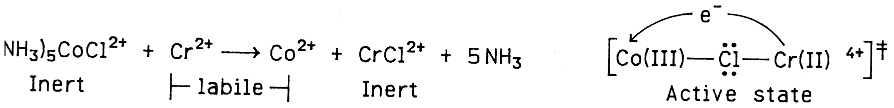

The result is the same whether one chooses to call either of these processes electron transfer followed by transfer of labilized ligand (O^{2-} or Cl^-) or atom transfer resulting in a net electron transfer in the opposite direction. In each case, electron transfer would produce states in which the bond that breaks would have become labilized and the bond formed would have become inert. Electron transfer as the primary action is consistent with the Franck-Condon principle that electron transitions in atomic systems are very rapid compared with nuclear motions, but one cannot experimentally determine that it is primary unless there is detection of intermediate complexes—in this case preceding and following formation of the oxygen or chlorine bridge.

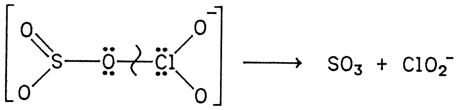

This complex, in which electrons have been transferred from S to Cl, could also hydrolyze to give $2H^+$, SO_4^{2-}, and ClO_2^-. In most cases the order of events following formation of the active state—electron transfer, hydrolysis, O–Cl bond scission, and so forth—cannot be determined. (This powerful *isotopic tracer* method of observing atoms being transferred in redox reactions from an inert reactant to form an inert product was pioneered by Henry Taube, who received the Nobel Prize in 1984.) For electron transfer to occur, there must be contact between electron donor and acceptor, adequate potential to effect transfer and overcome any barriers, and a mechanism for conduction of electron(s) from donor to acceptor. Conduction may take place through delocalized molecular orbitals as in the conduction bands of metals or π-bonding systems as in graphite. Reactions have been observed to occur with a breakdown in Arrhenius plots of the temperature coefficient of reaction rate. Electron transfers involving no energy of activation are thought to occur by quantum-mechanical tunneling. Electron transfer reactions over long distances are of great current interest in the study of redox phenomena in biological systems, where currents are found to be carried by electrons through connected orbital systems, by tunneling, and by series of coupled redox reactions as in the respiratory chain below. In this overall process oxygen molecules accept electrons from NADH. The electrons are transmitted by a series of electron transfer reactions between metal centers embedded in enzymes and labile organic redox couples in FAD and coenzyme Q. Cytochrome

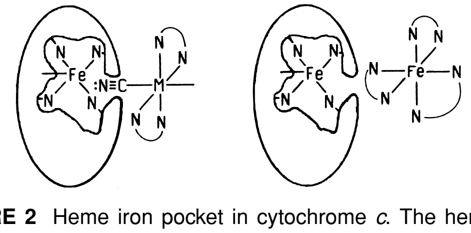

FIGURE 2 Heme iron pocket in cytochrome *c*. The heme iron redox center in cytochrome *c* exists in a hydrophobic pocket with a small opening to the surface of the protein, which provides means for alternative pathways for electrons to travel between heme iron and external redox centers. (Left) Pocket open to the surface of cytochrome *c* can be penetrated by a conducting ligand bound to a redox center (M). (Right) NN is ethylenediamine, which cannot conduct or penetrate the pocket.

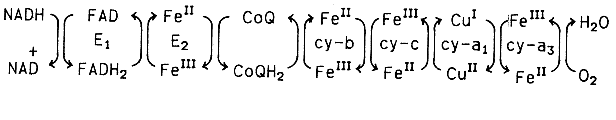

c has been isolated, its structure determined, and electron pathways to the heme iron center investigated by attaching metal ions to its surface or by attaching ligands to reducing metal ions that can probe the hydrophobic pocket in which the heme iron atom is found (see Fig. 2).

IV. ELECTRON TRANSFERS BETWEEN PAIRS OF ATOMS: NUMBERS OF ELECTRONS

There have been arguments for many years over the possibility of simultaneous multiple-electron transfer. The formation of electron pair bonds by donation from Lewis bases to Lewis acids suggests that a two-electron transfer might occur by such a route. Several reagents have been found to discriminate between one- and two-electron donors or acceptors in terms of products formed.

Nitrate ion (NO_3^-) is reduced to N_2O, NH_3OH^+, or NH_4^+ by two-electron donors, Zn, Sn(II), and so forth, and to NO_2 or NO by one-electron donors such as Cu, Fe(II), Ti(III), and VO^{2+}. Similarly, chlorate ion (ClO_3^-) is reduced to ClO_2(gas) by one-electron donors and to Cl^- by two-electron donors. In each case it appears that two-electron donors can bypass stable odd-electron molecules by donating electrons in pairs to the acceptor, even when several successive donations are required to reach the final product. Hydrazine is oxidized by one-electron acceptors by the following mechanism:

$$2H_2NNH_2 \rightarrow 2(e^- + H^+ + H_2NNH\cdot) \rightarrow$$
$$[H_2NNHNHNH_2]\ddagger \rightarrow N_2 + 2NH_3 + 2H^+,$$

but two-electron acceptors produce only N_2. Sulfite ion (SO_3^{2-}) is oxidized to SO_4^{2-} by two-electron acceptors and to dithionate ($S_2O_6^{2-}$) by one-electron acceptors. The latter oxidize SO_3^{2-} to $\cdot SO_3^-$, which dimerizes. (The ability of hydrazine and sulfite ions to discriminate between "mono-" and "di-delectronators" was observed in the 1920s by A. W. Browne. The concept of one-step two-electron transfer then fell into disfavor and is still treated with a fair amount of skepticism.)

V. INNER SPHERE AND OUTER SPHERE TRANSFERS

Many atom transfer reactions are also called inner sphere when donor and acceptor atoms are joined by a bridging atom bound to each redox center. The bridging atom may or may not be transferred in the opposite direction to the electron(s) as in the oxygen and chlorine atom transfers described above. $IrCl_6^{2-}$ is reduced to $IrCl_6^{3-}$ by Cr^{2+} without transferring a Cl^- to the Cr^{3+} product. By incorporating radioactive iridium into $IrCl_6^{2-}$, one can follow the electron exchange reaction:

$$^*IrCl_6^{2-} + IrCl_6^{3-} \rightarrow IrCl_6^{2-} + {}^*IrCl_6^{3-}.$$

Such a reaction, in which no change takes place in the coordination spheres of reactants and products, is called an outer sphere reaction, assuming no direct bridging atom or atoms bind donor and acceptor together in the activated state. Exchange reactions have been intensively studied, but only for one-electron processes. (Detailed theory concerning such processes is based on the work of Rudolf Marcus and Noel Hush.)

Probing the surface of cytochrome *c* for electron pathways to the heme redox center has been pioneered by Harry Gray. Conducting ligands like CN^- that can be inserted into the pocket cause deviations from the predictions of the Marcus relation for outer sphere electron transfer reactions, whereas nonconductors or ligands that cannot penetrate the pocket, like ethylenediamine complexes, are "well behaved." This indicates that various pathways with different energy barriers to electron transfer may be found for electrons entering and leaving redox centers in large biomolecules by outer sphere mechanisms.

VI. CLASSIFICATION OF ELECTRON TRANSFER STEPS

Several postulated combinations of numbers of electrons and numbers of pathways have been proposed for activated states in which redox centers exchange electrons. Structures of such states are deduced from experimental evidence such as rate laws, product analyses, isotopic tracer experiments, and deuterium isotope effects. Let

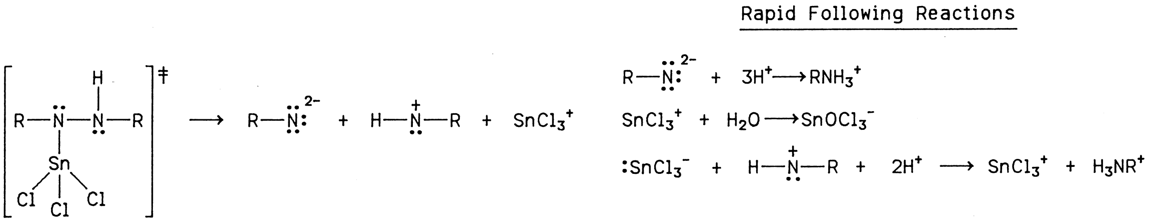

SCHEME 1

us assume that an individual orbital pathway may conduct one or two electrons and that more than one orbital pathway may lead to or from a given redox center. It is then possible for us to classify proposed electron transfer process in terms of combinations of numbers of pathways and numbers of electrons. Equations for overall reactions and formulas for postulated activated states that provide models for the structures in which electron transfers are thought to occur will be used to illustrate each classification.

A. One-Path Systems

1. Direct Transfer—Atom to Atom

a. One-electron transfers.

Reaction: $2Na + Cl_2 \rightarrow 2Na^+ + 2Cl^-$

Activated state(s): $[Na \cdots Cl—Cl]\ddagger$

$([Na \cdot\cdot Cl]\ddagger + Cl\cdot)$

Direct transfer of electrons from sodium atoms to chlorine molecules or atoms in the reacting systems results in the formation of $[Na^+Cl^-]$ ion pairs.

Reaction: $2Fe^{2+} + HNO_2 + H^+ \rightarrow$

$[FeNO]^{2+} + H_2O + Fe^{3+}$

Activated state: $[Fe(II) \cdots (NO^+)]\ddagger$

Electron transfer occurs by attack of Fe^{2+} on NO^+. The product NO forms a detectable complex with a second Fe^{2+} ion. The electron transfer step in most processes—especially in solution and even at electrodes—must be sorted out by intuition from a complexity of reactions leading to formation of the active state for electron transfer and also those leading from the activated state to formation of eventual products. Often it is clear that the activated state for the slow step in a reaction is not the state in which electron transfer occurs.

Polymerization:

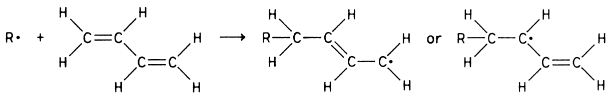

The attack of a radical (R·) on carbon C-1 of butadiene appears to transfer the odd electron on the radical to either C-4 or C-2, which creates a new radical. This radical can add to another monomer. The delocalized π-orbital in butadiene can "conduct" the intruding electron from C-1 to any other C, since it has a significant probability of being in valence orbitals associated with any participating carbon. It will end up most often on carbon atoms in which it can reside in the most stable half-filled nonbonding orbital, characterizing a new radical. One can also imagine that one of the two pairs of π electrons is "transferred" to the R–C bond and the delocalization of the second pair lowered from an orbital covering all four carbon atoms to one "localized" on C-2 and C-3. Seemingly, one might just as well talk of electron "scrambling" as of electron transfer; certainly one must be aware that an "electron transfer" process involves a change in the condition of all the valence electrons in the system connecting oxidant with reductant and reactants with products. One net result of all this electronic activity is the loss of electron(s) by the reductant and gain by the oxidant which we label electron transfer.

b. Two-electron transfers. Direct two-electron transfers presumably occur in the extreme case of a Lewis base's donating an electron pair to an acid, which forms a bond so polar that the electrons become a lone pair on the once acidic atom. Two-electron donors are often nonmetal atoms in complexes in which they exhibit oxidation numbers of $n-2$, where n is the number of the group in the periodic table in which they are found. Examples are $:SnCl_3^-$, $:SO_3^{2-}$, and Tl^+. $:SnCl_3^-$ is the active species when Sn(II) in aqueous hydrochloric acid is used as a reductant. It reduces the diazo group in methyl orange ($2{:}SnCl_3^- + RN{=}NR + 6H^+ + 6Cl^- \rightarrow 2SnCl_6^{2-} + 2RNH_3^+$). H^+ and $:SnCl_3^-$ attack the double-bonded nitrogen atoms to produce the activated state in Scheme 1.

2. Outer Sphere One-Electron Transfer

$$Fe^*(CN)_6^{4-} + Fe(CN)_6^{3-} \rightarrow Fe^*(CN)_6^{3-} + Fe(CN)_6^{4-}$$

The activated state is a collision complex with structures close enough in energy to enhance the probability of

electron transfer occurring without any eventual change in the two coordination spheres as radioactive iron equilibrates between the two oxidation states.

3. Inner Sphere One-Electron Transfer

These processes were described above in connection with chlorine atom transfer from a cobalt(III) complex to Cr^{2+} and with the electron transfer from Cr^{2+} to $IrCl_6^{2-}$ without accompanying chlorine atom transfer. Activated states probably contain Cl^- bridges in each case.

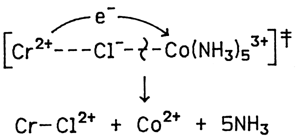

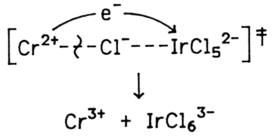

4. Inner Sphere Two-Electron Transfer

The oxygen atom transfer reaction described above has been shown as a two-electron inner sphere transfer. Oxidation of primary and secondary alcohols by MnO_4^- and by $HCrO_4^-$ have been rationalized as two-electron transfers that require removal of a proton from the carbon attached to oxygen. Manganese(V) has been detected as an intermediate product, and chromate ester precursors to reactions suggest the following activated states:

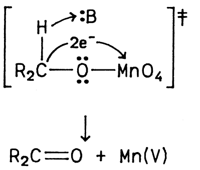

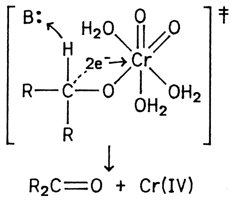

Tertiary alcohols without protons on the carbon are not oxidized. It is tempting to consider that removal of the proton in the activated states "frees" a pair of electrons to be transferred through the oxygen bridge to the metal ion. In the case of chromium(VI) oxidation of secondary alcohols there is general acid catalysis and a large deuterium isotope effect.

a. Hydride (H:⁻) transfer. The reaction of alcohols with MnO_4^- in basic solution is found to involve the reaction of alcoholate ion (R_2CHO^-) with MnO_4^- and is probably an example of direct transfer of hydride ion from C to form $HMnO_4^{2-}$.

$$[R_2C(O^-)—H \cdots OMnO_3^-]^{\ddagger} \rightarrow R_2C{=}O + HOMnO_3^{2-}$$

The neutral alcohol does not appear to react. Hydride transfer from neutral $R_2CH(OH)$ would involve charge separation of H^- from $R_2C^+(OH)$. Oxidation of C–H bonds in hydrocarbons by MnO_4^- has been found to generally involve hydrogen atom (H·) transfer.

b. Solvated electron. Hydrated electrons have stability enough to enable studies of the reduction of hundreds of other aqueous species. The $e^-(aq)$ has a hydration energy of −40 kcal/mol, an oxidation potential of ~2.5 V, and a k of only 16 M^{-1} sec^{-1} for reaction with H_2O. Diffusion-controlled reactions are observed with most paramagnetic species except alkyl radicals. Correlation between reactivity and redox potentials of electron acceptors is not likely. The availability of empty orbitals on transition metal ions and the energy gain on adding the electron are primary factors. Mn^{2+} is unreactive while Cu^{2+} reacts at about one-tenth the rate of diffusion control.

$$\cdot CO_2^- + HCrO_4^- \longrightarrow CO_2(g) + HCrO_4^{2-}$$

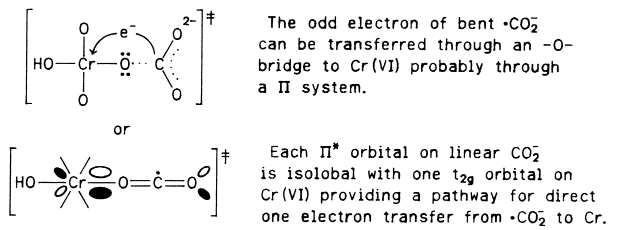

Chromium(VI) is an extraordinarily efficient radical trap even though its potential for forming chromium(V) does not appear to be particularly high. Empty t_{2g} orbitals as opposed to high potential make it a diffusion-controlled acceptor of hydrated electrons as well. It is notable that alkyl radicals are inert to hydrated electrons, which would form carbanions, and reactive to Cr(VI), which oxidizes them to carbonium ions.

B. Two-Path Systems

1. Two-Electron, Two-Path Transfers

a. Single donor—Two acceptors.

Reaction: $4VO_2^+ + N_2H_4 + 4H^+ \longrightarrow 4VO^{2+} + N_2 + 4H_2O$

Activated state:

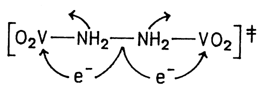

N_2H_4 is normally a discriminator between one- and two-electron acceptors. In this case its two-electron product (N_2) is observed and two one-electron acceptors appear in the activated state and are reduced. One can imagine the immediate result of two one-electron transfers from N to V(V) to be [V(IV)—NH=NH—V(IV)] + $2H^+$.

N_2H_2 is isoelectronic with O_2, with two half-filled π^* orbitals that are isolobal with half-filled t_{2g} orbitals on the V(IV) atoms resulting from the electron transfer step. This complex, if it is formed, is too unstable to detect due to the reaction $2N_2H_2 \rightarrow$ [HN—NH—NH—NH] $\rightarrow N_2 + N_2H_4$. Similar electron donors to hydrazine (N_2H_4) are oxalate ($^-O_2C—CO_2^-$) and thio-oxalate $[OSC—CSO]^{2-}$, which, when oxidized, break the C–C bond, which forms the gases CO_2 and CSO.

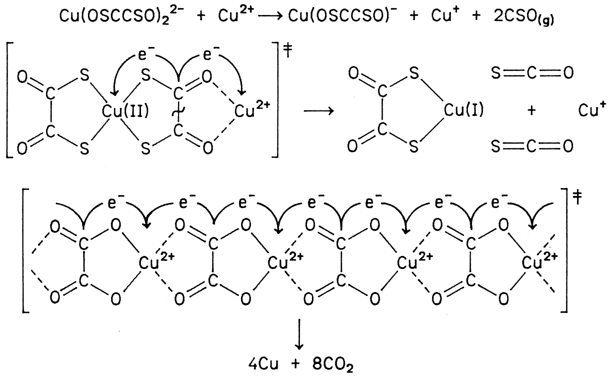

Copper ions have two t_{2g} orbitals with proper symmetry to interact with the π-orbitals in the planar oxalate ions, which provides a conduction path from each oxalate to two adjacent copper atoms. Mild heating causes smooth evolution of CO_2 and deposit of extremely fine copper crystals—a process used in the production of microelectronic devices.

b. Single acceptor—Two donors.

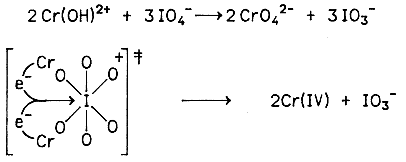

Two Cr^{3+} become coordinated to octahedral IO_6^{5-} to form an activated state for two one-electron transfers from Cr(III) to I(VII). Cr(IV) is unstable and disproportionates to Cr(VI) and Cr(III).

2. Four-Electron and Six-Electron Transfers

A multielectron process of great interest is the conversion of water to oxygen in the natural process of photosynthesis in green plants. Study of the photosystem has revealed that O_2 evolution maximizes on every fourth pulse of light, which suggests that the half-reaction

$$2H_2O \rightarrow O_2 + 4H^+ + 4e^-$$

may be effected in one step. The following reaction could be an example:

$$Mn(IV)_2 \text{ glucolate} \rightarrow 2Mn(II) \text{ gluconate} + O_2. \quad (2)$$

It occurs when Mn(IV) gluconate in 1.0*M* NaOH is brought to pH 12. A μ,μ-dioxo bridged dimer is proposed as the activated state:

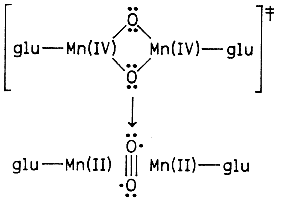

Two electrons from each bridging O^{2-} may be transferred to Mn(IV), which forms O_2 and two Mn(II) gluconate complexes.

A multiple-electron acceptor of interest is dinitrogen (N_2), which must accept six electrons to be converted to ammonia. A dinuclear complex of Zr(II) containing three ligated N_2 molecules reduces one N_2 to N_2H_4 when added to acid solution. The two-step mechanism with postulated electron transfers is illustrated below:

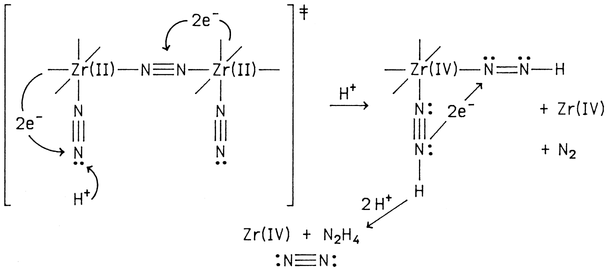

A highly conducting π-bonding system including t_{2g} orbitals on the zirconium atoms provides easy pathways for electrons impelled by the potential provided by proton attack on a terminal nitrogen atom.

A Mo(0) complex containing two N_2 and four substituted phosphine ligands, when added to acid, will reduce one N_2 to either N_2H_4 or $2NH_3$, which suggests that at least three orbital pathways exist for pairs of electrons on Mo to find their way to nitrogen under favorable potentials. Of course, one could also readily imagine that three successive two-electron transfers take place when the bound nitrogen forms ammonia.

Seemingly complicated activated states for electron transfer clearly arise when possibilities of direct production of stable products with most favorable geometries occur. A spectacular instance occurs in the oxidation of dimeric $(MoOH)_2^{4+}$ illustrated below. All oxidants give the same stoichiometry and product distribution. Mo(VI) as oxidant gives the same products by

$$6MoO_4^{2-} + 3(MoOH)_2^{4+} + 14H^+ \rightarrow$$
$$3Mo_2O_4^{2+} + 2Mo_3O_4^{4+} + 10H_2O$$

with Mo(VI) atoms equally distributed in the products. Evidently, $(MoOH)_2^{4+}$ on giving up electrons forms oligomers. The first that is able to break up into only stable products has 12 molybdenum atoms with an average oxidation state of 4.5.

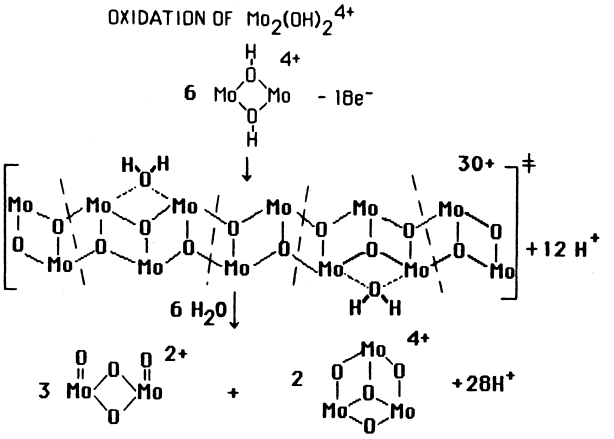

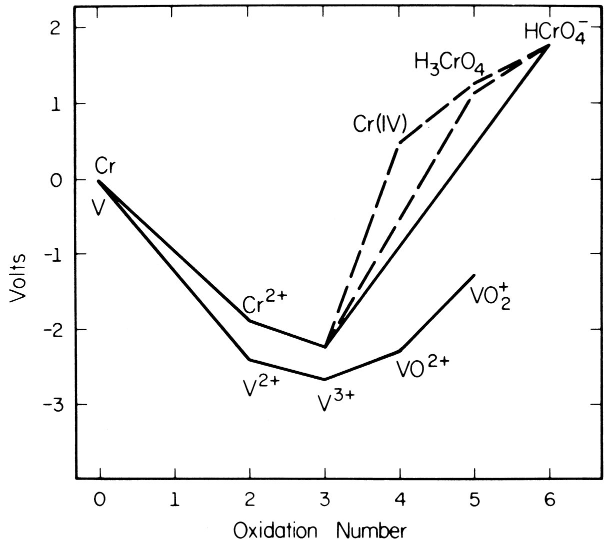

FIGURE 3 Oxidation state–potential diagrams for vanadium and chromium [1.0 *M* H^+(aq)].

VII. PATHWAYS AMONG OXIDATION STATES

Oxidation state–potential diagrams for nonmetallic and transition metal elements provide an interesting framework for analyzing the highly varied results obtained for redox reactions involving as many as nine oxidation states. So many different products and stoichiometries are obtained from the reduction of nitric acid that early work seeking patterns of reaction was abandoned after many years of frustrating effort.

Figures 3 and 4 show diagrams for the transition metals vanadium and chromium and for the nonmetal nitrogen, all in 1.0*M* aqueous acid solution. The slopes of lines joining redox couples represent the potentials for the half-reactions in question, a positive slope representing a reduction potential and a negative slope an oxidation potential. An intermediate state above tie lines joining higher and lower states will be unstable to disproportionation [e.g., Cr(V) and NO_2] while species below such tie lines are stable [e.g., Cr(III) and N_2]. The diagrams are a convenient way to postulate the feasibility of various possible one- and two-electron pathways in multistep redox processes involving a particular element.

A. Reduction of Nitric Acid

It is interesting to note that N_2 is seldom observed during reductions of nitric acid, which shows the importance of kinetic control over the course of multistep processes. One-electron reducing agents produce NO, which escapes as a gas from an open system, before nitrogen is reduced to oxidation number zero. Two-electron reducing agents (in excess) produce N_2O, NH_3OH^+, and NH_4^+, bypassing all states that require an odd number of electrons to be transferred to NO_3^-. HNO, which is isoelectronic with O_2, is apparently an active intermediate in all two-electron reductions of nitric acid. Most product patterns can be rationalized by postulating traps for HNO as follows:

$$HNO + HNO \rightarrow HONNOH \rightarrow N_2O + H_2O$$
(dimerization, no electron transfer).

Reducing agents:

$$HNO + :SnCl_3^- \rightarrow Sn(IV) + H{-}\ddot{N}{-}\ddot{O}:^{2-}$$
$$H{-}\ddot{N}{-}\ddot{O}:^{2-} + 3H^+ \rightarrow H_3NOH^+$$
(direct $2e^-$ transfer)

$$HNO + Mo(IV) \rightarrow [Mo{\equiv}N{-}\ddot{O}{-}H]^\ddagger \rightarrow$$
$$Mo(VI) + :\ddot{N}{-}\ddot{O}{-}\overset{2-}{H} \qquad \text{(direct } 2e^- \text{ transfer)}$$

The last case makes possible transfer of *two* unpaired t_{2g} electrons from Mo(IV) by forming a triple bond in the activated state using the π^* orbitals on NO^-, which are isolobal with two t_{2g} orbitals on Mo(IV). [Under similar circumstances Mo(IV) reduces two ClO_3^- to $\cdot ClO_2$ by separate one-electron transfers from the orthogonal

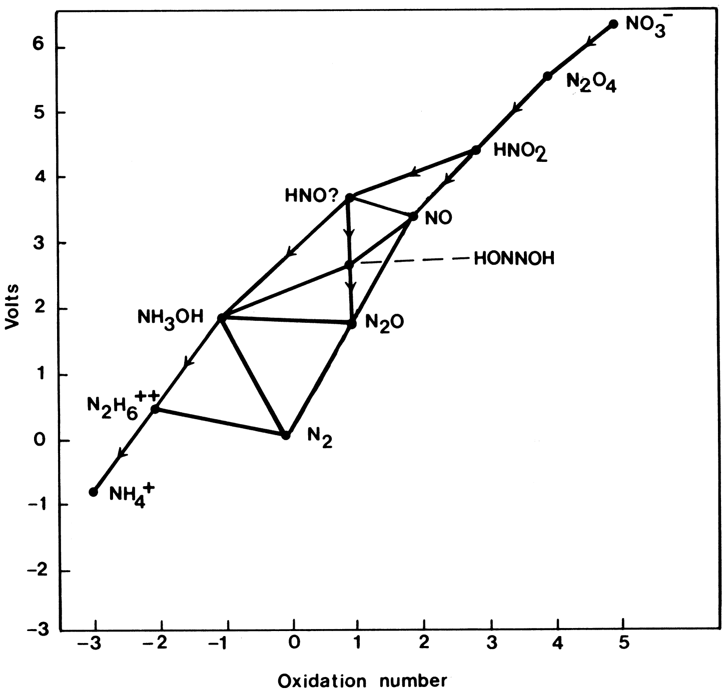

FIGURE 4 Oxidation state–potential diagram for nitrogen (1.0 M H^+).

t_{2g} orbitals to two different acceptors, probably by inner sphere one-electron transfer through oxygen bridges.]

Oxidizing agents:

$NO^- + NO^+ \rightarrow [:\ddot{O}{=}\ddot{N}{-}\ddot{N}{=}\ddot{O}:]^{\ddagger} \rightarrow 2\cdot NO$ or

$HNO + HNO_2 \rightarrow [HON \leftrightarrow NO_2H]^{\ddagger} \rightarrow 2\cdot NO + H_2O$

Coordination and bond scission or direct 1e⁻ transfer

$HNO + HNO_3 \rightarrow [H{-}O{-}N{\leftarrow}O{\rightarrow}NO_2H]^{\ddagger} \rightarrow 2HNO_2$ (2e⁻)

(Inner sphere 2e⁻ transfer and O-atom transfer)

$HNO + HCrO_4^- \rightarrow [H{-}N{\equiv}O{-}Cr(VI)]^{\ddagger} \rightarrow NO^+ + Cr(IV)$ (e⁻, e⁻)

2e⁻, 2 path transfer

From such an activated state one could reasonably expect a one-electron inner sphere transfer giving stable ·NO and CrO_4^{3-}. This does not occur. Figure 2 indicates that the potential for two-electron reduction of Cr(VI) is more favorable than for one-electron reduction. The octahedral activated state illustrated below can be constructed by incorporating two water molecules to rationalize the preference for two-electron transfer.

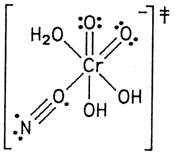

The octahedral activated state is favorable for formation of Cr(IV) and allows π* orbitals on NO⁻ to be isolobal with two t_{2g} orbitals on the Cr. Arguments are not changed if NO⁻ is N-bonded to Cr.

B. Reduction of Acid Chromate ($HCrO_4^-$)

Figure 5 indicates all the conceivable combinations of one- and two-electron processes that one could use to reach chromium(III) from chromium(VI). All pathways have been invoked to explain some process. The system lends itself to study, because it is possible to ascertain the formula of initial Cr(VI) species by equilibrium studies

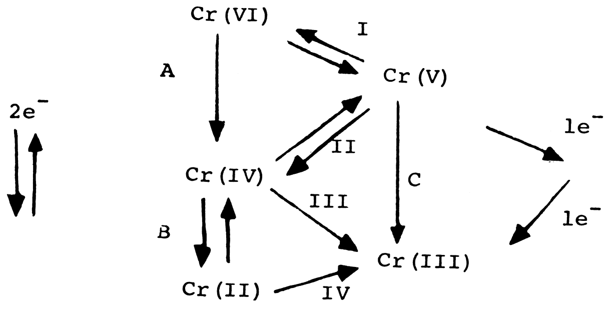

FIGURE 5 Electron transfer pathways from Cr(VI) to Cr(III).

and the inertia of Cr(III) complexes makes it possible to ascertain what is bound to Cr(III) when its precursor is reduced by electron transfer. The structures and properties of known (and postulated) species of chromium in each oxidation state are as follows.

1. Cr(VI)

In CrO_4^{2-}, esters ($ROCrO_3^-$), and metal complexes [Fe—$OCrO_3^+$], tetrahedral coordination dominates. Octahedral activated states for reduction of Cr(VI) to Cr(IV) or Cr(III) and containing *cis*-dioxo ligands are postulated by analogy to stable complexes of *cis*-MoO_2^{2+} (see Section VI.A.1.b). Mechanisms for substitution reactions on chromium(VI) postulate five-coordinate activated states. The potential for Cr(VI) to accept electrons increases as the number of electrons increases from one to three (Fig. 2).

2. Cr(V)

Tetrahedral CrO_4^{3-} and square pyramidal complexes of $Cr{\equiv}O^{3+}$ have been characterized. Octahedral complexes of *cis*-CrO_2^+ have been postulated as activated complexes for reduction to Cr(IV) and Cr(III). Cr(V) has a much higher potential for accepting two electrons than one and can disproportionate.

3. Cr(IV)

Chromium(IV) species are not detected during reductions of Cr(VI) to Cr(III). It can be inferred from kinetics and product distributions that Cr(IV) has a very high potential for accepting one electron and is very labile to substitution in octahedral complexes. It will disproportionate in the absence of oxidizable material in aqueous acid.

4. Cr(III)

Chromium(III) forms inert octahedral complexes. It is a one-electron donor of low potential.

C. Pathways from Cr(VI) to Cr(III) and Activated States (*)

1. Cr(VI)–Cr(V)–Cr(IV)–Cr(III)

a. Electrophilic donors—Fe^{2+}, VO^{2+}, Ti^{3+}, etc.

$$3Fe^{2+} + HCrO_4^- + 7H^+ \rightarrow 3Fe^{3+} + Cr^{3+} + 4H_2O$$

[Fe—O—CrO_3]*, [$(FeO)_2CrO_2(H_2O)_2^{3+}$]*, and [Cr(IV)—O—Fe(II)]* are all one-electron, inner sphere.

b. Nucleophilic donors—$Fe(CN)_6^{4-}$, Mo $(CN)_8^{4-}$, etc.

$$4Mo(CN)_8^{4-} + HCrO_4^- + 7H^+ \rightarrow 3Mo(CN)_8^{3-} + \left[Cr{-}N{\equiv}C{-}Mo(CN)_7^-\right] + 4H_2O$$

[$H_3CrO_4^+$, $(Mo(CN)_8^{4-}$]* (outer sphere) [Cr(V) or (IV)—N≡C—Mo(IV)]*. One or two $Mo(CN)_8^{4-}$ are bound to the Cr(III) product.

2. Cr(VI)–Cr(IV)–Cr(III) (Induced Reactions)

In acid solutions [$HCrO_4^-$ reacts slowly or not at all with I^- unless *induced* to do so by another reducing agent. If a two-electron agent is used, 0.5 mol I_2 is produced per mole of Cr(VI). The powerful oxidant Cr(IV) is capable of one-electron oxidation of I^- to I, which dimerizes to I_2.

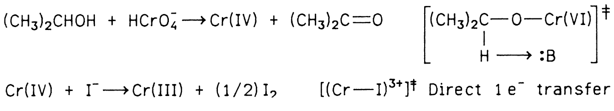

3. Cr(VI)–Cr(V)–Cr(III)

If I^- is present when some one-electron reducers are added to $HCrO_4^-$, 1 mol I_2 is produced per mole of Cr(VI) reduced. Chromium(V) has high potential as a $2e^-$ acceptor. (Its reaction as a one-electron acceptor with Fe^{2+} is the slow step in the sequence in Section VII.C.1 above.)

$$e^- + Cr(VI) \rightarrow Cr(V) + 2I^- \rightarrow Cr(III) + I_2$$

$$[Cr(V){-}O{-}I]\ddagger \rightarrow Cr(III) + OI^-$$

$$2H^+ + I^- + OI^- \rightarrow I_2 + H_2O$$

4. Cr(VI)–Cr(III) (Three-Electron Transfer Reactions)

The seemingly unlikely one-step three-electron reduction of Cr(VI) to Cr(III) has been found to take place when two ligands, one a two-electron donor and the other a one-electron donor, can both bind to *cis*-CrO_2^{2+} to give an octahedral activated state. Activated states for three-electron reductions of Cr(VI) by two sulfite ions (SO_3^{2-}), by two oxalate ions ($C_2O_4^{2-}$), and by an oxalate and an alcohol are shown below:

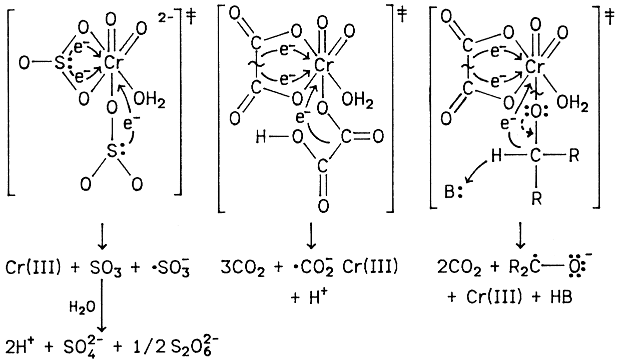

Chelated oxalate and sulfite ions have conducting Π-orbital systems that can include two t_{2g} orbitals on Cr, which creates the possibility of transferring one electron to each of those orbitals while the other ligand transfers an electron to the third. Such activated complexes make full use of the maximum potential available for reduction of chromium (VI) and give Cr(III) products directly with their most stable electron configuration. When the three-electron process involves two different electron donors (as in the case of oxalate and 2-propanol at right above), the process has been called cooxidation by its discoverer, Jan Rocek. How favorable the three-electron process can be is shown by the fact that $H_2PO_3^-$ has a rate constant about eight orders of magnitude smaller than that for isoelectronic HSO_3^-. Apparently the phosphite has an inert proton on the phosphorus(III) atom that inhibits the two-electron transfer from the P(III) center, and it is incapable of being a facile one-electron donor like the sulfite. It is also interesting that sulfite, which has been used to discriminate between one- and two-electron acceptors, is oxidized equally by one and two electrons by the three-electron acceptor Cr(VI).

VIII. ELECTRON TRANSFER IN BIOLOGICAL SYSTEMS

Space does not permit adequate description of the enormous effort and progress being made in the study of electron transfers in biological systems. The respiratory chain whose bare outline is given above has been under intensive study since the 1970s. The breakthrough that now provides detailed structural information on proteins and nucleic acids has made possible serious study of macromolecular mechanisms including electron transfer. Very elaborate enzyme systems with interesting new chemical structures are used by organisms to effect oxidation and reduction of small molecules that are the raw materials of life—H_2O, O_2, CO_2, N_2, NH_3, CH_4, and so forth. In the enzyme nitrogenase, for instance, several iron–sulfur clusters (Fig. 6) in one protein may serve as an electron sink poised to add four or six electrons to ahhhn inert N_2 molecule as it encounters a molybdenum center in a second protein in nitrogen fixing bacteria:

$$\left(N_2 + 6e^- + 6H^+ \rightarrow 2NH_3\right).$$

Oxidases may effect reduction of O_2 to H_2O_2 and/or $2H_2O$ in successive two-electron steps or one four-electron step. Photosystem II uses chlorophyll to effect the photochemical oxidation of H_2O to O_2 after every fourth light pulse, which suggests the possibility that the manganese centers present might be oxidized to an activated state capable of extracting four electrons from two proximate

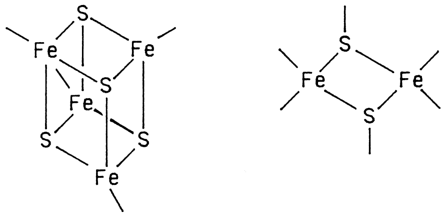

FIGURE 6 Iron–sulfur clusters for biological electron transfer. Distorted Fe_4S_4 "cubes" (left) are found in biological systems involved in electron transfer. Fe_2S_2 clusters (right) are active in electron transport systems in oxidases.

oxide ions to give O_2 directly [see Mn(IV) gluconate, Eq. (2)]. Any notions concerning actual electron transfer pathways in such multielectron systems remain conjectural as of this writing.

The advent of supercomputers will permit the massive calculations necessary to develop theoretical probes of pathways for electron transfer in large complex systems. An early result of just such a study by Atsuo Kuki and Peter Wolynes is shown in Fig. 7, about which Wolynes had this to say in 1988:

> Perhaps the ultimate level of description of an electron transfer process would be a movie showing how the electron leaves the reductant and flies to the reactant. There are two difficulties with this. First is the short time scale; the electron's leap, when it occurs requires only about 10^{-15} second. Second is the fact that the electron is a quantum-mechanical particle. Because of the uncertainty principle of quantum mechanics the electron does not follow a unique path, but follow simultaneously a whole family of paths. With modern computers it is possible, however, to simulate typical paths that an electron can follow. Such a calculation has been carried out (1985) at the University of Illinois. In Figure 7 is shown an electron path during the electron transfer between a ruthenium center bound to the surface of myoglobin and a heme-iron center (cf. cytochrome-*c*) in the interior of the protein. The quantum fluctuations cause it to deviate from a straight line. When families of such paths are generated they give an idea of which parts of the protein are most involved in electron transfer. Site directed mutagenesis of the protein changing its structure will allow experimental tests of these calculations.

By the end of the twentieth century, the ability of research chemists to determine detailed structures of proteins and DNA systems in which electron transfer reactions can be monitored on time scales ranging from seconds down to nano-, pico-, and femtoseconds has brought Wolynes' dream of a movie of an electron transfer process to the realm of possibility in biological oxidation–reduction systems. In protein chemistry several metalloenzymes containing buried metal ions such as Fe^{3+} in Fig. 2 have been modified by attaching other metal ions such as $Ru(bipy)_2^{2+}$ at various sites on the surface of the proteins

FIGURE 7 Computer-generated pathways (dashed lines) for the electron transfer from ruthenium(II) bound to the surface of myoglobin (lower right) to a heme iron center in the interior. Solid line segments outline the protein structure. Heavy shading for the surface structure and pathways fades to light shading in the interior.

and studying electron transfer processes induced by photoexcitation of the attached metal ion as shown in Fig. 7. Many natural proteins whose function includes electron transfer have structures with electron donor sites close enough to allow tunneling to holes, or acceptor sites for electrons. Space does not permit a detailed description of the elaborate structures, electron transfer pathways, and mechanisms occurring in biological systems. Interested readers are referred to the Bibliography, especially the articles dated from 1992 to 1999. The titles give an idea of what researchers are learning and seeking to learn about these very complicated reaction systems. We shall offer only a brief introduction to what has been learned and is being learned about the initial processes involved in natural photosynthesis.

A. Electron Transfer in Photosynthesis

Protein structures have evolved in photosynthetic organisms with an extraordinary ability to capture light and

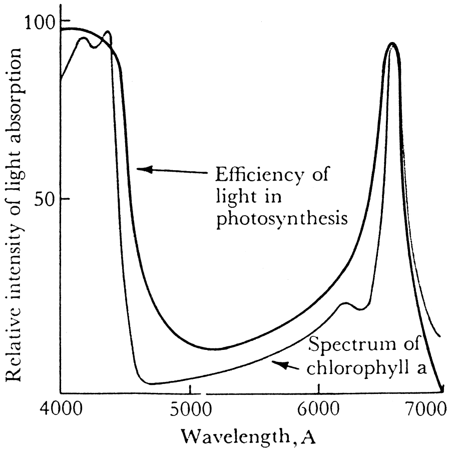

FIGURE 8 The relative effectiveness of chlorophyll to absorb different wavelengths of visible light and for those same wavelengths to initiat photosynthesis.

use the energy to drive a series of electron transfers to create a charge separation across a membrane capable of storing about 0.3 eV of chemical potential (Fig. 8). The protein structure includes 50–200 molecules of chlorophyll (Chl) in a light harvesting complex (LHC) and a membrane bound protein–pigment complex called the reaction center (RC). $Chl^{\#}$ formed by absorption of light donates an electron to a pheophytin (Ph) molecule in the RC in 2–3 psec. This forms a hole or positive charge on the chlorophyll (Chl^{+}). The electron on (Phe^{-}) is then passed to menaquinone in 100 p followed by hole filling at the oxidized (Chl) by reduced cytochrome *c* in the reaction center in ~10 n sec. A final charge shift from menaquinone to ubiquinone requires about 100 nsec. In 1999, Leslie Dutton proposed that electrons can be transferred through the protein medium for up to 14 Å by tunneling. For greater distances, successive tunneling processes are required. Such tunneling provides a very robust system for electron transfer since substrates bound to proteins can transfer electrons for faster than when they react with one another as independent molecules: they need only be close enough. Dutton discusses the evolution of biological oxidation–reduction systems in terms of natural engineering principles applied to structures for electron tunneling.

SEE ALSO THE FOLLOWING ARTICLES

BIOENERGETICS • CHEMICAL THERMODYNAMICS • ELECTROCHEMISTRY • ION TRANSPORT ACROSS BIOLOGICAL MEMBRANES • KINETICS (CHEMISTRY) • POTENTIAL ENERGY SURFACES • PROTEIN STRUCTURE • SUPERCOMPUTERS

BIBLIOGRAPHY

Anbar, M. (1965). Reactions of the hydrated electron. *In* "Solvated Electron," Chap. 6, Advances in Chemistry Series, Vol. 50, Am. Chem. Soc., Washington, D.C.

Barton, J. K. (1998). "DNA-mediated electron transfer: Chemistry at a distance," *Pure and Appl. Chem.* **70**(4), 873–879.

Bixon, M. *et al.* (1992). "Primary events in photosynthesis," *Isr. J. Chem.* **32,** 369–518.

Gray, H. B., and Malmstrom, B. G. (1989). "Long range electron transfer in multisite metalloproteins," *Biochemistry* **28,** 7499.

Gray, H. B., and Winkler, J. R. (1996). "Electron transfer in proteins," *Annu. Rev. Blochem.* **65,** 537–61.

Hemmerich, P. *et al.* (1982). "Scope and limitation of single electron transfer in biology," *Struct. Bonding (Berlin)* **48,** 93–123.

Lehninger, A. L. (1970). "Biochemistry," Chap. 17, Worth, New York.

Linck, R. G. (1976). Oxidation reduction reactions *In* "Survey of Progress in Chemistry," Vol. 7, pp. 89–147, Academic Press, New York.

Page, C. C. *et al.* (1999). "Engineering principles of electron tunnelling in biological oxidation–reduction," *Nature* **402,** 47–53.

Palmer, G. A., ed. (1991). "Long-Range Electron Transfer in Biology" (Vol. 75 of Structure and Bonding), Springer-Verlag, Berlin.

Scott, R. A., Mauk, A. G., and Gray, H. B. (1985). "Experimental approaches to biological electron transfer," *J. Chem. Educ.* **62,** 932–937.

Siegel, H., and Siegel, A., eds. (1991). Electron transfer reaction in metallo-proteins, *In* "Metal Ions in Biological Systems," Dekker, New York.

Taube, H. (1970). "Electron Transfer Reactions of Complex Ions in Solution," Academic Press, New York.

Wilker, J. J. *et al.* (1999). "Substrates for rapid delivery of electrons and holes to buried active sites in proteins," *Angew. Chem. Int. Ed.* **38,** 90–92.

Halogen Chemistry

Marianna Anderson Busch
Baylor University

I. The Elements
II. The Hydrogen Halides (Hydrohalic Acids)
III. Other Inorganic Halides
IV. Interhalogen Compounds
V. Halogen Oxides
VI. Oxyacids and Their Anions
VII. Other Inorganic Halogen Compounds
VIII. Astatine
IX. Organic Halogen Compounds

GLOSSARY

Azeotrope Constant-boiling mixture formed during distillation, when the composition of the vapor phase becomes identical to the composition of the liquid phase.

Carbonium ion Positively charged carbon ion that acts as a Lewis acid or electrophile.

Electron affinity Energy required to remove the most loosely held electron from an isolated negative ion in the gas phase in order to form a neutral atom in the gas phase. More positive electron affinities indicate that the electron is more tightly held.

Electronegativity Ability of a bonded atom in a molecule to attract electrons to itself. The greater the difference in the electronegativities of two atoms bonded to each other, the greater is the charge separation in the bond.

Free radical Species with one or more unpaired electrons.

Hydrogen bonding Attraction of a partially positive hydrogen bonded to atom A (generally N, O, or F) in one molecule to a partially negative atom B either in the same or another molecule. As the electronegativities of atoms A and B increase, the strength of the hydrogen bonding also increases.

Ionic and covalent Adjectives describing the way in which atoms are held together in a chemical compound. Ionic indicates that the interaction between atoms is primarily electrostatic. Covalent indicates that the atoms are held together through the sharing of electrons.

Ionization energy or ionization potential Energy required to remove the most loosely held electron from an isolated atom in the gas phase in order to form a positive ion in the gas phase. More positive ionization potentials indicate that the electron is more tightly held.

Lattice energy Energy released when ions come together from infinite separation to form one mole of a crystal.

More negative lattice energies indicate that the ions are held more tightly in the crystal.

Lewis acid Electron-pair acceptor (electrophile).

Lewis base Electron-pair donor (nucleophile).

Oxidation state or oxidation number Number of electrons lost or gained by the element as a result of compound formation. The number of electrons lost due to oxidation denotes a positive oxidation state, while the number of electrons gained due to reduction denotes a negative oxidation state.

Standard reduction potential Potential difference developed between two electrodes, where the reaction at one electrode is the oxidation of hydrogen gas at 1 atm pressure to H^+ at unit activity (about 1 *M* concentration) and the reaction at the second electrode is the reduction of interest. Higher positive values indicate a greater tendency for reduction.

THE HALOGENS, members of Group 17 of the periodic table (Group VIIA, older nomenclature), include the five elements fluorine (F), chlorine (Cl), bromine (Br), iodine (I), and astatine (At). Astatine, a radioactive element, does not occur naturally except in trace amounts. The remaining halogens do not exist in the free form, but are found primarily as anionic constituents in a large number of minerals and in marine water. All halogens are nonmetals and display many similarities in chemical behavior and in the properties of their compounds with other elements. There is a regular modification in these properties with increasing atomic weight of the halogen, and fluorine, the lightest halogen, displays some unique characteristics that tend to differentiate it from the remaining members of the group. Halogens and halogen-containing compounds are widely employed as refrigerants, propellants, lubricants, bleaches, antiseptics, water purification agents, pesticides, and gasoline additives. Other important commercial applications include photography and the prevention of tooth decay.

I. THE ELEMENTS

A. History

The name halogen, derived from the Greek roots *hal-* ("sea salt") and *-gen* ("to produce"), denotes the ability of the five elements in Group 17 of the Periodic Table to combine with sodium to give compounds that either exist in, or have properties similar to the components of, sea salt. The term halogen was first used by J. S. C. Schweigger in 1811 to describe chlorine, the only member of Group 17 known at that time. As additional elements of Group 17 were discovered, the meaning was extended to include all members of this family.

Compounds containing halogens have been known for thousands of years. Archeological evidence indicates that rock salt (NaCl) was used by people as early as 3000 B.C. and the Bible contains numerous references to the importance of this substance. Dibromoindigo (Tyrian purple) was employed as a dye by the Greeks and Romans, and medieval alchemists used *aqua regia*, a mixture of hydrochloric (HCl) and nitric (HNO_3) acids, to dissolve gold.

Chlorine was the first halogen to be isolated as a free element. In 1774, C. W. Scheele liberated chlorine by reaction of sodium chloride, sulfuric acid, and manganese dioxide,

$$4NaCl + 2H_2SO_4 + MnO_2 \xrightarrow{\text{heat}} 2Na_2SO_4 + MnCl_2 + 2H_2O + Cl_2(g), \quad (1)$$

but erroneously identified the yellowish-green gas as a compound. The true identity of the substance was not recognized until 1810, when H. Davy presented proof of its elementary nature to the Royal Society and suggested the name chlorine (Greek *chloros*, "yellowish-green") for the new element.

Iodine was isolated in 1811 by the industrial chemist B. Courtois. He treated seaweed ashes with hot, concentrated sulfuric acid and condensed the resultant violet vapor to black crystals, which he called "Substance X." In 1813, J. L. Gay Lussac recognized Substance X as an element similar to chlorine and proposed the name iodine (Greek *ioeidea*, "violet-colored").

In 1826, A. J. Balard isolated free bromine from concentrated natural brines. After first precipitating the sodium chloride and sulfate, he passed chlorine gas through the liquid residues and heated the resulting material with manganese dioxide and sulfuric acid. A red vapor was produced that condensed to form a dark liquid with an irritating smell. The similarity of this reaction to that used by Scheele to produce chlorine [Eq. (1)], led Balard to conclude that he had isolated a new element, muride, similar to chlorine. The element was later renamed bromine (Greek *bromos*, "stench") because of its odor.

Fluorine had been suspected as an element present in the mineral fluorite (CaF_2) and had been officially named in 1812 by A. M. Ampere and H. Davy (Latin *fluere*, "to flow," from the use of fluorite as a flux). Its isolation, however, remained one of the chief unsolved problems of inorganic chemistry for more than 70 years because of the great reactivity of this element. In 1886, the French chemist H. Moissan successfully prepared elemental fluorine by the electrolysis of a cooled solution of dry potassium hydrogen fluoride (KHF_2) in anhydrous hydrofluoric

acid (HF). For this achievement, among others, Moissan was awarded the Nobel Prize for Chemistry in 1906. The first purely chemical synthesis of elemental fluorine was not achieved until 100 years after Moissan's electrochemical synthesis. In 1986, K. O. Christe utilized the principle that certain unstable transition metal fluorides can be stabilized in the form of their corresponding MF_6^{2-} anions,

$$2KMnO_4 + 2KF + 10HF + 3H_2O_2 \xrightarrow{50\%\ \text{aqueous HF}} 2K_2MnF_6(s) + 8H_2O + 3O_2, \quad (2)$$

to produce elemental fluorine in high yield by a very simple reaction,

$$K_2MnF_6 + 2SbF_5 \rightarrow 2KSbF_6 + [MnF_4] \quad (3)$$

$$2[MnF_4] \rightarrow 2MnF_3 + F_2(g). \quad (4)$$

The underlying principle behind this synthesis is the displacement of a weaker Lewis acid, MnF_4, from its MnF_6^{2-} salt by the stronger Lewis acid, SbF_5. Since the liberated MnF_4 is thermodynamically unstable, it spontaneously decomposes to the lower fluoride, MnF_3, with the simultaneous evolution of elemental fluorine.

Astatine (Greek *astatos*, "unstable") has no stable or long-lived isotopes. It was first prepared by D. R. Corson, K. R. MacKenzie, and E. Segré in 1940 by alpha bombardment of Bi-209 in a cyclotron:

$$^{209}_{83}Bi + {}^{4}_{2}He \rightarrow {}^{211}_{85}At + 2\,{}^{1}_{0}n. \quad (5)$$

Some 27 isotopes of astatine are now known. The longest lived has a half-life of only 8.1 h, and the largest preparations of the element to date have given less than a microgram.

B. Occurrence

Except for astatine, the halogens occur rather widely in nature in the form of the halide (X^-) anion, with iodine also occurring as iodate (IO_3^-). Due to the great solubility of most halide salts, large quantities of chloride and bromide are concentrated in the ocean and in other natural brines. There are also more than 70 minerals containing a halogen as the sole or principal anionic constituent, although only a few of these are common. Most of the halogen-containing minerals are formed in one of four ways: (1) saline deposition by evaporation of sea water or other natural brines; (2) hydrothermal deposition; (3) surface alterations of silver, copper, lead, or mercury ores; and (4) deposition by sublimation near regions of geothermal or volcanic activity. Table I summarizes some of the more important terrestrial sources for the halogens.

Minute amounts of astatine have been detected in nature as a steady-state population produced from the decay of certain long-lived, naturally occurring radioactive elements such as ^{235}U. The total amount of astatine present on earth at any given time is estimated to be less than one ounce, making astatine the rarest naturally occurring terrestrial element.

TABLE I Important Natural Sources for the Halogens

Element	Source/remarks
Fluorine	Fluorite or fluorspar (CaF_2), cryolite (Na_3AlF_6), fluorapatite (calcium hydroxyphosphate where some hydroxide is replaced by fluoride)
Chlorine	Normal ocean water, other natural brines, halite (NaCl), sylvite (KCl), carnallite ($MgCl_2$, KCl, $6H_2O$), kainite ($MgSO_4$, KCl, $3H_2O$)
Bromine	Normal ocean water, other natural brines, bromide impurities in carnallite and in some other less abundant minerals such as bischofite ($MgCl_2$, $6H_2O$) and tackhydrite ($CaCl_2$, $2MgCl_2$, $12H_2O$)
Iodine	Some natural brines (especially from oil wells), lautarite [$Ca(IO_3)_2$], dietzeite [$7Ca(IO_3)_2$, $8CaCrO_4$], seaweed (*Laminaria* family)
Astatine	None, produced artificially

Table II compares the distribution of the halogens in various locations on earth, and on the moon and in the solar system. A few entries deserve special comment.

Airborne particulates typically contain increased concentrations of halogens near the ocean, in polluted areas, and in regions of volcanic activity. Fluoride concentrations are increased near aluminum and steel mills and phosphate-fertilizer plants. Bromide concentrations were once increased near urban areas as a result of the burning of gasoline additives (ethylene dibromide, a lead scavenger), but environmental legislation has resulted in a decline of this chemical's utilization. The enrichment of iodine in marine air as compared to sea water has been attributed to concentration of the element in organic surface films. Iodine-enriched material then enters the atmosphere in the form of spray.

Except for methyl chloride (CH_3Cl), most of the organic gases containing halogens are man-made. The chlorofluorocarbons (Section IX.F), which are particularly stable and can remain in the atmosphere for between 50 and 100 years, have been implicated in the depletion of the earth's ozone layer and in global warming (the greenhouse effect). Inorganic gases containing fluoride are detected only near polluted areas and in regions of volcanic activity. Hydrogen chloride is frequently found as a major component of acid rain.

In the ocean, the halogens form part of a group of elements classified as biounlimited. Elements in this group have concentration ratios that are constant in samples from all locations, from surface level to deep water. By measuring the concentration of one element in this group, the composition of all other biounlimited components can

TABLE II Occurrence of the Halogens (Estimated or Averaged Values)

Location	Fluorine	Chlorine	Bromine	Iodine
Solar system (relative abundance, normalized to Si)	780	4740	9.2	1.27
Moon (ppm,[a] *Apollo 11*)	140	14	0.1	—
Order of elemental abundance (terrestrial rocks)	13th	20th	46th	60th
Continental crust (ppm)[a]	544	126	2.5	0.46
Ocean water (ppm)[a]	1.3	19,400	67	0.06
Particles in marine air (ng/scm)[b]	0.2	5,000	7	
Atmospheric gases:				
Organic (ppt)[a]	1,000	2,500	20	3
Inorganic (ppt)[a]	—	1,000–2,000	1–10	1–5
Precipitation (rain and snow) (ppb)[a]	5–150	100–10,000	10	5

[a] ppm (parts per million), ppb (parts per billion), ppt (parts per trillion).
[b] nanograms/standard cubic meter.

be characterized. The factor normally selected for measurement is chlorinity, the total halide concentration in parts per thousand (grams per kilogram of sea water). Chlorinity is determined by titration with silver nitrate ($AgNO_3$) and is strictly defined as the total mass of silver needed to precipitate the halogens (chloride, bromide, and iodide) in 328.5233 g of sea water. Chlorinity is related to salinity, the total salt content in parts per thousand, by the following empirical relationship: salinity = 1.80655 chlorinity.

C. Human Biological Significance

In the human body, the halogens are generally present either as the halide ion or as part of complex organic molecules. Fluorine in its ionic form is found in bones and teeth. Prolonged exposure to fluoride ions can produce skeletal abnormalities or damage (fluorosis) ranging from stiffness to permanently crippling skeletal rigidity. However, the presence of only 0.8 to 1.0 ppm of fluoride in drinking water has been shown to produce a significant reduction in the incidence of dental caries without harmful side effects. Similar beneficial effects can be obtained from topical treatment with small amounts of fluorides or fluorophosphates in toothpaste.

Small quantities of ionic chlorine are found in blood and milk. In extracellular fluid, chloride ions help to regulate the osmotic pressure, while in salivary amylase the chloride ion activates the starch-splitting enzyme of saliva. Free hydrochloric acid is found in the stomach as part of the mixture of digestive fluids.

Although bromide and chloride ions readily interchange to some degree in body tissue, the biological function of bromine is unknown. Bromides act as depressants and have long been used for the treatment of nervous disorders.

The greatest concentration of iodine in the human body is present in the thyroid gland; it is here that iodine is converted to thyroxine and other hormones that regulate the rate of metabolism. Iodine is an essential element in the diet. Wherever dietary sources of iodine are low, goiter, a condition in which the thyroid gland becomes enlarged, is prevalent. Small quantities of iodide are often added to table salt to prevent iodine deficiency.

Astatine resembles iodine in that it concentrates in the thyroid gland where it causes localized destruction of tissue by α-particle emission. Radiotherapy using astatine is considered superior to that using iodine because considerable changes in thyroid tissue can be effected without noticeable alterations in the parathyroid gland or other peritrachial tissues.

In their elemental forms, all of the halogens are quite toxic. Exposure to fluorine causes very severe burns; extreme care must be taken to prevent the contact of fluorine with the skin or eyes. Many fluorine-containing compounds, especially inorganic ones, act in the same manner and should be considered equally dangerous. Concentrations of 15 to 30 ppm of chlorine gas in air are sufficient to cause irritation of the nose, throat, and lungs. Higher concentrations can result in death through suffocation. Contact with bromine causes almost instant injury to skin, and the painful burns are slow to heal. Bromine vapor is extremely toxic, although the strong odor generally gives sufficient warning to prevent inadvertent long-term exposure.

D. Atomic Properties

The halogens have few naturally occurring isotopes (Table III), and the outer electronic configurations of the atoms are very similar, each having one p electron less than that required for the next noble gas. As a result, the atoms have a strong tendency to acquire one additional electron, as indicated by their electron affinities (large positive values indicating that electron loss from the negative ion is very unfavorable). All of the halogen atoms are the smallest in their respective periods. The

TABLE III Atomic Properties of the Halogens

Property	Fluorine	Chlorine	Bromine	Iodine	Astatine[a]
Atomic number	9	17	35	53	85
Atomic mass	18.9984	35.453	79.904	126.9045	(210)
Stable isotopes (terrestrial %)	19 (100%)	35 (75.53%) 37 (24.47%)	79 (50.54%) 81 (49.46%)	127 (100%)	None
Electron configuration	[He]$2s^2$ $2p^5$	[Ne]$3s^2$ $3p^5$	[Ar]$3d^{10}$ $4s^2 4p^5$	[Kr]$4d^{10}$ $5s^2 5p^5$	[Xe]$4f^{14}$ $5d^{10} 6s^2 6p^5$
Ionization energy (kJ/mole)	1680.6	1255.7	1142.7	1008.7	(926)
Electron affinity (kJ/mole)	332.6	348.5	324.7	295.5	(270)
Electronegativity:					
Pauling	4.0	3.0	2.8	2.5	(2.1)
Allred–Rochow	4.10	2.83	2.74	2.21	(1.90)
Radius (pm):					
Covalent	72[b]	99	114	133	(140)
Ionic, X^-	133[c]	184[c]	196[c]	220[c]	(227)
van der Waals	135	180	195	215	—

[a] Because of the difficulties associated with obtaining experimental quantities of astatine, most physical properties of this element are either predicted from theory or obtained by extrapolation from the properties of the other halogens.
[b] Taken from the F–F distance in molecular fluorine. The value 64 pm gives better agreement with measured distances for organofluorine compounds.
[c] Varies somewhat with coordination number.

acquisition of the additional electron brings about a tremendous change in size, the X^- or halide ion being almost twice the size of the parent atom.

As indicated by their high positive ionization energies, the halogen atoms do not lose electrons readily. Ionization potentials show a decrease (greater ease of electron loss) with an increase in atomic number, as would be expected for the trend in atomic sizes (weaker binding of the valence electrons resulting from increased distance from the nucleus).

As shown by the data in Table III, fluorine displays a number of properties that cannot be obtained by extrapolation from the values observed for its heavier family members. Ionization energy and electronegativity are more positive than expected, while electron affinity and ionic and covalent radii are smaller than expected. Similar discontinuities are observed in the physical properties of the diatomic forms (Table IV) and in many properties of the halogen compounds.

In general, the differences between fluorine and chlorine are more pronounced than the corresponding differences between the first and second elements in other groups of the Periodic Table. Many of these differences can be accounted for in terms of the small size of

TABLE IV Some Properties of the Halogen Elements

Property	F_2	Cl_2	Br_2	I_2
Color and state (25°C, 1 atm)	Pale yellow gas	Greenish-yellow gas	Red-brown liquid	Black solid, violet vapor
Common oxidation states[a]	−1	−1, +1, +3, +5, +7	−1, +1, +3, +5, +7,	−1, +1, +3, +5, +7
Standard reduction potential ($2X^-/X_2$, V)	+2.87	+1.36	+1.07	+0.54
M.P. (°C)	−219.61	101.0	−7.25	113.5
B.P. (°C)	−188.13	−34.05	59.5	185.2
ΔH dissociation[b] (kJ/mole X_2)	158.8	242.58	192.77	151.10
ΔH fusion[c] (kJ/mole X_2)	0.51	6.41	10.57	15.52
ΔH vaporization[d] (kJ/mole X_2)	6.54	20.41	29.56	41.95
Temperature for 1% dissociation (°C) at 1 atm	765	975	775	575
Molar solubility in water at 25°C (moles/liter)	Reacts	9.1×10^{-2}	0.21	1.3×10^{-3}

[a] The free form of the element is considered to have an oxidation state of 0.
[b] Energy required to break 1 mole (Avogadro's number) of X—X chemical bonds. More positive bond energies indicate a stronger X—X bond.
[c] Energy required to convert 1 mole of solid to the liquid state at the melting point.
[d] Energy required to convert 1 mole of liquid to the gaseous state at the boiling point.

the fluorine atom, its unusually high electronegativity (Table III)—greater than that of any other element—and the unavailability of low-energy d-orbitals in fluorine for chemical bonding. In spite of these differences, there are closer similarities within the halogen family than within any other family in the Periodic Table (with the exception of the alkali metals, lithium through cesium).

E. Properties of the Elemental States

Under ordinary conditions, the elemental halogens (except astatine) exist as covalent, diatomic molecules, acquiring the electronic configuration of the next noble gas by sharing one pair of electrons between two atoms. Their appearance ranges from a pale yellow gas (F_2), through a dark red liquid (Br_2), to an almost black, crystalline solid (I_2). Bromine is unique in being the only nonmetallic element that exists as a liquid under ordinary conditions. Iodine crystals do not melt at atmospheric pressures, but sublime directly into the gas phase.

The high volatilities and relatively low heats of vaporization and fusion (Table IV) reflect the weak intermolecular interactions expected for the covalent nature of these molecules. The stabilities of the X—X bonds are indicated by their high dissociation energies (higher energies indicating stronger bonds). By comparison to the other halogens, the F—F bond displays an anomalously low dissociation energy and large bond distance, attributable to electron–electron repulsion around the small fluorine atoms, or to the lack of a d-orbital component in the bond, or to both.

As indicated by their large, positive standard reduction potentials, all of the halogen molecules have a strong tendency to be reduced (i.e., to act as oxidizing agents). Fluorine is the most powerful chemical oxidizing agent of all elements in the Periodic Table. This great reactivity is due primarily to the low energy of the F—F bond. The general tendency for halogen molecules to be reduced accounts for their natural occurrence as X^- or halide ions. The oxidizing power of fluorine is so great that this element does not normally exist in any oxidation state other than -1 and 0; however, the remaining halogens can display oxidation states up to $+7$ if combined with a sufficiently electronegative element such as oxygen.

F. Commercial Preparation and Use

Because of its great reactivity, fluorine is prepared commercially by electrolysis. The modern-day procedure is similar to the original preparation by Moissan and utilizes a 1:2 mixture of anhydrous KF and HF. The electrochemical reaction produces hydrogen gas (H_2) at the cathode and fluorine gas at the anode. The two gases will react explosively and must be kept apart.

The majority of commercially produced F_2 is used for the manufacture of uranium hexafluoride (UF_6, nuclear power generation), sulfur hexafluoride (SF_6, an important

trifluoride (ClF_3), and the hexafluorides of tungsten and rhenium (used for vapor deposition of the metal). Fluorine derivatives of hydrocarbons are used as refrigerants (Freon®), lubricants (Kel-F), and nonstick plastics (Teflon®).

Chlorine is produced industrially on a large scale in the "Chloralkai" process, electrolysis of aqueous sodium chloride or natural brine solutions. The most commonly employed cell uses an asbestos diaphragm to separate the chlorine gas formed at the cathode from the sodium hydroxide (NaOH) that concentrates in the residual solution:

$$2NaCl(aq) + 2H_2O \rightarrow Cl_2(g) + H_2(g) + 2NaOH(aq). \quad (6)$$

Electrolysis of molten NaCl is also carried out on a large scale, yielding sodium metal at the cathode rather than hydrogen. Still other processes involve the electrolysis of fused magnesium chloride ($MgCl_2$) or the oxidation of hydrogen chloride by oxygen or air in the presence of a copper catalyst.

The major uses for elemental Cl_2 are the production of organic and inorganic compounds and bleaches. Some of the more important chlorinated compounds are used as solvents, antifreeze, and plastics (e.g., polyvinyl chloride).

Bromine is produced by oxidation of bromide ion using Cl_2 gas (chlorine displacement):

$$2Br^-(aq) + Cl_2(g) \rightarrow 2Cl^-(aq) + Br_2(g). \quad (7)$$

Elemental bromine is blown out of the mixture as a vapor using either steam or air and then condensed to form an impure product. Purification may involve reduction with sulfur dioxide to reform the bromide ion,

$$Br_2 + SO_2 + 2H_2O \rightarrow 2HBr + H_2SO_4, \quad (8)$$

followed by a second displacement [Eq. (7)] using chlorine gas. Alternatively, bromine can be added to sodium carbonate (Na_2CO_3) solution to produce bromide and bromate:

$$3CO_3^{2-} + 3Br_2 \rightarrow 5Br^- + BrO_3^- + 3CO_2. \quad (9)$$

On acidification, the bromine is regenerated:

$$5Br^- + BrO_3^- + 6H^+ \rightarrow 3Br_2 + 3H_2O \quad (10)$$

Until recently, almost all commercially prepared bromine was converted to ethylene dibromide and used as a lead scavenger in gasoline. Other important applications now include the production of pesticides, fire retardants, drilling fluids, dyes, pharmaceuticals, and photographic chemicals.

The commercial production of iodine depends on the source of the element. From natural brines, the process is similar to bromine recovery: displacement of iodide ion (I^-) by chlorine, blowout of the impure iodine, and repurification by sublimation. Other processes employ iodide precipitation by silver nitrate ($AgNO_3$), separation on ion-exchange resins, or oxidation of iodide by sulfuric acid (somewhat similar to the original procedure used by Courtois).

When the naturally occurring source is iodate, the process typically employs sodium bisulfite reduction to produce iodide:

$$IO_3^- + 3HSO_3^- \rightarrow I^- + 3HSO_4^-. \quad (11)$$

More iodate is added and the solution is acidified:

$$5I^- + IO_3^- + 6H^+ \rightarrow 3I_2 + 3H_2O. \quad (12)$$

The iodine precipitates and is purified by sublimation.

Elemental iodine has many commercial uses. Much is incorporated into a wide variety of organic compounds that find application as catalysts for the manufacture of synthetic rubber, as supplements for animal feed, and as stabilizers, dyes, antiseptics, and photographic chemicals.

G. Chemical Reactions

Most metals combine directly with all of the halogens (X_2) and react particularly readily with fluorine. Many nonmetals also react. The reactivity of fluorine is so great that almost all of these reactions can be initiated at ordinary temperatures and will proceed with the evolution of considerable heat and light until the fluorine has been completely consumed. Some metals, such as aluminum, nickel, iron, and copper, form protective fluoride coatings that block further reaction unless the temperature is raised.

The reactivity of the halogen decreases with atomic number. Consequently, a halogen of lower atomic number will displace, or oxidize, a halide ion (X^-) of higher atomic number [Eq. (7)], both when the ion is in solution and in a crystal lattice. Fluorine (and chlorine to a lesser extent) will also react with both metals and nonmetals to produce higher states of oxidation than do bromine and iodine. Thus, the nonmetal sulfur is converted to SF_6 by fluorine, to SCl_2 by chlorine, and to S_2Br_2 by bromine. Compounds with S—I bonds are known, but sulfur iodides cannot be prepared by direct reaction of the elements. The highest thermally stable states resulting from the halogenation of the metal rhenium are ReF_7, $ReCl_6$, $ReBr_5$, and ReI_4.

All of the halogens are soluble to some extent in water, but they may also react to give a number of products depending on the temperature and the amount of acid or base present in the solution. Fluorine rapidly oxidizes water to give mainly oxygen and fluoride ion,

$$2F_2 + 2H_2O \rightarrow O_2 + 4F^- + 4H^+, \quad (13)$$

although small amounts of hydrogen peroxide (H_2O_2), oxygen difluoride (OF_2), and ozone (O_3) may be formed as well. In the case of chlorine, the reaction analogous to Eq. (13) tends to be slow, and the initial result is disproportionation (self-oxidation and reduction):

$$Cl_2 + H_2O \rightarrow HOCl + H^+ + Cl^+. \quad (14)$$

The hypochlorous acid (HOCl) that is formed decomposes slowly to give oxygen. Bromine does not react with water under acid conditions. In the case of iodine, the partial pressure of oxygen in the air is sufficient to oxidize iodide ion back to the elemental form [analogous to Eq. (13) in reverse].

If base is present, disproportionation is rapid for chlorine, bromine, and iodine:

$$2OH^- + X_2 \rightarrow XO^- + X^- + H_2O. \quad (15)$$

Further disproportionation of the XO^- ion to give XO_3^- may follow:

$$3XO^- \rightarrow 2X^- + XO_3^- \quad (16)$$

Reaction (16) is rapid for IO^-, less rapid for BrO^-, and even slower for ClO^-. Consequently, at room temperature, a basic solution of chlorine gives ClO^-, while bromine gives a mixture of BrO^- and BrO_3^-, and iodine gives IO_3^-, Increasing the temperature favors the formation of XO_3^-. At 50 to 80°C in base, Br_2 is quantitatively converted to BrO_3^-. The formation of ClO_3^- in base also becomes fairly rapid above 75°C.

Crystalline hydrates or clathrates of chlorine ($Cl_2 \cdot 7.3H_2O$) and bromine ($Br_2 \cdot 8.5H_2O$) are formed by freezing water in the presence of the halogens. The hydrogen-bonded, open arrangement of water molecules which forms on freezing acts as a trap for the halogen molecules. Iodine also combines with starch to give a deep blue color, due to the formation of another complex clathrate in which iodine molecules are trapped within the helical structure of the starch molecule. Formation of this blue color is used as a sensitive test for the presence of iodine.

The halogens are generally more soluble in organic solvents than in water. Carbon tetrachloride and chloroform readily extract chlorine, bromine, and iodine from water to give yellow-, red-, and violet-colored solutions, respectively.

Chlorine, bromine, and especially iodine react with Lewis bases such as benzene, alcohols, ethers, ketones, and amines to give highly colored solutions that are characteristic of the base and halogen. Part of the energy associated with the halogen-base bond is attributable to a transfer of charge between the donor atom and the halogen, thus giving the name charge-transfer complex to the species which is produced.

Halogen molecules dissociate into atoms on heating (Table IV) and on absorption of light. Halogen atoms are sometimes able to initiate chain reactions between other substances. Specific examples include the chlorine-sensitized explosion of hydrogen with oxygen, the bromine-sensitized decomposition of ozone, the iodine-sensitized decomposition of hydrogen peroxide, and the halogenation of hydrocarbons. Small quantities of iodine often serve as catalysts in such organic reactions as halogenation, dehydration, and isomerization.

H. Analysis

Quantitative determination of the halogens can be accomplished by a number of procedures. Accurate analysis of fluorine is the most difficult, and is generally carried out either by (1) calcium fluoride precipitation, (2) lead chlorofluoride precipitation, or (3) titration with thorium nitrate using sodium alizarin sulfonate as an indicator:

$$Th(NO_3)_4(aq) + 4KF(aq) \rightarrow ThF_4(s) + 4KNO_3(aq). \quad (17)$$

More methods are available for chlorine. As free chlorine, the element may be analyzed by reduction to chloride using iodide, arsenite, alkaline hydrogen peroxide, sulfur dioxide, or sodium thiosulfate ($Na_2S_2O_3$), or determined colorimetrically by treatment with *ortho*-toluidine in hydrochloric acid. Chloride ion may be precipitated as silver chloride or titrated with silver nitrate in the presence of potassium chromate (K_2CrO_4).

Free bromine and iodine are determined by reduction with sodium thiosulfate. Both bromide and iodide ions are typically analyzed by precipitation or titration using silver nitrate or by titration with potassium dichromate ($K_2Cr_2O_7$).

All six of the naturally occurring halogen isotopes have been studied by nuclear magnetic resonance (nmr) spectroscopy. Nmr sensitivity and ease of obtaining ^{19}F spectra are second only to ^{1}H. All five of the naturally occurring isotopes of Cl, Br, and I can be investigated by nuclear quadrupole resonance (nqr) spectroscopy. The ^{127}I and ^{129}I isotopes are the only halogens meeting the necessary requirements for observation and study by the Mössbauer effect.

II. THE HYDROGEN HALIDES (HYDROHALIC ACIDS)

A. Preparation and Use

The hydrogen halides (HX) make up one of the most important classes of inorganic compounds, containing the halogens in the −1 oxidation state. They are prepared in a number of different ways.

Anhydrous hydrogen fluoride is usually produced commercially by reacting hot, concentrated sulfuric acid with fluorspar:

$$CaF_2 + H_2SO_4 \rightarrow CaSO_4 + 2HF. \quad (18)$$

The principal use for anhydrous HF is in the preparation of other inorganic fluorides for fluoridation of water, for use as fluxes and catalysts, and for the manufacture of glass and ceramics.

Hydrogen chloride is produced by a reaction analogous to Eq. (18) using NaCl as the source of chloride. Alternatively, sodium chloride may be treated with a mixture of sulfur dioxide, air, and water (the Hargreaves process):

$$4NaCl + 2SO_2 + O_2 + 2H_2O \rightarrow 2Na_2SO_4 + 4HCl. \quad (19)$$

When very-high-purity HCl is required, hydrogen and chlorine gases are combined directly in a specially designed burner. A large percentage of commercially available HCl is obtained as a by-product of the chlorination of organic materials.

Most commercial HCl is used for the production of vinyl chloride and chlorinated solvents, for the manufacture of a large variety of inorganic chemicals, especially ammonium chloride (NH_4Cl), metal salts and bleaches, and for the pickling of metals to remove oxide scale. Food-related applications include the hydrolysis of starch to glucose and the manufacture of gelatine.

Hydrogen bromide is prepared by direct combination of the elements at elevated temperatures in the presence of a catalyst. Hydrogen iodide can also be made in this way, but is more often prepared as the aqueous acid by reaction of I_2 with hydrazine or hydrogen sulfide:

$$2I_2 + N_2H_4 \rightarrow 4HI + N_2, \quad (20)$$

$$H_2S + I_2 \rightarrow 2HI + S. \quad (21)$$

A convenient laboratory preparation involves the reduction of bromine or iodine with red phosphorus and water:

$$2P + 6H_2O + 3X_2(X = \text{Br or I}) \rightarrow 6HX + 2H_3PO_3, \quad (22)$$

$$H_3PO_3 + H_2O + X_2 \rightarrow 2HX + H_3PO_4. \quad (23)$$

A reaction analogous to Eq. (18) may be employed if the acid is nonoxidizing (e.g., H_3PO_4), and sodium bromide or sodium iodide serves as the halogen source.

Hydrogen bromide is used in the manufacture of inorganic and alkyl bromides. There is no large-scale use for HI outside of the laboratory.

TABLE V Physical Properties of the Hydrogen Halides

Property	HF	HCl	HBr	HI
M.P. (°C)	−83.6	−114.6	−88.5	−50.9
B.P. (°C)	19.5	−85.1	−67.0	−35.0
Liquid range (°C, 1 atm)	102.9	29.1	21.5	15.9
Dipole moment, D	1.86	1.11	0.79	0.38
Dielectric constant, ϵ	84 (0°C) 175 (−73°C)	9.28 (−95°C)	7.0 (−85°C)	3.39 (−50°C)
ΔH dissociation (kJ/mole HX)	574	432	363	295
Bond length (pm)	91.7	127.4	141.4	160.9
Solubility in water (0°C)	Miscible	500 vols.	600 vols.	425 vols.
		42%	68%	70%
Composition/B.P.[a]	38% HF	20% HCl	48% HBr	57% HI
Aqueous azeotrope	112°C	109°C	124°C	127°C
pK_a in Water (25°C)	3.2	−7.0	−9.5	−10

[a] 1 atm pressure.

B. Physical and Chemical Properties

At 20°C, all of the hydrogen halides exist as gases (Table V). They are extremely soluble in water where they ionize to give acid solutions. (Aqueous solutions of HX are called hydrohalic acids—e.g., hydrofluoric acid, hydrochloric acid). All of the hydrogen halides except HF are strong acids, meaning that dissociation in water to form acid and halide ions is essentially 100%. The increase in acid strengths (more negative pK_a values) down the group parallels a trend in decreasing hydrogen–halogen bond dissociation energies (Table V). The strength of HF as an acid increases with its concentration in water, due to the formation of ions such as HF_2^- and other more complex species.

When solutions of water and HX are distilled, the liquid mixture forms a maximum-boiling azeotrope. Thereafter, the mixture continues to boil at the same temperature with no further change in composition. These constant-boiling azeotropes represent the maximum degree of purification that can be achieved for aqueous HX by simple distillation (Table V).

In the crystalline state, HF forms zig-zag, polymeric chains in which adjacent HF molecules are held together by hydrogen bonds between the partially positive hydrogen on one HF unit and the partially negative fluorine on another. Hydrogen bonds are weaker than regular covalent bonds and play a significant role in determining molecular properties only when the intramolecular covalent bond between hydrogen and another atom bonded to it is very polar (i.e., the electronegativity difference between the bonded atoms is especially large, as in H—F, H—O, and H—N). The hydrogen bonding in HF is so strong that even gaseous HF is made up of a mixture of monomers and hydrogen-bonded polymers. The anomalously high melting and boiling points and dielectric constant of HF (Table V) are also attributable to hydrogen bonding.

As expected from the lower electronegativities of chlorine, bromine, and iodine (Table III), the other hydrogen halide molecules are not associated in the gaseous or liquid phases. However, the low-temperature forms of crystalline HCl and HBr display weakly bonded, zigzagged chains similar to HF. When the temperature is raised, the links between individual molecules are broken, and the crystalline structures become disordered.

The hydrogen halides display many typical acid reactions, including the liberation of hydrogen gas with electropositive metals such as Zn, Mg, etc.,

$$Zn + 2HCl \rightarrow ZnCl_2 + H_2, \tag{24}$$

the formation of salts with bases, and the liberation of carbon dioxide by reaction with carbonates,

$$CaCO_3 + 2HCl \rightarrow CaCl_2 + H_2O + CO_2. \tag{25}$$

Hydrochloric acid can be oxidized to chlorine only by very strong oxidizing agents such as potassium permanganate ($KMnO_4$) or manganese dioxide [Eq. (1)]. Hydroiodic acid liberates iodine readily with many oxidizing agents including oxygen in the air [analogous to Eq. (13) in reverse].

C. The Hydrogen Halides as Solvents

After water, liquid HF is one of the most generally useful of all solvent systems. Some of its primary advantages (Table V) include a high dielectric constant, low viscosity, large liquid range, and ability to dissolve many inorganic and organic compounds which are not soluble in water.

Self-ionization or autodissociation of the HF solvent system,

$$3HF \rightarrow H_2F^+ + HF_2^-, \quad (26)$$

occurs to a greater extent than the analogous reaction for water. Most inorganic fluorides dissolve in HF to give HF_2^- ions, which have an anomalously high conductance and make the resulting solutions quite conductive. Inorganic compounds other than fluorides generally react with the solvent to produce the corresponding fluoride. Liquid HF is also used in biochemical research to solubilize certain carbohydrates and complex proteins that dissolve with only minor chemical changes.

Acid–base and oxidation–reduction reactions in HF have been thoroughly studied. As an acid, HF will readily protonate water, alcohols, carboxylic acids, and other organic solutes having unshared pairs of electrons. Because the tendency for oxidation of fluoride to fluorine is very low, many inorganic and organic compounds can be fluorinated by the electrochemical insertion of F^- using the HF solvent system.

The other hydrogen halides, with lower boiling points, shorter liquid ranges, and negligible self-dissociation, are less useful as solvents. Considerably lower dielectric constants, as compared to HF, also mean that these compounds do not, in general, solubilize ionic compounds very readily. Nevertheless, work with HCl has indicated that this solvent system provides a convenient medium for the preparation of a number of chlorinated or protonated inorganic and organic products.

III. OTHER INORGANIC HALIDES

A. Preparation

The halogens form compounds of the type M_aX_b with most elements (M) in the Periodic Table. The method of synthesis depends on the properties of the desired product. If hydrolysis (reaction with water) is not a problem, then dissolution of the element [Eq. (24)] or its oxide,

$$MgO + 2HCl \rightarrow MgCl_2 + H_2O, \quad (27)$$

carbonate [Eq. (25)], or hydroxide in aqueous hydrohalic acid usually provides a convenient route to the appropriate halide. If the product is unstable in water, direct reaction of the element M with the halogen,

$$S + 3F_2 \rightarrow SF_6, \quad (28)$$

or with the anhydrous hydrogen halide [Eq. (24)] may be employed.

There are numerous alternative routes, including halogen displacement [as in Eq. (7)] and high-temperature halogenation of metal oxides in the presence of carbon or carbon tetrachloride:

$$UO_2 + CCl_4 \rightarrow UCl_4 + CO_2. \quad (29)$$

The range of applicability of the method, the reaction conditions, and the products obtained from the reaction will vary from halogen to halogen.

B. Classification

Binary halides can be grouped into two very broad categories: ionic and covalent. In ionic halides, the halogen acquires the electronic configuration of the nearest noble gas by appropriating one electron from atom M. Both atoms then become charged ions. In covalent halides, the bonding electrons are more shared than transferred, and the degree of charge separation between M and X is characteristically less. There is an almost continuous gradation in the nature of the bonds formed in inorganic halides, from nearly completely ionic to nearly completely covalent. This gradation is reflected in the chemical and physical characteristics of the resulting compounds.

The ionic halides can be distinguished by their higher boiling and melting points, lower volatilities, and greater degree of conductivity when fused. For the same metal cation, boiling and melting points generally decrease down the group (fluorid > chloride > bromide > iodide), reflecting a gradual increase in covalent character. Most ionic halides dissolve in water to form hydrated metal ions and halide ions. For the same metal cation, halide solubility generally increases down the group (fluoride < chloride < bromide < iodide), with dissolution of the smaller fluoride ions being less favored because of a higher crystal lattice energy (the energy holding the ions together in the solid state).

The covalent halides are often called acid halides because they react with water to give hydroxy compounds that are acidic. Reactions with other Lewis bases (electron donors) such as alcohols, ammonia, and substituted amines also occur. Covalent halides are generally more soluble in nonpolar solvents such as benzene and carbon tetrachloride.

There are several factors which can be used to predict the degree of ionic or covalent character in a halide. First, ionic character is markedly increased by an increase in the electronegativity difference between M and X. The halides of the Group IA and IIA metals, which have especially low electronegativities, as well as those of the lanthanides and actinides, tend to be ionic. Halides of metals with higher electronegativities, such as those of many transition metals, exhibit more covalent character. Halides of nonmetals, which have the highest electronegativities, are predominantly covalent.

Ionic character is also affected by the total charge present on M and the size of the halogen. If a given metal can have more than one oxidation state, the lowest

oxidation state (smallest charge) forms the most ionic halide. In any series of halides of the same metal, the smaller fluorides are the most ionic, while the larger iodides have the most covalent character.

C. Structure

In the solid state, the binary ionic halides exist as crystals made up of an ordered array of halide anions and metal cations (M^{n+}). The arrangement of the crystalline array is determined by the lattice energy of the crystal, and the relative numbers (stoichiometry) and sizes of the anions and cations which are present. Because of the small size of the F^- anion, fluorides often differ in structure from other halides of the same metal.

The actual arrangement of ions in the solid state can frequently be predicted by a rather simple procedure. The larger ions (usually the X^- anion) are stacked in a three-dimensional, closest-packed array like billiard balls, and the smaller ions (usually the M^{n+} cation) are evenly distributed in the holes left in this structure. If the cations and anions are approximately the same size, the most efficient lattice for maximizing cation–anion interaction is one in which eight ions of one type surround one ion of the second type. If the halide has a fair amount of covalent character, a chain or layer, structure may result in which the internuclear distance between layers is greater than within a layer.

Covalent halides exist as discrete molecules that persist throughout the solid, liquid, and gaseous phases. The forces between two or more molecular units in the crystalline state are weak, thus accounting for high volatilities and low melting and boiling points. Intermolecular forces are greatest for iodides and weakest for fluorides. Consequently, for the same nonmetallic element M, boiling and melting points of the halides generally increase down the group: fluoride < chloride < bromide < iodide. The crystal structures of the covalent halides are primarily determined by the arrangements of the atoms which make up the individual molecules.

D. Halide Complexes

All of the halide ions can act as ligands (Lewis bases or electron pair donors) toward the majority of metal ions and a number of molecular halides (Lewis acids or electron-pair acceptors), forming complex species such as AlF_6^{3-}, $AgCl_2^-$, $SbBr_4^-$, and HgI_4^{2-} [See Eq. (2)]. Halide ligands may also be present with ligands of many other types: $NbOCl_4^-$, $[Co(NH_3)_4Br_2]^+$, $Mn(CO)_5I$, and so on. The bonds formed by this attachment are called coordinate covalent, indicating that the ligand has contributed both electrons to the shared pair.

Studies to determine the relative stabilities of complex halides with respect to dissociation into their constituent ions in aqueous solution have shown that two types of behavior exist. Small, highly charged metal cations, called type A or hard Lewis acids (Be^{2+}, Fe^{3+}, Ce^{4+}, etc.), tend to form their most stable complexes with fluoride ion ($F^- > Cl^- > Br^- > I^-$), while larger metal cations of lower charge, called type B or soft Lewis acids (Ag^+, Pt^{2+}, etc.), tend to form their most stable complexes with iodide ion ($F^- < Cl^- < Br^- < I^-$).

Complexes formed by a transition-metal ion and halide ligands are typically highly colored as a result of ligand-induced splitting or differentiation of the metal d-orbital energies. Comparison of the ultraviolet–visible spectra of these complexes indicates that the extent of splitting decreases according to the sequence $F^- > Cl^- > Br^- > I^-$. The degree of differentiation between the metal d-orbitals has been related to the charge-to-radius ratio of the ligand, and the strength and type (σ or π) of the metal–ligand bond.

IV. INTERHALOGEN COMPOUNDS

A. General Survey

The halogens combine with each other to form four types of binary, neutral, interhalogen compounds: XY (all possible combinations), XY_3 (Y = F only), XY_5 (Y = F only), and XY_7 (X = I and Y = F only), where X is the heavier halogen (Table VI). The greater the electronegativity difference (Table III) between the central atom X and the terminal atoms Y, the greater the total number of Y atoms that can be bound in the molecule. Thus, iodine can bind up to seven F atoms, but only a maximum of three Cl atoms or one Br atom. The structures of these molecules can generally be predicted by simple valence-shell electron-pair repulsion (VSEPR) theory, in which the bonded and

TABLE VI Binary Interhalogen Molecules

General formula[a]			
XY	XY_3	XY_5	XY_7
ClF	ClF_3	ClF_5	
BrF	BrF_3	BrF_5	
IF[b]	IF_3	IF_5	IF_7
BrCl			
ICl	I_2Cl_6[c]		
IBr			

[a] The oxidation state of Y is −1. The oxidation state of X is equal to the number of Y atoms present.
[b] Observed spectroscopically.
[c] Dimer of ICl_3.

nonbonded valence electrons are arranged on X so as to minimize electrostatic repulsions between electron pairs.

A few ternary compounds, such as $IFCl_2$ and IF_2Cl, are also known. As can be seen from the formulas, the neutral interhalogen molecules always contain an even number of halogen atoms. A variety of polyhalide ions have also been identified. Many contain an odd number of halogen atoms.

Chemically, all of the interhalogens are rather reactive. They are good oxidizing agents and attack almost all elements to produce mixtures of halides. Most are readily hydrolyzed in water, yielding hypohalic acids (HOX) and halide ions under appropriate conditions.

B. Diatomic Interhalogens, XY

All six of the possible diatomic compounds between F, Cl, Br, and I are known (Table VI) and, except for BrF and IF, which are too unstable with respect to disproportionation to permit isolation at room temperature, they can be prepared by direct combination of the elements X_2 and Y_2. The properties of the compounds tend to be intermediate between those of the pure, parent halogens. Most add to carbon–carbon double bonds (Section IX. C), and some are useful as nonaqueous solvents. Liquid ICl, in particular, dissolves the chlorides of Group IA to give highly conducting solutions.

The stabilities of the diatomic interhalogens are variable. The diatomic interhalogen ClF is the most stable and IF the least. Like their pure halogen parents, interhalogen molecules dissociate into free atoms at elevated temperatures. The diatomic interhalogen ICl resembles I_2 by dissolving in a variety of organic solvents and reacts with molecules having unshared electrons to form stable, charge-transfer complexes.

C. Tetra-atomic Interhalogens, XY_3

The four known interhalogens of the XY_3 type (Table VI) can also be prepared by direct reaction of the elements, but conditions must be carefully chosen to avoid the formation of mixtures of interhalogens with different stoichiometries. Another synthetic approach involves reaction of a lower interhalogen with a halogen:

$$ClF + F_2 \rightarrow ClF_3. \qquad (30)$$

The two iodine-containing compounds have not been studied extensively, but BrF_3 and especially ClF_3 are extremely useful chemical reagents.

Chlorine trifluoride is a very powerful oxidizing agent and one of the most reactive chemicals known. It attacks many materials normally considered inert (e.g., asbestos, xenon gas) and for this reason has been employed in the production of incendiary bombs and experimental rocket motors. It is an exceptionally good fluorinating agent and is manufactured on a moderately large scale for the preparation of UF_6 in nuclear fuel processing.

Bromine trifluoride is somewhat less reactive than ClF_3, but is also a useful fluorinating and brominating agent. Liquid BrF_3 has a high specific conductance and has been exploited as a nonaqueous, ionizing solvent.

D. Hexa-atomic, XY_5, and Octa-atomic, XY_7, Interhalogens

Only four interhalogens with the formula XY_5 or XY_7 are known (Table VI). Synthesis involves direct fluorination of the element or a lower interhalogen fluoride. Fluorination of appropriate metal salts may also be employed.

$$KBr + 3F_2 \rightarrow KF + BrF_5; \qquad (31)$$

$$PdI_2 + 8F_2 \rightarrow PdF_2 + 2IF_7. \qquad (32)$$

All of these molecules are excellent fluorinating agents, with the general sequence of reactivity for the halogen fluorides being $ClF_3 > BrF_5 > IF_7 > ClF > BrF_3 > IF_5 > BrF > IF_3$.

E. Polyhalide, Polyhalonium, and Halogen Ions

A large class of anions is formed by the reaction of a halogen or interhalogen molecule and a halide ion:

$$Y_2 + X^- \rightarrow Y_2X^-; \qquad (33)$$

$$X'Y_n + X^- \rightarrow XX'Y_n^-. \qquad (34)$$

The halogens involved may or may not be of the same kind. Although compounds formed from these anions tend to be unstable, decomposing to a metal halide and neutral halogen or interhalogen molecule, stabilities may be enhanced by the presence of large cations, such as Cs^+ or tetraalkylammonium ions (R_4N^+).

Iodine forms the most extensive group of polyhalide anions, with triiodide, I_3^-, being the best-known example. The formation of this anion is responsible for the increased solubility of I_2 in water on addition of potassium iodide (KI). Triiodide is used extensively in analytical chemistry, many analytical procedures being based on the release or uptake of iodine and its subsequent titration with sodium thiosulfate (iodometry). The largest polyhalide anion known, I_{16}^{4-}, consists of an alternate arrangement of triiodide anions and neutral iodine molecules.

Fluorine shows the least tendency for polyhalide formation. The F_3^- ions does not exist under normal conditions. Species such as $IBrF^-$ have been identified, but the fluorine atom never occupies a center position in these structures.

Polyhalonium cations are also known, with iodine-containing cations being the most numerous and best characterized. There is no evidence for simple salts containing an X^+ ion; however, X_3^+ ($X = Cl, Br$) as well as the mixed species XY_2^+ and XYZ^+ (X, Y, Z = Cl, Br, or I) can be formed by reaction of halogens or interhalogens with strong oxidants. The halogen or interhalogen may also serve as the oxidant. Thus, gold dissolves in BrF_3 to give BrF_2^+ and AuF_4^- ions. Solutions containing these cations are frequently highly colored. Penta- and heptaatomic cations are also known (ClF_4^+, BrF_4^+, ClF_6^+, and IF_6^+, for example).

The halogens, X_2 ($X = Cl, Br, I$), dissolve in strongly oxidizing solvents such as oleum (a solution of SO_3 in concentrated H_2SO_4, also called fuming sulfuric acid) to give cationic species X_2^+. Both Br_2^+ and I_2^+ can be isolated as salts, but the presence of the Cl_2^+ ion has, so far, only been inferred from spectroscopic data. Other halogen cations include X_3^+ ($X = Cl, Br, I$), I_4^+, and X_5^+ ($X = Br$ and I only).

V. HALOGEN OXIDES

A. Oxygen Fluorides

Compounds of oxygen and fluorine are more properly called oxygen fluorides, because the electronegativity of fluorine is greater than that of oxygen. Several oxygen fluorides are known (Table VII), the most stable being OF_2 and the least stable, O_4F_2. Reasonably stable fluorinated peroxides have also been characterized.

OF_2, a colorless gas at room temperature, can be prepared by passing F_2 gas rapidly through a 2% aqueous sodium hydroxide solution:

$$2F_2 + 2NaOH \rightarrow OF_2 + 2NaF + H_2O. \quad (35)$$

TABLE VII Halogen Oxides

Fluorine	Chlorine	Bromine	Iodine[a]
OF_2	Cl_2O	Br_2O	
O_2F_2			
	Cl_2O_3[b]		
	ClO_2	BrO_2	
		Br_2O_3	
O_4F_2[c]	Cl_2O_4		I_2O_4
			I_2O_5
	Cl_2O_6[d]		
	Cl_2O_7		
			I_4O_9

[a] Decompose on heating.
[b] Explodes even below 0°C.
[c] Unstable even at −150°C.
[d] Dimer in equilibrium with ClO_3.

The compound is a powerful oxidizing and fluorinating agent, reacting with many metals to give oxides and fluorides. It is readily hydrolyzed by base, reacts slowly with water, and liberates other halogens from their acids or salts.

B. Chlorine Oxides

Chlorine forms a number of well-known oxides (Table VII) which are generally unstable and prone to explosion. Only ClO_2 and Cl_2O are employed to any extent commercially, where they are used to make chlorinated solvents and chemicals for water treatment, or function as important bleaching agents for wood pulp and textiles.

Dichlorine oxide (Cl_2O) is prepared commercially by several methods, including the reaction of Cl_2 gas with moist sodium carbonate:

$$2Cl_2 + 2Na_2CO_3 + H_2O \rightarrow 2NaHCO_3 + 2NaCl + Cl_2O(g). \quad (36)$$

The gas is not used directly because of a tendency to explode when heated or sparked. However, since Cl_2O is the anhydride of hypochlorous acid (HOCl), it is easily converted to hypochlorite salts, such as $Ca(OCl)_2$, by treatment with aqueous base. These salts are more stable and safer to handle.

Chlorine dioxide (ClO_2) may be prepared by reduction of sodium chlorate with sulfur dioxide in strongly acidic solution:

$$2NaClO_3 + SO_2 + H_2SO_4 \rightarrow 2ClO_2 + 2NaHSO_4. \quad (37)$$

It also has a tendency to explode if present in concentrated amounts and must be carefully prepared at the point of use. ClO_2 is soluble in water, forming solutions which decompose to chloride and chlorate (ClO_3^-) when exposed to light. In base, a mixture of chlorite (ClO_2^-) and chlorate is formed.

As a gas, chlorine dioxide decomposes thermally and in the presence of ultraviolet light to produce the short-lived chlorine oxide radical, ClO. This same radical (a species with an unpaired electron) is also produced by the photolysis of chlorofluorocarbons such as $CFCl_3$ and CF_2Cl_2 and has been implicated in reactions leading to depletion of ozone in the earth's upper atmosphere (Section IX.F).

C. Bromine and Iodine Oxides

There are only three reasonably well-established oxides of bromine. All three have low thermal stabilities and have not been extensively investigated. Of the oxides of iodine (Table VII), I_2O_5 is the most stable and useful.

The iodine oxide I_2O_5, prepared by dehydration of iodic acid (HIO_3), is a white, crystalline solid at room temperature, stable to 300°C. This compound is extremely soluble in water, reforming iodic acid. It is an important reagent for the determination of carbon monoxide (CO) in gaseous mixtures. The reaction,

$$5CO + I_2O_5 \rightarrow I_2 + 5CO_2, \quad (38)$$

proceeds rapidly and quantitatively at room temperature, and the iodine that is formed is titrated using sodium thiosulfate (iodometry).

The remaining two oxides of iodine are not well characterized. Oxides I_2O_4 and I_4O_9 are only moderately stable and decompose on heating to give I_2O_5 and iodine, or iodine and oxygen, respectively.

VI. OXYACIDS AND THEIR ANIONS

A. General Survey

All of the halogens form oxyacids and salts of these acids. The names of these compounds are determined by the oxidation state of the halogen.

+1, HOX (hypohalous acid); OX^- (hypohalite anion)
+3, HXO_2 (halous acid); XO_2^- (halite anion)
+5, HXO_3 (halic acid); XO_3^- (halate anion)
+7, HXO_4 (perhalic acid); XO_4^- (perhalate anion)

The only oxyacid of fluorine is HOF. Numerous oxyacids are known for the other halogens (Fig. 1), although most cannot be isolated pure and are stable only in aqueous solution or as salts.

The oxyacids become stronger acids as the number of oxygen atoms increases (pK_a: HOCl, 7.52; $HClO_2$, 1.94; $HClO_3$, −3; $HClO_4$, +10). The perhalic and halic acids ionize essentially completely in aqueous solution and are considered strong acids. Halous acids are moderately strong, and hypohalous acids are weak. For a series of analogous oxyacids, the acid strength increases in the order I < Br < Cl (i.e., HOI < HOBr < HOCl).

In water, many of the oxyacids and their anions are unstable with respect to disproportionation (self-oxidation and reduction). The tendency for this kind of instability may be conveniently determined from the reduction potential diagrams shown in Fig. 1. A large, positive standard reduction potential (the number over the arrows) indicates a strong tendency for the particular reaction indicated by the arrow (a reduction). A large, negative standard reduction potential indicates a strong tendency for change in the opposite direction (an oxidation). A particular oxyacid or its anion will not be stable with respect to self oxidation and reduction if a reduction potential to its immediate left is more positive than a reduction potential to its immediate right.

Reduction potentials are altered by changing the concentrations of the species present. Figure 1 is strictly valid only for unit activity (about 1 *M* concentration of the species involved). Two different sets of diagrams are provided: one for unit activity of acid and a second for unit activity of base.

To illustrate the use of these diagrams, the stability of I_2 in 1 *M* base will be considered. The diagram for iodine-containing species in base shows I_2 will disproportionate to I^- and IO^- [Eq. (15)]. IO^- should, however, also be unstable, undergoing disproportionation to I^- and IO_3^- [Eq. (16)]. Further disproportionation of IO_3^- is not expected because the reduction potential involving formation of IO_4^- is more positive than any reduction potential to the left of IO_3^-. It should be noted that these diagrams only predict what reactions are allowed to happen; they say nothing about how fast the reactions will occur (see Section I.G.).

B. Hypohalous Acids and Hypohalite Salts

Hypofluorous acid is formed by passing fluorine gas at low pressure over water at 0°C:

$$F_2 + H_2O \rightarrow HOF + HF. \quad (39)$$

Although the oxidation state of F in HOF is technically +1, the actual charge is estimated to be somewhat intermediate to that of F in HF and OF_2.

HOF is only marginally stable at room temperature, decomposing to HF and O_2 with a half-life of about 30 min at room temperature. HOF also reacts rapidly with water, the predominant products being hydrogen peroxide and HF under acidic conditions and O_2 and HF under alkaline conditions.

The other hypohalous acids are all very reactive oxidizing agents that are relatively unstable. They are most conveniently prepared by the disproportionation of the parent halogen, X_2, in water [Eq. (14)]. Addition of HgO or Ag_2O precipitates the halide ion and shifts the equilibrium so as to favor additional hypohalite formation. Attempts to prepare pure samples from aqueous solution lead to decomposition.

All three acids disproportionate in water, the rate and products of this reaction being influenced by temperature, concentration, and solution pH. HOCl is more stable than HOBr or HOI. Base converts the acids to the anions, which disproportionate less readily. Anion stability decreases in the order $ClO^- > BrO^- > IO^-$.

HOCl is the most commercially useful hypohalous acid, being employed primarily for bleaching and sterilizing. It is generally manufactured by disproportionation of Cl_2 using a strong base such as sodium or calcium hydroxide,

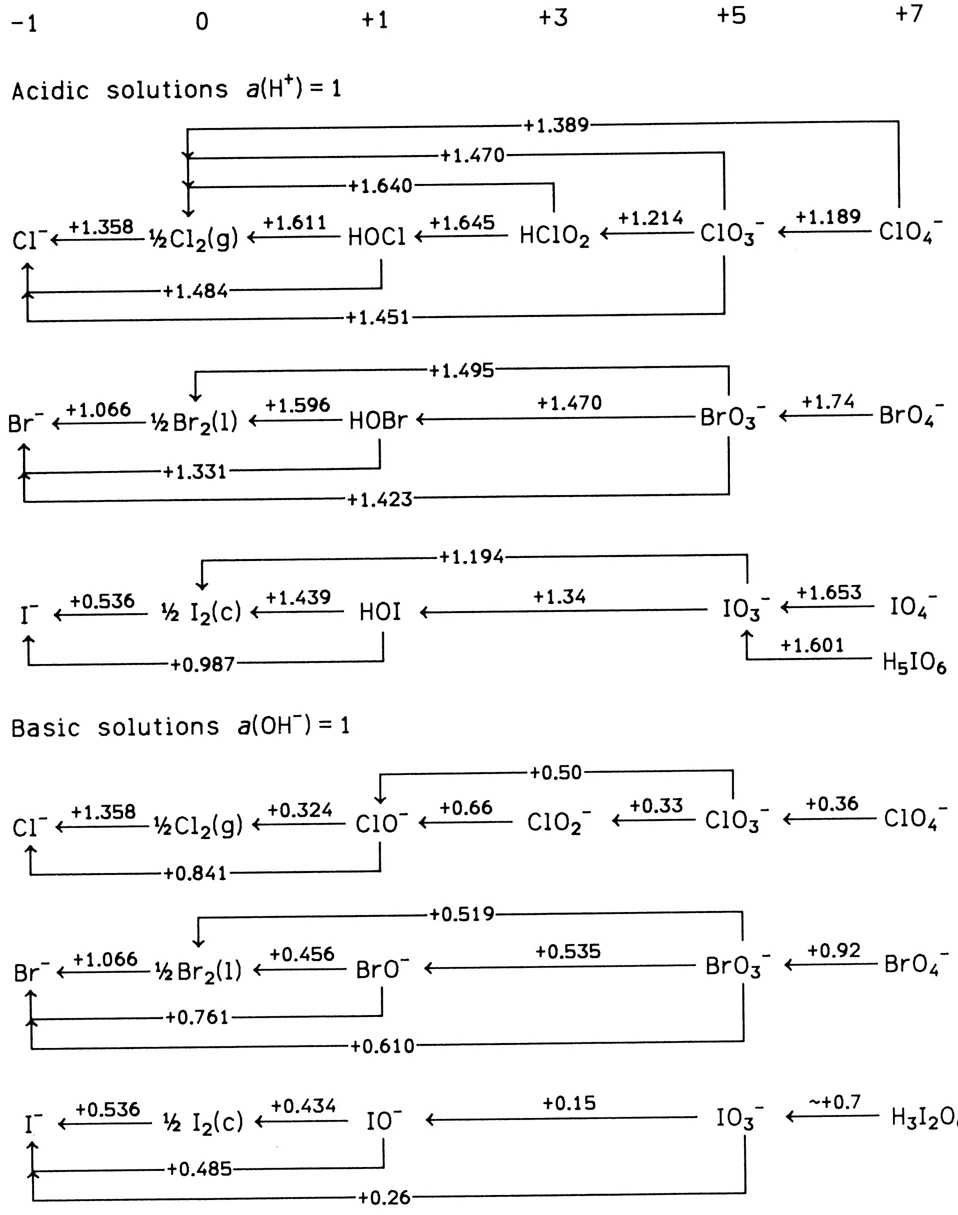

FIGURE 1 Standard reduction potentials for Cl, Br, and I species in acid and alkaline aqueous solutions.

or by treating ClO_2O with water. The hypochlorite anion, OCl^-, is also an effective bleach. Calcium hypochlorite is used for swimming-pool sanitation and bleaching powder. Liquid bleach is an alkaline solution of NaOCl with a chlorine content ranging from 5 to 12%.

Hypochlorites react with ammonia and organic amines to form chloramines. The "chlorine" odor of water treated with hypochlorite is actually due to the chloramines produced by action of the acid on bacteria. Hypobromites oxidize amines to N_2.

Hypohalous acids are useful halogenating agents for both aromatic and aliphatic compounds, the ease of aromatic halogenation increasing in the order $OCl^- < OBr^- < OI^-$. The reaction of hypoiodite with methyl ketones forms the basis of the iodoform (CHI_3) test for $CH_3C{=}O$ groups in organic compounds:

$$RC({=}O)CH_3 + 3OI^- \rightarrow RC({=}O)O^- + 2OH^- + CHI_3. \qquad (40)$$

HOCl is also used industrially to manufacture hydrazine, chlorhydrins, and α-glycols.

C. Halous Acids and Halite Salts

Chlorous acid is the least stable of all the oxyacids of chlorine. It can be prepared by treating a suspension of

barium chlorite with sulfuric acid followed by removal of the precipitated barium sulfate:

$$Ba(ClO)_2(aq) + H_2SO_4(aq) \rightarrow BaSO_4(s) + 2HClO_2(aq). \quad (41)$$

$HClO_2$ exists only in aqueous solution. It decomposes rapidly in base to give chlorite and chlorate ions and in acid to give chlorine dioxide and chlorate and chloride ions. There is some indirect evidence for the existence of bromous and iodous acids, but they are even less stable than $HSIO_2$.

A number of metal chlorite salts have been isolated. They are normally prepared by reduction of an aqueous solution of ClO_2 in the presence of the metal hydroxide or carbonate:

$$2ClO_2 + O_2^{2-} \rightarrow 2ClO_2^- + O_2. \quad (42)$$

Peroxide is the preferred reducing agent because it adds no contaminant to the resulting chlorite solution. Heavy metal chlorites tend to explode when heated or subjected to pressure. Chlorite salts of Groups 1 and 2 are more stable, but $NaClO_2$ is the only one that is of any commercial importance.

Neutral or basic solutions of $NaClO_2$ disproportionate so slowly at room temperature that they are considered stable. Heating or exposure to light speeds up the rate of reaction, and the solutions gradually decompose to chloride and chlorate ions. The main uses of $NaClO_2$ are in bleaching and removal of pollutants from industrial off-gases.

D. Halic Acids and Halate Salts

Chloric and bromic acids exist only in aqueous solution, but iodic acid can be isolated in the free state by dissolving I_2O_5 in a minimum amount of hot water. White crystals of iodic acid precipitate out on cooling. Alternatively, an aqueous suspension of iodine may be oxidized electrolytically, or with concentrated nitric acid, hydrogen peroxide, or ozone.

Aqueous solutions of chloric and bromic acids are formed by disproportionation of Cl_2 or Br_2 in hot alkaline solution [Eq. (15) and (16)] or by treating the appropriate barium halate salt with sulfuric acid and removing the precipitated barium sulfate [similar to Eq. (41)]. Concentration of these solutions leads to decomposition of the acid.

Sodium chlorate, $NaClO_3$, is the most commercially important halate salt. It is prepared commercially on a large scale by electrolyzing hot brine and allowing the chlorine gas liberated at the anode to disproportionate in the basic solution that forms at the cathode. The major uses of sodium chlorate are as a bleaching agent for paper pulp, as a defoliant, and as an intermediate in the production of other chlorates and perchlorates. Potassium chlorate, $KClO_3$, is employed as an oxidizer in fireworks, flares, and safety matches. Heating potassium chlorate in the presence of a transition-metal catalyst such as MnO_2 is a convenient laboratory method for the preparation of small amounts of oxygen:

$$2KClO_3 \rightarrow 2KCl + 3O_2. \quad (43)$$

Bromate and iodate salts are prepared on a much smaller scale than chlorates. Under appropriate conditions, these ions undergo oscillating chemical reactions known as "chemical clocks." The best known clock reaction is observed when an acidified solution of sodium sulfite (Na_2SO_3) is mixed with an excess of iodate in the presence of starch indicator. After a suitable induction period allowing for sodium sulfite reduction of iodate to iodide [Eq. (44)], the blue, starch-iodine color periodically appears and disappears as the iodide is oxidized to iodine [Eq. (45)], and the iodine is reduced back to iodide [Eq. (46)].

$$IO_3^- + 3SO_3^{2-} \rightarrow I^- + 3SO_4^{2-}; \quad (44)$$

$$5I^- + IO_3^- + 6H^+ \rightarrow 3I_2 + 3H_2O; \quad (45)$$

$$3I_2 + 3SO_3^{2-} + 3H_2O \rightarrow 6I^- + 6H^+ + 3SO_4^{2-}. \quad (46)$$

E. Perhalic Acids and Perhalate Salts

Perchloric and periodic acids and their salts have been known for some time and are well characterized. Perbromic acid was not prepared until 1968 using beta-decay of radioactive ^{83}Se.

Perchlorates are the most stable oxy-compounds of chlorine, both as solids and in solution at room temperature. They are, however, very strong oxidizing agents and undergo violent reactions with readily oxidizable organic or inorganic materials, especially when heated. While aqueous solutions at room temperature may be slow to react, the anhydrous form of the acid is particularly dangerous; great care must be exercised when preparing or handling it. Concentrated $HClO_4$ should never be added to organic solvents, even if the solution is chilled.

Perchlorates are manufactured on a large scale by the electrolytic oxidation of sodium chlorate. On a smaller scale, the acid is prepared by treating anhydrous sodium or barium perchlorate with concentrated HCl, filtering off the precipitated chloride salts, and concentrating the acid by distillation. $HClO_4$ is commercially available in concentrations of 60–62% or 70–72% by weight, the composition of the water–acid azeotrope boiling at 203°C. The anhydrous acid is prepared by distillation of the concentrated acid under reduced pressure in the presence of a dehydrating agent such as fuming sulfuric acid.

Most commercial perchloric acid is used to manufacture perchlorate salts. Perchlorates of almost all metals are known, and except for potassium, rubidium, and cesium, they are quite soluble in water. The perchlorates of greatest industrial importance are NH_4ClO_4 (a solid rocket propellent), $Mg(ClO_4)_2$ (an electrolyte in dry-cell batteries), and $KClO_4$ (used in fireworks and fiares).

Perchlorate salts have been widely used in laboratory studies to adjust the total electrolyte concentration because the anion was thought to be noncoordinating. Thus, addition of perchlorates in almost any amount could be made without affecting the identity of complex ions also present in the solution. This assumption is now known to be incorrect, and coordinated perchlorate has been identified in a number of cases involving both main group and transition metal ions. The donor ability of perchlorate is quite weak, however, and the use of this ion as an inert electrolyte in aqueous solution is still widespread.

Perbromate can be prepared only using the most powerful oxidizing agents, such as fluorine gas and XeF_2, or electrolysis. The best synthesis involves oxidation of bromate by F_2 gas in 5 *M* sodium hydroxide under carefully controlled conditions:

$$BrO_3^- + F_2 + 2OH^- \rightarrow BrO_4^- + 2F^- + H_2O. \quad (47)$$

Solutions of $HBrO_4$ can be concentrated up to 6 *M* without decomposition and are stable for prolonged periods. Some perbromate salts have been isolated and appear to be reasonably stable. Even NH_4BrO_4 can be heated to around 170°C.

Periodates are made by oxidation of iodide, iodine, or iodate in aqueous solution. The industrial process involves the electrolytic oxidation of $NaIO_3$, or oxidation of sodium chlorate using chlorine gas.

$$IO_3^- + 6OH^- + Cl_2 \rightarrow IO_6^{5-} + 2Cl^- + 3H_2O. \quad (48)$$

The product is actually dihydrogen orthoperiodate, $Na_3H_2IO_6$, the parent acid being H_5IO_6.

The chemistry of periodates is complicated by the number of species which are formed by deprotonation, dehydration, and aggregation of the parent acid, H_5IO_6. In aqueous solution, periodic acid exists primarily as the IO_4^- ion plus lesser amounts of several orthoperiodates such as H_5IO_6 (the parent acid), $H_4IO_6^-$ (deprotonation of the parent), and $H_3IO_6^{2-}$ (further deprotonation). An increase in pH results in progressive deprotonation, dehydration, and dimerization, the principal species being IO_4^-, $H_4IO_6^-$, $H_3IO_6^{2-}$, $H_2IO_6^{3-}$, and $H_2I_2O_{10}^{4-}$.

Most periodate salts, other than those with the IO_4^- ion, contain an IO_6^- unit of some sort. Periodates are good oxidizing agents, especially in acid solution. They are commonly used in organic chemistry to cleave adjacent functional groups such as alcohols, ketones, and amines. In rigid systems, the reaction is specific for cis-functional groups, making periodates extremely useful in natural product, carbohydrate, and nucleic acid chemistry.

Unlike perchlorates, periodates form many stable complexes with transition metals in which the IO_6^- unit is coordinated to the metal through two oxygens rather than only one. Coordination involving periodate sometimes stabilizes unusual metal oxidation states such as Ni(IV), Cu(III), and Ag(III).

VII. OTHER INORGANIC HALOGEN COMPOUNDS

A. Oxyfluorides

There are a number of halogen oxyfluorides (Table VIII) in which X (Cl, Br, or I) is bonded to both O and F, forming compounds of the general formula, F_nXO_m. The center halogen is always X, and the chemistry of these compounds resembles that of the halogen fluorides, XF_n. Most are very powerful oxidizing and fluorinating agents and react with fluoride donors and acceptors to give mixed oxyfluoro anions and cations.

Five chlorine oxyfluorides have been definitely characterized (Table VIII). Their stabilities range from FClO, which decomposes with a half-life of about 25 at room temperature, to $FClO_3$ (perchloryl fluoride), which is thermally stable to about 400°C.

The highly unstable FClO is prepared by hydrolysis of ClF_3 or photolysis of a mixture of ClF_3 and ozone in Ar at very low temperatures. F_3ClO is prepared by fluorination of Cl_2O using F_2 gas in the presence of NaF or some other metal fluoride. It is a very powerful oxidizing and fluorinating agent, reacting slowly at room temperature, but rapidly when heated or irradiated with ultraviolet light. $FClO_2$ is prepared by fluorination of ClO_2 using ClF_3:

$$6NaClO_3 + 4ClF_3 \rightarrow 6FClO_2 + 6NaF + 2Cl_2 + 3O_2. \quad (49)$$

It is also a good fluorinating agent and a moderately strong oxidizing agent, but it tends to explode in the presence of strong reducing agents.

TABLE VIII Neutral Halogen Oxyfluorides

Oxidation state[a]	Chlorine	Bromine	Iodine
+3	FClO		
+5	$FClO_2$	$FBrO_2$	FIO_2
	F_3ClO	F_3BrO	F_3IO
+7	$FClO_3$	$FBrO_3$	FIO_3
	F_3ClO_2		F_3IO_2
			F_5IO

[a] Central halogen, Cl, Br, or I.

The synthesis of F_3ClO_2 involves a sequence of fluorine-transfer reactions starting with $FClO_2$. F_3ClO_2 is extremely reactive, but forms a stable anion, $[F_2ClO_2]^-$ by fluoride transfer to acceptors such as BF_3. The remaining chlorine oxyfluoride, $FClO_3$, can be prepared by the electrolysis of sodium perchlorate in anhydrous HF. However, the most convenient route for industrial-scale manufacture involves the fluorination of a perchlorate salt using antimony pentafluoride (SbF_5) in the presence of $HOSO_2F$ or HF:

$$KClO_4 + 2HF + SbF_5 \rightarrow FClO_3 + KsbF_6 + H_2O. \quad (50)$$

By comparison to the other chlorine oxyfluorides, perchloryl fluoride is a mild fluorinating agent and has been used for the preparation of fluorinated steroids. $FClO_3$ also reacts with phenyl lithium to form the unstable perchloryl benzene, $C_6H_5ClO_3$, and lithium fluoride.

Bromine oxyfluorides have not been as thoroughly studied as their chlorine analogs, but appear to be less thermally stable and somewhat more reactive chemically. Bromyl fluoride, $FBrO_2$, and perbromyl fluoride, $FBrO_3$, hydrolyze readily in water and even attack glass.

The iodine oxyfluorides tend to be polymeric, rather than monomeric. Unlike chlorine, no oxyfluoride compound with iodine in the 3+ oxidation state is known; however, iodine oxide pentafluoride, F_5IO, (but not F_5ClO) has been characterized. F_5IO does not hydrolyze readily and is obtained when IF_7 reacts with water, silica, glass, or I_2O_5.

B. Derivatives of Oxyacids

Replacement of hydrogen in oxyacids such as perchloric, fluorosulfuric, or nitric, by a halogen yields compounds of the type $XOClO_3$, $XOSO_2F$, and $XONO_2$ where X equals F, Cl, Br, and I in the +1 oxidation state. In addition, derivatives such as $X(ONO_2)_3$ and $X(OSO_2F)_3$ as well as metal (M) complexes of the type $M[X(ONO_2)_2]$, $M[X(ONO_2)_4]$, and $M[X(OSO_2F)_4]$ are known, where X equal Br and I in the 3+ oxidation state.

Most of these compounds must be prepared at low temperatures and have a tendency to explode. In general, the thermal stability decreases with increasing atomic number of the halogen. The halogen nitrates are less stable than the perchlorates, while the fluorosulfates form the most stable derivatives of all.

C. Compounds of the Noble Gases

Prior to 1962, the noble gases were thought to be completely inert because of the stability of their electron configurations. A variety of fluoride, oxide, and oxyfluoride compounds and ions are now known for xenon (with a less extensive series for krypton), in which the noble gas has oxidation states ranging from +2 to +8. No stable compounds of He, Ne, or Ar have ever been found. Some evidence for a difluoride of radon has been obtained from radiochemical tracer studies. Of the other halides, $XeCl_2$, $XeBr_2$, and $XeCl_4$ have been detected as the nuclear decay products of their ^{129}I analogs using Mössbauer spectroscopy.

The three xenon fluorides, XeF_2, XeF_4, and XeF_6, can all be prepared by direct reaction of xenon and fluorine gases under pressure, but conditions must be carefully controlled to obtain the desired product. Xenon tetrafluoride is produced in nearly quantitative amounts when a 1:5 mixture of Xe and F_2 is heated to 400°C under 6 atm pressure. Xenon difluoride is formed by the same procedure if xenon is in excess. The preparation of XeF_6 requires 1:20 volume mixtures of xenon and fluorine at 250–300°C and 50–60 atm pressure.

The reaction of Xe and F_2 can also be induced at room temperature by any source of energy capable of dissociating the F_2 molecule, such as ultraviolet light, ionizing radiation, and electrical discharges. Pure XeF_2 can be prepared by the simple action of sunlight on a glass bulb containing a mixture of xenon and fluorine.

The reactivity of the xenon fluorides increases with the number of fluorine atoms in the molecule. XeF_2 is stable in water if acid is present, although the resulting solution is a powerful oxidizing agent. When base is added, hydrolysis produces Xe, HF, and O_2. XeF_4 hydrolyzes instantly in water, and XeF_6 is so reactive that it fluorinates silica and cannot be handled in glass containers. The hydrolysis of the two higher fluorides produces XeO_3, a highly explosive compound.

XeF_2 is a mild fluorinating agent and useful for the addition of fluorine to carbon–carbon double bonds and for aromatic fluorination. XeF_4 is more reactive, but somewhat less useful. XeF_2 is a good F^- donor, readily forming $[XeF]^+$ and the $[Xe_2F_3]^+$ dimer. Only XeF_6 is a good F^- acceptor, reacting with Group 1 fluorides to form compounds with the formula $MXeF_7$ (M = Rb, Cs) and M_2XeF_8(M = Na, K, Rb, Cs).

Three stable oxyfluorides have been characterized: $XeOF_4$ and XeO_2F_2 with Xe in the +6 oxidation state, and XeO_3F_2 with Xe in the +8 oxidation state. These are obtained by controlled hydrolysis of xenon fluorides or by fluorination of xenon trioxide. The oxyfluoro anions, $[XeO_3F]^-$ and $[(XeOF_4)_3F]^-$ result when the hydrolysis products of XeO_3 and $XeOF_4$ are treated with F^-.

Krypton difluoride, KF_2, is obtained by passing an electric discharge through Kr and F_2 at −183°C, or by irradiation of these two gases using high-energy electrons or protons. KF_2 is a volatile, white solid that decomposes slowly at room temperature. Radon has only a short half-life (^{222}Rn, 3.825 days), and evidence for RnF_2 and RnF^+ is obtained from tracer studies.

D. Pseudo-halogens

Pseudo-halogens are not true halogens, but other diatomic molecules which contain two relatively electronegative units (X) that are symmetrically bound together, e.g., cyanogen (NC—CN), oxocyanogen (NCO—OCN), and thiocyanogen (NCS—SCN). Like true halogens, the pseudo-halogens reduce to anions X^- (CN^-, OCN^-, SCN^-) and to molecular pseudohalides (e.g., CH_3—CN). They form compounds among themselves (NC—SCN) and with the halogens. Analogs to the polyhalide ions, $[I(SCN)_2]^-$, are also known.

In common with the halogens, pseudo-halogens add to carbon–carbon double bounds, react with a number of metals to give salts containing X^- ions, and form complexes with metal ions $[Co(NCS)_4]^{2-}$. Not all comparisons are strictly analogous, however. The pseudo-halogen hydrides, HX, are very weak acids by comparison to the hydrohalic acids (pK_a: HCl, −7.4; HCN, 8.9), and the stabilities of the metal complexes formed by the halogens and the pseudohalogens tend to differ widely.

VIII. ASTATINE

A. Preparation, Isolation, and Purification

Astatine is the heaviest member of the halogen family. With no stable or long-lived isotopes, it must be synthesized artificially through nuclear reactions. The short half-lives of even the longest-lived isotopes make it extremely difficult to obtain weighable amounts of the element. Although the identification of some astatine compounds can be made directly by mass spectrometry, most investigations of the chemistry of this element have been carried out by tracer techniques using extremely dilute solutions (10^{-8} M or less).

The chemistry of astatine is usually studied using ^{211}At. This isotope is prepared by the alpha-bombardment of ^{209}Bi using energies in the range of 26 to 28 MeV [Eq. (5)]. The isotope ^{211}At has a half-life of 7.2 h and decays either by electron capture (59%) or by alpha-emission (41%). It is removed from the target by distillation in a stream of nitrogen at a temperature of 200 to 600°C and purified by redistillation. Alternatively, the target is dissolved in perchloric acid containing a little iodine, the Bi is removed by precipitation with phosphate, and the aqueous solution of AtI is used as is or the AtI is extracted into an organic solvent such as carbon tetrachloride or chloroform. Further extractions are carried out to obtain the purified product. The isotope ^{211}At is assayed by counting the alpha-particles or X-rays resulting from its nuclear decay.

B. Chemistry

Five oxidation states for astatine (−1, 0, +1, +5, and +7) have been definitely established, and a + 3 state has been postulated. The aqueous potentials (V, 0.1 M H^+) are estimated to be as follows (compare Fig. 1):

$$At^- \xleftarrow{+0.3} At(0) \xleftarrow{+1.0} HAtO \xleftarrow{+1.5} AtO_3^- \xleftarrow{>+1.6} AtO_4^-. \quad (51)$$

In aqueous solution, astatine is usually found in the free (0) state. However, unlike the other halogens, astatine(0) is not diatomic. It can be volatilized from solution and extracted (like iodine) into organic solvents such as benzene and carbon tetrachloride. Coextraction with halogens, X_2, into chloroform produces interhalogen compounds, AtX (X = Cl, Br, I). Reaction with halide ion, X^-, yields polyhalide ions, AtX_2^- (X = Br, I) and $AtIBr^-$, which can be extracted into isopropylether.

The astatide ion (At^-) is formed by reducing free astatine using moderately strong reducing agents (zinc with acid or SO_2). The astatate ion (+5), AtO_3^-, is obtained by reaction of lower states of astatine with more powerful oxidants such as Ce^{IV}, $S_2O_8^{2-}$, and IO_4^-. XeF_2 in alkaline solution is used to oxidize astatine to perastatate (+7).

A few organic compounds of astatine have been characterized. Most are prepared by displacement of iodide from the desired compound. Astobenzene, C_6H_5At, is formed by reaction of iodobenzene and AtI,

$$C_6H_5I + AtI \rightarrow C_6H_5At + I_2, \quad (52)$$

or by reaction between iodobenzene vapor and astatide ion,

$$C_6H_5I + At^- \rightarrow C_6H_5At + I^-. \quad (53)$$

A number of normal and *iso*-alkyl astatides have been prepared by reaction between the vapor of the analogous alkyl iodide and At^- ion at elevated temperatures. Demercuriation reactions have produced aromatic aminoacids, steroids, and imidazoles containing astatine.

IX. ORGANIC HALOGEN COMPOUNDS

A. General Survey

Organic halogen compounds are derivatives of organic compounds in which one or more hydrogen atoms have been replaced by an equal number of halogen atoms (F, Cl, Br, or I). Almost any class of organic compounds (e.g., alcohols, ketones, carboxylic acids) can contain halogen atoms. Very few halogenated compounds occur naturally. Most are produced synthetically in the laboratory or as a result of industrial processes.

Substitution of hydrogen by the halogen atom results in an increase in the boiling point, melting point, and density of the organic compound. (Fluorocarbons containing up to four carbon atoms boil somewhat higher than their corresponding hydrocarbons, but the reverse is true of fluorocarbons with more than four carbons.) This increase is greater the heavier the halogen and, in general, the larger the number of halogen atoms present. However, in polyhalogenated compounds, the positions of the halogens relative to each other are also an important consideration. If this molecular orientation is symmetrical, a substantial decrease in the melting and boiling points may result.

When halogens are present, they occupy terminal positions on the carbon chain and modify the reactivity of a portion of the molecule in their immediate vicinity. Since carbon is less electronegative than any of the halogens, the shared pair of electrons in the C—X bond is displaced or polarized towards the halogen. For saturated carbons (carbons with only single bonds), the result of the inductive effect associated with this difference in electronegativities is to make the halogen partially negative and the halogenated carbon partially positive. The carbon atom then becomes susceptible to attack by reagents which are electron-rich (nucleophilic).

Equation (54) shows an example of a reaction which is controlled by the inductive effect. Nucleophilic attack by the negative hydroxide ion (the nucleophile) on the partially positive carbon atom in methyl bromide results in replacement of the bromide to form methyl-alcohol:

$$\mathrm{HO{:}^- + \overset{\delta+}{CH_3}\!-\!\overset{\delta-}{Br} \longrightarrow CH_3\!-\!OH + {:}Br^-.} \qquad (54)$$

The displacement of the electrons in the methyl bromide molecule is indicated by the symbols $\delta+$ and $\delta-$, where δ means that partially positive or negative charges result on the atoms in question. The curved arrows are used to indicate the direction of electron movement, with the arrowheads pointing to the atoms which accept electrons.

If the halogen is attached to an unsaturated carbon (one that has a double or triple bond), the unshared pairs of electrons on the halogen interact with the carbon–carbon multiple bond. This interaction involves a partial loss of electrons from the halogen and gives the carbon–halogen bond some multiple character.

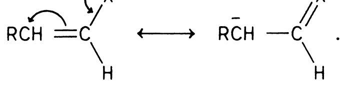
(55)

In Eq. (55), the double-headed arrow indicates that the actual state of the molecule is between the two extreme or "resonance" forms as shown. The shift in electrons, shown by the curved arrows, is now in a direction opposite to that expected from the inductive effect. The resonance effect alters the chemical reactivity of the molecule in two ways. First, the partially positive halogen atom is much less susceptible to nucleophilic attack than in saturated halides [Eq. (54)]. Second, the partially negative carbon in the multiple bond becomes more susceptible to attack by reagents that are electron-poor (eletrophilic).

Equation (56) shows the addition of hydrogen bromide to vinyl bromide where the direction of addition is controlled by the resonance effect. The positive hydrogen, H^+, adds to the partially negative carbon on the double bond, while the negative bromide ion adds to the carbon that is already halogenated:

$$\mathrm{H_2\overset{\delta-}{C}\!=\!\overset{\delta+}{CH\!-\!Br} \xrightarrow{H^+} H_3C\!-\!\overset{+}{CH}\!-\!Br \xrightarrow{:Br^-} CH_3CHBr_2.} \qquad (56)$$

The situation is more complex when halogens are present in extensively unsaturated or aromatic ring systems. If only one halogen is bound directly to a benzene ring, interaction of the halogen electrons with the multiple bonds on the ring produces partial negative charges on the ring carbons that are ortho and para to the halogen atom. The charge movement resulting from this resonance effect is shown in Eq. (57), where the double-headed arrows are again used to indicate that the actual state of the molecule is somewhere between the four extreme forms.

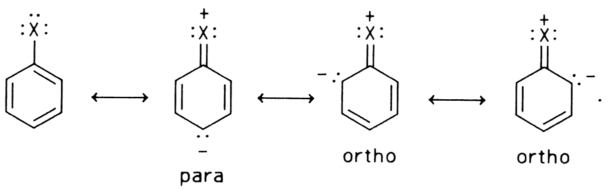

(57)

The effects on chemical reactivity are to make the halogen relatively inert to nucleophilic substitution and to direct electrophilic substitution to the ortho and para positions.

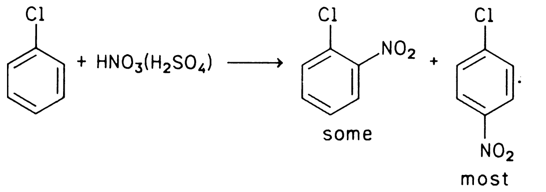

(58)

However, because the inductive effect of the halogen also acts to withdraw electron density from all carbons throughout the ring, the halogen is said to be "deactivating," and the rates of electrophilic substitution may be depressed. As one example, the rate of nitration of chlorobenzene [Eq. (58)] is slower than that of toluene, $C_6H_5CH_3$, because the methyl substituent (CH_3—) is both ortho–para directing and electron-releasing.

If an extensively unsaturated molecule is highly halogenated, the electron-withdrawing effect of the halogens may remove so much charge from the system that all of the carbons become quite positive and susceptible to nucleophilic attack. Both polychlorinated olefins and polychlorinated aromatics readily undergo nucleophilic fluorination by potassium fluoride, the reaction producing a whole range of polyfluorinated compounds in good yields.

B. Saturated Monohalides

There are three common methods for preparing compounds containing only one halogen atom: (1) addition of hydrogen halides, HX, to the C═C double bond in an alkene (olefin), (2) replacement of hydroxyl groups (—OH) in alcohols, and (3) direct halogenation of saturated hydrocarbons. The reactivity of HX for double bond addition decreases in the order HI > HBr > HCl > HF. With an unsymmetrical olefin, the halogen adds selectively to the carbon with the smaller number of hydrogen atoms (Markownikoff's rule):

$$CH_3CH{=}CH_2 + HI \rightarrow CH_3CHICH_3. \qquad (59)$$

Exceptions to Markownikoff's rule occur, as when HBr reacts in the presence of oxygen.

Replacement of hydroxyl groups in alcohols is typically carried out using anhydrous or concentrated aqueous solutions of hydrogen halides, phosphorus halides, thionyl chloride ($SOCl_2$), or thionyl bromide:

$$R{-}OH + SOCl_2 \rightarrow R{-}Cl + SO_2 + HCl; \qquad (60)$$

$$R{-}OH + HX \rightarrow R{-}X + H_2O. \qquad (61)$$

In these equations, R symbolizes the alkyl group (the carbon chain with all of its attached hydrogen atoms). For reactions using hydrogen halides, the relative rates of reaction are HI > HBr > HCl > HF for the hydrogen halides and tertiary > secondary > primary for the alcohol. Tertiary alcohols have three alkyl groups attached to the hydroxyl carbon (R_3C—OH), secondary have two (R_2CH—OH), and primary have one (RCH_2—OH). Various catalysts such as sulfuric acid or zinc chloride are sometimes added to increase the reaction rate.

Direct halogenation of saturated hydrocarbons or alkanes (compounds with no double or triple bonds) works satisfactorily only with elemental chlorine and bromine. The reaction proceeds via the formation of halogen atoms [Eq. (62)], which are highly reactive free radicals (species containing an unpaired electron):

$$Cl_2 \xrightarrow{\text{light}} 2Cl^{\cdot}; \qquad (62)$$

$$CH_4 + Cl^{\cdot} \longrightarrow CH_3^{\cdot} + HCl; \qquad (63)$$

$$CH_3^{\cdot} + Cl_2 \longrightarrow CH_3Cl + Cl^{\cdot}. \qquad (64)$$

Since the halogen atoms consumed in the second step [Eq. (63)] is regenerated in the third step [Eq. (64)], the process is called a chain reaction. In principle, one chlorine atom could induce the chlorination of an infinite number of hydrocarbon molecules through a cycle of reactions (63) and (64). In practice, several chain-termination reactions also occur that result in the destruction of the free radicals:

$$CH_3^{\cdot} + Cl^{\cdot} \rightarrow CH_3Cl; \qquad (65)$$

$$Cl^{\cdot} + Cl^{\cdot} \rightarrow Cl_2; \qquad (66)$$

$$CH_3^{\cdot} + CH_3^{\cdot} \rightarrow CH_3CH_3. \qquad (67)$$

Because the halogen atoms are very reactive, more than one substitution product is usually formed, with the extent of substitution depending on the halogen–hydrocarbon ratio. If monohalogenation is desired, a large excess of hydrocarbon is advantageous.

When alkyl halides react, the order of reactivity can generally be predicted by the relative ease with which the respective carbon–halogen bonds are broken: iodides > bromides > chlorides > fluorides, and tertiary (R_3C—X) > secondary (R_2CH—X) > primary (RCH_2—X). One typical reaction is nucleophilic substitution of the halogen by electron-rich groups such as ammonia (NH_3, to form amines), cyanide (CN^-), hydroxide ion [to form alcohols, Eq. (54)], alcohols (to form ethers), hydride ion (H^-), or even another halogen. Substitution of one halogen for another provides a convenient route for alkyl halide synthesis. Alkyl iodides are produced by iodide replacement of chlorine or bromine using sodium or potassium iodide as the reagent. Alkyl fluorides can be made by the exchange of F for Br or Cl using reagents such as antimony trifluoride or mercuric fluoride.

A second reaction typical of alkyl halides is elimination of the halogen to regenerate the C═C double bond. Halogen elimination occurs to some extent whenever alkyl halides react with base (_OH^-), but tends to become the main reaction if the alkyl halide is tertiary:

$$(CH_3)_3C{-}I + OH^- \rightarrow (CH_3)_2C{=}CH_2 + I^- + H_2O. \qquad (68)$$

A third reaction typical of alkyl halides involves the formation of free radicals in the presence of very active metals such as those of Groups 1 and 2. Subsequent reaction of the free radicals can lead to the formation of organometallic compounds (an organic compound with a metal substituent),

$$R{-}I + Mg \rightarrow R^{\cdot} + {}^{\cdot}MgI \rightarrow R{-}Mg{-}I. \qquad (69)$$

or coupling of the alkyl radicals, $R^{\cdot}$, to produce longer carbon chains, R—R.

C. Saturated Polyhalides

There are a number of methods for introducing more than one halogen into an organic molecule. Some of these procedures are selective, while others produce complex mixtures of products.

Reaction of aldehydes or ketones with phosphorus halides or other halogenating agents yields compounds in which two halogens are attached to the same carbon atom:

$$PCl_5 + CH_3C(=O)CH_3 \rightarrow POCl_3 + CH_3CCl_2CH_3. \quad (70)$$

Alternatively, two HX molecules may be added to a carbon–carbon triple bond in an alkyne. Dihalides in which the two halogens are attached to different carbons are formed by reaction of the diatomic halogen X_2 or interhalogen XY molecule with double bonds in alkenes, or, less effectively, by halogenation of compounds that contain more than one alcohol group (glycols). Trihalogen compounds, in which all three halogen atoms are on the same carbon, can be prepared by addition of haloforms (CHX_3) to alkenes:

$$CH_2{=}CH_2 + HCX_3 \rightarrow CH_3CH_2CX_3. \quad (71)$$

Reaction (71) proceeds via the formation of two free radicals, $^{\cdot}CH_2CH_2CX_3$ and $^{\cdot}CX_3$. Unless conditions are controlled carefully, coupling of the radicals may also occur, resulting in a mixture of products containing carbon chains of different lengths.

Direct halogenation of saturated hydrocarbons using elemental chlorine and bromine has been previously mentioned in the preparation of monohalogenated alkanes. (Direct iodination does not occur.) Analogous reactions using larger halogen–hydrocarbon ratios can also be used to produce highly halogenated molecules. Fluorination is so vigorous that there is almost no selectivity in replacement of the hydrogen atoms. (Some reactions involving fluorine and adamantanes or steroids are very selective.) Bromination tends to occur more readily at tertiary hydrogen atoms, followed by secondary and primary hydrogens in that order. Halogenation selectivity for chlorine is intermediate to that of fluorine and bromine. Improved selectivity for fluorination can be achieved by first preparing the polychlorinated or polybrominated compounds and then exchanging the chlorine or bromine for fluorine.

The reactions of polyhalogenated alkanes are similar to those of monohalogenated alkanes, except that the presence of more than one halogen on the same carbon results in a marked decrease in reactivity. For example, monofluorinated alkanes are quite unstable, but polyfluorinated alkanes are exceptionally resistant to chemical attack and thermal decomposition. Highly halogenated alkanes mainly undergo elimination reactions in which either HX or X_2 is lost with the resulting formation of alkenes or alkynes.

D. Unsaturated (Nonaromatic) Halides

Unsaturated halogenated compounds containing double bonds can be classified into two groups: vinyl halides and allyl halides. Vinyl halides (e.g., $CH_2{=}CHCl$) are those in which the halogen is attached to a carbon atom bearing a double bond. Allyl halides (e.g., $ClH_2C{-}CH{=}CH_2$) contain a halogen attached to a carbon which is one atom removed from the double bond. The preparations and chemical reactivities of these two types of compounds differ because of the different spatial relationships of the halogen atom to the site of unsaturation.

Vinyl halides are typically prepared by three methods: (1) addition of HX, X_2, or HCX_3 to a triple bond, (2) elimination of HX (dehydrohalogenation) from polyhalogenated alkanes, or (3) elimination of X_2 from polyhalogenated alkanes. Dehydrohalogenation is often accomplished by heating with alkali, while elimination of X_2 is carried out by heating with zinc dust in ethanol.

As discussed in Section IX.A, interaction of the unshared pairs of electrons on the halogen with the C=C double bond makes the C–X bond stronger than in ordinary alkyl halides and one of the carbon atoms in the C=C bond electron rich. As a result, vinyl halides do not undergo nucleophilic substitution reactions unless the double bond is extensively halogenated. The most common reactions of vinyl halides are (1) electrophilic addition of positive groups to the double bond, (2) free-radical addition to the double bond, and (3) formation of organometallic halides. Halogenated alkenes (such as vinyl chloride, $CH_2{-}CHCl$), which contain only two carbon atoms, readily polymerize to form long chains (polyvinyl chloride).

Allyl halides are frequently prepared by reaction of HX with allyl alcohols. Allyl halogens are very reactive because loss of the halogen as X^- produces a particularly stable carbonium ion with partial positive charge distributed over two sites:

$$CH_2{=}CH{-}{}^{+}CH_2 \leftrightarrow {}^{+}CH_2{-}CH{=}CH_2. \quad (72)$$

Again, the double-headed arrow indicates that the actual state of the ion is between the two resonance forms. Attack by an electron-rich nucleophile may occur at either of the two positive carbons, making allyl halides more susceptible to nucleophilic substitution of the halogen than ordinary alkyl halides.

Compounds containing halogen atoms directly joined to triply bonded carbon (haloalkynes) are formed either by (1) reaction between molecular halogen and a metallic derivative of the alkyne,

$$RC{\equiv}CNa + I_2 \rightarrow RC{\equiv}CI + NaI, \quad (73)$$

or by (2) elimination of X_2 or HX from halogenated alkanes or alkenes. The products of these reactions tend to be unstable, and the lower molecular weight compounds are prone to explosion. In general, stability of the haloalkynes increases in the order F < Cl < Br < I. The particular instability of the fluoroalkynes has been attributed to electron-pair repulsions between the unshared pairs on the fluorine atom and the adjacent triple bond.

Due to resonance effects similar to those shown in Eq. (55), a halogenated alkyne is more resistant to nucleophilic substitution than halogenated alkanes. Consequently, many nucleophiles react with haloalkynes first by addition to the triple bond and then by elimination of hydrogen halide:

$$\begin{aligned} ClC{\equiv}CCl + NH_3 &\rightarrow ClCH{=}C(NH_2)Cl \\ &\rightarrow HCl + ClC{\equiv}CNH_2 \\ &\rightarrow CH_2ClC{\equiv}N. \quad (74) \end{aligned}$$

In Eq. (74), ammonia (the nucleophile) adds to dichloroacetylene. The initial product, 1,2-dichloroaminoethylene, then loses HCl to give an alkyne, which isomerizes to give chloroacetonitrile as the final product.

In principle, nucleophilic attack can occur at several different locations in a haloalkyne: at the halogenated carbon in the triple bond [Eq. (75b)], at the halogen itself [Eq. (75a)], and at the second carbon in the triple bond [Eq. (75c)]. All three of these possibilities are observed in reactions with haloalkynes and sodium methoxide in methanol. The mechanisms of some of these substitution reactions are not clear, and acetylide ion intermediates, $RC{\equiv}C{:}^-$ may be involved.

Haloalkynes also undergo spontaneous polymerization reactions. In some cases, these reactions can be regulated so that trimerization to halogenated benzenes or benzene derivatives occurs.

E. Aromatic Halides

Halogenated aromatic compounds are derived from extensively unsaturated benzene-type (benzenoid) systems and are classified into two groups: aryl halides in which the halogen is attached directly to a ring carbon, and halides in which the halogen forms part of an alkyl group attached to the ring (an alkyl side chain). The preparation and reactivity of the two groups of compounds are quite different.

There are three main methods for introducing halogens directly onto an aromatic ring. The first involves electrophilic substitution of hydrogen by a halogen (Cl, Br, or I) using elemental halogen, hypohalous acids, halogenated amides, or hypohalites as the halogenating agent:

$$5C_6H_6 + 2I_2 + HIO_3 \rightarrow 5C_6H_5I + 3H_2O; \quad (76)$$

$$C_6H_6 + Br_2 \xrightarrow{FeCl_3} C_6H_5Br + HBr. \quad (77)$$

Ferric chloride, aluminum chloride, or boron trifluoride may be used as a catalyst in chlorination and bromination. Nitric acid is added in iodination.

All four halogens can be introduced into the ring via a diazonium salt, a method involving replacement of an amino group ($-NH_2$). The aromatic amine ($Ar{-}NH_2$, where Ar stands for any aromatic ring system) is converted to a diazonium salt ($Ar{-}N^+{\equiv}N\ X^-$), and the diazonium group is then replaced with halogen using cuprous chloride, cuprous bromide, or potassium iodide. Fluoride substitution is produced by heating the diazonium salt in the presence of fluoroborate ion, BF_4^-. Very pure products are produced because substitution of the halogen occurs only at the position originally occupied by the amino group.

A third method involves loss of HX or X_2 from polyhalogenated cyclohexanes or cyclohexenes in which the six-membered alkane or alkene ring is transformed into a six-membered aromatic benzene ring. Heating in aqueous alcohol and base leads to elimination of HX and heating with zinc or iron in ethanol removes X_2 to produce a mixture of halogenated aromatic products.

As discussed in Section IX.A, the presence of one Cl, Br, or I decreases the reactivity of the benzene ring and directs further substitution into the ortho and para positions. Aryl halides are much more resistant to nucleophilic attack than are alkyl halides, unless the halogen on the ring is activated by the presence of other electron-withdrawing groups in the molecule (e.g., nitro, $-NO_2$, ortho or para to the halogen) or the reaction conditions are especially severe (high temperatures and the presence of strong base). The presence of fluorine also directs further substitution to the ortho and para positions, but does not deactivate the ring.

The residual hydrogens in aryl halides are generally susceptible to electrophilic attack and can be halogenated, nitrated (substitution by $-NO_2$), or sulfonated (substitution by $-SO_2$). In highly halogenated ring systems, residual hydrogens become acidic because of the

$$C_6H_5C{\equiv}CX + CH_3O{:}^-Na^+ \begin{cases} \nearrow C_6H_5C{\equiv}CH & (75a) \\ \rightarrow C_6H_5C{\equiv}COCH_3 + C_6H_5CH{=}CXOCH_3 & (75b) \\ \searrow C_6H_5C(OCH_3){=}CHX & (75c) \end{cases}$$

electron-withdrawing properties of the halogens. Such species readily form organometallic compounds by hydrogen–metal exchange. Bromine and iodine on the ring are easily replaced by active metals to form organometallics. Chlorine reacts very slowly, while fluorine is inert to substitution by metals.

Halogens on alkyl side chains generally resemble halogens in alkyl halides. As with alkyl halides, preparation is typically carried out by (1) substitution of side-chain hydroxyl groups or (2) addition of HX or X_2 to side-chain olefins. Free-radical reaction with halogen molecules, X_2, yields a mixture of products and works best for chlorination or bromination.

If the halogen is attached to the carbon which links the alkyl group to the ring system (e.g., $Ar{-}CX_2CH_3$), the halogen is somewhat more susceptible to nucleophilic attack. The degree of reactivity is intermediate between that of the corresponding alkyl and allyl halide. When halogens are not attached to the carbon atom adjacent to the benzene ring, the reactivity of the halogen is essentially that of the analogous alkyl halide.

F. CFCs and Their Substitutes

The acronym CFC (*c*hloro*f*luoro*c*arbon) is used to designate perhalogenated derivatives of methane (CH_4) and ethane ($CH_3{-}CH_3$) that contain both chlorine and fluorine. As a class, these compounds are unusually stable with very low toxicities. Such properties—plus high densities and large heats of vaporization, low boiling points, viscosities, and surface tensions, nonflammability, and lack of odor—make CFCs uniquely suitable as refrigerants, propellants, blowing agents, and solvents.

CFCs have been among the most effective and widely used synthetic organic compounds in modern society. However, in a series of satellite observations made from 1987 to 1994, the Cl-containing decomposition products of these compounds wer shown to play a significant role in reducing the earth's stratospheric ozone level. On a global basis, the ozone layer has shrunk an average of about 3% since 1978, with the greatest depletions occurring in the polar regions, especially over the Antarctic.

Loss of stratospheric ozone has two major detrimental effects. First, ozone acts as a natural shield against biologically damaging ultraviolet radiation from the sun. Epidemiological studies suggest that each 1% depletion of ozone might lead to a 1–3% increase in skin cancer among fair-skinned people. Other effects include increased susceptibility to eye injuries and suppression of the immune system. Second, the absorption of solar energy by stratospheric ozone is a major source of heat for the upper atmosphere. Alteration of stratospheric temperature could significantly alter global wind systems and climate. Finally, CFC accumulation in the lower atmosphere could also contribute to global warming through the greenhouse effect.

In 1989, almost all nations of the world agreed to phase out CFC production by the year 2000. Then, following increasingly alarming evidence for ozone depletion, this agreement was amended in 1990 and again in 1992, setting an advanced deadline for complete, rather than partial phase-out of CFC production. December 31, 1995, marked the end of production of virtually all CFCs in the industrialized world. There are two exceptions to a CFC ban in the United States: (1) use as a propellant in inhalers for asthma patents, and (2) use in the manufacture of methyl chloroform to clean O-ring seals in the Space Shuttle.

HCFCs (*h*ydro*c*hloro*f*luoro*c*arbons) and HFCs (*h*ydro*f*luoro*c*arbons) have been developed as reasonable, but probably temporary, substitutes for CFCs. The hydrogen atoms in these substitutes make them subject to oxidation in the lower atmosphere, thus theoretically less able to carry chlorine up to stratospheric ozone. However, the identity and effects of the Cl-containing decomposition products of HCFCs are still incompletely known, and a portion of HCFC emissions and their degradation products may still reach the stratosphere, giving these compounds some potential for ozone depletion. While HCFCs are replacing CFCs in a number of commercial applications, HCFCs are also scheduled for total phase-out by 2030.

The chemistry required to make HCFC and HFC substitutes for CFCs is typically two to four times more complex than for CFC production. While simple HCFCs and HFCs can be prepared by halogen exchange,

$$CHCl_3 \xrightarrow{HF} CHCl_2F + CHClF_2 + CHF_3, \qquad (78)$$

the one-carbon products have unacceptably low boiling points. To match CFCs in physical properties requires substitute compounds that contain two carbon atoms. The two-carbon requirement tends to increase production costs for a number of reasons. First, more steps, generally involving halogen addition/elimination as well as substitution, are usually required. This produces more complex mixtures, increasing separation difficulties. To make matters worse, hydrogen fluoride, which is present in both addition and exchange reactions used to prepare the final product, tends to form hard-to-manage azeotropes with many HFCs. Finally, because HFCs and HCFCs are designed to be less stable than CFCs, they tend to decompose on catalyst surfaces, deactivating the catalyst. In two-carbon HCHC systems, a significant amount of HCl may be eliminated on some catalyst surfaces, producing toxic side products which must also be removed from the final product.

CFCs and their partially hydrogenated derivatives are identified by a series of numbers related to the formula of the compound. From right to left, the first digit gives the number of fluorine atoms, the second digit is one more than the number of hydrogen atoms, and the third digit is one less than the number of carbon atoms. Zero is always omitted. Any remaining positions are assumed to be occupied by chlorine atoms. Isomers may be given letter designators. Examples of this numbering system are CFC-12 (CCl_2F_2), CFC-113 ($C_2Cl_3F_3$), HFC-134a ($CH_2F—CF_3$), and HCFC-123 ($C_2HCl_2F_3$). If bromine is also present, the compounds are called Halons. The first digit on the right represents the number of bromine atoms, the second digit gives the number of chlorine atoms, the third gives the number of fluorine atoms, and the fourth gives the number of carbon atoms. In this system, zero is designated. Examples are Halon-1211 ($CBrClF_2$) and Halon-2402 ($C_2Br_2F_4$).

G. Other Halogenated Organics: Uses and Hazards

Commercial applications for halogenated organic compounds have been mentioned throughout this article, CFCs and their derivatives were specifically discussed in the preceding section. Many other organic halogen compounds have direct commercial applications, or are used in industry or the laboratory to synthesize other compounds with useful properties, such as dyes and medicinal agents. While it would be impossible to discuss thoroughly the wide range of industrial applications for halogenated organic compounds, some mention should be made of a few of the more important uses. Again, some of these compounds, especially those containing chlorine, are no longer employed as extensively as they once were because they are toxic or their presence represents an environmental hazard.

Small polychlorinated alkanes and alkenes have been widely used as solvents and fire retardants (carbon tetrachloride, CCl_4, and several Halons: 1211, 1301, and 2402) and anesthetics (chloroform, $CHCl_3$, mixed with acetone and ether). However, carbon tetrachloride can form phosgene ($COCl_2$), a very poisonous gas, when heated in the presence of oxygen, and its use in fire extinguishers has been discontinued. Chloroform, now known to cause liver damage has been replaced by the anesthetic halothane ($CF_3—CHBrCl$). Halothane has the advantages of nonflammability, high anesthetizing power, and a general lack of postnarcotic effects. Toxic effects are possible if it is not properly administered. Ethyl chloride ($CH_3—CH_2Cl$), once widely used for the manufacture of tetraethyllead, is now used to some extent as an ethylating agent in the synthesis of dyes and fine chemicals.

Larger polychlorinated molecules have been employed as insecticides—aldrin, DDT, chlordane, dieldrin, endrin, gammexane, and isodrin, for example. One of the earliest was DDT (*d*ichloro*d*iphenyl*t*richloroethane), which is prepared by the condensation of chlorobenzene and chloral in the presence of sulfuric acid (H_2SO_4):

$$2C_6H_5Cl + CCl_3CHO \rightarrow (p - ClC_6H_4)_2CHCCl_3 + H_2O. \quad (79)$$

Other polychlorinated molecules function as herbicides: 2,4-D (2,4-dichlorophenoxyacetic acid), 2,4,5-T (2,4,5-trichlorophenoxyacetic acid), diquat, paraquat, and Teklon. Many of these compounds are no longer used because their stability in the environment allows them to accumulate in the fat of fish, birds, and mammals.

Another example of industrially useful polychlorinated molecules that have been found to have long-term deleterious environmental and health effects are the polychlorinated biphenyls or PCBs: Aroclor, Clophen, Fenclor, Kanechlor, Phenoclor, Pyralene, and Santotherm. (Commercial PCBs are mixtures.) These substances have been listed as carcinogens by the U.S. Environmental Protection Agency, but they were once widely used as hydraulic fluids, plasticizers, adhesives, fire retardants, lubricants, and in carbonless reproducing paper. They are still found in older electrical capacitors and electrical transformers and are widely identified in the environment and chemical dump sites. Newer transformers and capacitors use alternative fluids.

Completely fluorinated polymers have low intermolecular forces, resulting in a low coefficient of friction and excellent lubricating properties. The small fluorine atoms replace hydrogen atoms with very little distortion of the molecule and shield the carbon atoms from chemical attack. As a result, polyfluorinated polymers have exceptional thermal stabilities as well as lubricating properties. Some of the most commercially important are the high-molecular-weight fluoroplastics and elastomers derived from tetrafluoroethylene, hexafluoropropylene, vinylidene fluoride, and vinyl fluoride. The fluorinated plastic, Teflon PTFE® [polytetrafluoroethylene, $—(CF_2—CF_2)_n—$], has a service temperature from –196 to 260°C and is used to pack bearings in motors. Other important fluoropolymers include Teflon FEP® (a plastic copolymer of tetrafluoroethylene and hexafluoropropylene), Kel-F® [$—(CF_2—CFCl)_n—$], and Viton® (an elastomeric terpolymer of hexafluoropropylene, tetrafluoroethylene, and vinylidene fluoride having excellent thermal, chemical, and oxidative stability). The lower-molecular-weight fluoropolymers are liquid and are employed as lubricants. The monomer, carbon tetrafluoride (CF_4), is used as a degreasing agent for the plasma etching of semiconductor devices.

Very large chlorinated polymers also have special properties which make them commercially valuable. The most important of these, the polyvinyl chlorides (PVCs), are used for electrical insulation, rubber substitutes (tubing, belting, and gaskets), and the production of water-resistant, artificial textiles.

Highly fluorinated molecules are very unreactive. Experiments with small mammals have shown that blood can be entirely replaced by certain biochemically inert perfluoroorganics. Life is sustained by the fluorocarbon blood substitute, which has the ability to dissolve, transport, and release oxygen by simple solubility. Experiments suggest that there is no apparent ill effect, and the animal is subsequently able to regenerate its own blood supply as the fluorocarbon is gradually exhaled through the lungs. Perfluorooctyl bromide ($C_8F_{17}Br$) is a nonirritating, radioopaque material used for the X-ray inspection of organs.

Small, lightly fluorinated molecules often exhibit toxic properties. Ethyl fluoroacetate and fluoroacetic acid were among the first nerve gases. Sodium monofluoroacetate is a rodenticide, and monofluoroacetamide has been used as a systemic insecticide. Both are dangerous to humans.

The introduction of a single fluorine atom into biologically significant molecules or established drugs frequently increases the efficacy of the drug or creates an enzyme-blocking agent. The compound 5–fluorouracil is thought to interfere with the biochemical operation of living cells and has been used successfully in the treatment of some forms of cancer.

SEE ALSO THE FOLLOWING ARTICLES

Bonding and Structure in Solids • Hydrogen Bonds • Ligand Field Concept • Mössbauer Spectroscopy • Nuclear Magnetic Resonance (NMR) • Organic Chemistry, Synthesis • Periodic Table (Chemistry) • Pollution, Environmental

BIBLIOGRAPHY

Cotton, F. A., Wilkinson, G., Murillo, C. A., and Bochmann, M. (1999). “Advanced Inorganic Chemistry,” 6th ed., Wiley, New York.

Cox, P. A. (1989). “The Elements: Their Origin, Abundance, and Distribution,” Oxford University Press, England.

Das, K. V. (1997). “Main Group Elements and Their Compounds,” Springer-Verlag, New York.

Davenport, J. W., and Wylie, D. M. (1996). “New Refrigerants for Air Conditioning and Refrigeration Systems,” Prentice Hall, Englewood Cliffs, NJ.

Emsley, J. (1998). “The Elements,” 3rd ed., Oxford University Press, New York.

Fabian, P., and Singh, O. N., eds. (1999). “Reactive halogen compounds in the atmosphere,” *In* “Handbook of Environmental Chemistry,” Vol. 4, part E., Springer-Verlag, New York.

Greenwood, N. N., and Earnshaw, A. (1997). “Chemistry of the Elements,” 2nd ed., Butterworth-Heinemann, Oxford, U.K.

Hagen, A., ed. (1991). “Inorganic Reactions and Methods: The Formation of Bonds to Halogens (Part 2),” Vol. 4, VCH Publishers, New York.

“Kirk-Othmer Encyclopedia of Chemical Technology,” 4th ed., Vols. 2 (1992), 5 (1993), 6 (1993), 11 (1994), and 14 (1995), Wiley, New York.

March, J. (1992). “Advanced Organic Chemistry: Reactions, Mechanisms, and Structure,” 4th ed., Wiley, New York.

Olah, G. A., Prakash, G. K. S., and Chambers, R. D., eds. (1992). “Synthetic Fluorine Chemistry,” Wiley, New York.

Perry, D. L., and Phillips, S. L., eds. (1995). “Handbook of Inorganic Compounds,” CRC Press, Boca Raton, FL.

Rappoport, Z., Hudlicky, M., and Zupan, M. (1989). “The Formation of Carbon Halogen Bonds,” Wiley, New York.

“Ullmann’s Encyclopedia of Industrial Inorganic Chemicals and Products” (1998). Vol. 6, Wiley, New York.

Inclusion (Clathrate) Compounds

Jerry L. Atwood
University of Alabama

I. Historical Perspectives
II. Inorganic Hosts
III. Organic Hosts
IV. Biochemical Relationships

GLOSSARY

Calixarene Cyclic oligomer made by the base-catalyzed condensation of a phenol and formaldehyde.

Clathrate Inclusion compound in which the guest is completely surrounded by the host.

Crown ether Macrocyclic polyether so called because of its appearance in molecular models.

Cyclodextrin One of a family of cyclic oligosaccharides produced by the enzymatic degradation of starch.

Guest Molecule or ion that is held within a molecule (or ion) or within a host lattice without the formation of a covalent bond.

Host Molecule, ion, or lattice capable of entrapping other molecules or ions (guests).

Inclusion compound Arrangement of two substances that are intimately linked, but not with covalent bonds.

Intercalation Reaction of a guest molecule (or ion) with a layered host lattice.

Zeolites Extensive group of porous tectosilicates.

INCLUSION COMPOUNDS are those formed between two substances that are intimately linked, but not with covalent bonds. One substance is designated as the host and the other as the guest. The original designation, clathrates, was used to describe the situation in which the guest was completely encapsulated by the host. The field has expanded vastly since the initial elucidation of the clathrate structures in the late 1940s.

I. HISTORICAL PERSPECTIVES

The concept of inclusion is as old as humankind. The hand is capable of a variable assortment of inclusions, and many analogies are appropriate. The first verified examples of inclusion compounds date from the early 1800s. It is instructive to list the dates of record for the preparation of inclusion compounds of various types: the chlorine clathrate hydrate by Faraday in 1823, graphite intercalates in 1841, the β-quinol H_2S clathrate in 1849,

cyclodextrin inclusion compounds in 1891, Hofmann's clathrate in 1897, tri-*o*-thymotide aromatic inclusion compounds in 1909, Dianin's compound in 1914, choleic acid inclusion compounds in 1916, phenol clathrates in 1935, urea inclusion compounds in 1940, and amylose inclusion compounds in 1946. These early studies were hard to understand since the compounds were often non-stoichiometric. A firm knowledge of any of the systems had to await developments in X-ray structure determination. All events came to a junction when H. M. Powell carried out his pioneering studies of β-quinol clathrates in 1947. We also owe to Powell the designation of the term clathrate.

Not all of the host–guest systems listed above fit under the meaning of the term clathrate, and we now use the designation inclusion compound to encompass solution behavior as well as many different types of solid-state phenomena. The area has grown rapidly since 1970 and is now recognized as an important interdisciplinary subject. In 1983, a periodical, the *Journal of Inclusion Phenomena*, was launched to collect work in the inclusion area. The maturity of this field is measured in part by the award of the Nobel Prize for Chemistry in 1987 to D. J. Cram, J.-M. Lehn, and C. J. Pedersen.

II. INORGANIC HOSTS

A. Werner Compounds

Werner compounds are named after the coordination chemist who made important contributions to inorganic chemistry at the turn of the century. Specifically, these hosts have the formula MX_2A_4, where M stands for practically any divalent transition metal cation; X represents an anionic ligand; and A is a neutral ligand, most commonly a substituted pyridine. The structure of one of the most studied, $Ni(NCS)_2$(4-methylpyridine)$_4$, is shown in Fig. 1. The molecular conformation is a propeller, in which the pyridine rings are twisted about 50° from a coplanar arrangement. In the solid state the molecules pack in layers. Guest molecules may pack between the layers in a space bounded by the NCS^- ligands. This is seen most clearly with reference to Fig. 2, which shows the naphthalene inclusion compound. There are rather large openings between the cavities occupied by the guests, and these are connected by two-dimensional windows. This is similar to the situation in zeolites discussed below.

Werner compounds have been used to effect separations between closely related molecules, for example, the

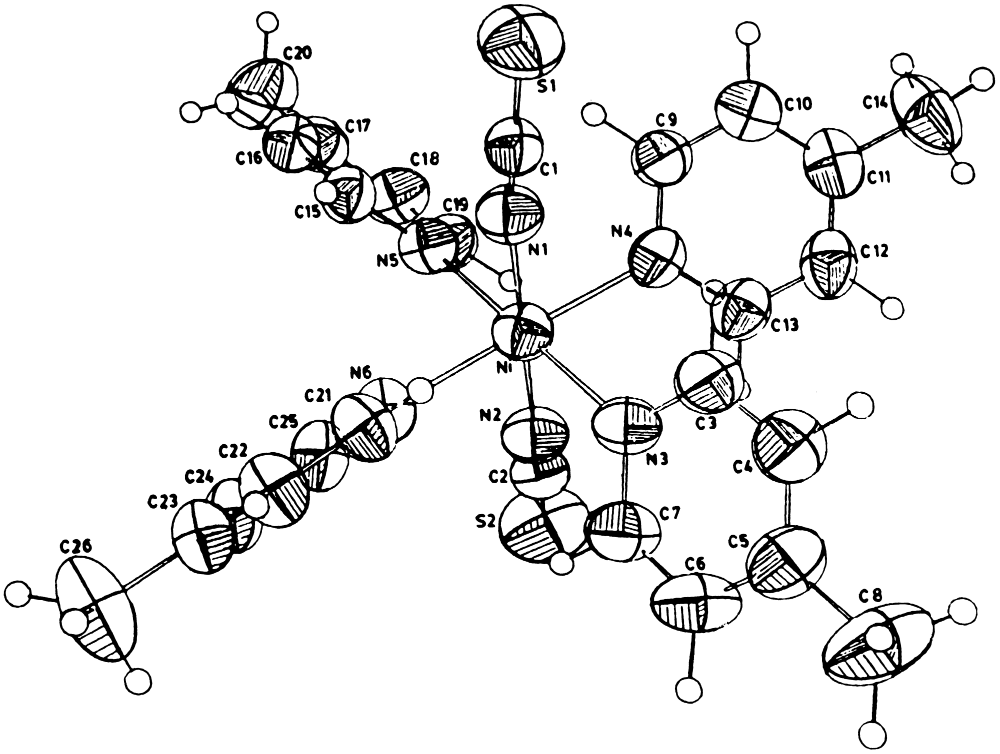

FIGURE 1 Structure of $Ni(NCS)_2(4\text{-}MePy)_4$. [From Atwood, J. L., Davies, J. E. D., and MacNicol, D. D., eds. (1984, 1985). "Inclusion Compounds," Vols. 1–3, Academic Press, Orlando.]

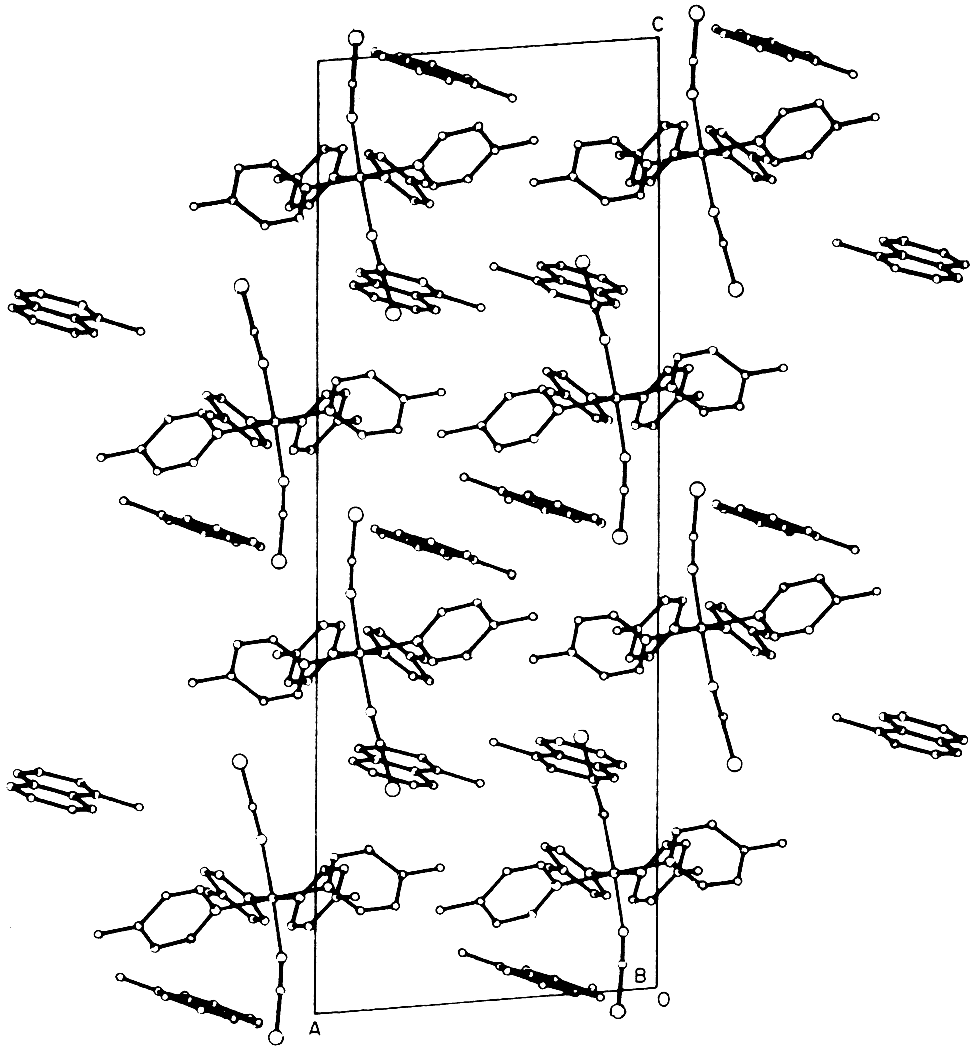

FIGURE 2 Packing of 1-methylnaphthalene in the lattice of $Ni(NCS)_2(4\text{-}MePy)_4$.

xylene isomers. In these situations it is important to consider both the shape of the cavities and the kinetics of the absorption and desorption processes.

B. Hofmann-Type Compounds

The compound as initially formulated by Hofmann was $Ni(CN)_2 \cdot NH_3 \cdot C_6H_6$. However, it is now recognized that the actual formulation is $Ni(NH_3)_2 \cdot Ni(CN)_4 \cdot 2C_6H_6$. There are two kinds of nickel atoms, one that exhibits square planar four-coordination [tetracyanonickelate(II)] and one that exhibits an octahedral array of nitrogen atoms around the nickel. The host has a layered structure, with the NH_3 units protruding into the layers. The cavities thus formed are illustrated in Fig. 3. The benzene is completely enclosed, and the compound is a true clathrate. Because of the limitation in space, only molecules smaller than substituted benzenes can be entrapped.

The original Hofmann clathrate may be modified in several ways to produce new inclusion compounds. First, the ammonia molecule may be changed for another amine, even a bi- or tridentate one. Second, the square planar

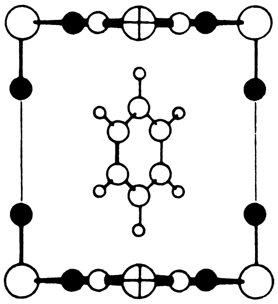

FIGURE 3 Hofmann's benzene clathrate, $Ni(NH_3)_2\ Ni(CN)_4 \cdot 2C_6H_6$.

nickel may be replaced by another square planar metal or by a tetrahedral one (for example, cadmium in $Cd(CN)_2$). Third, bulky substituents may be introduced into the amine.

C. Gas Clathrate Hydrates

These substances, first characterized by Faraday in 1823, are based on the ice structure. The gases are included in voids in the hydrogen-bonded network. There is a geometrical similarity between these materials and the zeolites in that both are based on three-dimensional four-connected nets. The guests range from dioxane down to argon. Also considered under this topic are the quaternary ammonium salt hydrates and the alkylamine hydrates. With a number of guests the gas clathrate hydrate structure is thermodynamically more stable than that of ice. Indeed, several have melting points in the range of 0°–15°C and one is reported to melt at 31.5°C.

The true gas clathrate hydrates, with few exceptions, crystallize in one of two structures, I and II. In general, the smaller guests belong to structure I and the larger ones to structure II, while those of intermediate size may belong to either under slightly different conditions. The ideal unit cell contents for a type I is $6X \cdot 2Y \cdot 46H_2O$ and for a type II, $8X \cdot 16Y \cdot 136H_2O$, where Y refers to the guests in a 12-hedra and X to those in 14-hedra or higher. The polyhedra can be understood with reference to Fig. 4. X and Y type spaces may both be filled by a small molecule. For example, the ideal stoichiometry is $8CH_4 \cdot 46H_2O$ for the gas clathrate hydrate of methane. It is also possible to form mixed hydrates in which a smaller guest is trapped in the smaller cavity and the larger in the more spacious void.

Structure I belongs to the cubic space group Pm3n and can be viewed as a close packing of 12- and 14-hedra sharing faces in the ratio of 1:3. Structure II falls in the cubic Fd3m group and is viewed as 12- and 16-hedra sharing faces in the ratio of 2:1. A hexagonal hydrate structure (type H) requiring both large and small guests to stabilize the lattice has been found to be isostructural with dodecasil-1H. Lower symmetry structure types III–VII have been observed for the ammonium salt hydrates and alkylamine hydrates. Description of these structures is beyond our scope, but it is instructive to note the differences between the ammonium or amine structures and those of the gases. In the case of simple salts that contain anions such as F^-, the latter is not surprisingly found involved with the hydrogenbond framework. For anions such as benzoate, the oxygen atoms are a part of the framwork, while the phenyl group is located in a void. The cations are entrapped, but much larger voids are required when an ion as large as $[N(i\text{-}C_5H_{11})_4]^+$ is utilized. Alkylamine hydrates are hydrogen bonded to the framework and penetrate the cavities as well. Figure 5 illustrates this situation.

Gas clathrates are of considerable importance industrially, even though they have gained some infamy by being held responsible for plugging the Alaska natural gas pipeline. The methane clathrate has a melting point well above that of ice itself, so the substance can crystallize

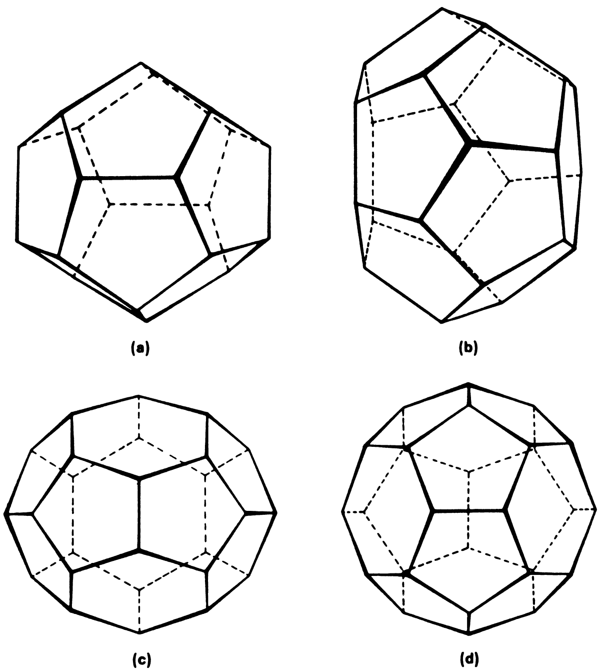

FIGURE 4 Clathrate hydrate voids: (a) 12-hedra, (b) 14-hedra, (c) 15-hedra, and (d) 16-hedra.

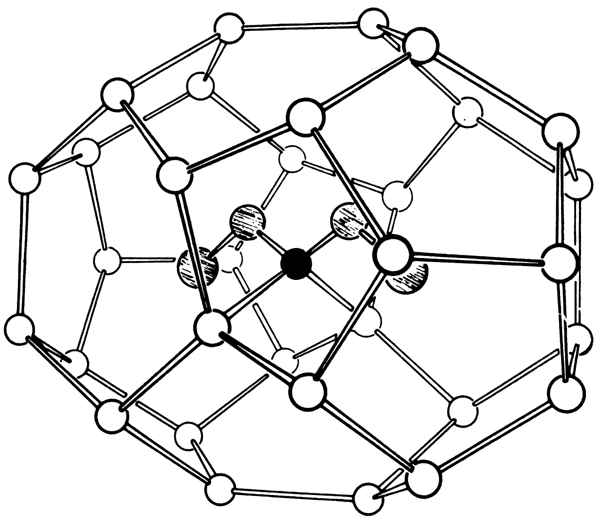

FIGURE 5 Structure of the diethylamine hydrate $12(CH_3CH_2)_2NH \cdot 104H_2O$. The nitrogen atom is the dark sphere; the carbon atoms of the ethyl groups are shaded spheres.

at temperatures above the freezing point of water. This very property has also caused speculation about the use of the substances as heat-storage media. It is possible to allow an underground reservoir to freeze in Minnesota and then use the ice as a source of air conditioning during the summer. The gas clathrates have nearly the same heat of fusion as ice, and a reservoir of a high-melting one could conceivably be used in a like manner in Georgia.

D. Zeolites

Zeolites are porous tectosilicates of typical formulas such as $Li_2[Al_2Si_4O_{12}] \cdot 2H_2O$ (bikitaite), $Ca_4[Al_8Si_{28}O_{72}] \cdot 24H_2O$ (heulandite), or $(Na_2,Ca,Mg)_{29}[Al_{58}Si_{134}O_{384}] \cdot 240H_2O$. Approximately 60 naturally occurring framework topologies exist, and many new ones have been synthesized. Each of the topologies gives rise to a unique system of cavities and channels that characterize its structure. The exchangeable cations (Li in bikitaite) may share cavities or channels along with guest molecules or ions. However, there are many more positions for guests than the exchangeable ions can inhabit. Framework structures are shown in Figs. 6 and 7. The networks are rigid, but access to cavities may be controlled by the type of guests present. For example, a zeolite with rather vast cavities may be rendered useless for adsorption purposes by the presence of smaller ions that specifically block channels giving access to the large cavities.

The internal channel systems may be classified as one-, two-, or three-dimensional. When the channels are too small to permit diffusion of the guest between them, then only one-dimensional diffusion is possible. An example of channel patterns is given in Fig. 8. The window concept is of importance in understanding molecular diffusion. The most important windows are of 8, 10, and 12 rings. The openings are themselves constrained by the supporting framework. The 8-ring structures may be nearly planar (in which case the opening is about 4.2 Å) or substantially elongated. A schematic representation is shown in Fig. 9. As an example of practical importance, consider the sorption of organic molecules by ZSM-5. The 10-ring openings, as shown in Fig. 9, allow entrance to *n*-parafins and simple aromatics. However, the opening is so narrow that benzene or *p*-xylene (critical dimension ~6.3 Å) may be differentiated by the rate of sorption from *o*-xylene, 1,2,4-trimethylbenzene, or naphthalene (~6.9 Å) and will exclude pentamethylbenzene or 1,3,5-trimethylbenzene (~7.8 Å).

Zeolites have found uses in many areas: adsorptive separation of hydrocarbons, purification of gases and liquids,

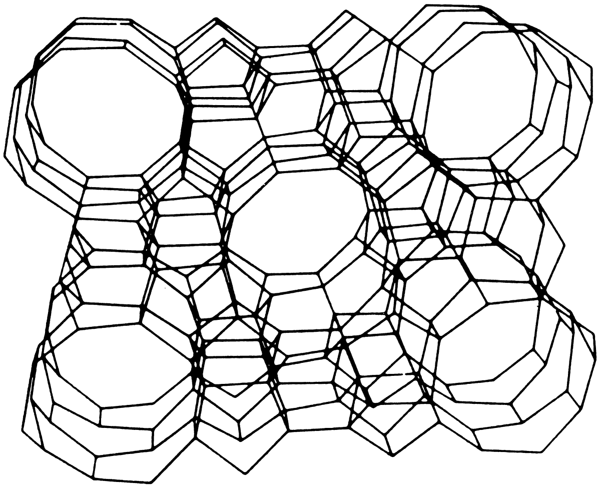

FIGURE 7 Structure of zeolite ZSM-5.

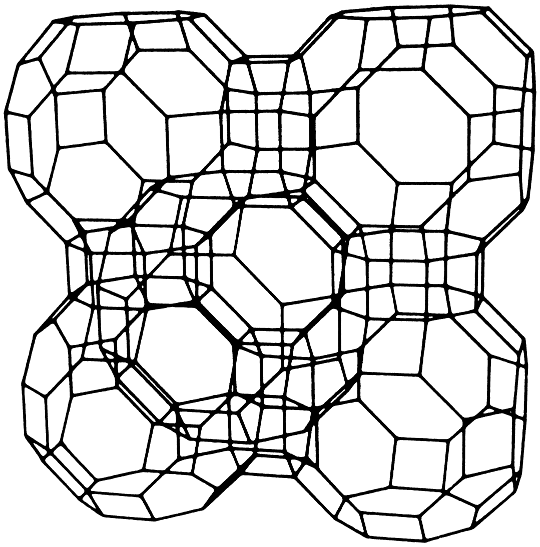

FIGURE 6 Framework structure of zeolite RHO.

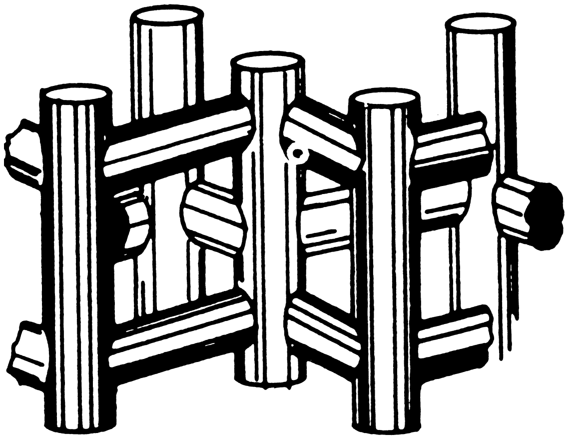

FIGURE 8 Channel structure of ZSM-5.

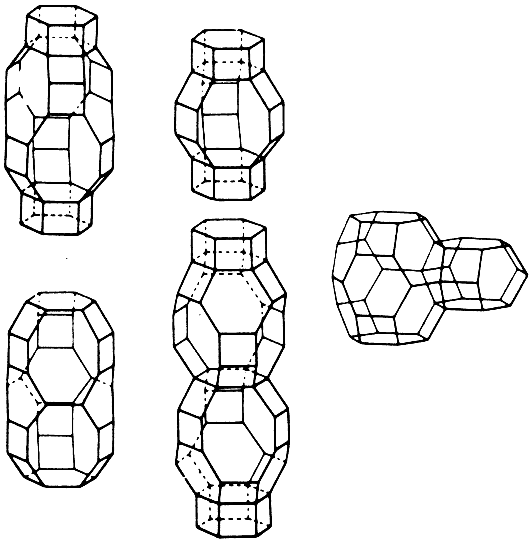

FIGURE 9 Openings between cavities in zeolites.

catalytic cracking of hydrocarbons, and ion exchange, to name the largest applications. Further developments in shape selective catalysis, molecular electronic devices, and sensors are anticipated.

E. Intercalates

Intercalation compounds are produced by the insertion of an atomic or molecular species into a host lattice. Many

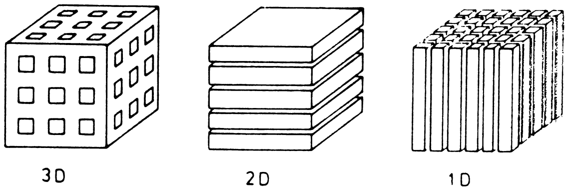

FIGURE 11 Host dimensionality.

common solid materials possess this property: graphite (structure shown in Fig. 10), MoO_3, H_xMoO_3 (a hydrogen bronze), V_2O_5, $Zr(HPO_4)_2$, FeOCl, and many clays to mention but a few. The reactions that lead to the intercalated substances are classified as reversible, topotactic solid-state reactions. These are therefore processes in which the solid matrix is essentially unchanged with regard to structure and composition. The reaction may conveniently be divided into two types: (1) intercalation of mobile guest species into an empty host lattice that provides adequate free volume and appropriate geometry and (2) intercalation by exchange reactions with a host that already contains a guest. In these reactions temperature is a very important factor. If the temperature is too low, the solid lattice is too rigid, but if the temperature is too high, the lattice may disintegrate.

Structurally, there are three types of hosts, as shown in Fig. 11: three-dimensional, layered, and chain structures. The concept of staging is important, and it may be visualized with reference to Fig. 12.

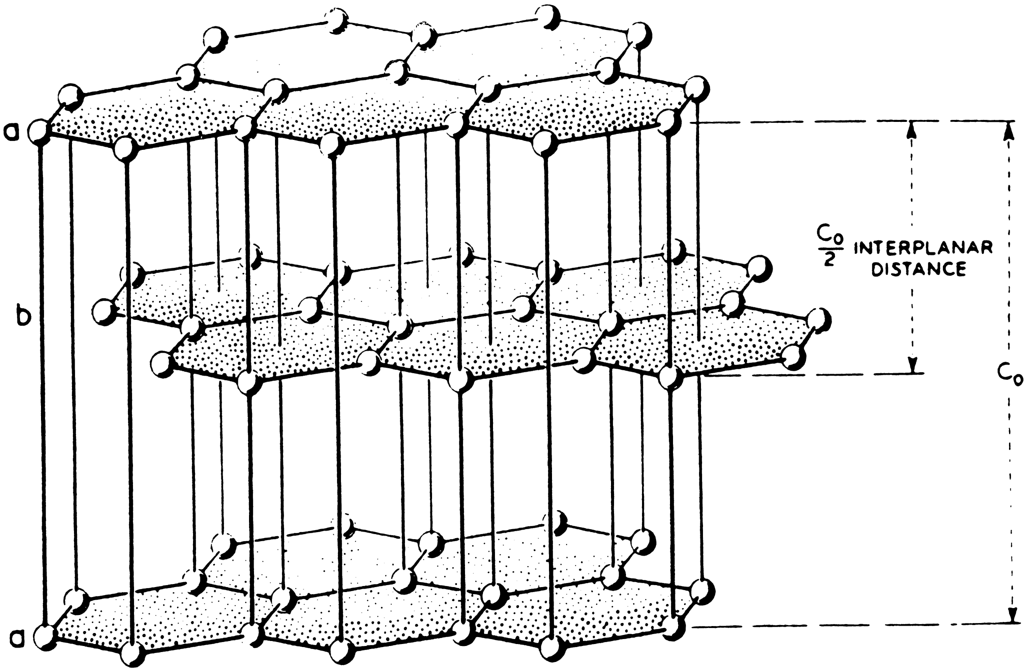

FIGURE 10 Layered structure of hexagonal graphite.

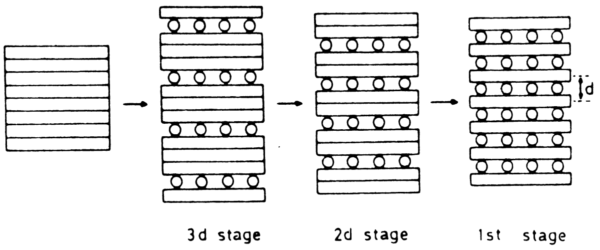

FIGURE 12 Staging in intercalation reactions of layered host lattices.

Applications of intercalates have been numerous. Sorption and ion exchange properties of zeolites and related substances are regarded under this heading. Catalysis of the heterogeneous type is emerging on the industrial level. Hosts with conductivity properties are seeing activity in energy storage. On the laboratory scale, new analytical techniques are being based on this type of phenomenon.

F. Cyclophosphazenes

This class of materials is composed of paddle wheel-shaped molecules, and the way in which the molecules pack in the solid state is illustrated in Fig. 13. The combination of layer types 1 and 2 gives the tunnel, as depicted in Fig. 14. The view leads one to expect that long-chain aliphatics should be preferentially entrapped. This is most dramatically realized by exposing crystals to a mixture of *n*-heptane and cyclohexane. The long-chain aliphatic is adsorbed to the total exclusion of the cyclic one. It is also worthwhile to note that the adsorption process is quite rapid, even though large crystals are used.

Molecular motion in the channels has been studied in detail and has been related to solid-state polymerization results (inclusion polymerization). It was found that *p*-bromostyrene can be polymerized, but styrene cannot be. The explanation was found in the orientation of the molecules in the tunnels.

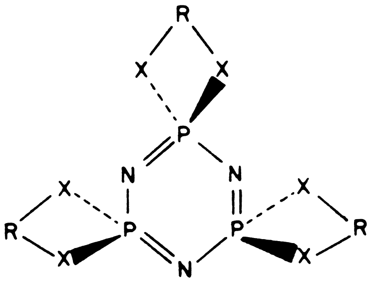

FIGURE 13 Paddle-wheel-shaped molecule of the host cyclophosphazene.

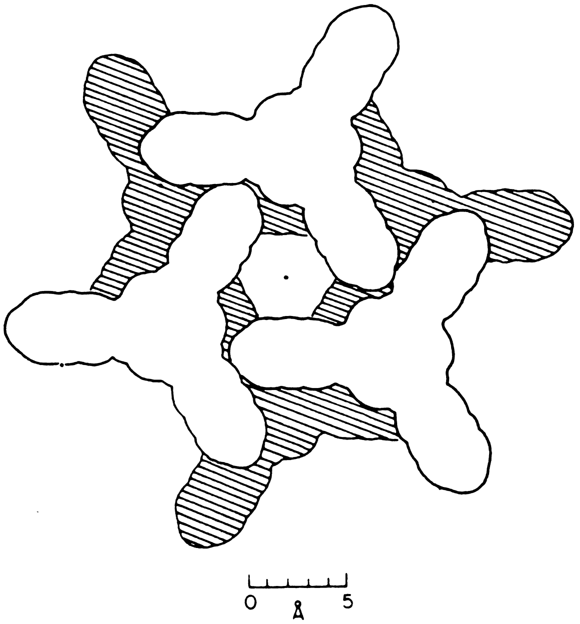

FIGURE 14 View of the tunnel that results from the packing of layer type 1 and layer type 2 upon each other.

G. Liquid Clathrates

The term *liquid clathrate* presents a paradox. Clathrates are by definition solid substances, but it is possible to apply the same basic concepts to liquids as well. A liquid clathrate is a member of a group of liquid inclusion compounds that form upon the interaction of aromatic molecules (guests) with certain species related geometrically to salts such as $[NMe_4][Al_2(CH_3)_6I]$. The substance thus formed contains a certain maximum number of guest molecules and is immiscible with excess aromatic. The hydrocarbon molecules in the liquid clathrate are trapped as they would be in a solid clathrate and can be freed by a change in temperature and reclaimed unaltered.

A model for liquid clathrate behavior is presented in Fig. 15. It is believed that the ions interact in a cooperative manner. One cation may be associated with two or more anions and vice versa. The cation–anion interaction must be strong, or the ions will separate and a normal solution will result. The aromatic molecules are necessary constituents of the layerlike structure. They are guests, but

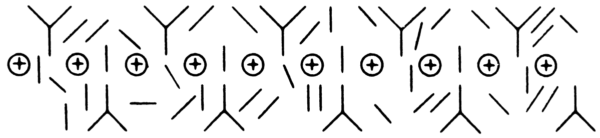

FIGURE 15 Two-dimensional model of liquid clathrate behavior.

they are also in effect components of the host. The analogy to certain solid-state inclusion compounds of the Werner type is to be noted.

Of the several interesting applications of liquid clathrates is in the area of separations. Since the behavior is found for aromatic molecules but not for aliphatic ones, a separation is possible. It is possible to envision even difficult problems such as the separation of the xylene isomers being attacked by liquid clathrates. Liquid clathrates have also been reported to be useful as solvents for the liquefaction of coal.

III. ORGANIC HOSTS

A. Crown Ethers and Cryptates

Crown ethers are cyclic polyethers, and typical examples are shown in Fig. 16. They were first recognized as a new class of macrocyclic compounds in 1967, but thousands of articles on aspects of the subject have been published since then. Crown ethers form the simplest models for the structured complexation that is central to the function of enzymes. They are also useful as models for ion transport. Indeed, the hole in the crown ether can be tailored so as to fit any simple cation: K^+ is best accommodated by 18-crown-6, while Na^+ fits into 15-crown-5. Recently, substantial effort has been expended in the study of the complexation of neutral molecules and anions by crown ethers.

Crown ethers are essentially two-dimensional complexing agents. Macrobicycles, first reported by Lehn in 1968, represent an important move to three-dimensionality. Simple examples of these so-called cryptates are shown in Fig. 17. Three-dimensionality has also been imparted to crown ethers by the addition of one or more side chains onto the crown (lariat ethers). The construction of hosts with specific complexing ability has proved to be an interesting area of synthetic organic chemistry. Since the number of naturally occurring organic hosts is limited, important advances in medicinal chemistry can be expected in this area.

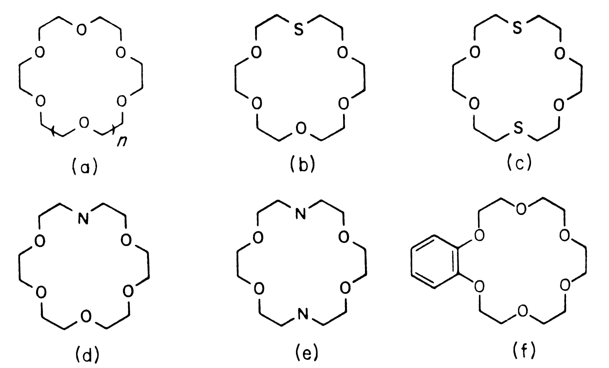

FIGURE 16 Crown ethers. (a) $n=0$, 15-crown-5; $n=1$, 18-crown-6; $n=2$, 21-crown-7. (b) Thia-18-crown-6. (c) 1,10-Dithia-18-crown-6. (d) Aza-18-crown-6. (e) 1,10-Diaza-18-crown-6. (f) Benzo-18-crown-6.

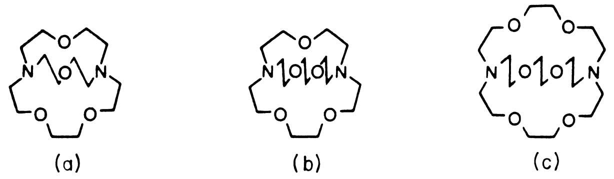

FIGURE 17 Cryptates. (a) Cryptand [2.1.1], (b) cryptand [2.2.1], and (c) cryptand [2.2.2].

B. Cyclodextrins

Cyclodextrins are cyclic oligosaccharides formed by the enzymatic degradation of starch. In the process, one portion of the starch helix is hydrolyzed off, and the ends are joined together. The most common results are molecules made up of six, seven, or eight glucose units; α-, β-, or γ-cyclodextrins, respectively. A schematic view of these structures is shown in Fig. 18.

Since the glucose unit is a rigid one, the cyclodextrins possess cavities even as isolated molecules in the absence of guests. All cyclodextrins have a height of about 8.0 Å and an outer diameter of 15–18 Å. The diameter of the cavity is 4.7–5.2 Å for α-, 6.0–6.4 Å for β-, and 7.5–8.3 Å for γ-cyclodextrin. These values are comparable to molecular dimensions for many simple organic molecules. Figure 19 shows a model view of the complex of p-iodoaniline with α-cyclodextrin.

It is significant to note that the cyclodextrins have good water solubilities. They are finding extensive use in the pharmaceutical industries of some countries as vehicles either to solubilize drugs or to protect them as they pass through the digestive system. Other applications in such diverse areas as that of food additives and in pesticide formulations have been realized.

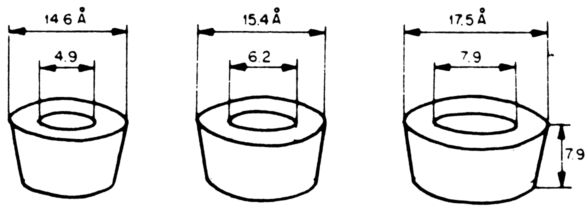

FIGURE 18 Representations of the structures of α-, β-, and γ-cyclodextrins. (The α-cyclodextrin is the smallest.)

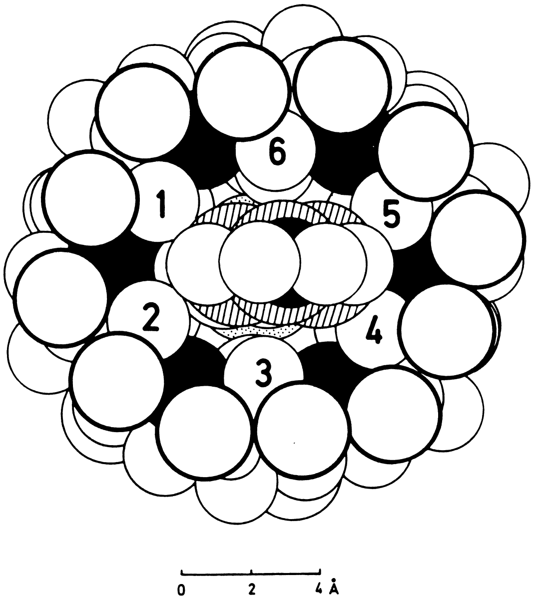

FIGURE 19 Structure of the complex of α-cyclodextrin and *p*-iodoaniline. Space-filling models have been used.

C. Urea and Thiourea

In 1940 the simple organic molecule urea, $(NH_2)_2C{=}O$, was discovered to form adducts. These differ from the previous two examples in this section in that the host–guest interaction occurs only in the solid state. Urea crystallizes in the presence of long-chain hydrocarbons, as illustrated in Fig. 20. Thiourea behaves in the same fashion with only minor modifications.

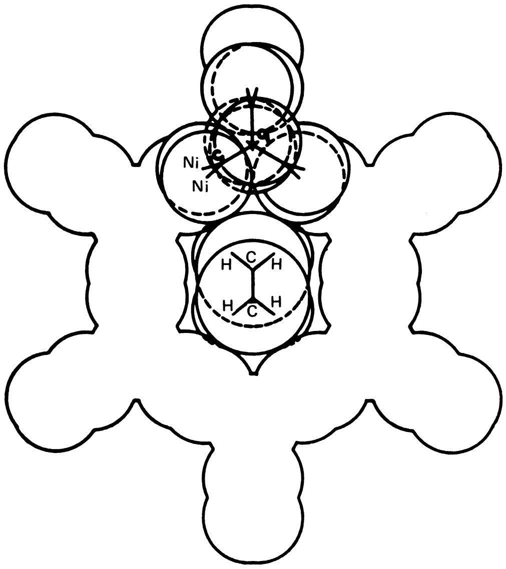

FIGURE 20 The inclusion compound formed by urea (the host) and a normal hydrocarbon (the guest).

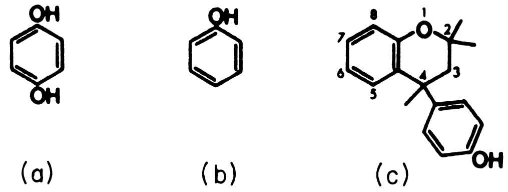

FIGURE 21 Formula representations of (a) hydroquinone, (b) phenol, and (c) Dianin's compound.

Since urea is a common, abundant substance, it is of interest to exploit its inherent selectivity toward hydrocarbons. Attempts have been made to use it to separate benzene and cyclohexane from *n*-heptane, but commercial reality has not been achieved.

D. Hydroquinone, Phenol, and Dianin's Compound

These molecules, represented schematically in Fig. 21, exhibit host lattices based on the use of hydrogen bonding to build a hexameric unit. In the case of Dianin's compound, the hexamer consists of three molecules of one configuration, R, pointing upward, and three of the other configuration, R′, pointing downward. When these units pack in the solid state, the result is the formation of a cavity, as shown in Fig. 22.

The extension of the naturally occurring hexameric units to synthetic analogs is significant. The hexa hosts, shown in Fig. 23, have the same overall geometry as the phenolic hosts, but the hydrogen bonding in the latter has been replaced with full covalent bonds in the former. The result is particularly important since it shows that molecules can be constructed or engineered to have a specific shape.

There are several uses for these hosts in the area of separations, but none are industrially important as yet. It is

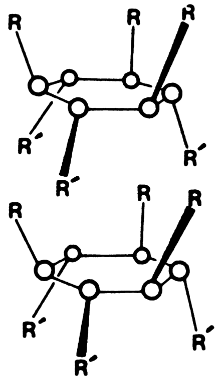

FIGURE 22 Schematic view of the packing of two hexameric units to form a cavity. The O—O represents a hydrogen bond.

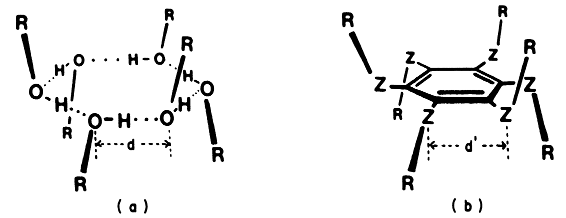

FIGURE 23 Analogy of the hydrogen-bonded hexameric unit (a) to the hexahost (b). Z denotes a general atom: S, for example.

instructive to note that the inclusion compound of SF_6 and Dianin's compound has been used as a method of storage of SF_6. This aspect of inclusion may prove to be important for a wide variety of reactive or unstable molecules.

E. Calixarenes

Calixarenes, shown schematically in Fig. 24, are prepared by the condensation of *p*-tert-butylphenol with paraformaldehyde. In the cone conformation, calix[4]arene has the shape of a chalice or vase. Figure 25 exhibits this geometry, and the inclusion of a toluene molecule is apparent. Closer observation of Fig. 25 shows that an Na^+ ion is also held in the base of the chalice. Thus, this calixarene can include both neutral molecules and ions at the same time. The similarity to the cyclodextrins is clear, but the calixarenes are not as rigid.

F. Other Organic Hosts

The synthesis of new types of inclusion hosts is an active area of organic research. The number and diversity of such materials makes even a summary treatment beyond the scope of this presentation. This section contains representative examples only.

Deoxycholic acid, $C_{24}H_{40}O_4$, has an arched shape (Fig. 26) and forms inclusion compounds of the channel type with a wide variety of organic molecules.

Perhydrotriphenylene, $C_{18}H_{30}$, has the schematic structure shown in Fig. 27 and forms inclusion compounds with

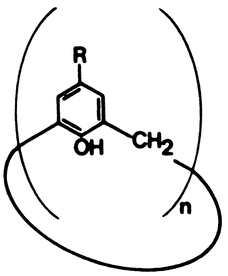

FIGURE 24 Schematic view of the structure of a calix[*n*]arene. The most common values of *n* are 4, 6, and 8.

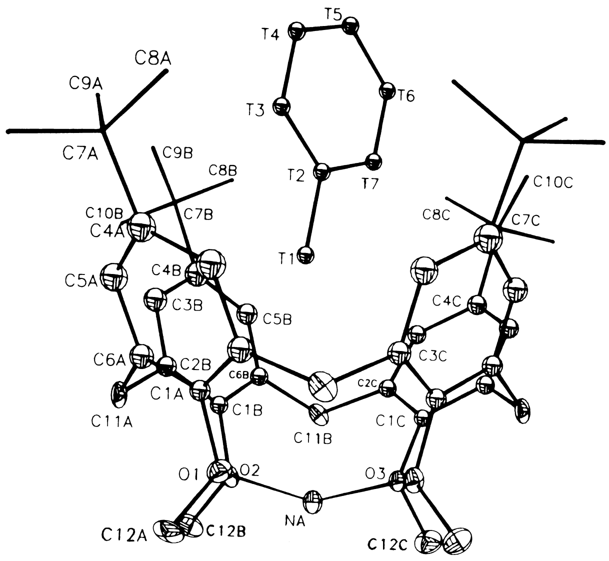

FIGURE 25 The methyl ether of calix[4]arene with included toluene (T) and sodium ion.

linear and branched chain hydrocarbons and with macromolecular compounds such as polyethylene.

Cyclotriveratrylene, $(C_9H_{10}O_2)_3$, has the shape of a saucer (Fig. 28a). The molecule can be used as a base upon which to chemically construct the so-called octopus molecules (Fig. 28b). These molecules can be used to include molecules in solution as well as in the solid state.

Tri-*o*-thymotide (Fig. 29a) exists in a propellerlike configuration and has features in common with the trianthranilides (Fig. 29b).

IV. BIOCHEMICAL RELATIONSHIPS

A. Enzyme Models

The chemist seeks enzyme mimics or models so as to bridge the gap between chemical reactions in the laboratory and those of the life processes. Since the way in which most biological transformations occur is obscure, model

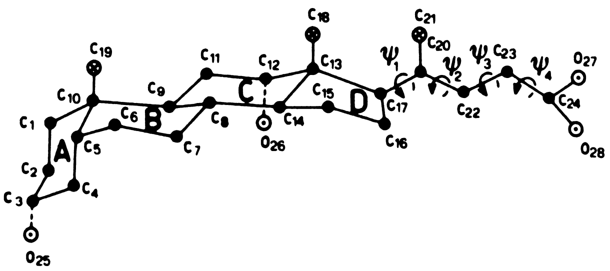

FIGURE 26 Structure of deoxycholic acid: ● represents C; ⊙, O; and ⊗, CH_3.

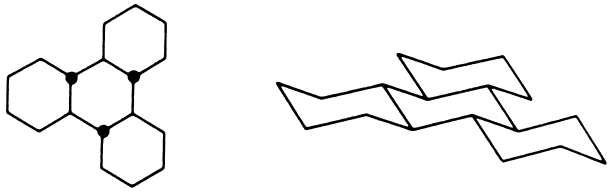

FIGURE 27 Two representations of the structure of perhydrotriphenylene.

reactions can provide insight. Reactions out of the realm of true biochemistry have two features in common: They are catalyzed very effectively, so that they occur rapidly even under mild conditions, and they are very selective. A true enzyme mimic must exhibit both of these features.

The most studied class of enzyme mimics is the cyclodextrins. The rigid hydrophobic cavity is rimmed with hydroxyl groups that may be further functionalized.

As an example of a well-studied biomimetic process, consider the chlorination of anisole:

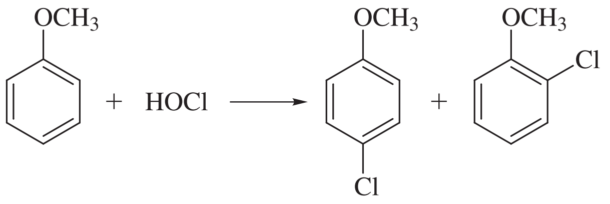

In aqueous solution both the *ortho* and the *para* isomers are produced (in ratio of about 40:60, respectively). Addition of α-cyclodextrin changes the ratio of 4:96. The *ortho* position is clearly shielded from attack, as is shown

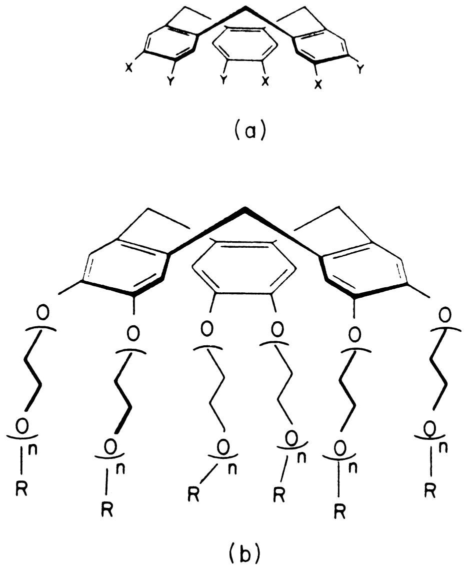

FIGURE 28 (a) Saucerlike structure of cyclotriveratrylene and (b) related octopus molecule.

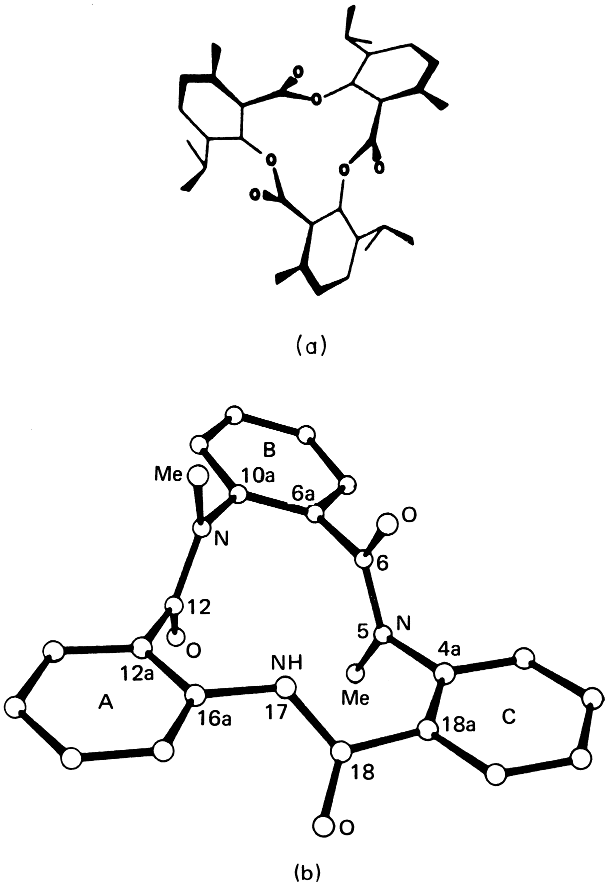

FIGURE 29 (a) Propellerlike structure of tri-*o*-thymotide and (b) related structure of *N*, *N*′-dimethyltrianthranilide.

in Fig. 30. The cyclodextrin also has the effect of substantially speeding up the chlorination of anisole. This catalysis is due to the existence of a new pathway for the reaction, which is also shown in Fig. 30.

The construction of synthetic iron(II) dioxygen carriers as a model for myoglobin has long been sought. Advances based on transition metal complexes of cyclidenes have now provided the result. Cyclidenes, given in Fig. 31, are composed of two fused rings, one which is useful for metal coordination and the other for molecular design purposes. A model which serves to illustrate the biological discrimination of O_2 over CO is displayed in Fig. 32.

The synthesis of molecules with shapes and functional group orientation (Fig. 33) appropriate for catalytic functions has been achieved by the use of the Kemp triacid as a structural unit to effect U-turns. This strategy has led to hosts capable of the recognition of numerous substrates such as is shown for chiral alcohols in Fig. 34.

Many other classes of enzyme mimics are under investigation, but the general principles are covered in the examples above. One of the first benefits expected from

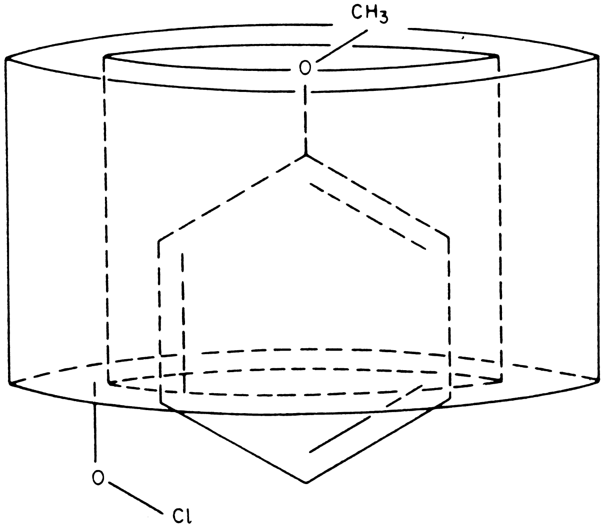

FIGURE 30 Schematic view of the structure of the complex of anisole with cyclodextrin.

studies of this type is a new way to catalyze known chemical reactions.

B. Cation Transport

A necessary feature of the life process is the solubilization of cations in low dielectric constant media. The way in which both electrolytes and nonelectrolytes cross membranes has received much study. A useful model of cation transport is the motion of ions affixed to macrocycles. Crown ethers and cryptates have been studied the most. One of the features of biological transport is selectivity. The simple crown ethers are particularly suited for experiments on selectivity, since the hole or cavity is of rather specific size. Thus, 15-crown-5 is better matched to Na^+ than to K^+, while the reverse is true for 18-crown-6.

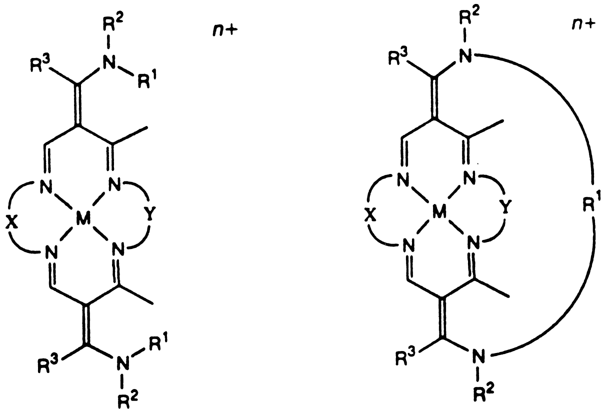

FIGURE 31 General cyclidene structure. [From Atwood, J. L., Davies, J. E. D., and MacNicol, D. D., eds. (1991). "Inclusion Compounds," Vol. 5, Oxford Univ. Press, Oxford, UK.]

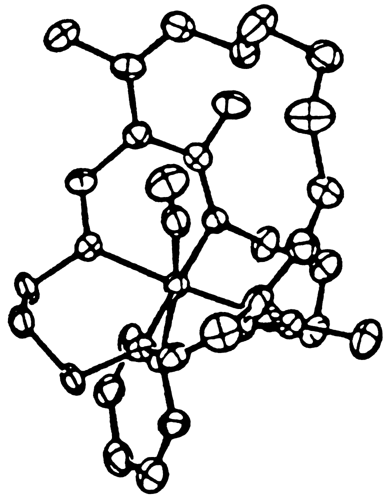

FIGURE 32 Cyclidene complex of iron(II) with bonded carbon monoxide.

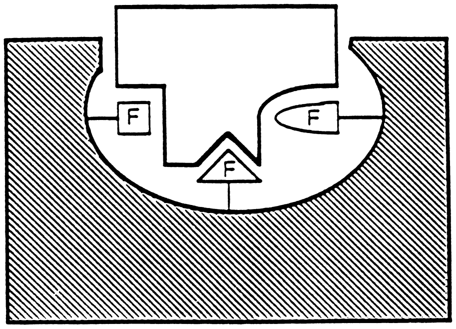

FIGURE 33 Schematic view of U-shaped host. [From Atwood, J. L., Ed. (1990). "Inclusion and Molecular Recognition," Plenum Press, New York.]

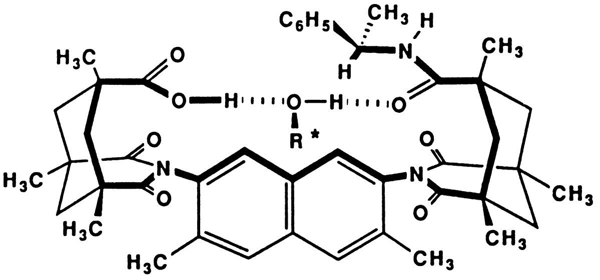

FIGURE 34 Rigid, U-shaped molecule capable of binding chiral alcohols.

SEE ALSO THE FOLLOWING ARTICLES

CATALYSIS, INDUSTRIAL • ENZYME MECHANISMS • HYDROGEN BOND • MICROPOROUS MATERIALS: ZEOLITES,

CLAYS, AND ALUMINOPHOSPHATES • ORGANIC MACROCYCLES • SOLID-STATE CHEMISTRY

BIBLIOGRAPHY

Atwood, J. L., Ed. (1990). "Inclusion Phenomena and Molecular Recognition," Plenum Press, New York.

Atwood, J. L., Davies, J. E. D., and MacNicol, D. D., Eds. (1984, 1985). "Inclusion Compounds," Vols. 1–3, Academic, New York.

Atwood, J. L., Davies, J. E. D., and MacNicol, D. D., Eds. (1991). "Inclusion Compounds," Vols. 4–5, Oxford Univ. Press, Oxford, UK.

CIBA Foundation Symposium (1991). "Host–Guest Molecular Interactions: From Chemistry to Biology—Symposium No. 158," Wiley, New York.

Inoue, Y., and Gokel, G. W. (1990). "Cation Binding by Macrocycles: Complexation of Cationic Species by Crown Ethers," Marcel Dekker, New York.

Mintova, S., Olson, N. H., Valtchev, V., and Bein, T. (1999). *Science*, **283**(5404), 958–960.

Occelli, M. L., and Kessler, H. (1996). "Synthesis of Porous Materials: Zeolites, Clays, and Nanostructures," Marcel Dekker, New York.

Sloan, E. D., Jr. (1998). "Clathrate Hydrates of Natural Gases," 2nd ed., Marcel Dekker, New York.

Steed, J. W., Johnson, C. P., Barnes, C. L., Juneja, R. K., Atwood, J. L., Reilly, S., Hollis, R. L., Smith, P. H., and Clark, D. L. (1995). "Supramolecular chemistry of *p*-sulphonatocalix [5] arene: A water-soluble, bowl-shaped host with a large molecular cavity," J. Am. Chem. Soc. **117,** 11426.

Inorganic Exotic Molecules

Joel F. Liebman
University of Maryland, Baltimore County

Kay Severin
Thomas M. Klapötke
Ludwig Maximilians University of Münich

I. Atoms and the Nature of Matter
II. Hydrogen and the Alkali Metals
III. Cations and/or Anions: Plemeioelectronic and Hermaphroditic Species
IV. Three-Atom 16-Valence-Electron XYZ Species: Isoelectronic Analogues
V. Ethylene and Beyond: Analogues, Cages, and Cleavage
VI. Reversing the Squashing: Boron Hydrides
VII. Polyphosphorus and Polynitrogen Species, Their Analogues and Derivatives
VIII. Noble Gases
IX. Transition Metal Complexes with Exotic Ligands and Geometries
X. Nano-Sized Molecules: Clusters, Fullerenes, and Self-Assembled Metal Complexes
XI. Conclusion

GLOSSARY

Alkalide Salt in which one of the alkali metals is the anion.

Connectivity The set of connections between atoms, where no distinction is made between single, multiple, or fractional bonds.

Fullerene Ball-shaped cluster or cage of interconnected trigonal or sp^2 carbon atoms. Derivatives include replacement of some carbons by hetero atoms, the presence of atoms inside the cluster/cage, and functionalization by reactions involving the formal double bonds connecting the carbons.

Harcourt structure Valence structures that involve more electrons in bonding than Lewis structures that are limited to electron-pair bonds and electron lone pairs (also "increased valence structure").

Heavy atom Any atom other than hydrogen.

HEDM (high-energy-density material) Species with highly exothermic decomposition pathways as well as high material density. As applied to fuels and explosives, respectively, more Btu's and bang to the barrel.

Hermaphroditic species Two species having the same composition and connectivity, but with opposite charges.

Homopolyatomic A group, ion, or molecule composed of only one type of atom.

Increased valence structure See Harcourt structure.

Isoelectronic species Two species having the same number of electrons and the same number and the same connectivity of heavy atoms.

Lewis structure A valence-bond structure that has (a) the maximum number of electron-pair bonds permitted by the rules of valence (e.g., the Lewis–Langmuir octet rule for first-row elements) and (b) places electron

pair bonds only between pairs of adjacent atoms (also "standard valence-bond structure").

Matrix isolation The study of the structure, reactivity, and spectroscopy of otherwise unisolable atomic, molecular, and ionic species under cryogenic conditions in extreme dilution in inert solvents.

Nano-sized molecule Molecule with a size between 1 and 100 nm^3.

Period Referring to position in the periodic table (also see "row"). In the current study, the second period elements include carbon and oxygen, and the third row elements include silicon and sulfur. *Note*: Period and row are not always synonymous in their numbering.

Plemeioelectronic species Two species having a different number of electrons and the same connectivity of heavy atoms.

Pseudohalogen A linear or planar univalent radical that, like the halogens, can form anions, salts, and covalent derivatives.

Row Referring to position in the periodic table (also see "period"). In the current study, the first row elements include carbon and oxygen, and the second row elements include silicon and sulfur. *Note*: In the literature these elements are often considered second and third row, respectively.

Self-assembly Controlled formation of larger structures by noncovalent interaction of two or more molecules.

Squashing The conceptual, theoretical process of adding the proton that was part of an X—H bond to the X nucleus, thereby decreasing the hydrogen count by one and increasing the nuclear charge of the heavy atom X by one.

Standard valence-bond structure See Lewis structure.

Transition metal complex Coordination compound containing the d- and f-block elements.

Valence isoelectronic species Two species having the same number of valence electrons and the same number and connectivity of heavy atoms.

VSEPR The valence shell electron pair repulsion model, originally introduced by Nyholm and Gillespie (with antecedents from Sidgwick and Powell), which assumes that molecular geometry associated with a central atom is determined by the number of groups (single bonds, double bonds, triple bonds, or lone pairs) surrounding that atom.

WE BEGIN by acknowledging the difficulty of defining the word "exotic." The words "beautiful," "weird," and "counterintuitive" come to mind, for which three aphorisms and a hitherto unpublished poem may help.

(i) From the Elizabethan philosopher and essayist Francis Bacon: "There is no exquisite beauty without something unusual in its proportions."[1]

(ii) From the early 20th century biophysicist J. S. B. Haldane (quoted in Sacks, 1995): "The universe is not only queerer than we might imagine, it is queerer than we can imagine."

(iii) From the contemporary superconductivity scientist . . . . . : "Things are counterintuitive only when you have intuition."

(iv) And poetry from one of the authors of this study:

Let us try to answer 'what is exotic?'
We don't respond that 'it is 'odd, ick'
Though it be real, somehow incomprehensible
Descriptions many, none quite sensible
The answer, Señor Panza, is quixotic
Indeed to answer, may be quixotic

This obviously suggests subjectivity in the choice of what is "exotic." As authors, we cannot profess unanimity in the species chosen, and, quite obviously, we cannot assume complete agreement with all readers. What is "exotic" also involves the Zeitgeist: depending on what else has been discovered or uncovered, a compound may be exotic for one generation and prosaic for the next, or even the other way around. A compound found in a minimal context may be a source of glory and beauty in a more expansive, complete story: a compound that participates in exotic phenomena is assumed to belong in this article as well. Some of the molecules we will discuss are long known, seemingly well understood, and thus commonplace and not exotic to some readers. Even for these species, we ask that the reader join us in our wandering and wondering. Dare we agree with T. S. Eliot (1943):

We shall not cease from exploration
And the end of all our exploring
Will be to arrive where we started
And know the place for the first time.

It is now incumbent on us to try to define the term "inorganic compound." As with most contemporary studies, we do not take this to mean the absence of carbon, as opposed to where carbon is not the dominant feature. To leave out species with carbon would force us to omit endohedral metallofullerenes, organometallics, and metal carbonyls. We also do not want to leave out simple species such as the binary carbon oxides CO and CO_2 as well as the hydrides C_2H_4 and C_2H_6,

[1] From the essay "On Beauty," quoted in Edgar Allan Poe's "Ligea" and inscribed over the Poe Gate at the U.S. Military Academy, West Point, NY.

which we will discuss for our own enunciated and idiosyncratic, internally and intellectually consistent, reasons. Having decided to include such species (and likewise some simple, classically well characterized and classic inorganic compounds), we conclude that "exotic" does not necessarily mean ephemeral, fragile, or even rare, and "inorganic" has long not meant the absence of carbon. Again, poetry more than chemistry from one of the article contributors is offered as an answer:

Molecules long-lived and transient,
From creative minds, fingers agile
Some molecules new, some ancient,
Like glass, fluid, frozen, fragile
Flowing like the tidal currents
Like the sands and like the sea
Lessened carbon occurrence
To students of chemistry

Finally, we turn to the relatively prosaic question of sources of information. We would have preferred to recommend only suitably advanced textbooks and articles in review journals and monographs. Somehow these sources appear more permanent than papers in the primary research journals, yet by definition secondary and tertiary sources of information are more dated. Wonders abound in all of them. We admit arbitrariness in our choices—no universal criterion for their inclusion other than the presence of exotic chemistry can be offered. There was too much, rather than too little, to choose among. After all, we were not allowed to write our own volume, "The Encyclopedia of Exotica." We close the introduction with two quotes that provided us a guideline. The first is from a psalm that provides implicit chastisement for whatever choice we made; the second is from the Mishnah, the legal core of the Talmud, which offers a source of reassurance for our efforts.

(i) "The stone that the builders rejected has become the chief cornerstone" (Psalm 118:22, Revised Standard Bible).
(ii) "It is not up to you to finish the work, yet you are not free to avoid it" Pirke Avot 2:16; Kravitz and Olitzky, 1993).

Now to the science.

I. ATOMS AND THE NATURE OF MATTER

Atoms and molecules are not part of conventional, daily human experience.

A. Energy and Length

We start our study with a brief interlude on units. We care about energy and length but the relevant size to us as chemists is not relevant to us as human beings. As chemists, we have two generally commonly used set of units, kcal mol^{-1} and kJ mol^{-1}. In this study we will use the latter, where by definition 1 kcal mol^{-1} equals 4.184 kJ mol^{-1}. In chemical discussions, the unit of length—atomic sizes, bond lengths (interatomic distances)—has typically been Å (angstroms), where, again by definition, 1 Å equals 10^{-8} cm or 10^{-10} m because that is the typical interatomic spacing. More recently, length is often written in picometers (pm; 1 Å equals 100 pm). Purely for personal reasons, we have rarely done so. Objects of scientific and technological interest have gotten smaller—"nanotechnology" has become a word for our era and a hope for the next. Molecular species have gotten bigger—the nanometer (nm; 10 Å equals 1 nm) is a convenient length scale and "nano" is a convenient, confluent prefix. In this text we will use both angstroms and nanometers length units, depending on the context.

B. A Review of Atoms—Hydrogen and Its Components

We start our study of exotic inorganic compounds with a brief review of atoms to emphasize the strangeness of ordinary chemical reality. We deal here with the simplest of chemically relevant species, and perhaps the most surprising phenomena. To chemists these species and associated phenomena may appear "normal" and so our discussion may appear either prosaic or philosophical. Accordingly, the reader may feel our text belongs, at best, in a freshman chemistry course or one in physics and/or philosophy. We shall simply tell our stories and hope the reader will continue on to read the following vignettes about the science of "bigger" species, those with more nuclei and electrons.

Consider atomic hydrogen and its components. In its most common isotopic form, it has one proton and one electron. The mass ratio of these two components is nearly 2000:1. Why are the two parts so different in mass? Protons are so massive that they, individually and therefore in assemblages, may be assumed to be stationary. From this the concept of molecular and geometric structure arises: bond lengths and angles require fixed positions. The mass of the electron is so low that we should consider electrons inherently delocalized. From this the concept of orbitals and electronic structure unavoidably arises: we should not talk about dots and lines that describe fixed electrons. At least as importantly, atoms, molecules, and all the chemical-based reality from legumes to lepidoptera

to lions to lakes that surround us do not collapse. Atoms have size. Molecules have size and shape. Despite this difference in heft, locality, and localizability of protons and electrons, their charge ratio is seemingly precisely $1{:}-1$. This allows for discrete elements: there is no element that interpolates oxygen and sulfur to allow us to understand better the plethora of species containing these two elements in the same group in the periodic table. It allows for neutral atoms and molecules as well as those with discrete, integer charges. There is no element that interpolates carbon and nitrogen to allow us to understand species with these elements.

All neutral atoms and molecules have singly positively charged counterparts from the loss of an electron, some (but, most assuredly, not all) form negatively charged counterparts by the gain of an electron, and some form multiply positive or negative counterparts. Atomic multiple positive ions, in isolation, are "stuck" that way. Atomic multiple negative ions, in isolation, are always unstable relative to loss of an electron. In isolation, multiply positive and multiply negative ions very often are unstable with regard to bond cleavage to minimize charge repulsion. This instability is not what we may recall from our "chemical childhood." Then again, the study of atomic and molecular matter in isolation is very often a study of "exotica," however common the species when in solution or as a pure liquid or solid. We will return to these ions later and simply ask now why any neutral atom or molecule that definitionally has an equal, and therefore balanced, number of protons and electrons would "want" to add another electron. Suffice it to say, we may view all chemical matter as exotic. We will not, clearly we cannot, discuss the almost 20 million known chemical species, or even the sizable minority that are called inorganic or even organometallic.

C. Helium

Consider helium. Atomic helium with its most stable nuclear and electronic arrangement of two protons, neutrons and electrons, offers few surprises, not even its phenomenal inertness because of the $1s^2$ electron configuration. Despite the exotica in Section VIII.B, helium normally occurs simply as the atom, as He, and not as the dimer, trimer, or any oligomer. Likewise, save in stellar interiors, helium fails to trimerize to form carbon, or four higher oligomers that may be recognized as oxygen, neon, magnesium, silicon, or sulfur: these processes are, in fact, highly exothermic This is perhaps no surprise—there is a high electrostatic (Coulomb, charge repulsion) barrier to these reactions—but had this not been so, chemistry as we know it would not exist. Certainly, we chemists would not exist nor would the condensed-matter, nuclear, and astro-physicists who study these and other exotic (both low- and high-temperature) phenomena involving helium.

D. Lithium

We close our discussion of atoms with lithium. Its three electrons do not result in even greater inertness. It does not have a $1s^3$ electron configuration, but rather $1s^22s^1$, and so more resembles atomic hydrogen than it does helium because of the half-filled, singly occupied valence level s orbital. We can thank, or alternatively blame, the Pauli exclusion principle for this, and will consider this principle, like the conservation of charge (and the conservation of mass and of atom types in a chemical reaction), absolutely inviolate. It is easy to forget how strange all of these rules are, even if, by always assuming their validity, we must turn to more complicated species to be labeled exotic in the discussion that follows. For example, we will see that lithium and hydrogen chemistry are very distinct, perhaps starting with the simple observation that elemental lithium is normally found as a solid metal and elemental hydrogen is a diatomic gas.

II. HYDROGEN AND THE ALKALI METALS

A. Univalent Cations, Acids, and Bases

The normal oxidation state for hydrogen and the alkali metals is +1, and indeed their unipositive cations have long been known to the chemical community. It is not by accident that these elements are called group 1 or group 1A. The alkali metal cations abound in solid (and molten) salts and in solution. By contrast, H^+ exists only as complexes, where its bonding with the molecules of the condensed phase (i.e., solid, liquid, solution) media is so strong that one should not refer to this monatomic cation in beginning texts, but instead to quite common ions such as $[H_3O]^+$ and much more exotic ones such as $[H_2F]^+$. (The former polyatomic ion is also a relatively common ion in salts, although these salts are also, and generally better, describable as hydrates of strong acids.) That these two ions are isoelectronic and isostructural with NH_3 and H_2O, respectively, does not make $[H_2F]^+$ less exotic—perhaps this is because we usually think of HF as an acid and not as a base. In nonaqueous media, HF is both. In gaseous media, HF is both an acid and base also, but we know of no neutral hydrogen-containing species that is not an acid, and no neutral species at all that is not a base: we recognize H^- and $[H_3]^+$ as the conjugate base and conjugate acid of the well known H_2.

B. Univalent Anions, Hydride, and Alkalide Salts

Hydrogen also forms the anion H^-, and numerous hydride salts such as LiH and CaH_2 are known. The alkali metals likewise form alkalide ions. The binding of an electron by the alkali metals is of comparable strength to that to atomic hydrogen; the electron affinities of H and the alkali metals are very similar. Salts of Na^-, K^-, Rb^-, and Cs^- are all known. One such salt is $[Li(CH_3NH_2)_n]^+ Na^-$, known as both solid and liquid with varying n, and formed from a 1:1 mixture of Li and Na with methylamine. Since sodium is less electronegative than lithium, and both the ionization energy and electron affinity of Na are smaller than those of Li, it is surprising that the isomer $[Na(CH_3NH_2)_n]^+ Li^-$ is unobserved, much less preferentially formed. What is also surprising is that there are seemingly no Li^- salts known, while Na^- salts arise from all alkali metal/sodium combinations, including species that contain both Na^+ and Na^-. This may look familiar from the finding that, as defined by EMF potentials in water, lithium is more reducing than sodium, but then again, the aqueous order for the alkali and other metals runs counter to any periodic trends.

C. Polylithium Species

Perhaps to appease the chemist for the seeming paucity of anionic salts, lithium forms a collection of polar binary compounds with exotic stoichiometries, at least when compared with their formal binary counterparts with hydrogen. For example, paralleling CH_4, NH_3, H_2O, HF, and H_2S are CLi_4, Li_3N, Li_2O, LiF, and Li_2S, but there are also the unprecedented CLi_3 and CLi_5, NLi_4, Li_3O and Li_4O, Li_2F and Li_3F, and Li_4S all with close Li—Li contacts and seemingly intermetallic bonding. However, before one concludes that interlithium bonding is always stabilizing, one should recall that Li_2O, as a triatomic molecule and not salt, is linear. It is not bent like its hydrogen analogue, water. Mixed hydrogen/lithium species are rare. We note that one such species, triatomic molecular and not salt LiOH, is also linear.

D. Electride Salts

We extend the discussion of these alkalide salts and note the existence of numerous species containing a second alkali metal ion but now found as complexed (with a crypt and/or crown ether) cation. These cations may be understood as solvated but with a well-defined solvation shell, both in terms of structure and stoichiometry. The solvation has made it easier to remove an electron from the alkali metal—so much easier that the electron may be put on another alkali metal atom, as we have said; and so much easier that the electron may be taken off and left as an anion unto itself. These are so-called electride salts. While these species may be recognized as a form of "expanded metal" and we are also used to writing e^- in an electrochemical or otherwise redox context, it is nonetheless a surprise to see a free electron as part of a structure or crystalline lattice.

E. Ions of Gold

Such metal clustering as found for the above neutral polylithium species is found for cationic polygold species in salts and/or solution with stoichiometries such as $[(LAu)_3O]^+$, $[N(AuL)]_4^+$, and even $[C(AuL)_5]^+$ and $[C(AuL)_6]^{+2}$, where L is a triarylphosphine, typically Ph_3P, wherein $Ph = C_6H_5$ = phenyl. Aha! Carbons in great numbers appear. And oh, yes, there are also Au^- salts that might otherwise be considered "merely" alloys. Interestingly, gold has another anionic form, $[AuF_6]^-$, in which the oxidation state is +5, otherwise unprecedented for either the alkali metals or the so-called coinage metals (Cu, Ag, Au).

III. CATIONS AND/OR ANIONS: PLEMEIOELECTRONIC AND HERMAPHRODITIC SPECIES

A. Transition Metals

This section attempts to answer why the aforementioned alkalide salts are at all exotic. We suspect the answer is because we are used to the alkali metals being cations, to metals being cations, and to not having a given species appear in both positive and negative charge states. Thus a choice of charge states is not a surprise. That is essentially the hallmark of transition metals, for example, the long-known sets of aquated cations Fe^{2+} (green) and Fe^{3+} (yellow) and the tetrahedral anions $[MnO_4]^-$ (purple), $[MnO_4]^{2-}$ (green), and $[MnO_4]^{3-}$ (blue) with their central metals with positive oxidation states. That the same heavy (nonhydrogen) atom skeleton is roughly maintained as the number of electrons is varied is also not a surprise, sets of so-defined plemeioelectronic species are not particularly rare.

B. Nonmetal Ions

It is rare that ions of both signs are found. Some of the very few salt-forming hermaphroditic (and so likewise exotic) species include the following: $[O_2]^{+/-}$ (e.g., the dioxygenyl salt $[O_2]^+[PtF_6]^-$ and the superoxide

K^+ $[O_2]^-$; the ozonide $[O_3]^-$ is known in numerous salts, but no ozonium, $[O_3]^+$, salt is known); $[NO_2]^{+/-}$ (nitronium/nitrite), but not $[NO]^-$ or $[NO_3]^+$; $[ClO_2]^{+/-}$ but no hypochlorite, chlorate, or perchlorate-like cations; $[XeF_5]^{+/-}$ (but not XeF_3, known only as the cation, and not XeF_7, known only as the anion); and the hexafluoro species $[EF_6]^{+/-}$, where E = Cl, Br, and I (E = Re is also known). A plausible assumption is that one wants an intermediately high oxidation state, but this is contradicted by the case of alkali metal cations and anions and the pair of doubly charged ions $[S_4]^{2+}$ and $[S_4]^{2-}$. Also note that the geometry of the cations and anions may be greatly different: $[XeF_5]^+$ is a C_{4v} square pyramid, whereas $[XeF_5]^-$ is one of but two binary species of the stoichiometry AB_5 with D_{5h} pentagonal symmetry, and $[S_4]^{2+}$ and $[S_4]^{2-}$ are, respectively, a 6-π-electron, square-shaped aromatic and an alkane-like (but gauche, not staggered) extended chain. We parenthetically add that these two last species may be also recognized as valence isoelectronic analogues of $[O_4]^{2+/2-}$, both unknown in these dimeric states, as opposed to their aforementioned monomers $[O_2]^{+/-}$, while the sulfur compounds are not known monomerically in the condensed phase save as the $[S_2]^-$ anion as a source of color for an uncommon mineral, "green ultramarine."

C. Can Alkali Metals Have Higher Oxidation States?

We close this section with a brief mention of higher valence alkali metal species. By this we do not mean highly ionized atomic ions such as $[Na]^{11+}$—verily any atom can be stripped of any, many, and even all of its electrons, but that is not what is meant. We do not mean species like KO_2 that have univalent K^+ accompanying superoxide, $[O_2]^-$, and are not tetravalent oxides like the covalent CO_2 and ionic UO_2 nor even divalent peroxides like BaO_2. What about CsF_3? Known as a matrix-isolated species, cesium trifluoride seemingly contains univalent, and thus commonplace, Cs^+ with the trifluoride ion, $[F_3]^-$, which, while, it has a precedent in other trihalide ions such as $[I_3]^-$, still qualifies as an example of exotica. There is no evidence for this being an ion pair of $[CsF_2]^+$ and F^-, the cation of which was suggested years ago as a plausible species because it is isoelectronic to XeF_2. It is still unrealized.

D. Trihalide Ions

Then again, similarly isoelectronic to XeF_2 is trihalide ion, $[IF_2]^-$. It is a plausible, indeed known, but still hardly explored species, unlike its better known valence isoelectronic chlorine and bromine analogues, both $[ICl_2]^-$ and $[ClF_2]^-$, and $[IBr_2]^-$ and $[BrF_2]^-$. It is perhaps surprising as well as disappointing that while the oxidation state of iodine goes from −1 to +7 and that of xenon from 0 to +8, cesium, and *a fortiori* the other alkali metals, is limited to +1 . . . and dare we forget, −1.

IV. THREE-ATOM 16-VALENCE-ELECTRON XYZ SPECIES: ISOELECTRONIC ANALOGUES

A. Old and New Species

Several isoelectronic analogues of CO_2 have been known for a long time and are well characterized. These include neutral N_2O and the ionic species $[N_3]^-$ (see below), $[CN_2]^{2-}$, and $[NO_2]^+$. Interestingly, the list does not include $[BO_2]^-$ ion. The so-called, long-known "metaborate" ion with this formula is found in numerous salts, but structurally it appears only as a trimer or polymer.

More recently, great progress has been made in the area of these simple 22-electron (16-valence-electron) X=Y=Z species. All of the possible $[X{=}Y{=}Z]^n$ systems that contain X, Y, and Z elements of the first row (second period) and net charges ($-4 \le n \le +4$) were studied using quantum chemical methods and many new ions were predicted to be locally stable. Meanwhile several of these unknown species have been prepared and characterized, for example, $[CBN]^{4-}$ and $[C_3]^{4-}$, and these species together with their heavier CS_2 analogues are discussed in the following paragraphs.

B. Bond Lengths and Angles

The structurally well-characterized ionic, isoelectronic analogues of CO_2 are summarized in Table I. We also include three isoelectronic ions corresponding to CS_2, the heavier, valence isoelectronic homologue of CO_2. The $[BAs_2]^{3-}$ anion, which is isoelectronic to CSe_2, has also been reported, with d(B—As) = 1.87 Å.

In all cases the bond lengths in the ions isoelectronic to CO_2 and CS_2 are suggestive of at least partial multiple bonding, and therefore significant $(p\text{–}p)\pi$ bonding has

TABLE I Structural Parameters[a] for N_2, $[N_3]^-$, and $[N_5]^+$

	N_2	$[N_3]^-$	$[N_5]^+$
Symmetry	$D_{\infty h}$	$D_{\infty h}$	C_{2v}
d(N—N, terminal)	1.10	1.18	1.11
d(N—N, central)			1.30
θ(NNN)		180	110, 166

[a] Bond lengths d in angstroms; angle θ in degrees.

to be considered. Even in the $[PCS]^-$ ion the C—S bond length (1.62 Å) is shorter than the expected value for a typical single bond (1.82 Å); then again, both resonance structures {$P\equiv C{-}S^-$} and {$^-P{=}C{=}S$} look exotic with their carbon–phosphorus triple and double bonds, respectively.

An interesting comparison involves the difference of bond lengths between corresponding bonds in corresponding first and second row species. For example, the difference of the CO and CS bonds in CO_2 and CS_2 is $1.55 - 1.16 = 0.39$ Å. By contrast, the difference of the same bonds in $[NCO]^-$ and $[PCS]^-$ is enigmatically increased to $1.62 - 1.13 = 0.49$ Å. Table II presents the collected bond lengths d(XY) and d(YZ), and the interrow differences Δd(XY) and Δd(YZ). No explanation is apparent for the spread of difference values.

With the counterion-dependent exception of the $[C_3]^{4-}$ ion, all species quoted in Table I can be regarded as linear.

In all ions isoelectronic to CO_2 the most electropositive atom always occupies the central Y position in the most stable X=Y=Z species. There is the pseudohalogen, CNO, with a central nitrogen of intermediate electronegativity to that of its bonding partners. That it is unstable is reflected in its trivial name "fulminate," as opposed to the C-centered but variously (O, N)-attached isomer cyanate/isocyanate. The remaining isomer, CON, with the electronegative oxygen in the center remains unknown and may safely be assumed to be even less stable.

C. Some Synthetic Chemistry

Most of the anionic 16-valence-electron species that are isoelectronic to CO_2 and CS_2 were synthesized by high-temperature solid-state reactions in ampules made of the refractory metal niobium or tantalum. For example, the compounds $Sr_3(BN_2)_2$ and $K_3(BP_2)$ were prepared at 1000°C from strontium nitride and graphitic BN, or from potassium and diamond or zinc-blende-like BP, respectively. The compounds $Ca_3Br_2(CBN)$ and $Sr_3Cl_2(CBN)$ were synthesized at 950°C from the corresponding metal, its dihalide, boron nitride, and graphite. By analogy, $Ca_3Cl_2C_3$ was formed from calcium, $CaCl_2$, and graphite at 900°C. The synthesis of the first compound containing an isolated $[PCS]^-$ ion was achieved in glyme (dme, 1,2-dimethoxyethane) solution,

$$S{=}C(OC_2H_5)_2 + [(CH_3)_3Si]_2P{-}Li \rightarrow [Li(dme)_3]^+[PCS]^- + 2C_2H_5OSi(CH_3)_3. \quad (1)$$

The $[SNS]^+$ ion was classically obtained by oxidation of a mixture of tetrasulfur tetranitride, S_4N_4, and elemental sulfur with AsF_5 as both the oxidant and fluoride-accepting Lewis acid:

$$S_4N_4 + \tfrac{1}{2}S_8 + 6AsF_5 \rightarrow 4[SNS]^+[AsF_6]^- + 2AsF_3. \quad (2)$$

However, two more recent laboratory syntheses are more convenient as they do not involve the use of explosive S_4N_4:

$$[S_8]^{2+}[AsF_6]_2^- + NaN_3 \rightarrow [SNS]^+[AsF_6]^- + NaAsF_6 + N_2 + \tfrac{3}{4}S_8 \quad (3)$$

$$[N(SCl)_2]^+[AlCl_4]^- + SnCl_2 \rightarrow [SNS]^+[AlCl_4]^- + SnCl_4. \quad (4)$$

TABLE II **CO_2 and CS_2 and Their Ionic, Isoelectronic Analogues XYZ, Experimentally Determined Bond Lengths d(XY) and d(YZ), and the Differences between the Distances for Corresponding Bonds with First Row and Second Row Elements Δd(XY) and Δd(YZ)[a]**

XYZ	d(XY)	d(YZ)	XYZ	d(XY)	d(YZ)	Δd(XY)	Δd(YZ)
OCO	1.16		SCS	1.55		0.39	
$[ONO]^+$	1.15		$[SNS]^+$	1.46		0.31	
$[NNN]^-$	1.18						
$[NCO]^-$	1.21	1.13	$[PCS]^-$	1.56	1.62	0.35	0.49
$[NCN]^{2-}$	1.23						
$[NBN]^{3-}$	1.36		$[PCP]^{3-}$	1.77		0.41	
$[CBN]^{4-}$	1.44	1.38					
$[CCC]^{4-}$	1.35						

[a] All distances are in angstroms.

V. ETHYLENE AND BEYOND: ANALOGUES, CAGES, AND CLEAVAGE

We now consider another simple species and see where our logic leads us. We start with the "organic compound" ethylene, C_2H_4. With its double bond, its banana bonds, its σ and π bonds, it is an archetype for numerous organic species, as well as the inorganic species that constitute the purview of this article. Let us now proceed to diverse exotica and with many forks in the road; there is no unique route or even destination.

A. Metal Complexes

Let us now consider metal complexes. Transition metal complexes of olefins, alkynes, and arenes and other organic π systems have become quite common in both the textbook and research literature: some exotica of this type will be discussed in a later section. We start with an ethylene complex with the simplest metal ion, Li^+. The cation is definitionally electrophilic, the olefin has an energetically accessible pair of electrons, and the complex is really quite sensible. We may recognize it as analogous to the better known olefin–silver complexes

such as $C_2H_4{\bullet}Ag^+$, simple carbo-cations such as the hydrogen-bridged, nonclassical ethyl cation, $[C_2H_5]^+$ ion, and to more normal solute/solvent complexes such as $Li^+{\bullet}(H_2O)_n$ with n ranging from 1 to "∞" (i.e., from a "super-simple" ion–molecule cluster to infinitely dilute aqueous solutions). It is related also to the corresponding propylene (methylethylene) complex by a simple substitution process, $CH_3CH{=}CH_2{\bullet}Li^+$. None of this is particularly surprising. However, this last ion is the product of the gas-phase reaction of Li^+ and isopropyl chloride,

$$Li^+ + (CH_3)_2CHCl \rightarrow CH_3CH{=}CH_2{\bullet}Li^+ + HCl. \quad (5)$$

This is reminiscent of the really quite ancient organic chemistry elimination reaction of an alkyl halide using a strong base (i.e., some alkali metal hydroxide) but now employing the metal half of the latter reagent.

B. "Squashing" Ethylene to Imines, En Route to Cages

Another set of interrelations arises when we take the hydrogens of ethylene and squash them in the carbon nuclei. We first produce $CH_2{=}NH$, known as either methylenimine or formaldimine. This species is unknown in the condensed phase but is known in the gas phase and as an interstellar molecule. It is the archetype of a large number of organic compounds. Although this is more within the province of organic than inorganic compounds, we note how the reaction

$$CH_2O + NH_3 \rightarrow CH_2NH + H_2O \quad (6)$$

does not proceed as written but instead goes on to form the tetraazaadamantane cage product hexamethylene tetramine $(CH_2)_6N_4$. Admittedly "organic," this species presages σ-bonded, electron-precise inorganic cage species such as phosphorus and arsenic oxides and sulfides. Recall such common species as phosphorus pentoxide P_4O_{10}—we note that the formula of this species is often written P_2O_5, which is the correct formula for an altogether different and much more exotic species with the structure $(O{=})_2P{-}O{-}P({=}O)_2$.

C. Carbonyl Compounds—To the Organic and Inorganic Chemist

Squashing results in a choice of two compounds and derivatives. The first is $CH_2{=}O$, known as formaldehyde or methanal. No surprises here with this organic molecule. Again, we recognize this species as the archetype of a large variety of compounds, $RR'CO$, so-called carbonyl compounds to the organic chemist. Some R and R′ are hydrogen, alkyl, or aryl groups—these are aldehydes and ketones. Or we may have halogen, oxygen, nitrogen-forming acyl halides, carboxylic acids and their esters and anhydrides, and amides. There are some unusual features of these species and some are indeed exotic, but, alas, they are organic. Or the groups may be metals and so we have a special type of carbonyl compound—the same term, but with a different meaning, since a metal attached to CO and nothing more is even a generally classical type of carbonyl compound, to the inorganic chemist. If the group is a main group metal, then there is novelty. For example, Li_2CO has the carbon and oxygen of the CO bridged by the two metal atoms, a quite unusual geometry even for those accustomed to the variety of structures and bonding types of metal carbonyls. Introduction of valence isoelectronic silicon, sulfur, and other elements of the second row and beyond into the discussion generates the exotic blue/purple disilylketones $(R_3Si)_2CO$, monomeric silanones $R_2Si{=}O$, the blue thioketones $R_2C{=}S$, and a plethora of doubly modified compounds of the type $R_2E{=}E'$ such as germaselones with quite obviously the third row Ge and Se. We note that many of these modified species energetically "prefer" to be polymers and that is their natural form to the laboratory scientist and layperson alike (e.g., silicone polymers). Then again, formaldehyde itself forms a polymer in an exothermic reaction, despite its rich chemistry as a monomeric tetratomic molecule.

D. Azo Compounds, Isodiazenes, and Peroxynitirites

The alternative squashing yields N_2H_2, alternatively known as diimide and diazene, with natural derivatives $R{-}N{=}N{-}R'$. Well known to the organic chemist, this is the archetype of generally red, orange, or yellow azo compounds. Paralleling the above is the blue $R_3SiNNSiR_3$, a rather rare variety of dinitrogen complexes en route to reduction and cleavage, and analogues such as the rare $RP{=}NR'$ (as opposed to common R_3PNR' species). We also recall N_2F_2 and hyponitrite salts $[N_2O_2]^{2-}$. These are seemingly normal, albeit unstable species. However, they have the surprising feature that the *cis* or *Z* isomer is more thermodynamically stable than the *trans* or *E* form, despite greater lone-pair, charge, and/or dipolar repulsion in the former. We should also not forget the isomeric species with the general formula $RR'N{=}N$, and while many are transient intermediates either forming dinitrogen or trapping it, there are also isolable isodiazene complexes containing such species as ligands. And, being fond of isoelectronic analogues, we note that $(O^-{-})_2\,N^+{=}O$ is more stable than its counterpart $O^-{-}N{=}O^+{-}O^-$, where we recognize these last two species respectively to be the ancient nitrate ion and (an unimportant resonance structure of) the increasingly important, but still exotic, peroxynitrite ion.

E. Nitroso and Isonitroso Compounds and Some Sulfur Analogues

The next squashing generates the isomeric nitroso and isonitroso species RNO and RON. For most R, the former isomer is more stable. The relative stability depends on the electronegativity of the R. For the electropositive $R = Li$, the LiON form is the more stable. Isoelectronic analogues are known having one or the other structure, for example, Me_2NNS and NSF; there is a plethora of nitrogen–sulfur compounds, most of which lack corresponding analogues with nitrogen and oxygen, such as S_4N_4, $N_4S_4F_4$, and $N_3S_3Cl_3$, in counterpoint to monomeric NO and NOF, actually ONF, and NOCl, actually ONCl. (Monomeric NSF and NSCl are also known but these are sulfur-centered, not nitrogen-centered.)

F. Elemental Oxygen, Elemental Sulfur, and Sulfur–Oxygen Species

The final squashing results in elemental dioxygen, O_2, an altogether normal, commonplace, well-known species that is one of the few non-transition-metal species with unpaired electrons that do not polymerize or oligomerize under normal situations. Indeed, its polymers are all but unknown. Whereas there is some indirect evidence for O_4 and we know of none for O_8, for the valence isoelectronically related sulfur, S_8 is the normal form for elemental sulfur, where S_2 is the exotic species and neutral S_4 remains largely unknown, as opposed to the aforementioned $[S_4]^{2-}$ and $[S_4]^{2+}$ ions found in salts. Speaking of salts, but now within the context of mixed sulfur–oxygen species, sulfites and sulfates, $[SO_3]^{2-}$ and $[SO_4]^{2-}$, are commonplace anions, while the "lower" oxoanions $[SO]^{2-}$ and $[SO_2]^{2-}$ remain essentially unknown, and this, despite the well-characterized situation for the isoelectronic chlorine–oxygen anions, $[ClO_n]^-$ for $n = 1, 2, 3$, and 4, and the importance of the redox chemistry of sulfur–oxygen radical anions $[SO_n]^{\bullet -}$ for $n = 2, 3$, and 4 in at least the aqueous solution of $[S_2O_4]^{2-}$, HSO_3^-, and $[S_2O_8]^{2-}$, respectively.

G. Cleavage Reactions and Fluorinated Derivatives

Another source of interesting chemistry arises from consideration of the formal cleavage reaction of ethylene into methylene, of the parent olefin into the parent carbene,

$$C_2H_4 \rightarrow 2CH_2. \tag{7}$$

This reaction per se, like that of most simple derivatives of ethylene, is not particularly relevant here—it is too "organicky." However, the conflict between weakly bonded but tetravalent ethylene analogues with higher group 14 elements in their divalent state is an interesting study. Consider, for example, tetrafluoroethylene and difluorocarbene, C_2F_4 and CF_2, not to be confused with carbon difluoride. CF_2 is a rather stable example of divalent carbon. While the carbon–carbon double bond in ethylene is considerably stronger than the corresponding carbon–carbon single bond in ethane (no surprise!), the former bond in tetrafluoroethylene is weaker than the carbon–carbon single bond in hexafluoroethane. The bond is not that weak—CF_2 is still recognized as a quite reactive carbene. Proceeding down the column, we have less and less tendency for the essentially olefinic species, and, instead, polar, if not ionic, compounds. We thus generate the toothpaste additive stannous fluoride, which does not contain Sn^{2+} in the crystal (unlike aqueous solution), but rather the tetrameric fluoro-cation ring $[(SnF)_4]^{4+}$ with fluorides bridging the tins within the oligomeric cation and between oligomers.

H. Di- and Tetravalent Oxides

We see this behavior in the divalent oxides as well. Carbon monoxide is a well-defined diatomic gas that has the strongest bond in any neutral molecule and a dipole moment almost precisely zero. It shows no tendency to dimerize—the formal ethylene-like species O=C=C=O has entertained, educated, and evaded numerous chemists; now, clearly, it cannot be the instability of the =C=O unit per se, as this is found in so many of the metal carbonyls enunciated above. Traversing the length of the column gets us to lead oxide, a long-known, quite ionic solid with at least formal Pb^{2+} ions. This does not mean that group 14 oxides never want to associate. Carbon dioxide, CO_2, is a well-defined triatomic gas (with a much more sensible zero dipole moment than the negligible one for CO because of the symmetry of the former). The triatomic SiO_2 also exists, but as a high-temperature gas. It readily forms an extended solid with an extensive collection of forms with poetic-sounding names, tridymite, cristobalite, and coesite, as well as the more prosaic sand, amorphous silica, silicalite, and quartz. Because of this diversity of forms, we consider silicon dioxide as an exotic species despite its ubiquity in both the natural and human-derived environment.

VI. REVERSING THE SQUASHING: BORON HYDRIDES

A. Relating Organic and Inorganic Species

Let us return to ethylene and reverse the squashing procedure, going to diborane(6), from C_2H_4 to B_2H_6, and thereby from organic carbon- to inorganic

boron-containing species. The latter species is so common that it is easy to forget its uniqueness as the archetype of species with three-center/two-electron bonds, of electron-deficient as opposed to electron-precise species, of boron compounds, and the general cluster and cage chemistry that arises from these structural and electronic features. We will not consider boron compounds or cluster species in any of their traditional glory. These are studies for other sections and other chapters, and their authors have also had to keep many of the highly interesting stories left unsaid. Rather, we recall the simple equilibrium between diborane(6) and the formally simpler borane(3), BH_3:

$$B_2H_6 \rightleftarrows 2BH_3. \tag{8}$$

This is so "simple" that we often speak of diborane and borane without the designations of "(6)" and "(3)." We say "formally" because BH_3 lacks "off-the-shelf chemistry": it spontaneously dimerizes. The simple one- and two-carbon hydrides CH_4 and C_2H_6 are both easily isolated and separated, as are one- and two-nitrogen hydrides NH_3 and N_2H_4 and one- and two-oxygen hydrides H_2O and H_2O_2: methane, ethane, ammonia, hydrazine, water, and hydrogen peroxide have very ancient and venerable names reflecting very ancient and venerable chemistry. BH_3 is more like CH_2, with which it is isoelectronic.

B. The BH_3/CH_2 Comparison: Triboron Species

Even here the chemistry of borane(3) shows some surprises and introduces us to some exotic compounds, only some of which have been isolated by experimentalists. To the extent that BH_3 and CH_2 are conceptually related, we would expect to find an entire homologous series $(BH_3)_n$ analogous to cycloalkanes $(CH_2)_n$. Not so; while the $n = 3$ carbon case of cyclopropane is well known, the corresponding triborane(9) qualifies as ephemeral, fragile, and exotic, and indeed, there is no isolable binary boron hydride with but three borons. The corresponding anion made by formal deprotonation of the latter, $[B_3H_8]^-$, is stable enough to be isolable as salts, whereas protonated cyclopropane, $[C_3H_7]^+$, is only known in gaseous or other nonnucleophilic media.

C. Tetraboranes

The $n = 4$ case results in the even less well known tetraborane(12)—four borons want but 10 hydrogens. That the stoichiometries of two of the earliest known boron hydrides, B_2H_6 and B_4H_{10}, are so familiar from hydrocarbon chemistry, and the formulas of other boron hydrides even more distinct, no doubt added to considering even these boron compounds as exotic. The simplest structure for diborane(6), long known to be wrong, is that of an ethane molecule in which the two carbons are replaced by borons. Now, clearly, this is too simplistic since two electrons are missing. Nonetheless, tetraborane(10) can be logically understood as the corresponding butane derivative. Now let us consider the more current structure of diborane(6), that of ethylene, where the two carbon–carbon bonds have been replaced by two B—H—B units. Accordingly, tetraborane(10) is related to diborane(6) much as butadiene, C_4H_6, is related to ethylene. There are other C_4H_6 isomers, all of which are considerably higher in energy. Recall that there is no isolable B_3 hydride. However, the correct structure for B_4H_{10} contains two fused B_3 rings and the most logical structure, most simply B_2H_5—B_2H_5, is not even an experimentalist's exotica—it remains the fancy of theorists.

D. Simple Clusters

We could talk about strain energies and delocalization energies, differences between σ and π bonds, as a way of organizing these boron and carbon hydrides. We will not. Instead we close this section with an apologetically brief mention of simple boron clusters, also containing four borons, with the generic formula B_4X_4. We do so because their special, symmetric, tetrahedral shape presages the plethora of triangulated, deltahedral boron clusters, their isoelectronic and isolobal analogues, and also of the likewise nonmetal tetrahedron, P_4. That P_4 is an ancient species, known since the interface of alchemy and chemistry, has a special symmetric shape, and is related to more current species adds to its exotic character. It would appear that both boron and phosphorus chemistry offer chemists numerous "exotica" to add to their amusement and aggravation. The next section discusses P_4 and related polyphosphorus and polynitrogen species.

VII. POLYPHOSPHORUS AND POLYNITROGEN SPECIES, THEIR ANALOGUES AND DERIVATIVES

In the introduction we defined *exotic* as "beautiful, exceptional, weird, paradoxical, and counterintuitive." We also indicated that such species could represent fragile and rare as well as simple and well-characterized classic inorganic compounds. In this section we will look at two of the simplest inorganic classes of compounds: polyphosphorus and polynitrogen species. We will dwell on the following elementary question: Why is it that polyphosphorus allotropes of the element are well known (white phosphorus; black phosphorus in its orthorhombic, rhombohedral, and cubic forms; red, amorphous phosphorus),

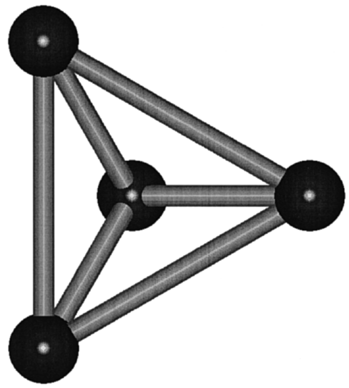

FIGURE 1 Molecular structure of white phosphorus, the tetrahedral P_4.

but in the case of nitrogen only one (kinetically) stable form, N_2, has been found?

A. Homopolyatomic Phosphorus Compounds

Since polyphosphorus species are far more common than polynitrogen compounds, in contrast to their order of appearance in the periodic table (N, P, As, Sb, Bi), here we discuss the neutral homopolyatomic phosphorus compounds first. As stated above, phosphorus occurs in three main forms: white, black, and red. White phosphorus consists of tetrahedral P_4 molecules (Fig. 1) and forms a molecular lattice that melts already at 44°C, and even the boiling point is rather low at 280°C. In accord with its molecular structure, P_4 is soluble in many organic nonpolar solvents but is insoluble in water—indeed, P_4 is usually stored under water because it is spontaneously flammable in air.

The remaining forms of elemental phosphorus, namely black and red phosphorus, are insoluble polymers that are much less reactive than white phosphorus. Black orthorhombic phosphorus is the most thermodynamically stable form of this element and can be obtained by heating white phosphorus under pressure. Red phosphorus, in contrast to the black allotrope, is not crystalline but amorphous and is readily obtained by heating P_4 up to 400°C in a sealed container. Red phosphorus consists of polymers obtained by partial opening and conjoining (or catenation) of the P_4 tetrahedra.

When white phosphorus is heated in organic solvents in the presence of certain cyclopentadienyl transition metal carbonyl complexes, new complexes containing the monocyclic P_6 analogue of benzene are found (Fig. 2). There are also a few compounds having metal atoms on both sides of a P_5 ring that can be recognized as the analogue of the cyclopentadienyl anion, $[C_5H_5]^-$.

B. Homopolyatomic Nitrogen Compounds—Ionic and Covalent Azides

In contrast to phosphorus, due to the high thermodynamic stability of the N_2 molecule, other homopolyatomic nitrogen species are very rare. Dinitrogen, N_2, was first isolated in 1772 by D. Rutherford and also by C. W. Scheele and H. Cavendish (Fig. 3). Over 100 years later hydrazoic acid, HN_3, was prepared for the first time by T. Curtius, and numerous metal azides containing the linear, isolated $[N_3]^-$ ion have been characterized (Fig. 3). The best known salt, NaN_3, can be prepared by adding powdered $NaNO_3$ to fused $NaNH_2$ at 175°C or by passing N_2O into the same molten amide at 190°C:

$$NaNO_3 + 3NaNH_2 \rightarrow NaN_3 + 3NaOH + NH_3 \quad (9)$$

$$N_2O + 2NaNH_2 \rightarrow NaN_3 + NaOH + NH_3. \quad (10)$$

In covalently bound azides the N_3 group behaves as a pseudohalogen (for example, HN_3 and the halogen azides FN_3, ClN_3, BrN_3, and IN_3). Although potential allotropes of nitrogen such as N_3—N_3 (analogous to Cl_2) and $N(N_3)_3$ (analogous to NCl_3) have not yet been isolated, these compounds have been extensively studied by quantum chemical methods (see below). The predicted high instability of any potential homopolyatomic nitrogen species stems from the particularly strong N≡N triple bond in N_2 with a bond energy of 945 kJ mol^{-1}, much higher than three typical N—N single bonds ($480 = 3 \times 160$ kJ mol^{-1}),

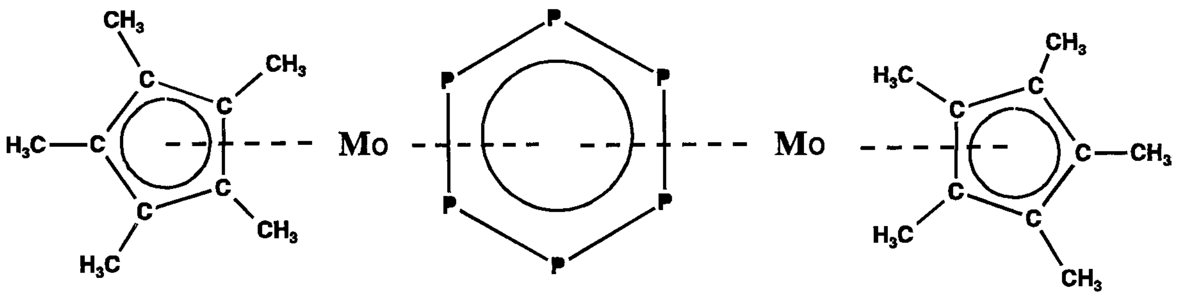

FIGURE 2 Structure of $[(C_5(CH_3)_5$—Mo—(P_6)—Mo—$C_5(CH_3)_5]$.

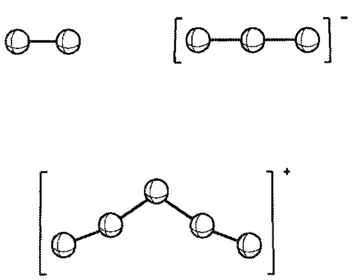

FIGURE 3 Structures of the isolated homopolyatomic polynitrogen species N_2, $[N_3]^-$, and $[N_5]^+$ as found in the gaseous, solid, and solid phases, respectively.

and 1.5 times the average N=N double bond energy ($630 = 1.5 \times 420$ kJ mol^{-1}) or the sum of one single and one double bond ($580 = 160 + 420$ kJ mol^{-1}). The superb stability of N_2 also accounts for the strong reducing power of aqueous azide, as seen in the electrochemical half-reaction

$$[N_3]^- \rightarrow \tfrac{3}{2}N_2 + e^-, \qquad (11)$$

and indeed NaN_3 is one of the very few sodium salts that is unstable relative to the elements.

C. The N_5^+ Cation and Its Analogues: Theory and Experiment

Quite recently, there was a report of the surprisingly straightforward preparation and characterization of the salt $[N_5]^+[AsF_6]^-$ containing the novel $[N_5]^+$ cation (Fig. 3), which represents only the third known example of a homopolyatomic nitrogen species that can be isolated on a macroscopic scale:

$$[N_2F]^+[AsF_6]^- + HN_3 \rightarrow [N_5]^+[AsF_6]^- + HF. \qquad (12)$$

The new compound, $[N_5]^+[AsF_6]^-$, is a white solid with marginal stability at room temperature that can be stored for weeks at −78°C.

The $[N_5]^+$ cation was first predicted to possess a planar V-shaped C_{2v} structure on the basis of quantum chemical calculations. In the most recent experimental study, the $[N_5]^+$ cation was investigated by means of $^{14/15}$N NMR, vibrational (IR, Raman) spectroscopy, and X-ray crystallography. The structural parameters for the three well-characterized homopolyatomic nitrogen species are given in Table II.

The symmetric triatomic azide ion $[N_3]^-$ is isoelectronic with N_2O (see below) and its structure can easily be rationalized using the classic VSEPR model. The standard Lewis (**1** and **3**) and increased-valence Harcourt structures (**2** and **4**) are displayed in Fig. 4. The increased-valence Harcourt structures, which may be derived from

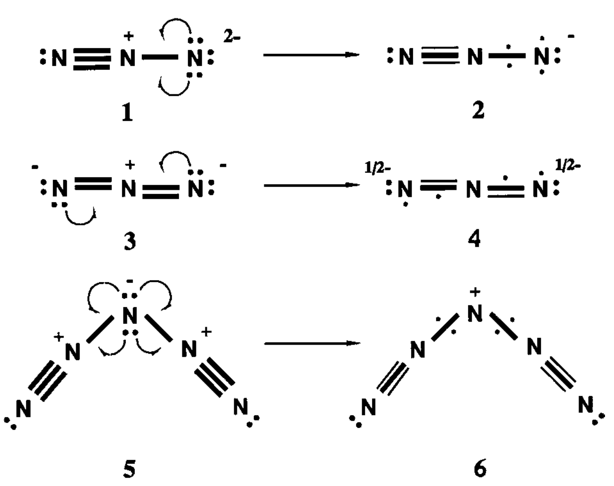

FIGURE 4 Standard Lewis and increased-valence Harcourt structures for $[N_3]^-$ and $[N_5]^+$.

the standard Lewis structures via the one-electron delocalizations indicated, involve smaller formal charge separations and are thus more stable (and therefore more important) than the Lewis structures. Resonance between the increased-valence structures (with their symmetry-related mirror-image structures) shows more clearly than does resonance between the standard Lewis structures that the N—N bond lengths of 1.18 Å (Table II) are shorter than the conventional estimate of 1.24 Å for an N=N double bond. Similarly, for $[N_5]^+$, which is isoelectronic to $C(CO)_2$, structures **5** and **6** are analogous standard Lewis and increased-valence structures. Inspection of structure **6** makes it clear why the central and terminal bonds are shorter than the N—N single bond (1.45 Å) and similar to that of N_2, respectively.

In addition to $[N_5]^+$ and the isoelectronic neutral 34-electron (24-valence-electron) species $C(N_2)_2$ and $C(CO)_2$, other known pseudohalide 34-electron ions have been reported. One example is the kinetically stable and bent anion [N≡C—N—C≡N]$^-$, which forms many salts but is a "Cinderella" of inorganic chemistry in not appearing in common textbooks. Even the "single-phosphorus" analogue [N≡C—P—C≡N]$^-$ has been made and characterized. A cumulene valence structure is also appropriate for the well-known linear carbon suboxide, O=C=C=C=O, whose sulfur analogues are also known. A reorganization of the nuclear charges yields the cyanoether N≡C—O—C≡N. The permutation of these atoms gives cyanogen isocyanate, N≡C—N=C=O, which has also been reported. Even the highly explosive isoelectronic cyanogen azide N≡C—NNN has recently attracted considerable attention both experimentally and theoretically. This highly reactive molecule behaves like a Lewis base and, like numerous other nitriles, can be coordinated to

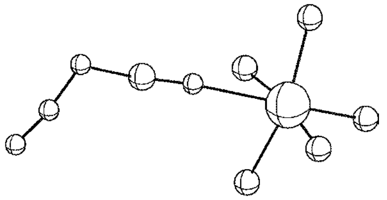

FIGURE 5 Molecular structure of the cyanogen azide–arsenic pentafluoride Lewis acid/Lewis base complex, $F_5As \cdots N{\equiv}C{-}NNN$.

strong Lewis acids such as arsenic pentafluoride (Fig. 5). Another isoelectronic analogue is boron oxide, B_2O_3, known in the gas phase as a bent pentatomic molecule and as a polymer with tricoordinated boron and dicoordinated oxygen in the solid.

D. Other Polynitrogen Species

Reiterating, only three homopolyatomic nitrogen species have been unequivocally isolated: N_2, $[N_3]^-$, and $[N_5]^+$. It is perhaps surprising that the $[N_5]^+$ ion does not react with additional HN_3 to form N_8 and eventually N_2. Other experimental studies of polynitrogen compounds have shown the transient existence of the $N_3^\bullet$ radical and the $[N_6]^{\bullet -}$ radical anion from which it presumably arises. Interestingly, the N_4 neutral remains undetected, while both its corresponding radical cation and anion have been observed. Many more homopolyatomic nitrogen compounds have been quantum chemically calculated with respect to the question of whether their potential as high-energy-density materials (HEDM) can be realized. The most comprehensive theoretical study in this area reported that other than N_2, the thermodynamically most stable N_n molecules are all based on pentazole units. Pentazole ($H{-}N_5$) and its anion $[N_5]^-$ (D_{5h}; Fig. 6) were established to be as aromatic as their isoelectronic analogues, for example, furan, pyrrole, and the cyclopentadienide anion. The C_s symmetric azidopentazole ($N_5{-}N_3$; Fig. 6) is the lowest energy N_8 isomer, but is still 825 kJ mol^{-1} higher in energy than four separated N_2 molecules. Octaazapentalene (D_{2h}; Fig. 6), with 10π electrons, is also aromatic. Finally, the bispentazole with D_{2d} symmetry (Fig. 6) is the lowest energy N_{10} isomer, but is still 1090 kJ mol^{-1} higher in energy than five separated N_2 molecules.

Among all possible cyclic isomers of the N_6 molecule, only the analogues (see Fig. 6) of Dewar benzene (C_{2v}), benzvalene (C_{2v}), prismane (D_{3h}), and a twisted cyclotriene (D_2 form) have been found to represent stable minima. By contrast, the planar aromatic benzene analogue (D_{6h}) of this last cyclic triene was found to be a second-order saddle point, i.e., it is not even a transition state. The twisted open-chain diazide molecule (C_2), is the most stable N_6 isomer.

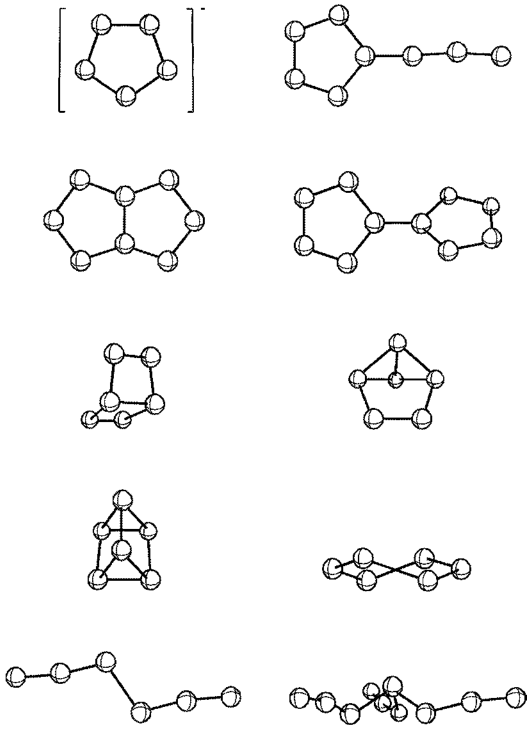

FIGURE 6 Structures of some quantum chemically investigated, still hypothetical, homopolyatomic nitrogen species. Proceeding from top left to bottom right: pentazole anion (D_{5h}), azidopentazole (C_s), octaazapentalene (D_{2h}), bispentazole (D_{2d}), hexaaza Dewar benzene (C_{2v}) hexaazabenzvalene (C_{2v}), hexaazaprismane (D_{3h}), twisted boat (D_2), diazide (C_2), nitrogen triazide (C_3).

For the elusive nitrogen triazide species N_{10} (also see Fig. 6), the *cis* structure (C_3) was calculated to be the most energetically favorable form but significantly less stable than the D_{2d} symmetric bispentazole (see above). We close this section by noting that none of these novel and still hypothetical polynitrogen species corresponds to any of the known allotropes of phosphorus.

VIII. NOBLE GASES

A. Identity and Alternate Names

Noble gases are the elements He, Ne, Ar, Kr, Xe, and Rn. These elements are also called "rare gases," although with Ar composing some 1% of the atmosphere, they are not particularly rare. There is also the earlier name "inert gases," which was belied some 40 years ago, and the briefly suggested, but never adopted, "aerogen" or "air-former."

B. Helium-Containing Species

As mentioned in an earlier section, all neutral species are able to bind with protons—they all are bases. Helium is the

least basic of the lot and binds a proton by almost 180 kJ mol^{-1}. While this so-called proton affinity is small, and indeed helium is the least basic of all neutral species, this binding energy is comparable to the iodine–iodine bond in elemental I_2 as well as the oxygen–oxygen bond in many peroxides. $[HeH]^+$ is rare and exotic, not because of its σ bond and being isoelectronic to the well known H_2, but because the helium–proton bond is both weak and labile: proton transfer to anything else in its chemical environment is exothermic and rapid. Isoelectronic to $[HeH]^+$ is $[LiH]^{2+}$, but this latter species is seemingly unknown and unbound. Unbound, but not unknown, is the isoelectronic $[He_2]^{2+}$. This seems like a contradiction in terms: what we mean to say is that there is a potential well, the species has a finite lifetime, but it is unstable relative to its separation products $2He^+$. We will not discuss its metastability other than to mention that it is related to the nonoligomerization of neutral helium and the slowness of most radioactive decay by α-particle emission. The process is called "tunneling," a wonderfully exotic phenomenon that is regrettably more in the province of the physicist than the inorganic chemist in the current context. We also note that this behavior is also found for most simple multiply charged cations: it is only the presence of "lots" of solvent, or an electrostatically stabilized counterion, that makes Ca^{2+}- and Fe^{3+}-containing species normal chemical species and not exotic as are the subvalent Ca^+ and Fe^+ seen in pulse-radiolysis experiments.

What about neutral helium-containing compounds? Atomic helium has been trapped inside dodecahedrane and buckminsterfullerene, analogous to other "endohedral" species to be discussed later. Are the resulting species $C_{20}H_{20}He$ and $C_{60}He$ organohelium compounds, or are they better understood as related to the long-known noble gas clathrates?

C. Xenon-Containing Species

We now jump to xenon. As mentioned earlier, xenon occurs with oxidation states 0–8. [Isolable Xe(I) species seem not to have been made, despite the seeming formation of $XePtF_6$ some 40 years ago that began "conventional"—pardon the oxymoron—noble gas chemistry.] With the value of 8, xenon shares the highest oxidation state value known in chemistry; only Os and Ru form analogous isolable (but in these cases, nonexplosive) tetraoxides. There is the value $+1/2$ as well, which is found in $[Xe_2]^+$. Having as precedents other $[NgNg']^+$ including $[He_2]^+$ as well as other noble-gas "ion–molecule complexes" such as $[ArN_2]^+$ and $[XeCO]^+$, $[Xe_2]^+$ is a rather stable ion. What is different is that the dixenon compound lacks the electron voracity of the helium and the other species. As such, despite a smaller dissociation energy and thus weaker bond than $[He_2]^+$, $[Xe_2]^+$ is capable of isolation as a solid salt. Xenon forms numerous species with the oxidation state $+2$ starting with XeF_2 and with a variety of other electronegative groups as well as salts containing the fluorine-conjugate acids $[XeF]^+$ and $[Xe_2F_3]^+$ ions.

There are also numerous species of the type HXeY that are perhaps best described as ion pairs HXe^+Y^- that are frozen in their matrix and so cannot revert and rearrange by proton transfer to form $Xe + HY$ from whence they came. The tetravalent and hexavalent XeF_4 and XeF_6 have chemistry generally not unlike XeF_2. A big difference is their anion chemistry: the former reacts with fluoride salts to form the aforementioned $[XeF_5]^-$ ion, the latter is the thermally highly stable $[XeF_8]^{2-}$ with its nine electron pairs but the very rare square antiprism geometry. Furthermore, the hydrolysis of XeF_4 and XeF_6 readily gives the explosive, isolable (at one's risk) xenon trioxide and xenon tetraoxide. Interestingly, the equally sensible xenon monoxide and dioxide remain uncharacterized and all but unknown and unstudied, a situation reminiscent of the valence isoelectronic oxyanions of sulfur. There is much that is known and much that remains strange about noble gas chemistry and the seemingly related chemistry of other nonmetals.

D. Compounds of the Other Noble Gases

What about neon, argon, krypton, and radon? We close this section with brief notes about these other noble gases. Pun intended, there is nothing new about neon. The chemistry of argon has been revolutionalized by the formation of H—Ar—F and its stability up to 27 K. The question of whether any argon compound will be isolable under ambient conditions remains tantalizingly plausible, with still unknown $[ArF]^+$ salts. The chemistry of krypton remains dominated by the binary, divalent fluoride KrF_2 that has the interesting property of being thermodynamically and kinetically stable with regard to the cleavage of one bond but not both, while being immune to the latter for a variety of extrathermodynamic reasons. (In fact, this is not unique to KrF_2: formaldehyde has the same bond-cleaving characteristics and is only metastable relative to $CO + H_2$.) And radon? We only wonder what exotic chemistry would arise from radon (and its neighbors such as the heaviest alkali metal, francium, and heaviest halogen, astatine) were it not so radioactive as to dissuade the general chemical community from its study.

It is to be acknowledged now that a result being exotic does not preclude its intelligibility nor even the absence of "simple" explanations. Such is the case with the existence of compounds of the heavier noble gases, krypton and xenon (and radon) as opposed to (at least, currently) those of the lightest noble gases, helium and neon. Noble gases do not want to accept electrons; their singly negative

ions are unbound. Helium and neon are particularly loathe to lose electrons: their ionization energies (ionization potentials) exceed those of any other element or group. To date, helium and neon remain inert. Argon also has a high ionization energy and so ArF_2 remains unobserved. By contrast, the proton affinity of argon is sufficiently high (ca. 369 kJ mol^{-1}) to make HAr^+ quite stable, both on its own and as part of a major resonance contributor to H—Ar—F. Accordingly, this last species enjoys existence under at least cryogenic conditions.

IX. TRANSITION METAL COMPLEXES WITH EXOTIC LIGANDS AND GEOMETRIES

The geometries and reactivities found for transition metal complexes are very diverse. This can partly be attributed to the fact that transition metals tolerate a variety of oxidation states and coordination numbers. Furthermore, the electronic situation of the participating ligands can change dramatically upon coordination to the metal ion. It is therefore not surprising that many unusual molecules are found within this class of compounds.

A. Stabilizing Highly Reactive Molecules

The strong influence of transition metals on the reactivity of coordinated ligands is highlighted by the fact that a variety of molecules known to be intrinsically difficult to synthesize have been isolated in the form of metal complexes. The antiaromatic cyclobutadiene, for example, is highly reactive and its isolation generally requires low-temperature matrices (ca. −260°C). Coordinated to a metal fragment, the stability is significantly enhanced, as highlighted by the fact that the iron carbonyl complex (**7**; mp 27°C) can be distilled for purification (bp 48°C, 3 mm). A similar situation is encountered with the extremely strained alkyne benzyne, which was stabilized in the coordination sphere of an organometallic zirconium complex (**8**; (Me = CH_3, Cp = C_5H_5).

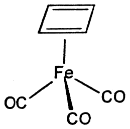

7

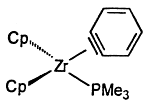

8

B. Planar Tetracoordinate Carbon

In 1874 J. H. van't Hoff and J. A. Le Bel proposed independently a tetrahedral geometry for tetracoordinated carbon atoms. Despite heavy initial criticism, this concept became one of the fundamental principles of modern organic chemistry. In organometallic chemistry, however, the situation can be different. Albeit still a rarity, a tetracoordinated carbon atom can adopt a planar geometry when it is surrounded by one or more metal fragments, with zirconocenes ["Cp_2Zr" or $Zr(C_5H_5)_2$] being especially suited (**9**). The smallest (fewest number of electrons as well as fewest number of atoms) molecular species with a planar tetracoordinated carbon atom is $[Al_4C]^-$. Other tetracoordinated nonmetals may presumably also be coerced into a planar geometry. The square planar phosphonium cation (**10**) was recently characterized, so far the only example of its kind.

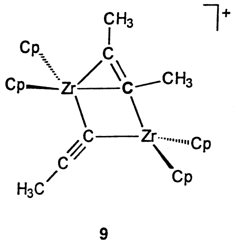

9

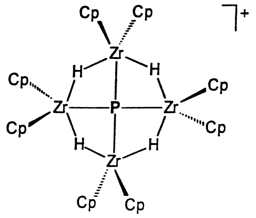

10

C. Unusual Coordination Numbers for Main Group Elements

In the presence of transition metals, main group elements not only can adopt rare geometries but can also display unusual coordination numbers. In 1995 the synthesis of a phosphido complex with a terminal P_1 ligand was described (**11**). A triple bond to a unicoordinate phosphorus atom was proposed similar to the phosphaalkynes (R—C≡P). Hypervalent carbon atoms with the coordination number six were found for the aforementioned gold complex (**12**). Structurally related are the carbido (**13**) and the nitrido cluster (**14**) in which a carbon and nitrogen atom are surrounded by six ruthenium carbonyl and five iron carbonyl fragments, respectively. Just about the time that precedents are being established for six-coordinated carbon, high-level computational theory has suggested that its realization in a planar hexagonal geometry may be realizable in $[CB_6]^{2-}$, CB_6H_2, and (three isomers, no less!) C_3B_4.

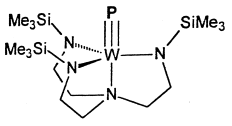

11

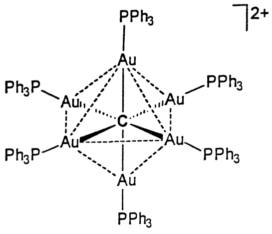

12

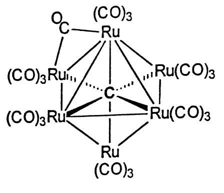

13

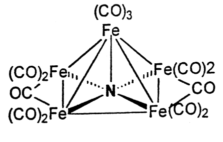

14

D. Carbon Monoxide as a Ligand

Carbon monoxide is a ligand of central importance in organometallic chemistry. Most transition metals form homoleptic carbonyl complexes (CO as the only ligand), several of which can be isolated under ambient conditions. The reason for the success of CO is its ability to act as a good σ-donor/π-acceptor ligand. This electronic flexibility was the basis for some unexpected discoveries in recent years. The transition metals chromium and iridium are commonly found in positive oxidation states. Surrounded by carbonyl ligands, however, negative oxidation states such as −IV in $[Cr(CO)_4]^{4-}$ and −III in $[Ir(CO)_3]^{3-}$ were observed. These "superreduced" carbonyl metallates can be considered modern extensions of the well known $[Fe(CO)_4]^{2-}$, the alkyl derivatives of which have found applications in organic synthesis. The variability of CO as a ligand is highlighted by the synthesis of carbonyl cations such as $[Fe(CO)_6]^{2+}$ and $[Ir(CO)_6]^{3+}$ as well as of the calcium and uranium mixed cyclopentadienyl/carbonyl complexes $[C_5(CH_3)_5]_2Ca(CO)$ and $[C_5(CH_3)_4H]_3U(CO)$. Remarkably, the ν(CO) stretching bands in the infrared spectra of the iridium carbonyls $[Ir(CO)_3]^{3-}$ and $[Ir(CO)_6]^{3+}$ differ by more than 600 cm^{-1}.

E. Metals Bridged by Unsaturated Elemental Carbon Chains

Dinuclear complexes in which the two metal atoms are bridged by polyyne, unsaturated elemental carbon chains (**15**–**17**), have received considerable attention due to their unique properties. For example, upon oxidation, these complexes form metallacumulenes of the general formula $[L_nM{=}(C{=}C)_p{=}ML_n]^{2+}$, where L includes pentamethylcyclopentadienyl, [Cp*, $C_5(CH_3)_5$], triarylphosphine, [Ar_3P, Ar = Ph, C_6H_5, and Tol, p-$CH_3C_6H_4$], aryl, CO, and NO. With the fragment $[C_5(CH_3)_5]Re(NO)[P(C_6H_5)_3]$ as the capping, complex molecules with chains containing up to 20 carbon atoms have been synthesized. For compound **17** a rhenium–rhenium distance of 2.87 nm was estimated. These complexes can be considered the first step toward metal-capped, one-dimensional carbon allotropes.

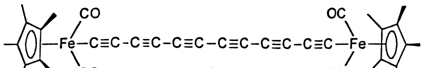

15

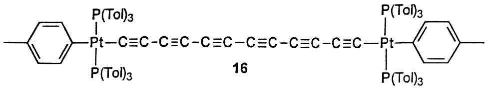

16

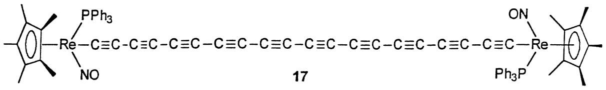

17

Following the same structural motif but going to the other extreme—short instead of long bridges—results in a single carbon atom surrounded by two metal atoms. A complex of this kind has been synthesized having a (TPP)Fe fragment on one side and an $Re_2(CO)_9$ fragment on the other (TPP = tetraphenylporphyrinato). The Fe—C bond length in (TPP)FeCRe$_2$(CO)$_9$ is only 1.60 Å, representing the shortest metal–carbon bond known, not that much larger than the C—C bonds found in the porphyrin assemblage or phenyl substituents.

F. Sandwich Compounds

In the early 1950s ferrocene (**18**), the first sandwich complex, was one of the most exotic inorganic molecules. Soon after, a variety of η^5-cyclopentadienyl complexes were discovered and ferrocene slowly come to be considered "normal." In 1965 it was shown that the open-cage carborane $[C_2B_9H_{12}]^{2-}$ ("dicarbollide") can be used instead of $[C_5H_5]^-$ ("cyclopentadienide") (**19**) (see Fig. 7), where in a formal way, we may say that the former contains 6-coordinated carbon. Since then, the coordination chemistry of carboranes has also flourished. An interesting feature of carborane ligands is that they are especially well suited to construct structurally unique compounds: the multidecker complexes. These rodlike molecules can be considered expanded sandwich complexes. So far, up to five metal ions have been staggered between slices of heteroaromatic ring systems. The hexadecker complex **20** (also shown in Fig. 7) was structurally characterized and contains four Co^{III} centers (with two associated hydrido ligands) and, remarkably, one Co^{IV} center.

Textbooks on organic chemistry depict molecules with single, double, and triple bonds between elements. For a certain class of dinuclear transition metal complexes this description is not sufficient and a quadruple bond between the two metal centers has to be introduced. The fourth bond is due to overlapping d orbitals with δ symmetry. Especially interesting are Cr_2L_4 complexes (L = bidentate, anionic ligand), some of which show extremely short metal–metal bonds (<2.00 Å). For $[Cr_2(5\text{-}CH_3\text{—}2\text{-}CH_3OC_6H_3)_4]$ (**21**) a chromium–chromium distance of only 1.83 Å was determined, the shortest metal–metal bond known.

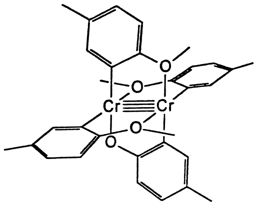

21

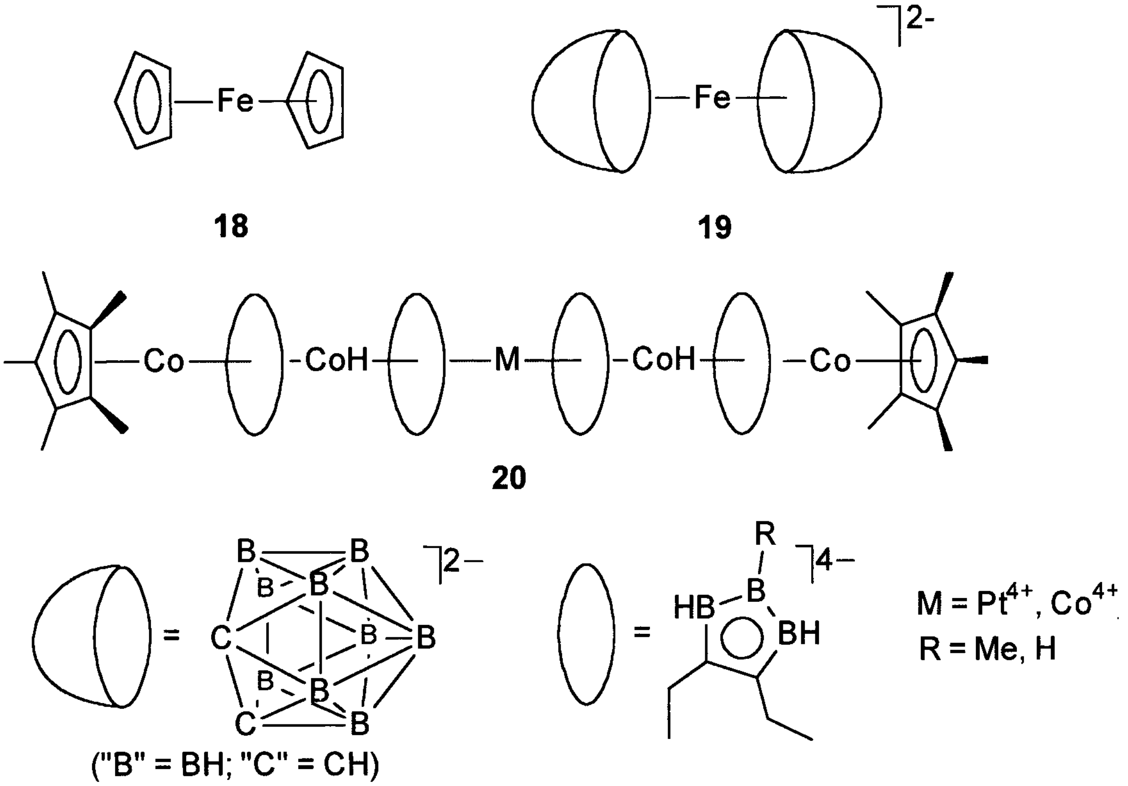

FIGURE 7 Structures of ferrocene (**18**), the related iron(II) bisdicarbollide anion (**19**), and a hexadecker, mixed cyclopentadienyl/triboracyclopentadienyl pentametal sandwich complex (**20**).

X. NANO-SIZED MOLECULES: CLUSTERS, FULLERENES, AND SELF-ASSEMBLED METAL COMPLEXES

"Nano-size," "clusters," "fullerenes," and "self-assembly" are key words in the description of "large" inorganic molecules. Rather than giving explicit definitions here, we give examples we hope will suffice.

A. "Moly Blue"

Soluble molybdenum blue (moly blue) is obtained if acid molybdate [Mo(VI)] solutions are reduced by chemical or physical means. Although these deeply colored solutions have been known for more than 200 years, it was not until recently that a more detailed structural characterization succeeded. Remarkably, the basic building blocks

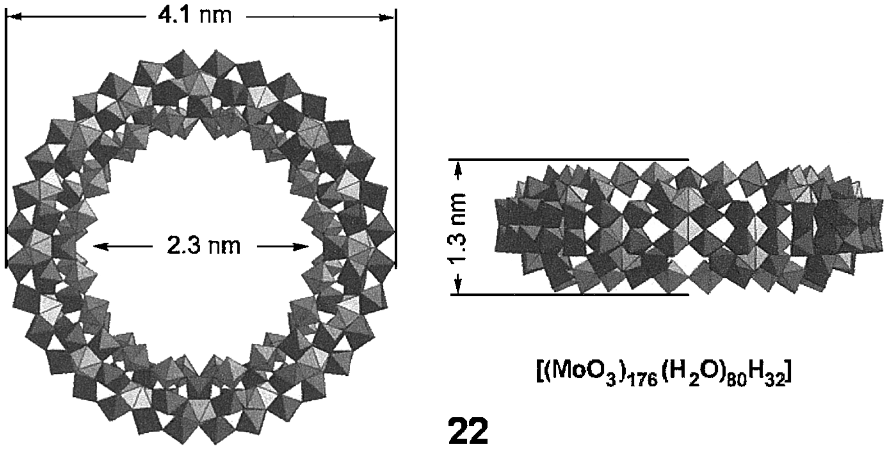

FIGURE 8 The nano-sized cluster "moly blue" (**22**).

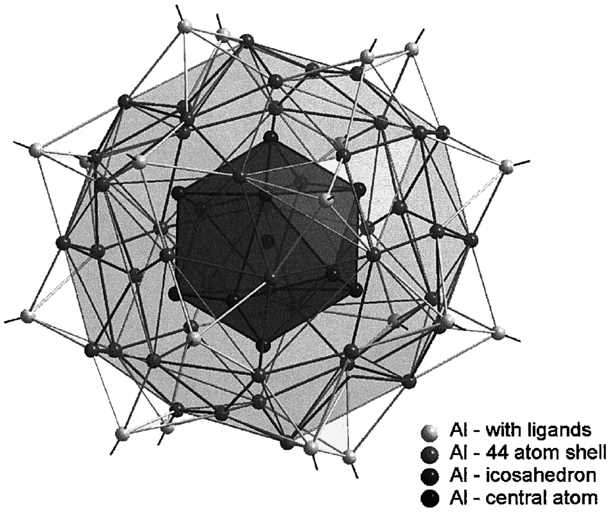

23

FIGURE 9 A-77 aluminum cluster (**23**).

correspond to giant wheel-shaped clusters made out of partially reduced MoO_3 units. Among others, the nano-sized cluster **22** was isolated. As shown in Fig. 8, **22** contains 176 Mo and 608 oxygen centers, representing one of the largest structurally characterized inorganic molecules. In the solid state, wheel-shaped clusters of this kind can form nanochannels or can encapsulate other, smaller clusters.

B. A 77-Aluminum Cluster

The largest molecular species containing metal–metal bonds that was characterized by X-ray diffraction is the Al_{77} cluster (**23**) as shown in Fig. 9. A central Al atom is surrounded by three concentric polyhedral shells containing 12, 44, and 20 Al atoms. Aggregation to form bulk metal is prevented by 20 $[N(SiMe_3)_2]$ ligands. Overall, the cluster can be considered an intermediate species to the formation of bulk, solid elemental aluminum.

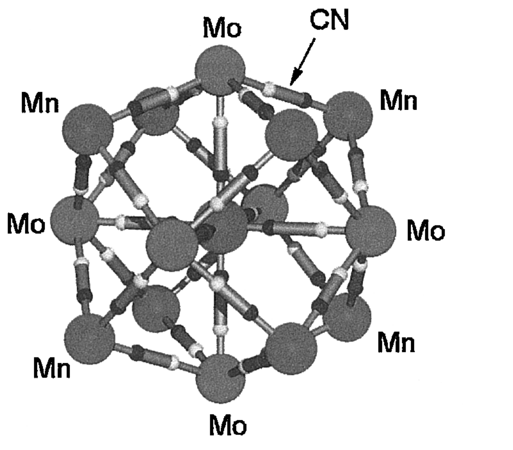

24 S = 51/2

FIGURE 10 An idealized structure for the core of an $S = 51/2$ Mn/Mo cluster (**24**).

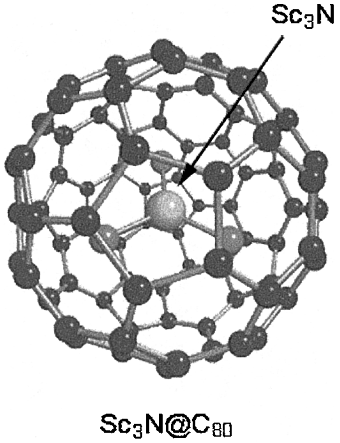

25

FIGURE 11 An endohedral scandium nitride fullerene cluster (**25**).

C. A Really High-Spin Molecule ($S = 51/2$)

Evidence that transition metal clusters can display highly unusual physical properties was recently provided by

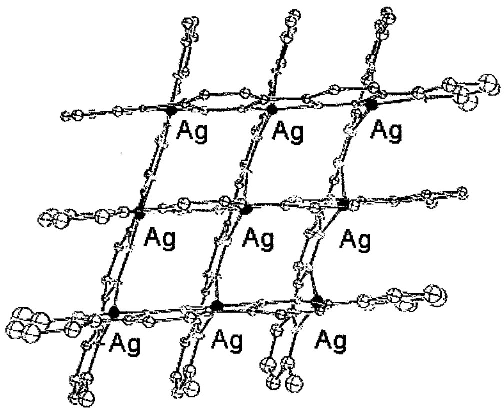

26

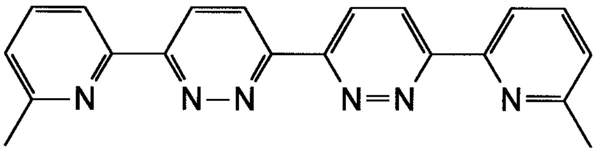

27

FIGURE 12 A grid formed with Ag^+ (**26**) and the hexacoordinating ligand itself (**27**).

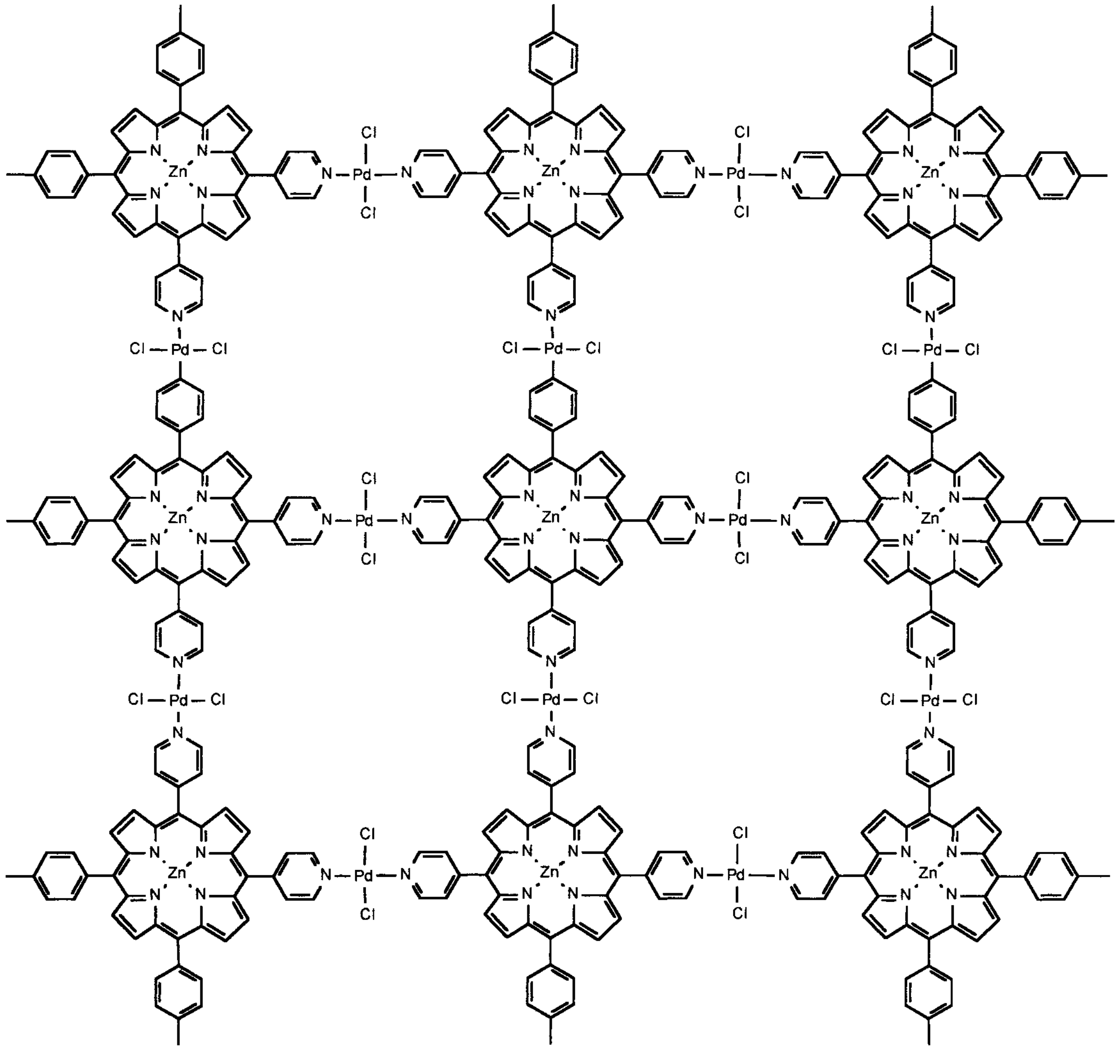

28

FIGURE 13 A zinc porphyrin–palladium(II) grid (**28**).

synthesizing the cyano-bridged cluster $[Mn^{II}\{Mn^{II}(MeOH)_3\}_8(\mu\text{-}CN)_{30}\{Mo^{V}(CN)_3\}_6]$ (**24**; an idealized structure without terminal ligands is depicted in Fig. 10). This compound, consisting of nine Mn^{II} ions ($S = 5/2$) and six Mo^{V} ions ($S = 1/2$), contains 51 unpaired electrons, the highest value found for a discrete molecule.

D. Fullerenes and Their Derivatives

Fullerenes are probably the most prominent ball-shaped molecules in organic chemistry. Repeatedly, this class of compounds has astonished the chemical community. One of these surprises was that fullerenes can encapsulate metal atoms as well as noble gases and atomic hydrogen (in formulas symbolized with "@," e.g. $Sc@C_{82}$). Endohedral metallofullerenes have been obtained with group 3 metals (M = Sc, Y, La), most of the lanthanides, group 2 metals (M = Ca, Sr, Ba), alkali metals (M = Li, Na, K, Cs), and some tetravalent metals (M = U, Zr, Hf). Remarkably, the metal atoms can stabilize fullerene geometries that are not known in the free form, such as C_{66}. Despite their unusual structures, metallofullerenes could have been considered "exotic" just because the synthetic yields are extremely low (0.1–0.01%). However, this might change in the future. An early step is the recent discovery that C_{80} fullerenes can encapsulate nitrido clusters such as Sc_3N with yields in excess of 3% (**25**; see Fig. 11).

This species may be considered multiply exotic. While widely studied, fullerenes remain exotic as a class of compounds; C_{80} is a very rare state of carbon aggregation.

Scandium chemistry is hardly commonplace; the Sc_3N core is unexpected.

C_{60} is a highly electrophilic molecule and numerous addition reactions of nucleophiles and electrons (to give C_{60}^{n-}, $n = 1$–6) are known. Another surprise was therefore the recent report of the protonated $[HC_{60}]^+$. To stabilize this unusual acid, the exceptionally inert $[CB_{11}H_6X_6]^-$ carborane anion was used (X = Cl and Br). (Have we become so jaded not to consider the anion "exotic" because its framework interpolates the "superaromatic" icosahedral $[B_{12}H_{12}]^{2-}$ and its dicarbon isoelectronic relatives, the isomeric *o*-, *m*-, and *p*-carboranes, $B_{10}C_2H_{12}$, and their numerous and diversely substituted derivatives?)

E. Molecular Grids

The synthesis of molecules of nanoscopic dimensions by controlled self-assembly is a rapidly growing field in inorganic chemistry. Based on defined transition metal–ligand interactions, amazingly complex and exotic structures have been built, such as one-dimensional helicates and tubes, two-dimensional polygons, as well as three-dimensional cages and polyhedra. The 3 × 3 molecular grid $[\mathbf{26}]^{9+}$ shown in Fig. 12 was synthesized in 99% yield by reaction of ligand **27** with 1.5 equiv of $[Ag(CF_3SO_3)]$. The structure of $[\mathbf{26}]^{9+}$ in the crystal reveals a rhombus-shaped geometry.

Another remarkable example of a grid like molecule was obtained by palladium(II)-directed self-assembly. The self-organization proceeds by coordination of nine zinc porphyrins having pyridine side chains to 12 $PdCl_2$ units, resulting in the 25-nm^2 grid (**28**) shown in Fig. 13. Interestingly, the assembly forms columnar clusters on silica surfaces that can be visualized by atomic force microscopy.

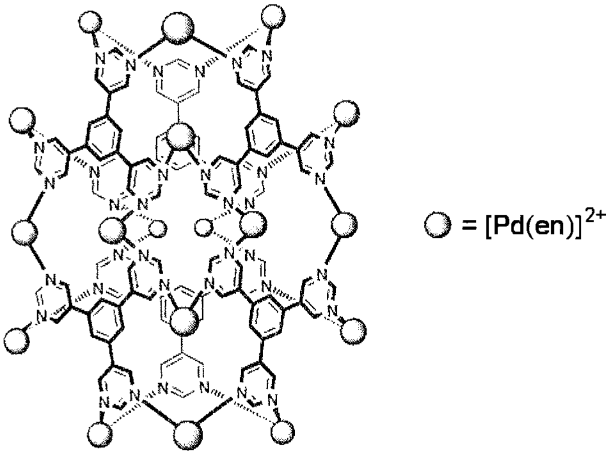

29

FIGURE 14 A palladium(II) trispyrimidylbenzene nanocage (**29**).

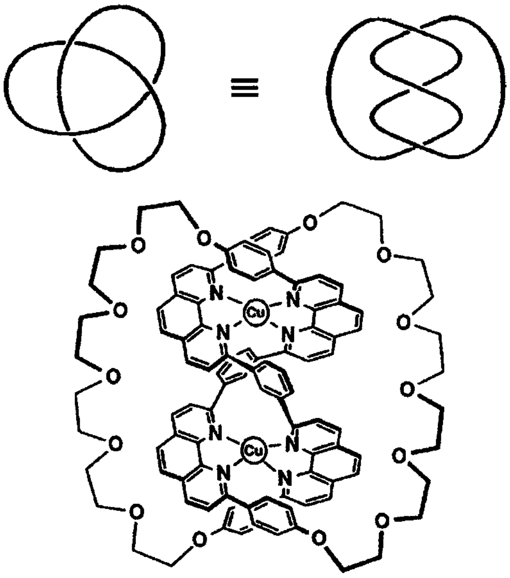

30

FIGURE 15 A trefoil copper phenanthroline knot (**30**).

F. Large Cages

Three-dimensional cages have been obtained using rigid C_3 symmetric ligands in combination with appropriate transition metals. One of the largest assemblies synthesized (**29**) is depicted in Fig. 14. The nanocage consists of six 1,3,5-tris(pyrimid-5-yl)benzene ligands and 18 $[Pd(en)]^{2+}$ (en = ethylene diamine) fragments and has dimensions of 3 × 2.5 × 2.5 nm. With an internal volume of about 0.9 nm^3, the polynuclear complex **29** is an ideal host for the encapsulation of large guest molecules.

G. Large Knots

To make a knot is a task easily accomplished by a child playing with a rope, or even by a careless adult with shoelaces. For a chemist playing with molecules this is an intrinsically difficult problem and so far only a few of these topologically interesting compounds have been synthesized. A strategy that finally led to success is based on the self-assembly of double-helical copper phenanthroline complexes. The helix represents the core structure from which the trefoil knot **30** in Fig. 15 is obtained in a final cyclization step. It is important to note that a trefoil knot is chiral. The resolution of the two enantiomers was recently accomplished by fractional crystallization of the diastereoisomers obtained with a chiral counterion.

XI. CONCLUSION

In this article we have assembled a collection of exotic species. The definition of the word "exotic" remains

awkward if atoms and self-assembled trefoil complexes can both cogently belong in our discussion, along with a variety of species of diverse stoichiometry, symmetry, and size that also qualify. Maybe it should suffice to paraphrase the platitude and say that the exotic, like the beautiful, is in the eye of the beholder. And the mind.

SEE ALSO THE FOLLOWING ARTICLES

Metal Cluster Chemistry • Nanosized Inorganic Clusters • Noble-Gas Chemistry • Organometallic Chemistry • Quantum Chemistry

BIBLIOGRAPHY

Atwood, J. L., Davies, J. E. D., Macnicol, D. D., and Vögtle, F. (eds.). (1996). "Comprehensive Supramolecular Chemistry," Vol. 9, "Templating, Self-Assembly, and Self-Organization," Pergamon Press, Oxford.

Berson, J. A., Birney, D. M., Dailey III, W. P., and Liebman, J. F. (1988). "Ethylenedione, its ions and analogues." *In* "Modern Models of Bonding and Delocalization" (J. F. Liebman and A. Greenberg, eds.), p. 391, VCH, New York.

Bochmann, M. (1994). "Organometallics 2: Complexes with Transition Metal–Carbon π-Bonds," Oxford University Press, New York.

Cotton, F. A., Wilkinson, G., Murillo, C. A., and Bochmann, M. (1999). "Advanced Inorganic Chemistry," 6th ed., Wiley, New York.

Dembinski, R., Bartik, T., Jaeger, M., and Gladysz, J. A. (2000). "Toward metal-capped one-dimensional carbon allotropes: Wire-like C_6–C_{20} polyynediyl chains that span two Redox-active (η^5-C_5Me_5)Re(NO)(PPh_3) endgroups," *J. Am. Chem. Soc.* **122,** 810.

Dietrich-Buchecker, C., Rapenne, G., Sauvage, J.-P., De Cian, A., and Fischer, J. A. (1999). "Dicopper(I) trefoil knot with *m*-phenylene bridges between the ligand subunits: Synthesis, resolution, and absolute configuration," *Chem. Eur. J.* **5,** 1432.

Dyson, P. J. (1999). "Chemistry of ruthenium–carbide clusters $Ru_5C(CO)_{15}$ and $Ru_6C(CO)_{17}$," *Adv. Organomet. Chem.* **43,** 43.

Ecker, A., Weckert, E., and Schnöckel, H. (1997). "Synthesis and structural characterization of an Al_{77} cluster," *Nature* **387,** 379.

Eliot, T. S. (1943). "Little Gidding," Part V. *In* "Four Quartets," Harcourt, Brace and Co., New York.

Ellis, J. E. (1990). "Highly reduced metal carbonyl anions: Synthesis, characterization and chemical properties," *Adv. Organomet. Chem.* **31,** 1.

Elschenbroich, C., and Salzer, A. (1992). "Organometallics. A Concise Introduction," Wiley-VCH, Weinheim.

Exner, K., and Schleyer, P. V. R. (2000). "Planar hexacoordinate carbon: A viable possibility," *Science* **290,** 1937.

Greenwood, N. N., and Earnshaw, A. (1984). "Chemistry of the Elements," Pergamon Press, Oxford.

Graham, L., Graudejus, O., Jha, N. K., and Bartlett, N. (2000). "Concerning the nature of $XePtF_6$," *Coord. Chem. Rev.* **197,** 321.

Harcourt, R. D. (2000). "Increased-valence structures for qualitative valence-bond representations of electronic structure for electron-rich molecules," *Eur. J. Inorg. Chem.* 1901.

Hunter, E. P., and Lias, S. G. (2000). "Proton affinity evaluation." *In* "NIST Chemistry Webbook," NIST Standard Reference Database Number 69, http://webbook.nist.gov (W. G. Mallard and P. J. Linstrom, eds.), National Institute of Standards and Technology, Gaithersburg, MD.

Jacox, M. E. (2000). "Vibrational and electronic energy levels of polyatomic transient molecules." *In* "NIST Chemistry Webbook," NIST Standard Reference Database Number 69, http://webbook.nist.gov (W. G. Mallard and P. J. Linstrom, eds.), National Institute of Standards and Technology, Gaithersburg, MD.

Klapötke, T. M. (1994). "New ionic, isoelectronic analogs of CO_2 and CS_2," *Angew. Chem. Int. Ed. Engl.* **33,** 1575.

Klapötke, T. M. (1999). "Ionic polyatomic nitrogen compounds." *Angew. Chem. Int. Ed. Engl.* **38,** 2536.

Klapötke, T. M., Schulz, A., and Harcourt, R. D. (1998). "Quantum Chemical Methods in Main-Group Chemistry," Wiley, Chichester, U.K.

Kraichtchev, L., Pettersson, M., Runeberg, N., Lundell, J., and Räsänen, M. (2000). "An isolable argon compound," *Nature* **406,** 874.

Larionova, J., Gross, M., Pilkington, H. A., Stoeckli-Evans, H., Güdel, H. U., and Decurtins, S. (2000). High-spin molecules: A novel cyano-bridged MnMo molecular cluster with a $S = 51/2$ ground state and ferromagnetic intercluster ordering at low temperatures. *Angew. Chem. Int. Ed. Engl.* **39,** 1605.

Leininger, S., Olenyuk, B., and Stang, P. J. (2000). "Self-assembly of discrete cyclic nanostructures mediated by transition metals," *Chem. Rev.* **100,** 853.

Li, X., Wang, L.-S., Boldyrev, A. I., and Simons, J. (1999). "Tetracoordinated planar carbon in the Al_4C^- anion. A combined photoelectron spectroscopy and ab initio study," *J. Am. Chem. Soc.* **121,** 6033.

Liebman, J. F., Chickos, J. S., and Simons, J. (1988). "Aspects of the estimation of physical properties of boron compounds by the use of isoelectronic and plemeioelectronic analogies." *In* "Advances in Boron and the Boranes: A Volume in Honor of Anton B. Burg" (J. F. Liebman, A. Greenberg, and R. E. Williams, eds.), p. 491, VCH, New York.

Liu, S., and Sun, S. (2000). "Recent progress in the studies of endohedral metallofullerenes," *J. Organomet. Chem.* **599,** 74.

Kravits, L., and Olitzky, K. M. (eds.). (1993). "Pirke Avot: A Modern Commentary on Jewish Ethics," UAHC Press, New York.

Mallard, W. G., and Linstrom, P. J. (eds.). (2000). "NIST Chemistry Webbook," NIST Standard Reference Database Number 69, http://webbook.nist.gov National Institute of Standards and Technology, Gaithersburg, MD.,

Meot-Ner (Mautner), M., and Lias, S. G. (2000). "Binding energies between ions and molecules and the thermochemistry of cluster ions." *In* "NIST Chemistry Webbook," NIST Standard Reference Database Number 69, http://webbook.nist.gov (W. G. Mallard and P. J. Mallard, eds.), National Institute of Standards and Technology, Gaithersburg, MD.

Müller, A., and Serain, C. (2000). "Soluble molybdenum blues—'des Pudels Kern,'" *Acc. Chem. Res.* **33,** 2.

Parsons, S., and Passmore, J. (1994). "Rings, radicals and synthetic metals: The chemistry of SNS^+," *Acc. Chem. Res.* **27,** 101.

Paul, F., and Lapinte, C. (1998). "Organometallic molecular wires and other nanoscale-sized devices. An approach using the organoiron (dppe)Cp*Fe building block," *Coord. Chem. Rev.* **178–180,** 431.

Pyykkö, P., and Runeberg, N. (1991). "Ab initio studies of bonding trends. Part 9. The dicyanamide–carbon suboxide–dicyanoether–cyanogen azide isoelectronic series A═B═C═D═E," *J. Mol. Struct. (Theochem)* **234,** 279.

Pyykkö, P., and Zhao, Y.-F. (1990). "Ab initio study of bonding trends. 4. The 22-electron A═B═C series: Possible new anions down to NCB^{4-}, possible new cations up to FNF^{3+}," *J. Phys. Chem.* **94,** 7753.

Quadbeck-Seeger, H.-J., Faust, R., Knaus, G., and Siemeling, U. (1999). "World Records in Chemistry," Wiley-VCH, Weinheim.

Rawls, A. (1999). "N_5^+ cation makes explosive debut," *Chem. Eng. News.* **1999**(January 25), 7.
Reed, C. A., Kim, K.-C., Bolskar, R. D., and Mueller, L. J. (2000). "Taming superacids: Stabilization of the fullerene cations HC_{60}^+ and $C_{60}^{\bullet +}$," *Science* **289,** 101.
Röttger, D., and Erker, G. (1997). "Compounds containing planar-tetracoordinate carbon," *Angew. Chem. Int. Ed. Engl.* **36,** 812.
Sacks, O. (1995). "An Anthropologist on Mars," Knopf, New York.
Scheer, M. (1995). "Terminal E_1 ligands from elements of group 15," *Angew. Chem. Int. Ed. Engl.* **34,** 1997.
Scherer, O. J. (1999). "P_n and As_n ligands: A novel chapter in the chemistry of phosphorus and arsenic," *Acc. Chem. Res.* **43,** 752.
Stephan, D. W. (2000). "'Breaking the rules': A planar phosphonium cation," *Angew. Chem. Int. Ed. Engl.* **39,** 501.
Wang, X., Sabat, M., and Grimes, R. (1995). "Organotransition-metal metallocarboranes. 44. construction of pentadecker and hexadecker sandwiches from triple-decker building blocks," *J. Am. Chem. Soc.* **117,** 12227.
Wojaczynski, J., and Latos-Grazynski, L. (2000). "Poly- and oligometalloporphyrins associated through coordination," *Coord. Chem. Rev.* **204,** 113.

Liquid Alkali Metals

C. C. Addison
University of Nottingham

I. Some Modern Applications
II. Basic Physical and Chemical Properties
III. Manipulation of the Liquids
IV. Purification
V. Alkali Metal Mixtures
VI. Species Formed by Dissolved Elements
VII. Electrical Resistivity
VIII. Reactions between Dissolved Elements
IX. Corrosion by the Liquid Alkali Metals

GLOSSARY

Coolant Fluid used to carry away heat from the core of a reactor.

Eutectic Term applied to the particular mixture of two or more substances that has the lowest melting point.

Fast nuclear reactor Reactor in which the neutrons are not slowed down by moderators.

Getter Element (usually a solid metal) that reacts with, and thereby removes, dissolved impurities in liquid metals by forming insoluble products.

Ionization potential Energy required to detach an electron from an isolated gaseous atom of the element.

Solute Constituent of a solution that is considered to be dissolved in a liquid, termed the solvent.

Solvation Process whereby an atom or ion dissolved in a liquid attracts to itself atoms or molecules of the liquid medium, with consequent release of energy.

THE ALKALI METALS lithium, sodium, potassium, rubidium, and cesium constitute the first group of elements in the periodic table and have quite exceptional properties. They have low melting points and can be manipulated readily in the liquid state. The liquids are finding ever-increasing use as coolant fluids in, for example, fast nuclear reactors and high-temperature storage batteries. The liquids also have low viscosity, low density and high thermal conductivity, which makes them particularly suited for use as heat-transfer media. The liquid alkali metals can also act as solvents for other elements such as carbon, oxygen, nitrogen, hydrogen, and heavier elements. The presence of these elements in solution renders the liquid metals corrosive, but techniques have now been developed for their monitoring and removal.

I. SOME MODERN APPLICATIONS

Sodium and lithium have wide industrial application, and two examples of this are given below. Other promising future applications include the use of sodium in solar power plants, in which the sun's energy is concentrated by mirrors onto a central receiver, from which heat is removed by flowing sodium. Potassium is finding application in turbine technology. The thermal efficiency of a heat cycle is increased by raising the peak temperature of the cycle, but corrosion problems usually restrict the available upper temperature. Efficiency can be increased by the use of an intermediate cycle, the *topping cycle*, which is stable at a higher peak temperature. Potassium is the most useful fluid for this purpose because of its availability, compatibility with steels, and vapor pressure. No large-scale applications have yet been found for rubidium or cesium, but these may well develop when their properties are better understood. They have been studied for use in vacuum tubes and photoelectric cells, ion propulsion engines, and power generation by means of magneto-hydrodynamics and thermionic conversion. These applications take advantage of the very low ionization potentials of the rubidium and cesium atoms.

A. Nuclear Reactors

The fast nuclear reactor provides the best example of the use of a liquid alkali metal on a large scale. Neutrons in a fast nuclear reactor are not slowed down by moderators, and high reactor temperatures are involved. The coolant must be capable of removing large quantities of heat from the reactor, and only a liquid metal can satisfy all the requirements. An experimental reactor, the Dounreay fast reactor (DFR), was assembled during 1950–1959 and employed 120 metric tons of a mixture of sodium and potassium. This alloy was chosen because at the eutectic composition the alloy is liquid down to $-12°C$. After several years experience with this alloy, the use of pure sodium alone as coolant was no longer a problem. Relevant physical properties of sodium are given in Section II. In particular, its wide liquid range of temperature is ideally suited to reactor conditions. A prototype fast reactor (PFR) was then built at Dounreay, in 1974, that used 1150 metric tons of liquid sodium as coolant. Because of its low density and low viscosity, the sodium can be circulated at rates as high as 3000 l/sec. Much larger reactors are now envisaged; the planning and design of the first commercial demonstration fast reactor (CDFR) is well advanced and will incorporate up to 7000 metric tons of liquid sodium.

Liquid lithium may play a key role in the fusion reactors of the future. Increasing effort is being devoted throughout the world, notably in the United States, Russia, Japan, and Europe, to means of tapping the limitless supply of energy that is potentially available from the thermonuclear fusion of light nuclei. The reaction most likely to be exploited is fusion of deuterium and tritium. The latter can be produced by irradiation of the ^{6}Li isotope with thermal neutrons, and fast neutrons (>1 MeV) can yield significant additional tritium from ^{7}Li. This yield can be an important contribution in attaining a breeding rate above unity. The core of the reactor may be surrounded by a blanket of liquid lithium, but at this stage of development many other substances (e.g., Pb_4Li) are under consideration as blanket fluids. The unique property of lithium is therefore that it can serve both as a tritium breeder and as a heat-transfer medium.

B. Rechargeable Batteries

A new generation of batteries is under development that has distinct advantages over the traditional lead–sulfuric acid batteries both in terms of weight and energy density, and which can be adapted to road or rail transport. Most attention to date has been applied to the sodium–sulfur battery, in which liquid sodium and liquid sulfur are separated by a diaphragm of β-alumina. The cell is operated at 300–350°C, and the cell reaction is

$$2Na + 3S = Na_2S_3$$

Corresponding cells containing liquid lithium and sulfur have not yet been developed to the same extent, though higher specific energies are theoretically possible; Because of its higher reactivity toward the diaphragm, there are more problems in handling liquid lithium than with liquid sodium.

The lithium–chlorine battery is light in weight and is unsurpassed in the high level of energy (20 times that of the lead–acid battery) that can be achieved. One modification of this battery can be operated at temperatures around 350°C, but its wide application is again restricted by problems of corrosion.

II. BASIC PHYSICAL AND CHEMICAL PROPERTIES

A. Physical Properties

Some important properties of the alkali metals are collected in Table I. Unless otherwise stated, values are quoted for 200°C, at which temperature all the alkali metals are liquid, and corresponding values for water and mercury are quoted for comparison. The alkali metals clearly show the influence of increasing atomic mass

TABLE I Physical Properties of the Liquid Alkali Metals

	Li	Na	K	Rb	Cs	H_2O	Hg
Melting point (°C)	180.5	97.8	63.2	39.0	28.5	0	−39
Boiling point (°C)	1317	883	754	688	671	100	357
Liquid range (°C)	1138	785	697	649	642	100	396
Density (kg/m^3 at 200°C)	507	904	797	1390	1740	990 (50°C)	13,100
Viscosity (cp) at 200°C	0.565	0.450	0.300	0.346	0.350	0.55 (50°C)	1.01
Surface tension at 200°C (N m^{-1} × 10^{-3})	398	195	103	76 (39°C)	74 (105°C)	68 (50°C)	436
Vapor pressure (Torr) at 200°C	10^{-9}	1.5×10^{-4}	0.006	0.04	0.08	92 (50°C)	17
Heat of fusion (kJ mol^{-1})	2.93	2.64	2.39	2.20	2.09	6.01	2.3
Heat of vaporization (kJ mol^{-1})	147	99.2	79.1	75.7	66.5	41.1	59.1
Specific heat at 200°C (J mole^{-1} deg^{-1})	3.51	1.34	0.786	0.463	0.447	4.18 (50°C)	0.134
Thermal conductivity at 200°C (J cm^{-1} sec^{-1} deg^{-1})	0.42	0.84	0.56	0.31	0.21	0.0067 (50°C)	0.12
Electrical resistivity at 200°C ($\mu\Omega$ cm)	29.1	13.5	20.6	35.8	56.6	$>10^6$	114
Volume increase on melting (%)	1.5	2.17	2.41	2.54	2.66	−0.014	3.6

and size on the physical properties of the bulk liquid. Thus, melting and boiling points, surface tension, viscosity, heats of fusion, and vaporization and specific heat all decrease along the series lithium to cesium, while vapor pressure and volume change upon fusion increase steadily along the series. In some properties, for example, density, lithium appears to be anomalous; this is due to the exceptionally small size and high charge–radius ratio of the Li^+ ion. It should be noted that the melting point of cesium is below blood temperature, so that a sample of cesium in a glass vessel can be melted in the hand. Also, the density and viscosity of liquid sodium are not greatly different from the values for water, so that operations such as pouring, pumping, stirring, and general manipulation of the liquid in the laboratory on a liter scale are much more like those for water than for mercury.

B. Chemical Properties

The major difficulty encountered in the manipulation of the liquid metals on a laboratory or industrial scale arises from their vigorous chemical reactivity with other elements and compounds; the vigorous nature of their reaction with water is well known, and other examples are mentioned in later sections. In most cases, reactivity increases with electropositive nature from lithium to cesium. Thus, lithium reacts gently with water, sodium reacts vigorously, potassium ignites, and rubidium and cesium explode. On the other hand, liquid lithium reacts readily with nitrogen, whereas the other alkali metals do not. Apparatus for handling the liquid metals are therefore necessarily designed with this reactivity in mind.

III. MANIPULATION OF THE LIQUIDS

A. The Cover Gas

The free space inside any equipment that contains a liquid alkali metal must be filled with a gas that will not react with the metal, and because of the chemical reactivity mentioned above, the choice of an acceptable cover gas is limited. All the alkali metals react with hydrogen and oxygen, but only lithium reacts with nitrogen. Therefore, nitrogen is a suitable cover gas for liquid sodium, potassium, rubidium, and cesium, but not for liquid lithium. Argon is the ideal cover gas, and because of its chemical inertness it can be used for any of the alkali metals. It is the most common cover gas used in industry. As with nitrogen, however, it must be scrupulously purified. As an indication of this, argon that is available commercially with greater than 99.99% purity will cause a film to form almost immediately at the clean surface of a liquid alkali metal. Elaborate gas purification trains have been devised involving the use of molecular sieves and passing the gas over hot calcium, titanium, or uranium chips. As a final treatment the gas can be bubbled through liquid sodium–potassium alloy.

B. Container Materials

Glass has very limited use. No glass is inert toward liquid lithium, and attack begins almost immediately upon contact. The glass first darkens, and its structure then collapses. Liquid sodium attacks glass more slowly, and Pyrex® glass can be used to contain liquid sodium at lower temperatures. Attack is evident by discoloration of the glass through yellow and brown to black; at 200 and

300°C, attack becomes evident in 3 days and in several hours, respectively. The discoloration of glass is due partly to the elemental silicon produced by the reduction process

$$4M + SiO_2 = 2M_2O + Si$$

and partly by penetration of alkali metal atoms into the glass. Attack on glass by liquid potassium, rubidium, and cesium is somewhat slower than that by sodium at similar temperatures. However, because of their lower melting points, these metals can be handled as liquids at lower temperatures. A sample of cesium that had been kept under argon in a glass vessel at room temperature gave no sign of attack after 4 years.

In practice, the liquid alkali metals are handled almost entirely in equipment constructed from transition metals. The refractory metals (e.g., titanium, zirconium, vanadium, chromium, molybdenum, and tungsten) are all useful, but they are expensive and sometimes difficult to fabricate and are reserved for parts of the industrial plant where their special properties are needed. The element that finds by far the widest use is iron, and by alloying iron with chromium and nickel it is possible to devise steels that are appropriate for the various experimental conditions and temperatures. All the main components of a steel have some slight solubility in liquid sodium, and where many tons of sodium are circulating in steel containers this can be significant. Some relevant solubility values are quoted in Table II. With liquid sodium, steels can be devised in which this solubility problem is minimized, but the chemistry of liquid lithium–steel interactions is different in two important respects. First, since nitrogen has a considerable solubility in liquid lithium (1.7 mol% at 420°C), it replaces oxygen as the element mostly responsible for corrosion of steels by liquid lithium. Second, the solubility of iron and the alloying elements (especially nickel) are much higher in liquid lithium than in liquid sodium, and even for short-term laboratory experiments it is desirable to contain liquid lithium in pure iron vessels.

C. Stirring

Stirring the liquid alkali metals inside suitable containers is more difficult than with most liquids because of the need to maintain perfect protection from the atmosphere. However, since the liquid is a metal it is possible to take advantage of the electromagnetic effect, and all the liquid alkali metals can be stirred readily by rotating a permanent magnet outside the containing vessel. This technique has now been generally superseded by the electromagnetic pump, which employs the principle that if a conductor carrying a current is placed at right angles to an applied magnetic field, there will be a mechanical force on the conductor in a direction perpendicular to both the magnetic field and the direction of the current. Small pumps can be incorporated into steel containers for laboratory work, at temperatures up to 500°C. Extensive use of electromagnetic pumps has also been made for circulating the alkali metal in sodium-cooled fast reactors; these are large-capacity pumps requiring correspondingly high currents and powerful electromagnets and are now being superseded by mechanical (centrifugal) pumps.

TABLE II Approximate Solubilities of Some Metals at 650°C in Liquid Lithium and Liquid Sodium

Solute metal	Solubility (ppm by weight)	
	In liquid lithium	In liquid sodium
Ni	1000	1.7
Cr	15	0.12
Fe	16	1.0

IV. PURIFICATION

The solubility in the liquid alkali metals of those metals that can be used as containers is quite small and can usually be measured in parts per million. The solubility of most of the nonmetals is also small. Nevertheless, it is these small concentrations of metals and nonmetals that are responsible for many of the problems that arise in the industrial use of the liquid alkali metals. For this reason, much attention has been paid to methods of purification and analysis of the liquid metals. Heavy metal impurities are introduced as a result of corrosion of structural metals either during production or storage. The main metallic impurity in sodium is calcium, which results from the production of sodium by electrolysis of $NaCl–CaCl_2$ mixtures. The main nonmetallic impurities are hydrogen and oxygen (from contact with the atmosphere and moisture), carbon (from structural steels) and nitrogen, which is only important in the case of lithium. Some solubility values are given in Table III. They illustrate the influence of temperature and the very high solubility of oxygen in liquid rubidium and cesium, which is exceptional. There are three main methods of purification, involving filtration, gettering, or distillation.

A. Filtration

The liquid metals can be readily filtered by passage through sintered plates made from glass or steel. Simple filtration at constant temperature will merely remove suspended foreign matter, but advantage is taken of the fact that solubilities in the alkali metals decrease with

TABLE III Solubilities of Nitrogen and Oxygen in the Liquid Alkali Metals

	Solubility (at.%)					
		Oxygen in				
Temp. (°C)	Nitrogen in lithium	Li	Na	K	Rb	Cs
50	—	—	—	—	—	19.7
100	—	—	0.0004	0.24	21.0	20.3
150	—	—	0.0015	0.44	23.3	22.7
200	0.086	0.0009	0.0039	0.67	24.2	25.1
300	0.416	0.0099	0.0185	1.46	26.4	26.2
400	1.450	0.051	0.0534	3.70	31.2	27.6

decreasing temperature. It is clear from Table III, for example, that if sodium is filtered at a temperature near its melting point, the oxygen content will be reduced to a few parts per million. This is the function of the "cold traps" that are inserted in metal coolant circuits. A second method by which a soluble impurity can be rendered insoluble, and thus filterable, is to add another element that will form an insoluble product with the impurity. Using the removal of calcium from sodium as an example, the free energies of formation of the two oxides lead to the equation

$$Na_2O + Ca \rightarrow CaO + Na \qquad (-240 \text{ kJ/g atom O})$$

so that the forward reaction is favorable and calcium impurity is precipitated as calcium oxide by addition of oxygen. Excess oxygen is removed by filtration of the sodium at its melting point.

B. Gettering

Gettering is a general term for the removal of impurities (usually nonmetals) by converting them into more stable compounds that are insoluble in the liquid metal. The elements (usually metals) that are added for this purpose are termed *getters* and are usually insoluble in the liquid metals. The getter can thus be immersed in the liquid metal, held there until it has collected the impurity, and then withdrawn. The use of insoluble getters on an industrial scale is termed *hot trapping*. In the general equation

$$L[X] + M \rightarrow MX + L \qquad (-\Delta G)$$

the efficiency with which the getter M will remove impurity X from the liquid metal L to produce the insoluble surface film MX on the getter will be dictated, in the first place, by the magnitude of the free energy change associated with this reaction. Taking oxygen as a typical example, reference can be made to the values for the free energies of formation of the oxides given in Table IV. The

TABLE IV Values of Free Energy of Formation ($-\Delta G_f^\circ$) for Metal Oxides at 327°C [a]

Oxide	$-\Delta G_f^\circ$	Oxide	$-\Delta G_f^\circ$	Oxide	$-\Delta G_f^\circ$
Li_2O	497	MgO	543	Y_2O_3	574
Na_2O	333	CaO	573	TiO_2	419
K_2O	273	SrO	530	ZrO_2	489
Rb_2O	248	BaO	500	ThO_2	556
Cs_2O	224	Fe_2O_3	231	UO_2	490
		Cr_2O_3	326	Al_2O_3	496
		NiO	184		

[a] Kilojoules per gram atomic oxygen.

greater the difference between the $-\Delta G$ values for the getter oxide and the oxide of the liquid metal, the greater will be the potential value of the metal M as a getter. It is evident that all the metals listed in the third column of Table IV have potential use as getters for sodium, potassium, rubidium, and cesium but that only yttrium and thorium are likely to remove oxygen from liquid lithium. Similar comparisons of the free energies of formation of the hydrides, nitrides, and carbides of the metals can be made. It is often possible, particularly in the laboratory, to maintain an impurity at very low concentration by suitable choice of container materials. For example, in experiments in which the reactivity of sodium with various other materials is being studied, the oxygen content of the sodium can be kept low by the use of zirconium crucibles. Again, one of the best getters for carbon dissolved in liquid sodium is stainless steel (e.g., austenitic-type 316 steel), and therefore liquid sodium in a stainless steel container always has a low carbon content.

C. Distillation

Because of the relatively high vapor pressure of the alkali metals compared with most other metals, distillation is an acceptable method of purification. Distillation under reduced pressure lowers the distillation temperature and thereby reduces the risk of contamination from the condenser. Vapor pressures increase from lithium to cesium (Table I). In the case of cesium (and also rubidium), the vapor pressure is sufficiently high that the type of glass still used for molecular liquids (e.g., water or alcohol) can be used for the alkali metal also. Removal of transition metals by distillation is virtually complete. With cesium, the high solubility of oxygen renders the filtration method unsuitable, whereas distillation is efficient.

With potassium, sodium, and lithium the vapor pressures become progressively lower, and distillation of appreciable quantities of these metals in glass apparatus is not practicable. For special cases, equipment can be designed, in steel, in which the vapor distance is reduced, but

these three metals are more readily purified by filtration and gettering.

D. Continuous Monitoring of Impurities

When a liquid metal is used as a coolant fluid, it is pumped around a circuit that carries away heat from the heat source. In the case of liquid sodium in the nuclear reactor, for instance, it is essential that information of any change in impurity levels should be available immediately, as would be the case if leakage of water, for example, into the circuit was to occur. For this reason, sampling and chemical analysis by traditional methods are no longer acceptable, and the withdrawal of liquid metal samples could itself introduce impurities. A simple device that has been in use for some years is the *plugging meter*. Part of the sodium flow is diverted through a bypass that carries an orifice, the temperature of which can be controlled. As the temperature of the bypass is decreased, the saturation temperature of the impurity (e.g., oxygen) is eventually reached, and precipitation of the impurity (e.g., sodium oxide) restricts the flow of the liquid sodium. This occurs at the *plugging temperature*, and with suitable calibration the plugging temperature can be related directly to the impurity concentration. For example, if the impurity were oxide and the plugging temperature 200°C the impurity level would be about 10 parts per million by weight of oxygen. The plugging meter is a rather crude instrument since it cannot be specific for any one impurity; nevertheless, it is still regarded as a most reliable and rugged indicator of total impurity levels.

Methods are now available that provide a continuous record of specific impurities. These are mostly electrochemical in nature, but an interesting alternative technique has been developed in the United Kingdom, the United States, France, The Netherlands, and Russia, for metering hydrogen in solution. This technique is based on the ability of hydrogen to diffuse, from solution in sodium, through a thin nickel membrane. The methods differ in detail, but all employ the same principle. A tube carrying a nickel membrane is inserted into the sodium stream. Hydrogen diffusing from solution through the membrane is swept away in a stream of argon, and its concentration measured by ion pump or Katharometer. The rate and extent of this diffusion can give a direct measure of the hydrogen in solution. A technique employing a similar principle is in use for the determination of carbon in liquid sodium. The instrument makes use of a tube incorporating an α-Fe membrane, the inner surface of which has been oxidized to form a film of iron oxide. When immersed in liquid sodium (at 500–750°C) carbon diffuses through the iron membrane. Upon reaching the inner surface, the carbon reacts with the iron oxide film to form gaseous oxides of carbon (CO and CO_2) that are swept away by a flow of argon gas. The rate at which carbon diffuses through the membrane is proportional to the activity of carbon in the sodium.

Methods based on electrochemical cells come closest to satisfying the demands for continuous monitoring of specific impurities, and such meters for hydrogen, oxygen, and carbon in solution in sodium have been the subject of extensive research. They not only provide the basis for reactor instrumentation but are also finding increasing use in the research laboratory. The meters are, in effect, concentration cells and thus incorporate two electrodes and a conducting electrolyte; one electrode is the liquid metal. In the case of the hydrogen meter, a mixture of calcium chloride with calcium hydride forms the electrolyte, and the reference electrode is a lithium metal–lithium hydride mixture that provides a fixed hydrogen activity at a fixed temperature. The electrochemical oxygen meter differs from the hydrogen meter in that a solid electrolyte is available that is compatible with liquid sodium. The electrolyte in common use is a solid solution of yttrium oxide (Y_2O_3) in thorium oxide (ThO_2) through which electrical conduction takes place by migration of oxygen ions. A platinum–air reference electrode system has been widely used both in the United States and the United Kingdom, and reference electrodes consisting of metal–metal oxide couples (particularly the indium couple In–In_2O_3) are also suitable. In the carbon meter, attention has been centered around liquid electrolytes. During the 1970s, cells were described that used solutions of acetylides (e.g., CaC_2 in molten $CaCl_2$ or Li_2C_2 in molten LiCl–KCl mixture) as electrolytes. These appear to be unsuitable, partly because of their chemical instability, and in 1982 a satisfactory meter was described that used a molten mixture of anhydrous sodium carbonate and lithium carbonate. This electrolyte is held between electrodes of thin iron, and cementite (Fe_3C) provides the reference electrode. The meter responds rapidly to changes in carbon content of the sodium, but the use of the carbon meter to determine actual carbon content remains a major problem. Unlike hydrogen and oxygen, carbon in solution in sodium is present both as dimeric (C_2) and monomeric (C) units, and the electromotive force of the concentration cell cannot be converted immediately into carbon concentration. Furthermore, the solubility of carbon in sodium is extremely small (Table V).

The fact that is has been possible to develop meters that can record concentrations in liquid sodium as low as a few parts per million represents a remarkable achievement. Some of the permeation and electrochemical meters can, in principle, be used for liquid lithium, but in practice problems arise due to corrosion and the different solubility of nonmetals in liquid lithium (Tables III and V). Lithium meters are in an early stage of development.

TABLE V Solubility of Carbon in Liquid Lithium and Sodium

Temperature °C	Liquid lithium (at. ppm)	Liquid lithium (wt. ppm)	Liquid sodium (at. ppm)	Liquid sodium (wt. ppm)
200	2	3	0.38×10^{-6}	0.2×10^{-6}
400	66	114	10.7×10^{-2}	5.6×10^{-2}
600	460	800	10.5	5.5
800	1550	2700	184	96

V. ALKALI METAL MIXTURES

The alkali metals resemble one another in atomic structure and in the physical and chemical properties of the bulk metals, and it might be expected that the properties of mixtures would lie close to the mean of the separate liquids. Some properties do, in fact, vary linearly with composition; they include density, viscosity, compressibility, and specific heat. On the other hand, some properties of mixtures deviate widely from values that would be calculated additively from the properties of the separate components.

A. Miscibility

The heavier elements sodium to cesium are miscible with one another in all proportions in the liquid state, and only in the case of mixtures with lithium does immiscibility arise. Lithium–sodium mixtures are miscible in all proportions above 305°C, but below this temperature the mixture separates into two separate phases. At 171°C, the immiscibility gap extends from 10.1 to 97.0 at.% of lithium. Liquid lithium is even less miscible with the heavier alkali metals. When liquid lithium and liquid potassium are mixed, two immiscible liquid phases are formed; at 300°C the lithium phase contains 0.43 at.% of potassium, and the potassium phase contains only 0.024 at.% of lithium. The miscibility of lithium with rubidium and cesium is negligible.

B. Melting Points

The sodium–potassium system has been the most fully explored because at one time it seemed possible that the eutectic mixture (NaK) might become the accepted coolant for fast nuclear reactors. At the eutectic composition, 67.8 at.% potassium, the mixture is liquid at temperatures down to −12.5°C. This low temperature relative to the melting points of the two pure metals (97.8 and 63.2°C, respectively) is remarkable and must be related to their different atomic sizes. An inflection in the phase diagram suggests the presence of a compound Na_2K; presumably the atoms can pack into a solid structure of this composition, and there is no evidence of Na_2K molecules being present in the liquid state. The sodium–rubidium and sodium–cesium phase diagrams are similar to that for sodium–potassium, and the binary mixtures are liquid at temperatures down to −5 and −29°C, respectively.

With mixtures of three of the alkali metals, the remarkable feature is again the very low melting points that can be achieved. Because of its immiscibility with the heavier alkali metals, lithium is not suitable as a major component of a lowmelting alloy. Of the other four metals, four ternary systems are possible, and the lowest melting points that can be achieved are as follows:

System	Melting point (°C)
Na–K–Rb	−25
Na–Rb–Cs	−37
K–Rb–Cs	−38
Na–K–Cs	−78

These are claimed to be the lowest melting points of any known metallic systems, and the alkali metals can therefore be obtained as liquids at temperatures as low as are normally available with organic solvents.

C. Other Properties

Electrical resistivity measurement is the major technique used to study reactions in solution, so it is relevant to note that the resistivity of any liquid alkali metal mixture is greater than that of either of the separate metals. The extent of this excess resistivity varies remarkably with difference in atomic size of the components; the excess for sodium–lithium mixtures is very small indeed, whereas that for sodium–cesium mixtures is 10 times the resistivity of sodium alone.

The surface tension of a liquid alkali metal mixture also shows pronounced deviation from the mean value. The surface tension of liquid cesium ($74\ N\ m^{-1} \times 10^{-3}$), lies much below that for sodium ($197\ N\ m^{-1} \times 10^{-3}$), and since surface tension reflects the attraction between atoms in the liquid, the concentration of cesium in the surface of the liquid metal mixture should be much greater than in the bulk of the liquid. Consistent with this, the surface tension of pure sodium falls rapidly upon addition of cesium, and in the range 40–100% cesium the surface tension is near to that for pure cesium. A similar behavior has been observed for sodium–potassium mixtures. Many chemical reactions of the liquid alkali metals and their mixtures involve reaction with gases, and care must then be exercised in relating reaction rates with bulk composition when it is the surface composition that is the relevant factor.

VI. SPECIES FORMED BY DISSOLVED ELEMENTS

A. Types of Species

Various elements, both metallic and nonmetallic, will dissolve in the liquid alkali metals, and it is these dissolved elements, although usually present only in small concentrations, that are responsible for many of the problems (e.g., corrosion) encountered in the use of the alkali metals on a large scale. In order to understand corrosion and other reactions, attempts have been made to define the species in solution, but with only limited success. This is because a solute dissolved in a liquid metal is immersed in a sea of electrons, and it is the number of these electrons, their energy, and the extent to which they are localized on the metal medium that now determines the chemistry of dissolved substances. For example, does oxygen dissolved in cesium exist as O_2, O^-, or O^{2-} species, and will nitrogen give solutions consisting of N_2, N^-, N^{2-}, or N^{3-} in liquid lithium? Spectroscopic methods, which are so useful with aqueous solutions, are not applicable to metallic-type solutions, and many of the conclusions on the nature of dissolved species have to be arrived at by indirect methods such as kinetics, phase equilibria, electrical conductivities, electrochemical measurements, and the like. A brief outline of some conclusions based on such measurements will now be given.

The noble gases undergo negligible electronic interaction with the liquid metals, and solubility is very small indeed (on the order of 1×10^{-7} to 1×10^{-8} M of solution per atmosphere at 300°C). Solubility decreases with increasing size of the noble gas atom and increases only slightly with increasing temperature. All these properties are consistent with a simple concept in which the solubility represents the number of noble gas atoms that can be accommodated in holes of appropriate size between the metal atoms.

With respect to diatomic molecules, a general guide to solubility and dissolved species is provided by the simple chemistry of the binary systems. For example, lithium (solid or liquid) reacts readily with nitrogen to form the stable product Li_3N, and so nitrogen has appreciable solubility in liquid lithium. In contrast, sodium and nitrogen do not yield a corresponding nitride, and so nitrogen is insoluble in liquid sodium. Some fairly firm conclusions have been reached regarding the species formed by hydrogen, oxygen, and nitrogen in solution. With hydrogen, both pressure measurements and cryoscopy indicate that solution involves the process

$$H_2\ (\text{gas}) \underset{+2e}{\overset{+2e}{\rightleftharpoons}} 2H^-\ (\text{in solution})$$

in which the hydrogen molecule dissociates into atoms, which are then converted to H^- ions by electrons from the conduction band of the metal. Oxygen dissolves in all the alkali metals. Cryoscopic studies on solutions of oxygen in rubidium and cesium show that the oxygen is monatomic in solution. Hall coefficient values indicate that two electrons are removed from the conduction band per atom of oxygen, so that solution involves the process

$$O_2\ (\text{gas}) \xrightarrow{+4e} 2O^{2-}\ (\text{in solution})$$

There is no corresponding direct evidence as to the nature of the species formed on solution of nitrogen, but the extensive chemistry of nitrogen solutions is entirely consistent with the process

$$N_2\ (\text{gas}) \xrightarrow{+6e} 2N^{3-}\ (\text{in solution})$$

Metallic solutes fall into two classes. The first is represented by the alkaline earth metals calcium, strontium, and barium; these metals dissolve as monomeric species, and their solubility in the liquid alkali metals increases with atomic weight. The chemical reactivity of these metals is not inhibited by solution in the liquid metal, and a solution of barium in sodium, for example, behaves as though sodium were no more than an inert diluent for the barium. From the chemical point of view, it is convenient to regard the valence electrons in the liquid alkali metal medium as being free from the atoms and existing in a conduction band in the liquid medium. Liquid sodium, for instance, is then treated as an assembly of Na^+ ions in a sea of free electrons. Solutions of the alkaline earth metals are then regarded as containing M^{2+} units, with two electrons from each atom added to the conduction band of the alkali metal medium.

The second class of metallic solutes is represented by the less electropositive metals. Here, the situation is the reverse of that discussed above. Sodium amalgam is widely used in industry and in the laboratory and is a good example of this class. Upon addition of mercury to liquid sodium, the reactivity of the sodium toward aqueous solutions is vastly reduced, and reaction with hydrogen is slower by an order of magnitude than that for pure sodium. This fact is important in the operation of the Solvay cell for the industrial production of sodium hydroxide by electrolysis of brine, in which sodium amalgam forms one of the electrodes. In such amalgams, valency electrons from the conduction band of liquid sodium, which would normally be responsible for its chemical reactivity, are partially localized on the mercury atoms, thus inhibiting the reactivity of sodium.

B. Solvation

As indicated above, elements dissolved in the liquid alkali metals form, in solution, species that are usually monomeric and vary in type from X^{n-} (formed by

collecting electrons from the medium) to X^{n+} (formed by donating electrons to the medium). The chemical behavior of these solutions cannot be fully explained if we assume that these dissolved species have no further interaction with the medium. In fact, these charged ions collect around themselves atoms of the liquid metal concerned, the number of such atoms being determined by such factors as the charge and size of the dissolved ion. It has been calculated that in liquid sodium, the fluoride ion has six sodium atoms coordinated around it in an octahedral arrangement, and the chloride ion is surrounded by a coordination shell of eight sodium atoms in a cubic arrangement. This phenomenon is termed solvation, and since it occurs as a result of attraction between the solute ion and atoms of the medium, energy is released in the process. The phenomenon is well established in aqueous solutions, and it is of interest that the solvation energy of the chloride ion is similar in magnitude in water and in liquid sodium (−381 and −305 kJ/g ion, respectively). Some values for solvation energy are given in Table VI. As expected, the values increase considerably with the charge on the dissolved ion but are not influenced greatly by change in the alkali metal that is used as solvent.

These energy values have practical significance. When water comes (by accident) into contact with one of the liquid alkali metals, the hydroxyl ion OH^- is produced within the metal, which may then dissociate as

$$OH^- + 2e \rightleftharpoons H^- + O^{2-}$$

and the change in solvation energy that is involved in the dissociation is one of the factors that determines the extent of the dissociation. In practice, it is found that dissociation is complete in liquid lithium; no dissociation occurs in liquid potassium, rubidium, or cesium, and there is an equilibrium in liquid sodium, with all three species present in the solution.

TABLE VI Solvation Energies in Liquid Alkali Metals

Solvent metal	Dissolved anion	Solvation energy (kJ/g ion)
Li	H^-	−425
	Cl^-	−343
	O^{2-}	−1960
	N^{3-}	−3473
Na	H^-	−344
	Cl^-	−305
	O^{2-}	−1721
K	H^-	−362
	Cl^-	−316
	O^{2-}	−1642
Rb	Cl^-	−286
Cs	Cl^-	−280

VII. ELECTRICAL RESISTIVITY

For the study of the behavior of dissolved substances in the liquid alkali metals, and their interactions, the most useful technique has been found to be the measurement of changes in electrical resistivity. This is understadable, since the electrons in the bulk metal that are responsible for electrical conductivity are also those that are involved in the solution process. All available evidence supports the belief that the introduction of a solute into the metal solvent leads to scattering of the conduction electrons, and the important practical result is that the resistivity of the pure alkali metal is invariably increased by the introduction of any foreign element. The technique has been used with success for following the rates of solution or precipitation, to determine solubilities, and to define phase diagrams. When two solutes are present, resistivity change is additive, but if they interact, then this is revealed in the resistivity value.

A remarkable feature about resistivity changes is that for dilute solutions, the resistivity (ρ) increases linearly with concentration (x) at a rate that is entirely characteristic of the particular solute in a given alkali metal. This can be defined in terms of a resistivity coefficient $d\rho/dx$, which expresses the increase in resistivity ($\Omega m \times 10^{-8}$) caused by solution of 1 mol% of the solute. Some values are given in Table VII, and a few broad generalizations are possible. Thus, coefficients increase with increase in ionic radius of the dissolved atom or ion, so that the size of a dissolved species is more important than its charge in determining the resistivity coefficient. The coefficients are largely independent of the alkali metal used as solvent.

TABLE VII Resistivity Coefficients for Solutes in the Liquid Alkali Metals $d\rho/dx$[a]

Solvent metal	Solute	$d\rho/dx$	Solute metal	Solute	$d\rho/dx$
Na	H^-	4.5	Li	N^{3-}	7.0
	O^{2-}	1.8		H^-	4.9
	Li	0.04		O^{2-}	2.1
	K	1.14		Si	10.4
	Rb	3.4		Pb	9.0
	Cs	4.2	K	F^-	3.9
	Sr	0.2		Cl^-	5.7
	Ba	2.5		Br^-	6.9
	Pb	11.2		Na	1.2
	Ag	2.8		Rb	0.22
	Au	5.0		Cs	1.61
	Hg	4.1	Cs	O^{2-}	3.2
				H^-	4.7
				Na	5.71
				K	1.01

[a] $\Omega m \times 10^{-8}$ per mol% solute.

For alkali metals dissolved in each other, the coefficients are relatively small when the metals adjoin one another in the group (e.g., lithium in sodium) but increase as the solute and solvent metals are further separated in atomic number (e.g., sodium in cesium).

VIII. REACTIONS BETWEEN DISSOLVED ELEMENTS

Many species dissolved in the liquid alkali metals do interact when present together, but often in ways that cannot be anticipated from existing knowledge of the chemistry of these species in other liquid media. Two examples will illustrate this.

A. The Nitrogen Group II Metal Reaction in Liquid Sodium

The technical significance of this reaction arises from the observation that dissolved calcium (the main metallic impurity in sodium) permits some nitrogen to dissolve in the sodium, and this in turn promotes the nitriding of steel containers. However, when excess nitrogen is present, this corrosion is diminished. Because of the small solubility of calcium in sodium, the solutions are difficult to study, but barium has a higher solubility, and the chemistry of barium solutions is similar to that of the calcium solutions. In a typical experiment a solution of barium (about 4 at.%) in sodium was exposed to progressive aliquots of nitrogen gas at 300°C. The nitrogen continued to dissolve until the nitrogen:barium ratio reached 1:4. The N^{3-} ion is held in solution as a result of the high solvation energy arising from the solvation of each N^{3-} ion by four barium atoms. When further nitrogen is added, precipitation of barium nitride commences, some of the barium atoms in the Ba_4N unit have to be replaced by sodium atoms, and the solvation shell becomes weaker and eventually collapses. With excess nitrogen, pure liquid sodium remains, and the precipitate is a barium nitride of composition Ba_2N. Such behavior has been found in many other liquid metal solutions and is quite different from the chemistry of these species that is normally observed in molecular liquid media.

B. The Nitrogen–Carbon Reaction in Liquid Lithium

Nitrogen and carbon are the main impurities in liquid lithium, and for the competent handling of liquid lithium on an industrial scale it is necessary to determine the species actually present in the liquid. To this end, elemental carbon was added to an unsaturated solution of nitrogen in lithium; reaction occurred, giving a residue of lithium cyanamide, Li_2NCN. The same product was formed when the reactants were added in the reverse order. The remarkable feature here is that the simple cyanide LiCN is not produced, and all attempts to isolate it from liquid lithium have failed. Once again, the chemical behavior of common elements in the electronic environment of a liquid metal is quite unusual; in this case, the cyanamide ion NCN^{2-} has highest stability, though the cyanide ion CN^- is stable in liquid sodium.

IX. CORROSION BY THE LIQUID ALKALI METALS

Whenever a liquid metal has to be stored, and manipulated, on a large scale, the problem of corrosion of containers is of paramount importance. The general principles governing corrosion by liquid metals bear very little resemblance to those involved in corrosion of metals by aqueous media; they have been defined largely as a result of research on liquid sodium, but they apply to the other alkali metals also. Essentially, corrosion results from the solution of the container metal (or one of the constituents in the case of an alloy such as steel) in the liquid alkali metal, and this can be augmented by intergranular attack of the solid metal. A phenomenon known as *thermal gradient mass transfer* is one of the most important and most troublesome consequences of this solubility. When used as a coolant, sodium contained in (say) steel is in constant circulation; one part of the loop (the hot leg) is receiving heat, and at another region (the cold leg) heat is being withdrawn. If the temperature difference amounts to several hundred degrees, structural metal will dissolve in the hot leg and deposit in the cold leg; this is thermal gradient mass transfer.

Corrosion also results from chemical reaction with nonmetals dissolved in the liquid metal. Oxides, nitrides, or carbides are then formed on the container surface as surface layers, which can thicken or be swept away in the stream of flowing liquid metal. The formation of such films, however, is a highly selective process and depends on the free energies of formation of the compounds involved. Thus, the high value of $-\Delta G_f^\circ$ for lithium oxide (Table IV) ensures that oxygen dissolved in liquid lithium will stay in the liquid rather than react with most of the transition metals used as containers. This suggests that oxygen in lithium should not act directly as a corrosive impurity, and this is found to be the case in practice. However, because of the lower free energies of formation of sodium oxide and potassium oxide, solutions of oxygen in these two liquids are more reactive toward transition metal surfaces. Some of the corrosion products formed on the surface of various metals are shown in Table VIII. While

TABLE VIII Some Products of Corrosion

Container metal	Product: In liquid sodium — Oxides	In liquid lithium — Nitrides	In liquid lithium — Carbides
Fe	—	Li_3FeN_2	Fe_3C
Cr	$NaCrO_2$	Li_9CrN_5	Cr_3C_2, $Cr_{23}C_6$
V	$NaVO_2$	VN, Li_7VN_4	V_2C
Nb	Na_3NbO_4	Nb_2N	Nb_2C
Ta	Na_4TaO_4	Ta_2N	Ta_2C
Ti	Na_4TiO_4	Ti_2N	Ti_2C
Zr	Na_2ZrO_3	Li_2ZrN_2	—
Mo	—	MoN	Mo_2C

oxygen usually remains in liquid lithium, nitrogen and carbon impurities are more readily transferred from solution to the solid metal container surface. This is because the $-\Delta G_f^\circ$ values for Li_3N and Li_2C_2 at 625°C are only 45 and 178 kJ/mol, respectively, compared with 455 for Li_2O. In practice, therefore, nitrogen and carbon in lithium may play a corrosive role similar to that of oxygen in sodium, and some examples of the nitrides and carbides formed at the surface of various metals are given in Table VIII.

The corrosion rates are normally quite slow (often not more than a few milligrams per square centimeter per year) and the solid metal surfaces tend to develop a layer that is resistant to further corrosion. Most research has been carried out on stainless steel in liquid sodium, and this provides an interesting illustration of the effect. The steel components iron, chromium, and nickel react toward liquid sodium containing oxygen in different ways. Chromium reacts to form the ternary oxide $NaCrO_2$ (chromite), and this reaction takes place at virtually all oxygen concentrations in the sodium. The iron component does not develop an iron oxide film; nickel shows no reaction, but has a relatively high solubility in the liquid metal and is preferentially dissolved relative to the other alloying elements. The net result is that a surface layer of $NaCrO_2$ forms on the stainless steel. In time, the surface reaches an equilibrium composition and the rate of corrosion decreases.

SEE ALSO THE FOLLOWING ARTICLES

Batteries • Chemical Thermodynamics • Nuclear Power Reactors

BIBLIOGRAPHY

Addison, C. C. (1984). "The Chemistry of the Liquid Alkali Metals," Wiley (Interscience), New York.

Borgstedt, H. U., and Mathews, C. K. (1987). "Applied Chemistry of the Alkali Metals," Plenum, New York and London.

Charnock, W., Haigh, C. P., Horton, C. A. P., and Marshall, P. (1979). "C.E.G.B. Research," Berkeley (UK).

Foust, O. J., ed. (1972). "Sodium-NaK Engineering Handbook," Gordon and Breach, New York.

Gruen, D. M. (1972). "The Chemistry of Fusion Technology," Plenum, New York.

Mausteller, J. W., Tepper, F., and Rodgers, S. J. (1967). "Alkali Metal Handling and Systems Operating Techniques," Gordon and Breach, New York.

Ohse, R. W., ed. (1985). "Handbook of Thermodynamic and Transport Properties of Alkali Metals," I.U.P.A.C. Chemical Data Series No. 30, Blackwell, Oxford.

Main Group Elements

Russell L. Rasmussen, retired
Wayne State College

Joseph G. Morse
Karen W. Morse
Utah State University

I. Boron
II. Aluminum, Gallium, Indium, and Thallium
III. Carbon
IV. Silicon
V. Germanium, Tin, and Lead
VI. Multiple-Bond Compounds
VII. Nitrogen
VIII. Phosphorus
IX. Arsenic, Antimony, and Bismuth
X. Oxygen
XI. Sulfur
XII. Selenium and Tellurium

GLOSSARY

Anisotropic Characterized by having physical properties that vary along different axes, for example, the electrical conductivity of graphite.

Concatenate To link together to form chains of like atoms.

Diamagnetism Repulsion of a chemical species by a magnetic field, an indication that all electrons are paired.

EC (enzyme code number) Specific code number assigned to an enzyme to indicate the type of reaction it catalyzes and the type of molecule (substrate) it acts on.

Electron deficient Characterized by an insufficiency of electrons around the central atom relative to the octet rule. The following structure is electron deficient, having six rather than eight electrons surrounding boron:

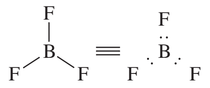

Electronegativity Measure of the relative attraction of an atom for the electrons in a bond. Nonmetals have high electronegativity values; metals tend to have low values.

Hydrogen bonding Intermolecular force arising from the attraction of a hydrogen atom covalently bonded to a highly electronegative atom (fluorine, oxygen, or nitrogen) for a second nearby electronegative atom, as shown below for hydrogen bonding between water

molecules. Hydrogen bonding dramatically affects physical properties.

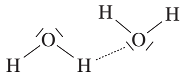

Ionization energy Minimum energy necessary to remove an electron from a gaseous atom. The first ionization energy corresponds to the first electron removed.

Main group element Element whose atoms are characterized by the filling of s or p orbitals of the outermost shell (the occupied electronic shell with the greatest quantum number). Referred to also as a representative element.

Mohs hardness scale Empirical scale by which the hardness of solids can be determined by comparison with 10 reference minerals ranked from 1 to 10: 1, talc; 2, gypsum; 3, calcite; 4, fluorite; 5, apatite; 6, orthoclase; 7, quartz; 8, topaz; 9, corundum; and 10, diamond.

Molecular orbital theory Quantum mechanical explanation of bond formation as the occupation by electrons of clouds (orbitals) that characterize the entire molecule.

Valence-shell electron-pair repulsion theory (VSEPR) Explanation for the geometric arrangements and angles of unshared and shared electron pairs around the central atom by consideration of repulsions among electron pairs.

[Note: Before discussing current knowledge about the main group elements, we must first define how groups in the periodic table will be identified. In the following discussion, the periodic group notation is in accord with actions by the IUPAC and American Chemical Society nomenclature committees. The elements in groups headed by the numbers 13–17 are considered the main group elements and correspond to filling of the outermost p energy level. Since many references still use the older Chemical Abstracts Service (CAS) system, each group is referred to by its number and its former CAS designation (IIIA–VIIA). Thus, the nitrogen family is designated Group 15 (VA). Only Groups 13 (IIIA) to 16 (VIA) are covered in this article.]

THE CHEMISTRY OF THE MAIN GROUP ELEMENTS has great variety and many practical applications. It is a chemistry that is fascinating and well worth knowing. It ranges from gases vital to life processes (O_2 in respiration, N_2 in nitrogen fixation) to polymeric materials that give us a quality of life unknown to our ancestors.

To help the reader identify and follow the properties of and trends among these elements, several tables are provided. Table I gives the names and symbols of the elements and the appropriate periodic notation. Table II describes physical and atomic properties of representative elements. Table III lists the elements in order of abundance in crustal rocks. Table IV ranks the top 50 chemicals produced in the United States. Reference to these tables is made during discussion of the elements and their chemistry. Discussion begins with Group 13 (IIIA), the group headed by boron.

TABLE I Names, Symbols, and Atomic Numbers of the Main Group Elements

Symbol	Name	Atomic number
Group 13 (IIIA): Boron–aluminum family		
B	Boron	5
Al	Aluminum	13
Ga	Gallium	31
In	Indium	49
Tl	Thallium	81
Group 14 (IVA): Carbon–silicon family		
C	Carbon	6
Si	Silicon	14
Ge	Germanium	32
Sn	Tin	50
Pb	Lead	82
Group 15 (VA): Nitrogen–phosphorus family		
N	Nitrogen	7
P	Phosphorus	15
As	Arsenic	33
Sb	Antimony	51
Bi	Bismuth	83
Group 16 (VIA): Chalcogens		
O	Oxygen	8
S	Sulfur	16
Se	Selenium	34
Te	Tellurium	52
Po	Polonium	84
Group 17 (VIIA): Halogens		
F	Fluorine	9
Cl	Chlorine	17
Br	Bromine	35
I	Iodine	53
At	Astatine	85
Special		
H	Hydrogen	1

I. BORON

Boron is a relatively rare element [9 parts per million (ppm) of crustal rock] and ranks only thirty-eighth in abundance among all elements. Boron does not occur free in

TABLE II Some Physical and Atomic Properties of Main Group Elements, Groups 13–16 (IIIA–VIA)

Symbol	Density (g/cm^3)	mp (°C)	bp (°C)	ΔH_{vap} (kJ/mol)	Atomic radius (Å)	Electronegativity[a]	First ionization energy (kJ/mol)	Relative abundance in crustal rock (order in ranking)[b]	ΔH_f° hydride (kJ/mol)
B	2.34	2180	3650	505	0.88	2.0	801	38	—
Al	2.70	660	1467	291	1.43	1.5	578	3	—
Ga	5.91	30	2403	270	1.22	1.6	579	33 (tie)	—
In	7.31	157	2080	232	1.62	1.7	558	61	—
Tl	11.85	304	1457	166	1.71	1.8	589	58	—
C	2.25	3570	4830	715	0.77	2.5	1086	17	−74.9
Si	2.33	1414	2680	383	1.18	1.8	786	2	34.3
Ge	5.32	937	2830	328	1.22	1.8	761	53	—
Sn	7.30	232	2270	296	1.41	1.8	708	48	—
Pb	11.35	328	1750	178	1.46	1.9	715	36	—
N	(1.25 g/liter)	−210	−196	2.8	0.70	3.0	1402	33 (tie)	−46.2
P	1.83	44	280	12.4	1.10	2.1	1012	11	5.4
As	5.73	800	Sublimes	32.4	1.21	2.0	947	51	66.4
Sb	6.69	631	1580	194.8	1.41	1.9	834	62	145.1
Bi	9.75	271	1564	178.5	1.46	1.9	703	69	277.8
O	(1.43 g/liter)	−218	−183	3.4	0.66	3.5	1319	1	−286
S	2.07	112	444	12.6	1.04	2.5	1004	16	−20.2
Se	4.79	217	685	14.0	1.21	2.4	941	66	29.7
Te	6.24	450	990	49.9	1.41	2.1	869	72 (tie)	99.6
Po	9.32	254	962	—	1.65	2.0	813	—	—

[a] Pauling values.
[b] See Table III for more details.

nature. Like silicon, which it resembles in several respects, it is essentially always found bonded to oxygen. Vast deposits of the three most important borate minerals, borax ($Na_2[B_4O_5(OH)_4] \cdot 8H_2O$), kernite ($Na_2[B_4O_6(OH)_2] \cdot 3H_2O$), and colemanite ($Ca_2[B_3O_4(OH)_3]_2 \cdot 2H_2O$), are found in dry lake beds in California, Turkey, and other arid regions. Borax and kernite are often shown as $Na_2B_4O_7 \cdot 10H_2O$ and $Na_2B_4O_7 \cdot 4H_2O$, respectively; however, these are simplified representations of these two important minerals, neither of which contains a $B_4O_7^{-2}$ ion. A good rule of thumb in boron chemistry is never to assume that things are as simple as they first appear.

Boron of ~95% purity can be prepared from the oxide by reaction with powdered magnesium:

$$B_2O_3 + 3Mg \rightarrow 2B + 3MgO$$

High-Purity boron (>99.9%) can be obtained by passing a mixture of BCl_3 or BBr_3 and hydrogen over a heated tantalum filament:

$$2BBr_3\,(g) + 3H_2\,(g) \xrightarrow{1000-1200^\circ C} 2B\,(s) + 6HBr\,(g)$$

Because elemental boron exists in so many allotropic modifications, the exact determination of physical properties is no easy matter. The melting point of 2180°C and the boiling point of 3650°C are approximate values commonly listed in tables; they apply to the β-rhombohedral form, the most stable modification. Pure crystalline boron is brittle, hard, low in density (2.35–2.45 g/cm^3), and high in electrical resistance—clearly properties of a nonmetal.

In most of its allotropic forms, elemental boron exists in B_{12} icosahedral structural units. An icosahedron has 12 vertices and 20 faces, each of which is a triangle. The manner in which the B_{12} clusters are linked together to produce a large three-dimensional network accounts for the high melting point and extreme hardness of this element.

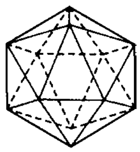

Because boron is the only nonmetal with just three valence electrons at its disposal, it must resort to clever stratagems in its bonding and structure. All the other elements in Group 13 (Group IIIA) are metals; their chemistries are reasonably straightforward and relatively

Periodic table of the elements

New notation / CAS version

1 Group IA	2 IIA	3 IIIB	4 IVB	5 VB	6 VIB	7 VIIB	8 VIII	9 VIII	10 VIII	11 IB	12 IIB	13 IIIA	14 IVA	15 VA	16 VIA	17 VIIA	18 VIIIA
1 H 1.0079																	2 He 4.00260
3 Li 6.941	4 Be 9.01218											5 B 10.81	6 C 12.011	7 N 14.0067	8 O 15.9994	9 F 18.9984	10 Ne 20.179
11 Na 22.9898	12 Mg 24.305											13 Al 26.9815	14 Si 28.0855	15 P 30.9738	16 S 32.06	17 Cl 35.453	18 Ar 39.948
19 K 39.0983	20 Ca 40.08	21 Sc 44.9559	22 Ti 47.88	23 V 50.9415	24 Cr 51.996	25 Mn 54.9380	26 Fe 55.847	27 Co 58.9332	28 Ni 58.69	29 Cu 63.546	30 Zn 65.39	31 Ga 69.72	32 Ge 72.59	33 As 74.9216	34 Se 78.96	35 Br 79.904	36 Kr 83.80
37 Rb 85.4678	38 Sr 87.62	39 Y 88.9059	40 Zr 91.224	41 Nb 92.9064	42 Mo 95.94	43 Tc (98)	44 Ru 101.07	45 Rh 102.906	46 Pd 106.42	47 Ag 107.868	48 Cd 112.41	49 In 114.82	50 Sn 118.71	51 Sb 121.75	52 Te 127.60	53 I 126.905	54 Xe 131.29
55 Cs 132.905	56 Ba 137.33	57 La ★ 138.906	72 Hf 178.49	73 Ta 180.948	74 W 183.85	75 Re 186.207	76 Os 190.2	77 Ir 192.22	78 Pt 195.08	79 Au 196.967	80 Hg 200.59	81 Tl 204.383	82 Pb 207.2	83 Bi 208.980	84 Po (209)	85 At (210)	86 Rn (222)
87 Fr (223)	88 Ra 226.025	89 Ac ▲ 227.028	104 Unq[a] (261)	105 Unp[a] (262)	106 Unh[a] (263)	107 Uns[a] (262)											

★ Lanthanide series	58 Ce 140.12	59 Pr 140.908	60 Nd 144.24	61 Pm (145)	62 Sm 150.36	63 Eu 151.96	64 Gd 157.25	65 Tb 158.925	66 Dy 162.50	67 Ho 164.930	68 Er 167.26	69 Tm 168.934	70 Yb 173.04	71 Lu 174.967
▲ Actinide series	90 Th 232.038	91 Pa 231.036	92 U 238.029	93 Np 237.048	94 Pu (244)	95 Am (243)	96 Cm (247)	97 Bk (247)	98 Cf (251)	99 Es (252)	100 Fm (257)	101 Md (258)	102 No (259)	103 Lr (260)

Note: Atomic masses shown here are the 1983 IUPAC values (maximum of six significant figures). a Symbols based on IUPAC systematic names.

much simpler. However, the chemistry of boron is unique in that the bonding and structures of boron are built up in a fashion unparalleled even by carbon chemistry. The complexities of the borides, borates, halides, boranes, carboranes, and other derivatives of this remarkable element offer myriad exciting and unusual examples.

TABLE III Abundance of Groups 13–16 (IIIA–VIA) Elements in Crustal Rocks

Element	Symbol	ppm (by mass)	Rank among all elements
Oxygen	O	456,000	1
Silicon	Si	273,000	2
Aluminum	Al	83,600	3
Phosphorus	P	1,120	11
Sulfur	S	340	16
Carbon	C	180	17
Nitrogen	N	19	33 (tie)
Gallium	Ga	19	33 (tie)
Lead	Pb	13	36
Boron	B	9	38
Tin	Sn	2.1	48 (tie with europium)
Arsenic	As	1.8	51
Germanium	Ge	1.5	53
Thallium	Tl	0.7	58
Indium	In	0.24	61
Antimony	Sb	0.20	62
Selenium	Se	0.05	66
Bismuth	Bi	0.008	69
Tellurium	Te	0.001	72 (tie with iridium)

A. Boron Carbide

Boron carbide is often represented as "B_4C," but this is only a rough empirical formula. The compound is thought to consist of dodecahedral clusters of 12 boron atoms associated with linear rods of 3 carbon atoms, but the stoichiometry is highly variable and can range from "B_6C_5" to "B_4C." Boron carbide is extremely hard (9.3 on the Mohs scale) and is used as an abrasive.

B. Boron–Nitrogen Compounds

Two of the early nitrogen derivatives of borane were $NR_3 \cdot BH_3$ and $[(NH_3)_2BH_2^+][BH_4^-]$. These resulted, respectively, from symmetric cleavage of B_2H_6 ($BH_3 + BH_3$) and unsymmetric cleavage of B_2H_6 ($BH_2^+ + BH_4^-$). Many studies have shown that Lewis acid–base ($BH_3 \cdot$ base) products are common in borane chemistry due to the electron-deficient nature of boron. Phosphorus, arsenic, oxygen, and sulfur acid–base adducts are all known. Borane (BH_3) is commonly stored and marketed as its tetrahydrofuran adduct.

Among the compounds that contain B—N bonds, two of them, boron nitride (BN) and borazole ($B_3N_3H_6$), merit special mention because of their resemblance to familiar carbon species. Boron nitride, a white, crystalline solid, has been compared to graphite because the layer structures

TABLE IV Top 50 Chemicals Produced in the United States During 1990

Rank by mass	Name	Formula	Billions of kilograms	Molecular weight	Billions of moles	Rank by moles (top 20)
1	Sulfuric acid	H_2SO_4	39.5	98	403	5
2	Nitrogen	N_2	24.4	28	873	2
3	Oxygen	O_2	17.2	32	536	4
4	Ethylene	C_2H_4	15.9	28	568	3
5	Ammonia	NH_3	15.4	17	903	1
6	Lime	CaO	15.0	56	268	6
7	Phosphoric acid	H_3PO_4	10.5	98	107	14
8	Chlorine	Cl_2	10.2	71	143	9
9	Sodium hydroxide	NaOH	10.1	40	252	7
10	Propylene	C_3H_6	9.24	42	220	8
11	Sodium carbonate	Na_2CO_3	8.98	106	84.7	18
12	Nitric acid	HNO_3	7.26	63	115	11
13	Urea	N_2H_4CO	7.03	60	117	10
14	Ammonium nitrate	NH_4NO_3	6.87	80	85.9	17
15	Ethylene dichloride	$C_2H_4Cl_2$	6.22	99	62.8	
16	Benzene	C_6H_6	5.30	78	67.9	20
17	Carbon dioxide	CO_2	4.92	44	112	12
18	Vinyl chloride	C_2H_3Cl	4.37	62.5	69.9	19
19	Ethyl benzene	C_8H_{10}	4.19	106	39.5	
20	Terephthalic acid	$C_8H_6O_4$	3.78	166	22.8	
21	Styrene	C_8H_8	3.70	104	35.6	
22	Methanol	CH_4O	3.25	32	102	15
23	Formaldehyde	CH_2O	2.90	30	96.5	16
24	Toluene	C_7H_8	2.65	92	28.9	
25	Xylene	C_8H_{10}	2.64	106	24.9	
26	Ethylene glycol	$C_2H_6O_2$	2.50	62	40.3	
27	*p*-Xylene	C_8H_{10}	2.50	106	23.6	
28	Ethylene oxide	C_2H_4O	2.42	44	55	
29	Hydrochloric acid	HCl	2.39	36.5	65.5	
30	Methyl *tert*-butyl ether	$C_5H_{12}O$	2.26	88	25.7	
31	Ammonium sulfate	$(NH_4)_2SO_4$	2.14	132	16.2	
32	Cumene	C_9H_{12}	2.06	120	17.2	
33	Phenol	C_6H_6O	1.77	94	18.8	
34	Acetic acid	C_2H_4O	1.74	60	29.0	
35	Potash (mixture)	—	1.52	—	—	
36	Propylene oxide	C_3H_6O	1.45	58	25.0	
37	Butadiene	C_4H_6	1.40	54	25.9	
38	Carbon black	"C"	1.32	12	110	13
39	Acrylonitrile	C_3H_3N	1.19	53	22.5	
40	Acetone	C_3H_6O	1.14	58	19.7	
41	Vinyl acetate	$C_4H_6O_2$	1.12	86	13.0	
42	Cyclohexane	C_6H_{12}	1.09	84	13.0	
43	Aluminum sulfate	$Al_2(SO_4)_3$	1.07	342	3.12	
44	Titanium dioxide	TiO_2	1.00	80	12.5	
45	Calcium chloride	$CaCl_2$	0.87	111	7.6	
46	Sodium silicate	Na_2SiO_3	0.80	122	6.6	
47	Adipic acid	$C_6H_{10}O_4$	0.75	146	5.1	
48	Sodium sulfate	Na_2SO_4	0.73	122	5.9	
49	Isopropyl alcohol	C_3H_8O	0.65	60	10.8	
50	Caprolactam	$C_6H_{11}NO$	0.60	113	5.3	

are analogous. Graphite, however, is black and an electrical conductor; BN is a nonconductor. Boron nitride can also be obtained in a modification with the cubic diamond structure. This form is called borazon and approaches diamond on the Mohs hardness scale.

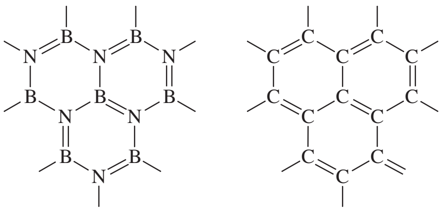

Boron Nitride Graphite

Borazole, sometimes called borazine, is a cyclic hexagonal compound that resembles benzene (C_6H_6). Often referred to as inorganic benzene, borazole is synthesized by reacting NH_4Cl with BCl_3 and then reducing with $NaBH_4$:

$3BCl_3 + 3NH_4Cl \xrightarrow{\Delta}$ 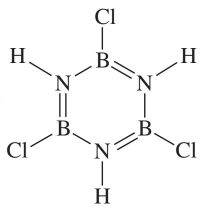 $+ 9HCl$ (1)

$$2B_3N_3Cl_3H_3 \xrightarrow{6NaBH_4} 2B_3N_3H_6 + 6NaCl + 2B_2H_6 \quad (2)$$

The structures and physical properties of borazole and benzene are much closer than the properties of BN and graphite; however, the chemical properties are quite different. The densities and surface tensions of benzene and borazole are virtually the same; however, benzene has a higher melting point (6 vs –57°C) and a higher boiling point (80 vs 55°C). Numerous interesting derivatives of borazole have been prepared by replacing the hydrogen atoms with other atoms or groups.

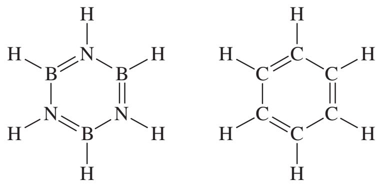

Borazole Benzene

C. Boron Halides

Boron forms two simple series of lower halides, BX_3 and $B_2X_4(X_2B{-}BX_2)$. The highly reactive trihalides are volatile covalent compounds whose molecules have the expected trigonal planar geometry. The molecules of the other series are also planar in the solid state; however, in the gaseous state, the chloride and the bromide probably assume a different shape in which the halogen atoms on one of the borons are perpendicular to the rest of the molecule.

The melting points and boiling points of the trihalides are presented for purposes of comparison. It is interesting that at room temperature the physical states of the trihalides are the same as those of the parent halogens.

	BF_3	BCl_3	BBr_3	BI_3
mp (°C)	−127	−107	−46	+50
bp (°C)	−100	+12.5	+91	+210
Physical state at room temperature	Gas	Gas	Liquid	Solid

Unlike the iodide, the other three BX_3 compounds can be prepared by directly combining the elements. Widely used as an industrial catalyst in organic synthesis, BF_3 is prepared on a large scale by the reaction of fluorspar, borax, and sulfuric acid:

$$6CaF_2 + Na_2[B_4O_5(OH)_5] \cdot 8H_2O + 8H_2SO_4$$
$$\rightarrow 4BF_3 + 15H_2O + 2NaHSO_4 + 6CaSO_4$$

Boron also forms several higher halides, B_4Cl_4, B_8Cl_8, B_9Cl_9, and B_9Br_9. These are not simple linear or cyclic structures; rather, they are polyhedral clusters of boron atoms to which halogen atoms are attached at the vertices.

D. Boron Oxides and Boric Acid

Boron oxide, B_2O_3, can be prepared by burning boron at temperatures higher than 700°C. It can also be prepared by dehydrating orthoboric acid, which is written either as H_3BO_3 or as $B(OH)_3$:

$$2B(OH)_3 \rightarrow B_2O_3 + 3H_2O$$

B_2O_3 is a glassy white solid that will dissolve in hot water to reform the acid.

Orthoboric acid, also called boracic or boric acid, is usually made by precipitation from a solution of borax on treatment with sulfuric acid. The acid is a solid at room temperature and is only sparingly soluble in water. Dilute aqueous solutions are often used as mild antiseptics. Orthoboric acid is a very weak Lewis acid that, on reaction with water, produces hydronium ions as follows:

$$B(OH)_3 + 2H_2O \rightarrow B(OH)_4^- + H_3O^+$$

$B(OH)_3$ is the product of the hydrolysis of numerous boron compounds:

$$B_2H_6 + 6H_2O \rightarrow 2B(OH)_3 + 6H_2$$

$$BX_3 + 3H_2O \rightarrow B(OH)_3 + 3HX \qquad (X = Cl, Br, I)$$

E. Borates

Borates constitute a class of about four dozen minerals that almost rival silicates in diversity and complexity. The basic building block of many borates is a boron surrounded by three oxygen atoms; however, boron may also be surrounded by four oxygens in a tetrahedral configuration like that of the silicates. Borates may contain simple $[BO_3]^{3-}$ ions or complex rings and chains. The most important borate is borax, $Na_2[B_4O_5(OH)_4] \cdot 8H_2O$, which contains the cyclic $[B_4O_5(OH)_4]^{2-}$ anion in which boron atoms are attached to either three or four oxygen atoms.

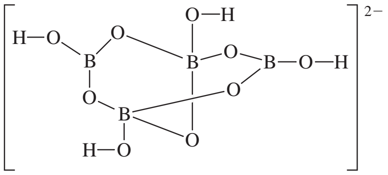

In addition to its importance as the compound from which orthoboric acid is made, borax is used to prepare washing compounds and to soften water.

F. Boranes

The structures and reactions of boron hydrides have been studied since being pioneered by Stock, who developed high-vacuum techniques to handle them.

The synthesis and reaction chemistry of boranes and their derivatives have been extensively examined. Most boranes belong to either the B_nH_{n+4} series (stable) or the B_nH_{n+6} series (unstable). The usual terminology has a prefix signifying the number of boron atoms followed by a numeral showing the number of hydrogen atoms; thus, B_6H_{10} is hexaborane-10. Diborane (B_2H_6) serves as the starting material for almost all boranes by either heating or addition (or both) of hydrogen to the higher boranes. Boron skeletons of the higher boranes can be considered to be fragments of octahedra or of icosahedra, with $B_{12}H_{12}^{2-}$ being the basic icosahedral structure. The boranes are particularly interesting because they are electron-deficient compounds; that is, there are insufficient valency electrons for adjacent atoms to be held together by electron-pair bonds. It is useful to invoke the concept of three-center bonds (three atoms are bound together by two electrons) to rationalize the hydrogen-bridge bonding and boron–boron bonds (open and closed, three-centered). W. N. Lipscomb has extensively developed the bonding ideas related to boron hydrides.

Neutral boranes (B_nH_m) and borane anions ($B_nH_m^{x-}$) have been classified into five series according to structure and stoichiometry: *closo*boranes (consisting of complete, closed, polyhedral clusters of n boron atoms); *nido*boranes [having nonclosed clusters in which the B_n portion occupies n corners of an $(n+1)$-cornered polyhedron]; *arachno*boranes [having more clusters in which B atoms occupy n contiguous corners of an $(n+2)$-cornered polyhedron]; *hypho*boranes [having the most open clusters in which the boron atoms occupy n corners of an $(n+3)$-cornered polyhedron]; and *conjuncto*boranes (having structures formed by linking two or more of the latter types of clusters together).

G. Hydroborates (Borohydrides)

Tetrahydroborate (BH_4^-) is the most familiar hydroborate. It is made from NaH and $B(OMe)_3$ and is commercially available. Different cations (Na^+, Li^+, R_4N^+, etc.) result in differing reducing capabilities toward organic functional groups. A wide range of reactivity has also been provided by substitution of different groups onto the boron itself, giving trialkyl hydroborates, $[R_3BH^-]$, carboxylatotrihydroborates, $[H_3BCO_2^{2-}]$ and $[H_3BCO_2R^-]$, and cyanotrihydroborate, $[BH_3CN^-]$. Tetrahydroborate and its derivatives have shown important reducing capabilities toward organic functional groups and have assisted in the establishment of the nature of hydroborate bonding to metals.

H. Carboranes

Carboranes are polyhedral boranes in which a BH^- unit has been formally replaced by an isoelectronic CH unit. An entire class of carboranes can be prepared from an alkyne and a borane by pyrolysis or by reaction in a silent electric charge. Derivatives are known, including those derived by reaction of lithium carboranes with a variety of reactants (CO_2, HCHO, I_2, NOCl).

Sulfur- and phosphorus-containing boranes are also known, such as carbaphosphaborane ($B_{10}CPH_{11}$) and the thiaborane ion $B_{10}SH_{10}^{2-}$. An entire class of metallocarboranes has been developed by M. F. Hawthorne and colleagues.

I. Biologically Active Boron Compounds

A relatively new area of boron chemistry concerns boron compounds having biological activity. B. F. Spielvogel, the pioneer in this field, developed the first boron analogues of α-amino acids and related compounds. Examples include aminecyanoboranes, amine(ethylcarbamoyl) boranes, and amine carboxyboranes and their esters. An example of a boron analogue of an α-amino acid is trimethylaminecarboxyborane, $Me_3\overset{+}{N}\overset{-}{B}H_2COOH$, the protonated boron analogue of the dipolar amino acid betaine $[Me_3^{(+)}NCH_2COO^-]$. Other important derivatives may be represented by the following general

formulation: amine: BHRX ($X = BH_2CN$, $\cdot BH_2CO_2H$, $\cdot BH_2CONHCH_2CH_3$). Boron analogues have shown significant antiarthritic, antitumor, antiinflammatory, hypolipidemic, and hypocholesteremic activity in mice. Not only are these compounds biologically active, but if they can be selectively incorporated into a tumor, irradiation with thermal neutrons could lead to cellular destruction *in vivo*. Interesting developments in boron neutron capture theory (BNCT) include the synthesis of backbone-boronated oligonucleotides and base-boronated nucleic acids. Another major advance is the encapsulation of certain boron compounds (which by themselves do not necessarily exhibit tumor affinity) in phospholipid vesicles that are capable of selective localization within cancer cells.

II. ALUMINUM, GALLIUM, INDIUM, AND THALLIUM

This family of elements, with boron, constitutes one of the least regularly varying families in the periodic table. It is noteworthy, however, that the trends from boron and aluminum through the Group III elements (scandium, yttrium, and lanthanum) are quite regular. This points out the importance of the underlying core of electrons to the chemical properties of atoms, noble gas in this case, while gallium, indium, and thallium have a d^{10} core. In contrast to boron, each of these elements is metallic in its physical properties. The first two members are notoriously amphoteric chemically; that is, they and their oxides are soluble in either strong acid or strong base. Rather than the smooth trend in ionization energies decreasing from aluminum through thallium, which is observed for aluminum through lanthanum, the values for gallium are comparable to those for aluminum followed by a substantial decrease at indium and an *increase* at thallium such that the first ionization energy is greater than that of aluminum. (This parallels the trend for zinc, cadmium, and mercury.) Metallic and ionic radii vary in a similarly irregular way, with gallium quite comparable to aluminum, and indium and thallium quite similar to one another but different from aluminum and gallium. The trend in electronegativity is even more remarkable and shows an increase from aluminum to thallium rather than the expected decrease.

		B	Al	Ga	In	Tl
Ionization energy	I	800.5	577.4	578.6	558.2	589.1
(kJ/mol)	II	2426.5	1816.1	1978.8	1820.2	1970.5
	III	3658.7	2744.1	2962.3	2704.0	2877.4
Ionic radius	I	—	—	120	140	150
(pm)	III	—	53.5	62.0	80.0	88.5
Electronegativity (Pauling)	—	2.0	1.5	1.6	1.7	1.8

These irregularities in the periodic trend in atomic properties are reflected in similar irregularities in chemical properties. For example, Ga_2O_3 is more acidic than Al_2O_3. The Lewis acidities of aluminum and gallium halides are comparable, and the sequence of strengths depends on the specific Lewis base considered; nitrogen and oxygen bases generally prefer aluminum, whereas sulfur and phosphorus bases prefer gallium. Indium compounds are only slightly amphoteric, and the oxides of thallium are clearly basic. Indium and, especially, thallium show a significant tendency to form univalent compounds (e.g., TlOH); Tl(III) salts are good oxidants in aqueous solutions. In fact, TlI_3 is best formulated as $Tl^+I_3^-$.

A. Aluminum

Aluminum is the most abundant metal in the earth's crust and has assumed a major technological role since the development of the Hall–Herault metallurgical process. Among its compounds, the various aluminum oxides, lithium aluminum hydride, and aluminum chloride are the most important, though the fluoride is important in the metallurgical process itself and organoaluminum nitrides are of current structural interest.

B. Aluminum Chloride

Aluminum chloride is noteworthy as a Lewis acid and is extensively used as such in the Friedel–Crafts alkylation and acylation of aromatic hydrocarbons. This property is evidenced in the structure of the compound. While the crystal consists of an "ionic" lattice, with each aluminum ion surrounded by six chloride ions in an octahedral array, the compound becomes a dimeric molecule in the nonconducting liquid phase and in the gas phase. This molecule, Al_2Cl_6, consists of tetrahedrally coordinated aluminum with two chlorine atoms bridging the two aluminum atoms, effectively a Lewis acid–base adduct of one monomer to another.

C. Aluminum Oxides

Aluminum oxides and related compounds have long been technologically important as abrasives (corundum) and in refractories and ceramics in the α-crystalline modification. In the γ modification, a more open, defect structure, aluminum oxide becomes "activated alumina" and is useful in chromatography and in catalysis. A third modification occurs on the surface of the metal on exposure to air and serves as the well-known protective oxide. A more recent technological achievement is the production of remarkably uniform cylindrical fibers of Al_2O_3. These fibers can be incorporated in a variety of fabrics, papers, ropes, and so on, which gain the advantage of stability to very

high temperatures (1400°C), resistance to corrosion except by a very strong acid or base, a high tensile strength, and a remarkably silky texture. Composites made with metals reinforced by fibers gain in thoughness and benefit from the low density of the fibers.

A related compound, often called β-alumina, is actually sodium β-alumina (idealized as $NaAl_{11}O_{17}$). The compound can be prepared by heating Na_2CO_3 with any form of Al_2O_3. The structure consists of layers of tightly bound aluminum and oxygen in a spinel-like array alternating with loosely packed layers containing the Na^+ ions. This highly "defect" structure, has many more available sites than Na^+ ions, with the consequence that the Na^+ ions can be exchanged for many other univalent cations in suitable molten salt media and, more important for the present, that the Na^+ ions are highly mobile under the influence of an electric field. This property has proved to be important in the continuing effort to develop high-energy density and practical storage batteries. There remains substantial interest in the sodium sulfur cell in which sodium β-alumina serves as the membrane to separate molten sodium and molten sulfur. The Na^+ ions produced on discharge of the cell migrate through the solid electrolyte membrane to neutralize the sulfide ions produced simultaneously and complete the electrical circuit. The migration is reversed on recharging of the cell. The relatively low operating temperature (300–350°C) and the very high energy storage per unit mass make this cell attractive for many applications.

A second crystalline modification of similar composition, called sodium β''-alumina, permits exchange for Na^+ by metal ions and supports the rapid migration of most cations in the periodic table, including multivalent ones. Because it can serve as a single crystal or powder host for multivalent cations, sodium β''-alumina has a variety of potential uses as a solid electrolyte and in optical and electrical devices and has excited much current interest.

Related to the aluminas, especially the β-aluminas, are tricalcium aluminate and its hydrated derivatives. These are major components of Portland cement and of high-alumina cement. A structural modification and the heat released on hydration are factors in the "setting" process of these cements.

D. Aluminum Hydrides

Aluminum hydride, AlH_3, seems to be the unique binary hydride of aluminum. This is indeed a dramatic contrast to the extensive hydride chemistry of boron. In fact, this example is remarkably recent as a well-defined compound because solvents useful in its preparation tend to remain bound in the crystals. The hydride can form at least six crystalline modifications. The most stable form, the α form, has a saltlike structure, with aluminum octahedrally coordinated by hydrogen. In the gas phase it apparently has some tendency to form a dimer analogous to B_2H_6. The compound is a strong reducing agent, but it has a reactivity pattern quite different from that of $LiAlH_4$. It is, however, thermally unstable, is difficult to prepare and maintain in pure form, and has not, in consequence, assumed a very large place in synthetic chemistry. The important $LiAlH_4$ is prepared by direct reaction of sodium, hydrogen gas, and aluminum at a high pressure and temperature and subsequent displacement of the Na^+ by Li^+. The resulting ether-soluble compound has become a standard reagent in the organic chemist's laboratory for accomplishing many otherwise tedious or dangerous reduction reactions. There is substantial covalent interaction between the Li^+ cation and the AlH_4^- anion in the crystal and in solution. The extent of aggregation, and consequently the reactivity, varies with the concentration and solvent. The reactions of organoaluminum compounds with amines give rise to a remarkably complex series of cluster compounds containing Al—N bonds in the framework. There is as yet no clearly defined pattern to these structures, and this remains an active area of investigation.

E. Gallium

Gallium is far less abundant than its predecessor and for many years was notable mainly for having been predicted by Mendeleev. As indicated earlier, it is similar in its chemistry to aluminum but is physically quite different. Its very low melting point (29.78°C) ensures that it is not of structural value but that it is of value where low-melting metal or alloys are desired. Remarkably, the liquid metal does not boil until 2403°C, somewhat higher than the boiling point aluminum, giving it the largest liquid range of any substance known. Its major economic value at present derives from its role in semiconductor technology. Several of its binary compounds with nitrogen family elements [the Group 13–15 (IIIA–VA) semiconductors] are of significant commercial value by virtue of their possessing appropriate band gaps for various applications. For example, $GaAs_xP_{1-x}$ is used in light-emitting diode display devices. The Group 13–15 (IIIA–VA) compounds can be prepared directly from the elements at high temperatures or alternatively by means of the reactions of the hydrides of the elements, for example, that of gallium with NH_3 or Me_3Ga with EH_3 (E = As, P, Sb). Most of the Group 13–15 (IIIA–VA) compounds are subject to chemical attack, which limits their utility to encapsulated forms. Methods for producing crystalline samples of semiconductor grade are still under development and are largely proprietary.

In general, gallium forms compounds analogous to those of aluminum, though there are significant

differences in properties. As mentioned above, Ga_2O_3 is more acidic than Al_2O_3. The β-crystalline form of Ga_2O_3 is the more stable, in contrast to Al_2O_3. The Lewis acidity of Ga^{3+} is similar to that of Fe^{3+}, a consequence of the similar size and the same charge. Gallium (III) has been found useful, therefore, in studies of the role of iron in biochemistry when a diamagnetic analogue of the Fe(III) is required. GaH_3 is a viscous liquid of even more limited thermal stability than AlH_3, decomposing to the elements at room temperature. $LiGaH_4$ can be prepared from LiH and $GaCl_3$ ($LiAlH_4$ can be prepared analogously) but slowly decomposes at room temperature and is a much weaker reducing agent than is $LiAlH_4$. In contrast to aluminum, however, gallium does exhibit some variation in oxidation number, several Ga(I) species having been characterized in crystals and solution as well as in the gas phase.

F. Indium and Thallium

Both indium and thallium are rare metals, and only indium has achieved a significant role in technology. Indium finds use in low-melting alloys and solders and has a place in semiconductor technology, like gallium, in Group 13–15 (IIIA–VA) semiconductors and as a dopant for germanium *p–n* junction devices. Thallium is so far of mainly academic interest, though there is potential in that TlBr and TlI are transparent to infrared radiation. Like its neighbor, mercury, the metal and its compounds are extremely toxic.

Chemically, neither indium nor thallium has been as thoroughly explored as aluminum and gallium. Noteworthy is the variable valence exhibited by both. Indium and, especially, thallium are observed in the I and III oxidation states. In fact, the preferred oxidation state for thallium is I. Indium and gallium are the only members of the family yet observed in the II oxidation state, in $In_2X_6^{2-}$, which have an ethane-like structure with an In—In bond, and in the corresponding gallium anions. Even here, the atoms are trivalent. Other apparently divalent compounds consist of mixtures of I and III species, for example, $Tl^+[TlCl_4^-] =$ "$TlCl_2$."

III. CARBON

A. Allotropes

Only two nonmetallic elements, carbon and sulfur, were known to the ancients; however, carbon was not recognized as an element until the eighteenth century, by which time diamond and graphite were known to be different forms of the same element.

Carbon exists free in nature as graphite and diamond; it occurs in combined form in carbonate rocks (chalk, limestone, marble, calcite, and dolomite) and in carbon dioxide gas in the atmosphere. Surprisingly, carbon is not plentiful compared with many elements; it ranks only seventeenth in order of abundance.

Although six allotropic forms of pure carbon exist, only two are considered: diamond and hexagonal (or α) graphite. These two crystalline forms are drastically different. The diamond lattice is a three-dimensional structure in which each carbon atom is attached by covalent bonds to four neighbors tetrahedrally arranged around it at a distance of 1.54 Å. Graphite is composed of planar hexagonal rings in which each carbon atom is attached to three neighbors at a distance of 1.42 Å. The planes in graphite lie at a distance of 3.35 Å, and since these planes are not held by chemical bonds, they readily slide past one another and give the substance a greasy feel.

The properties of diamond and α-graphite are compared in the following tabulation:

Property	Diamond	α-Graphite
Hardness (Mohs scale)	10	1–2
Color	Transparent	Black, opaque
Density (g/cm^3)	3.51	2.27
Electrical conductivity	Negligible	Good in the direction along planes
ΔH_f° (kJ/mol)	1.90	0.00 (standard state)
Chemical reactivity	Relatively insert, burns at ~800°C	Relatively reactive, burns at 400°C; undergoes attack by oxidizing agents and oxo acids at room temperature

At room temperature graphite is more stable than diamond; however, at high pressures and temperatures, graphite can be transformed into diamond if molten chromium, iron, or nickel is present as a catalyst. Although these synthetic diamonds are not gem quality, they are useful in drills and saw blades.

Less glamorous than the synthesis of diamonds but far more important is the industrial manufacture of three impure graphite forms of carbon: carbon black (soot), coke, and activated charcoal.

Carbon black, which consistently ranks about thirty-fifth among the top 50 chemicals produced in the United States, is manufactured by partially oxidizing the residual hydrocarbons from petroleum refining; coke is made by heating coal in the absence of air to remove volatile components; and activated charcoal is made by heating sawdust or peat in the presence of certain metal salts. More than 90% of the 1.14 billion kg of carbon black produced annually is used by the rubber industry, mostly for reinforcing the rubber in tires. The demand for carbon black is easily understood when it is pointed out that the 4 tires on an automobile require more than 15 kg of carbon black

and the 18 tires on a truck require more than 160 kg of carbon black.

Coke is used as a reducing agent in the pyrometallurgy of iron. The stoichiometric process, but not the mechanistic process, is represented by the following equation:

$$2Fe_2O_3 + 3C\,(\text{coke}) \rightarrow 4Fe + 3CO_2$$

Activated charcoal is used to decolorize sugar, to purify air and other gases, and to treat water. One gram of charcoal provides an adsorption surface of roughly 300 to 2000 m^2—about half the area of a football field.

B. The Buckminsterfullerene

In 1985, researchers at Rice University vaporized graphite with lasers and produced what might be regarded as a new modification of carbon: a surprisingly stable, highly symmetric molecule containing 60 carbon atoms. The molecule is envisioned as an aromatic spheroidal cluster with 60 vertices and 32 faces, 20 of which are hexagons and 12 of which are pentagons. The proposed structure, formally described as a truncated icosahedron, has the geometry of the surface of an ordinary soccer ball. Indeed, soccerballene would be an apt name for the C_{60} species, but the discoverers settled on the whimsical name buckminsterfullerene (also known as buckyball) to honor R. Buckminster Fuller, whose pioneering efforts with polygonal structures led to the development of geodesic domes. The basic structural feature of all geodesic domes, however, is actually the triangle.

The C_{60} cluster has a diameter of ~7 Å and an inner cavity of ~5 Å. Vaporization of graphite impregnated with lanthanum results in a species LaC_{60}, which is assumed to be a buckyball sphere inside which the lanthanum atom is trapped. Other clusters containing an even number of carbon atoms ranging from 44 to 76 also encapsulate lanthanum, but the LaC_{60} complex predominates.

It has been speculated that buckyballs might occur in outer space around carbon-rich stars, and, rather surprisingly, they may even exist at the cores of mundane soot particles, which tend to be spherical. In recent years, fullerenes of C_{70} and C_{50} have been proposed as stable even clusters of carbon atoms.

C. All-Carbon Cyclic Molecules: The Cyclo(*n*) Carbons

Elegant chemical syntheses at UCLA have resulted in the unambiguous structural characterization of monocyclic all-carbon molecules. Cyclo(18) carbon and other species have been prepared and characterized. Neutral cycles satisfying the general formula $4n + 2$ atoms are predicted to be closed-shell aromatic molecules with special stability. This new class of monocyclic molecules, which might well be regarded as synthetic or unnatural allotropes of carbon, will be systematically named the cyclo(n) carbons (where n = the number of carbon atoms present). Evidence indicates that the rings consist of carbon atoms with alternating C≡C and C—C bonds. A general structure is shown below.

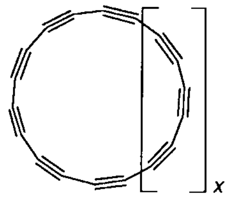

D. Carbonates and Carbonic Acid

Carbon dioxide in an aqueous solution can be described by the following equilibrium:

$$CO_2 + H_2O \rightleftharpoons \underset{\text{Carbonic acid}}{H_2CO_3} \rightleftharpoons H^+ + \underset{\text{Bicarbonate ion}}{HCO_3^-}$$

$$\rightleftharpoons 2H^+ + \underset{\text{Carbonate ion}}{CO_3^{2-}}$$

Less than 1% of the dissolved carbon dioxide exists as carbonic acid or its dissociation products. Carbonic acid, a weak acid with a pK of ~6.38, serves as an important buffer in blood.

All the C—O bonds in the carbonate ion are equal in length, but the three resonance structures of this flat triangular species show one double and two single bonds:

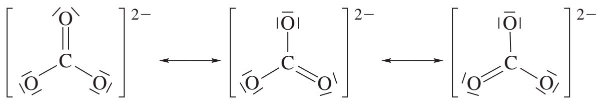

More than 70 minerals containing the carbonate ion are recognized, and some of these are fairly abundant in nature. Important natural carbonates include calcite, $CaCO_3$ (calcium carbonate); siderite, $FeCO_3$ (ferrous carbonate); magnesite, $MgCO_3$ (magnesium carbonate); smithsonite, $ZnCO_3$ (zinc carbonate); dolomite, $CaMg(CO_3)_2$ (calcium magnesium carbonate); witherite, $BaCO_3$ (barium carbonate); cerussite, $PbCO_3$ (lead carbonate); malachite, $Cu_2CO_3(OH)_2$ (basic copper carbonate); natron, $Na_2CO_3 \cdot 10H_2O$ (hydrous sodium carbonate); and trona, $Na_3H(CO_3)_2 \cdot 2H_2O$ (hydrous sodium acid carbonate). Smithsonite, witherite, cerussite, and malachite are useful ores and serve as sources of the metals present in each.

Carbonates containing relatively small and highly charged metal ions can be decomposed by heating. For example, calcium carbonate can decompose as follows:

$$CaCO_3\,(s) \xrightarrow[\text{heat}]{} CaO\,(s) + CO_2\,(g)$$

The calcium oxide (quicklime) produced by the thermal decomposition of limestone and chalk exceeds 13 billion kg annually and earns lime sixth place among the manufactured chemicals.

Ranked eleventh among chemicals, Na_2CO_3 is important in glassmaking and the preparation of detergents. This chemical was once produced synthetically in vast quantities by the Solvay process.

Carbonation:

$$NaCl + H_2O + NH_3 + CO_2 \rightarrow NaHCO_3 + NH_4Cl$$

Ammonia recovery:

$$2NH_4Cl + Ca(OH)_2 \rightarrow 2NH_3 + CaCl_2 + 2H_2O$$

Heating:

$$2NaHCO_3\,(s) \rightarrow Na_2CO_3\,(s) + H_2O\,(g) + CO_2\,(g)$$

Now, however, this process is being phased out because of the cost of ammonia and the availability of huge natural deposits of natron in Wyoming. A major disadvantage of the Solvay process involves the ammonia recovery step. The by-product $CaCl_2$ finds some use as a deicer on highways and sidewalks and as a concrete additive, but the quantities of $CaCl_2$ produced far exceed the demand. The disposal of excess $CaCl_2$ from the Solvay process creates a serious environmental problem.

E. Oxides

When carbon is burned in a sufficiency of air or oxygen, CO_2 results; but if the supply of oxygen is limited, highly toxic CO is the major combustion product. Other, higher oxides of carbon can be formed by indirect methods; for example, C_3O_2, carbon suboxide (tricarbon dioxide), results from the dehydration of malonic acid, a three-carbon dicarboxylic acid. The Lewis structures of these three oxides indicate the presence of multiple bonds:

At room temperature, carbon monoxide is a colorless, odorless, and tasteless gas; its boiling point is −192°C, and its melting point is −205°C. The extreme toxicity of CO arises from its capacity to bind to the iron ion in hemoglobin molecules, thus reducing the capacity of hemoglobin to bind and carry O_2.

Carbon monoxide has a number of important industrial uses as a fuel [Eq. (3)], as a reducing agent in metallurgy [Eq. (4)], and as a reactant in the preparation of important organic compounds [Eqs. (5) and (6)]:

$$2CO\,(g) + O_2\,(g) \rightarrow 2CO_2\,(g) + \text{heat}$$
$$\Delta H = -566\ \text{kJ} \qquad (3)$$

$$Fe_2O_3\,(s) + 3CO\,(g) \rightarrow 2Fe\,(s) + 3CO_2\,(g) \qquad (4)$$

$$CO + 2H_2 \xrightarrow[\text{catalyst}]{\text{heat}} \underset{\text{Methanol}}{CH_3OH} \qquad (5)$$

$$CH_3OH + CO \rightarrow \underset{\text{Acetic acid}}{HC_2H_3O_2} \qquad (6)$$

Methanol (number 22) and acetic acid (number 34) both rank among the top 50 chemicals produced in the United States.

Carbon dioxide, the other important oxide of carbon, earns the rank of seventeenth among chemicals produced. It is recovered mainly as a by-product of other processes, for example, the thermal decomposition of carbonates and the fermentation of carbohydrates.

Carbon dioxide is a colorless, odorless gas. When cooled at atmospheric pressure, it solidifies to form dry ice. This solid sublimes at atmospheric pressure and a temperature of −78°C. All three physical states of CO_2 are useful: more than half the solid CO_2 produced annually is used as a refrigerant, liquid CO_2 is used as an aerosol propellant, and gaseous CO_2 is used primarily to carbonate beverages.

A significant amount of CO_2 is used to manufacture urea, which ranks thirteenth by weight among the top 50 chemicals produced in the United States:

$$CO_2 + 2NH_3 \xrightarrow{\text{pressure}} H_2N{-}\overset{\overset{\displaystyle O}{\|}}{C}{-}NH_2 + H_2O$$

IV. SILICON

After oxygen (45.5 wt%), silicon (27.2 wt%) is the most abundant element in the earth's crust. It is never found free in nature, and it is usually found combined with oxygen. Unlike carbon, silicon does not readily concatenate; instead, it forms stable Si—O—Si bonds, and it is these bonds that are found in the bewildering and complex variety of minerals called silicates.

Relatively crude silicon can be prepared by the reduction of silicon dioxide (sand or quartzite) with coke in an electric furnace at ∼3000°C:

$$SiO_2\,(s) + 2C\,(g) \rightarrow 2CO\,(g) + Si\,(s)$$

The crystal structure of silicon is similar to that of diamond; however, the Si—Si bonds (226 kJ/mol) are weaker than the C—C bonds (356 kJ/mol), and silicon is not nearly as hard. There is no graphitic allotrope of silicon. Crystalline silicon is a blue–gray, somewhat shiny, brittle element that certainly appears metallic; however, it is classified as a nonmetal or metalloid because it is a semiconductor; that is, at low temperatures it is an insulator. However, when heated sufficiently, its electrical conductivity increases markedly. Very pure silicon for transistors is produced by reducing silicon tetrachloride prepared by

reacting silicon with Cl_2. The $SiCl_4$ is a volatile liquid that can be purified by fractional distillation before reduction with hydrogen gas:

$$Si\,(s) + 2Cl_2\,(g) \rightarrow SiCl_4\,(l)$$

$$SiCl_4\,(g) + 2H_2\,(g) \rightarrow Si\,(s) + 4HCl\,(g)$$

Very pure silicon for electronic applications is prepared by zone refining of the silicon obtained from $SiCl_4$ reduction.

A. Silanes (Silicon Hydrides)

Unlike carbon, silicon does not form a large number or variety of hydrides; however, several colorless, volatile compounds with the general formula Si_nH_{2n+2} have been synthesized and are called silanes, a name proposed by Alfred Stock to reflect the similarity to alkanes, C_nH_{2n+2}.

A comparison of the boiling points of silanes and alkanes indicates the lower volatility of the former:

	SiH_4	CH_4	Si_2H_6	C_2H_6
bp (°C)	−112	−162	−14	−88
	Si_3H_8	C_3H_8	Si_4H_{10}	C_4H_{10}
bp(°C)	+53	−42	+108	−0.5

Despite the parallels in physical properties, silanes and alkanes are markedly different chemically. Silanes are extremely reactive and ignite spontaneously in air:

$$SiH_4\,(g) + 2O_2\,(g) \rightarrow SiO_2\,(s) + 2H_2O\,(g)$$

In contrast, alkanes have little affinity for most chemical reagents and are often called paraffins (Latin, *parum*, "little"; *affinis*, "reactivity"). The reactivity of the Si—H bond can be used to advantage in the synthesis of organosilicon compounds and in special reduction reactions.

B. Silicides

Silicides are binary compounds of metals and silicon. Formulas are difficult to predict, and the bizarre stoichiometries often appear to be the reaction products found on freshman examinations. Silicides of most representative metals except beryllium are known, and most of the transition elements except silver, gold, and a few others form various silicides. The heavy metals mercury, thallium, lead, and bismuth do not react with silicon; indeed, the molten metals are not even miscible with liquid silicon.

C. Halides

The tetrahalides of silicon, SiF_4, $SiCl_4$, $SiBr_4$, and SiI_4, are all known and can be synthesized by direct reaction of the halogen with elemental silicon. The fluoride can also be synthesized by the reaction of hydrofluoric acid and silica:

$$SiO_2 + 4HF\,(aq) \rightarrow SiF_4\,(g) + 2H_2O\,(l)$$

As noted earlier, the chloride is important in the preparation of ultrapure silicon for use in transistors, but it also serves as a valuable reagent for preparing silicon esters and silanes:

$$SiCl_4\,(l) + 4C_2H_5OH \longrightarrow Si(OC_2H_5)_4\,(l) + 4HCl\,(g) \qquad (7)$$

$$SiCl_4 + LiAlH_4 \xrightarrow{\text{ether}} \underset{\text{Silane}}{SiH_4\,(g)} + LiCl\,(s) + AlCl_3\,(s) \qquad (8)$$

Silicon esters are important in the preparation of new high-technology ceramic materials.

D. Silica

Silicon dioxide is an intriguing, highly complex compound that has been the subject of more scientific scrutiny than any substance except water. Dozens of forms are known: α-quartz, chalcedony, chert, agate, onyx, jasper, and many others.

The term *silicon dioxide* is a misnomer in the sense that no individual SiO_2 molecules are known. In its numerous crystalline modifications, SiO_2 exists in the form of giant three-dimensional network molecules in which each silicon atom is surrounded tetrahedrally by four oxygen atoms to form a hard, rigid lattice:

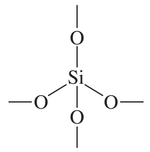

On the Mohs hardness scale, quartz is assigned a value of 7; diamond is 10.

Some of the types of SiO_2 employed for industrial purposes include high-purity α-quartz, vitreous silica, silica gels, and diatomaceous earth. The use of very pure quartz crystals in oscillators and other electromechanical devices constitutes one of the most important applications of high-grade quartz. Such oscillators are the heart of quartz watches and also enable radio stations to remain on an assigned frequency.

The fusion of sand and sodium carbonate yields sodium silicate (ranked number 46 among the top 50 chemicals produced in the United States), which is converted to silica gel or used in the manufacture of detergents and cleaning agents:

$$SiO_2\,(s) + Na_2CO_3 \rightarrow Na_2SiO_3\,(s) + CO_2\,(g)$$

Concentrated aqueous solutions of Na_2SiO_3 are often sold in hobby shops under the name of water glass.

When white sand is fused at 1500°C with a mixture of sodium and calcium oxides and carbonates, the result is a molten mixture of silicates, Na_2SiO_3, $CaSiO_3$, and silica. Cooling this liquid produces ordinary soda glass, an amorphous transparent substance that gives the appearance of a solid.

Variations in the proportions of the three basic starting materials and additions of a few other ingredients will produce a variety of glasses with modified properties. If calcium is replaced with lead, a flint glass with a higher refractive index results; SiO_2 partially replaced with P_4O_{10} yields crown glass. The addition of boron oxides to soda glass yields a borosilicate glass (Pyrex) with greatly improved thermal-shock properties that result from the reduced coefficient of expansion.

E. Silicones

The simple organosilicon derivative $(CH_3)_2SiCl_2$, which can be prepared by several methods, serves as a starting point synthesis of an important class of polymers called silicones. Hydrolysis of $(CH_3)_2SiCl_2$ followed by condensation–polymerization results in long-chain molecules with a host of valuable and interesting properties:

$$(CH_3)_2SiCl_2 + 2H_2O \longrightarrow (CH_3)_2Si(OH)_2 + 2HCl$$

Hydrolysis

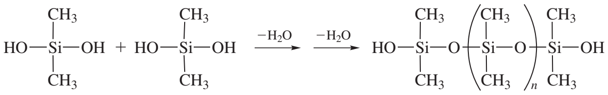

Condensation-polymerization

Cross-linked polymers can also be made:

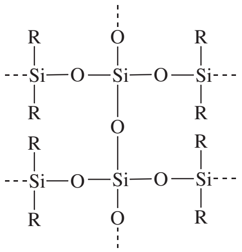

Variations in the length of chains, the organic groups, and the degree of cross-linking produce silicones that vary widely in their physical properties. Silicones may be fluids (oils), greases, or even rubberlike solids. All possess a host of desirable traits: resistance to temperature extremes, water repellency, antistick properties, chemical inertness, and lack of physiological activity.

F. Silicate Minerals

Silicon has often been referred to as the "earth maker," for nearly 95% of the earth's crust is composed of silicate minerals if quartz (SiO_2) is considered a silicate. The basic structural feature of silicates is a silicon atom tetrahedrally surrounded by four oxygen atoms. These SiO_4 tetrahedra can exist as discrete ions (as in the orthosilicate ion, SiO_4^{4-}) or can share oxygen atoms at a corner to build up larger, more complex entities.

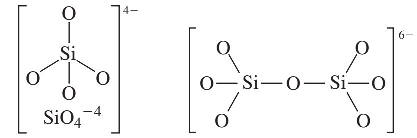

Orthosilicate ion in nesosilicates   Pyrosilicate ion in sorosilicates

The classification of silicates is based on the number of shared oxygen atoms per tetrahedron and the nature of the arrangements of tetrahedra into rings, chains, or sheets. Thus, in addition to the *neso*silicates and *soro*silicates illustrated, there are *cyclo*silicates (closed ring structures), *ino*silicates (continuous chain or ribbon structures), *phyllo*silicates (continuous sheet structures), and *tecto*silicates, (continuous three-dimensional structures). Quartz is an example of a *tecto*silicate, that is, a silicate in which all four oxygen atoms at the corners of the tetrahedron are shared, to give a three-dimensional structure reminiscent of that in diamond.

G. Asbestos

Defining *asbestos* is difficult, for the term is an imprecise commercial designation referring to several fibrous inorganic silicates with a high tensile strength and considerable heat resistance. Various silicate minerals that usually crystallize in nonfibrous rock forms can, under special geological conditions, crystallize in bundles of tough, flexible fibers—the so-called asbestiform habit. Two mineral groups are recognized: the serpentines and the amphiboles. Serpentines have the generalized chemical formula $Mg_6(SiO_4O_{10})(OH)_8$, and one serpentine asbestiform variety called chrysotile (white asbestos) represents ~95% of world production. The amphiboles with asbestiform habit include a blue asbestos (crocidolite), $Na_2Fe_3^{2+}Fe_2^{3+}Si_8O_{22}(OH, F)$, and a brown asbestos (cummingtonite–grunerite), $(Mg^{2+}, Fe^{2+})_7Si_8O_{22}(OH)_2$.

In the mid-1980s, panic regarding the toxicity of asbestos caused the demand to plummet to less than a third of that in 1973, the peak year. The demand now is for asbestos abatement services to remove safely and quickly the huge quantities of asbestos that were employed as fireproofing and insulation in the thousands of office buildings, schools, and municipal buildings constructed in the 1960s and early 1970s.

High exposure to asbestos causes pulmonary fibrosis (asbestosis), lung cancer, and gastrointestinal cancers.

Victims of asbestosis suffer acute shortness of breath, which in extreme cases may occasion heart failure. There is little agreement among researchers on the nature of the toxicity and carcinogenicity of asbestos. Particle size is probably a factor, and there is some evidence that asbestos may facilitate entry of carcinogenic hydrocarbons into cells. For instance, exposure to asbestos enhances the risk of lung cancer among cigarette smokers.

A safe replacement for asbestos might be Saffil, specially prepared fibrous forms of Al_2O_3 and ZrO_2, for which, fortunately, there is no documented evidence of toxicity. The soft, silky fibers of Saffil can be made into yarn, cloth, fiber mats, blankets, solid heat shields, and high-temperature insulation.

H. Silicon Carbide

Although silicon carbide, carborundum, was first synthesized before the turn of the century, new syntheses and applications for this important compound are still being developed. The name *carborundum* derives from its hardness (9.3 on the Mohs hardness scale) and was coined to indicate that SiC falls between carbon (diamond = 10.0) and corundum (sapphire, $Al_2O_3 = 9.0$).

SiC exists in several crystalline modifications, one of which, α-SiC, is prepared commercially by reacting sand and coke in an electric furnace at 2000 to 5000°C:

$$SiO_2 + 3C \rightarrow SiC + 2CO$$

Slightly iridescent and dark blue–black, the hard impure crystalline product is an excellent abrasive used in grinding wheels and powders.

Another modification of silicon carbide, β-SiC, results from heating very pure graphite and silicon at 1500°C. This purer modification is almost colorless and is similar to diamond in crystal habit.

In recent years, ceramic fibers and whiskers of SiC have gained in importance. When added to aluminum, these materials greatly enhance tensile strength and nearly double stiffness.

By means of a complex series of steps, SiC fibers can be fabricated from dimethyldichlorosilane, $(CH_3)_2SiCl_2$, the starting material for silicones. SiC whiskers, which are much shorter and finer than fibers, can be prepared by heating rice hulls to temperatures of ~2000°C.

The direct synthesis of high-purity, ultrafine SiC powders by means of a sophisticated plasma technology is currently under development. These high-technology ceramic powders, as well as whiskers, will find ever-increasing use in automobile engines and turbochargers. Engine parts reinforced with ceramic materials can withstand high operating temperatures and thus enhance engine efficiency.

I. Silicon Nitride

Silicon nitride (Si_3N_4) has long been considered a promising material for use in ceramic gas turbines. A hard network solid (~9 on the Mohs scale), Si_3N_4 features a structure in which each nitrogen atom is surrounded by three silicon atoms, and each silicon atom is tetrahedrally surrounded by four nitrogen atoms.

Si_3N_4 can be synthesized by the direct combination of the elements at 1250–1450°C:

$$\text{(a)} \qquad 3Si_{(s)} + 2N_{2(g)} \xrightarrow[\sim 1,300^\circ C]{} Si_3N_{4(s)}$$

$$\text{(b)} \qquad 3SiCl_{4(g)} + 4NH_{3(g)} \rightarrow Si_3N_{4(s)} + 12HCl_{(g)}$$

Because axial turbine rotors made of Si_3N_4 are still not completely reliable, research efforts continue to focus both on improving injection molding techniques and on strengthening the silicon nitride material systems. A ceramic composite of Si_3N_4 reinforced with silicon carbide whiskers may reduce structural failures and provide better high-temperature performance than monolithic ceramic parts.

V. GERMANIUM, TIN, AND LEAD

Germanium, tin, and lead complete the members of Group 14 (IV A) elements, and the change from nonmetallic properties in carbon to weakly metallic properties in lead is readily observable.

A. Occurrence, Preparation, and Uses

Germanium minerals are not abundant, and the element is usually recovered from coal ash or the flue dust of zinc ores, with which germanium often occurs. Recovery of germanium is effected by preparing the tetrachloride (bp, 83°C), distilling, hydrolyzing to GeO_2, and reducing with charcoal:

$$GeCl_4\,(l) + 2H_2O\,(l) \rightarrow GeO_2\,(s) + 4HCl$$

$$GeO_2\,(s) + 2C\,(s) \rightarrow Ge\,(s) + 2CO\,(g)$$

The cooled germanium crystallizes with a diamond structure and, when highly purified, finds its greatest use in transistors. It is a brittle, gray–white metalloid.

Cassiterite, SnO_2, is readily reduced by hot carbon, a process known to the ancients and still employed in the pyrometallurgy of the element:

$$SnO_2\,(s) + 2C\,(s) \rightarrow 2CO\,(g) + Sn\,(s)$$

Tin exists in two allotropic forms: a gray form and a white metallic form. The white or metallic form (density, 7.31 g/cm^3) is stable from the melting point, 232°C, down to 13°C, at which temperature it changes to crumbly, gray

form with a diamond structure (density, 5.75 g/cm^3). This transformation from the shiny metallic allotrope to the crumbly form was known in the past as "tin pest" or "tin disease."

Because tin is rather expensive, it is rarely used alone; however, it finds wide application in coatings, in platings, and in solders and alloys (bronze and pewter), in which it can be extended by use with a less expensive metal.

Lead, like tin, is a metal with which the ancient world was familiar. The rather simple pyrometallurgy permitted easy recovery of lead from the mineral galena, PbS.

$$2PbS\,(s) + 3O_2\,(g) \rightarrow 2PbO\,(s) + 2SO_2\,(g)$$

$$PbO\,(s) + C\,(s) \rightarrow Pb\,(l) + CO\,(g)$$

$$PbO\,(s) + CO\,(g) \rightarrow Pb\,(l) + CO_2\,(g)$$

The largest use of lead is in storage batteries, from which more than 80% is recovered and recycled. Lead is also used in ethyl gasoline and in paints, but both uses are being phased out. Lead is also found in certain types of solders and pipes. The toxicity of lead is well known, but its congeners, tin and germanium, have not been shown to be poisonous.

B. Hydrides

Germanes, the hydrides of germanium, are somewhat similar to silanes in their chemical and physical properties. The general formula Ge_nHe_{2n+2} ($n = 1$–5) recalls that of C_nH_{2n+2} for alkanes and that of Si_nH_{2n+2} for silanes. Germanes are less volatile and flammable than silanes and are somewhat less reactive toward alkali. The two known stannanes, SnH_4 and Sn_2H_6, are much less stable than silanes; and the one plumbane, PbH_4, decomposes readily. In fact, its existence is still questioned.

C. Halides

Lead, tin, and germanium form two distinct series of halides, MX_2 and MX_4. The dihalides are more ionic and have higher melting points and boiling points; the tetrahalides are generally covalent with a tetrahedral geometry. $SnCl_2$ is a colorless, crystalline solid that dissolves in water, melts at 246°C, and boils at 623°C, whereas $SnCl_4$ is a colorless volatile liquid that dissolves in nonpolar hydrocarbon solvents, melts at −33°C, and boils at only 114°C.

The stability of dihalides follows the order $GeX_2 < SnX_2 < PbX_2$; that of tetrahalides is $GeX_4 > SnX_4 > PbX_4$. The lead dihalide $PbCl_2$ is much more stable than $PbCl_4$. The latter is explosive when warmed to 105°C; however, $PbCl_2$ can be heated to 500°C, its melting point, and then up to 953°C, at which temperature it boils without decomposition.

D. Oxides

All three elements, lead, tin, and germanium, form both a monoxide and a dioxide. The order of stability for monoxides is $GeO < SnO < PbO$; that for dioxides is $GeO_2 > SnO_2 > PbO_2$. PbO_2 functions as the positive plate of lead storage batteries. A mixed oxide of lead, Pb_3O_4, is called red lead. It is used as a pigment and primer and as an additive to leaded glass.

E. Organometallic Compounds

Tetraethyllead, $Pb(C_2H_5)_4$, is added to gasoline to reduce knocking; however, its use will continue to decline as a switch is made to other, less environmentally hazardous antiknock agents.

In terms of the number and variety of industrial applications, organotin derivatives are the most valuable of any organometallic compounds. Polyvinyl chloride plastics are readily degraded by heat and light unless stabilized by the addition of dioctyltin compounds. Other organotin compounds function as curing agents for another important type of polymer, the silicones. Certain triorganotin derivatives have been found to function as highly selective, versatile pesticides. These pesticides have additional advantages; they are safe and readily biodegradable.

VI. MULTIPLE-BOND COMPOUNDS

Considerable progress in the determination of quantitative values for bond strengths in silicon compounds has been realized. These thermochemical data gain additional significance in light of the continuing success with syntheses of stable silicon compounds containing multiple bonds. In fact, startlingly rapid advances in the double-bond chemistry of silicon and phosphorus, as well as other members of Groups 14 and 15 (IVA and VA), have created a need for increasingly reliable thermodynamic data to provide coherence and direction for further work.

Only a few years ago, students were taught that silicon and germanium formed no multiple bonds to anything. Textbooks emphasized that these elements, as well as other, heavier main group elements, were simply not able to self-link through double bonds to yield stable compounds analogous to those of alkenes, the important family of unsaturated hydrocarbons with C═C bonds. Now the facile synthesis of multiple bonds in heavier main group elements is routinely reported, and doubtless the detailed thermochemistry will keep apace.

One of the reasons for the lack of success in early attempts to synthesize multiple-bond compounds of heavier elements can be attributed to the failure to recognize that two single bonds (two σ bonds) are more stable than one

double bond (one σ and one π bond). Rather than remain double-bond monomers, the heavier elements form cyclic oligomers:

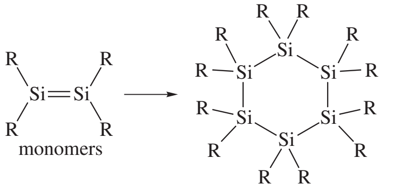

R = same organic group

If, however, sufficiently bulky R groups are present, their steric requirements will preclude oligomerization and will effectively shield the double bond. Some of the stable compounds that have been synthesized include the following:

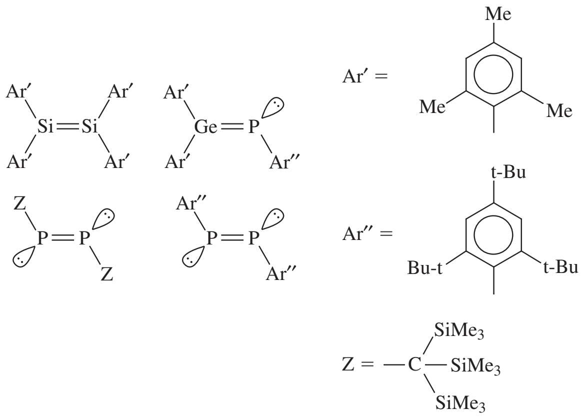

Proof that a double bond is present is best illustrated by the reactions of a germanium phosphorus compound, an orange crystalline solid. If treated with HCl, HOH, or CH_3OH, the compound undergoes an addition reaction similar to alkenes, and its orange color is discharged as it forms a saturated colorless product:

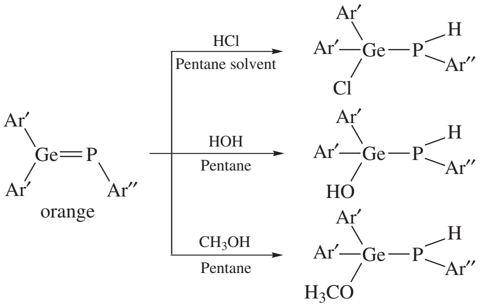

colorless products

VII. NITROGEN

Although the air is ~75% elemental nitrogen by weight, nitrogen-containing compounds are not abundant in the earth's crust. Only two minerals, saltpeter (KNO_3) and Chile saltpeter ($NaNO_3$), are found in significant amounts in crustal rocks. Because both these nitrates are highly soluble in water, they are not widely distributed and are usually found only as major evaporites in northern Chile and other extremely arid regions of the globe.

In terms of abundance, nitrogen ranks thirty-third among all elements; but this low ranking belies its importance, as evidence by the fact that 5 chemical compounds containing nitrogen appear among the top 15 chemicals produced in the United States. These five, along with top-ranked sulfuric acid, are listed in order of rank for the year 1989, below and in Table IV.

Chemical	Rank by mass	Billions of kilograms	Billions of moles	Rank by moles
Sulfuric acid, H_2SO_4	1	39.5	368	5
Dinitrogen, N_2	2	24.4	703	2
Ammonia, NH_3	5	15.4	865	1
Nitric acid, HNO_3	12	7.3	116	11
Urea, $(NH_2)_2CO$	13	7.0	108	13
Ammonium nitrate, NH_4NO_3	14	6.9	80	17

Year in and year out sulfuric acid is the top chemical produced by weight; but if the rankings were based on moles, not kilograms, both ammonia and nitrogen would be ranked ahead of H_2SO_4.

Atmospheric nitrogen is the ultimate source of all commonly used nitrogen compounds. The liquefaction and fractional distillation of air provide the N_2 from which the important compounds are synthesized. Ammonia is made from N_2 (the Haber process) by reaction with H_2 from natural gas, nitric acid is made from ammonia in several steps, ammonium nitrate is made from the reaction of nitric acid with ammonia, urea is made from ammonia and carbon dioxide, and ammonium sulfate is prepared by the reaction of ammonia and sulfuric acid.

A. Hydrides

Ammonia (NH_3), hydrazine (N_2H_4), and hydrazoic acid (HN_3) are the most important binary compounds of hydrogen and nitrogen. The first two are bases, but hydrazoic acid, as its name implies, is weakly acidic.

Ammonia, the most important of the three hydrides of nitrogen, is one of the most important of all industrial chemicals. It is produced by the Haber process, which brings about the fixation of nitrogen by the direct combination of nitrogen and hydrogen under high pressure and in the presence of a catalyst:

$$N_2\,(g) + 3H_2\,(g) \xrightleftharpoons{Fe, Al_2O_3\cdot K_2O,\ 450^\circ C,\ 250-600\ \text{atm}} 2NH_3\,(g) + 92.2\ \text{kJ}$$

Research with an alkali-promoted (potassium or K_2O) ruthenium catalyst has demonstrated that ammonia synthesis can be effected at lower temperatures and pressures than those required by the Haber process. As the price of energy increases, ruthenium catalysis might become increasingly important, because the energy-expensive compression process could be avoided. Another advantage of ruthenium if its diminished susceptibility to poisoning by H_2O and CO. Ruthenium catalysts can carry out the direct synthesis of ammonia from N_2, CO, and H_2O:

$$3H_2O + 3CO + N_2 \xrightarrow{Ru-K_2O} 3CO_2\,(g) + 2NH_3\,(g)$$

Ammonia, a colorless gas with a distinctive, highly irritating, penetrating odor, is a potent heart stimulant. It is highly soluble in water, boils at −33°C, and melts at −78°C. The shape of the ammonia molecule is that of a trigonal pyramid; the lone pair on the nitrogen atom helps to explain the highly polar nature and the basicity of the molecule.

Liquid ammonia has certain solvent properties like those of water; however, liquid ammonia will dissolve the alkali metals (sodium, potassium, etc.) and the heavier alkaline earth metals (calcium, strontium, barium) to give intensely blue, conducting solutions. The sodium solution is widely used as a reducing agent in organic syntheses. The unbalanced equation is presented in textbooks as follows:

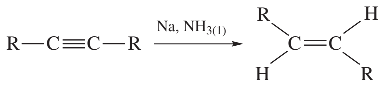

The primary use of ammonia (∼80%) in the United States is in fertilizers, either as anhydrous ammonia or as the salts ammonium nitrate and ammonium sulfate. Other uses include conversions to nitric acid and urea. The reaction for the syntheses of the ammonia derivatives are as follows.

1. Ammonium nitrate:

$$NH_3 + NHO_3 \rightarrow NH_4NO_3$$

2. Ammonium sulfate:

$$2NH_3 + H_2SO_4 \rightarrow (NH_4)_2SO_4$$

3. Nitric acid:

$$4NH_3\,(g) + 5O_2\,(g) \rightarrow 4NO\,(g) + 6H_2O\,(g)$$

$$2NO\,(g) + O_2\,(g) \rightarrow 2NO_2\,(g)$$

$$3NO_2 + H_2O \rightarrow HNO_3 + NO$$

4. Urea:

$$2NH_3 + CO_2 \xrightarrow{\text{heat,pressure}} H_2N{-}\overset{\overset{\displaystyle O}{\|}}{C}{-}NH_2 + H_2O$$

Hydrazine, N_2H_4, is a colorless liquid with a weakly ammoniacal odor. Its density, boiling point (114°C), and melting point (2°C) are fairly close to those of water. Hydrazine and its monomethyl and dimethyl derivatives are used as rocket fuels. A more mundane application of hydrazine is its use in water treatment and in cleaning steam boilers.

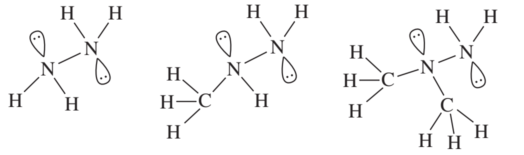

Hydrazine Monomethylhydrazine Dimethylhydrazine

Hydrazoic acid, HN_3, is a colorless, explosive liquid. It is a weak acid whose salts are called azides. Heavy-metal azides, like the acid, are unstable and are employed as detonators for explosives. Sodium azide, NaN_3, is used by biochemists to study cellular respiration. The linear, symmetric azide ion, $[N{=}N{=}N]^-$, serves as an inhibitor of the key electron transfer step.

B. Halides

The important nitrogen halides include the following: NF_3, N_2F_2, N_2F_4, NCl_3, NBr_3, and NI_3. The structures of the four fluorides have been determined and are not unexpected in terms of valence-shell electron-pair repulsion theory (VSEPR) for predicting molecular geometries.

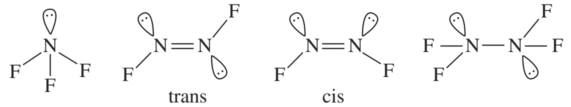

trans cis

The trihalides of nitrogen provide sharp contrasts in their stability and reactivity. NF_3 is a stable gas that resists hydrolysis by water, NCl_3 is an unstable liquid that decomposes explosively and hydrolyzes readily, and NBr_3 is very unstable and decomposes explosively even at very low temperatures. Pure NI_3 has not been isolated. Crystals resulting from the action of iodine on ammonia are represented by the formula $NI_3 \cdot NH_3$. This unstable adduct, often prepared for chemical demonstrations, can be exploded by the slightest tickling with a feather.

C. Nitrogen Oxides

Nitrogen forms several oxides, some of which were known to investigators of the eighteenth century. A brief tabular presentation of the oxides appears in Table V.

The three nitrogen oxides NO, NO_2, and NO_3 are paramagnetic, odd-electron species. Both NO and NO_2 are important in the synthesis of nitric acid from ammonia;

TABLE V Nitrogen Oxides

Formula	Name	Structure	Description
N_2O	Nitrous oxide, dinitrogen monoxide		"Laughing gas"; colorless; used as an anesthetic and a propellant or aerating agent in canned whipped cream
NO	Nitric oxide, nitrogen monoxide	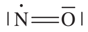	Paramagnetic, odd-electron species; colorless gas; serious air pollutant
N_2O_3	Dinitrogen trioxide	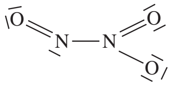	Exists as a blue solid at low temperatures, dissociates into NO_2 and NO gases at higher temperatures; formal acid anhydride of nitrous acid:
	not (older symmetrical representation)	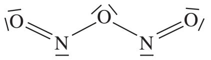	$N_2O_3 + H_2O \rightarrow 2HNO_2$
NO_2	Nitrogen dioxide	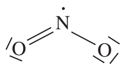	Paramagnetic, odd-electron species; brown gas; serious air pollutant
N_2O_4	Dinitrogen tetroxide	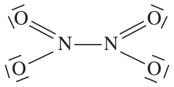	Dimer of NO_2: $2NO_2\,(g) \rightarrow N_2O_4\,(g) + \text{heat}$
N_2O_5	Dinitrogen pentoxide	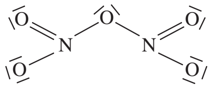	White ionic solid at room temperature $[NO_2]^+[NO_3]^-$; at the formal anhydride of HNO_3: $N_2O_5{+}H_2O \rightarrow 2HNO_3$
NO_3	Nitrogen trioxide	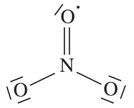	Transient, odd-electron, paramagnetic species; if recent environmental studies had not implicated this unstable compound as a serious pollutant, it would scarcely merit mention among the oxides

both are also important as the NO_x species of air pollution. Recent research is beginning to provide a modified view of the relative seriousness of SO_2 and NO_x as pollutants. In the past, SO_2 and SO_3 were regarded as the worst culprits of air pollution because they produced most of the acid rain; now, however, studies have shown that NO_x and ozone cause serious damage to terrestrial foliage even though they may not be responsible for "killing" lakes. Measures to reduce SO_2 emissions should be continued and intensified, but corresponding emphasis on reducing NO_x, especially from automobiles, should accompany these efforts.

In fact, a considerable amount of research is under way to find economically sound technologies that will make it possible for industries to comply with the more stringent regulations expected for NO_x emissions. One area of research is concerned with the development of better furnaces and burners capable of substantially lowering NO_x formation; another is concerned with the treatment of flue gases containing high levels of NO_x. In the latter approach, NO_x is reduced to nitrogen by ammonia in the presence of a highly selective catalyst.

Unfortunately, the catalytic reduction of NO_x in flue gases is not cost effective in the United States, but it has been employed in Japan. However, a different reduction technique, electrogenerative reduction, is currently being developed at the University of Wisconsin, and it shows considerable promise as an econimically viable commercial process.

In electrogenerative reduction, NO_x pollutants are electrocatalytically reduced in a special cell to yield both electrical energy and any of three useful chemical by-products: ammonia, hydroxylamine (NH_2OH), and nitrous oxide. The percentage of NO_x converted is generally high, and the relative proportions of the three products can be easily adjusted by modifying the reaction conditions. Further refinements of the electrogenerative reduction technique are still necessary, but any process with three points in its favor, that is, elimination of NO_x pollutants, generation of electrical energy, and production of valuable chemicals, would seem to have a good chance of commercial success.

D. Oxoacids and Oxoanions

Although nitrogen forms several oxoacids, only three are discussed here: (meta)nitric acid (HNO_3), orthonitric acid (H_3NO_4), and nitrous acid (HNO_2).

The alchemists referred to nitric acid as *aqua fortis* ("strong water") out of respect for its capacity to dissolve silver from alloys of gold. Its industrial synthesis from ammonia has been described earlier; however, small amounts

are also produced in the atmosphere from nitrogen oxide pollutants (NO_x) and from NO produced during lightning storms:

$$N_2\,(g) + O_2\,(g) \xrightarrow{\text{lightning}} 2NO\,(g)$$

$$2NO\,(g) + O_2\,(g) \rightarrow 2NO_2\,(g) + \text{heat}$$

$$3NO_2\,(g) + H_2O \rightarrow 2HNO_3 + NO\,(g)$$

Pure nitric acid, a colorless liquid that readily fumes in moist air, is rarely encountered; rather it is the concentrated aqueous solution of commerce with which most persons are familiar. A comparison of the physical properties of the pure acid versus the solution is made in the following tabulation:

	Anhydrous HNO_3	**Concentrated HNO_3**
Density (g/cm^3)	1.504	1.405
Boiling point (°C)	82.6	120.5
Melting point (°C)	−41.6	—
Concentration (%)	100	68 by weight

Nitric acid is the most stable and important of the nitrogen oxoacids; however, the pure acid decomposes on heating to yield a mixture of oxides, one of which is the brown gas NO_2. A powerful oxidizing agent, HNO_3 reacts with a host of metals and nonmetals.

Nitrates, the salts of nitric acid, contain the flat, triangular nitrate ion:

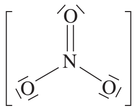

The most important industrial use of nitric acid is the preparation of the salt ammonium nitrate, NH_4NO_3, which is used in the manufacture of fertilizers and explosives. In fact, more than 80% of the nitric acid produced annually is devoted to the preparation of fertilizers.

Nitrous acid, HNO_2, is an unstable, weak acid that is known only in solution. It is prepared by adding a strong acid to a solution containing a nitrite (e.g., $NaNO_2$, KNO_2):

$$H^+ + Cl^- + Na^+ + NO_2^- \rightarrow Na^+ + Cl^- + \underset{\text{Nitrous acid}}{HNO_2}$$

Nitrite salts are more stable than the parent nitrous acid and, like nitrates, are generally soluble in water. Sodium nitrite is the most important nitrite salt, and its use in preserving meat (sausage, bacon, etc.) has a long history. Unfortunately, nitrites have been linked to the production of nitrosoamines, compounds that have been demonstrated to be carcinogenic.

$$\underset{\text{A secondary amine}}{R{-}\underset{\underset{R}{|}}{N}{-}H} + HONO \rightarrow \underset{\text{A nitrosoamine, carcinogenic}}{R{-}\underset{\underset{R}{|}}{N}{-}N{=}O} + H_2O$$

Orthonitric acid, H_3NO_4, which is analogous to orthophosphoric acid, H_3PO_4, has not been prepared. The hydrate of nitric acid, which is represented by the formula H_3NO_4, has been identified by Raman spectroscopy to be merely hydronium nitrate:

$$\text{“}H_3NO_4\text{”} \equiv H_3O^+ + NO_3^-$$

Successful attempts to synthesize orthonitrate salts of sodium and potassium have been reported:

$$NaNO_3 + Na_2O \xrightarrow[\substack{300°C\\ \text{for 1}\\ \text{week}}]{\substack{\text{silver}\\ \text{crucible}}} Na_3NO_4$$

Not surprisingly, the NO_4^{3-} ion has been found to have the same tetrahedral geometry as its analog, the PO_4^{3-} ion.

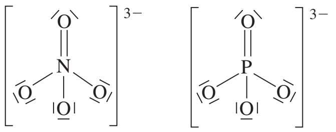

Unlike the stable orthophosphate ion, the orthonitrate ion is easily destroyed; it readily reacts with the water and carbon dioxide present in air to yield the nitrate ion:

$$NO_4^{3-} + H_2O + CO_2 \rightarrow NO_3^- + OH^- + HCO_3^-$$

VIII. PHOSPHORUS

Phosphorus was first isolated in 1699 from urine, not an inappropriate source inasmuch as the element is important in numerous bioorganic phosphate compounds as well as in typical "inorganic" compounds. Among all elements, phosphorus ranks eleventh in order of abundance in the lithosphere. Essentially all phosphorus is found as orthophosphate (PO_4^{3-}) minerals, the most important of which is apatite, which is written either as $Ca_5(PO_4)_3$ (OH, F, Cl) or as $Ca_3(PO_4)_2 \cdot Ca_2(PO_4)$(OH, F, Cl). The following idealized equation indicates how elemental phosphorus is currently produced by heating sand and coke with apatite:

$$2Ca_3(PO_4)_2 + 6SiO_2 + 10C \xrightarrow[1500°C]{1400°C} 6CaSiO_3 + 10CO\,(g) + P_4\,(g)$$

Phosphorus exists in several allotropic forms, but only two are considered: the white and the red. The phosphorus vapor generated by the reduction of apatite is highly flammable, so it is condensed under water to give white phosphorus, a low-density (1.82 g/cm3), low-melting (mp 44°C), highly reactive waxy species in which the four phosphorus atoms occupy the corners of a tetrahedron. White phosphorus stored under water for a long time is gradually converted to the less toxic, more stable polymeric red phosphorus.

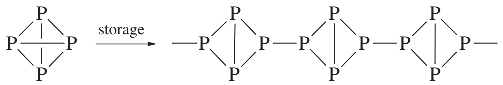

White phosphorus (known configuration)   Red phosphorus (proposed configuration)

A. Phosphides

A majority of the elements in the periodic table form stable binary compounds with phosphorus. If the element is a metal, the binary compound formed is referred to as a phosphide. Many stoichiometries are known, and some metals form several different phosphides. Nickel, for example, forms eight known compounds.

Phosphides can be produced by reaction of red phosphorus with a metal at an elevated temperature in an inert atmosphere:

$$3Ca + 2P \rightarrow Ca_3P_2$$

$$Al + P \rightarrow AlP$$

Most phosphides are industrially worthless; however, a few are valued for some special property. Aluminum phosphide finds application as a semiconductor, and Ca_3P_2 is employed in sea flares to produce flammable phosphine gas (PH_3):

$$Ca_3P_2 + 6H_2O \rightarrow 2PH_3 + 3Ca(OH)_2$$

$$4PH_3\,(g) + 8O_2\,(g) \rightarrow P_4O_{10}\,(s) + 6H_2O\,(g)$$

B. Phosphines

The hydrides of phosphorus are called phosphines. The general formula for this homologous series of very poor thermal stability is P_nH_{n+2} ($n = 1$–6). Other, even less stable homologous series are also known.

The most important phosphine is PH_3, a colorless, poisonous, highly reactive gas. PH_3 is used in naval flares, and it and organic derivatives can serve as ligands that bind to metal atoms.

C. Halides

Three series of phosphorus halides, PX_3, P_2X_4, and PX_5, are known, and all 12 possible compounds have now been synthesized; however, not all have been well characterized because of their instability. The shapes of the halides in the gas phase are as follows (X = F, Cl, Br, I):

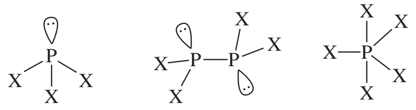

Trihalides (trigonal pyramidal)   Diphosphorus tetrahalides   Pentahalides (trigonal bipyramidal)

Pentahalides, however, may exist as ions in the crystalline phase, for example, $[PCl_4^+]\,[PCl_6^-]$.

D. Oxides

Only the two most important stable binary oxides, P_4O_6 and P_4O_{10}, are considered, but many others are known, even the diatomic species PO, whose electronic spectrum has been characterized.

P_4O_6 hydrolyzes in cold water to yield $H(O)P(OH)_2$, phosphorous acid (phosphonic acid), a diprotic acid:

$$P_4O_6 + 6H_2O \longrightarrow 4H(O)P(OH)_2,$$

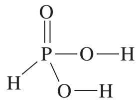

Phosphonic acid

The most important oxide P_4O_{10}, is often referred to as phosphorus pentoxide. It hydrolyzes in water to yield H_3PO_4, orthophosphoric acid, a triprotic acid:

$$P_4O_{10} + 6H_2O \longrightarrow 4H_3PO_4,$$

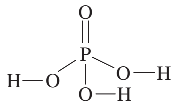

Orthophosphoric acid

E. Oxoacids and Oxoanions

Phosphorus forms more oxoacids than any other element, and the number of oxoanions and oxo salts ranks second only to silicon. Phosphoric acid, H_3PO_4, ranks seventh among the top 50 chemicals in production, and sodium tripolyphosphate, $Na_5P_3O_{10}$, ranks just outside the top 50. $Na_5P_3O_{10}$ may be regarded as a salt of triphosphoric acid, $H_5P_3O_{10}$, whose structure is as follows:

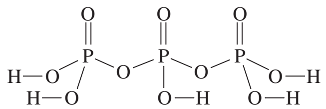

$Na_5P_3O_{10}$ is not formed by the reaction of NaOH with $H_5P_3O_{10}$ but, rather, is produced by fusion of the dibasic and monobasic sodium salts of phosphoric acid at a 2:1 ratio:

$$2Na_2HPO_4 + NaH_2PO_4 \xrightarrow{\Delta} Na_5P_3O_{10} + 2H_2O$$

Concentrated H_3PO_4 is one of the most important acids of the chemical industry; more than 10 billion kg are produced annually. The reactions for the preparation and use of phosphoric acid can be summarized as follows:

$$\underset{\text{Phosphate rock}}{Ca_5(PO_4)_3F} + 10H_2O + 5H_2SO_4$$
$$\rightarrow \underset{\text{Impure acid}}{3H_3PO_4} + 5CaSO_4 \cdot 2H_2O + HF$$
$$\underset{\text{Elemental phosphorus (prepared from phosphate rock)}}{P_4} + 5O_2 \rightarrow P_4O_{10}$$

then

$$P_4O_{10} + 6H_2O \rightarrow \underset{\text{Pure phosphoric acid}}{4H_3PO_4}$$

About 95% of the impure phosphoric acid is used to prepare fertilizers; the remainder is made into pure phosphoric acid for metal treatment or use in foods, detergents, and pharmaceuticals.

F. Metaphosphate Ions

Until fairly recently, the monomeric metaphosphate ion (PO_3^-) was assumed not to exist. Now, however, important work has provided evidence that the metaphosphate ion, which is analogous to NO_3^-, may be an important intermediate in the hydrolysis of bioorganic phosphate esters.

A proposed two-step mechanism invokes the formation of PO_3^- ion and its subsequent attack by H_2O:

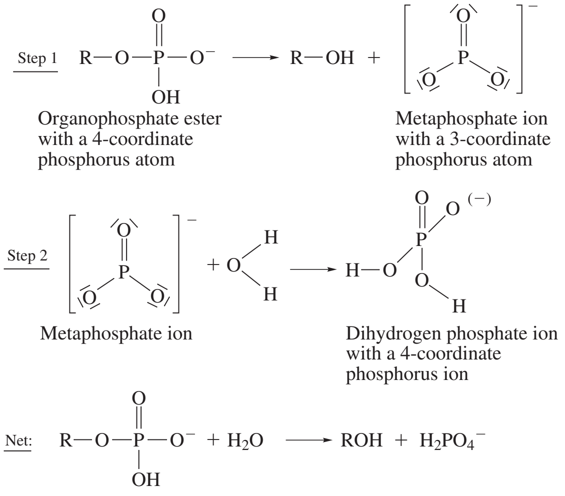

In the first step, the coordination number of phosphorus decreases from 4 to 3, thus producing a metaphosphate ion, which then adds a water molecule to yield a four-coordinate dihydrogen phosphate ion.

This reaction, as well as other biochemical reactions in which PO_3^- can be an intermediate, is gaining increased attention. Mechanisms involving bioorganic phosphate esters are extremely important in elucidating the reactions of the enzymes known as kinases, phosphorylases, and phosphotransferases, all of which involve phosphate esters or anhydrides.

G. Aluminophosphates

A new family of aluminophosphate molecular sieves has been developed. The aluminophosphates are microporous inorganic solids with structural and chemical properties similar to those of zeolites, which are naturally occurring and synthetic aluminosilicates. Natural zeolites find applications as molecular sieves, ion exchangers, water softeners, and desiccating agents. The new aluminophosphate sieves ($AlPO_4$) are strongly hydrophilic and preferentially adsorb water over hydrocarbons. Their potential use as desiccants in drying large volumes of natural gases has been suggested. Unlike the zeolites, however, the aluminophosphates apparently lack ion-exchange capability. Of greater importance to the chemical industry is the possible application of the aluminophosphates as catalysts and catalyst supports in reforming and isomerizing hydrocarbons.

H. Phosphazenes

Phosphazenes contain the basic structure unit $-X_2P{=}N-$. Although some monomeric forms are known, most are obtained initially as six- or eight-membered rings. The rings consist formally of alternating double and single bonds, but the uniform dimensions of the rings indicate delocalization. Structural variation with substituents indicates that the degree of delocalization is sensitive to those substituents. The simplest interpretation incorporates (p–d) π bonds, although the extent of d-orbital participation remains a subject of intense debate.

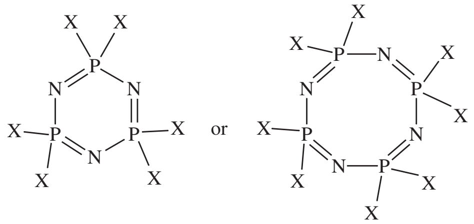

$[X_2PN]_3$ $[X_2PN]_4$

The ring structures are readily prepared by means of the reaction of PCl_5 with NH_4Cl. The transformation of the product, $(Cl_2PN)_{3,4}$ rings, into chain polymers, which results simply from heating the materials past melting, was first observed in the 1890s. The rubbery product is highly insoluble and subject to ready hydrolysis in moist air, so has no practical utility.

The chlorine atoms in the $(Cl_2PN)_{3,4}$ rings are readily replaced by fluorine, amino, or alkoxy groups. When so

derivatized, however, the chain polymerization reaction no longer occurs, in general. It was determined, however, that the polymerization reaction occurs in two stages. The first stage leaves a soluble, low molecular weight polymer on which the same substitution reactions can be accomplished. Further heat treatment gives fully substituted high polymers, many of which have highly desirable properties. Several are in current small-scale commercial production.

Synthesis problems remain, however, in providing the complete range of potentially useful polymer substituents and functional groups. One approach to this lies in the development of alternative routes to the polymers. A recent report describes a condensation–polymerization route in which alkyl substituents and, in some circumstances, mixed alkyl substituents can be introduced.

The high polymers are characterized by a highly flexible backbone, which permits facile conformational changes and leads in most cases to materials that retain their elastomeric character to very low temperatures. The freedom to introduce a wide variety of substituent groups onto the polymer chain makes possible a wide array of properties. For example, when the side chain is an amino function (e.g., NHMe), the high polymer is water soluble and retains significant activity as a ligand for transition metals. In contrast, when the substituent groups are $—OCH_2CF_3$, the polyphosphazene is so water repellant that it does not interact with living tissue, making it a good candidate for use in artificial organ devices. This ease of functionalization also shows promise in providing polymer-attached therapeutic agents, catalysts, and polymeric solid electrolytes.

I. Phosphorus Ylides

Phosphorus ylides are dipolar species in which positive and negative charges are located on adjacent atoms. A typical example is the following:

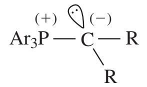

Ar = Phenyl group
R = H or Alkyl group

These strange-looking species are not merely interesting laboratory curiosities; on the contrary, they are extremely valuable laboratory workhorses that facilitate the conversion of an aldehyde or ketone to an alkene via intermediates known as betaines and oxaphosphatenes:

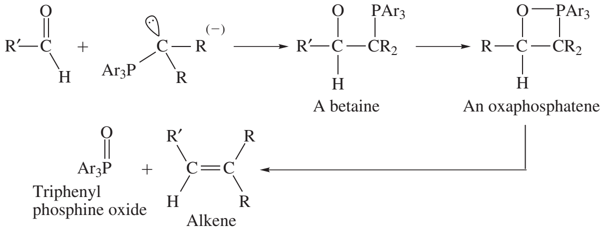

This series of reactions, one of the most useful and versatile for alkene synthesis, is usually called the Wittig reaction to honor its discoverer and developer, the German chemist Georg Wittig. In 1979, Wittig shared the Nobel Prize in chemistry with H. C. Brown, whose boron reagents also made possible the facile syntheses of numerous organic compounds. Wittig reagents are practical and economical, and they have even been adopted by chemical and drug firms for the large-scale commercial syntheses of special pharmaceuticals and bioorganic molecules.

IX. ARSENIC, ANTIMONY, AND BISMUTH

Arsenic, antimony, and bismuth are the last three members of Group 15 (VA). The first two members of the family, nitrogen and phosphorus, are decidedly nonmetallic; however, arsenic is a metalloid, antimony is partially a metalloid, and bismuth is definitely a metal. Arsenic and antimony, like phosphorus, exist in allotropic modifications. Arsenic, antimony, and bismuth occur in nature in both the free state and combined states, usually as sulfides. The principal ores of arsenic are realgar (As_2S_2), orpiment (As_2S_3), and arsenopyrite (FeAsS); the principal ore of antimony is stibnite (Sb_2S_3); and the major ore of bismuth is bismuthinite (Bi_2S_3). None of the elements is abundant in crustal rock; the parts-per-million value of arsenic is 1.8, that of antimony is 0.20, and that of bismuth is only 0.008. In terms of abundance, the rankings among all elements are fifty-first for arsenic, sixty-second for antimony, and sixty-ninth for bismuth.

The pyrometallurgy of all three elements is similar; the sulfide is first roasted and then reduced with carbon (E = As, Sb, Bi):

$$2E_2S_3 + 9O_2 \rightarrow 2E_2O_3 + 6SO_2$$

$$E_2O_3 + 3C \rightarrow 2E + 3CO$$

A considerable amount of bismuth is recovered as a byproduct of the processes involved in refining the metals lead, zinc, and copper.

Arsenic is a gray crystalline solid that does not melt at atmospheric pressure but simply volatilizes to give a dense, malodorous yellow vapor. Its main use as an element is to harden lead–antimony alloys, for example, those in storage batteries or lead shot. Arsenic compounds are highly toxic; hence, many have been used as potent herbicides and insecticides.

Antimony, more metallic than arsenic, is an opaque, lustrous, tin–white, brittle solid. Both the element and its compounds are poisonous. Like arsenic, antimony is used to improve the properties of lead alloys.

As expected, bismuth is more metallic and more lustrous than either arsenic or antimony. A brittle, white metal

with a slight reddish tint, bismuth is one of the few substances that expands on freezing. Most bismuth is used to prepare low-melting alloys composed of bismuth, tin, and lead. Rose's metal, which contains 50% bismuth, 25% lead, and 25% tin, melts at 94°C; and Wood's metal, in which half the tin is replaced with cadmium, melts at only 65.5°C. These remarkably low-melting alloys are used in automatic sprinkler systems and fire alarms.

A minor use of bismuth, which has not been demonstrated as being poisonous, is its application in pharmaceutical compounds.

A. Hydrides

The three hydrides of arsenic, antimony, and bismuth are arsine (AsH_3), stibine (SbH_3), and bismuthine (BiH_3); all are thermally unstable and have high positive enthalpies of formation: 166, 145, and 278 kJ/mol, respectively. The three hydrides are colorless, poisonous gases that decompose on heating to give the elements. The decomposition temperatures for AsH_3, SbH_3, and BiH_3 are about 250, 30, and −45°C, respectively.

B. Halides

Both trihalides and pentahalides are known for arsenic, antimony, and bismuth. The 12 possible trihalides, all of which are known are as follows:

AsF_3	SbF_3	BiF_3
$AsCl_3$	$SbCl_3$	$BiCl_3$
$AsBr_3$	$SbBr_3$	$BiBr_3$
AsI_3	SbI_3	BrI_3

Only five pentahalides are known, and one of these, the thermally unstable $AsCl_5$ (decomposition temperature, about −50°C), was not synthesized until the mild-1970s. The five known pentahalides are the following:

AsF_5	$AsCl_5$
SbF_5	$SbCl_5$
BiF_5	

No pentaiodides or pentabromides for any of the three elements have been prepared.

X. OXYGEN

Oxygen is the most abundant element on the earth's surface. As the free element, it makes up 23% of the atmosphere by weight; in combination with hydrogen, it makes up 89% of the hydrosphere; and in combination with silicon and numerous other elements, it makes up nearly 50% of the minerals in crustal rocks. Combined with carbon, hydrogen, nitrogen, and lesser amounts of sulfur and phosphorus, oxygen is one of the major elements of the bioorganic compounds of living organisms—the lipids, carbohydrates, proteins, and vitamins.

Among the top 50 chemicals produced in 1989, oxygen ranked third, with 17.2 billion kg; however, in terms of moles it would have earned fourth place, with 536 billion mol.

Nearly all oxygen is prepared by fractional distillation of air, and most of the huge amount produced is used for steelmaking and welding purposes. Oxygen finds considerable application in medicine, and a significant quantity of liquid oxygen is employed as the oxidant in rocket fuels.

A. Allotropes

Oxygen exists in two allotropic forms: dioxygen (O_2) and ozone (O_3). The properties of the two are compared in Table VI.

In the stratosphere, the region of the atmosphere from 10 up to 50 km, ozone is synthesized from dioxygen in a complex cycle of reactions. Thanks to its strong absorption of ultraviolet radiation in the range between 232 and 290 nm, ozone provides a protective shield for the plant and animal life on the earth's surface. Because no other atmospheric species can absorb the intense radiation in this range, the ozone layer is absolutely critical to the earth's inhabitants and has been the focus of numerous investigations. A major concern is the possible depletion of the ozone layer by nitrogen oxides from automobile exhausts and by Freons from aerosal sprays.

In the troposphere, that part of the lower atmosphere from the earth's surface up to 10 km, ozone is present in only trace amounts, roughly 0.04–0.07 ppm during the summer growing season. Because ozone is one of the most damaging gaseous pollutants to vegetation, even these

TABLE VI Properties of Dioxygen and Ozone

	Dioxygen	Ozone
Formula	O_2	O_3
Structure	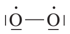	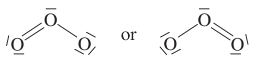
Magnetic properties	Paramagnetic	Diamagnetic
Odor	Odorless	Pungent
Melting point (°C)	−218	−193
Boiling point (°C)	−183	−112
Color	Gas, colorless	Gas, blue
	Liquid, pale blue	Liquid, deep blue
	Solid, pale blue	Solid, violet black
Stability	Stable	Explosive in solid and liquid states

small amounts can reduce crop yields without apparent injury to plant foliage. How ozone produces these effects is not understood, but research has established that ambient levels of ozone can significantly reduce net photosynthesis in both tree and crop species, with a concomitant reduction in growth. The deleterious effects of ozone on terrestrial systems may ultimately prove to be as serious as those of acid rain on aquatic systems. In contrast, studies indicate that acid rain has little negative effect on photosynthesis in certain arboreal species.

B. Water and Hydrogen Peroxide

Water and hydrogen peroxide (H_2O_2) are the two important hydrides of oxygen. Water is abundant and widely dispersed over the earth. It is indispensable to industry and life, and its unique nature and importance were recognized by the ancients, who regarded it as one of the four "elements": water, air, fire, and earth.

Some of the important physical and molecular properties of water and hydrogen peroxide are compared in the following tabulation:

	H_2O	H_2O_2
Structure	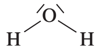	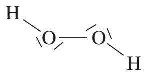
Boiling point (°C)	100	150
Melting point (°C)	0	−0.43
Density (g/cm^3)	1.00 (liquid)	1.44 (liquid)
	0.92 (solid)	1.64 (solid)
Color	Colorless	Very pale blue

Water is an anomalous substance with many unusual properties, most of which result from hydrogen bonding. Water has an abnormally high melting point and boiling point, a high specific heat, a high enthalpy of vaporization, a high entropy of vaporization, and a high surface tension. It is a superior solvent, and much of the value of water results from its extraordinary capacity to dissolve so many substances—both ionic and covalent.

C. Oxides, Peroxides, and Superoxides

All the elements form oxides except the three lightest noble gases, helium, neon, and argon, which form no stable compounds with any element. Oxides are often classified as acidic, basic, or amphoteric on the basis of their acid–base properties in aqueous solution.

1. *Acidic*. (a) Most oxides of nonmetallic elements (Cl_2O, SO_2, SO_3, NO_2, N_2O_5, P_4O_{10}, CO_2); (b) oxides of transition elements in high oxidation states (CrO_3, MoO_3, WO_3, Mn_2O_7).

2. *Basic*. (a) Oxides of electropositive representative elements (Na_2O, K_2O, MgO, BaO, Tl_2O); (b) oxides of electropositive transition elements in lower oxidation states (Sc_2O_3, O_3, TiO_2, ZrO_2).

3. *Amphoteric*. (a) Oxides of less electropositive representative elements (BeO, Al_2O_3, GeO, SnO, Sb_2O_3); (b) oxides of less electropositive transition elements or those in intermediate oxidation states (Cr_2O_3, ZnO).

When active metals react with oxygen, they do not always form the simple, "normal" oxides. Elements from Groups 1 (IA) and 2 (IIA) may also form peroxides and superoxides. The Lewis structures for these ions are as follows:

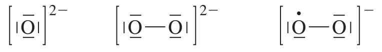

Oxide ion	Peroxide ion	Superoxide ion
Oxidation state −2	Oxidation state −1	Oxidation state $-\frac{1}{2}$

K_2O is potassium oxide, K_2O_2 is potassium peroxide, and KO_2 is potassium superoxide.

The term *superoxide* is something of a misnomer if it leads one to assume that the ion is somehow superreactive. Both the unusual oxidation state of $-\frac{1}{2}$ for oxygen and the odd number of electrons have prompted many to expect an unusual chemistry for this species; however, superoxide is not a reactive electron transfer oxidant of either organic or inorganic substrates. Despite its odd electron, superoxide does not resemble organic radicals in terms of reactivity.

The superoxide ion appears as a common intermediate of cellular reduction of oxygen and has become the subject of special biochemical studies dealing with respiration in both normal and cancerous cells. If O_2 is only partially reduced by gaining two electrons, highly toxic hydrogen peroxide is produced:

$$O_2 + 2H^+ + 2e^- \rightarrow 2H_2O_2$$

If, however, O_2 in a cell gains only one electron, the product is the toxic superoxide ion:

$$O_2 + e^- \rightarrow O_2^-$$

In 1968 it was discovered that respiring cells are protected from superoxide by the action of an enzyme called superoxide dismutase (SOD). Superoxide dismutase (EC 1.15.1.1) converts the toxic superoxide ion to hydrogen peroxide, which is then rapidly decomposed to water and dioxygen by the action of catalase (EC 1.11.1.6), an extremely active enzyme whose function has been known for several decades:

$$2H^+ + 2O_2^- \xrightarrow{\text{SOD}} H_2O_2 + O_2$$

$$2H_2O_2 \xrightarrow{\text{catalase}} 2H_2O + O_2$$

The cytotoxic nature of superoxide is not completely understood, but one explanation suggests that the superoxide ion, or possibly the hydroxyl radical (·OH) produced in a side reaction, can function as an oxidant of certain cellular materials, particularly the unsaturated fatty acids of membrane lipids. Other evidence indicates a strong link between the various oxygen radicals (O_2^-, ·OH, ·OOH) and carcinogenesis, but the significance of the relative rates of formation and destruction of O_2^- in tumor cells remains obscure. Further investigations to ascertain the relationship between O_2^- concentrations and SOD activity in tumorous tissue may provide the information needed to develop novel approaches to preventing and treating certain types of cancer.

D. Hydrogen Peroxide

Hydrogen peroxide is used industrially to bleach wood pulp, textiles, straw, and leather. It is also used extensively in pollution control efforts. It is a valuable reagent in the syntheses of both organic chemicals (epoxides, peroxy compounds, and oxides) and inorganic chemicals (perborates and percarbondates). Familiar domestic uses of dilute 3% solutions of hydrogen peroxide include its application as a hair bleach and as a mild disinfectant. The efficacy of H_2O_2 as an antiseptic and bacteriocide is, however, somewhat dubious; consequently, the household use of peroxide has declined in recent years.

The most important future application of H_2O_2 may be its use in agriculture. Recent studies have shown that dilute alkaline treatment of wheat straw, corncobs, and cornstalks can render these poorly digestible crop residues far more nutritious to sheep and other ruminants. In one study, sheep fed treated straw gained 235 g/day, about the same gain they would realize if fed shell corn; however, sheep fed only untreated straw lost 106 g/day. If alkaline H_2O_2 treatment of fibrous agricultural waste products becomes feasible, then an inexpensive, almost-unlimited food source will be made available for livestock production.

E. High-Energy Oxidizers

Space technology has led to extensive research into the synthesis and properties of high-energy oxidizers for potential use in rocket engines. Among the products of such research is dioxygen difluoride, FOOF. The compound is prepared by passing a low-pressure mixture of F_2 and O_2 through a silent discharge. A very unstable compound, it decomposes at a rate of ~4%/day at −160°C. A potentially important use of this powerful oxidant has been developed at the Los Alamos Scientific Laboratory for recovery of waste and scrap plutonium. Volatile PuF_6 is produced on contact of a variety of forms of the metal and its compounds, with gaseous FOOF allowing transport and collection of the product. The yields are not quantitative in many cases, however, and this oxidant may be displaced by the even more exotic KrF_2.

XI. SULFUR

Sulfur (atomic number 16) ranks sixteenth in order of abundance among the elements. Its total contribution—both free and combined—to crustal rock is 340 ppm; this is only about one-third the value listed for phosphorus (1120 ppm), but it is nearly twice the value for carbon (180 ppm).

Sulfur occurs free in many volcanic regions of the world and in extensive underground deposits in Louisiana and Texas. Although these American deposits lie buried under nearly 200–300 m of clay, sand, and gravel, their recovery by means of the Frasch process dates from the turn of the century. In the combined state, sulfur is found as metal sulfides, as metal sulfates, and as H_2S and organosulfur compounds in petroleum and coal. Some of the important sulfide ores (which also serve as a source of the metal) include galena (PbS), molybdenite (MoS_2), pyrite (FeS_2), sphalerite (ZnS), and cinnabar (HgS). The most important sulfates are those of the Group 2 (IIA) metals and include epsomite ($MgSO_4 \cdot 7H_2O$), gypsum ($CaSO_4 \cdot 2H_2O$), celestite ($SrSO_4$), and barite ($BaSO_4$).

Sulfur for commercial purposes is derived mainly from elemental sulfur mined by the Frasch process or from the sulfur by-products of purified "sour" natural gas and petroleum. (The term *sour* is generally associated with high-sulfur petroleum products.) During World War II, sulfur was first produced commercially from sour natural gas; by the early 1970s, sulfur from sour natural gas and organosulfur compounds in crude oil already exceeded that produced by mining elemental sulfur.

Often found in forbidding, Hades-like regions of volcanic activity, elemental sulfur was known to prehistoric peoples, and over the millennia a certain mystique has been associated with it. Probably no other element, with the exception of gold ("the lust for gold," "the golden touch," "the glint of gold," "the golden fleece") has enjoyed this mystical aura. The fact that rock sulfur burned was obviously impressive to the ancients, but the horrible choking fumes of the sulfur dioxide produced must have been equally impressive. Sulfur was called brimstone (*brennstein*, "the stone that burns"), and it was frequently associated with Stygian origins and infernal punishments.

In later centuries, sulfur was central to the efforts of alchemists, who vainly labored to transmute lead to gold by transferring the yellow color of sulfur into the base metal. Sulfur was also associated with the phlogiston theory of

combustion introduced by Georg Stahl (1660–1734). This theory proposed that the more phlogiston an object contained, the more easily it burned. On being burned, the object lost its phlogiston and became a new substance incapable of being burned further. Inasmuch as sulfur could be burned with almost no residue, it was thought to be essentially pure phlogiston.

Even in modern times it is easy to ascribe a mystical, mythic nature to sulfur. The discovery of its numerous allotropic modifications (perhaps 30 or more) would suggest that sulfur is the element of Proteus, the Greek sea deity with knowledge of the past, present, and future. Proteus had the extraordinary ability to assume different shapes and forms to avoid those who would force him to prophesy.

A. Allotropes

Ordinary sulfur is a pale-yellow solid at room temperature and consists of puckered rings of S_8 molecules, but there are other cyclic allotropes with more or fewer atoms. The two common crystalline S_8 varieties are called orthorhombic and monoclinic sulfur, for which the melting points are listed as 113 and 119°C, respectively. These values, however, are difficult to observe because some of the rhombic sulfur is converted to the monoclinic form, and the resulting allotropic mixture melts at only 115°C and forms a thin, straw-colored liquid still containing S_8 molecules. If liquid sulfur is heated further to temperatures near 160°C, the S_8 rings rupture and the ends of the chains combine to form S_{16}, S_{24}, and S_{32} species. The melt darkens to a rich orange–brown, and a tremendous increase in viscosity (10,000-fold) is observed as the long chains twist and tangle. Above 190°C the viscosity decreases as the extended chains break into shorter fragments, and when the boiling point (444°C) is finally reached, liquid sulfur is once again very thin and runny. Sulfur vapor consists of acyclic S_8, S_6, S_4, and S_2 molecules, with the smaller molecules dominating at higher temperatures. At 1000°C, most of the molecules are probably S_2, which, like O_2 molecules, are paramagnetic. At 2000°C, nearly half the diatomic S_2 molecules are estimated to be dissociated into sulfur atoms.

Although sulfur is found in the native state, it is really quite reactive and combines directly with most other elements at elevated temperatures. It does not, however, combine directly with certain nonmetals (iodine, tellurium, nitrogen, the noble gases) or with unreactive metals (iridium, platinum, gold).

B. Sulfanes

The hydrides of sulfur are called sulfanes. Hydrogen sulfide, H_2S, is the most important and most stable. It is a colorless, vile-smelling, poisonous gas whose putrid odor is recognized as that of rotten eggs. It can be prepared by treating metal sulfides with an acid or by directly combining molten sulfur and hydrogen gas at elevated temperatures. A number of polysulfanes, $H_2S_x (x = 2-8)$, are also known, but they are unstable and readily decompose to sulfur and H_2S.

C. Halides

Sulfur halides include several fluorides (SF_2, SF_4, SF_6, S_2F_2, SSF_2, S_2F_{10}), some chlorides (SCl_2, SCl_4, S_2Cl_2), and some poorly characterized bromides. Even a compound of sulfur and iodine is claimed; however, the S—I bond is notoriously unstable and cannot be formed by direct reaction of the elements.

Both SF_6 and S_2Cl_2 are important compounds that can be synthesized directly from the elements. Unlike the other fluorides, most of which are readily hydrolyzed to HF and an oxide of sulfur, SF_6 is a truly unreactive species. It is a colorless, insoluble gas that will not burn, has no taste or odor, and is nontoxic. It can be bubbled through molten sodium, but boiling sodium will decompose it to NaF and Na_2S. The chemical inertness of SF_6 is used to advantage in high-voltage transformers, where the compound is employed as an insulating gas. S_2Cl_2 is used mainly to vulcanize rubber, and for this purpose alone great quantities are produced annually.

D. Sulfur Oxides

More than a dozen oxides of sulfur are known, but some of them are rather unimportant cyclic monoxides formed by treating a puckered ring of 5 to 10 sulfur atoms with a peroxy acid, and others are unstable acyclic species. Two of the acyclic oxides, however, are extremely important: sulfur dioxide (SO_2) and sulfur trioxide (SO_3). In the decade of the 1980s, when *acid rain* became a household word, these two compounds and their roles in acid rain formation became as familiar to the educated laity as carbon monoxide and carbon dioxide.

Sulfur dioxide is made on a vast industrial scale by burning sulfur, by burning H_2S, or by roasting sulfide ores as part of the pyrometallurgy of zinc, molybdenum, and other metals. The burning of high-sulfur coals and fuel oil serves as the major source of SO_2 produced as an environmental pollutant.

Most of the commercially prepared SO_2 is converted to SO_3, which is subsequently used to manufacture sulfuric acid, H_2SO_4. Other uses of SO_2, albeit on a much-smaller scale, include its application as a refrigerant, food preservative, and bleaching agent.

Sulfur dioxide is a bent molecule in the gaseous state, whereas SO_3, gas molecules are planar triangular. In the liquid and solid state, SO_3 trimerizes to form S_3O_9:

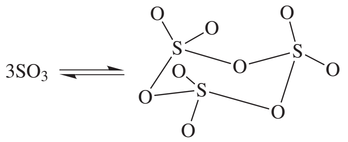

In the presence of a trace of H_2O, SO_3 will polymerize to form needles of crystalline β-SO_3 [actually $HO(SO_3)_xH$, where x is very large].

E. Oxoacids and Oxoanions

Of the approximately 10 oxoacids, only 2 are considered: H_2SO_4 and H_2SO_3. Sulfur trioxide is the acid anhydride of sulfuric acid, H_2SO_4, the most important commercially prepared compound. Its total synthesis from sulfur is as follows:

$$S_8 + 8O_2\,(g) \rightarrow 8SO_2\,(g)$$

$$2SO_2\,(g) + O_2\,(g) \xrightarrow[\text{catalyst}]{V_2O_5} 2SO_3\,(g)$$

$$SO_3\,(g) + H_2SO_4\,(l) \rightarrow H_2S_2O_7\,(l)$$

$$H_2S_2O_7\,(l) + H_2O \rightarrow 2H_2SO_4$$

Although sulfuric acid results from the reaction of $SO_{3(g)}$ with H_2O, a for or mist of tiny H_2SO_4 droplets forms in the reaction chamber. The formation of this mist can be avoided if the SO_3 is dissolved in pure H_2SO_4 to form pyrosulfuric acid, $H_2S_2O_4$, which is then allowed to react with water to yield H_2SO_4.

In terms of mass, H_2SO_4 ranks first among the chemicals produced annually in the United States. In 1989, ~40 billion kg was manufactured; this amounts to nearly 160 kg for each person in the nation. The main uses of H_2SO_4 are the manufacture of phosphate and ammonium fertilizers, the synthesis of other chemicals, petroleum refining, and metallurgical applications.

Sulfur dioxide is the acid anhydride of sulfurous acid, H_2SO_3, a weak acid that does not exist in the free state. The salts of the acid, the sulfites, are stable and are commercially important in food processing, the paper industry, and photography. In 1985, the Food and Drug Administration restricted the use of sulfites on fresh produce. Sulfites are used as "freshening agents" to preserve color and retard wilting in fruits and vegetables; however, asthmatics and other sulfite-sensitive persons may experience violent reactions. Victims often require hospitalization, and some deaths have even been reported. The rapidly increasing number of salad bars necessitated the ban on using sulfites on fresh produce, but sulfites are also added to alcoholic beverages, frozen potatoes, fresh seafood, and even prescription medicines. The sulfites commonly employed are sodium sulfite (Na_2SO_3), sodium bisulfite ($NaHSO_3$), potassium bisulfite ($KHSO_3$), and SO_2.

F. Sulfur–Nitrogen Compounds

The study of binary compounds of sulfur and nitrogen has been spurred both by the problems they pose to simple bonding theory and by the observation that polysulfur nitride is metallic in its properties.

Although oxygen and sulfur are in the same periodic family, there is virtually no parallel between nitrogen oxides and nitrogen sulfides. The relatively poor capacity for π bonding among second long-row elements is reflected by the lack of evidence for the existence of NS and NS_2, the sulfur analogues of NO and NO_2, the two common oxides of nitrogen.

The easiest of the sulfur nitrides to prepare, and the starting point for most of the others, is tetrasulfur tetranitride, S_4N_4. The compound can be prepared from liquid ammonia and elemental sulfur or by warming a mixture of ammonia and S_2Cl_2 or SCl_2. It is kinetically inert in air but may decompose explosively to the elements on being struck. This instability is due to the very strong bond in N_2 rather than to the inherent weakness of the S—N bonds. The compound assumes a boatlike ring form in which there may be some transannular S—S bonding, making the structure more like a cluster. No single satisfactory bonding structure can be written for the compound, but rather an extensive series of resonance structures must be considered. As in other such cases, the bonding is best treated by molecular orbital theory.

Other nitrides include S_2N_2, S_3N_2, $S_{11}N_2$, $(S_7N)_2S_x$, and S_5N_6. Each of these is a colored compound and, with the possible exception of $(S_7N)_2S_x$, defies simple two center–two electron bonding descriptions. Noteworthy is that the first three are ring structures whose essential planarity about the nitrogen atoms suggests some degree of π bonding to the sulfur atoms ($S_{11}N_2$ is bicyclic). S_4N_2 is formally analogous to the important oxide, N_2O_4, but has no comparable acyclic structure. In fact, only the 1,3-diazahexasulfane ring isomer is known. $(S_7N)_2S_x$ has two eight-membered rings joined by an S_x (x = 1–5) chain at the two nitrogens. This structure allows a simple Lewis bonding structure in which a trivalent nitrogen replaces one sulfur atom in the S_8 ring. S_5N_6 assumes a cage (or quadricyclic) structure. Each of these structures retains some. Lewis base character.

In addition to the neutral binary compounds, a number of binary cations and anions have been isolated and structurally characterized. These have contributed to the

discussions regarding the bonding between these elements. After S_4N_4, the most important of these binary compounds is doubtless S_2N_2, which is best prepared by the catalyzed (silver wool) thermal decomposition of S_4N_4. Like its parent, this compound is unstable with respect to the elements, decomposing explosively to the elements on being heated above 30°C or when struck. Interest in S_2N_2 arises from the observation that it spontaneously polymerizes when allowed to stand in the solid phase to give $(SN)_x$, poly(sulfur nitride). The mechanism of this polymerization has been the object of much study, which shows that polymerization is facilitated by the nearly square-planer geometry of the monomer. The resulting polymer retains a nearly planar array of alternating sulfur and nitrogen atoms arranged in a zigzag pattern in which the bond angles have opened from about 90 to 111–113°.

Poly(sulfur nitride) forms golden crystals with a metallic sheen and is the first "nonmetallic metal" to have been described. The fibrous crystals exhibit true metallic conductivity, which increases with decreasing temperatures until superconductivity is reached below 0.33 K. The conductivity is, however, anisotropic. The conductivity along the fibers is ~50 times that perpendicular to them, but this may be due more to the nature of the crystals than to anisotropy at the molecular level. There is disagreement regarding the exact bonding structure that permits this polymer to behave as a metal. Part of this disagreement lies in some remaining uncertainty in the exact structure of the crystals. Qualitatively, the structure may be regarded as having alternating π bonds along the length of the chains, with one "extra" electron from each sulfur atom occupying a delocalized π antibonding orbital or band of the polymer metal.

Poly(sulfur nitride) apparently oxidizes slowly in air and has not achieved significant utility. Halogenated $(SN)_x$ has been shown to have even higher conductivity than the parent polymer, and these derivatives continue to be the subject of intense study. The remarkable properties of poly(sulfur nitride) have spurred extensive research in the general area of conducting polymeric materials as a consequence of the obvious potential utility of such materials.

XII. SELENIUM AND TELLURIUM

The last two chalcogens from Group 16 (VIA) to be considered are selenium and tellurium, both of which resemble sulfur to some extent. Radioactive polonium not is considered since it is radioactive and extremely rare.

Both selenium and tellurium are also rather rare, and their commercial values and chemical uses are insignificant compared with those of the exciting congeners oxygen and sulfur. Selenium ranks sixty-sixth in abundance among elements (0.05 ppm in crustal rock); tellurium ranks a lowly seventy-second (0.001 ppm). Sulfur has ~30 allotropic forms; selenium has only 6 (3 red forms, each consisting of Se_8 rings but differing slightly in stacking patterns; 1 gray, metallic forms consisting of extended helical chains of Se atoms; and 1 black, brittle vitreous form). Tellurium has but one crystalline allotrope; it consists of helical polymeric chains like those of gray selenium.

Selenium and tellurium both occur free in nature and in combination in minerals called selenides and tellurides. The native elements as well as the minerals are found closely associated with sulfur and sulfur minerals. Inasmuch as selenium and tellurium minerals are not abundant, no commercially exploitable ore deposits are known. The elements are usually obtained from the anodic sludge resulting from the electrochemical refining of copper.

A. Hydrides

Both H_2Se and H_2Te are known. Like H_2S, they are extremely toxic, highly malodorous gases.

B. Oxides

Both SeO_2 and TeO_2 are known; however, they do not exist as discrete, V-shaped gas molecules like those of SO_2. Both SeO_2 and TeO_2 occur as polymeric solids and can be formed by direct combination of the elements with oxygen.

The trioxides, SeO_3 and TeO_3, are also known, but they are not obtained by oxidation of the dioxide as is the case with SO_3. The selenium and tellurium trioxides are usually prepared by dehydration of their respective oxoacids, H_2SeO_4 and $Te(OH)_6$ or (H_6TeO_6).

C. Halides

A variety of halides of selenium and tellurium has been synthesized, but their somewhat specialized chemistries and structures are not considered.

D. Oxoacids

Unlike H_2SO_3, both H_2SeO_3 and H_2TeO_3 can be isolated in stable form. Both are white solids that can be easily converted to the respective dioxide by dehydration in a jet of dry air.

The higher acids, H_2SeO_4 and H_6TeO_6, are also known; these correspond to the +6 oxidation state for the sulfur atom in sulfuric acid, H_2SO_4.

E. Uses

Tellurium has no major uses; however, a small amount is used in alloys and steel production. Selenium has several important commercial uses, the most important of which is xerography, a process that takes advantage of the photoconductor properties of gray selenium. Selenium is also used to color glass. SeO_2 and certain organoselenium compounds are gaining favor as versatile reagents in specialized organic syntheses, but these applications are minor and will not greatly increase the demand for selenium.

Despite the fact that selenium and its compounds are poisonous, trace amounts of selenium are required by most higher animals. Health food stores promote selenium as the wonder mineral of the decade. It is allegedly effective in reducing the risk of cancer, alleviating problems associated with high blood pressure, preventing cataracts, and reducing the pain of arthritis. If the faddists are correct, selenium is even valuable in slowing the aging process and protecting against infertility.

SEE ALSO THE FOLLOWING ARTICLES

ALUMINUM • BORON HYDRIDES • HALOGEN CHEMISTRY • METAL HYDRIDES • PERIODIC TABLE • SILICON, HYDROGENATED AMORPHOUS • TIN AND TIN ALLOYS

BIBLIOGRAPHY

Abelson, P. H. (1985). "Air pollution and acid rain," *Science* **230,** 617.
Allcock, H. R. (1976). *Science* **194,** 1214.
Allcock, H. R. (1979). *J. Am. Chem. Soc.* **101,** 606.
Allcock, H. R. (1985). *Chem. Eng. News* **Mar. 18,** 22, 212.
Baum, R. M. (1985). "Science: Laser vaporization of graphite gives stable 60-carbon molecules," *Chem. Eng. News* **Dec. 28**.
Brown, H. C. (1972). "Boranes in Organic Chemistry," Cornell University, Press, Ithaca, NY.
Cowley, A. H. (1984). "Stable compounds with double bonding between the heavier main-group elements," *Acc. Chem. Res.* **17,** 386.
Curl, R. F., and Smalley, R. E. (1988). "Probing C_{60}," *Science* **242,** 1017.
Dagani, R. (1988). "Ceramic composites emerging as advanced structural materials," *Chem Eng. News* **Feb. 1,** 7.
Diederich, F., Rubin, Y., Knobler, C. B., Whetten, R. L., Shriver, K. E., Houk, K. N., and Li, Y. (1989). "All-carbon molecules: Evidence for the generation of cyclo[18] carbon from a stable organic precursor," *Science* **245,** 566.
Escendie, J., Courte, C., Stage, J., Andrianarison, M., and Andrinizake, J. D. (1985). "2,2,-Dimesityl-1-(2,4,6-tri-tert-butyl phenyl) germaphosphene: The first stable compound with a germanium–phosphorus double bond," *Am. Chem. Soc.* **107,** 3378.
Greenwood, N. N., and Earnshaw, A. (1984). "Chemistry of the Elements," Pergamon, Oxford.
Grimes, R. N. (1970). "Carboranes," Academic Press, New York.
Haggin, J. (1990). "Zeolite catalyst breaks down nitric oxide," *Chem. Eng. News* **Jan. 15,** 38.
Klein, C., and Hurlbut, C. S., Jr. (1985). "Manual of Mineralogy," Wiley, New York.
Liotta, D. (1984). "New organoselenium methodology," *Acc. Chem. Res.* **17,** 28.
Muetterties, E. L. (ed.) (1975). "Boron Hydride Chemistry," Academic Press, New York.
O'Sullivan, D. A. (1985). "European concern about acid rain is growing," *Chem. Eng. News* **Jan. 28,** 12.
Rai, S. B., and Rai, D. K. (1984). "Electronic spectra of diatomic oxides of 5A elements," *Chem. Rev.* **84,** 73–78.
Reich, P. B., and Amundson, R. G. (1985). "Ambient levels of ozone reduce net photosynthesis in tree and crop species," *Science* **230,** 566.
Rubin, Y., and Diederich, F. (1989). "Precursors to the cyclo[19] carbons: $[4n+2]$- and $[4n]$ annuleness with unusual stabilities," *J. Am. Chem. Soc.* **111,** 6870.
Sanders, H. J. (1984). "Hightech ceramics," *Chem. Eng. News* **July 9,** 26.
Worthy, W. (1985). "Useful chemicals from NO_x emissions," *Chem. Eng. News* **May 6,** 39.
Zurer, P. S. (1985). "Asbestos, the fiber that's panicking America," *Chem. Eng. News* **Mar. 4,** 28.

Mesoporous Materials, Synthesis and Properties

Robert Mokaya
University of Nottingham

I. Introduction and Background
II. Synthesis
III. Compositions
IV. Pore Geometry
V. Pore Size Control
VI. Characterization Techniques and Properties
VII. Potential Applications

GLOSSARY

Liquid crystal An array of highly ordered molecules in solution.

Mesophase Pertaining to the morphology of a mesostructure.

Mesoporous Having pores of size 2–50 nm in diameter.

Mesostructure Pertaining to the structure of a mesoporous material.

Micelle A number of surfactant molecules forming a sphere, rod, or other shape to minimize repulsive interactions between their hydrophobic tails and aqueous solution.

Microporous Having pores less than 2 nm in diameter.

Supramolecular Pertaining to a large array of molecules.

THE SYNTHESIS and properties of porous solids generally referred to as mesoporous materials, is described here. Although there is a large variety of materials that can loosely be described as mesoporous, this report concentrates on *mesoporous molecular sieves*, which possess a regular arrangement of uniform (mesopore) channels in a solid inorganic framework. The main distinguishing feature of mesoporous molecular sieves, compared to other molecular sieves, is the size of pores they possess and the way in which the pores are arranged. In terms of their structure, they offer highly unusual textural characteristics such as uniform pore sizes greater than 2 nm, surface areas in excess of 1000 m^2/g, and long-range order in the packing of pores. These physical characteristics offer exciting properties that may find applications in (heterogeneous) catalysis, adsorption, molecular sieving, and guest–host chemistry. In general, the mesoporous materials currently available can also be distinguished from zeolites by the fact that their pore walls are amorphous rather than crystalline. Their ordering lies in the arrangement of the pore channels rather than within the pore walls.

Another common feature of mesoporous materials is that they are derived from assemblies of surfactants (or other similar aggregates), which act as templates for the organisation of inorganic components into a structurally well-defined framework.

This article describes the preparation, properties (including characterization techniques), and potential applications of mesoporous materials. The article begins by examining the chemistry of surfactant/inorganic precursor solutions and discusses its application to the synthesis of mesoporous materials. The most common methods of characterization and the properties of the materials are described and finally potential applications are mentioned. This article is therefore intended to provide a general overview of the synthesis, formation mechanisms, characterization, properties, and applications of mesoporous molecular sieves.

I. INTRODUCTION AND BACKGROUND

Materials commonly referred to as molecular sieves obtained their name from the observation that they only adsorb molecules that are small enough to fit through their pore channel apertures. The implication of this is that they can be used to separate molecules of different sizes. According to IUPAC (International Union of Pure and Applied Chemistry) definitions, molecular sieves are defined as one of three different types, depending on the size of the pores they possess—microporous (<2 nm), mesoporous (2–50 nm), and macroporous (>5 nm). Microporous molecular sieves, such as zeolites, have been known for a long time. Indeed, zeolites were first reported in 1756 by the Swedish geologist, Cronstedt, when he noticed that on heating an unidentified silicate mineral in a blowpipe flame, it appeared to boil—the word *zeolite* is derived from the Greek words *zeo*—boil—and *litho*—stone. Today, the basic synthetic procedure for producing microporous molecular sieves (zeolites) is relatively straightforward and is generally carried out in a high-pressure autoclave at elevated temperatures. The inorganic precursor—for example, colloidal silica (and alumina if the zeolite is to be an aluminosilicate)—is mixed with a specific organic molecule or a large cation (the template) and heated to between 100 and 200°C. This process allows the inorganic precursor to form into an open structure, surrounding the suspended molecular templates. Finally, the solid porous zeolite product is obtained by burning away the template molecule (at ca. 500°C in air). The resulting zeolite has a highly regular and precise network of channels (micropores) whose size (and nature) can be varied by changing the template, inorganic precursor or preparation conditions.

In recent years, fundamental and industrial demands have meant that considerable effort has been devoted, particularly in the last 20 years, to expanding the pore size range of well ordered zeolite-type (zeotype) materials into the mesoporous range. Using traditional zeolite synthesis methods, the largest pore sizes achieved are in the range 0.8–1.3 nm (in, for example, VPI-5, UTD-1, and Cloverite). The development of mesoporous molecular sieves owes much to the considerable synthetic effort that, over the last two decades, has been devoted to developing porous solids that bridge the gap between microporous (e.g., zeolites) and macroporous (e.g., amorphous aluminosilicates) materials. The hope was that new mesoporous materials would overcome the limitations imposed by the size of microporous zeolite pore channels. One such group of materials, developed early on in the search for mesoporous solids, are pillared clays. Pillared clays are prepared by the "propping" apart of layered clay minerals (usually of the smectite type, e.g., montmorillonite) with a variety of nano-sized pillars. The pillars are normally metal oxides, which hold apart the clay layers and expose intracrystal clay surfaces. This increases the surface area of the clay. The pore channels in pillared clays are determined by the interlayer and interpillar spaces. Pillared clays have been shown to act as molecular sieves, adsorbents, and catalysts. However, they are not truly mesoporous since they contain a heterogeneous mix of pore channel sizes ranging from the microporous to the mesoporous range. A breakthrough for increasing pore sizes into the mesoporous range came in the early 1990s when truly mesoporous molecular sieves were synthesized by researchers in the United States (at the Mobil Corporation) and in Japan. Since then there has been a global resurgence in interest in mesostructured materials that have uniform pore channels whose size is in the mesoporous domain. Such mesostructured materials are of great interest for a number of reasons. They are unique in that they possess extremely large uniform pores whose size can be easily tailored in a wide pore size range.

The formation of mesoporous molecular sieves is essentially due to the use of surfactant molecular arrays (so-called supramolecular aggregates) as template rather than the single solvated organic molecules or cations traditionally used for the synthesis of microporous zeolites. It is worth noting that the extent to which actual templating occurs varies in zeolites and mesoporous molecular sieves. In zeolites, the organic molecule rarely acts as a true template but typically directs structure or fills space in the porous product. The single organic template molecules are able to rapidly rotate in solution and therefore their orientation is not fixed. Furthermore, the atomic sizes of the organic molecule, which are comparable to the size of the framework building units, means that only a rather

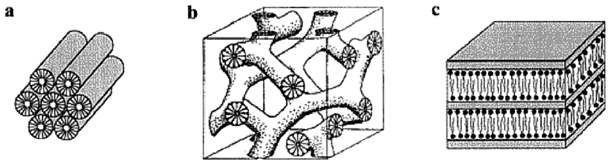

FIGURE 1 Three structure types observed for silica–surfactant mesophases: (a) hexagonal; (b) cubic bicontinuous, *Ia3d*; (c) lamellar.

indirect correlation of the shape and size of the organic molecule is obtained in the structure and volume of the cavity created in the final inorganic framework. In contrast, in mesoporous mesophases the organic supramolecular array clearly acts as template, and there is a direct correlation of the surfactant array size (and shape) to the final pore size and geometry in the mesophase. The intimate template–framework association is facilitated by the flexibility and compliance of the precursor inorganic networks, which are built up of relatively small oligomers and by the large radius of curvature of the organic template.

The initial reports on the synthesis of mesoporous molecular sieves described two types of materials, the M41S family and FSM-16 type materials. Since then much scientific interest has been focused on the three groups of M41S materials—the hexagonal (designated MCM-41), cubic (MCM-48) and lamellar (MCM-50) phases—which are depicted in Fig. 1. The similarity between the different M41S phases and known liquid-crystal phases hinted at a link between the two. For this reason it was initially suggested that so-called liquid-crystal templating (LCT) mechanisms were responsible for formation of M41S mesoporous molecular sieves. As discussed later, recent developments in synthesis methodologies have added new varieties of mesoporous molecular sieves and expanded/clarified the formation mechanisms.

II. SYNTHESIS

In general, the procedures used for the preparation of mesoporous materials are similar to those utilized in the synthesis of zeolites except that a surfactant instead of an inorganic cation or base is used as the template. Mesoporous materials (e.g., mesoporous silica) are prepared under room temperature or mild hydrothermal conditions (typically below 150°C) in the presence of anionic, cationic, or neutral surfactants, in either basic or acidic conditions.

A. Assembly of the Surfactant System

Surfactant chemistry is key to the formation of mesoporous materials. The inorganic species also play an important role in the organization of the surfactant molecules. In general, the interaction (electrostatic, Van der Waals, hydrogen bonding) between the inorganic species and surfactant molecules determines the morphology and pore geometry of the resulting mesophase. In order to understand the necessary reaction conditions for obtaining a particular mesoporous structure, it is useful to look at the behavior of surfactant molecules in an aqueous solution.

1. Behavior of Surfactants in Solutions

In aqueous solution, surfactant molecules exist as very active components with variable structures in accordance with increasing concentrations. At low concentrations, surfactant molecules exist as monomolecules, but with increasing concentration the surfactant molecules aggregate together to form micelles, which has the effect of decreasing the entropy of the solution. The driving force for the aggregation of surfactant molecules to micelles is to minimize repulsive interactions between their hydrophobic tails and water. The resulting micelles are either spherical or rod-shaped. The initial concentration at which the surfactant molecules begin to aggregate into micelles is called the critical micelle concentration, CMC. As the surfactant concentration increases further, hexagonal close packed arrays of micelle rods appear, producing hexagonal phases (such as those that lead to the formation of MCM-41). The next step, as the surfactant concentration increases, is the formation of a lamellar phase, which is sometimes but not always preceded, by the formation of a cubic phase. The changes are illustrated in Fig. 2. The particular phase of the surfactant does not only depend on its concentration, but also on the nature of the surfactant molecules and their environment. Important environmental factors include variables such as the length of the surfactant hydrophobic (alkyl) carbon chain, the nature of the surfactants' hydrophilic head group, the properties of the counterion, pH, temperature, ionic strength, and the presence of other additives/dopants. It has been found that in most cases the CMC decreases with increase of chain

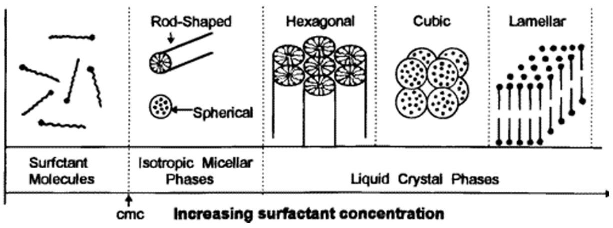

FIGURE 2 Phase sequence of a surfactant/water system. The scheme shows the formation of micelles after the critical micelle concentration (CMC) and the sequence of phases as the concentration of surfactant increases beyond the CMC.

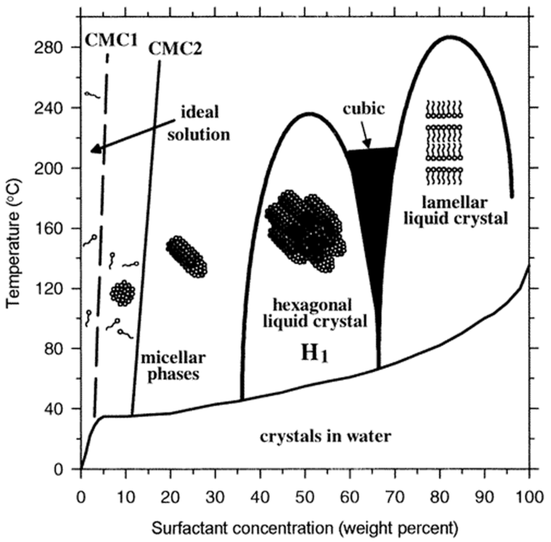

FIGURE 3 A phase diagram showing the relationship between temperature, concentration, and liquid-crystal structure for a surfactant/water system.

length of the surfactant, and the valency of the counterions. Conversely the CMC increases with increasing counterion radius, pH, and temperature.

As stated above, the extent of micellization, the shape of the micelles, and the aggregation of micelles into liquid crystals depends on the surfactant concentration and other factors such as temperature. A more detailed illustration of the micellization process is shown in Fig. 3. At very low concentration, the surfactant is present as free molecules dissolved in solution. At the critical micelle concentration (CMC1 in Fig. 3), the individual surfactant molecules form small, spherical aggregates (micelles). At higher concentrations (CMC2 in Fig. 3), the amount of solvent present between the micelles decreases and as a result the spherical micelles can coalesce to form elongated cylindrical micelles. These cylindrical micelles can then pack together into various liquid crystal (LC) phases. Initially, rod-like micelle aggregate to form hexagonal close-packed LC arrays. As the concentration increases, cubic bicontinuous LC phases form followed by LC lamellar phases.

B. Synthesis Mechanisms

The key feature in the preparation of mesoporous molecular sieves is that the templates used are surfactant aggregates instead of the traditional single organic molecule or metal ion. The mechanisms responsible for the formation of mesoporous molecular sieves, such as the M41S family of materials, from their precursors have for the past decade attracted much attention and speculation. A number of mechanisms have been suggested, each apparently supported by a body of evidence. The following section attempts to explain the prevailing mechanisms and the underlying factors that determine mesophase formation.

There are two general methods used to prepare mesoporous molecular sieves:

1. Assembly of dissolved inorganic species around surfactant arrays via liquid crystal templating (LCT) mechanisms
2. Intercalation of surfactant ions into layered silicates via a folded sheet mechanism (FSM materials).

1. Liquid Crystal Templating (LCT) Mechanisms

The key aspect of the LCT mechanism is that the liquid crystalline mesophases or micelles act as templates rather than individual single molecules or ions. Accordingly, the final product is an inorganic (e.g., silicate) skeleton that contains voids, mimicking the shape of the surfactant mesophases. This mechanism, first proposed by researchers at the Mobil Corporation for the synthesis of M41S materials, is based on similarities between liquid-crystalline surfactant assemblies and the resulting mesoporous solid product. The whole process can be described by two possible mechanistic pathways, which are represented schematically in Fig. 4.

Pathway 1: The liquid crystal mesophases form prior to the addition of the inorganic species, allowing the inorganic species to form directly around the structure.
Pathway 2: The inorganic species added to the reaction mixture influences the ordering of the isotropic, rod-like micelles into the resulting liquid crystal phase (e.g., hexagonal/cubic, etc.)

The influence of altering key parameters such as alkyl chain length and pH on the pore size of mesoporous materials is consistent with well-documented surfactant chemistry, and can be taken as strong evidence for the

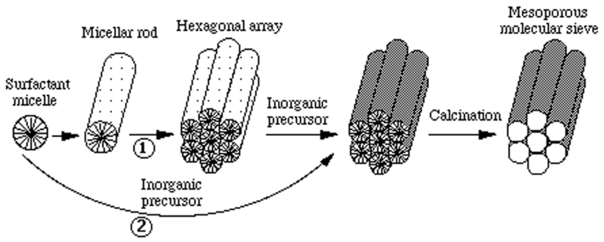

FIGURE 4 Schematic illustration of two possible LCT mechanistic pathways to the formation of mesoporous molecular sieves. In pathway 1 the liquid crystal phase is intact before the inorganic precursor is added; in pathway 2, addition of the inorganic precursor mediates the ordering of the encased surfactant micelles.

LCT mechanism. At present, there is a broad consensus that the formation of M41S materials (in the presence of charged surfactants) takes place via a cooperative mechanism where the interactions between the inorganic and surfactant ions play a key role in determining the morphology of the resulting mesophase. Pathway 2 is therefore now largely accepted as the most likely formation mechanism. Liquid crystal mesophases (according to pathway 1) are not expected to exist at the low surfactant concentrations usually used for synthesis of M41S materials. However, if a much higher concentration of surfactant is present, pathway 1 can be employed to prepare mesoporous materials. Indeed, pathway 1 is operative when surfactant concentrations greater than 30 wt% are employed. In this case, a liquid crystal phase is formed which then acts as a cast or mold in which the inorganic network polymerizes throughout the aqueous regions of the liquid-crystalline phase. The formation of the ordered mesophase is therefore largely independent of surfactant/inorganic interfacial interactions. This pathway is now dubbed "true liquid-crystal templating."

Three LCT-based formation models have been suggested. A common feature of all the models is that surfactants in solution conduct the ordering of the materials, but the type of interactions between the surfactants and inorganic species are different. The three models discussed here are (i) the puckering layered model, (ii) the silicate rod assembly model, and (iii) the cooperative charge density matching model. For simplicity, the following discussion on the LCT models assumes that the inorganic species are silicate ions and that a hexagonal mesophase is formed.

a. Puckering layered model. This model is based on the assumption that the hexagonal surfactant phases are present and that the inorganic (i.e., silicate) source dissolves into the aqueous regions around the surfactant arrays. The dissolved silicates ions are organized into layers (or sheets) with cylindrical surfactant micellar rods intercalated between the layers. These silicate sheets and hexagonal surfactant phases then give rise to hexagonal silica-surfactant mesophases via puckering of the silicate sheets.

b. Silicate rod assembly model. This model proposes that randomly ordered, rod-like micelles form initially and interact with inorganic (i.e., silicate) species to form surfactant rods encapsulated by 2–3 monolayers of silica; these species then spontaneously assemble into a hexagonal structure that has long-range order. Since the hexagonal phase does not form until addition of the inorganic species, this model is consistent with pathway 2 of the LCT mechanism described above.

c. Cooperative charge density matching model. This model involves

1. Cooperative nucleation of inorganic and organic (surfactant) species.
2. Liquid-crystal formation with molecular inorganics.
3. Inorganic polymerization and condensation.

The model proposes that when charged surfactants are used, the initial step is preferential ion exchange of the surfactant counterions with polycharged oligomeric inorganic (i.e., silicate) species. These silicate species serve as multidentate moieties, and can bind several surfactant molecules and screen the repulsive forces between the headgroups within a surfactant aggregate. This can reduce the local curvature and allow the aggregate to grow in size. The charge screening afforded by the silicate ions can reduce the thickness of the double layer that keeps the micelles separated. At the appropriate concentration, this can allow attractive interfacial forces to dominate the inter-aggregate repulsive forces and can induce self-assembly into a new ordered (hexagonal) morphology.

Before concluding the discussion on the LCT models, it is worth pointing out that under certain conditions a true cooperative self-assembly of inorganic ions (e.g., silicates) and surfactants is possible. For example, at low temperature and high pH, conditions that prevent condensation of silicate ions, the formation mechanism schematically represented in Fig. 5 can be operative. According to this mechanism, the formation of mesoporous materials occurs via so-called "silicatrophic liquid crystals" (SLC). Three steps are involved in the synthesis pathway:

1. Assembly of the surfactant system and the formation of ion pairs between surfactant molecules that interact with polydentate and polycharged inorganic species.
2. Self-organization of ion pairs into a mesophase with usually a liquid-crystal structure (hexagonal, lamellar, or cubic), the nature of which depends on the composition of the mixture, the pH, the temperature, and the reaction time.
3. Polycondensation of the inorganic (e.g., silicate) species leading to the formation of a rigid inorganic framework.

Finally, to conclude the description of LCT mechanisms, it is worth noting that no clear and universally accepted mechanism has emerged. However as mentioned above, it is now generally accepted that pathway 2 of the LCT mechanism is responsible for the formation of a majority of mesoporous materials currently available. It is, however, also important to point out that none of the models described above explicitly address mesoporous

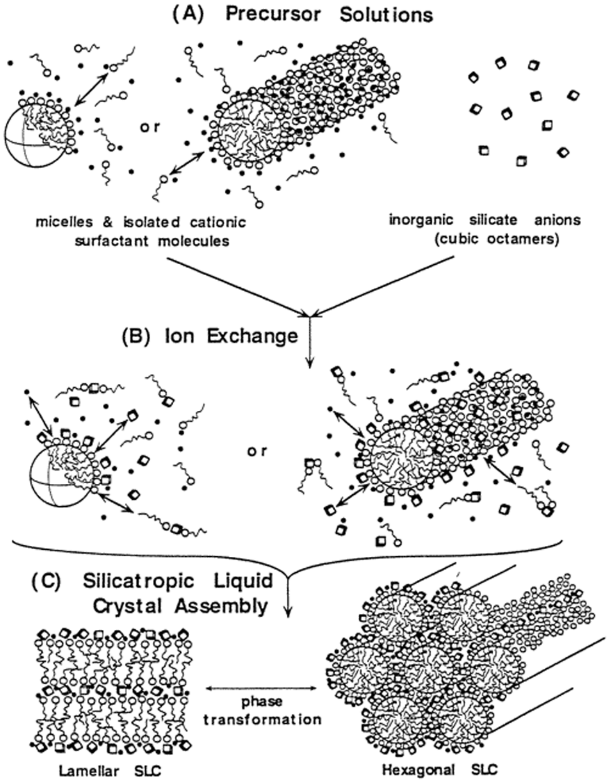

FIGURE 5 Scheme showing the formation of the silicatropic liquid-crystal phase(s).

molecular sieve synthesis where strong electrostatic interactions are absent—for example when neutral surfactants are used. Neutral surfactants have a much greater tendency to form aggregates in water than charged surfactants, and their strong tendency to aggregate in combination with hydrogen-bonding interactions is apparently sufficient to allow the formation of mesophases.

2. Folded Sheet Mechanism

The second general formation mechanism for mesoporous molecular sieves involves the intercalation of surfactants into the layers of a layered silica, kanemite, followed by conversion into a hexagonal phase structure. This mechanism is therefore based on the intercalation of ammonium surfactant in kanemite, a type of hydrated sodium polysilicate composed of single layered silica sheets. After the surfactants are ion exchanged into the layered structure, the silicate sheets are thought to fold around the surfactants and condense into a hexagonal mesostructure as shown in Fig. 6.

C. Generalized LCT Pathways

As mentioned above, it is now generally accepted that pathway 2 of the LCT mechanism described above is responsible for the formation of a majority of mesoporous materials currently available. Key to this mechanism is the interaction between the surfactant molecules and inorganic species. Based on pathway 2 of the LCT mechanism, the interaction between anionic (negatively charged) inorganic species (I^-) and cationic (positively charged) quaternary ammonium surfactants (S^+) is categorized as S^+I^- interaction. There are at least four different electrostatic reaction pathways/interactions that can be explained by a LCT type of mechanism.

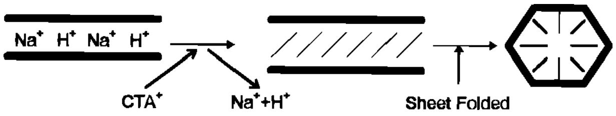

FIGURE 6 Scheme showing the folding sheet mechanism for the formation of mesoporous materials.

1. The (S^+I^-) route: In this case, cationic surfactants (S^+) are used as structure directors for anionic inorganic species (I^-). This is recognized as the pathway for the syntheses of M41S mesoporous materials.
2. The (S^-I^+) route: In this pathway anionic surfactants (S^-) interact with cationic inorganic species (I^+).
3. The ($S^+X^-I^+$) route: Here both the surfactant and the inorganic species are cationic. This pathway is mediated by negatively charged counterions ($X^- = Cl^-$, Br^- etc).
4. The ($S^-M^+I^-$) route: In this case both the surfactant and the inorganic species are anionic and positively charged counterions ($M^+ = Na^+$, K^+, etc.) mediate the structure formation.

This classification is very useful especially for other types of surfactant–inorganic interactions such as those involving neutral surfactants as structure directors (templates). Such interactions can be denoted as follows:

1. S^0I^0, where both the surfactant (S^0) and inorganic species (I^0) are neutral. The surfactant–inorganic interaction is due to hydrogen bonding.
2. N^0I^0, where both the template, nonionic polyethylene oxide (N^0) and inorganic species (I^0) are neutral. The organic–inorganic interaction is due to hydrogen bonding.

The interactions listed above represent the majority of synthesis pathways to mesoporous molecular sieves. However, pathways involving other structure directing agents, such as polymers, lyotropic liquid crystals, and emulsions are also possible. Similarly, a wide range of inorganic species may be used as discussed in Section III.

D. Typical Synthesis Procedures

Three general steps are involved in forming mesoporous molecular sieves: synthesis, drying, and template removal. The four main components (reagents) of the synthesis gel (mixture) are the structure director (template), a source of the inorganic species, a solvent, and a catalyst (an acid or a base). The synthesis is usually performed under room temperature or mild hydrothermal conditions (typically below 150°C). The choice of inorganic species is crucial in determining the preparation procedure, as illustrated in the following example for mesoporous silica. When nonmolecular silica sources (such as fumed silica or water glass) are used, a gel that contains all of the reagents is formed from a nonhomogeneous solution. The gel is then treated hydrothermally at between 50 and 150°C for several hours to several days. For this procedure, surfactant concentrations in the range 10–30 wt% can be used. For molecular silica sources, e.g., alkoxysilanes (such as tetraethyorthosilicate), the aqueous surfactant solution and catalyst are first combined to form a homogeneous micellar solution to which the molecular alkoxide (silica source) is added. The inorganic/surfactant mesophase forms almost immediately and surfactant concentrations as low as 0.5 wt% can be used.

Once the inorganic species and surfactant are assembled into a surfactant/inorganic mesophase, the surfactant (template) is removed leaving behind a well-ordered solid inorganic framework. The diameter of pores in the resulting material is determined primarily by the size of the template surfactant molecules. The pores can be tailored in the 2.0–300 nm range. The materials exhibit specific surface areas typically in the range 500–1500 m^2/g and pore volumes greater than 0.5 cm^3/g associated with a uniform or narrow distribution of pore sizes. The method and conditions used to remove the template can affect the final pore volume fraction, porosity, and the pore size of the materials, but (except under extreme conditions) not the connectivity or arrangement (geometry) of the pores. Various methods are commonly used to remove the template. This include solvent extraction, calcination, oxygen plasma treatment, and supercritical extraction.

A typical synthesis procedure for mesoporous silica is given here to illustrate the key preparation steps.

> 40.4 g of water (solvent) and 6.2 g of cetyltrimethylammonium bromide (template) are mixed and stirred at room temperature until all the template is dissolved. Then, to the surfactant solution, 10 g of a 20% TEAOH solution (catalyst) is added. Finally, 4.1 g of Fumed silica (silica/silicate ions source) is added. The mixture is stirred at 70°C for 2 hours and then aged at room temperature for a further 24 hours. The mixture is then transferred into a Teflon-lined autoclave and heated at 150°C for 48 h under autogenous pressure. After the hydrothermal treatment the autoclave is cooled to room temperature and the as-synthesized mesoporous silica obtained via filtration. The as-synthesized mesoporous silica is then washed with plenty of distilled water, air-dried, and finally calcined in air at 550°C for 10 hours to remove the template resulting in the mesoporous silica.

III. COMPOSITIONS

The key property required of the inorganic species is ability to build up (polymerize) around the template molecules into a stable framework. As is already evident in this article, the most commonly used inorganic species are silicate ions, which yield a silica framework. The silica can be doped with a wide variety of other elements (heteroatoms), which are able to occupy positions within the framework. For example, addition of an aluminium source to the synthesis gel provides aluminosilicate ions and ultimately an aluminosilicate mesoporous molecular sieve. Other nonsilica metal oxides can also be used to construct stable mesoporous materials. These include alumina, zirconia, and titania. Metal oxide mesophases, of varying stability, have also been obtained from metals such as antimony (Sb), iron (Fe), zinc (Zn), lead (Pb), tungsten (W), molybdenum (M), niobium (Nb), tantalum (Ta), and manganese (Mn). The thermal stability, after template removal, and structural ordering of these mesostructured metal oxides, is far lower, however, than that of mesoporous silica. Other compositions that are possible include mesostructured metal sulfides (though these are unstable to template removal) and mesoporous metals (e.g., platinum, Pt).

A. Compositional Modification

Pure silica mesoporous molecular sieves are the most common mesoporous materials. In the following discussion, M41S type (i.e., MCM-41 or MCM-48) mesoporous silica is used to illustrate the compositional flexibility of mesoporous materials. The chemical composition of mesoporous silica can be easily modified to generate new materials with altered properties. It is however worth noting that compositional modification of mesoporous silica has structural implications; in most cases the introduction of a "guest" heteroatom reduces the long-range structural ordering. In some cases the pore size is also altered.

The compositional modification of silica frameworks by other elements (often metals) is achieved via a number of methods. The most frequently used method is the direct addition of the guest elements' precursors to the synthesis solution (gel). Hence, the modifying elements are incorporated into the solid structure along with silica during mesophase formation. This method enables a uniform distribution of the guest element in the resulting framework. A second modification route is to introduce the guest element after formation of the silica mesostructure. This can

be done before or after template removal. If it is done after template removal, the guest element is anchored onto the silica framework via hydroxy (silanol) groups present on the surface. A third method is deposition of guest elements (e.g., metals) onto the silica mesoporous structure via the so-called incipient wetness impregnation technique. The most common modified mesoporous silica materials are those containing aluminum. Incorporation of transition metals into the silica structure is also fairly common.

Indeed, the compositional flexibility of mesoporous materials is such that it is possible to prepare mesoporous organosilicas with organic groups (e.g., ethene) inside the pore walls. An unusual property of mesoporous silicas is that they can themselves be used as templates for the formation of mesoporous carbon. The mesoscopically ordered nanoporous (or mesoporous) carbon molecular sieves are prepared by carbonizing sucrose (or other carbon precursors) inside the pores of mesoporous silica molecular sieve. The mesoporous carbon is obtained after subsequent removal of the silica template by dissolution in HF (hydrofluoric acid) or NaOH (sodium hydroxide) solution.

B. Morphology

Mesoporous materials can be made in a variety of forms. These include bulk powders (the most common form), monolithic gels, and thin films, hierarchically ordered fibrous/tubular forms, and "hard" spheres. The form obtained depends on the synthesis conditions and in particular the rate of precipitation of the inorganic species. For silica materials, low pH values are used to slow down the rate of silicate precipitation, thus making it easier to control the morphology and form.

IV. PORE GEOMETRY

The surfactant/inorganic interactions determine the pore geometry of the resulting mesoporous material. For example, the M41S family contains three distinctly different mesophases; a hexagonal (space group $p6m$) phase referred to as MCM-41, a cubic phase (space group $Ia3d$) known as MCM-48, and a nonstable lamellar phase (space group $p2$). MCM-41 possesses nonintersecting (one-dimensional) pores while MCM-48 has a bicontinuous three-dimensional pore structure (see Fig. 1). Other mesophases, which illustrate the breath of inorganic/surfactant interactions are SBA-1, cubic phase (space group $Pm3n$), and SBA-2, hexagonal phase (space group $P6_3/mmc$) with supercages instead of unidimensional channels. In addition, other less well-ordered phases have been observed. These include HMS and MSU-n, which consist of highly disordered wormhole-like arrays of channels, and KIT, with a highly branched network of pores similar to the L_3 surfactant phase.

V. PORE SIZE CONTROL

One of the most attractive properties of mesoporous molecular sieves is the ability to control/tailor their pore size over a wide range. Pore size in mesoporous materials can be controlled by the length of the surfactant, addition of auxiliary organics, the template removal method, and processing conditions.

A. Surfactant Chain Length

Some limited control of pore size is possible simply by changing the length of the surfactant chain. A good example is for trimethylammonium bromide (CnTMABr, $n = 8$, 10, 12, 14, 16, 18) surfactants, where the pore size increases by roughly 2.25 Å for each increase of one carbon in the surfactant. This means that even-numbered carbon chain length surfactants can be used to increase the pore size by increments of ∼4.5 Å. A limitation of this method of pore size control is that the shortest chain surfactant from which mesophases can be made is $n = 8$ (imposing a lower limit of pore size of ∼15 Å). An upper limit of possible pore size is ∼45 Å due to the limited solubility of surfactants with $n > \sim 18$ carbons which cannot therefore be used.

B. Adding Auxiliary Organics

Mesophases can be made with regular pore diameters up to ∼80 Å by dissolving hydrophobic molecules into the interior of the surfactant aggregates prior to extensive condensation of the inorganic framework. Auxiliary organics that can be used include paraffins, aromatics, and alcohols. For example, 1,3,5-trimethylbenzene (TMB) provides a nearly linear increase in pore size with increasing concentration up to a TMB/Si ratio of 2.5.

C. Hydrothermal Restructuring

Surfactant-containing silica and aluminosilicate mesophases can be hydrothermally restructured at elevated temperatures (100–175°C) in alkaline solutions resulting in pore size expansion.

D. Processing Conditions

Reaction (synthesis) time, degree of framework condensation, or template removal conditions can affect the pore

size. Changes in these synthesis parameters can be used to tailor the pore size.

VI. CHARACTERIZATION TECHNIQUES AND PROPERTIES

Many different techniques are used to characterize mesoporous materials. Often several techniques are used in combination, in order to provide conclusive structural information. The most valuable methods for structure elucidation include powder x-ray diffraction (XRD), transmission electron microscopy (TEM), scanning electron microscopy (SEM), and adsorption (porosity) measurements.

Powder XRD provides direct information on the pore geometry and structural ordering of materials. Due to the limited ordering in mesoporous materials, the diffraction patterns only have reflection peaks in the low-angle region, i.e., 2-theta degrees ($2\theta/^{\circ}$) between 1 and 10. No reflections are seen at higher angles because the pore walls are largely amorphous. The ordering observed by XRD lies in the pore structure rather than in the pore walls. Fortunately, the low-angle diffraction peaks are sufficient to allow indexing according to pore geometry. A typical powder XRD pattern for MCM-41 is shown in Fig. 7. Figure 8 shows a typical XRD pattern for a well-ordered MCM-48 material.

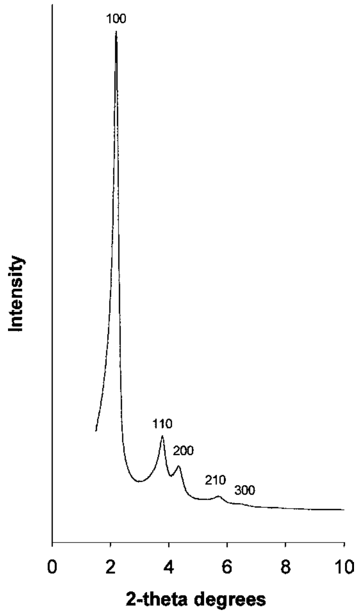

FIGURE 7 Powder X-ray diffraction pattern of MCM-41 mesoporous material. The peaks are indexed according to hexagonal (space group *p*6*m*) geometry.

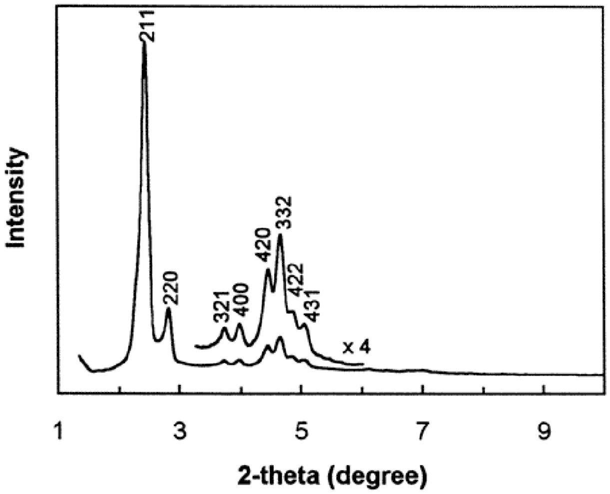

FIGURE 8 Powder X-ray diffraction pattern of MCM-48 mesoporous material. The peaks are indexed according to cubic (space group $Ia\bar{3}d$) geometry.

TEM is a powerful technique for visualizing the pore ordering in mesoporous materials. Figures 9 and 10, for example, show the TEM images of MCM-41 at two different projections. TEM images are useful in estimating the pore size, and wall thickness, and in detecting any defects in the pore structure. SEM is used to identify particle size and morphology.

Adsorption techniques are used to determine the porosity and pore uniformity of the materials. It is possible from the adsorption data to calculate a number of important textural properties such as surface area, pore volume, and pore

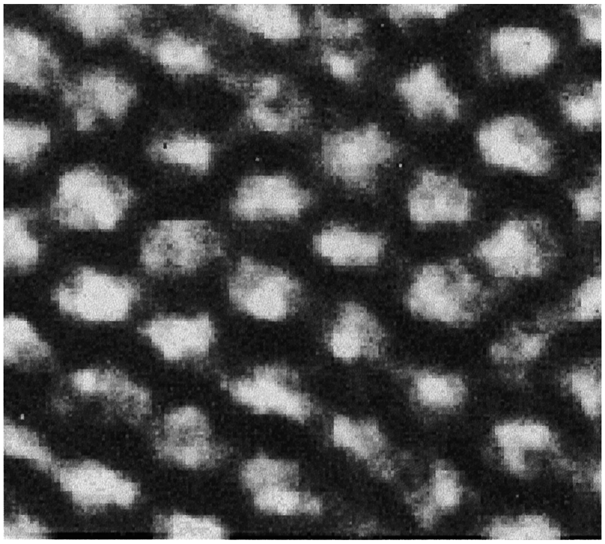

FIGURE 9 TEM image of MCM-41 as viewed down the pore axis. The pore ordering can be clearly observed.

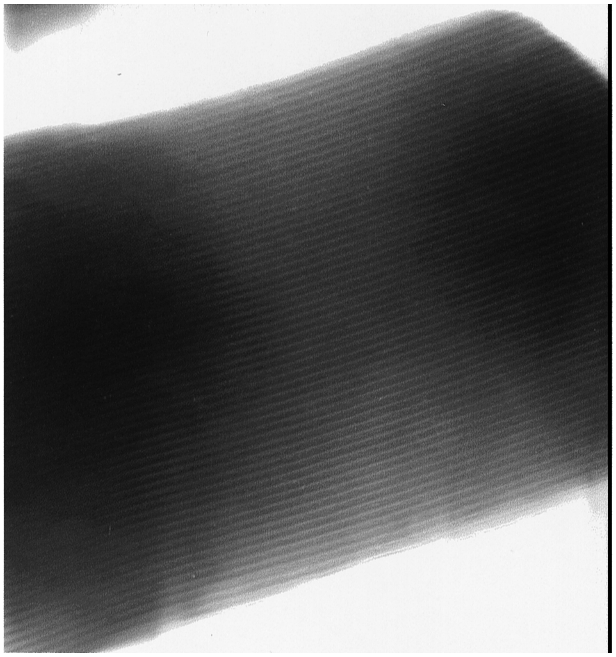

FIGURE 10 TEM image of MCM-41 viewed perpendicular to the pore axis. The pores are clearly observed.

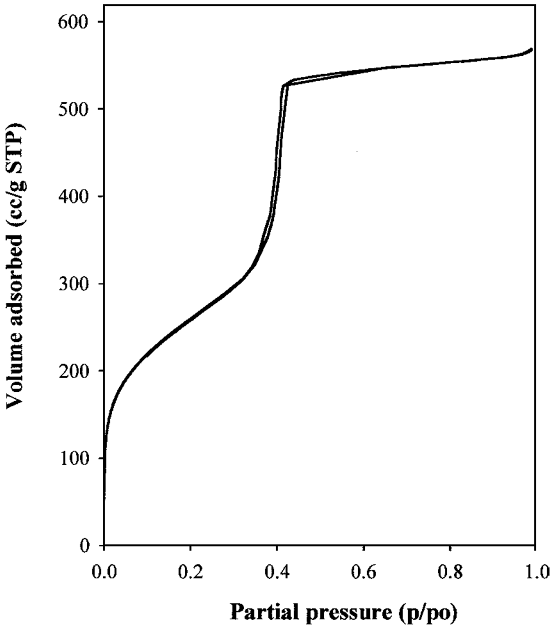

FIGURE 11 Adsorption–desorption isotherm of nitrogen at 77 K on an MCM-41 sample.

size. The spread of pore sizes (pore size distribution) can also be determined; a variety of models for calculating the pore size distribution are available. The most commonly used adsorbate is nitrogen, though argon and water may also be used. Mesoporous materials exhibit a type IV (according to the IUPAC definition) adsorption–desorption (sorption) isotherm. A typical example is shown in Fig. 11 for MCM-41. The type of isotherm is mainly determined by the pore size and pore uniformity. The isotherms are largely insensitive to pore geometry. MCM-41 and MCM-48 materials of similar pore size and pore uniformity would exhibit similar sorption isotherms. In Fig. 11, at low relative pressures (p/po ≤ 0.2) adsorption only occurs as a thin layer (monolayer coverage) on the pore walls of the mesoporous material. Depending on the pore size, a sharp increase in adsorption is observed at relative pressures above 0.2. This adsorption corresponds to capillary condensation of the adsorbate into the mesopores. It is therefore an indication of a mesopore-filling step. The sharpness of the step reflects the uniformity of the pore sizes and the height indicates the pore volume. The position of the step is an indication of the average pore size. The partial pressure at which pore filling occurs increases with the pore size.

Other important characterization techniques for mesoporous materials include solid state NMR. ^{29}Si-MAS-NMR (MAS: magic angle spinning) spectroscopy is used to study the degree of condensation in the pore walls of mesoporous silica materials. The method has been very useful in clarifying that the walls of mesoporous silica are similar to amorphous silica and different from crystalline zeolites. ^{27}Al-MAS-NMR spectroscopy is used to distinguish between tetrahedrally and octahedrally coordinated aluminum in mesoporous aluminosilicate frameworks. ^{129}Xe-NMR is in some cases used to study the porosity of mesoporous materials. NMR methods are also useful in clarifying formation mechanisms and in tracking the incorporation of a variety of heteroatoms into silica frameworks. There are other methods that can also be used to obtain information about the incorporation of other elements (heteroatoms) into the siliceous framework. Diffuse reflectance Fourier transform infrared (FTIR) spectroscopy, ultraviolet-visible (UV-vis) spectroscopy, X-ray photoelectron spectroscopy (XPS), X-ray absorption near the edge structure (XANES), and extended X-ray absorption fine structure (EXAFS) can, for example, provide valuable information regarding the incorporation of heteroatoms.

VII. POTENTIAL APPLICATIONS

Mesoporous molecular sieves present very high surface areas with very regular pore size dimensions. These properties alone, even in the absence of active (e.g., catalytic) sites, have great potential for a wide range of applications.

Potential areas of application for mesoporous materials include use as catalysis, adsorbents, and molecular sieves, and as hosts in the preparation of advanced composite materials. Their potential applications therefore span the areas of heterogeneous catalysis, molecular sieving, and host/guest chemistry.

A. Catalysis

The unique structural properties of mesoporous materials make them highly desirable for catalytic applications. Their large pore sizes limit diffusion restrictions of reactant and product molecules, and thus enable the processing of bulky molecules, which are beyond the size range of microporous zeolites. Furthermore, unlike in microporous zeolites, their large surface area and pore volume allows the grafting of large active species within the mesoporous framework thus increasing the range of possible reactive sites. Mesoporous materials can therefore be used as solid acid catalysts, base catalysts, or reduction/oxidation (redox) catalysts depending on the nature of active sites. The versatility of active sites that can be introduced in these materials greatly expands their catalytic possibilities.

1. Acid Catalysis

Given the absence of active sites and ion-exchange capacity, purely siliceous mesoporous materials are of limited use as catalysts. To generate active and ion exchange sites, doping by isomorphous substitution with a number of metals is performed. The metals used include aluminum (Al), zirconia (Zr), gallium (Ga), and titanium (Ti). The most popular choice of metal dopant for generating ion exchange and acid sites is aluminum. Adding an acidic ingredient such as a heteropolyacid, an ultrastable Y (USY) or an Al-containing ZSM-5 zeolite can also generate acid sites in mesoporous silicates. These additions result in materials that are essentially physical mixtures. The mesoporous silica therefore simply performs the role of a support. For example, by mixing mesoporous silica with zeolites it is possible to create a unique composite catalyst in which a mesoporous shell surrounds a zeolite core. Such a catalyst can be used as follows: the mesoporous shell can provide a high surface area to support metal functionalities (e.g., for hydrogenation), and the zeolite core can provide the acid sites for other process such as cracking. The composite material is essentially a dual (bifunctional) catalyst, capable of performing both hydrogenation and cracking.

Although acidic (e.g., aluminosilicate) mesoporous materials are only moderately acidic, they can be useful catalysts for processes that do not require very strong acid sites. Such processes include hydrocracking, demetalization, hydroisomerization, and olefin oligomerization. Acid mesoporous materials can also be used as catalysts for organic synthesis and production of fine chemicals in, for example, Friedel–Crafts alkylation, acylation, acetalyzation, and Beckmann rearrangement reactions. Common for all these fine chemical synthesis reactions is the increased activity of mesoporous catalysts when the size of the reacting molecules increases. These reactions often involve bulky reactants and products, and in many cases they are carried out in liquid phase where diffusion problems can be severe. The use of a mesoporous material reduces or eliminates these diffusion limitations. An added attraction of mesoporous materials is that the large pore size can produce desired product distributions not achievable on microporous zeolites. Organic synthesis is therefore certainly a field in which acidic mesoporous materials are expected to make a significant contribution.

2. Base Catalysis

Mesoporous materials can also be used as base catalysts—for example, when the negative charge on a mesoporous aluminosilicate is compensated by metal ions such as sodium (Na) or cesium (Cs). Amines anchored on mesoporous silica can also be used as base catalysts. Successful utilization of basic sites requires the total absence of acid sites since the two functions tend to drive reactions through different pathways. There are, however, some cases where adjacent acid/base sites are desirable.

3. Redox Catalysis

The ability to introduce transition metals into the walls of mesoporous materials imparts redox catalytic properties. Transition metal-substituted mesoporous solids represent a very useful and versatile group of potential redox catalysts. In particular, they extend redox catalysis by ordered porous solids beyond the microporous (zeolite) range. Zeolites are limited, due to structural constraints, by the size of transition metal, which can be introduced into their framework. This limitation is largely absent in the case of the ordered mesoporous materials. Though transition metal-containing mesoporous materials are intrinsically less active than Ti-zeolites, they are able to process much bulkier substrates. They are therefore more active than zeolites for processes involving large molecules. The biggest disadvantage however in transition metal-containing mesoporous catalysts is that the activity and selectivity strongly decreases when the level of the metal is increased.

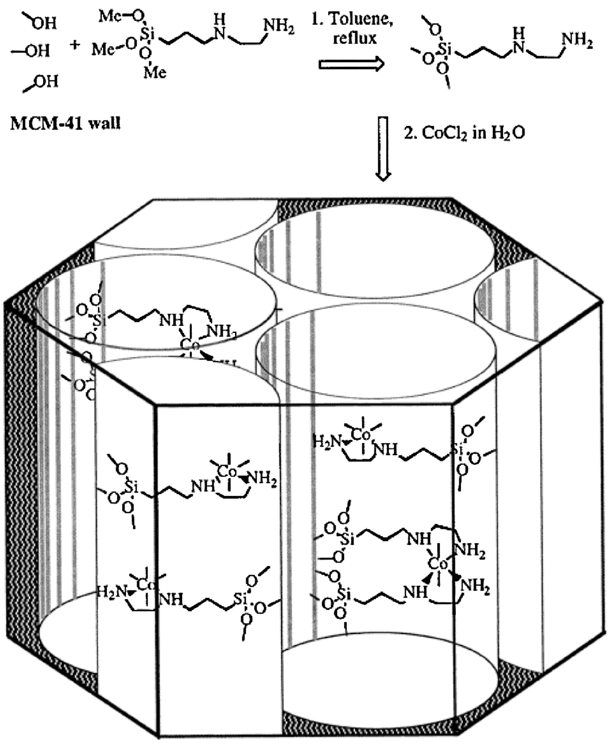

FIGURE 12 Scheme showing the reaction sequence for the anchoring of amino ligand-based Co(II) chelate into a mesoporous material (MCM-41) host.

4. Mesoporous Materials as Catalyst Supports

As described above, mesoporous materials can be used as supports for metals, oxides, acids, and bases. However, perhaps the most intriguing and exciting application is in catalysis involving large active molecules such as organometallics and transition metal complexes immobilized within the pores, as illustrated in Fig. 12. The large surface areas of mesoporous materials makes the materials very attractive as supports for such active phases.

To conclude the discussion on potential catalytic applications, it is clear that mesoporous materials have certainly expanded the range of porous catalysts beyond microprous zeolites into the mesopore range. Their discovery has doubtless created new opportunities not only in catalysis but also in a number of key areas in advanced materials applications. As far as catalysis is concerned, mesoporous materials have shown promising performances in a number of acid, base, and redox processes. The observed improvement compared to more conventional catalysts often stems from increased surface area and greater accessibility of active sites. Furthermore, in a number of potential applications mesoporous molecular sieves can act as supports for catalytically active materials and bring about significant catalytic improvement above that of conventional or commercial catalysts. This is again due to the larger pore size of mesoporous materials, which allow easy access of reactants to the active ingredients and subsequent product release. For transition metal modified mesoporous molecular sieves, innovative applications dealing particularly with bulky molecules relevant to fine chemical synthesis are possible. Another important area is the deposition of transition-metal complexes within the channels and cavities of mesoporous molecular sieves resulting in materials that are likely to be useful as enzyme-mimicking catalysts.

B. Thin Films and Membranes—Separation

In order to be used in thin film or membrane applications, mesoporous materials must be manufactured in the form of defect-free oriented thin films. These films should have controllable pore directions as well as variable thickness. Thin films of mesoporus materials can be grown onto a substrate (e.g., mica) or at the interface between air and water. A major disadvantage of unidimensional mesoporous thin films is that their pores tend to be aligned parallel to the substrate or interface that they are grown at. In potential applications such as biomolecular separation membranes and sensors for large molecules, the pores must preferentially be perpendicular to the solid substrate or interface. One possible way of dealing with this problem is to synthesize three-dimensional mesoporous films. Alternatively, external forces such as a magnetic field can be applied to direct the pore ordering of mesoporous films.

C. Adsorbents—Gas/Liquid Adsorption

The huge pore volume, surface area, and compositional flexibility of mesoporous materials can be exploited for adsorption (and retention) of a wide range of liquids or gases. Here there is a wide range of possible uses, ranging from improving the efficiency of gas (e.g., methane) storage to selective adsorption of heavy metals. For the latter, the mesoporous material has to be functionalized with appropriate adsorption sites.

D. Molecular Hosts

The large uniform-shaped cavities of mesoporous molecular sieves can provide many interesting possibilities for the fabrication and hosting of quantum-sized particles. An example is the fabrication of stable carbon wires in the pore structure of mesoporous materials by polymerizing acrylonitrile within the channels. It is also possible to fill the mesopores with a semiconductor such as germanium. This type of molecular and quantum wires may have many

applications within high technology electronic equipment. The regular system of large channels in mesoporous materials also offers unique opportunities for the preparation of nanostructured composite materials. For example, by combining organic polymers with inorganic fillers, the mechanical strength of the polymers can be greatly enhanced.

Mesoporous materials also have potential use in the following areas:

1. As a stationary phase in normal phase high-performance liquid chromatography (HPLC). The acidic and/or basic properties of mesoporous materials are suitable in the chromatographic separation of acidic, neutral, and basic compounds.
2. As hosts for photoinduced electron transfer reactions in the preparation of uniform nanoscopic products. For example, 2,4,6-triphenylpyrilium confined in mesoporous silica is an efficient electron transfer agent, and in the presence of long wavelength radiation it has been used as sensitizer in the conversion of *cis*-stilbene to *trans*-stilbene.

SEE ALSO THE FOLLOWING ARTICLES

Liquid Crystals • Micelles • Microporous Materials • Stochastic Description of Flow in Porous Media • Surfactants, Industrial Applications

BIBLIOGRAPHY

Raman, N. K., Anderson, M. T., and Brinker, C. J. (1996). Template-based approaches to the preparation of amorphous, nanoporous silica. *Chem. Mat.* **8,** 1682–1701.

Sayari, A. (1996). Catalysis by crystalline mesoporous molecular sieves. *Chem. Mat.* **8,** 1840–1752.

Clearfield, A. (1998). Organically pillared micro- and mesoporous materials. *Chem. Mat.* **10,** 2801–2810.

Moller, K., and Bein, T. (1998). Inclusion chemistry in periodic mesoporous hosts. *Chem. Mat.* **10,** 2950–2963.

Ying, J. Y., Mehnert, C. P., and Wong, M. S. (1999). Synthesis and applications of supramolecular-templated mesoporous materials. *Angew. Chem. Int. Ed.* **38,** 56–77.

Øye, G., Sjöblom, J., and Stöcker, M. (2001). Synthesis, characterisation and potential applications of new materials in the mesoporous range. *Adv. Colloid Interface Sci.* **89–90,** 439–466.

Metal Cluster Chemistry

D. F. Shriver
Northwestern University

I. Introduction
II. Representative Transition Metal Cluster Compounds
III. Early Transition Metal Clusters with Halide and Alkoxide Ligands

GLOSSARY

Butterfly geometry An array of atoms consisting of two triangles that share a common edge, where the metal atoms are located at the vertices of the triangles.

Electron count The number of valence electrons on an atom or molecule.

Halides The elements in column 17 of the periodic table: F, Cl, Br, I, and At.

Ligand An anion or neutral molecule that bonds to a metal atom by donating a pair of electrons to the metal.

Main group metals The elements in the first two columns of the periodic table, excluding hydrogen.

Metal–metal bond A bond between two metal atoms in a metal cluster compound.

Transition metals The elements located in columns 3–10 in the periodic table.

Valence electrons The outermost electrons on an atom, which may form bonds with valence electrons on adjacent atoms.

X-ray diffraction The reflection of an X-ray beam by a solid, which may be analyzed to determine molecular structure.

A METAL CLUSTER compound usually consists of a polyhedral array of metal atoms that are held together by metal–metal bonds. This metal cluster is surrounded by ligands that may be small molecules or ions, such as CO or Cl^-. An important tool in the development of metal cluster chemistry is single-crystal X-ray diffraction, which is used to determine the arrangement of the atoms in metal clusters. The structures illustrated in this section were determined by X-ray diffraction. It is important to note that the formation of cluster compounds is not limited to the metal elements. Nonmetal clusters are also known such as P_4 and C_{60}.

I. INTRODUCTION

Many of the early discoveries of metal cluster compounds occurred in the research laboratory of Professor Walter Hieber at the University of Munich in the early 1900s. Hieber's cluster compounds consisted of transition metals that have metal–metal bonds, and carbon monoxide ligands are attached to the metal cluster. However, Hieber knew only the composition of his newly discovered compounds. Eventually their structures were determined by

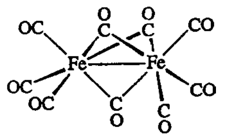

FIGURE 1 Structure of $Fe_2(CO)_9$.

X-ray single crystal diffraction, and this method remains one of the most valuable tools for the characterization of newly synthesized metal cluster compounds. In particular, the presence of short metal atom distances, determined by X-ray diffraction, indicate the presence of metal–metal bonds in clusters. The X-ray diffraction data also indicate the identity and disposition of ligands, such as CO, which usually surround the metal cluster core. A simple metal carbonyl cluster compound is $[Fe_2(CO)_9]$, (Fig. 1).

It is possible to systematize the structures of many organometallic metal cluster compounds according to the number of cluster valence electrons. This correlation was developed by K. Wade and D. M. P. Mingos in the England and by J. Lauher in the United States. It is often referred to as Wades rules. In the following discussion, we will employ the Wade–Mingos–Lauher electron counting rules to describe a variety of metal clusters. For a neutral cluster, the number of cluster valence electrons is the sum of the valence electrons on the metal framework, plus the number of electrons donated by ligands attached to the cluster. For a positively charged cluster, we subtract the charge number, and for a negative cluster, we add the charge number to determine the total valence electron count.

II. REPRESENTATIVE TRANSITION METAL CLUSTER COMPOUNDS

Clusters with triangular metal arrays are common and typically clusters in this class contain 48 cluster valence electrons. Examples include $Fe_3(CO)_{12}$, (Fig. 2) and $[Fe_3(CO)_{11}]^{2-}$. A good illustration of the influence of electron count, on the chemistry of a cluster compound, is the reduction of the neutral molecule $Fe_3(CO)_{12}$, which has a triangular array of iron atoms. When this cluster is reduced by sodium, two electrons are transferred to $Fe_3(CO)_{12}$, and to accommodate these electrons, a CO ligand (which is a two-electron donor) is expelled to form $[Fe_3CO_{11}]^{2-}$. The total electron count (48) is preserved, and the triangular array of metal atoms is unchanged in this process.

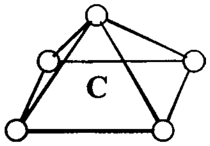

FIGURE 3 A square pyramidal cluster.

A tetrahedral array of metal atoms is generally found for four-metal clusters having a 60 e^- count; an example is $[Fe_4CO_{13}]^{2-}$. When the electron count of the four-metal clusters is increased to 62 by a two-electron reduction, a more open butterfly geometry for the metal atoms results.

Five-metal transition cluster compounds adopt a wide variety of geometries. Those having 72 cluster valence electrons often have a trigonal bipyramidal arrangement of metal atoms. The main group metal clusters $[Sn_5]^{2-}$ and $[Pb_5]^{2-}$ also adopt this geometry (Fig. 4), but unlike the transition metal clusters, many of these main group clusters do not have ligands attached to the metal atoms.

Examples of trigonal bipyramidal clusters are observed for five metal transition metal clusters, such as $[Os_5(CO)_{16}]$ and $[Ni_5(CO)_{12}]^{2-}$. The correlation of valence electron count with structure varies for many of the five-metal clusters. A substantial number of five-metal clusters, that have a 76 valence of electron count, adopt a trigonal bipyramidal geometry; examples include $[Ni_5(CO)_{12}]^{2-}$ and $[Rh_5(CO)_{15}]^{-}$. Five-metal cluster compounds that contain iron group metals (iron, ruthenium, and osmium) and a 74-valence electron count often adopt a square pyramidal geometry, as illustrated in Figure 4. Some clusters in this class also have a main group element, such as carbon in the center of the square base, examples are $[Fe_5C(CO)_{15}]$, $[Ru_5N(CO)_{14}]^{-}$, and $[Os_5S(CO)_{15}]$. A variety of other metal atom arrays are found for five-metal clusters.

The largest group of metal clusters contain six transition metal atoms in an octahedral geometry. The majority of these octahedral clusters have an 86 valence electron count. Examples of these 86-electron clusters

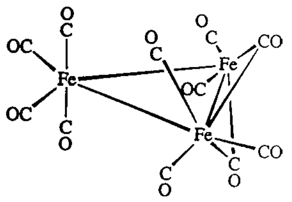

FIGURE 2 Structure of Fe_3CO_{12}.

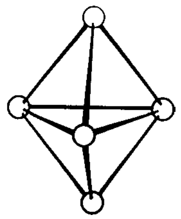

FIGURE 4 Structure of $[Pb_5]^{2-}$.

are $[Co_6(CO)_{16}]$ and $[Ir_6(CO)_{16}]$. Six metal clusters that have a higher electron count adopt more open structures, such as the nearly flat arrangement for the metal atoms in $[Fe_3Pt_3(CO)_{15}]^{2-}$, which has a 90-valence electron count. Osmium, which is a cogener of iron, forms a significant number of clusters containing ten Os atoms with a carbon buried inside the cluster, such as $[Os_{10}C(CO)_{24}]^{2-}$.

III. EARLY TRANSITION METAL CLUSTERS WITH HALIDE AND ALKOXIDE LIGANDS

To this point the descriptions of metal clusters has focused on transition metals ranging from the middle to the right of the periodic table in low oxidation states. We now turn to cluster compounds containing transition metals on the left of the periodic table, which are often referred to as early transition metals. In general, the early transition metal clusters have a strong affinity for halide and oxide ligands, referred to as hard ligands, which contrast with the soft ligands such as CO and organic groups that dominate the metal cluster chemistry of the late transition metals described above. The metal atoms in the early transition metal clusters have positive oxidation states. As with some of the late transition metal clusters, some of the early transition metal clusters have a nonmetal atom such as carbon or boron in the middle of the cluster; an example is $[(Zr_6C)(Cl_{15})]^-$, where a carbon atom resides inside a Zr_6 octahedron and the Cl ligands surround the Zr_6 cluster. The early transition metal cluster complexes often form extended arrays of cluster, which are joined by halide ions that bridge between the apexes of the component clusters.

SEE ALSO THE FOLLOWING ARTICLES

Ligand Field Concept • Metal Forming • Metal Hydrides • Metal Particles and Cluster Compounds

BIBLIOGRAPHY

Braunstein, P., Oro, L. A., and Raithby, P. R. (1999). "Metal Clusters in Chemistry," Vol. 2, Wiley—VCH, New York.

Chisholm, M. H., ed. (1995). "Early Transition Metal Clusters with π-Donor Ligands," VCH, New York.

Cotton, F. A., and Walton, R. A. (1993). "Multiple Bonds between Metal Atoms," 2nd ed., Clarendon Press, Oxford.

Fackler, J. P., ed. (1990). "Metal–Metal Bonds and Clusters in Catalysis," Plenum Press, New York.

Shriver, D. F., Kaesz, H. D., and Adams, R. D., eds. (1990). "The Chemistry of Metal Cluster Complexes," VCH, New York.

Metal Hydrides

Holger Kohlmann
University of Geneva

I. Introduction
II. Preparation and Characterization
III. Crystal Structures and Properties
IV. Applications
V. Conclusion and Outlook

GLOSSARY

Alloy Mixture of metals, intermetallic compounds and/or nonmetals.

Cu type Crystal structure isotypic to Cu, space group $Fm\bar{3}m$, Cu in 4*a* 0, 0, 0; in the literature also called fcc (face centered cubic) or ccp (cubic closest packed).

M Metallic element.

Metal deuteride Metal hydride containing hydrogen in an isotopic purity $>99\%$ D.

Metal hydride Chemical compound of one or more metals with hydrogen (H); generally H consists of the natural isotopic mixture of 99.985% ^{1}H (protium) + 0.015% ^{2}H (deuterium, D); the term metal hydride is also used as a collective name for hydrogen compounds of all isotopes, i.e., protides, deuterides, and tritides.

Mg type Crystal structure isotypic to Mg, space group $P6_3/mmc$, Mg in 2*c* 1/3, 2/3, 1/4; in the literature also called hcp (hexagonal closest packed).

Intermetallic compound Chemical compound from two or more different metals with a stoichiometric or close to stoichiometric composition and in general an ordered crystal structure.

Solid solution Homogeneous solid phase with variable composition, e.g., $Cu_{1-x}Au_x$, also called mixed crystal. In general boundary phases have isotypical crystal structures, similar atomic radii, electronegativity, and valence electron concentration.

W type Crystal structure isotypic to W, space group $Im\bar{3}m$, W in 2*a* 0, 0, 0; in the literature also called bcc (body centered cubic).

HYDROGEN reacts with most of the metals to form chemical compounds—metal hydrides. Their properties, crystal structures and chemical bonding cover a wide range, including features of typical ionic, covalent, metallic and complex compounds. Metal hydrides are particularly useful for reversible storage of hydrogen in applications as an energy carrier.

I. INTRODUCTION

The first report on the reaction of hydrogen with a metal dates from 1866, when *Graham* observed the absorption of hydrogen by palladium up to 935 times its own volume.

TABLE I Binary Metal Hydrides[a]

1a	2a	3b	4b	5b	6b	7b	8b	8b	8b	1b	2b	3a	4a	5a
LiH	**BeH_2**													
NaH	**α-MgH_2** *γ-MgH_2*											**AlH_3**		
KH	**CaH_2**	**$ScH_{0.3}$** ScH_2	**$TiH_{0.9}$** **$TiH_{1.5}$**	V_2H LT V_4H_3 LT VH LT	CrH	*$MnH_{0.4}$*	*$FeH_{0.4}$* *FeH*	*$CoH_{0.2}$* *$CoH_{0.3}$* *$CoH_{0.5}$*	(NiH)	CuH	ZnH_2	GaH_3 Ga_2H_6		
RbH	**SrH_2**	**YH_2** **YH_3**	**ZrH_2**	Nb_4H_3LT **NbH** LT	Mo	Tc	Ru	Rh	PdH	Ag	Cd	(InH_3)	Sn_2H_6 **SnH_4**	
CsH	**BaH_2**	LaH_2 **$LaH_{2.3}$** **LaH_3**	**HfH_2**	**Ta_2H LT** Ta_4H_3 LT TaH LT	W	Re	Os	Ir	Pt	Au	Hg	(TlH) (TlH_3)	(PbH_4)	BiH_3
Fr	Ra	AcH_2												

CeH_2 **$CeH_{2.3}$** **CeH_3**	PrH_2 **$PrH_{2.4}$** PrH_3	NdH_2 **$NdH_{2.4}$** **NdH_3**	Pm	SmH_2 $SmH_{2.3}$ SmH_3	**EuH_2**	GdH_2 GdH_3	**TbH_2** **$TbH_{2.3}$** TbH_3	DyH_2 **DyH_3**	HoH_2 **HoH_3**	ErH_2 ErH_3	TmH_2 TmH_3	**YbH_2** **$YbH_{2.4}$**	LuH_2 LuH_3
ThH_2 **Th_4H_{15}**	PaH_3	α-UH_3 **β-UH_3**	NpH_2 NpH_3	PuH_2 PuH_3	AmH_2 AmH_3	CmH_2	Bk	Cf	Es	Fm	Md	No	Lr

[a] Integer stoichiometric indices are used for fully ordered structures. Transition metal hydrides have broad nonstoichiometry ranges, but precise formulae are only given where necessary for the distinction of different phases. Greek symbols are used only for the distinction of different phases of the same stoichiometry, i.e., they do not represent α and β phases as presented in Fig. 1. **Bold**:Crystal structure fully characterized (see II.C), in general by neutron diffraction on the deuteride. (In parentheses): Existence not yet clear. *Italics*:High pressure phase (prepared under high H_2 or hydrostatic pressures). LT:Low temperature modification.

Ever since many more metal–hydrogen systems have been studied, and today we know that most elements form chemical compounds with hydrogen, called hydrides (Table I). The focus of this article are compounds consisting of metals and hydrogen only. Hydrides containing other nonmetals will be mentioned only briefly.

Hydrogen is the lightest of all elements containing only one proton and one electron (^1H). Because the electron configuration $1s^1$ lies in between the more stable ones, $1s^0$ and $1s^2$, hydrogen shows Janus-head-like chemical properties with parallels to both the alkaline metals and the halogens. This unique feature and its medium electronegativity ($\chi = 2.2$) largely determine its behavior in metal hydrides. A fascinating characteristic of metal–hydrogen systems is the existence of a vast number of phases of different stoichiometry, crystal and electronic structures, properties, and applications. In terms of the classical concepts of chemical bonding, metal hydrides can be typical ionic compounds, such as NaH (NaCl type structure), covalent, such as SnH_4 (discrete tetrahedral SnH_4 molecules), or metallic compounds with hydrogen in interstices of a closest metal atom packing, such as in $PdH_{0.7}$. However, gradual rather than abrupt transitions occur and many hydrides combine features of different bonding types. The orthodox classification as ionic, covalent, and metallic (interstitial) hydrides is therefore abandoned here, and a more natural sequence is adopted according to the metal's position in the periodic table. After a brief introduction in preparation and characterization of metal hydrides (II) we will discuss first structures and properties of main group metal hydrides (III.A), then turn to the transition metal hydrides including lanthanides and actinides (III.B), and finally consider a group of hydrides containing both main group and transition metals, the complex hydrides (III.C).

Metal hydrides find a wide range of applications of which the most prominent is reversible hydrogen storage (IV.A). This is of great importance in view of a possible future hydrogen economy in which hydrogen would replace fossil fuels as an energy carrier. Other fields of application include heat pumps, hydrogen purification, isotope separation, and moderation in nuclear reactors (IV.B). Because of this multiformity and its impact on both basic and applied research, metal hydrides have always been the subject of

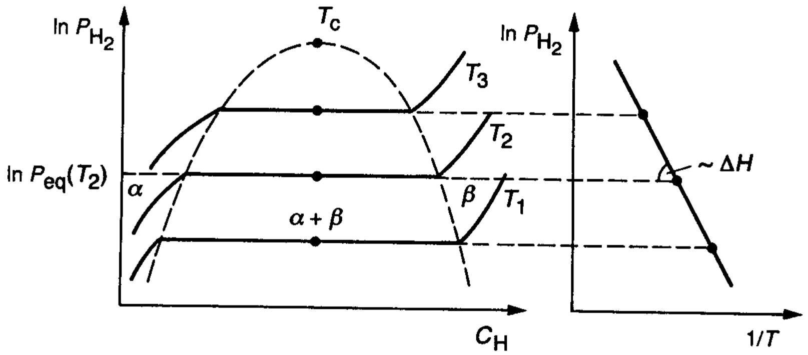

FIGURE 1 Pressure–composition isotherms (*left*) and *van't Hoff* plot (*right*) for the reaction of a metal or intermetallic compound with hydrogen. p_{H2}, hydrogen pressure; c_H, hydrogen concentration in the solid phase; T, absolute temperature; α, solid solution phase of hydrogen in the metal or intermetallic compound; β, metal hydride phase; p_{eq}, equilibrium pressure of metal hydride formation; T_c, critical temperature; ΔH, enthalpy of hydride formation. [From Schlapbach, L., Meli, F., and Züttel, A. (1995). Intermetallic hydrides and their applications. *In* "Intermetallic Compounds: Principles and Practice" (J. H. Westbrook and R. L. Fleischer, eds.), Vol. 2, pp. 475–488. Reproduced with permission from John Wiley & Sons, New York.]

interdisciplinary work involving chemists, crystallographers, engineers, materials scientists, metallurgists, and physicists.

II. PREPARATION AND CHARACTERIZATION

A. Hydrogenation of Metals and Intermetallic Compounds: Thermodynamics

Most binary metal hydrides are synthesized by a solid–gas reaction between the metal and hydrogen. As shown in the idealized pressure–composition isotherms (Fig. 1), at low hydrogen pressure p_{H2} a solid solution of hydrogen in the metal forms in which H occupies interstitial places in the metal host lattice (α-phase). When the equilibrium pressure p_{eq} is reached a metal hydride (β-phase, sometimes called α') forms and the pressure remains constant until the α-phase is entirely converted into the β-phase at the end of the plateau region. Temperature and pressure of the plateau region define the conditions for the preparation of metal hydrides and of reversible hydrogen storage in these materials. The hydrogen concentration (c_H) at the end of the plateau and the length of the plateau region determine the maximum hydrogen uptake and the capacity useful for reversible storage, respectively. In the single-phase region β following the plateau, the pressure rises again drastically with only small compositional changes. This region may be followed by further plateau regions at higher pressures. Above a critical temperature T_c the two-phase region vanishes and the hydrogen concentration in the metal hydride can vary continuously. The enthalpy of metal hydride formation ΔH which is in general negative and the reaction entropy ΔS can be derived from a *van't Hoff* plot ln p_{eq} vs $1/T$ using the equation $\ln p_{eq} = \Delta H/RT - \Delta S/R$ (R, gas constant; Fig. 1, right). Thermodynamical data of some metal hydrides are summarized in Table II. For stability considerations it is sufficient to discuss ΔH values, since ΔS is fairly constant for most systems and corresponds to the entropy of hydrogen gas (130 J/K mol) that is lost on absorption by the metal or intermetallic compound. Thus,

TABLE II Thermodynamic and Hydrogen Storage Properties for Selected Metal Hydrides[a]

Hydride	ΔH (kJ/mol H_2)	Weight fraction of H (%)	H density (g/L)
LiH	−180	12.7	98
NaH	−112	4.2	58
MgH_2	−74	7.7	109
CaH_2	−188	4.8	93
AlH_3	−8	10.1	149
TiH_2	−136	4.0	152
$MnH_{0.5}$	−16	0.9	62
$FeH_{0.5}$	+20	0.9	59
$PdH_{0.7}$	−41	0.7	72
LaH_2	−208	1.4	73
UH_3	−127	1.3	137
Mg_2FeH_6	−98	5.5	150
Mg_2CoH_5	−86	4.5	125
Mg_2NiH_4	−64	3.6	97
$FeTiH_2$	−30	1.9	96
$LaNi_5H_6$	−31	1.4	92
$ZrCr_2H_{3.8}$	−96	2.0	111

[a] For comparison, the density in liquid and gaseous hydrogen in 70.9 and 0.084 g/L, respectively.

in general a ΔH value of less than -38 kJ/mol is required to fulfill the necessary condition $\Delta G = \Delta H - T\Delta S < 0$ for hydride formation at room temperature (ΔG: free enthalpy of hydride formation). This idealized thermodynamic picture does not take into account kinetic effects. Thus, in real systems the plateaus are not completely flat and a hysteresis is often observed on absorption and desorption of hydrogen indicating a nonequilibrium situation. The purity and homogeneity of the materials are critical in this context.

B. Methods of Synthesis

Many metal hydrides can be synthesized by a solid–gas reaction of hydrogen with a metal, an intermetallic compound, or mixtures of metals or binary hydrides and metals. Because of the limited thermal stability of the resulting hydrides, the hydrogenation is usually carried out at moderate temperatures (<800 K). While many metals and intermetallic compounds easily take up hydrogen, others form hydrides only under high hydrogen pressure, i.e., equilibrium pressures p_{eq} vary from 10^3 to 10^9 Pa. Depending on the pressure required, silica apparatus, standard steel, or special high-pressure autoclaves (<25 MPa, <1 GPa) are used. High hydrostatic pressures up to 10 GPa, as produced, for instance, in a belt-type apparatus or in a multianvil press, can be used for solid-state reactions between binary hydrides or binary hydrides and metals. High-pressure syntheses allow the stabilization of new metal hydride phases with high coordination numbers or high oxidation states of the metals, e.g., Sr_2MgH_6, $K_2Pt^{IV}H_6$ or FeH.

Solution methods are rarely applied, but are in some particular cases the only successful route. The synthesis of the first complex transition metal hydride, K_2ReH_9, from an aqueous solution is such a remarkable exception. Other examples are CuH, ZnH_2, and the hydrides of groups 3a and 4a. Alternative methods are ion implantation, ball-milling in a hydrogen atmosphere (hydrogen storage materials), and electrochemical synthesis (e.g., CrH). Many metal hydrides are air sensitive and have to be kept in an inert gas atmosphere. Those containing heavy alkaline metals are extremely reactive and have to be handled with the utmost care. The synthesis of metal hydrides yields samples that are often fine powders and contain by-products. This causes difficulties for structure analysis and the study of physical properties. The growth of single crystals is rarely successful because metal hydrides are in general insoluble in common solvents, and high-temperature methods do not apply because of the low thermodynamical stability. In some cases the addition of LiH as a flux agent has been helpful for single crystal growth. Hydrogen shows the greatest isotope effect of all elements, but this mainly alters some physical and hardly any chemical properties. Therefore, the deuterides are generally synthesized under the same experimental conditions as the hydrides.

C. Chemical and Crystal Structure Analysis

The determination of the exact composition of a metal hydride phase requires precise chemical analysis of the hydrogen content. This may be done by gravimetric or volumetric methods on hydrogen absorption or desorption, heating of the hydride in oxygen atmosphere with subsequent gravimetrical analysis of the water produced, neutron radiography, or interferometry. The analytically found hydrogen content has to be consistent with the result of a structure refinement.

Structure determination of metal hydrides is more difficult than for most other inorganic compounds because of two obstacles: (1) the unavailability of single crystals in most cases, and (2) the difficulty using X-ray diffraction data of precisely locating hydrogen in the presence of heavy elements. Thus, most crystal structures of metal hydrides are solved by a combination of X-ray and neutron *powder* diffraction using the complementary character of the two techniques. Crucial steps for the structure determination are the synthesis of a well-crystallized and preferably single-phase sample and the collection of high-quality diffraction data. Unit cell dimensions, space group, and metal atom positions are determined from X-ray data, and the hydrogen atoms are located from neutron data, both generally on powder samples. The space group determined from X-ray data has to be verified by the neutron data as sometimes pseudo-symmetry of the metal lattice occurs. The deviation from more symmetrical structures can be exceedingly small, which makes the use of high-resolution X-ray (synchrotron) and neutron data indispensable. Pseudo-symmetry can cause microtwinning as seen by anisotropic line broadening, which is a further problem for structure determination. For the refinement of the whole crystal structure including the D positions, joint refinements are often advantageous as this makes full use of the complementary character of X-ray and neutron diffraction using the two data sets simultaneously.

In neutron diffraction deuterides are used instead of the hydrides because of their more favorable coherent scattering and much less pronounced incoherent scattering. No significant differences are found for their crystal structures besides slightly smaller cell volumes of the deuterides due to the lower thermal displacement of ^2H compared to ^1H. Some elements, such as Cd, Eu, Sm, and Gd, exhibit an excessively high neutron absorption cross section,

σ_a. Neutron diffraction studies on compounds containing these elements require either the use of the isotope effect, i.e., generally very expensive isotopic pure materials, or the use of the wavelength dependence of σ_a, which often makes it necessary to choose rather short wavelengths.

Because of the progress in structure solution from powders and in neutron diffraction, more than 300 crystal structures have already been fully determined, most of them during the past two decades. Here, crystal structures are only considered as fully characterized if all atomic positions have been determined and refined to an acceptable precision. The *hydride fluoride database* (*HFD*) provides a comprehensive, critical compilation of crystal structure data of metal hydrides. The power of the method described of combining X-ray and neutron powder diffraction may be illustrated by the example of $Mg_6Co_2D_{11}$, whose rather complex crystal structure, which contains 63 free positional parameters, was solved *ab initio* from high-resolution synchrotron and neutron powder diffraction data. Because of the main problems discussed in this section, the accuracy of metal hydride structural parameters is generally lower than for other inorganic compounds.

D. Electronic Structure and Spectroscopy

Quantum mechanical calculations are being increasingly used to determine the nature of the chemical bonding in metal hydrides, the site preferences of hydrogen, and the factors limiting the hydrogen capacity of storage materials. Depending on the complexity of the crystal structure, semiempirical methods such as Extended Hückel or self-consistent methods (LMTO, LAPW) are used. As for experimental techniques such as X-ray absorption near-edge structure spectroscopy (XANES) and photoelectron spectroscopy (PES), difficulties arise from the unavailability of single crystals and the low thermodynamical stability under experimental conditions (ultrahigh vacuum).

Diffraction methods provide a detailed picture of the crystal structure averaged over space and time, but fail to give information on local structures and coordinated dynamics in materials. Here, spectroscopic methods such as inelastic neutron scattering (INS) are better suited for the study of metal–hydrogen and hydrogen-hydrogen interactions, nuclear magnetic resonance (NMR), infrared (IR), Raman, Mössbauer, and muon spin rotation spectroscopy (μSR) for local structure and dynamics of hydrogen. Because of the high incoherent scattering of ^{1}H, INS can also be used to locate hydrogen positions in hydrides with very low H concentrations where diffraction techniques fail. Many other characterization techniques such as electrical transport are often not feasible because of the low sample quality (powder, multiphase).

III. CRYSTAL STRUCTURES AND PROPERTIES

Hydrogen with its electron configuration $1s^1$ bonds to metals in different ways. Uptake of a further electron leads to a stable helium $1s^2$ configuration, which may be achieved by combination with very electropositive metals. The resulting hydride anion H^- is extremely deformable and less stable than He because of its charge. With less electropositive metals hydrogen can donate its s-electron in a covalent σ-bond. Finally, hydrogen can form interstitial metal hydrides of a variable composition and with a metallic character. There are intermediates, and in ternary hydrides different bonding patterns may be combined. The crystal structure and properties are largely determined by the nature of the chemical bond in metal hydrides.

A. Hydrides of Main Group Metals: From Ionic to Covalent

1. Binary Main Group Metal Hydrides

Following the trend in electronegativities χ of the main group metals, hydrogen ($\chi = 2.2$) forms ionic hydrides with alkaline metals such as K, Rb, Cs ($\chi = 0.9$) and covalent compounds with group 4a and 5a metals such as Sn ($\chi = 1.7$). Crystal structures, e.g., extended solid KH (NaCl type) vs discrete SnH_4 molecules, and properties resemble those of other typical ionic or covalent compounds. However, there is a gradual transition between these two extremes for the metals with medium electronegativities.

All main group metal hydrides are colorless, diamagnetic, nonmetallic, stoichiometric compounds with a low mobility of hydrogen in the crystal structure and a fixed hydrogen content determined by the metal valence. On electrolysis of molten ionic hydrides, hydrogen is produced at the anode, proving the anionic character of hydrogen. Ionic (often called saline or saltlike) hydrides are characterized by a high electron localization at the hydride anion, H^-. This has a huge polarizability far surpassing that of all other anions because of the high charge ratio of 2/1 between valence shell and nucleus, and this strongly influences its crystal chemistry. In the series of the isotypical alkaline hydrides LiH–NaH–KH–RbH–CsH (NaCl type structure), the ionic radius $r(H^-)$ varies as 128–142–148–150–152 pm, showing the strong dependence of the polarizing effect of the cation. Such radius values are close to that of F^- (133 pm), causing some structural similarities between ionic hydrides and fluorides, known as the *hydride fluoride analogy*. Some hydrides form solid solutions with the corresponding fluorides, $MH_{x-y}F_y$. In comparison to the fluorides, metal hydrides are thermodynamically less

stable. Enthalpies of formation of ionic hydrides range typically from −70 to −180 kJ/mol (Table II) while those of metal fluorides are generally found to be −250 to −600 kJ/mol. The enthalpy of formation of the hydride ion $\Delta H = -72$ kJ/mol by the reaction $H_{(g)} + e^- \rightarrow H^-_{(g)}$ is much less negative than that of the corresponding reaction for the fluoride anion (−333 kJ/mol). Binary metal hydrides decompose under 10^5 Pa H_2 atmosphere upon heating before they melt because of the low thermodynamic stability. As an exception LiH melts at 953 K without decomposition. As H^- is a very strong base, ionic hydrides react violently with water, producing H_2 gas. Ionic hydrides are not soluble in common solvents. They are used as reducing agents, e.g., for the reduction of oxides to metals, for the convenient production of pure hydrogen on a laboratory scale, but are thermodynamically too stable for reversible hydrogen storage (Table II).

As for the alkaline earth metal hydrides, the covalent character increases in the series BaH_2–SrH_2–CaH_2–MgH_2–BeH_2. Unlike the corresponding fluorides, BaH_2, SrH_2, and CaH_2 adopt the $PbCl_2$ type structure. MgH_2 crystallizes in the rutile type and BeH_2 in its own type with a framework of corner-sharing BeH_4 tetrahedra (H–Be–H bond angles between 107° and 113°). AlH_3 is often described as a covalent hydride, and 3-center-2-electron bonds Al–H–Al (bond angle 141°) are discussed in analogy to boranes. However, it is an extended solid with a typical fluoride structure of corner-sharing AlH_6 octahedra (VF_3 type structure), which derives from hexagonal closest packed Al (Mg type) by filling one-third of the octahedral holes with H. GaH_3 is less stable and decomposes at room temperature to the elements. Its solid structure is unknown; in the gas phase it dimerizes to digallane, Ga_2H_6. The existence of InH_3, TlH_3, and TlH is not yet proven. Distinct molecules as expected for typical covalent compounds are found in GeH_4 and SnH_4. SnH_4 is a very volatile hydride (melting point 123 K, boiling point 221 K) that decomposes at room temperature. In the solid state, weak Sn–H interactions between neighboring tetrahedral SnH_4 units are present. In the gas phase, distannane Sn_2H_6 has also been reported. The existence of PbH_4 is not yet clear. BiH_3 seems to be extremely unstable and has never been produced in high yields.

2. Ternary Main Group Metal Hydrides

Ternary hydrides containing alkaline and alkaline earth metals only adopt typical ionic structure types and are very air sensitive. In the following discussion Eu and Yb are included as they are divalent in hydrides only (except binary $YbH_{2.4}$) and greatly resemble Sr and Ca in their hydrides because of their almost identical ionic radii. EuH_2 and YbH_2 crystallize as the dihydrides of Ca, Sr, and Ba in the $PbCl_2$ type structure. In contrast to the main group hydrides, those with Eu are colored (red, brown, or violet) and are ferromagnetic semiconductors. Simple ionic structure types are adopted by many ternary hydrides of the type $A_aM_mH_{a+2m}$ (A = Li–Cs, M = Mg–Ba, Eu, Yb), e.g., the perovskite-type structures. Examples of the latter are $RbMgH_3$ (hexagonal perovskite ($BaTiO_3$) type), $NaMgH_3$ (orthorhombic perovskite ($GdFeO_3$) type), $CsCaH_3$, $SrLiH_3$, $BaLiH_3$, and $EuLiH_3$ (cubic perovskite ($SrTiO_3$) type). In the last structure (Fig. 2, left) Eu is surrounded by 12 H cuboctahedrally and Li by 6 H octahedrally. Despite the different stoichiometry there is a close relationship to the crystal structure of $EuMg_2H_6$ (Fig. 2, right), a further ternary metal hydride with ionic character. Every other Eu layer is missing in the latter with respect to the former as required by the electroneutrality on replacing Li^+ by Mg^{2+}. This surprising structural resemblance may be explained by the diagonal relationship between Li and Mg. Some examples of ternary hydrides with group 3a and 4a metals are $NaAlH_4$ ($CaWO_4$ type), $NaGaH_4$ ($CaSO_4$ type), Na_3AlH_6 (cryolite (Na_3AlF_6) type), and Ca_3SnH_2 (anti-$CsCu_2Cl_3$ type). The alkaline aluminum and gallium hydrides show complex anions $[AlH_4]^-$, $[GaH_4]^-$, and $[AlH_6]^{3-}$ in which hydrogen is covalently bonded to the metal. These compounds are soluble in ethoxyethane. Alanates with transition metals have also been reported, such as $Ti(AlH_4)_4$ and $Fe(AlH_4)_2$, but not structurally characterized. The AlH_4^- unit also serves as a ligand in organometallic complexes. With BeH_2, MgH_2, and CaH_2, ternary hydrides $A(AlH_4)_2$ (A = Be, Mg, Ca) are formed with a more covalent character. AlH_3 reacts with diborane to give $Al(BH_4)_3$ and with gallane to give $Ga(AlH_4)_3$. $LiAlH_4$ is widely used in preparative chemistry as a versatile reducing agent.

Some ternary main-group metal hydrides are very metal rich and were first reported as being new intermetallic compounds with unusual properties, as hydrogen has been overlooked in the X-ray structure determination. Common sources of hydrogen are the commercially available divalent metals Ca, Sr, Ba, Eu, Sm, Yb used for synthesis, which may contain as much as 10–20 at% H. Unrecognized hydrogen content has led to confusion in view of valence electron rules in compounds considered as Zintl phases, e.g., the compounds of the formerly assigned "β-Yb_5Sb_3" type structure. It was shown that the true composition is A_5M_3H (A = Ca, Sr, Ba, Sm, Eu, Yb; M = Sb, Bi), and the crystal structure and properties are in agreement with the ionic formula $(A^{2+})_5(M^{3-})_3H^-$. Further examples for metal rich main group hydrides are A_3MH_2 (A = Ca, Yb; M = Sn, Pb) with the ionic formula $(A^{2+})_3M^{4-}(H^-)_2$. $Ba_5Ga_6H_2$ contains both a

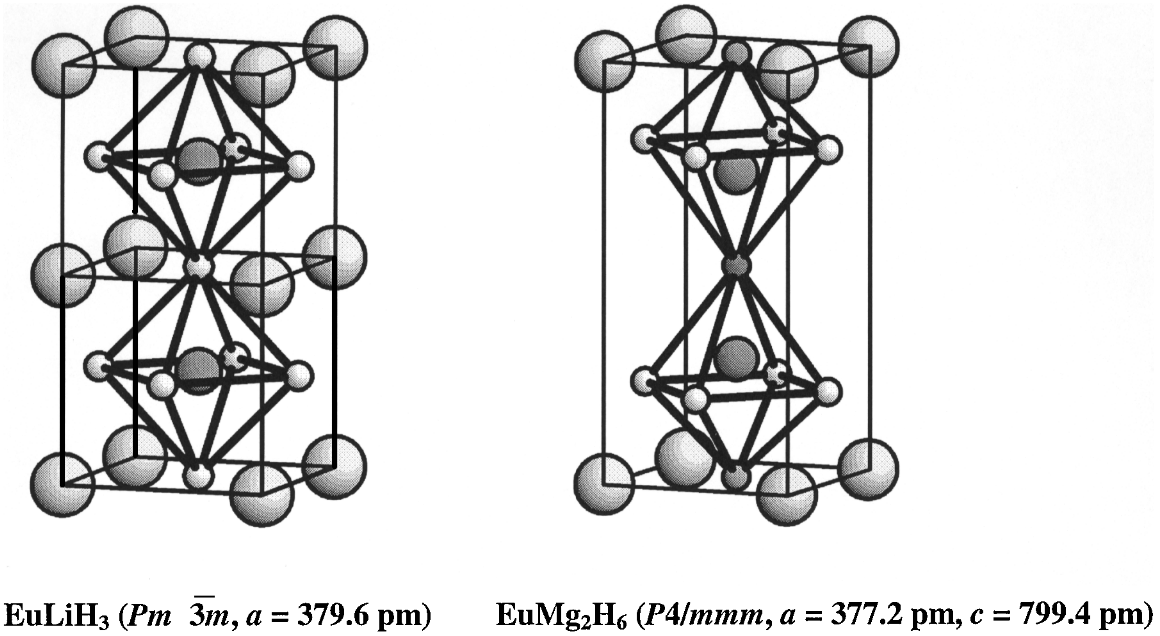

FIGURE 2 View of the crystal structures of the ternary ionic hydrides $EuLiH_3$ (two unit cells shown) and $EuMg_2H_6$. Large spheres represent Eu, middle-sized spheres Li and Mg, respectively, and small spheres H. The structure of $EuMg_2H_6$ (right) is related to that of $EuLiH_3$ (left, cubic perovskite type structure) by doubling the *c*-axis and omitting every other Eu layer. [Reprinted from *Physica B 276–278*, H. Kohlmann, Crystal structure solution of hydrides containing ^{nat}Eu from neutron powder diffraction data., 288–289, **2000,** with permission from Elsevier Science.]

hydride (H^-) and a cluster anion Ga_6^{8-} which satisfies the Wade–Mingos rules. A similar situation seemingly occurs in $Na_{15}K_6Tl_{18}H$, and for both compounds the bonding situation is in full agreement with valence electron rules after the hydrogen content is correctly assigned. All these compounds are stoichiometric and have semiconducting or insulating properties. Ternary hydrides with a nonmetal, such as hydride halides AHX (A = Ca, Sr, Ba, Eu, Yb; X = Cl, Br, I) or $Th_6Br_{15}H_7$, oxide hydrides ($Ba_{21}Ge_2O_5H_{24}$), and hydride nitrides (Ba_2HN, Sr_2HN, Li_4NH), will not be discussed.

B. Transition Metal Hydrides

Transition metals and intermetallic compounds consisting of transition metals form only hydrides, which often derive from closest packing of the metal atoms with hydrogen filling tetrahedral and/or octahedral voids. Therefore, they are often called *interstitial hydrides*. Structures and properties of transition metal hydrides (including lanthanides and actinides) range from nonstoichiometric compounds with broad composition ranges and metallic properties to valence compounds with a more saltlike or covalent character. Ternary hydrides including nontransition metals are excluded here. The most important group among them, the complex transition metal hydrides, will be discussed in section III.C.

1. Binary Transition Metal Hydrides

The thermodynamic stability of binary transition metal hydrides decreases with increasing group number in the periodic table of the elements (see ΔH values in Table II). Metals of groups 6b–8b (with the notable exception of Pd) form hydrides only under extreme high hydrogen pressures, e.g., FeH, which is likely to play an important role in the geochemistry of the earth's core. Binary transition metal hydrides are in general nonstoichiometric compounds with a disordered H distribution, high H diffusivity, and metallic properties.

The lanthanides (except Eu, Yb) and group 3b metals (Y, Sc, La, Ac) show a rather complex behavior on hydrogenation. They form nonstoichiometric dihydrides MH_2 in which the metal atoms adopt a Cu type arrangement, in contrast to the parent metals, most of which crystallize in an Mg-type structure. All tetrahedral voids of the Cu-type structure of M are occupied by hydrogen, i.e., the dihydrides MH_2 crystallize in a fluorite type structure (Fig. 3, left).

The dihydrides easily take up further hydrogen, which is accommodated successively in octahedral voids. For M = La, Ce, Pr the cubic structure is retained until all octahedral voids have been filled according to a limiting stoichiometry MH_3 (CeD_3 type structure). For the heavier rare earths (Nd, Sm, Gd–Tm, Lu), the cubic dihydride

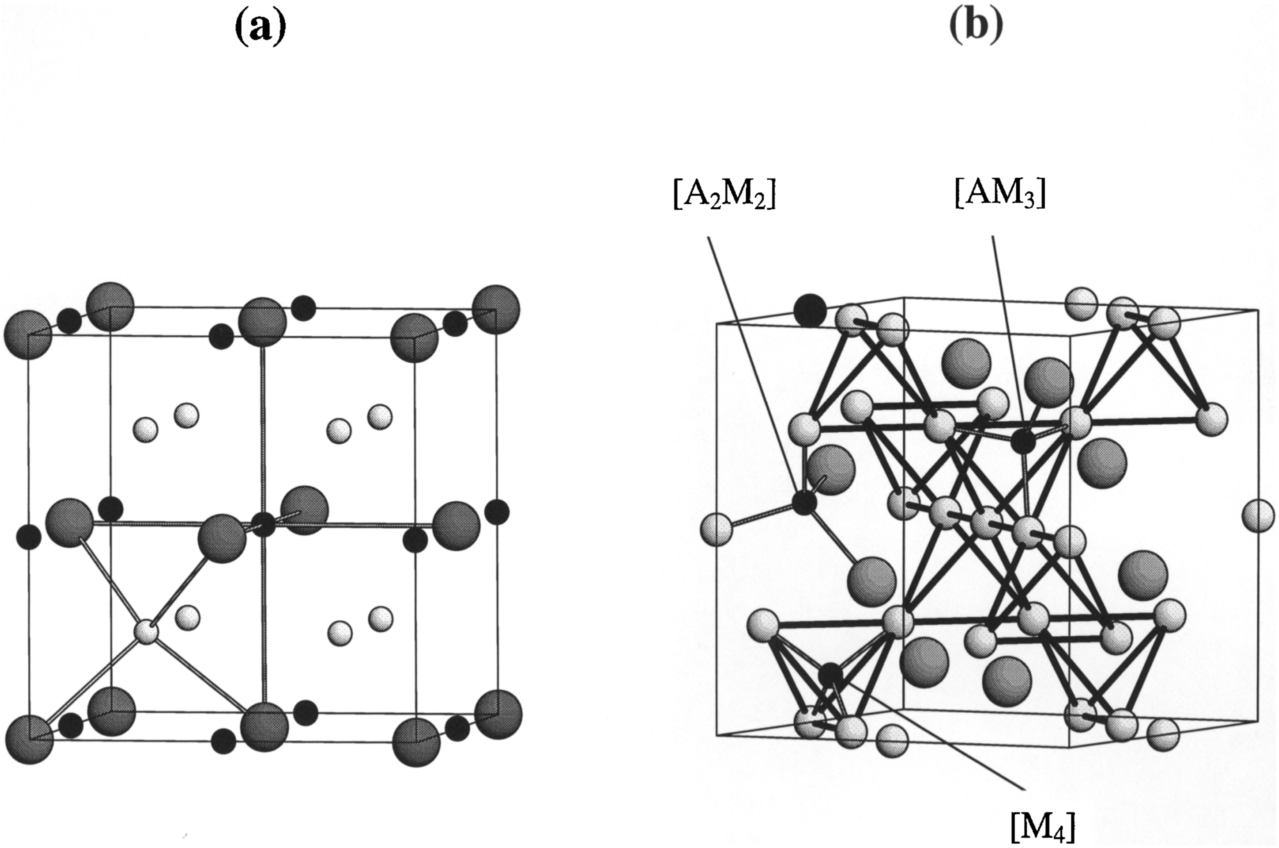

FIGURE 3 Interstitial sites in (a) a Cu type structure (cubic closest packed structure, ccp) and (b) a cubic Laves phase ($MgCu_2$ type, C15). (a) In a Cu-type arrangement of *n* metal atoms (large spheres), *n* octahedral (small filled spheres), and 2*n* tetrahedral voids (small empty spheres) are found. The surroundings of one representative of each is shown. (b) In a cubic Laves phase AM_2 (M_4 tetrahedra drawn out), three types of tetrahedral voids are available for hydrogen: those surrounded by two A and two M, [A_2M_2], by one A and three M, [AM_3], and those surrounded by M only, [M_4]. For the sake of clarity only one representative of each type of interstice is shown with its surroundings.

structure undergoes a reconstruction to a trigonal trihydride phase (HoD_3 type structure) on hydrogen uptake. The balance between attractive M–H and repulsive H–H interactions determines which one of the two trihydride structures will be more stable. As the atomic radius decreases along the lanthanide series and the void radius for hydrogen occupation decreases as well, H–H repulsion becomes more important, favoring the trigonal over the cubic structure for the heavier rare earths. In trihydrides of the cubic CeD_3 type, the octahedrally coordinated hydrogen atoms perform large anharmonic vibrations. This leads to a structural description in which those hydrogen positions are displaced by about 20 pm along the cell diagonal $[111]_{cub}$ away from the middle of the octahedral interstice. A similar displacement in the trigonal HoD_3 type structure is presumably due to H–H repulsion. Both the dihydrides MH_2 and the trihydrides MH_3 exhibit considerable nonstoichiometry ranges. In both the metal adopts the oxidation state of +III, causing good metallic conductivity in MH_2 ($M^{3+}e^-(H^-)_2$) and nonmetallic behavior in MH_3 ($M^{3+}(H^-)_3$) due to the presence or absence of itinerant electrons, respectively. Consequently, approaching the maximum hydrogen content MH_3 leads to a metal–semiconductor transition. The accompanying transition in the optical properties can be used to produce switchable mirrors (Fig. 4). The unusual feature of a decrease in the unit cell volume on hydrogen uptake from MH_2 to $MH_{2.4}$ and an enhanced sensitivity toward air for samples $MH_{>2.2}$ points at an increasing saltlike character with increasing hydrogen content x in $MH_{2<x<3}$. For these intermediate compositions the octahedral holes are only partially filled, i.e., H has got a partially disordered structure and an order–disorder transition occurs accompanied by a tetragonal distortion. EuH_2 and YbH_2 are saltlike hydrides that adopt the $PbCl_2$ type structure as the corresponding dihydrides of Ca, Sr, and Ba. YbH_2 may take up further hydrogen to form the mixed-valent $YbH_{2.4}$.

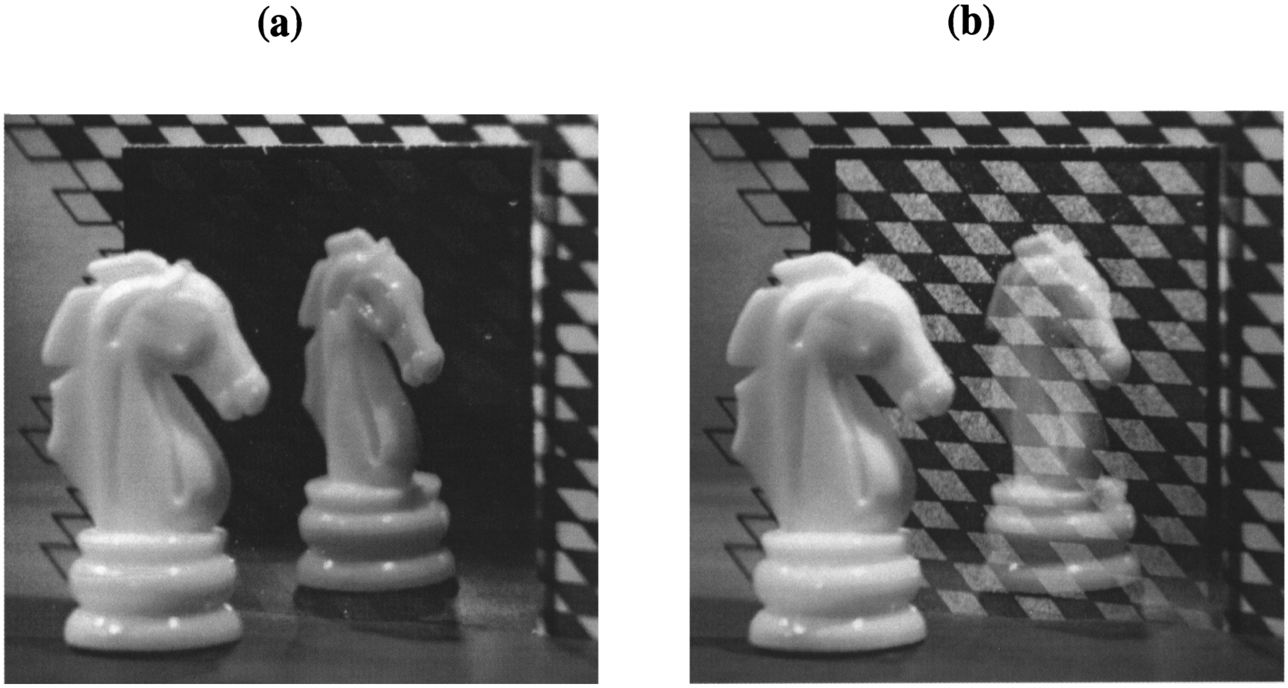

FIGURE 4 Change of optical properties on hydrogenation of yttrium. A 500-nm-thick yttrium film covered with a 20-nm-thick palladium protection layer in a hydrogen atmosphere ($p_{H2} = 10^5$ Pa). (a) The dihydride phase YH_{2-x} ($x \approx 0.2$) is formed after 1 min hydrogen exposure. Its metallic-like optical reflectivity can be seen by the mirror image of the knight in front. (b) After formation of the trihydride YH_{3-x} the film becomes transparent, as now the chessboard pattern behind is visible. The faint mirror image of the knight is caused by reflection from the Pd layer. (Photographs courtesy of Prof. R. Griessen, University of Amsterdam.) [Reprinted from Huiberts, J. N., Griessen, R., Rector, J. H., Wijngaarden, R. J., Dekker, J. P., de Groot, D. G., and Koeman, N. J. (1996). Yttrium and lanthanum hydride films with switchable optical properties. *Nature* **380,** 231–234, with permission from *Nature*.]

The elements of group 4b and Th also form dihydrides MH_{2-x} with broad compositional ranges ($0 \leq x \leq 0.5$). Those with a composition close to that of the dihydride MH_2 adopt a tetragonally distorted fluorite-type structure. The distortion is driven by electronic factors, i.e., lowering the density of states (DOS) at the Fermi level E_F by lifting a degeneracy, as shown by quantum mechanical calculations.

The binary hydrides of group 5b are based on the W-type arrangements of the parent metals by filling tetrahedral voids with hydrogen. The phase diagrams are rather complicated and show several superstructures with a distorted W-type structure and an ordered hydrogen distribution with stoichiometries M_2H, M_4H_3, and MH, but only those of β-NbH (*Cccm*) and β_1-Ta_2H ($C222$) are fully structurally characterized.

The crystal structures of the two modifications of CrH that may be prepared by electrochemical and high-pressure methods are based on Cu- and Mg-type structures of Cr, respectively, but the H positions have not yet been determined. Manganese, iron, and cobalt hydrides can only be synthesized under very high hydrogen pressure. They crystallize with a metal atom substructure of the Cu type (Mn) or of the Mg type (Fe, Co) with hydrogen occupying octahedral interstices.

The best-investigated metal–hydrogen system is Pd–H (Fig. 5a). The Cu type structure of Pd is retained on hydrogenation and H enters octahedral cavities. As a Cu type arrangement of n atoms accommodates n octahedral interstices (Fig. 3, left), the limiting stoichiometry is PdH with a NaCl type crystal structure. The phase boundary at $T = 50$ K (50 K anomaly, Fig. 5) is considered to belong to an order–disorder transition. Pd is remarkable insofar as it is the only metal of groups 6b–8b readily forming a hydride.

The red-brown CuH and the white ZnH_2 cannot be prepared by direct hydrogenation of the metals, but only by solution methods. They are very reactive, presumably nonmetallic, and stoichiometric solids with a pronounced covalent character. CuH probably crystallizes in a wurtzite-type structure.

Crystal structures and properties of the binary transition metal hydrides underscore the difficulty of a strict categorization of metal hydrides according to their chemical

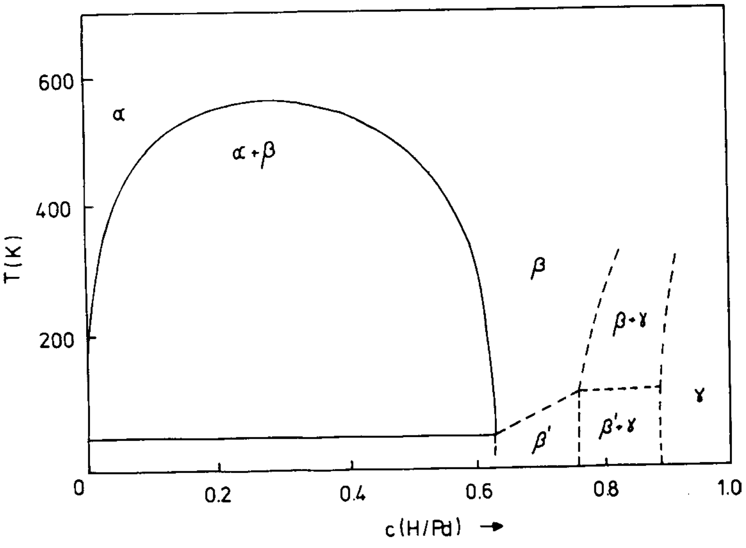

(a)

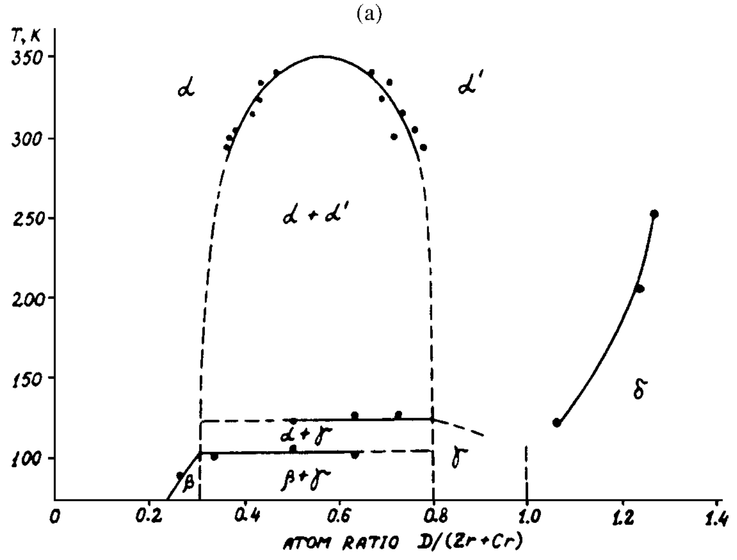

(b)

FIGURE 5 Phase diagrams of the systems Pd–H (a) and $ZrCr_2$–D (b). Continuous lines represent phase boundaries considered to be known; broken lines represent conjectured boundaries. For crystal structure drawings; see Fig. 3. Note the close resemblance of the upper part of the phase diagrams and the pressure composition isotherms in Fig. 1. (a) T, temperature; c(H/Pd), concentration of hydrogen as atom ration H/Pd; α, β, γ, palladium hydride phases with disordered H distribution; β', palladium hydride phase with probably ordered H distribution. [Reprinted from *Journal of the Less-Common Metals 49*, J. K. Jacobs and F. D. Manchester, Thermal and Motional Aspects of the 50 K Transition in PdH and PdD, 67–73, **1976,** with permission from Elsevier Science.] (b) T, temperature; α, α'; zirconium dichromium hydride phases with disordered H distribution; β', γ, δ, zirconium dichromium hydride phases with ordered H distribution. [Reprinted from *Journal of the Less-Common Metals 101*, V. A. Somenkov and A. V. Irodova, Lattice Structure and Phase Transitions of Hydrogen in Intermetallic Compounds, 481–492, **1984,** with permission from Elsevier Science.]

bonding type. As typical interstitial hydrides in which hydrogen occupies interstices of the parent metal, only those of Pd, V, Nb, and Ta may be considered. Hydrides of the groups 3b, 4b and the lanthanides show a complex behavior with both reconstructive and displacive structural changes and metal–semiconductor transitions as a function of hydrogen pressure and temperature. However, all binary transition metal hydrides show broad compositional ranges, and order–disorder transitions frequently occur (III.B.3).

2. Ternary Transition Metal Hydrides

Many ternary transition metal hydrides $A_aM_mH_h$ are based on intermetallic compounds A_aM_m (A, M = transition metal). On hydrogenation the crystal structure of the intermetallic is expanded and possibly distorted. Frequently the degree of distortion increases with increasing hydrogen content because of the growing importance of H–H repulsion and with decreasing temperature. A complete reconstruction of the intermetallic structure on hydrogenation happens less often. In many cases the hydrogen uptake is reversible, i.e., the intermetallic can be recovered by decomposing the hydride. In the ternary transition metal hydride, the hydrogen atoms occupy interstices of the intermetallic substructure, often octahedrally or tetrahedrally surrounded by metal atoms, analogous to the situation in the binary interstitial hydrides (III.B.1) such as PdH_x. These hydrides show pronounced compositional ranges according to a variable occupancy of crystallographical positions and generally exhibit metallic conductivity. Good hydrogen absorbers A_aM_m are based on at least one transition metal that forms a stable binary hydride (see III.B.1 and Table II) and they often show multiplateau behavior on hydrogen absorption as described in Section II.A. According to an empirical model introduced by *Miedema*, *Buschow*, and *van Mal*, the stability of ternary transition metal hydrides AM_mH_{2h} (A = Sc, Y, La, Ti, Zr, Hf, Th, U, Pu; M = any transition metal) can be predicted. The estimated value for the enthalpy of formation $\Delta H(AM_mH_{2h}) = \Delta H(AH_h) + \Delta H(M_mH_h) - \Delta H(AM_m)$ should be less than −38 kJ/mol to form a stable ternary hydride at a H_2 pressure around 10^5 Pa and room temperature, i.e., at least one of the metals A and M should form a stable hydride (large negative ΔH) and the thermodynamic stability of the intermetallic compound AM_m should not be too high (*rule of reversed stability*). For many systems the decomposition into the binary hydrides is thermodynamically favored over the formation of a ternary transition metal hydride AM_mH_{2h}. However, this reaction often has a high activation energy, and thus at moderate *p*–*T* conditions the ternary hydrides are formed as metastable compounds. A purely geometrical approach to hydride formation is given by the *Westlake criterion*, according to which the minimal hole radius in a metal matrix to accommodate a hydrogen atom is $r_{min} = 33$ pm. In real systems, however, only voids with $r_{min} > 40$ pm are being occupied. Together with the further condition of a minimum H–H distance of 210 pm and the assumption that the largest holes are occupied first, this model predicts preferred site occupation of hydrogen in an intermetallic compound. Besides these geometrical factors, the enthalpy of metal hydride formation ΔH also depends on electronic structure as accounted for by *Griessen* and *Driessen*'s band structure model. According to this semiempirical approach, ΔH depends on the difference between the energies of the Fermi level and the lowest conduction band of the intermetallic compound. The band structure model and the criteria just mentioned apply for main group metals, as well, e.g., for the ionic hydrides of the alkaline metals.

The important application for the ternary transition metal hydrides (reversible hydrogen storage), their relative insensitivity toward air, and the huge combinatorial potential of intermetallic compounds make them the by far most investigated subclass within the metal hydrides. From the vast number of A_aM_m–H systems, only some prominent representatives can be discussed in detail. Table III gives an overview of some hydride phases of important subclasses of A_aM_m intermetallic compounds.

An important and numerous class of intermetallic compounds AM_2 are the cubic Laves phases ($MgCu_2$ type, C15). Many representatives with A or M being one of the transition metals forming stable binary hydrides (see III.B.1) absorb considerable amounts of hydrogen up to compositions AM_2H_7. Hydrogen occupies tetrahedral interstices of the crystal structure, thereby expanding it.

TABLE III Composition and Space Group of Some Intermetallic Compounds and Their Hydrides[a]

ZrV_2 ($Fd\bar{3}m$, $MgCu_2$ type)	$ZrV_2H_{4.5}$ ($Fd\bar{3}m$), $ZrV_2H_{1<x<4}$ ($Fd\bar{3}m$, 360 K), $ZrV_2H_{3.6}$ ($I4_1/a$ 230 K), ZrV_2H_3 ($P2_1/c$, 77 K), $ZrV_2H_{1.9}$ ($C2/c$, 100 K)
$ZrCr_2$ ($Fd\bar{3}m$, $MgCu_2$ type)	$ZrCr_2H_{3.8}$ ($Fd\bar{3}m$, 298 K), $ZrCr_2H_{3.8}$ ($C2/c$, 1.6 K)
$ZrCr_2$ ($P6_3/mmc$, $MgZn_2$ type)	$ZrCr_2H_{3.8}$ ($P6_3/mmc$, 298 K), $ZrCr_2H_{3.8}$ ($R\bar{3}c$, 100 K)
FeTi ($Pm\bar{3}m$, CsCl type)	FeTiH ($P222_1$), $FeTiH_2$ ($Cmmm$)
$LaNi_5$ ($P6_3/mmm$, $CaCu_5$ type)	$LaNi_5H_3$ ($P6_3/mmm$), $LaNi_5H_6$ ($P31m$), $LaNi_5H_{6.7}$ ($P6_3mc$)
Y_6Mn_{23} ($Fm\bar{3}m$, Th_6Mn_{23} type)	$Y_6Mn_{23}H_{30}$ ($Fm\bar{3}m$, 295 K), $Y_6Mn_{23}H_{30}$ ($P4/mmm$, 4 K)

[a] All hydride phases (right column) represent hydrogen filled, some of them distorted, variants of the intermetallic structure (left column).

According to a purely geometrical approach, [A_2M_2] type interstices (Fig. 3, right) are preferred for low H concentrations if the lattice parameter $a < 800$ pm and [AM_3] type interstices are preferred for $a > 800$ pm. For high H concentrations usually both [A_2M_2] and [AM_3] are occupied. Because of the high crystallographic multiplicity of these positions and the closeness of neighboring equivalent positions their occupancy is generally low, i.e., H is statistically disordered over the tetrahedral interstices. Temperature-dependent structural transitions from these cubic phases with disordered H distribution to a lower symmetric low-temperature phase with an at least partially ordered H distribution frequently occur. Some examples are summarized in Table III. In all cases crystallographic group–subgroup relationships prove the structural relationship between the ordered (low temperature) and the disordered (high temperature) modification, suggesting the possibility of second-order (displacive) phase transitions. Unlike the Laves phases discussed so far, those containing a nontransition metal, such as AMg_2 (A = La, Ce, Sm), transform into stoichiometric, nonmetallic phases such as ternary ionic hydrides (III.A.2), but like the other Laves phases and unlike typical ionic hydrides they show a pronounced structural similarity to the parent intermetallic.

Another example of hydrogen-induced structural distortion is the class of H-absorbing AM compounds with the cubic CsCl type structure, such as the technologically relevant FeTi used for reversible hydrogen storage. FeTi forms a solid solution phase (called α) of approximate composition $FeTiH_{0.06}$. On increasing the hydrogen pressure a so-called β-phase (see Fig. 1), orthorhombic FeTiH, crystallizes in which H occupies octahedral positions in a deformed CsCl type FeTi substructure. A stronger distortion of the metal atoms structure is found in the higher hydride $FeTiH_2$ (called γ), clearly showing the dependence of the degree of structural distortions on the H concentration.

To date the most important class of intermetallics for reversible hydrogen storage is that based on the hexagonal $CaCu_5$ type structure. $LaNi_5$ forms a solid solution phase (α) $LaNi_5H_{0.3}$ and several higher hydrides, hexagonal $LaNi_5H_3$, trigonal $LaNi_5H_6$, hexagonal $LaNi_5H_{6.7}$ (Table III). All hydrides have $LaNi_5$ arrangements that are distorted $CaCu_5$ type structures with H occupying distorted tetrahedral and distorted octahedral positions.

The metal atom substructure may also differ completely from the intermetallic structure, i.e., the intermetallic compound may suffer a reconstruction during formation of the metal hydride. On hydrogenation of ZrCo (CsCl type structure), a hydride $ZrCoH_3$ with a completely rearrange ZrCo substructure (CrB type) is formed. The reverse reconstruction is found for EuPd (CrB type structure), which forms a hydride $EuPdH_3$ with the EuPd substructure of the CsCl type.

The vast majority of metal hydrides are crystalline phases. Sometimes, however, hydrogenation induces an amorphization, e.g., in the cubic Laves phase $CeFe_2$, $GdFe_2$, $SmNi_2$ whose hydrides are amorphous materials. the reverse process is known as well, i.e., the formation of a crystalline metal hydride from an amorphous material, e.g., the hydrogenation of amorphous $Zr_{0.33}Ti_{0.67}$ yielding the crystalline spinel type $ZrTi_2H_4$.

3. Hydrogen as a Lattice Gas and Order–Disorder Transitions

Hydrogen disturbs the crystal structure of a metal or an intermetallic compound much less than other nonmetals (low *defect power*), most of which do not form interstitial compounds, but in a reconstructive reaction form compounds completely distinct in structure and properties from the former metal. Further elements capable of forming interstitial compounds are, for instance C, N, O. Some of the interstitial carbides, nitrides, and oxides take up hydrogen to form mixed compounds such as $Zr_3V_3OH_x$ or $ZrC_{1-x}H_y$. As a first approximation interstitial hydrides can be described as host–guest systems in which hydrogen can be treated by a *lattice gas* model. Hydrogen can migrate in the metal hydride nearly freely, and the H–H interactions are mainly long-range attractive forces and short-range repulsion as in the pair potential for gas particles. Self-diffusion constants at room temperature are high, e.g., $D = 4 \times 10^{-4}$ mm^2/s for hydrogen in $PdH_{0.7}$, which is comparable to that of protons in water. Hydrogen concentration can be changed continuously, i.e., a solid solution MH_x is formed with x covering a broad stoichiometric range. Below a critical temperature T_c two distinct phases of different density are in equilibrium: a gas and a liquid in the model, or two phases MH_x and MH_y with nonoverlapping solid solution regions x and y in the real hydride systems. As an example, Fig. 5 shows the phase diagrams of the systems Pd–H and $ZrCr_2$–D. Below $T_c = 570$ K the uniform Pd–H phase disproportionates into two phases, α and β, with a miscibility gap in between. The same behavior is found for $ZrCr_2$–D with $T_c = 350$ K. This *lattice gas–liquid transition* is driven by short-range order effects. In phases of the lattice liquid or gas type, low occupancies of hydrogen in interstices are often observed, i.e., hydrogen is disordered statistically. However, the interstices are not filled in a totally random manner. A short-range order is introduced by the H–H repulsion, which blocks nearest neighbor sites around each H atom within a radius of 210 pm. This is evident by a "liquid-like," very broad peak at $d = 210$ pm in neutron diffraction patterns on disordered metal hydrides. Such

hydrogen substructures have a *configurational entropy* different from zero and thus are likely to be unstable at low temperatures. As a consequence a further transition occurs that can be described as a *crystallization of the lattice liquid*. Here, the repulsive interaction of neighboring H atoms comes into play, and a long-range order in the hydrogen sublattice is introduced. The "liquid-like" peak in the neutron diffraction patterns vanishes on ordering of the H substructure. Hydrogen ordering is accompanied by a reduction in symmetry and often a drastic drop in H mobility.

The lattice gas approach is valid within certain limits for typical metallic hydrides, binaries as well as ternaries. Deviation from this idealized picture indicates that metallic hydrides are not pure host–guest systems, but real chemical compounds. An important difference between the model of hydrogen as a lattice gas, liquid, or solid and real metal hydrides lies in the nature of the phase transitions. Whereas the crystallization of a material is a first-order transition according to Landau's theory, an order–disorder transition in a hydride can be of first or second order. The structural relationships between ordered and disordered phases of metal hydrides have been proven in many cases by crystallographic group–subgroup relationships, which suggests the possibility of second-order (continuous) phase transitions. However, in many cases hints for a transition of first order were found due to a surface contamination of the sample that kinetically hinders the transition to proceed.

4. Electronic, Magnetic, and Mechanical Properties

Hydrogen entering the crystal structure of a metal or an intermetallic obviously influences its electronic, magnetic, and phonon structure. The main effects are that of the generally observed *lattice expansion*, the electronic interaction between hydrogen and the neighboring metal atoms (*M–H bonding*), and the *H–H interactions*. Hydrogen may influence the electronic and magnetic properties in many ways: On hydrogenation, metal–semiconductor transitions may occur (YH_2–YH_3), ferromagnetism may appear (Th_6Mn_{23}–$Th_6Mn_{23}H_{30}$) or change into antiferromagnetism (Gd–GdH_2), paramagnetic metals may become diamagnetic (Pd–$PdH_{0.6}$), antiferromagnetic metals may become ferromagnetic semiconductors (Eu–EuH_2), metal valences may change ($Ce^{IV}Ru_2$/$Ce^{III}Ru_2H_x$, $Eu^{III}Rh_2$/$Eu^{II}Rh_2H_{5.5}$), or heavy fermion behavior may appear ($CeH_{2.6}$ with a *Sommerfeld* coefficient $\gamma = 110$ mJ/mol K compared to $\gamma = 10$ mJ/mol K for γ-Ce).

As for the electronic structure, the ridid band approximation assumes that the energy bands in the metal or intermetallic compound remain unchanged on hydrogenation. This leads either to the protonic model for hydrogen in case the H 1*s* band lies above the conduction band in the metal or intermetallic compound (H as e^- donator) or to the anionic model if it lies below (H as e^- acceptor). Accordingly, the free electron carrier concentration should increase or decrease, respectively. A more realistic approach accounts for the H-induced changes of the conduction band (*Switendick's hybrid band model*). Quantum mechanical calculations and photoelectron spectroscopy have indeed shown that hydrogen strongly influences the metal conduction band and induces new low-lying energy states some electron volts below the Fermi level E_F (M–H bonding). From electronic structure considerations, the maximum hydrogen content of hydrides can often be explained. The prediction that Pd can accommodate 0.76 additional electrons corresponds nicely to the fact that Pd readily takes up hydrogen to form $PdH_{0.7}$. In contrast to the H *s*, metal *d* overlap in transition-metal and rare-earth hydrides, the M–H bonding in actinide hydrides seems to be dominated by interaction between H 1*s* and M 5*f* electrons (M = actinide metal). β-UH_3 may also be considered as a heavy fermion compound ($\gamma = 28.7$ mJ/mol K as compared to $\gamma = 9.88$ mJ/mol K for U). Examples for superconducting hydrides are PdH ($T_c = 9.5$ K) and PdD ($T_c = 11$ K) with a reverse isotope effect, and Th_4H_{15} ($T_c = 8$ K). As superconductivity is based on a strong electron–phonon coupling, both altering the phonon modes and the density of states (DOS) at the Fermi level E_F on introducing hydrogen in a metal or intermetallic compound are critical. Because of the additional electrons of hydrogen, E_F in the hydride is often shifted to regions of lower DOS as compared to the metal or intermetallic, and T_c of superconductors often drops on forming the hydride.

Because of the complex interplay of volume expansion (variation of interatomic distances) and the DOS at E_F (Stoner criterion), the changes of magnetic bulk properties on hydride formation are manifold. Ferrimagnetic Y_6Mn_{23} and Pauli-paramagnetic Th_6Mn_{23} crystallize with the same cubic structure (Th_6Mn_{23} type). On hydrogenation the former loses its magnetic order while the latter becomes a ferromagnet. This different behavior was explained by a structural transformation (cubic–tetragonal) that takes place in $Y_6Mn_{23}H_{30}$ (Table III), but not in the homologous Th compound. Ce often changes its valency in compounds from IV+ to III+ on formation of hydrides, causing for example the appearance of ferromagnetism in Pauli-paramagnetic $CeNi_3$ by hydrogenation.

The formation of metal hydrides deteriorates mechanical properties of materials, which is a serious problem in engineering. The precipitation of H_2 in voids and cracks of a material causes high internal pressure and the hydride formation in areas of high stress lowers the cohesion

of a material. Inhomogeneities during hydrogenation often introduce internal strain and stress, and conversely, mechanical stress may introduce hydrogen concentration inhomogeneities. The latter is utilized in *Gorsky effect* measurements, in which the hydrogen redistribution after mechanical deformation of a sample is studied, in order to investigate long-range hydrogen diffusion. The lattice expansion on formation of a metal hydride cracks the metal or intermetallic compound into a fine powder. The volume effect upon hydrogenation can be as large as 25% for the fully hydrided $LaNi_5H_7$ as compared to $LaNi_5$. Even higher values are found for the system $CeRu_2$ (37% volume increase for $CeRu_2H_5$) due to a valence change for Ce. As a rule of thumb a volume increase of $2–3 \times 10^6$ pm^3 per absorbed hydrogen atoms occurs. On repeated hydrogen absorption–desorption cycles phase segregation may occur. The formation of very small Ni clusters in $LaNi_5$ powder cycled 1500 times was observed by the occurrence of a magnetic hyperfine splitting in ^{63}Ni Mössbauer spectroscopy. The high surface area of cycled materials engenders a higher sensitivity toward contaminants such as oxygen or water.

C. Complex Transition Metal Hydrides

The characteristic part of a complex transition metal hydride is the anionic homoleptic transition metal (M) hydrido complex $[M_mH_h]^{x-}$, which is balanced by the cation A^+ or A^{2+} (A = Li–Cs, Mg–Ba, Eu, Yb). The formation of an extended solid is a consequence of the attractive electrostatic Coulomb interaction between cations and complex anions, whereas within the $[M_mH_h]^{x-}$ complex, hydrogen is bound covalently to the metal M. The hydride fluoride analogy known from ionic hydrides is less pronounced for complex transition metal hydrides; however, some representatives show structural resemblance to the corresponding halides. The hydrido complexes follow the 18-electron rule known from coordination chemistry, e.g., $[ReH_9]^{2-}$ in K_2ReH_9 or $[NiH_4]^{4-}$ in $CaMgNiH_4$. They may also contain free hydride anions H^- that are not part of the complex anions, e.g., in K_3PtH_5 $(=(K^+)_3[PtH_4]^{2-}H^-)$. According to their bonding properties, complex transition metal hydrides are stoichiometric, electron-precise compounds that often are colored, are nonmetallic, and have an ordered hydrogen distribution. However, because of the high mobility of hydrogen as a ligand, some of them undergo a transition to a disordered high-temperature phase. In metal-rich compounds with less electropositive elements A (=Li, Mg), metal–metal interactions may occur, and they are border cases toward metallic metal hydrides, whereas for heavier, electropositive metals A (= Rb, Cs, Ba) a more saltlike character is found. No dihydrogen complexes as found in metal organic coordination chemistry are known for inorganic homoleptic complex hydrides. Also, no hydrido complexes of rare earth or actinide elements are known. Some 80 complex transition metal hydrides are known and well characterized at present.

1. Thermodynamic and Chemical Properties

Complex hydrides of the late transition metals (M = 8b group element) are formed at relatively moderate hydrogen pressures with generally low oxidation states for M, e.g., $[Pt^{II}H_4]^{2-}$ in K_2PtH_4. Synthesizing compounds with higher oxidation states such as $[Pt^{IV}H_6]^{2-}$ in K_2PtH_6 or complex hydrides of transition metals other than from group 8b requires much higher hydrogen pressures. A remarkable exception is the solution synthesis of the first complex metal hydride ever reported, $K_2Re^{VII}H_9$. No compounds for M = 3b, 4b, or 5b elements are known thus far. A possible explanation for this fact might be the higher thermodynamic stability of the binary hydrides of the early as compared to the late transition metals. Hydrido complexes of Ag, Au, and Hg are also unknown. The scarce thermodynamic data on complex hydrides suggest a thermal stability between those of ionic hydrides and metallic hydrides (Table II) with hydride enthalpy of formation ΔH ranging between −64 (Mg_2NiH_4) and −137 kJ/mol ($Yb_4Mg_4Fe_3H_{22}$). As, in contrast to ternary hydrides containing transition metals only, the complex transition metal hydrides are usually not based on stable intermetallic compounds, the models for the prediction of the enthalpy of hydride formation as discussed in Section III.B.2 are of limited use here. Considering the high weight and volume efficiencies for hydrogen storage, e.g., that of Mg_2FeH_6, which is more than twice that of liquid hydrogen, the less stable complex transition metal hydrides are interesting candidates for hydrogen storage applications. Most complex transition metal hydrides are air sensitive and insoluble in commonly used solvents. Compounds with organometallic cations such as $[MgBr(THF)_2]_4[FeH_6]$ (THF = tetrahydrofuran) show a moderate THF solubility.

2. Geometry and Properties of Transition Metal Hydrido Complexes

The geometries found for transition metal hydrido complexes resemble those in inorganic transition metal coordination compounds following the well-known rule that a total of 18 electrons are required for a stable complex. Examples for 18-electron complexes are the tricapped trigonal prismatic $[Re^{VII}H_9]^{2-}$, octahedral $[Mn^IH_6]^{5-}$, $[Re^IH_6]^{5-}$, $[Fe^{II}H_6]^{4-}$ (Fig. 6), $[Ru^{II}H_6]^{4-}$, $[Os^{II}H_6]^{4-}$, $[Rh^{III}H_6]^{3-}$, $[Ir^{III}H_6]^{3-}$, $[Pt^{IV}H_6]^{2-}$, square pyramidal $[Co^IH_5]^{4-}$ (Fig. 6), tetrahedral $[Mn^{II}H_4]^{2-}$, $[Ni^0H_4]^{4-}$ (Fig. 6), $[Pd^0H_4]^{4-}$, $[Cu^IH_4]^{3-}$, $Zn^{II}H_4]^{2-}$ and $[Cd^{II}H_4]^{2-}$. Electron-deficient complexes show different

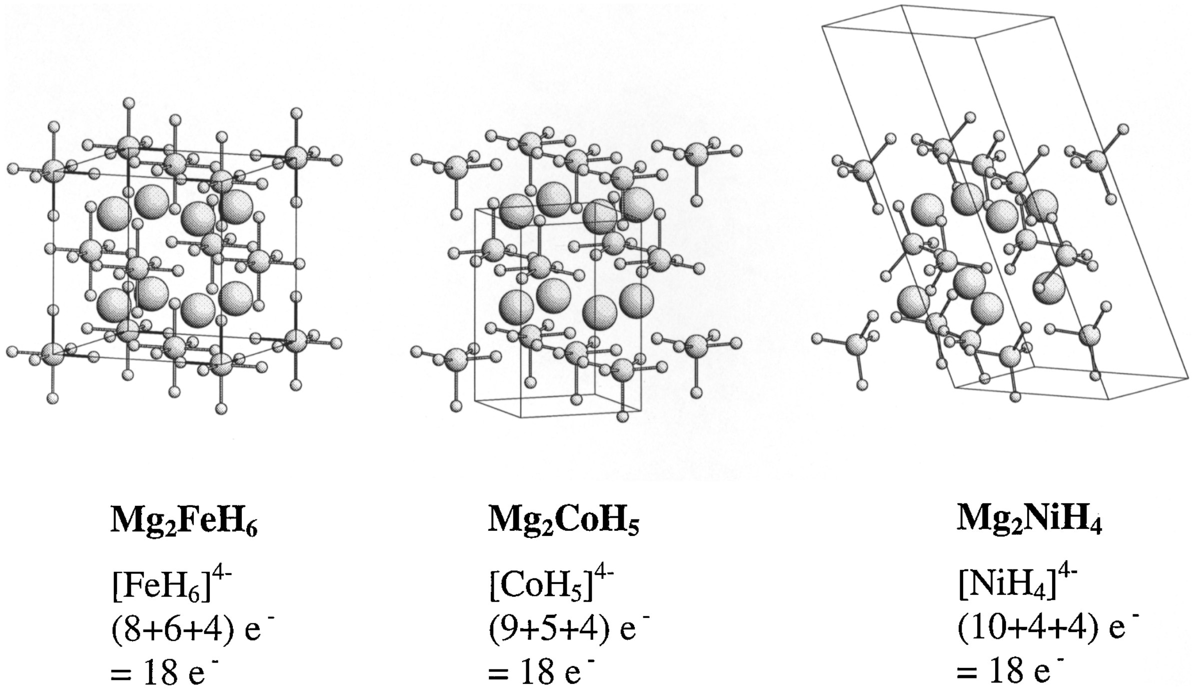

FIGURE 6 Crystal structures of cubic Mg_2FeH_6 (K_2PtCl_6 type), tetragonal Mg_2CoH_5, and monoclinic Mg_2NiH_4. Large spheres represent Mg, middle-sized spheres the transition metal M (Fe, Co, Ni), and small spheres H. M–H bonds in the transition metal hydrido complexes are drawn out. For Mg_2NiH_4, an incomplete unit cell is shown. Note the close resemblance of the geometrical arrangements of Mg cations and transition metal complex anions in all three structures.

geometries such as the 16-electron octahedral $[Re^{III}H_6]^{3-}$, the square plamar $[Rh^{I}H_4]^{3-}$, $[Pd^{II}H_4]^{2-}$, $[Pt^{II}H_4]^{2-}$, triangular $[Pd^{0}H_3]^{3-}$, and the linear 14-electron complexes $[Pd^{0}H_2]^{2-}$ and $[Pt^{0}H_2]^{2-}$. Other formally electron-deficient complexes form metal–metal bonds to obey the 18-electron rule as indicated by crystal structure, properties, and quantum mechanical calculations, such as binuclear $[Pt_2H_9]^{5-}$ in $Li_5Pt_2H_9$, $[Ru_2H_6]^{12-}$ in Mg_3RuH_3, or polymer $[Ru_nH_{4n}]^{4n-}$ in Mg_2RuH_4. Metal–metal interactions occur also in Na_2PdH_2 and Li_2PdH_2 ($NaHgO_2$ type structure), which are remarkable insofar as they melt before decomposing and show low-dimensional metallic behavior. Owing to their electron configuration (d^0, low-spin d^6, d^8, d^{10}) and geometry, complex transition metal hydrides are diamagnetic. Exceptions are those with Eu and $A_3Mn^{II}H_5$ (A = K, Rb, Cs) which show Curie–Weiss paramagnetism. The former order ferromagnetically at low temperatures, the latter antiferromagnetically. K_3ReH_6 shows Van Vleck paramagnetism.

Bond distances M–H as derived from structure analysis within the transition metal hydrido complex are close to the sum of the covalent radius for the transition metal M and a radius of 28 pm for the hydrogen atom, supporting the picture of a covalent M–H bond within the hydrido complexes $[M_mH_h]^{x-}$. H–H distances are longer than 210 pm, the blocking radius of an H atom (see III.B.3). Deviations from these expected values may be caused by partial occupancy of H atoms, unusual coordination numbers, or a matrix effect of the surrounding A cations.

3. Structural Relationships and Order–Disorder Transitions

The interplay between the two factors governing structural chemistry and properties of complex transition metal hydrides—the *18-electron rule* and the *high hydrogen mobility*—may be best explained by the series Mg_2FeH_6–Mg_2CoH_5–Mg_2NiH_4. These consist of Mg^{2+} and isoelectronic 18-electron complexes $[Fe^{II}H_6]^{4-}$, $[Co^{I}H_5]^{4-}$, and $[Ni^{0}H_4]^{4-}$ for which the electron counts (transition metal *d* electrons + hydrogen electrons + charge of the complex) are $8+6+4=18$, $9+5+4=18$, $10+4+4=18$ for the three complexes. They crystallize in closely related structures (Fig. 6). Mg_2FeH_6 is isotypical to cubic K_2PtCl_6; Mg_2CoH_5 and Mg_2NiH_4 adopt tetragonal and monoclinic distortion variants of the former. The 18-electron rule controls the hydrogen content of the complexes, which are then necessarily lower symmetric for $[CoH_5]^{4-}$ and $[NiH_4]^{4-}$ as compared to $[FeH_6]^{4-}$. The structures have to accommodate these lower symmetric

entities, which leads to the formation of distortion variants of the K_2PtCl_6 type as shown in Fig. 6. On the other hand, the dynamical behavior of hydrogen with its high mobility gives rise to order–disorder transitions. Mg_2CoH_5 transforms from the tetragonal room-temperature structure with ordered hydrogen distribution at 488 K into a disordered cubic high-temperature modification in the K_2PtCl_6 type (Fig. 6) in which five hydrogen atoms are disordered over six crystallographically equivalent positions resulting in an occupation probability of 5/6 ($[CoH_{6*5/6}]^{4-}$). A similar order–disorder transition occurs at 483–513 K for Mg_2NiH_4 from the monoclinic to a cubic modification with four hydrogen atoms on six sites ($[NiH_{6*2/3}]^{4-}$). Further transitions with ordered low-temperature structures derived from the cubic K_2PtCl_6 type occur for $A_{2-x}Eu_xIrH_5$ (A = Ca, Sr; $0 \leq x \leq 2$) and A_2PtH_4 (A = Na–Cs, square planar $[PtH_4]^{2-}$ in two different orientations depending on A). For K_2PtH_4 a rigid motion-type disorder was evidenced by NMR spectroscopy. For other disordered hydrogen-deficient cubic K_2PtCl_6-type structures such as Mg_2IrH_5 and Sr_2RhH_5, no transition to an ordered phase was observed. Further order–disorder transitions occur in A_3PtH_5 (A = K–Cs, $[PtH_4]^{2-}/[PtH_{6*2/3}]^{2-}$ for ordered and disordered phase, respectively, K_3PdH_3 ($[PdH_2]^{2-}/[PdH_{6/3}]^{2-}$) and in A_3ReH_{10} (A = K, Rb, $[ReH_9]^{2-}/[ReH_{24*9/24}]^{2-}$). In contrast to these examples some hydrogen-deficient compounds do not transform to an ordered modification, such as the metal-rich $CaPdH_2$, $SrPdH_{2.7}$ (cubic perovskite type), $MgRhH_{1-x}$, $MgIrH_x$ (derived from cubic perovskite type), and Mg_4IrH_5 (unique type). Such compounds have a metallic appearance and are border cases between complex hydrides and interstitial hydrides.

IV. APPLICATIONS

A. Hydrogen Storage

The most important application of metal hydrides is hydrogen storage. As pointed out in the preceding chaptes many metals and intermetallic compounds can take in considerable amounts of hydrogen reversibly. The hydrogen density of metal hydrides often exceeds that in liquid hydrogen (Table II). An ideal material for hydrogen storage applications would have broad plateau regions (high reversible hydrogen storage capacity), p_{eq} close to 10^5 Pa at room temperature, fast absorption–desorption kinetics, no deviation from the idealized thermodynamic behavior (Fig. 1), a good cycle life (many hundreds of cycles), a high weight and volume efficiency, a high resistance to surface-poisoning gases such as oxygen and water, and low production costs, and it would not contain toxic materials.

The need for safe and convenient hydrogen storage systems is driven by the idea of *a hydrogen economy* using hydrogen as an ecologically clean, cheap fuel that would replace fossil fuels with their limited availability and ecological problems. In a hydrogen economy electricity would be produced preferably by renewable energies, such as solar, wind, and water. Electricity cannot be stored and transported very efficiently. These shortcomings are overcome by using hydrogen as an energy carrier that can be produced using electricity, for instance by electrolysis of water. For the storage and transportation of hydrogen the metal hydrides come into play as more volume- and weight-efficient alternatives to tanks for gas or liquid hydrogen. Hydrogen can be used in most of today's end-user systems as a fuel without major modifications, e.g., in automobiles, heating systems, or ovens. In constrast to fossil fuels, hydrogen is nonpolluting, as it burns to H_2O with only trace amounts of NO_x and a high efficiency (close to 100% in catalytic converters).

Instead of producing heat by combustion, the energy of hydrogen can also be retransformed to electricity in batteries. Commercially very successful is the nickel–metal hydride rechargeable battery (Ni-MH), which can be considered as a successor of the nickel–cadmium battery. It has several advantages over the latter, e.g., the prevention of ecologically problematic Cd, a higher storage capacity, a greater energy density (80 Wh/kg, 250 Wh/L), faster charge, and a high cycle rate (500) with a comparable operating voltage to that of Ni–Cd. A general cell reaction involves the reversible intercalation (on charging, C) and reintercalation (on discharging, D) of hydrogen in a storage material M in an aqueous potassium hydroxide solution as electrolyte:

$$MH + NiOOH \underset{C}{\overset{D}{\rightleftharpoons}} M + Ni(OH)_2$$

Ni-MH rechargeable batteries are available commercially containing hydrogen storage materials such as M = $LaNi_5$ (MH = $LaNi_5H_6$) and M = $ZrCr_2$ (MH = $ZrCr_2H_{3.8}$) and their substitutional variants, e.g., $LaNi_{3.55}Mn_{0.4}Al_{0.3}Co_{0.75}$ and $ZrMn_{0.5}Cr_{0.2}V_{0.1}Ni_{1.2}$. The substituents on Ni and Cr sites improve the reversibility of the cell reaction, the cycle stability, and the corrosion behavior. Ni-MH batteries have been widely used since the 1990s in portable devices such as cellular phones or laptops, in battery-driven cars, and in aeronautics.

For use in vehicles with internal combustion engines or fuel cells, a high volume and weight efficiency is required. Shortcomings of the commercially available systems are their weight, bulkiness, and high cost. New developments in the area include hydrogen storage in quasicrystals and carbon nanotubes and the catalytic decomposition of light-weight hydrides such as $LiAlH_4$. Several producers are running test cars and trucks with liquid hydrogen, metal hydride tanks, or hydrogen fuel cells. DaimlerChrysler recently announced the first commercially available

hydrogen fuel cell buses (CITARO) to be delivered by the end of 2002. In Zollbrück, Switzerland, the house and a hydrogen driven van of M. Friedli is powered exclusively by photovoltaically produced hydrogen that is stored in a metal hydride tank. Iceland with its abundant geothermal and water power sources recently launched an initiative to become a hydrogen economy by 2025.

B. Other Applications

Besides reversible hydrogen storage, metal hydrides have found other important fields of application. The enthalpy of formation of a metal hydride is rather a problem for the storage of hydrogen as a fuel, as it has to be removed continuously during charging with hydrogen. However, it may also be utilized in heat pumps in which the heat of decomposition of a metal hydride is recovered at a different place by recombination of the produced hydrogen in a second reservoir with a hydride-forming material. In TRIGA-type reactors, ZrH_2 is used as moderator with a negative temperature dependence of moderating efficiency, i.e., those reactor types have an inherent safety. In chemical synthesis hydride formation is of use for the purification of reaction gases (H_2 getter) and metal hydrides as precursors for the preparation of finely divided metal powders, e.g., uranium by thermal decomposition of UH_3, and in the HDDR process (hydrogenation–disproportionation–desorption–recombination) for the synthesis of magnetic materials such as $Nd_2Fe_{14}B$ and $SmCo_5$. Vanadium is being used for isotope separation of H and D via formation of the hydrides/deuterides. The temperature dependence of the desorption pressure of metal hydrides is the basis for their use in thermal compressors and fire detectors.

V. CONCLUSION AND OUTLOOK

The pronounced variety in crystal structures and properties of metal hydrides does not justify a strict categorization according to chemical bonding types, i.e., ionic, covalent, and metallic (interstitial) hydrides. However, within the framework of the differentiation in main-group, transition-metal, and complex hydrides, some trends become apparent. For binary hydrides there is a clear distinction between the hydrides of main group and transition metals including the rare earths. Characteristic general features as summarized in Table IV show main group metal hydrides as stoichiometric, nonmetallic valence compounds with an ordered hydrogen distribution in the crystal structure and a low hydrogen mobility. In contrast, transition-metal hydrides may be regarded as nonstoichiometric, often metallic compounds with a variable content of hydrogen that is disordered and very mobile in the crystal structure. Structural relationships between the metal and the hydride crystal structure are obtained for some transition metals, but not for main group metals. This phenomenological approach to a classification of binary metal hydrides does not make any statement about the specific type of chemical bonding, thus avoiding difficulties of assigning chemical bonding in borderline cases such as BeH_2.

TABLE IV Characteristic Features of Binary Main Group and Transition Metal Hydrides[a]

	Main group metal hydride	Transition metal hydride
Composition	Stoichiometric	Nonstoichiometric
Crystal structure (H distribution)	Ordered	Disordered, order–disorder transitions
H content determined by	Metal valence	Geometrical and electronic factors
H diffusivity	Low	High
Electrical conductivity	Insulating or semiconducting	Metallic or semiconducting
Appearance	Nonmetallic	Metallic
Air sensitivity	High (H^- as base)	Low
Density	Higher than metal	Lower than metal

[a] Not all listed properties may apply for a given compound. Some exceptions are discussed in the text.

The major exceptions to this simplified picture are probably CuH and ZnH_2, which are reported to be stoichiometric, nonmetallic solids like the main group metal hydrides, but their crystal structures and physical properties are not well characterized. Borderline cases are the rare earth hydrides, which show a hydrogen concentration-dependent semiconductor–metal transition. EuH_2 and YbH_2 behave like alkaline earth dihydrides because of the special electron configuration of Eu^{2+} ($4f^7$) and Yb^{2+} ($4f^{14}$).

Ternary hydrides containing main group and transition metals in the same compound show an interesting combination of features of the two groups. In complex transition metal hydrides $A_a[M_mH_h]$ (A = Li–Cs, Mg–Ba, Eu, Yb; M = transition metal) ionic (between A^+ or A^{2+} and $[M_mH_h]^{x-}$) and covalent bonding (M–H) predominates as in main group metal hydrides. Furthemore, they are nonmetallic, stoichiometric compounds with an H content determined by metal valencies (18-electron rule). On the other hand, in some cases order–disorder transitions, structural relationships to the underlying intermetallic or border cases with metallic character, are observed, resembling the typical features of transition metal hydrides (Table IV). Thus, complex hydrides combine features of both groups.

For future research, those metal hydrides representing border line cases in view of chemical bonding and the classification just given are particularly interesting. An enhanced use of theoretical calculations to account for the electronic structure of metal hydrides, limiting hydrogen concentrations, and preferred site occupancies in

hydrides is expected to play a vital role, as well as the explorative synthesis of new materials with unusual properties, i.e., high oxidation states by high-pressure synthesis. A largely unexplored field is the reaction pathway for hydrogenation of metals and intermetallic compounds. Unfortunately, physical properties of metal hydrides are most often not as well characterized as their crystal structure. This is largely due to the difficulty of synthesizing single-phase samples and single crystals of sufficient size and quality—another challenge for future research. The developments of the past decade brought a breakthrough in metal hydride technology in some areas, such as the Ni-MH battery. One hopes that this encouraging progress and the continued interest of both basic and applied research in metal hydrides will guarantee that this is not the end of the story.

SEE ALSO THE FOLLOWING ARTICLES

Boron Hydrides • Chemical Thermodynamics • Hydrogen Bond • Metal Cluster Chemistry • Metal Forming • Superconductivity

BIBLIOGRAPHY

Bronger, W., and Auffermann, G. (1998). New ternary alkali-metal–transition-metal hydrides synthesized at high pressures: Characterization and properties. *Chem. Mat*. **10,** 2723–2732.

Buschow, K. H. J. (1984). Hydrogen absorption in intermetallic compounds. *In* "Handbook on the Physics and Chemistry of Rare Earths" (K. A. Gschneidner, Jr., and L.Eyring, eds.), Vol. 6, pp. 1–111. North-Holland Physics Publishing, Amsterdam.

Fukai, Y. (1993). "The Metal–Hydrogen System," Springer-Verlag, Berlin.

Furrer, A. (ed.) (1994). "Neutron Scattering from Hydrogen in Materials," World Scientific, Singapore.

Gingl, F., Gelato, L., and Yvon, K. (1997). The hydride fluoride crystal structure database, HFD. *J. Alloys Compounds* **253–254,** 286–290.

Libowitz, G. G., and Maeland, A. J. (1979). Hydrides. *In* "Handbook on the Physics and Chemistry of Rare Earths" (K. A. Gschneidner, Jr., and L. Eyring, eds.), Vol. 3, pp. 299–336. North-Holland Physics Publishing, Amsterdam.

Moyer, R. O., Jr., Lindsay, R., and Marks, D. N. (1978). Results of reactions designed to produce ternary hydrides of some rarer platinum metals with europium ytterbium, *Adv. Chem. Ser*. **167,** 366–381.

Sastri, M. V. C., Viswanathan, B., and Srinisawa Murthy, S. (1998). "Metal Hydrides," Narosa Publishing House, New Delhi.

Schlapbach, L. (ed.) (1988). "Hydrogen in Intermetallic Compounds I/II," Vol. 63/64, "Topics in Applied Physics." Springer-Verlag, Berlin.

Thomas, G., and Sandrock, G. (2000). Hydride Information Center, http://hydpark.ca.sandia.gov/.

Wang, Q. D., and Lei, Y. Q. (eds.) (1999). "Proceedings of the International Symposium on Metal–Hydrogen Systems—Fundamentals and Applications, Hangzhou, China, October 4–9, 1998," *J. Alloys Compounds* **293–295**.

Winter, C. J., and Nitsch, J. (eds.) (1988). "Hydrogen as an Energy Carrier," Springer-Verlag, Berlin.

Yvon, K. (1994). "Hydrides: Solid state transition metal complexes," *In* "Encyclopedia of Inorganic Chemistry" (R. B. King, ed.), Vol. 3, pp. 1401–1420. Wiley, New York.

Yvon, K. (1998). Complex transition-metal hydrides. *Chimia* **52,** 613–619.

Metal Particles and Cluster Compounds

Allan W. Olsen
Kenneth J. Klabunde
Kansas State University

I. Metallic Elements
II. Metal Particles
III. Metal Cluster Compounds

GLOSSARY

Arachno Polyhedron two vertices short of close configuration (weblike).

Closo Deltahedron (all triangular faces, closed configuration).

Cluster Group of atoms bound together.

Colloid Particle small enough to remain suspended in solution or a gas.

Coordination sphere Immediate vicinity around a metal atom.

Coordinative unsaturation Open binding site(s) on a metal atom due to loss of a ligand.

Fermi level Energy difference between electron filled and unfilled levels in a semiconductor (the chemical potential at 0 K).

Isolobal Two molecular fragments with similar orbital energies and symmetries.

Knudsen cell High-temperature furnace with one small pin hole exit for high-temperature vapors to escape.

Ligand Molecule bound to a metal atom or cluster.

Ligation Act of bonding a metal with a ligand.

Nanocrystal A crystalline piece of solid matter less than 100 nm in diameter.

Nanoparticle A crystal or aggregate of crystals of solid matter less than 100 nm in diameter.

Nido Polyhedron one vertex short of closo configuration (nest like).

Nuclearity Number of metal atoms bound together.

Plasmon Collective oscillation of electrons in a solid, often of characteristic frequency.

Sintering Growth of metal particles by movement and agglomeration of smaller particles.

Sol Similar to a colloidal particle; a particle that remains suspended in a solution.

Work function Energy to pull an electron off of a bulk metal.

VERY SMALL pieces of metal, each made up of only a few atoms, constitute an unusual form of matter. These metal particles/clusters by themselves exhibit high chemical and catalytic reactivity, as well as unusual magnetic and spectroscopic properties. In addition, these metal

particles can be surrounded and stabilized by ligands to yield new chemical compounds. These ligands can be inorganic, such as halide ions, or organic such as alkenes, alkynes, and carbon monoxide. As of 1999 the known well-characterized metal cluster compounds are of the form M_xL_y (M = metal atom, L = ligand molecule), where x = 2–55.

I. METALLIC ELEMENTS

Humans have used and shaped metals since the Mesopotamian era (3500–1500 B.C.). The first metals to be fabricated were gold, copper, and tin. Gold has been a fascination for over 4000 years, especially in the period 1000–1600 A.D. when alchemists tried to produce pure gold by transmutation of base metals. Much was learned about chemical processing of metals because of the alchemists' dreams. In addition, chemical processing and shaping of iron, beginning in 1500 B.C., yielded much more information about metals.

As the science of chemistry slowly grew out of alchemy and all the elements were painstakingly discovered and systematized, it became apparent that much of our material universe is made up of metals or chemical compounds of metals. The periodic chart displays more than 70 elements that are considered metals. Some of these substances are hard and brittle whereas some are soft, malleable, and low melting. The extreme of course is mercury which melts at minus −39°C (bp = 357°C), whereas tungsten melts at 3410°C (bp = 5660°C). These physical properties reveal the strength of the bonding interaction between the individual metal atoms. Another property that is an even better measure of the bonding strength between metal atoms is the heat of formation, which is roughly a measure of the energy needed to vaporize the element (to break all chemical bonds). Figure 1 shows a periodic chart listing mp, bp (atmospheric pressure), and heat of formation of the elements.

	Osmium	Iridium	Platinum	Gold	Mercury
Distance between atoms (Å)	2.6754	2.714	2.746	2.8841	3.005
Heat of formation (kcal)	187	160	135	88	15

Also shown in Fig. 1 are the bond lengths between individual atoms of the elements. This is another crude measure of the strength of bonding for elements in the same row, although many things must be taken into account. Note the correspondence of heat of formation with bond length presented in the table above.

The atoms pack differently for the metallic elements. There are three common packing geometries as shown in Fig. 2. For two layers the packing is the same, the second layer of atoms resting in the declivities of the other. This is the densest arrangement. When the third layer is added two possibilities arise. The atoms can be placed directly over the first layer giving hexagonal symmetry (hexagonal close packed, hcp) or slightly displaced with respect to the first layer to give cubic symmetry (cubic close packed, ccp). A third less common packing arrangement is body centered cubic (bcc) where each atom has only eight instead of twelve nearest neighbors, although there are six next nearest neighbors that are only 15% farther away. The bcc arrangement is 92% as dense as the ccp and hcp arrangements. Of course, some metals can exist in more than one geometrical arrangement (e.g., Ca, Sr, Ti, Zr, Hf, Fe, and Co). The important metals Rh, Ir, Ni, Pd, Pt, Cu, Ag, and Au take on ccp geometry while V, Nb, Ta, Cr, Mo, and W prefer bcc. Most other metals prefer hcp geometries.

As more and more atoms pack together to form large metal particles (say 10^4–10^{25} atoms) the typical metallic properties are assumed. Long-range effects are observed such as ferromagnetism, reflectivity, conductivity, and malleability.

When growth stops there naturally must be edges, corners, steps, and kinks formed on the particle surface as shown in Fig. 3. Metal atoms that find themselves in such positions are much more chemically reactive, due to their accessibility and their coordinative unsaturation. These sites are believed to be very important in some catalytic processes. Likewise many catalysis experts believe that only certain geometrical arrangements of metal atoms are capable of carrying out a specific chemical (catalytic) transformation of an adsorbed molecule (the so-called ensemble effect). We will deal with these subjects in more detail later.

II. METAL PARTICLES

A. Atoms

The smallest metal particle is a single atom. In recent years atoms of metallic elements have attracted a great deal of interest. First, their formation by evaporation of the bulk element has been studied extensively. It is possible to evaporate metals that vaporize under vacuum at temperatures below 2000°C by using electrical resistive heating of ceramic crucibles (such as aluminium oxide coating on a tungsten wire basket). The metals listed below all evaporate nicely using this method. All but Sn, As,

Example
Pt
2043 ← mp (K)
4100 ← bp (K)
135 ← Heat of formation (kcal/mol)
2.746 ← Bond length (Å)

Li 452 1590 39 3.039	Be 1556 3243 78 2260														
Na 371 1156 26 3.7157	Mg 923 1383 35 3.1971											Al 933 2740 78 2.863	Si 1683 2628 107 2.3517		
K 336 1030 21 4.544	Ca 1124 1755 42 3.947	Sc 1812 3000 82 3.212	Ti 1941 3533 113 2.8956	V 2163 3273 123 2.6224	Cr 2148 2472 95 2.4980	Mn 1517 2370 67 2.7311	Fe 1810 3273 100 2.4823	Co 1766 3373 101 2.5061	Ni 1726 3003 103 2.4916	Cu 1356 2855 80 2.5560	Zn 693 1180 31 2.6694	Ga 303 2676 69 2.442	Ge 1210 3103 90 2.4498	As 1090 886 72 2.49	Se 490 958 54 2.321
Rb 312 961 20 4.95	Sr 1043 1653 39 4.302	Y 1782 3473 86 3.551	Zr 2123 4650 145 3.179	Nb 2741 5200 172 2.8584	Mo 2883 5833 159 2.7251	Tc 2443 5303 155 2.703	Ru 2583 4392 155 2.6502	Rh 2233 4000 133 2.6901	Pd 1825 3020 89 2.7511	Ag 1234 2483 68 2.8894	Cd 594 1040 27 2.9788	In 430 2348 58 3.2511	Sn 505 2960 72 2.8099	Sb 904 1908 63 2.90	Te 725 1663 47 2.864
Cs 302 978 19 5.309	Ba 1002 1910 42 4.347	La 1193 3727 104 3.739	Hf 2503 5473 145 3.1273	Ta 3269 5700 187 2.86	W 3683 6203 202 2.7409	Re 3443 5903 186 2.741	Os 3323 4500 187 2.6754	Ir 2716 4662 160 2.714	Pt 2043 4100 135 2.746	Au 1336 3081 88 2.8841	Hg 234 630 15 3.005	Tl 576 1730 43 3.4073	Pb 600 2024 47 3.5003	Bi 548 1833 50 3.09	Po 527 1235 34 3.345
Ce 1071 3530 97 3.650	Pr 1208 3290 85 3.649	Nd 1289 3400 77 3.628	Pm 1441 2733	Sm 1343 2173 50	Eu 1099 1712 43 3.989	Gd 1585 3273 82 3.573	Tb 1629 2753 87 3.525	Dy 1680 2608 71 3.503	Ho 1743 2993 75 3.486	Er 1795 2783 75 3.468	Tm 1818 1998 56 3.447	Yb 1089 1466 40 3.880	Lu 1948 3588 102 3.435		
Th 2023 4073 135 3.595	U 1405 4091 117 3.058														

FIGURE 1 Periodic chart showing mp, bp (atmospheric pressure), heat of formation, and bond lengths for metallic elements.

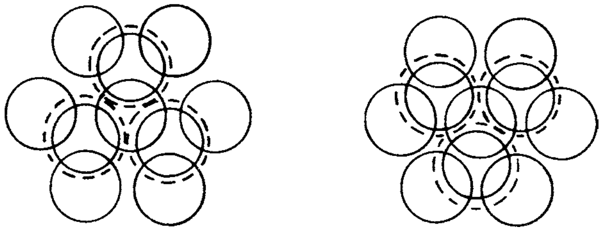

FIGURE 2 Illustration of the most common packing geometries of metallic elements. [From West, A. R. (1984). "Solid State Chemistry and It's Applications," Reprinted by permission of John Wiley & Sons, Ltd.]

Sb, Bi, Se, and Te evaporate monatomically according to mass spectrometric data.

Li	Mg	Li	Mg	Cr	Mn	Fe	Co	Ni	Cu	Zn	Ga	Ge	As	Se
Na	Ca	Na	Ca					Pd	Ag	Cd	In	Sn	Sb	Te
K	Sr	K	Sr						Au	Hg	Tl	Pb	Bi	
Rb	Ba	Rb	Ba	(and most lanthanides)										

These metals can also be evaporated (atomized) by laser heating or electron-beam heating. These methods allow many other elements to be evaporated, even those vaporizing under vacuum at temperatures of 2000°C–4000°C. A series of these high-temperatures evaporants are shown below.

											B	C
		Sc	Ti	V								Si
		Y	Zr	Nb	Mo		Ru	Rh				
			Hf	Ta	W	Re	Os	Ir	Pt			
Th	U											

A final evaporation method is called sputtering where gaseous ions are accelerated and allowed to collide with metallic surfaces. The energy of the collision causes metal atoms to be ejected (as well as some metal ions). Thus, there are well-established methods for generating the smallest of metal particles, the single atom.

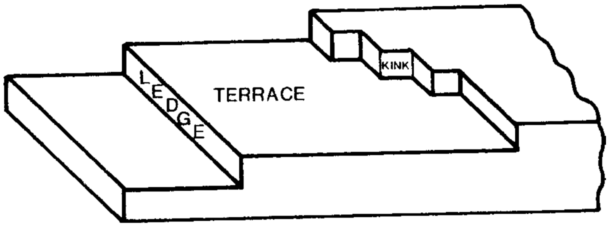

FIGURE 3 Edges, corners, steps, and kinks on a metal surface. [From Davis, S. C., and Klabunde, K. J. (1982). *Chem. Rev.* **82,** 152–208. Copyright 1982 American Chemical Society.]

In order to demonstrate what the composition was of the material coming off the evaporating surface for each element, ingeneous methods of detection of single atoms, dimers, and higher aggregates have been devised. The most useful has been mass spectrometry where the metal is heated in a Knudsen cell (hot oven with a pinhole exit) and the vapor escapes through a small hole, exits into a chamber in which the particles are ionized, and is mass analyzed magnetically. In this way the composition of the vapor in thermal equilibrium is determined.

A serious problem with the Knudsen cell is that it may not give an accurate picture of a vapor's composition (M, M_2, M_3, etc.) emitting from an open surface of hot metal, which is not in thermal equilibrium. More research is certainly needed in this area. A second problem is that mass spectrometry requires that the metal particle be ionized before mass analysis. Just the process of ionization may cause fragmentation of M_2, M_3, etc. Further research using very gentle ionization methods (using energetically controlled photons instead of electrons) is needed in this area as well.

A second method of studying vapor composition is to trap the atoms in a cold, inert material such as frozen argon or xenon. This can be done by employing liquid helium as a coolant (4 K) or special refrigeration units that can go down to below 20 K. A cold window can be employed inside a vacuum chamber, and the vapors coming off the hot metal source can be condensed on the cold window simultaneously with excess argon gas (atoms). In this way the metal particles can be surrounded and trapped in a frozen inert "ice." Then the trapped atoms can be analyzed spectroscopically. This method is called matrix isolation spectroscopy and will be discussed in more detail in Section IL.B.2.

What properties of single metal atoms are of great interest? Generally three areas come to mind: (1) ionization potentials and other electronic energy levels, (2) chemical reactivity, and (3) repolymerization to form metallic films and large metal particles.

Ionization potentials are quite revealing. The first ionization potentials of single metal atoms are listed in Table I. For comparison the work functions of the bulk metal are also listed. Note the much lower work functions as compared to the ionization potential for the atoms. So as atoms agglomerate $M \rightarrow M_2 \rightarrow M_3 \rightarrow\rightarrow M_x$ the ionization potential I. P. usually becomes lower and lower until the work function of the bulk metal is reached.

For most metals the formation of the atoms from the bulk element demands a great deal of energy. This gives the atoms a high level of potential energy (steric availability and orbitals poised for bonding) and high reactivity. Thus, reaction chemistry of free atoms and particles has been extremely fruitful and has made vapor synthesis or

TABLE I Ionization Potentials of Metal Atoms and Work Functions of Bulk Metals

Element	First ionization potential of atom (eV)	Work function (contact potential method) (eV)
Ag	7.574	4.21
Al	5.984	3.38
As	9.81	—
Au	9.22	4.46
Ba	5.21	1.73
Be	9.32	3.10
Bi	7.287	4.17
Ca	6.111	3.33
Cd	8.991	4.00
Ce	5.6	—
Co	7.86	4.21
Cr	6.764	4.38
Cs	3.893	4.46
Cu	7.724	—
Dy	6.8	—
Er	6.08	—
Eu	5.67	—
Fe	7.87	4.40
Ga	6.	3.80
Gd	6.16	—
Ge	7.88	4.50
Hf	7.	—
Hg	10.43	4.50
In	5.785	—
Ir	9.	4.57
K	4.339	1.60
La	5.61	—
Li	5.39	2.49
Lu	—	—
Mg	7.644	3.58
Mn	7.432	4.14
Mo	7.10	4.08
Na	5.138	1.60
Nd	5.51	—
Ni	7.633	4.32
Os	8.5	4.55
Pb	7.415	3.94
Pd	8.33	4.49
Po	8.43	—
Pr	5.46	—
Pt	9.0	5.36
Pu	5.1	—
Ra	5.277	—
Rb	4.176	—
Re	7.87	—
Rh	7.46	4.52
Rn	10.746	—
Ru	7.346	4.52
Sb	8.639	4.14
Sc	6.54	—
Se	9.75	4.42
Si	8.149	4.2
Sm	5.6	—
Sn	7.342	4.09
Sr	5.692	—
Ta	7.88	3.96
Tb	5.98	—
Tc	7.28	—
Te	9.01	4.70
Th	6.95	3.46
Ti	6.82	4.14
Tl	6.106	3.84
Tm	5.81	—
U	6.08	4.32
V	6.74	4.44
W	7.98	4.38
Y	6.38	—
Yb	6.2	—
Zn	9.391	—
Zr	6.84	3.60

metal atom/vapor chemistry an established field in inorganic and organometallic chemistry. Metal atoms undergo low-temperature chemical reactions smoothly, and many unusual new compounds have been prepared by combining metal atoms with organic molecules. These studies have not only led to new molecules but have also contributed to a more fundamental understanding of metal—organic interactions, which of course is important in catalysis and other surface chemistry phenomena.

Basically the low-temperature reaction chemistry of free atoms and particles can be illustrated as follows. Some classic chemical reactions are shown as examples:

Oxidative addition

$$Ni + C_6F_5Br \rightarrow C_6F_5{-}Ni{-}Br$$

$$SiF_2 + C_6F_6 \rightarrow C_6F_5SiF_3$$

Electron transfer

$$Li_{atom} + (NC)_2C{=}C(CN)_2 \rightarrow Li^+(NC)_2C{=}(CN)_2^-$$

Abstraction

$$Ag_{atom} + CF_3I \rightarrow AgI + \cdot CF_3$$

Simple orbital mixing

$$Cr_{atom} + C_6H_6 \rightarrow \underset{\text{benzene sandwich compound}}{(C_6H_6)_2Cr}$$

Substitution

$$2Ag_{atom} + (CF_3)_2CFI \rightarrow AgI + AgCF(CF_3)_2$$

Disproportionation and ligand transfer

$$2Ni_{atoms} + (CH_2{=}CHCH_2)_4Sn$$

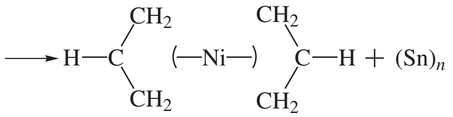

Cluster formation

$$Mg_{atom} + Mg_{atom} \rightarrow Mg{-}Mg \xrightarrow{CH_3Br} CH_3MgMgBr$$

In the absence of some added reactant, condensation of free atoms does not lead to new chemical compounds, but instead to metal clusters (particles) and then to metal films. With the availability of excellent high-vacuum technology and high-temperature sources, industry has made great use of this process.

B. Atom Agglomerates (Particles/Clusters)

Attention will now be given to small metal particles (atom agglomerates) M_2 through $M_{1,000,000}$. We will be concerned first with smaller particles M_2–M_{100}, and in Section IV with larger particles (M_{100}–$M_{1,000,000}$).

The general topic of small metal particles has received a great deal of attention recently. Much of this interest is due to the fact that these particles bridge the gap between the chemist's detailed knowledge of small molecular systems and the physicist's understanding of the collective behavior of matter.

Historically, Michael Faraday must be credited with some of the earliest work on small particles, his gold colloid preparations are still used today over 200 years later. In 1925, Richard Zsigmondy received the Nobel Prize for his study of colloidal metal solutions. Today microclusters of metals constitute one of the most important of man's synthetic materials; they are vital in heterogeneous catalysis on which 20% of the GNP of the United States is dependent. Among other numerous applications of small metal particles are thin films and coatings, latent image development, and photographic films.

The theory and applications of nucleation and cluster growth have taken great strides in recent years. First the theory will be considered followed by further discussion of experimental evidence.

1. Theoretical Studies

Consider metal atoms in the vapor state striking normal to the surface of a substrate. An individual atom, upon hitting the surface, rapidly loses kinetic and thermal energy. The loss of kinetic energy is a result of an inelastic collision of the atom with the surface. It loses most of its kinetic energy normal to the surface but may have some kinetic energy parallel to the surface. Depending upon how "hot" the impinging atom is and how effective the substrate is toward dissipating the heat of the atom, it loses a certain amount of thermal energy. The efficiency of the substrate to thermally stabilize an atom striking its surface is influenced by the heat of desorption Q_{des}. This is the energy that a thermally equilibrated atom on the surface must acquire in order to escape to the vapor phase. The degree of thermal equilibration actually achieved is also dependent on many other parameters as well. A measure of this equilibration efficiency is given by the accommodations coefficient α_T as

$$\alpha_T = \frac{T_1 - T_R}{T_1 - T_S} = \frac{E_1 - E_R}{E_1 - E_S}$$

where T_1, T_S, and T_R are the temperatures of the incident atoms, the substrate, and the desorbed atoms, respectively, and E refers to their kinetic energies. Since Q_{des} depends upon the interaction between an impinged atom and the surface, its value is very sensitive toward the condition of the surface and its cleanliness. If Q_{des} is much greater than kT, where T is the temperature of an incident atom, an atom rapidly becomes thermally equilibrated and its mean stay time on the surface, before being desorbed, is long. During its stay time on the surface an atom is considered to be absorbed and is called an adatom. If $Q_{des} \sim RT$, thermal equilibration is approached slowly and an adatom remains "hot." This "hot" atom has a very short stay time. The thermally equilibrated atom spends it stay time diffusing about on the substrate surface. The distances $\bar{X}$ that an equilibrated adatom diffuses over the surface are given by the Einstein relation for Brownian movement:

$$\bar{X} = \sqrt{2}a \exp \frac{Q_{des} - Q_d}{2kT}$$

where a is the distance between absorption sites on the surface and Q_d is the activation energy for a surface diffusion jump. This theory assumes that the adatom migrates in the form of jumps between potential energy wells on the surface. Therefore, Q_d is another parameter that is sensitive to the surface condition. If there are other adatoms within $\bar{X}$ of a given adatom, two of these may form a pair which may or may not be stable depending mainly on the substrate temperature. The pairing of two adatoms marks the beginning of the nucleation process (Fig. 4). Nucleation theories can now be used to evaluate the nucleation of adatoms. Two nucleation theories, yielding the same qualitative results, will be used. The first is the capillarity

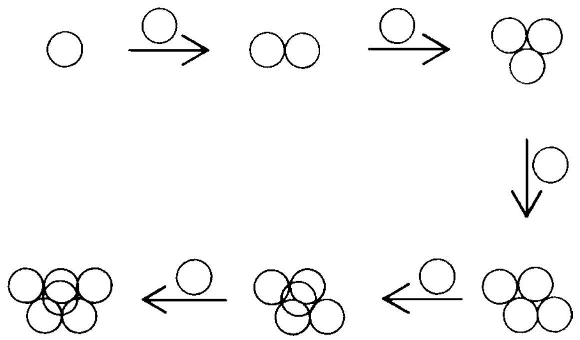

FIGURE 4 Illustration of metal atom accretion to particles (clusters).

theory which shows the relationship between the size of a spherical particle and its total free energy. The total free energy ΔG_0 needed to form a spherical particle of radius r is taken as the sum of the energy needed to create a surface (surface energy) and the volume energy of condensation. Subcritical nuclei ($r < r^*$), formed by collisions of thermally equilibrated adatoms jumping around on the surface, grow with an initial increase in free energy until a critical size is reached, greater than which growth continues with a decrease in free energy. Agglomerates (particles) smaller than r^*, the radius of the critical nucleus, are unstable and decompose, while larger clusters spontaneously grow to form stable particles. It can be seen now that an incident atom that instantaneously thermally equilibrates upon striking the surface can hop around on the surface for a finite length of time. If it collides with a critical nucleus or larger particle it becomes stabilized on the surface of that particle. If this atom collides with a subcritical nucleus the resultant particle may become stable if the critical size results or if other adatoms collide with this subcritical nucleus before dissociation occurs. The final fate of a migrating atom which fails to become part of a stable nucleus is to desorb. If an incident atom becomes incorporated into a stable cluster it is considered to be condensed. The probability that an impinging atom will condense is called the condensation coefficient. The second nucleation theory, the atomistic theory, supports the capillarity theory. The main difference between the two theories is that the capillarity theory treats a continuously varying cluster size in terms of a continuously varying free energy while the atomistic theory considers the change in the number of atoms in a cluster in terms of discontinuous changes in the binding energy of the adatoms comprising the cluster. Both theories define the nucleation rate I as being proportional to the product of the concentrations of critical nuclei and the rate at which adatoms join these critical nuclei by diffusion. It is important to note that an adatom within an area $\sim\pi \bar{X}^2$ of a critical nucleus will diffuse to that nucleus. Since $\pi \bar{X}^2$ is much larger than the physical area of the critical nucleus, there is a much greater probability for the nucleus to capture atoms by diffusion than by direct impingement.

The size of a critical nucleus of Ag, for example, can be roughly estimated by using the capillarity theory with bulk parameters and a typical deposition rate of 0.1 nm/sec at 300 K, yielding $r^* = 2.2$ Å. This suggests that critical nuclei are of atomic dimension.

Thus, these various models usually give rise to the notion of a critical-sized particle. Particles below this critical size decay faster than they grow. Of course, this critical size will vary with the type of metal under study, the surface material and temperature, and other factors.

The fate of the heat of condensation has been studied in several theoretical models and is quite interesting. The internal and translational temperatures are not necessarily in thermal equilibrium. Small agglomerates may well be "liquid" because of this extra energy and because of the fact that melting point decreases with cluster size.

While the kinetics and theory of agglomeration attempt to give size distributions, other theoretical approaches attempt to describe the detailed electronic structure of individual particles. The usual approach taken by chemists is to construct the particle from individual atoms and minimize the electronic energy as a function of shape (bonding geometry). In this way the evolution from small agglomerates toward the bulk is clarified. In contrast the physist's approach is to start with a band-type description of the bulk phase and to investigate how this breaks down as the size gets smaller. In the latter case, a primary goal is often the calculation of the density of states function of metals. Early in this century there was considerable progress made in describing the color of colloids such as gold by means of Mie's theory and the idea of plasmon responses. More recently, plasmons have been invoked in an attempt to explain the surface-enhanced Raman effect. The calculation of the electronic properties of small metal particles becomes complicated because the spacing between adjacent levels may become large compared to kT, and classical continuum models break down. It becomes clear that quantum mechanical effects are very important when considering the electronic band structure of small metal clusters.

When comparing theoretical calculations on metal microclusters the location of the d and s bands and their degree of overlap is sometimes used as a guide to their accuracy. In bulk metals the s band is contained within the d band, and for copper clusters of eight atoms or more the Xα – SW theoretical approach predicts s and d overlap. However, another method, Hartree–Fock, predicts distant s and d bands for the same eight atom copper agglomerates. Most calculational methods agree with the

Hartree–Fock results, but it can be seen that substantial disagreement is still prevalent with theorists when electronic structures are involved.

Due to computational limitations, *ab initio* calculations (more basic, fewer approximations) have been limited to very small particles such as dimers or trimers. Lithium has been treated the most extensively. The assumption that the core electrons can be treated as a pseudopotential (the same for each metal) allows the extension of these calculations to other metals. For example, particles up to ten atoms have been treated theoretically for Ni, Pd, Cu, and Ag. These calculations become so complex even for high-speed computers, that fixed-particle geometry is often assumed. Thus, no structural information can be derived although various electronic energies can be estimated.

Calculations of the binding energy indicate a significant *increase* in binding energy per atom with increase in cluster size for certain metals. Lithium and copper clusters up to 13 atoms show a nearly linear relationship between number of atoms and binding energy. It appears that the dimer has a binding energy of one-fourth that of the bulk value and the 13-atom particle has roughly two-thirds that of the bulk value.

Calculation of ionization potentials provides a good test of theoretical models. In general, there is a decrease by roughly a factor of two from the ionization potential of the atoms to the work function of the bulk metal. The decrease is not monatomic, but depends very much on particle geometry. There is also an odd–even alternation with the odd-atom clusters having a lower ion-ization potential, presumably because they are odd-electron systems as compared to closed-shell structures for the even-electron systems. These results agree fairly well with the few experimental results available for comparison.

Theoretical calculations of particle geometries have also been carried out by several methods. These calculations have spanned the complete range of bond types including van der Waals clusters of rare gas atoms, ionic clusters of salts, and metal clusters. Somewhat surprisingly the rare gases and metals often are predicted to have similar shaped clusters perhaps reflecting the nondirectionality of the binding forces. A common goal of these calculations is to try and predict the bulk three-dimensional crystal structure. In general, this goal has not been met as the small particles often have quite different structure from the bulk, and the transition to bulk geometries occurs only gradually and for rather large particles (>500 atoms). As an example of the difficulty, most calculations for rare gases (and metals) predict clusters with fivefold symmetry while it is commonly known that no extended three-dimensional structure may have fivefold symmetry.

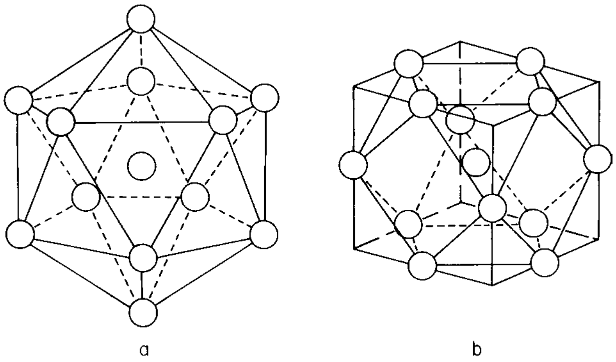

FIGURE 5 Icosahedran (a) and cuboctahedran (b) show two different 13-atom clusters.

Further calculations on rare gas atom clusters, which are believed to model many metal atom clusters, have shown that tetrahedral groupings of atoms are usually preferred over octahedral groupings.

The 13-atom case is most interesting because it represents the smallest structure that can have an internal atom, i.e., one which is not on the surface. Two of the most important 13-atom structures are the cuboctahedran and the icosahedran (Fig. 5). The cuboctahedran is derived from the face-centered cubic (fcc, closest packed) structure and may be pictured as a central atom in a cube surrounded by 12 equivalent atoms at the centers of each edge. This figure has eight triangular faces and six square faces. The icosahedran consists of a central atom surrounded by layers of five atoms each above and below. Each of these layers has in turn a central atom capping the figure. All twenty faces are triangular and all twelve vertices have fivefold symmetry. This leads to a more closely packed surface for the icosahedran than for the cuboctahedran. The icosahedran can be constructed from twenty tetrahedral figures packed so that they each share three faces with only minimal distortion (the dihedral angle of a tetrahedron is 70.53° as compared to 72° for the pentagonal angles). The icosahedral structure is dynamically the most stable 13-atom cluster. Inclusion of small three-center forces does not change this conclusion.

There exist some 988 distinct minimal 13-atom structures in these dynamic calculations. Much amorphous and/or fluctional character to these small particles is expected. One might even wish to ask whether they are solid or liquid.

Various experiments involving the condensation of gases show the presence of "magic numbers," i.e., clusters with certain numbers of atoms that are significantly more prevalent than others. Often these magic numbers correspond in size to the nearly spherical Mackay icosahedra (1, 13, 55, 147, 309, 561, 932, ...). Continuous deformations of these structures can lead to fcc cuboctrahedral

structures. These deformations involve the transformation of sites of tetrahedral symmetry to sites of octahedral symmetry.

In addition to the problem represented by the fact that icosahedra (tetrahedra) cannot form extended three-dimensional structures, the Mackay icosahedra do not grow smoothly from one into another by simply placing new atoms in the centers of each triangular face. Such a growth pattern by the formation of caps might be expected to be energy efficient and does lead to other magic numbers which are experimentally seen. For the larger particles a highly symmetrical geometry was assumed and the evolution, if any, of the particle with time was followed.

While these calculations using pair potentials can be extended to agglomerates of several hundred atoms, they are only appropriate to systems, such as the rare gases, in which non-nearest neighbor interactions can be neglected. This is clearly not the case for metal clusters where valence electrons move readily from atom to atom and electronic band structures are important. Because of computational difficulties most *ab initio* calculations start with an assumed geometry and look for electronic properties. Early calculations on lithium clusters seem to favor linear chains over planar or three-dimensional structures. However, inclusion of $2p$ orbitals seems to destroy this preference for linear structures.

There have been some attempts to use CNDO and extended Hückel calculations to address the geometry issue. Again linear structures appear to be more stable for many metals such as silver. The relative stability of icosahedral versus cuboctahedral structures would appear to depend on the d orbital occupation. Thus palladium with a $d^{9.2}s^{0.8}$ configuration prefers an icosahedral structure whereas silver with a $d^{10}s^{1}$ configuration is predicted to be cuboctahedral. Qualitatively these results may be understood in terms of the more closely packed surface of the icosahedral structure. This leads to a larger d-orbital bandwidth and to a higher energy for a completely filled d band. As with the pair potential calculations the energy does not vary strongly with geometry and many structures are calculated to be nearly isoenergetic.

For metal clusters, it is now possible, through first principle theoretical (calculational) approaches, to predict and better understand vibrational spectra, optical band gaps, polarizability, quantum confinement, and structural predictions. One modern approach is to use pseudopotential density functional methods (PDFM), in particular to predict optical and dielectric properties. Similarly, using molecular dynamics simulations, it is possible to create models for cluster structures. This has been especially valuable for predicting a three-dimensional image for mixed metal clusters. Figure 6 illustrates computed structures for Cu-Ru bimetallic clusters. Note that in this case the dynamics simulation predicted an enrichment of Cu at the edges and corners of the polyhedral structure. Indeed, this prediction was supported by later experimental catalysis data.

Now let us turn our attention to experimental methods and results for the generation and characterization of small metal particles. There are three catagories: molecular beams, matrix isolation, and clusters on surfaces, all of which were introduced very briefly earlier.

2. Experimental Studies

The mass analysis of an effusive beam of metal particles from a Knudsen cell allows us to calculate the equilibrium constants for the formation of dimers, trimers, etc. Performing similar studies over a wide range of temperatures then allows us to obtain the complete set of thermodynamic quantities: free energy, enthalpy, and entropy of formation. Unfortunately, the multimer concentrations are typically so small that this technique is limited to an analysis of the thermodynamics of only dimers except in favorable cases. Nevertheless, these studies provide a convenient check for spectroscopic measurements of bond energies.

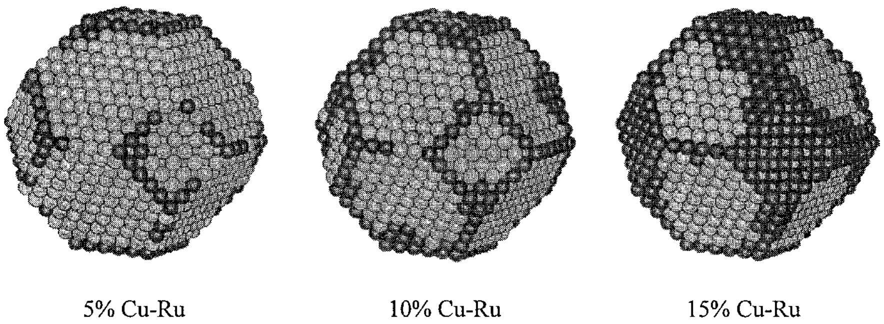

FIGURE 6 Computed structure for Cu-Ru bimetallic clusters. Note enrichment of Cu at edges and corners.

In recent years there have been numerous studies using supersonic beams. In this case a high-pressure gas expands adiabatically through a small nozzle and cools greatly. Now either the supersaturated gas itself or another material seeded into the gas condenses forming clusters. The low temperature of the seeded beams not only produces condensation but greatly simplifies the electronic spectra allowing the detailed study of even weakly bound molecules such as van der Waals complexes. However, even with the simplification caused by the low temperature, only small systems such as dimers and trimers have been studied in detail. Our interest is with larger agglomerates.

In a seeded beam a condensable material is mixed with a large excess of a rare gas (usually helium) which does not condense under the experimental expansion conditions. This technique is used with metals and other materials which have too low a vapor pressure to be expanded directly. Low boiling metals, such as the alkalis and alkaline earths, can be heated in a simple Knudsen cell. Stronger heating has been used for the more refractory transition metals. Most recently laser evaporation has been used to produce beams of many metals. This technique, which uses a pulsed, focused laser to evaporate metal from a rod, is well suited to the use of a time-of-flight mass spectrometer for cluster analysis. Analysis by laser-induced fluoresence or laser ionization also allows many spectroscopic studies to be conducted in small clusters. In this way bond lengths and other parameters have been determined for dimers of Cr, Cu, and Sn to name just a few.

For larger clusters much spectroscopic detail is lost, but measurements of the photoionization thresholds provide information concerning cluster ionization potentials. Sodium clusters show a relatively smooth decrease in ionization potential from 5.1 eV for the atom to 3.5 eV for the 14-atom cluster. This is still significantly above the 1.6-eV work function of bulk sodium. For the smaller clusters the odd sizes have a lower ionization potential than the neighboring even-sized clusters because of effects due to open versus closed shell configurations. Recently measurements have been made of the ionization potential of iron clusters up to 25 atoms. In this experiment the ionization potentials were bracketed by the use of various ionizing lasers. There is a decrease in the ionization potential from 7.870 eV for an iron atom to the 4.4-eV work function of the bulk metal, but the trend is by no means linear. Thus, the ionization potential of Fe_2 is about 5.9 eV, while those of Fe_3 and Fe_4 are above 6.42 eV. Clusters in the range of 9–12 atoms have ionization potentials below 5.58 eV while those in the range of 13–18 atoms are above 5.58 eV. The ionization potential of the 25-atom cluster still exceeds the bulk value by 0.3 eV (6.9 kcal/mol).

Chemical reactions of metal clusters in a beam are just beginning to be studied. Sodium clusters (Na_n) react with chlorine atoms by the abstraction of a sodium atom forming NaCl and electronically excited Na_{n-1}. Similarly, rate constants for reaction of H_2 with iron clusters have been made. In these studies the hydrogen always appears to add as a dimer and the reaction rate is a very strong function of cluster size. Clusters below four atoms are slow to react as are clusters of 15–18 atoms. There appears to be a strong correlation between low ionization potential and fast reaction rate, but more work needs to be done to confirm this.

In the technique of matrix isolation the atoms of the metal to be studied are mixed with a large excess of an inert gas upon condensation on a cold surface. The inert gas is often argon in excess by a factor of about 1000, and the temperature is in the neighborhood of 10 K. This technique has the advantages of freezing quite reactive atoms/clusters, concentrating them by collecting over time, and holding them for more leisurely study. Often spectral lines are very sharp, although they can be broadened by inhomogeneous lattice effects. In some cases laser excitation can give sharp line emission from only a limited number of sites. Matrix relaxation also leads to line broadening.

A principal difficulty with matrix isolation studies is that they are often limited to small clusters of indeterminate size. Large dilutions favor monomer deposition. Comparison of the growth of spectral features as a function of dilution ratio with statistical models allows us to correlate these new spectra with various sized particles. However, there is significant migration of atoms within the growing surface before the condensing gas becomes rigid. The degree of this migration can be enhanced by increasing the temperature, either during or after the deposition, or by using the lower melting gas. Silver atoms undergo a photomigration when they are excited in an argon matrix with atom absorptions being bleached and dimer absorptions growing.

While many spectroscopic studies have been published on dimers, the most extensive polymer studies have been with Ag, Na, and Cu clusters. As might be expected much of the interest in silver relates to the photographic process where it appears that a four-atom silver cluster on a silver halide surface leads to reduction by developer, whereas a three-atom cluster does not. The electron spin resonance (ESR) spectrum of sodium in argon confirms that the trimer is covalently bonded and not an equilateral triangle. Ultraviolet photoelectron spectroscopy (UPS) of Cu clusters indicates that the d band is separate from the s band, unlike in the bulk or in the $X\alpha$ calculations mentioned earlier.

Even under matrix isolation conditions some chemical reactions occur. A large number of reactions with atoms (especially the alkalis) have been observed. Reactions between CO and Cu or Ni clusters have been studied by

infrared spectroscopy. The CO stretching frequencies on clusters of one to four nickel (or copper) atoms rapidly approach the values found for CO chemisorbed on the polycrystalline bulk metal. Thus, the CO to metal bonding appears to be local as expected.

In mixed deposits of metal, methane, and argon only A1 atoms of some 18 metals tried appears to react at 10 K without photolysis. The reactivity of A1 appears to be unique and probably due to its radical like ^2P state. Theoretical studies lend support to the idea that atoms with partially filled *p* orbitals would be most reactive in C—H insertion processes.

The question as to whether clusters or atoms are more reactive in carbon-halogen bond breaking processes was recently considered. It was found that in an argon matrix at 10 K Mg_2 and Mg_3 reacted with CH_3Br (presumably to form CH_3Mg_2Br and CH_3Mg_3Br), but Mg atoms did not. This higher reactivity was attributed to the lower ionization potential of these small clusters and to the fact that in the free state Mg_2 and Mg_3 are very weakly bound, but in the product should be strongly bound. Similar results have been found for Ca, Ca_2, and Ca_3. *Ab initio* theoretical studies convincingly support these experimental results. However, even after numerous attempts, these cluster compounds have eluded isolation, and are apparently quite unstable.

Kinetic studies of metal atom aggregation in cold matrices has received some attention. A statistical frozen matrix approach (calculating probability that M and M are neighbors and react to give M_2), and a highly mobile metal atom approach (diffusion being rapid in quasiliquid layer) have been used. It was found that the diffusion mechanism was supported best by the experimental results. The eventual M_2 concentration was found to be proportional to the square of the M/substrate ratio. Concentrations of higher metal aggregates vary as some higher power of the M/substrate ratio.

Since the statistical approach underestimates the formation of clusters in the matrix, further analysis has been done. Both dilute and high-concentration matrices have been dealt with experimentally and mathematically. The best model was found to be one which simulates freeze-out by assuming the reactions to stop abruptly after a certain time. It should also be pointed out that the trend in product distribution as a function of metal concentration is adequately described by this model and greatly aids spectroscopic assignment of bands to metal atoms and clusters.

A film produced by deposition of atoms or particles on a surface forms in several stages: (1) nucleation, (2) cluster growth, (3) coalescence, (4) further thickening, and (5) recrystallization (perhaps). We will be concerned with steps (1)–(3).

Clusters on surfaces, or supported clusters, lend themselves to a variety of X-ray and electron spectroscopies, such as extended X-ray absorption fine structure (EXAFS), X-ray and ultraviolet photoelectron spectroscopy (XPS and UPS), and transmission electron microscopy (TEM) to name a few. Most studies of model systems have used sodium chloride or carbon substrates and ultrahigh-vacuum techniques.

Several authors have modeled the kinetics of cluster growth. Nucleation occurs at specific sites, often associated with lattice defects on the substrate. Cluster growth commences as atoms impinge near each other; in a series of experiments it was found that gold atoms will be captured if they land within 6.5 A of a growing cluster.

As cluster growth continues the energetics regarding two- or three-dimensional growth must be considered. Calculations indicate that if the heat of vaporization of the metal Λ_0 is greater than three times the heat of desorption of the metal atom from the surface, E_{des}, three-dimensional clusters should form. However, if the heat of metal vaporization is less than three times the energy of desorption minus the energy of diffusion E_{diff}, two-dimensional cluster growth is favored. Depending on the surface, E_{des} and E_{diff} will vary:

$$\Lambda_0 \gtrsim 3E_{des}$$

(three-dimensional growth favored)

$$\Lambda_0 \lesssim 3E_{des} - E_{diff}$$

(two-dimensional growth favored)

These theoretical considerations predict that metal clusters growing on most clean metal surfaces and semiconductors would grow initially in two dimensions, and this is found experimentally.

Small clusters on surfaces have some unusual properties. Their geometrical shapes usually do not resemble the bulk element. For example, using Moire interference patterns and TEM the smallest colloids of gold are shown to have pentagonal symmetry. The presence of multiple twinned tetrahedra such as icosahedra, again suggests that icosahedral structures are preferred over the bulk structure during the initial growth phase.

If perfect crystallites are not formed in the initial stages of growth, there will be some strain energy in the cluster. As metal thickness increases, the desorption energy of a metal atom on the surface changes. For Na on a tungsten surface, E_{des} is initially 2.5 ± 0.2 eV, but after four layers are deposited becomes 1.06 eV, which corresponds closely to the bulk heat of vaporization of Na. Since the Na—Na bonding energy is so high initially, lattice relaxation via two-dimensional dislocations is difficult so more strain energy is created in the growing Na cluster.

The importance of these unusual growth characteristics has stimulated theoretical work on the kinetics of surface cluster growth, and often cluster growth has been treated as a polymer growth problem. The growth process becomes governed by an equilibrium between impingement and desorption which is indicated by a constant value of monomer concentration over a considerable time period. So at a certain substrate temperature it should be possible to establish equilibria with very small cluster sizes. However, at low substrate temperatures no such equilibria can be established, and cluster concentration and nucleus concentrations rise very steeply. Generally the cluster growth for Au under low-temperature conditions (80 K) on a clean surface involves an induction period of 10^{-5} sec, twin formation until 10^{-3} sec, constant growth to 10^{-1} sec, and then coalescence to a film.

Small clusters on surfaces can also be affected electronically, and so supported clusters have been extensively investigated. Of particular interest is the behavior of the *d* electrons. X-ray photoelectron spectroscopy indicates that the *d* electron binding energy decreases and the *d* electron bandwidth increases with increasing cluster size. These effects can be explained in terms of changes in the d–$s(p)$ orbital hybridization. Thus, the $3d^84s^2$ configuration of atomic nickel becomes $3d^94s^1$ in bulk nickel. Similar increases in *d* orbital occupation with increasing cluster size are expected for other metals. Because of their more localized nature, *d* electrons are repelled more by the core electrons and the electron binding energy is expected to decrease with increasing *d* orbital occupancy (cluster size). From a simple molecular orbital picture, the larger the number of like neighbors, the larger should be the *d* electron bandwidth. Because of overlap integral effects, this increasing width is asymmetric with the weakly bonding and antibonding orbitals shifting more; i.e., the binding energy decreases with increasing size (number of neighbors). An UPS study of silver and iodine-covered silver clusters has led to a similar interpretation of cluster size effects upon the *d* electron bandwidth and ionization potential.

Gold clusters on weakly interacting substrates, such as carbon or alkali halides, have been most extensively studied. In this case, changes in *d* electron binding energy as a function of cluster size are exactly paralleled by similar changes observed in gold–cadmium alloys as a function of gold concentration. The only important parameter appears to be the average number of like nearest neighbors. Dilute gold alloys behave like small clusters. Thus, there is a linear increase in *d* electron binding energy with decreasing concentration. When the substrate has localized *p* or *d* orbitals which overlap the *d* orbitals of the cluster there is a strong interaction which usually leads to a decrease in the *d* electron binding energy.

Unfortunately, until very recently experimental studies of small metal particle structure usually lacked the resolution necessary to observe differences between various geometries. In most cases only average particle sizes or size distributions are obtained and these usually assume simple cubic or spherical geometries. Technology was not available (and is still not very accessible) to study local surface disorders on an ordered core of a small particle. Some structural differences between small metal particles produced in different ways have been observed, however. These may be compared to large cluster compounds whose detailed structure can be determined by X-ray crystallographic methods (see Section III).

New technology is now available, however, and dramatic recent advances in microscopy techniques now allow imaging of surfaces at the atomic level. Scanning Tunneling Microscopy (STM) especially has made great strides in this area. This technique depends on the movement of a probe tip over a surface, not touching but very close. An electrical potential between the probe tip and the surface causes electrons to tunnel through the space between them. Automatic movement of the probe to maintain a constant tunneling current as the surface is scanned essentially plots out, with atomic resolution, the geography of the surface. These exciting developments allow the imaging of atoms and clusters, rows, and arrays of atoms. Truly, the age of "seeing" atoms is now with us.

Metal atoms nucleating on a [100] NaCl plane take on one of two structural orientations, depending on the metal. These are the [001] plane initially for Ni > Cu > Ag > Au > Al. Upon further deposition this expitaxial growth preferred the [111] orientation. High-resolution electron microscopy showed that twinned particles with external shapes of either decahedron or icosahedron were formed. No gaps or dislocations were observed. Slightly diverging lines in the lattice images were interpreted as particles being formed from a nucleus of several atoms forming the smallest unit of either a decahedron or icosahedron. Growth proceeded layer by layer of atoms on the nucleus in the most closely packed form. These structures are present for particles even less than 20 Å in diameter, but they no longer kept their initial structures when they grew beyond 150 Å in size.

A supersonic free jet mixture of metal particles in argon has been studied by electron diffraction. Particles of Bi, Pb, and In of 40–95 Å were measured. Changes in crystal structure from that of bulk metal were observed for clusters in the 50–60 Å diameter range (2000–4000 atoms/particle). Indium growing particles changed from tetragonal to face-centered cubic as size increased. Lattice parameters of the microcrystals were found to decrease as the cluster size increased. Apparently a high proportion of surface atoms in small clusters favors crystal defects

in surface regions of high curvature. The resulting defects may play an important role with regard to cluster stability in dictating a change from tetrahedral to face-centered cubic indium.

Further studies of supported clusters by X-ray diffraction and electron microscopy have shown that Ni clusters of about 21 Å diameter supported on Al_2O_3 or SiO_2 have a great deal of strain attributed to internal pressure buildup in small particles to counter the surface tension or deformation of fcc structures. Using the most sophisticated technology available, rhodium clusters of as few as five atoms have been observed by high-resolution electron microscopy. The outline of each atom was observable, and the atomic "spots" measured 2.7 ± 0.2 Å in diameter compared with the atomic diameter of Rh as 2.74 Å. The spacings between the spots measured 3.5–4.0 Å, which is in good agreement with the lattice spacings given for the fcc structure of Rh of 3.8 Å.

So modern technology is beginning to allow the physical study and observation of the smallest metal particles. The future holds a great deal of progress, information, and new uses for these interesting species.

Most metal particles are supported or attached to a surface. This surface is often a high surface area powder, such as SiO_2, Al_2O_3, MgO, or C. How mobile are metal particles on these surfaces? What are the electronic effects of the surfaces (supports) on the small metal particles? These are vital questions in the field of heterogeneous catalysis.

The growth of supported metal particles by movement and agglomeration is called sintering. Sintering can occur by two different mechanisms: (1) migration and coalescence and (2) dissociation of single atoms and movement of the atoms to other particles. It can be seen that these are the same phenomena discussed prevously for particles on surfaces. However, in catalysis other reactants are present and it is possible for mechanism (2) to operate by chemical reaction of surface metal atoms to yield a volatile compound which can be transported to another cluster, decompose, and deposit the atom. For example, Ni particles are easily sintered in a CO atmosphere:

$$(\mathrm{Ni})_\mathrm{n} + 4\mathrm{CO} \rightarrow (\mathrm{Ni})_{n-1} + \mathrm{Ni(CO)_4}$$

$$(\mathrm{Ni})_\mathrm{m} + \mathrm{Ni(CO)_4} \rightarrow \mathrm{Ni_{(m+1)}} + 4\mathrm{CO}$$

Generally these mechanisms and theories of sintering predict a movement of atoms from smaller particles to larger ones, eventually reaching unisized particles. Indeed, experimentally it has been found that the broader the starting particle size distribution, the faster the sintering. Likely driving forces are the reduction of internal strain and reduction of surface free energy.

Sintering of supported metal particles can occur over a wide range of temperatures depending on the metal and the support. Generally 200–600°C is the range where common catalysts may age by sintering.

Of course, the bonding of the support to the metal particle will affect the ease of sintering, and may also affect the electronic properties of the metallic particle. Thus, strong support effects are the subject of much current research. The support TiO_2 has the most pronounced support effect because it is capable of shuttling electrons to and from the metallic particle. This is apparently due to the fact that TiO or TiO_2 (Ti^{2+} or Ti^{4+}) is available on the surface.

One of the most pronounced differences between small particles and bulk ferromagnetic metals (e.g., Fe, Co, Ni) is their magnetic behavior. Such differences were first reported in 1896. By 1930 small metal particles were referred to as "magnetic drops," which were predicted to be the smallest units which display ferromagnetism and were a minimum of 10^{-4} cm. in diameter. By 1938 there was evidence that small metal particles behaved as tiny magnets. By 1946 the smallest domain structure of ferromagnetic bodies was calculated to be 2×10^{-6} cm. Smaller particles should therefore exhibit quite different magnetic properties from bulk specimens. Theories then developed and experiments were performed showing that particles below 300 Å in diameter act like paramagnetic "atoms" with very large magnetic movement. This phenomenon has been termed superparamagnetism or collective paramagnetism.

This knowledge has allowed magnetic measurements to be used to measure metal particle sizes, even down to less than 50 Å (modern electron microscopy now allows measurements down to 1 Å). During the years that magnetic measurements were used for particle size measurements it was noted that chemisorbed hydrogen had a significant effect. Oxygen and nitrogen also had effects. These observations led to the use of magnetic measurements to elucidate chemisorption mechanisms on particles.

The Curie temperature, or that temperature where ferromagnetic substances become merely paramagnetic, has also been used to study small metal particles. Although magnetic effects are of great use in the study of small particles of ferromagnetic metals, great care must be exercised since chemisorbed species and the oxidation state of surface atoms can have dramatic effects on the experimental results. A few additional comments about electronic properties, as they depend on particle size, are in order.

Theoretical treatments have shown that the average spacing δ between energy levels in a statistical collection of small metal particles is inversely proportional to the size of the particles. In bulk metals δ is smaller than any of the relevant energy parameters such as kT. In small particles, however, δ may no longer be considered small. Thermal

properties, heat capacity, and magnetic susceptibilities, for example, may be very different for small particles relative to the bulk due to the increase in S. This would be expected to be especially relevant at low temperature where $\delta \geqq kT$.

Defects in small particles have been considered by theorists. Density of states at the Fermi level in 13-atom clusters of Fe, Ni, and Cu showed the highest densities in Fe. The d bandwidth for the case of a 13-atom Ni particle was much smaller than that of the bulk. The model used in these calculations was varied to include special surface features such as steps. Plotting orbital charge densities for states near the Fermi level revealed strongly charged lobes extending above the step atoms and terminating in the plane below the step for the Ni case (see Fig. 7). In general, stepped surfaces show a variety of bonding orbitals not present on flat surfaces, and this may explain the higher catalytic activities of stepped surfaces for some chemical reactions.

Experimental evidence has been reported that changes from a discrete set of electronic levels to a spectrum characteristic of bulk metal are continuous, and the bulk spectrum is reached when the particle contains about 100 atoms. As a result of this, Auger electron spectra reveal no changes due to particle size variations for Ag-, Cu-, Au-, and Ni-evaporated ultrathin films on amorphous carbon.

3. Inherent Chemical Reactivities of Small Metal Particles

Previous discussion has indicated that small metal particles have several different properties as compared to bulk metal. Electronic spectra are different, energy levels are different, defect sites such as steps or kinks lie at higher energy levels than similar sites on bulk samples, and even preferred geometries are sometimes different.

Knowing this it should not come as a surprise that small metal particles behave differently in chemical reactions than bulk samples. Qualitatively there is a great deal of evidence available indicating that higher reaction rates, more complete conversions, and varying reaction selectivities are possible using small metal particles (as compared with bulk metals). However, sorting out surface area effects, support effects, oxidation state changes, and the behavior of defects has caused a great deal of confusion and inherent reactivities of metal atoms versus bulk metal have been difficult to ascertain. However, it has been learned that certain chemical reactions are more sensitive to surface structure than others. These reactions are (1) C—C bond breaking (hydrogenolysis and skeletal isomerization) and formation (dehydrocyclization), (2) D_2 exchange with benzene, and (3) various oxidation reactions. The implication is that a certain array of metal atoms (ensemble) perhaps with certain defect sites are necessary for these reactions to take place. This in turn suggests some mechanistic features of the reactions where the organic reactants must lie down on the surface in a specific way in order for the reaction to take place. An example is shown in Fig. 8.

Studies of free atoms and free metal particles (not supported but either in a frozen matrix of argon at 10 K or in the gas phase) have recently been initiated. Interestingly, in every case where a comparison of reactivity of M atoms versus $M_2, M_3, \ldots, M_n$ ($n < 20$) could be made, dimers, trimers, and higher clusters showed increased activities over M atoms. For example, at a very low temperature of 150 K (−130°C) C—C bond cleavage occurred on Ni_n but not Ni atoms. Interestingly clean Ni films (bulk) do not react with alkanes to give C—C bond cleavage at such low temperatures. Thus, small metal particles seem to be more reactive than atoms or bulk metal. Similar results

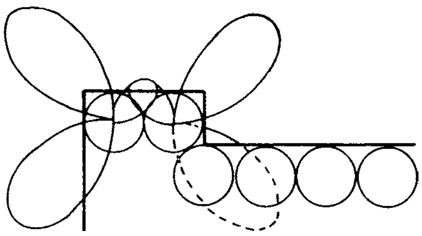

FIGURE 7 Representation of orbital charge densities of states at step sites on a nickel surface. [From Davis, S. C., and Klabunde, K. J. (1982). *Chem. Rev.* **82,** 153–208. Copyright 1982 American Chemical Society.]

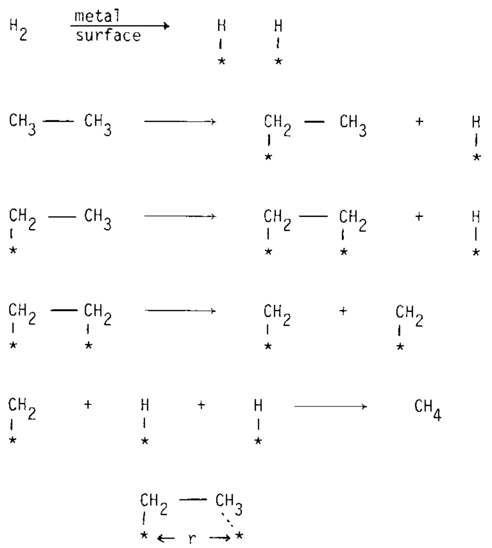

FIGURE 8 Example of the mechanism for a structure-sensitive reaction: * denotes attachment to a metal atom. The critical parameter is r which affects the efficiency of dissociative adsorption.

were found with Mg atoms versus Mg_2 and Mg_3 reacting with CH_3Br at 10 K. Only Mg_2 and Mg_3 reacted whereas Mg atoms and bulk Mg did not. In addition, the recent development of techniques for producing and studying gas phase metal clusters has led to a great deal of new knowledge about cluster reactivities. Careful studies of Fe_x, Nb_x, Pt_x, C_x, Al_x, and others (where $x = 2-100$) produced in gaseous streams of helium followed by reaction with CH_4, H_2, H_2O, NH_3, or O_2 have led to many intriguing results. Reactivity appears to be sensitive to cluster size and probably structure as well. In some cases, the ionization energy of the metal cluster is important in determining relative reactivity. Also, it has been noted that heating of the gas phase clusters sometimes leads to a lowering in relative reactivity (for example, Fe_x with H_2). This finding is compatible with the idea that the gas phase cluster growth process may lead, by kinetic control, to structures with many reactive defect sites. Upon raising their temperature, the clusters may anneal to more compact, less reactive structures.

Thus, recent experimental evidence seems to support the idea that growing small particles have maximum chemical reactivities, and certain sized/shaped small particles may have the *highest* reactivities. What size and/or shape varies with the metal in question and the reaction in question? This information strongly supports three ideas: (1) structure sensitivity in chemical reactions on metal surfaces is very important, (2) more than one atom is necessary to carry out at least some bond breaking processes, and (3) defect sites on growing small particles are extremely reactive (see Fig. 9). It has also been possible by pulsed laser vaporization to produce many types of gas phase metal clusters. Particularly interesting have been reactivity studies of niobium clusters Nb_x where $x = 5$–20. A definite cluster size dependence on reactivity was observed. Exposure

$$Nb_x + C_6H_6 \rightarrow Nb_xC_6 + 3H_2$$

of Nb_8 or Nb_{10} to benzene caused no reaction. On the other hand Nb_5, Nb_6, Nb_9, and Nb_{11} reacted vigorously

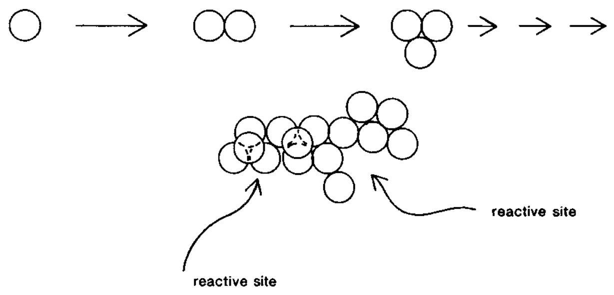

FIGURE 9 Illustration of possible reactive sites on a growing metal particle (low-temperature growth, not in equilibrium).

to form Nb-carbide species with loss of hydrogen. It was concluded that the closed structure of Nb_8 and Nb_{10} render them less reactive, while the reactive clusters were capable of a lower activation energy entry to benzene, and the reaction went to completion driven by the exothermicity of Nb–C bond formation and H_2 bond formation.

In an investigation of CO_2 reactions, reaction channels

$$Nb_x + CO_2 \rightarrow (OCNb_xO) \nearrow OCNB_xO \text{ (larger clusters)}$$
$$(OCNb_xO) \searrow Nb_xO + CO \text{ (smaller clusters)}$$

were dependent on cluster size.

Interestingly, small Nb clusters favored Nb_xO formation while larger ones favored $OCNb_xO$. Possibly this results because larger clusters can internally stabilize the "hot" $OCNb_xO$ intermediate while the smaller adducts fly apart since energy cannot be dissipated well enough.

These studies again clearly showed that geometrical structure coupled with electronic structure (open shell with unpaired electrons, or closed with no unpaired electrons) are important in determining relative reactivates. However, it still remains in large part a mystery why certain clusters are reactive or unreactive, or why ionization energies vary so much with cluster size.

Reactivity of much larger gas phase metal clusters have also been examined in recent years. An example is the determination of binding sites for NH_3 gas on Ni_x and Fe_x where $x = 50$–147. The adsorption of ammonia on gas phase metal clusters can lend information, since the number of binding sites would vary with cluster structure. For Ni clusters, the number of ammonia molecules adsorbed showed pronounced minima in the 50–116 atom range for those specific clusters that are particularly stable (those that are a "magic number" are in larger amounts than statistically predicted (see Fig. 10)).

These clusters probably arise from closing of shells and subshells of the MacKay icosohedra; indeed the ammonia adsorption data support this idea. However, for clusters with a more open structure, more than the predicted amount of ammonia was adsorbed. Evidence for such open shell structures was found more prevalently for Fe_n than Ni_n. It seems that d-electron-rich metal atom clusters more readily form close-packed structures (Ni) but d-electron-poor clusters growth is more controlled by kinetic factors, and many unusual, metastable structures appear to be possible even at as high a room temperature.

In another example of the interesting behavior of small metal clusters, the ability to produce small gas phase metal clusters, and to slow them down so they can be "soft-landed" on a surface, has been utilized in an ingenious

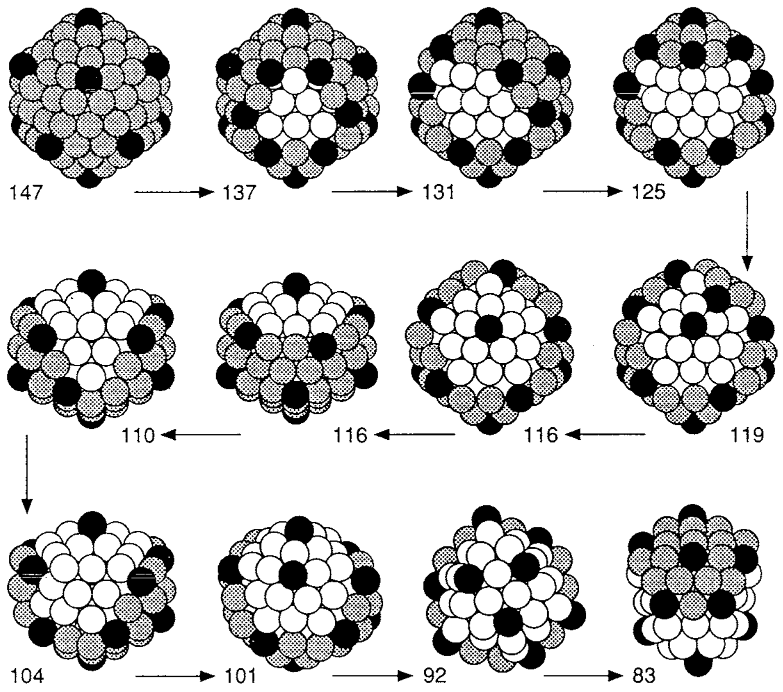

FIGURE 10 Drawings of closed (sub) shell clusters in the proposed growth sequence from n = 83–147. Black denotes primary NH_3 adsorption sites; gray, third shell atoms; and white, second shell atoms.

way to elucidate how the classic silver-silver bromide photographic process works. Woste and coworkers soft-landed Ag_2, Ag_3, and Ag_4 clusters (positively or negatively charged) on a surface of silver bromide. It was found that only the Ag_4 cluster was capable of catalytically enhancing the photographic development process subsequently carried out. These data suggest that Ag_4 is a key species that is formed when silver-bromide-containing photographic film is exposed to light. Indeed, it has been estimated that about 10 photons are needed to produce one Ag_4 species (according to the proposed mechanism, four would be the minimum number required).

Based on these results, it has been proposed that at defect sites on the AgBr surface photons caused free elections to be formed, which migrate to the surface and reduce Ag^+ to Ag^0. These Ag^0 atoms aggregate to form Ag_4, and this is a thermodynamically favored species. The presence of Ag_4 then can later serve as a catalyst for further silver ion reduction to silver metal in the photographic developer solution.

Thus, it is again clear that the study of small metal clusters can yield a great deal of useful information.

4. Larger Particles (M_{100}–$M_{1,000,000}$)

In recent years unprecedented progress has been made in synthesis and characterization of comparatively large metal particles, say 2–100 nm in diameter, or M_{100}–$M_{1,000,000}$. Although one million metal atoms sounds like a larger number, it is still small compared to Avogadro's number. This size range is in the nanometer regime where it has been found that numerous physical and chemical properties change and are dependent on the exact size in this range. Optical properties (including color) change with size, as do melting points, magnetic properties, and surface chemistry. For example, gold nanoparticles suspended in solution can be blue, red, or purple depending on the size due to changes in plasmon resonance (a collective phenomenon where the particle generates its own molecular orbitals and, in a sense, behaves like one giant atom). Another interesting point is that a 5-nm gold particle melts 50°C lower than bulk gold.

A unique development here was the synthesis of a class of ligand-stabilized metal clusters by Schmid and coworkers. These represent giant clusters when considered in the light of normal ligand-stabilized clusters, which are covered in Section III. For example, $Au_{55}(PPh_3)_{12}Cl_6$ and $Pd_{561}(Phen)_{36}O_{190-200}$ exemplify better than any others the crossover between molecular metal clusters and metal particles. Thus, they are soluble molecular species.

Although these represent "giants" in molecular clusters, they are small compared to what has been prepared in the nanoscale metal particle area, which will now be discussed.

New preparative methods and better techniques for characterization have allowed considerable progress in this field of endeavor.

One synthetic approach involves the codesposition of metal vapors with vapors of hydrocarbon solvents at liquid nitrogen temperatures (77 K). This approach has been termed the solvated metal atom dispersion (SMAD) method for preparation of ultrafine metal powders. In a typical experiment 1–2g of metal (almost any metal) is vaporized from a high temperature crucible and codeposited over 1–2 hr with 100 g of hydrocarbon in a 3-liter vacuum chamber cooled to liquid nitrogen. Upon warming form 77 K to room temperature, the nanoscale metal particles form by atom aggregation, and the growth process is controlled by choice of solvent, and warmup rate. As the particles grow, atom by atom, they become less mobile, and growth stops as weak solvation completes favorable with slower and slower particle movement. The SMAD method has been used to prepare a wide variety of useful nanomaterials including catalysts, nonaqueous colloids, metal particles in polymers, and bimetallic magnetic and catalytic materials, and synthetic apparatus as been built to allow 100-g quantities to be produced over several hours.

Chemical-reducing agents have also been used to advantage to prepare metal particles through atom-by-atom growth. Metal ions in solution (polar organic solvents or water) can be reduced to metal atoms, which then aggregate to particles. Some metal ions, such as those of gold (Au^{3+}), silver (Ag^{+}), cobalt (Co^{2+}), and nickel (Ni^{2+}) can be reduced by sodium borohydride ($NaBH_4$) resulting in metallic nanoparticles. For metals that are more difficult to reduce, stronger reagents have been used, such as potassium metal or alkyl borohydrides, so that even magnesium, aluminum, titanium, chromium, and other fine, reactive small particles can be produced.

In recent years a most notable advance has been the controlled growth of metal particles in the small pockets of inverse micelles. Micelles are formed in a sea of water when dissolved surfactant molecules aggregate with long hydrocarbon chains together. Inverse micelles are formed in a sea of hydrocarbon (gasoline, kerosene, octane, etc.) where the polar end groups of the surfactant aggregate. Small amounts of water are collected in these regions, and these aqueous pockets can serve as nanometer sized reactor zones. Metal salts can be dissolved in these reactor pockets and chemically reduced to zero-valent metal particles. Indeed, by varying the amount of water and surfactant, the size of these reactor pockets can be controlled and this can be used to roughly control the size of the resultant metal nanoparticles (Fig. 11).

Under certain conditions tubular shaped pockets can be formed and there have been reports of the synthesis of cylindrical shaped metal particles by use of these tubular shapes (vesicles).

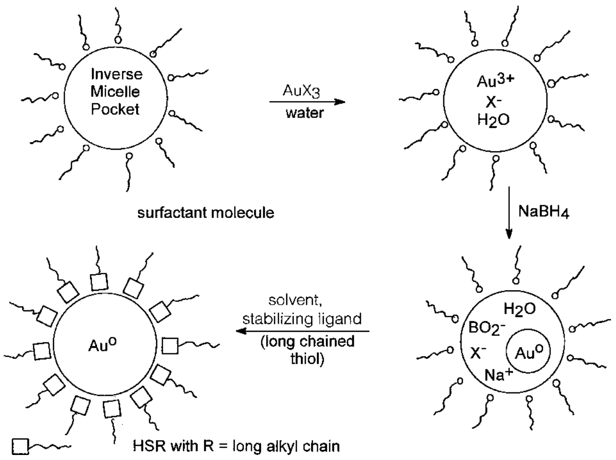

FIGURE 11 Illustration of the synthesis of gold nanocrystals in an inverse micelle pocket.

There is considerable promise in the inverse micelle "nanoreactor" approach since there are many kinds of surfactants available, including cationic, anionic, and neutral molecules (Fig. 12).

Likewise, water content, surfactant concentration, and polarity of organic solvent can be adjusted to yield different sizes and shapes of the nonreactor pockets. However, particle synthesis and growth is a dynamic process, with rapid exchange of micelle contents occurring, and so only a rough control of resultant nanoparticle size and shape can be expected.

Numerous other metal particle growth and entrapment environments have been reported. These include silica-alumina zeolites, bridge polysilesquioxanes, gels, and phosphates.

One of the consequences of being able to prepare metal particles in the nanometer size range, and with very narrow size distribution, is that these particles begin to behave as "super atoms." For example, when 6-nm spherical gold particles were ligand-stabilized by adding a long chained thiol they were found to readily form nanocrystal superlattices. Figure 13 shows electron microscope pictures of ordered arrays of 6-nm gold particles in two and three dimensions. This represents a new type of crystal, and is an ordered assembly of nanocrystals. Such materials are expected to exhibit a range of new properties, and are just now becoming available for detailed studies.

III. METAL CLUSTER COMPOUNDS

A. Importance and Background

Many transition-metal cluster compounds, where the metal particle (cluster) is surrounded and stabilized by

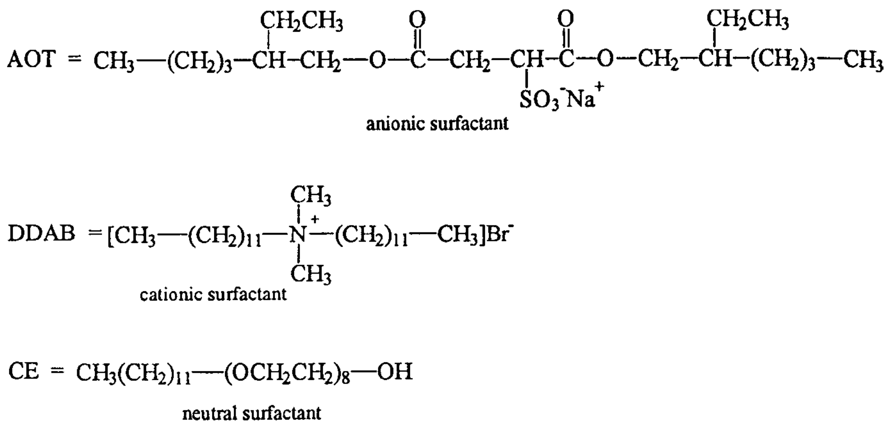

FIGURE 12 Typical surfactants used in preparing inverse micelles.

ligands, have been synthesized and structurally characterized. The symmetries of many cluster compounds of various sizes have been similar to those predicted during the lowest energy growth process from 1 to 13 atoms. Many unusual geometries have been observed in cluster compounds, mostly due to the nature of the stabilizing ligands and formal change of the cluster unit. However, a general trend in geometry is toward that of a polytetrahedral icosahedron.

The connection between small metal particles and metal cluster compounds is that the latter can be structurally characterized and hopefully could serve as good models for small metal particles. However, large cluster compounds where the M_n core is large ($n > 20$) are extremely difficult to synthesize. It has not been possible to synthesize a cluster compound large enough such that it would be stable with or without ligands (e.g., reversible ligand exchange with a support surface).

However, great progress is being made, and metal cluster compounds are in the "spotlight" in the field of chemistry. Recently clusters such as $[Pt_{19}(CO)_{22}]^{4-}$ have been characterized. The $[Pt_{38}(CO)_{44}]$ dimer has been recently mentioned and interestingly exhibits a ccp structure found in bulk Pt.

Even larger clusters, such as $Au_{55}(PPh_3)_{12}Cl_6$ and $Au_{18}Ag_{20}Cl_{14}[P(tolyl)_3]_{12}$ have been reported. Indeed there appears to be an extensive series of silver-gold clusters based on linked icosahedra.

This is an exciting, developing area that holds great theoretical and practical promise. In the discussion that follows the reader will be made familiar with this relatively new area of chemistry.

The scientific community did not realize the importance of cluster compounds for nearly 40 years after their discovery. In the early 1900s tantalum halides of the general formula $[Ta_6X_{12}]^{2+}$ were being prepared. In 1907 the chloride was incorrectly reported as $TaCl_2$. In 1910 the proper formula was reported for the bromine analog. We now know these to contain an octahedron of Ta atoms with extensive metal–metal bonding. However, it was not until the mid-1940s that X-ray crystallography provided direct evidence for such bonding by establishing the presence of an octahedral core of Mo atoms.

Crystallographic techniques are of paramount importance to cluster research. Until the collection of crystallographic data was aided by computerization the field of metal cluster chemistry remained relatively unexplored. While waiting for technology to provide the means for rapid acquisition of structural data, theories of bonding in polyhedra were being developed. Many of these polyhedral bonding theories were developed for boron cluster compounds since these were most familiar. These advances in boron cluster chemistry greatly aided the field of metal cluster chemistry; this will become clear in later sections.

Before proceeding any further we should explicitly define a metal cluster compound. The term cluster should be reserved for those compounds which contain three or more metal atoms and enough metal–metal bonding to constitute a bonded triangle of metal atoms; M_3 triangles are important structural units as they are the basic geometric building block for higher nuclearity clusters. Nature's choice of this simple building block is far from arbitrary, and is it not unique to cluster compounds. Bulk metals, with their close-packed crystal structures, can be viewed as being constructed from triangular building blocks. The dominance of the triangular geometry is due to the fact that it is this geometry which provides the means of maximum electron delocalization between three metal atoms. Since it is the delocalization of electrons between atoms which constitutes a bond, the strongest bonding or structural integrity is achieved when the subunits are of a triangular form. In order to look more closely at the metal–metal bond we will begin our consideration of metal clusters

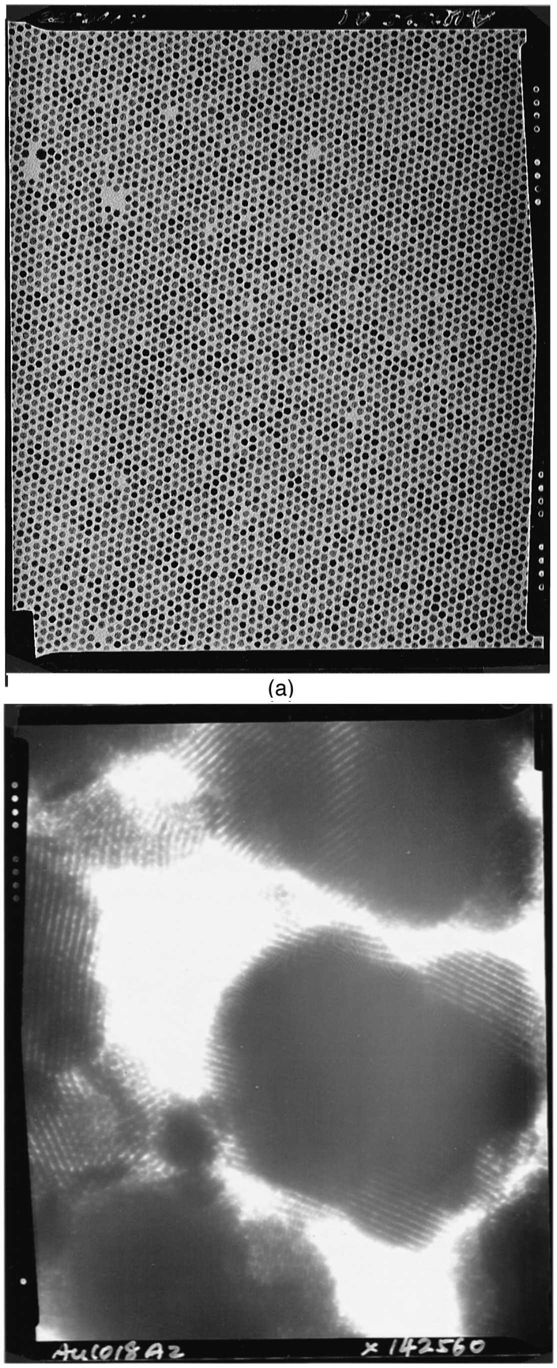

(a)

(b)

FIGURE 13 (a) Two-dimensional array of 6-nm gold nanoparticles ligated with an organic thiol. (b) Three-dimensional array.

with what might be considered their precursors, metal–metal bonded dimers.

B. The Metal–Metal Bond

When two metal atoms are brought together, in principle, one sigma, two pi, and two delta bonds may be formed.

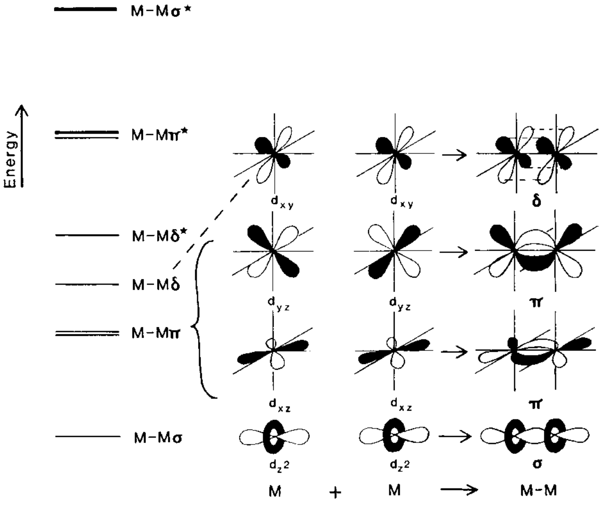

FIGURE 14 *d*-Orbital–*d*-orbital overlap leading to σ, π, and δ bonds and the relative energy ordering of metal–metal bonding and antibonding orbitals.

Figure 14 shows the orbital overlap leading to each type of bond. The antibonding interactions (not pictured) are the out-of-phase combination of those interactions pictured. Consider the approach of two metal atoms and let the internuclear axis be the z axis. The σ bond is the result of the overlap of two d_{z^2} orbitals. The highly directional nature of these orbitals is responsible for a large overlap and therefore a strong bond. A pi bond is formed by the overlap of coplanar d orbitals on adjacent metal atoms. Each metal has an orthogonal pair of d_{xz} and d_{yz} orbitals which participate in this type of bonding thereby allowing for the formation of two orthogonal, degenerate π bonds. A bond between two parallel d orbitals is a δ bond. Within our defined coordinate system the pair of d_{xy} orbitals and the pair of $d_{x^2-y^2}$ orbitals could each form a δ bond. However, in a ligated metal–metal dimer one of these sets of orbitals would be dedicated to the formation of metal–ligand σ bonds, consequently only one δ bond may be formed.

As the degree of orbital overlap decreases from σ to π to δ so does each bond's contribution to the overall metal–metal bond strength decrease. Despite the weakness of the π and particularly the δ bond relative to the sigma bond their presence in a molecule can have a dramatic effect. Several structural aspects of a compound, metal–metal bond distance, for example, provide evidence for multiple bonds. There have been many attempts to correlate the metal–metal bond distance to the order of a metal–metal bond. Generally, the higher the bond order is between two metal atoms the closer the equilibrium distance between these two atoms will be, and these bond distances usually are in the 2.4–3.0 Å range. The shortest metal–metal bond distance ever observed is 1.83 Å. This incredibly

short distance is that for the Cr—Cr quadruple bond in $Li_6[Cr_2(\sigma\text{-}C_6H_4O)_4]Br_2$. From the spectroscopic data of bare Cr—Cr dimers, studied under matrix isolation condition, an even shorter Cr—Cr distance of 1.71 Å has been inferred. This nonligated dimer has a $d^{10}s^2$ electron configuration, hence, a sextuple bond has been postulated. The remarkably short Cr—Cr distance seems congruent with a sextuple bond. The Mo—Mo single bond in $(C_5H_5)(CO)_3$ Mo—Mo$(CO)_3(C_5H_5)$ has a bond distance of 3.21 Å and is the longest distance between two metal atoms which are considered to have a formal metal–metal bond. In general, if two metal atoms which are not bridged by any ligands come within 3.2 Å of each other they may be considered to have a metal–metal bond. The restriction of this generalization to nonbridged metal atoms is important as bridges may have a considerable effect on the metal–metal distance. The specific effect that a bridging ligand will have on a metal–metal bond depends on what ligand is acting as the bridge. Bridging hydride ligands, for example, are generally associated with metal–metal bonds that are longer than similar nonbridged bonds. Carbonyl ligands, on the other hand, have the opposite effect, they tend to shorten the metal–metal bonds they bridge. When comparing bond distances we must be careful to consider what type of ligands are present in the molecules. So that ligand consideration might be diminished it would be advantageous to have a complete series of metal–metal bonded dimers with the same ligands all of which are coordinated in the same fashion. This, however, is not available so bond distances alone do not provide sufficient information for a good correlation to be made between bond length and bond order.

Another structural feature of a metal dimer which may imply the presence of multiple metal–metal bonding is the stereochemical configuration of the molecule. In $[Re_2Cl_8]^{2-}$, the compound for which the first quadruple bond was proposed, the effects of the multiple bond on the stereochemical configuration are clearly seen; $[Re_2Cl_8]^{2-}$ has no bridging chloride ligands. As such, we might expect this compound to adopt a staggered configuration; however, this is not the case. An eclipsed configuration is maintained despite the fact that the short Re—Re bond of 2.24 Å brings the chloride ligands closer together than the sum of their van der Waals radii. This seemingly high energy configuration is necessitated by the presence of a δ bond as it is only in this configuration that a full δ bond will remain intact. A 45° rotation about the Re—Re bond giving the staggered conformation, would result in zero overlap between the two d_{xy}-orbitals and total destruction of the δ bond. The δ bond, however, is quite tolerant to rotation about the metal–metal bond. Even at a 30° rotation, 50% of the δ bond overlap remains. Therefore, quadruply bonded metal dimers may alleviate some steric congestion by a rotation about the metal–metal bond without a serious loss in δ bonding.

One further tool for establishing the presence and order of metal–metal bonds is theoretical analysis. Such analysis has provided results which are consistent with the simple d orbital-d-orbital mixing ideas which lead to the one σ two π, and one δ bond. The energy of the bonding orbitals is inversely proportional to the degree of atomic orbital overlap, the opposite being true for the antibonding orbitals. The energy ordering scheme up through the σ antibonding orbital is shown in Fig. 14. Since metal–metal bonding essentially occurs through the d-orbitals, the d orbital occupancy, or the oxidation state of the metals, necessarily dictates the upper limit of the bond order which may be obtained. Filling the orbitals of the energy diagram clearly shows that the eight electrons of a d^4–d^4 system, such as $[Re_2Cl_8]^{2-}$ can produce a metal–metal quadruple bond. The isoelectronic Mo(II)–Mo(II) compound $[Mo_2Cl_8]^{4-}$ has also been structurally characterized. The Mo—Mo quadruple bond distance of 2.138 Å is about 0.1 Å shorter than that of the Re—Re quadruple bond. With all the ligand environment of the metal being identical in these two compounds the difference in the metal–metal bond length may be wholly attributed to the inherent differences of each metal.

Another type of quadruply bound metal dimer is found in compounds with the general formula $M_2(L_2CR)_4$ where M = Cr, Mo, W and L = O, S, N. One example is $Mo_2(O_2CH)_4$, with a Mo—Mo distance of 2.091(2) Å. In these compounds the metal–metal bond is bridged by four uninegative, bidentate ligands giving a paddlewheel geometry to the compounds (Fig. 15). In such compounds the configurational requirements of the ligands as well as the presence of a δ bond confine these molecules to an eclipsed configuration. As well as restricting the rotation about the metal–metal bond these bidentate ligands can influence the metal–metal bond distance. Variations in the

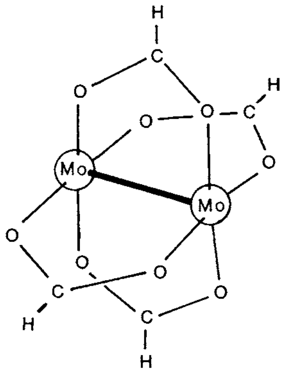

FIGURE 15 Structure of $Mo_2(O_2CH)_4$. Note the paddle-wheel geometry typical of carboxylate-bridged metal dimers.

electronic properties of these ligands can be achieved by changing the heteroatom donor from O to N or S or by changing the R group in the (L_2CR) ligands. The R group can also play an important role sterically. Certainly the hydrogen atom of the (O_2CH) ligand is stereochemically inactive but R groups as large as 2-phenylphenyl have been utilized. In such compounds the steric demands of the ligand should be considered. In $[M_2L_8]^{n-}$ or $[M_2(LL)_4)]$ systems the metal atoms are one ligand shy of being octahedrally coordinated. The vacant coordination sites lie along the z axis opposing the metal–metal bond. Coordination does occur at these sites. The sensitivity of the metal–metal bond distance to this coordination varies from metal to metal. Chromium dimers, which show the greatest tendency to accept axial ligands, are the most sensitive. Some Cr dimers have been observed to increase the Cr—Cr distance by ~42% upon the axial coordination of pyridine.

There are two ways of forming a M—M triple bond. The triple bond electron configuration of $\sigma^2\pi^4$ is provided by a d^3–d^3 system. This situation exists in M_2L_6 compounds when M = Mo, W and L = NR_2, OR, X. One example is $Mo_2(NMe_2)_6$, with a Mo—Mo triple bond distance of 2.21 Å. A triple bond can be obtained from a d^5–d^5 system as well. This involves metal–metal bond order reduction via the population of antibonding orbitals. Triple bonds of this sort have an electron configuration of $\sigma^2\pi^4\delta^2\delta^{*2}$. Completely filling the δ^* orbital annihilates the δ bond. A half-filled δ^* orbital would result in a metal–metal bond with an order of 3.5. Thus, $[Re_2Cl_8]^{2-}$ undergoes one-electron reduction to $[Re_2Cl_8]^{3-}$. The trianion will have the 3.5 bond order electron configuration $\sigma^2\pi^4\delta^2\delta^{*1}$. Reducing the δ bond contribution to the overall bond order to one-half should loosen the grip the δ bond has on the eclipsed configuration. The trianion is electrochemically generated in solution and has a very short lifetime. Therefore, structural studies have not verified this expectation. The metal–metal bond length would also be expected to increase.

A two-electron reduction of $[Re_2Cl_8]^{2-}$ may be carried out chemically by treatment with $P(C_2H_5)_3$. The d^5–d^5 product, $Re_2Cl_4(P(C_2H_5)_3)_4$, has a metal bond electron configuration of $\alpha^2\pi^4\delta^2\delta^{*2}$. δ Bond destruction results in a net bond order of three. However, the expected concomitant isomerization to a staggered conformation does not occur. Staggering the phosphorus atoms places the bulky ethyl groups in closer contact with each other than when the phosphorus atoms are eclipsed, therefore, the complex is less sterically crowded in an eclipsed configuration.

Further bond order reduction can be achieved by continuing to populate the metal–metal antibonding orbitals. For example, $Ru_2(O_2C\text{-}C_3H_7)_4Cl$ with its $\sigma^2\pi^4\delta^2\delta^{*2}\pi^{*1}$ electron configuration has a bond order of 2.5; the corresponding bond length is 2.281 Å. Total population of the π^* orbitals leaves only the σ bond intact. $Rh_2(O_2CCH_3)_4$ with its two d^7 Rh(II) atoms has the single bond electron configuration $\sigma^2\pi^4\delta^2\delta^{*2}\pi^{*4}$. The Rh—Rh single bond distance is 2.386 Å.

All of these examples have been cases in which all of the valence d electrons on each metal atom have paired in either bonding or antibonding orbitals. For zero-valent metal carbonyl dimers only one of the many valence d electrons on each metal is shared; hence, only single bonds are known for these systems. The reason why the earlier transition metals in nonzero valent oxidation states form up to quadruple bonds and the later zero-valent transition metal carbonyls form only single bonds can be understood by considering the electronic needs of these different metal centers.

The coordination about a transition metal and the chemistry of transition metal complexes is often dictated by the electronic needs of the metal center. The stabilization of compounds when the elements present acquire a closed-shell configuration is well known. For a transition metal, with its nine valence orbitals (one s, five d, and three p orbitals), the stabilizing closed-shell configuration is obtained when the electron count about the metal center reaches 18. When a metal center has fewer than 18 electrons in its valence shell it is said to be electronically unsaturated. One step toward alleviating this electronic unsaturation is the formation of metal–metal bonds. Because of their covalent nature, metal–metal single bonds are considered to add one electron to the valence shell of each metal atom. The electron donation from one metal atom to the other mirrors the bond order so a quadruple bond increases the valence count of each metal by four electrons.

Consider the carbonyl complexes of Fe, Co, and Ni. Iron, a d^8 metal, requires ten more electrons to reach the eighteen required for stabilization. The coordination of five CO ligands, each of which donates two electrons, would satisfy this electronic requirement. Nickel, a d^{10} metal, requires four CO ligands to become electronically saturated. In fact, $Fe(CO)_5$ and $Ni(CO)_4$ are stable forms of these metal carbonyls. A problem arises, however, with the intermediate d^9 cobalt. There is no way in which a mononuclear, 18-electron binary metal carbonyl can be formed from a d^9 metal; $Co(CO)_4$ and $Co(CO)_5$ would be 17- and 19-electron complexes, respectively. Given that a metal–metal single bond supplies one additional electron to each metal center an 18-electron cobalt carbonyl can be formed via the dimerzation of two 17-electron $Co(CO)_4$ units. Thus, $Co_2(CO)_8$ is a stable 18-electron complex with a single Co—Co bond. This is a d^9—d^9 system in which only one electron on each cobalt atom was used for metal–metal bonding unlike the earlier transition-metal dimers in higher oxidation states in which all valence d-electrons are used for metal–metal bonding. The earlier transition

metals, which form multiply bonded dimers, have fewer *d* electrons than the later transition metals. When the early transition metals are in a high oxidation state, as in the dimers, they find themselves quite short of achieving the 18-electron, closed-shell configuration. The formation of multiple metal–metal bonds is required to electronically saturate each metal center. It is for this reason that when two such metals come together all valence electrons are used for metal–metal bonding.

C. Bonding in Metal Clusters: The 18-Electron Rule

When used to analyze metal clusters, the 18-electron rule finds its greatest success when applied to metal carbonyl clusters. The rule does, however, hold for some nonzero-valent clusters as well. Take, for example, $[Re_3Cl_{12}]^{3-}$ (Fig. 16) in which the Re—Re bond distance of 2.46 Å is indicative of strong metal–metal bonding. This distance is between the length of the Re—Re quadruple bond in $[Re_2Cl_8]^{2-}$(2.24 Å) and the length of the Re—Re single bond in $Re_2(CO)_{10}$ (3.04 Å). Assigning a Re—Re double bond in the Re trimer is not only consistent with the observed bond lengths but also satisfies the 18-electron rule at each metal center. This can be taken as further support or evidence for Re—Re double bonds.

The stability of the $M_3(CO)_{12}$ clusters (M=Fe,Ru,Os) is easily explained by the 18-electron rule. The M_3 cluster frame is held together by metal–metal single bonds. Each d^8 metal atom needs ten more electrons to satisfy the 18-electron rule. Two metal–metal single bonds to each metal atom supply two of the needed ten electrons. Four CO ligands per metal atom is sufficient to electronically saturate each metal center. In the Ru and Os clusters the four carbonyls per metal atom are all terminally bound. In the Fe cluster one Fe—Fe bond is bridged by two carbonyl ligands. As such, this Fe—Fe bond is shorter than the other two and the Fe_3 triangle is best described as isosceles whereas the Os and Ru cluster have equilateral cores (Fig. 17). The tendency for carbonyls to bridge 3*d*–4*d* metal bonds more than 4*d*–4*d* and 5*d*–5*d* metal bonds is a general phenomenon. In fact no μ_2- or μ_3-carbonyls have been observed bridging a 5*d*–5*d* metal bond.

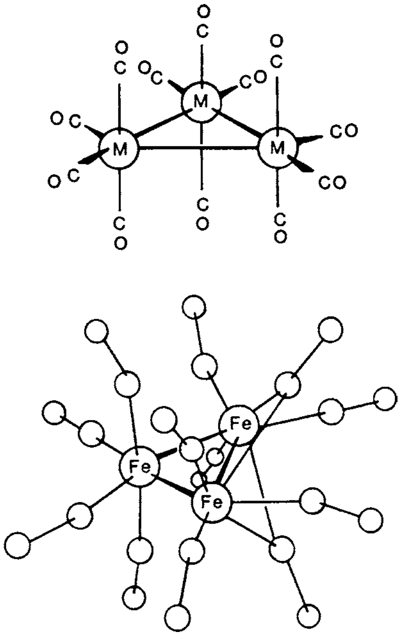

FIGURE 17 Structure of $M_3(CO)_{12}$(M=Fe, RU, Os). One Fe—Fe bond is bridged by two carbonyl ligands whereas the Ru and Os clusters have only terminal carbonyls.

$Fe_5C(CO)_{15}$ is a particularly interesting cluster, whose stability may also be rationalized by the 18-electron rule. The Fe_5 skeleton forms a square-based pyramid (Fig. 18). Each iron atom has three terminally bound CO ligands and the carbide resides 0.08 Å below the base of the pyramid. The apical iron atom with four single metal–metal bonds and three carbonyls, satisfies the 18-electron rule. The basal iron atoms with only three metal–metal single bonds, would only acquire 17 valence electrons if it were not for the presence of the carbide. If the carbon donates one of its four valence electrons to each basal iron atom they become electronically saturated.

For mononuclear transition metal complexes the adherence to the 18-electron rule is extraordinary. The widespread applicability speaks well for the concept. The adherence to the 18-electron rule by cluster compounds

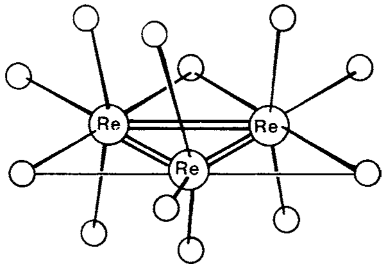

FIGURE 16 Structure of $[Re_3Cl_{12}]^{3-}$, formally containing Re—Re double bonds.

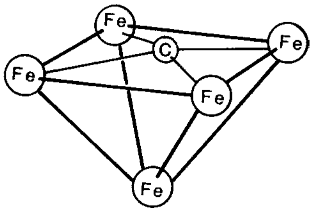

FIGURE 18 Structure of $Fe_5C(CO)_{15}$. The carbide slightly protrudes out of the square-based pyramid core. (Terminal carbonyls are not shown for clarity.)

has also been demonstrated. There are, however, many clusters that defy rationalization from within the 18-electron rule constructs. The mononuclear cases for which the 18-electron rule works so well represents the limit of metal dispersion. The other extreme is bulk metal for which the 18-electron rule has no significance. As a cluster increases in nuclearity the nature of the metal core becomes more like bulk metal. In general, the usefulness of the 18-electron rule decreases with the increasing nuclearity of clusters.

It became necessary to develop new approaches for predicting electron closed-shell structures, and ideas came from Williams, Wade, Mingos, and Rudolph, which now make up the polyhedral skeletal electron pair theory (PSEPT). The bonding in clusters can sometimes be described in terms of edge-localized, two-center two-electron bonds. Thus, through the formation of element-element bonds, the atoms of a polyhedron can acquire an effective inert gas configuration (8 valence electrons for a main group element and 18 for a transition metal atom).

In addition to the valence electrons that a metal atom can donate, it is important to know how many electrons attached ligands generally donate. Typical one-electron donors are H, CH_3, C_6H_5, and SiR_3; two-electron donors: CO, CS, CNR, CR_2, SO_2; three-electron donors: PR_2, SR, OR, NO, Br, I, P; four-electron donors: PR, S, O; and five-electron donors: Cl, Br, I, OR (face bridging such as μ_3 or μ_4).

Interstitial atoms can be very versatile electron donors. For example, B is a three-electron donor; C, Si, Ge are four-electron donors; and P, As, Bi, Sb are five-electron donors. Even nine-electron donors (Rh, Co), ten (Pt, Pd), and eleven (Au, Ag) have been observed in cluster structure.

Other similar approaches to understanding electron filling have been developed by Lauher and Wade.

Lauher's approach to analyzing cluster compounds is to determine how many valence electrons a cluster with a given nuclearity and geometry can accommodate. This method, like the 18-electron rule, seeks to electronically saturate a metal center, but instead of this metal center being an isolated metal atom it is the entire cluster core. By carrying out extended Hückel calculations on bare metal cluster the number of electrons the cluster can accommodate is determined. Thus, the bonding capabilities of that cluster are also known. (For example, how many two-electron-donating CO ligands can the cluster accept.)

The molecular orbital calculations provide the orbital energy levels of the cluster and typically an energy gap of about 1 eV separates a group of low-lying energy levels from a group of high-lying levels. The division occurs near the energy of the atomic p orbitals of the isolated metal atom. Those molecular orbitals whose energies lie above the atomic p level are classified as high-lying antibonding orbitals (HLAOs) and those with an energy below the atomic p level are classified as cluster valence molecular orbitals (CVMOs). The HLAOs are assumed to lie too high in energy to be used for metal–metal or cluster–ligand bonding, whereas the energy levels of the CVMOs are suitable for these functions. The number of CVMOs dictates how many electrons a metal skeleton can accept and therefore the bonding capabilities of a particular cluster.

A linear combination of n atomic orbitals will always generate n molecular orbitals. Therefore, an M_3 cluster with nine atomic orbitals per metal will have 27 molecular orbitals. The calculation for an equilateral triangle shows that three of these 27 are high enough in energy to be classified as HLAOs, leaving 24 CVMOs. With orbital occupancy being limited to two electrons, 48 electrons are required to electronically saturate an M_3 equilateral triangle cluster. In fact, 48 electrons is the number of valence electrons found in a host of three-metal clusters. $Fe_3(CO)_{12}$ and $Co_3(C_5H_5)_3(CO)_3$, for example, both have 48 valence electrons.

There are several reasonable geometries that the metal atoms of a four-atom cluster may adopt. The number of CVMOs for a four-atom cluster depends on which geometry the metal skeleton possesses. A tetrahedron, derived from a metal atom capping the face of an equilateral triangle precursor, is the closest packed arrangement. It is, therefore, not surprising that the tetrahedron is the most frequently observed arrangement of four-atom clusters. Extended Hückel calculations indicate that a tetrahedral core of metal atoms generates 30 CVMOs. $M_4(CO)_{12}$ (M = Co, Rh, Ir) and $Ni_4(CO)_6(PR_3)_4$ are clusters with a tetrahedral core of metal atoms and are all electronically saturated with 60 cluster valence electrons. Note the structures of the Co and Ir clusters (Fig. 19). The cobalt cluster has three bridging carbonyls whereas the 5d Ir cluster has only terminally bound CO.

When a tetrahedron is distorted by lengthening one of its edges the symmetry is lowered to C_{2v}. This skeletal change is accompanied by an increase in the number of CVMOs from 30 to 31. The metal core of $[Fe_4(CO)_{13}H]^-$, described as having a butterfly structure, has this C_2 symmetry (Fig. 20). In this compound one CO ligand acts as a four-electron donor thereby bringing the number of cluster valence electrons to 62, exactly the number needed to electronically saturate the Fe_4 core. If 62 electrons were placed into the orbitals of a tetrahedral core of metal atoms one HLAO would be filled. If this HLAO were a metal–metal antibonding orbital the cleavage or lengthening of a metal–metal bond would be expected. This is totally consistent with the preceding discussion.

The addition of a fifth skeletal atom which caps the face of a tetrahedron creates a cluster with a trigonal bipyramid

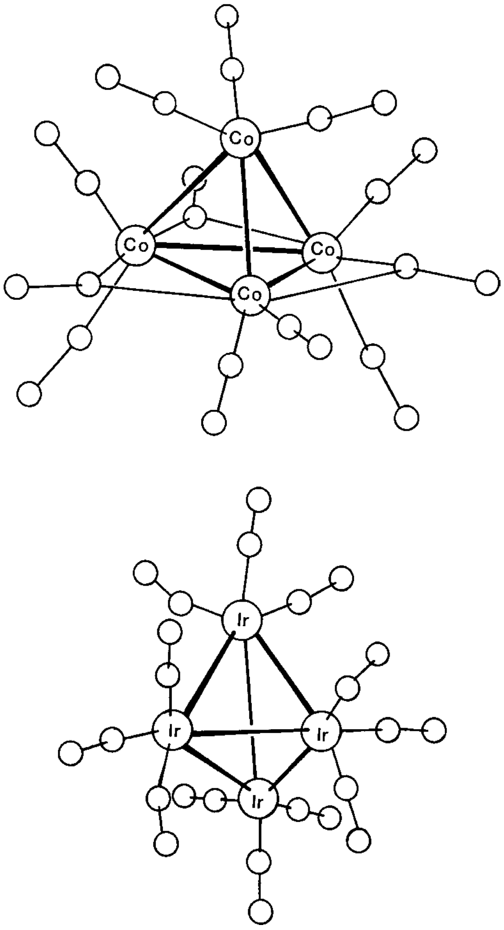

FIGURE 19 Structure of $M_4(CO)_{12}$, where M = Co, Ir. Both clusters have a tetrahedral core of metal atoms. The Co cluster has three bridging carbonyls. The Ir cluster, a third row transition metal cluster, has only terminal carbonyls.

geometry and 36 CVMOs. One compound exhibiting this geometry is $Os_5(CO)_{16}$. The five d^8 Os atoms and 16 two-electron-donating carbonyls provide the 72 electrons needed to electronically saturate the trigonal bipyramid metal core. As is expected for a third-row transition-metal cluster, all of the carbonyl ligands are terminally bound. The Os to CO ratio of 5:16 precludes an even distribution of the sixteen carbonyl ligands. Four of the five Os atoms have three terminally bound carbonyls. The four remaining carbonyls are bound to the fifth Os atom. This unique Os atom is positioned in an equatorial site of the trigonal bipyramid. Because of the asymmetrical placement of the CO ligands about the cluster there is a core distortion from a pure trigonal bipyramid geometry.

Three possible geometries for a cluster containing six metal atoms are the octahedron, the capped square pyramid, and the bicapped tetrahedron which possess 43, 43, and 42 CVMOs, respectively. The 86 cluster valence electrons of $Co_6(CO)_{16}$ suggest the bicapped tetrahedron would be an unstable cluster configuration since this would place two electrons in an HLAO. The observed octahedral geometry with its 43 CVMOs can accommodate the 86 cluster valence electrons.

It is interesting to consider $Os_6(CO)_{18}$ and $Os_6(CO)_{18}H_2$. Emperically these compounds appear very similar yet structurally they differ significantly (Fig. 21). The two additional valence electrons of the dihydride can account for this structural difference. The osmium core of $Os_6(CO)_{18}$ defines a bicapped tetrahedron; therefore, 42 CVMOs are available and filled by the 84 cluster valence electrons. The two additional electrons of the dihydride $Os_6(CO)_{18}H_2$ would occupy an HLAO unless a structural change in the Os_6 skeleton occurs. Rearrangement to a capped square pyramid increases the CVMO count by one to a net 43 which is sufficient to accept all 86 cluster valence electrons.

Lauher's method is one in which the nuclearity and structural geometry of a cluster core is assumed and the binding capabilities or the number of electrons which that cluster can accommodate is determined. A somewhat opposite but complimentary approach to cluster bonding has been taken by K. Wade. In Wade's model a cluster's structure is determined or rationalized by the number of electrons present.

One shortcoming of the 18-electron rule when applied to clusters is its dependence on a two-electron-two-center bond model. Recalling the nature of electrons in bulk metal (extensive delocalization through a band structure)

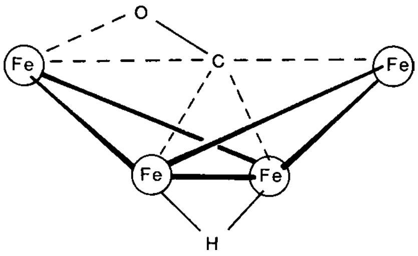

FIGURE 20 Structure of $[Fe_4(CO)_{13}H]^-$. The Fe core has a butterfly arrangement with one CO metal between the wings. (Terminal carbonyls are not shown.)

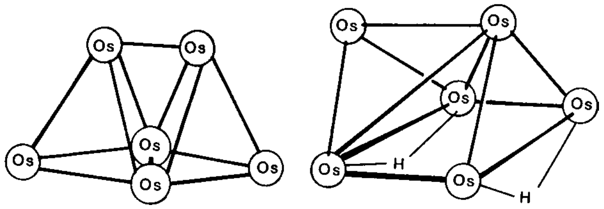

FIGURE 21 Structure of $Os_6(CO)_{18}H_2$. Osmium atoms define a bicapped tetrahedron. (Terminal carbonyls are not shown.)

a multicenter bonding model would seem much more appropriate for cluster compounds. The polyhedral skeletal electron pair (PSEP) theory developed by Wade is one such model. This bonding model was developed to explain boron cluster compounds but has been successfully extended to transition-metal cluster compounds. Perhaps the PSEP theory would best be understood by first seeing how it applies to the borane systems for which is was developed, keeping in mind the method also works for metal cluster compounds.

Borane clusters are divided into four categorise depending on the structure they adopt. The relationship between polyhedra in each class are shown in Fig. 22. Clusters with the general formula $B_nH_n^{2-}$ and the isoelectronic carboranes ($C_2B_{n-2}H_n$, for example) are called closo compounds due to the closed-cage type structure of the cluster skeleton. Each B—H unit has four valence electrons. Of these four electrons two are needed for a B—H bond leaving two electrons which are available for the bonding needs of the cluster skeleton. A cluster with this general formula will therefore have $n + 1$ electron pairs for cluster bonding (one pair from each BH unit and one pair from the overall charge on the complex). In general, compounds with $n + 1$ electron pairs are found to have closo geometries.

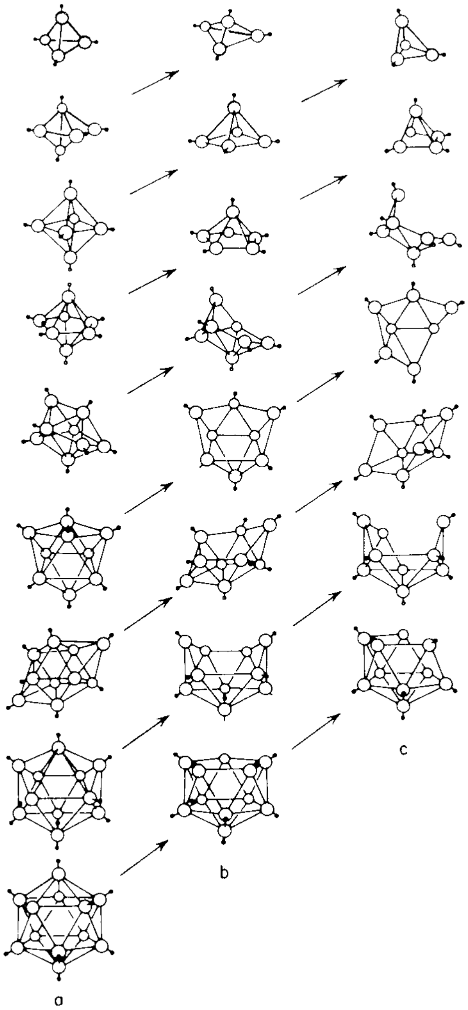

FIGURE 22 Closo (a), nido (b), and arachno (c) cluster cores are shown in the vertical columns. The diagonal lines show how they are related by the removal of vertices. [After Rudolph, R. W., and Pretzer, W. R. (1972). *Inorg. Chem.* **11,** 1974. Copyright 1972 American Chemical Society.]

A second type of borane clusters are those with the general formula B_nH_{n+4}. These are classified as nido boranes. Isoelectronic carboranes of the general formula $C_xB_{n-x}H_{n+4-x}$ are produced by replacing a BH unit with a C. Nido refers to the nest-like structure of these compounds. Such a structure is obtained by the removal of one vertex from a closo structure (Fig. 22). Compounds of the general formula, B_nH_{n+4} will have n electron pairs (one from each BH unit) plus four electrons or two pairs from the four additional hydrogen atoms. The total of $n + 2$ electron pairs will be used for skeletal bonding. Generally, any cluster compound with $n + 2$ skeletal electron pairs will adopt a nido structure.

The arachno class of cluster compounds, with a weblike configuration, are those boranes with the general formula of B_nH_{n+6}. Their structural relationship to closo boranes is that of having two vertices missing from a closo configuration (Fig. 22). The n skeletal electron pairs from the n(BH) units are augmented by three more pairs from the additional hydrogens. In general, clusters with $n + 3$ skeletal electron pairs will be found to have an arachno configuration.

Clusters which are three vertices shy of having a closo configuration are classified as hypo clusters. The general formula for these boranes is B_nH_{n+8}, and, therefore, $n + 4$ skeletal electron pairs result in a hypo or netlike configuration.

To understand why this empirical method developed for borane clusters may be successfully applied to transition metal clusters requires that we look at the orbitals that the boron vertex atoms utilize for cluster bonding and how these orbitals are related to the orbitals a metal atom would use for cluster bonding. This is an isolobal comparison or analogy. The isolobal notion compares the orbital likeness between two molecular fragments. If a comparison reveals that two molecular fragments have similar orbitals—similar with respect to the number, symmetry, energy ordering, and directionality—then one fragment may be a suitable substitute for the other within a compound. The boron vertex orbitals and the similar orbitals of a metallic molecular fragment are shown in Fig. 23.

The linear arrangement of the H—B cluster core suggests sp hybridization of the boron center. The two

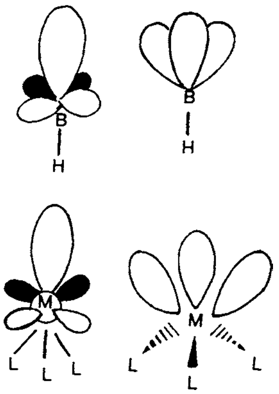

FIGURE 23 Isolobal relationship between B—H and ML_3 fragments. Two alternative ways of viewing the hybridization are shown. The B—H group may be considered to be *sp* hybridized in which case a metal $d_{z^2} p_z$ hybrid mimics the radially oriented *sp* orbital on boron. The sp^3 hybridization of a B—H group may be mimicked by the orbital lobes of an ML_3 unit which are directed to three facial octahedral sites.

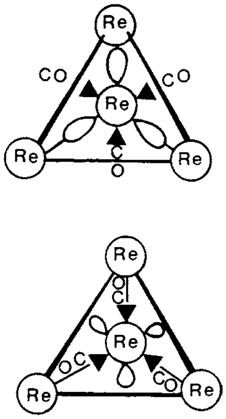

FIGURE 24 Structures of $Re_4(CO)_{12}H_4$ and $[Re_4(CO)_{12}H_6]^{2-}$. The carbonyls of $Re_4(CO)_{12}H_4$ are staggered with respect to the tetrahedral edges. The carbonyls of $[Re_4(CO)_{12}H_6]$ eclipse the tetrahedral edges.

p-orbitals which remain unhybridized are oriented tangentially to the cluster. The *sp* hybrid points inward to the cluster core and can participate in significant bonding interactions as shown below for an octahedral cluster. The unhybridized *p*-orbitals are oriented such that they may contribute to surface bonding. These "surface" orbitals allow for interactions between adjacent cluster vertices as well as contributing to cluster–ligand interactions. The orbitals of a metal fragment can easily mimic those of the *sp* hybridized boron. A $d_{z^2} p_z$ hybrid of a metal can play the role of the radially oriented *sp* hybrid while $d_{xz} p_x$ and $d_{yz} p_y$ hybrids play the role of the tangentially oriented *p* orbitals.

The *sp* hybridization is just one of many ways to look at the bonding in the borane polyhedra. Alternatively, an sp^3 hybridization may be considered. The B—H bond utilizes one of the four orbitals in sp^3 hybridization leaving three orbitals to participate in cluster bonding. The orbitals a metal could use to imitate the sp^3 hybrid are easily conceptualized. Imagine an octahedral ML_6 species being stripped of three facial ligands and the resulting ML_3 unit being incorporated into a cluster. The orbitals directed toward the three vacant coordination sites are those orbitals which are similar to the sp^3 orbitals and can be used for cluster bonding (Fig. 23). One advantage of considering an $M(CO)_3$ molecular fragment to be isolobal with an sp^3 hybridized boron vertex is realized when attempting to rationalize the observed stereochemical configuration of some metal carbonyl clusters. The sp^3 type vertex orbitals may be oriented along the edges of the triangular units of a cluster. This orbital orientation, which suggests two-electron–two-center bonds, results in the carbonyl ligands of the $M(CO)_3$ unit being staggered with respect to the polyhedral edges. $Re_4(CO)_{12}H_4$ is one compound in which such carbonyl orientation is observed (Fig. 24). Alternatively, the sp^3-like vertex orbitals may be rotated 60° thereby directing the orbital lobes over the triangular faces of the polyhedron. This orientation, which suggests three center bonding interactions over the tetrahedral faces, causes the carbonyl to eclipse the polyhedral edges. This configuration is seen in $[Re_4(CO)_{12}H_6]^{2-}$ (Fig. 24).

In order to predict or rationalize a geometry of a metal cluster by the PSEP theory, the number of cluster valence electrons must be determined. The electron donation from a metallic molecular fragment [$M(CO)_3$, for example] is determined as follows. Assume all nine valence orbitals are used. Through the isolobal analogy three of these nine orbitals of the metal are used for cluster bonding. This leaves six orbitals to serve in metal–ligand bonding or nonbonding (lone pair) capacities. These six orbitals will accommodate 12 electrons. Therefore, the electron donation to a cluster from a metallic molecular fragment is the total valence electron count at the metal center less 12 electrons. For example, $Fe(CO)_3$ has a 14-electron count at the iron center [d^8Fe + three (2-electron) donors]. Of these 14 electrons 12 are allocated to the Fe—CO bonds and nonbonding or lone pair orbitals which leaves two electrons to be supplied to the cluster. Likewise, the molecular fragment $Co(C_5H_5)$ contains 14 electrons at the metal center (d^9Co + 5 electron donor), which makes this a two-electron donor to a cluster. These two metallic molecular fragments each donate two electrons as do (BH) and (CH^+) units. Therefore, it is not surprising that these isolobal fragments are interchangeable giving rise to a large family of cluster compounds known as metalloboranes and metallocarboranes.

Metalloboranes or metallocarboranes are compounds in which one or more vertices of a parent borane/carborane

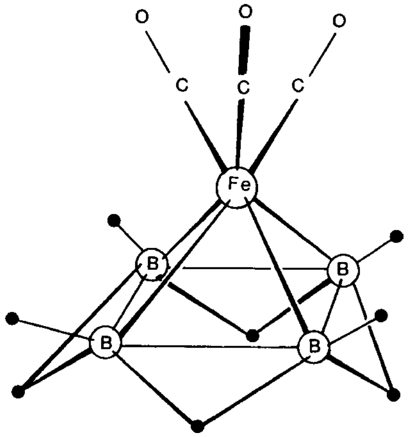

FIGURE 25 Structure of $B_4H_8Fe(CO)_3$. The metalloborane derived from the isolobal replacement of B—H by $Fe(CO)_3$.

is replaced with a transition metal molecular fragment. For example, the reaction of *nido*-B_5H_9 with $Fe(CO)_5$ proceeds with the loss of a BH vertex and the incorporation of the isolobal transition metal fragment $Fe(CO)_3$ to give *nido*-$B_4H_8Fe(CO)_3$ (Fig. 25).

Reaction of the *closo*-1,5-$C_2B_3H_5$ carborane with either $Fe(CO)_5$ or $(C_5H_5)Co(CO)_2$ results in cage expansion to the closo structure depicted in Fig. 26. Further reaction of $Fe(CO)_3C_2B_3H_5$ with $Fe(CO)_5$ produces the pentagonal bipyramidal metallocarborane $(Fe(CO)_3)_2$ $C_2B_3H_5$. Consecutive replacement of (BH) or (CH) vertices with ML_x units will ultimately lead to metal cluster compounds. The structure of many metal cluster compounds can be understood by using the PSEP theory as the following few examples will demonstrate.

$Rh_6(CO)_{16}$ is an octahedral cluster with six $Rh(CO)_2$ vertices and four triply bridging carbonyls. Being a closo, six-vertex cluster the PSEP theory would predict this cluster to contain seven skeletal electron pairs. Each $Rh(CO)_2$ vertex contributes one electron to the cluster core and each (μ_3-CO) contributes two electrons. The total skeletal electron count being 14 or 7 pairs as the theory would predict.

There are numerous metal cluster-alkyne complexes which have the C≡C unit of the alkyne positioned such that it occupies two vertices of a regular polyhedron (Fig. 27). For example, there are many octahedral clusters with an M_4C_2 core. There is a significant distortion from pure octahedral symmetry due to the differing M—M, M—C, and C—C bond distance which define the edges of the octahedron. The PSEP theory successfully describes these clusters as well. Within the PSEP theory constructs the C—R vertices are considered to be three electron donors. Of carbon's four valence electrons one is used in a covalent C—R bond, the remaining three are donated to the cluster. Therefore, we can see why $Co_4(CO)_{10}C_2Et_2$ has such a core. The four $Co(CO)_2$ vertices each donate 1 skeletal electron ($d^9Co + 2e^-/CO - 12 = 1$). The two ($\mu_2 - CO$), as always, donate two electrons and each C—Et vertex donates three electrons. The total electron count is seven or $(n + 1)$ skeletal pairs. Remember the PSEP theory states that $(n + 1)$ skeletal electron pairs will result in a closo structure which for a six-vertex cluster can be the octahedron.

When the atoms of a ligand occupy a cluster vertex they tend to be low coordinate vertices. This is not evident in M_4C_2 clusters as all vertices of an octahedron are of equal coordination. It is clear in trigonal bipyramidal M_3C_2 cluster cores. The apexes are three coordinate and the three

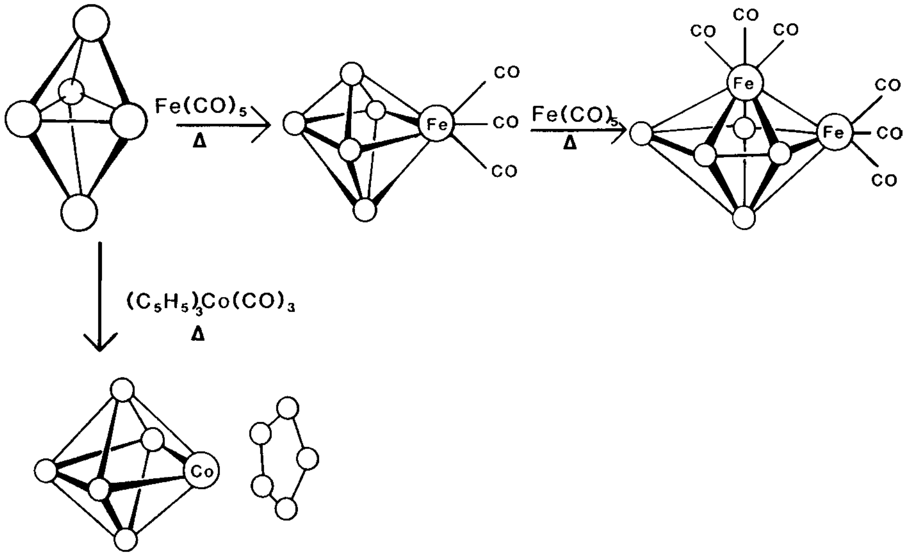

FIGURE 26 Production of metallocarboranes $Fe(CO)_3C_2B_3H_5$, $(Fe(CO)_3)_2C_2B_3H_5$, and $Co(C_5H_5)C_2B_3H_5$.

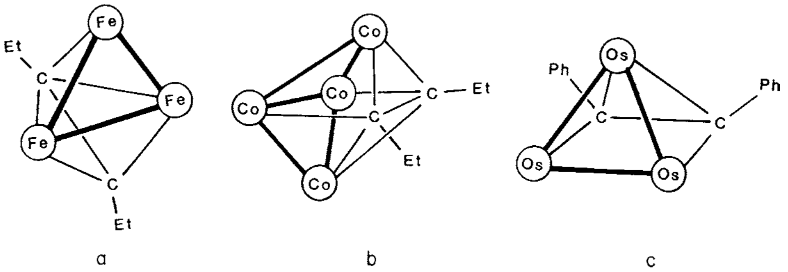

FIGURE 27 Polyhedra cluster cores may be defined by both metal and ligand atoms. The M_3C_2 trigonal bipyramid in (a) $Fe_3(CO)_9C_2Et_2$, the M_4C_2 octahedron in (b) $Co_4(CO)_{10}C_2Et_2$, and the M_3C_2 square based pyramid of (c) $Os_3(CO)_{10}C_2Ph_2$ are depicted here.

equatorial vertices are four coordinate. Six skeletal electron pairs would be necessary to give this five-vertex, closo geometry. Consider $Fe_3(CO)_9C_2Et_2$, one axial (low-coordinate) site is occupied by a carbon atom rather than the alternative of having both carbon atoms occupying the four coordinate equatorial sites.

When an M_3C_2 unit constitutes the five vertices of a cluster with seven skeletal bond pairs a nido structure should be observed. This situation is observed in $Os_3(CO)_{10}C_2Ph_2$. The Os_3C_2 core forms a squared-based pyramid which has the high coordinate apex occupied by an Os atom, again demonstrating the aversion carbon has to high-coordinate vertices.

Alkynes in metal cluster compounds are perhaps more commonly considered to be a four-electron-donating entity rather than two separate three-electron donors. This difference being due to the fact that the PSEP theory is based on a delocalized bonding model whereas the four-electron-donating models are based upon two-electron–two-center bonding schemes. In the four-electron-donating models the four π electrons in C≡C are reassigned to M—C σ and π bonds, one of each type originating from each carbon. A single C—C remains keeping the "alkyne" unit intact.

D. Ligands

The discussion of ligands in metal cluster compounds has so far been quite limited. It is the goal of this section to elucidate some of the specifics of metal–ligand bonding in cluster compounds. Ligands serve many important functions in cluster compounds, and their importance must not be overlooked. First, it is the ligand field which is responsible for stabilizing a bare cluster or particle. As demonstrated earlier, metal clusters require an electron count which is greater than the metals can themselves provide. The ligands, by supplying these electrons, stabilize the cluster. Second, the variation and manipulation of ligands provide an interesting chemistry through which we can learn more about metal clusters. These reactions also fuel the hopes that we may realize practical applications for these compounds.

There are numerous ligands known to stabilize clusters, and many of these ligands are capable of coordinating to the cluster in a variety of ways. To specify the manner in which a ligand is bound, the qualifiers μ_x and η^x are used. When a ligand is bound to more than one metal atom the symbol μ_x identifies the number of metal atoms x to which the ligand is bound. For example, a ligand which bridges the edge of a polyhedron is interacting with two metal atoms and is designated as μ_2 (a nonsubscripted μ implies μ_2). A ligand that caps the triangular face of a polyhedron would be designed as μ_3. The symbol η^x is used to indicate how many atoms of a ligand are coordinated to the metal center. In $[Fe_4\text{-}(CO)_{13}H]^-$, for example, one CO interacts with all four Fe atoms using both C and O (Fig. 20). The formula is more explicitly expressed as $[Fe_4(\mu_4, \eta^2\text{-}CO)(CO)_{12}(\mu_2\text{-}H)]^-$. The ($\mu_2$-H) indicates that the hydride bridges two Fe atoms. When the cyclopentadienyl ligand is designated as (η^5-C_5H_5) this indicates that all five carbon atoms of the aromatic ring are interacting with the metal center.

Species that are suited particularly well for cluster bonding are unsaturated molecules or molecular fragments. By virtue of their unsaturation these ligands have an abundance of electron density which can be made available to the cluster. In addition to their electron-donating ability many unsaturated ligands impart further stabilization by accepting electron density back from the metal center. This synergistic or cooperative bonding interaction is known as backbonding. Alkenes, alkynes, nitrosyl, and carbonyl ligands are among those ligands capable of participating in this type of bonding. We will use the metal–carbonyl bond to outline the principles of this bonding.

Carbon monoxide can bind to a metal center in a variety of ways. When only the carbon atom of CO is interacting with a metal center it is acting as a two-electron donor regardless of the number of metals to which it is bound. That is, terminal doubly bridging (μ_2) and triply bridging (μ_3) carbonyls all donate two electrons. The donation occurs

from the highest occupied molecular orbital which calculations confirm to be primarily a carbon lone pair orbital.

The sigma donation of a carbon lone pair should have little effect upon the strong C—O bond. The fact that significant changes in the C—O bond do occur upon coordination to a metal center suggest that some other bonding interaction is involved. This additional bonding interaction is the π-backbonding briefly mentioned earlier. π-Backbonding involves a π-type overlap of occupied metal d orbitals with the vacant π^* orbitals of CO. The metal to ligand donation populates an orbital which is antibonding between carbon and oxygen, the results being a reduction of the C—O bond order. The reduction in C—O bond order is experimentally observed as a longer C—O bond distance and a reduced C—O stretching frequency. Free CO has a C—O bond distance of 1.128 Å and a ν_{CO} of 2143 cm^{-1}. The effects of coordination become apparent upon bonding to just one metal atom (i.e., terminal CO). The typical C—O bond distance increases to about 1.15 Å in metal carbonyls and typical stretching frequencies are in the range of 1800–2150 cm^{-1}.

Doubly bridging or μ_2-carbonyls participate in very similar bonding, that is a sigma donation of the lone pair on carbon to vacant metal orbitals as well as d–π^* backbonding from the metal to CO. The symmetry-allowed interactions are depicted in Fig. 28 which depicts the sigma donation of the carbon lone pair. Figure 28b–e show backbonding interactions. In Fig. 28c–e only the CO_{π^*} lobes located on carbon are shown interacting with the metal atoms. Figure 28b and c show the same interaction from different perspectives. Carbon monoxide contains two degenerate, orthogonal π^* bonds. The $M_\pi \rightarrow CO_{\pi^*}$ and the $M_\delta \rightarrow CO_{\pi^*}$ donation involve the same π^* orbital on CO. Although they are symmetry allowed the interactions are very weak due to poor overlap and energy match. The strongest $M_d \rightarrow CO_{\pi^*}$ donation involves the other CO π^* orbital and an M—M antibonding orbital. Donation from a metal–metal antibonding orbital should strengthen the M—M bond. Recall M—M bonds are generally shortened when bridged by CO. Note that there are now two metal atoms supplying electron density into the CO π^* orbital; hence, an increased effect on the CO bond is observed. The CO stretching frequencies for μ_2-carbonyls typically occur between 1700–1850 cm^{-1}.

For triply bridging (μ_3) carbonyls the same situation exists, a sigma donation by the carbon lone pair (Fig. 29a) and d–π^* backbonding occurs. Again, only the CO lobes located on carbon are shown interacting with the M_3 triangle. As is apparent by the C—O stretching frequencies for μ_3-carbonyls (as low as 1625 cm^{-1}) the amount of d–π^* backbonding is even greater than it is for μ_2-carbonyls. Upon progressing from an M_2 to an M_3 species the number of electrons available for $d \rightarrow \pi^*$ backbonding increases. This additional electron supply certainly contributes to the increase in backbonding which occurs. More importantly, however, there are now significant interactions involving both of the orthogonal, π^* orbitals. It is the increase in π^* orbital involvement to which the further reduction in ν_{CO} may be attributed.

All of the bonding modes for CO thus far described are ones which result in a two-electron donation of the carbon lone pair. Additional sources of available electron density include the C—O π bond and the oxygen lone

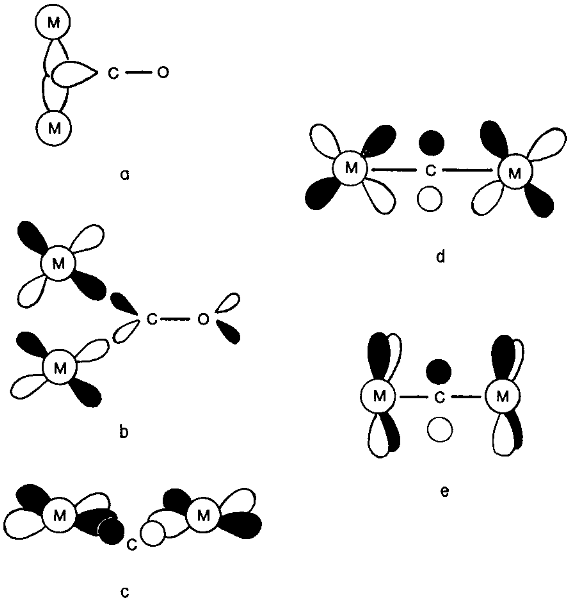

FIGURE 28 M_2–CO orbital interactions. (a) Sigma donation of carbon lone pair, (b) and (c) backbonding interaction of $M_{\pi^*} \rightarrow CO_{\pi^*}$ donation, (d) $M_\pi \rightarrow CO_{\pi^*}$, and (e) $M_\delta \rightarrow CO_{\pi^*}$.

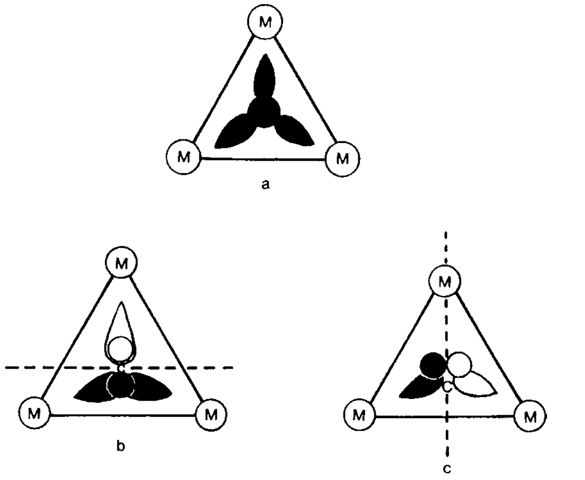

FIGURE 29 M_3–CO orbital interactions. (a) Sigma donation of carbon lone pair, (b) and (c) degenerate M_3 interactions backbonding to orthogonal CO_{π^*} orbitals.

pair. Utilizing either of these electron sources brings the net electron donation of the CO ligand to four. This type of bonding should be indicated with a μ^2 bonding descriptor.

A (η_2, μ^2-CO) is observed in $Mn_2(CO)_5$-(Ph_2PCH_2 $PPh_2)_2$. The CO stretching frequency of 1645 cm^{-1} responds to the removal of π-bond density as well as π^* orbital population. The asymmetric attachment of CO reduces the overlap responsible for backbonding from the Mn atom receiving the carbon lone pair sigma donation. However, the side-on bonding of CO to the other Mn atom offers another means by which backbonding can occur. Figure 30 shows this side-on bonding of CO. This same type of interaction is also responsible for the side-on bonding of olefins to metal centers.

Another example of a four-electron-donating carbonyl is found in $[Fe_4(\mu_4, \eta^2\text{-CO})(CO)_{12}H]^-$ (Fig. 20). The (μ_4, η^2-CO) sits inside the wings of the Fe_4 butterfly. The elongation of the C—O bond to 1.26 Å is indicative of the electronic demands that the cluster has placed on this CO ligand.

The high degree of unsaturation in the cyclopentadienyl ligand makes this an effective cluster ligand. This aromatic ligand can donate six electrons to a cluster core which allows cluster stabilization to be achieved with relatively few ligands. The cluster compounds that best demonstrate this are $Ni_6(\eta^5\text{-}C_5H_5)_6$ and its cation $[Ni_6(\eta^5\text{-}C_5H_5)]_6^+$ (Fig. 31). These were the first homoleptic metal cluster–cyclopentadienyl compounds discovered.

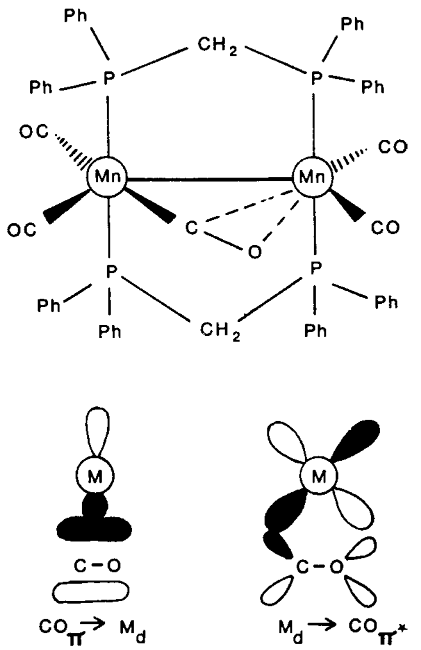

FIGURE 30 Structure of $Mn_2(CO)_5(Ph_2PCH_2PPh_2)_2$. Asymmetric bridging of one CO allows side-on bonding to one Mn. The Dewar–Chatt–Duncanson model of olefin bonding to metal centers is applicable.

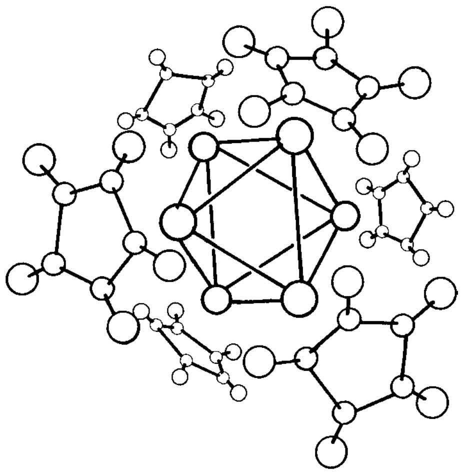

FIGURE 31 Structure of $[Ni_6(C_5H_5)_6]^+$. This cluster and the parent neutral cluster are the first cluster compounds to contain only the (C_5H_5) ligand. One symmetrical (C_5H_5) ligand is associated with each vertex of the Ni_6 octahedron.

In these clusters it is not the electron count which determines the cluster core geometry but the steric demands of the ligand field. The neutral and cationic clusters have electron counts of 90 and 89, respectively. From these electron counts a trigonal prismatic core is expected; however, an octahedral core is observed. An octahedral core can only accommodate 86 electrons before HLAOs begin to be filled. The lowest lying HLAOs are a set of triply degenerate orbitals. $[Ni_6(\eta^5\text{-}C_5H_5)_6]^+$ with its three extra electrons would half fill this triply degenerate level. Placing the four extra electrons of the neutral $Ni_6(\eta^5\text{-}C_5H_5)_6$ into a triply degenerate level results in an electronic configuration which is subject to a Jahn–Teller distortion. This could account for the observed distortion from octahedral symmetry in the neutral cluster whereas the cation is not distorted. It has been suggested that the steric crowding between cyclopentadienyl ligands, which would occur with a trigonal prismatic geometry, prevents this structure from being energetically favorable despite the fact that HLAOs are occupied when the cluster adopts the octahedral geometry.

$Ni_6(\eta^5\text{-}C_5H_5)_6$), prepared by the reduction of the mononuclear sandwich compound nickelocene, is unusual in that it contains no hydride lignands whereas other metal cluster–cyclopentadienyl compounds prepared in similar manners do. $[Co_4(\eta^5\text{-}C_5H_5)_4(\mu_3\text{-}H)_4]$ and $[Rh_3(\eta^5\text{-}C_5H_5)_4\text{-}(\mu_3\text{-}H)]$ are examples. The cobalt cluster consists of a tetrahedron of Co atoms each of which has one (η^5-C_5H_5) ligand associated with it. The four hydride ligands cap each face of the Co tetrahedron. The Rh_3 cluster is unusual in that it contains a (μ_3, η^5-C_5H_5) ligand, typically the (η^5-C_5H_5) ligand is bound to just one metal atom. Here the Rh_3 triangle is capped by a cyclopentadienyl ligand.

This causes the ring centroids of the other three (η^5-C_5H_5) ligands, each associated with a cluster vertex, to be bent out of the Rh_3 plane. These three (η^5-C_5H_5) ligands are bent toward the face of the Rh_3 triangle which is capped by the smaller hydride ligand.

From a practical point of view the cyclopentadienyl ligand may be important for several reasons. Clusters can be stabilized with relatively few ligands and these ligands may be capable of changing their mode of coordination. The change in coordination is accompanied by change in the electron donation made to the metal center. In mononuclear–cyclopentadienyl chemistry the conversion of (η^5-C_5H_5) $\rightarrow$ (η^3-C_5H_5) is important in catalytic reactions; perhaps conversions of this sort will prove to be important in cluster–cyclopentadienyl chemistry as well. From an aesthetic point of view the symmetry inherent to the (η^5-C_5H_5) ligand in consort with the symmetry of a cluster core makes these compounds particularly attractive.

The importance of ligand unsaturation such that there is an abundance of electrons available to a metal center has been demonstrated. The extreme of unsaturation is the bare atom, and bare atoms constitute an important class of cluster ligands. Bare atoms that have been observed as cluster ligands include: from Group I—H; from Group IV—C, Si, Ge, and Sn; from Group V—N, P, As, and Sb; from Group VI—O, S, and Se and all of the Group VIII halogens except At.

Two types of bare atom ligands are observed: interstitially bound and surface bound. When interstitially bound or encapsulated by a cluster framework, all of the valence electrons of that atom are donated to the cluster. As an atom's ability to accommodate lone pairs of electrons increases (i.e., electronegativity increases) there is an increased tendency to adopt surface over interstitial coordination. This is best demonstrated by the halogens for which there are no known examples of interstitial coordination.

Hydride ligands are typically introduced to a cluster by the protonation of an anionic precursor as in the following reactions:

$$[Co_6(CO)_{15}]^{2-} \underset{-H^+}{\overset{+H^+}{\rightleftarrows}} [HCo_6(CO)_{15}]^-$$

$$[Ru_6(CO)_{18}]^{2-} \underset{-H^-}{\overset{+H^+}{\rightleftarrows}} [HRu_6(CO)_{18}]^-$$

$$[Re_3(CO)_{12}]^{3-} \underset{-H^+}{\overset{+H^+}{\rightleftarrows}} [HRe_3(CO)_{12}]^{2-}$$

$$\underset{-H^+}{\overset{+H^+}{\rightleftarrows}} [H_2Re_3(CO)_{12}]^-$$

$$[Os_3(CO)_{12} \underset{-H^+}{\overset{+H^+}{\rightleftarrows}} [HOs_3(CO)_{12}]^+$$

Hydrides are known to coordinate both as interstitial and surface ligands. As a surface ligand, a hydride may be terminally bound or it may bridge two or three metals. As in boron cluster compounds the hydride ligands preferentially select the more highly coordinated (μ_3-H) position, participating in multicenter bonding rather than the terminal hydride position. In fact, terminal hydrides are quite rare. Of the two hydrides in $H_2Os_3(CO)_{11}$ one is terminally bound while the other is a bridging μ_2-H. The Os atom with the terminal hydride is also one of the bridged atoms. Removal of one CO to produce $H_2Os_3(CO)_{10}$ causes the terminal hydride to adopt a bridging mode. Both hydrides now bridge the same Os—Os bond. In order to remain electronically saturated this doubly bridged Os—Os bond must have a bond order of two. As in organic chemistry this double bond is a seat of reactivity. Many new triosmium clusters may be derived from this reactive cluster.

As an interstitial ligand the highest coordination number of a hydride observed to date is six. This situation exists in $[(\mu_6\text{-H})Nb_6I_{11}]$, the first compound in which the existence of an interstitial hydride was established. The hydride occupies the octahedral cavity created by the Nb_6 core. Alternatively, an interstitial hydride may occupy a tetrahedral cavity as is the case in $[(\mu_4\text{-H})Os_{10}(\mu_6\text{-C})(CO)_{24}]^-$ (Fig. 32). The arrangement of Os atoms in this cluster is such that both an octahedral cavity and tetrahedral cavities exist. Four tetrahedral cavities are created by four $Os(CO)_3$ units capping four faces on an octahedral Os_6 core. The hydride cannot occupy the central octahedral cavity as it is already occupied by a carbon atom or carbido ligand which brings us to Group IV atomic donors.

All of the Group IV elements, except lead, have been observed as atomic donor ligands. For Sn, Ge, and Si there

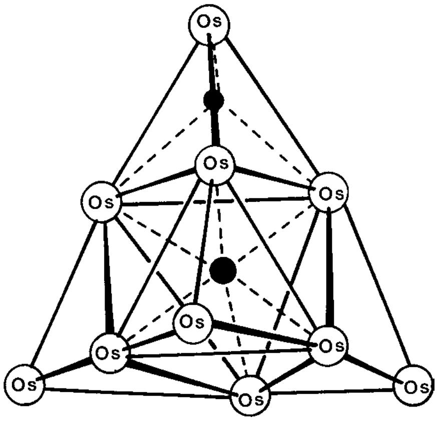

FIGURE 32 Structure of $[(\mu_4\text{-H})Os_{10}(\mu_6\text{-C})(CO)_{24}]^-$. An interstitial hydride occupies one of four tetrahedral cavities while the central octahedral cavity is occupied by a carbide. (Terminal CO are not shown.)

are relatively few examples known. Note in the examples, shown below, that they are each μ_4-donors thereby retaining their typical tetrahedral coordination. They are all acting as surface μ_3-donors to an M_3 triangle while being capped by a fourth metal. The distance between this fourth metal atom and the M_3 base precludes metal–metal bonding so these atomic donor ligands would rightly be considered surface type donors rather than interstitials. This designation is not merely one of semantics since the susceptibility of a ligand to attack is markedly greater for a surface ligand than it is for an interstitial ligand.

Carbido ligands on the other hand commonly participate in interstitial bonding. The highest coordination number for a carbido ligand observed to date is eight. In $[Co_8(\mu_8\text{-}C)(CO)_{18}]^{2-}$ the central carbide occupies the cavity of a tetragonal antiprism (Fig. 33). This unusual geometry for a cluster core certainly derives some of its stability from the presence of the μ_8-C. To set the organic chemist at ease, carbon atoms with coordination numbers greater than four have been referred to as inorganic carbon.

Interstitially bound atoms seem to impart stabilization to unusual cluster core geometries. The previously mentioned square antiprism is one example while the trigonal prism is another. In $[Rh_6(\mu_6\text{-}C)(CO)_{15}]^{2-}$ the carbide occupies the trigonal prismatic cavity created by the Rh core. Clusters of two trigonal prisms which have their square face in common are capable of holding two carbon atoms in the cluster cavity. This situation occurs in the bimetallic cluster $[Co_6Ni_3(\mu_6\text{-}C)_2(CO)_{16}]^{2-}$ (Fig. 34). Viewing the two interstitial carbon atoms as independent carbide ligands rather than a C_2 species in which there is C—C interaction is supported by both electronic and structural considerations. Primarily, the cluster core geometry is such that 116 cluster valence electrons are needed for stabilization. This can only be accomplished if all eight of the valence electrons available from the two carbon atoms are donated to the cluster. This would preclude direct C—C interaction. However, the short C—C distance of 1.49 Å might be taken as evidence for C—C interaction. This short distance is the result of steric demands imposed by the cluster core. The centroids of the trigonal prismatic cavities are separated by the same distance of 1.49 Å.

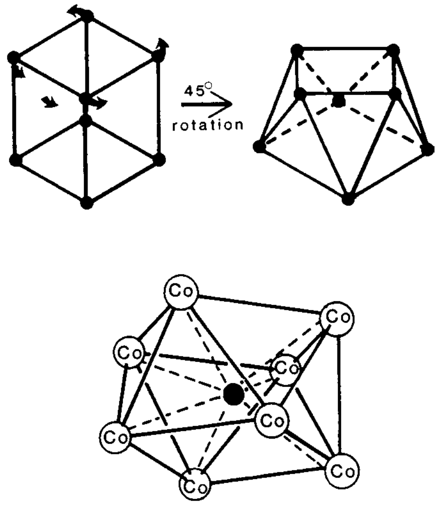

FIGURE 33 Structure of $[Co_8(\mu_8\text{-}C)(CO)_{18}]^{2-}$. The Co atoms of this cluster define a square antiprism, the center of which is occupied by a carbon atom. The relation between a cube and a square antiprism is also shown.

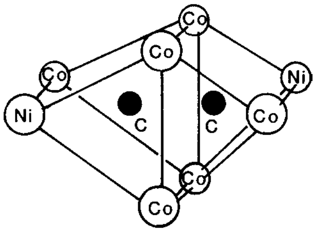

FIGURE 34 Structure of $[Co_6Ni_2(\mu_6\text{-}C)_2(CO)_{16}]^{2-}$. Two Co_5Ni trigonal prisms share a common Co_4 square face. Each trigonal prism encapsulates one carbon atom. (Terminal CO are not shown.)

Direct C—C interaction between two interstitial carbon atoms occurs in $[Rh_{12}C_2(CO)_{25}]$. The complex Rh_{12} core can be described as two fused polyhedra whose cavity centers are separated by a distance greater than the observed C—C distance. This suggests a bonding interaction exists between these two carbon atoms.

A more common role for an interstitial carbide is the occupancy of an octahedral cavity, as in $[Fe_6(\mu_6\text{-}C)(CO)_{16}]^{2-}$. Although interstitial carbides stabilize clusters by supplying electrons, it is difficult to imagine their active participation in reaction chemistry since the cluster framework isolates the carbide. Before their utility can be realized the cluster core must open so as to expose the carbide. Consider, for example, the removal of one Fe vertex from $[Fe_6(\mu_6C)\text{-}(CO)_{16}]^{2-}$ to yield $[Fe_5(\mu_5\text{-}C)(CO)_{15}]^{2-}$ which has a square based pyramid structure (Fig. 18). The carbido ligand protrudes slightly out of the Fe_5 nest (toward the vertex missing from the octahedron) and the transition from interstitial to surface-bound carbides may be considered to begin with this type of carbide exposure. Further exposure and surface character of a carbido ligand is observed in the arachno structure of $[HFe_4(\mu_4\text{-}C)(CO)_{12}]^-$. This carbido ligand sits between the wings of the iron butterfly cluster. The exposure is sufficient to allow direct attack to occur at the μ_4-C.

Moving to Group V many similarities to Group IV are seen, particularly between nitrido and carbido clusters. The following isoelectronic complexes make this clear: $[Fe_6(\mu_6\text{-}C)(CO)_{15}]^{2-}$ and $[Ru_6(\mu_6\text{-}N)(CO)_{15}]^{2-}$ both find the atomic donor ligand occupying the cavity of an

octahedral core. The square-based pyramid $[Fe_5(\mu_5\text{-}C)(CO)_{15}]$ has a Group V counterpart in $[HFe_5(\mu_5\text{-}N)(CO)_{14}]$. The butterfly geometry of $[HFe_4(\mu_4\text{-}C)(CO)_{12}]^-$ is observed in the nitrido cluster $[Os_4(\mu_4\text{-}N)(CO)_{12}]^-$.

There are also differences to be noted upon changing from Group IV to Group V atomic donor ligands. The heavier Group V atoms (P, As, Sb) do occupy interstitial bonding sites whereas carbon is the only Group IV atom to do so. In addition, the tendency to occupy surface sites increases as demonstrated by $[(\mu_3\text{-}As)Co_3(CO)_9]$ and $[(\mu_3\text{-}As)_2Fe_3(CO)_9]$. The arsenic atoms cap the M_3 triangles giving overall tetrahedral and trigonal bipyramid geometries, respectively. When bonded in this fashion As is acting as a three-electron donor leaving two electrons to reside on As as a lone pair.

In order for an atomic donor ligand to be interstitially bound, the cluster core cavity must be large enough to accommodate the donor. Since P, As, and Sb are significantly larger than N they are not found within octahedral cavities since this does not provide enough space. Closo structures which do host the larger Group V atomic donors include the bicapped square antiprism of $[Rh_{10}(\mu_8\text{-}L)(CO)_{22}]^{3-}$ (L=P, As) and the icosahedron as observed in $[Rh_{12}(\mu_{12}\text{-}Sb)(CO)_{27}]^{3-}$. To further illustrate the necessity for a large cavity, compare the structure of $[Co_6(CO)_{16}]$ with that of $[Co_6(\mu_6\text{-}P)(CO)_{16}]^-$. Note the non-closo structure of the anionic phosphide cluster (Fig. 35) whereas the core of the similar $[Co_6(CO)_{16}]$ possesses pure octahedral symmetry. There is no way a phosphide ligand can occupy the cavity of a Co_6 octahedron; nor is a Co_6 trigonal prism capable of encapsulating a P atom. The only alternative is to open the cluster core exposing the phosphide. Realizing the anionic phosphide cluster carries with it six more electrons than $Co_6(CO)_{16}$, Lauher's or Wade's approach may be taken to rationalize the cage opening.

A further increase in the preference for surface bonding relative to interstitial bonding is observed on moving to Group VI.

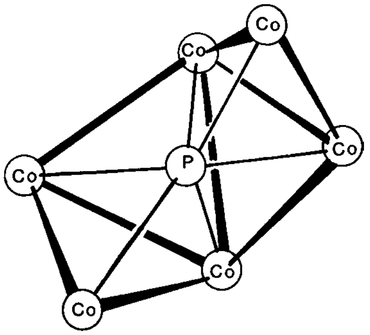

FIGURE 35 Structure of $Co_6(\mu_6\text{-}P)(CO)_{16}$. The open structure of the Co_6 core is necessary to accommodate a μ_6-P. (Terminal CO are not shown.)

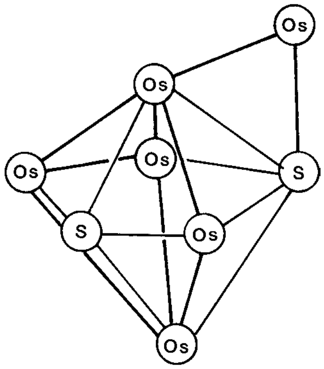

FIGURE 36 Structure of $Os_6(\mu_4\text{-}S)_2(CO)_{17}$. A pentagonal bipyramid core is defined by an Os_5S_2 unit. The sulfido ligands occupy nonadjacent equatorial sites. One $Os(CO)_4$ group bridges an OS_{axial}—$OS_{equatorial}$ bond.

The two μ_4-sulfido ligands present in $[Os_6(\mu_4\text{-}S)_2(CO)_{17}]$ are exposed surface-like atoms as is clearly depicted in Fig. 36 the two μ_4-sulfido ligands occupy the two equatorial nonadjacent vertices of a pentagonal bipyramid. The five remaining vertices of the cluster core are occupied by Os atoms. This leaves one Os atom unaccounted for. An $Os(CO)_4$ unit bridges an axial to equatorial Os—Os bond.

As μ_2 and μ_3 surface ligands, oxygen and sulfur both serve as four-electron donors, $[W_3\text{-}(\mu_2\text{-}S)_3(\mu_3\text{-}S)F_9 \cdot 3H_2O]$ and $[Mo_3(\mu_2\text{-}S)_3(\mu_3\text{-}S)\text{-}(C_5H_5)_3]$ being two cases in point. In both of these compounds each edge of the M_3 triangle is bridged by a sulfur atom, and one face of the triangle is capped by a μ_3-S. Selenium also can supply four electrons as a μ_3-surface ligand as in $[Co_3(\mu_3\text{-}Se)(CO)_9]$. Although it is more common to observe a Group VI donor as a surface ligand, interstitially bound examples are known. $[Rh_{17}(\mu_9\text{-}S)_2(CO)_{32}]^{3-}$ and $[Rh_{10}(\mu_8\text{-}S)(CO)_{22}]^{2-}$ which have interstitially bound sulfido ligands again demonstrate the need for large cluster cavities to accommodate the larger atomic donor ligands (Fig. 37). In each of these clusters the geometry of the Rh atoms that are nearest neighbors to the sulfido ligand is a square antiprism.

While discussing Group VI ligands, Fe–sulfide clusters of extreme biological significance should be mentioned. In nature Fe–S clusters are found in proteins and enzymes. Nitrogenases, for example, are Mo dependent Fe–S enzymes that catalytically participate in the six-electron reduction of elemental nitrogen to ammonia, a more biologically useful form of nitrogen. Nitrogenases promote many other reductive processes including the reduction of acetylene to ethylene. The active site in these enzymes are thought to be Fe–S cores or Mo–Fe–S cores. In the laboratory many cluster compounds have been synthesized to act as models of these enzymes.

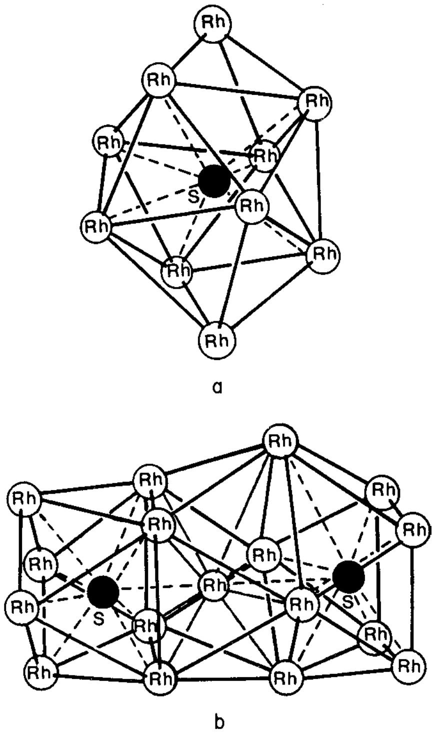

FIGURE 37 Structure of (a) $[Rh_{10}(\mu_8\text{-}S)(CO)_{22}]^{2-}$ and (b) $[Rh_{17}(\mu_9\text{-}S)_2(CO)_{32}]^{3-}$. The Rh_{10} cluster is a bicapped square antiprism. A sulfido ligand occupies the square antiprism cavity. The Rh_{17} cluster contains three square antiprisms. The cavity of the center one is occupied by an Rh atom. The two outer square antiprisms each encapsulate a one sulfur atom. (Terminal CO are not shown.)

One such model recently synthesized is $[Fe_8S_6I_8]^{3-}$ (Fig. 38). This cluster is unique in that the Fe_8 core forms an almost perfect cube. The six faces of the cube are capped by (μ_4-S) ligands and each Fe vertex has one terminal iodide ligand. Although the Fe—Fe distances of 2.71–2.73 Å in this cluster supports the presence of metal–metal bonding many of the naturally occurring Fe–S proteins, and many synthesized model complexes do not possess extensive metal-metal bonding. The lack of M—M bonding in these clusters may be due to the low Fe:S ratios. The abundance of sulfide ligands makes these clusters electron rich. Perhaps population of M—M antibonding orbitals is the result.

Our brief look at atomic donor ligands will conclude with the halogens. The reluctance of a halogen to share all seven of its valence electrons with a cluster is made evident by the rarity of cluster compounds which contain an interstitially bound halogen. As a surface ligand halogens may be terminally bound to a metal atom, in which case it is serving as a one-electron donor, or they may act as three-electron donors by adopting a bridging mode of coordination. Both μ_2- and μ_3-bridges are common.

This group of atomic donor ligands is unique in that they stabilize a host of binary cluster compounds. In fact, the first compounds recognized to have a cluster framework were octahedral metal chlorides. Two common forms of octahedral metal halide clusters exist (Fig. 39). One type is seen in $[(Ta_6(\mu_2\text{-}Cl)_{12}))Cl_6]^{4-}$ where all twelve edges of the tantalum octahedron are bridged by chlorine atoms. The other six chlorine atoms are terminally bound, one to each Ta vertex, and may be removed to produce the dication $[Ta_6(Cl_{12})]^{2+}$. $[(Mo_6(\mu_3\text{-}Cl)_8)Cl_6]^{2-}$ exhibits the second common structural form where all eight faces of the octahedron are capped by triply bridging chlorides. The six-terminal chlorides in this cluster may also be removed.

A precursor of the prevalent $[(M_6(\mu_3\text{-}X_8)X_6]^{2-}$ core is seen in $[(Mo_5(\mu_3\text{-}Cl)_4(\mu_2\text{-}Cl)_4Cl_5]^{2-}$. This is related to $[(Mo_6(\mu_3\text{-}Cl)_8)Cl_6]^{2-}$ by the removal of a Mo–Cl vertex (this is a conceptual relationship and not one achieved chemically). The nido Mo_5 cluster contains four (μ_2-Cl) ligands which would be μ_3-chlorides if the sixth vertex of the octahedron were in place.

The bulk of binary metal–halide clusters involve the early transition metals, however, later transition metal–halide clusters are known. $[Pt_6(\mu_2\text{-}Cl)_{12}]$ is one example.

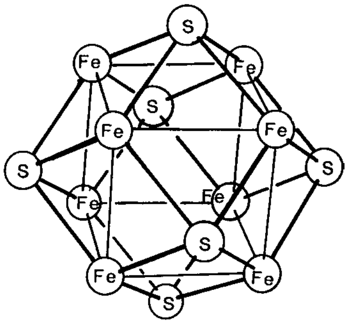

FIGURE 38 Structure of $Fe_8S_6I_8$. Each square face of the Fe_8 cube is capped by a sulfur atom. (One terminal I per Fe is not shown.)

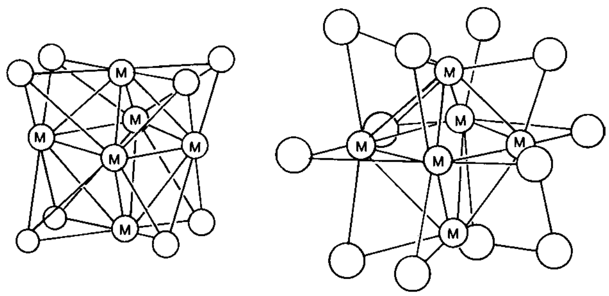

a b

FIGURE 39 Two common cores for octahedral metal halide clusters of the general formulas (a) $[M_6X_{12}]^{2+}$ and (b) $[M_6X_8]^{4+}$.

A distortion from pure cotahedral symmetry creates two types of Pt—Pt bonds. Note must be taken of these long Pt—Pt "bond" distances which average 3.32 and 3.40 Å. This suggests *very* weak Pt—Pt interaction meaning the bridging chloride ligands contribute significantly to the structural integrity of this cluster.

The lack of late transition-metal halide clusters and the poor bonding which results when they are formed can be easily rationalized. In binary metal halide clusters the metal atoms are in a high oxidation state. The valence orbital contraction in these high oxidation state metals is much greater for the later transition metals than it is for the early ones. The diminished radical extension of the valence shell inhibits metal–metal bonding.

E. Cluster Compound Reaction Chemistry

In this last section we will discuss some of the reaction chemistry which has been observed with cluster compounds. Volumes could be written on this aspect of metal clusters alone. We will simply discuss the cluster–surface analogy as well as demonstrate the variety of reactions in which cluster compounds may participate. In doing so the complexity and difficulties of cluster chemistry will surely become apparent.

Because the nuclearity and geometry of clusters are so dependent on electron count, gross structural changes often occur during the course of a reaction.

The susceptibility of metal clusters to change their nuclearity is shown in the following reactions:

$$Co_4(CO)_{12} \xrightarrow{100^\circ C} Co_6(CO)_{16}$$

$$Ru_4(CO)_{12} \xrightarrow{100^\circ C} Ru_6(CO)_{16}$$

$$Ru_3(CO)_{12} \xrightarrow{180^\circ C} Ru_6(\mu\text{-C})(CO)_{16}$$

$$Os_3(CO)_{12} \xrightarrow{210^\circ C} Os_6(CO)_{18} + Os_8(CO)_{23} + Os_7(CO)_{21} + Os_5(CO)_{16}$$

$$Os_3(CO)_{12} + Os_5(CO)_{15}C \xrightarrow{250^\circ C} \text{(products of the 210°C pyrolysis)} + Os_8(CO)_{21}$$

Two extremes of metal-mediated reactions are those that occur on bulk metal sufaces versus those that occur in mononuclear metal complexes. Each extreme has its advantages as well as disadvantages. Consider, for example, the properties of activity and selectivity, two properties that are usually inversely related. The metal surface extreme possesses high activity at the expense of poor selectivity. The high activity on a surface can be attributed to the cooperative nature of the extended array of metal atoms. An electronic cooperation occurs through the band structure present in bulk metals. The high density of active sites on a metal surface provides another type of cooperation. The bond activation of surface-adsorbed species is facilitated by the close proximity of active sites. Metal clusters have, to a lesser extent, this cooperative influence on cluster ligands. The high selectivity and low activity associated with mononuclear complexes is due to the presence of only one active site, whereas surfaces (and clusters) provide a multitude of these active sites. The active sites on a metal surface are often considered to be located at surface defects. By definition, a surface atom has a low coordination number. The atoms defining the boundary of a surface defect will have an even lower coordination number. The coordination number of the metal atoms in a small metal cluster is generally low. In this aspect small metal clusters are more like surface defect sites. Large clusters, however, may serve as models for the extended surfaces of bulk metal. $[Rh_{13}(CO)_{24}\text{-}H_3]^{2-}$, for example, contains an Rh_{13} core with a hexagonal close-packed arrangement while $[Rh_{14}(CO)_{25}]^{4-}$ exhibits a body-centered ccp of Rh atoms.

$Os_3(CO)_{12}$ is a molecule in which three active sites have been brought together. The effect of this on the selectivity of its reactions is clearly seen. Consider the reaction of $Os_3(CO)_{12}$ with triphenylophosphine where the three sites in this one molecule promote intramolecular reactions. Three of the *nine* reaction products are the simple substitution products $Os_3(CO)_{12-x}(PPh_3)_x$ ($x = 1, 2, 3$). The remaining six oxidative addition products have an assortment of ligands which are quite varied, a few are noted below.

$HOs_3(CO)_9(PPh)_3)(PPh_2C_6H_4)$ (Fig. 40) is produced when an ortho positioned C—H bond in the disubstituted precursor, $Os_3(CO)_{10}(PPh_3)_2$, oxidatively adds to a core osmium atom. This intramolecular reaction utilizes two adjacent Os sites and creates a five-member Os–P–C–C–Os ring. The hydride bridges these same two Os atoms.

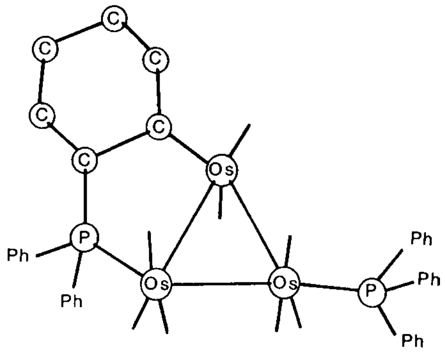

FIGURE 40 Structure of $HOs_3(CO)_9(PPh_3)(PPh_2C_6H_4)$. The five-member chelate ring formed from the oxidative addition of CH to the Os_3 core is shown.

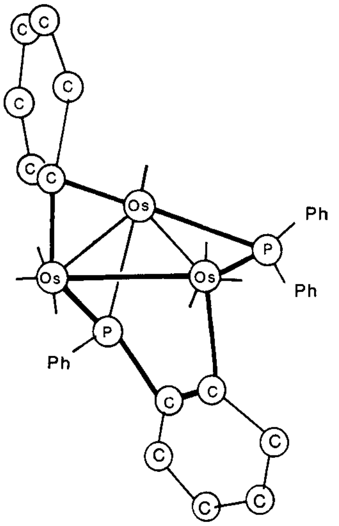

FIGURE 41 Structure of $Os_3(CO)_8(PPh_2)Ph(PPhC_6H_4)$. Note the μ_3 bonding of the $(PPhC_6H_4)$ ligand and the two-electron, three-center bond interaction with the C_6H_5 ligand.

In the production of $Os_3(CO)_8(PPh_2)$-(Ph)$(PPhC_6H_4)$ (Fig. 41) all three Os atoms become involved. All three edges of the Os_3 core are bridged in this product. Note the presence of the $(PPhC_6H_4)$ ligand. It is very similar to the $(PPh_2C_6H_4)$ ligand of the previously mentioned cluster. It is similar in that an ortho CH bond in a C_6H_5 group has oxidatively added to an adjacent Os atom forming another five member ring. There is, however, one less phenyl group in this ligand. The loss of a phenly group is compensated for by the phosphorus forming a bond to the third Os atom. Ultimately this ligand achieves μ_3-coordination. The second Os–Os edge is bridged by a C_6H_5 ligand. This is a unique two-electron–three-center bond between a carbon of C_6H_5 and an Os–Os edge. The near planar C_6H_5 ring lies nearly orthogonal to the Os—Os bond which it bridges. The third Os–Os edge is simply bridged by the phosphorus of PPh_2.

$Os_3(CO)_7(PPh_2)_2(C_6H_4)$ (Fig. 42) is another product of the $Os_3(CO)_{12} + PPh_3$ reaction. The most noteable feature of this compound is the presence of a benzyne ligand. Benzyne intermediates have been proposed in the surface activation of arenes. This, the first isolated benzyne compound, is a good model for arene activation. Other products of the $Os_3(CO)_{12} + PPh_3$ reaction include $HOs_3(CO)_8(PPh_2C_6H_4)$ and $HOs_3(CO)_7$-$(PPh_2)(C_6H_4)(PPh_3)$.

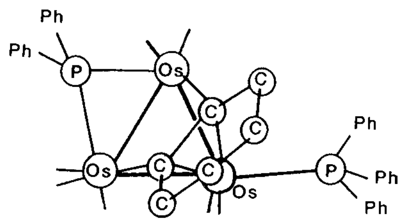

FIGURE 42 Structure of $Os_3(CO)_7(PPh_2)_2(C_6H_4)$ containing a benzyne ligand interacting with the Os_3 core.

It was stated earlier that the carbide in $[HFe_4(\mu_4\text{-C})(CO)_{12}]^-$ is sufficiently exposed to allow direct attack at the (μ_4-C). Formation of a methyne (CH) ligand can be achieved by prolonged treatment of the carbide cluster with HCl yielding the neutral $HFe_4(\mu_4\text{-CH})(CO)_{12}$. More significantly, perhaps, is an alternate route to this same methyne cluster compound. The dianion $[Fe_4(\mu_4\text{-C})(CO)_{12}]^{2-}$, when oxidized by $AgBF_4$ in the presence of H_2, yields $HFe_4(\mu_4\text{-CH})(CO)_{12}$. The cluster–surface analogy draws strength from this hydrogenation of a surfacelike carbide atom from H_2.

Fischer–Tropsch chemistry, involving the reduction of CO by H_2 to yield hydrocarbons and some oxygen-containing products (alcohols, ketones, and aldehydes) has been postulated to proceed via the dissociative chemisorption of CO on a metal surface. The carbide atoms may be hydrogenated, combine to form the backbone of larger chain hydrocarbon, or react with incoming CO. Total hydrogenation will yield methane, and partial hydrogenation produces surface-bound alkane fragments. The selectivity of Fischer–Tropsch synthesis for producing n-alkanes in much greater yields than branched alkanes suggests that hydrogenation of carbides to CH_2 units must be an important process. The presence of oxygen-containing compounds suggests that CO may insert into metal–carbide or metal–alkyl fragments. The diversity of Fischer–Tropsch chemistry has been responsible for many, some seemingly contradictory, mechanisms to be postulated. It seems probable that more than one mechanism is operative during the synthesis. We have to this point discussed a number of related Fe_4C cluster compounds which provide the cluster analogs of proposed Fischer–Tropsch intermediates. Figure 43a shows the proposed surface-bound intermediates, and Fig. 43b shows the isolated cluster analogs to show the similarities.

Another Fe_4C cluster, $Fe_4(CO)_{12}(\mu_4\text{-CCO}_2Me)$, (Fig. 43) strengthens the cluster-surface analogy. This cluster is derived from $[Fe_6(\mu_6\text{-C})(CO)_{16}]^{2-}$. Oxidation of this cluster causes the removal of two Fe vertices. The protected (μ_6-C) now becomes a (μ_4-C) and is susceptible to attack. In the presence of CO and methanol, $Fe_4(CO)_{12}(\mu_4\text{-CCO}_2Me)$ is formed. Hydrogenation of this cluster releases the (μ_4-CO_2Me) ligand as methylacetate. This reaction involves the formation of a C—C bond from a carbide and CO and leads to a useful organic compound. This example also demonstrates the utility of an encapsulated μ_6-carbide.

By studying cluster core–ligand interactions we may gain insight to the chemisorption processes so important

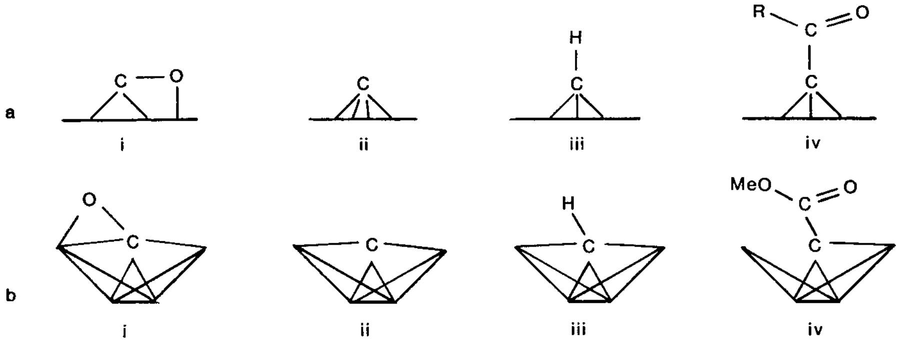

$[HFe_4(CO)_{13}]^-$ $[HFe(C)(CO)_{12}]^-$ $HFe_4(CH)(CO)_{12}$ $Fe_4(CCO_2Me)(CO)_{12}$

FIGURE 43 (a) Proposed surface-bound intermediates and (b) their isolated cluster analogs.

to surface catalysis. On this basis clusters serve as models of the catalyst. However, some clusters are themselves catalysts. Many catalytic processes have been studied in which metal cluster compounds were present at the start of the reaction. However, these clusters are frequently referred to as catalyst precursors as reaction conditions often promote cluster degradation to reactive mononuclear species. There are, however, several catalytic reactions for which there is evidence supporting cluster involvement.

Both $Co_3(CO)_9(\mu_3\text{-CPh})$ and $Co_4(CO)_8(\mu_2CO)_2(\mu_4\text{-PPH})_2$ are thought to remain intact while catalyzing hydroformylation reactions. Hydroformylation, an important industrial process, is the production of an aldehyde via the reaction of CO and H_2 with an alkene. The basis for thinking that the clusters retain their integrity is the recovery of unchanged clusters at the end of the long reactions (>100 h). This in and of itself is not conclusive evidence for cluster involvement as it is conceivable that mononuclear species, once part of cluster, could recombine forming the original cluster. This type of regeneration is most easily conceived for binary metal carbonyl clusters. The unlikelihood that clusters containing (μ_3-CPh) and (μ_4-PPh) ligands could be degraded and regenerated with no other Co-containing compounds being formed argues for intact cluster catalysis. The specific hydroformylation reactions these clusters have been found to catalyze are the conversions of 1- and 2-pentene to aldehydes. Under relatively mild reaction conditions ($T = 90-150°C$) the yields were excellent and the selectivity encouraging. Specifically, the hydroformylation of 1-pentene at 110°C gave a 94% yield of the terminal 1-hexanal and the branched products 2-methylpentanal and 2-ethylpentanal. The ratio of normal to branched products was 4.7.

Another system in which intact cluster catalysis seems likely is the synthesis gas (CO/H_2) production of ethylene glycol catalyzed by an anionic rhodium cluster of uncertain or undisclosed identity. From high-temperature and -pressure infrared studies it is believed that $[Rh_{12}(CO)_{30-34}]^{n-}$ are abundant at reaction conditions as well as lesser quantities of $[HRh_6(CO)_{15}]^-$ and $[Rh_{13}(CO)_{24}H_3]^{2-}$. The high selectivity, producing as much as 75% ethylene glycol, can be affected by addition of various cationic promoters. This also suggests that anionic species are involved in the catalysis. However, unequivocal proof of intact cluster catalysis has not yet been demonstrated.

Much effort has been expended so that we may further understand molecular clusters. As clusters bridge the gap between the mononuclear and bulk metal regimes they offer unique chemical and physical properties. Attempts to bridge this gap have been made in the following way. Well-characterized cluster compounds have been used as precursors to well-defined supported metal clusters. The idea is that the cluster compound, of known nuclearity, would be absorbed on a catalyst support, and the ligands stripped away by heating or photolysis, leaving a bare, known nuclearity cluster on the surface. Unfortunately, almost all of these attempts have failed, with the possible exception of very stable, strongly bound osmium clusters. In most cases the complete removal of ligands is difficult, and the deposited cluster is rather more labile and fragile than was initially expected. Nevertheless, this is an area for much successful future work.

Clearly there are many reasons for the continued interest in cluster compounds. Recall it was just 80 years ago that $[Ta_6Cl_{12}]^{2+}$ was synthesized. Over 40 years passed before the true nature of this compound was realized. In the 40 years that have followed the realization that metal cluster compounds do exist great progress has been made in our understanding of these systems. However, for the thousands of cluster compounds known today it is probably safe to say that only a small fraction of their reaction chemistry has been uncovered. With the persistent interest in these compounds many more thousands are sure to be

discovered. The magnitude of possibilities will certainly help sustain research in this area. With continued research we will hopefully realize much of the great potential which these systems possess.

ACKNOWLEDGMENT

The support of the National Science Foundation and the Army Research Office is acknowledged with gratitude.

SEE ALSO THE FOLLOWING ARTICLES

Bonding and Structure in Solids • Ligand Field Concept • Metal Cluster Chemistry • Nanosized Inorganic Clusters • Noble Metals • Periodic Table • Sintering

BIBLIOGRAPHY

Baetzold, R. C., and Hamilton, J. F. (1983). *Prog. Solid State Chem.* **15,** 1–53.

Cotton, F. A., and Walton, R. A. (1982). "Multiple Metal Bonds Between Metal Atoms," Wiley, New York.

Cotton, F. A., and Wilkinson, G. (1980). "Advanced Inorganic Chemistry," 4th ed. Wiley, New York.

Davis, S. C., and Klabunde, K. J. (1982). *Chem. Rev.* **82,** 153–208. American Chemical Society Publishers, Washington, D.C.

El-Sayed, M. A. (1991). *J. Phys. Chem.* **95,** 3898.

Fendler, J. H. (1987). *Chem. Rev.* **87,** 877.

Gates, B. C., Guczi, L., and Knozinger, H. (1986). "Metal Clusters in Catalysis," Elsevier, Amsterdam.

Henglein, A. (1989). *Chem. Rev.* **89,** 1861.

Johnson, B. F. G., ed. (1980). "Transition Metal Clusters," Wiley, New York.

J. Organomet. Chem. **213**(1). Special Issue dedicated to the late Professor Paolo Chini.

Klabunde, K. J. (1994). "Free Atoms, Cluster, and Nanoscale Particles," Academic Press, San Diego.

Klabunde, K. J. (1980). "Chemistry of Free Atoms and Particles," Academic Press, New York.

Klabunde, K. J., and Mohs, C. (1998). *In* "Chemistry of Advanced Materials, An Overview" (L. V. Interrante and M. J. Hampden-Smith, eds.), pp. 271–327, Chapter 7, Wiley-VCH Publishers, New York.

Klabunde, K. J., Jeong, G. H., and Olsen, A. (1990). Ground state metal atoms and clusters in low temperature C—H and C—C activation: Periodic trends and unusual steric effects. *In* "Molecular Structure and Energetics," Vol. 12. (J. A. Davies, P. L. Watson, J. F. Liebman, and A. Greenberg, eds.) VCH Publishers, New York.

Lin, X. M., Wang, G. M., Sorensen, C. M., and Klabunde, K. J. (1999). *J. Phys. Chem. B* **103,** 5488–5492.

Mason, M. G. (1983). *Phys. Rev. B* **27,** 748.

Mingos, M. P., and Wales, D. J. (1990). "Introduction to Cluster Chemistry," Prentice Hall, Englewood Cliffs, New Jersey.

Muetterties, E. L., Rhodin, T. N., Band, E., Brucker, C. F., and Pretzer, W. R. (1979). *Chem. Rev.* **79,** 91–138.

Neuman, R. D., and Ibrahim, J. H. (1999). *Langmuir* **15,** 10.

Pileni, M. P. (1997). *Langmuir* **13,** 3266.

Polyhedron Symposium-in Print Number 1 (1984). *Polyhedron* **3**(12). Recent Advances in the Structure and Bonding in Cluster Compounds.

Schmid, G., ed. (1994). "Clusters and Colloids," VCH Publishers, Weinheim.

Schugart, K. A., and Fenske, R. F. (1989). *J. Am. Chem. Soc.* **108,** 5094.

Stave, M. S., and DePristo A. E. (1992). *J. Chem. Phys.* **97,** 3386.

Takasu, Y., Zhang, X. G., Minoura, S., and Murakami, T. (1997). *Appl. Surf. Sci.* **121–122,** 596.

Teo, B. K., and Keating, K. (1984). *J. Am. Chem. Soc.* **106,** 2224.

VanderWiel, D. P., Pruski, M., and King, T. S. (1999). *J. Catalysis* **188,** 186–202.

Vasiliev, I., Ogut, S., and Chelikowsky, J. R. (1999). *Phys. Rev. Lett.* **82,** 1919.

West, A. (1984). "Solid State Chemistry and its Applications," Wiley, New York.

Nanosized Inorganic Clusters

Leroy Cronin
Achim Müller
University of Bielefeld, Germany

Dieter Fenske
University of Karlsruhe, Germany

I. From Clusters to the Boundary of the Metallic State
II. From Clusters to Segments of Solid-State Structures
III. From Building Blocks Via Clusters to Solids
IV. Conclusions and Perspectives

GLOSSARY

Cluster Group of atoms bound together.
Colloid Particle small enough to remain suspended in solution or gas.
Icosahedron A polyhedron having 20 faces and 12 vertices.
Ligand Molecule bound to a metal atom or cluster.
Nucleation The condensation or aggregation process by which crystals are formed on a minute amount of substance that acts as a nucleus for subsequent crystalline growth.

NANOSIZED CLUSTERS or "nanoclusters" is a term given to particles of any kind of matter, the size of which is greater than that of typical molecules, but is too small to exhibit characteristic bulk properties. Examples of such materials include the family of carbon-based fullerenes, weakly bound van der Waals clusters observed in the gas phase, metal carbonyl clusters, boron carbides and hydrides, metal clusters surrounded by protecting ligands, and metal ions connected by bridging ligands. Of special relevance in this article are those clusters that are sufficiently well-defined and large enough to be at the borderline between the molecule and the bulk. It is in this area that materials with extremely interesting properties have begun to have a profound influence on basic science as well as technology from catalysis to electronically interesting materials. Such materials become even more interesting when they are themselves, as building blocks, organized into a bulk material in a predesigned, desired manner. It is the fabrication of inorganic nanoclusters that lies at the cutting edge of nanodesign and technology today and promises many exciting discoveries and applications tomorrow. We refer here to three important classes of molecular clusters which have been thoroughly characterized and can be seen to be entering the size regime of mesoscopic materials.

I. FROM CLUSTERS TO THE BOUNDARY OF THE METALLIC STATE

Giant metal-based clusters serve as a bridge between molecular clusters and bulk metals. This has implications

for the development of electronic materials, new catalysts and, from an academic point of view, can be used to examine the transition from clusters to the boundary of the metallic state. To examine clusters that lie on the relevant borderline it is important to synthesize systems that do not interact with each other and undergo coalescence, destroying the individuality of the cluster.

To synthesize giant metal-based clusters a preparative approach has to be taken that can yield the metal atoms in their preferable zero-valent oxidation states. Generally, the preparation of these clusters requires the precursor complexes to be dissolved in solution followed by the reduction of the metal ions to a zero-valent state. Once the reduction has occurred—the reduction step can be achieved by metals such as sodium and substrates such as hydrazine, sodium tetrahydroborate, carbon monoxide, and hydrogen—the lifetime of the metal atoms in solution is very short and they tend to coalesce quickly into larger arrangements. The decisive step during the synthetic procedure of clusters of a distinct size, and also with colloids, is to stop the metal-metal aggregation/growth process at the right moment to prevent the formation of a bulk metal. In the gold, platinum, and palladium species this growth can be limited by introducing stabilizing π-acceptor-type ligands, such as phosphines, phenanthroline, and bipyridyl. The role of such ligands is vital in the synthesis of discrete clusters as these ligands act as protecting groups preventing the coalescence of the clusters to form a bulk material.

One example of a material that can be prepared in this manner is given by the gold cluster $Au_{55}(PPh_3)_{12}Cl_6$ which is a two-shell cluster consisting of a central atom that is embedded by two close packed shells of 12 and 42 atoms and is terminated with the protective ligand sheath of twelve triphenylphosphine ligands. The synthesis of this Au_{55} cluster has been improved further by the introduction of a thiol-terminated dendrimer which removes the phosphine ligands and acts as a matrix. The synthesis of other clusters using this approach has shown that the number of metal atoms in the core can follow a set of "magic-numbers," see Fig. 1. Such numbers were postulated since metal skeletons of large molecular clusters could be similar in their structures to small metal crystallites formed on the basis of close-packed (face-center) cubic or hexagonally close-packed arrangements of metal atoms. In the case of the 12-vertex polyhedra, a metal skeleton in the shape of a cuboctahedron or anticuboctahedron was expected as derived from these packing arrangements. The magic numbers can be derived from the formula:

$$N = \frac{1}{3}(10m^3 + 15m^2 + 11m + 3)$$

(N is the magic number and m is the number of shells of the metal atoms packed around the central metal atom in the symmetry of a cuboctahedron or anticuboctahedron). A range of clusters has been synthesized which correspond to magic numbers, for instance M_{13} (one-shell) = $[Au_{13}(diphos)_6](NO_3)_4$, M_{55} (two-shell) = $Au_{55}(PPh_3)_{12}Cl_6$, M_{309} (four-shell) = $Pt_{309}Phen_{36}O_{30\pm10}$ and M_{561} (five-shell) = $Pd_{561}Phen_{60}(OAc_{180})$—the largest cluster to be synthesized and separated preparatively. The five-shell cluster, $Pd_{561}Phen_{60}(OAc_{180})$, results if an acetic acid solution of palladium(II) acetate is reduced by gaseous hydrogen in the presence of small amounts of phenanthroline (phen) followed by the controlled addition of oxygen. In this synthesis the Pd_{561} is the smallest of three different cluster species formed which are 3.60, 3.15, and 2.20 nm in diameter, respectively (without the ligand shell). The electron microscopic study of these particles proves that the different particles are characterized by a distinct number of atomic planes: the 3.60-nm cluster consists of 17 planes, the 3.15-nm cluster of 15 planes, and the 2.20-nm particles of 11 planes. These numbers are compatible with the existence of the magic numbers for each of these cluster types, as described above. In principle, the nth shell consists of $10n^2 + 2$ atoms. Following this model

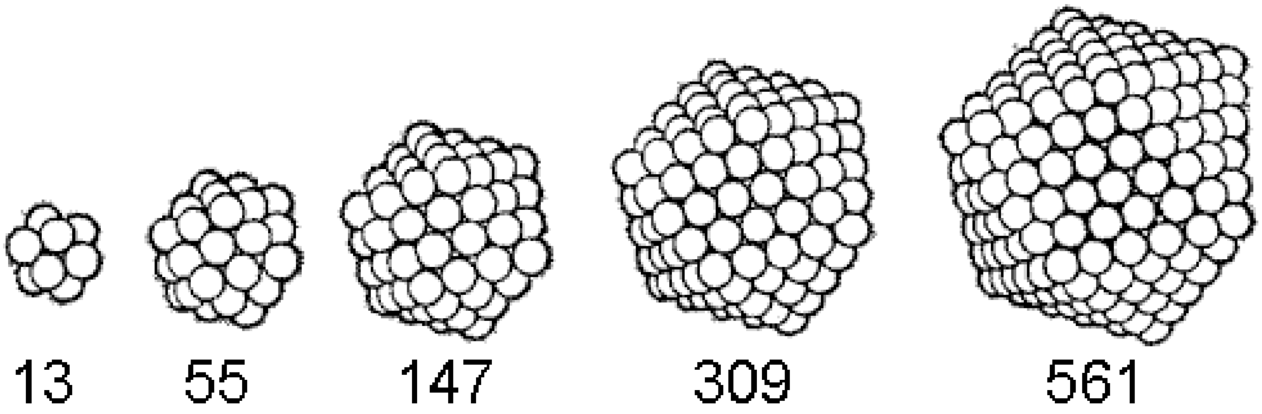

FIGURE 1 A representation of the magic numbers of clusters obtained by surrounding a given atom by successive shells of atoms (the figure shows the cuboctahedral polyhedra formed by the atoms).

the 17 planes in the 3.60-nm clusters are formed by 2057 atoms 15 planes by 1415 atoms and the 11 planes by 561 atoms. Overall, these numbers correspond, for example, to the eight-, seven-, and five-shell clusters with formulas equating to: $Pd_{2057}Phen_{84}O_{1600}$, $Pd_{1415}Phen_{60}O_{1100}$, and $Pd_{561}Phen_{36}O_{200}$, respectively.

Naturally electron microscopy cannot determine the exact number of metal atoms. However, considering the observation that more than 90% of the particles detected with the electron microscope occur with one of the discussed number of planes, it would appear that the natural packing distribution of these assemblies tends toward the description given by the magic numbers. However, in cases where the number of metal atoms in the cluster approaches several hundreds, a set of imperfect clusters/colloids are formed with a certain distribution with respect to size and chemical composition.

The use of colloidal dispersions in the synthesis of metal-based clusters has also afforded routes to ligand-stabilized bimetallic clusters that offer other opportunities to tune the properties of the overall cluster formed. The aim of such work in the future lies in both stabilizing and geometrically linking such cluster entities into 2-D and 3-D networks. If such work was to succeed then new types of storage devices and electronic components of "minute dimensions" may become accessible that probably will never be reached by established methods such as nanolithography.

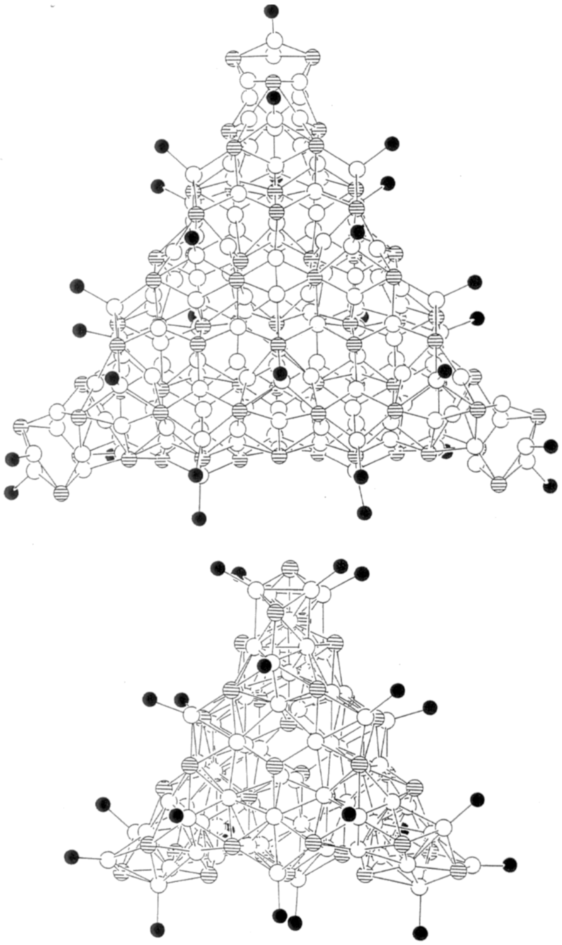

FIGURE 2 Structure of $[Cu_{70}Se_{35}(PEt_3)_{22}]$ and $[Cu_{146}Se_{73}(PPh_3)_{30}]$ (without Et and Ph groups). The Cu atoms are shown as empty spheres, the Se atoms are shown as hatched spheres, and the P as black spheres.

II. FROM CLUSTERS TO SEGMENTS OF SOLID-STATE STRUCTURES

An alternative class of metal clusters which may also provide routes to interesting systems of scientific and technological relevance are derived from metal chalcogenides. During the last few years interest in this class of compounds has increased dramatically, as they can be used as precursors in the production of semiconducting metal selenides and tellurides. A considerable number of multinuclear metal selenide cluster complexes are known now which are protected by a ligand shell thus avoiding further reaction to stable binary selenides. Examples include $[Ni_{34}Se_{22}(PPh_3)_{10}]$, $[Cu_{70}Se_{35}(PEt_3)_{22}]$, and $[Cu_{146}Se_{73}(PPh_3)_{30}]$. These compounds are formed by the reaction of PR_3 complexes (R = organic group) of metal halides with $Se(SiMe_3)_2$, Scheme 1.

The mechanism for cluster formation, and thus the molecular structure of the products, is strongly influenced by the special reaction conditions (temperature, type of copper salt used, type and size of the PR_3 ligand). As expected very often the thermodynamically stable metal chalcogenides are formed, however, calculations have shown that the PR_3-stabilized cluster complexes are metastable.

It is possible to obtain copper chalcogenide clusters which can be approximately described as a section of the structure of the binary Cu_2E phase (E = S, Se, Te) surrounded by PR_3 ligands. Though spherical cluster cores with up to 62 copper atoms do not permit a direct comparison with the binary copper chalcogenides, with increasing cluster size, a tendency toward a layered Cu_2E-type skeleton can be seen. Fragments of the structure of the binary Cu_2Se phase can be recognized for the clusters $[Cu_{70}Se_{35}(PEt_3)_{22}]$ and $[Cu_{146}Se_{73}(PPh_3)_{30}]$ (Fig. 2). In particular, the relation to the Cu_2Se structure can be seen by comparing the Se sublattices of the two cluster compounds. In both clusters a layered segment is formed by the Se ligands, consisting of layers with 10, 15, and 10 Se ($\{Cu_{70}\}$) and 21, 31, and 21 Se atoms ($\{Cu_{146}\}$ cluster), respectively (Fig. 3). Most of the Cu atoms are positioned in the tetrahedral surroundings spanned by the Se atoms.

$$\mathrm{CuX + PR_2R'} \xrightarrow[-\mathrm{SiMe_3X}]{\text{1. organic solvent; 2. } +\mathrm{E(SiMe_3)_2}} \mathrm{[Cu_{2n}E_n(PR_2R')_m]} \qquad \begin{array}{l} \mathrm{X} = \mathrm{Cl, OAc} \\ \mathrm{R, R'} = \text{org. group} \\ \mathrm{E} = \mathrm{S, Se} \end{array}$$

SCHEME 1 General route to the preparaton of metal chalcogenides.

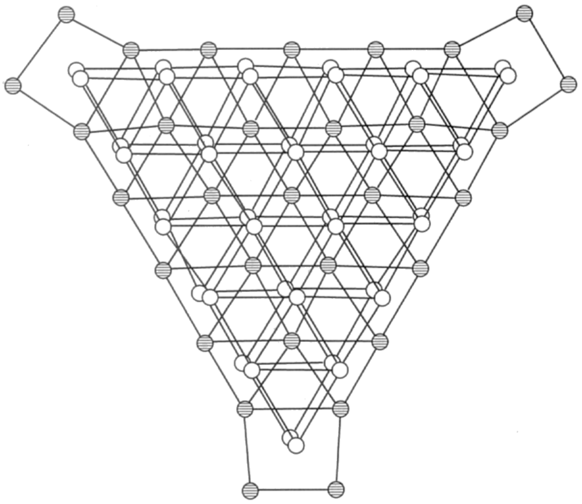

FIGURE 3 Structure of the Se network in $[Cu_{146}Se_{73}(PPh_3)_{30}]$. The Se atoms on the first and third layers are shown as empty spheres and those of the middle layer as hatched spheres.

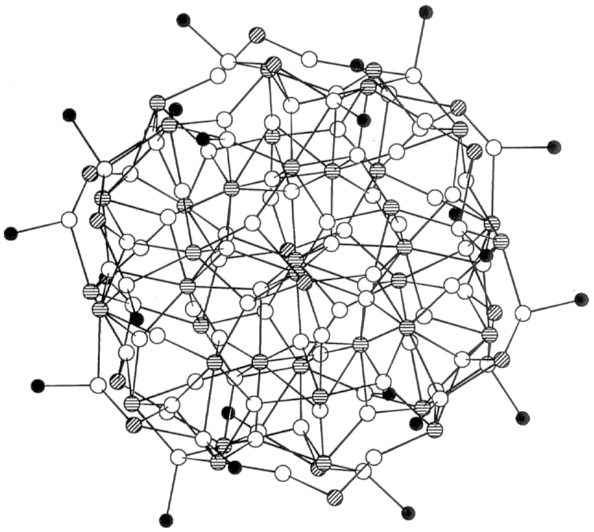

FIGURE 4 Structure of $[Ag_{90}Se_{38}(Se^tBu)_{14}(PEt_3)_{22}]$ without C atoms. Ag atoms are shown as empty spheres, Se atoms are depicted as horizontally hatched spheres, and the Se atoms of the Se^tBu groups are hatched spheres.

The reaction of AgCl, for example, with $Se(SiMe_3)_2$ in the presence of PR_3 usually affords insoluble Ag_2Se, while the corresponding reaction with $R'TeSiMe_3$ preferably provides silver clusters with Te^{2-} and TeR^- ligands. The structures of the compounds formed depend very much upon the type of the tertiary phosphane used and also on the organic group R′. Examples of related compounds with known structures are $[Ag_6(\mu_3\text{-}Te^nBu)_4(\mu\text{-}Te^nBu)_2(PEt_3)_4]$, $[Ag_{10}(TePh)_{10}(PMe_3)_2]_\infty$, $[Ag_{30}(TePh)_{12}Te_9(PEt_3)_{12}]$, $[Ag_{32}(\mu_3\text{-}Te^nBu)_{18}Te_7(PEt_3)_6]$, $[Ag_{46}(TeMes)_{12}Te_{17}(PEt_3)_{16}]$, and $[Ag_{48}(\mu_3\text{-}Te^nBu)_{24}Te_{12}(PEt_3)_{14}]$. Other Ag clusters can be isolated from the reaction of silver carboxylates with $RSeSiMe_3$ (R = organic group) and PR_3 or bidentate phosphanes. The reaction of P^nPr_3 with $^tBuSeSiMe_3$ and silver benzoate in pentane at −40°C affords $[Ag_{30}Se_8(Se^tBu)_{14}(P^nPr_3)_8]$ (Scheme 2). Using the same reaction conditions with PEt_3 as ligands, only the formation of $[Ag_{90}Se_{38}(Se^tBu)_{14}(PEt_3)_{22}]$ can be observed.

However, the $\{Ag_{90}\}$ cluster (Fig. 4) shows no similarity with the corresponding binary phase Ag_2Se but exciting structural details: The Se atoms form a torus-shaped polyhedron, which is built up from Se_3 faces (Fig. 5). The reaction of $Ag(C_{11}H_{23}CO_2)$ with $^nBuSeSiMe_3$ and P^tBu_3 yields $[Ag_{114}Se_{34}(Se^nBu)_{46}(P^tBu_3)_{14}]$ (Fig. 6). If the monodentate phosphane ligands are replaced by bis(diphenylphosphino) propane (dppp), under the same reaction conditions (Scheme 3) (−30°C) the largest known Ag cluster $[Ag_{172}Se_{40}(Se^nBu)_{92}(dppp)_4]$ is formed (Fig. 7).

The layer clusters of the type $\{Ag_{114}\}$ and $\{Ag_{172}\}$ are structurally different from the aforementioned systems, for instance, from the spherical $\{Ag_{30}\}$ and $\{Ag_{90}\}$ clusters. There is a remarkable agreement between the Se skeletons in the $\{Ag_{114}\}$ and $\{Ag_{172}\}$ clusters and that of Ag_2Se (Fig. 8). The cluster structures can realistically be described as sections of the binary phase Ag_2Se. With increasing cluster size, the distribution of the Ag atoms in the molecular structure becomes more random. Obviously there is a tendency to a kind of disordering of the Ag atoms which is also observed in the bulk material Ag_2Se.

$$\mathrm{[Ag_{90}Se_{38}(Se^tBu)_{14}(PEt_3)_{22}]} \xleftarrow[\mathrm{PEt_3}]{\mathrm{^tBuSeSiMe_3}} \mathrm{Ag(C_6H_5CO_2)} \xrightarrow[\mathrm{P^nPr_3}]{\mathrm{^tBuSeSiMe_3}} \mathrm{[Ag_{30}Se_8(Se^tBu)_{14}(P^nPr_3)_8]}$$

SCHEME 2 Synthetic route to Ag_{90} and Ag_{30} clusters.

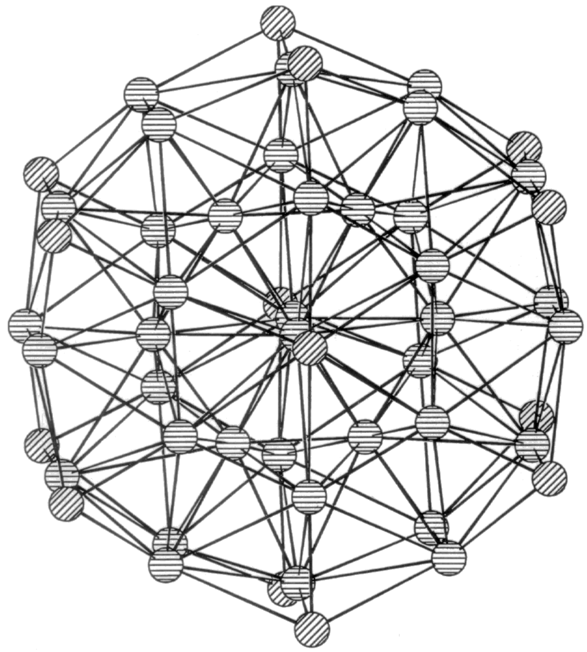

FIGURE 5 Se skeleton in $[Ag_{90}Se_{38}(Se^tBu)_{14}(PEt_3)_{22}]$. Se atoms are shown by the horizontally hatched spheres and the Se atoms of the Se^tBu groups as diagonally hatched spheres.

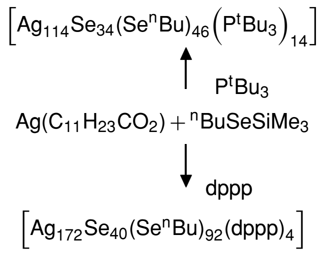

SCHEME 3 Synthetic route to the Ag_{114} and the Ag_{172} clusters.

III. FROM BUILDING BLOCKS VIA CLUSTERS TO SOLIDS

The one-pot synthesis of ring-shaped and spherical polyoxometalates, based on a set of structurally conserved building blocks, has been another highly successful route to clusters of nanoscopic dimensions containing cavities and, in principle, pores. Such syntheses have been found to be based upon a building block principle with units that are suggested to have intrinsic properties (variable charge and flexible coordination modes) that facilitate the self-assembly of clusters containing many thousands of atoms in solution (Fig. 9). In this respect, the use of pentagonal-type building groups, with different symmetries, plays a key role in the formation of these systems as pentagonal units allow the construction of clusters with curvature that in turn prevents immediate growth to bulk materials.

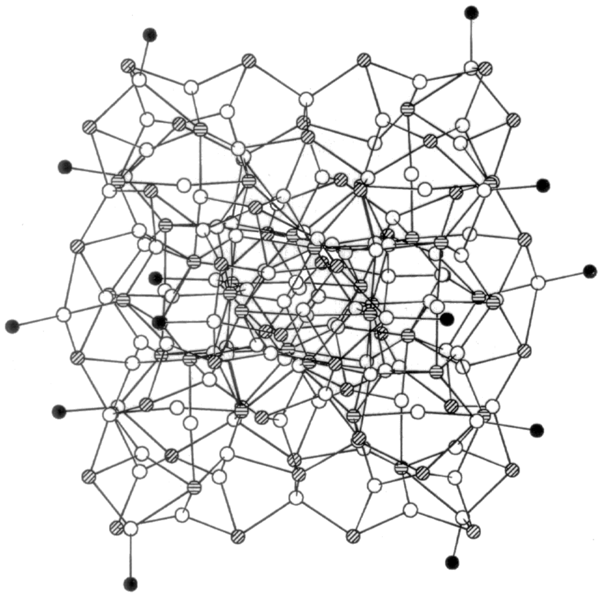

FIGURE 6 Molecular structure of $[Ag_{114}Se_{34}(Se^nBu)_{46}(P^tBu_3)_{14}]$. Ag atoms are shown as empty spheres, Se atoms depicted as horizontally hatched spheres, and the Se atoms of the Se^nBu groups as diagonally hatched spheres.

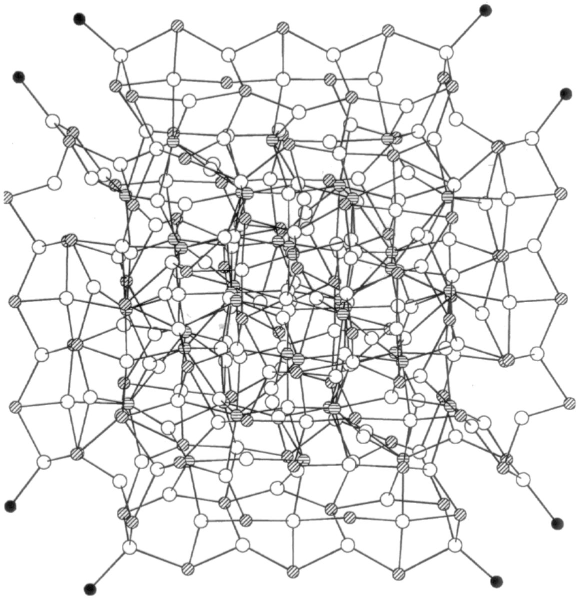

FIGURE 7 Molecular structure of $[Ag_{172}Se_{40}(Se^nBu)_{92}(dppp)_4]$. Ag atoms are shown as empty spheres and Se atoms depicted as horizontally hatched spheres, the Se atoms of the Se^nBu as diagonally hatched spheres, and the P atoms as black spheres.

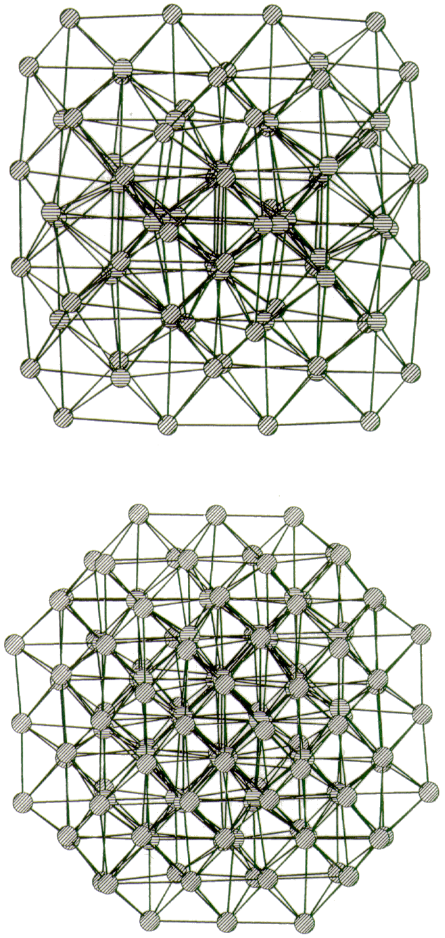

FIGURE 8 Se skeleton in $[Ag_{114}Se_{34}(Se^{n}Bu)_{46}(P^{t}Bu_{3})_{14}]$ (above) and $[Ag_{172}Se_{40}(Se^{n}Bu)_{92}(dppp)_{4}]$ (below). Se atoms are depicted by the horizontally hatched spheres and the Se atoms of the $Se^{n}Bu$ groups as diagonally hatched spheres.

The most important strategy to promote growth of polyoxometalate clusters requires the generation of sufficiently negatively charged fragments/intermediates formed during the aggregation process. This can be attained not only by substituting some lower valence metal centers for ones of higher oxidation state or by substituting less positively charged for higher positively charged groups (e.g., by exchanging $[Mo(NO)]^{3+}$ for $[MoO]^{4+}$), but mainly by the presence of an appropriate reducing agent or even different types of these. The growth processes are promoted by the overall solubility of the growing cluster in solution-preventing aggregation, which can be achieved by avoiding nucleophilicity of the peripheral oxygen atoms that is too high. The presence of numerous H_2O ligands causes high solubility in protic media and terminal double-bonded oxygen atoms of the O=Mo groups prevent aggregation.

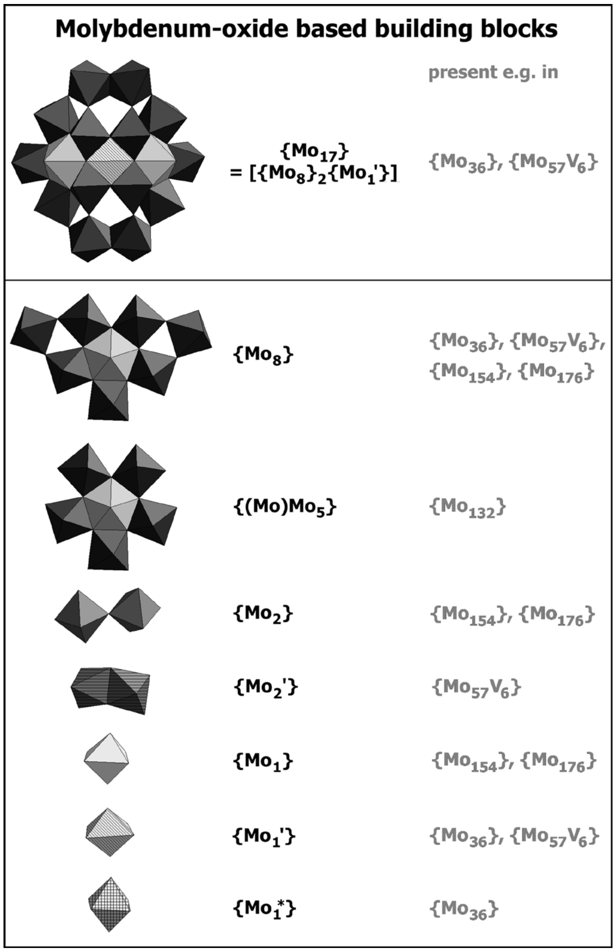

FIGURE 9 Molybdenum-oxide-based building blocks.

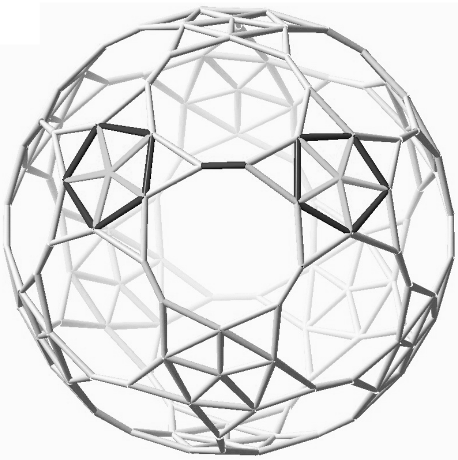

$\{Mo_{132}\}$

FIGURE 10 Schematic representation of the 132 molybdenum atom framework of the Keplerate cluster highlighting its spherical nature. Two pentagonal $\{(Mo)Mo_5\}$ groups linked by an $\{Mo^{V}\text{-}Mo^{V}\}$ bridge are emphasized.

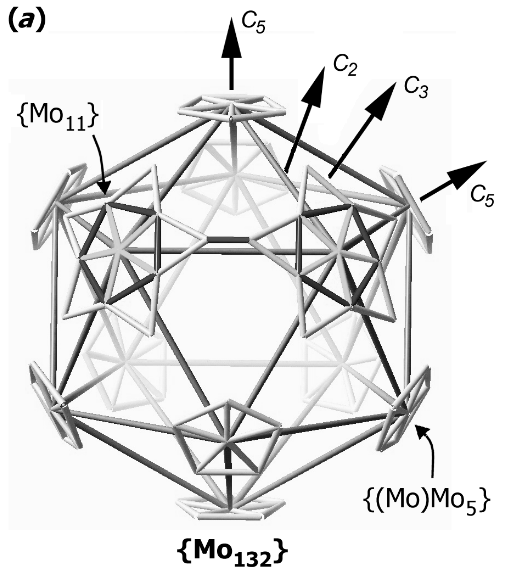

FIGURE 11 Schematic representation of the icosahedron spanned by the centers of the {(Mo)Mo_5} subfragments of the {Mo_{132}}-type cluster. Two of the {Mo_{11}} units each formed by the {(Mo)Mo_5} groups and the five related Mo centers of the five neighboring {$Mo^V{}_2O_4{}^{2+}$} bridges are emphasized.

A. Superfullerene Clusters with Icosahedral Symmetry

It is possible to construct a giant species similar in size and shape to spherical viruses with icosahedral symmetry (i.e., having C_5, C_3, and C_2 axes) from a reaction system in which pentagonal units with C_5 symmetry can first be generated, then get linked and placed at the 12 corners of an icosahedron. In the case of polyoxomolybdates, these pentagonal units of the type {(Mo)Mo_5} consist of a central pentagonal bipyramidal MoO_7 unit sharing edges with 5 MoO_6 octahedra. The {(Mo)Mo_5} unit is itself a constituent of the {Mo_8}-type unit abundant in many giant polyoxomolybdates (see below) in which two additional MoO_6 octahedra are bound (sharing corners) to the {(Mo)Mo_5} unit. In the presence of linkers, units which are capable of bridging two (or more) building blocks, for instance, those of the classical $[Mo^V{}_2O_4]^{2+}$ type (typically formed in reduced molybdate solutions in the presence of bidentate ligands), an icosahedral molecular system with 12 of the mentioned pentagons and 30 of the mentioned linkers is formed with the stoichiometry $[Mo^{VI}{}_{72}\,Mo^V{}_{60}O_{372}(CH_3COO)_{30}(H_2O)_{72}]^{42-}$ ({Mo_{132}}).

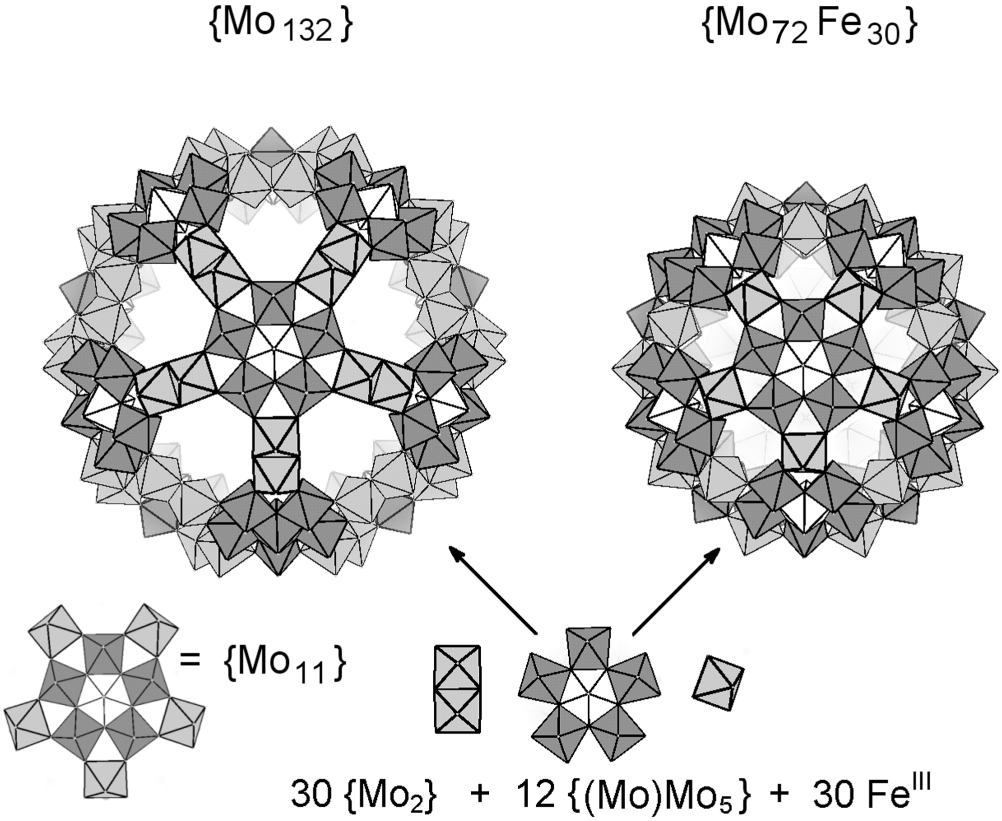

FIGURE 12 Comparison of the polyhedral representations of the {Mo_{132}} (left-hand side) and {$(Mo)^0(Mo_5)^I(Fe_{5/2})^{II}$}$_{12}$ (right-hand side) spherical clusters. The pentagonal centers of the {Mo(Mo_5)} are shown in white, the {Mo_2} groups and Fe-based octahedra are shown as light gray polyhedra, and the remaining (Mo_5) as dark gray polyhedra.

The central Mo positions of the 12 {(Mo)Mo_5} pentagons define an icosahedron and the 30 [$Mo^V{}_2O_4{}^{2+}$] a truncated icosahedron. This corresponds to the formulation [{(Mo) $Mo_5O_{21}(H_2O)_6$}$_{12}${$Mo^V{}_2O_4(CH_3COO)$}$_{30}$]$^{42-}$. The ball-like structure (Fig. 10) is also documented in the crystal structure (space group F$m\bar{3}$) with cubic closest-packed spheres in the salt $(NH_4)_{42}[Mo^{VI}{}_{72} Mo^V{}_{60}O_{372}(CH_3COO)_{30}(H_2O)_{72}]$ • ca. 300 H_2O • ca. 10 CH_3COONH_4.

This molecular system with its 60 MoO_6 subunits, corresponding to the 12 related {(Mo)Mo_5} pentagons, represents a topological model for spherical viruses, e.g., the most simple satellite tobacco necrosis virus (STNV) with 60 identical protein subunits coded only by one gene. These form the 12 pentagonal capsomers (morphology units), each capsomer consists of five protomers.

Such spherical {Mo_{132}}-type clusters have been referred to in the literature as Keplerates corresponding to Kepler's model of the cosmos and his concept of planetary motion, as described in his early opus *Mysterium Cosmographicum*. In accordance with this speculative model, Kepler believed that the distances between the orbits of the planets could be explained if the ratios between the successive orbits were designed to be equivalent to the spheres successively circumscribed around and inscribed within the five Platonic solids.

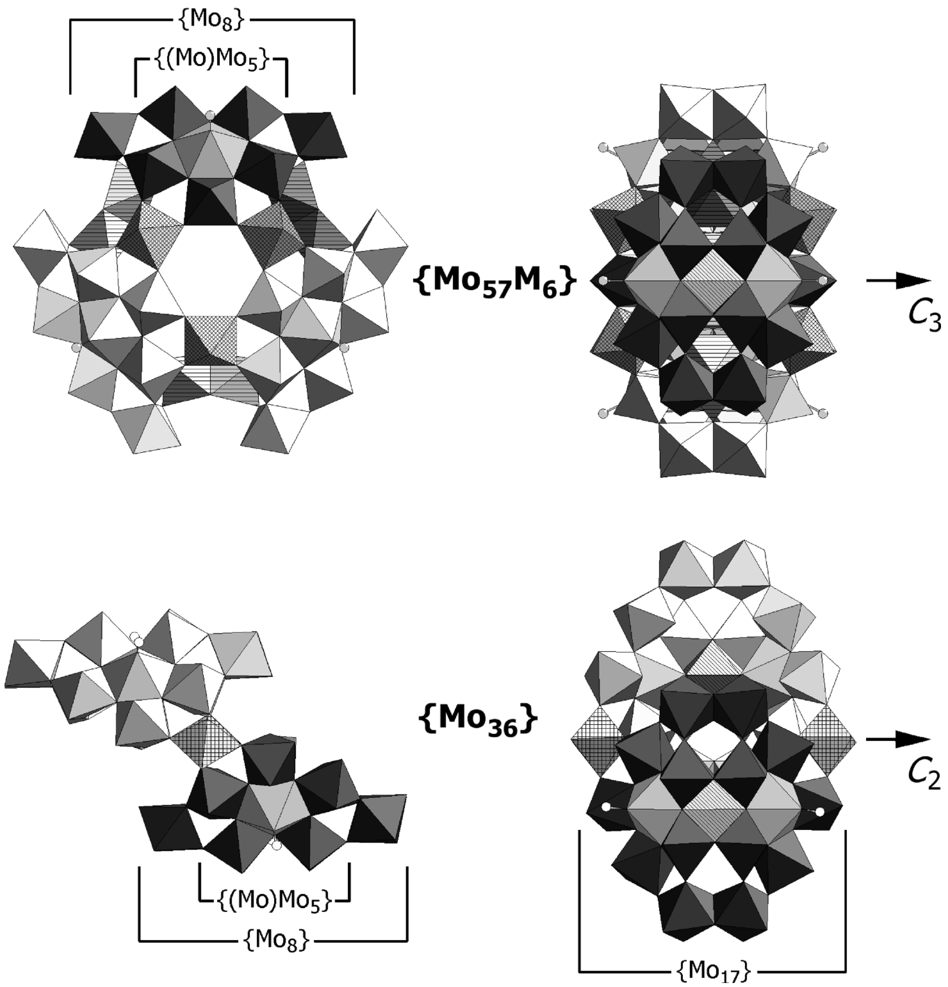

FIGURE 13 Polyhedral representation of the {$Mo_{57}M_6$} cluster with its basic building blocks and their constituents along the C_3 (upper left) and along one of the three C_2 axes (upper right). On the upper right, one {Mo_{17}} building block consisting of one {Mo_1'} and two {Mo_8} groups, and on the upper left, one {Mo_8} unit is shown by dark gray shading. Also shown by dark gray shading are one {Mo_2'} group (built up from two face-sharing octahedra) and one MO_6 unit (cross hatched). For comparison, the polyhedral representations of the {Mo_{36}} cluster structure, consisting of two {Mo_{17}} building blocks linked by two {Mo_1^*} units, are shown in the related views, also highlighting one {Mo_8} (bottom left) and one {Mo_{17}} building block (bottom right). It is important to recognize the relationship between the {Mo_8} and the pentagonal {(Mo)Mo_5} groups (see text). ({Mo_8}: light gray (central MoO_7 pentagonal bipyramid: white), {Mo_2'}: black, {Mo_1'}: hatched, {Mo_1^*}: cross hatched)

In analogy, the cluster correspondingly shows spherical shells of terminal oxygen and molybdenum atoms in which an icosahedron spanned by the centers of the 12 {(Mo)Mo_5} pentagons—the Mo atoms of the central MoO_7 bipyramids—is inscribed (see Fig. 11). The {Mo_{132}}-type cluster has been the starting point for the development of a Keplerate-type chemistry illustrated by the fact that these types of species are stable in aqueous solution and allow the encapsulation of different types of guests into the cavity. It is possible to replace the {Mo_2^V}-type linker units by Fe^{III} ions which results in a {$((Mo)Mo_5)_{12}Fe_{30}$}-type cluster (a discrete cluster with the largest number of paramagnetic centers known). Such exchange reactions also allow resizing of the cluster shells while keeping the icosahedral symmetry (Fig. 12).

B. The Route to Wheel and Giant-Wheel Structures

In generating large complex molecular species the corresponding natural processes are effected by the (directed as well as nondirected) linking of (a huge variety of) basic and well-defined preorganized (or stepwise organized) fragments. An impressive example of this is the self-aggregation/reconstitution process of the tobacco mosaic virus (TMV) from preorganized units. This process more or less meets the strategy of controlling the linking of fragments to form larger units and linking the latter again. The linking of building blocks containing 17 metal atoms ({Mo_{17}} units) to form cluster anions consisting of two or three of these units provides an archetypal example. The resulting 2- or 3-fragment clusters are of the {Mo_{36}} ($[\{MoO_2\}_2\,\{H_{12}Mo_{17}(NO)_2O_{58}(H_2O)_2\}_2]^{12-} = [\{Mo_1^*\}_2(\{Mo_8\}_2\{Mo_1'\})_2]$) or of the {$Mo_{57}M_6$} type (e.g., $[\{VO(H_2O)\}_6\,\{Mo_2(\mu\text{-}H_2O)_2\,(\mu\text{-}OH)\}_3\,\{Mo_{17}\,(NO)_2O_{58}(H_2O)_2\}_3]^{21-} \equiv [\{VO(H_2O)\}_6\{Mo_2'\}_3(\{Mo_8\}_2\{Mo_1'\})_3]$) (Fig. 13).

The structure of the {Mo_{17}} unit can be reduced to two {Mo_8}-type groups which are symmetrically linked by an {Mo_1'}-type unit. The {Mo_8} building block, found in many other large polyoxometalate structures, is itself (as mentioned above) built up from a densely packed

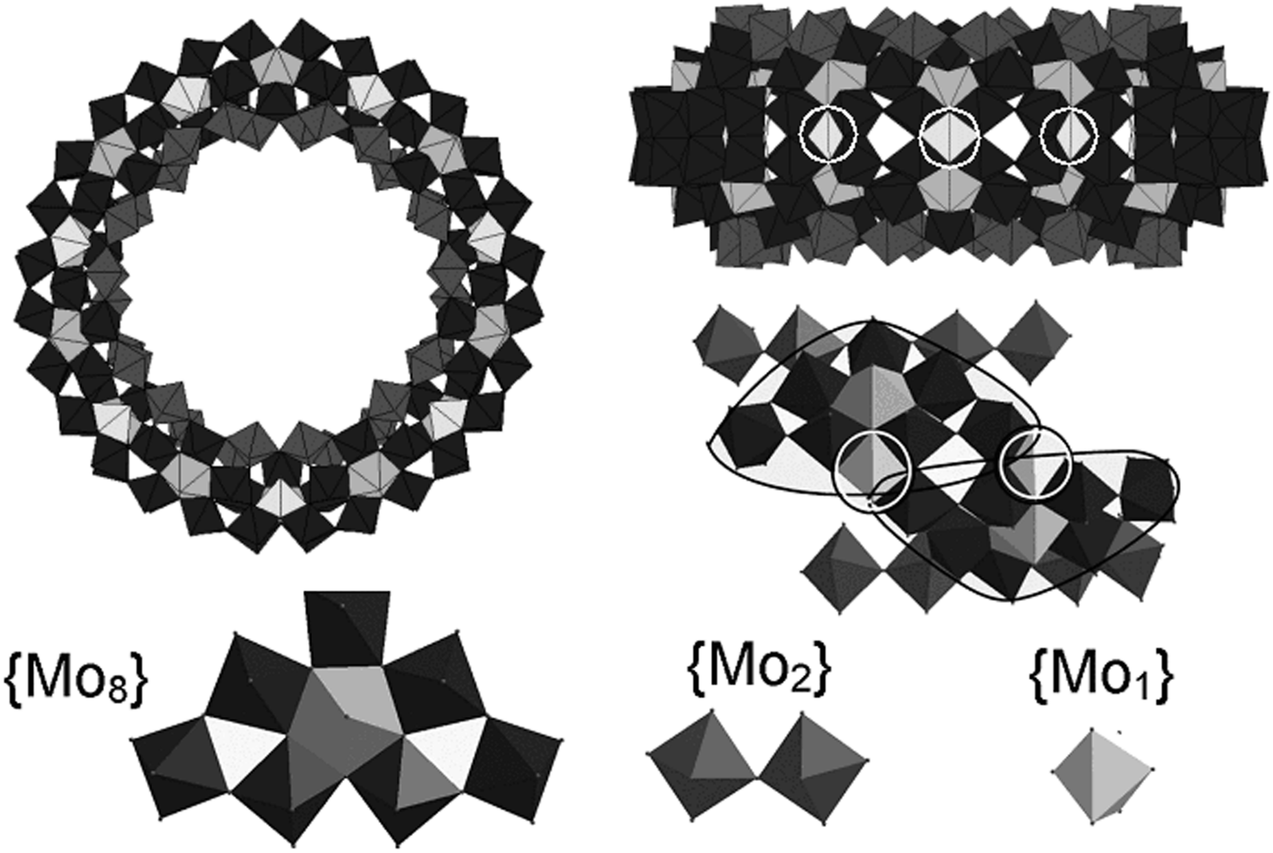

FIGURE 14 Schematic representation of the general architecture principle for the Giant-Wheel-type clusters, using the {Mo_{154}} cluster (top view left-hand side and side view right-hand side) as an example. The structural building blocks for all Giant-Wheel clusters can be formulated as comprising {Mo_8} units that are connected together via the {Mo_2} units on the inner side of the wheel. Finally, the {Mo_1} units form the equatorial plane of the ring linking the {Mo_8} units together above and below the equator (the {Mo_1} units are circled in the side view of the cluster for clarity).

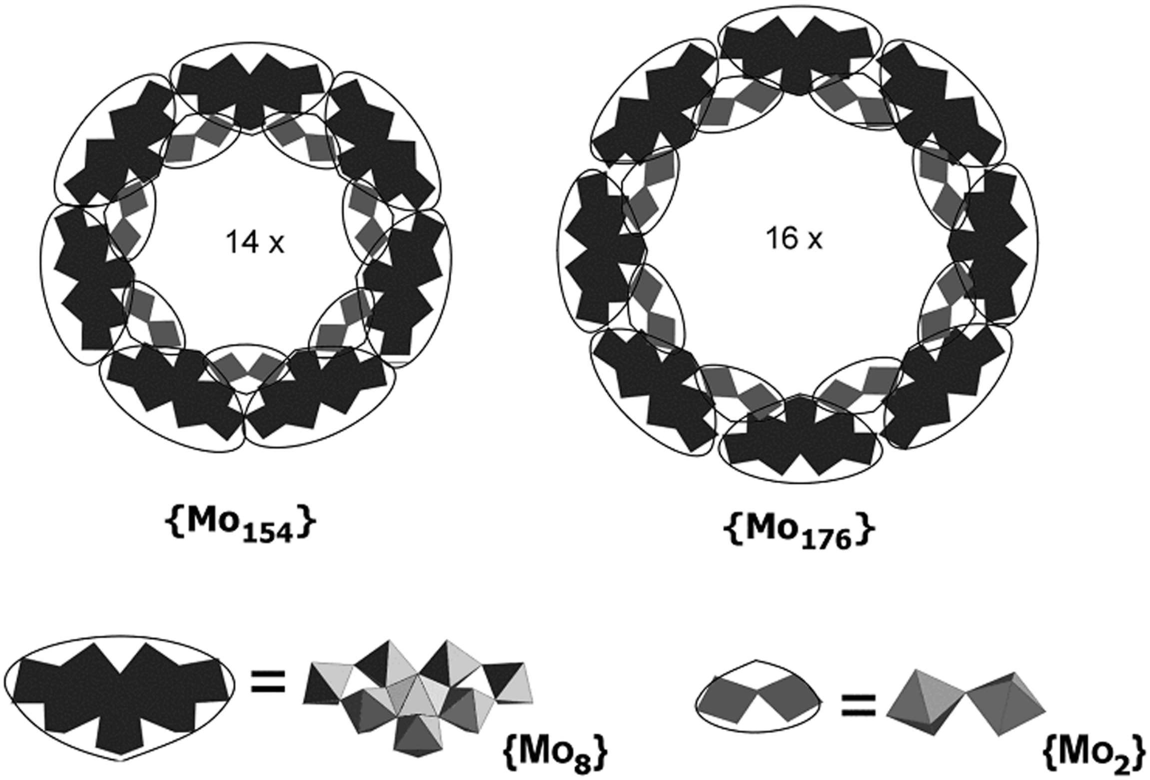

FIGURE 15 A representation of the upper halves of the tetradecameric $\{Mo_{154}\}$ and the hexadecameric $\{Mo_{176}\}$ Giant-Wheel clusters. The $\{Mo_8\}$ and $\{Mo_2\}$ building blocks are shown below. The equatorial $\{Mo_1\}$ building blocks, which connect the two sides of the Giant-Wheels together are not visible in this representation.

pentagonal $\{(Mo)Mo_5\}$ unit—containing a central MoO_7 or $MoO_6(NO)$ bipyramid sharing edges with five MoO_6 octahedra—with two more "weakly bound" (sharing only corners) MoO_6 octahedra which can be more easily removed. The pentagonal unit with a high formation tendency is, for instance, responsible for the formation of curved structures and, therefore, icosahedral symmetry like the $\{Mo_{132}\}$-type cluster (see Fig. 11).

With $\{Mo_8\}$-, $\{Mo_2\}$-, and $\{Mo_1\}$-type building blocks (Fig. 9) even larger and unusual clusters can be built up, for example, the 3.5-nm-diameter, wheel-shaped metal-oxide-based cluster anion containing 154 molybdenum atoms $[(MoO_3)_{154}(H_2O)_{70}H_{14}]^{14-}\equiv[\{Mo_2\}_{14}\{Mo_8\}_{14}\{Mo_1\}_{14}]^{14-}$ ($\{Mo_{154}\}$). The cluster above contains 14 of the mentioned $\{Mo_8\}$ groups linked by 14 $\{Mo_2\}$- and 14 $\{Mo_1\}$-type units, respectively (Figs. 14 and 15).

Overall, the complete ring system consists formally of 140 MoO_6 octahedra and 14 pentagonal bipyramids of the type MoO_7, see Fig. 14. The basic building blocks of the tetradecameric wheel are 14$\{Mo_8\}$ units with a central MoO_7 group. This MoO_7 group is symmetrically connected to five MoO_6 octahedra by edge sharing resulting in

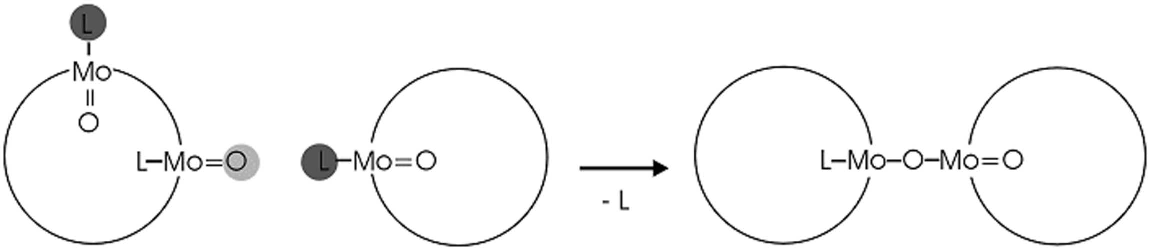

FIGURE 16 Schematic representation of the basic assembly principle of the Giant-Wheel-shaped cluster units forming the networks and layers. The formation is based on the synergetically induced functional complementarity of the $\{Mo_2\}$ units O=Mo(L) (L=H_2O, $H_2PO_4^{2-}$).

an $\{(Mo)Mo_5\}$ pentagon. Four of the MoO_6 octahedra are linked to two MoO_6 octahedra via corners to form the basic $\{Mo_8\}$ unit. Continuing from the $\{Mo_8\}$ unit the complete $\{Mo_{154}\}$ cluster ring is built up as follows: (1) those two MoO_6 octahedra which are not directly connected to the central MoO_7 bipyramid are fused to neighboring $\{Mo_8\}$ units through corners; (2) neighboring $\{Mo_8\}$ groups are additionally fused together by the $\{Mo_2\}$ units, thereby completing the inner-ring parts of the upper and lower half of the ring structure; and (3) the complete ring is constructed when the second half is rotated around 360/14 degrees relative to the first and fused to it through the 14 $\{Mo_1\}$ groups, which are located at the equator of the complete ring, see Fig. 14.

The synthesis of the tetradecameric $\{Mo_{154}\}$ cluster type can be related to that of the hexadecameric $\{Mo_{176}\}$ cluster. The most important change is that this requires reaction conditions with a pH lower than in the smaller ring system and the presence of an increased concentration of molybdate. The $\{Mo_{176}\} \equiv [\{Mo_2\}_{16}\{Mo_8\}_{16}\{Mo_1\}_{16}]^{16-}$ cluster with the formula $[(MoO_3)_{176}(H_2O)_{80}H_{16}]^{16-}$ comprises two extra $\{Mo_8\}$, $\{Mo_2\}$, and $\{Mo_1\}$ units, respectively, when compared to the smaller $\{Mo_{154}\}$ cluster, see Fig. 15.

C. Introduction of Defects and Linking the "Giant-Wheel" Clusters to Chain and Layer Networks

It is possible to obtain Giant-Wheel-type clusters that are structurally incomplete, i.e., comprising defects when compared to the original $\{Mo_{154}\}$ cluster. Such defects manifest themselves as missing $\{Mo_2\}$ units. (These defects can sometimes be seen as underoccupied $\{Mo_2\}$ units when the distribution suffers from rotational or translational disorder within the crystal structure.) It should be noted, however, that as the introduction of defects increases the overall negative charge, the rings can be linked together into chains and layers. In general, this type of linking reaction occurs via the terminal $\{Mo_2\}$-based $H_2O{-}Mo{=}O$ groups (see Fig. 16). For example, an

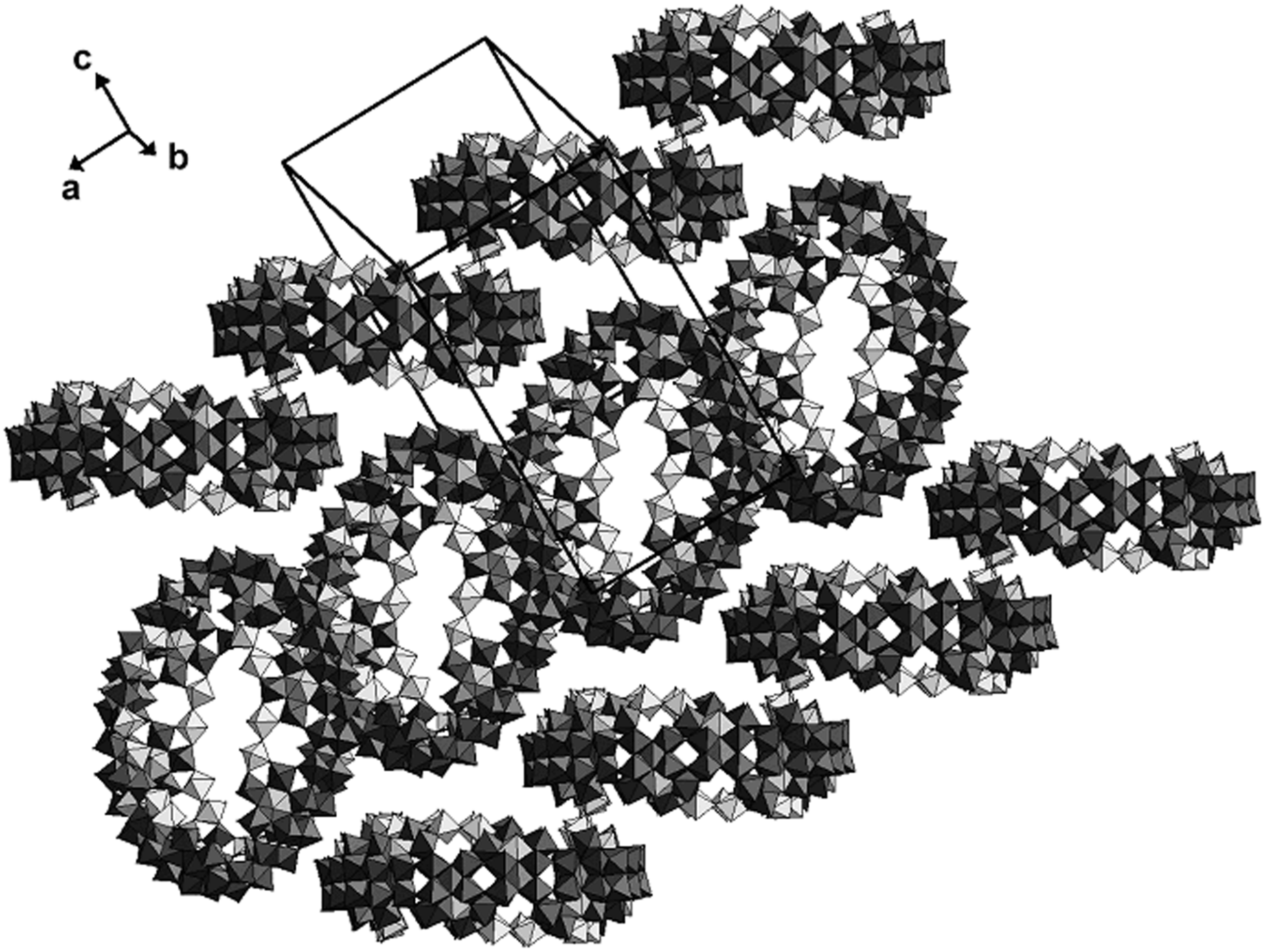

FIGURE 17 Polyhedral representation of $\{Mo_{144}\}$ units linked to chains. Linking occurs via the $\{Mo_2\}$ units.

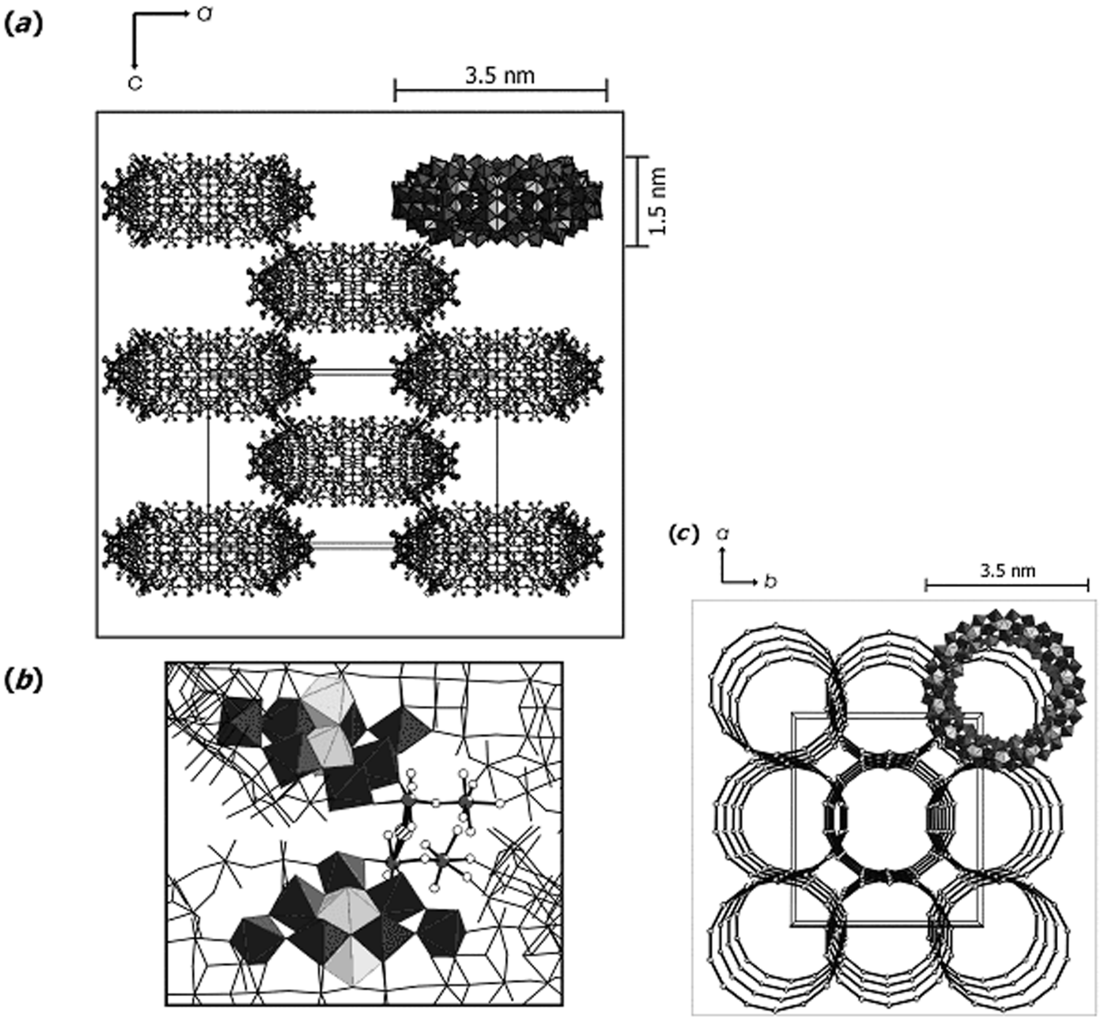

FIGURE 18 Ball and stick representation of the "packing" of the linked rings (in the direction of the *b* axis) in crystals of $Na_{16}[Mo^{VI}_{124}Mo^{V}_{28}O_{429}(\mu_3\text{-}O)_{28}H_{14}(H_2O)_{66.5}]$. XH_2O (X ≈300) ({Mo_{152}}) viewed along the crystallographic *b* axis. (a) Each ring is connected to surrounding rings via Mo-O-Mo bridges of the O=Mo-O-Mo-OH_2 units, thus forming layer networks parallel to the *ac* plane. One ring is shown as basic unit in polyhedral representation. (b) Detailed view of the bridging region between two cluster rings. One {Mo_8} unit of each ring along with one {Mo_1} unit is shown in polyhedral representation and one $\{Mo_2\}^{2+}$ $(=\{Mo^{VI}{}_2O_5(H_2O)_2\}^{2+})$ unit per ring in ball and stick representation. (c) Perspective view along the crystallographic *c* axis showing the framework with nanotubes that are filled with H_2O molecules and sodium cations. For clarity, only one ring is shown in a polyhedral representation. For the other rings only the equatorial {Mo_1} units are given and connected.

{Mo_{144}} defect cluster can be linked to chains (see Fig. 17) and an {Mo_{152}} cluster can be linked in the construction of a layered compound (see Fig. 18).

D. Nucleation Processes within a Cluster Cavity—from an {Mo_{176}} to an {Mo_{248}} Cluster

Under special types of reducing conditions (using ascorbic acid as a reducing agent) the {Mo_{176}} cluster can be observed to grow; during this process a further two {Mo_{36}} units are "added" to each side of the cluster forming a spherical disk-shaped cluster comprising 248 Mo atoms. The hubcaps were found in the mixed-crystal compound to have an occupation of 50%, see Fig. 19. This appears to be a remarkable result when it is considered that the larger wheel cluster "cap," the $[Mo_{36}O_{96}(H_2O)_{24}]$-type fragment, is nearly identical to a segment of the solid-state structure of the compound Mo_5O_{14} (see Fig. 20). This extraordinary structure (the largest discrete inorganic structure to be characterized by single crystal X-ray diffraction to date) offers the possibility of model crystal growth

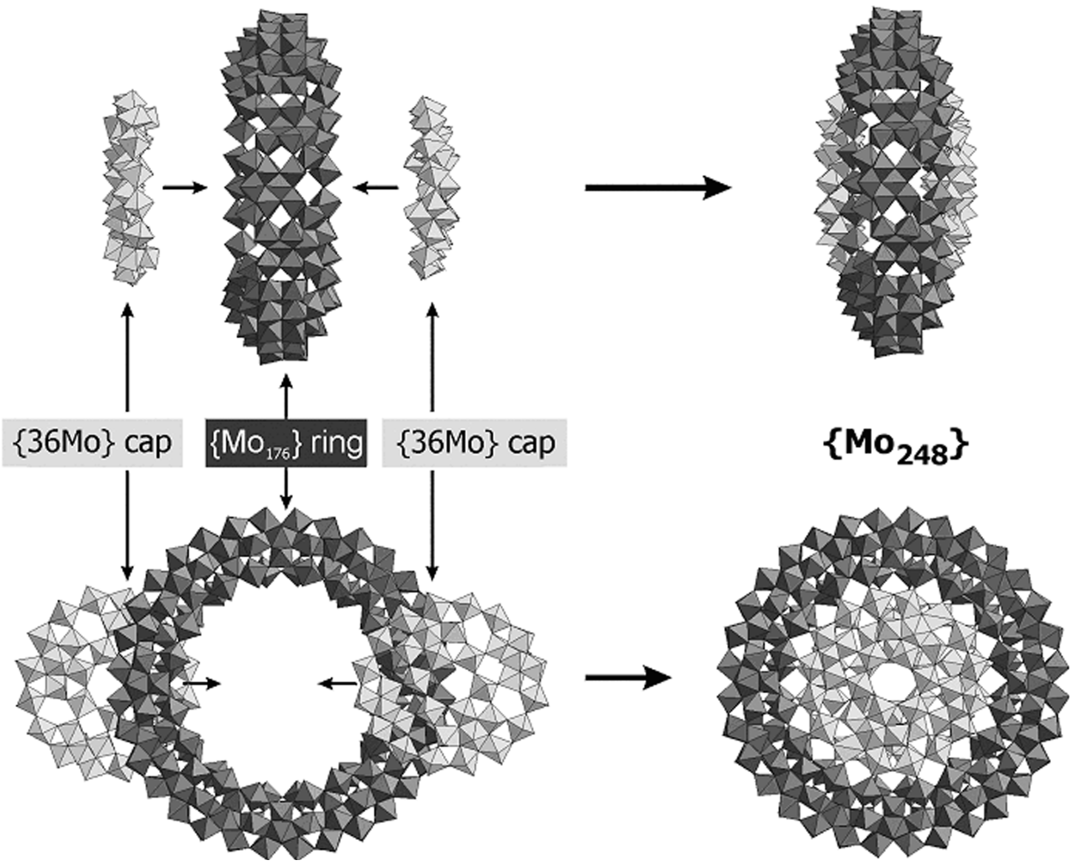

FIGURE 19 Schematic representation of the growth process $\{Mo_{176}\} \rightarrow \{Mo_{248}\}$. The structure of one $\{Mo_{248}\}$ cluster can formally be decomposed into one $\{Mo_{176}\}$ ring and two $\{Mo_{36}O_{96}(H_2O)_{24}\}$ "hubcaps."

under boundary conditions, especially the related nucleation process. Of particular note is that the growth event can be considered to start from the inner $\{Mo_2\}$ groups, see Fig. 19.

IV. CONCLUSIONS AND PERSPECTIVES

It seems to be worthwhile to try to correlate aspects of nanostructured giant discrete clusters and related solid-state structures, which is possible for molybdenum-oxide, metal-chalcogenide, and pure metal-based systems. On investigating the border region between the molecular and the macroscopic world, several questions arise, for instance, whether the size of such cluster systems has a limit or whether we can fabricate ever larger assemblages approaching (the limit of) the macroscopic world. The synthesis of gold, palladium, and related clusters protected with ligands or as colloidal dispersions may provide a direct route to new materials with novel electronic properties. From another point of view, the nanosized polyoxomolybdate clusters provide model objects for studies on the initial nucleation steps of crystallization processes, an interesting aspect for solid-state chemists and physicists as the initial steps for crystal growth are not known. It is remarkable that using the same reaction type, i.e., the acidification of aqueous solutions of the most simple tetrahedral oxoanions of the early transition elements of the type $MO_4{}^{n-}$, the (resulting) products span the three important areas of matter, from the micro-, through the meso- (or nano-), to the macrostructures, the latter being characterized by periodicity or translational invariance. The use of the above-mentioned fundamental linkable building units, e.g., in the form of Platonic solids such as tetrahedra or octahedra, enables the generation of molecular systems of higher structural variability and versatility compared to arrangements of aggregated metal atoms with spherical symmetry. It appears that through the synthesis of inorganic clusters man is developing a level of control from the molecular through the nanoscale to bulk material that will allow the construction of materials having a massive impact both in our understanding of conservative self-organization processes and the development of materials of interest for technology.

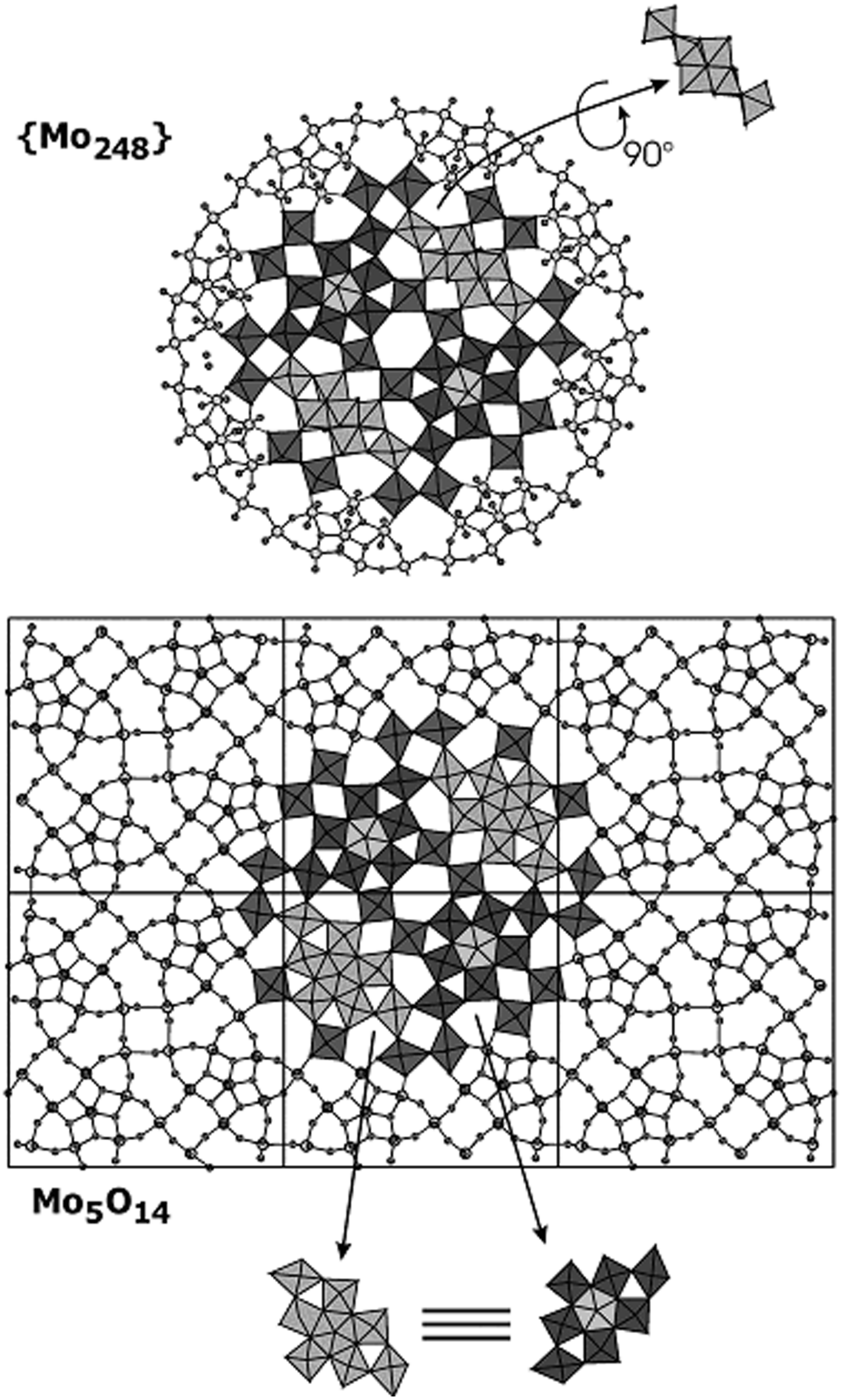

FIGURE 20 Structural comparison of the hubcap motif of the $\{Mo_{248}\}$ cluster (above) and the related segment of the solid-state structure $\{Mo_5O_{14}\}$ (below).

SEE ALSO THE FOLLOWING ARTICLES

Metal Cluster Chemistry • Metal Particles and Cluster Compounds • Solid-State Chemistry

BIBLIOGRAPHY

Cronin, L., Kögerler, P., and Müller, A. (2000). *J. Solid State Chem.* **152,** 57.

Kozitsyna, N. Y., and Moiseev, I. I. (1995). *Russ. Chem. Rev.* **84,** 47.

Müller, A., Fenske, D., and Kögerler, P. (1999). *Curr. Op. Solid State Mater. Chem.* **4,** 141.

Müller, A., Kögerler, P., and Bögge, H. (2000). *Struct Bonding* **96,** 203.

Müller, A., Kögerler, P., and Kuhlmann, C. (1999). *Chem. Commun.* 1347.

Schmid, G. (1996). In "From Simplicity to Complexity in Chemistry—and Beyond," (A. Müller, A. Dress, and F. Vögtle Part I, eds.), Vieweg Braunschweig, Wiesbaden, Germany.

Noble Metals (Chemistry)

Hubert Schmidbaur
Technical University of Munich, Garching

John L. Cihonski
Engelhard Corporation

I. Occurrence, Properties, and Chemistry
II. Applications
III. Toxicity

GLOSSARY

Black Dull black metallic powder obtained by reduction and precipitation from solutions or by condensation from the vapor phase.

Doré metal Silver–gold alloy usually derived from noble metal refining.

Filled Product with a gold or gold alloy coating mechanically clad to the surface.

Fineness Term used to define the degree of purity of gold or silver. Fineness is given as parts of the metal concerned per 1000 parts by weight.

Karatage K, term to express the degree of purity of gold. The karatage is expressed as pads of gold in 24 pads of alloy by weight. Pure gold is 24 karat or 1000 fine.

Mud Impure noble metals concentrate produced by removal of base metal from a predominately base metal anode.

Native Term used to describe a metal found as such in nature in relatively pure form.

Placer Alluvial, marine, or glacial deposit containing particles of valuable minerals, especially gold.

Platinum group metals (PGM) Second and third row Group VIII transition metals. These metals—platinum, palladium, iridium, rhodium, osmium, and ruthenium—are usually found together in nature.

Rolled Rolled gold or other metal product means the surface has been clad mechanically with a coating of gold or other metal. Rolled gold products carry thinner films of gold than do gold filled products.

Sponge Metal in porous form, usually prepared by reduction without sintering.

Sweeps Noble metal wastes from used items or production scrap.

THE NOBLE METALS, or precious metals, consist of gold, silver, and the platinum group metals (PGM)—platinum, palladium, iridium, rhodium, osmium, and ruthenium. These metals are known for their stability in corrosive environments, physical beauty, and unique physical and chemical properties. They command a premium price because of their low abundance in nature. The noble metals are used in many applications with great success and often with few, if any, substitutable materials.

I. OCCURRENCE, PROPERTIES, AND CHEMISTRY

A. Natural Occurrence

1. Gold

Gold is found in about 3.5 ppb in the earth's crust, often as 75–90% pure native gold that has been released by

weathering of sedimentary and igneous rocks. It accompanies silver and the base metals, copper and nickel, as the sulfides and selenides. Gold is also found in the telluride minerals, calaverite and sylvanite. The largest suppliers of gold are South Africa, Russia, and Canada, in their order of importance. In the U.S., about 60% of the gold produced is from ores and about 40% is a by-product of base metal production. Most U.S. production is in the Midwest and West (South Dakota, Nevada, Utah, and Arizona).

2. Silver

Silver is estimated at about 0.1 ppm in the earth's crust. Silver minerals are most commonly found with those of lead, but they can also be found in ores of copper, zinc, and gold. Ores with silver as the main component—argentite (Ag_2S), cerargyrite (AgCl), polybasite ($Ag_{16}Sb_2S_{11}$), proustite (Ag_3AsS_3), pyrargyrite (Ag_3SbS_3), and stephanite (Ag_5SbS_4)—are most often associated with igneous rocks of intermediate felsic composition. Native silver also occurs but most deposits of this type have been worked out. The majority of the world's silver is found in Mexico, U.S., Peru, Canada, Russia, Australia, and Japan. The major U.S. source is the Coeur d'Alene in Idaho.

3. Platinum and Palladium

The platinum group metals (PGM) are usually found together and are thus produced together. Their ratio depends on the ore location. Platinum is found in about 0.01 ppm in the earth's crust. The major forms are sperrylite ($PtAs_2$), cooperite (Pt, Pd)S, braggite (Pt, Pd, Ni)S, and as native metals in platinumiridium and palladiplatinum. The ores and metal are found in placer deposits derived from basic/ultrabasic igneous rocks. In sedimentary and igneous rocks the platinum is associated with chromite, magnetite, ilmenite, iridium, and osmium. The PGM deposits in the Merensky Reef in South Africa are found with iron, nickel, and copper ores. The total PGM concentration in the ore is in the 4–10 ppm range. In Canada, the Sudbury Area of Ontario is the major source of PGMs, where they are a by-product of nickel and copper production. The Ural Mountain and East Siberian deposits in the Russia are obtained as a by-product of nickel production.

Palladium has a concentration of about 0.005 ppm in the earth's crust. Beside cooperite and braggite, palladium is also found as potarite (PdHg or Pd_3Hg_2) or stibiopalladinite (Pd_3Sb) or as native palladium. The ratio of platinum to palladium varies with location but together these two metals account for about 90% of the PGMs. The Russia is the largest palladium producer, with Canada and South Africa following. The ores in the Russia are about 30% platinum and 60% palladium, whereas those in Canada are 43% platinum and 43% palladium, and in South Africa, approximately 64% platinum and 26% palladium.

4. Iridium and Osmium

Iridium and osmium are both found in the earth's crust in concentrations of about 0.001 ppm. These metals are most often found together in the alloys osmiridium or syserkite (less than or equal to 60% iridium and about 35% osmium), iridiosmium or neuyanskite (greater than 60% iridium and about 20% osmium), and osmium in lauritite (Ru, Os)S_2. Estimates indicate that the Russia is the largest supplier of iridium and South Africa has the largest supply of osmium.

5. Rhodium

Rhodium is present at about 0.001 ppm in the earth's crust. Its production is estimated to be as low as 2% and as high as 10% of the platinum production. Russia is thought to have about half of the world's supply.

6. Ruthenium

Ruthenium is estimated at 0.001 ppm in the crust and is isolated with the other noble metals mainly from laurite (Ru, Os)S_2.

B. Processing and Production

1. Gold

Gold is obtained as free metal in placer deposits or by mining of vein gold, with a minimum of about 3 ppm gold being required for its economic recovery. Approximately 92–96% of the gold is recovered from the ore and is often isolated with silver to produce doré metal. The method of separating gold and silver from each other depends on the relative concentrations. The most popular method is cyanidation with amalgamation being of secondary importance.

2. Silver

Silver is obtained through open pit and sub-surface mining chiefly as a low grade ore associated with copper, lead, and zinc. Silver is produced in the largest volume of all the noble metals, and it is separated by amalgamation and cyanidation.

3. Platinum Group Metals

The PGMs are isolated mainly for platinum and palladium. Iridium, osmium, rhodium, and ruthenium production is

TABLE I 1979–1983 World Noble Metal Production[a]

Year	Au	Ag	Pt	Pd	Ir	Rh	Os	Ru
1979	38,807	343,848	2755	3058	99	195	66	314
1980	39,197	339,382	2910	3212	105	207	72	330
1981	41,227	362,308	2875	3248	108	206	72	326
1982	42,713	372,528	2600	3200	101	192	66	287
1983	42,710	390,000	2600	3200	101	193	65	287

[a] Data times 1000 troy ounces. From the Bureau of Mines "Minerals Year Book," Mineral Industry Surveys—Platinum Quarterly, and "Metal Statistics 1984" from American Metal Market.

of secondary importance in mining because of the low concentrations of these elements in the ore. It is difficult to obtain more than an estimate of the production volumes of the rarer PGMs. The U.S. has only small occurrences of PGMs and is almost totally dependent on foreign production for them.

Table I shows the noble metal production for a recent five-year period from worldwide mining operations. This is new metal that has become available to the market and does not include scrap metals being recovered.

Separation and purification of gold, silver, and the PGMs are dependent on the ore, the metal concentration, and potential contaminating metals, such as base metals. Isolation of the noble metals is illustrated in Figure 1, which outlines the separation of the metals from an anode slime produced from a copper–nickel ore similar to that found in the Sudbury mines. The scheme can be altered depending on the relative metal concentrations and other metals present. The scheme shown depends on precipitation technology, but solvent extraction techniques that can change the order of metal separation have been developed. In South Africa, where the PGMs are found in higher concentrations, the base metal separation is not as significant a step.

Noble metal recovery from scrap can be difficult because of the heterogeneity of the material. Sometimes, it is more difficult to obtain metals in pure form from scrap than from ore. If proper allowances in refining are not made to account for contaminants, products may be obtained that are unsuitable for demanding applications.

The noble metals usually come from refiners in the form of sponge or ingot with 99.9% minimum purity. Sponge is a convenient form for catalyst and chemical preparation, whereas ingots are preferred for sheet, tube, and wire production. The metals are sold by the troy ounce with the price determined by purity, the general economy, and sudden changes in supply and demand.

C. Metal Properties

Noble metals are known for their stability, unusual physical properties, and beauty. Some useful properties are tabulated in Table II. Physical properties can vary significantly with minor changes in metal purity.

1. Gold

Gold is known mainly for its color, electrical conductivity, ductility, and corrosion resistance. The malleability of gold is the highest of all metals; 1.0 troy ounce can be spread to approximately 300 ft^2 of foil. Gold by itself is not strong enough for many applications and must be alloyed. It is resistant to oxygen, sulfur, selenium, and most reagents, even in the presence of air. It will react with tellurium at approximately 475°C and with the halogens in the presence of moisture. Dry chlorine above 80°C is corrosive to gold as are fluorine above 310°C and iodine above 480°C. The metal will react with aqua regia, hot H_2SO_4, or cyanide and alkali in the presence of an oxidizing agent and HCl/Cl_2, and arsenic and phosphorous acids. Gold has the highest atomic weight and ionization potential of the noble metals and the second lowest boiling point. It has one naturally occurring isotope, ^{197}Au, and 26 unstable ones, of which the most often used is ^{198}Au, with a half-life of 2.7 days. Gold and its alloys are available in many forms, such as ingot, wire, tubing, sheet, ribbon, sponge, and powder.

2. Silver

Silver, the whitest metal, has the highest thermal and electrical conductivity and good resistance to corrosion. It is less noble than gold, platinum, and palladium but nobler than copper. It has high resistance to alkali and oxygen at ambient temperatures and to organic acids. It resists anhydrous HF at high temperatures and HCl up to 225°C, but it has low resistance to chlorine above room temperature. Silver is tarnished by sulfur or sulfur compounds and is attacked by ozone, low-melting metals, hydrogen halides, alkaline cyanide with an oxidizing agent, nitric acid with a trace of nitrous acid, and hot H_2SO_4. Molten silver will dissolve about ten times its volume of oxygen (about 0.32 wt %) and eject it violently just prior to solidification, which can be a potential hazard. Solid silver will dissolve

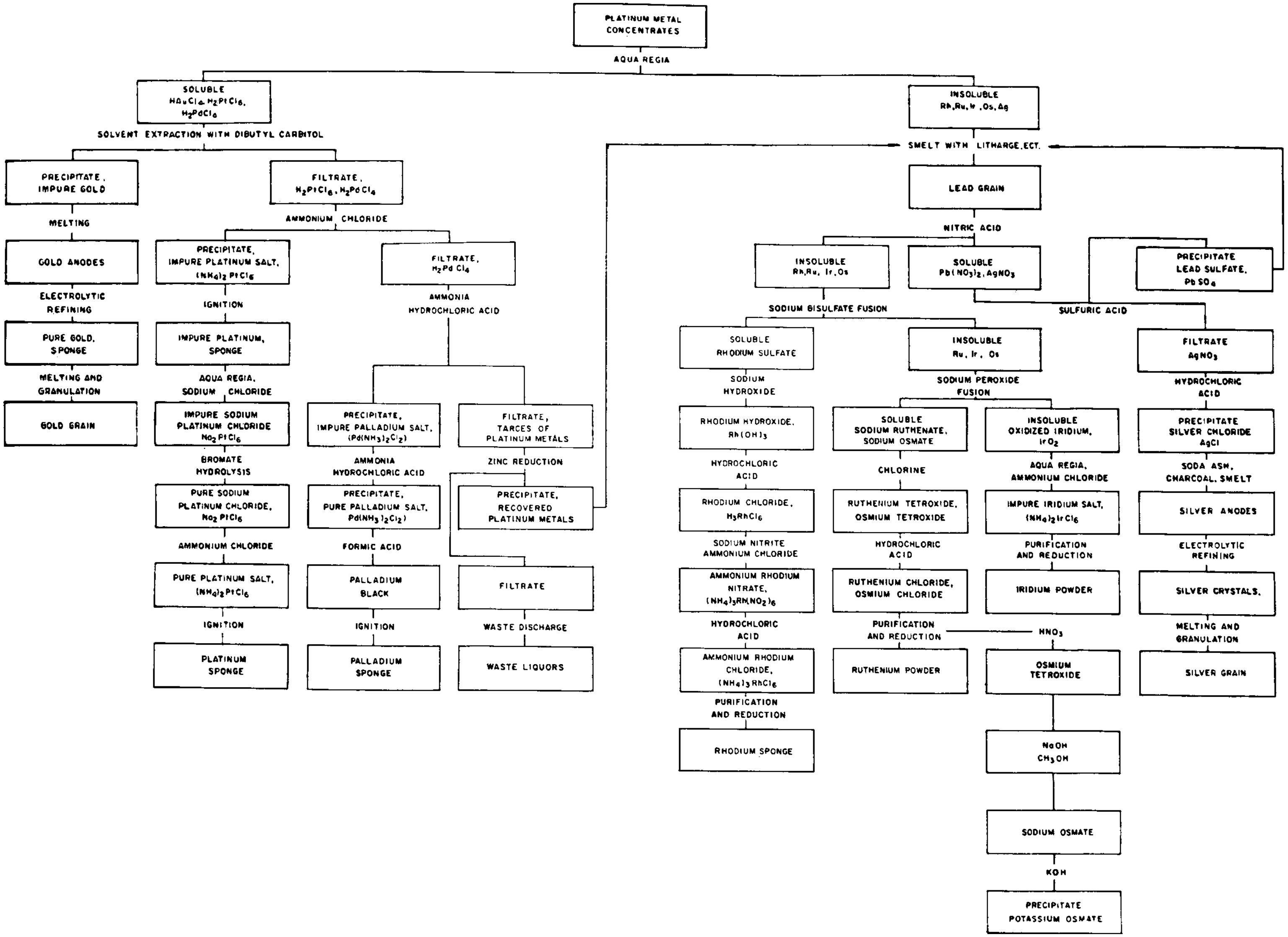

FIGURE 1 Noble metals process route at International Nickel Acton refinery. [Reprinted from Kirk, R. E., and Othmer, D. F. (eds.) (1982). "Encyclopedia of Chemical Technology," 3rd ed. Wiley, New York. Copyright 1982 John Wiley and Sons, New York.]

TABLE II Properties of Noble Metals[a]

Properties	Platinum	Palladium	Iridium	Rhodium	Osmium	Ruthenium	Gold	Silver	Units
Atomic Number	78	46	77	45	76	44	79	47	
Atomic Weight	195.09	106.4	192.2	102.905	190.2	101.07	196.967	107.870	Amu
Naturally Occurring Isotope	194 190 195 192 196 198	102 104 105 106 108 110	191 193	103	184 186 187 188 189 190 192	96 98 99 100 101 102 104	197	107 109	
Distance Closest Approach of Atoms	2.774	2.751	2.715	2.689	2.7341	2.7056	2.884	2.889	Angstrom Units
Crystal Structure	FCC	FCC	FCC	FCC	HCP	HCP	FCC	FCC	
Lattice Constant a	3.9231	3.8898	3.8394	3.8031	2.7341	2.7056	4.0786	4.0862	Angstrom Units
c/a					1.5799	1.5820			
	(Pt at 25°C)	(Pd at 25°C)	(Ir at 26°C)	(Rh at 25°C)	(Os at 26°C)	(Ru at 25°C)	(Au at 25°C)	(Ag at 25°C)	
Valence Electrons	$5D^9 6S^1$	$4D^{10}$	$5D^7 6S^2$	$4D^8 5S^1$	$5D^4 6S^2$	$4D^7 5S^1$	$5O^{10} 6S^1$	$^4D^9 5S^2$	
Chemical Valence	2, 4	2, 4	3, 4	3	4, 6, 8	3, 4, 6, 8	1, 3	1, 2, 3	
Magnetic Susceptibility	.971	5.23	0.133	.9903	.052	.427	−0.15	−0.181	X10-^{6} cgs units/gm
Ionization Potential	9.0	8.3	9	7.46	8.7	7.364	9.22	7.542	Electron Volts
Work Function Thermionic Emission	5.32–5.47	4.99	5.4	4.8	4.7	—	4.25	4.31	Electron volts
Thermal Neutron Capture Cross Section	8.8	8.0	440	149	15.3	2.56	98.8	63	Barns
Density at 20°C	21.45	12.02	22.65	12.41	22.61	12.45	19.32	10.49	g/cm^3
Vapor Pressure Pressure (mm Hg) 10^{-6}	1490	990	1810	1470	2160	1720	953	684	Temp. °C
10^{-5}	1610	1080	1950	1580	2310	1850	1038	751	
10^{-4}	1750	1190	2110	1710	2490	1990	1140	828	
10^{-3}	1910	1320	2290	1860	2690	2150	1260	918	
10^{-2}	2100	1460	2500	2040	2920	2350	1403	1028	
10^{-1}	2320	1650	2770	2250	3190	2590	1574	1163	
1	2590	1880	3090	2510	3530	2860	1786	1330	
10^1	2920	2180	3480	2840	3930	3210	2055	1543	
10^2	3340	2570	3980	3250	4440	3630	2412	1825	
Melting Point	1772	1554	2447	1963	3045	2310	1064.43	961.93	Temp. °C
Boiling Point	3800	2900	4500	3700	5020	4080	2808	2210	Temp. °C
Specific Heat	0.0314	0.0584	0.0307	0.0589	0.0309	0.0551	0.03077	0.0559	cal/gm
Thermal Conductivity 0–100°C	0.17447	0.182	0.354	0.3585	0.208	0.25083	0.743	1.0	cal-cm/sec-cm^2°C
Linear Coefficient of Thermal Expansion	9.1	11.6	6.8	8.3	6.1	9.1	14.2	19.68	X10–^{6}in/in.-°C
Electrical Resistivity	9.85	9.93	4.71	4.33	8.12	6.80	2.06	1.59	microhm-cm
Temperature Coefficient of Electrical Resistance	0.003927	0.003802	0.00427	0.00463	0.0042	0.0042	0.004	0.0041	0–100°C., per °C
EMF Vs. Pt at 1000°C	—	11.46	12.74	14.10	—	9.74	12.34 (at 800°C)	10.70 (at 700°C)	Millivolts
Tensile Strength (wire)	32–35,000 (50% cold worked)	47–60,000 (50% cold worked)	300–360,000 (hot drawn)	200–230,000 (cold drawn)	—	72,000 (hot swagedbar)	30–32,000 (60% cold worked)	42,000 (50% cold worked)	psi

continues

TABLE II Properties of Nobel Metals[a] (*continued*)

Properties	Platinum	Palladium	Iridium	Rhodium	Osmium	Ruthenium	Gold	Silver	Units
Tensile Strength									
Annealed (wire)	18–24,000	21–33,000	160–180,000	120–130,000	—	—	18–20,000	18.2–27,000	psi
Percent Elongation Annealed									
(2″ length wire).......	30–38	29–34	20–22	30–35	—	—	39–45	43–50	
Percent Elongation (2″ length wire).......	1.0–2.0 (50% cold worked)	1.5–2.0 (50% cold worked)	5–18 (hot drawn)	2.0 (cold drawn)	—	3 (as hot worked)	4 (60% cold worked)	3–5 (50% cold worked)	
Hardness (wire).........	90–95DPN (50% cold worked)	105–110DPN (50% cold worked)	650–700DPN (hot drawn)	530DPN (cold drawn)	—	—	55–60DPN (60% cold worked)	—	
Hardness Annealed (wire)	37–42DPN	37–44DPN	200–240DPN	120–140DPN	—	200–350DPN	25–27DPN	25–30DPN	
Hardness, as cast........	43DPN	44DPN	210–240DPN	—	800DPN	170–450DPN	33DPN	—	
Young's Modulus at 20°C									
Static................	24.8	16.7	75	46.2	81	60	11.2	10.3–11.3	$\times 10^4$psi
Dynamic.............	24.5	17.6	76.5	54.8	—	69			$\times 10^4$psi
Modulus of Rigidity at									
20°C	8.8	6.5	30.4	21.6	—	24.6	4.0	3.9–4.2	$\times 10^4$psi
Poisson's Ratio	0.39	0.39	0.26	0.26	—	0.30	0.42	0.37	

[a] From "Platinum Palladium Gold and Their Alloys." (Reprinted with permission from the Engelhard Corporation.)

hydrogen as well as oxygen. When silver is cold worked, its density is lowered, which may be due to oxygen incorporation into the lattice. The two stable isotopes are ^{107}Ag and ^{109}Ag, but there are 25 reported radioisotopes. The commercial forms of silver are similar to those of gold.

3. Platinum

Platinum is harder than gold, softer than silver, and can be cold worked to increase its hardness. It is resistant to acids at room temperature, $FeCl_3$, HCl without an oxidizing agent, SO_2, H_2SO_4, persulfuric acids, Na_2CO_3 to 800–900°C under nonoxidizing conditions, sulfides with alkali, molten glass, and urban sulfur. Platinum is attacked by aqua regia, HCl with oxidizing agents, HBr with bromine, free halogens at elevated temperatures, cyanides, and some phosphates. It is attacked slightly by oxygen at temperatures greater than 750°C. It can absorb a large volume of hydrogen and, in a finely divided state, reject the gas violently on heating. The metal is available in the same forms as are gold and silver.

4. Palladium

Palladium is the second most important PGM. Similar to gold and platinum, it can be beaten into leaf and is easily cold and hot worked. Contamination with low-melting metals causes embrittlement; with base metals, hardening and a decrease in corrosion resistance; and with silicon, a loss in hot strength. Palladium absorbs over 800 times its volume of hydrogen, which is expelled when heated. The metal also acts as a diffusion barrier for hydrogen purification. Hydrogen can be used as a deoxidizer to produce very dense ingots. Other suitable deoxidizing agents are aluminum, calcium boride, and carbon monoxide.

Palladium is less resistant to corrosion than is platinum, but it is inert to HF(aq), $HClO_4$, and H_3PO_4 at ambient temperatures and molten $NaNO_3$ or KNO_3. Palladium will tarnish with SO_2 and be slowly attacked by H_2SO_4, HOAc, HCl, and HBr. More potent agents are HNO_3, $FeCl_3$, HCl, moist halides, Na_2O_2, and Na_2CO_3. The commercial forms are similar to those found for platinum.

5. Iridium

Iridium is the only known metal that can be used up to 2000°C in oxygen without catastrophic failure. This element is difficult to fabricate because it rapidly work-hardens and crumbles to a powder. It is worked at 1200–1500°C and drawn into wire at 600–700°C. Working at lower temperatures increases hardness and lowers ductility. Iridium is not attacked by oxygen, common acids, hot H_2SO_4, or aqua regia at ordinary temperatures. It is attacked by aqua regia at elevated temperature and pressure and by NaClO. The common commercial forms are similar to platinum.

6. Rhodium

Rhodium has the highest electrical conductivity, thermal conductivity, and reflectivity of any PGM. It is similar to iridium. It is difficult to fabricate and is resistant to corrosion. The major corrosive agents are moist iodine, NaClO, hot H_2SO_4, and hot HBr.

7. Osmium

Osmium melts at 3045°C. It is a hard, heavy element that is easily oxidized in air to toxic OsO_4. The ease with which this oxide is formed demands caution. Osmium is difficult to work with because of its hardness at low temperatures and the possible formation of OsO_4 at elevated temperatures. It is very resistant to rubbing wear, resistant to H_2SO_4 and 40% HF at ambient temperatures, and 36% HCl at 100°C but is easily attacked by oxygen, HNO_3, and aqua regia.

8. Ruthenium

Ruthenium is one of the hardest elements known. It has good corrosion resistance and is not attacked by common acids, aqua regia up to 100°C, H_2SO_4 up to 500°C, or most molten metals in the absence of oxygen. It is slowly attacked by alkaline hypochlorites and is more rapidly attacked by chlorine and Na_2O_2. Ruthenium cannot be cold worked and is hot worked only with difficulty.

D. Alloys

Alloys, multicomponent elemental compositions in solid solution, exist in the substitutional or interstitial forms depending on the relative size of the elements. Substitutional alloys form when the components have similar radii so that one element can easily be replaced by another without disrupting the overall lattice. If the radii vary by approximately 15% or more, the resulting lattice structure may be different from that of the elements because of packing preferences. In general, the more ordered the alloy, the more ductile, malleable, and better conducting it is compared to a disordered structure. If the alloying element is small enough, it will not disrupt the structure, but it will fit into the interstitial positions in the lattice to give the material different properties. Some elements capable of forming this type of structure are hydrogen, boron, carbon, and nitrogen. By varying the size, electronic structure, and ratio of the alloying elements, a series of materials with useful properties can be fabricated. This section addresses the most commonly used precious metal alloys and the properties that make them important.

1. Gold

Gold alloys are used in a wide variety of applications. Most alloys with greater than 50% gold are resistant to tarnish and corrosion. The scale for rating gold alloys used in jewelry fabrication is the karatage scale: pure gold is 24 karat (or 1000 fine). The karat rating relates to the amount of gold in an alloy and does not relay any information concerning the makeup of the remainder of the alloy. For example, a 12-karat gold item will have 50% gold. Alloys below 14 karats are susceptible to stress corrosion cracking.

Common gold alloys, including Au–Ag, are soft and malleable. Gold–copper alloys are harder, more fusible, and have higher tensile strength than does pure gold. Iron alloys of gold have a lower melting point than does pure gold, and the iron-rich phase is ferromagnetic. Gold–platinum alloys have good corrosion resistance and better mechanical properties than does gold itself. By varying the ratio of gold, silver, and copper, the green, yellow, and red golds can be produced; Au–Ni–Cu(Zn) alloys are white golds. Gold has been alloyed with elements of the main group, transition group, and some of the lanthanide elements.

Zinc is commonly added to gold jewelry alloys to deoxidize, lighten the color, decrease the hardening that may occur on air cooling, and lower the melting point. Fractional percentages of iridium or rhodium together with ruthenium reduce the grain size of the alloy, which will impart increased strength, hardness, and toughness to the alloy.

Aside from the structured alloys, gold has been studied in several glassy metal, amorphous forms. Widely referenced are Au_4Si, which was the first commercially produced glass ribbon, $La_{80}Au_{20}$, which has superconducting properties, $Co_{62}Au_{38}$, $Fe_{60}Au_{40}$, and Au–Ge–Si. These glassy systems are produced by rapidly cooling a liquid system to a solid while maintaining the disorder of the liquid. The glasses crystallize to an ordered structure on heating. The amorphous alloys generally are magnetically soft, mechanically strong, show high electrical resistivities and superconductivity as a type II or "dirty" superconductor, corrosion resistant because of the lack of structural defects and grain boundaries, and will become brittle on mild heating.

2. Silver

Silver alloys with a substantial number of metals such as aluminum, silicon, nickel, copper, zinc, gallium, germanium, cadmium, indium, tin, paltinum, gold, mercury, tellurium, and lead are known. The most common Ag–Cu alloy is sterling silver, 92.5 Ag–7.5 Cu, known for its wear resistance and hardness. As the copper content is increased, the melting point, electrical conductivity, and thermal conductivity are lowered. The oxygen content in the alloy is decreased by the addition of a trace amount of phosphorous. In alloys such as Ag–Mg, the magnesium is oxidized on heating, which serves to harden the alloy to more than double its original strength. In general, trace amounts of oxidizable impurities harden the alloy and restrain grain growth. Tarnish resistant silver and silver alloys can be obtained by either coating with nickel then rhodium or by adding 50% palladium or 70% gold to

the silver. The glassy metal alloys consisting of $Cu_{50}Ag_{50}$ and $Pd_{90}Ag_{10}$ have been characterized.

3. Platinum

Platinum has been used frequently as the predominant metal in alloy mixtures. In general, sulfur attacks alloyed platinum more readily than it does the unalloyed metal. Platinum hardness can be increased in the general order tungsten > nickel > ruthenium > osmium > copper > gold > iridium > rhodium > palladium, with the last yielding the softest alloy. The electrical resistivity can also be related to the alloying element with tungsten > copper > ruthenium > osmium > nickel > iridium > palladium > rhodium, in order of decreasing resistivity.

Some of the most common platinum alloys involve Pt–Pd. Where palladium comprises 25% of the alloy, it performs similarly to platinum. The resistance to HNO_3 decreases as the palladium content increases. Platinum–iridium alloys of approximately 10% iridium have good tarnish and corrosion resistance; resistance to aqua regia increases as the iridium content increases, and workability decreases. Platinum–iridium use is not recommended above 800°C in air because a black oxide film will form. Commercial Pt–Rh alloys contain 5–40% rhodium but most commonly contain 10% rhodium. These alloys are preferred to platinum in high-temperature oxidizing conditions, and they can be hot or cold worked. Above 40%, rhodium fabrication can be difficult. The Pt–Ru alloy is similar to the Pt–Ir alloy except that less ruthenium is required for similar properties. For example, 5% ruthenium will act similarly to 10% iridium. The ruthenium alloy is not suitable for high-temperature service under strong oxidizing conditions because ruthenium can volatilize as the oxide; Pt–Rh–Ru alloys have high tensile strengths, hardness, good corrosion resistance, weldability, and stability in electrical uses. These alloys are sensitive to impurities. They are very slowly attacked by aqua regia. Platinum–cobalt alloys with approximately 50 at. % cobalt make excellent permanent magnets for use in many specialty applications; Pt–Ni and Pt–W are alloys that are known for both their hardness and strength. At high temperatures under oxidizing conditions, selective oxidation of the nickel and tungsten occurs.

4. Palladium

Common palladium alloys include Pd–Ag with 1–60% Pd; this material is tarnish resistant at greater than 50% Pd. The alloys are attacked by HNO_3 and cyanide but are resistant to HCl except in the presence of oxidizing agents; Pd–Ag–Cu, Pd–Ag–Au, and Pd–Au alloys also show good corrosion resistance; and Pd–Cu, Pd–Ni, and Pd–Ru alloys are harder than palladium. Rhodium and ruthenium are often used together with palladium as with platinum to improve hardness and mechanical strength. Examples of palladium glassy alloys are $Pd_{80}Si_{20}$, which has high strength and good ductility, and $Pd_{90}Ag_{10}$.

5. Iridium

Iridium is most often used as the minor component in alloy mixtures, often with less than 20% iridium. Above 20% iridium, the alloy loses ductility and becomes difficult to process. Common alloys are Ir–Os, osmiridium. Iridium containing a small percentage of ruthenium melts several hundred degrees higher than iridium. Iridium is used to increase palladium and platinum hardness and corrosion resistance. The intermetallic compounds Ti_3r, $ThIr_2$, Nb_2Ir, and Th_7Ir_3 have been shown to possess superconducting properties. Iridium–tungsten alloys have increased tensile strengths, especially at high temperatures. Glassy metal alloy systems such as $Ta_{55}Ir_{45}$ and $Nb_{55}Ir_{45}$ are known.

6. Rhodium

Rhodium is most commonly alloyed with platinum and palladium to improve corrosion resistance and mechanical properties at high temperatures. Rhodium improves the corrosion resistance of chromium and titanium to nonoxidizing acids. Alloys of titanium, approximately 3% max, increase the tensile strength of the rhodium. The alloy $Ni_{63}Rh_{37}$ shows better corrosion resistance than does 14-karat gold. Rhodium does not form a continuous series of solutions with osmium or ruthenium because they crystallize in different structures. The rhodium-containing amorphous alloys $Ta_{55}Rh_{45}$, $Nb_{60}Rh_{40}$, $Nb_{55}Rh_{45}$, and $Mo_{82}Rh_{18}$ have been characterized.

7. Osmium

Osmium is used mostly as a hardening agent in alloys, but this application has limited use because of formation of the toxic OsO_4. The known alloys osmiridium, found naturally, and 85Os–15Pt are extremely hard and are used in some specialty applications where hardness is of primary importance.

8. Ruthenium

Ruthenium is used most often as a hardening agent for platinum and palladium. The major alloy is Pt–Ru with 10–15% ruthenium. Special alloys with 30–70% ruthenium are used in applications in which resistance to severe wear and corrosion is required. Ruthenium is replacing iridium as a hardening agent because it is more effective and less expensive. The glassy metal alloy Mo_xRu_{1-x} is known to have superconducting properties.

E. Chemistry

The noble metals, while being relatively unreactive in the metallic state, have a rich and varied chemistry. In general,

the second-row metals and their compounds are more reactive than their third-row counterparts. This introduction to noble metal chemistry deals mainly with the diversity of compounds and their preparations. A complete list of the common compounds is not given here because there are several excellent compilations.

The precious metals form a variety of salts, coordination complexes, and organometallic compounds. The metals are discussed individually to gain some understanding of how the compounds are formed and what ligands will stabilize a particular oxidation state.

1. Gold

Gold compounds are known in the (−I), (I), (II), (III), and (V) oxidation states. The linearly two-coordinate gold(I) and square planar four-coordinate gold(III) complexes are the most common.

Common gold salts are obtained in a number of reactions from the metal: $[Au(CN)_2]^-$ by reaction with cyanide, alkali, and oxygen; $AuCl_3$ by reaction with chlorine; and $HAuCl_4$ by reaction with aqua regia. Figure 2 is a tabulation of some representative gold chemistry.

Gold(I), d^{10}, compounds are the largest group of gold-containing species and include salts, complexes, and organometallic derivatives. Most salts (e.g., AuCl) are unstable in aqueous solution and will disproportionate to the gold(III) salt and metal. All binary gold(I) sulfides are thermodynamically unstable, accounting for the noble character of gold. The complexes of gold(I) usually involve the halides or pseudohalides and phosphorus, arsenic, sulfur, and nitrogen-containing ligands. Gold(I) is a "soft" metal center with a preference for "soft" donor atoms. Substitution reactions follow this pattern. Organometallic derivatives include alkyl, aryl, alkenyl, alkynyl, and carbene complexes. They are usually formed by ligand exchange using a Grignard or organolithium reagent with a gold(I) halide. Gold(I) π-complexes with olefins are not as stable as the platinum analogs. The Au–C bond can be stabilized with PR_3, AsR_3, R_2S, and RNC. Alkylgold(I) complexes can undergo oxidative addition with CH_3l or halogen to yield four-coordinate gold(III) derivatives.

$Na[Au(CN)_2]$ and $K[Au(CN)_2]$ are used extensively for electrochemical or electroless guilding and in the recovery and recycling of gold. Gold(I) thiosulfate, thiomalate, and thiogluconate esters are important gold drugs (chrysotherapy of polyarthritis). Gold thiolates are the basis for "liquid golds" in gold plating.

Gold(III), d^8, is isoelectronic with platinum(II) and is responsible for the second largest portion of gold chemistry. The halides are known as well as binary and ternary oxides. Complexes, especially the gold halides, form readily and numerous examples are known with nitrogen, phosphorus, arsenic, sulfur, and selenium donor atoms. Complexes with bi- and tridentate phosphino and amino ligands are also formed. The complexes can be prepared by ligand exchange or by oxidative addition to a gold(I) compound. Gold(III) organometallic compounds with up to four organic groups bound to the central

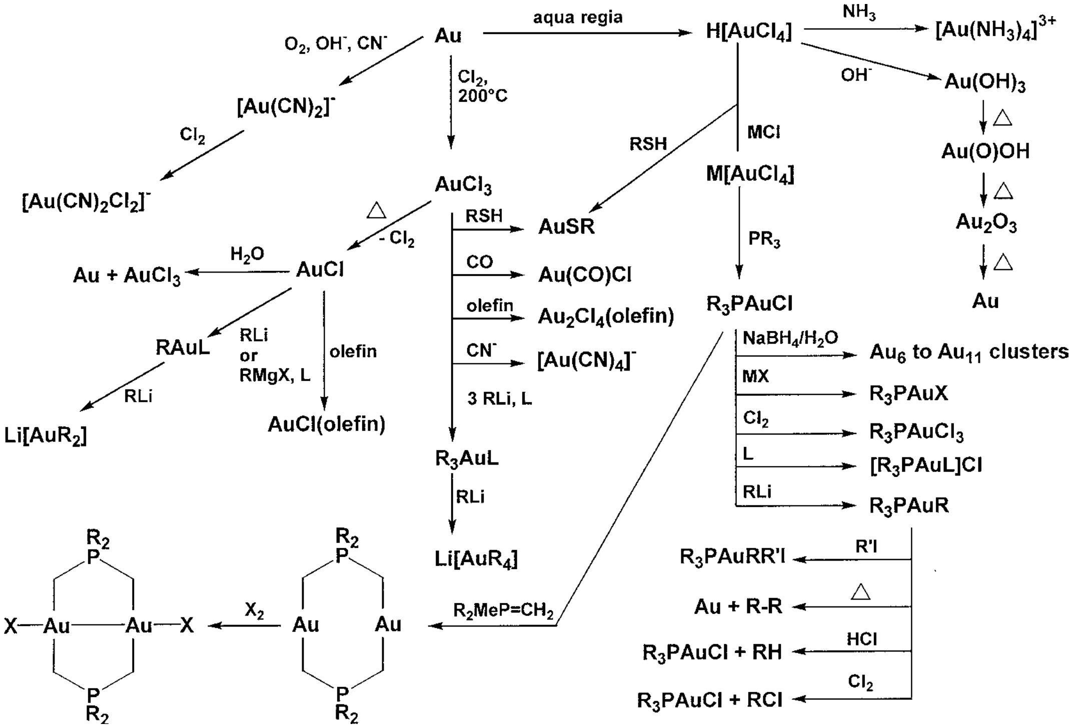

FIGURE 2 Representative gold chemistry.

atom are available. Reductive elimination reactions lead to organogold(I) compounds.

Gold(−I) is formed when the metal is reacted with elemental cesium or with sodium or lithium in liquid amonia to yield CsAu, NaAu, or LiAu. Gold(II), d^9, is present in dinuclear gold compounds with direct Au–Au bonding, mainly in metalla-bicyclic prototypes, which are formed by oxidative addition of halogen across the rings. Mononuclear gold(II) species are found in dithiolene, dithiolate, and dicarbollyl complexes. Phosphorus ylides $R_3P = CH_2$ form a particularly large class of stable organogold compounds (Fig. 2) of gold(I), gold(II) and gold(III).

Gold(V), d^6, is known in AuF_5 and in $[AuF_6]^-$ salts that are prepared by the action of fluorine on the metal.

2. Silver

Silver(I), (II), (III) compounds are known. Silver metal will react with cyanide in air, HNO_3, or the halogens to form the commercially important salts $[Ag(CN)_2]^-$, $AgNO_3$, AgCl, and AgBr, respectively. Figure 3 illustrates some common silver chemistry beginning with the metal. Silver halides and pseudohalides are generally known for their insolubility in water, but the nitrate, chlorate, and perchlorate are soluble. The halides are light sensitive and are used extensively in photographic emulsions.

Most silver(I), d^{10}, compounds can easily be obtained by ligand exchange with $AgNO_3$. A partial list of the salts includes halides, cyanide, azide, acetylide, carbonate, chromate, oxide, sulfide, sulfite, permanganate, phosphate, thiocyanate, and thiosulfate, as well as the soluble salts mentioned previously. Silver(I) linear two-coordinate complexes are known with amines, cyanide, nitrile, halide, phosphine, arsine, sulfide, and selenide ligand systems. Coordination complexes involving oxygen donor ligands are less common. If excess ligand is present, small amounts of three- and four-coordinate products will form. Complicated polynuclear systems result when polydentate ligands are used, because of their inability to bond in a linear fashion around a single metal center. The organometallic chemistry of silver(I) is very limited, with unstable olefin compounds making up the major fraction. Silver alkyl and aryl species are much less stable than both the copper and the gold analogs. Phosphorus ylides form the most stable organosilver(I) compounds (Fig. 3). With F_3C substituents, even organosilver(III) complexes can be isolated. The olefin complexes can be obtained by direct reaction with a silver(I) salt.

Silver(II), d^9, is paramagnetic and is present in salts such as AgF_2, a strong oxidizing agent. AgO is diamagnetic and is, in fact, a mixed valence system $Ag^IAg^{III}O_2$. Silver(II) complexes are mainly known for nitrogen donor ligands (e.g., pyridine and *o*-phenanthroline) and are four-coordinate square planar. The complexes are often prepared by peroxysulfate or ozone oxidation of silver(I).

Silver(III), d^8, salts are limited in number and are only confirmed for a series of ternary oxides. The four-coordinate silver(III) complexes of ethylenedibiguanidine and porphyrin have been isolated. Complexes of the anions $[AgF_4]^-$ and $[Ag(OH)_4]^-$ are strong oxidants.

3. Platinum

Platinum forms compounds in the (−I)–(VI) oxidation states. The four-coordinate platinum(II) and

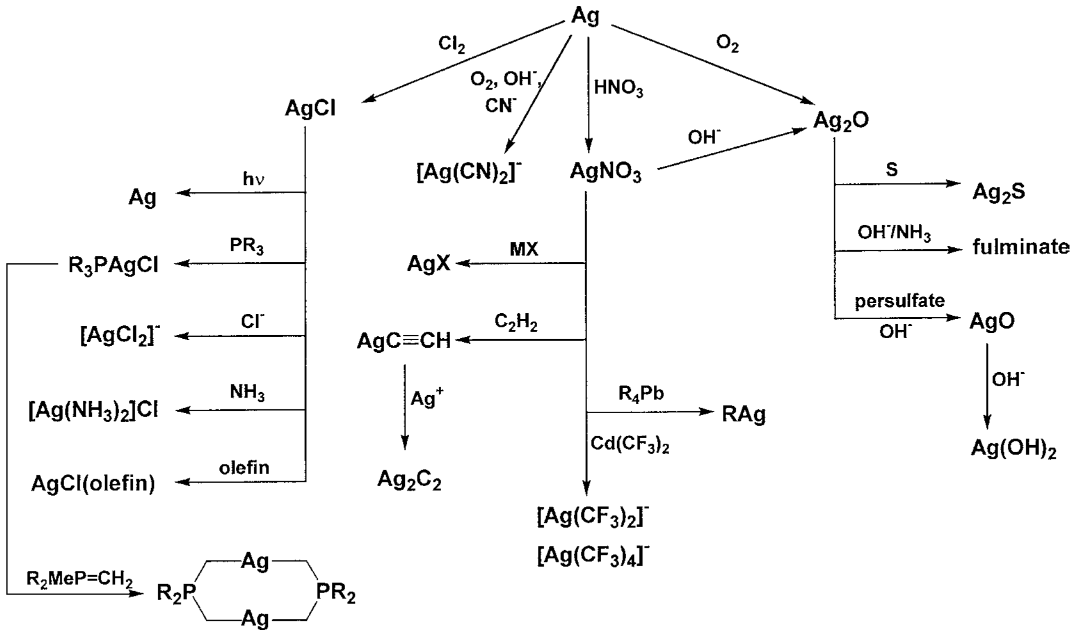

FIGURE 3 Representative silver chemistry.

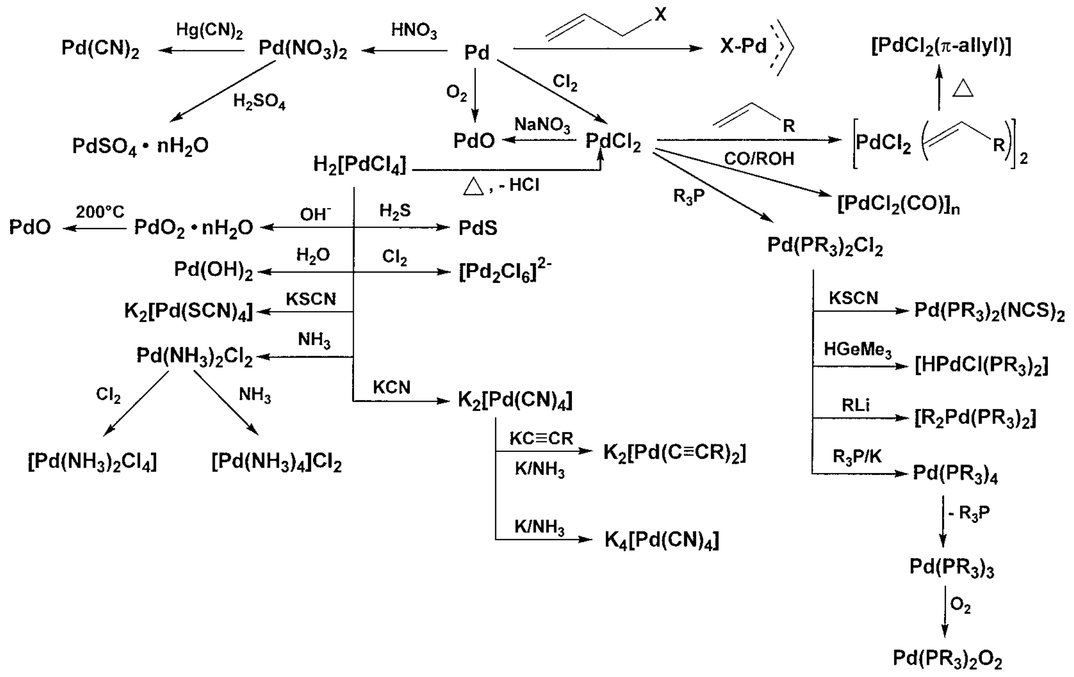

FIGURE 4 Representative palladium chemistry.

six-coordinate platinum(IV) complexes are the most common. Platinum chemistry is similar to that of palladium but the higher oxidation states are more stable for platinum than for palladium. (Figure 4 illustrates some common *palladium* chemistry). The metal will react with HCl and oxygen, aqua regia, chlorine, fluorine, and molten oxides.

Platinum(0) complexes form with phosphine, amine, and carbonyl ligands (e.g., $Pt(PR_3)_4$ and $[Pt(CO)_2]_n$). These complexes are produced either by reduction of a platinum(II) compound in the presence of the ligand or by direct reaction of the metal with a ligand such as PF_3.

Platinum(II), d^8, compounds are similar to those of palladium, but in general they are less reactive. The halides, except for PtF_2, and the oxide and hydroxide are well known. Pt(II) complexes are mainly square planar but there are some five-coordinate species. The most common ligands involve halogen, nitrogen, phosphorus, arsenic, sulfur, selenium, and carbon donor atoms. Little preference is shown for hard bases, such as fluoride and oxide, but nitrate, sulfate, carbonate, and acetylacetonate compounds are known. Because of the stability of the complexes, they have been widely used as models in reaction mechanism studies. Platinum(II) complexes can undergo oxidative addition, but the reaction tends to be reversible because of the stability of the Pt(II) state. Platinum forms bridged complexes of the formula $[Pt_2X_6]^{2-}$, where X is an anionic ligand. Compounds of the type $[Pt(NH_3)_4][PtCl_4]$, Magnus green salt, can stack by metal–metal interaction along the z axis to form columnar structures. The complexes are formed by ligand addition or exchange with an easily obtained compound (e.g., $PtCl_2$ or $K_2[PtCl_4]$). $[Pt(NH_3)_4]Cl_2 \cdot H_2O$ is used as a catalyst (for hydrogenation) and in galvanization. $K_2[Pt(NO_3)_4]$ and the explosive $[(NH_3)_2Pt(NO_3)_2]$ are also used in electrochemistry, because they are free of chlorine. *Cis*-$[(NH_3)_2PtCl_2]$ is an important drug in cancer therapy (*cis*-platinum).

The extensive organometallic chemistry of platinum(II) involves carbonyl, acyl, isocyano, alkyl, aryl, olefin, diene, and acetylene complexes. The carbonyl, isocyanide, olefin, diene, and acetylene compounds are formed by direct addition of the ligand to the salt or complex. The alkyls and aryls are prepared by an exchange reaction using a Grignard or organolithium reagent. The acyl compound is obtained from the alkyl derivative by CO insertion. Organoplatinum(II) compounds are important catalysts in organic synthesis.

Platinum(IV), d^6, salts with halides and pseudohalides or with ligands featuring oxygen, sulfur, selenium, and tellurium as donor atoms are known. Chloroplatinic acid, $H_2[PtCl_6]$, is easily prepared from the metal (with aqua regia), and it is the most important synthetic starting material (as is the hexahydrate). Like its potassium salt, it is deep yellow. The hexahydroxo complex $H_2[Pt(OH)_6]$ is insoluble in water. It is used as a precursor for the preparation of catalysts such as $PtO_2 \cdot H_2O$. $H_2[PtCl_6]$ is the basis for the preparation of Speier's catalyst for hydrosilylation. Mixed ligand platinum(IV) complexes can be prepared by oxidative addition to platinum(II) compounds.

The organometallic chemistry of platinum(IV) is limited to the alkyl derivatives. They are formed either by oxidative addition starting with platinum(II) or by displacement using a Grignard reagent.

The formal platinum(−I) state is present in cluster compounds such as $[Pt_3(CO)_3]^{2-}$ and other Pt–Pt bonded species such as $[C_5H_5Pt(CO)]_2$. Platinum(III), d^7, has been proposed in PtX_3, $X = $ Cl, Br, I, and $Pt(NH_3)_2Br_3$, but the compounds are mixed valence species of platinum (II) and platinum(IV). Platinum(V), d^5, and platinum(VI), d^4, are represented by fluoro and oxyfluoro derivatives [e.g., PtF_5, $PtOF_3$ for platinum(V) and PtF_6, $PtOF_4$, and PtO_3 for platinum(VI)]. These compounds are strong oxidizing agents.

4. Palladium

Palladium is found in the (0) through (IV) oxidation states. The four-coordinate square planar complexes of palladium(II) are the most common. Figure 4 outlines some common palladium chemistry. The metal is easily oxidized. It dissolves in aqua regia and in HCl or HNO_3 in the presence of oxygen to form $H_2[PdCl_4]$.

The palladium(0) complexes [e.g., $Pd(PPh_3)_4$ and $[Pd(dba)_2$ (dba = dibenzylidene-acetone)] are formed by reduction of the palladium(II) analog. Alkyne, alkene, and nitroso derivatives are also known, the more stable palladium(0) complexes being formed with ligands having strong π-acceptor ability.

Palladium(II), d^8, salts include the halide, oxide, hydoxide, sulfide, selenide, telluride, nitrate, sulfate, cyanide, and thiocyanide derivatives. $PdCl_2$ is a coordination polymer, insoluble in water, but soluble in aqueous chloride solution. It is used in catalysis and for galvanization. Stable complexes are formed with halide, nitrogen, phosphorus, arsenic, and antimony donor atoms. $[Pd(NH_3)_2Cl_2]$, $[Pd(NH_3)_4]Cl_2$, $[Pd(NH_3)_2(NO_3)_2]$, and $[Pd(CH_3COO)_2]_3$ are important commercial products for the electronics industry. Oxygen donor and fluoro complexes do not form as readily. An exception to this is the high stability of the acetylacetonate complex. Palladium—like platinum—forms ligand bridged complexes. In four-coordinate Pd(II) complexes the fifth and sixth coordination sites are taken up by weakly bound solvent molecules. As with platinum(II), palladium(II) complexes are well suited for structural and mechanistic studies.

The organometallic chemistry of palladium(II) is similar to that of platinum(II) except that the palladium compounds are less stable. This lability permits a wide variety of useful catalytic reactions (e.g., palladium olefin complexes in the Wacker process). Prominent examples are the formation and reaction of π-allyl complexes. The π-allyl complexes can be formed from an olefin bound to palladium(II) on heating or by the reaction of an allyl halide or alcohol with palladium(0). More π-allyl complexes are known with palladium than with any other metal.

Palladium(IV), d^6, is the second most common oxidation state for palladium, but it is not as common as the platinum(IV) state. The salts include mainly the fluoride, oxide, and nitrate counterions. Six-coordinate complexes are known involving fluoro, chloro, phosphine, arsine, and amine ligands, but most compounds are only stable in the presence of excess oxidizing agent.

Palladium(I), d^9, is found in a few complexes of the type $[PdCl(CO)]_n$ and $PdCl(CO)PPh_3$. Palladium(III), d^7, is formally present in "PdF_3" and "$Pd(NH_3)_2Cl_3$". However, the paramagnetism of "PdF_3" has been shown to be caused by high-spin palladium(II) in $Pd^{II}[Pd^{IV}F_6]$ and not by the d^7 configuration of palladium(III).

5. Iridium

Iridium compounds are known for oxidation states (−II)–(VI); the (I), (III), and (V) states are the most common. The metal itself is very noble and will not dissolve in aqua regia, but it will react with oxygen or chlorine at red heat to give the respective salts, and it can be converted to IrO_2 by peroxide fusion. The oxide, IrO_2, can also be obtained by reaction of the metal with alcohol and KNO_3. It is used for catalysts and for electrodes. The chloride is formed by reaction with chlorine and KCl or HCl and $NaClO_4$. Iridium(0) complexes are derived from iridium(I) and iridium(III) compounds by reduction. The $[Ir(CO)_4]_n$ and $Ir_4(CO)_{12}$ cluster species are standard examples.

In the absence of auxiliary ligands, the iridium(I), d^8, salts are limited to the chloride, bromide, and iodide, which are obtained by decomposition of the iridium(III) analogs. The major chemistry of this oxidation state involves complexes and organometallics. Iridium(I) complexes, in general, incorporate π-acceptor ligands to stabilize the low oxidation state, and they undergo oxidative additions easily to form iridium(III) complexes. The species commonly have carbonyl, nitrosyl, phosphine, arsine, olefin, diene, and acetylene ligands. Two of the most important iridium(I) complexes are Vaska's compound, $IrCl(CO)(PPh_3)_2$, which is a good model for the activation and oxidative addition of simple molecules (e.g., hydrogen, chlorine, oxygen, and HCl), and $[Ir(COD)Cl]_2$ (COD = cyclooctadiene-1,5), which is a catalyst.

Simple iridium(III), d^6, salts may contain halide, oxide, hydroxide, sulfide, and selenide ligands. $IrCl_3 \cdot (H_2O)_n$ is soluble in water and is the basis for the preparation of many other products (catalysts, electrodes etc.). The complexes are usually six-coordinate and rather inert. A large number of complexes are known, incorporating ligands with donor atoms such as oxygen, nitrogen, phosphorus, arsenic, and antimony. Iridium(III) forms a particularly large number of hydride complexes, mainly with phosphine and

arsine donor ligands. The complexes are formed by reduction of iridium(IV) species or by oxidative addition to iridium(I) compounds. The organometallics comprise carbonyl, alkyl, aryl, and π-complexing ligands. The carbonyls can be prepared by direct reaction of CO with the iridium(III) halide salt. The alkyl and aryl complexes are synthesized using Grignard or lithium alkyl reagents.

Iridium(IV), d^5, salts of halides, hydroxide, sulfide, selenide, and telluride have been reported. The commercial product $H_2[IrCl_6] \cdot 6H_2O$ is water soluble and acts as a catalyst. IrO_2 is prepared from the hexahydroxo complex. Iridium(IV) does not form many complexes, but the six-coordinate halides (excluding the iodo species), and some amine and pyridine complexes are known. Compounds with phosphorus, arsenic, and sulfur donor atoms are not stable; these ligands reduce iridium(IV) to the iridium(III) state.

Iridium(V), d^4, and iridium(VI), d^3, compounds are limited to the fluoride and oxide derivatives. Known species are IrF_5 and $[IrF_6]^-$ for iridium(V), and IrF_6 and IrO_3 for iridium(VI).

6. Rhodium

Rhodium has chemistry similar to that of iridium, but its compounds are more labile than their iridium analogs. Figure 5 is an outline of some common rhodium chemistry, with many of the reactions also applying to iridium. Rhodium is found in oxidation states (—I) through (V). The most common states are (I) and (III), with coordination numbers of four (square planar) and six (octahedral), respectively.

The metal is inert to aqua regia but $Rh(OH)_3$ can be prepared by fusing rhodium with sodium bisulfate followed by water and alkali. Rhodium(0) complexes are derived from $RhCl_3$ by direct reaction with CO to form $Rh_2(CO)_8$, and the clusters $Rh_4(CO)_{12}$ and $Rh_6(CO)_{16}$.

Rhodium(I), d^8, compounds are comprised almost entirely of π-acceptor ligand complexes, which serve to stabilize the low oxidation state. The most significant ligands are carbonyl, phosphine, arsine, stibine, π-acceptor nitrogen compounds, nitrosyl, cyanide, cyclopentadienyl, olefin, diene, acetylene, and allyl species. Complexes containing hydride, halide, and oxygen donor ligands (e.g., acetate and acetylacetonate) are known in combination with π-acceptor ligands. Rhodium(I) complexes are prepared by ligand exchange with another rhodium(I) complex or by reducing a rhodium(III) species with alcohol, $SnCl_2$, or $CO \cdot [(CO)_2Rh(acac)]$, $[(CO)Ph_3P)Rh(acac)]$, $[RhH(CO)(PPh_3)_3]$, and $[Rh(COD)Cl]$ are the most common catalysts (acac = acetylacetonate; COD = cyclooctadiene-1,5). $[ClRh(PPh_3)_3]$ is known as Wilkinson's catalyst (for hydrogenation).

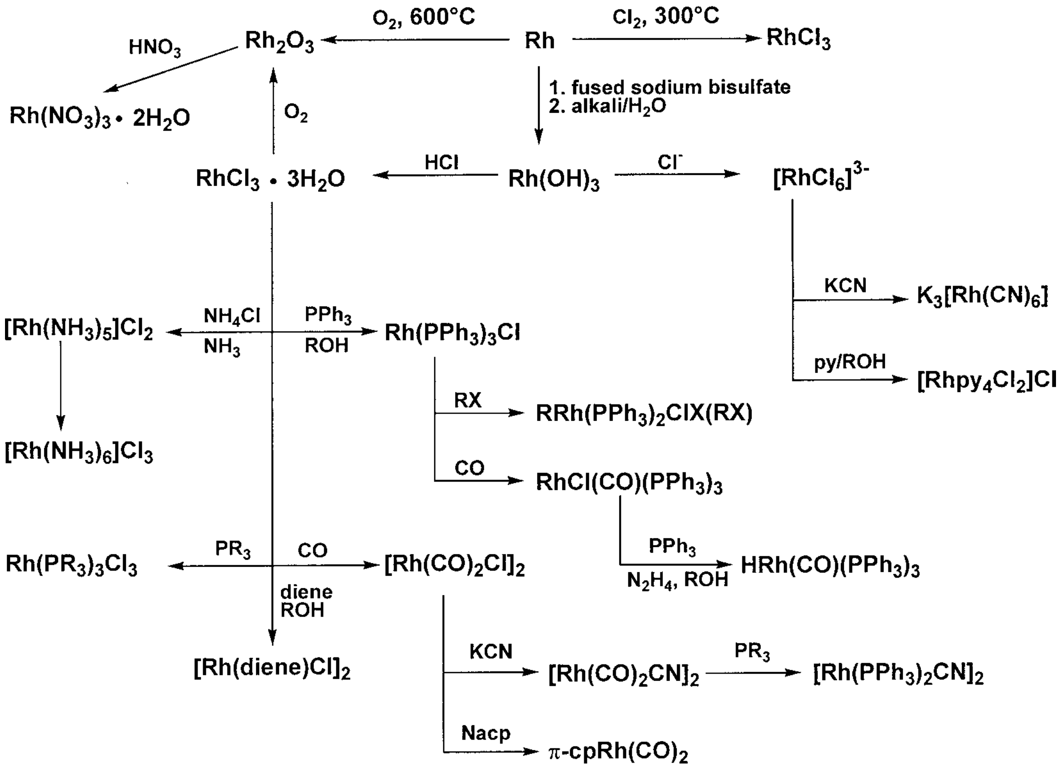

FIGURE 5 Representative rhodium chemistry.

Rhodium(II), d^7, is present in dinuclear metal–metal bonded complexes of the type $[Rh_2(CH_3COO)_8] \cdot H_2O$, with bridging acetate groups.

Rhodium(III), d^6, is the most common oxidation state. The water soluble hydrate of $RhCl_3$ and the hexaquo complex $[Rh(H_2O)_6]_2(SO_4)_3$ are valuable starting materials for other rhodium compounds. The most common ligands are the halides (except iodide), cyanide, thiocyanide, amines and other nitrogen donors, nitrate, sulfate, carboxylate, and polydentate donors such as ethylenediaminetetraacetic acid (EDTA). Few compounds containing phosphine and arsine ligands are known. Rhodium(III) has an extensive organometallic chemistry involving carbonyl, thiocarbonyl, alkyl, aryl, π-allyl, cyclopentadienyl, olefin, and diene ligands. The alkyls and aryls are often prepared by oxidative addition to rhodium(I) compounds. The rhodium(III) olefin complexes are unstable and very few are known.

Rhodium(−I) is found in complexes with π-acceptor ligands to stabilize the low oxidation state. Examples of this state are $[Rh(CO)_2(PPh_3)_2]^-$, and $[Rh(PF_3)_4]^-$.

Rhodium(II), d^7, is present in dinuclear carboxylato complexes with four bridging ligands and Rh–Rh bonding.

Rhodium(IV), d^5, is known in several fluoride, chloride, and oxide compounds. Rhodium(IV) can be obtained either by oxidation of rhodium(III) with ozone, sodium bimuthate, ceric sulfate, or by anodic oxidation, or by reduction of rhodium(VI).

Rhodium(V), d^4, derivatives are known as the fluoride and chloride salts and the complex $Cs[RhF_6]$.

Rhodium(VI), d^3, appears in RhF_6 and $K_2[RhO_4]$.

7. Osmium

The chemistry of osmium and ruthenium is similar but, except for a few areas, their chemistry does not parallel that of iron. Figure 6 illustrates some of the chemistry of ruthenium, which in general also applies to osmium. The osmium derivatives are usually more stable than the ruthenium analogs, and osmium has more stable higher oxidation states. Osmium is found in the (−II)–(VIII) states with (III), (IV), and (VI) as the most common, showing a preference for six-coordination.

The metal will react readily with oxygen, chlorine, or fluorine to yield the respective products. The metal will also react slowly with nitric acid to give OsO_4. Osmium(0) compounds involve several carbonyls, as well as phosphine, amine, arene, diene complexes, and the well-studied osmium clusters. The compounds are usually prepared by reducing an osmium salt in the presence of the appropriate ligand and, if necessary, a halide acceptor such as copper, silver, or zinc salts.

Osmium(III), d^5, compounds consist of the halide salts, except fluoride, and complexes involving halides, amines, and acetylacetonate, as well as some mixed ligand species involving phosphines and arsines. These complexes are

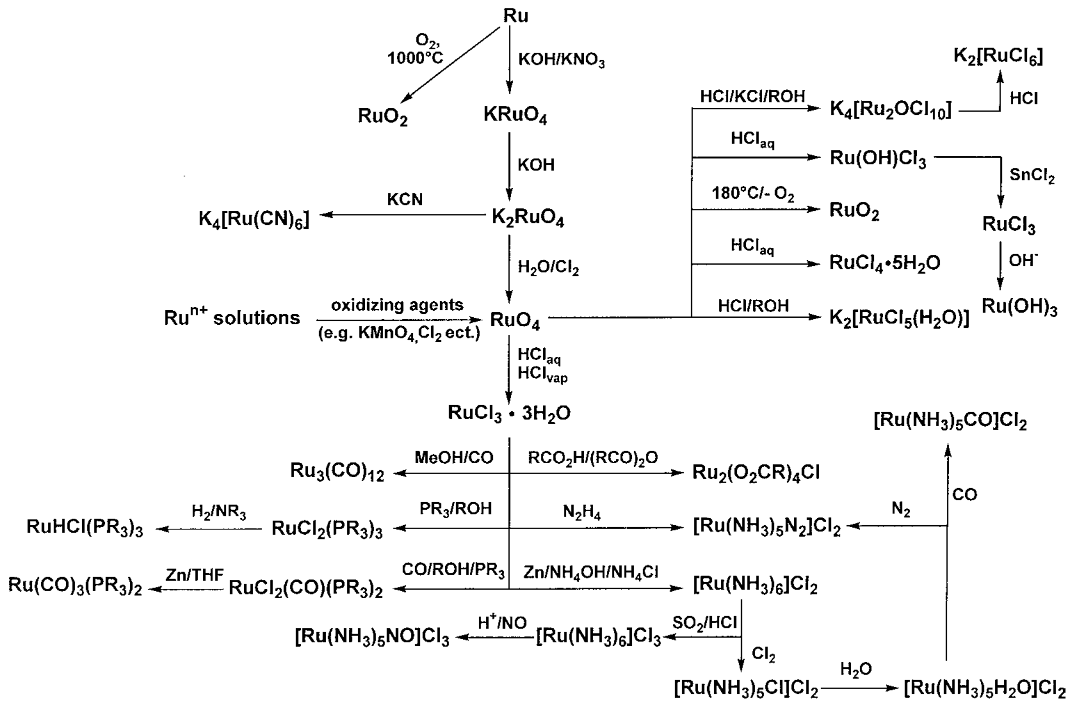

FIGURE 6 Representative ruthenium chemistry.

usually prepared by substitution of osmium(III) or by reducing an osmium(IV) derivative.

Osmium(IV), d^4, halides are the most important osmium salts, with $K_2[OsCl_6]$ as the most prominent example. The most common complexes of osmium(IV) involve oxygen donor ligands.

Osmium(VI), d^2, is present in OsF_6, $OsOF_4$, and $OsOCl_4$. OsF_6 is the most stable of the PGM hexafluorides. OsO_3 has been detected only in the vapor phase. Other complexes prepared by reduction of OsO_4, include $[OsO_2(OH)_4]^{2-}$, $[OsO_2Cl_4]^{2-}$, $[OsO_5]^{4-}$, $[OsO_6]^{6-}$, and $[OsO_2(NO_3)_2(NO_2)_2]^{2-}$.

For osmium(−II), the complexes $[Os(CO)_4]^{2-}$ and $[Os(PF_3)_4]^{2-}$ are known. Osmium(I), d^7, is found in polynuclear complexes like $[Os(CO)_4Cl]_2$ and $Os(C_5H_5)(CO)$, and in a series of carbonyl hydrides [e.g., $H_4Os_4(CO)_{12}$].

Osmium(II), d^6, occurs in OsI_2 and in a number of π-acceptor ligand complexes (e.g., cyanide, nitrosyl, phosphine, arsine, stibine, and carbonyl). The most interesting species are the dinitrogen complexes $[Os(NH_3)_5N_2]^{2+}$, $[Os(NH_3)_4N_2]^{2+}$, and $OsCl_2(PEt_3)_2N_2$, which are prototypes for nitrogen fixation models. Osmium(II) complexes are prepared by reducing osmium(III) or osmium(IV) compounds. Osmium(V), d^3, species are limited to OsF_5 and $[OsF_6]^-$.

Osmium(VII), d^1, is found in OsF_7 and $OsOF_5$ obtained from the metal or from OsO_2.

Osmium(VIII), d^0, compounds are foremost represented by the strong oxidizing agent OsO_4 and the osmiamates $[OsO_3N]^-$ and $OsO_3=N(i\mathrm{Bu})$. The tetroxide is volatile and toxic so proper care must be taken with its use. It has a simple tetrahedral structure, but is soluble in water to form hydrates. Usage is generally limited due to the high toxicity of most compounds with osmium in high oxidation states.

8. Ruthenium

Ruthenium is known in oxidation states (−II)–(VIII), the (II), (III), and (IV) states, with six-coordination being the most common. Figure 6 outlines some typical ruthenium chemistry. The metal is inert to mineral acids, but will react with fluorine, bromine, BrF_3, or oxygen at 1000°C. It will also react with KOH and KNO_3 to yield $K[RuO_4]$, which is a good starting material for other compounds. Ruthenium(0) carbonyl complexes and clusters are obtained by the reduction of a ruthenium(III) halide [e.g., $Ru(CO)_5$, $Ru_2Os(CO)_{12}$, and $Ru_6C(CO)_{17}$].

Ruthenium(II), d^6, is known as the binary bromide and as $[RuCl_4]^{2-}$. The richer complex chemistry involves stable compounds with cyanide, amines, halides, water, nitrosyl, carbonyl, hydride, phosphine, arsine, stibine, arene, and cyclopentadienyl ligands. $[RuCl_2(PPh_3)_2]$ is used as a catalyst. Ruthenium(II) is a good π-donor and was the first metal ion found to complex dinitrogen (as $[Ru(NH_3)_5N_2]^{2+}$), as was discussed for osmium. Ruthenium(II) forms many cationic, neutral, and anionic species with nitrosyl ligands that serve as models for understanding the role of the nitrosyl function in coordination chemistry. Ruthenium(II) species are usually derived from ruthenium(III) salts or other ruthenium(II) complexes.

Ruthenium(III), d^5, is ruthenium's most stable oxidation state and resembles rhodium(III) and iridium(III) more than osmium(III). The salts include the halides, hydroxides, and oxides; $RuCl_3 \cdot 3H_2O$ is most important because it is a good starting material for other compounds and reacts readily with olefins and phosphines. Complexes of this oxidation state are known with water, cyanide, oxygenated organics, such as β-diketones and carboxylates, pyridines, carbonyls, cyclopentadienyls, phosphine, and arsine ligands. A notable difference between ruthenium(II) and ruthenium(III) is the absence of ruthenium(III) nitrosyl complexes.

Ruthenium(IV), d^4, forms a more limited number of complexes involving mainly the halides (except the iodide), oxalate, and sulfate, together with π-acceptor nitrogen donor ligands. RuO_2 is used as a catalyst and as an electrode material.

The ruthenium(I), d^7, chloride, bromide, and iodide salts have been characterized in solution but not as solids. The complexes involve π-acceptor ligands [e.g., $[Ru(CO)Br]_n$ and $[(C_5H_5)Ru(CO)_2]_2$]. The compounds are derived from ruthenium(III) salts. Ruthenium(V), d^3, compounds are limited to RuF_5, $[RuF_6]^-$, and the oxide Ru_2O_5. Ruthenium(VI), d^2, is known in RuF_6, $RuOF_4$, $[RuO_4]^{2-}$, and $H_2[RuO_2Cl_4]$; the first three are prepared from the metal. The ruthenium(VII), d^1, state is present in $K[RuO_4]$ and the ruthenium(VIII), d^0, state in RuO_4. RuO_4 is a stronger oxidizing agent than OsO_4, and is less stable. It can decompose explosively at temperatures greater than 180°C to yield RuO_2 and oxygen.

F. Analytical Procedures

Analysis of the precious metals is very important when the economics of metal recovery from ore or scrap is considered. The purity of refined metal is also critical because trace impurities can be responsible for a product's lack of performance. For these reasons, it is important to have dependable analytical methods.

The method of sample preparation and analysis will depend on the form of the metal (ore, complex, metal, etc.), its concentration, and the presence of potentially interfering species. If noble metals are mixed with base metals, the latter must be removed first, followed by noble metal separation. The chemistry of noble metal separation is similar to that used in the refining of the metals, but it can be greatly simplified by knowning what elements are present.

1. Gold

In most cases, the gold sample involves gold metal or salts that can be converted easily to the chloride complex for further analysis. This method of putting the gold into solution can be used for samples that are predominantly gold (e.g., ingot) or predominantly extraneous material (e.g., alloy or ore). Gold is usually converted to $[AuCl_4]^-$ by dissolving it in aqua regia, purifying to remove NO_x and then concentrating the sample by solvent-extraction if necessary. The most common analytical methods are gravimetric, titration, and spectrometric. Fire assaying involves fusing the sample with fluxes, litharge, and a reducing agent to obtain a lead button containing the precious metals. The base metals and lead can be removed to yield the gold, silver, and PGMs, which can then be analyzed further. The precipitation of gold from a $[AuCl_4]^-$ solution can be done by using $C_2O_4^{2-}$, SO_2, or hydroquinone. Hydroquinone is best because it does not bring down the PGMs. A third gravimetric method involves the precipitation of a gold complex. The common chelating agents used in this method are dimethylglyoxime, tetraamisole, thiophenol, and 8-quinolinol. Determination of gold by the titration of gold(III) to gold(0) can be followed potentiometrically or coulometrically using hydroquinone as the reducing agent. Interference by other metals can be decreased by extraction of the gold complex into an organic solvent (e.g., diethyl ether, ethyl acetate, methylisobutyl ketone, or dichloromethane–tetrahydrofuran). Very small quantities of gold in other metals or trace impurities in gold can be determined by emission spectroscopy, atomic absorption spectroscopy, and neutron activation.

2. Silver

The methods used for silver analysis are similar to those used for gold. Spectrophotometrically, silver can be determined to trace levels by a rhodanine derivative, with mercury and iron interfering, or a pyrogallol red complex, where common anions can interfere. Cation interference can be minimized by using EDTA as a masking agent. Silver can be determined volumetrically, either indirectly, by reacting copper metal with silver(I) and then titrating the resulting copper(II) with EDTA, or directly, by titrating silver (I) with a halide using dithizone in carbon tetrachloride as an indicator. Gravimetric determinations can be made using 1,2,3-benzotriazole and its derivatives in acid, 1-amidino-2-thiourea in base, or a halide. Silver can be determined electrochemically by amperometric titration using sodium diethyldithiocarbamate or by polarography. As with gold, silver can be determined by atomic absorption, emission spectroscopy, and neutron activation.

3. Platinum

High concentrations of platinum can be determined with X-ray emission spectroscopy (e.g., as platinum metal or in alloys). Low to trace levels of metal can be analyzed with optical emission spectroscopy or by spectrophotometric analysis using stannous chloride and *p*-nitrosodimethylaniline. Platinum analysis can be done by gravimetric analysis using thermal decomposition of a compound, but since no specific reagent is known, the metal must be isolated from the interfering elements. The platinum must be in the (IV) state and free of nitrate. The platinum is isolated by treatment with NH_4Cl, followed by reduction with an agent such as formate. Atomic absorption is an excellent method as long as the sample can be put into solution. Methods for polarographic and X-ray fluorescence techniques are also known. Volumetric methods, in general, are not satisfactory for platinum or the other PGMs.

4. Palladium

For the other PGMs, aside from atomic absorption, the most common analytical methods are gravimetric and spectrophotometric. For the palladium gravimetric procedure, there are over 50 reagents; the most common are the oximes. Gold is the only interfering metal, and it can be removed by reduction with oxalate. Since PdO will form on burning, the combustion product must be treated with methanol vapor to reduce the surface oxide to the metal. The common colorimetric reagents are thiocyanate, *p*-nitroaniline derivatives, and 8-mercaptoquinoline. The colorimetric method does not have a significant advantage over the gravimetric method.

5. Iridium

Iridium is best determined gravimetrically as IrO_2, which can be reduced to the metal. There are no specific gravimetric reagents for iridium. Spectrophotometrically, the $[IrCl_6]^{2-}$ complex can be used to determine iridium, or the reagent $SnBr_2$ can be used if rhodium, palladium, and platinum are absent.

6. Rhodium

Rhodium is quantified spectrophotometrically with $SnBr_2$ or gravimetrically by precipitating the rhodium with H_2S, burning, and then reducing with hydrogen.

7. Osmium

Gravimetric analysis of osmium is accomplished by the reaction of osmium(VIII), as OsO_4 with 1,2,3-benzotriazol

to yield the complex $Os(OH)_3(C_6H_4N_2NH)_3$, which is then dried and weighed. Spectrophotometrically, thiourea and its derivatives are used for this determination.

8. Ruthenium

Spectrophotometric analysis of ruthenium is the same as that used for osmium. Gravimetrically, there is no specific reagent, so it is analyzed by conversion to RuO_4 precipitated, and then reduced at approximately 750°C to yield the metal.

II. APPLICATIONS

An attempt was made to break the precious metal applications down into major subsections to allow for their similar chemistry or use. In Table III, the U.S. noble metal usage for the years 1979–1983 is tabulated. Data for 1983 show that U.S. gold consumption was approximately 3,081,000 troy oz. A rough breakdown shows 1,696,000 troy oz used in jewelry and decorative applications, 1,030,000 troy oz in industrial applications, 352,000 troy oz in dental and medical uses, and approximately 3000 troy oz for investment purposes. Table IV lists the major silver uses for 1983, and Table V is a tabulation of 1983 U.S. consumption of the platinum group metals by application.

A. Plating

Noble metal plating is used where improved appearance, protection, special surface properties, or engineering or mechanical properties are required. Examples of the importance of this technique are found in electronics and solar reflectors or absorbers.

The metals are commonly applied by means of electrolytic plating, nonelectrolytic catalytic plating, and solutions contaning organometallic compounds that can be fired to yield a metallic coating. Electrolytic plating, in which a metallic anionic salt is plated onto an article acting as the anode, is the oldest technique. Nonelectrolytic electroless plating can be accomplished by two methods. Immersion plating is done by reducing a salt of the metal to be coated with the less noble metal from which the article is made. Immersion deposits can be powdery and the deposits cannot be built up to a thickness comparable with that obtained by the electrolytic method. The second method, autocatalytic plating, involves the controlled chemical reduction of the salt, which is catalyzed by the metal already deposited. A catalyst, usually $PdCl_2$ reduced with $SnCl_2$, is required to start the deposition process. This method has the advantages of unlimited throwing power, little or no excess deposit on high points, excellent physical and chemical properties, and the ability to coat hard to reach places such as the insides of items. The disadvantages are the need for a reducing agent and the cost. A third coating technique uses an organometallic complex or stable colloid system that will adhere to the surface. It is fired to leave a smooth film. Low-firing

TABLE III 1979–1983 U.S. Noble Metal Consumption[a]

Year	Au	Ag	Pt	Pd	Ir	Rh	Os	Ru
1979	4785	157,200	1409	1133	17	83	1	113
1980	3215	124,700	1118	912	24	74	1	78
1981	3276	116,600	873	889	8	62	1	88
1982	3448	118,800	780	926	11	50	1.4	87
1983	3081	120,000	789	825	5	100	1.4	144

[a] Data times 1000 troy ounces. Tabulated from "Metal Statistics 1984." American Metal Market.

TABLE IV 1983 U.S. Silver Consumption by Application[a]

Application	Consumption
Photography	51,800
Electrical	27,800
Sterling silver	7,100
Jewelry	7,100
Brazing/soldering	6,900
Electroplating	3,500
Coins, bullion	3,000
Batteries	3,000
Catalysts	2,400
Dental/medical	1,600
Mirrors	1,000
Miscellaneous	4,800
Total	120,000

[a] Data times 1000 troy ounces. From "Metal Statistics 1984." American Metal Market.

TABLE V 1983 U.S. Platinum Group Metals Consumption by Application[a]

Application	Pt	Pd	Ir	Rh	Os	Ru
Automotive	508	172	0.04	82	—	—
Chemical	65	40	0.6	4	0.4	55
Petroleum	38	50	1.0	—	—	0.2
Glass	15	0.1	0.04	2	—	—
Electrical	69	216	1.0	2	—	71
Dental/medical	16	280	0.1	0.2	1.0	0.2
Jewelry/decorative	10	6	0.8	2	—	1
Miscellaneous	68	60	1.3	8	—	17
Total	789	824.1	4.3	100.2	1.4	144.4

[a] Data times 1000 troy ounces. Data is tabulated from "Metal Statistics 1984." American Metal Market.

materials (approximately 260°C) have been introduced, which make it practical to consider firing fiberglass and high-temperature plastics. Other plating methods are hot dipping, chemical vapor deposition sputtering, and vacuum evaporation. Multiple metal coatings are used for special purposes. These alloy coatings require more care to produce, but similar results cannot be obtained from single metal coatings.

1. Gold

Gold was deposited by coating the article with a Au–Hg alloy and then heating it to remove the mercury. Currently, electrolytic gold plating is done using $[Au(CN)_2]^-$ or, to a lesser extent, $[Au(SO_3)_3]^{3-}$, usually as the potassium salt. Baths have been formulated using acidic, neutral, and basic solutions to which agents are added to tie up impurities and to brighten, harden, and control the metal grain size. Gold alloys have been prepared with antimony, tin, nickel, copper, silver, indium, and cobalt. Many of these coatings were developed for use in the jewelry and electronics industry. Electroless plating uses a palladium catalyst with reducing agents such as hydrazine or hypophosphite. Once the gold starts to deposit, it becomes the catalyst for further plating. The organometallic golds known as liquid golds can be prepared by reacting $AuCl_3$ with sulfurized Venice turpentine to yield an ink or paint. Recently, the liquid golds have been composed of alkyl and aralkyl mercapto gold compounds. If oxidizable metals, such as bismuth, tin, or vanadium, are present in the paint, they can form a good bond with glass, porcelain, or metal. Gold leaf (23K gold) is also used for coating.

2. Silver

For the electrochemical plating of silver, a 99.9% silver anode is used with an electrolyte composed of $[Ag(CN)_2]^-$ and other required additives. Silver should not come into direct contact with steel or severe corrosion can occur. Steel parts can be protected by first coating with copper or nickel. Silver coating is commonly used for flatware, holloware, jewelry, electrical, and mechanical applications. Chemical methods are available to apply silver as a coating to plastic or glass.

3. Platinum

Platinum electroplating is done on a commercial scale. The plating solutions are usually based on H_2PtCl_6 and its salts. Liquid platinum, platinum sulforesinates, and alkylmercaptides in organic solvents have been used to coat platinum on glass and ceramics. Platinum can also be coated on metallic and nonmetallic articles by the vapor deposition of $Pt(CO)_2Cl_2$ or $Pt(acetyl\text{-}acetonate)_2$ followed by firing.

4. Palladium

Electrolytic plating of palladium uses the salts $Pd(NH_3)_2(NO_2)_2$ palladium P salt; $Na_2[PdCl_4]$; and $[Pd(NH_3)_4]X_2$, where X is Cl or NO_2. Palladium is considered as a viable substitute for gold in many plating operations because it is less dense and is less expensive than gold. Two plated alloys 80Pd–20Ni and 50Pd–50Ni have been used in printed circuits, connectors, and contacts because of the cost benefit over pure gold or palladium. $[Pd(NH_3)_4]^{2+}$ salts with hydrazine are used for electroless plating. Liquid palladium solutions are available which incorporate such compounds as dichloro(di-*n*-butylsul-fide) palladium(II).

5. Iridium

Methods to plate iridium are known but have not been of much importance.

6. Rhodium

Rhodium is the most commonly plated PGM. It is noted for its brilliant finish, tarnish resistance, reflectivity, and hardness. If the coating is to tin, lead, zinc, cadmium, aluminum, iron, or steel, a precoating of silver or nickel is required to prevent faulty adhesion. Rhodium can be directly deposited on silver, copper, nickel, brass, phosphor-bronze, and some copper alloys. Electrolytic deposition of rhodium uses an acid solution and rhodium sulfate, sulfamate, fluoroborate, or phosphate salts. The exact species present in the electrolyte are not known. Vapor-phase plating involves rhodium fluorocarbon-β-diketonate complexes. Rhodium plating is used for searchlight reflectors, heat concentrators in infrared ovens, cutlery, jewelry, and electrical applications. The maximum thickness usually recommended is approximately 0.002 in., and the minimum is 0.00002 in. to protect against tarnish. Thick coatings of rhodium have a tendency to crack.

7. Osmium

Methods for plating osmium have been described, but due to the tendency of osmium to oxidize to toxic OsO_4, they have remained laboratory curiosities.

8. Ruthenium

Laboratory-scale ruthenium electroplating solutions involving complexes such as $Na_2[Ru(NO)(NO_2)_4OH]$ and $(NH_4)_2[Ru(NO)Cl_5]$ have been developed.

B. Brazing and Soldering

Alloys used for soldering and brazing have two different functions. Solders are used to make mechanical,

electromechanical, or electronic connections and may not be relied on for mechanical strength. Solders are low melting point alloys that can be tailored to wet the metals of interest with the proper heat and flux. Brazing alloys are used where bonding strength is required, and they are designed to create a bond below the melting point of the metals to be joined. The alloy is drawn into the close fitted joint by capillary action. Alloying of the brazing agent and the metal can occur, which may result in an unfilled joint.

Soldering and brazing alloys containing lead, zinc, or cadmium should be used with proper ventilation. The noble metals themselves present no direct problems because the reactive osmium is not used in these alloys.

1. Gold

Gold, silver, and palladium are the most frequently used precious metals in solder and brazing alloy formulations. A large number of gold alloys are available; they are well suited for applications in which good conductivity under oxidizing conditions is necessary. Gold alloys with copper, silver, indium, silicon, silver, tin, cadmium, zinc, nickel, chromium, molybdenum, tantalum, palladium, and platinum are known mainly as two- and three-component alloy systems, with gold the major component. Low-melting alloys, such as 73Au–27In, 94Au–6Si, 88Au–12Ge, and 80Au–20Sn, have good corrosion resistance and are used in transistor technology. Alloys of Au–Cu, Au–Ni, and Au–Cu–Ni have low metal vapor pressures and have been used in high-vacuum applications. The Au–Pd–Ni brazing alloys are used to join tungsten, molybdenum, nickel, and stainless steel parts. The 35Au–35Ni–30Mo and 60Au–10Ni–30Ta blends are used in brazing with graphite. These two alloys are resistant to molten fluorides. One of the most oxidation-resistant alloys is 92Au–8Pd. Gold alloys have found applications in the electronics, nuclear, and aerospace industries. Gold brazing alloys are used to join some jet engine components.

2. Silver

Silver alloys provide the ability to wet and join base metals at low temperatures while providing good strength. Because low temperatures can be used for silver soldering and brazing, the risk of surface oxidation and heat distortion is reduced. Silver alloys usually comprise eutectic mixtures of tin, zinc, or copper, with lead and cadmium being used in some applications. The Ag–Cu alloys have been used with ceramics to produce electrical parts, and they have been used to braze carbide inserts to drills. The carbide inserts can easily be adjusted or replaced by melting the alloy.

3. Palladium

Palladium alloys in general are high-temperature solder or brazing alloys that have low vapor pressures, excellent wetability, and minimum penetration into austenitic alloys. The alloy components are usually silver, copper, manganese, nickel, and/or chromium. The Pd–Ag alloy is used to braze stainless steel, Inconel, and other heat-resistant alloys. A Pd–Ag–Mn brazing alloy was used to join nickel tubing for the liquid hydrogen engines used in the Saturn rocket. Engines on the Apollo spacecraft were joined with a Pd alloy. Use of the other PGMs in brazing and soldering is almost nonexistent.

C. Electrical and Electronic Applications

The precious metals are important in electrical applications because of their durability, conductivity, and tarnish resistance. Tarnish-free conductors and contacts are especially important where low voltages and currents are used. The alloy mixtures provide a method of varying the resistance and the mechanical and thermal properties.

1. Gold

Gold is widely used in electronics in contacts, connectors, and printed circuits, mainly in alloyed form. Gold is alloyed with silicon, germanium, tin, or indium to yield the low-melting eutectics used to make semiconductor connections. The Au–Sb alloys are used for n-type and Au–In for p-type semiconductors. The alloy mixture 94Au–6Si, which has a eutectic at 370°C, can be brittle and cause p-type semiconductivity, which may require countermeasures. The Au–Pd alloys form a continuous series of solutions that offers a wide range of resistivities for resistor and potentiometer applications. An advantage of these alloys is their minimum temperature coefficient of resistivity. The alloy Au–0.4Mn is recommended for resistance thermometry at cryogenic temperatures. The Au–Pd alloys are useful as thermal limit fuses for electric furnaces because of their narrow melting range. Au–Ag–Cu alloys are used as brazing agents in electrical applications and as slip rings and brushes for electrical instruments. Gold, electroplated to a thickness of 0.05-mil, has been used as stop-offs in ferric chloride and chromic acid etching of printed circuits. Powders involving Au–Pd–Pt alloys with high surface areas and small particle size are used in inks for hybrid circuits. The Au–Pd–Ag based alloys are used in electronic applications where a vacuum is required.

2. Silver

Use of silver in electronics is second only to its use in photography. Silver is important because it has high electrical

and thermal conductivity and excellent oxidation resistance. The most frequent use of silver and its alloys is in electrical contact materials. The advantage is that its contact resistance is not increased by oxidation at normal temperatures by arcing. Silver with 15–25% Cd, 7.5–28% Co, 3–10% Pd, 10% Au, or 3% Pt is used for minimal demand switching. When greater demands are placed on the contacts, silver alloys with either 0.25–10% C or 10–40% Ni are used. Heavy-duty electrical contacts utilize the internally oxided alloys Ag–0.41MgO–0.25Ni or Ag–2.5–15CdO. These two alloys are used in springs in electrical equipment such as miniature and micro relays. The Ag–CdO alloy has good sticking and welding resistance, and it does not arc erode easily. Silver with 50–60% Mo, 50–70% W, or 10–60% WC is used for heavy switching demands. The Ag–Pd alloys are used as resistance windings and Ag–Mg is used in relays as spring members. Silver paints are available to produce conducting surfaces on nonconductors. An example is their use in rear window defrosters in cars. Paints that require firing are available for ceramics, glass, and mica. Wood, paper, and plastics can be coated by air drying paints.

3. Platinum

Platinum and its alloys are used in high-frequency conductors where silver corrodes and at high temperatures where gold might stick. Rhodium and palladium can also be used in these applications. Platinum is wetted by, but not attacked by, mercury, which makes it useful in special electrical relays. Platinum with either palladium or ruthenium is used in electrical contacts; the ruthenium alloy is better suited for heavy-duty use. 96Pt–4W was used in aircraft spark plugs because of its high resistance to spark erosion and to lead. This alloy is also used in electronic tubes, such as microwave and X-ray tubes, as a control grid because it gives a minimum of electron emissions. Platinum, molybdenum, or tungsten wire has also been used for this application. The alloy 92Pt–8W is used as potentiometer wire because of its low noise and good wear characteristics. This alloy is also used in heater elements and glow wires for copiers. The alloy Pt–10–4ORh is used in furnace windings. The alloy Pt–Ni is remarkably free of hysteresis and is used in applications such as electric meters. The alloy Pt–Rh–Ru is very versatile with uses in potentiometers, galvanometers, suspension strips, contacts, copier wires, and explosive bridge wires. The alloy Pt–Ir is used as fuse wire for detonators. The magnetic alloy Pt–Co has electrically related uses due to its minimum space requirements and stable temperature performance. Its uses include focusing magnets, hearing aid magnets, magnetic phonograph cartridges, electric watch magnets, and digital magneto-optic recording. Platinum-based resistors can be made by firing platinum complexes onto glass, mica, or quartz in a variety of forms.

4. Palladium

Palladium is extremely important in the construction of electronic relays that are free of tarnish for reliable noise-free transmission. The most commonly used alloy is 60Pd–40Ag, which is used in contact points for telephone switching equipment. Solid-state switches may diminish this use. Pd–Ag alloys are used also as precision resistance wires. 60Pd–40W is used in electrical contacts in which the current is in the milliampere range. Pd–Ag–Cu alloys have good wear resistance and spring properties and are used in contacts in which sliding wear can occur. Zinc or platinum can be used to assist in age hardening these alloys.

5. Iridium

Iridium is used mainly as an additive (e.g., Pt–Ir) that is used in electrical contacts and precision resistance wiring applications. The alloys Ti_3Ir, $ThIr_2$, $ZnIr_2$, Nb_3Ir, and Th_7Ir_3 are superconductors. Iridium is also used in conductive inks and pastes for electronic applications.

6. Rhodium, Osmium, and Ruthenium

Rhodium alloys find most of their applications in electrical contacts for radio frequency circuits, precision potentiometers, and spark plug electrodes. The trend is toward lower usage in electronics, mainly because of price. Osmium has minor uses in electrical equipment, mainly in contacts. Ruthenium is used in electrical contacts and high-voltage relays up to 500°C because even RuO_x is conductive. A ruthenate thick-film paste is used for printed circuit resistance elements. The ruthenate is converted to RuO_2, which has very low resistance drift, ~0.10%.

D. Industrial Applications

This section accents the indirect uses of the noble metals in industry. This excludes chemical and catalytic uses of precious metal compounds where they are part of the process itself. The majority of the precious metal usage in industry is related to the unreactive nature of the metals and the ability to recover the metal after its usefulness has been exhausted.

1. Gold

Gold, because of its corrosion resistance, is used to line autoclaves for phosphate handling up to 500°C and in closure gaskets for obtaining zirconium by the iodine method. Gold or Au–Pt is used in rupture disks for service with corrosive materials such as fluorine. The alloy of 70Au–30Pt

is used in spinnerets through which cellulose acetate and rayon fibers are extruded. This alloy is being replaced by 90Pt–10Rh in some applications.

The alloys are used in thermocouples for use with liquid helium and for temperatures as high as approximately 1300°C. Gold coatings make excellent reflectors for use in solar energy collection, radiant heating and drying devices using infrared radiation, thermal barrier windows, and as a protective coating for space craft and space suits.

2. Silver

Silver is used as a coating on mirrors because of its good reflectance properties. This application has potential in solar energy collection. The coating is produced by pretreating the glass with $SnCl_2$ followed by $AgNO_3$ or an ammonia complex with a reducing agent such as sugar, Rochelle salt, or formaldehyde. Silver is also coated over copper, nickel, or carbon steel for use in the food, drug, and chemical industries in which a high degree of product purity is required in a corrosive environment. These coated products are used to concentrate chemicals where flavor and stability problems may exist. Hormones and vitamins often are prepared in this type of container. Evaporating pans are used to concentrate high-purity KOH, NaOH, and organic acids. At temperatures up to approximately 325°C, silver tubes have been used as condensers for 70% HF(aq) and HF vapors during UF_6 preparation. Fluorophosphoric acid has been prepared in a silver-lined reactor for corrosion protection from the phosphoric anhydride and anhydrous HF. Steel bearings with a palladium coating followed by a silver coat are used as engine bearings because of their good lubrication properties, moderate hardness, good thermal conductivity, and low solubility in iron.

3. Platinum

Platinum is used in high-temperature measurement. This application requires high-purity (99.999%) platinum, which is sometimes designated as Pt67. The resistivity of platinum can change considerably depending on the impurity identity and its concentration. Platinum/platinum–rhodium can be used as thermocouples at 1500 to 1850°C depending on the rhodium content. Platinum–rhodium spinneretts are used in fiberglass production. Platinum and Pt–Ir alloys are used for crucibles and to line melt furnaces used for high-purity glass (e.g., manufacturing optical glass). Platinum–iridium crucibles are used at temperatures up to 2100°C in the process to grow yttrium–aluminum–garnet (YAG) crystals, which are used to project laser and maser beams. Platinum with approximately 3.5% rhodium is used in crucibles and heated high-pressure vessels. Electrodes composed of platinum or 80Pt–20Pd are used as anodes in ship hull cathodic protection because of platinum's corrosion resistance in salt water, as well as to protect pipelines. Electrodes of 90Pt–10Ir are used in several electrochemical processes. The metal is used to line autoclaves for ethyl chloride production at approximately 1000°C, as well as to line a container for mixtures of phosphates and fluorides up to 500°C. Alloys containing 10–40% Rh are used as furnace heater coils for continuous operation. With 40% rhodium, a 1500–1800°C furnace temperature can be maintained in an oxidizing atmosphere. Platinum and Pt–Rh alloys have thermal expansion coefficients very similar to those of high quality glass (e.g., optical glass) and along with their corrosion resistance are very useful for making glass–metal seals. These seals are important when good temperature resistance and ductility is required (e.g., camera lenses, eyeglasses, and television tubes). The Pt–Rh–Ru alloys are used in strain gages. Platinum with 4–10% Ru is used in aircraft magnetos and aircraft spark plug electrodes.

4. Palladium

Palladium is often substituted for the more expensive platinum. Conversion of urea to melamine at 275–595°C is done in palladium-lined equipment; in this application, platinum is attacked rapidly. Palladium is also used in trays for firing phosphors in oxidizing environments. A hard alloy, 60Pd–40Cu, is used when metal contact is involved (e.g., springs and brushes made from the same material). Palladium and Pd–Ag alloys are used as septa to purify hydrogen gas.

5. Iridium

Iridium is usually used in alloys; the pure metal is difficult to forge or fabricate. Iridium is most commonly used with platinum to impart additional corrosion resistance. An example of its use is the Pt–Ir crucible. Thermocouples of iridium and Ir–Rh can be used up to 2000°C. An Ir–W alloy is used for springs that must function at high operating temperatures. Iridium can be used with mercury because it will not be wet.

6. Rhodium

Rhodium is used mainly in platinum alloys; the rhodium imparts additional corrosion resistance and good high-temperature characteristics. A rhodium coating on steel or brass is effective for corrosion prevention, especially in sea water. The coating must be very thin to justify its cost. Rhodium has very high optical reflectance and has been used in optical equipment, especially where tarnish might be a problem. Sometimes, it is coated on to silver

to improve the reflective quality. Rhodium is also used with platinum in the molten glass industry, in spinnerets in the fiber industry, and with iridium in high-temperature thermocouples.

7. Osmium

Osmium has limited usage due to the formation of toxic volatile oxide. It is used when a very hard and wear resistant alloy is required (e.g., spindle pivots).

8. Ruthenium

Ruthenium is not as industrially important as other noble metals, but it is used as RuO_2 to coat the dimensionally stable titanium anodes used in the production of chlorine, chlorate, and caustic, as well as oxygen in water electrolysis. Ruthenium has also found some use as a binder for high-temperature cemented carbides.

E. Batteries

Noble metal usage in batteries is essentially limited to silver which includes both primary and secondary batteries.

Primary batteries, sold in a charged state and not intended for recharge, use Ag_2O and AgO as cathodic materials. The primary silver oxide/zinc cell has a high energy output per unit weight and a fairly constant voltage during discharge, but due to its high cost, applications are limited mainly to wet cell uses with the military. Commercial uses of minature dry cells include hearing aids, watches, and photoelectric exposure devices. The silver oxide cell is a good reference voltage source. Open circuit voltage is 1.85 V for AgO/Zn and 1.60 V for Ag_2O/Zn. Discharge voltage is $\sim$1.5 V in each case. Commercial cells use Ag_2O, but an AgO cell is being developed because its electrical capacity per gram would be twice that of the Ag_2O cell. Primary lithium batteries are known with a variety of silver oxidizing agents (e.g., Ag_2CrO_4, AgF, and AgCl). The advantages of these cells are the low equivalent weight of lithium and its excellent reducing ability for making a high-energy-density battery.

Rechargeable secondary batteries using silver are the Ag/Zn, Ag/Cd, Ag/Fe, and an experimental Ag/H system. The most widely known secondary battery, lead–acid, is not direct competition for the silver cells. The Ni/Cd system has the majority of this specialty battery market. The Ag/Zn battery currently has the highest energy density of the rechargeable systems. The cell has a 95–100% efficiency in charge acceptance and one of the flattest voltage curves of any practical battery. Life is approximately 10–30 cycles for high rate of discharge and approximately 100–300 cycles for low rate of discharge. The wet life of the cell is approximately two years. The Ag/Cd cell has an energy density close to that of the Ag/Zn system but with the advantage that it is nonmagnetic. This cell has a 95% efficiency of charge acceptance, but battery performance declines below 0°C and above 40°C. This cell is used in appliances, power tools, and satellites, where nonmagnetic properties are important, and to power submarine simulator target drones. The Ag/Fe cell has the advantage of a high discharge rate capability with the cycling characteristics of the iron electrode. The discharge voltage is approximately 1.1 V. The energy density is similar to that of the Ag/Zn system, but it can be recharged up to 500 times without performance changes. Applications include emergency power; telecommunications systems in tethered balloons; and small button cells used in hearing aids, calculators, and electric razors. The Ag/H cell is in the research and development stage, but it shows promise. The Ag/Zn and Ag/Cd systems have higher power/weight or unit volume ratings than the lead–acid, Ni/Zn, and Ni/Cd systems, but the silver systems are more expensive.

F. Electrodes

The noble metals are used in the construction of anodes because they will not dissolve as some materials have a tendency to do. They also assist in the reduction of overpotential at the interface between the electrode and the solution.

Platinum can be used by itself or as a coating for titanium or tantalum to produce anodes that are useful in the production of sodium hypochlorite, dimethylsebacate, and tetraalkylthioramdisulfide. Anodes of Ti–Pt and Ti–Pt–Ir are used for cathodic protection and sodium chlorate production. Titanium by itself will build up a layer of surface oxide that is nonconducting; platinum or Pt–Ir prevents this from occurring by giving additional stability to the system. Platinum and Ti–Pt anodes are used in noble metal plating solutions. A titanium electrode coated with 70Pt–30Ir is used in chlorine and sodium chlorate production because of its high current efficiency and low overpotential for chlorine evolution and high overpotential for oxygen evolution. The iridium is present as the dioxide and it is the species responsible for the improved overpotential. Anodes of Ti–Ru are used in the chloroalkali industry. The electrode is composed of a titanium core with a Ru_2O_3 and RuO_2 conductive coating to protect the system. Electrodes composed of Ta_2O_5 with an IrO_2 coating have been proposed for use in oxygen generation. Anodes that are coated with platinum are stable in mercury cells and have a lifetime of 3–5 yr in a chlorine cell and 2–4 yr in a sodium chlorate cell.

In general, precious metal electrodes or precious metal coated electrodes are used in batteries, fuel cells,

electroplating, and synthetic chemistry (e.g., the preparation of organic and organometallic compounds). They are also used in the commercial production of zinc, manganese, and cobalt.

G. Fuel Cells

The fuel cell, a special case of a primary battery, involves the continuous feeding of high-energy reactants such as hydrogen, hydrocarbons, ammonia, or hydrazine and an oxidant such as pure oxygen, air, or peroxide. Fuel cells have been used in the space program and show promise in areas such as peaking and intermediate power for electric utility generation and onsite cogeneration for residential, commercial and industrial buildings. The direct use of hydrocarbon fuels is not currently efficient, but the fuels can be converted to hydrogen-rich streams in situ, e.g., by steam reforming.

The system closest to commercialization is the hydrocarbon–air–phosphoric acid electrolyte cell. It is tolerant of carbon dioxide impurities. The molten carbonate electrolyte fuel cell is in an earlier stage in its development cycle, but it has the potential for higher efficiency. The solid oxide electrolyte fuel cell is also relatively early in its development cycle, and, because of its high operating temperature, it is expected that hydrocarbon fuels can be converted directly to hydrogen bearing gas at the fuel electrode. Alkaline electrolyte fuel cells have been used effectively and at very high efficiency in the space program; but commercially viable versions will require additional development, and their use with carbonaceous fuels will be limited because of their carbon dioxide intolerance.

To date, the catalysts for low-temperature fuel cell electrodes (phosphoric acid and alkaline cells) have been the precious metal blacks and, more recently, precious metals on carbon supports. Development of fuel cell catalysts using precious metals remains very active. Also, some work is being done on systems that may be substituted for the noble metals. For example, tungsten carbide based anode catalysts have been shown to have good durability over long periods, but they are not as active as platinum.

H. Catalysis

Noble metals are widely used in homogeneous and heterogeneous catalysis. Their advantages are high activity under mild reaction conditions and improved selectivities compared to base metal catalysts. Precious metal catalyst systems are expensive initially because of the metal costs, but because PGMs can be recovered, the overall cost of using these catalysts may actually be lower than that of a less active or selective base metal system.

The precious metals have been used successfully in most types of catalytic reactions, and as their chemistry becomes better understood new applications should open up as well as improvements to the state of the art.

1. Gold

Gold has been studied frequently as a catalyst or cocatalyst, and it can show good or even improved selectivities but is less active than other noble metal systems. Supported gold catalysts are usually prepared from $HAuCl_4$ by reduction. Gold is used primarily as an activity modifier with other PGMs (e.g., in Pd–Au used in vinyl acetate production). The catalysts can hydrogenate olefins, dienes, and acetylenes, but severe conditions are required and coking problems result. Oxydehydrogenations can also be carried out with gold. For example, ketones can be converted to α, β-unsaturated ketones in 70–94% selectivity and 22–48% conversion at 400–600°C and ethyl benzene can be converted to styrene in 94% selectivity and 53% conversion at 700°C, but more effective catalysts are available.

2. Silver

Silver catalysts are uniquely suited for direct oxidation of ethylene to the important industrial chemical ethylene oxide. Silver will also catalyze the dehydrogenation of methanol to formaldehyde or other appropriate alcohols to yield acetone or methylisobutylketone. Ethylene glycol and air over Ag/Ag_2O yield glyoxal. Commonly used oxidation catalysts for sugars, olefins, and diols are Ag_2CO_3 and Ag_2CO_3/Celite. Ag_2SO_4 is used as a catalyst to determine the chemical oxygen demand (COD) in waste water, and it has also been used for the reduction of aromatics to cyclohexanes. Silver has also shown activity in the isomerization of carbon–carbon bonds in strained ring systems (e.g., cubane can be converted to cuneane). Acrylates and acrylamides can be polymerized with $AgClO_4$.

3. Platinum

In commercial applications probably the platinum catalyst most widely known to the general public is that used in the automobile catalytic converter, which currently accounts for approximately 60% of U.S. platinum usage. The two-way converter, used between 1975 and 1980 to remove carbon monoxide and hydrocarbons, is a Pt–Pd catalyst with roughly a 7:3 ratio of metal. In 1980, the three-way catalyst (Pt–Pd–Rh or Pt–Rh), which removes carbon monoxide, hydrocarbons and nitrogen oxides, was introduced. It is well documented that lead has significant effects on the catalyst, from changing product selectivity

to complete deactivation. This is seen when leaded gasoline is used in a car equipped with a catalytic converter. Platinum on a monolithic honeycomb support has been used in a large number of odor and pollution abatement applications. The Pt–Re and Pt–Ir catalysts on acid supports are used in the petroleum industry for re-forming low-octane naphthas into high-octane branched hydrocarbons and aromatics. The platinum acts as a hydrogenation/dehydrogenation catalyst, and the acid support is responsible for the isomerization, cracking, and cyclization reactions. This process also serves as a source of aromatics for other purposes. Product stream octane ratings as high as 104 are produced. A 90Pt–10Rh gauze is used to produce nitric acid from ammonia and oxygen. The nitric acid is used in fertilizers and explosives. The alloy 90Pt–5Rh–5Pd is also used. During HNO_3 production, platinum loss can be reduced by the use of a getter, which is a palladium-based gauze, downstream. The 90Pt–10Rh is used to convert ammonia, methane, and oxygen into HCN. Platinum is used on glass wool or asbestos in catalytic heaters to burn hydrocarbons or alcohols. It was first used for H_2SO_4 production, in which it catalyzed the oxidation of SO_2 to SO_3. This is one of the few areas in which noble metals have lost ground, with the platinum being replaced by a base metal system.

Platinum is used in hydrogenation reactions. The most commonly used catalytic systems for chemical synthesis are PtO_2, Pt/C, and Pt/Al_2O_3. Platinum will catalyze reductive alkylations, NO_x to NH_2OH, cyclohexanone oxime to caproiactam for use in Nylon 6, and selectively reduce nitro groups in halonitroaromatics. Homogeneous systems [e.g., $Pt(PPh_3)_4$] will catalyze oxidation reactions such as the conversion of cyclohexanone to adipic acid and carbon monoxide to carbon dioxide. Pt/Al_2O_3 is a versatile dehydrogenation catalyst useful for producting alkenes and aromatics. Platinum(II) and platinum(IV) will activate C—H bonds in saturated molecules for H–D exchange in D_2O. This type of system is used to produce heavy water. Platinum catalyzes many other reactions such as dimerizations, hydrosilations, oxygen removal, and water gas shift.

4. Palladium

Commercial uses for palladium catalysts include hydrocracking, vinly acetate production, and the Wacker process, which is used to convert olefins into aldehydes or ketones. The best known example is the conversion of ethylene to acetaldehyde. The process is catalyzed by $[PdCl_4]^{2-}$, which is reduced to palladium(0) as the olefin is converted to the aldehyde. The metal is reoxidized with $CuCl_2$. The homogeneous system is attractive here because the product is easy to separate from the catalyst. This is an advantage that heavier products may not enjoy in homogeneous systems in which separation would be more difficult. Like platinum, the palladium systems are widely used for reductions. For example, nitro, olefin, acetylene, diene, aldehyde, and ketone groups can readily undergo hydrogenation and substituted systems having benzyl or halide functions can undergo hydrogenolysis. Palladium is used in petrochemical purifications to remove acetylene or diolefins from olefins and unsaturates from a saturate stream. Palladium is also used in the synthesis of hydrogen peroxide. It has been used to control or eliminate oxygen by catalyzing the hydrogen–oxygen combination reaction. On the exploratory front, the palladium glasses mentioned earlier are being tested in hydrogenation reactions when it is thought that their disordered structure might lead to some novel chemistry.

5. Iridium

Iridium has little commercial use in catalysis. Its main function is as a synergist with other PGMs (e.g., Pt–Ir, which was mentioned earlier as a re-forming catalyst). Iridium compounds, mainly homogeneous, have been shown to catalyze olefin and acetylene hydrogenation, olefin isomerization, hydroformation, and oxidation reactions, as well as H–D exchange in saturated hydrocarbons. In general, iridium is not as good a catalyst as rhodium.

6. Rhodium

Rhodium is an excellent catalyst for many reactions. It is used commercially as a homogeneous catalyst (e.g., $[Rh(CO)_2I_2]^-$ and CH_3I) to produce acetic acid or acetic anhydride from methanol and carbon monoxide. Another process is the hydroformylation of propylene using $RhH(CO)(PPh_3)_3$ to yield mainly the desired n-butanal and 2-methylpropanal. It has been shown that the product isomer ratio can be varied by changing the alkyl or aryl group on the phosphine. As discussed earlier, rhodium is now used in catalytic converters to control NO_x pollution. The complex $RhCl(PPh_3)_3$, Wilkinsons catalyst, was the first homogeneous catalyst that would hydrogenate olefins and other unsaturated compounds at ambient temperatures and 1 atm of pressure. The system was found to be versatile since it will also catalyze olefin isomerizations, hydroformylations, decarboxylations, hydrosilylations, and oxidations. Work is being done to anchor catalysts such as Wilkinson's onto a polymer backbone to avoid the separation problems inherent in a homogeneous system.

An impressive application of rhodium is in asymmetric synthesis. A *bis*-phosphine rhodium complex using an asymmetric phosphine is used to prepare L-DOPA (dihydroxyphenylalanine), a chiral compound used to treat Parkinson's disease, in high optical yield. Asymmetric synthesis is a very active and promising area of research. Rhodium has been used as a dimerization catalyst in

the preparation of 1-butene from ethylene and *trans*-1,4-hexadiene from butadiene and ethylene. In a reaction similar to that in the Wacker process, $RhCl_3$ and $Cu(ClO_4)_2$ or $Cu(NO_3)_2$ will convert alkenes and oxygen into methyl ketones. The cluster complex $Rh_6(CO)_6$ will catalyze the oxidation of cyclohexanone to adipic acid and CO to CO_2. Cubane can be converted to *syn*-tricyclooctadiene as an example of strained ring isomerization. Rhodium will also catalyze H–D exchange with saturated hydrocarbons. Cluster compounds (e.g., $[Rh_{12}(CO)_{34}]^{2-}$ and $[Rh(CO)I]_x$) will catalyze the water gas shift reaction. Cluster compounds have also been shown to form ethylene glycol from synthesis gas.

7. Osmium

Osmium has only minor uses as a catalyst. The most useful reaction is the conversion of olefins to cis diols using OsO_4. In the process, the OsO_4 is converted to $OsO_2(OH)_2$, but the tetroxide can be regenerated using H_2O_2 or ClO^- to make the reaction catalytic. $HOsCl(CO)(PPh_3)_3$ can convert alkynes to *cis* alkenes and $Os_3(CO)_{12}$ shows some activity for the hydroformylation of olefins.

8. Ruthenium

Ruthenium can be used alone or as a synergist. It is a good catalyst for reducing carbonyls to alcohols, aromatics to cyclohexanes, and for the methanation of CO. Other reductions for which ruthenium catalysts are well suited include the selective reduction of 1-alkenes and nitriles to amides. Alcohols can be dehydrogenated to aldehydes or ketones using $RuCl_3$. Primary amines can be oxidatively dehydrogenated to nitriles with $RuCl_3$. Ruthenium is also a good catalyst for a variety of coupling reactions, hydroformylation, and the Fischer–Tropsch reaction. The examples listed can be accomplished with homogeneous catalysts or heterogeneous catalysts such as Ru/C or Ru/Al_2O_3.

Ruthenium tetroxide is a stronger oxidizing agent than OsO_4 and can perform many oxidation reactions. It will cleave olefins to aldehydes or ketones, oxidize aldehydes to acids, alcohols to aldehydes or ketones, ethers to esters, and amides to imides. Its use can be made catalytic by regenerating the RuO_4 from lower valent ruthenium species with strong oxidizing anions (e.g., hypochlorite, chlorine, bromate, prime or permanganate). Ruthenium in $[tris(2,2'\text{-bipyridine})\text{ruthenium(II)}]^{2+}$ type complexes and in $Pt/TiO_2/RuO_2$ is photolytically active. The systems have potential for the production of hydrogen and oxygen from water because of their photo-activity.

A word of caution should be mentioned concerning the use of dispersed reduced noble metal catalysts. When they are allowed to come into contact with oxygen and an oxidizable material, a potential fire hazard exists, as is often noted in the literature. For safety, the catalysts should be kept under an inert atmosphere and wet if possible. The reduced catalysts are available commercially in a water-wet form to reduce the fire hazard.

I. Dental Applications

Noble metal alloys, wires, and solders are used in dentistry because they are nontoxic, biocompatible, stress and wear resistant, noble in the oral environment, and have good casting properties. The alloys selected for use must have good fluidity and low gas absorption when molten for good reproduction in the preparation of partials, bridges, crowns, and orthodontic appliances and in filling cavities. The standards for dental alloys are set by the American Dental Association Specifications.

1. Gold

The use of gold is decreasing because more economical metals are being used, but it is still the preferred color. Gold foil and matte gold have been used in the direct filling of certain types of cavities but these fillings are not as strong as those made with other alloys. Gold used in dentistry involves various alloyed combinations with platinum, palladium, silver, iridium, rhodium, copper, zinc, and nickel. The exact composition depends on the end use. Copper and silver are added to obtain a solid solution and hardening; palladium and platinum are used to increase the potential for precipitate hardening; palladium preserves the nontarnish property as gold content decreases and silver content is increased; zinc is a deoxidizer; and iridium and ruthenium are used to reduce the grain size in castings. Gold alloys also use palladium and platinum to raise the solidus temperature and lower the coefficient of expansion to match ceramics when a porcelain covered crown is prepared. Dental solders commonly have compositions involving Au–Ag–Cu–Sn–Zn, with the copper and silver varied to control the color and working characteristics. For crown and bridge work 22-karat wrought gold and high-strength wires are assembled and soldered. Low-temperature solders are preferred to limit the effect of temperature on the part. Solders having a high silver content flow freely and high copper solders attach to the substrate, which is useful in building up a deficient site.

2. Silver

The greatest use of silver is in dental amalgams for restoring lost tooth structure. The amalgams, involving $65_{min}\%$ Ag–$29_{max}\%$ Sn–$6_{max}\%$ Cu–$3_{max}\%$ Hg–$2_{max}\%$ Zn, are used because of their good mechanical properties but they are attacked by inorganic acids and can undergo slight

corrosion and tarnish in the oral environment. Thus, these fillings are less noble and less permanent than the gold-based alloys just discussed.

3. Platinum Group Metals

Platinum usage is decreasing for the same reason as for gold. Less expensive metals are being substituted for it (e.g., palladium and other alloys).

Palladium is used to a greater extent than platinum. Alloys such as 30Pd–40Ag–30Au with indium or tin are used in porcelain veneering because of their lower cost, good strength, ability to handle porcelain baking at approximately 1000°C, and the previously discussed ability to closely match the thermal expansion coefficients of the alloy and the porcelain. Some alloys have as high as 88% palladium with the remainder being predominately silver. The iridium and tin will oxidize to yield a surface oxide coating that readily forms bonds with the porcelain to give a good alloy–porcelain bond. Alloys of Pd–Ag–Cu are beneficial when age hardening is desired.

Iridium and ruthenium are used as minor components, mainly in gold alloys, to reduce the grain size in castings. Rhodium and osmium have not had significant use in this area.

J. Medical and Biological Applications

Noble metal applications fall into two classifications: metals and their alloys used in medical application because of their lack of reactivity and metal compounds and radioisotopes used because of the special reactions they undergo in biological systems.

1. Gold

Gold-198 prepared by irradiation of natural gold is implanted in granular form in cancerous tissue or infused in colloidal form as a treatment for bladder cancer. Gold-195m is used in a similar manner. Gold compounds have been used in the past to treat tuberculosis and are currently being used to treat arthritis (e.g., Auranofin). Gold(I) thiols are water soluble and have been useful for rheumatoid arthritis. Some Gold(I) chloride complexes have been found to suppress adjuvant arthritis in rats, through oral administration, without harm to the kidneys. Gold treatments in general can cause pain, insomnia, and anxiety, as well as affect the bone marrow and produce stomatitis and histamine reactions. Work is being done to find less toxic derivatives. The gold complexes $[Au(CN)_2]^-$, $[AuCl_4]^-$, and $[AuI_4]^-$ are used to label enzymes and proteins in X-ray diffraction studies. Gold colloids are used are used as a cytochemical marker.

2. Silver

Silver is used in many states as a prophylactic against ophthalmia by placing a 1% $AgNO_3$ solution in the eyes of new born infants. Other applications include using a 10–20% $AgNO_3$ solution or solid $AgNO_3$ to remove warts or cauterize wounds. Silver sulfadiazene is effectively and widely used in preventing infections in burn victims. Silver metal itself has an oligodynamic effect, which makes it lethal to bacteria, and the insolubility of the metal makes it nontoxic to higher life forms so it can be a useful disinfectant.

3. Platinum

The most widely known medical application of platinum is in chemotherapy. Its compounds, the best known being cisplatin, *cis*-dichloro diammineplatinum(II), have been successful in treating testicular and ovarian cancers both alone and in combination with other drugs. Cisplatin has also shown promise in the treatment of other genitourinary, head and neck tumors, some forms of lung cancer, as well as various pediatric cancers. It is speculated that the platinum complex inhibits cell division by binding the DNA or by making the cancer cell susceptible to the body's immune system. While this treatment is successful, these complexes, primarily cisplatins, are toxic to the kidneys. The toxicity can be reduced by increasing urinary output to dilute the platinum passing through the kidneys. Carboplatin, a likely commercial prospect, is less toxic than cisplatin. The platinum thymine blues, aside from their antitumor activity, react specifically with DNA to assist in the visualization of nuclear components. The complexes cisplatin and *cis*-diamminediaquoplatinum(II) nitrate are active against Rous sarcoma and fowl pox viruses. Zeise's salt, $K[(C_2H_4)PtCl_3]$ will detect Hepatitis B in blood sera, erythematosis, and rheumatoid arthritis.

The metal and its alloys are commonly used in the medical field. Platinum and 90Pt–10Ir are used in catheters, electrodes in heart pacemakers, and body implant probes to reduce pain. For the latter application, an electrode can be implanted in the brain to stimulate excretion of endorphins to relieve pain. An example of this is in the treatment of arachnoiditis, a painful inflammatory condition of one of the spinal cord coverings. Platinum electrodes have also been used in exploratory work to assist sight and hearing. Alloys of Pt–Ir and Pt–Ru are used in hypodermic needles and surgical instruments because of their sharpness and durability. Magnets made of Pt–Co are found in medical applications such as assisting in the control of artificial eyes, retention of implant artificial dentures, systems for delivery of magnetic emboli via a guided catheter to specific cerebral arteries, and for removing foreign objects.

In the biological, as opposed to medical, related uses the platinum–protein interaction is capitalized on to provide a heavy metal center to assist in X-ray diffraction studies and as a model to understand how platinum interacts with various biological systems in antitumor medication. Many derivatives display bacteriostatic and bacteriocidal properties (e.g., $(NH_4)_2[PtCl_4]$ and the corresponding iridium, osmium, and palladium derivatives and $(NH_4)_2[PtCl_6]$ and its corresponding ruthenium derivative). $PtCl_2$ acts as a lipid stain because of its ability to interact with the olefinic group.

4. Palladium

Palladium alloys are used as replacements for damaged arthritic bones and joints in which there is a load-bearing requirement. Palladium(II) complexes have shown some antitumor activity on initial screening, and $Pd(OH)_2$ was tested in treating obesity.

5. Iridium

As discussed with platinum, iridium is a component in alloys used in pacemakers. The isotope ^{191m}Ir, derived from ^{191}Os, is useful in radioangiography because it has a short half-life, 4.9 sec, and it decays to a nontoxic product. Because the exposure is minimal, it is well suited for serial radiological studies. This has been applied to the study of heart defects in children. The human-made isotope ^{192}Ir can be placed in a platinum container, which allows gamma rays to pass while absorbing potentially damaging beta ray emission. The container is then implanted into the tumor for treatment. Breast cancer has been treated by this method.

6. Rhodium

The major medical use of rhodium is in radiotherapy. The isotopes $^{106}Ru/^{106}Rh$ have been shaped into cups that are coated with silver and then used to treat retinoblastoma. Rhodium(II) carboxylates may be antitumor agents based on initial screening and $RhCl_3(DMSO)$ has been shown to have activity against leukemia in mice. Several rhodium(II) pyrimidine derivatives show bacteriostatic and bacteriocidal properties.

7. Osmium

Surprisingly, OsO_4 has been found to be an effective treatment for inflammatory arthritis of the knee. This application of osmic acid was approved in Sweden and Norway in 1978, but its use is controversial. The potential of damage from the OsO_4 to healthy tissue has prompted a search for other osmium derivatives. Work is being done on osmium carbohydrate polymers to avoid the potential side effects. OsO_4 is a useful biological fixative and specific stain for lipid-containing structures. Because the compound reacts selectively with olefinic bonds, $Os_2O_6py_4$ will react with the 2- and 3-hydroxyl groups in nucleosides, and osmium amine complexes are used as a specific stain for polysaccharides.

8. Ruthenium

Ruthenium(III) complexes involving chloro, ammine, and carboxylato ligands have shown antitumor activity on initial screening. Ruthenium(II) 1,10-phenanthroline derivatives have been investigated for their antibacterial activities mainly against gram-positive microorganisms. Ruthenium Red, prepared by the air oxidation of $[Ru(NH_3)_6]Cl_3$, is used to stain polysaccharides and elastic tissue fibers. Of more theoretical interest to biological systems is the work on electron exchange being done with Ru^{II}/Ru^{III} complex systems. This system is important because it is resistant to substitution in both oxidation states, making it easy to study. $[Ru(NH_3)_5H_2O]^{2+}$ is hydrophilic and remains solvated even though it is bound tightly to a protein and the oxidation–reduction potentials of the systems studied are in the range of those found in biological systems.

K. Jewelry

In general, the noble metals, because of their attractive appearance, stability, and perceived value, have been treasured in jewelry, art, and decoration.

1. Gold

The popularity of gold is due to its social acceptance, color, lack of allergenic properties in the metallic form, as well as for the properties discussed for the precious metals in general. Gold is used predominately in jewelry and is rated on a karatage or a fineness system. The karatage system is the one in predominant use in the U.S. and Great Britain. In the jewelry industry in the U.S. gold must be a minimum of $10\frac{1}{2}$ karat. Jewelry is commonly labeled gold filled or rolled gold plate, with the rolled gold plate having a lower gold content. Bonding of the gold to a base is done by soldering, brazing, welding, or mechanical methods. The soldering or brazing alloy is usually Au–Ag–Cu with the Ag–Cu ratio varied to adjust the melting point. The most common alloys are Au–Ag–Cu, yellow gold; Au–Ni–Cu–Zn, white gold; and Au–Pd, a more expensive but more corrosion resistant white gold. White golds that are rich in silver can tarnish. Depending on the application, the two white gold alloys may be interchangeable. The color of the gold can be changed by varying its composition (e.g., red gold is high in copper, and green gold is high in gold and

silver and low in copper). As discussed earlier, gold can be plated by several methods for art and decorative purposes, (e.g., china decoration). Colored gold in the form of purple of Cassius is used as a coloring agent for glass. A high gold:glass ratio (1:50,000) gives a ruby red color and a low gold:glass ratio (1:100,000) gives a rose-red color.

2. Silver

The most common form of silver in the decorative area is sterling silver, Ag–Cu, which is used in silverware and was also widely used in coinage because of its hardness and wear resistance. Sterling, 92.5% silver, will tarnish, but work has been done to find a nontarnishing sterling silver. A rhodium coating will protect the silver but it is cost-prohibitive for most uses. Plated silver is 99.99% pure and is usually put on a blank, such as steel or nickel silver, which is a Ni–Cu alloy containing no silver. Finely powered silver metal is used as a pigment. Polychromic glass contains AgCl and Ag_2MoO_4, and Ag_2SO_4 imparts a yellowish-red color to glass bulbs.

3. Platinum

Prior to 1974, the greatest use of platinum was in jewelry, but since then, its use in automobile catalytic converters has taken the lead. It is popular in settings for the finest jewelry because of its high intrinsic worth and the way it sets off diamonds. Platinum with either 5–15% iridium, 5% ruthenium, or 5% rhodium is used to harden the metal. These alloys are used for small delicate pieces such as small chains. Rhodium is also used to finish the platinum piece for additional whiteness as well as wear resistance. The Pt–Pd alloys are commonly used in jewelry in Europe, but the biggest outlet is in Japan.

4. Palladium

Palladium has characteristics similar to platinum and is finding increased use. It is less costly, and because of its lower density, it is used where weight is important (e.g., earrings). Palladium pieces, like platinum, are often finished with rhodium for the same reasons. The alloy 95Pd–4Ru–1Rh is popular for jewelry use because of its mechanical strength and hardness. The "white" alloy 95.5Pd–4.5Ru sets off diamonds well and is a standard for palladium use in the U.S. Palladium is used as a protective and decorative coating on ceramics, leather, metal, and wood.

5. Iridium

Iridium, at less than a 20% level, is used in diamond settings with platinum. Iridium black is used as a black pigment to decorate fine porcelain or china.

6. Rhodium

The main use of rhodium is as a component in alloys for hardening and as a coating to whiten the alloys. It is used to coat prongs and claws to hold diamonds because of its highlighting effect. It is also used to coat costume jewelry, cigarette lighters, and low-karat white gold, which is sensitive to corrosion caused by perspiration. Small amounts of rhodium are also used in the manufacture of liquid gold.

7. Osmium

Osmium is not used in jewelry or decorative applications. In fact, pains are taken to eliminate it from gold because small amounts can streak a polished gold surface.

8. Ruthenium

Ruthenium is used as a hardening agent, which is its only significant use in jewelry or decoration.

L. Photography

Photography, the largest single use for silver, is too broad a topic to be covered in any depth here so the discussion is limited to the mechanism of its use and does not include details such as positive and negative imaging.

Silver salts are used because they are photochemically reduced under mild conditions. The most common salts are the halides: chloride, bromide, and iodide, but other compounds such as mercaptides can be used. The film is prepared by mixing $AgNO_3$ and the appropriate mixture of sodium or potassium halide to form a silver halide emulsion of crystals containing approximately 10^{12} atoms. The emulsion is spread on a backing and kept from coalescing by locking the crystals in a gel. There is a trade-off: the larger the crystals, the faster the speed of the film or the better the photosensitivity; but because of the large crystal size, the resolving power or sharpness of the photograph decreases. Silver halides are sensitive only to blue and ultraviolet light, which are responsible for the reduction of the silver. Several options are available to increase the sensitivity of the film to visible light. The easiest change is to shift from low-sensitive AgCl to the more photosensitive AgI. Going from the chloride to iodide requires less energy to reduce the silver, which results in a shift in film sensitivity to the lower-energy visible light. For low-sensitivity film, AgCl, AgCl/AgBr, or AgBr are used; and for high-sensitivity film, AgBr with up to 10% AgI is used. Polymethine-type dyes are used to make the salts more sensitive to the green and red regions. This is termed spectral sensitization and there are even dyes available that will sensitize the film to the infrared region. Another method, chemical sensitization, does not alter the light absorbing properties of the silver halide but it does improve

the efficiency with which the blue photons are absorbed and thus the efficiency with which the image is formed. The most popular compounds for chemical sensitization are silver sulfide and gold salts (e.g., gold thiocyanate and $K[AuCl_4]$). Compounds such as K_2PtCl_4, $PdCl_2$, and their phosphine/halide complexes have also been studied as chemical sensitizers. Platinum salts were used in the early days of photography, in the same manner as that in which silver salts are used today, to yield excellent prints from the platinotype process.

The silver halide, when exposed to light, is split into silver metal and a halide radical that can migrate into the gel and react or less likely, recombine with the silver metal. This trace amount of silver metal on the crystal sensitizes it to further reduction. The silver present is termed the latent image and is too light to be detected visually. When the film is treated (developed) with a mild reducing agent (e.g., hydroquinone, catacol, aminophenol, *p*-phenylenediamine, or ascorbic acid), an enhancement of approximately 10^{10} to the latent image occurs. The reducing agent is of prime importance because it must be strong enough to reduce the centers with the silver metal but not strong enough to reduce the centers without the metal (i.e., those centers that were unexposed). This treatment will yield dark silver spots where the light impinged on the film and result in a negative image. At this point, the unreduced silver halide must be removed or it will develop on further exposure to light and thus diminish the quality of the photograph. The silver salt is removed with a "fixer" solution, which is a complexing agent such as sodium thiosulfate that yields the complex $[Ag(S_2O_3)_2]^{3-}$ with a stability constant of approximately 1.7×10^{13}. At this point, the photograph consists of a negative image, which is further processed to give the positive image.

For color film, the silver halides are used in conjunction with a series of dyes and filters to allow for selective reduction by the various spectral regions. Color film is too complicated an area to be addressed in any depth here.

III. TOXICITY

When determining toxicity, the metal should be considered in its bulk metallic state, the more reactive finely divided metallic state and its compounds, which should be judged on a case by case basis. Unfortunately, for compounds that are not commonly used in industry, toxicity information may be difficult to obtain.

This section deals with generalities and is not intended as a substitute for a specific search regarding the compounds or metal forms of interest. In general, the noble metals themselves are nontoxic and no major problems have been reported when they are worked on in areas with the proper ventilation. Caution must be used with osmium because the metal is easily oxidized to OsO_4.

A. Gold

Gold compounds are the most toxic of the copper, silver, and gold subgroup. When gold compounds are used medically, it is found that their excretion is slow, approximately 20% in two weeks and less thereafter. The side effects include urticaria (hives), itching, purpura, and skin rashes; damage to the blood forming organs and the nervous system has also been described. The effects can be long lasting and require some treatment. Gold can be chelated with thiols to accelerate its excretion. Antidotes for gold poisoning include 2,3-dimercapto-1-propanol(bal), sodium hyposulfite, calcium gluconate, sodium formaldehyde sulfoxylate, vitamin C, and pencillamine.

B. Silver

Chronic exposure to silver or its alloys in poorly vented areas can result in the irreversible absorption of silver into the body tissue, where it precipitates as a gray to purple pigment. This condition, argyria, is disfiguring but apparently it is harmless. With proper hygiene and ventilation this malady has become uncommon. Silver compounds, in general, can yield the skin effects discussed previously as well as be an irritant to the skin and the mucous membranes. As a reminder, care should be taken with alloys such as Ag–Cd because of the potential hazard due to cadmium. The same caution should be taken with other alloys containing toxic components. Compounds of silver may be misleading in their lethal concentration data (e.g., LD_{50}) in that their insolubility may make them appear to be less of a hazard than they may be.

C. Platinum

Platinosis, the allergic reaction caused by small quantities of anionic platinum salts, can be recognized by coughing, wheezing, running nose, tightness of the chest, shortness of breath, and dermatitis. This is not seen with the metal itself, even in a finely divided state. Cisplatin, used in cancer treatment, can cause damage to the renal tubules, gastrointestinal epithelium, and spleen and can cause bone marrow depression. In humans, it can cause nausea, vomiting, peripheral neuropathy, and high-frequency hearing loss. Platinum compounds and other PGMs are generally toxic to the kidneys. Also, as a general rule, as PGM valence increases the curarelike effects increase.

D. Palladium

Palladium compounds, like platinum, can cause damage to the organs (e.g., heart, liver, and kidney) and be dermal irritants as well.

E. Iridium

Very little information is available on iridium and its compounds mainly because it is so little used in industry.

F. Rhodium

Rhodium, like iridium, has little data available, but OSHA has set an air standard. Some LD_{50} (rat) data are available for a few of the common complexes (e.g., $RhCl_3$).

G. Osmium

Osmium metal and most of its compounds are probably safe to handle with proper precautions, but OsO_4 and OsF_8 are highly toxic. The compound OsO_4 is a hazard to the eyes, nose, and throat and readily oxidizes organic matter. It can cause dermatitis and ulceration of the skin on contact, as well as cause conjunctivitis, corneal irritation, halo effects, and temporary blindness.

H. Ruthenium

It is generally assumed that ruthenium behaves in a manner similar to that of osmium.

SEE ALSO THE FOLLOWING ARTICLES

Analytical Chemistry • Batteries • Catalysis, Homogeneous • Catalysis, Industrial • Electrochemical Engineering • Isotopes, Separation and Applications • Metallogeny • Mining Engineering • Organometallic Chemistry • Periodic Table (Chemistry) • Photographic Processes and Materials

BIBLIOGRAPHY

Bailar, J. C., Emeleus, H. J., Nyholm, R., and Trotman-Dikenson, A. F. (eds.). (1973). “Comprehensive Inorganic Chemistry.” Pergamon, New York.

Cubberly, W. H., et al. (eds.). (1979). “Metals Handbook,” 9th ed. American Society for Metals, Metal Park, Ohio.

Hightower, J. (1977). “Platinum Group Metals,” National Academy of Sciences, Washington, D.C.

Kirk, R. E., and Othmer, D. F. (eds.). (1978). “Encyclopedia of Chemical Technology,” 3rd ed. Wiley, New York.

Robbins, P., and Lee, D. (1979). “Guide to Precious Metals and Their Markets.” Van Nostrand-Reinhold, New York.

Wilkinson, G., Stone, F. G. A., and Abel, E. W. (eds.). (1982). “Comprehensive Organometallic Chemistry.” Pergamon, Oxford.

Noble-Gas Chemistry

Gary J. Schrobilgen
McMaster University

I. Historical Background
II. Preparative Methods for the Binary Fluorides
III. Xenon Compounds
IV. Krypton Compounds
V. Radon Compounds
VI. Prospects for Argon Compounds
VII. Applications

GLOSSARY

Argon, Ar At. no. 18, at. wt 39.948, mp −189.2°C, bp −185.7°C. Argon is the most abundant of the noble gases (0.93% of dry air) and is used in light bulbs, as an inert shield in arc welding, and for metal production (Ti, Si). Argon has the ground state electronic configuration $[Ne]3s^23p^6$ and forms some clathrates but no stable bulk compounds, except excited state species and one species isolated in a low-temperature argon matrix, HArF.

Element-118 See ununoctium.

Helium, He At. no. 2, at. wt 4.00260, mp −272.2°C, bp −268.934°C. Helium is one of the noble gases (5.2×10^{-4}% in dry air and up to 7% in some natural hydrocarbon gases). It is found in some radioactive minerals as a product of radioactive decay (the α-particle is an He^{2+} cation) and is separated by liquefaction. Helium is used to provide an inert atmosphere for arc welding and for Ti, Zr, Si, Ge production; as a coolant in the liquid state for superconducting magnets; with 20% O_2 as an atmosphere for divers; and for pressurizing liquid fuel rockets and for filling balloons and lighter-than-air craft. Helium has the ground state electronic configuration $1s^2$ and has no normal chemistry, although excited state species containing bound He are formed in discharge tubes. Liquid He has no triple point and cannot be solidified at atmospheric pressure. Liquid He_{II} exhibits superconductivity and can flow against gravity over the edge of vessels. It changes to He_I at 2.2 K.

Krypton, Kr At. no. 36, at. wt 83.80, mp –156.6°C, bp −152.3°C. Krypton (1.14×10^{-3}% in dry air) is used (with Ar) for fluorescent lights, high-intensity miniature incandescent lamps, and in certain photographic flash lights. The ground state electronic configuration is $[Ar]4s^24p^6$. Krypton forms a limited range of compounds containing Kr—F, Kr—O, and Kr—N bonds and some clathrates. Among the chemical compounds it forms are linear krypton difluoride, KrF_2 (formed by the low temperature reaction of Kr with F atoms that are formed by dissociation of F_2 under photolytic, electric discharge, or thermal conditions), $Kr(OTeF_5)_2$, and $HCNKrF^+AsF_6^-$. Krypton difluoride also reacts with

Lewis acid fluorides to form KrF^+ and $Kr_2F_3^+$ salts. The KrF^+ cation is the strongest oxidative fluorinating agent known.

Neon, Ne At. no. 10, at. wt 20.179, mp −248.67°C, bp −246.05°C. Neon is a relatively abundant noble gas (1.82×10^{-3}% of dry air) and is widely used in fluorescent tubes (neon lights), Geiger-Müller tubes, gas lasers, and electrical equipment. The ground state electronic configuration is $[He]2s^2 2p^6$, and Ne forms no stable chemical compounds.

Noble gases Sometimes referred to as the rare gases or inert gases (the latter is a misnomer). They are the elements helium, neon, argon, krypton, xenon, radon, and element-118. All except element-118 occur as minor constituents of the atmosphere. Helium, neon, argon, krypton, and xenon are separated by fractionation of liquid air. Helium is also a minor component of some natural hydrocarbon gases. They are used (particularly, He and Ar) to provide an inert atmosphere, e.g., for welding, and in electric light bulbs and discharge tubes (Ne) and high-intensity photographic lamps (Xe). Liquid helium is used in cryogenic applications, such as the coolant for superconducting magnets. The amounts of He and Ar formed in minerals by radioactive decay can be used to determine the age of a specimen. Xenon, and to a lesser extent Kr and Rn, have a chemistry; the other noble gases do not form bulk chemical compounds, but an example of an argon compound has been detected in trace amounts at low temperature.

Radon, Rn At. no. 86, at. wt 222, mp −71°C, bp −61.8°C. Radon is an intermediate radioactive decay product of ^{226}Ra. ^{222}Rn, the most stable isotope of radon, is obtained as a gas from aqueous solutions of $^{226}RaCl_2$ and has been used as a radiation source and as a gaseous tracer. It is a considerable hazard in uranium mines. In some areas, radon in basements and in ground water is a potential health hazard because of its radioactivity. The ground state electronic configuration of radon is $[Xe]4f^{14}5d^{10}6s^2 6p^6$. Because radon is intensely radioactive, the chemistry of radon has only been investigated on the tracer scale. Radon forms compounds, particularly a fluoride (likely RnF_2), and solid adducts between the fluoride and Lewis acid fluorides.

Ununoctium, Uuo Name and symbol are temporary; at. no. 118, at. wt 293. Ununoctium is a synthetic or transuranium element that was first made in 1999 in a cyclotron by the nuclear reaction of 449 MeV $^{86}Kr + {}^{208}Pb$. The nucleus of $^{293}118$ decays within less than 1 msec by emission of an α-particle into element-116. No physical and chemical properties of ununoctium have been directly determined, as only a few atoms have been produced by this method. It is likely that element-118 may be a solid at room temperature. Like radon, the chemistry of ununoctium is expected to reflect its anticipated metalloid properties. The unconfirmed ground state electronic configuration is $[Rn]5f^{14}6d^{10}7s^2 7p^6$.

Xenon, Xe At. no. 54, at. wt 131.29, mp −111.9°C, bp −107.1°C. Xenon (8.6×10^{-6}% in dry air) is used in lamps and discharge tubes and is moderately soluble in water. Xenon exhibits the most extensive chemistry of all the noble gases. It has the ground state electronic configuration $[Kr]5s^2 5p^6$ and shows oxidation states (examples in parentheses) $+\frac{1}{2}(Xe_2^+)$, +2 (XeF_2 and salts of XeF^+, $Xe_2F_3^+$), +4 (XeF_4, XeF_3^+ salts), +6 (XeF_6, $XeOF_4$, XeO_2F_2, XeO_3, and salts of XeF_5^+, $XeOF_3^+$, XeO_2F^+, XeF_8^{2-}, XeF_7^-, $XeOF_5^-$, $XeO_2F_3^-$, and XeO_3F^-), and +8 (XeO_2F_4, XeO_3F_2, XeO_4, and salts of XeO_6^{4-} and $XeO_3F_3^-$). Both XeO_3 and XeO_4 are treacherous explosives and are exceedingly difficult to handle. Bonds to elements other than xenon, oxygen, or fluorine are known, namely, carbon, nitrogen, and gold. These are exemplified as the $C_6F_5Xe^+$, $HCNXeF^+$, and $AuXe_4^{2+}$ cations, respectively.

I. HISTORICAL BACKGROUND

The noble gases had been characterized for many years as inert and incapable of forming compounds with other elements. Numerous attempts to induce chemical reactivity over the years led to the myth of their chemical inertness and the inviolability of the noble-gas valence shell octet of electrons, the so-called "octet rule." Several unsuccessful attempts to synthesize noble-gas compounds were published in the 1930s, as well as theoretical speculations by Linus Pauling that noble-gas compounds should exist. Failed attempts to discover noble-gas chemistry likely served to entrench the doctrine of the octet rule. The discovery of noble-gas reactivity played a key role in inaugurating a new era in inorganic chemistry. The first authentic noble-gas compound was discovered by Neil Bartlett in 1962 at the University of British Columbia. He recognized that molecular oxygen was oxidized by PtF_6 to give $O_2^+PtF_6^-$ and that PtF_6 must therefore be an oxidizer of unprecedented strength. He also noted that the first ionization energies of molecular oxygen (1.176 MJ mol^{-1} for $O_2 \rightarrow O_2^+ + e^-$) and Xe (1.167 MJ mol^{-1}) are very similar and surmised that PtF_6 should also oxidize xenon. He proceeded to show that deep red-brown PtF_6 vapor spontaneously oxidized xenon gas at room temperature to produce a yellow-orange compound which he formulated

as "$Xe^{+}PtF_6^{-}$." Within a very short time, a number of other xenon compounds, a krypton fluoride, and a radon fluoride, were reported.

The heavy noble gases—krypton, xenon, and radon—have been shown to react with fluorine and other powerful oxidants to form a number of stable products. Xenon has the most extensive chemistry in this group and exhibits the oxidation states $+\frac{1}{2}$, +2, +4, +6, and +8 in the compounds it forms. Since the discovery of noble-gas reactivity, xenon compounds, including halides, oxides, oxofluorides, oxosalts, and numerous covalent derivatives in which xenon is covalently bonded to other polyatomic ligands, have been prepared. Additionally, the fluorides and oxofluorides of xenon form a variety of fluoro- and oxofluorocations and anions in their reactions with strong Lewis acid acceptors and fluoride ion donors, respectively. Examples of xenon covalently bonded to fluorine, oxygen, nitrogen, carbon, and gold are now known. The chemistry of krypton is far less extensive than that of xenon. Krypton has been shown to form a difluoride and a series of complex salts derived from krypton difluoride. Several examples of krypton bonded to nitrogen are now known, and a single compound containing krypton bonded to oxygen has been reported.

Radon lies on the diagonal of the Periodic Table between the true metals and nonmetals and is classed as a metalloid. As the heaviest and most metallic of the naturally occurring noble gases, radon has the lowest ionization energy of the group (1030 kJ mol^{-1}); consequently, it is expected to be the most reactive. The chemistry of radon is, however, less extensive than the chemistries of krypton and xenon and is rendered considerably more difficult because no stable isotopes of this element exist. The inherent radiation hazard that accompanies the intense radioactivity of radon requires tracer level experimentation. Nevertheless, evidence has been obtained that radon forms a difluoride and several complex salts.

Thus far, no stable bulk compounds of the lighter noble gases, helium, neon, and argon, have been found, although HArF has been observed spectroscopically. Element-118, or ununoctium, a synthetic (transuranium) element, was first made in 1999 in a cyclotron by colliding krypton-86 ions with a lead-208 target at an energy just sufficient to fuse their nuclei together and to loose one neutron. Only a few atoms of the isotope having the mass number 293 have been produced by this method. Ununoctium-293 decays within less than 1 msec after creation into another transuranium element, element-116, by emitting an alpha particle. Although no physical and chemical properties of element-118 can be directly determined at this time, it has been proposed that element-118 may be a solid at room temperature.

II. PREPARATIVE METHODS FOR THE BINARY FLUORIDES

The only way to "fix" krypton, xenon, and radon gases is through reaction with fluorine or a reactive fluoride so that their chemistries are ultimately derived from the binary fluorides.

Amounts of the binary xenon fluorides suitable for synthetic work are generally prepared by heating mixtures of xenon and fluorine to 250–400°C in nickel or Monel vessels. Although all three fluorides coexist in equilibrium, suitable adjustments of the temperature, pressure, and xenon/fluorine ratio can be made to yield primarily the difluoride, tetrafluoride, or hexafluoride. Xenon difluoride can be prepared photochemically by exposing xenon and fluorine, contained in a Pyrex flask, to either direct sunlight or to ultraviolet light from a mercury arc lamp. Other methods, including electric discharges, proton and electron beams, and γ-rays, have been employed for the preparation of xenon fluorides, but are rarely used today. Xenon difluoride can also be prepared by the interaction of Xe and F_2 in the dark when the reaction takes place in anhydrous HF.

Both XeF_2 and XeF_4 can be manipulated in glass vacuum systems, but XeF_6 must be handled in either fluorine-passivated metal or fluoroplastic (e.g., Teflon, Kel-F, FEP) vacuum systems, since Pyrex and quartz are attacked to form initially $XeOF_4$, which can react further to form XeO_2F_2 and treacherously explosive XeO_3. Safety measures, such as the use of protective glasses, face and apparatus shields, and other personal protective covering, are essential for work involving the tetrafluoride and hexafluoride, owing to the adventitious formation of highly explosive XeO_3 by inadvertent exposure of the compounds to moisture (the tetrafluoride disproportionates in water according to the reaction, $6\ XeF_{4s} + 12\ H_2O_l \rightarrow 2\ XeO_{3s} + 4\ Xe_g + 3\ O_{2g} + 24\ HF_{aq}$).

Krypton difluoride cannot be synthesized by the standard high-pressure, high-temperature means used to prepare xenon fluorides because of the low thermal stability of KrF_2. There are three low-temperature methods which have proven practical for the preparation of gram and larger amounts of KrF_2. High-voltage electric discharges through a 1:1 mixture of krypton and fluorine at −183°C over a period of several hours result in product deposition on the cold walls of the cell. The second method involves the resistive heating of a nickel filament, inside in a metal vessel (usually stainless steel, copper, or aluminum), cooled to −196°C and containing solid krypton condensed on its walls and fluorine in the gas phase. Fluorine atoms formed by thermal dissociation of F_2 at the hot surface of the nickel filament diffuse to the reactor walls,

reacting with krypton over a period of several hours to form KrF_2. An excellent and experimentally simpler photochemical method for the preparation of KrF_2 has been developed which involves the photolysis of solid krypton/liquid fluorine mixtures at −196°C. Krypton difluoride can routinely be obtained in yields of several grams to several tens of grams using low-temperature photochemical means and generally requires no further purification. It can be stored indefinitely at temperatures of −78°C or below. However, great care must be exercised in avoiding inadvertent contact with organic substances and the introduction of moisture into solid KrF_2 samples, as the potent oxidant properties of KrF_2 result in the rapid oxidation of organic compounds and water. For example, violent explosions have been known to occur upon warming of moisture-contaminated bulk samples to or near room temperature.

Radon fluoride is most conveniently prepared by reaction of radon gas with a liquid halogen fluoride (ClF, ClF_3, ClF_5, BrF_3, or IF_7) at room temperature. Millicurie or larger amounts of radon react spontaneously with gaseous or liquid fluorine in a small volume (25 or 50 mL flask) within about 30 min. The radon behaves as both activator and reactant. The product is nonvolatile and hence remains in the reaction vessel when the excess reagent is removed by vacuum distillation.

III. XENON COMPOUNDS

The principal neutral, cationic, and anionic fluorides; oxide fluorides; and oxides of xenon are listed in Table I along with their geometries.

A. Halides

Xenon fluorides (and $XeOF_4$) and their complexes are the only thermodynamically stable xenon compounds. Xenon difluoride (XeF_2), xenon tetrafluoride (XeF_4), and xenon hexafluoride (XeF_6) are stable, colorless, crystalline solids which can be sublimed under vacuum at 25°C. The mean thermochemical bond energies are XeF_2, 132.3 ± 0.7 kJ mol^{-1}; XeF_4, 130.3 ± 0.5 kJ mol^{-1}; and XeF_6, 125.3 ± 0.7 kJ mol^{-1}. Xenon hexafluoride is yellow-green as a liquid or gas. Reports of xenon octafluoride, XeF_8, in the early noble-gas chemistry literature remain unsubstantiated. Xenon difluoride is a linear symmetrical molecule [Xe—F, 1.9773(15) Å], and XeF_4 is a square planar molecule [Xe—F, 1.953(4) Å]. Experimental evidence is consistent with a distorted octahedral structure for gaseous XeF_6 arising from the presence of an extra pair of nonbonding electrons in the xenon valence shell. Solid XeF_6 exists in at least four phases which consist of tetrameric and hexameric rings of virtually undistorted square pyramidal XeF_5^+ cations (see Section III.E) linked together by fluoride ion bridges.

Xenon dichloride ($XeCl_2$) and XeClF have been prepared by photochemical and electric discharge methods and have been examined at low temperatures by matrix-isolation techniques. The dichloride has a linear structure like that of XeF_2. Evidence for the existence of $XeCl_2$, $XeBr_2$, and $XeCl_4$ has been obtained from ^{129}Xe Mössbauer studies. The compounds were obtained by γ-decay of the corresponding ^{129}I compounds. Owing to their thermal chemical instabilities, no dihalide other than the binary fluorides have been prepared in macroscopic amounts. Other examples of Xe(II)—Cl bonds are C_6F_5XeCl and $(C_6F_5Xe)_2Cl^+$ (see Section III.F.3).

Unstable monohalides of xenon (XeF, XeCl, XeBr, and XeI) have been produced in the gas phase by electron bombardment methods and in solid matrices by gamma and ultraviolet irradiation methods. Although short lived in the gas phase, these halides are of considerable importance as light-emitting species in gas lasers.

B. Oxides

Two oxides of xenon are known: xenon trioxide (XeO_3) and xenon tetroxide (XeO_4). Xenon trioxide is most efficiently prepared by the hydrolysis of XeF_6 or by the reaction of XeF_6 with $HOPOF_2$. The XeO_3 molecule has a trigonal pyramidal shape [C_{3v} point symmetry; Xe—O, 1.76(3) Å], and XeO_4 has a tetrahedral shape in the gas phase [T_d point symmetry; Xe—O, 1.736(2) Å]. Xenon tetroxide has also been studied in solution by ^{129}Xe and ^{131}Xe NMR spectroscopy. Xenon tetroxide is prepared by the interaction of concentrated sulfuric acid with sodium or barium perxenate (Na_4XeO_6, Ba_2XeO_6). Both oxides are thermodynamically unstable, explosive solids which must be handled with the greatest care. On decomposing to the elements, solid XeO_3 and gaseous XeO_4 release 402 and 642 kJ mol^{-1}, respectively. Xenon trioxide has a negligible vapor pressure at room temperature and readily dissolves in water to give stable solutions containing mainly molecular XeO_3 and xenic acid anion, $HXeO_4^-$, which is vanishingly small ($K \approx 3 \times 10^{-11}$ for $XeO_{3aq} + 2\,H_2O_l - HXeO^-_{4aq} + H_3O^+_{aq}$), except in basic solution ($K \approx 1.5 \times 10^3$ for $XeO_{3aq} + OH^-_{aq} - HXeO^-_{4aq}$). Xenon tetroxide is volatile at 25°C, but frequently decomposes explosively well before this temperature is reached.

C. Oxide Fluorides

The oxide fluoride $O(XeF)_2$ is isoelectronic with the $Xe_2F_3^+$ cation and is also pale yellow in color and has

TABLE I Fluoro- and Oxofluorocations and Anions of Xenon, Their Parent Compounds, and Geometries

	Parent compound	Structure[a]	Cation(s)[b]	Structure[a]	Anion(s)	Structure[a]
Xe(II)	XeF_2	(Linear, $D_{\infty h}$)	XeF^+	(Linear, $C_{\infty v}$)		
			FXe--F--XeF^+	(V-shape, C_{2v})[b]		
	FXeOXeF	(V-shape, C_{2v})	FXeOXe--$FXeF^+$	(Bent chain, C_s)		
Xe(IV)	XeF_4	(Square plane, D_{4h})	XeF_3^+	(T-shape, C_{2v})	XeF_5^-	(Pentagonal planar, D_{5h})
	$XeOF_2$	(T-shape, C_{2v})			$XeOF_3^-$	(Planar, C_{2v})
Xe(VI)	XeF_6	(Monocapped octahedron, C_{3v}	XeF_5^+	(Square pyramid, C_{4v})	XeF_7^-	(Monocapped octahedron, C_{3v})
			F_5Xe--F--XeF_5^+		XeF_8^{2-}	(Square antiprism, D_{4d})
	$XeOF_4$	(Square pyramid, C_{4v})	$XeOF_3^+$	(Disphenoid, C_s)	$XeOF_5^-$	(Pentagonal pyramid, C_{5v})
					$(XeOF_4)_3F^c$	
	XeO_2F_2	(Disphenoid, C_{2v})	XeO_2F^+	(Trigonal pyramid, C_{2v})	$XeO_2F_3^-$	(Square pyramid, C_s)
			FO_2Xe--F--XeO_2F^+			
	XeO_3	(Trigonal pyramid, C_{3v})			XeO_3F^-	[d]
Xe(VIII)	XeO_2F_4	(Pseudooctahedron, D_{4h})[e]				
	XeO_3F_2	(Trigonal bipyramid, D_{3h})			$XeO_3F_3^-$	(Pseudooctahedron, facial arrangement, C_{3v})
	XeO_4	(Tetrahedron, T_d)			$XeO_4F_2^{2-}$	(Distorted octahedron, mixture of isomers *cis* (C_{2v}) and *trans* (D_{4h}))

[a] Point group symmetries are given in parentheses.

[b] Cations that are mononuclear in xenon and the F_5Xe--F--XeF_5^+ ($Xe_2F_{11}^+$) and the FO_2Xe--F--XeO_2F^+ ($Xe_2O_4F_3^+$) cations interact with their fluoroanions through one or more fluorine bridges. The $Xe_2F_3^+$ cation forms no fluorine bridges with its fluoroanion. The XeF_5 groups in $Xe_2F_{11}^+$ have square pyramidal geometries and the XeO_2F groups in $Xe_2O_4F_3^+$ have trigonal bipyramidal geometries similar to that of XeO_2F_2.

[c] Three $XeOF_4$ molecules, having essentially square pyramidal geometries, are coordinated through the xenon atoms to a single fluoride ion to give a trigonal pyramidal arrangement about the fluoride ion.

[d] The structure consists of open polymeric chains, $[XeO_3F^-]_n$, with two fluorine bridges to each xenon atom.

[e] Predicted geometry.

a V-shaped geometry. The only known synthetic route to $O(XeF)_2$ is by displacement from the $FXeOXeFXeF^+$ AsF_6^- salt (see Section III.V) using the fluoride ion donor NOF. Xenon oxide difluoride ($XeOF_2$) is formed as an unstable yellow solid by the interaction of XeF_4 with a stoichiometric amount of water. Xenon oxide tetrafluoride, $XeOF_4$, [square pyramidal geometry with the oxygen trans to the electron lone pair; Xe—F, 1.703(15) Å; Xe—O, 1.900(5) Å] is a volatile colorless liquid, and XeO_2F_2 [trigonal bipyramidal geometry with both oxygens and the electron lone pair in the equatorial plane, Xe—F, 1.714(4) Å; Xe—O, 1.899(3) Å] is a colorless solid. The compound $XeOF_4$ is formed by the interaction of XeF_6 with equimolar amounts of water, $NaNO_3$, or POF_3. The reaction of stoichiometric amounts of N_2O_5 and $XeOF_4$ affords XeO_2F_2. Two additional oxofluorides are known, XeO_3F_2 and XeO_2F_4. Xenon trioxide difluoride is formed by reaction of XeF_6 with Na_4XeO_6. The structure of XeO_3F_2 has been determined by vibrational spectroscopy and ^{17}O, ^{19}F, and ^{129}Xe NMR spectroscopy. Xenon dioxide tetrafluoride is prepared by reaction of XeO_3F_2 with XeF_6 in $XeOF_4$ solvent. Although XeO_2F_4 has been characterized by mass spectrometry, the structure of XeO_2F_4 has not been established by experiment. Both XeO_3F_2 and XeO_2F_4 are thermodynamically unstable.

D. Xenates and Perxenates

Alkali metal xenates of composition $MHXeO_4 \cdot 1.5H_2O$, where M is sodium, potassium, rubidium, or cesium, have been prepared by freeze drying mixtures of xenon trioxide and the corresponding metal hydroxides in 1:1 molar ratios. The xenates are unstable, explosive solids.

When XeF_6 is hydrolyzed in a strongly alkaline solution, part of the xenon is lost as gas, but a large fraction precipitates as a perxenate (XeO_6^{4-}) salt in which xenon is in the +8 oxidation state. Among the salts

that have been prepared in this manner, or by alternative procedures, are $Na_4XeO_6{\cdot}6H_2O$, $K_4XeO_6{\cdot}9H_2O$, $Li_4XeO_6{\cdot}2H_2O$, and $Ba_2XeO_6{\cdot}1.5H_2O$ [average Xe—O bond length, 1.864(12) Å]. The salts are kinetically very stable, losing water gradually when heated, for example, $Na_4XeO_6{\cdot}6H_2O$ becomes anhydrous at 100°C and decomposes at 360°C. A number of transition metal and actinide perxenates have been prepared, but are not thoroughly characterized, and include those of copper, lead, silver, zinc, thorium, and uranium. Perxenates are powerful oxidants in aqueous solution and are capable of oxidizing iodate ion to periodate and manganous ion to permanganate.

E. Ionic Complexes and Molecular Adducts of Xenon

The majority of the known complexes of xenon can be classified as cation or anion derivatives of binary fluorides, oxofluorides, and XeO_3 (Table I). Although complex compounds derived by the interaction of a noble-gas fluoride or oxofluoride with a strong fluoride acceptor are generally written as ionic formulations, the cations and anions interact with one another by means of weak covalent interactions of the cation with one or more fluorines on the anion, an interaction that is termed "fluorine bridging," e.g., $F—Xe^{+}{-}{-}{^-}F—AsF_5$ ($XeF^+AsF_6^-$) and $F—Xe{-}{-}F{-}{-}Xe—F^+$ (V-shaped $Xe_2F_3^+$ cation).

Xenon difluoride behaves as a fluoride ion donor towards many metal pentafluorides to form complex salts containing the XeF^+ and $Xe_2F_3^+$ cations. In reactions with the pentafluorides of arsenic, antimony, and ruthenium, for example, it forms the salts $Xe_2F_3^+AsF_6^-$ [Xe—$F_{terminal}$, 1.929(6) Å; Xe--F_{bridge}, 2.157(3) Å] $XeF^+AsF_6^-$ [Xe—$F_{terminal}$, 1.873(6) Å; Xe--F_{bridge}, 2.212(5) Å], $Xe_2F_3^+SbF_6^-$, $XeF^+SbF_6^-$, $XeF^+Sb_2F_{11}^-$, $Xe_2F_3^+RuF_6^-$, $XeF^+RuF_6^-$, and $XeF^+Ru_2F_{11}^-$. Bartlett's original compound, "$Xe^+PtF_6^-$," was subsequently shown by him to be of this general type, i.e., a mixture of $XeF^+PtF_6^-$, $XeF^+Pt_2F_{11}^-$, and PtF_5. Adducts with the weak fluoride ion acceptors $MoOF_4$ and WOF_4 are known in which XeF_2 interacts with the metal by formation of asymmetric Xe—F--M bridges (M = Cr, Mo, or W), e.g., F—Xe—F--CrF_4, F—Xe—F--(CrF_4)--F—Xe—F, F—Xe—F--MOF_4, F—Xe—F--$MoOF_4(MoOF_4)_2$. A crystal structure of $XeF_2{\cdot}WOF_4$ exhibits the bond lengths Xe—F_{bridge}, 2.04(3) Å; W--F_{bridge}, 2.18(3) Å; and Xe—$F_{terminal}$, 1.89(3) Å. The compound $Ag(XeF_2)_2^+AsF_6^-$ provides an example in which the XeF_2 molecules are weakly coordinated to the Ag^+ ion. Xenon difluoride also forms a related fluorine bridged adduct cation, F—Xe—F---$BrOF_2^+$, in the compound $XeF_2{\cdot}BrOF_2^+AsF_6^-$ and a number of molecular complexes in which the molecular parameters are essentially the same as in the pure compound; these include $XeF_2{\cdot}IF_5$, $XeF_2{\cdot}XeOF_4$, and $XeF_2{\cdot}XeF_4$.

Xenon difluoride reacts with hydronium ion salts, $H_3O^+MF_6^-$ (M = As, Sb) in HF solvent to give $FXeOH_2^+MF_6^-$ and $FXeOXeFXeF^+MF_6^-$. The latter salt is deep red to magenta in color and is the precursor used to generate the only other oxide fluoride of xenon in the +2 oxidation state, $O(XeF)_2$ (see Section III.C).

The only example of xenon in a fractional oxidation state, $+\frac{1}{2}$, is the bright emerald green, paramagnetic dixenon cation, Xe_2^+. Mixtures of xenon and fluorine gases react spontaneously with liquid antimony pentafluoride in the dark to form solutions of $XeF^+Sb_2F_{11}^-$, in which Xe_2^+ is formed as an intermediate product that is subsequently oxidized by fluorine to the XeF^+ cation. Spectroscopic studies have shown that xenon is oxidized at room temperature by solutions of XeF^+ in SbF_5 solvent to give the Xe_2^+ cation. The dixenon cation has been isolated as the $Sb_4F_{21}^-$ salt in which Xe_2^+ has the bond length 3.087(1) Å.

Xenon tetrafluoride is a much weaker fluoride ion donor and only forms stable complex salts with the strongest fluoride ion acceptors: $XeF_3^+SbF_6^-$ [Xe—F_{axial}, 1.906(14) Å; Xe—$F_{equatorial}$, 1.835(10) Å; Xe--F_{bridge}, 2.485(10) Å], $XeF_3^+Sb_2F_{11}^-$, and $XeF_3^+BiF_6^-$. Xenon tetrafluoride has also been shown to behave as a weak fluoride ion acceptor toward alkali metal fluorides and the naked fluoride ion source $N(CH_3)_4^+F^-$ to give salts of the novel pentagonal planar XeF_5^- anion [Xe—F, 2.012(3) Å], the first example of an AX_5E_2 (A = central atom, X = ligand atom, and E = valence electron lone pair) VSEPR (valence shell electron pair repulsion) arrangement. Xenon oxide difluoride is a fluoride ion acceptor, forming the only other anion containing xenon in the +4 oxidation state, the $XeOF_3^-$ anion in $Cs^+XeOF_3^-$.

Xenon hexafluoride is both a strong fluoride ion donor and acceptor. Examples of salts containing the XeF_5^+ cation are numerous, with counteranions such as PtF_6^-, AuF_6^-, SbF_6^-, CrF_5^-, BF_4^-, and GeF_5^-. A representative crystal structure is that of $XeF_5^+PtF_6^-$ (Xe—F_{axial}, 1.81 Å; Xe—$F_{equatorial}$, 1.88 Å). There are several examples of salts that contain the fluoride bridged $Xe_2F_{11}^+$ cation that have a number of counteranions in common with those of the XeF_5^+ salts, e.g., $Xe_2F_{11}^+NiF_6^-$, $Xe_2F_{11}^+VF_6^-$. The structure of the $Xe_2F_{11}^+$ cation is exemplified in the crystal structure of $Xe_2F_{11}^+AuF_6^-$ [Xe—F_{axial}, 1.82(1) Å; Xe—$F_{equatorial}$, 1.84(1) Å]. Xenon(VI) fluorometalates(III) and (IV) of the rare earth elements (including Y and La) have the formulations $6XeF_6{\cdot}YF_3$, $XeF_6{\cdot}2CeF_4$, $XeF_6{\cdot}4PrF_4$, $XeF_6{\cdot}2TbF_4$, $3XeF_6{\cdot}DyF_3$, $6XeF_6{\cdot}HoF_3$, $6XeF_6{\cdot}ErF_3$, $6XeF_6{\cdot}TmF_3$, $6XeF_6{\cdot}YbF_3$, and $6XeF_6{\cdot}LuF_3$. Vibrational spectra are in accordance with the formulation of these compounds

as salts of the XeF_5^+ cation with polymeric ($XeF_6{\cdot}4MF_4$ and $XeF_6{\cdot}2MF_4$) or monomeric anions ($3XeF_6{\cdot}MF_3$) and salts of the $Xe_2F_{11}^+$ cation with monomeric anions ($6XeF_6{\cdot}MF_3$).

A number of salts in which XeF_6 behaves as a fluoride ion acceptor towards alkali metal fluorides are known which contain the XeF_7^- and XeF_8^{2-} anions. Several nonalkali metal salts have been shown by X-ray crystallography and vibrational spectroscopy to contain the anions XeF_7^-, and XeF_8^{2-} and include $NF_4^+XeF_7^-$, $Cs^+XeF_7^-$, $[NF_4^+]_2XeF_8^{2-}$, and $[NO^+]_2XeF_8^{2-}$. The XeF_7^- anion in $Cs^+XeF_7^-$ is a capped octahedral structure with an Xe—F bond to the capping F atom that is remarkably long [2.100(6) Å]. The XeF_8^{2-} anion in $[NO^+]_2XeF_8^{2-}$ is a square antiprism with Xe—F bond lengths of 1.946(5)–2.099(5) Å. Reaction of NO_2F and XeF_6 (1:2 mole ratio) affords $NO_2^+Xe_2F_{13}^-$. The $Xe_2F_{13}^-$ anion structure is composed of an XeF_6 molecule bridged by two long Xe--F bonds to an XeF_7^- anion such that the bridge fluorines avoid the axial nonbonding electron pair of the XeF_6 molecule.

The oxofluorides of xenon +6, $XeOF_4$ and XeO_2F_2, exhibit analogous fluoride ion donor and acceptor properties. Salts of both the $XeOF_3^+$ and XeO_2F^+ cations are known, as well as a salt of the fluoride bridged cation $Xe_2O_4F_3^+$, and include $XeOF_3^+SbF_6^-$ [Xe—O, 1.69(2) Å; Xe—F_{axial}, 1.88(2) Å; Xe—$F_{equatorial}$, 1.82(2) Å; Xe--F_{bridge}, 2.53(2) Å], $XeOF_3^+Sb_2F_{11}^-$, $XeO_2F^+Sb_2F_{11}^-$, $XeO_2F^+AsF_6^-$, and $Xe_2O_4F_3^+AsF_6^-$. Several alkali metal fluoride complexes with $XeOF_4$ are known, such as $3KF{\cdot}XeOF_4$, $3RbF{\cdot}2XeOF_4$, $CsF{\cdot}XeOF_4$, and $CsF{\cdot}3XeOF_4$. Structural studies show that the CsF complexes are best formulated as $Cs^+XeOF_5^-$ and $Cs^+(XeOF_4)_3F^-$ [Xe—O, 1.70(5) Å; Xe—F, 1.90(3) Å; Xe--F_{bridge}, 2.62(1) Å]. The $N(CH_3)_4^+$ and NO^+ salts of $XeOF_5^-$ are also known. The $XeOF_5^-$ anion has a pentagonal-pyramidal geometry with the O atom and the electron lone pair in the apical positions [Xe—O, 1.710(2) Å; Xe—F, 1.995(4) Å]. The only complexes between XeO_2F_2 and a strong fluoride ion donor are the salts $Cs^+XeO_2F_3^-$ and $[NO_2^+][XeO_2F_3{\cdot}nXeO_2F_2^-]$.

Alkali metal fluoroxenates $KXeO_3F$, $RbXeO_3F$, $CsXeO_3F$ (decompose above 200°C) and chloroxenates $CsXeO_3Cl$ (decomposes above 150°C) have been prepared by evaporating aqueous solutions of XeO_3 and the corresponding alkali metal fluorides and chlorides. The alkali metal fluoroxenates are the most stable solid oxygenated compounds of xenon(VI) known. X-ray crystallography shows that $KXeO_3F$ is best formulated as $nK^+[XeO_3F^-]_n$, in which each XeO_3 group is bonded to two fluorine atoms which bridge adjacent XeO_3 groups to give an open chain polymeric structure [Xe—O, 1.77(1) Å; Xe--F_{bridge}, 2.42(1) Å]. Similarly, the X-ray crystal structures of the compounds $2.25\ MCl{\cdot}XeO_3$ (M = Rb, Cs) feature infinite chains of $[XeO_3Cl]^-$ units linked by nearly linear chlorine bridges (Xe—O, 1.55–1.78 Å; Xe—Cl, 2.93–2.97 Å). The $CsXeO_3Br$ compound is unstable even at room temperature.

No complex salts or molecular adducts derived from the known oxofluorides and oxide of xenon in the +8 oxidation state, namely, XeO_3F_2, XeO_2F_4, and XeO_4, are known.

F. Compounds of Xenon Bonded to Polyatomic Groups

1. Xenon Bonded to Oxygen

The greatest variety of polyatomic ligand groups bonded to xenon occur for xenon in its +2 oxidation state, and those bonded through oxygen are most plentiful. Both mono- and disubstituted derivatives having the formulations FXeL and XeL_2 are known where L = $OTeF_5$, $OSeF_5$, OSO_2F, $OP(O)F_2$, $OClO_3$, ONO_2, $OC(O)CH_3$, $OC(O)CF_3$, OSO_2CH_3, OSO_2CF_3, and $OIOF_4$. With the exception of $OIOF_4$ and $OP(O)F_2$, the syntheses involve HF elimination reactions of the parent acid HL with XeF_2 (e.g., $XeF_2 + x\ HL \rightarrow F_{2-x}XeL_x + x\ HF$; $x = 1, 2$). Among the most stable derivatives are those of the pseudo-octahedral and highly electronegative $OSeF_5$ and $OTeF_5$ groups. For example, $FXeOTeF_5$ (pale yellow liquid at room temperature; mp −24°C) and $Xe(OTeF_5)_2$ (white solid; mp 35–37°C) decompose at 130 and 120°C, respectively. The selenium analogues $FXeOSeF_5$ (pale yellow liquid; mp ca. −13°C) and $Xe(OSeF_5)_2$ (pale yellow solid; mp 69°C) decompose at 100°C. The crystal structures of $Xe(OSeF_5)_2$ [Xe—O, 2.09(3) Å] and $Xe(OTeF_5)_2$ [Xe—O, 2.12(2) Å] are known. Upon dissolution of equimolar amounts of $Xe(OTeF_5)_2$ and $Xe(OSeF_5)_2$ in $CFCl_3$ solvent, an equilibrium mixture of the starting materials and the mixed ligand compound $Xe(OTeF_5)(OSeF_5)$ was observed by NMR spectroscopy. The yellow solids $XeOTeF_5^+AsF_6^-$ (mp 160°C) and $XeOSeF_5^+AsF_6^-$ are formed by reaction of $FXeOTeF_5$ and $FXeOSeF_5$ with AsF_5. The crystal structures of $XeOSeF_5^+AsF_6^-$ [Xe—O, 2.04(4) Å] and $XeOTeF_5^+AsF_6^-$ [Xe—O, 1.966(4) Å] have been determined. Displacement of AsF_5 by SbF_5 results in the formation of $XeOTeF_5^+Sb_2F_{11}^-$, which is a light yellow-orange solid at room temperature. In BrF_5 solution at −48°C, $XeOTeF_5^+AsF_6^-$ undergoes solvolysis to give the bridging cation $FXe{-}{-}F{-}{-}XeOTeF_5^+$, which is structurally similar to the V-shaped $Xe_2F_3^+$ and $Kr_2F_3^+$ cations (see Section III.E) with a $OTeF_5$ group and a fluorine in terminal positions.

Reaction of *cis*-$(HO)_2TeF_4$ with $Xe_2F_3^+AsF_6^-$ in HF solvent affords the yellow solid *cis*-FXeO—TeF_4—OXe^+

AsF_6^-, which is stable at room temperature (dec 89°C). The crystal structure of orange $HOTeF_4$—$OXe^+AsF_6^-$, obtained from HF solvent, has been shown to be HF·HO—TeF_4—$OXe^+AsF_6^-$ [Xe—O, 1.962(9) Å].

The —$OTeF_5$ derivatives of xenon in its +4 and +6 oxidation states are well characterized. The derivative $Xe(OTeF_5)_4$ is the only example known where xenon in the +4 oxidation state is coordinated exclusively to oxygens. The compound is prepared by reaction of XeF_4 with $B(OTeF_5)_3$. It is a dark yellow solid which decomposes at 72°C to give $Xe(OTeF_5)_2$ and F_5TeO—$OTeF_5$. The X-ray crystal structure of $Xe(OTeF_5)_4$ reveals square planar coordination at xenon and an average Xe—O bond length of 2.032(5) Å. The mixed ligand derivatives $FXe(OTeF_5)_3$, *cis*- and *trans*-$F_2Xe(OTeF_5)_2$, and $F_3XeOTeF_5$ have been observed in $CFCl_3$ solution and result from the ligand redistribution upon mixing XeF_4 and $Xe(OTeF_5)_4$. The mixed ligand cations $FXe(OTeF_5)_2^+$, $F_2XeOTeF_5^+$, and $Xe(OTeF_5)_3^+$ are formed by the reaction of $Xe(OTeF_5)_4$ with SbF_5 solvent at 5°C. The reddish-violet solid $Xe(OTeF_5)_6$ is prepared by reaction of XeF_6 and $B(OTeF_5)_3$ at −40°C in perfluoro-*n*-pentane solvent. An incomplete X-ray analysis of $Xe(OTeF_5)_6$ suggests that, unlike XeF_6, solid $Xe(OTeF_5)_6$ is monomeric and isostructural with $Te(OTeF_5)_6$, with possible C_{3v} or D_{3d} local point group symmetry around xenon. The colorless compound O═$Xe(OTeF_5)_4$ (mp 56°C) is prepared by hydrolysis of $Xe(OTeF_5)_6$ or by reaction of O═XeF_4 with $B(OTeF_5)_3$. Slow decomposition (over several months) at room temperature produces $F_5TeOTeF_5$ and $O_2Xe(OTeF_5)_2$. The mixed ligand derivatives O═$XeF(OTeF_5)_3$, O═$XeF_2(OTeF_5)_2$, and O═$XeF_3(OTeF_5)$ are formed by reaction of O═$Xe(OTeF_5)_4$ and O═XeF_4 in $CFCl_3$ or $XeOF_4$ solvents. The cations O═$Xe(OTeF_5)_3^+$, O═$XeF(OTeF_5)_2^+$, and O═$XeF_2(OTeF_5)^+$ are formed upon dissolution of O═$Xe(OTeF_5)_4$ in SbF_5 solution at 5°C. Colorless $O_2Xe(OTeF_5)_2$ may be prepared by reaction of O_2XeF_2 with $B(OTeF_5)_3$ or from slow decomposition of O═$Xe(OTeF_5)_4$ at room temperature. The X-ray crystal structure of $O_2Xe(OTeF_5)_2$ reveals a local geometry at xenon which may be described as a pseudo-trigonal bipyramid or a distorted tetrahedron. The average Xe═O double bond lengths are 1.729(5) Å, and the Xe—O single bond lengths are 2.022(4) Å. The mixed ligand compound $O_2XeF(OTeF_5)$ is formed in SO_2ClF solution by reaction of excess O_2XeF_2 and $B(OTeF_5)_3$. The $O_2XeOTeF_5^+$ cation is formed by decomposition of the O═$XeF(OTeF_5)_2^+$ cation in SbF_5 solvent at 5°C. Decomposition of the $O_2XeOTeF_5^+$ cation also occurs in SbF_5 solution at 5°C, forming oxygen and the $XeOTeF_5^+$ cation.

The pseudo-octahedral and highly electronegative $OIOF_4$ group exists as a mixture of *cis* and *trans* isomers and forms derivatives with xenon in its +2 and +4 oxidation states. The interaction of IO_2F_3 dimer and XeF_2 in SO_2ClF (−5°C) and $CFCl_3$ (24°C) solvents produces the xenon(II) compounds $Xe(OIOF_4)_2$ and $FXeOIOF_4$. The compound $FXeOIOF_4$ is also prepared by the stoichiometric reaction of XeF_2 with $Xe(OIOF_4)_2$. Both compounds are isomeric mixtures in which the oxygen bonds in the pseudo-octahedrally coordinated $OIOF_4$ ligands are cis or trans to one another, i.e., *cis*,*cis*-$Xe(OIOF_4)_2$, *cis*,*trans*-$Xe(OIOF_4)_2$, *trans*,*trans*-$Xe(OIOF_4)_2$, *cis*-$FXeOIOF_4$, and *trans*-$FXeOIOF_4$. The mixture of *cis*- and *trans*-$FXeOIOF_4$ is a pale yellow liquid which is stable for periods exceeding 1 h at room temperature (mp −5 to 0°C). Pure *cis*,*cis*-$Xe(OIOF_4)_2$, prepared by the reaction of $Xe(OTeF_5)_2$ and $HOIOF_4$ at 0°C in $CFCl_3$ solvent or neat, is a yellow solid which decomposes rapidly at room temperature. Combination of $Xe(OTeF_5)_2$ and *cis*,*cis*-$Xe(OIOF_4)_2$ results in the formation of the mixed ligand species *cis*-$F_4OIOXeOTeF_5$ and *trans*-$F_4OIOXeOTeF_5$ in $CFCl_3$ solvent at 5 and 24°C. Solvolysis of $FXeOIOF_4$ in SO_2ClF solvent at −5°C results in the formation of *cis*-$FO_2SOXeOIOF_4$ and *trans*-$FO_2SOXeOIOF_4$. The xenon(IV) derivative, $F_3XeOIOF_4$, has been prepared by reaction of XeF_4 and IO_2F_3 in $CFCl_3$ solution at 24°C.

The fluorosulfate derivatives $FXeOSO_2F$ (mp 36.6°C) and $Xe(OSO_2F)_2$ (mp 43–45°C) are colorless and light yellow solids, respectively, at room temperature. The thermal decomposition of $Xe(OSO_2F)_2$ provides a method for the preparation of very pure $S_2O_6F_2$, which is formed in quantitative yield with the liberation of xenon gas. The crystal structure of $FXeOSO_2F$ has been determined [Xe—O, 2.155(8) Å; Xe—F, 1.940(8) Å]. The solids $FXeOSO_2CF_3$ and $FXeOSO_2CH_3$ are yellow and stable at 0°C, but decompose explosively when warmed to room temperature. The complex salt $Xe_2F_3^+AsF_6^-$ reacts with HSO_3F in HF or in HSO_3F solvent to form the $(FXeO)_2SOF^+$ cation as the pale yellow salt $(FXeO)_2SOF^+AsF_6^-$. Alternatively, $(FXeO)_2SOF^+AsF_6^-$ has been prepared by the reaction of XeF_2 with HSO_3F and AsF_5 in HF solvent. The $(FXeO)_2SOF^+$ cation is V-shaped, similar to $Xe_2F_3^+$, with the fluorosulfate group in the bridging position. The $XeOSO_2F^+$ cation has been observed as the product resulting from the solvolysis of $XeOTeF_5^+AsF_6^-$ in HSO_3F solution. The compounds $FXeOPOF_2$ and $Xe(OPOF_2)_2$ are both orange solids and are formed in the reaction of XeF_2 with one and two equivalents of $P_2O_3F_4$, respectively, at −22°C in $CFCl_3$ solvent. Both compounds rapidly decompose at 22°C. The perchlorate derivatives $FXeOClO_3$ [colorless solid, mp (dec),

16.5°C] and $Xe(OClO_3)_2$ [yellow solid, mp (dec), 0°C] are violent detonators. The compounds $Xe(OC(O)CF_3)_2$ and $FXeOC(O)CF_3$ are pale yellow solids which decompose within a few hours at room temperature, but can detonate above −20°C if thermally or mechanically shocked. The nitrates $FXeONO_2$ and $Xe(ONO_2)_2$ have not been isolated, but have been inferred from analysis of the decomposition products of the reaction of XeF_2 with pure HNO_3.

The formation of xenon–oxygen bonded species in the reaction of XeF_2 with excess WOF_4 at low temperature (−121°C) in SO_2ClF has been observed by NMR spectroscopy and is formulated as $FXe{-}OWF_5(WOF_4)$ and $FXe{-}OWF_5(WOF_4)_2$. The fluorine bridged adducts $FXeFMOF_4$ (M = W, Mo) undergo solvolysis in HSO_3F solvent (−80°C) to give the fluorosulfate bridged species $FXe{-}O(F)S({=}O)O{-}MOF_4$ (M = Mo, W), which is in equilibrium with $FXeOSO_2F$ and MOF_4.

Currently, only two examples of cations containing —O—Xe—F linkages are known. The reaction of $(CF_3)_2S{=}O$ with $XeF^+SbF_6^-$ in HF solvent at −65°C results in the species $(CF_3)_2S{=}O{-}XeF^+SbF_6^-$ (white solid), which is reported to be stable at −78°C, but is prone to detonate if mechanically disturbed. The salt $CF_3C(OH)NH_2^+AsF_6^-$ reacts with XeF_2 in BrF_5 solvent by an HF elimination reaction to give the novel Xe—O bonded $CF_3C(OXeF)NH_2^+$ cation.

2. Xenon Bonded to Nitrogen

Several ligand groups form compounds containing xenon–nitrogen bonds. The first xenon–nitrogen bonded compound, $FXeN(SO_2F)_2$, was prepared by reaction of $HN(SO_2F)_2$ and XeF_2 at 0°C in CF_2Cl_2 solvent, and Xe—N bonding in this compound was conclusively established by X-ray crystallography. The Xe—N and Xe—F bond distances are 2.200(3) and 1.967(3) Å, with trigonal planar coordination around the nitrogen atom. The compound is a white solid at room temperature, decomposing rapidly and quantitatively at 70°C to XeF_2, Xe, and $[N(SO_2F)_2]_2$. The fluoride ion donor properties of $FXeN(SO_2F)_2$ have been studied by reaction with the strong fluoride ion acceptors AsF_5 and SbF_5. The reaction of $FXeN(SO_2F)_2$ with AsF_5 results in a yellow solid, $XeN(SO_2F)_2^+AsF_6^-$, which decomposes at 22°C under vacuum to the yellow solid $F[XeN(SO_2F)_2]_2^+AsF_6^-$. The cation consists of two $XeN(SO_2F)_2$ groups with planar nitrogen centers joined by a bridging fluorine atom, similar to the $Xe_2F_3^+$ cation (see Section III.E). Crystalline $XeN(SO_2F)_2^+Sb_3F_{16}^-$ has been isolated by dissolution of $XeN(SO_2F)_2^+AsF_6^-$ in SbF_5 at 0°C. The X-ray crystal structure shows that the compound contains $XeN(SO_2F)_2^+$ cations fluorine bridged to the $Sb_3F_{16}^-$ anion through the xenon atom [Xe--F bridge bond distance = 2.457(8) Å]. The Xe—N bond length is 2.02(1) Å. The disubstituted compound $Xe[N(SO_2F)_2]_2$ is a white solid and is prepared by the reaction of XeF_2 and $HN(SO_2F)_2$ in a 1:2 molar ratio or by the reaction of $FXeN(SO_2F)_2$ with $HN(SO_2F)_2$ in a 1:1 molar ratio. Quantitative decomposition to xenon and $[N(SO_2F)_2]_2$ occurs rapidly at 22°C. The compound $Xe[N(SO_2CF_3)_2]_2$ is a white solid prepared by reaction of $(CH_3)_3SiN(SO_2CF_3)_2$ with XeF_2 in CF_2Cl_2 at −22 to 10°C and is stable indefinitely at room temperature. Rapid decomposition at 72°C produces xenon, C_2F_6, $(CF_3SO_2)_2NCF_3$, and $CF_3SO_2NSO_2$.

Fluorine bridge formation between the cation and fluoroanion in complex XeF^+ salts (see Section III.E) in the solid state indicates that the XeF^+ cation is a strong Lewis acid. Nitrogen bases have been shown to displace the anion, forming Lewis acid-base adduct cations containing —N—Xe—F linkages, e.g., $HC{\equiv}N{:} + F{-}Xe^+{-}{-}F{-}AsF_5^- \rightarrow HC{\equiv}N{-}Xe{-}F^+ + AsF_6^-$. Suitable nitrogen bases that are resistant to oxidation by the strongly oxidizing XeF^+ cation have been successfully predicted by choosing bases whose first adiabatic ionization potentials are greater than or equal to the estimated electron affinity of the XeF^+ cation (10.9 eV). The thermally unstable, colorless salt $HC{\equiv}NXeF^+AsF_6^-$ [Xe—F, 1.936(2) Å; Xe—N, 2.235(3) Å] is prepared by reaction of $HC{\equiv}N$ with $Xe_2F_3^+AsF_6^-$ or $XeF^+AsF_6^-$ in anhydrous HF solvent or by reaction of $HC{\equiv}NH^+AsF_6^-$ with XeF_2 in BrF_5 solvent. Other nitrile adduct cations, $RC{\equiv}N{-}XeF^+$ (R = CH_3, CH_2F, CF_3, C_2H_5, C_2F_5, n-C_3F_7, C_6F_5), have been prepared as AsF_6^- salts using methods similar to those used for the preparation of $HC{\equiv}NXeF^+AsF_6^-$. The alkyl and C_6F_5 derivatives are generally thermally less stable than $HC{\equiv}NXeF^+AsF_6^-$ or the perfluorinated alkyl derivatives. The structures of the $H_3CC{\equiv}NXeF^+AsF_6^-{\cdot}HF$ [Xe—F, 1.947(5) Å; Xe—N, 2.179(7) Å] and $(H_3C)_3CC{\equiv}NXeF^+AsF_6^-$ [Xe—F, 1.952(3) Å; Xe—N, 2.212(4) Å] salts have also been determined, and the C—N—Xe angles are found to be significantly bent by 175.0(8) and 166.9(4) degrees, respectively. The fluoro(perfluoropyridine)xenon(II) cations 4-$RC_5F_4N{-}{-}XeF^+$ (R = F, CF_3) have been observed by NMR spectroscopy in HF and BrF_5 solutions (stable up to −30°C), and their AsF_6^- salts (colorless solids) have been isolated from BrF_5 solutions. Low-temperature Raman and NMR spectroscopic results are consistent with planar cations in which the xenon atom is directly bonded to the aromatic ring through the lone pair of electrons on the nitrogen atom. The fluoro(perfluorodiazine)xenon(II) cations 1,2-C_4F_4NN

—XeF^+ and 1,3-C_4F_4NN—XeF^+ have been synthesized as the AsF_6^- salts by analogy with the fluoro(perfluorodiazine)xenon(II) salts in BrF_5 solvent. The colorless solid, *s*-$C_3F_3N_2N$-$XeF^+AsF_6^-$, is currently the only salt in this series of compounds which is stable at room temperature and is prepared by the reaction of XeF^+ AsF_6^- with liquid *s*-trifluorotriazine, *s*-$C_3F_3N_3$, at room temperature. The salts having the formulations L—$XeF^+AsF_6^-\cdot 2.5BrF_5$ have been characterized by low-temperature X-ray crystallography, where L is *s*-$C_3F_3N_2N$- [Xe—F, 1.931(5) Å; Xe—N, 2.316(6) Å], C_5F_5N- [Xe—F, 1.932(6) Å; Xe—N, 2.287(8) Å], 1,2-C_4F_4NN- [Xe—F, 1.956(8) Å; Xe—N, 2.247(9) Å], and 1,3-C_4F_4NN- [Xe—F, 1.90(2) Å; Xe—N, 2.28(3) Å]. In all cases, the prefluorinated heterocycle and N-coordinated XeF group are coplanar.

Other examples of xenon(II) bonded to inorganic nitrogen base centers are known. The reaction of $F_3S{\equiv}N$ with L = XeF^+, $XeOSeF_5^+$, and $XeOTeF_5^+$ leads to the formation of the corresponding $F_3S{\equiv}N$—L^+ cations. The $F_3S{\equiv}N$—L^+ cation is formed by reaction of $XeF^+AsF_6^-$ with liquid $F_3S{\equiv}N$ at −20°C or in HF solvent to form the $F_3S{\equiv}NXeF^+$ cation. The cation undergoes a two-step fluorination in HF to yield two further cations, $F_4S{=}NXe^+$ and $F_5SN(H)Xe^+$. The tellurium analogue of the latter cation, $F_5TeN(H)Xe^+$, is synthesized from F_5TeNH_2 and $XeF^+AsF_6^-$ in HF solvent at low temperatures. The $F_5TeN(H)Xe^+$ cation has been obtained as the AsF_6^- salt and has been shown to interact strongly through the Xe atom with the AsF_6^- anion in the solid state, forming a Xe--F—As bridge [Xe—N, 2.044(4) Å; Xe--F, 2.580(3) Å].

3. Xenon Bonded to Carbon

A number of structurally well-characterized compounds containing Xe—C bonds are known. In all cases they occur as colorless salts of xenonium cations, R—Xe^+ (R = a fluorophenyl or alkynyl group). The formation of the pentafluorophenylxenon(II) cation, $C_6F_5Xe^+$, in CH_2Cl_2 (−30°C) and $CH_3C{\equiv}N$ (0°C) solutions with the anions $B(C_6F_5)_3F^-$, $B(C_6F_5)_2F_2^-$, and $B(C_6F_5)F_3^-$ has been established. The salts are formed by the reaction of XeF_2 with the ligand transfer reagent $B(C_6F_5)_3$. The X-ray crystal structure of $[CH_3C{\equiv}N{-}Xe{-}C_6F_5]^+$ $[(C_6F_5)_2BF_2]^-$ shows that the xenon atom is weakly coordinated to the nitrogen atom of a $CH_3C{\equiv}N$ molecule [Xe—N, 2.681(8) Å; Xe—C, 2.092(8) Å]. This salt decomposes slowly at 14°C. Reaction of $[CH_3C{\equiv}N{-}Xe{-}C_6F_5]^+[(C_6F_5)_2BF_2]^-$ with AsF_5 in $CH_3C{\equiv}N$ solution results in $[CH_3C{\equiv}N{-}Xe{-}C_6F_5]^+AsF_6^-$. Solutions of this compound in $CH_3C{\equiv}N$ are stable for up to 1 day at room temperature. The compound $C_6F_5Xe^+AsF_6^-$ was also prepared by displacement of $(C_6F_5)_2BF$ from $C_6F_5Xe^+(C_6F_5)_2BF_2^-$ using AsF_5. The thermal stability of the melt (125°C) is surprisingly high. The Xe—C distances of 2.079(6) and 2.082(5), Xe--F distances (cation–anion contacts) of 2.714(5) and 2.672(5), and C-Xe-F angles of 170.5(3) and 174.2(3) degrees are observed in the X-ray crystal structure.

The reactions of XeF_2 with the boron ligand transfer reagents B(*m*-$CF_3C_6H_4)_3$ and B(*p*-$FC_6H_4)_3$ in CH_2Cl_2 solution at −45 to −50°C result in the formation of the white solids [*m*-$CF_3C_6H_4Xe]^+$[*m*-$CF_3C_6H_4BF_3]^-$ and [*p*-$FC_6H_4Xe]^+$[(*p*-$FC_6H_4)_2BF_2]^-$. The former compound is stable for up to 1 h in $CH_3C{\equiv}N$ at −41°C, whereas the latter compound decomposes below −40°C when an attempt is made to dissolve it in the coordinating solvent $CH_3C{\equiv}N$. The 2,6-$C_6H_3F_2Xe^+$ cation has been prepared as the BF_4^- salt. The X-ray structure shows that xenon is bonded to carbon [Xe—C, 2.090(6) Å] and weakly coordinated to a single F atom of the tetrafluoroborate anion [Xe--F, 3.096(4) Å]. The xenonium salt $Xe(2,4,6\text{-}F_3C_6H_2)^+BF_4^-$ is prepared by the reaction of $B(C_6H_2F_3)\cdot$thf and XeF_2 in the presence of $BF_3\cdot O(CH_3)_2$ in CH_2Cl_2 solution at −40°C, is stable for up to 21 days at room temperature in dry air, and is hydrolyzed slowly over 7 days in aqueous $CH_3C{\equiv}N$ solution. Arylxenon trifluoromethanesulfonates are directly prepared by reaction with $CF_3CO_2XeO_3SCF_3$. The reaction of $Xe(O_2CCF_3)_2$ and CF_3SO_3H gives the highly reactive intermediate $CF_3CO_2XeO_3SCF_3$. Benzene derivatives containing electron-withdrawing substituents, such as F, CF_3, Cl, or NO_2, undergo electrophilic attack by $CF_3CO_2XeO_3SCF_3$ to yield arylxenon trifluoromethanesulfonate salts containing the 2,4,6-$F_3H_2C_5CXe^+$, 2,5-$F(O_2N)H_3C_5CXe^+$, 2,5-$F(CF_3)H_3C_5CXe^+$, and 3,5-$(CF_3)_2H_3C_5CXe^+$ cations. The molecular structure of 2,6-$F_2H_3C_5CXe^+O_3SCF_3^-$ has been determined by X-ray crystallography [Xe—C, 2.09(1) Å]. The xenon atom of the arylxenon unit is also weakly coordinated to one O atom of the $CF_3SO_3^-$ anion.

Reaction of $Me_3SiC_6F_5$/$[Me_4N]F$ with XeF_2 in propionitrile, propionitrile/acetonitrile, acetonitrile, or CH_2Cl_2 yields $Xe(C_6F_5)_2$, the first example of xenon bonded to two carbon atoms. When the same reaction is carried out in a 1:1 stoichiometry, C_6F_5XeF is the predominant product. Reaction of C_6F_5XeF with $Me_3SiOSO_2CF_3$ gives $[C_6F_5Xe]^+OSO_2CF_3^-$. The reaction of $C_6F_5Xe^+AsF_6^-$ with 4-$ClC_5H_4N\cdot HCl$ in CH_2Cl_2 at −78° gives 85% C_6F_5XeCl, the first example of the bulk preparation of a xenon(II)–chlorine bonded species (see Section III.A). The reaction of $C_6F_5Xe^+AsF_6^-$ with Me_3SiCl in CH_2Cl_2 at −78° gives 91% $(C_6F_5Xe)_2Cl^+AsF_6^-$, which was characterized

by X-ray crystallography [Xe—C, 2.11(1) Å; Xe—Cl, 2.816(3) Å].

Hydrogen-containing (polyfluorocycloalken-1-yl)xenon(II) salts (2-H-hexafluoro-1,4-cyclohexadien-1-yl) xenon(II) and (2-H-octafluorocyclohexen-1-yl)xenon(II) hexafluoro-arsenates and tetrafluoroborates have been obtained together with their perfluorinated analogs on reacting the corresponding (2,3,4,5-tetrafluorophenyl)xenon(II) salts with XeF_2 in anhydrous HF. An example of an acyclic alkenylxenon(II) compound, trifluorovinylxenon(II) tetrafluoroborate, $F_2C{=}C(F)Xe^+BF_4^-$, is known; it was synthesized from XeF_2 and $F_2C{=}C(F)BF_2$ and was characterized by ^{13}C, ^{19}F, and ^{129}Xe NMR spectroscopy.

Examples of alkynyl xenonium tetrafluoroborates are known and are prepared by reaction of lithium acetylides or triphenylsilyl acetylenes with XeF_2 and $BF_3{\cdot}O(CH_3)_2$ at low temperatures (−78 to −40°C) in CH_2Cl_2 solvent. The known alkynyl derivatives are $(CH_3)_3C{-}C{\equiv}C{-}Xe^+BF_4^-$, $(CH_3)_3Si{-}C{\equiv}C{-}Xe^+BF_4^-$, $CH_3CH_2{-}C{\equiv}C{-}Xe^+BF_4^-$, and $CH_3CH_2CH_2{-}C{\equiv}C{-}Xe^+BF_4^-$. All of these species decompose in solution or as solids below 0°C.

The first organoxenon(IV) compound, $[C_6F_5XeF_2][BF_4]$, was prepared by reaction of $C_6F_5BF_2$ with XeF_4 in CH_2Cl_2 at −55°C and is obtained as a yellow solid. The cation geometry is analogous to that of the T-shaped XeF_3^+ cation in which the unique equatorial fluorine is replaced by the C_6F_5 group.

The existence of the $XeCH_3^+$ cation has been established in the gas phase. The Xe—C bond energy of the $XeCH_3^+$ cation has been estimated to be 180 ± 33 kJ mol^{-1} and, more recently, 231 ± 10 kJ mol^{-1} by ion cyclotron resonance (cf. XeF_2 and XeF^+; the respective bond energies are 132 and 201 kJ mol^{-1}). The compound $Xe(CF_3)_2$ is reported to be a waxy white solid having a half-life of ca. 30 min at room temperature. The synthesis involved the addition of XeF_2 to a trifluoromethyl plasma, but the characterization of this compound is limited and has not been independently confirmed.

4. Xenon Bonded to Other Elements

The first metal–xenon compound, $AuXe_4^{2+}(Sb_2F_{11}^-)_2$, contains gold–xenon bonds and was prepared by reduction of AuF_3 with elemental xenon. The square planar $AuXe_4^{2+}$ cation has an Au—Xe bond length of 2.74 Å. The bonding between gold and xenon is of the σ-donor type, resulting in a charge of approximately 0.4 per xenon atom.

There are a number of novel xenon-element bonds which have been characterized in species that have not been obtained in bulk quantities but have been identified by mass spectrometry or by matrix-isolation spectroscopy in the solid state. The identification and characterization of such species provide direction and incentive to synthetic chemists who pursue the syntheses of noble-gas compounds that contain novel bonds to other elements. Photolysis of H_2S in a Xe matrix at 7.5 K has afforded HXeSH, the first and only example of an Xe—S bond. The structure was determined by infrared spectroscopy. The gaseous trifluorosilylxenon cation F_3SiXe^+, a species with an Si—Xe bond, was obtained under mass spectrometric conditions from the nucleophilic displacement of HF by Xe from protonated SiF_4.

IV. KRYPTON COMPOUNDS

A. Krypton Difluoride

Krypton is the lightest of the noble gases that forms isolable chemical compounds in bulk amounts. The simplest of these compounds is KrF_2, a colorless crystalline solid which can be sublimed under vacuum at 0°C but is thermodynamically unstable and slowly decomposes to the elements at ambient temperatures. It can, however, be stored for indefinite periods of time at −78°C. The KrF_2 molecule has been shown, like XeF_2, to be linear in the gas phase, in the solid state, and in solution. The standard enthalpy of formation (derived from calorimetric measurements of the gaseous compound at 93°C) is 60.2 kJ mol^{-1}. Consistent with its thermodynamic instability, krypton difluoride is a powerful oxidative fluorinating agent and is capable of oxidizing xenon to XeF_6 and gold to AuF_5. The heat of atomization for KrF_2 is only 97.8 kJ mol^{-1} and is substantially less than that of F_2 (157.7 ± 0.4 kJ mol^{-1}), making it a better low-temperature source of fluorine atoms and an aggressive fluorinating agent at even low temperatures. Although the first krypton compound to be prepared was described as the tetrafluoride, the properties ascribed to this material have been shown to be those of the difluoride. No other molecular fluoride of krypton is known, so all krypton compounds are derived from KrF_2. Krypton difluoride is a powerful oxidizing agent and is capable of oxidizing and fluorinating xenon gas to XeF_6 and gold metal to AuF_5.

B. The Fluorocations of Krypton and Their Salts

The KrF^+ and $Kr_2F_3^+$ cations are formed in reactions of KrF_2 with strong and weak fluoride ion acceptors to give complex salts that are analogous to those of XeF_2. Salts

of KrF^+ and $Kr_2F_3^+$ are formed with the pentafluorides of Group 15 elements and those of platinum and gold: $KrF^+BiF_6^-$, $KrF^+SbF_6^-$, $KrF^+Sb_2F_{11}^-$, $Kr_2F_3^+SbF_6^-$, $KrF^+AsF_6^-$, $Kr_2F_3^+AsF_6^-$, $Kr_2F_3^+PF_6^-$, $KrF^+Nb_2F_{11}^-$, $KrF^+TaF_6^-$, $KrF^+Ta_2F_{11}^-$, $KrF^+PtF_6^-$, and $KrF^+AuF_6^-$. Unlike their xenon analogues, the majority of these salts decompose at or below room temperature, but at least three, $KrF^+AsF_6^-$, $KrF^+SbF_6^-$, and $KrF^+Sb_2F_{11}^-$, are moderately stable at room temperature. As in XeF^+ salts (see Section III.E), KrF^+ interacts rather strongly with the anion by means of a fluorine bridge, e.g., $KrF^+AsF_6^-$ [Kr—$F_{terminal}$, 1.765(2) Å; Kr--F_{bridge}, 2.131(2) Å]. The $Kr_2F_3^+$ cation, like $Xe_2F_3^+$, is V shaped, e.g., $Kr_2F_3^+AsF_6^-$ [Xe—$F_{terminal}$, 1.792(8) Å; Xe--F_{bridge}, 2.055(7) Å]. The KrF^+ cation ranks as the most powerful chemical oxidizer presently known and is capable of oxidizing gaseous xenon to XeF_5^+; gaseous oxygen to O_2^+; NF_3 to NF_4^+; and chlorine, bromine, and iodine pentafluorides to the ClF_6^+, BrF_6^+, and IF_6^+ cations, respectively. Adducts with the weak fluoride ion acceptors $CrOF_4$, $MoOF_4$, and WOF_4 are known in which KrF_2 interacts with the metal center by formation of asymmetric Kr—F--M bridges (M = Cr, Mo, W), e.g., F—Kr—F--MOF_4, F—Kr—F--$MoOF_4(MoOF_4)_2$.

C. Other Krypton Derivatives

Despite the strong oxidizing properties of the KrF^+ cation, it has been shown to behave as a Lewis acid towards a limited number of Lewis bases at low temperatures. These bases are resistant to oxidation by the strongly oxidizing KrF^+ cation and, as in the case of the XeF^+ cation, they have first adiabatic ionization potentials that are greater than or comparable to the estimated electron affinity of the KrF^+ cation (13.2 eV). The Lewis acid-base cations are all thermally unstable above ca. −40°C and consist of HC≡N—KrF^+, F_3CC≡N—KrF^+, F_3CCF_2C≡N—KrF^+, and n-$F_3CF_2CF_2C$≡N—KrF^+, all having AsF_6^- as the counteranion. These cations comprise the only examples of krypton bonded to nitrogen. The compound $Kr(OTeF_5)_2$ provides the only reported example of a compound in which krypton is bonded to oxygen. The existence of the $KrCH_3^+$ cation has been established in the gas phase by ion cyclotron resonance spectroscopy. The Kr—C bond energy of the $KrCH_3^+$ cation has been estimated to be 199.6 ± 10.5 kJ mol^{-1} and is considerably more stable than the Kr—F bonds of KrF_2 (mean thermochemical bond energy of 48.9 kJ mol^{-1}) and KrF^+ (∼155 kJ mol^{-1}). No compounds in which krypton is bonded to elements other than fluorine, oxygen, and nitrogen have been isolated. The nonexistence of simple oxides or oxofluorides is consistent with the lack of a higher oxidation state of krypton.

V. RADON COMPOUNDS

A. Radon Fluoride

All radon chemistry, of necessity, has been done at the radiotracer level, precluding the possibility of obtaining detailed structural support for the species that are proposed.

When a mixture of trace amounts of radon-222 and fluorine gas are heated to approximately 400°C, a nonvolatile fluoride is formed. The intense γ-radiation of millicurie and curie amounts of radon provides the activation, allowing radon in such quantities to react spontaneously with gaseous fluorine at room temperature and with liquid fluorine at −196°C. Radon is also oxidized by chlorine and bromine fluorides, IF_7 and NiF_6^{2-} in HF to give stable solutions of radon fluoride. The products of these fluorination reactions have not been analyzed because of their small masses and intense radioactivity. It has nevertheless been possible to deduce that radon forms a difluoride, RnF_2, and derivatives of the difluoride by comparing reactions of radon with those of krypton and xenon. Electromigration and ion exchange studies show that ionic radon is present in many of these solutions and is believed to be RnF^+ and Rn^{2+}. The chemical behavior of radon is similar to that of a metal fluoride and is consistent with its position in the Periodic Table as a metalloid element.

B. The Fluorocations of Radon

Radon reacts at room temperature with solid oxidants such as $O_2^+SbF_6^-$, $O_2^+Sb_2F_{11}^-$, $N_2F^+SbF_6^-$, and $BrF_2^+BiF_6^-$ to form nonvolatile complex salts, which are believed to be $RnF^+SbF_6^-$, $RnF^+Sb_2F_{11}^-$, and $RnF^+BiF_6^-$, by analogy with krypton xenon, which form the well-characterized salts $NgF^+SbF_6^-$, $NgF^+Sb_2F_{11}^-$, and $NgF^+BiF_6^-$ where Ng = Kr or Xe (see Section III.E and IV.B).

VI. PROSPECTS FOR ARGON COMPOUNDS

The photolysis of HF in a solid Ar matrix gives Ar fluorohydride (HArF), which has been identified by infrared spectroscopy. Theoretical calculations indicate that HArF is intrinsically stable, owing to significant ionic and covalent contributions to its bonding, thus confirming computational predictions that Ar should form a stable hydride species with properties similar to those of the analogous matrix-isolated Xe and Kr compounds.

Theoretical calculations indicate that argon difluoride may be unstable but that the ArF^+ cation will be stable in the presence of a suitable oxidatively resistant anion.

The corresponding HeF^+ and NeF^+ cations are predicted to be unstable. Experimental evidence for ArF^+ in the gas phase has been obtained, leading to $D_o(ArF^+) \geq 1.655$ eV and confirming the instability of HeF^+ and NeF^+ in their electronic ground states. The electronegativity values assigned to the compound-forming noble gases (Ar, 3.2; Kr, 2.9; Xe, 2.3; Rn, 2.1) and those predicted for the noble gases which presently do not form compounds (He, 5.2; Ne, 4.5) suggest that the values for argon and krypton are rather close and that efforts to synthesize an ArF^+ salt are realistic. The ArF^+ cation is expected to be an even stronger oxidant than KrF^+, making it an oxidizer of unprecedented strength. However, unlike KrF^+, which can only be synthesized from KrF_2, any synthesis of an ArF^+ salt cannot rely upon the difluoride precursor. Theoretical calculations also suggest that $HC{\equiv}N{-}ArF^+$ may be stable (see Sections III.E and IV.C).

VII. APPLICATIONS

Stable noble-gas compounds have no industrial uses at present but are frequently utilized in laboratories as fluorinating and oxidizing agents. Xenon difluoride and xenon tetrafluoride are relatively mild oxidative fluorinating agents and have been used for the preparation of phosphorus, sulfur, tellurium, and silicon derivatives. Xenon difluoride has proven to be a versatile and stable fluorinating agent for use in synthetic organic chemistry. It has been used for the fluorination of alkenes in fluorodecarboxylation and for the fluorination of thioethers and aromatic and aliphatic compounds. Xenon hexafluoride has been used to synthesize transition metal fluorides and oxofluorides, where the metal is in its highest oxidation state, e.g., $Xe_2F_{11}^+AuF_6^-$, TcO_2F_3. Krypton difluoride and its complex salts are extremely powerful oxidative fluorinating agents and can be used to oxidatively fluorinate gold, silver, and halogen fluorides to their highest oxidation states, e.g., AuF_5, AgF_4^-, ClF_6^+, BrF_6^+ (see Section IV). Krypton difluoride and XeF_6 have been used to form lanthanide(IV) fluorometallate complexes by the oxidation of Ln(III) in anhydrous HF solvent. Krypton species can also be used to fluorinate oxocompounds of elements that are already in their highest attainable oxidation states as is exemplified by the fluorination of OsO_4 to *cis*-OsO_2F_4 and TcO_2F_3 to $TcOF_5$ by KrF_2, and $XeOF_4$ to XeF_5^+ by KrF^+. Aqueous solutions of sodium perxenate and of xenon trioxide are intermediate in oxidizing strength and are useful for analyzing manganese and alcohols and carboxylic acids, respectively. Radon-222, an air contaminant in uranium mines, can be analyzed by means of oxidants that form nonvolatile radon salts, e.g., O_2^+ (dioxygenyl) cation salts.

SEE ALSO THE FOLLOWING ARTICLES

NOBLE METALS • PERIODIC TABLE (CHEMISTRY) • RARE EARTH ELEMENTS AND MATERIALS

BIBLIOGRAPHY

Bartlett, N., and Sladky, F. O. (1973). The chemistry of krypton, xenon and radon. *In* "Comprehensive Inorganic Chemistry" J. C. Bailar, Jr., H. J. Emeléus, R. Nyholm, and A. F. Trotman-Dickenson, eds.), Vol. 1, pp. 213–330, Pergamon, New York.

Hyman, H. H., ed. (1963). "Noble Gas Compounds," Univ. of Chicago Press, Chicago.

Laszlo, P., and Schrobilgen, G. J. (1988). *Angew. Chem. Int. Ed. Engl.* **27,** 479.

Schrobilgen, G. J., and Whalen, J. M. (1994). Helium-group gases, compounds. *In* "Kirk-Othmer Encyclopedia of Chemical Technology," 4th ed., pp. 38–53, Chap. 13, Wiley, New York.

Schrobilgen, G. J. (1992). Lewis acid properties of noble gas cations. *In* "Synthetic Fluorine Chemistry," (R. D. Chambers, G. A. Olah, and G. K. S. Prakash, eds.), pp. 1–30, Chap. 1, Wiley, New York.

Selig, H., and Holloway, J. H. (1984). Cationic and anionic complexes of the noble gases. *In* "Topics in Current Chemistry" (F. L. Boschke, ed.), Vol. 124, pp. 33–90, Springer-Verlag, Berlin.

Seppelt, K., and Lentz, D. (1982). Novel developments in noble gas chemistry. *In* "Progress in Inorganic Chemistry" (S. J. Lippard, ed.), pp. 167–202, Wiley, New York.

(1970). Edelgasverbindungen, *In* "Gmelins Handbuch der Anorganischen Chemie," 8th ed., Main Supplement, Vol. 1, VCH, Weinheim/New York.

Žemva, B. (1988). *Croat. Chem. Acta* **61,** 163.

Žemva, B. (1994). Noble gases: inorganic chemistry. *In* "Encyclopedia of Inorganic Chemistry," (R. B. King, ed.), pp. 2660–2680, Vol. 5, Wiley, New York.

Periodic Table (Chemistry)

N. D. Epiotis
D. K. Henze
University of Washington

I. Development of the Periodic System
II. Features of the Modern Periodic Table
III. Atomic Structure and Elementary Periodicity
IV. Tabular Trends
V. The New Valence Bond Interpretation of Chemistry
VI. The Colored Periodic Table
VII. The Hard/Soft Acid-Base (HSAB) Concept
VIII. Beyond the Isoelectronic and Isolobal Analogies
IX. Atomic Valence and the Colored Periodic Table

GLOSSARY

Arrow formula Representation of molecules by appending directional arrows on the valence atomic orbitals according to the electron occupancy.

Atom Smallest characteristic constituent particle of an element.

Atomic mass (atomic weight) Relative mass of an atom. By current international agreement, the standard for all atomic masses is the isotope carbon-12, which is arbitrarily assigned an atomic mass of exactly 12. Atomic mass was the original numerical basis for the periodic table.

Atomic number Number of protons in the nucleus of an atom. It is also the nuclear charge (in conventional electronic units) and the number of electrons in a neutral atom. The atomic number is the current numerical basis for the periodic classification of the elements.

Bond disociation energy (BDE) The energy difference between two atoms infinitely separated and at equilibrium geometry.

E-bond Bond due to Coulombic attraction of electron pairs and holes in the absence of charge transfer.

Electron Fundamental subatomic particle with a charge of $1.602 * 10^{-19}$ C and a rest mass of $9.110 * 10^{-31}$ kg. The number and arrangement of electrons in atoms is largely responsible for the chemical properties of elements and many of their physical properties.

Electron configuration The arrangement of electrons in the various energy levels, sublevels, and orbitals of an atom.

Electron shells (levels) Principal energy levels occupied by the electrons in an atom, specified by the principal quantum number n.

Element One of approximately 100 pure simple substances that cannot be decomposed into simpler ones by chemical means. Each individual element is made up of atoms of identical atomic number.

Family (group) Vertical column of the periodic table containing elements with similar chemical and physical properties and similar electron configurations, especially for the outer electrons. There are 18 such columns in the modern periodic table, although earlier versions sometimes grouped the members of certain adjacent columns into one family.

I-bond A bond represented by *two* arrows forming an open loop in the arrow formula.

Isotopes Atoms of the same element which differ in atomic mass, that is, in number of neutrons.

Isoelectronic Two atoms or molecular fragments which have the same number of valence, or outer, electrons.

Isolobal Two atoms or molecular fragments which bind by using atomic orbitals of the same symmetry type.

Isosynaptic Isoelectronic or isolobal groups bonding by the same mechanism (T, I, or E).

Orbital Electron cloud, generated from a wave function, that represents the probability of locating an electron as a function of three-dimensional spatial coordinates. Orbitals can be atomic (AO) or molecular (MO), depending upon the region to which the electron is constrained.

Period Horizontal row of the periodic table, over which the chemical and physical properties of elements usually change gradually with increasing atomic number. There are 7 periods, ranging in length from 2 to 32 elements.

Quantum number Number, in most cases an integer, specifying the fact that the associated energy, momentum, or other property of a system is restricted to certain values.

T-bond A bond represented by *two* arrows forming a closed loop in the arrow formula. When two electrons of opposite spin are spanned by the arrows, we have one T-bond. When the electrons have parallel spin, we have one T-antibond.

THE PERIODIC TABLE as it is adopted today is an arrangement of the elements in order of increasing atomic number. This classification suggests that elements with similar properties appear at regular, periodic intervals. For example, elements falling in vertical columns (called families or groups) have been assumed to have common characteristics because they contain the same number of valence electrons assigned to atomic orbitals (AOs) of the same symmetry. This is the *valence isoelectronic analogy*. Since the basis of elementary periodicity is atomic structure, we can think of today's long form of the periodic table as the legacy of physicists as well as exceptional chemists like its discoverers Mendeleev and Meyer, and we can call it the *physical periodic table*.

Chemistry is the science which investigates the change of matter. It is the science of reactions which reveals what is a stable and what is an unstable combination of atoms. Each chemical reaction is thus a declaration of chemical selectivity. In predicting the products, one effectively selects a subset from a list of many potential outcomes, i.e., one specifies the selectivity of the reaction. Hence, a primary goal of chemistry is to uncover the affinities of atoms for each other in order to explain why some products are formed but not others. To use the philosopher's terminology, the project of chemistry is selectivity.

During the last two decades of the 20th century, experimental and computational data, which progressively grew in volume, interpreted by Epiotis as being inconsistent with the standard notions of periodicity. A new interpretation of the molecular quantum mechanical wave function provided the theoretical underpinning of a *chemical periodic table*, which projects the intrinsic affinities of atoms for one of three possible mechanisms of chemical bonding and, by extension, the affinities of atoms for each other. This *colored periodic table*, named so because it is a painted version of the physical periodic table, reveals the selective ways in which elements combine to form the molecules and materials of the "chemical world." Here, we present a brief historical outline of the development of the traditional periodic table [for comprehensive histories, see the works of Van Spronsen (1969) and Puddephatt and Monaghan (1986)], and then we focus on the revolution promised by the colored periodic table.

I. DEVELOPMENT OF THE PERIODIC SYSTEM

A. Elementary and Atomic Concepts

The periodic table, the great classificatory scheme of chemistry, is based on two of the most fundamental concepts in physical science—elements and atoms. In their rudimentary forms, both of these ideas were inventions of the pre-Socratic Greek philosophers. The earliest of these thinkers was Thales of Miletus (ca. 624–545 BC), who subscribed to the idea that all matter is derived from one substance. While he considered water to be the elementary substance, others like Anaximenes, Heraclitus, and Anaximander favored air, fire, and *apeiron* (an eternal, unlimited element), respectively.

Some time around 450 BC, Empedocles (ca. 490–430 BC) appears to have synthesized some of these ideas in his argument that all matter is constituted of various mixtures

of four primordial substances—earth, air, fire, and water. The two greatest philosophers of classical antiquity, Plato (428–347 BC) and Aristotle (384–322 BC), adopted Empedocles's four elements, though Aristotle added a fifth, the *quita essentia*, which made up the crystalline spheres of the heavens. While some scholars accepted these elements as late as the 17th century, it is important to realize that these four elements were more philosophical constructs than specific entities with chemical consequences.

Similarly, atoms were proposed by the ancient Greeks not so much to explain specific natural phenomena as to account for permanence amid change. Atomists like Democritus of Abdera (ca. 460–370 BC) argued that a body could not be infinitely subdivided. The process ultimately had to stop at the level of an "uncuttable" particle, literally, $\alpha\tau o\mu o$s. The Roman poet, Lucretius (ca. 100–55 BC), claimed that atoms and the void constitute all things and elaborated that idea to explain meteorology and geology, sensation and sex, cosmology and sociology, and even life and the mind. In spite of such ambitious comprehensiveness, atoms were not as widely accepted as were the four earthly elements, largely because Aristotle rejected them. Nevertheless, the concept of ultimate particles of matter was occasionally invoked as a working hypothesis by scientists such as Gassendi, Galileo, Boyle, and Newton. Indeed, Newton went so far as to express this opinion: "It seems probable to me, that God in the Beginning form'd Matter in solid, massy, hard, impenetrable, movable Particles."

Thus, by 1700, the progress made in chemistry was calling the idea of four elements into serious question, while the idea of atoms was gaining scientific currency. The century which followed did much to further establish the latter and to overthrow the former. Antoine Laurant Lavoisier (1743–1794), the Frenchman often being credited with being the "Father of Modern Chemistry," enunciated a working definition of "simple substance" in his 1789 text, *Traité Élementaire de Chimie*. The first edition included a table of 33 elementary substances that could not be decomposed by chemical operations. Within this table, the elements were classified into groups such as *métalliques* and *non métalliques*. Most of the metals listed by Lavoisier (for example, antimony, silver, copper, and iron) had been known and used for centuries. This was also the case with certain of the nonmetals such as carbon and sulfur. However, Lavoisier's list also included hydrogen, oxygen, and nitrogen, three gases which had recently been isolated and, thanks to his theoretical system, correctly identified as specific, elementary substances. Essentially all of Lavoisier's original 33 substances still appear in a modern periodic table. Lavoisier's guess that the five "earths" he includes—lime, magnesia, baryta, alumnia, and silica—may in fact be complex substances has been substantiated. We now know them to be oxides of calcium, magnesium, barium, aluminum, and silicon. Two of his entries, light and heat, are not materials at all. Nevertheless, Lavoisier's concept of simple substances and his preliminary list proved to be of inestimable importance for the development of chemistry and the periodic classification of the elements.

For example, a clearly defined working concept of an element was essential for the elaboration of the atomic theory by John Dalton (1766–1844). In 1808, this English schoolmaster published *A New System of Chemical Philosophy* in which he put forth his postulates about the structure of matter. Each element, Dalton argued, is constituted of identical, immutable, and uniquely characteristic atoms. When elements combine to form compounds, their atoms unite in a fixed ratio that is characteristic of the compound. Because these numbers are fixed, the elementary composition of the compound, by mass, is also constant. This latter property could be quite accurately determined, even in Dalton's time. However, Dalton had no direct way of ascertaining the correct atomic ratio of the elements of any compound. As a consequence, he could not calculate, with confidence, the relative masses of the atoms of the various elements—their atomic masses or atomic weights. The atomic masses of the elements and the atomic ratios characteristic of specific compounds are manifested in the elementary mass composition of the compounds. Once the correct atomic ratio is known, atomic masses can be readily calculated from mass composition. Alternatively, knowledge of atomic masses permits conversion of composition by mass to composition by atomic ratio. However, Dalton faced the dilemma of an equation with two unknowns.

That dilemma continued to plague chemistry for 50 years and, hence, limited the utility of the atomic theory. Because of the importance of mass relationships in chemical reactions, there was a consensus that the characteristic atomic mass of an element was a significant property. However, there was little agreement on what the correct values were. Hydrogen was generally recognized to be the "lightest" element and, hence, was typically assigned an atomic mass of 1. Relative to this standard, the atomic mass of oxygen was approximately 8, according to some scientists, or 16, according to others. The situation had reached such a sorry impass that the progress of chemistry was being impeded. Therefore, a special international conference was convened in Karlsruhe, Germany, in 1860, with the expressed aim of resolving the confusion over atomic masses. Significantly, the two scientists most clearly associated with the development of the periodic table, the Russian Dmitri Ivanovich Mendeleev and the German Julias Lothar Meyer, were among those in attendance.

Once a set of reliable atomic masses was accepted by the scientific community [thanks in large measure to the application of Amadeo Avogadro's Hypothesis by Stanislao Cannizzaro (1826–1910)], the time was ripe for the formulation of the periodic law and the table based on it.

B. Early Discoveries of Periodicity

The fact that certain elements and compounds exhibit similar physical and chemical properties was well known long before the adoption of an accurate set of atomic masses. Indeed, some elements were first prepared in what appeared to be families. Humphry Davy's (1778–1829) experiments of the early 19th century led to the grouping of potassium and sodium into a family that has come to be called alkali metals and now includes lithium, rubidium, cesium, and francium as well. Not only do these elements share many common chemical and physical properties, but they form many compounds with similar properties. Davy also prepared magnesium, calcium, strontium, and barium and subsequently grouped them together to form the alkaline earths. As analytical methods improved, other elementary families were found, among them the halogens, a group of reactive and widely distributed nonmetals including fluorine, chlorine, bromine, and iodine. Clearly, the existence of these families was evidence for order in the great diversity of matter.

There were many different approaches to the task of grouping the elements. In 1817, Johann Wolfgang Döbereiner (1780–1849) proposed one of the first systems to organize the mineral world. His idea was to group elements into triads of related substances. Later, he focused on triads composed of the elements themselves, for example, lithium, sodium, and potassium. He found that within the triads he identified, the intermediate atomic mass was close to the arithmetic mean of the atomic masses of the other two. Moreover, other properties such as density, melting point, and boiling point behaved similarly.

Slightly later, another elementary system was proposed by Alexandre Emile Béguyer de Chancourtois (1820–1862). His idea was that the properties of elements are the properties of numbers. To demonstrate this, he arranged the elements in a three-dimensional spiral in order of increasing atomic mass. When thus ordered, elements with similar properties fell in vertical columns. The success of this numerological ordering was soon followed by a system created by J. A. R. Newlands. In 1863 or 1864, he assigned "ordinal numbers" to each element in order of increasing atomic mass. Hence, hydrogen was given an ordinal number of 1, lithium was 2, and so on. Next, the first seven elements were placed in a row, then the next seven were placed in a row directly below the first. In this way, elements with similar chemistry ended up being in the same column. Newlands even went so far as to leave blank spaces where he thought new elements should go, and he made predictions about the properties of these undiscovered atoms. Unfortunately, Newlands's idea, self titled the "Law of Octaves," received mostly criticism from the scientific community. He did not receive appropriate recognition until 1913, when H. G. Moseley established the physical reality behind the ordinal numbers of the elements.

C. The Periodic Table of Mendeleev

Dmitri Ivanovich Mendeleev is one of the most colorful characters in the history of chemistry. An account of his childhood reads like a plot by Dostoevsky. Of Russian and Mongolian ancestry, Mendeleev was born in Siberia in 1834, the youngest of 17 or 18 children. While Dmitri was still a child, his father, director of a secondary school, went blind. In order to support her family, Maria Kornileva Mendeleeva managed a glass factory. However, after some years, the factory burned down and the elder Mendeleev died of tuberculosis. Dmitri had just completed his secondary education and his obvious intelligence clearly called for further training. Therefore, his mother took her 16-year-old son and one of her daughters on a 1000-mile journey by horse-drawn vehicle to Moscow. Her efforts to obtain a place for Dmitri at the university there failed, but ultimately he was enrolled in the Central Pedagogic Institute at St. Petersburg.

Following his studies in St. Petersburg and a brief period as a school teacher, Mendeleev was allowed to continue his education and research in Paris and Heidelberg. Shortly after his return to Russia, he was appointed professor of chemistry at the Technological Institute of St. Petersburg. He held that position until 1890, when he resigned in a policy dispute with the administration. Subsequently, he assumed the post of Director of the Bureau of Weights and Measures. A strong individualist, Mendeleev appears to have been bold and outspoken in his educational, social, and political views. He was similarly courageous in putting forth his scientific ideas, a characteristic which is very evident in his approach to the classification of the elements. Indeed, it is probably Mendeleev's boldness in adhering to his classificatory scheme in the face of apparent contradictions and in making predictions based upon that scheme that has led to his identification with the periodic table.

Mendeleev also had another attribute essential for the task at hand—an encyclopedic knowledge of the chemical properties of the elements and thousands of their compounds. In 1869, he was summarizing much of that knowledge in a textbook, *Principles of Chemistry*. As part of this project, he was searching for a way to organize the great diversity of information into a pedagogically and

scientifically sound system. According to the historical account, on February 17, 1869, Mendeleev sat at his desk, arranging a stack of cards. Each carried the name, symbol, and atomic mass of a different element. In what has been likened to a game of patience or solitaire, he laid out the cards in rows in order of increasing atomic mass. Again, he saw what others had observed: when arranged in this fashion, elements naturally fall into families exhibiting similar chemical properties which periodically repeat themselves. In fact, the properties of the elements appear to be a function of the atomic mass, or in Mendeleev's words, "the size of the atomic weight determines the nature of the elements." That conclusion appeared in a paper on "The Relation of the Properties to the Atomic Weights of the Elements," read within a month of the February discovery.

Later that year, the first version of Mendeleev's periodic table appeared in a Russian scientific journal. The version shown in Fig. 1 dates from 1872 and was published in supplemental volume 8 of a German journal, *Annalen der Chemie*. It lists 63 known elements and leaves spaces for 31 more. The elements are arranged in eight major groups, seven of which contain two subgroups each to further refine the classification. The formulas heading each column represent characteristic formulas of the specified compounds of the elements below. Thus, the formula R^2O for Group I means that these elements form oxides that correspond to this atomic ratio, in modern symbolism, H_2O, Li_2O, etc.

Note in particular the spaces left in Group III for elements with atomic masses 44 and 68 and in Group IV for an element with atomic mass 72. If Mendeleev had not left these spaces, he could not have continued to group similar elements in the same vertical columns. They soon would have been scattered all over the table. Titanium would have appeared under boron, and the rest of row 4 would have been shifted one space to the left. Two additional leftward shifts would have occurred in row 5, and so on.

Characteristically, Mendeleev was not content to merely predict the existence of undiscovered elements; he also had the temerity to predict the properties of these elements and some of their compounds. His most successful predictions were for what he called ekaboron (the element below boron in his 1872 tabulation), ekaaluminium, and ekasilicon. When scandium, gallium, and germanium were ultimately discovered, their measured properties showed an amazing agreement with Mendeleev's calculations. Table I illustrates the accuracy with which he predicted the properties of germanium. Such predictive triumphs did much to establish the periodic table and assure its international acceptance.

TABLE I Predicted Properties of Ekasilicon and Observed Properties of Germanium

	Predicted	Observed
Atomic mass	72	72.6
Color of element	Gray	Gray
Density of element (g/cm^3)	5.5	5.36
Formula of oxide	XO_2	GeO_2
Density of oxide (g/cm^3)	4.7	4.703
Formula of chloride	XCl_4	$GeCl_4$
Density of chloride (g/cm^3)	1.9	1.887
Boiling point of chloride (°C)	<100	86

Reihen	Gruppe I. — R^2O	Gruppe II. — RO	Gruppe III. — R^2O^3	Gruppe IV. RH^4 RO^2	Gruppe V. RH^3 R^2O^5	Gruppe VI. RH^2 RO^3	Gruppe VII. RH R^2O^7	Gruppe VIII. — RO^4
1	H = 1							
2	Li = 7	Be = 9,4	B = 11	C = 12	N = 14	O = 16	F = 19	
3	Na = 23	Mg = 24	Al = 27,3	Si = 28	P = 31	S = 32	Cl = 35,5	
4	K = 39	Ca = 40	— = 44	Ti = 48	V = 51	Cr = 52	Mu = 55	Fo = 56, Co = 59, Ni = 59, Cu = 63.
5	(Cu = 63)	Zn = 65	— = 68	— = 72	As = 75	Ne = 78	Br = 80	
6	Rb = 85	Sr = 87	?Yt = 88	Zr = 90	Nb = 94	Mo = 96	— = 100	Ru = 104, Rh = 104, Pd = 106, Ag = 108.
7	(Ag = 108)	Cd = 112	In = 113	Su = 118	Sb = 122	Te = 125	J = 127	
8	Cs = 133	Ba = 137	?Di = 138	?Ca = 140	—	—	—	— — — —
9	(—)	—	—	—	—	—	—	
10	—	—	?Er = 178	?La = 180	Ta = 182	W = 184	—	Os = 195, Ir = 197, Pt = 198, Au = 199.
11	(Au = 199)	Hg = 200	Tl = 204	Pb = 207	Bi = 208	—	—	
12	—	—	—	Th = 231	—	U = 240	—	— — — —

FIGURE 1 Mendeleev's periodic table of 1871–1872. Originally published in *Annalen der Chemie*, Supplemetal Vol. 8, 1872. [Reprinted from Ihde, A. (1964). "The Development of Modern Chemistry," p. 245, Harper and Row, New York.]

D. Periodic Systems of Lothar Meyer and Others

Although Mendeleev is the major figure in the development of the periodic system of the elements, Julius Lothar Meyer proposed a very similar arrangement at about the same time. Trained as a physician, Meyer ultimately became professor of chemistry and rector of the University of Tübingen in southern Germany. Like Mendeleev, his motivation for organizing the elements was associated with writing a textbook. Some of Meyer's preliminary attempts at a periodic classification date from 1864, but his first real publication on the subject was in 1869. He stressed the importance of elementary combining powers, or valence, in his tabulation and emphasized the periodicity of certain physical properties. An example of the latter is Meyer's plot of atomic volume (the volume occupied by 1 g atomic mass of an element under specified conditions of temperature and pressure) versus atomic mass. This plot, shown in Fig. 2, illustrates the cyclic or periodic nature of the property. The maxima of the curve are occupied by lithium, sodium, potassium, and the other alkali metals that Mendeleev placed in his Group I.

Although Meyer and Mendeleev appear to have made their discoveries independently, they became involved in an unfortunate priority dispute. In retrospect, it seems clear that both deserve credit for their contributions to the periodic table, as do several of their contemporaries. Newlands and de Chancourtois have already been mentioned. Other, less well known contributors include William Odling and Gustavus Detlef Henrichs. Odling's system was based, in large measure, on the properties of compounds and the recognition of trends in the formulas of analogous compounds. For example, he noted the pattern formed by the nonmetal hydrides: CH_4, NH_3, H_2O, and HF. Henrichs was a European-born chemist who spent much of his career as a professor of physical science at the University of Iowa. He also came up with an elementary classification which suggested a periodic variation of chemical and physical properties as a function of atomic mass.

II. FEATURES OF THE MODERN PERIODIC TABLE

A. The Stable Elements

Disregarding for the time being the color designations, Fig. 3 is a modern version of a periodic table. In Mendeleev's original table, he divided what he called Groups I through VII into A and B subgroups. Nowadays, each column of the table gets its own number, ranging from 1 through 18 as prescribed by the International Union of Pure and Applied Chemistry (IUPAC).

The table shows that the length of a period is by no means constant. The first is only two elements long—hydrogen (H) and helium (He). Next come two periods with eight elements each, including some of the most abundant and important substances known. Nitrogen (N)

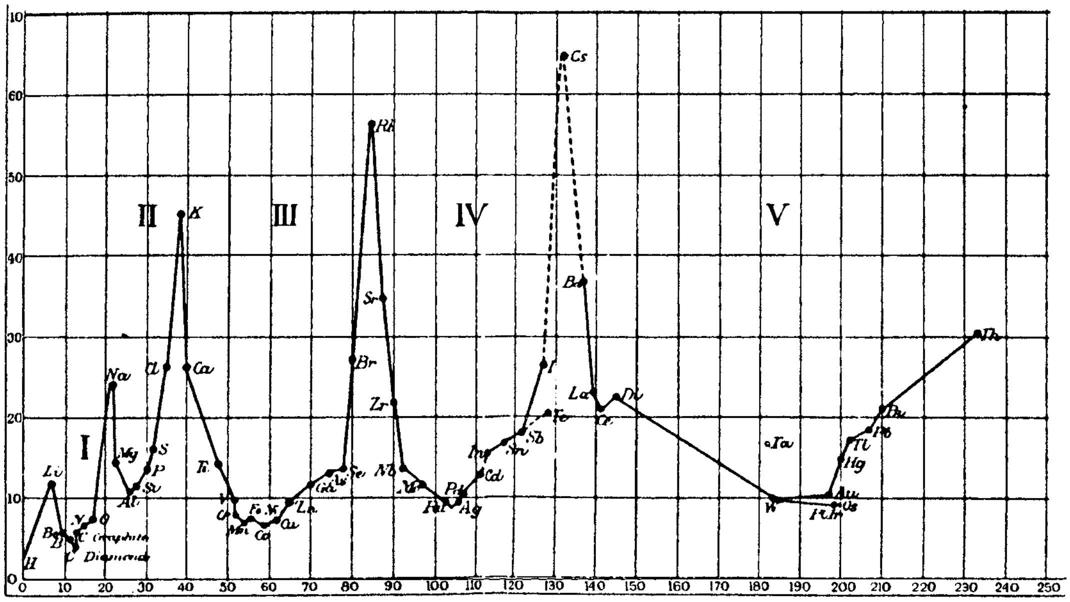

FIGURE 2 Meyer's plot of atomic volume versus atomic mass. Redrawn by T. Bayley for *Philisophical Magazine*, 1882, from Meyer's graph in *Annalen der Chemie*, Supplemetal Vol. 7, 1870. [Reprinted from Ihde, A. (1964). "The Development of Modern Chemistry," p. 251, Harper and Row, New York.]

The Modern Periodic Table

1	2	3	4	5	6	7	8	9	10	11	12	13	14	15	16	17	18
1 H																1 H	2 He
3 Li	4 Be											5 B	6 C	7 N	8 O	9 F	10 Ne
11 Na	12 Mg											13 Al	14 Si	15 P	16 S	17 Cl	18 Ar
19 K	20 Ca	21 Sc	22 Ti	23 V	24 Cr	25 Mn	26 Fe	27 Co	28 Ni	29 Cu	30 Zn	31 Ga	32 Ge	33 As	34 Se	35 Br	36 Kr
37 Rb	38 Sr	39 Y	40 Zr	41 Nb	42 Mo	43 Tc	44 Ru	45 Rh	46 Pd	47 Ag	48 Cd	49 In	50 Sn	51 Sb	52 Te	53 I	54 Xe
55 Cs	56 Ba	57 * La	72 Hf	73 Ta	74 W	75 Re	76 Os	77 Ir	78 Pt	79 Au	80 Hg	81 Tl	82 Pb	83 Bi	84 Po	85 At	86 Rn
87 Fr	88 Ra	89** Ac	104 Rf	105 Db	106 Sg	107 Bh	108 Hs	109 Mt	110 Uun	111 Uuu	112 Uub		114 Uuq		116 Uuh		118 Uuc

Lanthanides	* 58 Ce	59 Pr	60 Nd	61 Pm	62 Sm	63 Eu	64 Gd	65 Tb	66 Dy	67 Ho	68 Er	69 Tm	70 Yb	71 Lu
Actinides	**90 Th	91 Pa	92 U	93 Np	94 Pu	95 Am	96 Cm	97 Bk	98 Cf	99 Es	100 Fm	101 Md	102 No	103 Lr

= Blue   = Red   = Green

FIGURE 3 The modern long form of the periodic table. The color (shading) Scheme is discussed in Sections VI through IX.

and oxygen (O) are the two chief components in the atmosphere and are, of course, essential for life. Carbon (C) is so ubiquitous that an entire subdiscipline, organic chemistry, has been created to study its compounds. Silicon (Si) and aluminum (Al) are among the most plentiful elements in the earth's crust. These elements are members of a fairly large collection know as main group or representative elements. This category includes Groups 1, 2 (sometimes 12), and 13 through 17. They are called representative because they exhibit a wide range of properties and serve as prototypes for other elements. Because of the uncoupling of the subgroups, the fourth and fifth periods have 18 elements each. The 10 metals from scandium (Sc) through zinc (Zn) head columns labeled 3 through 12. They constitute the first transition series (though some authors exclude the elements of Group 12 from this classification and assign them to the representative elements). Members of the transition series exhibit certain similarities in chemical and physical properties. Changes from one element to the next are less pronounced than in the main group elements. Included among the transition elements are the metals that are most important in construction, alloying, and plating—vanadium (V), chromium (Cr), manganese (Mn), iron (Fe), nickel (Ni), copper (Cu), and zinc (Zn). After the transition elements comes gallium (Ga)—the ekaaluminum of Mendeleev, right where he predicted it. Five more elements, culminating in krypton (Kr), follow. The same pattern is repeated in row 5: an alkali metal, an alkaline earth, the 10 metals of the second transition series, and 6 more elements in Groups 13 through 18.

Row 6 demonstrates that the long-form periodic table is not enough. Element number 58, cerium (Ce), does not have sufficient chemical or physical similarity to titanium (Ti) or zirconium (Zr) to merit inclusion in Group 4. Instead, it is much more like 14 other elements called

lanthanide, rare earth, or inner transition series. These elements are similar and exhibit an even more gradual change in properties than do the transition metals. For this reason, and for reasons related to atomic structure, the lanthanides are grouped together in a row along the bottom of the table, with the understanding that they really fit between lanthanum (La) and hafnium (Hf). The third transition series follows, and the row is completed with the main group elements.

The seventh period begins, as do others, with an alkali metal and an alkaline earth. Thorium (Th) begins a series of 14 actinide elements corresponding to the actinides. All of these elements are radioactive, and those beyond uranium (U) do not occur in nature, at least not in appreciable quantities. Rather, they are all artificially made via nuclear reactions. They are among the products of modern atomic research, and their names refer to the places (Berkeley and California) and the people (Fermi and Lawrence) involved.

B. The New Discoveries

The newest and heaviest elements start a fourth transition series called the transfermium elements. These are also synthetic elements created in nuclear reactions, hence they have very short lifespans. In 1997, the IUPAC approved the names of elements 100–109; however, the elements after that are still referred to by their Latinized atomic number, for example, element 111 (Uuu) is unununium. The obvious cumbersome nature of such names has prompted another IUPAC committee to be formed which will soon approve names for elements 110 through 112. These last three elements were all discovered at the GSI (Gesellschaft für Schwerionenforschung) in Darmstadt, Germany, in 1994 and 1996. The newest element is ununoctium (Uuo, 118). It was created at Berkeley in 1999 and, due to rapid (0.12 msec) alpha decay, led to the first creation of element 116. This further decayed into a previously undiscovered isotope of element 114 [a different isotope of element 114 had been informally reported by Russian scientists at Dubna (Joint Institute for Nuclear Research) in 1999]. Due to the short lifespan of many of these elements, much of our knowledge about their properties has come from high-level calculations rather than experiment.

III. ATOMIC STRUCTURE AND ELEMENTARY PERIODICITY

One of the great achievements of modern atomic theory is the way in which it accounts for the periodic properties of the elements—the similarities in chemical and physical properties within a family and the gradual changes in properties as one moves down or across the periodic table. The fundamental correctness of the scheme developed by Mendeleev and his contemporaries has been verified through physical measurements and the computations of quantum mechanics. Today, the reason for the periodicity of the elements is well established; the explanation lies in the structure of the atom. Therefore, a discussion of tabular trends will be deferred until after this brief consideration of atomic structure and, in particular, the arrangement of electrons within atoms.

A. Radioactivity, Isotopes, and Atomic Mass

The contemporary conception of atomic structure is a product of the 20th century. Shortly before the turn of the century, a number of important experimental discoveries were made, chiefly in Europe. In late 1895, Wilhelm Röntgen (1845–1923) discovered X-rays in his Würzburg laboratory. Several months later, while investigating what he believed to be the same phenomenon, the French physicist Henri Becquerel (1852–1908) first observed natural radioactivity. In 1897, J. J. Thompson (1856–1923) of Cambridge University detected, in the rays emitted from the cathode of a partially evacuated gas discharge tube, negatively charged particles, later called electrons, which proved to be much less massive than hydrogen atoms. Ernest Rutherford (1871–1937) demonstrated that radioactive emissions consist of three major types: alpha particles with a charge of $+2$ and a mass of about 4 on the standard atomic mass scale, beta rays which are identical to (fast) electrons, and gamma rays which are massless manifestations of electromagnetic radiation. In collaboration with chemist Frederick Soddy (1877–1956), Rutherford went on to show that when an element emits alpha particles, it is spontaneously transmuted into the element lying two places to the left in the periodic table. Thus, uranium (U) becomes thorium (Th) after giving off alpha radiation. On the other hand, loss of beta "particles" (beta rays) transforms the emitting element into the element situated immediately to its right [thorium, for example, beta decays to protactinium (Pa)].

The process of radioactive decay led to the conclusion that atomic mass must not be a singularly identifying property of an element. Indeed, as Soddy demonstrated, not all of the atoms of any given element are identical. Most elements naturally exist as a mixture of atoms with differing atomic masses. Soddy called these different forms isotopes, literally emphasizing that all isotopes of the same element belong in the "same place" in the periodic table. The atomic masses determined for the elements from combining masses, gas densities, or other traditional chemical measurements are, in fact, weighted averages of the isotopic masses in the naturally occurring mixture. Thus, hydrogen consists almost exclusively of atoms of mass

1. However, one atom in 6500 has a relative mass of 2, an isotope called deuterium. In addition, there is a third isotope of hydrogen, a radioactive form called tritium, which has a mass of 3. The atomic mass for hydrogen, 1.0079, includes small contributions due to deuterium and tritium. For elements where the natural mixture of isotopes is less strongly biased towards a single species, the average atomic masses deviate considerably from whole numbers. Chlorine (atomic mass 35.453) and copper (atomic mass 65.546) are cases in point.

B. Nuclear Charge and Atomic Numbers

The existence of isotopes clearly indicates that, the periodic law notwithstanding, the properties of the elements cannot be a simple function of atomic mass. Atomic mass is not a sufficiently fundamental property. However, if atomic mass does not determine the identity and properties of an element, what does? The answer again came from Rutherford's laboratory. In 1909 he performed one of his most famous experiments, firing a stream of alpha particles at a thin gold foil and observing their trajectories. Most of the positively charged projectiles passed through the foil with very little change in path. Occasionally, however, the alpha particles would be deflected through large angles, in some cases almost completely reversing direction. "It was quite the most incredible event that has ever happened to me in my life," Rutherford observed, as an old and honored scientist looking back at this crucial experiment. "It was almost as incredible as if you fired a 15-inch shell at a piece of tissue paper and it came back and hit you." From this bizarre behavior, Rutherford calculated that an intense positive charge and most of the mass of the atom must be concentrated in a very small region of space. He assumed this extremely dense region would be at the center, or nucleus, of the atom. Thus was born the familiar and somewhat inaccurate picture of the atom as a miniature solar system, with electrons orbiting the positive and massive nucleus.

Four years later, two young men working with Rutherford made giant theoretical and experimental strides towards elaborating that model. The theoretician was the Dane Niels Bohr (1885–1962) who borrowed a revolutionary idea from the German physicists Max Planck (1858–1947) and Albert Einstein (1879–1955). These two had previously postulated that energy is quantized. Bohr then assumed that the energy of the single electron in a hydrogen atom is also quantized; that is, it can only have certain values, each corresponding to a circular orbit of specifically defined radii. Moreover, he derived mathematical expressions for both the energy and the radius. Bohr's calculations reproduced with amazing accuracy the frequencies which had been observed and measured for the spectral lines of hydrogen. Here, at last, was an atomic explanation for a phenomenon which had been used to identify the rare gases and many other elements.

The experimentalist Henry G. J. Moseley (1887–1915) was measuring the frequency of spectral lines—not in the visible region of the spectrum, but in the high-frequency X-ray region. He found that the frequencies of the most intense lines fell into a pattern. When the square roots of the frequencies are plotted against the atomic masses of the elements, a reasonably straight line is obtained. However, the line is not straight enough to satisfy a scientist's passion for order. So instead, Moseley plotted the same data against the ordinal numbers of the elements. These points exhibit almost perfect linearity, hence the ordinal number or atomic number, as Moseley called it, must represent a real physical property. "This quantity," he wrote, "can only be the charge on the central positive nucleus." The atomic number, not the atomic mass, determines the elementary identity of an atom. Thanks to Moseley's work, and that of his successors, we now know that the atomic number of an element is equal to the positive charge on the nucleus, determined by the number of positive particles or protons it contains. This number also equals the number of electrons in the electrically neutral atom. It increases integrally from hydrogen, atomic number 1, through uranium, atomic number 92, and beyond. All the isotopes of any given element have the same atomic number, that is, the same number of electrons and protons per atom. Thus, all atoms of carbon (atomic number 6) are made up of six electrons surrounding a nucleus containing six protons. However, carbon atoms differ in mass because of differences in the number of neutrons, the neutral particles also found in atomic nuclei. Therefore, the different isotopes of carbon have different amounts of neutrons in the nuclei. For example, a carbon-13 atom is made of seven neutrons, six protons, and six electrons, as opposed to carbon-12, which has six of each type of particle.

The fact that the atomic number of an element is a more fundamental property than its atomic mass means that the periodic law must be modified: the properties of the elements are periodic functions of their atomic numbers, not their atomic masses. This dependence also explains the several instances in the periodic table where the correct elementary placement results in a deviation from the normal trend of increasing atomic mass. Argon (Ar) has an atomic mass of 39.948, while potassium (K) has an atomic mass of 39.0983. Yet no one who knows anything about the properties of these elements would think of putting the highly reactive metal in Group 18 along with the inert gases or vice versa. Although argon does have a higher average atomic mass than potassium, its atomic number is 18 and that of potassium is 19. Similar atomic mass inversions occur for tellurium (Te, atomic number 52, atomic mass

127.60) and iodine (I, atomic number 53, atomic mass 126.905) and for cobalt (Co, atomic number 27, atomic mass 58.9332) and nickel (Ni, atomic number 28, atomic mass 58.69).

C. Quantum Numbers, Electron Shells, and Atomic Orbitals

The atomic number determines the identity of an element because the chemical properties of an element are almost exclusively due to its electrons. The quantum mechanical model, which was first proposed in the 1920s, treats matter as if it had wavelike characteristics. Solution of the Schrödinger wave equation for an atom yields a set of mathematical wave functions that can be related to the probabilities of locating the electrons both spatially and energetically. This function, when plotted in three-dimensional space, generates a probability cloud. We cannot be absolutely certain where the electron will be at any instant, but we do know the region of space that is most probably occupied over time.

The wave functions include four quantum numbers that emerge from the calculation. These numbers, in effect, provide a unique energetic and spatial "address" for each electron in an atom. Such information, in turn, helps increase our understanding of chemical properties and periodicity. The principal quantum number, symbolized n, is the chief indicator of the energy of the electron and the size of the electron cloud—in other words, how far, on the average, the electron is from the nucleus. This number can take on positive integer values: 1, 2, 3, etc. The fact that n can only have whole number values means that the energy of the atom is restricted to certain values, just as Bohr assumed in his model for the hydrogen atom. Electrons with the same value for the principal quantum number are said to be in the same shell or level.

The angular momentum of the electron is also quantized, and the azimuthal quantum number, l, specifies the permissible values. The number l can assume integer values between zero and $(n-1)$. Each value of l represents a subshell or sublevel of the principal shell. These subshells are usually identified by an alphabetical code based on old spectroscopic terms. Thus, $l=0$ is designated an s sublevel, $l=1$ is called a p state, $l=2$ is symbolized as d, $l=3$ corresponds to an f subshell, and so on in alphabetical order. The electronic distributions associated with various values of the azimuthal quantum number are also identified by this code. The designation is important because l reflects the shape of these electron clouds.

A third number which emerges from the wave equation is the magnetic quantum number, m_l. Its permissible integer values are determined by l. When l is 0, m_l can only be 0; if l equals 1, m_l can have values of $+1$, 0, or -1. In general, m_l can assume $2l+1$ values for each value of l: $m_l = 0, \pm 1, \pm 2, \ldots, \pm l$. Physically, the various values of the magnetic quantum number indicate the possible values of the quantized z component of the angular momentum of the electron. This means that m_l determines the spatial orientation of the corresponding electron cloud. Each distinct orientation is termed an atomic orbital, or simply an orbital. The spin quantum number, m_s, completes the set of four. It can assume only two possible values, $+1/2$ and $-1/2$. This differentiation takes into account the fact that an electron can be regarded as spinning either clockwise or counterclockwise.

D. Building Up the Elements: Electron Configurations

The rules governing the relationships among the four quantum numbers are used in the "buildup" of the elements. We start with the simplest atom, hydrogen, and successively add electrons to generate new atoms and elements. This process is guided by the Pauli Exclusion Principle which states that no two electrons in the same atom can have identical sets of all four quantum numbers. Therefore, as electrons are added, each is assigned a unique set of n, l, m_l, and m_s. The order of assignment is dictated by increasing energy. For each successive atom, the most stable electronic arrangement (or ground state) is that with the lowest energy. In general, the energy of an electron follows the sequence of increasing values for n and l, but there are exceptions that manifest themselves in the periodic table. The lowest energy level available to the single electron in a hydrogen atom is characterized by $n=1$, $l=0$, $m_l=0$, and $m_s = \pm 1/2$ (the value of the spin quantum number is of no energetic consequence in this case). The electronic configuration is designated $1s$ for $n=1$ and s for $l=0$. The electron can occupy other orbitals, corresponding to other values of n, l, and m_l, but these represent "excited" states of higher energy. Next comes helium, with atomic number 2. Its two electrons share the same values for the first three quantum numbers: $n=1$, $l=0$, $m_l=0$. However, in conformity with the Pauli Principle, they must differ in m_s. Thus, $m_s = +1/2$ for one of the electrons and $-1/2$ for the other. Since both electrons in a helium atom are in the $n=1$, $l=0$ orbital, the ground state for the element is written $1s^2$ with the superscript indicating the double occupancy. Note that these two sets of quantum numbers are the only possible sets for which $n=1$. This, then, is an electronic explanation for why hydrogen and helium are the only members of the first row of the periodic table.

The electronic configurations of the second and third row elements are shown in Table II. Since all possible combinations of quantum numbers for $n=1$ were used in the first row, the second row begins by letting $n=2$. First, the $2s$ shell fills in a manner similar to that of the first row. Then, because for $n=2$, l can equal 0 and 1, the $2p$ shell

TABLE II Electronic Configurations of the Elements in Periods 2 and 3

Period 2				Period 3			
Name	Symbol	Atomic number	Electronic configuration	Name	Symbol	Atomic number	Electronic configuration
Lithium	Li	3	$1s^2 2s$	Sodium	Na	11	$1s^2 2s^2 2p^6 3s$
Beryllium	Be	4	$1s^2 2s^2$	Magnesium	Mg	12	$1s^2 2s^2 2p^6 3s^2$
Boron	B	5	$1s^2 2s^2 2p$	Aluminum	Al	13	$1s^2 2s^2 2p^6 3s^2 3p$
Carbon	C	6	$1s^2 2s^2 2p^2$	Silicon	Si	14	$1s^2 2s^2 2p^6 3s^2 3p^2$
Nitrogen	N	7	$1s^2 2s^2 2p^3$	Phosphorus	P	15	$1s^2 2s^2 2p^6 3s^2 3p^3$
Oxygen	O	8	$1s^2 2s^2 2p^4$	Sulfur	S	16	$1s^2 2s^2 2p^6 3s^2 3p^4$
Fluorine	F	9	$1s^2 2s^2 2p^5$	Chlorine	Cl	17	$1s^2 2s^2 2p^6 3s^2 3p^5$
Neon	Ne	10	$1s^2 2s^2 2p^6$	Argon	Ar	18	$1s^2 2s^2 2p^6 3s^2 3p^6$

begins to fill with boron until all possible quantum number combinations are exhausted for $n = 2$ and $l = 1$ by the tenth atom, neon. Hence, the second row accounts for all possible quantum number combinations for $n = 2$. Similarly, the third row proceeds to fill the shells for all possible quantum number combinations for $n = 3$, $l = 0$ or 1. The similarities of the electron arrangements for members of the same family are apparent. Of particular importance is the configuration of the valence electrons. The conventional view is that atoms with the same number of outer electrons (isoelectronic atoms) exhibit similar chemical properties. Later on, we will see that a different scenario is supported by many pieces of data.

Starting with the first element of the fourth row, potassium, we see that in order for its valence configuration to be similar to that of the other alkali metals, it must begin filling the 4*s* shell, even though all possible $n = 3$ shells have not been filled [the 3*d* ($n = 3$, $l = 2$) shell is still empty]. This assignment is correct because it has been shown, experimentally and computationally, that the 4*s* energy level for potassium is lower than the 3*d*. The 3*d* does not begin to fill until scandium, the first of the transition elements.

This brings up the point that the assignment of quantum numbers indicates that orbital energy levels do not always follow the sequence of increasing *n* and *l* values. The valence electron configuration of the alkali metals and the alkaline earths are always *ns* and ns^2. Therefore, the elements of columns 1 and 2 are known as members of the *s* block. Groups 3 through 12 constitute the *d* block, because in these transition elements electrons are introduced into the *d* orbitals. The valence electronic configurations of this group follow a regular trend belonging to any one of three types: $(n-1)d^v ns^0$, $(n-1)d^{v-1} ns^1$, or $(n-1)d^{v-2} ns^2$, where v is the number of valence electrons. Interelectronic repulsion is a crucial determinant of the configuration type. Finally, the *p* block contains the elements of Groups 13 through 18, and the lanthanides and actinides comprise the *f* block.

IV. TABULAR TRENDS

A. Atomic Radius

Chemical and physical properties of the elements and their compounds constituted the evidence for the periodic system in the last half of the 19th century. Modern understanding of the arrangement of electrons within the atoms of the various elements has provided an explanation of these properties and their periodic nature. One property that is quite obviously associated with atomic structure is atomic size. For metallic elements, atomic radii can be determined using diffraction. Calculations are made from the angles at which the X-rays bounce off the atoms. Another experimentally based technique involves computing the distance between chemically bonded atoms from spectroscopic measurements. Quantum mechanical calculations also yield atomic radii, including those plotted in Fig. 4, which is a graph of atomic radius against atomic number. A periodic pattern is visible: the maxima are occupied by the alkali metals and the minima by the rare gases. Within any column or family, the radius increases with increasing atomic number. This is to be expected, since the atomic number equals the number of electrons in the atom. Each new shell increases the size of the atom. However, within any row or period, the atomic radius decreases with increasing atomic number. Here, the added electrons make the atom smaller. This latter trend is attributable to the fact that the positive nuclear charge (the number of protons) also increases along a row. The added outer electrons do not effectively screen the attractive force due to the protons, and hence, these forces increase with atomic number. This means the electrons are pulled closer to the nucleus and the atomic radius decreases.

B. Metallic Character and Ionization Energy

One readily observable periodic property is the variation in the metallic character of the elements. The members of the

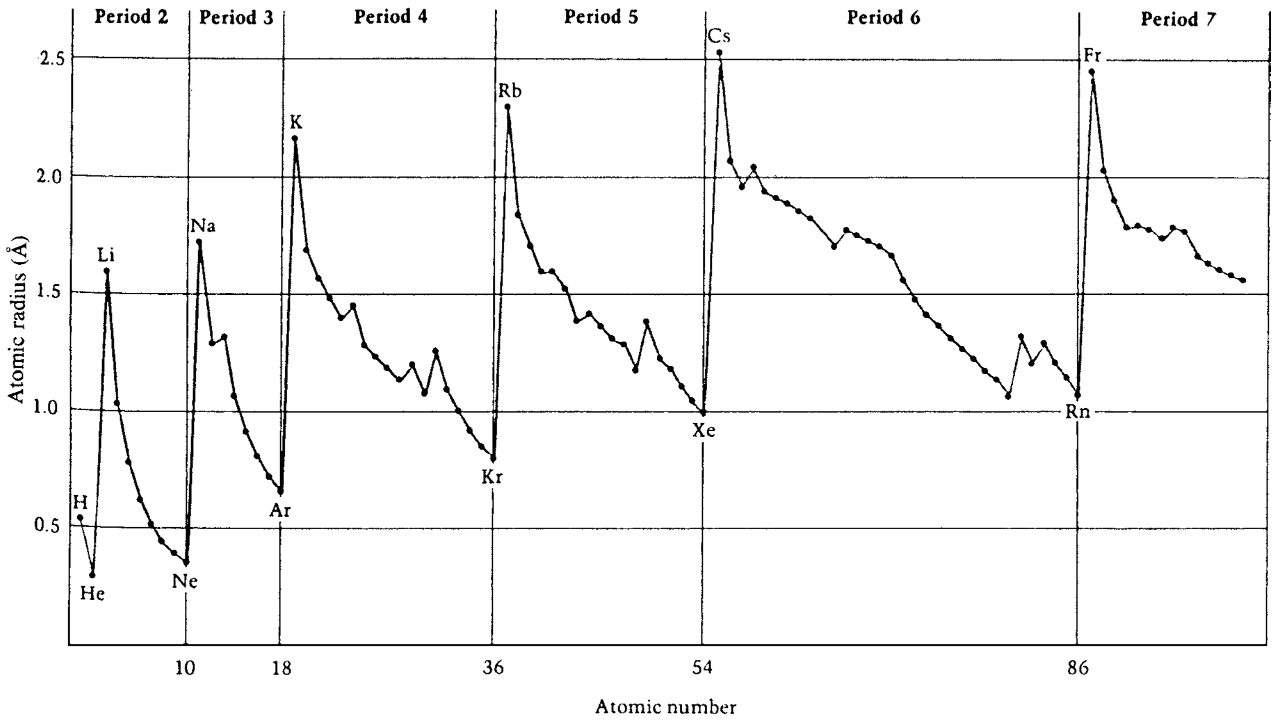

FIGURE 4 Plot of atomic radius versus atomic number. Data from Waber, J. T., and Cromer, D. T. (1965). *J. Chem. Phys.* **42,** 4116. [Reprinted from Ebbing, D. D. (1984). "General Chemistry," p. 181, Houghton, Boston.]

first two columns of the table are highly reactive metals—so reactive that the alkali metals and the alkaline earths are never found naturally in their uncombined forms. In the process of chemical combination, each alkali metal atom loses one electron. The positive particle that results has one more proton than electron. Hence, it is an ion with a charge equal to that of a proton (+1 in conventional units). This electron loss is termed oxidation, and the amount of energy required to remove an electron from a gaseous atom is called the ionization energy or ionization potential (IP).

The electrons removed in the ionization process are those least strongly attracted to the positive nucleus. In the case of the Group 1 elements, the single electron that is normally lost during a chemical reaction comes from the outermost *s* orbital: 2*s* for lithium, 3*s* for sodium, etc. This oxidation process yields ions with essentially the same electronic arrangement as the adjacent rare gases. Thus, Na^+ has the same electronic configuration as neon: $1s^22s^22p^6$. The two species are said to be isoelectronic. The fact that the rare gases are very unreactive (indeed, they were considered and called "inert" until 1962, when the first compounds of xenon were made) indicates that they have very little tendency to lose, gain, or share electrons. In other words, their electronic configurations, which involve fully filled subshells, are especially stable. Once that configuration is attained, as in Na^+, it is very difficult to remove a second electron. Sodium, in essentially all of its compounds, exists in this ionic form, and the other alkali metals behave similarly. This tendency to lose electrons and form positive ions is characteristic of metals. Moreover, the relative mobility of electrons within a bulk sample of these elements gives rise to electrical and thermal conductivity, malleability and ductility, and the bright, shiny appearance associated with metals. About 75% of the elements can be classified as metals. The degree of metallic character increases moving down any column of the periodic table, but it decreases moving from left to right along a row. In period 3, for example, aluminum is clearly metallic; silicon has some metallic properties; phosphorous is more nonmetallic; and sulfur, chlorine, and argon are obviously nonmetals. The elements that flank the boundary between metals and nonmetals are sometimes called metalloids because they are intermediate in properties. Indeed, it is not uncommon for metalloids to exist in two crystalline forms or allotropes, one more metallic and the other more nonmetallic. Not surprisingly, the trends in metallic character parallel ionization energies, but in different directions. The most aggressively reactive metals are those that are most easily ionized. Thus, metallic character increases as ionization energy decreases. Cesium, for example, has a lower ionization energy and greater metallic reactivity than sodium. The 6*s* electron in the larger atom is further from the nucleus than the 3*s* electron in sodium, and hence, it is easier to remove. Within a row

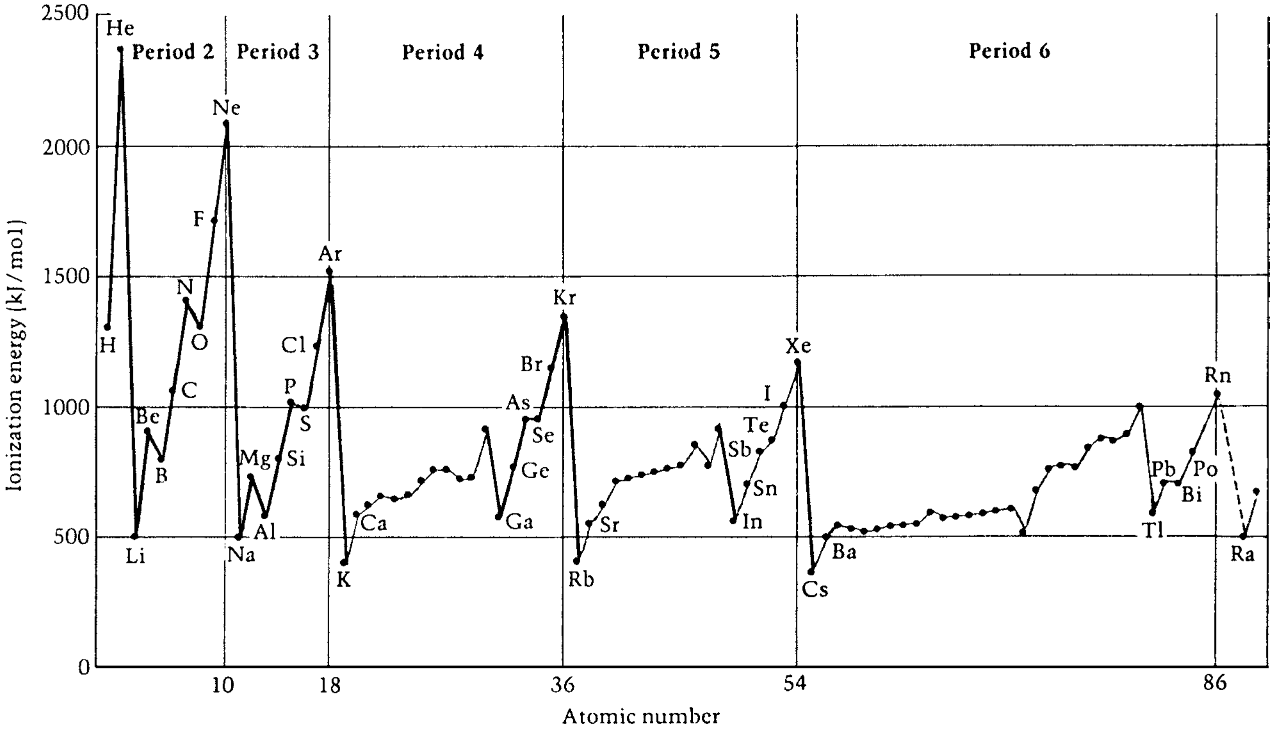

FIGURE 5 Plot of first ionization energy versus atomic number. [Reprinted from Ebbing, D. D. (1984). "General Chemistry," p. 184, Houghton, Boston.]

or period, ionization energy increases with atomic number, as the increasing unshielded nuclear charge enhances the electrostatic attraction experienced by the electrons. These trends are represented graphically in Fig. 5, a plot of the ionization energy required to remove one electron versus atomic number. The rare gases occupy the maxima on the curve, indicating how difficult it is to form positive ions from their atoms. The small zig-zags in the graph are important because they can be related to the details of electronic configuration. For example, the experimental values for ionization energy give evidence of energy differences between *s* and *p* orbitals in the same electron shell and the stability associated with half-filled and fully filled subshells. In fact, some of the best evidence for the correctness of the quantum mechanical model of the atom comes from such data.

C. Electron Affinity

A good deal of energy is required to form positive ions from the elements of Group 17. On the other hand, fluorine and the other halogens tend to gain one electron per atom in chemical reactions—a process called reduction. The negative ions that result are, once more, isoelectronic with the adjacent rare gas atoms. Thus, a chlorine atom, with a $1s^2 2s^2 2p^6 3s^2 3p^5$ electron configuration, becomes converted to a chloride ion, Cl^-, with the stable configuration of an argon atom: $1s^2 2s^2 2p^6 3s^2 3p^6$. The stability of the rare gas electron arrangement also helps explain why the atoms of oxygen and the other Group 16 elements gain two electrons during reaction to form ions such as O^{2-}. The formation of negative ions is one characteristic of reactive nonmetals.

A measure of the energy involved when a neutral atom in the gaseous state acquires one electron is called the electron affinity. When the negative ion thus formed is stable, energy is released and the electron affinity has a negative sign. When the ion is unstable, the electron affinity is positive. A comparison of Figs. 5 and 6 reveals that the variation of ionization potentials is much greater than that of the related electron affinities, and this is why ionization potentials serve better as singular indices of the electronic natures of different elements.

V. THE NEW VALENCE BOND INTERPRETATION OF CHEMISTRY

Vultures are flying over chemistry. In Horgan's *The End of Science*, chemistry assumes a secondary role smashed by the two behemoths of biology and physics as they themselves approach extinction. In *Ideas in Chemistry*, Knight proclaims the dicipline to be far past its golden days. Chemistry's icon Linus Pauling, in 1992, concurs: "I felt

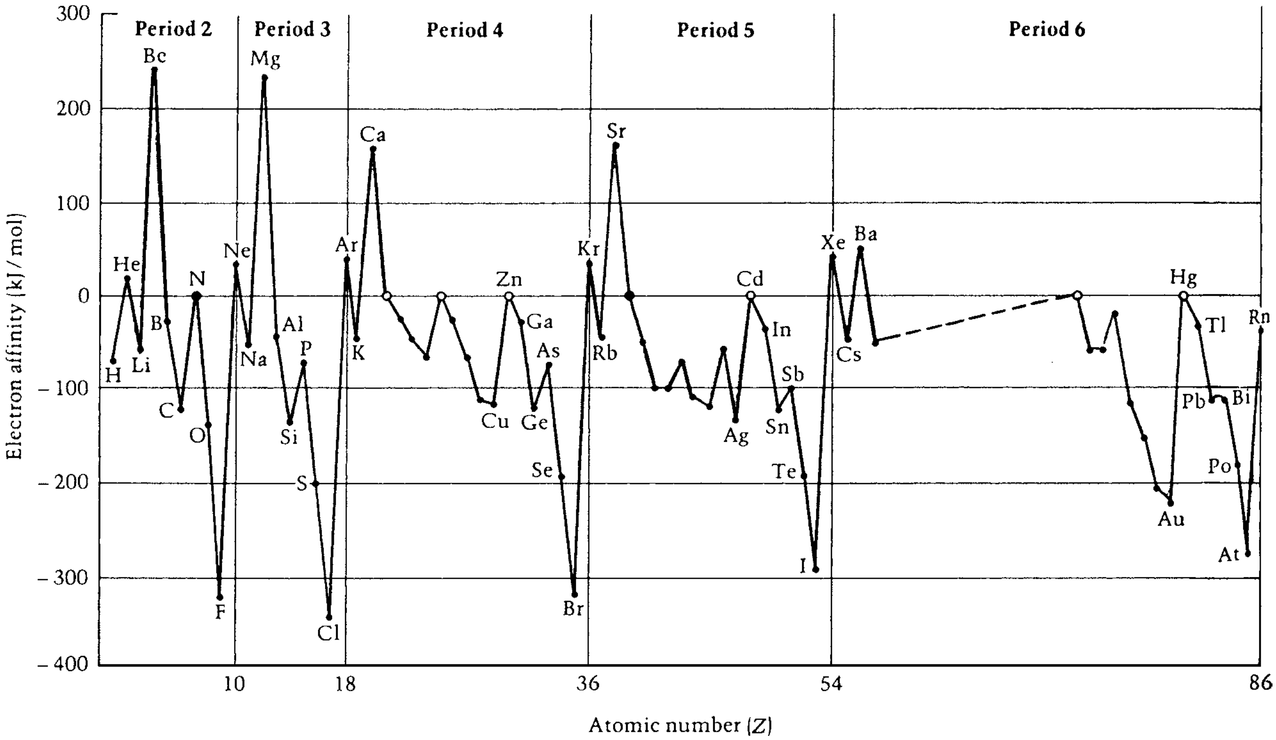

FIGURE 6 Plot of electron affinity versus atomic number. Elements indicated by open circles at zero form unstable negative ions. Their electron affinities are probably negative, but their exact values are unknown. [Reprinted from Ebbing, D. D. (1984). "General Chemistry," p. 186, Houghton, Boston.]

that by the end of 1930, or even the middle, that organic chemistry was pretty well taken care of, and inorganic chemistry and mineralogy–except sulfide minerals ...." Polemical in spirit, a new work proclaims the insufficiency of old ideas regarding molecular electronic structure and advances a new conceptual approach. This is explained and applied in a way that illustrates that there can still be excitement in an apparently dead science where presumably everything important has been discovered and all that remains is cleanup and service to biology. Quantum mechanics and Valence Bond (VB) theory were discovered within the first three decades of the 20th century. Since then a myriad of calculations and discussions of molecules have been published under a title that includes "VB" as part of an often-mysterious sounding acronym. Published in 1996, the monograph *Deciphering the Chemical Code: Bonding Across the Periodic Table* by Epiotis advances neither some new quantum mechanics nor some new brand of VB theory. Rather, it seeks to discover the proper chemical interpretation of the VB wave function so that the method can become a conceptual tool operative at the experimental frontier rather than a pedagogical vehicle for introducing one to quantum mechanical formalisms in conjunction with oversimplified molecular models (e.g., "pi system of benzene and aromaticity"). The conceptual breakthrough, for we are really talking about an epiphany rather than about some routine operation, can be stated simply as follows: molecules do *not* have a choice of two interatomic bonds—covalent and ionic. This covalent/ionic model is refuted by many long-known facts.

First, H_2 has a stronger bond that H_2^+, but exactly the *opposite* is true of Li_2 and Li_2^+. This means that the relative strengths of two- and one-electron covalent bonds are not qualitatively invariant but depend on atom electronegativity. Cr_2, with a formal sextuple, bond has a *shorter* bond but a *smaller* bond dissociation energy (BDE), 41 kcal/mol, than any of V_2 (57 kcal/mol), Ni_2 (48 kcal/mol), and Cu_2 (46 kcal/mol), which have fewer net-bonding and/or more antibonding electron pairs.

Our thesis is that there exists three types of bonds labeled T, I, and E, with the crucial indicator of the bonding mechanism being orbital or atom electronegativity. Hence, the periodic table in which atom electronegativity is a third dimension, as proposed by Allen and others, is a representation of atom affinity for one of the three bonding mechanisms.

In 1913, G. N. Lewis suggested that a line connecting two singlet-coupled electrons makes up one bond, giving birth to the concept of the electron pair bond and the Lewis electronic formula of a molecule. In *Deciphering*

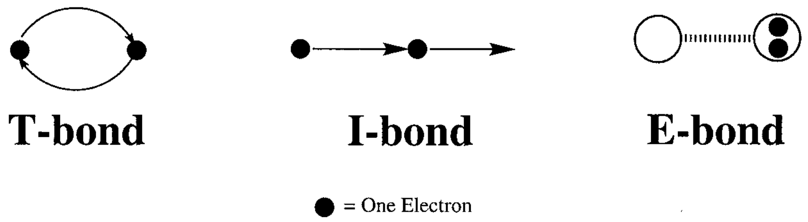

FIGURE 7 Schematic diagrams of the three types of bonding mechanisms: T, I, and E. Each arrow represents a one-electron "hop." Note that the I-bond promotes aggregation because a third party is needed at the head of one arrow. *Two* arrows count for *one* bond.

the Chemical Code: Bonding Across the Periodic Table, it is suggested that two arrows affixed on two singlet-coupled electrons constitute one bond. Superior bonds are formed when arrows are oriented in a codirectional (head to tail, HT) fashion. Two HT arrows can form either a closed or an open loop. The former corresponds to a T-bond promoting segregation of electron pairs, while the latter corresponds to an I-bond promoting aggregation because a third party is needed at the head (tail) of one arrow, as illustrated in Fig. 7.

At the limit of the hydrogen molecule, the T-bond is equivalent to the covalent bond of VB theory, i.e., the interaction of two diradical and two ionic VB configurations. By contrast, the concept of the T-bond leads to molecular formulae which are called T-formulae. These are fundamentally different from Lewis formulae as they constitute a representation of the molecule which reveals not only stoichiometry and shape but also intrinsic stability. At the limit of a metal solid, the I-bond can be said to be equivalent to the "metallic bond," although the last term is equivocally defined. Finally, the E-bond can be taken to be analogous to the ionic bond provided that induction and dispersion are also included in this definition. In summary, the new idea is that instead of classifying molecular experimental data according to the covalent/ionic gospel, one is now offered three receptacles in which to enter his observations: T, I, and E. This marks a new beginning for conceptual theoretical chemistry.

A. The Three Types of Bonds: T, I, and E

The recipe for the chemical implementation of VB theory is very simple: a molecule is made up of atoms, each in the electronic configuration deemed appropriate for bonding. Each atomic electronic configuration has any one or all of three elements: doubly occupied atomic orbitals (AOs), called "pairs"; singly occupied AOs, called "dots"; and vacant AOs, called "holes." The maximum electron delocalization which can be sustained by each one of the three elements, and which is consistent with the Pauli Exclusion Principle, is depicted by affixing arrows on each element. "Execution" of one, two, etc. arrows generates a unique ionic configuration. The allocation of arrows is made according to the *association rule:*

1. One arrow symbolizes the transfer of one electron ($1-e$ hop), and it causes kinetic energy reduction proportional to overlap.
2. A *dot* can have a maximum of one entering (inbound) and one exiting (outbound) arrow.
3. A *pair* can have a maximum of two exiting arrows.
4. A *hole* can have a maximum of two entering arrows.
5. Outbound arrows are called diastolic, and inbound arrows are called systolic.

The resulting molecular formula is called the *arrow formula*, and it displays pairs, dots, and holes connected by affixed arrows. Execution of one arrow, two arrows in all possible combinations, three arrows in all possible combinations, and so on generates an ensemble of VB configurations, the interactions of which are primarily responsible for binding. On the basis of energetic considerations, recognizing that two arrows acting concertedly (i.e., representing a single 2-e hop) achieve the same goal as the same two operating sequentially (i.e., representing two ordered $1-e$ hops), and that $1-e$ and $2-e$ hops interact, we focus attention on the possible $2-e$ hops. Here, we recognize two variants: an exchange $2-e$ hop which conserves charge and counts as one T-bond, and a charge transfer (CT) $2-e$ hop that engenders either inter- or intra-atomic charge separation and counts as one I-bond. Note that in each case two arrows are taken together to signify either a T- or an I-bond. Since the number of total arrows within the formula is conserved, we have a fixed number of pairwise arrow combinations and, hence, a fixed number of bonds (recall that two arrows count as one bond). Starting now from the arrow formula and specifying the pairwise arrow combinations (pictorially or symbolically) produces the formula called the *VB descriptor*. The linear combination of VB descriptors (each one corresponding to a linear combination of VB configurations) produces the operationally significant total VB wave function, a

resonance hybrid of VB descriptors. Depending upon the arrow combinations specified within each VB descriptor, each bond may be either of the T or the I variety. Hence, the overall resonance hybrid has a fixed number of bonds which have resonant T and I character. Bond character, T versus I, depends, to a first order, on atom electronegativity. I-bonding engenders CT and is favored by low electronegativity in homonuclear systems and by combinations of atoms differing greatly in electronegativity in heteronuclear systems. This leads to the rule that nonmetal atoms like H, C, N, O, and F (i.e., the atoms of "organic chemistry") support T-bonding, while semimetal and metal atoms increasingly support I-bonding. We have now broken ties with conceptual molecular orbital (MO) theory as presently practiced. Because of the conceptual intractability of this method, emphasis is placed on orbital symmetry and electron-count considerations. What we say here is that two molecules may have identical symmetry constraints and identical electron counts and yet can be fundamentally different on account of differing electronegativities which implies differing binding mechanisms, T versus I.

B. What Is a Multiple Bond?

Consider the double bond of ethylene produced by combining two methylenes, each containing one sp^3-hybridized carbon. Our first task is to allocate electrons to the constituent fragments in a way that minimizes energy consistent with potential bonding. This produces the reference configuration shown in Fig. 8a. Next, we affix the arrows according to the association rule in order to produce the arrow formula shown in Fig. 8b. Note how each dot gets one outbound and one inbound arrow as dictated by the association rule. There are a total of four arrows and, hence, a total of two (4 divided by 2) bonds. The *nature* of each bond (T or I) depends on how we combine two arrows to make one pair. Each arrow is labeled by a letter, and we use this lettering designation to define the possible combinations. One possible set of pairwise combinations is ab and cd. Each of these combinations represents a T-bond. This is one possible VB descriptor designated (ab/cd). A second possible set of combinations is ad and bc, each now representing an I-bond. This is a second possible VB descriptor denoted by (ad/bc). Note one characteristic difference: the two arrows span the same overlap region in the case of the T-bond, while they operate in two different overlap regions in the case of the I-bond.

In summary, the arrow formula of a double bond involves four arrows. There exist $(4-1)!$ pairwise (ij) combinations of arrows and $(3-1)$ quartet (ij/kl) selections. Each arrow pair represents one T- or I-bond. Each arrow

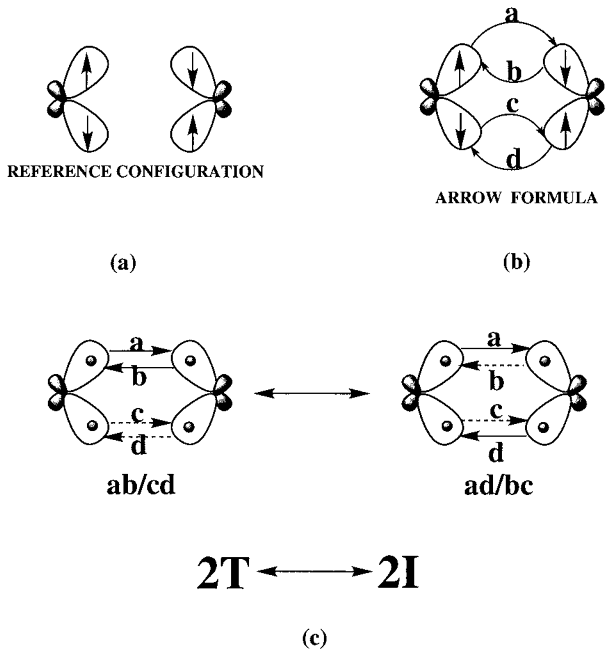

FIGURE 8 Sequential development of the electronic structure of a double bond. (a) The reference configuration. (b) Arrows are affixed on the electrons of the reference configuration in accordance with the association rule to create the arrow formula. (c) The most favorable ways of pairing the arrows to make a bond correspond to two (resonant) VB descriptors of the C=C bond. Arrows of the same type (solid or dashed) are paired.

quartet represents a pair of T-bonds or a pair of I-bonds. The three quartets represent the following bond combinations: (ab/cd): [T + T]; (ad/bc): [I(ROX) + I(ROX)]; (ac/bd): [I(OX) + I(RED)]. The term ROX denotes that CT causes simultaneous reduction and oxidation of one center, OX implies two-electron oxidation, and RED signifies two-electron reduction. The emerging viewpoint is that bonds have resonant T and I characters and that our C=C bond can be represented as a resonance hybrid of two VB descriptors as shown in Fig. 8c.

Additional VB descriptors can contribute to our resonance hybrid, but these are disregarded because the VB configurations which they span are high in energy. An example is the one involving the pairwise arrow combinations ac and bd. Such a contributor becomes important in the case of a highly heteropolar double bond. What is the principal character of the double bond of ethylene? Let us answer this question after we explicitly examine the consequences of the delocalization implied by the arrows. As shown below in Fig. 9, the ab (exchange $2-e$ hop) conserves charge by permitting each electron to occupy a different AO. By contrast, the bc (CT $2-e$ hop) confines two electrons in one AO at the price of severe interelectronic repulsion, measured by the index $J_{11} = IP - EA$,

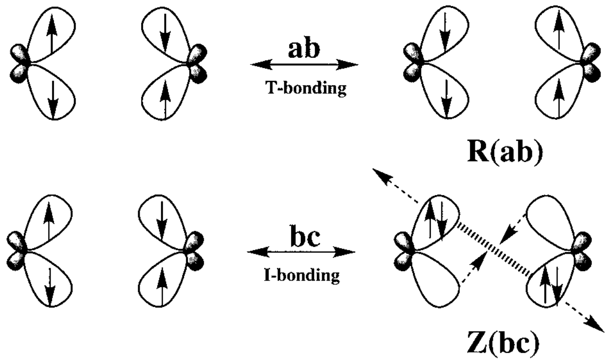

FIGURE 9 The effects of "executing" the different possible arrow pairs. In the top figure, the ab exchange conserves the charge of each atom, as in a T-bond. On the other hand, if the bc arrow pair is executed, as in an I-bond, one arrives at a configuration which confines two pairs of electrons to a single AO, causing severe electron-electron repulsion within the atoms. Relief of exchange repulsion (i.e., T-antibonding) can be affected by *transbending* as indicated by the dashed arrows.

where J_{11} is the self-repulsion bielectronic Coulomb integral, IP is the orbital ionization potential, and EA is the orbital electron affinity. This is only tolerable when the AOs are large in size or, saying the same thing in different language, if the atom has low IP, i.e., low electronegativity. Hence, we expect that replacing C by a heavier congener, such as Si, Ge, etc., will change the character of the double bond from T to I.

Two arrows make up either one bond or one antibond, and all depends on spin and electron count. Examples of T-antibonds are shown below in Fig. 10. We make a practice not to show T-antibonds in our arrow formulae so as not to clutter the picture.

With this in mind, let us now reassess the consequences of the configuration interaction (CI) characteristic of T- and I-bonding which were illustrated above in Fig. 9. It is clear that the bc arrow combination generates a VB configuration Z(bc) which features a "diagonal" double T-antibond, indicated by the hashed line. Trans-bending lowers the energy of Z(bc). Hence, trans-bending in heavy congener derivatives of ethylene and acetylene can be taken to be the fingerprint of predominant I-bonding. The strange, nonplanar, trans-bent geometries of disilenes (see the work of West, Fink, and Michl, 1981), digermenes, and distannenes are already a topic discussed in recent texts of inorganic chemistry (see Shriver, Langford, and Atkins, 1999). Noting the diversity of proposed explanations, the one most often cited is the "double singlet carbene" model of Pauling (1960). A barrage of reports in recent issues of *Chemical and Engineering News* (July 97, March 98, January 99) on the synthesis and characterization of heavy p-block multiple bonds is indicative of widespread interest in this topic. The well-known Cotton (Cotton and Walton, 1982) transition metal multiple bonds now await reinterpretation.

We are going one step further: the trans-bending of "heavy ethylene" has exactly the same origin as the square-to-rhombus deformation of the Li tetramer where I-bonding is expected to be predominant. This is illustrated (Fig. 11) by reference to the Z-type configuration produced by an I-type $2 - e$ hop starting from the lowest energy R-type tetraradical reference configuration of Li_4.

The following quotation is attributed to E. Schrödinger, a pioneer of quantum mechanics: "Suppression of details may yield results more interesting than a full treatment. More importantly, it may suggest new concepts. Pure quantum mechanics alone, in all its details, cannot supply a definition of, e.g., an acid or a base or a double bond." This is the philosophy espoused in this article.

VI. THE COLORED PERIODIC TABLE

We now set out to construct a two-dimensional mapping of molecules that reveals two things: the mechanism

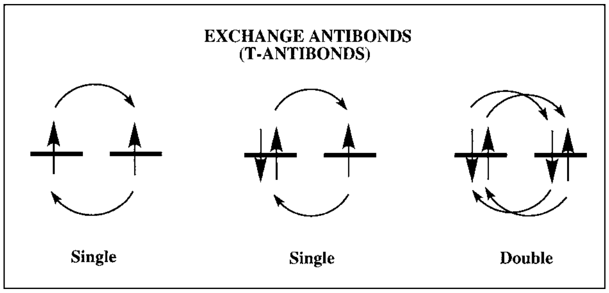

FIGURE 10 The different types of T-antibonds. These are left out of our formulae for clarity.

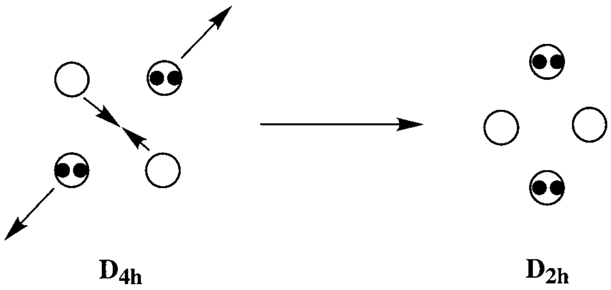

FIGURE 11 The origin of the deformation of square to rhombic Li_4. Compare with the Z(bc) formula of Fig. 9.

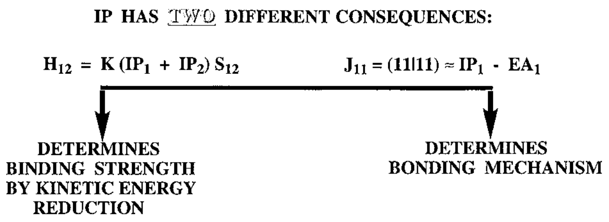

SCHEME 1

The Rules Of Chemical Bonding

	BLUE	GREEN	RED
BLUE	T		
GREEN	T T/I I	T T/I I	
RED	I E*	I E*	I

* In conjunction with electronegative blue or green atoms.

SCHEME 2

of bonding and the strength of the bond. Our quest is governed by four guidelines.

1. Kinetic energy reduction and, thus, bonding strength is related to the sum of the ionization energies of the overlapping AOs and, as a result, to the sum of atom ionization energies and atom electronegativities. The larger the sum is, the stronger the kinetic energy reduction and the stronger the bonding, everything else being equal.
2. The mechanism of delocalization, T or I, also depends on the sum of atom electronegativities, everything else being equal. In homonuclear molecules, strong bonding implies T-bonding and weak bonding goes hand in hand with I-bonding. The origin of the crucial effect of electronegativity on both the binding strength as well as on the bonding mechanism is emphasized in Scheme 1.
3. The condition for I-bonding is that the atoms support strong CT delocalization. For this to happen the sum of atom electronegativities, x^+, should be small and the difference of the atom electronegativities, x^-, should be large. However, this dual condition cannot be met because the limits are as follows: x^+ goes to zero as atom electronegativity goes to zero at which limit x^- is also zero. Thus, the "king of I-bonding" must involve some sort of compromise.
4. E-bonding is classical Coulomb attraction complemented by induction and dispersion. The conditions for optimization of E-bonding are the following:

   a. The interacting species are small and compact counterions formed from precursor neutral atoms of widely different electronegativities by transfer of one or more electrons from the more electropositive to the more electronegative atom. This maximizes classical Coulomb attraction.

   b. The interacting species are large polarizable neutral atoms. This maximizes the dispersive interaction.

   c. One species is a polar molecule or ion and the other is a polarizable neutral molecule. This maximizes the inductive interaction.

The proposed shading scheme for the periodic table has been displayed in Fig. 3. Our shading scheme should not be confused with artistic presentations in which color is often employed to indicate nonmetals, semimetals, and metals aside from attaining a visually pleasing result. There are three shades, each indicating the intrinsic affinity of each atom for one or more of the three bonding mechanisms. The affinities are blue atoms promote T-bonding, green atoms promote I-bonding or I/T-bonding and are tolerant to T-bonding, and red atoms promote either I- or E-bonding. The term I/T symbolizes *bimodal bonding* by which a single atom binds one set of ligands by I-bonds and another set by T-bonds. When a choice exists, exactly which type of bonding occurs depends on the precise combination of atoms. The matrix of atom combination and the forecast mechanisms are shown in Scheme 2. Note the tolerance of green and the intolerance of red atoms for T-bonding.

Examples of the different binding modes are given below.

One expectation is that green atoms can exhibit any one of three possible bonding modes: T, I, or bimodal. What is the electronic structure of the "hypervalent" trigonal

	BLUE	GREEN	RED
BLUE	T Organic Molecules (H,C,N,O,F) $(CH)_8$		
GREEN	T/I "Hypervalents", e.g., PF_5 Boranes SiHHSi I XeF_6 WF_6 T SiH_4	T/I "Hypervalents", e.g., PCl_5 $R_4G{=}GR_4$ trans-bent I $(P)_8$ T $R_4G{=}GR_4$ planar	
RED	I Organometallics, e.g., ferrocene LiHHLi E Ionic solids	I Phosphine TM Complexes E Ionic solids	I CP solids Metal Clusters e.g., Li_8

TM = Transition metal, CP = Closest packed

SCHEME 3

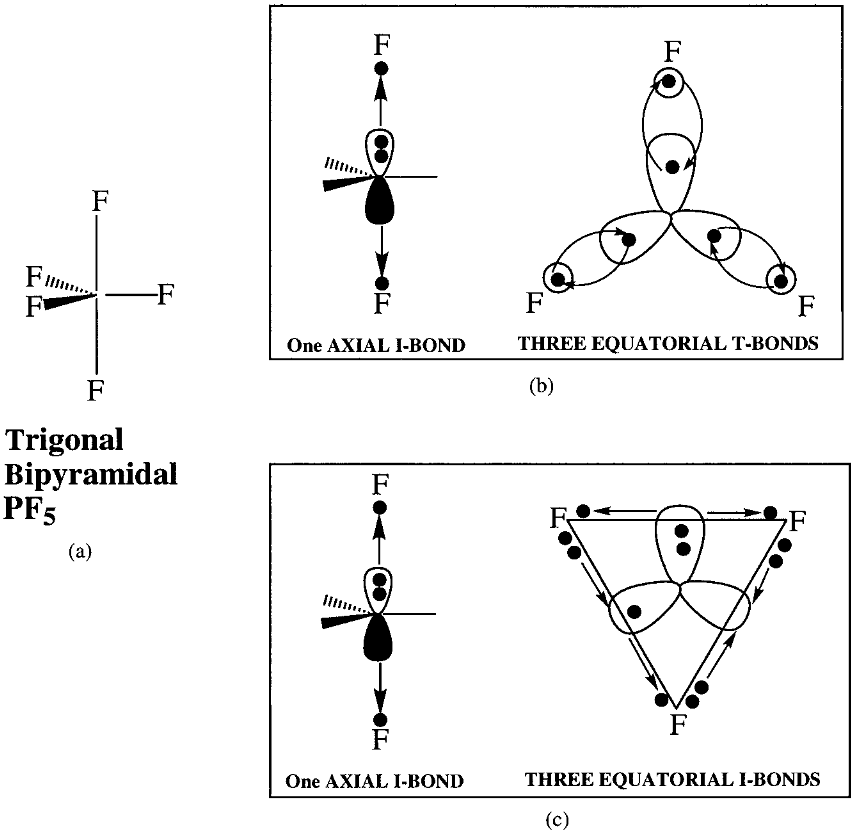

FIGURE 12 (a) The trigonal bypyramidal structure of PF_5. (b) T/I bimodal bonding. (c) Full I-bonding.

bipyramidal PF_5? As indicated in Fig. 12, there exist two different bonding schemes, Figs. 12b and 12c, which differ as follows: in Fig.12b, P binds five fluorines, each acting as an effective one-electron ligand, by three T-bonds and one I-bond. In Fig. 12c, P again binds to five fluorines, but now two of them act as one-electron and three as three-electron ligands, by four I-bonds. I-bonds are superior to T-bonds because electrons delocalize in different overlap regions, thus minimizing their interelectronic repulsion. The low electronegativity of P (say, relative to N) means that the low-spin P configuration involved in Fig. 12c is energetically accessible, and this “provokes” F to act fully or partly as a three-electron ligand so as to engender the superior I-bonds. Note that the number of arrows in each formula is conserved and that the only difference lies in the allocation of the arrows: a T-bond has two arrows spanning the same overlap region, but an I-bond has arrows spanning different overlap regions. Of course, the formula of Fig. 12c is only one of three (resonating) equivalent VB descriptors required for reproducing trigonal bipyramidal symmetry.

So, what is the electronic structure of PF_5, the formula in Fig. 12b or 12c? There exists an important periodic trend which seems not to have been recognized before: second row atoms have a greater affinity for ligands with actual (e.g., fluorine) or effective lone pairs (e.g., methyl). In other words, utilization of ligand lone pairs is triggered by atoms of (relatively) low electronegativity. Thus, we conclude that the better representation of PF_5 is that of the formula in Fig. 12c, while that of Fig. 12b may be the best representation of PR_3F_2 (fluorines axial). This explains directly why PH_5 is unknown: H is incapable of engendering CT by interaction with a P lone pair because of its low electronegativity, and it also lacks lone pairs. The two attributes that encourage I-bonding on the part of F are absent in H. It also explains why, while a C–H is stronger than a Si–H bond, the trend reverses when H is replaced by F: a Si–F is stronger than a C–F bond (in the tetracoordinate C and Si). Sulfuric acid can be thought of as a derivative of $(HO)_2S$ in which each of the two sulfur lone pairs are “capped” by an oxygen atom via an I-bond, see Fig. 13. Similarly, sulfur hexafluoride can be thought of as a derivative of F_2S in which each of the $3p$ and $3s$ lone pairs are capped by a pair of fluorine atoms in one I-bond. The strong electrophilic action of SO_3 can be understood by starting with an sp^2-hybridized S in which each one of the three sp^2 hybrid AOs are doubly occupied. Each oxygen atom caps one sp^2 lone pair

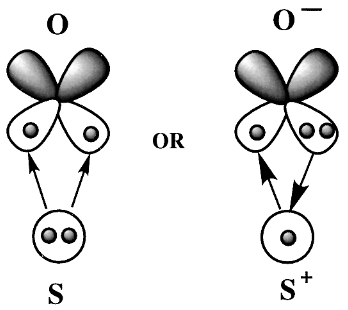

FIGURE 13 The capping of one lone pair of S by an oxygen atom via one I-bond. The two representations are essentially equivalent, differing only in the selection of the reference configuration.

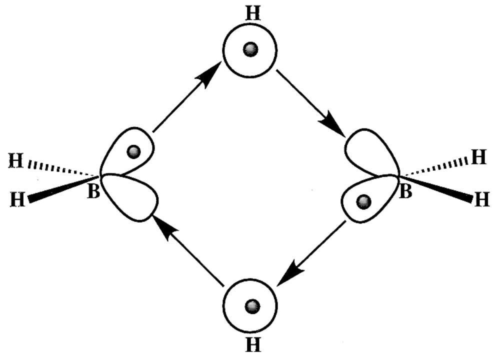

FIGURE 14 Bimodal T/I-bonding in Diborane. The four conventionally drawn B—H bonds are, according to the colored periodic table, T-bonds. However, the electrons responsible for the aggregation of the two ligands are connected via four HT arrows. Since one pair of arrows represents a single I-bond, there are a total of two I-bonds and four T-bonds.

by a pair of dots, while two oxygen lone pairs associate with the vacant $3p$ AO. We have a total of four I-bonds. This species is effectively the "I-analogue" of the CF_3^+ "T-prototype."

One can extend the approach described above to produce the most likely formulae of transition metal oxides. To do so, one takes transition metals in their low-spin electronic configurations, caps valence pairs by pairs of oxygen dots, and associates valence holes with oxygen lone pairs. Thus, the well-known oxidizer CrO_2Cl_2 can be formulated as Cr with three pairs plus three holes (the valence space is $3d$ plus $4s$), with each Cr pair tying up two ligand dots and each hole tying up two ligand lone pairs. Thus, this inorganic molecule has effectively two oxygen atoms and two chlorine atoms linked to chromium by six I-bonds.

Borane clusters were also key stimulants for the new VB interpretation. Boron is a gateway atom ambiguous about T- and I-bonding, advantageously combining both mechanisms as well as being tolerant to the expression of either one mechanism acting alone, generating a fantastic array of diverse chemical systems. An examination of the structural, experimental, and computational literature has produced the outlook presented in *Deciphering the Chemical Code: Bonding Across the Periodic Table.* Bridging is a consequence of either I- or E-bonding, never T-bonding (which favors electron pair segregation). Diborane, shown in Fig. 14, is an example of mixed T/I-bonding having four T- and two I-bonds.

As discussed before, we can envision transition metal oxides as binding through a low-spin metal electronic configuration with each oxygen atom acting through a pair of dots plus one lone pair to produce the maximum number of I-bonds permissible by the valence $(n-1)d/ns$ space of the metal. For example, OsO_4 has four tetrahedrally arranged Os pairs capped by four oxygens each acting by two dots plus one lone pair. Disengagement of one of the two oxygen dots at the expense of I-bond reduction (a form of promotional energy) generates an oxygen monoradical which can enter into hydrogen abstraction reactions much like the OH radical. Is it operationally significant to consider metal and semimetal oxides as sources of incipient oxygen radicals? Mayer (1998) has made a first step in answering this question, with the ultimate answer requiring an investigation of the mechanism of oxidation by main group oxides, e.g., XeO_3.

The BDEs of a series of fluorides that start with LiF and end with FF are as follows (in kcal/mol): LiF 137; BF 181; CF 127; NF 92; OF 55; FF 37. It is evident that BF stands out of the correlation. Now, the increase in the BDE in going from LiF to BF can be attributed to the increasing x^+. Also, the decrease in going from BF to CF can be attributed to the introduction of a three-electron pi antibond between one odd carbon electron and one fluorine lone pair. However, if this were all that was involved, the subsequent addition of antibonding electrons in going from CF to FF would have comparable consequences, and this is clearly not the case. One possible interpretation is that BF is actually a molecule with a very favorable I-bond as illustrated below.

Here, we can glimpse why I-bonding is intrinsically superior to T-bonding, i.e., why the famous "covalent bonding" actually represents a restriction. It can be seen

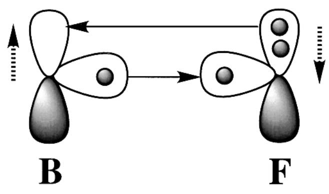

SCHEME 4

that interatomic CT specified by the two solid arrows is complemented by dispersion, i.e., intra-atomic CT, indicated by the two hatched arrows. This is the concept of overlap dispersion, the crucial underpinning of the I-bond which sends a clear message: without explicit recognition of electron-electron repulsion, one cannot arrive at a realistic theory of chemical bonding. Without the assistance of dispersion, (charge generating) I-bonding could never compete with (charge conserving) T-bonding. Using high-level ab initio computations, Davidson and co-workers (1993) discovered that this type of bonding mechanism, labeled "dynamic shielding of extramolecular correlation," is crucial in transition metal complexes, e.g., $Cr(CO)_6$.

The physical picture of overlap-dispersion I-bonding is electrons delocalizing without running into each other. Clearly, the sigma bond of BF does not belong to the catalog of conventional theory. Rather, it is a strong bond due to CT which is assisted by its environment, the latter being the pi space. The situation is expected to be the same in oxoboron molecules. Hawthorne commented in a 1998 UCLA faculty research lecture: "Boron especially likes to combine with oxygen. The nice thing about (boranes) is that when they burn they release large quantities of heat." So, could it be that the superiority of I-bonding points the way to rocket fuels? At the moment, we cannot dismiss the alternative viewpoint of T-bound BF_3, the stability of which can be explained by Pauling's notion of polar covalence (by vide infra).

The proposal of a new bonding pantheon and a colored periodic table is a beginning, not an end. We wish to emphasize this by giving explicit examples of our own uncertainty as to how things really are. Three simple illustrations are shown in Fig. 15.

VII. THE HARD/SOFT ACID-BASE (HSAB) CONCEPT

Many years ago, Pauling (1960) pointed out that "polar covalence" is responsible for the fact that many recombination reactions of the type shown below in reaction 1 are exothermic.

$$AA + ZZ \longrightarrow 2\,AZ \tag{1}$$

This trend applies when A and Z are nonmetals having different electronegativities. Examples of the "Pauling Trend" are given in part (a) of Table III. Note that in section a, all atoms have the same color—blue.

In 1958, Ahrland, Chatt, and Davies made a contribution of great significance. They pointed out that metal ions (Lewis acids) can be divided roughly into two classes depending on their ability to coordinate with specific donor atoms or groups (Lewis bases). Specifically, "class a" metal ions bind most strongly with first row donors (N, O, F), while "class b" ions form complexes of high stability in combination with donors from lower rows of the periodic table. In the early 1960s, Pearson (1969) made a related important contribution. He recognized that, if neutral metals and metal ions were classified as "hard" and "soft," the available thermochemical data implies that "soft likes to bind soft and hard likes to bind hard." Furthermore, Pearson recognized that the Hard Soft Acid-Base (HSAB) concept led to thermochemical predictions which were diametrically opposite to those of the Pauling "polar covalence" concept. Typical examples of the "HSAB Trend" are given in part (b) of Table III.

TABLE III Thermochemistry of Bond Interchange (in kcal/mol)

a. Pauling trend			
F—F + H—H	$\longrightarrow$	H—F + H—F	ΔE = −129
HO—OH + H—H	$\longrightarrow$	H—OH + H—OH	ΔE = −83
H_2N—NH_2 + H—H	$\longrightarrow$	H—NH_2 + H—NH_2	ΔE = −45
H_3C—CH_3 + H—H	$\longrightarrow$	H—CH_3 + H—CH_3	ΔE = −11
b. HSAB trend			
COF_2 + $HgBr_2$	$\longrightarrow$	$\underline{COBr_2}$ + HgF_2	ΔE = +85
CO + PbS	$\longrightarrow$	$\underline{CS}$ + PbO	ΔE = +71
H_2O + CaS	$\longrightarrow$	$\underline{H_2S}$ + CaO	ΔE = +37
HF + NaI	$\longrightarrow$	$\underline{HI}$ + NaF	ΔE = +32
c. Metal trend			
Li_2+ H_2	$\longrightarrow$	$\underline{LIH}$ + $\underline{LiH}$	ΔE = +13
Na_2+ H_2	$\longrightarrow$	$\underline{NaH}$ + $\underline{NaH}$	ΔE = +26
Cs_2+ H_2	$\longrightarrow$	$\underline{CsH}$ + $\underline{CsH}$	ΔE = +30

The HSAB concept marks a revolution. Selectivity of atom combination implies the existence of more than one mechanism of chemical bonding. The common denominator of all reactions in parts (b) and (c) of Table III is the existence of products which are combinations of atoms of different color: green/blue or red/blue combinations. For example, consider the red/blue Li—H. Ideally, Li has affinity for I-bonding and H has an affinity for T-bonding. Their combination is permissive of E-bonding provided that their electronegativity difference is large. This failing to be the case, we can conclude that Li—H is a *frustrated* molecule: none of the three mechanisms of chemical bonding, T, I, or E, is appropriate for this atom pair.

CS is a blue/green diatomic. It can exhibit bimodal T/I-bonding to the extent that the formal triple bond can be "2I + 1T." The problem lies in the fact that I-bonding couples overlap and dispersion, and a nonpolarizable blue atom is unable to support dispersion. Hence, blue/green diatomics or triatomics, like those on the product sides of the equations in part (b) of Table III, are said to be *frustrated*. A bonding principle emerges: atoms prefer to bind

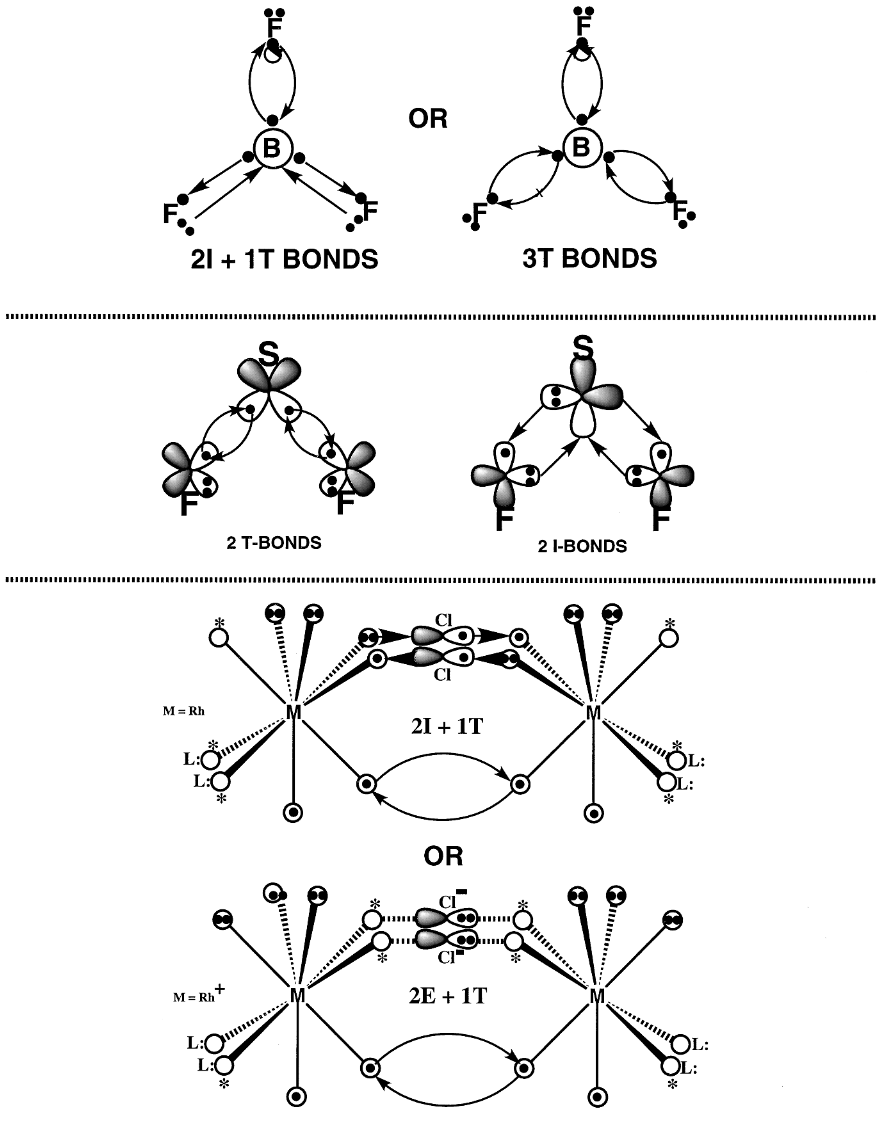

FIGURE 15 Candidate bonding mechanisms for three molecules.

in ways that ensure that the resulting molecule is uniformly colored. Note that the statement implies a comparison. The combination of atoms of the same color is relatively superior to the combination of atoms of a different color. This is the underpinning of the HSAB principle which, in turn, becomes a key piece of evidence in favor of the proposal of three mechanisms of chemical bonding.

The colored periodic table provides a theoretical basis for the HSAB concept. Consider the reaction shown below; lithium can be called soft and hydrogen hard. Hence, this reaction is the simplest embodiment of the HSAB concept. The terms soft and hard are now seen as inventions which serve the same purpose of differentiating between more than one mechanism of chemical bonding. Our interpretation of the endothermicity of the reaction is straightforward: the two H's taken together optimally engage in T-bonding ("homonuclear T-bonding"), while the two Li's taken together engage in I-bonding ("homonuclear I-bonding"). The LiH combination shown in reaction 2 involves frustrated bonding.

$$\underset{\mathrm{T}}{\mathrm{H{-}H}} + \underset{\mathrm{I}}{\mathrm{Li{-}Li}} \longrightarrow \underset{\mathrm{FR}}{2\,\mathrm{Li{-}H}} \quad \Delta E = +13\ \mathrm{kcal/mol} \tag{2}$$

Are atoms racist, as implied by the fact that atoms of like color prefer to bind each other? The answer turns out to be a resounding no! To see this, we recognize that reaction (2) represents only a part of the entire hypersurface. On the reactant side, the two diatomics can combine to form a van der Waals complex, while, on the product side, two

LiH molecules can form a much more stable rhomboidal dimer. Hence, we should transform the simple prototypical equation above to the one shown below in reaction (3). The bonding mechanisms operative in reactants and products are shown in Fig. 16.

$$\underset{\text{T}}{\text{H–H}} \text{- - - -} \underset{\text{T=FR}}{\text{Li–Li}} \longrightarrow \underset{\text{I}}{\text{Li–H–H–Li (rhombic)}} \quad (3)$$

On the reactant side, the T-bond in H_2 is partly localized, while the I-bond is converted to an unfavorable T-bond in Li_2. These are the "promotions" required for forming an intermolecular E-bond (due to induction/dispersion) indicated by a dashed line. One the product side, essential abolition of the T-bond of H_2 and the I-bond of Li_2 is the price necessary for establishing a very strong I-bond. The existing data suggests that the reaction is exothermic, something well explained by the superiority of I- to E-bonding.

VIII. BEYOND THE ISOELECTRONIC AND ISOLOBAL ANALOGIES

Oxygen has one 2*s*, three 2*p* AOs, and six valence electrons. Sulfur has one 3*s*, three 4*p* AOs, and six valence electrons. Oxygen and sulfur are *isoelectronic*. This explains the similarity of the shapes of HOH and HSH (both molecules are bent). By contrast, we say that the very similarity hides a fundamental difference in bonding mechanism due to the fact that S is more electropositive than O. As a result, HOH lies toward the T-delocalization limit, while HSH lies toward the I-delocalization limit. We expect that, in two other isoelectronic systems, the difference in bonding mechanisms will cause them to have radically different shapes.

BH has one radial *n* and two tangential *p* AOs of *a* and *e* symmetry (in C_{3v}) and two valence electrons. The C_{3v} $Fe(CO)_3$ fragment also has three frontier MOs of *a* and *e* symmetry and a total of two electrons. Hence, BH and $Fe(CO)_3$ are said to be isolobal. The analogies can be extended. All of the following fragments are *isolobal*, having one *a* and two *e* orbitals containing two valence electrons: C, Si, HC^+, HB, $Fe(CO)_3$, $Os(CO)_3$, $Co(CO)_3^+$, $Ir(CO)_3^+$. According to extended Hückel MO theory, replacing any one of these groups by another one should cause no change in the architecture of the molecule unless there is some problem of orbital mismatching or steric repulsion. The notion of "isolobality" was developed by Hoffmann and his school, and it motivated much fruitful research, most notably by Sone, Herrmann, and Huttner (1986). Nonetheless, our conclusions are at odds with the EHMO scenario: the shape of a molecule depends on the mechanism of bonding, i.e., whether T- or I-delocalization predominates. This depends on the electronegativity of the central atom. Thus, we expect that, for example, HC^+ and HB will combine with a given fixed fragment in a way which is stereochemically different despite the fact that they are isoelectronic and isolobal. In this sense, bonding theory starts after symmetry considerations have ended.

Here are some facts which make clear that it is the "color" of atom electronegativity that determines the bonding mechanism and, hence, their shapes and properties. Since a whole book can be written just on the differences of isoelectronic or isolobal species, we restrict our attention to the fragment series HC, HSi, N, P, $(CO)_3Co$, and $(CO)_3Ir$.

1. Nitrogen forms a strong triple bond to a second nitrogen, while phosphorus shows a preference to form rings, cages, and even deltahedral clusters (e.g., P_4).
2. C_2H_2 is linear with a carbon-carbon triple bond, while Si_2H_2 was computed to be "butterfly" by Lischka and Koehler (1983).
3. HC≡CH is a stable organic molecule, but $(CO)_3Co{\equiv}Co(CO)_3$ has not yet been made.

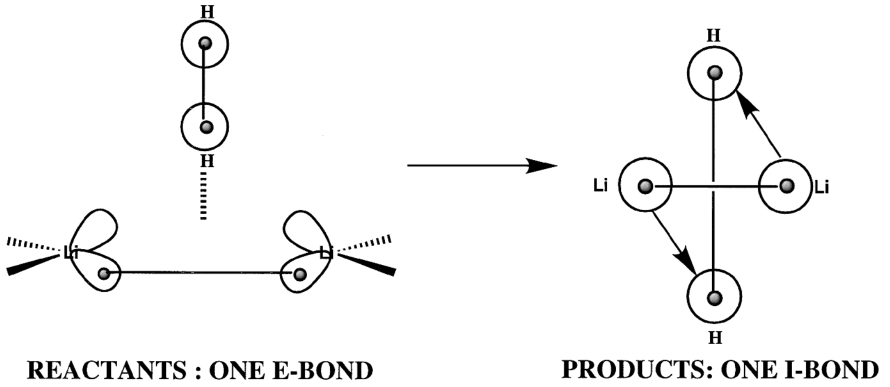

FIGURE 16 The expected energy minima of the Li_2H_2 hypersurface. A solid line connecting two dots implies a T-bond when overlap is substantial. For the "peculiar" bonding of the rhombus, consult Epiotis (1996).

4. Two acetylenes are more stable than one tetrahedrane. Similarly, tetrahedral N_4, irrespective of whether it is a secondary minimum or not, lies much higher than two N_2. By contrast, tetrahedral P_4 is more stable than two P_2 by 55 kcal/mol.
5. Similarly, $[Co(CO)_3]_4$ is tetrahedral involving carbonyls as bridging groups. By contrast, $[Ir(CO)_3]_4$ is a tetrahedron with no bridging carbonyls.

One of the major impulses toward the new VB interpretation was the observation that isoelectronic or isolobal species are not necessarily isostructural. For example, C and Si are isoelectronic and both are isolobal to $Fe(CO)_3$. Yet the structures of C-containing molecules are different from those of isoelectronic Si-containing molecules. By contrast, replacing Si by $Fe(CO)_3$ does not cause a gross change of molecular architecture. It was concluded that the difference between C and Si and between C and $Fe(CO)_3$ must be due to a difference in binding mechanism: C supports T-bonding, but the more electropositive Si and Fe support I-bonding. On the other hand, Si and $Fe(CO)_3$ must be essentially interchangeable within a molecule without causing a change of shape. We say that these two groups are isosynaptic. According to Epiotis (1989), "two groups are isosynaptic if they are isolobal or isoelectronic and they have the same color." Green and red isolobal groups are regarded, to a first approximation, as isosynaptic. For example, red $Fe(CO)_3$ is isolobal to green Si. Hence, they should also be isosynaptic. If disilaacetylene is a butterfly, then $Fe(CO)_3$ organometallics with butterfly structures must abound. Mere perusal of the monograph of Marko and Marko-Monostory (1981) makes evident that this is indeed the case.

We have seen that molecules in which atoms with the same number of valence electrons but different color can end up having different shapes. The other side of the coin is that molecules in which atoms have different numbers of valence electrons as well as different colors may have the same shape provided that T-bonds in one are replaced by I-bonds in the other. For example, NH_3, which features three N–H T-bonds, is pyramidal. The same thing is true of the isoelectronic XeO_3, ClO_3^{-1}, and SO_3^{-2}, in which the central atom is connected to each oxygen atom by one I-bond.

IX. ATOMIC VALENCE AND THE COLORED PERIODIC TABLE

One important utilization of the periodic table has been the connection of atomic number to atomic valence or atomic oxidation number. The term "valence" refers to the number of ligands which can be attached on a central atom. Modern electronic theory has attempted to rationalize this experimental observable. For example, from the electronic configuration of phosphorus (a 3*s* pair and three 3*p* dots), we can expect that this atom will be capable of forming a maximum of three covalent bonds to three univalent ligands. On such a basis, one expects that phosphorus is primarily trivalent. The fact that quadri- as well as penta-valent phosphorus compounds are known is more conveniently explained by the concept of formal oxidation state. This is equal to the number of electrons that can be transferred to a set of more electronegative ligands. The maximum (positive) oxidation state is equal to the number of valence electrons, i.e., five in the case of phosphorus.

The colored periodic table stands on very different theoretical grounds. In its ground electronic configuration, phosphorus contains two types of elements: one pair and three dots. But we have already seen that each atomic element (pair, dot, or hole) can receive a maximum of two arrows emanating or terminating at some ligand. Because each valence AO of an atom can be classified only as a pair, a dot, or a hole, it follows that the maximum valence of an atom equals twice the number of valence AOs. This means that the maximum coordination number of phosphorus within a molecule is eight, rather than three or five. Thus, the concept of the I-bond revolutionizes the concept of valence. The synthetic chemist can now throw away the inhibitory chains of conventional wisdom and attempt to make octavalent phosphorus (and high-valent green and red atoms) by judicious selection of ligands. A molecule in which each green or red atom employs each valence AO to tie up two elements is *associatively saturated*. We believe that there are many such examples in the literature which are obscured by the fact that coordinative saturation is different from associative saturation. For example, in the case of phosphorus, associative saturation requires the presence of eight elements around phosphorus. But these may be contained within fewer than eight ligands. Indeed, it is commonplace that an electronegative ligand, such as a halogen atom, may act via a dot plus one or two pairs (three- or five-electron ligand) to provide more than one element, rather than acting as a pure (one-electron) univalent ligand. The well-known PF_5 can be thought of as a molecule in which phosphorus acts with one 3*s* pair plus one 3*p* pair, and one 3*p* dot plus one 3*p* hole to tie up five fluorine dots and three fluorine lone pairs with four I-bonds (vide supra). Molecules containing phosphorus in a coordination state higher than five are not oddities. In fact, Holmes (1998) has reported hexacoordinate phosphorus to be implicated in enzymatic reactions. Hepta- and octacoordinate phosphorus (and, especially, heavier cogners) are expected to be realizable synthetic goals.

ACKNOWLEDGMENT

We are indebted to A. Truman Schwartz of Macalester College for composing most of the historical narrative which we abridged and modified.

SEE ALSO THE FOLLOWING ARTICLES

ACTINIDE ELEMENTS • ATOMIC PHYSICS • ATOMIC SPECTROSCOPY • CRYSTALLOGRAPHY • ELECTRON TRANSFER REACTIONS • HALOGEN CHEMISTRY • MAIN GROUP ELEMENTS • NOBLE METALS • ORGANIC CHEMICAL SYSTEMS, THEORY • QUANTUM CHEMISTRY • QUANTUM MECHANICS • QUANTUM THEORY • RADIOACTIVITY • RARE EARTH ELEMENTS AND MATERIALS • X-RAY ANALYSIS

BIBLIOGRAPHY

Ahrland, S., Chatt, J., and Davies, N. R. (1958). *Q. Rev. London* **12,** 265.

Allen, L. C. (1989). *J. Am. Chem. Soc.* **111,** 9003–9014. See also: Strong, L. E., ed. (1964). "Chemical Systems," Webster Division, McGraw-Hill, St. Louis. Produced by the Chemical Bond Approach Project.

Cotton, F. A., and Wilkinson, G. (1999). "Advanced Inorganic Chemistry," 5th ed., Wiley, New York.

Cotton, F. A., and Walton, R. A. (1982) "Multiple Bonds Between Metal Atoms," Wiley, New York.

Cowley, A. H. (1984). *Acc. Chem. Res.* **17,** 386–392.

Davidson, E. R., Kunze, K. L., Machado, F. B. C., and Chakravorty, S. J. (1993). *Acc. Chem. Res.* **26,** 628–635.

Epiotis, N. D. (1996). "Deciphering the Chemical Code: Bonding Across the Periodic Table," VCH/Wiley, New York.

Epiotis, N. D. (1989). "Topics in Current Chemistry," Vol. 150, p. 107, Springer-Verlag, New York.

Herrmann, W. A. (1986). *Angew. Chem. Int. Ed. Engl.* **26,** 56–75.

Hoffmann, R. (1982). *Angew. Chem. Int. Ed. Engl.* **21,** 711–723.

Holmes, R. R. (1998). *Acc. Chem. Res.* **31,** 535.

Horgan, J. (1996). "The End of Science," Addison-Wesley, Reading, MA.

Knight, D. M. (1992). "Ideas in Chemistry," Rutgers Univ. Press, New Brunswick, NJ.

Lewis, G. N. (1923). "Valence and the Structure of Atoms and Molecules," Chem. Catalog Co., New York.

Lischka, H., and Koehler, H.-J. (1983). *J. Am. Chem. Soc.* **105,** 6646–6649.

Marko, L., and Marko-Monostory, B. (1981). "The Organic Chemistry of Iron" (von E. A. K. Gustorf, F.-W. Grevels, and I. Fischler, eds.), Vol. 2, Academic Press, New York.

Mayer, J. M. (1998). *Acc. Chem. Res.* **31,** 441–450.

Pauling, L. (1960). "The Nature of the Chemical Bond," 3rd ed., Cornell Univ. Press, Ithaca, NY.

Pearson, R. G. (1969). "Survey of Progress in Chemistry" (A. Scott, ed.), Vol. 5, pp. 1–52. Academic Press, New York.

Puddephatt, R. J., and Monaghan, R. J. (1986). "The Periodic Table of the Elements," Clarendon, Oxford.

Shriver, D., Langford, C. H., and Atkins, P. W. (1999). "Inorganic Chemistry," 3rd ed., W. H. Freeman, New York.

West, T., Fink, M. J., and Michl, J. (1981). *Science* **214,** 1343–1344.

Van Spronsen, J. W. (1969). "The Periodic System of Chemical Elements: A History of the First Hundred Years," Elsevier, Amsterdam.

Rare Earth Elements and Materials

Zhiping Zheng
University of Arizona

John E. Greedan
McMaster University

I. The Rare Earth Elements
II. Chemical Physics of the Rare Earths
III. Rare Earth Materials
IV. Technological Applications
V. Catalysis and Other Chemical Applications

GLOSSARY

Bastnasite Common rare earth ore of composition $REFCO_3$ (fluorocarbonate) rich in La, Ce, Pr, and Nd.

Cathode ray tube An electron tube, or evacuated glass container, having at one end a cathode, or negative electrode, and a device called an electron gun that projects a beam of electrons against a luminescent screen at the opposite end of the tube.

Contrast agents Contrast agents are a class of pharmaceuticals that when administered to a patient, enter and pass through anatomic regions of interest to provide transient contrast enhancement.

Lanthanide contraction Systematic decrease in atomic and ionic size that occurs from lanthanum (La) to lutetium (Lu). The difference in size between adjacent elements is only about 1% but the cumulative effect is about a 20% reduction.

Liquid–liquid extraction Technique for the large-scale separation of the rare earth elements involving the countercurrent flow of two immiscible solvents.

Luminescence The phenomenon of the emission of light from materials under excitation is called luminescence. Luminescence may be divided into phosphorescence and fluorescence.

Mischmetal Alloy or mixture of La, Ce, Pr, and Nd metals that is cheapter to produce than separated metals.

Monazite and xenotime Rare earth ores of composition $REPO_4$ (phosphate). Xenotime is nearly pure YPO_4.

Permanent magnets Materials that retain their magnetic properties after having been exposed to a magnetic field.

Phosphors Solid-state materials exhibiting luminescence.

THE RARE EARTH elements are those from atomic numbers 57 (lanthanum) to 71 (lutetium) inclusive and elements 21 (scandium) and 39 (yttrium). They represent the largest group of chemically similar elements, but their physical properties differ markedly due to subtle features of electronic structure. Because of the similarity between

all of the rare earths, their separation and recovery in pure form have been extremely difficult. It was not until the 1940s that many of the properties of the individual rare earths and the materials containing these elements were investigated. The basic studies have greatly accelerated the pace at which rare earth materials are utilized in both fundamental scientific research and modern technology.

I. THE RARE EARTH ELEMENTS

Rare earth elements are a series of chemical elements of the periodic table, including the elements with atomic numbers 57 through 71, and, named in order, are lanthanum (La), cerium (Ce), praseodymium (Pr), neodymium (Nd), promethium (Pm), samarium (Sm), europium (Eu), gadolinium (Gd), terbium (Tb), dysprosium (Dy), holmium (Ho), erbium (Er), thulium (Tm), ytterbium (Yb), and lutetium (Lu). Yttrium (Y, atomic no. 39) and scandium (Sc, atomic no. 21) are sometimes included in the group of rare earth elements. The elements cerium (Ce, atomic no. 58) through lutetium (Lu, atomic number 71) are commonly known as the lanthanide series. As will be clearer later, there are ample reasons to include Y as a rare earth, but the inclusion of Sc is less common and more controversial.

In the usual short form of the periodic table, the lanthanides are segregated (along with the actinides, numbers 89 to 103) from the other elements giving the correct impression that they comprise a very closely related group with unique characteristics, but also the false impression that their properties are somehow unrelated or unconnected to the remaining elements. In the long form of the periodic table (shown in Fig. 1) it is clearly seen that the rare earths form a bridge between the very reactive metallic elements Cs and Ba and the transition element series beginning with hafnium (Hf), tantalum (Ta), and tungsten (W). Of course, the position of the rare earths in the periodic table of the elements and their chemical and physical properties follow more or less directly from the details of the atomic structure, also called their electronic configuration, which will be discussed in Section II.

A. Origin of the Names of the Elements

As will be clear from Section I.B, the general appellation for these elements as "rare earths" is inappropriate. Several decades of usage, however, make it unlikely that this term will soon disappear from the vocabulary of the working scientist or engineer. It arose, presumably, because many of these elements were first discovered as components of certain minerals that are indeed rare.

Table I gives the names of the rare earth elements together with other pertinent information regarding their origins. The identity of the discoverer is included as it was he, often, who enjoyed the privilege of naming the new element.

Note that many of the rare earths were first discovered in Sweden. In fact most were isolated from mineral samples mined from a quarry near Ytterby, a small village that has given various parts of its name to no fewer than four elements: yttrium, ytterbium, terbium, and erbium. Although their initial discovery was a Scandanavian event, the truly formidable task of separating, isolating, and identifying this group of 16 incredibly similar elements was an international affair drawing equally on the talents of the French spectroscopists, Demarcay, Lecoq de Boisboudran, and Urbain, the Austrian, von Welsbach, and many others.

In one sense Table I, while containing interesting historical facts, is somewhat misleading in an important way. It implies that most of the rare earths have been known since the late 19th and early 20th centuries (except for the "artificial" element prometheum). While this is true in a limited sense, samples of the rare earths of sufficient purity for modern chemical and physical studies were only prepared in the 1950s. Widespread commercial availability of these elements has come about even more recently. In a true sense, we are yet in an early stage of basic study and technological exploitation of this group of elements.

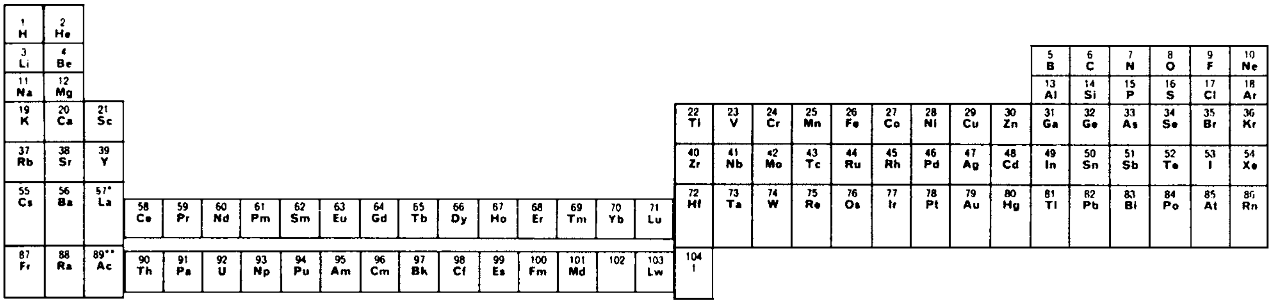

FIGURE 1 The "long form" of the periodic table of the elements. The rare earths are elements numbers 21 (Sc), 39 (Y), and 57 (La) to 71 (Lu) inclusive. This version emphasizes that the rare earths are a bridge between the reactive "alkaline-earth" elements Ca (20), Sr (38), and Ba (56) and the "transition metals" Ti (22), Zr (40), and Hf (72).

TABLE I Discovery of the Elements

Name	Discoverer (nationality) (year)	Origin
Lanthanum	C. G. Mosander (Swedish) (1839)	(Greek), lanthanein "to lie hidden"
Cerium	M. H. Kalproth (German) J. J. Berzelius (Swedish) W. Hinsinger (Swedish) (1803)	Ceres, an asteroid discovered only 2 years prior
Praesodymium and neodymium	C. A. von Welsbach (Austrian) (1885)	Separated from a mixture originally called didymia. (Greek) Prasios (green), neo (new), didymos (twin)
Promethium	J. A. Marinsky L. E. Glendenin and C. D. Coryell (American) (1945)	(Greek mythology) Prometheus, stole fire from the gods. All isotopes of prometheum are radioactive
Samarium	P. Lecoq de Boisboudran (French) (1879)	Samarskite, a mineral. The mineral was named for a Russian mining official Col. Samarski
Europium	E. A. Demarcay (French) (1901)	Europe
Gadolinium	J. C. G. Marignac (Swiss) (1886)	Gadolinite, a mineral. The mineral was named for J. Gadolin, a Finnish chemist
Terbium	C. G. Mosander (Swedish) (1843)	Ytterby, a Swedish village. Site of a quarry where many rare minerals containing "rare earths" were first discovered
Dysprosium	P. Lecoq de Boisbaudran (French) (1886)	(Greek) disprositos, "hard to get at" from the difficulty in isolating this element
Holmium	J. L. Soret (Swiss) P. T. Cleve (Swedish) (1878)	(Latin) Holmia, latin for Stockholm, Cleve's native city
Erbium	C. G. Mosander (Swedish) (1842) G. Urbain (French) (1905)	Ytterby, Swedish village. Mosander discovered erbium but Urbain first produced fairly pure material
Thulium	P. T. Cleve (Swedish) (1879)	Thule, ancient name for Scandanavia
Ytterbium	J. C. G. Marignac (Swiss) (1878)	Ytterby, Swedish village
Lutetium	C. A. von Welsbach (Austrian) G. Urbain (French) C. James (American) (1907)	Lutetia, ancient name for Paris
Yttrium	C. G. Mosander (Swedish) (1843)	Ytterby, Swedish village. Isolated by Mosander from mixture discovered by Gadolin (1794)

The reason for this surprising lag between initial discovery and the beginnings of a serious study and exploitation of the rare earths lies in the facts of their mineralogical origin and their great chemical similarity leading to enormous difficulties in separation and isolation of the individual elements. These issues are discussed in the following section.

B. Natural Occurrence and Abundance of the Rare Earths

1. Geological Distribution

The rare earths are very widely distributed in the earth's crust and exhibit a great diversity in the geological type of the deposits. They are found in all possible geological domains: igneous-hydrothermal, metamorphic, and sedimentary. They occur as an important constituent in more than 100 different minerals and in trace quantities in many others. In fact, the study of the distribution of rare earths at trace levels in minerals is of considerable importance as a geological tool to determine the evolutionary history of a given sample. This will be discussed briefly later on.

In spite of this great mineralogical diversity only a very few rare earth-bearing minerals occur in sufficient concentration to justify commercial exploitation as an ore. These are, roughly in order of current commercial importance, bastnasite (bastnaesite is another spelling), $REFCO_3$; monazite, $REPO_4$; and xenotime, YPO_4 (the same chemical formula as monazite but contains mostly yttrium). Here the symbol RE refers to a mixture of rare earths. In addition, apatites $(Ca, RE)_5(PO_4)_3F$ and uranium-bearing minerals such as uraninite and uranothorite contain commercial quantities.

Exploitable deposits of the above minerals are found on all six continents as shown in Table II, which lists world reserves in units of tons of Reoxide.

Note the striking fact that 80% of the world reserves of rare earths are located in China with 11% in North America and 5% in India. Both the Chinese (at Bayan Obo,

TABLE II World Rare Earth Reserves and Reserve Base[a,b]

	Lanthanides		Yttrium	
	Reserves[c]	Reserve Base[c]	Reserves[c]	Reserve Base[c]
United States	13,000,000	14,000,000	120,000	130,000
Australia	5,200,000	5,800,000	100,000	110,000
Brazil	280,000	310,000	400	1,500
Canada	940,000	1,000,000	3,300	4,000
China	43,000,000	48,000,000	220,000	240,000
Congo (Kinshasa)	—	—	570	630
India	1,100,000	1,300,000	36,000	38,000
Malaysia	30,000	35,000	13,000	21,000
South Africa	390,000	400,000	4,400	5,000
Sri Lanka	12,000	13,000	240	260
Thailand	—	—	600	600
Former Russia	19,000,000	21,000,000	9,000	10,000
Other countries	21,000,000	21,000,000	—	—
World total (rounded)	100,000,000	110,000,000	510,000	560,000

[a] Modified from Hedrick, J. B. (2000). "U.S. Geological Survey, Mineral Commodity Summaries," pp. 135, 189,

[b] Metric tons of rare earth oxide. Data may not add to totals shown because of independent rounding.

[c] The reserve base includes demonstrated resources that are currently economic (reserves), marginally economic (marginal reserves), and some of those that are currently subeconomic (subeconomic resources).

TABLE III World Mine Production in 1999[a]

	Lanthanides[b]	Yttrium[b]
United States	5,000	—
Australia	—	—
Brazil	1,400	15
Canada	—	—
China	65,000	2,200
Congo (Kinshasa)	—	—
India	2,700	55
Malaysia	250	7
South Africa	—	—
Sri Lanka	120	2
Thailand	—	—
Former Russia	2,000	125
Other countries	—	—
World total (rounded)	76,500	2,400

[a] Modified from Hedrick, J. B. (2000). "U.S. Geological Survey, Mineral Commodity Summaries," pp. 135, 189.

[b] Metric tons of rare earth oxide. Data may not add to totals shown because of independent rounding.

Nei Monggol Autonomous Region) and the United States deposits (Mountain Pass, CA) are primarily bastnasite. This latter deposit is of the highest grade yet discovered and is the only one mined principally for its rare earth content. Most economic monazite and xenotime deposits are in the form of beach sands in which wave action has concentrated the minerals. Such sands contain the Indian reserves and most of the remaining world reserves.

In terms of actual world production of rare earth elements and the capacity to produce them, the picture changes somewhat as seen in Table III.

North America (mostly the United States) with 10% of the world reserves accounts for nearly 50% of both production and capacity and Australia with less than 1% reserves is a strong second. Note that Scandanavia from whose mineral deposits most of the rare earths were first discovered is not presently a major producer.

2. Distribution of the Rare Earth Elements within the Various Ore Types

Bastnasite ores contain mostly rare earths near the beginning of the series, La, Ce, Pr, and Nd. For a typical deposit the figures would be approximately 30% La, 50% Ce, 4% Pr, and 15% Nd, leaving the remaining elements at the 1% level. Monazites are similarly constituted but contain somewhat less La and Ce and greater amounts of elements from Gd to Lu and Y. Xenotime ores contain up to 60% yttrium with the remainder mostly concentrated in the Gd to Lu half of the series with relatively little of La, Ce, Nd, and Pr. This information is summarized in Table IV.

3. Abundance of Rare Earths Relative to Other Elements

Thus La and Ce are the most abundant rare earths while Lu and Tm are the most scarce. This leads us finally to the issue of the inappropriate nature of the term "rare earth" to describe these elements. In fact, the most abundant "rare earth," Ce, has about the same abundance in the earth's crust as Cu (copper) and is more abundant than B (boron—a major constituent of all glass), Co (cobalt—a commonly used alloying agent in steelmaking). Ge (germanium—used to make the first transistor), Pb (lead—automobile batteries and gasoline), Sn (tin—as in cans), or U (uranium). Even Tm (thulium), the rarest of the rare earths, is more abundant than Cd (cadmium—a battery component), I (iodine—from the medicine chest), Hg (mercury—as in barometers and thermometers), and certainly Ag (silver), Au (gold), and Pt (platinum).

C. Recovery and Separation of the Rare Earths

The separation and purification of the rare earths were among the more spectacular chemical accomplishments

TABLE IV Rare Earth and Yttrium Contents of Major Source Minerals[a,b]

	Bastnasite		Monazite					
	(California)	(China)	(Eastern Australia)	(Western Australia)	(Florida)	(India)	(China)	Xenotime (Malaysia)
La_2O_3	32.00	27.00	20.20	23.90	17.47	23.00	23.35	0.50
CeO_2	49.00	50.00	45.30	46.03	43.73	46.00	45.69	5.00
Pr_6O_{11}	4.40	5.00	5.40	5.05	4.98	5.50	4.16	0.70
Nd_2O_3	13.50	15.00	18.30	17.38	17.47	20.00	15.74	2.20
Sm_2O_3	0.50	1.10	4.60	2.53	4.87	4.00	3.05	1.90
Eu_2O_3	0.10	0.20	0.10	0.05	0.16		0.10	0.20
Gd_2O_3	0.30	0.40	2.00	1.49	6.56		2.03	4.00
Tb_4O_7	0.01		0.20	0.04	0.26		0.10	1.00
Dy_2O_3	0.03		1.15	0.69	0.90	1.02		8.70
Ho_2O_3	0.01		0.05	0.05	0.11		0.10	2.10
Er_2O_3	0.01	1.00	0.40	0.21	0.04	1.50	0.51	5.40
Tm_2O_3	0.02		Trace	0.01	0.03		0.51	0.90
Yb_2O_3	0.01		0.20	0.12	0.21		0.51	6.20
Lu_2O_3	0.01		Trace	0.04	0.03		0.10	0.40
Y_2O_3	0.10	0.30	2.10	2.41	3.18		3.50	60.80
Total	100.00	100.00	100.00	100.00	100.00	100.00	100.00	100.00

[a] Hedrick, J. B. (1985). Rare earth elements and yttrium. "Mineral Facts and Problems," pp. 4–6. U.S., Bureau of Mines Bulletin 675.
[b] Percentage of total rare earth oxide. Analyses adjusted to 100% REO.

of the 20th century. To appreciate the difficulty of the task we recall again that the rare earths comprise a series of 16 very closely related elements of similar atomic size. Under the conditions of the deposition of these elements in the earth's crust and under the conditions that normally pertain during separation procedures neutral atoms are unimportant. Instead we must consider "ionized" states of the elements in which the outer or valence electrons are missing. The overwhelmingly predominant state of ionization of the rare earths, also called the valence or, preferably, the oxidation state, is one in which three electrons are lost giving tripositive ions, RE^{3+}. As with the neutral atoms, the relative sizes of the tripositive ions are similar and show the lanthanide contraction. Table V lists some useful ionic radii.

Note that the radii of the first four elements (La, Ce, Pr, Nd) are relatively large and also are more similar to each other than to the remainder of the series. This group is sometimes called the "cerium group" while the others are lumped as the "yttrium group." Recall that the relative distributions of REs in the various ore types, described in the preceding section, seem to mirror this subgrouping scheme. Note also that the radius of Y is between Ho and Er.

1. Recovery from Ores

The principal rare earth-bearing minerals, bastnasite, monazite, and xenotime, are separated from othermineral contaminants by standard procedures such as flotation and electrostatic and electromagnetic separation. Assuming that a reasonably pure mineral sample results from these techniques, the subsequent treatments depend on the chemical nature of the mineral, but the more common ores can be attacked by acids. Bastnasite, $REFCO_3$, can bedissolved in either sulfuric (H_2SO_4) or hydrochloric (HCl) acids. Monazite and xenotime, both phosphate minerals, can be treated similarly. These procedures result in aqueous (water) solutions containing the RE^{3+} ions along with some impurities such as Th^{4+} (thorium is a common constituent of rare earth minerals). Treatment with a

TABLE V Radii of Trivalent Rare Earth Ions

RE^{3+}	Radius (nm)[a]	RE^{3+}	Radius (nm)
La	0.132	Gd	0.120
Ce	0.128	Tb	0.118
Pr	0.128	Dy	0.117
Nd	0.126	Ho	0.116
(Pm)	0.124	Er	0.114
Sm	0.123	Tm	0.113
Eu	0.121	Yb	0.112
		Lu	0.111
		Y	0.115

[a] Derived by R. D. Shannon and C. A. Prewitt, 1 nm = 10^{-9} m.

strong base such as NaOH (sodium hydroxide) is an often preferred alternative in the case of monazites and xenotimes because the phosphate is removed more efficiently than by the H_2SO_4 treatment.

Subsequent treatment depends on the intended use of the rare earths. For some applications, particularly the older ones, it is not necessary to achieve a separation of the elements. For example, a mixture of the cerium group metals, called "mischmetal," has been used for decades for lighter flints. Thus from a bastnasite or monazite ore base, which contains predominantly the cerium group elements, little further separation work is necessary. However, for basic research into the properties of the elements and their compounds and in applications involving increasingly sophisticated technology the availability of the individual elements in a high purity form is essential.

2. Modern Separation Methods

First, it is relatively easy to separate cerium and europium (and in some cases samarium and ytterbium) from an aqueous mixture of RE^{3+} ions. Here one exploits the fact that in an aqueous environment only these elements can have stable oxidation states different from the prevailing 3+ state, that is, Ce^{4+} and Eu^{2+}. Cerium is normally removed first by a process of oxidation, an increase in valence or oxidation state from 3+ to 4+. In fact, for bastnasite ores this oxidation is often carried out before the acid treatment by heating the mineral in air, which contains oxygen, to 650°C producing CeO_2 (in which Ce is 4+) which is insoluble in the acid leach. For large-scale operations, other oxidation methods can be used such as electrolysis or chlorine gas. On the laboratory scale, chemicals called oxidizing agents such as permanganate (MnO_4^-) can be used according to the equations below:

$$3Ce^{3+} + MnO_4^- + 4H_2O \rightarrow 3CeO_2 \downarrow + MnO_2 + 8H^+,$$

where CeO_2 is insoluble and is removed from solution. To remove europium its oxidation state must be reduced from 3+ to 2+ and this requires a chemical called a reducing agent. On the laboratory scale, zinc (Zn) is used according to the following equations:

$$2Eu^{3+} + Zn \rightarrow 2Eu^{2+} + Zn^{2+}$$

$$Eu^{2+} + SO)_4^{2-} \rightarrow EuSO_4 \downarrow.$$

Addition of sulfate (SO_4^{2-}) following the reduction results in precipitation of $EuSO_4$. For large-scale operations, reduction by sodium amalgam (sodium dissolved in mercury) removes europium, samarium, and ytterbium. As a recent development, the separation of Eu can be achieved by photochemical means using lasers. That is, an intense light beam of uniform wavelength is applied to an aqueous solution of Eu^{3+} and Eu^{2+} results as shown below:

$$H_2O + Eu^{3+} \xrightarrow[190\text{ nm}]{\text{light}} Eu^{2+} + H^+ + OH.$$

Again, SO_4^{2-} can be present simultaneously with the photoreduction allowing precipitation as $EuSO_4$.

It is now time to separate the remaining 14 elements. Most chemical properties such as solubility of a salt or stability of a complex ion depend to some extent on the size of the species involved. As the sizes of the RE^{3+} ions are very similar, differences in solubilities or stabilities will be slight but will at least be systematic due to the lanthanide contraction. Separation techniques prevalent before the 1950s relied on the differences in solubilities of various rare earth salts such as the double nitrates. $RE(NO_3)_3 \cdot 2N\text{–}H_4NO_3 \cdot 4H_2O$, and were known as fractional crystallization or precipitation methods. These are exceedingly laborious methods and, since about 1950, ion-exchange methods have become the rule for separating the rare earths.

To perform an ion-exchange separation, a solution of rare earth ions is introduced at the top of a column containing cation-exchange resin, a polymeric material typically in the form of sodium polystyrene sulfonate. The RE^{3+} ions readily undergo ion exchange displacing Na^+ ions, thus forming a band of the lanthanide ions bound to the top of the column. Affinity of metal ions for most resins is based loosely on ionic size and charge. To move these rare earth ions down the column and effect a separation, a solution consisting of a negatively charged organic species (a ligand) is slowly passed through the column. The ligand, typically having a number of sites that are capable of metal binding (a chelating ligand), have greater affinities for the RE^{3+} ions than the resin by forming stable metal–ligand complex. Because the complexes formed between the ligand and the RE^{3+} possess a lower positive charge than the initial RE^{3+}, they are less tightly held by the resin, and are displaced from the ion-exchange material into the surrounding solution. The RE^{3+} cations with smallest radius are most strongly bound to the ligand and so these ions have the greatest tendency to be eluted first. The size difference between different RE^{3+} is small, but enough to produce an effective separation. Among the useful ligands are α-hydroxyisobutyric acid and ethylenediamine tetraacetate (EDTA) (Fig. 2). The

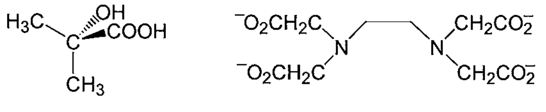

α-hydroxyisobutyric acid ethylenediamine tetraacetate (EDTA)

FIGURE 2 Molecular structures of two commonly used chelating ligands for ion-exchange separation of rare earth ions.

elutes are then treated with oxalate ion ($^{-}O_2C\text{–}CO_2^{-}$) and the precipitated RE oxalates ignited to the oxides. The low solubility of chelating ligands in aqueous solution, their high prices, and delicate and expansive recovery are some of the limitations of ion-exchange technique. When coupled with the disadvantages of using resins, namely, process discontinuity and low kinetics of ion exchange, this results in high cost for large-scale production of rare earths by this method. Presently only a few heavy rare earths are purified commercially on a small scale by ion exchange.

For large-scale production the chosen path is liquid–liquid extraction. The technique, using counter-current two-phase extraction procedure, relies on the differential partitioning of soluble rare earth complexes between immiscible aqueous and organic phases. A component will have a distribution coefficient, measured at equilibrium:

$$D = (\text{concentration in organic phase})/(\text{concentration in aqueous phase}).$$

For two components, RE_A and RE_B, both distributed between the organic and aqueous phases, a separation factor can be defined as $\beta^{A/B} = D_A/D_B$, where D_A and D_B are the distribution coefficients of RE_A and RE_B, respectively.

The closer the separation factor approaches 1 the more difficult it will be to separate those two components. The degree of separation is maximized by optimization of operating conditions and increase of separation stages (extraction and washing cycles). A simplified liquid–liquid counter-current extraction circuit is illustrated in Fig. 3. Continuity of operations is the predominant factor in the rapid expansion of liquid–liquid extraction, especially its ease in implementing counter-current techniques in the decanting mixers with a very high degree of automation. Solvent extraction technology is the most efficient and economical separation method presently available and today all large-scale commercial production is done in this way.

II. CHEMICAL PHYSICS OF THE RARE EARTHS

The rare earths have been the object of intensive studies by scientists from many disciplines, including condensed matter physics, solid-state chemistry, solution chemistry, biochemistry, and materials sciences. The scientific and technological interests in the rare earths are mainly due to their unique optical and magnetic properties. These interesting properties are a consequence of the atomic structure (also called electronic configuration) of the rare earth elements.

A. Atomic Structure: Electronic Configuration

Each atom of a given element contains, among other elementary particles, equal numbers of electrons and protons in quantities given by the atomic number of the element. Each electron in an atom occupies a state of well-defined energy which is characterized by a set of four indices called quantum numbers. To put it another way, each state can be thought of as a box or container, labeled by a unique set of four quantum numbers. If the number and relative energies of the available boxes are known for a given element, its electronic configuration can be easily determined

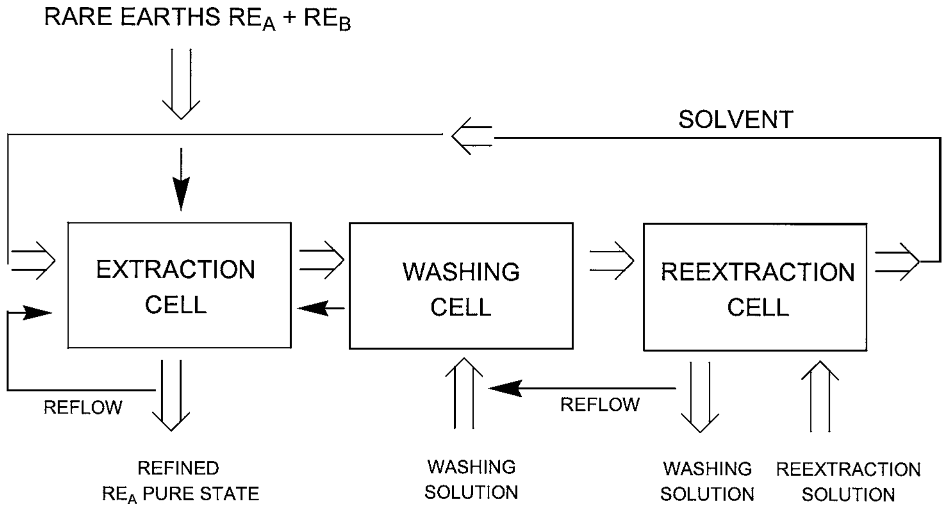

FIGURE 3 A schematized liquid–liquid counter-current extraction circuit for large-scale separation of rare earth ions. RE_A and RE_B are the two components of the mixture.

by simply filling the boxes beginning with that of the lowest energy and continuing until the appropriate number of electrons has been allotted.

The different quantum numbers together with their designation and symbol are n, principal; l, angular momentum; m, magnetic; and s, spin. Quantum numbers n, l, and m take only integral values and the possible values of l and m are restricted by the value of n in a manner given by the following relationships:

$$l = 0, 1, 2, \ldots, n - 1$$

for given n, $n \neq 0$

$$m = +l, +(l - 1), \ldots, -l$$

for a given l there care $2l + 1$ possible values of m.

It is found that s can have only the values $\pm\frac{1}{2}$. A widely used shorthand nomenclature exists to specify the angular momentum quantum number, l, according to the following.

l	Symbol
0	*s*
1	*p*
2	*d*
3	*f*
4	*g*
⋮	⋮

A box or level labeled by quantum numbers $n = 2$, $l = 1$ is thus called a $2p$ level, with $n = 3$, $l = 2$, we have a $3d$ level, and so on.

It is known that for a neutral atom in the absence of electrical or magnetic fields all levels with the same n and l values have the same energy (said to be degenerate levels). The number of degenerate levels associated with each n, l designation is easily computed from the relationships given above. For a $2p$ state we find three values of m, that is, $+1, 0, -1\,(2l + 1)$ which can each be associated with an s of $\pm\frac{1}{2}$ giving a total of six $2p$ levels. Similarly, a $3d$ level is 10-fold degenerate and a $4f$ level is 14-fold degenerate. The precise ordering of the energy states for a given atom is the result of a complex interplay of intratomic forces, but these orderings are known from experiment for all elements. At element 54, xenon, the energy levels are ordered in such a way that the sets $1s$, $2s$, $2p$, $3s$, $3p$, $3d$, $4s$, $4p$, $4d$, $5s$, and $5p$ are completely filled by the 54 electrons. Beginning with element 55 (Cs) the lowest unfilled levels are the $6s$, $5d$, and $4f$. For Cs to La, the order is $6s < 5d < 4f$ and the electronic configuration for La (57) is [Xe] $6s^2\,5d^1\,4f^0$, where the 54 "core" electrons are included in the symbol [Xe] and the number of electrons in each level is given by a superscript. But for element 58, Ce, the order is $6s < 4f < 5d$ so the configuration for Ce is [Xe] $6s^2, 4f^2$. This same ordering persists with minor anomalies at Gd (66) and Lu (71) until the $4f$ level is completely filled with 14 electrons. The electronic configurations of all of the lanthanides are shown in Table VI. Included are configurations for Sc (21) and Y (39) which are seen to be similar to La (57). Thus it is clear why there are 15 lanthanides and 17 rare earths. Sc, because it is rather smaller in atomic and ionic size than Y and the lanthanides, is sometimes excluded in the discussions that follow.

The filling of the $4f$ shell has profound consequences for the lanthanides. First there is the famous "lanthanide contraction." As electrons are being added to the same level, protons are also being added to the nucleus. As electrons in the same level are on average the same distance from the nucleus, they provide very poor mutual shielding of the nuclear charge. Thus, as electrons and protons are incrementally added across the series, the average radius of the $4f$ level decreases and, therefore, also the effective radius of the atom due to the unshielded increase in nuclear charge. This contraction is relatively small between adjacent elements, but the cumulative effect is quite significant

TABLE VI Electronic Configurations of the Rare Earth Elements[a]

Element	
21 Sc	[Ar] $4s^2\ 3d^1$
39 Y	[Kr] $5s^2\ 4d^1$
57 La	[Xe] $6s^2\ 5d^1$
58 Ce	[Xe] $6s^2\ 4f^2$
59 Pr	[Xe] $6s^2\ 4f^3$
60 Nd	[Xe] $6s^2\ 4f^4$
61 Pm	[Xe] $6s^2\ 4f^5$
62 Sm	[Xe] $6s^2\ 4f^6$
63 Eu	[Xe] $6s^2\ 4f^7$
66 Gd	[Xe] $6s^2\ 4f^7\ 5d^1$
65 Tb	[Xe] $6s^2\ 4f^9$
66 Dy	[Xe] $6s^2\ 4f^{10}$
67 Ho	[Xe] $6s^2\ 4f^{11}$
68 Er	[Xe] $6s^2\ 4f^{12}$
69 Tm	[Xe] $6s^2\ 4f^{13}$
70 Yb	[Xe] $6s^2\ 4f^{14}$
71 Lu	[Xe] $6s^2\ 4f^{14}\ 5d^1$

[a] The symbols [Ar], [Kr], and [Xe] refer to all filled core energy levels associated with the elements of atomic number 18 (Ar), 36 (Kr), and 54 (Xe). Explicitly they are [Ar] $\equiv 1s^2 2s^2 2p^6 3s^2 3p^6$, [Kr] $\equiv$ [Ar] $4s^2 3d^{10} 4p^6$, and [Xe] $\equiv$ [Kr]$5s^2 5d^{10} 5p^6$.

with the lutetium atom being about 20% smaller than lanthanum.

Second, as a rule, the rare earths have incomplete, partially filled $4f$ levels, Y, La, Yb, and Lu being the only exceptions. The presence of unfilled $4f$ levels conveys a rich variety of optical and magnetic properties on the rare earth elements and their compounds which has stimulated much basic research and has led to a number of useful applications as will be discussed in a later section.

Finally, although the different rare earths are distinguished by different numbers of $4f$ electrons, there is almost no correlation between the extent of filling of the $4f$ level and chemical properties. This is because the $4f$ electrons are on average held more closely to the atomic nucleus, that is, have a smaller average radial extent than either the $6s$ or $5d$ electrons. Indeed even the $5p$ and $5s$ electrons that belong to the Xenon-like core have a greater average radial extent than the $4f$'s. So the $4f$ electrons are well shielded from their environment and as the chemistry of elements is controlled largely by the nature of the outermost electrons, the valence electrons, and by atomic size, the chemical properties of the rare earths are indeed very similar. And as their valence electrons are of $6s$ and $5d$ character, their chemical properties will be related to both Ba and Hf as subsequent discussion will reveal.

B. Some Physical Properties of the Pure Elements

The rare earth elements as a group have chemical and physical properties that are normally described as metallic. In a later section, their chemical properties will be described but here we make some brief comments about a limited number of physical properties. First, though, it should be noted that many properties such as melting or boiling points and electrical conductivity depend very strongly on the state of purity of the element. Thus, it is only very recently, with the availability of relatively high purity samples, that some of these quantities have been determined definitively. The property most sensitive to impurities is the electrical conductivity. In spite of recent advances, impurity levels in even the best samples of the rare earth metals are a few orders of magnitude greater than has been achieved for other metals. Thus, the absolute magnitudes of the electrical conductivities for the lanthanides are rather higher than for other metals.

In Table VII are listed melting points, boiling points, crystal structure, and atomic volume at 24°C.

From the preceding, we begin to see that the rare earths are perhaps not so homogeneous a group of elements as we were led to believe from the behavior of their trivalent ions

TABLE VII Melting Points, Boiling Points, and Crystal Structures and Volume of the Rare Earth Elements

Element	Melting point (°C)	Boiling point (°C)	Crystal structure[a]	Atomic volume (cm^3/mol)
La	918	3464	dhcp	22.60
Ce	798	3433	ccp	20.70
Pr	931	3520	dhcp	20.80
Nd	1021	3074	dhcp	20.58
Pm	1042	—	dhcp	20.24
Sm	1074	1794	Complex hcp	20.00
Eu	822	1529	bcc	28.98
Gd	1313	3273	hcp	19.90
Tb	1365	3230	hcp	19.31
Dy	1412	2567	hcp	19.00
Ho	1474	2700	hcp	18.75
Er	1529	2868	hcp	18.45
Tm	1545	1950	hcp	18.12
Yb	819	1196	ccp	24.84
Lu	1663	3402	hcp	17.78
Y	1522	3338	hcp	19.89

[a] hcp, Hexagonal close packed; ccp, cubic close packed; bcc, body centered cubic; dhcp, double hexagonal close packed. These structures are diagrammed in Fig. 4.

in aqueous solution. For example, the melting points range from 819°C (Yb) to 1663°C (Lu) and these are adjacent elements! No fewer than five different types of crystal structure are exhibited, two of which are uniquely found in the rare earth series.

But there are predictable regularities. The melting points increase monotonically across the series with exceptions at Eu and Yb. This correlates well with the general decrease in atomic volume. The values for La (918°C) and Lu (1663°C) are reasonable when compared with their neighbors Ba (725°C) and Hf (2227°C) allowing for the differences in metallic valences (La and Lu are 3+, while Ba is 2+ and Hf is 4+).

Let us now turn to the anomalies at Eu and Yb where the melting points are much lower than expected. These two elements have atomic volumes that are much greater than those of the remaining members of the series and also different crystal structures. These properties can be understood in terms of a metallic valence of 2+ for both elements which follows from the electronic configurations of the atoms (Table VI and the special stability of half-filled ($4f^7$) and completely filled ($4f^{14}$) shells. This suggests that Eu and Yb have more in common with the group IIA elements, Ca, Sr, and Ba, than with their fellow rare earths. In fact, Eu and Yb are very similar in atomic volume to Sr (33.9 cm^3/atom) and Ca (26.1 cm^3/atom) and in melting point to Ca (839°C). Similar anomalies occur in the boiling points and even elements adjacent to Eu and Yb,

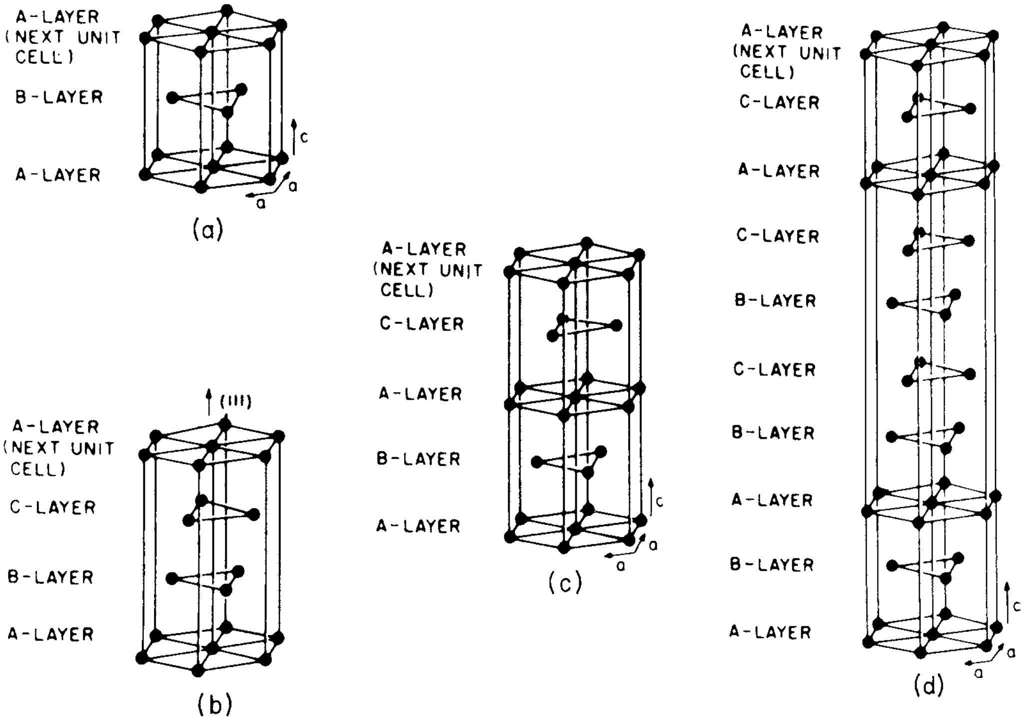

FIGURE 4 Crystal structures exhibited by the rare earth elements. (a) Hexagonal close packed (hcp), (b) cubic close packed (ccp), (c) double hexagonal close packed (dhcp), and (d) the complex structure of Sm. [From Gschneider, K. A., Jr. (1961). Crystallography of the rare-earth metals. *In* "The Rare Earths" (F. H. Spedding and A. H. Daane, eds.), p. 190, Wiley, New York.]

Sm and Tm, are involved. Although these latter elements are trivalent in the metallic state, they show a strong tendency to divalency in many compounds.

As mentioned, the rare earths exhibit five different crystal structures at room temperature. Three of these are common metallic structures, hexagonal close packed (hcp), cubic close packed (ccp), also called face-centered cubic fcc, and body-centered cubic. The first two are pictured in Fig. 4. The bcc structure is not pictured but consists of cubes of atoms surrounding another atom inserted into the geometric center or body-center of the cube. The two structures, unique to the rare earths are the double-hexagonal close packed structure (dhcp) found for La, Pr, Nd and Pm and the complex structure found for Sm. Both of these are variants of the hcp structure. Their occurrence for the early members of the series can be explained by postulating that the $4f$ electrons, which have relatively large radial extensions for the early elements, participate in the metallic bonding.

Finally, the physical properties that have attracted the most attention are the great variety of magnetic properties exhibited by the rare earths. The origin of magnetism in these elements lies in their electronic structure. The rare earths, as mentioned earlier, are characterized by partially filled $4f$ levels, and it is the detailed manner in which these $4f$ levels are occupied that determines the magnetic properties. Here we invoke principles first discovered by the early spectroscopists, which are called Hund's rules. We regard the $4f$ levels as 14 boxes labeled uniquely according to the quantum numbers as below: $l = 3$, $m_l = +3, +2, +1, 0, -1, -2, -3$.

$s = +\frac{1}{2}$ $\quad m_l = +3\ +2\ +1\ 0\ -1\ -2\ -3$

$s = -\frac{1}{2}$ $\quad m_l = +3\ +2\ +1\ 0\ -1\ -2\ -3$

We also need Pauli's exclusion principle which states that each box can contain only one electron. Hund's first rule requires that electrons be added to available boxes so as to maximize the total spin of the system, $S = \Sigma_i s_i$. Hund's second rule insists that, consistent with the first rule, the total magnetic quantum number $M_L = \Sigma_i m_{l_i}$ also be maximized. It is also standard to define $M_L(\max) \equiv L$, the total orbital angular momentum quantum number. With these ideas in mind it is easy to write down the total spin and orbital quantum numbers for all possible $4f^n$ configurations as shown in the following table.

n in $4f^n$	Typical rare earth ion	S	L	J
0	La^{3+}, Ce^{4+}	0	0	0
1	Ce^{3+}, Pr^{4+}	$\frac{1}{2}$	3	$\frac{3}{2}$
2	Pr^{3+}	1	5	4
3	Nd^{3+}	$\frac{3}{2}$	6	$\frac{9}{2}$
4	Pm^{3+}	2	6	4
5	Sm^{3+}	$\frac{5}{2}$	5	$\frac{5}{2}$
6	Eu^{3+}	3	3	0
7	Gd^{3+}, Eu^{2+}, Tb^{4+}	$\frac{7}{2}$	0	$\frac{7}{2}$
8	Tb^{3+}	3	3	6
9	Dy^{3+}	$\frac{5}{2}$	5	$\frac{15}{2}$
10	Ho^{3+}	2	6	8
11	Er^{3+}	$\frac{3}{2}$	6	$\frac{15}{2}$
12	Tm^{3+}	1	5	6
13	Yb^{3+}	$\frac{1}{2}$	3	$\frac{7}{2}$
14	Lu^{3+}, Yb^{2+}	0	0	0

Divalent and trivalent ions are listed for each $4f^n$ as all rare earth elements contain either trivalent or divalent ions, the remainder of the valence electrons, $6s$ and $5d$, having been donated to the sea or gas of "free" electrons which conduct the electrical current (called the conduction electrons).

C. Spectroscopic and Magnetic Properties of Rare Earth Ions

1. Transition in Rare Earth Ions: Absorption Spectroscopy

The excitation of an atom, ion, or molecule from its ground electronic level to higher lying level (excited state) may be effected by the absorption of light. When the incident light energy is exactly equal to the difference between the ground state and an excited state, a quantum of light will be absorbed. For rare earth elements, however, the majority of the electronic transitions involve a redistribution of electrons within the $4f$ orbitals, which by the spectroscopic Selection Rules are forbidden. This leads to the long excited state lifetimes in the micro- to millisecond range and the low extinction coefficients indicated by the pale colors of rare earth-containing compounds. Moreover, the electrons in the $4f$ orbitals are shielded by filled $5s$ and $5p$ shells. As a result of this shielding, the influence of the host lattice on transitions within the $4f$ shell is insignificant. In other words, optical spectra of rare earth materials are virtually independent of environment. Indeed, similar sharp line-like spectra are observed in gaseous, solution, and solid states.

2. Luminescence of the Rare Earths

Absorption of photon energy occurs when electrons from a lower-energy state are promoted to a higher-energy state. The reverse process, that is, the transition of electrons from an excited state to a lower-energy state corresponds to energy release via either radiative (light-emitting) or non-radiative (heat-releasing) pathways or both. The electromagnetic radiation emitted due to $4f$ transitions of the rare earth ions is usually in the visible range, but can also be in other spectral regions, such as the ultraviolet or infrared.

The trivalent cations of the rare earths have photoluminescent properties that are favorable for several kinds of applications. However, it is difficult to generate this luminescence by direct excitation of the lanthanide ion because of the forbidden nature of the f–f transition, as stated earlier. This difficulty can be overcome by some indirect means of excitation of the ion to an upper level. For example, the rare earth ions can be incorporated into a matrix or host of oxide or glass-forming materials. A carefully chosen impurity species, commercially called sensitizer, absorbs ultraviolet radiation and the energy is transferred to the emitter (activator) through the crystalline host lattice. The excited rare earth ion then decays to the ground state which will involve emission of light quanta corresponding to the energy differences with the ground level. The mechanism of such matrix-assisted energy transfer and subsequent luminescence is schematically shown in Fig. 5.

An ordered lattice facilitates this energy transfer but may simply serve to allow transfer to an inadvertent impurity ion that provides a mechanism for deactivation without emission. The degree of order of the lattice has to be optimized, as too does the concentration of the chosen emitter. Among the most efficient of commercial phosphors are those based on the red emission of Eu(III), the green emission of Tb(III), and the blue emission of Eu(II).

Another approach to sensitize rare earth luminescence is to prepare rare earth complexes with chelating ligands such as EDTA and the like. If the ligands contain organic functional groups (called chromophores) that are capable of absorbing light energy, highly luminescent rare earth complexes can be obtained. The chromophore acts like some sort of "antenna." The energy absorbed by such chromophores can be transferred to a nearby lanthanide ion, which is then able to emit its characteristic luminescence. The chelating ligands provide a protecting environment in such a way that deactivation of the excited state (or so-called quenching of luminescence) can be mitigated. Various lanthanide complexes containing organic chromophores are known to show efficient photoluminescence. The basic architecture of these systems is depicted in Fig. 6.

3. Magnetic Properties and Related Topics

All rare earth elements except La, Yb, and Lu have nonzero values of S and L. As both orbital and spin

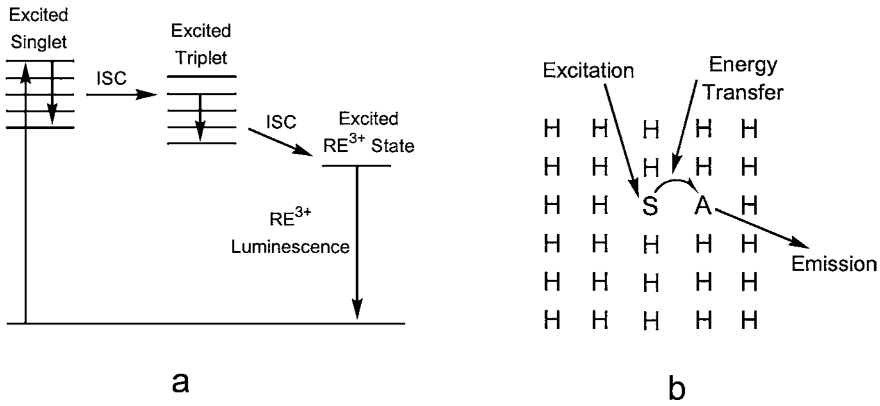

FIGURE 5 (a) Schematic representation of the mechanism of RE^{3+} luminescence (ISC, intersystem crossing). (b) Matrix-assisted luminescence of RE ions (S, sensitizer; A, activator).

angular momentum give rise to magnetic "moments," all rare earths except those mentioned have magnetic properties. In fact, for the rare earths, the magnetic moment is proportional to the total angular momentum $J = |L \pm S|$, where the minus sign is taken for $n = 1$ to 6 and the plus sign for $n = 8$ to 13. These values are also listed above. A magnetic moment may be visualized as a vector of magnitude proportional to J.

Recall our picture of the rare earth metals—a close packed array of trivalent ions (divalent for Eu), each with a magnetic moment proportional to J, imbedded in a sea of conduction electrons. As the $4f$ electrons have only a small radial extent, these moments are well localized on the ions. It is the interaction between these moments that gives rise to an ordered arrangement called "magnetic ordering." For the rare earths these interactions occur via the conduction electrons, the so-called RKKY (Ruderman–Kittel–Kasuya–Yosida) interaction. Magnetic ordering occurs only below a certain temperature called a critical temperature, T_c. Basically, there are two simple types of magnetic order—ferromagnetism in which all of the moments align parallel to each other along some direction in the crystal and antiferromagnetism in which for each magnetic moment pointing in some direction there is another moment exactly antiparallel to it. While there is only one way to achieve a truly ferromagnetic arrangement, a very large number of ways to realize antiferromagnetism exist. Now the rare earths exhibit both kinds of basic magnetic order and, in addition, several very complex forms in which the moments assume a spiral, helical, or even a sine-wave pattern. Critical temperatures range from about room temperature for Gd to near absolute zero.

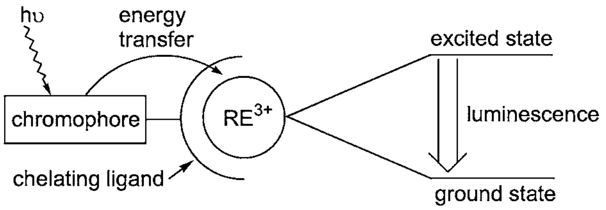

FIGURE 6 Sensitization of rare earth luminescence by energy transfer from an excited organic chromophore to a nearby rare earth ion.

Furthermore, a single element may show more than one type of order as a function of temperature. An attempt to summarize this very complex behavior is given in Table VIII.

Some of these structures for the rare earths Gd, Tb, Dy, Ho, Er, and Tm are pictured in Fig. 7. The origin of these very complex structures is thought to arise from the combined effects of the RKKY mechanism and giant magnetic anisotropy. The latter is the tendency for the moments to align along a particular direction in the crystal. Magnetic anisotropy is largest for ions with high values of L, the total orbital angular momentum, and the rare earths together with the actinides possess the largest L values of any groups of elements.

III. RARE EARTH MATERIALS

The rare earths are very reactive metals as expected from their position in the periodic table. They combine readily with nearly all of the other elements to form a wide variety of materials in both solid and solution states. In addition, the synthesis of rare earth-containing organometallic compounds has received considerable attention in the past 2 decades. The preparation and properties of these materials are briefly described here.

A. Solid-State Materials

1. Oxides

The rare earth oxides of the general composition of RE_2O_3 are well-defined and stable solids usually obtained as the

TABLE VIII Magnetic Properties of the Rare Earth Metals

Metal	T_c (K)	Type of order[a]
Ce	12.5	Af(?)
Pr	—	No order
Nd	19.2	AF
	7.8	AF
Pm	—	—
Sm	106	F
	13.8	Complex AF
Eu	91	AF
Gd	293	F
Tb	230	AF spiral
	225	F
Dy	146	AF spiral
	90	F
	133	AF spiral
	42	Complex
	20	F-Cone spiral
Er	80	Complex sine wave
	52	Complex
	20	F-Cone
Tm	56	Complex
	32	Complex

[a] AF, antiferromagnetic; F, ferromagnetic.

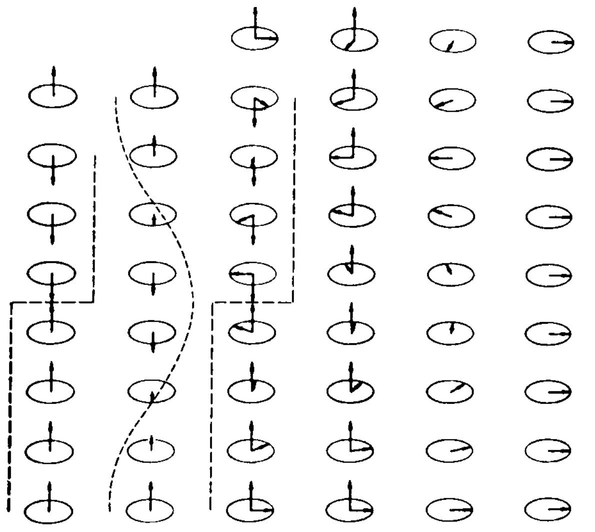

FIGURE 7 Magnetic structures of the rare earth elements Tm, Er, Ho, Dy, Tb, and Gd. The oval shape represents a plane normal to the unique direction of the crystal. This is the plane defined by seven, atoms of a hexagonal face in Fig. 2. The arrows represent the direction of the magnetic moments with respect to this plane. [From Koehler, W. C. (1972). Magnetic structures of rare earth metals and alloys. *In* "Magnetic Properties of Rare Earth Metals" (R. J. Elliot, ed.), p. 88, Plenum Press, New York.]

final product of the calcination in air of most RE metals and salts. This is a consequence of the high thermodynamic affinity of the rare earth elements for oxygen and the stability of their trivalent oxidation state. The three elements: cerium, praseodymium, and terbium, however, have stable oxides of different compositions, namely, CeO_2, Pr_6O_{11}, and Tb_4O_7, respectively. Cerium oxide, CeO_2 (also known as ceria) contains only tetravalent Ce, and is the most stable form produced when most cerium salts, Ce^{3+} or Ce^{4+}, are calcinated in air. For Pr and Tb, stable oxides with mixed $+3/+4$ composition result due to sufficient but limited stability of the tetravalent state. The coexistence of two valence state in the solid makes charge-transfer absorption bands possible and these two oxides are strongly colored. Mixed valence oxides RE_3O_4 (RE = for example, Eu or Sm), which can be formulated as $RE^{2+}(RE^{3+})_2(O^{2-})_4$, also exist.

Divalent oxides REO (RE = Nd, Sm, Eu, Yb) exist and may be prepared by reduction of RE_2O_3 with elemental rare earths at high temperature and pressure:

$$Ln_2O_3 + Ln \Rightarrow 3LnO$$

NdO, SmO exhibit lustrous golden yellow colors, exhibit metallic conductivity, and may be formulated as $RE^{3+}(O^{2-})(e^-)$, whereas EuO (dark red), YbO (greyish-white) are insulating genuine $RE^{2+}O^{2-}$. Such differences may be understood in terms of their electron configuration. It appears that the $[Xe]4f^n5d^1$ configuration is more stable than the $[Xe]f^{n+1}$ in some rare earth compounds, contributing a single electron per rare earth atom to a broad $5d$ band. The partially filled $5d$ band is believed to be responsible for the high electrical conductivity of NdO and SmO.

The rare earths also form a large number of "complex" oxides that involve one or more other metals in addition to a rare earth and oxygen. The most numerous and important type are oxides of composition $REFeO_3$, $RECrO_3$, and similar types called "perovskites" and those of composition $RE_3Fe_5O_{12}$ or $RE_3Al_5O_{12}$ called "garnets." The magnetic characteristics of rare earth garnets have been exploited for "magnetic bubble" memory in computer storage system. The best bubble materials are 20-μm films of $RE_3Fe_5O_{12}$.

2. Hydrides

All of the rare earths combine directly with hydrogen to form binary compounds of composition of REH_x, that except for Eu and Yb, have the fluorite (CaF) structure. Wide variations in composition make a continuous range from REH_2 to REH_3 possible. The light RE hydrides show a metal, REH_2, to a semiconductor, REH_3, transition; a color change can also occur, e.g., from a dark metallic green CeH_2 to a bronze CeH_3. The dihydride can be

formulated as $RE^{3+}(H^-)_2(e^-)$ with electrons delocalized in a metallic conduction band, accounting for their high conductivity for electricity. The trihydrides may be prepared at higher H_2 pressure, but these species are poor conductors for electricity, favoring the formation of RE^{3+} and $3H^-$.

3. Intermetallics

The rare earths form a large number of intermetallic compounds with transition elements. Of these intermetallic compounds, some most intensively studied are those with the elements Fe, Co, and Ni. A list of the typical RE–Ni materials gives an idea of the variety involved: RENi, RE_2Ni_3, $RENi_2$, $RENi_3$, RE_2Ni_7, $RENi_5$, and RE_2Ni_{17}.

The rare earth–transition metal intermetallics are to be distinguished from alloys that normally form between two or more metallic elements of similar size and crystal structure and can be regarded as "solid solutions." The rare earths are generally larger than most of the metallic elements so they tend to form compounds rather than alloys in combination. Many of these species form ternary hydrides:

$$\text{RE–M} + \text{Hydrogen} \Leftrightarrow \text{RE–M–Hydride}.$$

The crystalline structures containing atoms of disparate sizes offer a wide variety of interstitial sites, all of which can accommodate the small H atom. This inherent variety, along with a range of interatomic metal–metal contacts, allows for an inherent flexibility within the crystal lattice and a low activation energy for hydrogen absorption. Of the many RE–transition metal intermetallics, $LaNi_5$ has been found to absorb and desorb large amounts of hydrogen gas more or less reversibly under very mild conditions. The hydrogen content corresponds to $LaNi_5H_6$ and there has been intensive research into this compound as a medium for hydrogen storage.

4. Halides (Fluorides, Chlorides, Bromides, and Iodides)

The behavior of the rare earths with the halogen elements fluorine (F), chlorine (Cl), bromine (Br), and iodine (I) is somewhat similar to that with hydrogen. The rare earths lose their valence electrons, donating them to the halogens to form halide ions F^- (fluoride), Cl^- (chloride), Br^- (bromide), and I^- (iodide). If we represent a "halide" ion as X^-, compounds of composition REX_4, REX_3, and REX_2 form readily and have been known for some time. The REX_4 compounds are least common, existing only for X = F and RE = Ce, Pr, and Tb, those commonly exhibiting a 4+ valence. Not surprisingly, REX_3 compounds exist for all RE and all X. For X = F, the only REX_2 that exist have RE = Sm, Eu, and Yb. The most extensive series of REX_2 compounds occurs for X = I which numbers 11 at present. Only Y, Tb, Ho, and Er do not exist. The compounds formed when RE = La, Ce, Pr, and Gd all have high electrical conductivities and must be regarded as trivalent as with the hydrides.

In addition to the above "normal" valence materials, recent research has uncovered a number of mixed valence and apparent subvalent halides. For example, discreet compounds with halogen to rare earth ratios of 2:200, 2:167, and 2:140 have been observed for chlorides and bromides of Dy, Yb, Ho, and Sm. These are really mixed valence 3+, 2+ compounds with formulas such as Dy_5Cl_{11}, Yb_6Cl_{13}, and $Sm_{11}Br_{24}$. The complex structures of these materials have been the subject of considerable research.

Perhaps even more remarkable are the so-called subvalent materials Gd_2Cl_3 and GdCl. Formally, the rare earth valences in these compounds are less than 2+. In fact both compounds probably contain Gd^{3+}. In the Gd_2Cl_3 material the structural unit is a six-atom cluster of Gd atoms in the shape of a regular octahedron which share edges to form chains. The GdCl structure can be regarded as a condensation of the Gd_2Cl_3 octahedra to form layers of these octahedral units. Both are shown in Figs. 8 and 9. The GdCl compound has the same structure as ZrCl, indicating the kinship of the rare earths with their neighbors to the right in the periodic table.

5. Chalcogenides (Sulfides, Selenides, and Tellurides)

These are the elements related to oxygen in the periodic table and the rare earths form compounds of composition similar to those of the oxides which can be illustrated by examples from the sulfides, RES_2, RE_2S_3, RE_3S_4, and RES. Most similarities end with composition as these materials are very different from the oxides. RES_2, for example, does not involve the 4+ valence as part of the sulfur is present as S_2^{2-} (disulfide) and part as S^{2-}. One

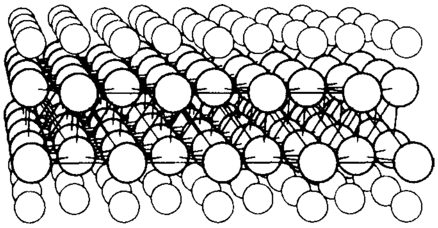

FIGURE 8 A view of the atomic arrangement (crystal structure) of GdCl, ScCl, etc. The large circles are Gd and these atoms form a metal–metal bonded double layer sandwiched between Cl atoms (smaller circles). [From Corbett, J. D. (1981). *Acct. Chem. Res.* **14,** 244.]

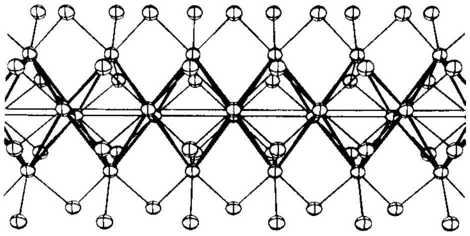

FIGURE 9 A view of the atomic arrangement (crystal structure) in Gd_2Cl_3, Y_2Cl_3, etc. The Gd atoms are in the shape of octahedra that share two edges forming an infinite chain shown in heavy outline. The Cl atoms are attached to the Gd atoms making up the chain. [From Corbett, J. D. (1981). *Acct. Chem. Res.* **14,** 243.]

cannot apply the same concepts that work with oxides to the chalcogenide family.

The compounds of composition RES are perhaps the most interesting. These form for all rare earths, yet only for Sm, Eu, and Yb is the rare earth valence 2+. In all other cases, physical measurements point to the 3+ valence and as only two of the valence electrons go to make S^{2-} the extra electron goes into the conduction electron sea making these materials good electrical conductors.

The rare earth carbides, nitrides, and borides have also been prepared, but these substances are much less well developed and will not be discussed here.

B. Coordination Compounds

1. General Features of Coordination Chemistry of Rare Earths

The rare earth ions typically exist in the trivalent oxidation state. The cations show similar properties, with gradual changes occurring across the lanthanide series, a size effect from the lanthanide contraction. Because of the large size of the cations, a coordination number greater than 6 (usually 8 to 9) in their compounds is often adopted. In addition, because the *f* electrons are well shielded from their environment, the effects imposed by the ligand(s) are insignificant, leading to the primarily ionic bonding in the coordination compounds. The lack of covalency in RE–ligand interaction implies that there are no orbital requirements for ligands around the metal center; the coordination polyhedra are determined by the steric requirement of the ligands and are therefore often ill defined. The ionic bonding character also causes the rapid ligand exchange, and as a result, stable complexes of the rare earth ions can only be obtained with chelating ligands. RE^{3+} cations display typical hard Lewis acid properties that prefer coordination with O and F–donor ligands. One indication is that the products isolated from an aqueous solution are often found containing aqua ligand(s).

2. Solution Chemistry of the Rare Earth Ions

Coordination chemistry of rare earth elements is an active research theme because of the importance of gadolinium complexes as contrast agents in magnetic resonance imaging, and luminescent europium and terbium complexes as probes in biochemistry. The extremely facile ligand exchange at *f* element centers makes the isolation of their coordination complexes difficult, particularly from aqueous solutions. A successful method of overcoming this is to increase the thermodynamic stability of the complexes by exploitation of the chelate and macrocyclic effects. Typical ligands used in such a strategy include β-diketonates, EDTA, and macrocyclic ligands such as crown ethers and cryptands (Fig. 10). Although the solution chemistry of the rare earth ions is predominantly that of the trivalent oxidation state, the chemistry of lanthanide ions of other oxidation states has also been studied, including those of Ce^{4+}, Sm^{2+}, Eu^{2+}, and Yb^{2+}.

C. Organometallics

The term "organometallics" defines compounds in which the rare earth atom is bound to carbon through single σ-bonds or through multiple π-bonding. The organometallic chemistry of the rare earths is arguably the most significant development in rare earth chemistry in the last 2 decades. As compared with other metals, the distinct features of rare earths include not only their highly positive characteristics, like that of alkali metals, but also a wide coordination sphere, like that of *d*-block elements. The properties and the structure of rare earth organometallics reflect the peculiarity of the electron arrangement of these metals. For example, rare earths cannot act as π-electron donors and, as a result, rare earth carbonyl compounds

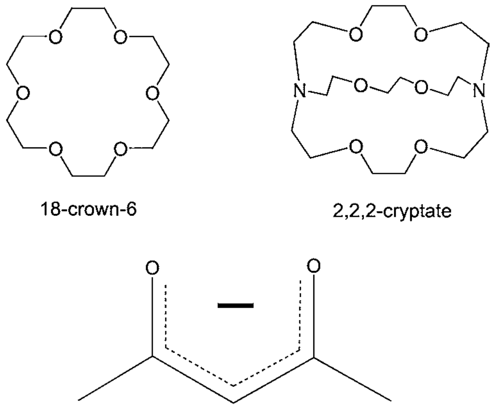

FIGURE 10 Molecular structures of three commonly used chelating ligands for rare earth coordination compounds.

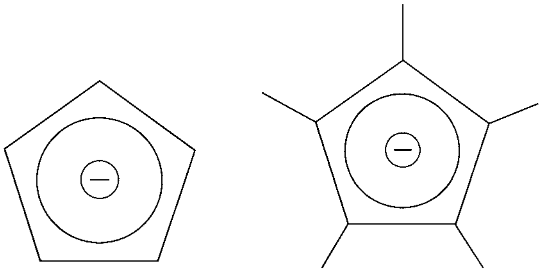

FIGURE 11 Molecular structures of three commonly used ligands for rare earth organometallic compounds.

(CO molecules as ligands) are not stable due to the lack of any significant back-bonding. The metal–ligand bonding is primarily ionic in character because of the contracted nature of the $4f$ orbitals. The highly carbanionic character of organic ligand and oxophilicity of rare earth ions render these substances extremely air and moisture sensitive. Although the organometallic chemistry of the rare earths is not as extensive as that of their d-block counterparts, the research is currently receiving a lot of attention, especially in the applications of these substances as highly efficient catalysts in organic synthesis and polymer chemistry.

The organometallic chemistry of the rare earths is predominantly, though not exclusively, that of cyclopentadienyl and substituted cyclopentadienyl compounds (Fig. 11). These complexes were the first organometallic rare earths to be synthesized and comprise three series: $RE(C_5H_5)_3$, $RE(C_5H_5)_2X$, and $RE(C_5H_5)X_2$. They are prepared by the reaction of the lanthanide chloride with the stoichiometric amount of NaC_5H_5:

$$RECl_3 + n\ C_5H_5Na \Rightarrow RECl_{3-n}(C_5H_5)_n + n NaCl.$$

The properties of cyclopentadienyl rare earth compounds are influenced markedly by the relationship between the size of the rare earth atom and the steric demand of the cyclopentadienyl group.

Rare earth organometallics have also been prepared with cyclooctatetraenyl (Fig. 11) and arene ligands, so have the σ bonded alkyls and aryl compounds. In the latter case, bulky and/or chelating ligands are typically used in order to achieve steric saturation around the rare earth center and hence the stability of the compounds.

Divalent rare earth organometallics for Eu, Yb, and Sm have also been prepared. The most important compounds are those of the pentamethylcyclopentadienyl ligands. The products have bent structures as have, surprisingly, the solvent free $(C_5Me_5)_2RE$ (RE = Sm, Eu). Remarkably, $(C_5Me_5)_2Sm$ reversibly complexes with dinitrogen, forming a dimeric compound with side-on bridging nitrogen (Fig. 12).

IV. TECHNOLOGICAL APPLICATIONS

Rare earth materials represent a growing market and group of technologies. These materials have expanding applications in markets as diverse as rechargeable batteries, advanced ceramics, permanent magnets, optical data storage, laser, fiber optics, glass, phosphors, and superconductors. Clearly it will be impossible to discuss each of these fully, so we will restrict our list to the major categories and treat only a few in modest detail.

A. Phosphors

A phosphor is a solid luminescent material that converts certain types of energy into light (electromagnetic radiation). The intense emissions and almost monochromatic tones obtained by diluting the rare earth-based activators in the appropriate host networks render rare earth compounds very attractive for phosphor application, especially to meet the very specific criteria for use that traditional band emission phosphors could not satisfy. A great variety of emissions can be obtained, depending on the type of activator brought into play and the respective positions of the excited or fundamental energy levels. Rare earth phosphors have now been extensively used in color television screens,

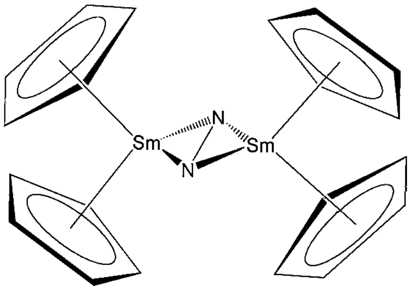

FIGURE 12 Molecular structure of a dinitrogen complex of samarium(II) pentamethylcyclopentadienylide, $(C_5Me_5)_2Sm$.

computer monitors, fluorescent lighting, and medical X-ray photography.

1. Luminescent Lighting

A prediction was made in early 1970s that a luminescent lamp with a high efficiency and high light quality could be obtained by combining three phosphors (luminescent materials) which emit in narrow wavelength intervals centered around 450 nm (blue), 550 nm (green), and 610 nm (red). Immediately, it was clear that phosphors doped with lanthanide ions were the most obvious choice to construct this tricolor luminescent lamp.

The perfection of phosphors using *blue* emissions from divalent europium, *green* emissions from trivalent terbium coactivated by cerium, and *red* from trivalent europium has made it possible to make trichromatic fluorescent tubes recently miniaturized in the form of compact lights for use in the home.

Giving off a color very close to that of incandescent lights, the trichromatic system of fluorescent light bulbs has a five to eight times greater light output than that of traditional light bulbs using an off-white band emitter. The life span for rare earth-based bulbs is more than a 1000 hr longer, resulting in significant savings to the user.

There has also been a marked increase in the use of phosphors in signs and signals. Numerous safety signs (exit lights, reflective safety bands, and highway markings, etc.) require the use of phosphorescence. Rare earths are part of the mineral phosphorescent product with the longest known phosphorescence duration.

2. Phosphors for Field Emission Display (FED)

In color television, the image is reproduced by selective excitation of three RE-phosphors (blue, green, and red) deposited on the internal face of the screen by a highly powerful electron beam originating from a metal electrode (cathode). Such an excitation technique is termed Cathode Ray Tube (CRT) technology. It is estimated that over 80% of the total worldwide display phosphor market will be utilized in the CRT industry (TVs and desktop PC monitors).

A new technology called Field Emission Display (FED) works on a principle similar to that of CRT, but instead of using just one "gun" spraying electrons against the phosphor-coated inside of the screen face, there are as many as 500 million of them (microtips). The main driver of this technology is the quest for brighter displays with less viewing angle dependence than liquid crystal displays (such as those currently used in laptop computers).

Any phosphor that is to be used in a FED must posses stringent properties in order to be successful: good chromaticity (high color purity), high luminance, high efficiency, low saturation, and good aging properties while it is operated at the low voltages and high current densities on portable displays. The materials currently used are sulfur-free rare earth compounds that are more stable than conventional CRT phosphors. FED devices are projected to become commercially significant around 2004 and to experience a strong growth rate for the rest of the decade and beyond. Initially, FEDs are likely to replace small LCDs in digital cameras and camcorders, but have the promise, eventually, to be deployed in laptop computers and other larger-area display applications.

3. Phosphors for Organic Light-Emitting Devices (OLEDs)

There is a strong demand to replace the cumbersome cathode ray tubes on televisions and computers with a large dimensional flat screen. This goal may be achieved by the FED technology as briefed above using more advanced RE-phosphors. It may also be achieved by the newly emerging organic light-emitting technology. An organic light-emitting diode (OLED) consists of a light-emitting junction layer sandwiched between two electrodes, one of which is transparent (Fig. 13). When an electrical current is passed through the OLED, the electrical energy is converted into light (electroluminescence), which passes out of the device through the transparent electrode. This conceptually simple design paves the way for thin, potentially flexible displays on plastic substrates and represents the future for flat-panel display technology. The properties of the light-emitting layer are critical to the performance of the OLED. The improvements in efficiency, lifetime, and ease of manufacturing that will be necessary for the realization of a low-cost, high-volume solution for flat panel displays, can only arise by careful optimization of the light-emitting layer.

In the lanthanide elements, f electrons residing are buried deep within the metal ion. The lack of any significant interaction between them and the surrounding ligands gives rise to two important features of rare earth phosphors

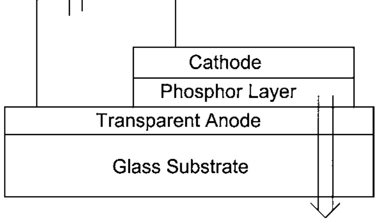

FIGURE 13 Schematic representation of an organic light-emitting diode.

(REPs): color purity and device processing flexibility. First, the emission occurs at a well-defined wavelength and the spectral bands are very narrow. Second, since the ligands have little influence on the core they can be modified without altering the emission wavelength. The ligands, being on the surface of the REP, largely determine its physical properties, such as solubility and volatility, which are so important for volume manufacture. Hence, these key determinants of the ease of processing can be "tuned" independently of the emission characteristics.

An additional and potentially great advantage of REPs is that devices containing REPs could operate with increased efficiency over those containing purely organic materials. The electrons in an electroluminescent device can be excited in two different states, singlets and triplets. In OLEDs containing purely organic systems only those electrons which are in singlet states can be responsible for the emission of light, imposing a limit of 25% on the efficiency of the device. The mechanism of light emission in REP materials is such that both singlet and triplet states can emit. The theoretical ceiling to device efficiency is therefore 100%.

B. Biological and Biomedical Applications of Rare Earth Luminescence

In luminescence research, attention has recently shifted from the development of solid-state phosphors (in television screens) and lasers (e.g., yttrium aluminum garnet (YAG) lasers) to solution-state methods exemplified by the development of probes for bioinorganic chemistry and the development of time-resolved luminescent labelings and assays.

1. Rare Earth Ion as Probe for Metal Binding Sites in Proteins

The importance of identifying Ca^{2+} in living systems is that it is an important intracellular secondary messenger of signal transduction. Changes in Ca^{2+} concentration trigger changes in cellular metabolism and are responsible for cell growth and regulation. Unfortunately, the study of Ca^{2+} is very difficult because it lacks any convenient spectroscopic property by which it can be studied. Because of the similar size and chemistry, it is possible to replace Ca^{2+} with a rare earth ion, such as Eu^{3+} or Tb^{3+}, which does have convenient spectroscopically useful traits. Study of the rare earth ions then gives the information otherwise unavailable directly for Ca^{2+}. Such replacements are a popular trick in bioinorganic chemistry and have yielded very useful structural information of metal-containing biomolecules.

2. Luminescent Immunological Assays and DNA Labeling

The detection and quantification of important biological molecules rely on immunoassays in solution. A typical analytical system consists of two components: a targeting group to recognize selectively and bind strongly to the target molecule of interest, and a reporter group which incorporates a radioisotope to allow detection at extremely low level of the target species. This approach provides high sensitivity for detection but also presents problems, including the potential of radiation exposure, high disposal costs, and limited shelf-lives of radioisotopes.

It has long been recognized that luminescence can potentially provide an equally sensitive detection method where the obvious drawbacks and problems associated with the radioactive substances do not arise. Using luminescent rare earth compounds not only eliminates these problems but also offers several advantages over the fluorescent organic dyes currently used in substitution of radioisotopes.

The emission bandwidths of the lanthanide ions are narrow, even at room temperature in fluid solution. As a comparison, the fluorescent dyes have emission bandwidths that overlap, sometimes making it difficult to distinguish between target species. In addition, because the lifetimes of the excited states of rare earth ions are relatively long (due to the forbidden nature of the f-electronic transitions), emission detection can be time-gated. In other words, a time delay is introduced between excitation and detection so that sources of interfering light such as scattered excitation light, Raman scattering, and impurity fluorescence have died down, allowing us to identify target molecules with greater accuracy.

The luminescent probe concept is by no means limited to immunological assays. It can be conveniently utilized in the labeling and mapping of DNA. Sequence information can offer insight into the location and function of genes, provide an understanding of the relationship between the variations in sequence and different genetic diseases, and serve as a basis for the prediction, treatment, and cure of those disease conditions.

C. Magnetic Applications

1. Permanent Magnets

Permanent magnets are materials that retain their magnetic properties after having been exposed to a magnetic field. They are found in a great variety of materials used in a significant and increasing number of industrial and commercial applications. These include micromotors and capacitors used in computers, audiovisuals (speakers, VCR's, etc.), automobiles (directional aids, power windows,

antilock brakes, dashboard computers, etc.), and household electronics (dishwashers, washing machines, air conditioners, etc.). Permanent magnets are also used as timing motors in industrial robots, military and space technology, and clocks and watches.

Among the commercially important families of permanent magnets, two contain rare earth elements, namely, the samarium–cobalt and neodymium–iron–boron. As compared with the non-rare-earth-containing permanent magnets, both rare earth-based permanent magnets have much higher-energy product (the figure-of-merit used to compare permanent magnets, which is a value proportional to the amount of stored magnetic energy per unit volume of magnet).

The samarium–cobalt magnets were discovered in the 1960s. Its performance made it possible to obtain intense magnetic energy in low volume, and subsequently, miniaturization utilized in timing motors, or, even more spectacularly, in audiovisuals where the use of the Sm–Co magnet, for example, made it possible to refine the miniature earphones used with Walkman®s.

But the most significant discovery in this area came in the 1980s with the discovery of neodymium–iron–boron ($Nd_2Fe_{14}B$) permanent magnets. This family of magnets has shown the fastest development of any permanent magnet yet discovered, and currently constitutes over 25% of the total worldwide market. The major driving force for the growth in the use of these magnets has been the significant size, weight, and performance advantage that they can provide over other magnets. These materials are now a key design feature in a wide range of high technology, high growth applications, notably spindle and stepper motors for the computer peripheral and consumer electronics industry. Virtually all of the hard disk drives manufactured worldwide employ spindle motors using $Nd_2Fe_{14}B$ magnets. Other major applications include motors for floppy disk drives, printers, fax machines, cameras, camcorders, and VCR's. Driven by these and other developing applications, the market for bonded neodymium–iron–boron is expected to continue growing.

2. NMR Shift Reagents

Since most complexes of trivalent RE are paramagnetic, they do not usually give useful NMR spectra. The resonances are at unusual chemical shifts and are often very broad. Nevertheless, certain complexes called lanthanide shift reagents are used to induce chemical shift changes selectively in other molecules via through space magnetic interactions. These complexes comprise a lanthanide ion surrounded by three β-diketonate ligands, such as in Fig. 14. The ligands are chosen such that the complexes are soluble in nonpolar solvents but still have reasonably accessible coordination sites so that the molecule being analyzed can form a bond via a heteroatom to the paramagnetic center. The use of lanthanide shift reagents in ^{1}H NMR can in certain cases dramatically simplifies the interpretation of the spectra and in other cases aids the assessment of the composition of complex mixtures.

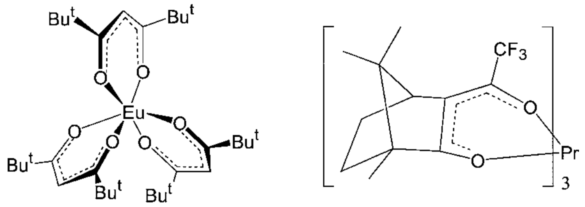

FIGURE 14 Molecular structures of two commonly used lanthanide shifts reagents in ^{1}H nuclear magnetic resonance (NMR) spectoscopy.

3. Contrast-Enhancing Agents for Magnetic Resonance Imaging

Whereas a quarter century ago activity was focused on the use of complexes of Eu, Pr, and Yb as chemical shift reagents for NMR spectroscopy, the current interest centers on the *in vivo* application of related paramagnetic gadolinium complexes as commercially important contrast agents in magnetic resonance imaging (MRI). This diagnostic imaging technique relies upon the detection of the spatially localized proton NMR signals of water present in living body fluids. The water signal intensity is dependent upon a number of factors particularly the values of the water proton relaxation time, which decreases substantially when the water oxygen is close to a highly paramagnetic substance such as a rare earth complex. These paramagnetic species are not themselves directly imaged but rather enhance contrast indirectly by affecting the nuclear magnetic relaxation times of the water protons in surrounding tissues, providing enhanced imaging contrast between normal and diseased tissues.

Paramagnetic "contrast" agents are now used routinely in clinical practice to enhance the signal intensity obtained in an MRI image. Attention is focused on the Gd^{3+} ion which couples a large magnetic moment ($S = 7/2$) with a long electron-spin relaxation time, two properties that allow efficient nuclear-spin relaxation. The contrast agents are administered as stable complexes to avoid toxicity of the free metal ions. The clinically approved contrast agents are highly stable and water-soluble complexes of Gd^{3+} with the ligands in Fig. 15 or their derivatives.

The MRI technique uses no invasive radiation such as X-rays, and to date no negative side effects have been demonstrated on the species under normal examination conditions. With the ever growth of MRI procedures,

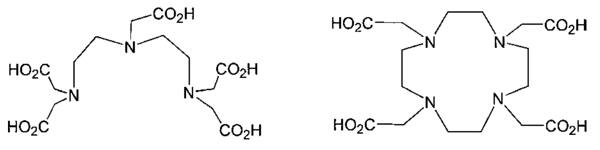

FIGURE 15 Molecular structures of ligands of rare-earth-based contrast agents for magnetic resonance imaging (MRI).

the contrast agents will certainly be playing accordingly critical roles for high-resolution diagnosis.

D. Other Miscellaneous Applications

1. Hydrogen Storage

Considering the decreasing resource of petroleum and growing environmental concern, the use of hydrogen as fuel is most attractive because it is abundant, nearly inexhaustible, and environmentally benign. However, liquid H_2 is difficult to store and transport because of its low density and low boiling point. In addition, H_2 forms explosive mixtures with air, adding further difficulty to its storage. The rare earth intermetallic compounds provide a means to store H_2 as a solid compound (hydride) from which it can be re-extracted. These properties of the alloys can be utilized for the hydrogenation of unsaturated organic compounds. The more important applications of rare earth intermetallic hydrides are in the technologically important areas. For example, the nickel rare earth hydride battery provides a source of energy storage to the new generation of electric vehicles. They are also extensively used in cordless tools, camcorders, cellular phones, and laptop computers. These rechargeable batteries are improving the performance of portable electronic devices by reducing their size and weight, while increasing the energy storage capacity. Moreover, because they contain no heavy metals such as cadmium, lead, and mercury, these batteries contribute to the protection of the environment.

2. Catalytic Converter

A well-tuned engine still produces many pollutants caused by the incomplete combustion of the fuel. The three regulated harmful compounds from exhaust gas mixtures are hydrocarbons (in the form of unburned gasoline), carbon monoxide (formed by the combustion of gasoline), and nitrogen oxides (created when the heat in the engine forces nitrogen in the air to combine with oxygen). Carbon monoxide is a poison for any air-breathing animal. Nitrogen oxides lead to smog and acid rain, and hydrocarbons produce smog.

A catalytic converter is a device that uses a catalyst to convert the three harmful compounds into harmless ones. The catalyst formulation comprises three key constituents: precious metals (platinum, palladium, rhodium), alumina, and rare-earth-based materials which enhance catalytic activity of the metals. Ceria is typically used in this capacity. It is white when pure, but is usually pale yellow on account of the nonstoichiometric phases between Ce_2O_3 and CeO_2. The nonstoichiometric ceria is responsible for the following functions to remove the pollutants from the motor vehicle engine exhaust:

a. Promotion of the water-gas shift reaction: $CO + H_2O \Rightarrow CO_2 + H_2$.

b. Enhancement of the NO_x reduction capability of rhodium.

c. Oxygen storage. In this role, ceria provides elemental oxygen in fuel-rich but air-poor conditions, to ensure oxidation of unburnt hydrocarbons and the removal of CO. It accomplishes this by going nonstoichiometric to CeO_{2-x}. In leaner (fuel-deficient, air-rich) conditions, it re-oxides to CeO_2, i.e., it stores oxygen during the air-rich periods.

Catalytic converters are an integral part of all automobile exhaust systems manufactured since the mid-1970s (in the United States as a result of the 1970 Clean Air Act).

3. Superconductors

Few events of recent times have received as much attention, both from the scientific community and the general public, as the discovery and characterization during the period late 1986 to 1988 of the so-called "high temperature superconductors." These are a series of structurally related, complex copper oxides, most of which contain rare earth elements as an integral component. Although the first material was discovered in early 1986, the report was not published until late in that year. The authors of this report, G. Bednorz and A. Muller, had found signs of "possible" superconductivity at temperatures as high as 29 K (the previous record was 23 K for Nb_3Ge) in a multiphase mixture of lanthanum, barium, and copper oxides. Other workers in Tokyo quickly identified the single compound responsible for the superconductivity as $La_{1.85}Ba_{.15}CuO_4$. Ironically, this exact compound had been synthesized earlier by several other groups, in one case in the mid-1970s, but no one had measured electrical conductivity down to sufficiently low temperatures until Bednorz and Muller.

This discovery generated much frenetic activity worldwide, and in early 1987 a large group at the Universities of Houston and Alabama-Huntsville reported another multiphase mixture with a superconducting transition temperature above 90 K. This was recognized as another breakthrough, as the transition temperature now exceeded 77 K,

the boiling point of liquid nitrogen, and significant commercial opportunities were forecast. The race to discover the chemical composition and crystal structure of the single phase responsible for the superconductivity was one of the most competitive and intense in the history of science. By late March 1987, because of reports from NRC Canada, Bellcore, AT&T Bell Laboratories, Argonne National Laboratories, McMaster University, and others, the compound was identified as $YBa_2Cu_3O_7$.

$YBa_2Cu_3O_7$ is an oxygen-deficient perovskite, the structure of which is shown in Fig. 16. It may be seen that there are two types of coordination about the copper ions—square planar and square pyramidal—and electron-spin resonance data indicate that there is a mixture of Cu^{2+} and Cu^{3+} ions distributed across the coordination sites (Fig. 16). Removal of oxygen from the partially shaded sites leads to the semiconducting $YBa_2Cu_3O_6$. Many other high *Tc* superconductor have been synthesized, including $Nd_{2-x}Ce_xCuO_4$ and $HgBa_2Ca_2Cu_3O_8$ (the current high *Tc* record holder at 133 K, and all feature puckered planes of CuO_2 (as does $Yba_2Cu_3O_7$) which are believed to provide a pathway for superconduction. Although the exact mechanism of superconductivity remains unclear, it is widely believed that in a superconducting material, pairs of electrons (known as Cooper pairs) move through the solid, the first electron distorting the lattice in such a way that the second can follow it very easily.

The commercial potentials of superconducting materials have yet to be realized because of the ceramic nature of the high *Tc* substances. The inherent brittleness of ceramics prevents their fabrication into wires, and it now seems that the most promising way forward is the deposition of thin films of superconductor onto metal oxide or silver surfaces to form flexible tapes.

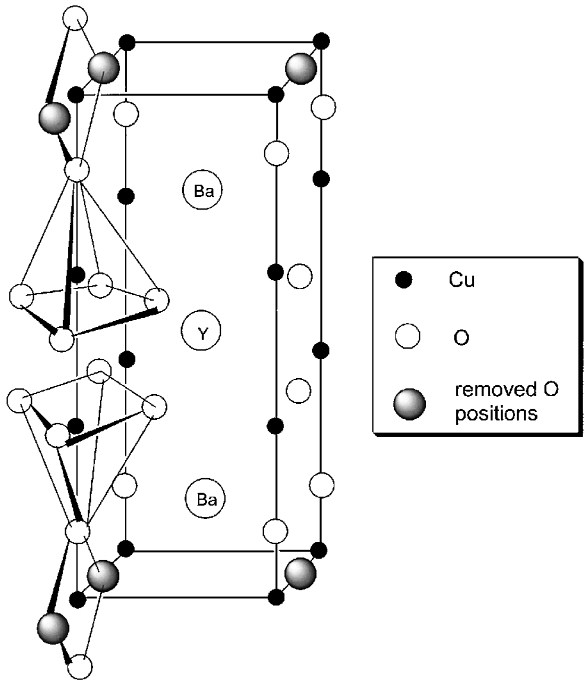

FIGURE 16 The unit cell for $YBa_2Cu_3O_7$.

V. CATALYSIS AND OTHER CHEMICAL APPLICATIONS

A. Rare Earth in Organic Synthesis

Organic synthesis with rare earth metals and their compounds has undergone considerable development over the last 2 decades. A great number of synthetic reactions have been explored with the use of rare earth reagents, wherein the synthetic utilities of earth metals and alloys, di-, tri-, or tetravalent rare earth compounds have been demonstrated. Applications cover almost every aspect of organic synthesis such as oxidation, reduction, and carbon–carbon bond-forming reactions, and some procedures have become indispensable protocols in modern organic synthesis. For example, unlike the common Lewis acids, some trivalent rare earths are stable in aqueous solutions. Due to this unique feature, they can be used in certain organic transformations where common Lewis acids may not even survive. In addition, many efforts in lanthanide-catalyzed reactions in aqueous and other environmentally friendly solvents proved to be very successful. This, along with the low to nontoxicity of rare earth compounds, makes them very promising in the field of green chemistry.

B. Rare Earth Catalysts in Petrochemical Industry

Rare earth compounds are also used in numerous catalytic reactions in petrochemical industry. One example is the use of rare earth salts to stabilize zeolites used for the catalytic cracking of crude oils to gasoline. Rare earth doping increases the activity of these zeolites with the consequence of higher gasoline yields. In addition, these rare earth-modified catalysts have found expanded application as a consequence of the refineries use of residual or "heavy" crude oils which contain "high" levels of nickel, vanadium, and sulfur which attack zeolites and reduce their activity; rare earths are more resistant to these catalytic "poisons."

The petrochemical industry is searching for more efficient and environmentally friendly processes for making monomers and complex hydrocarbons for downstream use as feedstocks for making polymers. Much emphasis has been placed recently on reducing the number of catalytic process steps required to make these hydrocarbons as well

as using less expensive starting feedstocks. This leads to the application of rare earth catalysts for the refinement of long-chained hydrocarbons to high-end monomers such as styrene. Cerium (as cerium carbonate) has traditionally been used in styrene monomer catalyst recipes as a catalyst promoter. Modern styrene monomer catalyst producers are increasing the levels of cerium in recipes to make "higher"-activity and "higher"-yield catalysts as well as using cerium to displace more toxic components such as chromium.

Another application of rare earth compounds in catalysis concerns with rare earth organometallics in polymer synthesis. Modern plastics and synthetic rubber manufacturers are discovering new uses of these compounds to improve the polymerization process and the selectivity of polymers.

C. Rare Earths in Catalytic Cleavage of DNA and RNA

Nonenzymatic phosphate ester cleavage is effectively facilitated by the RE^{3+} ions. The trivalent charge makes these cations strong Lewis acids for withdrawing electron density away from a phosphate diester substrate. They are also known for forming hydroxo species in aqueous solution by deprotonating coordinated water molecules. The requirement of rare earth ions for high coordination number allows the simultaneous coordination of the substrate and hydroxide nucleophiles. The disadvantages of RE^{3+} ions are their toxicity and the generally low stability of the complexes with regular ligands. Free RE^{3+} ions readily form RE^{3+} hydroxide precipitates and both forms are active in phosphate ester cleavage (Fig. 17), which makes kinetic control complicated. However, some stable RE^{3+} complexes have been successfully applied as RNA cleavers in antisense oligonucleotides. In addition, other dinuclear lanthanide complexes with macrocyclic ligands have been demonstrated to accelerate the cleavage of supercoiled DNA. Such efforts may eventually lead to the discovery of diagnostic and therapeutic agents for genetic diseases.

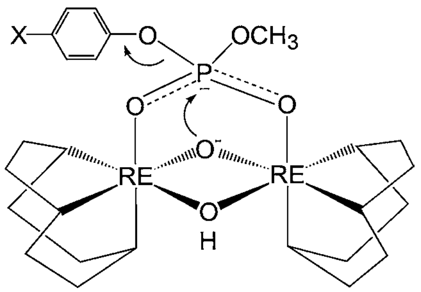

FIGURE 17 Double activation and cleavage of a diphosphate substrate by a rare-earth-hydroxo species.

Over the last few decades, the persistent efforts of the international community of scientists have led to a variety of new rare earth-containing materials and their applications, which extend beyond the traditional technological applications. These new applications are based on the unique $4f$ properties of the rare earth elements, and have become increasingly important. The demand for higher efficiency and more environmentally friendly materials and processes has led to a new era for rare earth materials. The new technologies, along with renovated traditional techniques, will continue to drive the rare earth markets well into the 21st century.

SEE ALSO THE FOLLOWING ARTICLES

Actinide Elements • Chemical Composition and Element Distribution in the Earth's Crust • Luminescence • Magnetic Materials • Periodic Table (Chemistry) • Superconductivity

BIBLIOGRAPHY

Cotton, S. A. (1991). "Lanthanides and Actinides," MacMillan Education, London.

Gschneider, K. A., Jr., and Eyring L. (eds.) (1978). "Handbook on the Chemistry and Physics of Rare Earths," North Holland, Amsterdam, Vols. 1–27 (published in 1978 to present).

Hedrick, J. B. (2000). "U.S. Geological Survey, Mineral Commodity Summaries," pp. 135, 189.

Imamoto, T. (1994). "Lanthanide in Organic Synthesis," Academic Press, Harcourt Brace & Company, Publishers, New York.

Kaltsoyannis, K., and Scott, P. (1999). "The f Elements," Oxford University Press, New York.